



Edited by
Michel TOUSSAINT
Dominique BONJEAN

The Scladina I-4A Juvenile Neandertal

Palaeoanthropology and Context

Andenne, Belgium



MAX PLANCK GESELLSCHAFT



Wallonie

Michel Toussaint & Dominique Bonjean (eds.), 2014.

*The Scladina I-4A Juvenile Neandertal (Andenne, Belgium)
Palaeoanthropology and Context*

Études et Recherches Archéologiques de l'Université de Liège, 134, 464 p.

Graphic design, layout, and cover art

Jean-François Lemaire,
Service public de Wallonie, DGO4

Front cover photographs

Transversal Profile C 32/31,
© Archéologie Andennaise

Hemimandibles, maxillary fragment,
and 16 isolated teeth of the juvenile
Neandertal of Scladina Cave,
© Archéologie Andennaise

Scladina Cave,
© Archéologie Andennaise

Back cover photographs

Left hemimandible Scla 4A-9 in situ,
© Archéologie Andennaise

Collection of ERAUL Editions

Université de Liège, Service de Préhistoire
Place du XX Août, 7, bât. A1
B-4000 Liège – Belgique
Tél.: +32/4/366.54.76 – Fax.: +32/4/366.55.51
E-mail: eraul@ulg.ac.be
<http://www.ulg.ac.be/prehist/>

**Centre archéologique de la grotte
Scladina, Archéologie Andennaise**

Rue Fond des Vaux, 339d
B-5300 Sclayn – Belgique
Tél.: +32/81/58.29.58
E-mail: direction@scladina.be
<http://www.scladina.be>

D/2014/0480/7

ISBN: 978-2-930495-20-0

All rights reserved. Not to be
reproduced without authorization

This monograph was awarded the
2014 Robert Beaujean Prize by the
King Baudouin Foundation
www.kbs-frb.be

The nineteen Neandertal fossils from Scladina Cave are grouped under the name 'Scladina I-4A', indicating the first (I) published Neandertal specimen found in Sedimentary Complex 4A. In addition, each of these fossils has its own code, from 'Scla 4A-1' to 'Scla 4A-20' (Scla 4A-10 is not assigned).

The Editors would like to express their deepest gratitude to Cheryl Roy and Rhylan McMillan (Vancouver Island University, Nanaimo, British Columbia, Canada), Rebecca Miller (University of Liège), as well as Jean-François Lemaire (Service public de Wallonie) for their valuable help in editing the English manuscript.

The Scladina I-4A Juvenile Neandertal

Andenne, Belgium

Palaeoanthropology and Context

Edited by Michel Toussaint & Dominique Bonjean

Michel Toussaint, Dominique Bonjean,
Grégory Abrams, Sanda Balescu,
Stefano Benazzi, Hervé Bocherens, Mona Court-
Picon, Freddy Damblon, Élise Delaunois,
Dorien De Vries, Kévin Di Modica,
Sireen El Zaatari, Christophe Falguères,
Paul Haesaerts, Catherine Hänni, Katerina
Harvati, Jean-Jacques Hublin, Kristin L. Krueger,
Kornelius Kupczik, Adeline Le Cabec,
Rhylan McMillan, Anthony J. Olejniczak,
Ludovic Orlando, Marcel Otte, Stéphane Pirson,
Donald J. Reid, Cheryl A. Roy, Matthew M. Skinner,
Tanya M. Smith, Paul T. Tafforeau,
Christine Verna, Yuji Yokoyama

Preface by

Jean-Jacques Hublin

The Scladina palaeoanthropological
project was made possible through
the long term implication of

Direction de l'Archéologie du
Service public de Wallonie

Max Planck Institute for
Evolutionary Anthropology

Archéologie Andennaise

With the support of

Université de Liège

Association wallonne
d'Études mégalithiques

Ville d'Andenne

Fédération Wallonie-Bruxelles

Institut du Patrimoine Wallon

Fondation Roi Baudouin

ERAUL 134

Études et Recherches Archéologiques de l'Université de Liège

Andenne, 2014

In memoriam
Jean Maes
President of Archéologie Andennaise
from 1983 to 2014

Table of Contents

PREFACE	9
Jean-Jacques HUBLIN	
CHAPTER 1 Overview and context of the Scladina palaeoanthropological project	13
Michel TOUSSAINT	
1. Introduction	13
2. Scientific context of the Neandertal child, Scladina I-4A	14
3. About human palaeontology	16
4. Scladina, palaeoanthropology in the field	17
5. Overview of the Scladina monograph	20
CHAPTER 2 Scladina Cave: archaeological context and history of the discoveries	31
Dominique BONJEAN, Grégory ABRAMS, Kévin DI MODICA, Marcel OTTE, Stéphane PIRSON & Michel TOUSSAINT	
1. Topography, geography, and geology of Scladina	31
2. History of the research	34
3. Sedimentary context	35
4. Archaeological context	35
5. The Scladina I-4A Neandertal Child: history of the discoveries	44
CHAPTER 3 The stratigraphic sequence of Scladina Cave	49
Stéphane PIRSON	
1. Introduction	49
2. History of the establishment of the stratigraphic record at Scladina Cave	50
3. Lithostratigraphy	51
4. History of the filling: sedimentary and diagenetic processes	61
5. Conclusions	65
CHAPTER 4 The palaeoenvironmental context and chronostratigraphic framework of the Scladina Cave sedimentary sequence (units 5 to 3-SUP)	69
Stéphane PIRSON, Mona COURT-PICON, Freddy DAMBLON, Sanda BALESU, Dominique BONJEAN, & Paul HAESAERTS	
1. Introduction	69
2. Palaeoenvironmental context	69
3. Chronostratigraphic framework	78
4. Conclusions and prospects	86
CHAPTER 5 Stratigraphic origin of the juvenile Neandertal remains from Scladina Cave: re-evaluation and consequences for their palaeoenvironmental and chronostratigraphic contexts	93
Stéphane PIRSON, Dominique BONJEAN & Michel TOUSSAINT	
1. Introduction	93
2. Methods	95
3. Reappraisal of the stratigraphic position of the juvenile Neandertal fossils	96
4. Discussion	110
5. Conclusions and prospects	115

CHAPTER 6	Non-Destructive Gamma-Ray Spectrometry of the Scladina Neandertal mandible (Scla 4A-1)	125
	Yuji YOKOYAMA & Christophe FALGUÈRES	
	1. Introduction	125
	2. Methods	125
	3. Results and discussion	125
CHAPTER 7	Taphonomy of the juvenile Neandertal remains from Sedimentary Complex 4A, Scladina Cave	127
	Dominique BONJEAN, Grégory ABRAMS, Élise DELAUNOIS, Kévin DI MODICA, Rhylan McMILLAN, Stéphane PIRSON, Cheryl A. ROY, & Michel TOUSSAINT	
	1. Introduction	127
	2. Material and methods	128
	3. Results	131
	4. Discussion: how to interpret the presence of the Scladina Neandertal remains	146
	5. Conclusions	150
	6. Annexes	150
CHAPTER 8	Dental development in and age at death of the Scladina I-4A juvenile Neandertal	155
	Tanya M. SMITH, Donald J. REID, Anthony J. OLEJNICZAK, Paul T. TAFFOREAU, Jean-Jacques HUBLIN & Michel TOUSSAINT	
	1. Introduction	155
	2. Material and methods	157
	3. Results	160
	4. Discussion	160
CHAPTER 9	Is sex determination of the Scladina I-4A juvenile Neandertal possible?	167
	Michel TOUSSAINT	
	1. Introduction	167
	2. Methods	168
	3. Results	171
	4. Discussion	172
	5. Conclusion	174
CHAPTER 10	The juvenile Neandertal mandible from Scladina (Scla 4A-1 & Scla 4A-9)	179
	Michel TOUSSAINT	
	1. Introduction	179
	2. Discovery and preservation	180
	3. Age and sex	181
	4. Mandibular morphology	181
	5. Morphometry	199
CHAPTER 11	3-D geometric morphometric analysis of the Scladina Neandertal child's mandible in a developmental context	215
	Katerina HARVATI & Michel TOUSSAINT	
	1. Introduction	215
	2. Materials and methods	215
	3. Results	217
	4. Discussion and conclusions	221

CHAPTER 12	The fragmentary right maxilla of the Scladina I-4A juvenile	223
	Christine VERNA & Michel TOUSSAINT	
1.	Introduction	223
2.	State of preservation	223
3.	Morphology	224
4.	Conclusions	231
CHAPTER 13	The dentition of the Scladina I-4A juvenile Neandertal	233
	Michel TOUSSAINT	
1.	Introduction	233
2.	Materials and methods	233
3.	Description of the Scladina I-4A teeth	235
4.	Discussion	302
CHAPTER 14	Enamel thickness in the Scladina I-4A Neandertal teeth	307
	Stefano BENAZZI, Michel TOUSSAINT & Jean-Jacques HUBLIN	
1.	Introduction	307
2.	Materials and methods	308
3.	Results	310
4.	Discussion and conclusions	312
CHAPTER 15	Interspecific and intraspecific taxonomic affinity based on permanent mandibular molar enamel-dentine junction morphology of the Scladina I-4A juvenile	315
	Dorien DE VRIES, Jean-Jacques HUBLIN, Michel TOUSSAINT & Matthew M. SKINNER	
1.	Introduction	315
2.	Materials and methods	315
3.	Results	318
4.	Discussion	321
5.	Conclusion	322
CHAPTER 16	Micro-Computed tomographic quantification of tooth root size and tissue proportions in the Scladina I-4A juvenile, a short-rooted Neandertal	325
	Adeline LE CABEC, Christine VERNA, Michel TOUSSAINT, Jean- Jacques HUBLIN & Kornelius KUPCZIK	
1.	Introduction	325
2.	Material and methods	326
3.	Results	329
4.	Discussion	337
5.	Conclusion	345
CHAPTER 17	Diet and ecology of the Scladina I-4A Neandertal Child: insights from stable isotopes	351
	Hervé BOCHERENS	
1.	Introduction	351
2.	Principles of isotopic tracking of Pleistocene terrestrial palaeoecosystems in Europe	351
3.	Material	352
4.	Methods	352
5.	Results and discussion	353

CHAPTER 18	Dental microwear texture analysis and the diet of the Scladina I-4A Neandertal Child	363
	Sireen EL ZAATARI, Kristin L. KRUEGER & Jean-Jacques HUBLIN	
1. Introduction		363
2. Materials		364
3. Methods		366
4. Results		367
5. Discussion		371
6. Conclusions		374
CHAPTER 19	Neandertal evolution and human origins: a tale from the Scladina I-4A Child	379
	Ludovic ORLANDO & Catherine HÄNNI	
1. Introduction		383
2. Results		383
3. Discussion		386
4. Perspectives: Neandertal genomics		389
CHAPTER 20	Scladina I-4A in the chronological context of the Neandertals from the Belgian Meuse Valley and northwest Europe	395
	Michel TOUSSAINT & Stéphane PIRSON	
1. Introduction		395
2. Methodological limits of the chronological approach		396
3. Chronology of the Belgian Meuse River Basin Neandertals		397
4. Northwest European context		402
5. Conclusion		403
CHAPTER 21	The Scladina I-4A juvenile Neandertal: a synthesis	409
	Michel TOUSSAINT, Dominique BONJEAN & Stéphane PIRSON	
1. Introduction		409
2. Main interdisciplinary results of the research at Scladina		409
3. Some perspectives for the Neandertal research in the Belgian Meuse River Basin		414
AN EXCAVATION JOURNEY		419
	Marcel OTTE	
	Scladina Cave from 1971 to 2014	423
	The Scladina Child	437
	Summaries/Résumés	439
	Figures and Tables	457
	Authors' addresses	462

Preface

Jean-Jacques HUBLIN

Neandertal studies are undoubtedly critical to understanding the human essence. Neandertals are our closest relatives in the evolutionary tree. Their lineage diverged from that of modern human ancestors about half a million years ago. The length of this separation was not enough for reproductive incompatibility to develop between the groups, but it resulted in the emergence of anatomical differences that surpass all the variability observed between living populations of our species. Along different pathways, the two lineages independently evolved large brains. Some degree of parallelism affected other aspects of their anatomy as well. Both developed very distinctive features. This combination of similarities and differences has often made Neandertals difficult to understand both biologically and behaviorally. The passion surrounding the scientific debates on these issues come as no surprise.

This particular situation and a long and rich record of discoveries in Europe and in the Levant have naturally caused Neandertals to be the most analyzed fossil hominins. Virtually all possible methods of investigation in the field of palaeoanthropology have been applied to Neandertals and, when a new technique emerges, it is almost inevitably first adjusted on Neandertal material before being used to investigate other fossil hominin groups.

The publication of “The Scladina I-4A Juvenile Neandertal” does not simply provide us with an exhaustive description of unpublished fossil remains. Like some previous monographic publications dedicated to specific sets of fossil remains, it offers a remarkable illustration of the current available techniques at a given stage of development of the discipline. The impressive effort taken to analyze the fragmentary remains of an eight-year-old Neandertal, who lived and died some 87,000 years ago in the Meuse Valley, have benefited from the spectacular methodological advances witnessed in the field of palaeoanthropology over the last two decades. Following two other volumes, one dedicated to the sedimentary filling of Scladina and its palaeoenvironment and the other to the archaeological material unearthed in the cave, this volume will therefore stand as a main reference along the continuous and disparate flow of Neandertal studies that have been produced since the first discoveries of these archaic humans in the middle of the nineteenth century.

The study of the Scladina Neandertal juvenile starts with the detailed analysis of its geological and archaeological context. Taphonomy has become a key issue to understand the occurrence of fossil hominins in archaeological sites. Specifically, the anthropogenic nature of their deposition cannot be taken for granted anymore; site formation and carnivore activities must be now seriously investigated. In Scladina Cave, the remains of a deceased child including at least the skull and the mandible, but possibly some other parts of the body, were dispersed inside a karstic cavity in relation with the formation of a gully, ending up in three different sedimentary environments. How these fossils entered the cave is still purely speculative. However, although fragmented, the bones were little weathered and are remarkably well preserved.

A large portion of the analysis of this fossil hominin was conducted at the Department of Human Evolution of the Max-Planck Institute for Evolutionary Anthropology in Leipzig, where the remains were loaned on several occasions and were CT-scanned. Dr. Michel Toussaint was hosted in the department for several periods of time, during which access to the fossil material by various specialists was made possible and intense collaborative works could take place. Several forms of sampling, including the preparation of histological thin sections, were also conducted. The well-preserved and rather complete dentition of the specimen allowed a detailed analysis of the dental tissues, from a quantitative and non-quantitative point of view. Imagery techniques were largely exploited for the visualization of internal structures and for the study of the dental surface microwear.

The sections of this volume where geometric-morphometrics were implemented to analyze shapes and forms are quite significant of the evolution of the field. They complement the detailed anatomical descriptions and allow the quantitative assessment of subtle morphological variations. This is particularly spectacular when dealing with fine internal structures such as the enamel-dentine junction in the dental crown. These mathematical tools also allow the Scladina individual to be repositioned in the developmental context of Neandertal mandibles, emphasizing that Neandertal juveniles seem more advanced along their growth trajectory than modern human juveniles of similar dental age.

Key aspects of the results obtained on the Scladina Neandertal relate to its immature nature. Changes in life history patterns and developmental rates played a central role in the establishment of the human niche among hominoids. Approaches based on life history theory have initially suggested that the human developmental pattern emerged at an early stage of the genus *Homo* evolution. However, empirical data provided by the fossil record brought no support to this notion. *Homo erectus* and most likely some later Pleistocene hominin forms did not display a modern developmental pattern. Specifically regarding Neandertals, the analysis of the Scladina juvenile's dental tissues has been pivotal in highlighting differences with modern humans. Enamel and dentine microstructures of this immature Neandertal demonstrate a clear discrepancy between its calendar age at death and a developmental age that could be estimated on modern standards for dental eruption. These results support the hypothesis of a faster dental and/or somatic development in Neandertals.

The Scladina juvenile was also one of the first Neandertals from which ancient DNA was extracted and sequenced, at a stage of development of palaeogenetics when only fragments of mitochondrial DNA could be analyzed.

Another pioneering study that has been conducted at Scladina addresses the stable isotopes of N and C in preserved organic molecules of the bony structure. The palaeodietary reconstruction it allowed confirms the importance of the consumption of open environment herbivores for Neandertals. This diet could have been driven by a choice; alternatively, other sources of game could have been difficult to access at the time the Scladina Child lived.

The Scladina hominin provides us with a wealth of information for Neandertals during a time period — the early Weichselian — that to date only yielded a limited fossil record in Western Europe. It provides invaluable information on the individual Neandertal development and shows that many of the distinctive features of the group are already present at a juvenile stage.

The events that allow the preservation of fossil hominins such as those from Scladina are extraordinary. The remains of a rare mammal of the Pleistocene landscape have miraculously

survived in the sediment of a cave for tens of millennia and unexpectedly escaped total oblivion. Facing the material evidence of extinct forms of hominins always provokes deep emotions in anyone perceiving their exceptional nature. The never-ending interest of the public for the Palaeolithic world is one of the most obvious expressions of this fascination. There is however a high risk of betraying the rich message that fossil hominins can deliver to us by turning them into inaccessible relics, overprotected in museum showcases. A long tradition of storytelling surrounds Neandertal remains. Some might be satisfied with it, but the truth is that only hard work by specialists can unveil some snapshots of these lost existences. The study of a fossil hominin can never be considered finished, as new methods of investigation constantly appear in the field of palaeoanthropology. It is therefore of the utmost importance to warrant access to the fossil material for the scientists. Still there are countless examples of restriction on this access. In sharp contrast, the discoverers and curators of the Scladina juvenile Neandertal showed exemplar flexibility and openness in supporting all possible studies of these precious remains. Their reward is a monograph that provides an impressive variety of results and will remain as a model of its kind.

Leipzig, the 18th of August 2014

Michel TOUSSAINT

*Michel Toussaint & Dominique Bonjean (eds.), 2014.
The Scladina I-4A Juvenile Neandertal (Andenne, Belgium)
Palaeoanthropology and Context*

Études et Recherches Archéologiques de l'Université de Liège, 134: 13–30.

1. Introduction

Many of the most famous Neandertal fossil discoveries occurred numerous decades ago: Gibraltar (1848), the Neandertal type site (1856), Krapina (from 1899), La Quina (from 1908), La Chapelle-aux-Saints (1908), La Ferrassie (from 1909), etc. As a result, their context is not precisely known by comparison to current standards of research, particularly in the absence of rigorous stratigraphic and chronological position as well as planimetric distribution or strict association with lithic material. Within the Meuse River Basin of southern Belgium (i.e. in the vicinity of Scladina) this same situation is encountered in a series of illustrious karstic discoveries (TOUSSAINT, 1992, 2001): in 1829-30 at Engis by Ph.-Ch. Schmerling (SCHMERLING, 1833-34; TILLIER, 1983), in 1866 at La Naulette in the Lesse Valley by E. Dupont (DUPONT, 1866; LEGUEBE & TOUSSAINT, 1988), and in 1886 at Spy (FRAIPONT & LOHEST, 1887). The same may be said about the lesser known discovery of some teeth and bones at Goyet around 1870 (ROUGIER et al., 2009, 2014) and of a partial femur in 1895 at Fonds de Forêt (TWIESSELMANN, 1961).

To finally have at our disposal Neandertal remains from Meuse River Basin caves which possess a precise enough context compatible with modern scientific requirements, we had to wait until the last three decades for the discovery of new Middle Palaeolithic human fossils in the sedimentary fillings of three other caves, successively in 1984 at Trou de l'Abîme (Couvin; TOUSSAINT et al., 2010), from the early 1990s onwards at Scladina (Sclayn-Andenne; TOUSSAINT et al., 1998) as well as in 1997 at Walou (Trooz; TOUSSAINT, 2011). At Couvin and Walou, however, the discoveries are limited to an isolated tooth, a deciduous mandibular right second molar and a mandibular left first premolar, respectively.

This explains the tremendous interest in the discovery of both halves of a mandible, a fragment

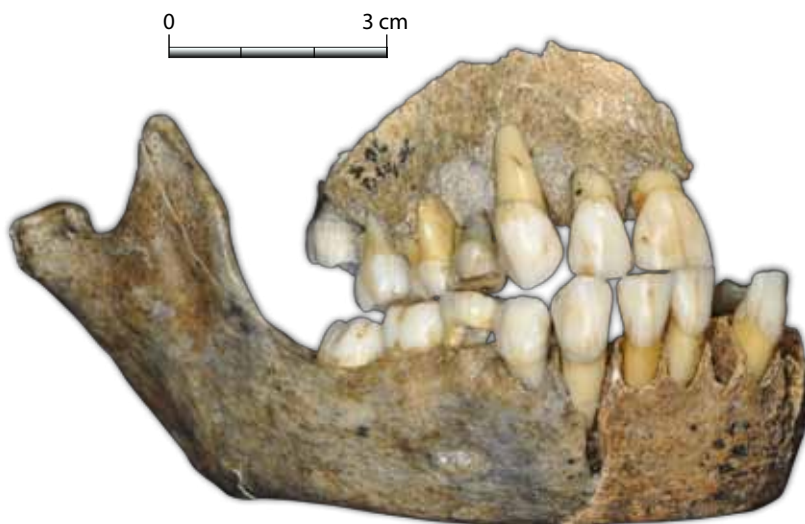


Figure 1: Refitting of most Scladina Neandertal fossils found in former Layer 4A (photograph Joël Éloy, AWEM).

of a maxilla, and a series of teeth, all from the same juvenile Neandertal (Figure 1), during the excavations of Scladina Cave, on the left bank of a small tributary of the Meuse Valley (Figure 2). Excavations at Scladina have been conducted almost without interruption since 1978 by the University of Liège and, at present, by Archéologie Andennaise. The importance accorded to the context of all the fossils and artefacts at Scladina was enhanced by the discovery of the right hemimandible (Scla 4A-1) of a child in 1993, the first Neandertal osseous element encountered in Belgium in 98 years. A very high degree of resolution has been achieved over the past 10 years based on the stratigraphic revision (PIRSON, 2007; Chapter 3, this volume) and an excavation method adapted to this stratigraphic complexity (Chapter 2, this volume; BONJEAN, 2009). In this regard, a unique field technique based on combined horizontal and vertical excavations on a reduced surface has recently been developed in order to obtain a very precise stratigraphical position for all lithic and faunal artefacts without the



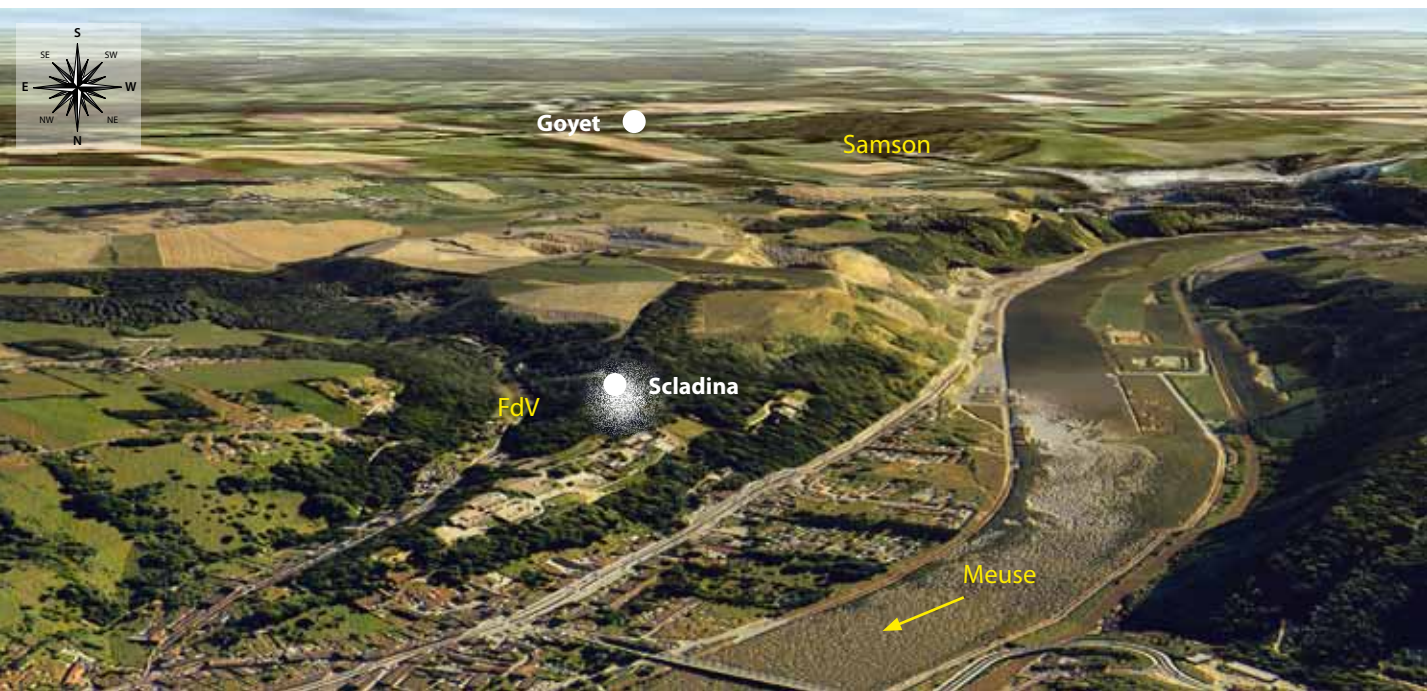


Figure 2: 3D representation of the Meuse Valley and two of its tributaries, Fond des Vaux (FdV) and Samson, with the location of Scladina and Goyet caves (Joël Éloy, AWEM).

loss of their planimetric distribution, as all the Cartesian coordinates are precisely recorded.

Scientific context of the 2. Neandertal child, Scladina I-4A —

The anthropological finds from Scladina derive from a prehistoric and palaeontological site of major importance to the Belgian Meuse Basin as well as northwest Europe. The application of the latest standards of modern multidisciplinary Quaternary research to the excavation of the site provides remarkable precision in the contextual allocation of these finds, amplifying their interest.

The human fossils found in former Layer 4A have each received a number, from 1 to 20 (for example Scla 4A-11 which refers to the isolated permanent maxillary right central incisor). In addition, as all these fossils of former Layer 4A belong to the same 8-year-old specimen, it has been decided to use the code 'Scladina I-4A' to refer to the juvenile as an individual.

The stratigraphical sequence of the cave had been partially described in the pioneering works of archaeologists (OTTE et al., 1983; BONJEAN, 1998^a) and geologists (DEBLAERE & GULLENTOPS, 1986; GULLENTOPS & DEBLAERE, 1992; HAESAERTS, 1992; BENABDELHADI, 1998) who had revealed the tremendous potential of the site. The recent

meticulous reappraisal of the sequence during the course of Stéphane Pirson's (2007) PhD thesis in geology at the University of Liège revealed the sequence of deposits was much more complex and rich in information than previously thought, with significant variability in the sedimentary and diagenetic processes as well as in the scale of the lateral variations of facies.

The cave is also rich in palaeontological and palynological information. In this regard, it has led to multiple research projects, published in numerous papers and PhD theses.

Initial projects focused on palynology (e.g. BASTIN & SCHNEIDER, 1984; BASTIN et al., 1986; SCHNEIDER, 1986), microfauna (Cordy in BASTIN et al., 1986), and macrofauna. Many of these contributions were developed in the first monograph dedicated to the site (OTTE (ed.), 1992; BASTIN, 1992; CORDY, 1992; SIMONET, 1992). Some more recent works deal with archaeozoology (e.g. PATOU-MATHIS, 1998^{a, b}; PATOU-MATHIS & LÓPEZ-BAYÓN, 1998; CRÉPIN, 2002) and taphonomy (PIONNIER, 2006; DELAUNOIS et al., 2012).

All this previous research referenced initial lower resolution stratigraphic records that have been improved in recent years (PIRSON, 2007). For example, the authors combined all data from what they called 'Layer 4' (SIMONET, 1992; PATOU-MATHIS, 1998^a), whereas this vast layer was actually very stratigraphically complex.

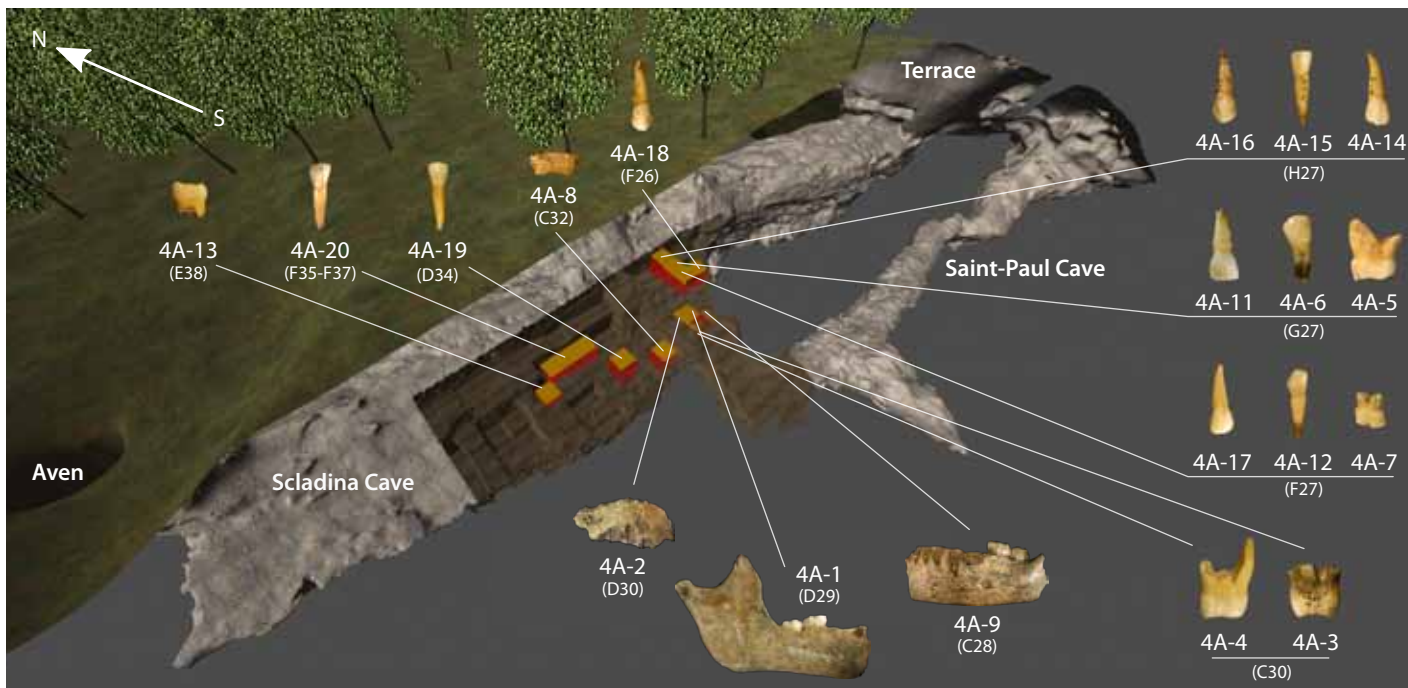


Figure 3: 3D reconstruction of Scladina Cave positioning the Neandertal fossils found in former Layer 4A (Joël Éloy, AWEM).

Despite this problem, the correlation of information gathered from old palaeontological data with recent palynological and anthracological data (Damblon & Court-Picon, in PIRSON, 2007) based primarily on the last stratigraphic revisions is possible. This association forms an innovative palaeoenvironmental synthesis, confirming the remarkable quality of preservation of the Scladina deposits (PIRSON, 2007).

A variety of dating methods provided numerous dates for Scladina: conventional radiocarbon dating of bones and stalagmites; AMS dating of animal bones and teeth; U/Th dating of concretions, stalagmitic floors, and teeth; TL dating of calcite, burned flint, and silt; gamma spectrometry of the Neandertal mandible, and ESR dating of bones (e.g. Gilot, Szabo & Aitken in OTTE et al., 1983; Gewalt in BASTIN et al., 1986; GEWELT et al., 1992; GILOT, 1992; HUXTABLE & AITKEN, 1992; DEBENHAM, 1998; BONJEAN, 1998^b; Falgùères & Yokoyama in TOUSSAINT et al., 1998; PIRUELLE, 2006; PIRSON, 2007; PIRSON et al., 2008). These dates are discussed in Chapter 4 and placed in the context of the general stratigraphic sequence of Scladina. With few exceptions, all these dates become gradually younger from sedimentary Unit 5, which yielded the richest prehistoric occupation of the Middle Palaeolithic – some 130,000 ± 20,000 years BP – up to sedimentary Unit T, near the top of the Pleistocene sequence, from which

a ¹⁴C date of 37,300 +370/–320 BP (GrA-32633; PIRSON, 2007) was recently obtained. Based on this set of dates, a palaeoenvironmental synthesis can tentatively be related to a hypothetical stratigraphic position, in which some benchmarks appear fairly clearly (see Chapter 4).

Another cave of the Meuse River Basin, Walou, located about sixty km east of Scladina, has also yielded a magnificent Pleistocene sequence whose chronostratigraphy is better known (DRAILY et al. (dir.), 2011; PIRSON et al. (dir.), 2011). The comparison of the stratigraphy of these two caves contributes to the establishment of a palaeoenvironmental and chronostratigraphic reference for Meuse River Basin caves to which other regional archaeological and palaeoanthropological discoveries can be correlated. For example, fossils found in an acceptable, albeit less complete, stratigraphy than those of Walou and Scladina, may be reinterpreted as is notably the case for the deciduous mandibular right second molar found at Trou de l'Abîme, in Couvin (TOUSSAINT et al., 2010, 2011).

In addition to its stratigraphic, palaeontological and palaeoenvironmental interest, Scladina yielded some essentially Middle Palaeolithic occupation layers (mainly units 5 and 1A). Numerous archaeological studies focusing on lithic typology, technology, spatial distribution and raw materials have been published (for example OTTE et al.

(dir.), 1998, DI MODICA & BONJEAN, 2004 and more recently DI MODICA, 2010, 2011).

The event which confers a major international appeal for Scladina was the *in situ* discovery (from 1993) of dental and osseous remains of a Neandertal child (Figure 3) although the first fragments (found in 1990) were not identified at that time. The studies offered in this monograph correspond only to the first stage of our understanding of the human palaeontological heritage of the cave as the potential for the discovery of Neandertal remains seems far from exhausted. A distributional comparison of the location of recovered hominin fossils with the large unexcavated areas of the cave provides an indication in this respect, notably by highlighting a concentration of teeth at the limit of the excavated area. The fact that the Neandertal face is only represented by a fragment of right maxilla adds another argument in this regard.

The outstanding state of preservation of the bone material, like that of numerous other limestone caves of the Meuse River Basin, allowed the extraction of fossil DNA, animal (ORLANDO et al., 2002) as well as human (ORLANDO et al., 2006). At that time one tooth of the child delivered the oldest fragment of the Neandertal sequence and this sample exhibited a larger genetic variability than more recent samples, for example those of the eponymous Feldhofer site. The $\delta^{13}\text{C}$ and $\delta^{15}\text{N}$ from Scladina bones, either belonging to mammals (BOCHERENS et al., 1997) or Neandertals (BOCHERENS & BILIOU, 1998; BOCHERENS et al., 1999, 2001), have also deepened our knowledge of the diets of extinct taxa. Some fragments of the TRAP protein were also recovered (NIELSEN-MARSH et al., 2009).

3. About human palaeontology —

Human palaeontology is a science whose complexity has been steadily increasing over the years. A scientist a quarter of a century ago could potentially publish alone and satisfy research demands by describing fossils anatomically and by comparing them statistically with the corpus of more or less similar hominins.

Today, numerous new disciplines yield information about fossils in diverse fields such as the details of the internal morphology; diet studied by means of isotopic biogeochemistry; DNA, both mitochondrial and nuclear, and the timing of dental development, microwear analysis, and

enamel thickness. A number of sophisticated techniques are also available: micro-CT scanning, synchrotrons, tooth histology, mass spectrometry, 3D statistical analysis, etc. Obviously, a palaeoanthropologist is unable to master them all. Wisdom suggests, and this summarizes the philosophy governing the present work, the acceptance of limitations and the adaptation to them. More than ever, multidisciplinary collaborations are imperative. For example, a single tooth has many messages to deliver. Accordingly, numerous chapters in this monograph take into account the wealth of signals recorded within the Scladina Child's teeth. They cover in particular the morphological description of the teeth; statistical comparisons; age determination by histological techniques; analysis of the roots; the diet analyzed through microwear of the occlusal surface; EDJ, and enamel thickness, etc.

Interest in the contextual study of human remains continues to increase. In the past, palaeoanthropologists were frequently relegated to laboratories where they studied human remains brought to them by archaeologists. They wrote reports annexed to archaeological publications or anatomical analyses of human remains with very little knowledge of the contexts or conditions of discovery.

Current palaeoanthropologists are now inclined to put the fossils they are studying in an ever more precise chronostratigraphical context which allows them to better understand the evolution of the taxa. They turn to microstratigraphy and dating techniques, classify fossils according to the isotopic stages, and closely analyze the conditions of introduction and modification of the fossils in the sediments (taphonomy).

Palaeoanthropologists are now more involved from the early stages of the field work: drawing or commenting on the distribution maps of bones and dental remains, trying to decipher burial practices, etc. A good example of the evolution of anthropological practices is provided by the comparison of a series of monographs on Neandertals. La Chapelle-aux-Saints (BOULE, 1911-1913), Mount Carmel (McCOWN & KEITH, 1939), or Shanidar (TRINKAUS, 1983), are all pure — but very interesting — laboratory projects as opposed to Kebara (BAR-YOSEF & VANDERMEERSCH (eds.), 1991) and Dederiyeh (AKAZAWA & MUHESEN, 2002), which reflect a real involvement of palaeoanthropologists from the beginning of the excavation.

Through numerous collaborations such as those currently underway at Scladina, which involve Neandertal remains and multidisciplinary

focus from the early stages of field work, the scientific adventure is coupled with an equally exciting human adventure, especially from all the personal meetings, discussions and passionate debates, etc.

Could we not say that the very purpose of our disciplines is to decipher the millions of years of the long adventure which slowly transformed our early ancestors into current humans, therefore, building bridges through the millennia? Somehow, palaeoanthropology finds parallels in the time machines that have haunted the dreams of so many authors like Henri Vernes in “The Dinosaur Hunters” (1957 for the original French edition), adapted into a comic book by Coria in 1984, and E.P. Jacobs in his comic book “The Time Trap” (1962 for the original French edition).

Scladina, palaeoanthropology 4. in the field

The exploration of Scladina Cave was initiated in 1971 with speleological work which quickly turned into a haphazard collecting of out-of-context archaeological artefacts. This went on

until 1977. From 1978, with Marcel Otte's involvement, the excavations immediately took on a scientific approach. Very early, the archaeologist looked for information relative to the palaeoenvironment and the age of the Palaeolithic layers which retained his interest. He initiated collaborations with specialists of the earth sciences, mainly geologists (Paul Haesaerts, Franz Gullentops), palaeontologists (Jean-Marie Cordy, Pierre Simonet, Marylène Patou-Mathis) and palynologists (Bruno Bastin), as well as with dating specialists (Etienne Gilot, Michel Gewalt, Yves Quinif, etc.).

However, the specialized in situ interventions remained rare. One of them involved Paul Haesaerts drawing a few sections on the terrace while another saw two sections in the cave itself analyzed by Christophe Deblaere and Franz Gullentops. Bruno Bastin was involved in palynological sampling and Yves Quinif in U/Th analysis. The palaeontologists were restricted to laboratory studies so their work had little impact on excavation. The excavation remained under the exclusive control of the archaeological team. No continuous geological recording of stratigraphy was possible in the course of the excavation.

Anthropological No.	Archaeological No.	Description	Unearthed	Identified	Square Metre
Scla 4A-1	Sc 1993-148-185	right half of the mandible	16/07/1993	20/07/1993	D29
Scla 4A-2	Sc 1992-1283-96-1	small part of right maxilla	18/02/1992	October 1993	D30
Scla 4A-3	Sc 1992-411-107-1	permanent maxillary right second molar	15/10/1992	October 1993	C30
Scla 4A-4	Sc 1993-330-127	permanent maxillary right first molar	14/12/1993	14/12/1993	C30
Scla 4A-5	Sc 1990-81-46	deciduous maxillary right second molar	13/03/1990	October 1993	G27
Scla 4A-6	Sc 1990-132-41	mandibular right first premolar (P3)	4/07/1990	October 1993	G27
Scla 4A-7	Sc 1991-574-11	deciduous maxillary right first molar	12/11/1991	October 1993	F27
Scla 4A-8	Sc 1995-286-7-1	permanent maxillary right third molar	14/07/1995	14/07/1995	C32
Scla 4A-9	Sc 1996-203-1	left half of the mandible	12/07/1996	12/07/1996	C28
Scla 4A-11	Sc 1990-81-47	permanent maxillary right central incisor	13/03/1990	May 2000	G27
Scla 4A-12	Sc 1990-90-1	permanent mandibular right canine	28/03/1990	July 2001	F27
Scla 4A-13	Sc 2001-262-44	deciduous mandibular right second molar	13/11/2001	13/11/2001	E38
Scla 4A-14	Sc 1990-37-1	permanent maxillary right lateral incisor	22/02/1990	14/12/2004	H27
Scla 4A-15	Sc 1990-37-25	permanent mandibular right central incisor	22/02/1990	14/12/2004	H27
Scla 4A-16	Sc 1990-49-1	permanent maxillary right canine	23/02/1990	16/12/2004	H27
Scla 4A-17 (= Scla 3-2)	Sc 1991-526-1	permanent maxillary left lateral incisor	17/10/1991	October 1993	F27
Scla 4A-18 (= Scla 3-3)	Sc 1991-590-1	permanent maxillary left canine	19/11/1991	October 1993	F26
Scla 4A-19 (= Scla 3-4)	Sc 1995-108-197-1	permanent mandibular left lateral incisor	8/03/1995	10/04/1995	D34
Scla 4A-20	Sc 2006-81-1	permanent mandibular right lateral incisor	12/07/2006	12/07/2006	F35 to F37

Table 1: List of all Scladina Neandertal remains unearthed in former Layer 4A.



Fortunately, the situation gradually improved: first at the instigation of Dominique Bonjean, archaeologist in charge of the excavation since 1991, followed by the involvement of Stéphane Pirson as part of his PhD in geology from the end of the summer 2003.

The first discoveries of Neandertal teeth took place in 1990 but were not identified as human at the time.

The first fossil discovered in situ in Scladina's former Layer 4A was the hemimandible Scla 4A-1 (Table 1). Found on Friday, July 16th 1993, the morphology of the specimen alerted the student (Claire Curvers) assigned to the square, who informed Dominique Bonjean. Interest increased when work resumed the following Monday. The nature of the mandible, however, remained uncertain. The decision was made to contact Marcel Otte, professor of prehistory at the University of Liège. The next day, during a visit to the site, Marcel suggested seeking the advice of the present author who rushed to the cave and identified the fossil as Neandertal (BONJEAN et al., 2009). Fortunately, the coordinates of the mandible had been recorded in

three dimensions (Figure 4), like most of the faunal remains, but no in situ pictures had been taken.

From that moment on, the excavation of the cave took another direction. The field team learned to recognize human teeth and bones.

In the cave, continuous attention was given to identifying the human remains in situ, and, indeed, numerous fossils were recognized at the moment of their discovery, such as the left half of the mandible, Scla 4A-9 (Figure 5), and the permanent maxillary right first molar Scla 4A-4 (Figure 6). The palaeoanthropologist advised the excavation team to contact him if they encountered more remains with suspicious morphology.

At the same time, a new review was conducted, this time with an anthropological focus, of all the skeletal and dental remains discovered earlier in the stratigraphic layers directly above and below the one in which the two hemimandibles were found. This allowed the identification of the series of Neandertal teeth unearthed in Scladina during the years 1990-1992 that had not been recognized during the excavation nor when the collections were classified.

The recent revision of the stratigraphy (PIRSON, 2007 and Chapter 3) represents a further step in the precise positioning of the Neandertal fossils within the sediments of the site. The identification of an important, previously unnoticed, longitudinal gully, 4A-CHE, which had reworked a portion of the cave sediments, was crucial to understanding how the fossils were deposited. As a result, the sediments from which the fossils came have been divided into three large stratigraphic units: the sediments before Stalagmitic Floor CC4, the 4A-CHE gully which is subdivided into at least 8 discontinuous lithofacies, as well as the four 4A-POC layers. The attempt to reposition all the Neandertal remains found earlier within these layers and lithofacies of the new Pirson stratigraphy was necessary. For that purpose, all fossils have been reviewed from a combination of plans, sections, and photographs corresponding to the time of their discoveries, and by virtually projecting them on the closest sections (Chapter 5). Through this procedure, most fossils could be repositioned within the gully (4A-CHE) or the group of layers immediately over it (4A-POC). With the help of a new excavation method that relies on vertical microstratigraphy, future finds will be positioned precisely in the context of the new, extremely precise stratigraphic sequence.

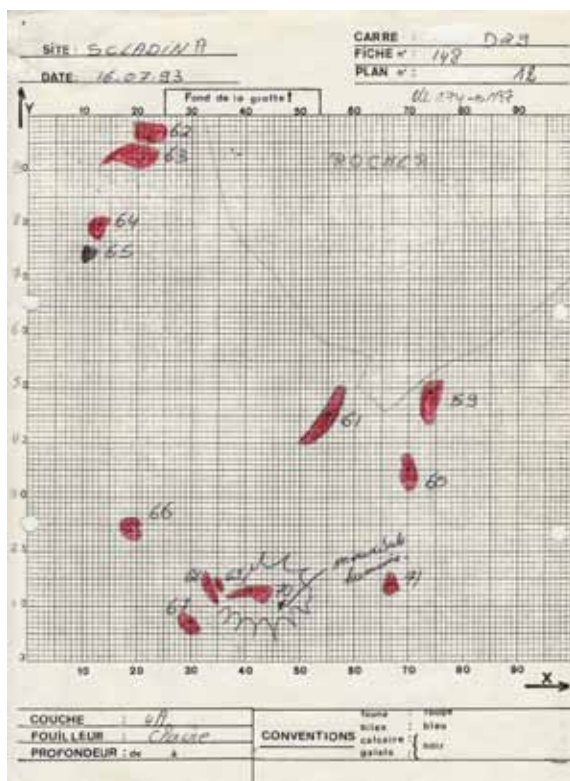


Figure 4: Technical sheet and field plan drawn up by a student during the in situ discovery of the right hemimandible Scla 4A-1.



Figure 5: Left half of the mandible, Scla 4A-9, in situ, on Section D/C 28 (photograph Dominique Bonjean, AA).



Figure 6: Permanent maxillary first right molar Scla 4A-4, in situ (Square C 30; photographs Dominique Bonjean, AA).

Prior to 1990, human remains had already been found in the upper part of the stratigraphic sequence; however, these discoveries have no bearing on the present palaeoanthropological project. For example, several fossils that might correspond to a Neolithic multiple burial comprising several individuals seem to have been found in the Holocene layers during the early work by speleologists (OTTE et al., 1988; OTTE, 1990). These are currently inaccessible and were never studied in detail. Later, a first metatarsal was found in 1982, in Layer 3, apparently in an area close to disturbed sediments. Its study was not conducive to a definitive taxonomic identification although it was probably associated with the Neolithic (LEGUEBE et al., 1989). This fossil was also lost. A few other human remains (teeth, vertebrae), whose study goes beyond the scope of the present monograph, have also been found in the sedimentary units 3 and 1B (TOUSSAINT et al., 1998).

The facial elements of Scladina I-4A have been the subject of a few preliminary reports describing the remains and presenting their context (e.g. OTTE et al., 1993; TOUSSAINT et al., 1994, 1998; BONJEAN et al., 1996; TOUSSAINT, 1996; PIRSON et al., 2005). Some detailed analyses were also published, such as the age at death (SMITH et al., 2007).

The current study of these fossils (Figure 1) is the subject of a large international collaboration. The following people took part in this monograph:

In Belgium:

Grégory Abrams, MA, Archéologie Andennaise

Dominique Bonjean, MA, Archéologie Andennaise

Mona Court-Picon (France), PhD, Belgian Royal Institute of Natural Sciences

Freddy Damblon, PhD, Belgian Royal Institute of Natural Sciences

Élise Delaunois, MA, Musée de la préhistoire en Wallonie/Prehistomuseum

Kévin Di Modica, PhD, Archéologie Andennaise

Paul Haesaerts, PhD, Belgian Royal Institute of Natural Sciences

Marcel Otte, PhD, Université de Liège

Stéphane Pirson, PhD, Direction de l'Archéologie, Service public de Wallonie

Michel Toussaint, PhD, Direction de l'Archéologie, Service public de Wallonie

At the Max Planck Institute for Evolutionary Anthropology, in Leipzig, Germany:

Stefano Benazzi (Italy), PhD, now also at the Department of Cultural Heritage, University of Bologna

Sireen El Zaatari (Lebanon), PhD, now at Tübingen University

Katerina Harvati (Greece), PhD, now at Tübingen University

Jean-Jacques Hublin (France), PhD

Kornelius Kupczik (Germany), PhD, now at the Friedrich-Schiller-Universität Jena.

Adeline Le Cabec (France), PhD, now at the ESRF, European synchrotron Radiation Facility, Grenoble

Anthony J. Olejniczak (USA), PhD

Matthew Skinner (Canada), PhD, now at University College London

Tanya Smith (USA), PhD, now at Harvard University

Christine Verna (France), PhD, now at the CNRS, Paris

In France:

Sanda Balescu (Belgium), PhD, Lille1 University

Hervé Bocherens, PhD, now at Tübingen University

Christophe Falguères, PhD, Museum National d'Histoire Naturelle, Institut de Paléontologie humaine, Paris

Catherine Hänni, PhD, École Normale Supérieure of Lyon

Ludovic Orlando, PhD, formerly at the École Normale Supérieure of Lyon, now at the University of Copenhagen, Centre for Geogenetics

Paul T. Tafforeau, PhD, ESRF, European Synchrotron Radiation Facility, Grenoble

Yuji Yokoyama (Japan), PhD, Museum National d'Histoire Naturelle, Institut de Paléontologie humaine, Paris

In Canada:

Cheryl A. Roy (USA), MA, Vancouver Island University

Rhylan McMillan, BA (Distinction), Vancouver Island University

In the USA:

Dorien De Vries (Netherlands), MA, Stony Brook University, New York,

Kristin L. Krueger, PhD, Department of Anthropology, Loyola University Chicago,

Chicago **Donald J. Reid** (UK), PhD, now at George Washington University

Overview of the Scladina

5. monograph

This monograph is the third about Scladina Cave: a first volume covered the stratigraphic context—before the recent revision of S. Pirson—and the palaeoenvironnement (OTTE (ed.), 1992), and a second one dedicated to the archaeology (OTTE et al. (dir.), 1998). Both were written in French, with the exception in each case, of one chapter in English concerning TL dating.

After the present overview, this third monograph proposes, in its second chapter, an overall presentation of the Scladina site with its geographic location, its topography and geology, the history of the excavations that have been conducted there for over a third of a century, as well as the archaeological context and history of the anthropological discoveries. The third chapter is an overview of the stratigraphic context of the Neandertal remains discovered at Scladina. The layers presented in that chapter are just those related with palaeoanthropological remains, namely former layers 4A/4B, as well as those directly below (former Layer 5) and above them (former Layer 3). The chapter then proceeds with an analysis of the sedimentary dynamics of the site and its implications for fossil deposition.



Figure 7: Evocation of the Scladina Child (Benoît Clarys, 2013, © Archéologie Andennaise).

The fourth chapter presents both a palaeoenvironmental overview of the site and a critical analysis of all dates obtained and integrates this data within the newly revised stratigraphy. The fifth chapter discusses in detail the stratigraphic position of each element of the partial face of the Scladina Neanderthal child.

In 1994, non-destructive gamma-ray spectrometry applied to the right hemimandible Scla 4A-1 provided an age of $127+46/-32$ ka BP, which allowed to think that the Scladina I-4A Child lived around 100,000 years ago (Chapter 6).

The taphonomy of the Neanderthal fossils from Scladina is analysed in Chapter 7, using four approaches: first, the fossils are examined for evidence of different surface modifications; second, their spatial and stratigraphic distribution is analysed; third, these observations are compared to the analysis of the faunal material found over the last ten years in the new stratigraphy as revised by S. Pirson; and finally, in the

discussion, these different approaches are integrated in order to build a model of successive chronological phases in relation to death, burial and postdepositional processes, as well as archaeological and/or palaeontological excavations.

The eighth chapter presents an estimation of the age of the child (Figure 7) as calculated from histological studies, with an age estimation of 8 years. This histological result, clearly the most reliable age determination technique, makes the Scladina Child younger than previously thought. Indeed, in previous papers we concluded that “If the criteria of age linked to dental eruption and to the formation of molar roots observed in modern humans are applied to Neandertals, the child of Sclayn [...] would have been at least 12-13 years old. The persistence of deciduous molars could however indicate a younger age, probably hardly more than about ten years” (TOUSSAINT et al., 1998: 738). This position was complemented in more recent syntheses: “Dental age determination compared with cutting

teeth and molar root formation in modern humans suggests the child died at the age of 12. Yet the persistence of deciduous molars is consistent with a younger age, but probably not less than 10. In addition, Granat and Heim's new method of Neandertal dental age determination seems to indicate the child could not have been older than 8.5" (TOUSSAINT & PIRSON, 2006: 382-383; see also TOUSSAINT et al., 2001, 2011).

Can sex be determined on the basis of a mandible or teeth not associated with coxal bones? This question is discussed in Chapter 9. The temptation is to suggest that the Scladina Child might be female; however, the accuracy of sex determination is questionable.

Chapter 10 systematically describes the mandible anatomically, while seeking to distinguish the plesiomorphic features from the derived ones. This chapter also aims to statistically compare the Scladina mandible to samples of subadult and adult Neandertals, and also modern humans. Chapter 11 develops these morphometric comparisons using 3D geometric analysis. The maxillary fragment of the child is presented in Chapter 12.

In Chapter 13, the teeth are described morphologically, with a focus on their taxonomic implications, before being statistically compared to a large collection of similar data. Particular aspects of the teeth, enamel thickness, enamel-dentine junction morphology, and micro-computed tomographic quantification of tooth root size and tissue proportions, are the subject of Chapters 14 to 16.

Two chapters concern the diet of the child, using isotopic biogeochemistry (C/N; Chapter 17) and dental microwear texture (Chapter 18). Both techniques indicate that the child was omnivorous but mainly ate meat: biogeochemistry indicates the consumption of open environment herbivores, while the microwear data also reveals a diet that most likely included small amounts of abrasive plant foods.

Chapter 19 deals with mtDNA extraction and demonstrates that the Scladina Neandertal Child was more distantly related to modern humans than more recent Neandertals, suggesting that the Neandertal population experienced a significant demographic bottleneck in the last 50-30 ka preceding their extinction.

Chapter 20 places Scladina I-4A within the chronological context of the other Neandertal remains from the Belgian Meuse River Valley and northwest Europe. It discusses the association of

the La Naulette and Scladina remains to MIS 5 or earlier, then addresses the absence of occupation during the second part of MIS 4 due to a major climatic deterioration, and finally evaluates the allocation of Late/Classic Neandertals to MIS 3.

The concluding chapter (21) integrates the key findings of this monograph from an multidisciplinary perspective, and discusses various ideas concerning regional Neandertal research.

Acknowledgements

A particularly pleasant duty, in the closing paragraph of this introduction to the first detailed report on the Scladina palaeoanthropological project, is to express a resounding and heartfelt tribute to Dominique Bonjean of Archéologie Andennaise (AA), the archaeologist responsible for the excavation for the better part of the last two decades. Without him, Scladina would not have gradually become a synonym of excellence. We also owe Professor Marcel Otte, from University of Liège, our gratitude for his determination; he set the process in motion in 1978 without any real means of imagining the future scale of its development, and he never stopped inspiring and controlling its positive evolution. The essential role of both Archéologie Andennaise and the City of Andenne, owner of the cave, should also be highlighted. In this respect, it is a pleasure to underline the role of Jean Maes, the president of the association, as well as that of Claude Eerdeken, the city mayor.

Thanks also to the teams of archaeologists, to the students of universities from numerous countries, and to the professional excavators present at Scladina for over thirty years, the last twenty three of which were full-time. Among these are the archaeologists Kévin Di Modica and Grégory Abrams and the excavators Gérard Bouchat, Marcel Chardon, Philippe Frison, Damien Samedi, and Michaël Servaes.

With considerable gratitude, we have to acknowledge the colleagues who participated in this project.

The collaboration with the researchers at the Max Planck Institute for Evolutionary Anthropology (MPI EVA), in Leipzig (Germany), was exceptional as much for their kindness as for the impressive quality of their scientific contribution. A warm thank you to Stefano Benazzi, Sireen El Zaatari, Katerina Harvati, Kornelius Kupczik, Adeline Le Cabec, Christina Nielsen-Marsh, Anthony Olejniczak, Mike Richards, Matthew Skinner, Tanya Smith, Christine Verna, and, in

particular, to Jean-Jacques Hublin, their director within the Department of Human Evolution, whose efficiency and interest were one of the keys to the present achievement. Thank you also to Svante Pääbo and Johannes Krause.

A very special thank to Stéphane Pirson, an outstanding Quaternary geologist, a specialist in cave entrance and rock shelter deposits but also a good friend, who was in charge of the Scladina stratigraphy in the course of his 2007 PhD thesis.

A great thank to Cheryl A. Roy and Rhylan McMillan (Vancouver Island University, Canada) for many constructive discussions relating to methods of field investigation and taphonomic analyzes of bones. We also wish to express our gratitude to Dr. Shara Bailey, palaeoanthropologist at New York University, for her precious advice on some anatomical details of the teeth. Many thanks to Ludovic Orlando, formerly at CNRS Lyon and now at the University of Copenhagen, to Catherine Hänni, CNRS Lyon and to Hervé Bocherens, Universität Tübingen Institut für Ur- und Frühgeschichte und Archäologie des Mittelalters – Arbeitsbereich Paläoanthropologie. Nora De Clerck (Antwerpen University) also provided helpful technical support.

Many thanks to Sylviane Lambermont and Joël Éloy (Association wallonne d'Études mégalithiques, AWEM) and Jean-François Lemaire (Service public de Wallonie, SPW).

Cheryl Roy and Rhylan McMillan (Vancouver Island University, Canada), Rebecca Miller (Université de Liège) and Jean-François Lemaire have helped to improve the English text of the French speaking researchers.

This research was mainly supported by:

– In Belgium, for the field work: the City of Andenne; the Direction de l'Archéologie du Service public de Wallonie, which provides the Département de Préhistoire de l'Université de Liège and the association Archéologie Andennaise with substantial annual grants,

– In Belgium, for the analysis of the fossils: the Direction de l'Archéologie du Service public de Wallonie which, for years, allowed their palaeoanthropologist and geologist to study the Scladina material,

– In Germany, the Max Planck Institute for Evolutionary Anthropology (MPI EVA), Leipzig, for the invaluable contribution of its researchers.

Finally, for all other people who have provided assistance and were not specifically mentioned: thank you.

References

AKAZAWA T. & MUHESEN S., 2002. *Neanderthal Burials. Excavations of the Dederiyeh cave, Afrin, Syria*. Kyoto, International Research Center for Japanese Studies, 394 p.

BAR YOSEF O. & VANDERMEERSCH B. (eds.), 1991. *Le squelette moustérien de Kébara 2*. Paris, Éditions du Centre national de la recherche scientifique, Cahiers de Paléanthropologie, 197 p.

BASTIN B., 1992. Analyse pollinique des sédiments détritiques, des coprolithes et des concrétions stalagmitiques du site préhistorique de la grotte Scladina (province de Namur, Belgique). In M. OTTE (ed.), *Recherches aux grottes de Sclayn, vol. 1 : Le Contexte*. Études et Recherches Archéologiques de l'Université de Liège, 27 : 59-77.

BASTIN B., CORDY J.-M., GEWELT M. & OTTE M., 1986. Fluctuations climatiques enregistrées depuis 125 000 ans dans les couches de remplissage de la Grotte Scladina (Province de Namur, Belgique). *Bulletin de l'Association française pour l'étude du Quaternaire*, 2^e série, 25-26: 168-177.

BASTIN B. & SCHNEIDER A.-M., 1984. Palynologie. In C. EK. & K.-H. Pfeffer (eds.), *Le Karst belge*. Kölner Geographische Arbeiten, 45: 87-93.

BENABDELHADI M., 1998. Étude sédimentologique de la coupe transversale 30/31 des carrés A, B, C et D de la grotte Scladina. In M. OTTE, M. PATOU-MATHIS & D. BONJEAN (dir.), *Recherches aux grottes de Sclayn, vol. 2 : L'Archéologie*. Études et Recherches Archéologiques de l'Université de Liège, 79: 25-37.

BOCHERENS H. & BILIOU D., 1998. Implications paléoenvironnementales et paléoolimentaires de l'étude isotopique du Néandertalien de la couche 4. In M. OTTE, M. PATOU-MATHIS & D. BONJEAN (dir.), *Recherches aux grottes de Sclayn, vol. 2 : L'Archéologie*. Études et Recherches Archéologiques de l'Université de Liège, 79: 311-328.

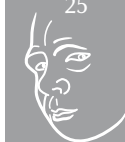
BOCHERENS H., BILIOU D., MARIOTTI A., PATOU-MATHIS M., OTTE M., BONJEAN D. & TOUSSAINT M., 1999. Palaeoenvironmental and Palaeodietary Implications of Isotopic Biogeochemistry of Last Interglacial Neanderthal and Mammal Bones in Scladina Cave (Belgium). *Journal of Archaeological Science*, 26: 599-607.

BOCHERENS H., BILIOU D., MARIOTTI A., TOUSSAINT M., PATOU-MATHIS M., BONJEAN D. & OTTE M., 2001. New isotopic evidence for dietary



- habits of Neandertals from Belgium. *Journal of Human Evolution*, 40: 497-505.
- BOCHERENS H., BILLIOU D., PATOU-MATHIS M., BONJEAN D., OTTE M. & MARIOTTI A., 1997. Isotopic biogeochemistry (^{13}C , ^{15}N) of fossil mammal collagen from Scladina cave (Sclayn, Belgium). *Quaternary Research*, 48: 370-380.
- BONJEAN D., 1998^a. La stratigraphie. In M. OTTE, M. PATOU-MATHIS & D. BONJEAN (dir.), *Recherches aux grottes de Sclayn, vol. 2 : L'Archéologie*. Études et Recherches Archéologiques de l'Université de Liège, 79: 15-23.
- BONJEAN D., 1998^b. Chronologie à la grotte Scladina. In M. OTTE, M. PATOU-MATHIS & D. BONJEAN (dir.), *Recherches aux grottes de Sclayn, vol. 2 : L'Archéologie*. Études et Recherches Archéologiques de l'Université de Liège, 79: 45-57.
- BONJEAN D., 2009. L'archéologie de terrain aujourd'hui : la fouille *made in* Scladina. In K. DI MODICA & C. JUNGELS (dir.), *Paléolithique moyen en Wallonie. La collection Louis Éloy*. Bruxelles, Collections du Patrimoine culturel de la Communauté française, 2: 28-32.
- BONJEAN D., MASY P. & TOUSSAINT M., 2009. L'enfant néandertalien de Sclayn. Petite histoire d'une découverte exceptionnelle. *Notae Praehistoricae*, 29: 49-51.
- BONJEAN D., TOUSSAINT M. & OTTE M., 1996. Scladina (Sclayn, Belgique) : l'homme de Néandertal retrouvé ! *Notae Praehistoricae*, 16: 37-46.
- BOULE M., 1911-1913. *L'homme fossile de La Chapelle-aux-Saints*. Annales de Paléontologie, 278 p.
- CORDY J.-M., 1992. Bio- et chronostratigraphie des dépôts quaternaires de la grotte Scladina (province de Namur, Belgique) à partir des micro-mammifères. In M. OTTE (ed.), *Recherches aux grottes de Sclayn, vol. 1 : Le Contexte*. Études et Recherches Archéologiques de l'Université de Liège, 27: 79-125.
- CRÉPIN L., 2002. *Étude archéozoologique de la couche 1b de la grotte Scladina (Sclayn-Belgique)*. DEA thesis, Museum National d'Histoire Naturelle, Institut de Paléontologie humaine, 63 p.
- DEBENHAM N. C., 1998. Thermoluminescence Dating of stalagmitic Calcite from La Grotte Scladina at Sclayn (Namur). In M. OTTE, M. PATOU-MATHIS & D. BONJEAN (dir.), *Recherches aux grottes de Sclayn, vol. 2 : L'Archéologie*. Études et Recherches Archéologiques de l'Université de Liège, 79: 39-43.
- DEBLAERE C. & GULLENTOPS F., 1986. Lithostratigraphie de la grotte Scladina. *Bulletin de l'Association française pour l'étude du Quaternaire*, 2^e série, 25-26: 178-181.
- DELAUNOIS É., ABRAMS G., BONJEAN D., DI MODICA K. & PIRSON S., 2012. Altération différentielle des ossements de l'ensemble sédimentaire 4A de la grotte Scladina (Andenne, Belgique). *Notae Praehistoricae*, 32: 5-18.
- DI MODICA K., 2010. *Les productions lithiques du Paléolithique moyen de Belgique : variabilité des systèmes d'acquisition et des technologies en réponse à une mosaïque d'environnements contrastés*. Unpublished PhD thesis. Université de Liège, Faculté de Philosophie et Lettres & Museum National d'Histoire Naturelle, Département de Préhistoire, 787 p.
- DI MODICA K., 2011. Variabilité des systèmes d'acquisition et de production lithique en réponse à une mosaïque d'environnements contrastés dans le Paléolithique moyen de Belgique. In M. TOUSSAINT, K. DI MODICA & S. PIRSON (sc. dir.), *Le Paléolithique moyen en Belgique. Mélanges Marguerite Ulix-Closset*. Bulletin de la Société royale belge d'Études Géologiques et Archéologiques *Les Chercheurs de la Wallonie*, hors-série, 4 & Études et Recherches Archéologiques de l'Université de Liège, 128: 213-228.
- DI MODICA K. & BONJEAN D., 2004. Scladina (Sclayn, province de Namur) : ensembles lithiques moustériens méconnus. *Notae Praehistoricae*, 24: 5-8.
- DRAILY C., PIRSON S. & TOUSSAINT M. (dir.), 2011. *La grotte Walou à Trooz (Belgique). Fouilles de 1996 à 2004, vol. 2 : Les sciences de la vie et les datations*. Namur, Service public de Wallonie, IPW, Études et documents, Archéologie, 21, 241 p.
- DUPONT E., 1866. Étude sur les fouilles scientifiques exécutées pendant l'hiver de 1865-1866 dans les cavernes des bords de la Lesse. *Bulletins de l'Académie royale des Sciences, des Lettres et des Beaux-Arts de Belgique*, 2^e série, XXII: 31-54.
- FRAIPONT J. & LOHEST M., 1887. La race humaine de Néanderthal ou de Canstadt en Belgique. Recherches ethnographiques sur des ossements humains découverts dans les dépôts quaternaires

- d'une grotte à Spy et détermination de leur âge géologique. Gand, *Archives de Biologie*, 7 (1886): 587-757, 4 pl. h.t.
- GEWELT M., SCHWARTZ H. P. & SZABO B. J., 1992. Datations $^{230}\text{Th}/^{234}\text{U}$ et ^{14}C de concrétions stalagmitiques de la grotte Scladina. In M. OTTE (ed.), *Recherches aux grottes de Sclayn, vol. 1 : Le Contexte*. Études et Recherches Archéologiques de l'Université de Liège, 27: 157-172.
- GILOT E., 1992. Sclayn : datation par ^{14}C du Moustérien final. In M. OTTE (ed.), *Recherches aux grottes de Sclayn, vol. 1 : Le Contexte*. Études et Recherches Archéologiques de l'Université de Liège, 27: 173.
- GULLENTOPS F. & DEBLAERE C., 1992. Érosion et remplissage de la grotte Scladina. In M. OTTE (ed.), *Recherches aux grottes de Sclayn, vol. 1 : Le Contexte*. Études et Recherches Archéologiques de l'Université de Liège, 27: 9-31.
- HAESAERTS P., 1992. Les dépôts pléistocènes de la terrasse de la grotte Scladina à Sclayn (province de Namur, Belgique). In M. OTTE (ed.), *Recherches aux grottes de Sclayn, vol. 1 : Le Contexte*. Études et Recherches Archéologiques de l'Université de Liège, 27: 33-55.
- HUXTABLE J. & AITKEN J., 1992. Thermoluminescence dating of burned flint and stalagmitic calcite from Grottes de Sclayn (Namur). In M. OTTE (ed.), *Recherches aux grottes de Sclayn, vol. 1 : Le Contexte*. Études et Recherches Archéologiques de l'Université de Liège, 27: 175-178.
- LEGUEBE A., ORBAN R. & SIMONET P., 1989. Un premier métatarsien humain découvert à Sclayn (Belgique). *Bulletin de l'Institut royal des Sciences naturelles de Belgique, Sciences de la terre*, 59: 191-205.
- LEGUEBE A. & TOUSSAINT M., 1988. *La mandibule et le cubitus de La Naulette, morphologie et morphométrie*. Cahiers de Paléanthropologie, 125 p., 8 pl.
- MCCOWN T. D. & KEITH A., 1939. *The Stone Age of Mount Carmel. The Fossil Human Remains from the Levallois-Mousterian*, vol. II. Oxford, Clarendon Press, 390 p. & 28 pl.
- NIELSEN-MARSH C., STEGEMANN C., HOFFMAN R., SMITH T. M., FEENEY R., TOUSSAINT M., HARVATI K., PANAGOPOULOU E., HUBLIN J.-J. & RICHARDS M. P., 2009. Extraction and sequencing of human and Neanderthal mature enamel proteins using MALDI-TOF/TOF MS. *Journal of Archaeological Science*, 36: 1758-1763.
- ORLANDO L., BONJEAN D., BOCHERENS H., THÉNOT A., ARGANT A., OTTE M. & HÄNNI C., 2002. Ancient DNA and the population genetics of cave bears (*Ursus spelaeus*) through space and time. *Molecular Biology and Evolution*, 19: 1920-1933.
- ORLANDO L., DARLU P., TOUSSAINT M., BONJEAN D., OTTE M. & HÄNNI C., 2006. Revisiting Neandertal diversity with a 100,000 year old mtDNA sequence. *Current Biology*, 16: R400-R402.
- OTTE M., 1990. L'occupation moustérienne de Sclayn (Belgique). *Ethnographisch-Archäologische Zeitschrift*, 31: 78-101.
- OTTE M. (ed.), 1992. *Recherches aux grottes de Sclayn, vol. 1 : Le Contexte*. Études et Recherches Archéologiques de l'Université de Liège, 27, 178 p.
- OTTE M., EVRARD J.-M. & MATHIS A., 1988. L'occupation du paléolithique moyen à Sclayn (Belgique). Actes du colloque « Cultures et industries paléolithiques en milieu loessique », Amiens 9-11 décembre 1986. *Revue archéologique de Picardie*, 1-2: 115-124.
- OTTE M., LÉOTARD J.-M., SCHNEIDER A.-M. & GAUTIER A., 1983. Fouilles aux grottes de Sclayn (Namur). *Helinium*, 23: 112-142.
- OTTE M., PATOU-MATHIS M. & BONJEAN D. (dir.), 1998. *Recherches aux grottes de Sclayn, vol. 2 : L'Archéologie*. Études et Recherches Archéologiques de l'Université de Liège, 79, 425 p.
- OTTE M., TOUSSAINT M. & BONJEAN D., 1993. Découverte de restes humains immatures dans les niveaux moustériens de la grotte Scladina à Andenne (Belgique). *Bulletins et Mémoires de la Société d'Anthropologie de Paris*, nouvelle série, t. 5, 1-2: 327-332.
- PATOU-MATHIS M., 1998^a. Origine et histoire de l'assemblage osseux de la couche 5. Comparaison avec la couche 4 sus-jacente, non-anthropique. In M. OTTE, M. PATOU-MATHIS & D. BONJEAN (dir.), *Recherches aux grottes de Sclayn, vol. 2 : L'Archéologie*. Études et Recherches Archéologiques de l'Université de Liège, 79: 281-295.
- PATOU-MATHIS M., 1998^b. Les espèces chassées et consommées par l'homme en couche 5. In M. OTTE, M. PATOU-MATHIS & D. BONJEAN (dir.), *Recherches aux grottes de Sclayn, vol. 2 : L'Archéologie*. Études



et Recherches Archéologiques de l'Université de Liège, 79: 297-310.

PATOU-MATHIS M. & LÓPEZ-BAYÓN I., 1998. Analyse spatiale des ossements de la couche 5. In M. OTTE, M. PATOU-MATHIS & D. BONJEAN (dir.), *Recherches aux grottes de Sclayn, vol. 2: L'Archéologie*. Études et Recherches Archéologiques de l'Université de Liège, 79: 377-395.

PIONNIER M., 2006. *Les carnivores de Scladina : grands prédateurs ou simples opportunistes ? Étude des restes osseux de la couche 1B du site de Sclayn (Belgique, Pléistocène supérieur) : caractéristiques archéozoologiques et taphonomiques d'une occupation de grotte par des carnivores*. Unpublished master thesis, Paris, Muséum National d'Histoire Naturelle, Institut de Paléontologie Humaine, 37 p.

PIROUELLE F., 2006. *Contribution méthodologique à la datation, par les méthodes Uranium-Thorium (U-Th) et Résonance de Spin Electronique (ESR), de sites Moustériens de Ligurie, de France et de Belgique*. Unpublished PhD thesis, Paris, Muséum National d'Histoire Naturelle, Institut de Paléontologie Humaine, 396 p.

PIRSON S., 2007. *Contribution à l'étude des dépôts d'entrée de grotte en Belgique au Pléistocène supérieur. Stratigraphie, sédimentologie et paléoenvironnement*. Unpublished PhD thesis, University of Liège & Royal Belgian Institute of Natural Sciences, 2 vol., 435 p. & 5 annexes.

PIRSON S., BONJEAN D., DI MODICA K. & TOUSSAINT M., 2005. Révision des couches 4 de la grotte *Scladina* (comm. d'Andenne, prov. de Namur) et implications pour les restes néandertaliens : premier bilan. *Notae praehistoricae*, 25: 61-69.

PIRSON S., COURT-PICON M., HAESAERTS P., BONJEAN D. & DAMBLON F., 2008. New data on geology, anthracology and palynology from the Scladina Cave pleistocene sequence: preliminary results. In F. DAMBLON, S. PIRSON & P. GERRIENNE (eds.), *Hautrage (Lower Cretaceous) and Sclayn (Upper Pleistocene). Field Trip Guidebook. Charcoal and microcharcoal: continental and marine records*. IVth International Meeting of Anthracology, Brussels, Royal Belgian Institute of Natural Sciences, 8-13 September 2008. Brussels, Royal Belgian Institute of Natural Sciences, Memoirs of the Geological Survey of Belgium, 55: 71-93.

PIRSON S., DRAILY C. & TOUSSAINT M. (dir.), 2011. *La grotte Walou à Trooz (Belgique). Fouilles*

de 1996 à 2004, vol. 1: Les sciences de la terre. Namur, Service public de Wallonie, IPW, Études et Documents, Archéologie, 20, 208 p.

ROUGIER H., CREVECOEUR I., BEAUVAL C., FLAS D., BOCHERENS H., WIßING C., GERMONPRÉ M., SEMAL P. & VAN DER PLICHT J., 2014. New fossils at the "Troisième Caverne" of Goyet (Belgium) and the mortuary practices of Late Neandertals. *Middle Palaeolithic in North-West Europe. Multidisciplinary approaches*, Book of Abstracts, Namur, Conference: March the 20th-21st: 35.

ROUGIER H., CREVECOEUR I., SEMAL P. & TOUSSAINT M., 2009. Des Néandertaliens dans la troisième caverne de Goyet. In K. DI MODICA & C. JUNGELS (dir.), *Paléolithique moyen en Wallonie. La collection Louis Éloy*. Bruxelles, Collections du Patrimoine culturel de la Communauté française, 2: 173.

SCHMERLING P.-C., 1833-34. *Recherches sur les ossements fossiles découverts dans les cavernes de la province de Liège*. Liège, P. J. Collardin, 167 & 195 p., 34 & 40 pl.

SCHNEIDER A.-M., 1986. Contribution à l'étude du dernier interglaciaire : résultats palynologiques à la grotte de Sclayn (Belgique). *Revue de Paléobiologie*, 5: 57-70.

SIMONET P., 1992. Les associations de grands mammifères du gisement de la grotte Scladina à Sclayn (Namur, Belgique). In M. OTTE (ed.), *Recherches aux grottes de Sclayn, vol. 1: Le Contexte*. Études et Recherches Archéologiques de l'Université de Liège, 27: 127-151.

SMITH T. M., TOUSSAINT M., REID D. J., OLEJNICZAK A. J. & HUBLIN J.-J., 2007. Rapid dental development in a Middle Paleolithic Belgian Neanderthal. *Proceedings of the National Academy Science of the United States of America*, 104, 51: 20220-20225.

TILLIER A.-M., 1983. Le crâne d'enfant d'Engis 2 : un exemple de distribution des caractères juvéniles, primitifs et néandertaliens. *Bulletin de la Société royale belge d'Anthropologie et de Préhistoire*, 94: 51-75.

TOUSSAINT M., 1992. The Role of Wallonia in the History of Palaeoanthropology. In M. TOUSSAINT (ed.), *Cinq millions d'années, l'aventure humaine*. Études et Recherches Archéologiques de l'Université de Liège, 56: 27-41.

TOUSSAINT M., 1996. D'Engis à Sclayn, les Néandertaliens mosans. In D. BONJEAN (sc. ed.), *Neandertal, Andenne*: 48-70.

TOUSSAINT M., 2001. *Les hommes fossiles en Wallonie. De Philippe-Charles Schmerling à Julien Fraipont, l'émergence de la paléanthropologie*. Carnet du Patrimoine, 33, Namur, Service public de Wallonie, 60 p.

TOUSSAINT M., 2011. Une prémolaire néandertalienne dans la couche CI-8 (anciennement C sup et C8) de la grotte Walou. In C. DRAILY, S. PIRSON & M. TOUSSAINT (dir.), *La grotte Walou à Trooz (Belgique). Fouilles de 1996 à 2004, vol. 2: Les sciences de la vie et les datations*. Namur, Service public de Wallonie, IPW, Études et Documents, Archéologie, 21: 148-163.

TOUSSAINT M., BONJEAN D. & OTTE M., 1994. Découverte de fossiles humains du Paléolithique moyen à la grotte Scladina à Andenne. In M.-H. CORBLIAU & J. PLUMIER (eds.), *Actes de la deuxième Journée d'Archéologie Namuroise*. Namur, Facultés universitaires Notre-Dame de la Paix, 26 février 1994, Ministère de la Région wallonne, Direction générale de l'Aménagement du Territoire et du Logement, Direction de Namur, Service des Fouilles: 19-33.

TOUSSAINT M., OLEJNICZAK A. J., EL ZAATARI S., CATTELAÏN P., FLAS D., LETOURNEUX C. & PIRSON S., 2010. The Neandertal lower right deciduous second molar from Trou de l'Abîme at Couvin, Belgium, *Journal of Human Evolution*, 58: 56-67.

TOUSSAINT M., OTTE M., BONJEAN D., BOCHERENS H., FALGUÈRES C. & YOKOYAMA Y., 1998. Les restes humains néandertaliens immatures de la couche 4A de la grotte Scladina (Andenne, Belgique). *Comptes rendus de l'Académie des Sciences de Paris, Sciences de la terre et des planètes*, 326: 737-742.

TOUSSAINT M. & PIRSON S., 2006. Neandertal Studies in Belgium: 2000-2005. *Periodicum Biologorum*, 108, 3: 373-387.

TOUSSAINT M., PIRSON S. & BOCHERENS H., 2001. Neandertals from Belgium. *Anthropologica et Praehistorica*, 112: 21-38.

TOUSSAINT M., SEMAL P. & PIRSON S., 2011. Les Néandertaliens du bassin mosan belge: bilan 2006-2011. In M. TOUSSAINT, K. DI MODICA & S. PIRSON (sc. dir.). *Le Paléolithique moyen en Belgique. Mélanges Marguerite Ulrix-Closset*. Bulletin de la Société royale belge d'Études Géologiques et Archéologiques *Les Chercheurs de la Wallonie*, hors série, 4 & Études et Recherches Archéologiques de l'Université de Liège, 128: 149-196.

TRINKAUS E., 1983. *The Shanidar Neandertals*, New York, Academic Press, 502 p.

TWIESELMANN F., 1961. *Le fémur néandertalien de Fond-de-Forêt (province de Liège)*. Bruxelles, Mémoires de l'Institut royal des Sciences naturelles de Belgique, 148: 164 p. & 2 pl.

Annexes

Lists of papers concerning directly or indirectly the Neandertal fossils of Scladina:

1. Papers written by researchers associated with the Scladina scientific team, in chronological order

(A) = announcement of the Scladina anthropological discoveries and evolution of research

(B) = studies of various scientific aspects

(C) = Scladina through syntheses on Neandertals

(D) = presentation to the public

1993 (A). Otte M., Toussaint M. & Bonjean D. Découverte de restes humains immatures dans les niveaux moustériens de la grotte Scladina à Andenne (Belgique). *Bulletins et Mémoires de la Société d'Anthropologie de Paris*, nouvelle série, t.5, 1-2: 327-332.

1994 (D). Bonjean D., Otte M. & Toussaint M. L'homme de Sclayn. *Archeologia*, 299, mars 1994: 26-30.

1994 (A). Bonjean D., Otte M. & Toussaint M. Andenne/Sclayn: découverte d'ossements néandertaliens. *Chronique de l'Archéologie wallonne*, Éditions du Ministère de la Région wallonne, Direction des Fouilles, Division des Monuments, Sites et Fouilles de la Direction de l'Aménagement du Territoire et du Logement, 2/1994: 135-136.

1994 (A). Toussaint M., Bonjean D. & Otte M. Découverte de fossiles humains du Paléolithique moyen à la grotte Scladina à Andenne. In M.-H. Corbiau & J. Plumier (eds.), *Actes de la deuxième Journée d'Archéologie Namuroise*. Namur, Facultés universitaires Notre-Dame de la Paix, 26 février 1994, Ministère de la Région wallonne, Direction générale de l'Aménagement du Territoire et du Logement, Direction de Namur, Service des Fouilles: 19-33.

1996 (A). Bonjean D., Toussaint M. & Otte M. Scladina (Sclayn, Belgique): l'homme de Néandertal retrouvé! *Notae Praehistoricae*, 16: 37-46.



- 1996 (C). Toussaint M. D'Engis à Sclayn, les Néandertaliens mosans. In D. Bonjean (sc. ed.), *Neandertal, Andenne*: 48-70.
- 1997 (A). Bonjean D., Toussaint M. & Otte M. Grotte Scladina (Sclayn, Belgique): bilan des découvertes néandertaliennes et analyse du contexte. In J. Plumier (dir.), *Actes de la cinquième journée d'Archéologie Namuroise*, Namur, Facultés universitaires Notre-Dame de la Paix, 22 février 1997, Ministère de la Région wallonne, Direction générale de l'Aménagement du Territoire, du Logement et du Patrimoine, Direction de Namur, Service des Fouilles: 19-27.
- 1997 (A). Bonjean D., Toussaint M. & Otte M. Andenne/Sclayn: seconde moitié de mandibule néandertalienne. *Chronique de l'Archéologie wallonne*, Éditions du Ministère de la Région wallonne, Direction des Fouilles, Division des Monuments, Sites et Fouilles de la Direction de l'Aménagement du Territoire et du Logement, 4-5: 168.
- 1997 (D). Bonjean D., Toussaint M. & Otte M. Andenne, Sclayn. La "Grotte Scladina". In M.-H. Corbiau (ed.), *Le patrimoine archéologique de Wallonie*, Namur, Service public de Wallonie: 114-116.
- 1998 (B). Bocherens H. & Biliou D. Implications paléoenvironnementales et paléoolimentaires de l'étude isotopique du Néandertalien de la couche 4. In M. OTTE, M. PATOU-MATHIS & D. BONJEAN (dir.), *Recherches aux grottes de Sclayn, vol. 2: L'Archéologie*. Études et Recherches Archéologiques de l'Université de Liège, 79: 311-328.
- 1998 (B). Toussaint M., Otte M., Bonjean D., Bocherens H., Falguères C. & Yokoyama Y. Les restes humains néandertaliens immatures de la couche 4A de la grotte Scladina (Andenne, Belgique). *Compte rendus de l'Académie des Sciences de Paris, Sciences de la terre et des planètes*, 326: 737-742.
- 1999 (B). Bocherens H., Biliou D., Mariotti A., Patou-Mathis M., Otte M., Bonjean D. & Toussaint M. Palaeoenvironmental and Palaeodietary Implications of Isotopic Biogeochemistry of Last Interglacial Neanderthal and Mammal Bones in Scladina Cave (Belgium). *Journal of Archaeological Science*, 26: 599-607.
- 2001 (B). Bocherens H., Billiou D., Mariotti A., Toussaint M., Patou-Mathis M., Bonjean D. & Otte M. New isotopic evidence for dietary habits of Neandertals from Belgium. *Journal of Human Evolution*, 40: 497-505.
- 2001 (D). Bonjean D., Otte M. & Toussaint M. La grotte Scladina à Sclayn (prov. de Namur). In C. Bellaire, J. Moulin & A. Cahen-Delhayé (eds.), *Guide des sites préhistoriques et protohistoriques de Wallonie*: 14-15.
- 2001 (C). Toussaint M., Pirson S. & Bocherens H. Neandertals from Belgium. *Anthropologica et Praehistorica*, 112: 21-38.
- 2004 (D). Bonjean D., Otte M. & Toussaint M. Andenne, Sclayn, La grotte Scladina. *Patrimoine exceptionnel de Wallonie*. Namur, Division du Patrimoine: 493-496.
2004. (B). Pirson S., Bonjean D., Di Modica K. & Toussaint M. Révision des couches 4 de la grotte Scladina (comm. d'Andenne, prov. de Namur) et implications pour les restes néandertaliens: premier bilan. *Notae praehistoricae*, 25: 61-69.
- 2005 (B). Semal P., Toussaint M., Maureille B., Rougier H., Crevecoeur I., Balzeau A., Bouchneb L., Louryan S., De Clerck N. & Rausin L. Numérisation des restes humains néandertaliens belges. Préservation patrimoniale et exploitation scientifique. *Notae praehistoricae*, 25: 25-38.
- 2006 (B). Orlando L., Darlu P., Toussaint M., Bonjean D., Otte M. & Hänni C. Revisiting Neandertal diversity with a 100,000 year old mtDNA sequence. *Current Biology*, 16: R400-R402.
- 2006 (C). Toussaint M. & Pirson S. Neandertal Studies in Belgium: 2000-2005. *Periodicum Biologorum*, 108, 3: 373-387.
- 2007 (B). Pirson S. *Contribution à l'étude des dépôts d'entrée de grotte en Belgique au Pléistocène supérieur. Stratigraphie, sédimentologie et paléoenvironnement*. Unpublished PhD thesis, University of Liège & Royal Belgian Institute of Natural Sciences, 2 vol., 435 p. & 5 annexes.
- 2007 (B). Smith T. M., Toussaint M., Reid D. J., Olejniczak A. J. & Hublin J.-J. Rapid dental development in a Middle Paleolithic Belgian Neanderthal. *Proceedings of the National Academy Science of the United States of America*, 104, 51: 20220-20225.
- 2008 (B). Olejniczak A. J., Smith T. M., Feeney R. N. M., Macchiarelli R., Mazurier A., Bondioli L., Rosas A., Fortea J., de la Rasilla M., Garcia-Taberner A., Radović J., Skinner M. M., Toussaint M. & Hublin J.-J. Dental tissue proportions and enamel thickness in Neandertal

- and modern human molars. *Journal of Human Evolution*, 55: 12-23.
- 2009 (A). Bonjean D., Masy P. & Toussaint M. L'enfant néandertalien de Sclayn. Petite histoire d'une découverte exceptionnelle. *Notae Praehistoricae*, 29: 49-51.
- 2009 (B). Le Cabec A., Kupczik K., Braga J. & Hublin J.-J. (2009) – Incisor Root Morphology in Neanderthals and Homo sapiens. 78th American Association of Physical Anthropologists meeting, Chicago, Illinois, United States of America. Published abstract in *American Journal of Physical Anthropology*, 138, S48: 263.
- 2009 (B). Nielsen-Marsh C., Stegemann C., Hoffman R., Smith T. M., Feeney R., Toussaint M., Harvati K., Panagopoulou E., Hublin J.-J. & Richards M. P. Extraction and sequencing of human and Neanderthal mature enamel proteins using MALDI-TOF/TOF MS. *Journal of Archaeological Science*, 36: 1758-1763.
- 2010 (D). Bonjean D., Di Modica K. & Abrams G. La grotte Scladina et l'Enfant néandertalien de Sclayn. Nature, patrimoine et public : une notion de respect! In E. Goemaere (sc. dir.), *Terres, pierres et feu en vallée mosane. L'exploitation des ressources naturelles minérales de la commune d'Andenne : géologie, industries, cadre historique et patrimoines culturel et biologique*. Collection geosciences. Service géologique de Belgique. Institut royal des Sciences naturelles de Belgique: 501-510.
- 2010 (B). Delaunois É. *L'altération différentielle des vestiges en archéologie paléolithique. Contribution à l'établissement d'une clé de contrôle stratigraphique et d'homogénéité des collections. L'exemple des couches 4A de Scladina (Namur, Belgique)*. Unpublished Master thesis. Université de Liège, 2 vol., 95 p. & 110 p.
- 2010 (B). Di Modica K. *Les productions lithiques du Paléolithique moyen de Belgique : variabilité des systèmes d'acquisition et des technologies en réponse à une mosaïque d'environnements contrastés*. Unpublished PhD thesis. Université de Liège, Faculté de Philosophie et Lettres & Museum National d'Histoire Naturelle, Département de Préhistoire, 787 p.
- 2010 (B). Kupczik K. & Hublin J.-J. Mandibular molar root morphology in Neanderthals and Late Pleistocene and recent Homo sapiens. *Journal of Human Evolution*, 59: 525-541.
- 2010 (B). Skinner M. M., Evans A., Smith T. M., Jemvall J., Tafforeau P. T., Kupczik K., Olejniczak A. J., Rosas A., Radovčić J., Thackeray F., Toussaint M. & Hublin J.-J. Brief Communication: Contributions of Enamel-Dentine Junction Shape and Enamel Deposition to Primate Molar Crown Complexity. *American Journal of Physical Anthropology*, 143: 157-163.
- 2010 (B). Smith T. M., Tafforeau P. T., Reid D. J., Pouech J., Lazzari V., Zermeno J. P., Guatelli-Steinberg D., Olejniczak A. J., Hoffman A., Radovčić J., Makaremi M., Toussaint M., Stringer C. B. & Hublin J.-J. Dental evidence for ontogenetic differences between modern humans and Neanderthals. *Proceedings of the National Academy Science of the United States of America*, 107, 49: 20923-20928.
- 2011 (C). Bonjean D., Di Modica K., Abrams G., Pirson S. & Otte M. La grotte Scladina: bilan 1971-2011. In M. Toussaint, K. Di Modica & S. Pirson (sc. dir.), *Le Paléolithique moyen en Belgique. Mélanges Marguerite Ulrix-Closset*. Bulletin de la Société royale belge d'Études Géologiques et Archéologiques *Les Chercheurs de la Wallonie*, hors-série, 4 & Études et Recherches Archéologiques de l'Université de Liège, 128: 323-334.
- 2011 (C). Pirson S. & Toussaint M. (dir.) *Neandertal, l'Européen*. Namur, Direction générale opérationnelle de l'Aménagement du Territoire, du Logement, du Patrimoine et de l'Énergie, Service public de Wallonie, 128 p.
- 2011 (C). Toussaint M., Semal P. & Pirson S. Les Néandertaliens du bassin mosan belge: bilan 2006-2011. In M. TOUSSAINT, K. DI MODICA & S. PIRSON (sc. dir.), *Le Paléolithique moyen en Belgique. Mélanges Marguerite Ulrix-Closset*. Bulletin de la Société royale belge d'Études Géologiques et Archéologiques *Les Chercheurs de la Wallonie*, hors-série, 4 & Études et Recherches Archéologiques de l'Université de Liège, 128: 149-196.
- 2012 (B). Benazzi S., Fornai C., Buti L., Toussaint M., Mallegni F., Ricci S., Gruppioni G., Weber G. W., Condemi S. & Ronchitelli A. Cervical and Crown Outline Analysis of Worn Neanderthal and Modern Human Lower Second Deciduous Molars. *American Journal of Physical Anthropology*, 149: 537-546.
- 2012 (D). Bonjean D., Abrams G. & Di Modica K. La grotte Scladina et l'Enfant de Sclayn. *Les*



Cahiers nouveaux, Trimestriel du Développement territorial et du Patrimoine. Grandes figures en Wallonie, 83: 14.

2012 (A). Bonjean D., Di Modica K., Abrams G., Otte M. & Pirson S. La grotte Scladina (Andenne, Province de Namur). Neuvième Congrès de l'Association des Cercles Francophones d'Histoire et d'Archéologie de Belgique. LVIIe Congrès de la Fédération des Cercles d'Archéologie et d'Histoire de Belgique, Liège, 23-26 août 2012. *Institut Archéologique Liégeois*. Actes, tome 1: 179-180.

2012 (C). Pirson S., Flas D., Abrams G., Bonjean D., Court-Picon M., Di Modica K., Draily C., Damblon F., Haesaerts P., Miller R., Rougier H., Toussaint M. & Semal P. Chronostratigraphic context of the Middle to Upper Palaeolithic transition: Recent data from Belgium. *Quaternary International*, 259: 78-94.

2013 (B). Le Cabec A. *Anterior dental loading and root morphology in Neanderthals*. PhD thesis. MPI-EVA, Leipzig University (Germany) & Université Toulouse III-Paul Sabatier (France).

2013 (B). Le Cabec A., Gunz P., Kupczik K., Braga J. & Hublin J.-J. Anterior tooth root morphology and size in Neanderthals: Taxonomic and functional implications. *Journal of Human Evolution*, 64: 169-193.

2014 (B). Benazzi S., Panetta D., Fornai C., Toussaint M., Gruppioni G. & Hublin J.-J. Technical Note: Guidelines for the Digital Computation of 2D and 3D Enamel Thickness in Hominoid Teeth. *American Journal of Physical Anthropology*, 153: 305-313.

2014 (A). Bonjean D., Abrams G., Di Modica K., Otte M., Pirson S., Toussaint M. The sedimentary context, archaeology, and anthropology of Scladina Cave (Belgium). *Middle Palaeolithic in North-West Europe: Multidisciplinary approaches*. Book of Abstracts. Namur, March the 20th-21st: 75.

2014 (B). El Zaatari S., Krueger K., Toussaint M. & Hublin J.-J. Dental Microwear Texture Analysis and the Diet of the Scladina Child. European Society for the Study of Human Evolution (ESHE), 4th Annual Meeting, Florence, Italy, 18-20 September. Proceedings of the ESHE 3: 64.

2014 (B). Verna C., Toussaint M., Hublin J.-J. & Richards M. P. Neandertal mobility patterns in the Meuse Valley: insights and perspectives through

strontium isotope analysis on dental enamel. *Middle Palaeolithic in North-West Europe: Multidisciplinary approaches*. Book of Abstracts. Namur, March the 20th-21st: 44.

2. Selection of books and papers making more or less extensive reference to the Scladina Neandertal fossils or using anthropological data from Scladina, written by researchers not associated with the Scladina palaeoanthropological project

1995. Heim J.-L. & Granat J. La mandibule de l'enfant néandertalien de Malarnaud (Ariège). Une nouvelle approche anthropologique par la radiographie et la tomographie. *Anthropologie et Préhistoire*, 106: 75-96.

1999. Coqueugnot H. *Le crâne d'Homo sapiens en Eurasie : croissance et variation depuis 100 000 ans*. Oxford, British Archaeological Reports, International Series, 822, 197 p.

1999. Maureille B. & Bar D. The premaxilla in Neandertal and early modern children: ontogeny and morphology. *Journal of Human Evolution*, 37: 137-152.

2002. Schwartz J. H. & Tattersall I. *The human fossil record. Volume one. Terminology and Craniodental Morphology of Genus Homo (Europe)*. New York, Wiley-Liss, 388 p.

2006. Excoffier L. Neandertal Genetic Diversity: A Fresh Look from Old Samples. *Current Biology*, 16: R650-R652.

2007. Moncel M.-H. & Condemi S. The human remains of the site of Payre (S-E France, MIS 5-7). Remarks on stratigraphic position and interest. *Anthropologie*, XLV: 19-29.

2012. Shackelford L. L., Stinespring Harris A. E. & Konigsberg L. W. Estimating the distribution of probable age-at-death from dental remains of immature human fossils. *American Journal of Physical Anthropology*, 147: 227-253.

2013 (B). Austin C., Smith T. M., Bradman A., Hinde K., Joannes-Boyau R., Bishop D., Hare D. J., Doble P., Eskenazi B. & Arora M. Barium distributions in teeth reveal early-life dietary transitions in primates. *Nature*, 498: 216-219, doi: 10.1038/nature12169.

Chapter 2

SCLADINA CAVE: ARCHAEOLOGICAL CONTEXT AND HISTORY OF THE DISCOVERIES

Dominique BONJEAN, Grégory ABRAMS,
Kévin DI MODICA, Marcel OTTE, Stéphane
PIRSON & Michel TOUSSAINT

*Michel Toussaint & Dominique Bonjean (eds.), 2014.
The Scladina I-4A Juvenile Neandertal (Andenne, Belgium)*

Palaeoanthropology and Context

Études et Recherches Archéologiques de l'Université de Liège, 134: 31-48.

Topography, geography, 1. and geology of Scladina

The village of Sclayn (City of Andenne, Province of Namur, Belgium; Figure 1) is situated on the border between High and Middle Belgium, along the south bank of the Meuse River, between Andenne and Namur: 5 km from Andenne and 14 km from Namur. At this location the river has cut deeply into the Palaeozoic limestone substratum, actively contributing to the development of a complex karstic network.

Scladina Cave, in Sclayn, is located on the west side of the small Fond des Vaux Valley, through which runs a small stream called Ri de Pontainne (or Pontine). This brook joins the Meuse River in the village approximately 750 m downstream from the cave. About fifteen caves are found within the west valley wall (DUBOIS, 1981). Scladina, the main one, opens towards the southeast approximately 7 m below a plateau that served as the interfluvial zone between the Meuse and the Ri de Pontainne, and about 30 m above the alluvial plain (Figure 2). The coordinates of the site are: 50° 29' 33" N and 5° 01' 30" E; the altitude is 137.7 m AMSL.

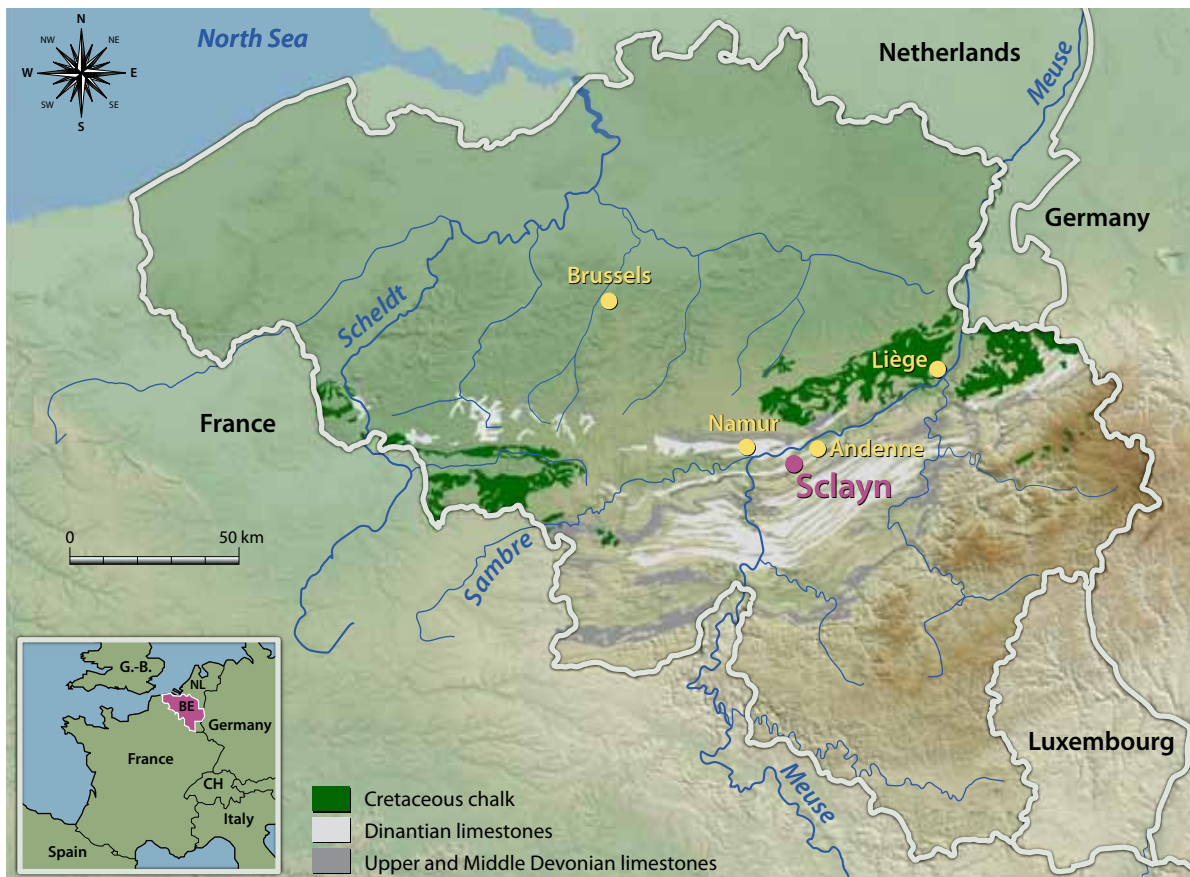


Figure 1: Situation of the village of Sclayn (Andenne) in Belgium; the Meuse Valley incises the Palaeozoic limestones and separates High Belgium to the south from the low plateaus of Middle Belgium to the north (graphics K. Di Modica, J.-F. Lemaire, SPW).





Figure 2: Scladina Cave is situated high in the west wall of a small valley adjacent to the Meuse River (map © IGN; top view © Google).

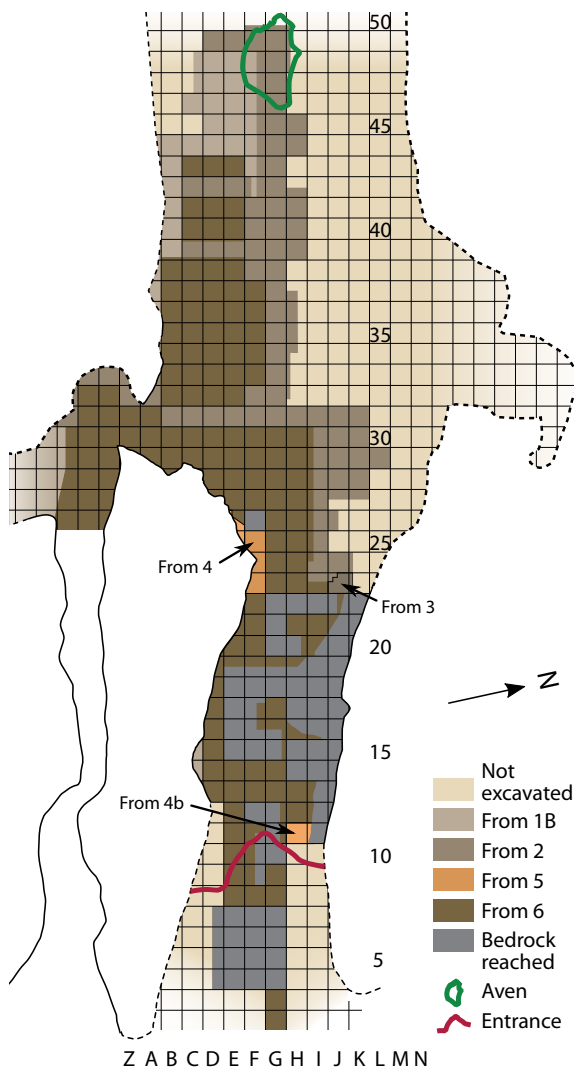


Figure 3: At Scladina, the archaeological research began on the terrace, from metre 2 to metre 10 and extends 39 m inside the cave, from metre 11 to metre 50.

The bedrock is composed of Visean Limestone (Lower Carboniferous), and Scladina is located within the superior portion of the Haut-le-Wastia Member of the Lives Formation (PIRSON, 2007).

Several other caves are found in the immediate area. Approximately 5 m south of Scladina at a similar elevation is Saint-Paul Cave which, 20 m to the northwest of its entrance, intersects Scladina. Several metres below Saint-Paul another gallery develops, called Sous-Saint-Paul. This gallery is connected to Saint-Paul by a chimney. A survey on Scladina's terrace (carried out in 1978) revealed another karst cavity, which corresponds to an expansion of Sous-Saint-Paul. These three caves (Scladina, Saint-Paul, and Sous-Saint-Paul) constitute a cave series known in literature as the *Grottes de Sclayn* (caves of Sclayn).

According to GULLENTOPS & DEBLAERE (1992), three terraces of the Meuse have been identified in Sclayn. The presence of ancient fluvial deposits was confirmed by the observation of water-worn river rocks on the plateau above Scladina, which range in size from pebbles to cobbles.

Scladina Cave is a long cylinder-like karst structure that extends along the axial plane of an anticline. Currently, the excavation of the sediment within the cave extends about 40 m from Scladina's entrance (50 m from the edge of the terrace; Figure 3), and speleological prospecting indicates that the cave extends for at least another 12m. The height of the gallery is approximately 6m. Its width is variable: for the first 12 m (corresponding to metres 10 to 21) the average is only 6m, beyond metre 21 it widens considerably. The



Figure 4: At the time of discovery, the cave was filled to the vault with sediments. In some areas, the Holocene stalagmitic floor is still partially attached to the stalactites (upper right; Photograph, July 2010).

total width is not known because the cave extension to the north remains concealed by sediment (Figure 4). Toward the south the cave joins Saint-Paul at about metre 30. The maximum width excavated to date is in the order of 12 m at metre

29; however, the total width is estimated to be about 20 metres (PIRSON, 2007).

Between squares K and L, from metres 22 to 25, a chimney is present in the ceiling of Scladina. Also, on the plateau, approximately 35 m from the

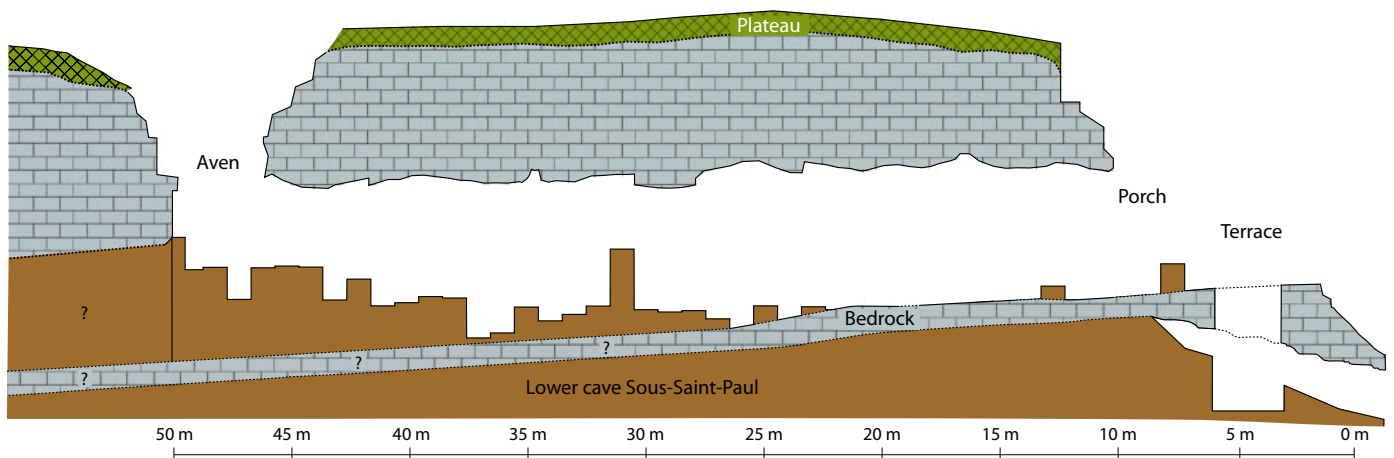


Figure 5: Longitudinal schematic section of Scladina Cave from the entrance to the aven (from PIRSON, 2007; section D. Bonjean, M. Chardon; graphics G. Abrams, K. Di Modica, E. Dermience & A. Laurys, RBINS, J.-F. Lemaire, SPW).



porch a depression of around 60 m² was visible before the excavation. This dolina indicated the presence of an aven, connecting the cave to the surface (Figure 5). This structure was discovered in 1997 (BONJEAN et al., 2002) and is situated on the hinge line of the anticline. Today, a concrete slab blocks the opening.

2. History of the research

From 1910, the karsts of Sclayn were of high interest because of their speleological potential (DONCEEL et al., 1910). Starting in 1949, the immediate area around Scladina was prospected by speleologists and amateur archaeologists from Namur. Both the Saint-Paul and Sous-Saint-Paul caves were exploited after their discoveries in 1951 and 1953, respectively (BONJEAN, 1998^a). A rich faunal and archaeological collection ranging from the Middle Palaeolithic to the Neolithic was exhumed during these excavations, including an important Neolithic burial. Unfortunately, the absence of recorded context and the dispersal of the material to several private collections (to which access is limited) prevented any interpretation.

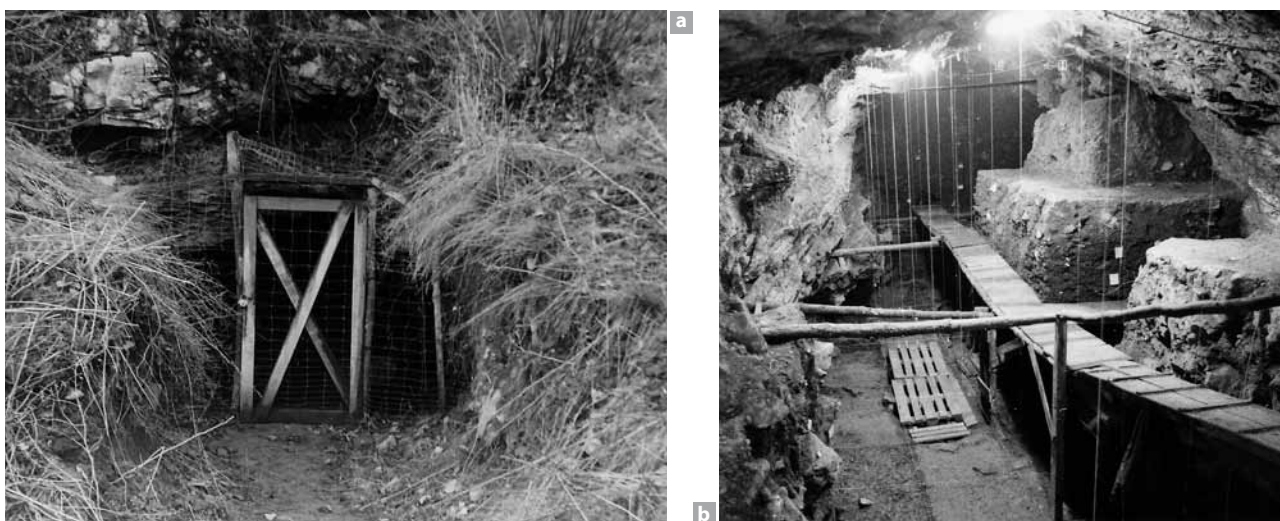
In 1971, Scladina Cave was discovered and named by speleologists and amateur archaeologists from Sclayn (OTTE et al., 1983; OTTE (ed.), 1992; BONJEAN 1998^a). At that time, the cave was filled to the vault with sediment. From 1971 through 1977 they unblocked the passage and started work on the first 15 m with the purpose of

opening a karstic site for tourism. In the process, the two metres of sediment directly under the ceiling were removed without respecting the stratigraphy. Following the discovery of the first artefacts, the speleologists contacted several professional archaeologists; this initiative, retrospectively, would save the cave.

In August 1978, the Department of Prehistory of the University of Liège, under the direction of Marcel Otte, collaborated with local amateurs from the Cercle Archéologique Sclaynois (CAS) to undertake the first scientific excavation (Figure 6). A 10 metre deep test pit on the terrace of the cave was opened in the middle of a chimney that leads to the lower network of Sous-Saint-Paul (Figure 5). Before long, the stratigraphy of the site was published for the first time (OTTE et al., 1983).

At present, the excavations are carried out by the nonprofit organization Archéologie Andennaise in conjunction with the University of Liège, with support from the City of Andenne and the Service public de Wallonie. Dominique Bonjean has been the director of the site and its excavation since 1991. In 1996, the cave was classified as an archaeological site and made *site exceptionnel de Wallonie* (exceptional site of Wallonia, protected by regional laws) (BONJEAN, 1998^a). The present team at Scladina is solely dedicated to research and is comprised of local personnel including three archaeologists, four workers, a laboratory assistant, and a secretary.

Figure 6: Scladina Cave and the evolution of the site excavation: a. A 2 metre deep trench opened on the terrace in the direction of the cave (1972); b-c. Two steps in the evolution of the site (1985 and 2005); d. Today's excavators are equipped with powerful halogen lights, permitting a careful observation of the geometry of the stratigraphy (photographs Cercle Archéologique Sclaynois, Archéologie Andennaise).



Over the first 15 years of field research, the interest in Scladina was essentially archaeological and was linked to the discovery of Middle Palaeolithic artefacts primarily recovered from former layers 5 and 1A (OTTE & BONJEAN, 1998), now understood and communicated as sedimentary units 5 and 1A after further sedimentological investigation (PIRSON, 2007). The study of the stratigraphic context, palaeontology, and palynology completed the approach and were the subjects of numerous publications (OTTE (ed.), 1992; OTTE et al. (dir.), 1998).

Since 1993, an emotional dimension has been part of the excavation at Scladina with the recovery of a mandible, a maxillary fragment, and 16 isolated teeth belonging to a juvenile Neandertal. This discovery, the most important made in Belgium in the 20th century, permitted Scladina to join several other Belgian sites that have yielded Middle Palaeolithic human remains (TOUSSAINT et al., 1994, 1998, 2001, 2011; BONJEAN, 1995; TOUSSAINT & PIRSON, 2006). The study of this Neandertal child's remains is the subject of this monograph.

3. Sedimentary context

Since the beginning of scientific research in 1978, multidisciplinary studies have been frequently carried out at the site (OTTE (ed.), 1992; OTTE et al. (dir.), 1998; PIRSON, 2007; PIRSON et al., 2008). These demonstrated that the sediment contained evidence of a number of climatic fluctuations belonging to the Upper Pleistocene. From a palaeoclimatic perspective, this is one of the most complete sequences available to researchers

in Belgium. The palaeoenvironmental context and the chronostratigraphic sequence of Scladina are the subject of a specific chapter within this volume (see Chapter 4).

The major units that make up the stratigraphic sequence were identified in the original works (Otte et al., 1983; DEBLAERE & GULLENTOPS, 1986; GULLENTOPS & DEBLAERE, 1992; HAESAERTS, 1992; BENABDELHADI, 1998); however, beginning in 2003, a detailed re-examination in the form of research for a PhD thesis found a previously unknown complexity in the sediment deposition (PIRSON, 2007). Presently, more than 120 layers, divided into 30 sedimentary units, have been identified in a sequence that is approximately 15 m thick. A large number of sedimentary processes (e.g., run-off, debris flow, torrential flow, solifluction, and settling) and post-depositional processes (e.g., deep frost, cryoturbation, bioturbation, precipitation of iron hydroxide and manganese dioxide) are understood, which makes Scladina an excellent reference site.

4. Archaeological context

Scladina is one of the major Palaeolithic archaeological sites in Belgium. Two important Middle Palaeolithic artefact series have been recovered here (the assemblages from units 5 and 1A), which have been studied from a variety of perspectives, including typology, technology, petrography, spatial distribution, and statistics (OTTE et al., 1988; OTTE et al. (dir.), 1998; BONJEAN et al., 2009^a). The excavation methods used in the field over the years have profoundly evolved and continue to do so. They now follow a



microstratigraphic approach in combination with horizontal and/or vertical excavation.

4.1. Excavation Methods: Evolution and Difficulties

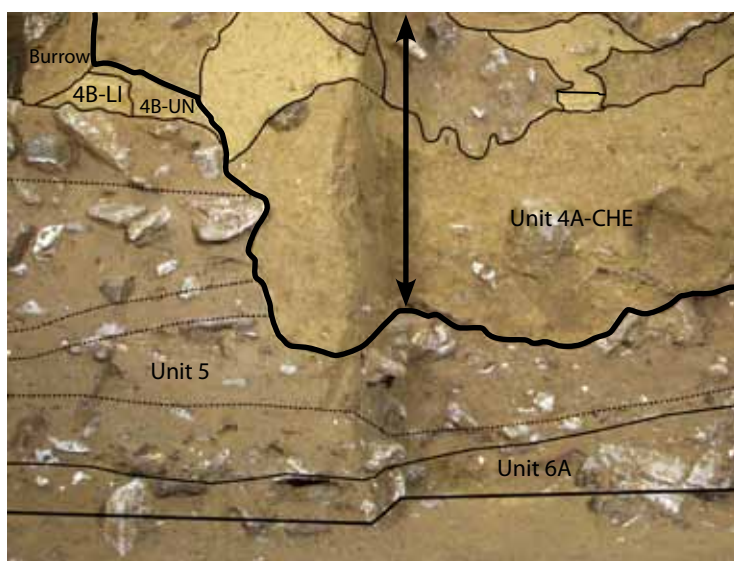
From its discovery in 1978, Scladina's Unit 5 revealed a surprising richness: the first square metres probed under the porch delivered tens of bones and lithic flakes. The exceptional concentration of artefacts with relatively fresh, sharp edges motivated the researchers to establish an excavation system based on the horizontal cleaning of square metres before observing the spatial relationships between the objects (OTTE, 1990). Currently, close to 20,000 artefacts and bone fragments from Unit 5 have been recorded and mapped according to their 3-dimensional coordinates. The contextualization of this material permitted the study of its distribution within its sedimentary context. In addition, systematic screening of the sediment through a 2.5 mm mesh added to the exhaustive recovery of material. The small pieces obtained through screening brought the total number of analyzable objects to nearly 100,000.

Hundreds of planimetric plottings of the material have been produced, allowing for a detailed study of their spatial and altimetric distributions. Unfortunately, they showed a mainly homogeneous distribution of artefacts in the first chamber of the cave (from the entrance to metre 23) in terms of the raw material, debitage techniques, and debitage typological classes (OTTE et al. (dir.), 1998; BONJEAN, 1998^b). No clearly circumscribed anthropogenic zones were recognized

through the examination of the spatial distribution of the objects. The burned bones and those with butchering marks were spread across the total surface of the first chamber (PATOU-MATHIS & LÓPEZ-BAYÓN, 1998). Large clusters of morphologically similar lithics were observed; some clusters contained only debitage, while others were comprised almost completely of larger flakes and blocks. These clusters have been interpreted as the possible evidence of activity zones (BONJEAN, 1998^b; BONJEAN & OTTE, 2004).

Recent stratigraphic observations (PIRSON, 2007) revealed the existence of a gully inside Unit 5, clearly visible on the stratigraphic Section H/I 23 (see Chapter 3, Figure 5). Coming from the terrace, the gully was the result of an erosional event that likely affected the first 12 m of the cave. The formation of this gully generated an intense reworking of both sediment and objects, which potentially originated several layers underneath. Such mechanisms caused by natural phenomena can distribute objects in a way that is seemingly anthropogenic. The concentration of artefacts numerically declines towards the back of the cave, which also indicates transportation of the material by erosion (BONJEAN et al., 2009^a). Referring again to the maps mentioned above, the refitting of lithics from different locations substantiates the same direction of movement (BONJEAN, 1998^b). Therefore, caution is necessary during the interpretation of data, especially when identifying the difference between anthropogenic and natural actions that occurred during sedimentary deposition. For this reason, an excavation method adapted for this stratigraphic complexity was established (BONJEAN, 2009).

Figure 7: View of a 1-metre-wide longitudinal section in the middle of Square F34. The stratified deposits (units 6A, 5 and layers 4B-LI and 4B-UN) were at first eroded by the event(s) that created the gully (Unit 4A-CHE). The different steps in the sedimentation of the gully represent a second phase. Pleistocene and Holocene bioturbations finished the reworking phase, visible on the sections, creating a mosaic of different types of sediment, whose genesis must be reconstituted before excavation.



The stratigraphy of Scladina is typical of cave environments: irregular, often oblique, and exhibiting complex sedimentary structures often caused by erosion (Figure 7). In retrospect, the traditional excavation method was inadequate because it did not allow for the observation of stratigraphic subtleties. Furthermore, this method can lead to the association of anachronistic remains based on their geographic proximity (BONJEAN et al., 2009^a).

To remedy the problem, a new field approach was conceived and applied. Implemented in 2004, the system combined horizontal excavation on a reduced surface (100 cm long, 10–50 cm wide) with stratigraphic observation and control made possible by the use of 2–4 adjacent vertical sedimentary sections. Therefore, everywhere in the cave archaeological investigations now begin by the meticulous cleaning of an existing section. The section is then photographed and printed. In the cave, the excavator annotates the photograph by adding the limits and the names of the layers, as well as some altimetric information.

The worker subsequently excavates by horizontally removing the sediment on the reduced surface, while observing the vertical sections adjacent to the excavation zone so the stratigraphic structure is respected (BONJEAN, 2009). In order to precisely observe the nature of the sediment that contains an object, the excavator establishes a small section at the object's base. This operation permits the verification of the homogeneity of the sediment surrounding the object and the excavator is also assured what layer the object is from. Simultaneously, the spatial distribution in three dimensions is recorded. All sediment that is removed from the cave is wet screened.

4.2. Prehistoric occupations

The sedimentary deposits of Scladina recorded numerous occurrences (Figure 8) of Neandertals frequenting the Ri de Pontainne Valley. After 35 years of investigation, each of the 30 observed sedimentary units (PIRSON, 2007) have provided at least some artefacts.

4.2.1. The principal assemblages

Two assemblages contain a considerable number of artefacts. Around 13,500 tools and knapping waste products of diverse rock types (e.g., flint, quartz, and quartzite) constitute the archaeological assemblages from units 5 and 1A.

4.2.1.1. The assemblage from Unit 5

The sedimentary Unit 5 is composed of several layers. The sedimentary dynamics in lower deposits (Layer 5-G) seem to be dominated by solifluction, while the top layer of the deposit (Layer 5-J) has heavily eroded the underlying layers, and is likely a debris flow (PIRSON, 2007; see Chapter 3). Archaeological material can be found in this unit across the cave, scattered by these processes. Most of the environmental elements, such as palynology, sedimentary dynamics, magnetic susceptibility, point to cold climatic conditions during its deposition. The combination of the available dates for the sequence and the other chronostratigraphic data suggests that Unit 5 was deposited during a cold phase of the Weichselian Early Glacial (PIRSON et al., 2008; see Chapter 4).

The lithic assemblage is characterized as much by the different types and geographic origins of raw material as by the nature of the artefacts. Flint was transported to the cave in the form of small, crudely sculpted nodules, as well as in the form of prepared products. The most likely source of this material is the Hesbaye region, located about 6 km north of the site on the opposite bank of the Meuse. Therefore, at one of the numerous passages found at confluences, the river must have been forded. Some quartz and quartzite pebbles, collected from the Meuse alluvium near the cave, were also brought to the cave either in their original form or, in some cases, anthropogenically modified. Blocks of limestone and chert available around the site and in the Ri de Pontainne Valley were also exploited (Figure 9). Finally, some rare pieces manufactured from other raw materials, such as fine grained flints or tertiary sandstones, perhaps attest to the exploitation of another geographic zone and could correspond to a tool kit that Neandertals took with them from place to place (VAN DER SLOOT, 1998).

Guided by a desire to economize material, as well as to employ the best type of rock based on its functional characteristics (Figure 10), these materials were exploited through flexible and complementary methods. Preferentially, flint had served to produce delicately created tools such as scrapers (Figure 11) and points, while the local material (quartz and quartzite) was used in the production of heavy, asymmetrical pieces (Figure 12) such as knives (Figure 13), which were easily grasped by their wide backs, opposed to



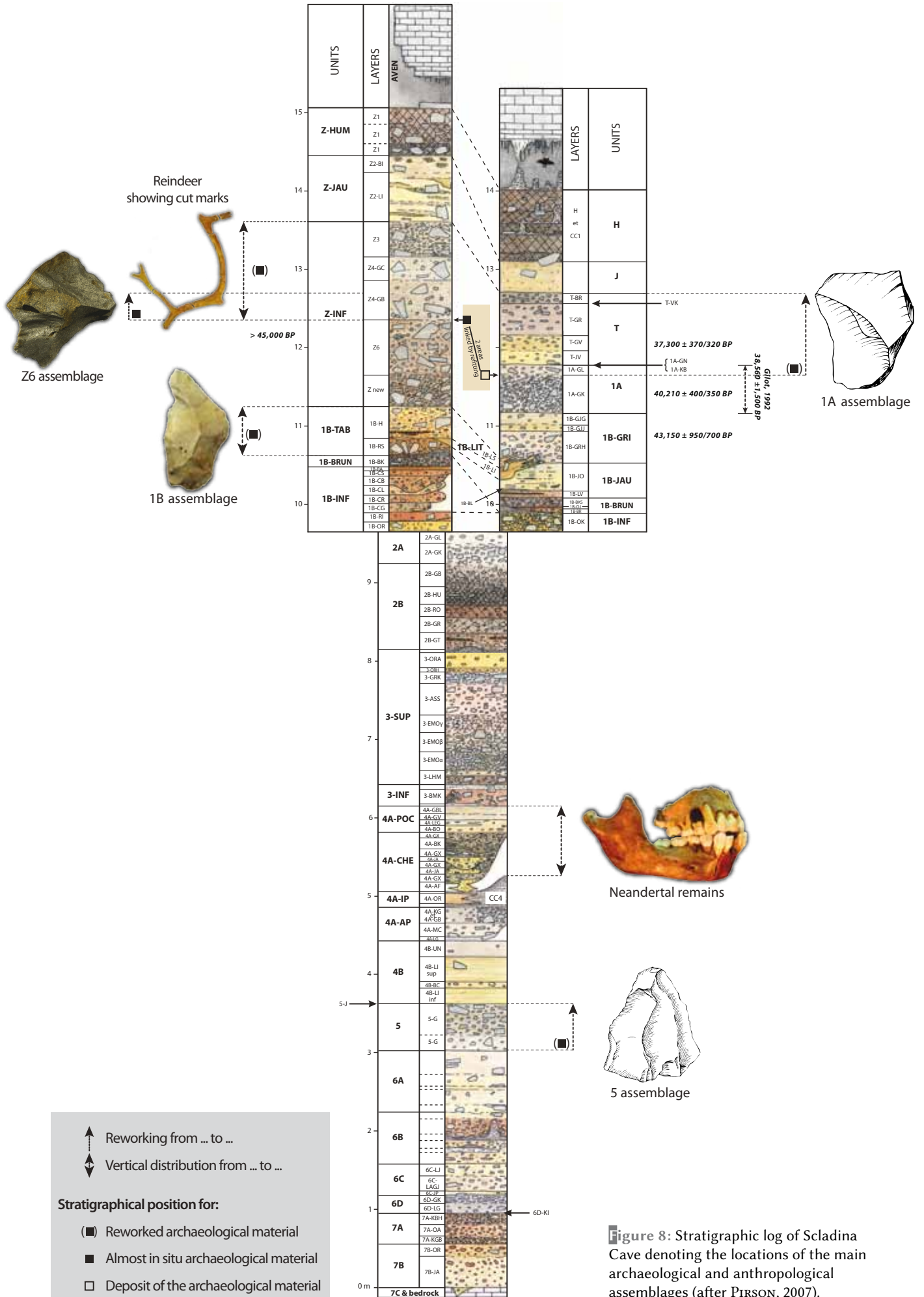


Figure 8: Stratigraphic log of Scladina Cave denoting the locations of the main archaeological and anthropological assemblages (after PIRSON, 2007).

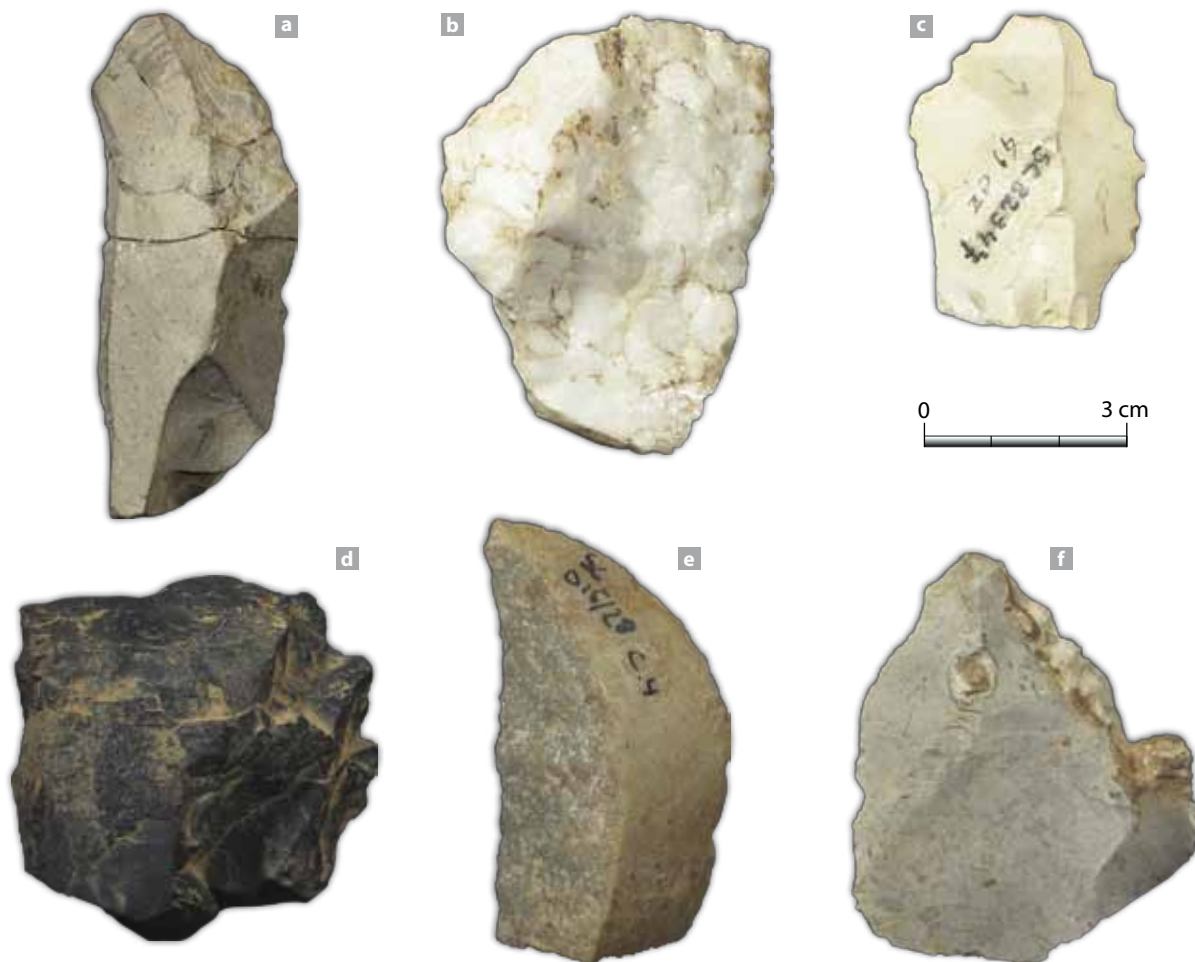


Figure 9: The raw material types worked in the assemblage from Unit 5: a. Limestone, b. Quartz, c. & f. Two types of flint, d. Chert, e. Quartzite.

their sharp edges (DI MODICA, 2010^a; DI MODICA, 2010^b; DI MODICA et al., in press).

The instruments necessary for the production of lithics have also been found. Tens of quartzite pebbles recovered from Unit 5 show the characteristics of their use as stone hammers (i.e. evidence of pecking; DI MODICA, 2010^b). Recently, evidence of the use of bone tools complemented the series of pebbles. In fact, an examination of a number of bone fragments permitted the identification of 26 large diaphyseal fragments that were used as retouchers (ABRAMS et al., 2013).

However, the acquisition and use of raw tool making materials as the explanation for Neandertals to use Scladina is not substantiated, since quality materials are absent for several kilometres around the site. Therefore, the motivation to stop at Scladina must be linked to other types of resource acquisition, such as the exploitation of animals from the hilly environment of the *Sillon Sambre-et-Meuse* (between the Sambre and Meuse valleys). The zooarchaeological data suggests that hunting with the purpose of building up a surplus of food may have been the

motivation for habitation at Scladina. Some bones show traces of flint cut marks, and faunal analysis shows that 6 whole chamois had been taken to the site and processed there in order to obtain skins, meat, tendons and marrow. It is suggested that they were likely packaged for transport to another site, which suggests that Scladina was a hunting camp (PATOU-MATHIS, 1998^a). The predation of small game was also illustrated by the presence of a coxal bone of a hare (Figure 14), bearing 18 butchery marks (BONJEAN et al., 2011). Finally, more than 1000 burned bone fragments have been collected, illustrating the existence of one or several hearths.

4.2.1.2. The assemblage from Unit 1A

Situated 2m higher in the stratigraphy, this group of artefacts was the first identified by the pioneers of the site. Its chronological position can be very precisely determined, even though diverse processes have reworked the artefacts, predominantly by debris flows and run-off. The first layer in which the assemblage appears is 1A-GL, which



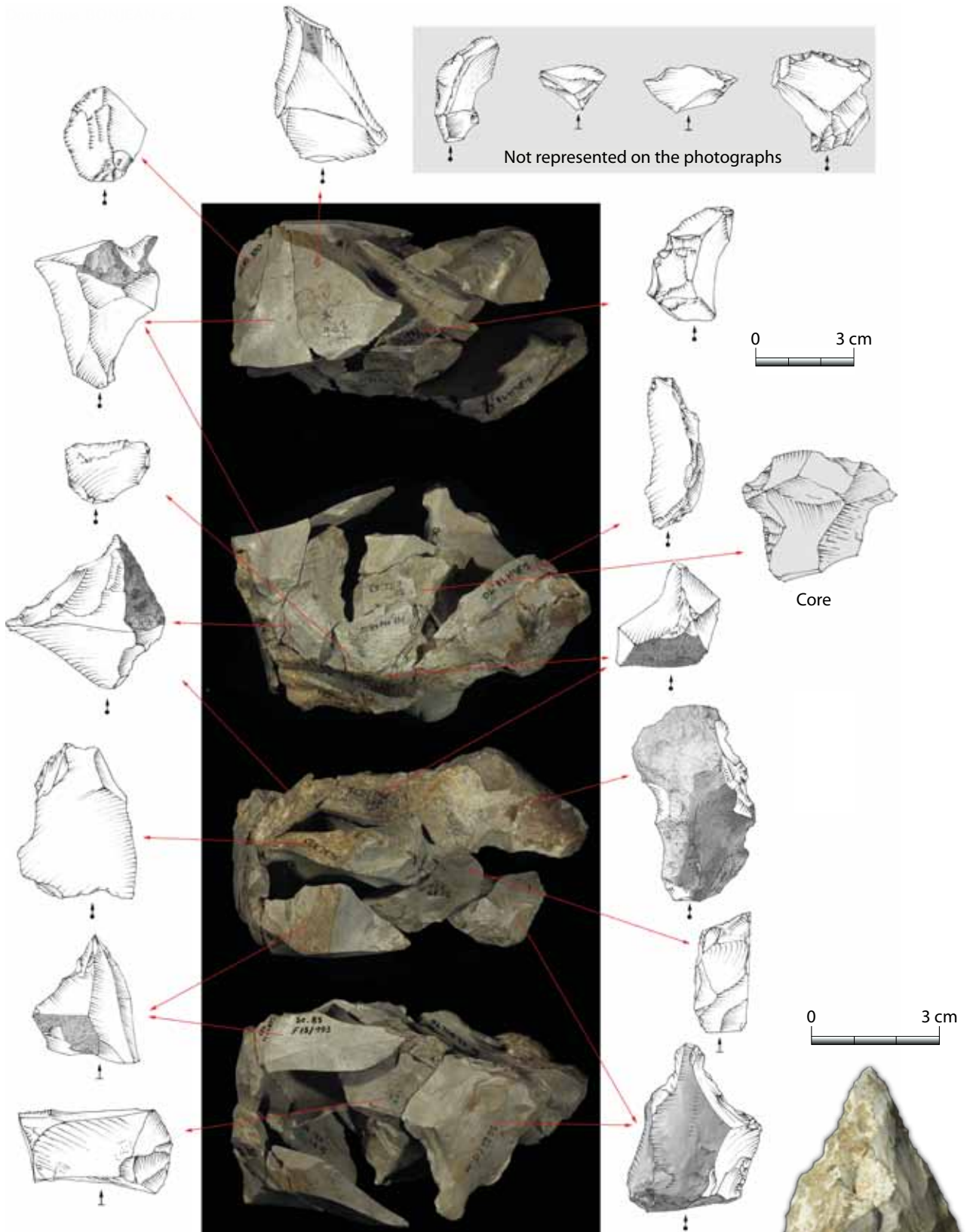


Figure 10: The flint nodules are roughly prepared. Their exploitation shows low standardization, which translates as an important flexibility in the concepts of tool making (drawings Sylviane Lambermont, refitting, photographs and graphics Kévin Di Modica).

Figure 11: Simple convex side scraper on a bulky, asymmetric flint flake coming from the assemblage of Unit 5.



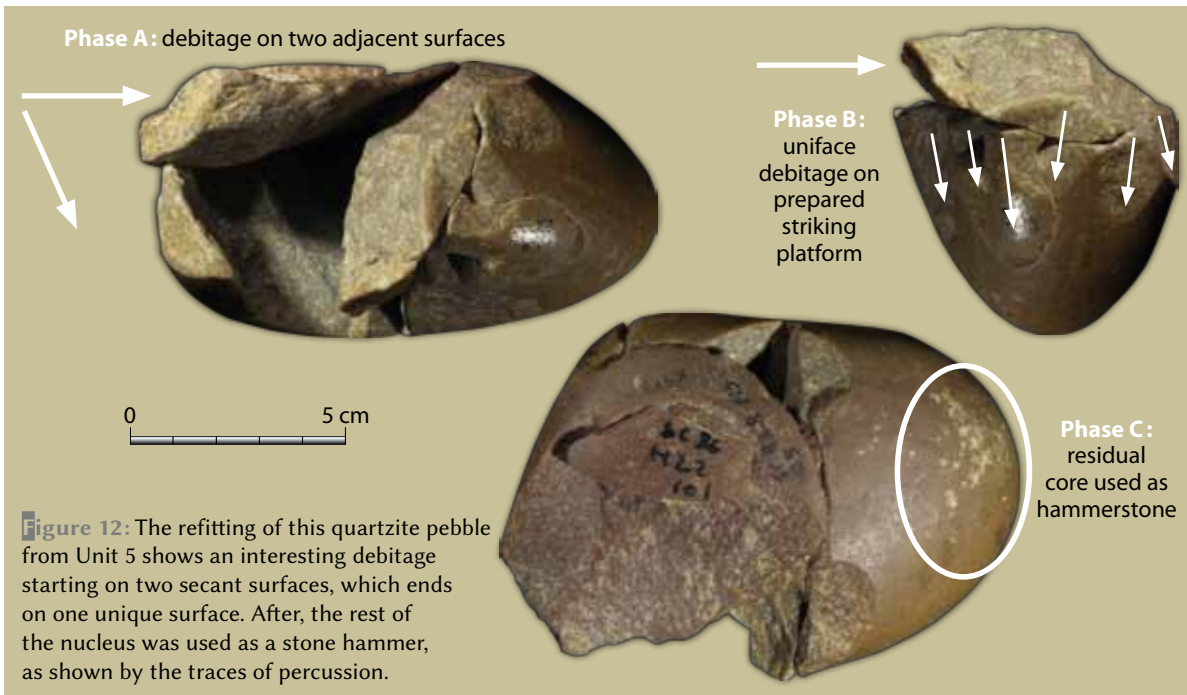


Figure 12: The refitting of this quartzite pebble from Unit 5 shows an interesting debitage starting on two secant surfaces, which ends on one unique surface. After, the rest of the nucleus was used as a stone hammer, as shown by the traces of percussion.



Figure 13: A massive quartzite asymmetrical knife from Unit 5.

Figure 14: Found in Unit 5, this hare coxal fragment attests to the hunting of small game. This bone exhibits 18 cut marks (drawing Sylviane Lambermont, AWEM).

is dated to between 40,210 +400/-350 BP (GrA-32635; PIRSON, 2007) and 37,300 +370/-320 BP (GrA-32633; PIRSON, 2007). These dates correspond to the Weichselian Middle Pleniglacial (MIS 3).

With approximately 4500 artefacts, the assemblage of Unit 1A is the second most valuable archaeological series of the site. Unlike the assemblage of Unit 5, the Unit 1A assemblage is characterized by a poorer state of preservation, heterogeneity of patina, highly abraded edges of the flint artefacts, as well as less circumscribed planimetric and stratigraphic distribution.

The differential use of the raw materials observed in this assemblage is essentially controlled by economic imperatives: small blocks and river pebbles of flint (Figure 15) or quartzite, complete exploitation, and immediate knapping without preparation. The series shows some behavioral similarities to that of Unit 5 in terms of flint importation strategies and the use of local raw materials. These similarities show the stability and balance attained by Neandertals in terms of their response to their needs and their exploitation of environmental resources. These analogies



Figure 15: Different faces (above) and schematic drawings (below) of the sequence of debitage (a-f) of a small alluvial flint pebble following the Quina conception, recovered in Unit 1A.

seem to ignore the ca. 70,000 years that separated the occupations, as well as the climatic and environmental variability (ORTE et al. (dir.), 1998; DI MODICA, 2010^b, DI MODICA et al., in press).

The analysis of faunal remains within Unit 1A indicated that less osseous material was present than teeth (LAMARQUE, 2003). Almost 148 cave bears were counted on their molars; but a minimum of only 9 individuals were represented by bones, which frequently exhibited

hyena gnawing marks (Figure 16). The poor preservation of bone impeded the observation of the relationship between Neandertals and fauna. If hunting was the major objective for stopping at Scladina, as previously suggested, the 1550 bones of ungulates recovered, corresponding to 17% of identified remains, exhibited no proof of predation by humans (BOURDILLAT, 2008). However, almost two hundred fragments of burned bone, some of which calcined, suggested the use of bone

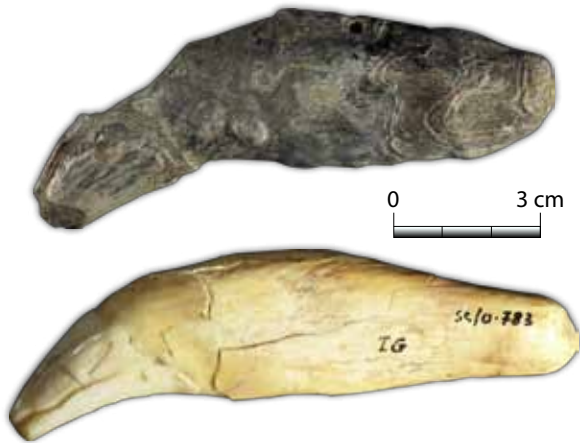


Figure 16: Two cave bear canines (*Ursus spelaeus*). One (up) is altered by the gastric acid of a cave hyena (*Crocuta spelaea*).

as fuel and, in fact, is the only proof of anthropogenic interaction with fauna found so far (ABRAMS et al., 2010).

As excavation at Scladina reached 35 m beyond the entrance, an aven became visible (BONJEAN et al., 2002). The opening of this aven was first observed in Layer 1B-TAB (PIRSON, 2007). The aven was totally filled with sediment from the plateau, creating a peculiar stratigraphic sequence that developed simultaneously with the sequence that was deposited from the entrance. In this new sedimentary sequence approximately 100 flint, quartz, and quartzite artefacts were recovered from the limit between layers Z6 and Z4, as well as the basal part of Z4. These artefacts were petrographically and technologically similar to the lithic series collected from Unit 1A. Two quartzite flakes from the two sedimentary sequences were refitted, demonstrating that both archaeological collections seem to represent a single human occupation.

4.2.2. The small lithic assemblages

The small lithic assemblages are an indicator that the cave and the surrounding region were frequented by Neandertals for approximately 100,000 years; however, their interpretation is complicated by the low number of anthropogenically modified objects. When faced with coherent assemblages composed of thousands of pieces, such as those from units 5 and 1A, the location and the type of activity, the contemporaneous relation to deposits, the consistency of assemblages, the reworking processes, and even the details of site function are questions that can

be addressed. However, with only a few tens of pieces, all these questions are more difficult to confront and to answer because of the absence of statistical parameters and contemporaneous links such as those established by refitting. Therefore, in small assemblages almost all artefacts can only be studied for themselves.

Flint flakes from units 2A, 2B and 3, all derived from very cryoclastic layers, were characterised by a very poor state of preservation of the ridges and cutting edges (Figure 17). The lithology of the units (particularly the abundance of limestone fragments) as well as the mode of deposition and the successive depositional reworking all had a powerful effect on the conservation of artefacts, and suggest the substantial displacement of material from its original context (DI MODICA & BONJEAN, 2004). In each case, is the reworked material contemporaneous with the sedimentary unit that contains it? Did this redistribution of artefacts in the cave come from one or several older archaeological deposits? Did the reworking of these pieces originate at the entrance of the cave or from the overlying plateau? At this time all these questions remain unanswered.

In some of the sedimentary units, the flint flakes have a very fresh appearance (Figure 17). This is the case for the few pieces found in the silts of units 6A, 6B and 6C, which are almost devoid of limestone fragments. The freshness of the material does not necessarily facilitate its interpretation. Does this indicate a taphonomic exception, or is this evidence of an occupation site? Again, this question remains unanswered due to the lack of material.

The archaeological interpretation of Layer 1B-TAB is also difficult. Directly below the aven, approximately 100 small, unweathered flint flakes and chips with the same white patina were recovered. In this place, silty sediment containing very few limestone fragments had slid from the plateau and had been moderately dispersed in the cave. All these factors indicate a coherent assemblage, including: freshness of the material, taphonomic homogeneity, and a concentration of small, relatively unmodified, knapped artefacts sparsely spread within the silt matrix. This seems to correspond to a location that was used by hominids for short periods of time, for which the question is whether this activity occurred on the plateau beside the aven or, less likely, in the cave under an opening that produced light.

Furthermore, under the aven, approximately 10 reindeer bones with butchery marks were



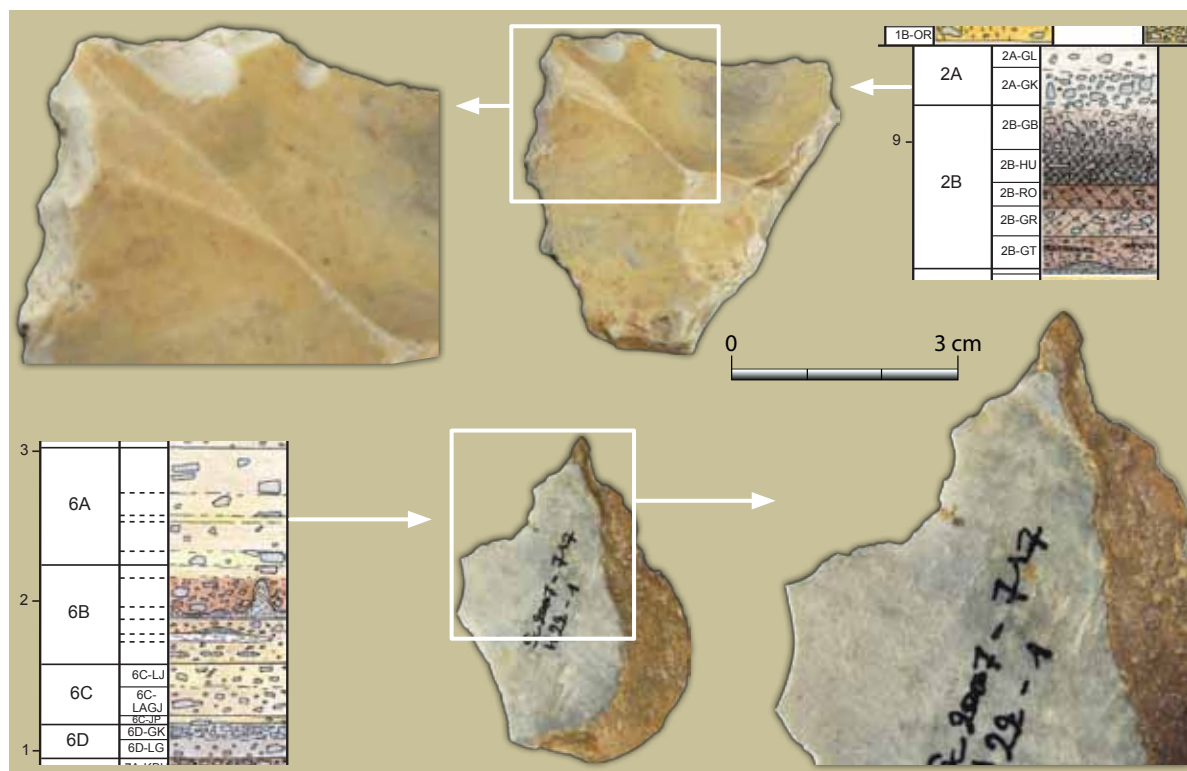


Figure 17: The flint artefacts of Unit 2A (above) are patinated with very blunt edges. On the other hand, the ones from Unit 6A (below) are fresh with sharp cutting edges.

found in Layer Z4. The bones seem to belong to a single individual. Their dispersal is limited, extended over only 9 m². Human activity is once again suggested to have occurred either on the plateau next to the aven, which functioned as a collector of waste, or in the cave where the dual advantage of both shelter and light was present.

Above the Middle Palaeolithic archaeological sequence, some pieces were excavated that belonged to later periods. These pieces, frequently extracted from perturbed sedimentary contexts (e.g. due to bioturbation), are of limited interest. Sediment reworked from the plateau to the cave through the aven, as well as several other chimneys, brought with it some Upper Palaeolithic and Mesolithic artefacts. A Neolithic group burial was also found at the entrance to the cave, as mentioned above. The activity of bioturbators also produced some of the most surprising anachronisms: a Roman tile fragment, ceramic pieces, and a clay pipe manufactured in Andenne during the 19th century were all incorporated into the cave through different types of burrows (OTTE et al. (dir.), 1998; OTTE, 1998; BONJEAN et al., 2010).

The Scladina I-4A Neandertal 5. Child: history of the discoveries

The first Palaeolithic hominid teeth were found at Scladina at the beginning of 1990.

The first 12 years of excavation had emptied the cave up to metre 27, during which several thousand faunal remains had been exhumed from the Sedimentary Complex 4A (see Chapter 3), mainly attributed to *Ursus spelaeus* (SIMONET, 1992; PATOU-MATHIS, 1998^b). The first palaeontological assessment of the site was done on this material (SIMONET, 1991).

Unfortunately, nobody had recognized the Neandertal remains at this time. The excavators did not identify the first 3 teeth of the Neandertal child (2 incisors and 1 canine) that were removed from excavation Square H27 on either February 22 and 23, 1990. Over the next 2 years, the excavation extended over 15 m² toward the back of the cave and 8 other teeth were recovered under the same conditions as the first 3; likely they were not recognized. The small maxillary fragment without teeth also passed unrecognized in 1992 during the excavation of Square D30.

The year 1993 compensated for these first failures. On July 16, Claire Curvers, a student from the University of Liège spotted the right hemimandible in Square D29 (Figure 18). It was precisely recorded in three dimensions. An anthropologist identified it as Neandertal four days later (BONJEAN et al., 2009^b).

From September 1993 on, part of the team continued excavation, while the other part took advantage of the collections and checked if some



Figure 18: Recreation of the geographic and stratigraphic position of the right hemimandible Scla 4A-1 discovered on July the 16th 1993. The sediment of Unit 4A-CHE (the gully) contains many limestone fragments and reworked speleothems (photomontage).

pieces of the Neandertal child had escaped the vigilance of the excavators and the first analysts. Through this process, the aforementioned 11 teeth and the maxillary fragment were recovered from bags stored over the preceding 4 years.

The field team was also fortunate: on December 14, 1993, an excavator from Archéologie Andennaise recognized the child's permanent maxillary right first molar in Square C30. After being photographed at the time of its removal (Figure 19), this tooth became the first Belgian Neandertal fossil to be pictured in the place of its discovery.

In 1995, 2 teeth escaped the observation of the excavators and were recovered during screening. However, the excavation being standardized and the planimetric map of the remains being sufficiently detailed the 2 pieces could be attributed to a precise sedimentary layer (see Chapter 5).

In 1996, the left hemimandible was found under spectacular circumstances, and it is by chance that its precise position could be recorded. Along the left wall of the cave, a limestone slab had detached from the roof, and, over time, had put pressure on the sediment in the underlying berm. A fracture developed and was about to cause the collapse of a small portion of the section. The director of the site made the decision to remove the fragile portion of the berm. On the new section, generated by the fracture, the left hemimandible was found (Figure 20).

Further excavations toward the back of the cave lead to the discovery of 2 more isolated teeth. The last hominid remain to have been discovered is the permanent mandibular right lateral incisor from zone F35-F37 that was recovered in 2006 during the screening of sediments derived from the collapse of an imposing berm weakened by several badger burrows.

This list closes with the discovery of the deciduous mandibular right second molar of the child, on November 13, 2001, in Square E38 (Figure 21). Although this is not the most recent Neandertal remain discovered at Scladina, it is world-renowned for being the element of the child that was analyzed by geneticists (see Chapter 19 and ORLANDO et al., 2006).

Acknowledgements

The authors would like to express their deepest gratitude to Cheryl Roy and Rhylan McMillan (Vancouver Island University, Nanaimo, British Columbia, Canada) as well as Jean-François Lemaire (Service public de Wallonie), for their valuable help in translating the manuscript into English. Many thanks to Anne Laurys and Eric Dermience of the Royal Belgian Institute of Natural Sciences (RBINS), Sylviane Lambermont, graphics artist at the Association wallonne d'Études mégalithiques (AWEM) for the line drawings.



Figure 19: Partial top view of Square C30. In the middle, the permanent maxillary right first molar appears in situ: $x = 12$ cm, $y = 50$ cm, $z = -466$ cm.

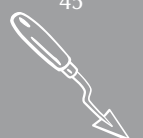




Figure 20: Detail of Section D/C 28. The left hemimandible Scla 4A-9 appears in situ: $x = 98$ cm, $y = 75$ cm, $z = -478.5$ cm. The fossil lays 2 cm from a stalagmite fragment reworked into the gully.

References

ABRAMS G., BELLO S. M., DI MODICA K., PIRSON S. & BONJEAN D., 2014. When Neanderthals used cave bear (*Ursus spelaeus*) remains: Bone retouchers from unit 5 of Scladina Cave (Belgium). *Quaternary International*, 326, 327: 274–287.

ABRAMS G., BONJEAN D., DI MODICA K., PIRSON S., OTTE M. & PATOU-MATHIS M., 2010. Les os brûlés de l'ensemble sédimentaire 1A de *Scladina* (Andenne, Belgique): apports naturels ou restes de foyer(s) néandertalien(s)? *Notae Praehistoricae*, 30: 5–13.

BENABDELHADI M., 1998. Étude sédimentologique de la coupe transversale 30/31 des carrés A, B, C et D de la grotte Scladina. In M. OTTE, M. PATOU-MATHIS & D. BONJEAN (dir.), *Recherches aux grottes de Sclayn, vol. 2: L'Archéologie*. Études et Recherches Archéologiques de l'Université de Liège, 79: 25–37.

BONJEAN D., 1995. Dans la foulée de l'Homme de Néandertal: Sclayn 1994. Résultats scientifiques préliminaires et diffusion médiatique. In J. PLUMIER & M.-H. CORBIAU (eds.), *Actes de la Troisième Journée d'Archéologie Namuroise*. Namur, Facultés universitaires Notre-Dame de la Paix, 26 février 1994, Ministère de la Région wallonne, Direction générale de l'Aménagement

Figure 21: In 2001, Square E38 yielded the deciduous mandibular right second molar Scla 4A-13 (inset). Top view of the square with the fossil in situ: $x = 88$ cm, $y = 57$ cm, $z = -481$ cm.



du Territoire, du Logement et du Patrimoine, Direction de Namur, Service des Fouilles: 45–48.

BONJEAN D., 1998^a. Situation géographique et historique. In M. OTTE, M. PATOU-MATHIS & D. BONJEAN (dir.), *Recherches aux grottes de Sclayn, vol. 2: L'Archéologie*. Études et Recherches Archéologiques de l'Université de Liège, 79: 9–14.

BONJEAN D., 1998^b. Répartition spatiale de l'industrie lithique. In M. OTTE, M. PATOU-MATHIS & D. BONJEAN (dir.), *Recherches aux grottes de Sclayn, vol. 2: L'Archéologie*. Études et Recherches Archéologiques de l'Université de Liège, 79: 340–376.

BONJEAN D., 2009. L'archéologie de terrain aujourd'hui: la fouille *made in* Scladina. In K. DI MODICA & C. JUNGELS (dir.), *Paléolithique moyen en Wallonie. La collection Louis Éloy*. Bruxelles, Collections du Patrimoine culturel de la Communauté française, 2: 28–32.

BONJEAN D., ABRAMS G., DI MODICA K. & OTTE M., 2009^a. La microstratigraphie, une clé de lecture des remaniements sédimentaires successifs. Le cas de l'industrie moustérienne 1A de *Scladina*. *Notae Praehistoricae*, 29: 139–147.

BONJEAN D., DI MODICA K. & ABRAMS G., 2010. Andenne/Sclayn: un nouveau témoin du Paléolithique supérieur à Scladina. *Chronique de l'Archéologie wallonne*, Éditions du Service public de Wallonie, Direction générale opérationnelle de l'Aménagement du Territoire, du Logement, du Patrimoine et de l'Énergie, Département du patrimoine, 17: 182–183.

BONJEAN D., DI MODICA K., ABRAMS G., PIRSON S. & OTTE M., 2011. La grotte Scladina: bilan 1971–2011. In M. TOUSSAINT, K. DI MODICA & S. PIRSON (sc. dir.), *Le Paléolithique moyen en Belgique. Mélanges Marguerite Ulrix-Closset*. Bulletin de la Société royale belge d'Études Géologiques et Archéologiques *Les Chercheurs de la Wallonie*, hors-série, 4 & Études et Recherches Archéologiques de l'Université de Liège, 128: 323–334.

BONJEAN D., LOODTS I. & LÓPEZ-BAYÓN I., 2002. La doline de Scladina (Sclayn, Andenne, province de Namur). Un second complexe sédimentaire. *Notae Praehistoricae*, 22: 15–19.

BONJEAN D., MASY P. & TOUSSAINT M., 2009^b. L'enfant néandertalien de Sclayn. Petite histoire d'une découverte exceptionnelle. *Notae Praehistoricae*, 29: 49–51.

BONJEAN D. & OTTE M., 2004. Une organisation

- fonctionnelle de l'espace d'habitat. Le cas de la grotte Scladina (Sclayn, Belgique). In N. J. CONARD (ed.), *Settlement Dynamics of the Middle Paleolithic and Middle Stone Age*, 2, Tübingen, Kerns Verlag: 261-271.
- BOURDILLAT V., 2008. *Hommes – Carnivores ? Caractériser l'action de l'hyène des cavernes : de l'utilisation des données fossiles pour l'interprétation des sites mixtes*. Unpublished PhD thesis. Paris, Muséum National d'Histoire Naturelle, 2 vol., 292 p. & 38 p.
- DEBLAERE C. & GULLENTOPS F., 1986. Lithostratigraphie de la grotte Scladina. *Bulletin de l'Association française pour l'étude du Quaternaire*, 2^e série, 25-26: 178-181.
- DI MODICA K., 2010^a. Contraintes naturelles et implantations moustériennes dans le bassin mosan (Belgique). In N. J. CONARD & A. DELAGNES (eds.), *Settlement Dynamics of the Middle Paleolithic and Middle Stone Age*, 3, Tübingen, Kerns Verlag: 307-328.
- DI MODICA K., 2010^b. *Les productions lithiques du Paléolithique moyen de Belgique : variabilité des systèmes d'acquisition et des technologies en réponse à une mosaïque d'environnements contrastés*. Unpublished PhD thesis. Université de Liège, Faculté de Philosophie et Lettres & Museum National d'Histoire Naturelle, Département de Préhistoire, 787 p.
- DI MODICA K., ABRAMS G., BONJEAN D., BOSQUET D., BRINGMANS P. M., JUNGELS C. & RYSSAERT C., in press. Le Paléolithique moyen en Belgique : variabilité des comportements techniques. In P. DEPAEPE, J.-L. LOCHT, E. GOVAL & H. KOEHLER (dir.), *Les plaines du Nord-Ouest : carrefour au Paléolithique moyen ?* Compte-rendu des journées de la Société Préhistorique Française, Amiens, 28-29 mars 2008. Paris, Mémoires de la Société Préhistorique Française.
- DI MODICA K. & BONJEAN D., 2004. Scladina (Sclayn, province de Namur) : ensembles lithiques moustériens méconnus. *Notae Praehistoricae*, 24: 5-8.
- DONCEEL P., VANDEBOSCH A. & DE RADZITZKY D'OSTROWICK I., 1910. Région Sclayn-Bonneville. *Bulletin de la Société royale belge d'Études Géologiques et Archéologiques* Les Chercheurs de la Wallonie, 4: 131-160.
- DUBOIS J., 1981. Prospection au Fond des Vaux à Sclayn. *Activités du SOS Fouilles*, 2: 86-89.
- GULLENTOPS F. & DEBLAERE C., 1992. Érosion et remplissage de la grotte Scladina. In M. OTTE (ed.), *Recherches aux grottes de Sclayn, vol. 1 : Le Contexte*. Études et Recherches Archéologiques de l'Université de Liège, 27: 9-31.
- HAESAERTS P., 1992. Les dépôts pléistocènes de la terrasse de la grotte Scladina à Sclayn (Province de Namur, Belgique). In M. OTTE (ed.), *Recherches aux grottes de Sclayn, vol. 1 : Le Contexte*. Études et Recherches Archéologiques de l'Université de Liège, 27: 33-55.
- LAMARQUE F., 2003. Les ours spéléens de la grotte de Scladina (Namur, Belgique): essai d'explication du déséquilibre entre la conservation des dents et des os de la couche 1A. In M. PATOU-MATHIS & H. BOCHERENS (eds.), *Le rôle de l'environnement dans les comportements des chasseurs-cueilleurs préhistoriques*. Actes du XIV^{ème} Congrès de l'Union Internationale des Sciences Préhistoriques et Protohistoriques, Section 3 : Paléoécologie. Colloque C3.1., Université de Liège, Belgique, 2-8 septembre 2001, Oxford, British Archaeological Reports, International Series, 1105: 111-119.
- ORLANDO L., DARLU P., TOUSSAINT M., BONJEAN D., OTTE M. & HÄNNI C., 2006. Revisiting Neandertal Diversity with a 100,000 year old mtDNA Sequence. *Current Biology*, 16: R400-R402.
- OTTE M., 1990. L'occupation moustérienne de Sclayn (Belgique). *Ethnographisch-Archäologische Zeitschrift*, 31: 78-101.
- OTTE M. (ed.), 1992. *Recherches aux grottes de Sclayn, vol. 1 : Le Contexte*. Études et Recherches Archéologiques de l'Université de Liège, 27: 182 p.
- OTTE M., 1998. Le Paléolithique supérieur. In M. OTTE, M. PATOU-MATHIS & D. BONJEAN (dir.), *Recherches aux grottes de Sclayn, vol. 2 : L'Archéologie*. Études et Recherches Archéologiques de l'Université de Liège, 79: 63-68.
- OTTE M. & BONJEAN D., 1998. L'outillage. In M. OTTE, M. PATOU-MATHIS & D. BONJEAN (dir.), *Recherches aux grottes de Sclayn, vol. 2 : L'Archéologie*. Études et Recherches Archéologiques de l'Université de Liège, 79: 127-179.
- OTTE M., EVRARD J.-M. & MATHIS A., 1988. Interprétation d'un habitat au paléolithique moyen. La grotte de Sclayn, Belgique. In H. DIBBLE & A. MONTET-WHITE (eds.), *Upper Pleistocene Prehistory of Western Eurasia*. Philadelphie, University Museum, Monograph, 54: 95-124.



- OTTE M., LÉOTARD J.-M., SCHNEIDER A.-M. & GAUTIER A., 1983. Fouilles aux grottes de Sclayn (Namur). *Helinium*, 23: 112-142.
- OTTE M., PATOU-MATHIS M. & BONJEAN D. (dir.), 1998. *Recherches aux grottes de Sclayn, vol. 2 : L'Archéologie*. Études et Recherches Archéologiques de l'Université de Liège, 79, 437 p.
- PATOU-MATHIS M., 1998^a, Les espèces chassées et consommées par l'homme en couche 5. In M. OTTE, M. PATOU-MATHIS & D. BONJEAN (dir.), *Recherches aux grottes de Sclayn, vol. 2: L'Archéologie*. Études et Recherches Archéologiques de l'Université de Liège, 79: 297-310.
- PATOU-MATHIS M., 1998^b, Origine et histoire de l'assemblage osseux de la couche 5. Comparaison avec la couche 4 sus-jacente, non anthropique. In M. OTTE, M. PATOU-MATHIS & D. BONJEAN (dir.), *Recherches aux grottes de Sclayn, vol. 2: L'Archéologie*. Études et Recherches Archéologiques de l'Université de Liège, 79: 281-295.
- PATOU-MATHIS M. & LÓPEZ-BAYÓN I., 1998. Répartition spatiale des ossements de la couche 5. In M. OTTE, M. PATOU-MATHIS & D. BONJEAN (dir.), *Recherches aux grottes de Sclayn, vol. 2: L'Archéologie*. Études et Recherches Archéologiques de l'Université de Liège, 79: 377-395.
- PIRSON S., 2007. *Contribution à l'étude des dépôts d'entrée de grotte en Belgique au Pléistocène supérieur. Stratigraphie, sédimentogenèse et paléoenvironnement*. Unpublished PhD thesis, University of Liège & Royal Belgian Institute of Natural Sciences, 2 vol., 435 p. & 5 annexes.
- PIRSON S., COURT-PICON M., HAESAERTS P., BONJEAN D. & DAMBLON F., 2008. New data on geology, anthracology and palynology from the Scladina Cave pleistocene sequence: preliminary results. In F. DAMBLON, S. PIRSON & P. GERRIENNE (eds.), *Hautrage (Lower Cretaceous) and Sclayn (Upper Pleistocene). Field Trip Guidebook. Charcoal and microcharcoal: continental and marine records*. IVth International Meeting of Anthracology, Brussels, Royal Belgian Institute of Natural Sciences, 8-13 September 2008. Brussels, Royal Belgian Institute of Natural Sciences, *Memoirs of the Geological Survey of Belgium*, 55: 71-93.
- SIMONET P., 1991. *Contribution à la connaissance des grands mammifères du pléistocène supérieur de Belgique et de Bretagne*. Unpublished PhD thesis, University of Liège, 565 p. & 362 tables.
- SIMONET P., 1992. Les associations de grands mammifères du gisement de la grotte Scladina à Sclayn (Namur, Belgique). In M. OTTE (ed.), *Recherches aux grottes de Sclayn, vol. 1 : Le Contexte*. Études et Recherches Archéologiques de l'Université de Liège, 27: 127-151.
- TOUSSAINT M., BONJEAN D. & OTTE M., 1994. Découverte de fossiles humains du Paléolithique moyen à la grotte Scladina à Andenne. In M.-H. CORBIAU & J. PLUMIER (eds.), *Actes de la deuxième Journée d'Archéologie Namuroise*. Namur, Facultés universitaires Notre-Dame de la Paix, 26 février 1994, Ministère de la Région wallonne, Direction générale de l'Aménagement du Territoire et du Logement, Direction de Namur, Service des Fouilles: 19-33.
- TOUSSAINT M., OTTE M., BONJEAN D., BOCHERENS H., FALGUÈRES C. & YOKOYAMA Y., 1998. Les restes humains néandertaliens immatures de la couche 4A de la grotte Scladina (Andenne, Belgique). *Comptes rendus de l'Académie des Sciences de Paris, Sciences de la terre et des planètes*, 326: 737-742.
- TOUSSAINT M. & PIRSON S., 2006. Neandertal Studies in Belgium: 2000-2005. *Periodicum Biologorum*, 108, 3: 373-387.
- TOUSSAINT M., PIRSON S. & BOCHERENS H., 2001. Neandertals from Belgium – Les Néandertaliens de Belgique. *Anthropologica et Praehistorica*, 112: 21-38.
- TOUSSAINT M., SEMAL P. & PIRSON S., 2011. Les Néandertaliens du bassin mosan belge: bilan 2006-2011. In M. TOUSSAINT, K. DI MODICA & S. PIRSON (sc. dir.), *Le Paléolithique moyen en Belgique. Mélanges Marguerite Ulix-Closset*. Bulletin de la Société royale belge d'Études Géologiques et Archéologiques *Les Chercheurs de la Wallonie*, hors-série, 4 & Études et Recherches Archéologiques de l'Université de Liège, 128: 149-196.
- VAN DER SLOOT P., 1998. Matières premières lithiques et comportements au Paléolithique moyen. Le cas de la couche 5 de la grotte Scladina. In M. OTTE, M. PATOU-MATHIS & D. BONJEAN (dir.), *Recherches aux grottes de Sclayn, vol. 2 : L'Archéologie*. Études et Recherches Archéologiques de l'Université de Liège, 79: 115-126.

Stéphane PIRSON

Michel Toussaint & Dominique Bonjean (eds.), 2014. The Scladina I-4A Juvenile Neandertal (Andenne, Belgium), Palaeoanthropology and Context Études et Recherches Archéologiques de l'Université de Liège, 134: 49–68.

1. Introduction

A sound knowledge of stratigraphy and an in-depth understanding of the genesis of sedimentary deposits are essential prerequisites for any prehistoric or palaeoanthropological study. This is particularly the case for cave entrances and rock shelters, where recent analyses have highlighted a critical and complex heterogeneity of deposits, including factors such as the diversity of sedimentary sources (Figure 1), the effects of variable local conditions, specific diagenetic phenomena, and the presence of sedimentary dynamics dominated by slope processes that successively redistribute sediment (e.g., TEXIER, 2000, 2001; FERRIER, 2002; BERTRAN (dir.), 2004; BERTRAN, 2005, 2006; GOLDBERG & SHERWOOD, 2006; PIRSON, 2007; LENOBLE et al., 2008; BERTRAN et al., 2009).

Because of the complexity of these heterogeneous deposits, only detailed stratigraphic studies that are built on a large number of cross-sections

from across the entirety of a site are able to provide a sufficient understanding of lateral sedimentary variations and lead to the development of an optimal sedimentary record. Such an approach is also necessary for determining the accurate stratigraphic positioning of anthropological, archaeological, or palaeontological discoveries. A reliable reconstruction of the genesis of deposits – and incidentally the nature and extent of the disturbances and hiatuses that occurred during their deposition – is also fundamental for understanding sedimentary depositional dynamics and evaluating the integrity of the material exhumed during excavation (e.g., BERTRAN & TEXIER, 1995, 1997; TEXIER, 2000, 2001; LENOBLE & BORDES, 2001; LENOBLE, 2005; BERTRAN et al., 2006, 2009, 2012; LENOBLE et al., 2008, 2009). Finally, a good understanding of sedimentary context is necessary for sampling strategies and analyses such as those that focus on the palaeoenvironmental and chronostratigraphic aspects of the stratigraphic sequence.

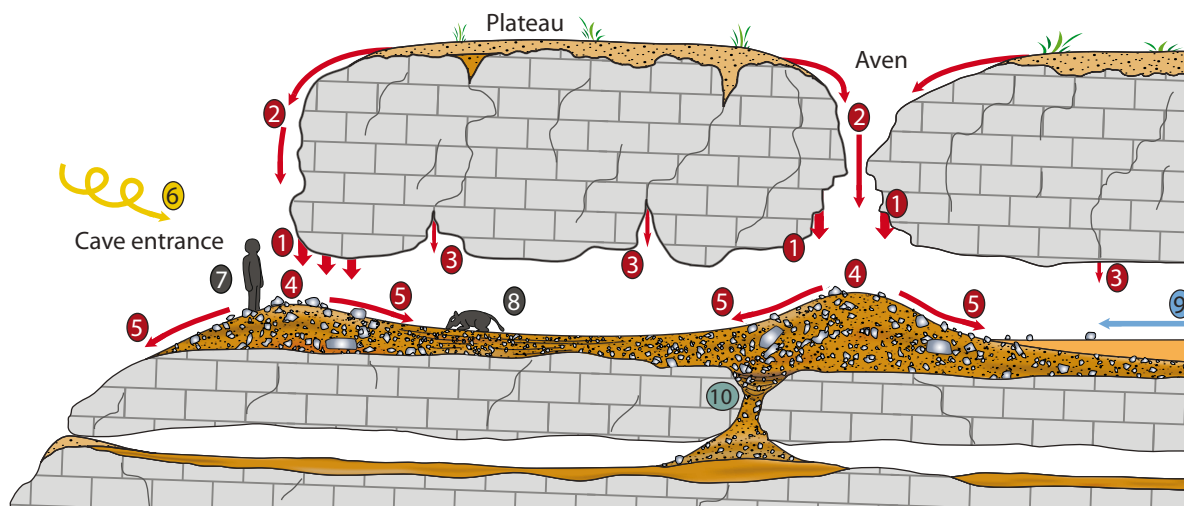
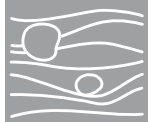


Figure 1: The complexity of the genesis of cave entrance sedimentary sequences (modified after FERRIER, 2002).

1. Fracturing of the limestone walls; 2. Gravity input from the plateau through the cave porch or avens; 3. Infiltration through fissures; 4. Main accumulation zone (rock fan); 5. Redistribution from the rock fans by several processes (solifluction, run-off, debris flow, etc.); 6. Aeolian input; 7. Anthropogenic input; 8. Faunal input; 9. Endokarstic alluviation; 10. Collapse of sediments (withdrawing) into a lower gallery. Graphics: Joël Éloy (AWEM).



In Belgium, much of the available data for fossil hominids has been collected from the numerous cave entrances found in the Palaeozoic limestones of the centre part of the country (PIRSON et al., 2008). More specifically, all the known Belgian Palaeolithic human remains were found at these karstic sites (TOUSSAINT & PIRSON, 2006; TOUSSAINT et al., 2011). However, amongst the 8 Belgian sites that have yielded such remains, only the sites that have been recently excavated have both a detailed stratigraphic log and a good understanding of the genesis of the sedimentary deposits (e.g., TOUSSAINT & PIRSON, 2007). Scladina and Walou caves are the most striking of these sites; Neandertal remains were discovered at both locations during the 1990s (PIRSON et al., 2006, 2007; PIRSON, 2007; PIRSON et al. (dir.), 2011; DRAILY et al. (dir.), 2011). Therefore, Scladina Cave holds a special significance in the study of fossil hominids in Belgium.

History of the establishment of the stratigraphic record 2. at Scladina Cave

The constitution of the stratigraphic sequence at Scladina Cave can be presented in 3 periods.

The first period began in 1971, the year the cave was discovered and explored by speleologists. Over the course of 7 years (1971–1977), those speleologists removed the top 2 metres of sediment from the first 10 horizontal metres of the site without recording any stratigraphic data. The discovery of lithic material prompted them to contact professional archaeologists and cease their excavations in 1977. As soon as 1978 the University of Liège began its first scientific excavation campaign at Scladina. A few stratigraphic records were taken at that time, which led to the definition of the main units of the sequence (OTTE & SLOOTMAEKERS, 1982; OTTE et al., 1983).

The second period, during which the initial stratigraphic system was supplemented, began with the collection of the first stratigraphic information from inside the cave by a geologist. These studies, as well as the first sedimentological analyses, were combined and then used as the framework for a university graduate thesis (DEBLAERE & GULLENTOPS, 1986; GULLENTOPS & DEBLAERE, 1992). Simultaneously, the geologist P. HAESAERTS (1992) studied the stratigraphic sequence of the cave entrance. Several years later,

another geologist undertook a sedimentological study devoted to the clarification of the context of the Neandertal remains (BENABDELHADI, 1998), focusing on only 1 small sedimentary profile. Finally, the archaeologist in charge of the excavations published new data about specific areas of the sedimentary sequence (e.g., TOUSSAINT et al., 1994; BONJEAN et al., 1996, 1997, 2002) and a synthesis of the stratigraphy was completed (BONJEAN, 1998^a; Figure 2). All in all, by the end of this period a total of about 10 sedimentary profiles were recorded and interpreted.

The third period corresponds with a PhD study in geology (PIRSON, 2007). October 2003 saw the beginning of the detailed stratigraphic recording of almost all accessible profiles in Scladina, totaling approximately 70, with each one covering vertical surfaces that ranged from 1 to 45 square metres. Simultaneously, a geological survey of the archaeological excavation was conducted as systematically as possible in close collaboration with D. Bonjean, the archaeologist in charge of the site. Following these new records,

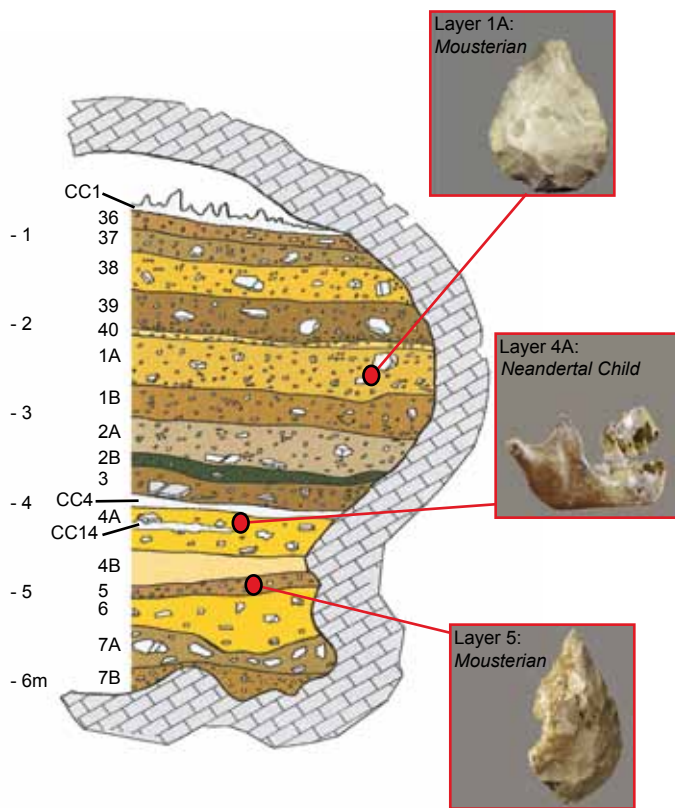


Figure 2: The former stratigraphic sequence of Scladina Cave (after the synthesis of BONJEAN, 1998^a based on OTTE et al., 1983 and GULLENTOPS & DEBLAERE, 1992). Graphics: Joël Éloy (AWEM).

the stratigraphy of the site appeared much more complex than previously thought. The number of identified layers expanded from 30 to almost 120, grouped into 30 distinct units (Figure 3). These units correspond roughly to the former layers (e.g., Unit 2B, which is comprised of 5 layers and corresponds to former Layer 2B). The differences between the new and the previous sequence are particularly striking for former layers 6, 4A, and 1B. The review of these 3 former layers led to the identification of 14 units, encompassing more than 50 layers in total. The field study also revealed complex geometries, numerous lithologies, a large variety of depositional and diagenetic processes, as well as a large number of climatic fluctuations that all demonstrate the exceptional nature of this stratigraphic sequence.

More recently, ongoing excavation and the examination of new profiles has led to the identification of some new layers, but only in the second, upper half of the sequence (e.g., units 1A and T; see BONJEAN et al., 2009).

3. Lithostratigraphy

Only the deposits that are related to the palaeoanthropological remains — i.e. former Layer 4A — are described below, as well as the layers directly below (former layers 5 and 4B) and above it (former Layer 3). The complete lithostratigraphic description is available in PIRSON (2007). It is worth mentioning here that below Scladina Cave another cave has been identified, called Sous-Saint-Paul Cave. Their respective deposits are locally connected through sinkholes, but the two sedimentary sequences are separated by an important hiatus (HAESAERTS, 1992; PIRSON, 2007; PIRSON et al., 2008).

3.1. The former stratigraphic record

In the previous stratigraphic system defined for the inside of the cave (OTTE et al., 1983; GULLENTOPS & DEBLAERE, 1992; BONJEAN et al., 1996, 1997; BONJEAN, 1998^a; Figure 2) there was, above Layer 5 and below Layer 3, from bottom to top:

- a silty layer, sometimes laminated (Layer 4B);
- a stony layer (Layer 4A);
- a thick in situ Stalagmitic Floor CC4¹.

¹ Several “calcitic crusts” (“*croûte de calcite*”) were identified in the former stratigraphic sequence, from CC1 to CC8. They correspond to either in situ stalagmitic floor, reworked speleothem or even in situ

Towards the entrance, where Stalagmitic Floor CC4 is absent, the top of former Layer 4A is altered. In some publications only a single Layer 4 was identified (OTTE et al., 1983; BASTIN, 1992; SIMONET, 1992; PATOU-MATHIS, 1998) in the same area where 2 layers would later be mentioned (GULLENTOPS & DEBLAERE, 1992; BONJEAN, 1998^a). A stalagmitic floor was also described inside Layer 4A (called CC14; BONJEAN et al., 1996; BONJEAN 1998^a).

3.2. The new stratigraphic record

The careful observation of the sedimentary profiles accessible between metres 23 and 43 led to a more accurate definition of the succession of lithostratigraphic units in former layers 4A and 4B, leading to the definition of Sedimentary Complex 4 (PIRSON et al., 2005; PIRSON, 2007). Before metre 23 almost nothing remains of this complex and beyond metre 43 it has not been excavated at this time (Figure 4).

To stay as consistent with the previous stratigraphic naming convention as possible it was decided that a trailing dash would be added to the previously given names, followed by letters relating to particular features of each new layer (see PIRSON, 2007). The new stratigraphy is presented below, from bottom to top (Figure 3 and Figures 5-7).

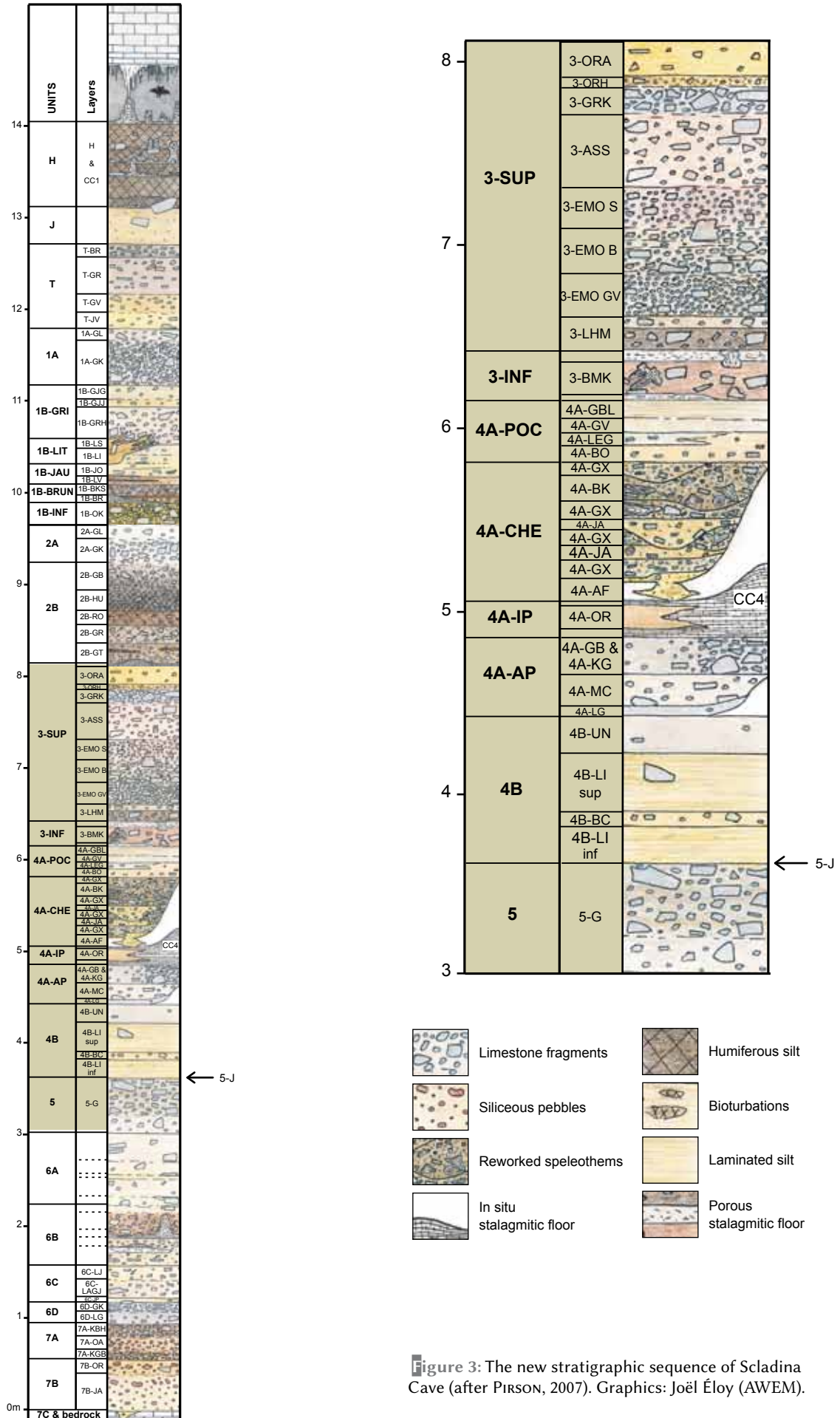
3.2.1. Unit 5

Layer 5-G is a silt that is rather rich in limestone fragments and contains a few small silicoclastic river pebbles. Much of the coarse components exhibit a strong preferential orientation, from planar to linear (*sensu* BERTRAN (dir.), 2004). The matrix is either grey-brown, light brown, or grey-beige with frequent iron staining (rust-coloured spots and planes). The structure is generally finely granular. At the bottom of the layer a thin (1 mm) platy structure has been locally observed. Several lithologies superimpose each other (5-GJAC, 5-GBG, 5-GRO, 5-GBLA, 5-GKBR), which are defined by variations in colour and concentration of limestone pebbles; however, their lateral extensions have not yet been ascertained. These lithologies might reflect different layers, but this has not yet been demonstrated. The bottom of

or reworked calcitic cementation of the matrix; besides, some of these calcitic crusts are lateral equivalent (see PIRSON, 2007).



LITHOSTRATIGRAPHY






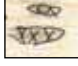

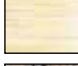


-  Limestone fragments
-  Humiferous silt
-  Siliceous pebbles
-  Bioturbations
-  Reworked speleothems
-  Laminated silt
-  In situ stalagmitic floor
-  Porous stalagmitic floor

Figure 3: The new stratigraphic sequence of Scladina Cave (after PIRSON, 2007). Graphics: Joël Éloy (AWEM).

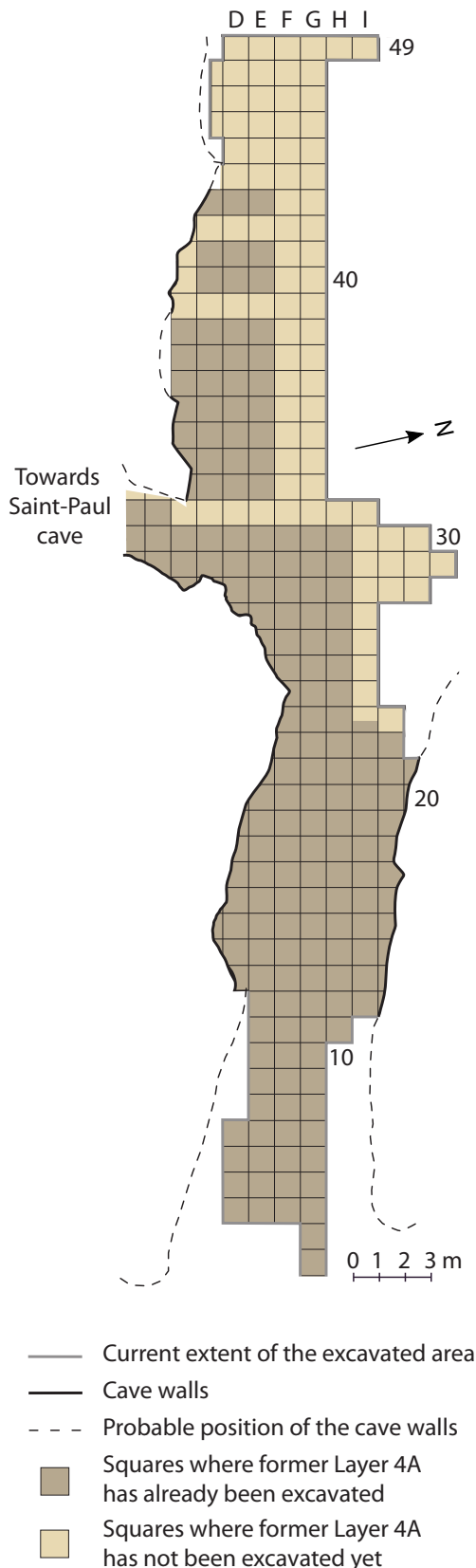


Figure 4: Map of the cave showing the extent of the area where Sedimentary Complex 4 has been excavated (modified after PIRSON et al., 2005). Graphics: Joël Éloy (AWEM).

Unit 5 has eroded the top of Unit 6A, creating small gullies in the process.

Above 5-G, **Layer 5-J** has been observed at some locations. It consists of a more heterogeneous silt that is grey-yellow in colour and includes numerous orange, grey, or beige aggregates (mud balls). When compared with 5-G, Layer 5-J contains fewer limestone fragments that do not have a clear preferential orientation. The clast-matrix relationship is matrix-supported (see TUCKER, 1991 and BERTRAN (dir.), 2004). The sediment is massive and has a rather coarse granular structure. The top of 5-J is locally hardened by calcite; the layer also locally develops into a gully.

Layer VB of the terrace (HAESAERTS, 1992) might correspond to a third layer of this unit.

Unit 5 contains the older of the 2 most important Middle Palaeolithic assemblages found in Scladina (Chapter 2).

3.2.2. Unit 4B

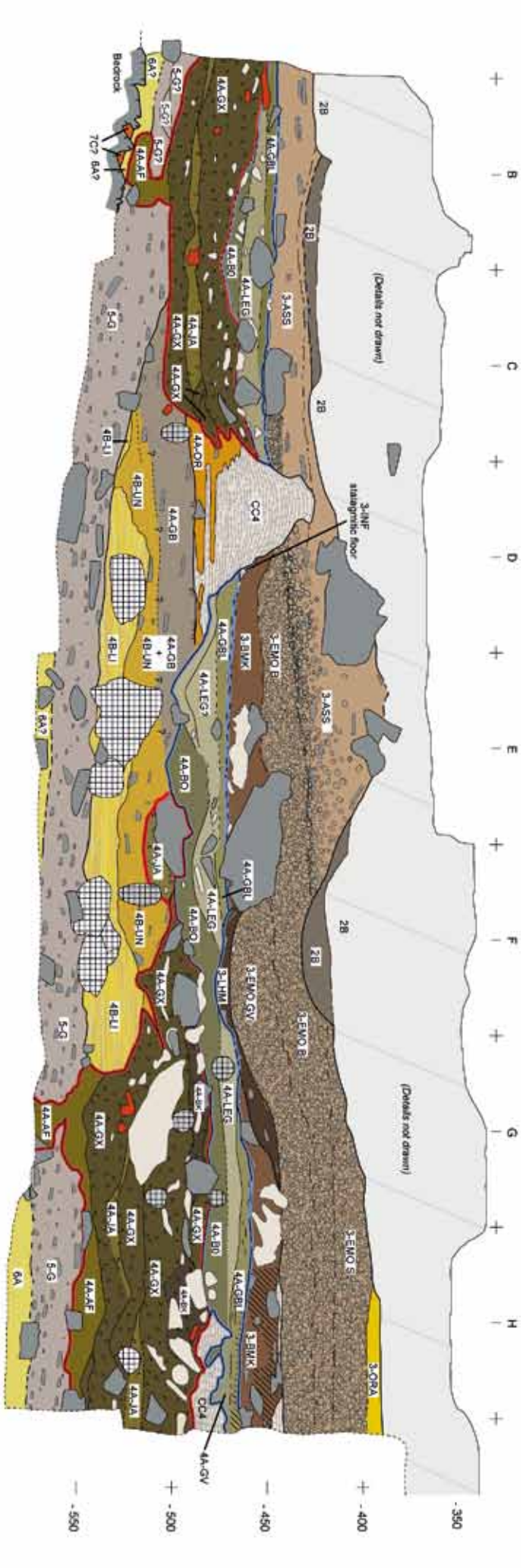
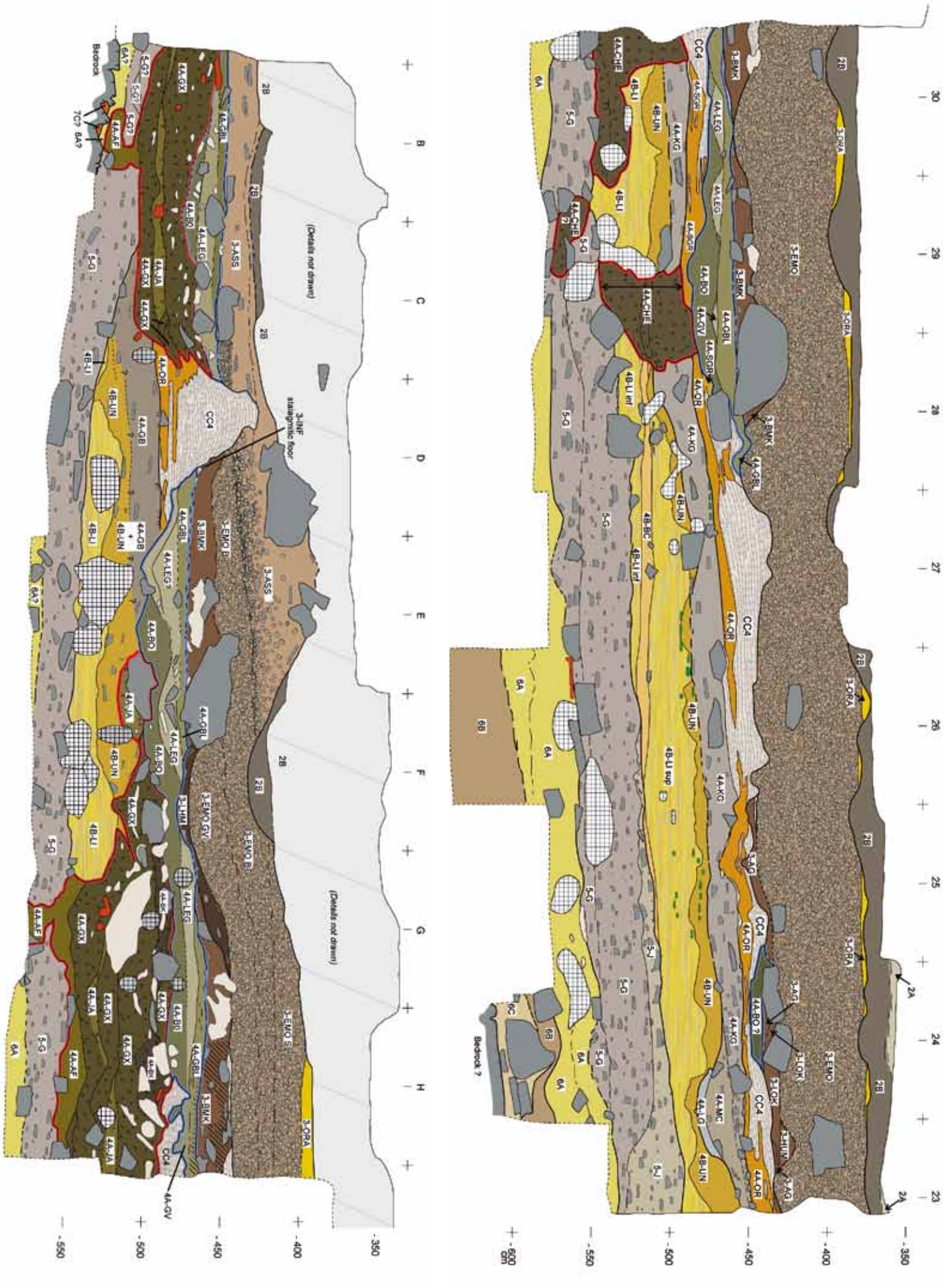
Layer 4B-LI is a finely laminated silt with almost no coarse elements. It is composed of alternating doublets ranging from less than a millimetre up to several millimetres thick. Each doublet is composed of a yellowish silty bed at the base and a darker clayey bed at the top. Although the internal stratification is mostly horizontal, the lower and upper limits of Layer 4B-LI dip towards the back of the cave. Massive and thicker (centimetric) laminae can regularly be observed, as well as small (centimetric) erosive phases that locally interrupt the horizontal bedding. Cross bedding can also be seen. The laminations are sometimes less obvious, particularly at the top of the unit. There are very few decimetric limestone fragments; underneath them the laminations are deformed. Some in situ calcareous concretions (1–5 cm) similar to loess dolls are present locally. From the top of the layer, evenly spaced (~30 cm) vertical narrow cracks developed downwards.

Frequently, the laminated Layer 4B-LI is interrupted by a decimetric, non-laminated, beige, silty facies that either contains a few scattered limestone fragments (**layers 4B-BC and 4B-IL**²) or none (**Layer 4B-LR**³). Area C-D 40-43 contains a rather loose silt with numerous large limestone slabs ranging in size from several decimetres to over a metre; the dominant type of clast-matrix relationship is clast-supported (**Layer 4B-KK**). The

² Facies “4B-LI b” of PIRSON et al., 2005.

³ Facies “4B-LI j” of PIRSON et al., 2005.





presence of these non-laminated layers interbedded in 4B-LI allows for the identification of 3 generations of 4B-LI (upper, middle, and lower). The large blocks from Layer 4B-KK sometimes deform the stratification of the lower generation of 4B-LI, whereas the upper generation fills the porosity between the limestone fragments at the top of 4B-KK.

Layer 4B-UN was the last layer of Unit 4B that was deposited. It is comprised of a rather homogeneous, greyish-beige clayey silt and contains few limestone fragments. The matrix is rich in aggregates (sand-sized and coarser) made of grey and compact clayey silt. Calcareous concretions similar to those from 4B-LI have been locally identified as well as some overall cementing of the matrix. A well-developed platy structure, 4–6 mm thick, is visible throughout this layer and the

overlying units 4A-AP and 4A-IP. The lower limit of Layer 4B-UN often appears sharp and erosive on underlying Layer 4B-LI. However, in some places the contact is diffuse and the fine lamination gradually disappears. **Layer 4B-UF** is a beige clayey silt with a few grey mud balls and rare limestone fragments. This layer is the likely lateral equivalent of 4B-UN beyond metre 30 (Figures 6 & 7), where it lies under 4A-GB.

3.2.3. Sedimentary Complex 4A: units 4A-AP, 4A-IP, 4A-CHE, and 4A-POC

The former Layer 4A, from which the Neandertal remains were unearthed, has been divided into 4 units, each comprised of several layers. The relationships between these 4 units are presented in Figure 8.

Unit 4A-AP, which is comprised of layers deposited before the formation of Stalagmitic Floor CC4, starts with **layers 4A-LG** and **4A-MC**. These are only visible in a small gully crosscutting Layer 4B-UN (Figure 5). The sediment is a grey to grey-beige clayey silt, either with a few limestone fragments (Layer 4A-MC) or without (Layer 4A-LG). Mud balls have also been observed. These deposits are affected by a well-developed platy structure (4–6 mm) that developed downwards through Layer 4B-UN and upwards up to Unit 4A-IP. **Layer 4A-KG** superimposes either

Figure 5 (facing page, above): Section H/I (after PIRSON, 2007). Limestone blocks under 10 cm were not drawn in the field; when they are shown (for units 5 to 3-SUP), it is with a textural pattern. Symbols as in Figure 7. Graphics: Joël Éloy (AWEM).

Figure 6 (facing page, below): Section 30/31 (after PIRSON, 2007). Limestone blocks under 10 cm were not drawn in the field; when they are shown (for units 5 to 3-SUP), it is with a textural pattern. Symbols as in Figure 7. Graphics: Joël Éloy (AWEM).

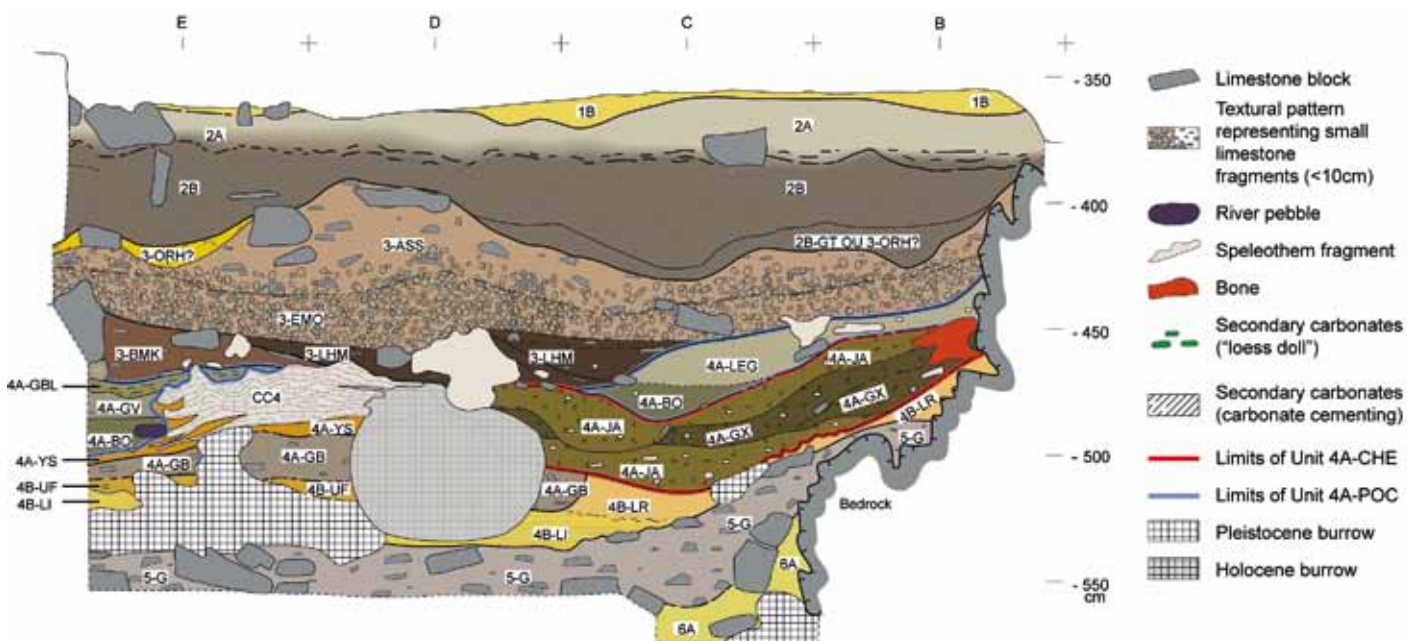
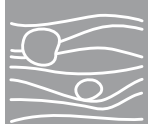


Figure 7: Section 32/31 (after PIRSON, 2007). Limestone blocks under 10 cm were not drawn in the field; when they are shown (for units 5 to 3-SUP), it is with a textural pattern (see graphic symbols). Graphics: Joël Éloy (AWEM).



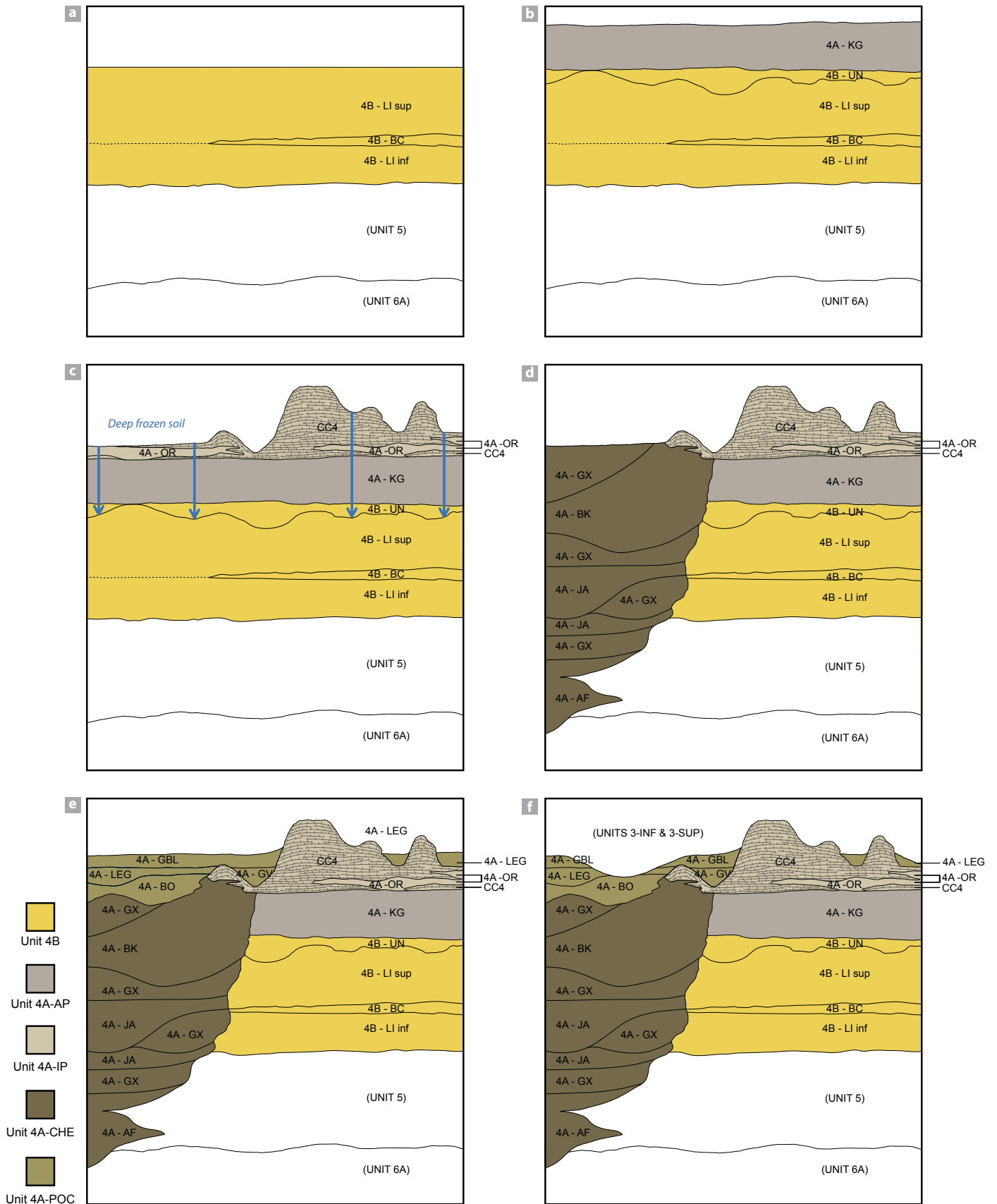


Figure 8: Diagrams presenting the stratigraphic relationships between the 5 distinct units of Sedimentary Complex 4. The 6 stages illustrate the succession of sedimentary and pedological events. a) deposition of Unit 4B over Unit 5; b) deposition of Unit 4A-AP; c) deposition of Unit 4A-IP, including the formation of Speleothem CC4; at the end of this stage, development of a deep frozen soil from the top of CC4; d) deposition of Unit 4A-CHE, eroding the underlying units; e) deposition of Unit 4A-POC; f) deposition of units 3-INF and 3-SUP on top of the Complex 4. Graphics: Joël Éloy (AWEM).

Layer 4B-UN or the small gully mentioned above. It consists of grey-beige silt, is more or less clayey, and is rich in limestone blocks ranging from 1 to 10 cm, sometimes up to several decimetres. Locally, at the top of the layer, the amount of coarser elements decreases. The proportion of coarse components also diminishes towards the back of the cave. Throughout the layer the coarse fragments do not exhibit any noticeable preferential orientation. The type of clast-matrix relationship is generally clast-supported, but matrix-supported relationships are not rare. The matrix contains numerous grey centimetric mud balls embedded in a more beige coloured sediment. Beyond metre 30, the likely equivalent of 4A-KG is **Layer 4A-GB**; the matrix is close to that of 4A-KG but with fewer limestone fragments. These 2 layers exhibit a platy structure, particularly well developed (4–6 mm) in 4A-GB.

Unit 4A-IP is comprised of CC4, an important stalagmitic floor, and the layers that were deposited during its formation. The thickness of the floor varies between a maximum of several decimetres thick at some locations and a minimum of only a calcitic lens less than 1 cm thick at others; also, it is occasionally completely absent. In some places this speleothem can be divided into three distinct generations. The sediment that was deposited between the generations of calcite is a massive silt, almost deprived of coarse elements. Locally, some small fragments of limestone, calcite, and stalactites have been observed within the silty matrix. The sediment that is interbedded in the speleothem is locally cemented by calcite. Three interbedded layers have been identified in different areas of the site, mainly on the basis of the colour of the matrix. **Layer 4A-OR** is a beige-orange homogeneous silt. **Layer 4A-SGR** is a silt with very few small limestone fragments. The matrix is either homogeneous (grey or orange) or heterogeneous (grey or orange lenses). It contains numerous sand-size aggregates as well as grey mud balls. **Layer 4A-YS** is a beige-yellow silt with no coarse fragments. Layers 4A-OR, 4A-SGR, and 4A-YS are affected by a thick platy structure (2–5 mm) that is often very well developed. The thick platy structure is present particularly where the overlying Stalagmitic Floor CC4 is absent or thin. Sometimes, a rather diffuse vertical component is superposed onto it (sub-angular blocky structure). The platy structure developed downwards to the base of Layer 4B-UN.

Unit 4A-CHE is the result of an important erosional phase that reworked both Stalagmitic

Floor CC4 and underlying deposits. It consists of a succession of cut-and-filled layers that developed within a large 2 m wide 0.5–1 m deep gully structure. Two distinct gullies have been identified locally. All in all, 4 main lithologies have been observed; they are facies rather than layers, for these lithologies alternate in a diverse order, or are present in different areas without any means of controlling their possible contemporaneity. The limits between these facies are generally quite sharp. Most coarse components do not exhibit any preferential orientation, except for some that are locally planar. Platy structures are absent throughout the whole unit.

– At the bottom of the unit, **Facies 4A-AF** consists of beige heterogeneous silt with no limestone fragments, but with many mud balls and tilted decimetric blocks of a laminated yellowish sediment which is similar to that from 4B-LI. This deposit filled small gullies with irregular walls that were caused by the erosion of underlying layers (units 5 and 6A) by undercutting them locally (scouring). The matrix exhibits a structure which is either massive or finely granular.

– **Facies 4A-GX**, which is particularly heterogeneous, consists of a mix between beige silt (same type as that of 4A-JA) and mud balls of various sizes (from 1 mm to several cm) that are composed of compact greyish clayey silt. These mud balls are sometimes so numerous the overall colour of the facies is grey and the sediment is very compact. Limestone blocks and speleothem fragments (from millimetric pieces to stalagmites several decimetres long) mostly represent the generally abundant coarse fraction. Most coarse components do not exhibit any preferential orientation. The sediment is massive, either clast- or matrix-supported, and the structure is granular, often quite coarse.

– **Facies 4A-JA** is a yellowish beige silt, sometimes slightly orange, with a few aggregates of grey compact clayey silt that are 1 mm to several cm in diameter. When the aggregates are more abundant, the facies is more similar to that of 4A-GX. The coarse elements are of the same nature as those from 4A-GX, although notably less numerous and smaller. The structure is massive or finely granular.

– **Facies 4A-BK** is a brown heterogeneous silt with many large speleothem fragments and a few limestone blocks. The sediment is massive, and either clast- or matrix-supported.



It contains sand-size aggregates and mud balls. The structure is granular.

Last unit of Complex 4A, **Unit 4A-POC**, is comprised of several layers that were deposited after the gully developed. These layers cover the deposits of both units 4A-IP and 4A-CHE. **Layer 4A-BO** is a rather heterogeneous beige-orange silt, often with numerous sand-size aggregates and mud balls, that changes into an orange silt interbedded with lenses of greyish or grey-beige silt (**Layer 4A-LEG**) towards the top. The structure of these two layers is mainly granular. The coarse elements (limestone blocks, speleothem fragments, and a few small silicoclastic river pebbles) are small (millimetric to centimetric), and sometimes quite numerous. **Layer 4A-GV** is a rather homogeneous greenish-grey clayey silt that developed into small gullies that are cutting 4A-BO; locally, the bottom of 4A-GV is pink-beige. Finally, **Layer 4A-GBL** is an often broadly stratified grey-beige silt with a few millimetric to centimetric coarse fragments (limestone blocks or calcite). The top of the layer is locally concretionary.

3.2.4 Unit 3-INF

This unit is very localised. Several layers have been identified (**3-BMK**, **3-HUM**, **3-CGO**, **3-AG**, **3-LOK**), but as of now the stratigraphic relationships have not been completely established. There is evidence of carbonate precipitation, both as calcite cementing (within 3-INF and at the top of Unit 4A-POC) and as thin stalagmitic floors at the top and bottom of the unit. These speleothems are highly porous and rather brittle. Blocks that are several decimetres in diameter are particularly frequent in this unit, as well as at the top of underlying Unit 4A-POC. Speleothem fragments, often quite large, have been observed, as well as a few small silicoclastic river pebbles. Layers 3-BMK and 3-HUM are the best represented; they both consist of heterogeneous silt that is middle to dark brown, rather loose, with numerous limestone fragments. The type of clast-matrix relationship is clast-supported. Numerous sand-size aggregates are present, as well as mud balls. The structure is granular.

3.2.5 Unit 3-SUP

Layer 3-LHM, which is observable only at a few places, exhibits important lateral variations. It is composed of a heterogeneous silt that is quite

loose at some locations, and can be a variety of colours: orange-beige, beige, grey, grey-beige, or brown. The concentration of coarse elements (limestone blocks and speleothem fragments) is highly variable. The sediment is massive and the type of clast-matrix relationship is either clast- or matrix-supported. Some facies are rich in sub-millimetric aggregates. The sediment from Layer 3-LHM eroded those of the underlying Unit 3-INF. Layer 3-LHM may in fact be several layers, but the current state of excavation does not make any verification possible.

Layer 3-EMO is a very stony deposit composed of very blunt, rounded, and rather well calibrated small limestone elements (1-4 cm), with some sparse blocks that are several decimetres large. The matrix is a rather clayey grey-beige silt composed almost exclusively of well-rounded sand-size aggregates. Under the large blocks, the sediment has an openwork structure; elsewhere, the voids between the clastic limestone elements are partially or totally filled with sand-size aggregates and the sediment exhibits a clast-supported structure. Three facies of 3-EMO are superimposed on sections H/I 23-30 and 30/31 F-H (3-EMO GV, 3-EMO B, and 3-EMO S⁴). The top of Layer 3-EMO is lighter in colour and regularly exhibits very strong iron and manganese staining. Locally, it is cemented by calcite.

From metre 30 towards the back of the cave, the proportion of limestone fragments within Layer 3-EMO lessens progressively upwards, and the gradual change into Layer 3-ASS can be observed. The transition to 3-ASS also happens towards the back of the cave between metres 32-34; there are no more traces of 3-EMO beyond that limit. **Layer 3-ASS** consists of a greyish beige clayey silt with characteristic pinkish shades. The limestone fragments are sometimes abundant, sometimes rather rare; some silicoclastic pebbles (up to 10 cm), as well as speleothem fragments, are also visible. There are traces of some diffuse internal stratification. A platy structure is visible throughout the layer; while rather coarse and noticeable at the top (3-4 mm), deeper it is less visible but sometimes very thick (3-10 mm). Manganese and iron spots as well as iron planes are visible. Similar to its lateral equivalent (3-EMO), the top of the layer is often lighter in colour. On the other hand, the bottom is darker, mouse grey, grey-pink, grey-brown, or red-brown, with a very diffuse boundary. Beyond metre 38, in the lower

⁴ = 3-EMO α , β and γ of Pirson, 2007

part of Layer 3-ASS there are many small weathered orange bone splinters almost always lying parallel to the stratification plane.

Unit 3-SUP contains other layers above 3-ASS and 3-EMO (Figure 3); their description is beyond the scope of this presentation.

Sedimentary Complex 4A is often directly superimposed by different layers, either those belonging to Unit 3-INF or Unit 3-SUP, depending on the location in the cave (Figures 5-7).

3.3. Correlations between the different stratigraphic records

Table 1 illustrates the correlation between the former stratigraphic interpretations and the current one. Depending on the area in the cave, former Layer 4A corresponds to 1 or several layers from units 4A-AP, 4A-IP, 4A-CHE, and 4A-POC. The comparison between the records that were taken of sections H/I (23-30) and 30/31 (B-H) before the stratigraphic reappraisal (Figure 9) and after it (Figures 5 & 6) helps to better understand the origin of the differences between the 2 systems.

Former Layer 4A was classically defined in the first 20 m inside the cave as a stony silt (GULLENTOPS & DEBLAERE, 1992; BONJEAN, 1998^a) situated above the silty Layer 4B, which is deprived

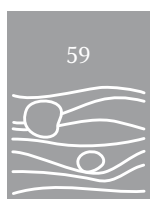
of any stone, and below the Stalagmitic Floor CC4. This, combined with the analysis of figures 5 and 9a, leads to the suggestion of the equivalence (at least partially) of former Layer 4A and Unit 4A-AP (mostly Layer 4A-KG).

Laterally, the transition to Unit 4A-CHE has not been understood. The huge gully has not been identified, even if cut-and-filled small channels were locally recognized (BONJEAN et al., 1997). The sediment from the 4A-CHE gully, rich in coarse components like 4A-KG and situated at similar depth, has been attributed to former Layer 4A (compare Figure 9b with Figure 6). The recent reappraisal of transverse cross-sections 30/31 and 32/31 (Figures 6 & 7) highlighted the important erosive boundary of the 4A-CHE gully, and showed that the coarse elements from units 4B, 4A-AP, and 4A-IP are deprived of any reworked speleothem fragments, while these are very frequent in units 4A-CHE and 4A-POC (Figures 5-7 and Figure 10).

The definition of Unit 4A-POC is linked to the problem of Stalagmitic Floor CC14 (PIRSON, 2007). This speleothem was found above a generation of former Layer 4A and below a second generation of former Layer 4A (BONJEAN, 1998^a; Figure 9a). In the system used at the time (Figure 2), former Layer 4A was older than Speleothem CC4.

TERRACE		CAVE			
Otte et al., 1983	Haesaerts, 1992	Otte et al., 1983	Gullentops & Deblaere, 1992	Bonjean, 1998a	Pirson, 2007
			DG-16 = 36 / CC1	36 / CC1	<i>H</i>
	II (top)		DG-15 = 37	37	<i>J</i>
II	II		DG-14 = 38	38	<i>T</i>
			DG-13 = 39	39	
			DG-12 = 40	40	transition <i>1A-T ?</i>
IA	IA	1A	DG-11 = 1A	1A	<i>1A</i>
IB	IB				
I	I	1B	DG-10 = 1B	1B	<i>1B-GRI</i> <i>1B-LIT</i> <i>1B-JAU</i> <i>1B-BRUN</i> <i>1B-INF</i>
		2A	DG-9 = 2A	2A	<i>2A</i>
III	III	2B	DG-8B = 2B	2B	<i>2B</i>
IV	IV		DG-8A = 2B1		<i>3-SUP (3-ORA)</i>
VA	VA	3	DG-7 = 3	3	<i>3-SUP</i>
					<i>3-INF (3-HUM)</i>
	V ocre	4 (top)	DG-6A / DG-6B (=CC4) / DG-6C	CC4	<i>4A-POC</i>
V		4	DG-5B = 4A	4A CC14	<i>4A-CHE</i> <i>4A-IP</i> <i>4A-AP</i>
	V gris		DG-5A = 4B	4A	<i>4B</i>
VB	VB	5	DG-4 = 5	4B	<i>5</i>
VI A	VI a			5	<i>6A</i>
VI B	VI b	6	DG-3 = 6	6	<i>6B</i> <i>6C</i> <i>6D</i>
VII	VII	7A	DG-2 = 7A	7A	<i>7A</i>
		7B	DG-1 = 7B	7B	<i>7B</i>

Table 1: Attempt at correlating the former stratigraphic systems and the new one (bold italic = units; roman = layers). Light brown background: part of the Scladina stratigraphic sequence concerned by this study.



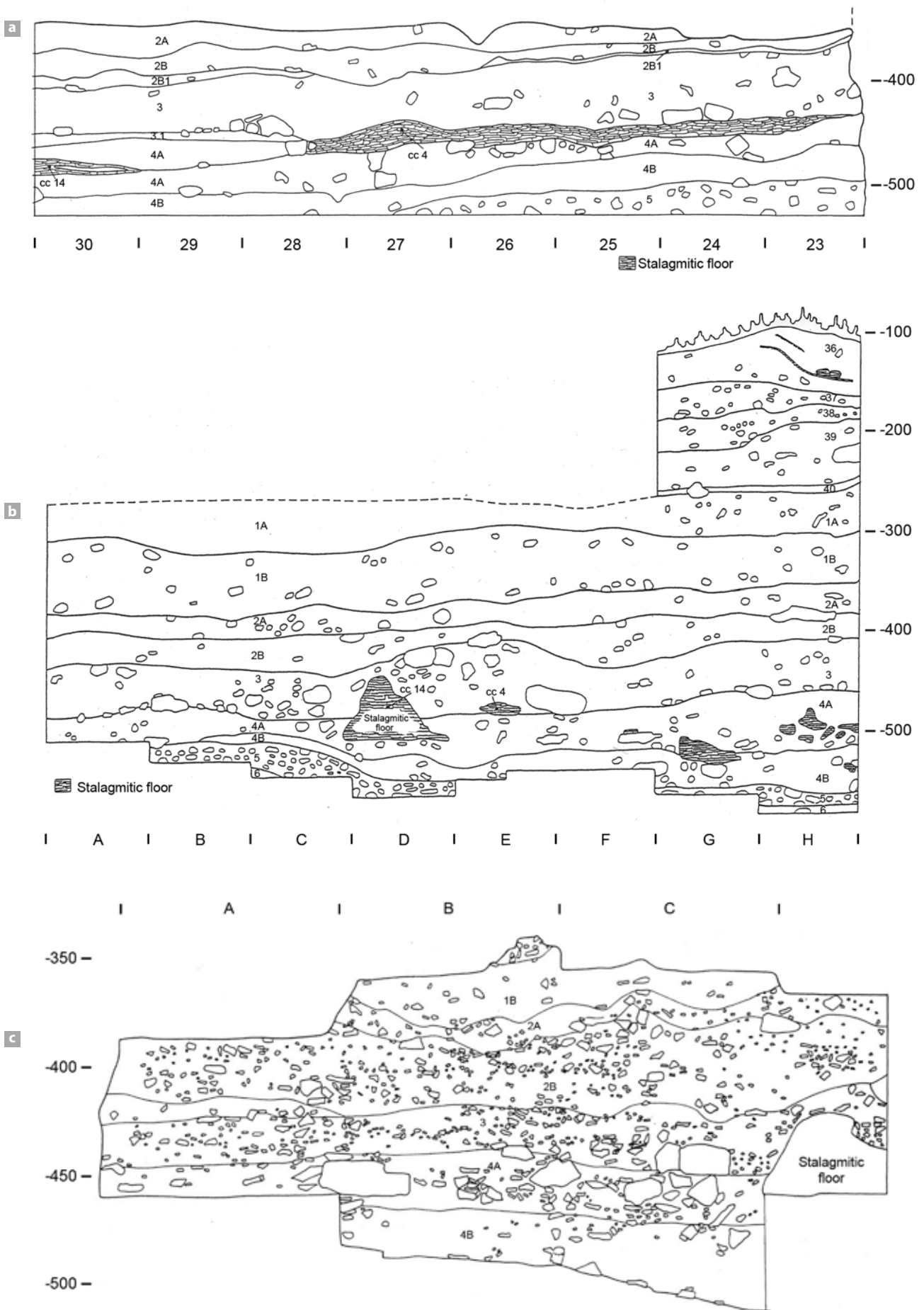


Figure 9: Previous stratigraphic records of profiles H/I (a) and 30/31 (b-c).
 a and b: after BONJEAN (1998^a); c: after BENABDELHADI (1998).

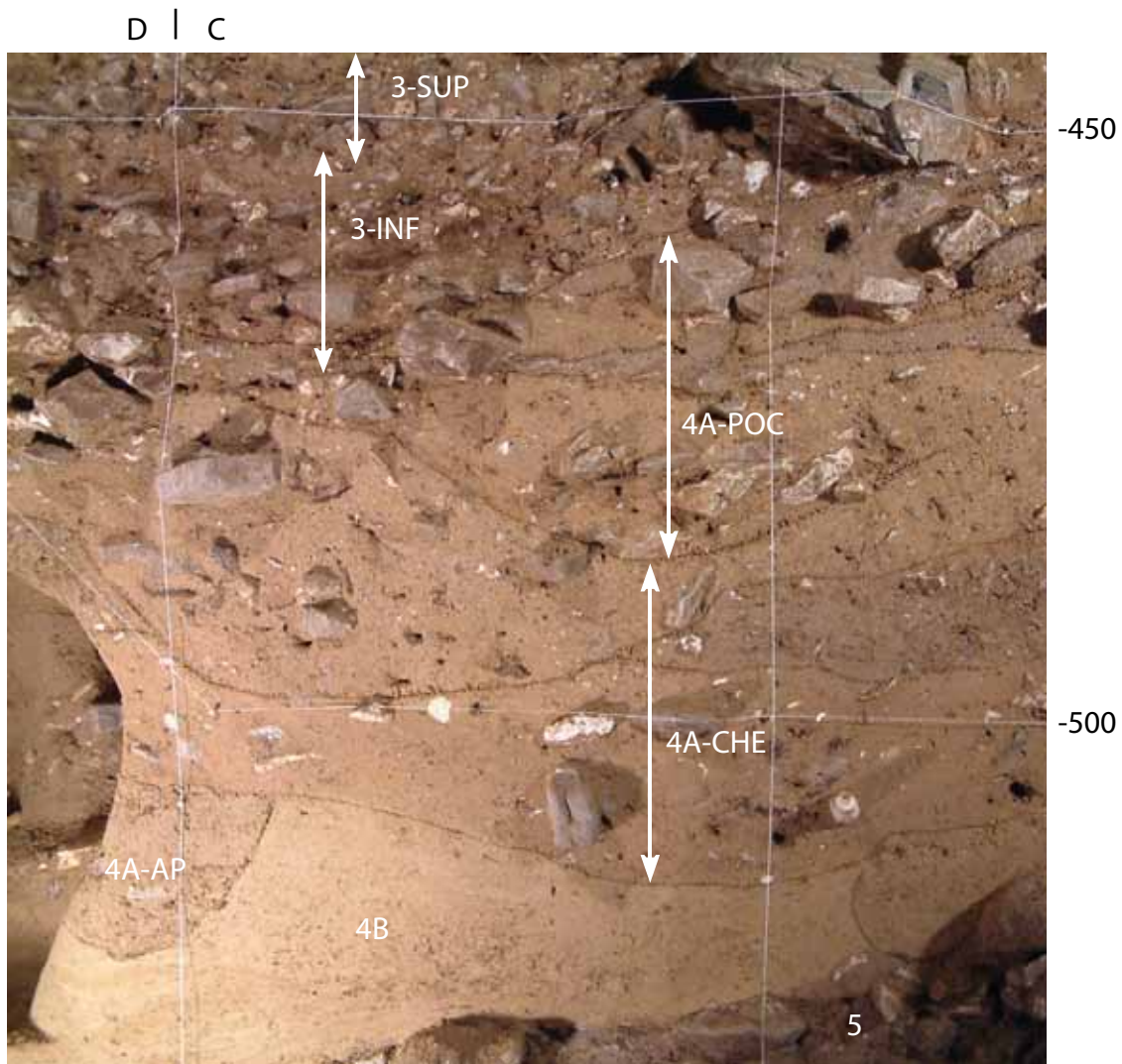


Figure 10: Picture of Section 32/31 showing the reworked speleothem fragments, signature of units 4A-CHE and 4A-POC. The labels are referring to units, not layers (photograph Dominique Bonjean, AA).

Therefore, this new speleothem covered by former Layer 4A had to be older than CC4 and had to lie inside former Layer 4A. According to the re-examination of data collected in the field, from the literature, and from documents relating to the previous excavations, nothing corroborates the existence of this Speleothem CC14. On the contrary, everything indicates that CC14 is nothing more than a lateral equivalent of CC4; the overlying sediment of former Layer 4A corresponds to Unit 4A-POC, which covers both CC4 and Unit 4A-CHE (Figures 3 & 5). It is worth mentioning here that the dates obtained from these 2 speleothems are very close (see summary in BONJEAN, 1998^b). This re-evaluation had major implications for the stratigraphic position of the Neandertal remains (see Chapter 5).

In some areas (beyond metre 34), the silty upper part of former Layer 4A (now called Unit 4A-POC)

was attributed in the previous stratigraphic system to the bottom part of former Layer 3, and more specifically to Layer 3-ASS. Again, this has implications for the positioning of the Neandertal child in the sequence, as 3 teeth that were apparently found in former Layer 3 probably came from 4A-POC (see PIRSON et al., 2005; see also Chapter 5).

History of the filling: sedimentary and 4. diagenetic processes

The sediment found in the Scladina sequence mainly consists of limestone blocks that have detached from the cave porch and walls and become embedded in loessic silt. A few allochthonous silicoclastic river pebbles and a



low percentage of sand, both resulting from the reworking of a terrace of the Meuse River that is preserved on the plateau above Scladina, complement the aforementioned two other dominant components. Slope processes govern the sedimentary dynamics. Blocks from the limestone hillside and sediment from the plateau accumulated together with aeolian deposits below the cave porch, forming a detritic cone from where they were later redistributed towards the inside of the cave (“*éboulis assistés*” *sensu* BERTRAN et al., 2004). Numerous sedimentary processes have been identified (PIRSON, 2007), including: debris flow, run-off, rock fall, solifluction, settling, torrential flow, and speleothem formation. Several post-depositional processes have also been recognised, such as: deep frost, cryoturbation, pedogenesis (on the cave terrace), formation of secondary phosphates, desiccation cracks, cementation of sediments by secondary carbonates, bioturbation, etc. Only the processes identified in units 5 to 3-SUP will be reviewed here, due to their pertinence for understanding the sedimentary context of the Neandertal child.

4.1. Unit 5

Layer 5-G may have been deposited by solifluction, as suggested by the overall planar to linear fabric of the limestone clasts (BERTRAN et al., 1997; BERTRAN & COUTARD, 2004). Also, the underlying deposits have been affected by deep frost, as attested by a thick platy structure visible throughout Unit 6A. It seems probable that Layer 5-G, with its iron staining, granular structure, and locally finely laminated structure corresponds to the upper part of this cryosol (active layer; see VAN VLIET-LANOË, 1988). This is compatible with the development of solifluction in 5-G.

In some sections, Layer 5-J has been observed superimposing 5-G. Its erosive lower boundary (gully) and matrix-supported sediment suggest that the main sedimentary process involved was a debris flow.

4.2. Unit 4B

The doublets observed in Layer 4B-LI (§ 3.2.2) exhibit a fining-upward pattern: the light-coloured lamina corresponds to the fast deposition of coarse particles (silt) and the overlying dark-coloured lamina to finer clayey particles. This normal graded bedding and the horizontality of the

laminations are two arguments that are consistent with a decantation deposit. Each doublet corresponds to a distinct input of sediments in a pool. The small erosive features and the unstratified massive centimetric lamina are indicative of more dynamic and turbulent phases of sediment input. The deformed laminations under some blocks are attributed to the collapse of these blocks from the cave ceiling into water-filled sediment. Periods of drying are evidenced by vertical cracks (shrinkage cracks). The massive deposits that have a granular structure interrupt 4B-LI and sometimes contain limestone blocks (i.e., layers 4B-BC, 4B-LR and 4B-IL) are probably linked to a decrease of the water depth, the development of rill wash periods, and the resulting transportation of the small limestone fragments. A rock fall episode took place during the decantation period (Layer 4B-KK), as indicated by 2 events: first, the deformation of the stratification by collapsing blocks and second, the covering of the resulting rockslide by new decantation deposits.

The combined observations for this part of Unit 4B allow for the reconstitution of a lateral sedimentary sequence with distinct areas:

- The source area of the sediments (erosion area) corresponds to the sedimentary cone located under the cave porch.
- The transport area corresponds to the first metres of the cave where the silty sediments have been redistributed by run-off. These sediments frequently exhibit diffuse laminations parallel to the slope and laterally change into massive facies (4B-IL); some horizontal laminations are also visible (4B-LI). These elements indicate that in this area the sedimentation took place through alternating periods of run-off and decantation. Some gullies have also been identified in the same area, on top of Unit 4B. Unfortunately, their stratigraphic positioning is delicate because the concerned cross-sections are disconnected from the rest of the site. These gullies might be the first evidence of the important gully 4A-CHE at the cave entrance, or, on the contrary, secondary small gullies related to Unit 4B, which would have transported some of the sediment from the sedimentary cone of the source area to the settling area.
- The third identified area corresponds to the settling area (distal area), where the dominant facies is 4B-LI. The decantation took place in a large closed basin, which evoked the formation of a small lake or a pool.

The deposition of Layer 4B-UN and its lateral equivalent 4B-UF lead to the erosion of the top of 4B-LI. Run-off is probably the process responsible for the deposition of these sediments, but the important period of deep frost that later affected these sediments (cf. infra) has eradicated any characteristic sedimentary structures. Similar cases of eradication of sedimentary structures by frost action have been described in different environments (e.g. VAN VLIET-LANOË, 1987; LENOBLE, 2005).

4.3. Sedimentary Complex 4A: units 4A-AP, 4A-IP, 4A-CHE, and 4A-POC

Layers 4A-LG and 4A-MC, which have developed in a small gully structure, may be the result of debris flow or hyperconcentrated flow (rill wash). The characteristics of the sediment from Layer 4A-KG also point to deposition by either a debris flow or rill wash. Near the back of the cave 4A-KG changes into 4A-GB, which indicates a diminution of the flow energy and suggests run-off.

An important stabilisation period took place after the deposition of Layer 4A-KG, causing the development of the Stalagmitic Floor CC4 in several phases. The interbedded detritic material observed in some places (layers 4A-OR, 4A-SGR, and 4A-YS) was probably deposited through run-off; as for 4B-UN, any characteristic sedimentary structures have been destroyed by the period of deep frost that later affected these layers (cf. infra).

The formation of Unit 4A-IP was followed by a period of deep frost that affected the sediment, as demonstrated by the thick platy structure identified in the sediments of units 4A-IP and 4A-AP, as well as in Layer 4B-UN, and down to the interface with Layer 4B-LI. In a loessic context, such a thick platy structure is associated with the continuing development of segregation ice lenses in the upper part of a permafrost throughout several seasons (HAESAERTS & VAN VLIET-LANOË, 1981; HAESAERTS, 1983; VAN VLIET-LANOË, 1988).

The development of this cryosol was followed by an extensive period of erosion that formed a large gully (Unit 4A-CHE), which locally reworked Stalagmitic Floor CC4 as well as the underlying layers from Unit 4A-IP down to Unit 5, sometimes even down to Unit 6A. Fragments of CC4 and underlying sediments have been incorporated into the gully. The different lithofacies present in

this complicated unit (§ 3.2.3) reflect important changes in the sedimentary dynamics:

- The facies that is rich in poorly sorted coarse components from 1 to several decimetres in diameter (limestone blocks, speleothem fragments, and mud balls) deprived of any preferential orientation and exhibiting a massive matrix either with matrix- or clast-supported structure (4A-BK and partly 4A-GX) is evocative of a flow with high sediment concentration, similar to a debris flow. The larger components are broken speleothems (up to 50 cm), which have probably not been transported over long distances; they are mostly found near in situ Stalagmitic Floor CC4 where it is broken. They have probably collapsed and been incorporated from the banks of the gully.

- The facies that contains less coarse components (or in which the coarse elements are smaller) exhibits a matrix-supported structure, and often contains numerous mud balls. It might be indicative of a rather strong rill wash (4A-GX *pro parte*). The massive aspect of the matrix is due to the presence of mud balls. In these facies the mud balls, the speleothem fragments, and the limestone blocks all measure about 1 cm. These well-sorted coarse elements are more support for the hypothesis of a rill wash (LENOBLE, 2005).

- The facies comprised of more homogeneous silt, either with less or no coarse components at all, would correspond to a lower energy run-off (4A-JA).

- A particular facies of heterogeneous silt (4A-AF) is found at the bottom of Unit 4A-CHE. It is deprived of coarse components and has developed inside a small gully that undercuts the anterior deposits. It may reveal a period of hyperconcentrated run-off reworking the sediment from Unit 4B, which occurred shortly after the debris flow episode that formed the gully.

4A-CHE may be interpreted as the result of the degradation of a deep frozen soil ('melting gully'). Some specific structures seem difficult to explain without this interpretation. The undercutting observed at the base of the gully in Unit 4A-CHE (facies 4A-AF), eroding Layer 5-G at the bottom of Section 30/31 in G (Figure 6), notably suggests the local thawing of frozen sediment. The presence of a well-documented deep frozen soil immediately preceding Unit 4A-CHE (see above) strengthens this hypothesis.



Because of the lack of cross-sections for several areas in the cave, the exact course of the large gully structure in Unit 4A-CHE could not be reconstructed in detail. Its general direction seems to coincide with the longitudinal axis of the cave, at least from metre 25 through metre 43 (see Chapter 5). A small relict section, which is in contact with the cave wall near the porch (Section D13/12), reveals an important erosive structure affecting the deposits of Unit 4B. This structure could correspond either to the gully or to the supply area associated with the decantation phase of Layer 4B-LI (cf. § 4.2). In the former case, this would mean that the gully would originate from the current cave entrance. Unfortunately, previous fieldwork did not provide any evidence of the entrance as the source since the 4A-CHE gully has only been identified during the new research conducted since 2003, after that part of the cave was already excavated. The only transverse section studied in that area before 2003 is Section 16/17 D-F (GULLENTOPS & DEBLAERE, 1992), but its authors did not record the presence of the gully since the base of that section only reached the top of Sedimentary Complex 4. BENABDELHADI (1998) studied transverse Section 30/31 where the gully would later be identified. He describes Layer 4A as a monolithic entity, homogeneous, subhorizontal, and without any internal stratification, all of which is contradicted by recent observations (PIRSON et al., 2005; PIRSON, 2007; Figure 6). Therefore, it seems probable that the gully structure in Unit 4A-CHE was excavated in the first 20 m of the cave without having been recognised as such.

After the constitution of 4A-CHE, Unit 4A-POC developed through a phase dominated by run-off. The silty deposits from 4A-POC indistinctly cover the deposits of units 4A-CHE and 4A-IP, including Speleothem CC4 (Figure 5). Some lenses and some stony deposits suggest concentrated run-off and/or debris flow, but the limited extent of these observations suggests that one must be cautious during the interpretation of these structures.

4.4. Unit 3-INF

A short period of stabilisation followed the deposition of Sedimentary Complex 4A; it is represented by the formation of a small speleothem and the concretioning of the top of 4A-POC. Unit 3-INF was then deposited. The limited observations in this part of the stratigraphy do not allow for a satisfactory reconstruction of the sedimentary dynamics, although it seems that debris flows played an important role. A period of rock

fall was also recorded, with the frequent presence of blocks several decimetres in width. Unit 3-INF ends with a new stabilisation phase marked by the development of a speleothem accompanied by calcitic cementing of the underlying sediment.

4.5. Unit 3-SUP

The deposits at the base of Unit 3-SUP (Layer 3-LHM) could not be observed well enough to allow a satisfactory reconstruction of the depositional context. It is probable that debris flow and run-off were the dominant sedimentary processes in this case as well.

On the contrary, the rest of Unit 3-SUP can be described in some detail. Very stony facies are characteristic of Layer 3-EMO, which contains very blunt and relatively well-sorted limestone fragments, with most clasts measuring between 1 and 4 cm. All of the limestone blocks are in contact (clast-supported sediment). The matrix is composed of well-rounded sand-size aggregates. The deposit locally exhibits an openwork structure. The longitudinal extension of 3-EMO is limited (ends around metre 34). These features suggest a 2-stage deposition process for Layer 3-EMO. During the first stage, an energetic flow (torrential flow), with a high sediment concentration, produced the sorting of the coarse elements transported as bottom load. These coarse elements were rounded in the process, while the fine particles were evacuated downstream. During the second stage, this coarse openwork deposit was partially infilled with sand-size aggregates. This second stage is indicative of the decrease of the energy of the flow, or of an additional phase of run-off. This 2-stage deposition process is demonstrated by the local presence of an openwork structure underneath large blocks, several decimetres wide. These large blocks prevented the infilling of the aggregates during the second stage.

Since the sequence was completely excavated between metre 23 and the cave entrance at the time of the stratigraphic revision, the impossibility of observation caused limitations for understanding the genesis of 3-EMO. The strike and dip of the layer situates its origin near the cave entrance. The process was probably initiated from the detritic cone under the cave porch. The related proximal facies could not be observed, nor the longitudinal variations of the facies of 3-EMO. However, data from the previous stratigraphic records allows one to visualise that this thick accumulation talus probably corresponds to the starting point of the

torrential flow. There must have been a gully in the area that would have concentrated the flow and allowed the transportation and sorting of the coarse elements, several centimetres large, that have been observed downstream.

The longitudinal Section E/F reveals that Layer 3-EMO ends between metres 32 and 34 and is progressively replaced by Layer 3-ASS towards the back of the cave. This Layer 3-ASS presents a facies that is notably less rich in coarse components and might correspond to the accumulation area of the fine component downstream from the area dominated by the torrential flow. Between metres 30 and 32, Layer 3-ASS also directly superimposes Layer 3-EMO; the facies richer in stones observed locally within Layer 3-ASS in this area may reflect more energetic flow pulses. Near metres 43-42, the bottom of Layer 3-ASS is totally lacking any coarse components and exhibits weak laminations, reflecting a distal phase of unconcentrated wash.

5. Conclusions

The meticulous study of the sedimentary profiles available at Scladina and the continuous geological survey of the archaeological excavation that has taken place there since October 2003 have both allowed for the complete reinterpretation of Sedimentary Complex 4. Rather than the previous succession of **Layer 4B/Layer 4A/Stalagmitic Floor CC4**, more than 20 layers have been identified with very different lithologies, but more importantly with a more complex distribution of the different lithostratigraphic units near Stalagmitic Floor CC4 than previously understood. All the layers that comprise Sedimentary Complex 4 are now divided into 5 distinct units: 4B, 4A-AP, 4A-IP, 4A-CHE, and 4A-POC.

Another major element of the new stratigraphic interpretation is the identification of an important gully (Unit 4A-CHE) in the upper part of Sedimentary Complex 4 that eroded Speleothem CC4 and the subjacent layers, locally down to units 5 and 6A.

The careful observation of sedimentary lithologies, geometries, and structures led to the reconstruction of the genesis of this part of the sequence. Following this genetic reconstruction it seems obvious that the filling of Scladina is quite complex and involves a large number of processes, both depositional and post-depositional. Several examples illustrate the existence of successive

lateral facies that were generated simultaneously by different processes intervening in certain specific areas of the cave, from the entrance to the back (e.g., layers 4B-LI and 3-EMO). These successions reflect the vast complexity of lithologies and geometries that can be found in a cave entrance sequence particularly well. They remind one that the isochronous limits are often notably distinct from the lithological limits, following the classic Walther's Law in stratigraphy.

Following the establishment of the new stratigraphic sequence the question of the exact position of the Scladina Neandertal remains became pertinent since all the fossils were found before the stratigraphic reappraisal. Therefore, the re-examination of all the available data was necessary in order to try to determine the objects' stratigraphic position in the new sequence. This is the objective of another chapter of this monograph (see Chapter 5; see also PIRSON et al., 2005; PIRSON, 2007).

Acknowledgements

I am very grateful to P. Haesaerts, who supervised my PhD study between 2003 and 2007. I benefited from his advice, his support, and numerous discussions about the Scladina sequence and stratigraphy in general. I also benefited from fruitful discussions on the field with my colleagues Pascal Bertran and Arnaud Lenoble about the sedimentary dynamics and I want to take this opportunity to warmly thank them.

I gratefully acknowledge Rhylan McMillan and Jean-François Lemaire for their valuable help in translating the manuscript into correct English, as well as to Joël Éloy (Association wallonne d'Études mégalithiques) for his technical assistance. Many thanks also to the staff at the association Archéologie Andennaise (Marie Rose Bouffioux, Gérard 'Gégé' Bouchat, Fred Chaplais, Marcel Chardon, Willy Dené, Philippe 'Fifi' Frison, Damien Samedi, Mike Servaes, and Tonino Verta) as well as to all the students who trained in the excavations for their enthusiasm.

Last but not least, I would like to express my deepest gratitude to Dominique Bonjean, Kévin Di Modica, and Grégory Abrams archaeologists at Archéologie Andennaise for their welcome on the site, their interest, and continuous encouragement. The numerous hours I spent with Dominique and Kévin over the last 10 years in front of the sedimentary profiles and the resulting



discussions were very enriching and stimulating and have definitively improved my understanding of the stratigraphy and the sedimentary dynamics of Scladina deposits. Many thanks to you!

This work was made possible by funding through an Action 2 project from the Belgian Science Policy.

References

- BASTIN B., 1992. Analyse pollinique des sédiments détritiques, des coprolithes et des concrétions stalagmitiques du site préhistorique de la grotte Scladina (province de Namur, Belgique). In M. OTTE (ed.), *Recherches aux grottes de Sclayn, vol. 1 : Le Contexte. Études et Recherches Archéologiques de l'Université de Liège*, 27 : 59-77.
- BENABDELHADI M., 1998. Étude sédimentologique de la coupe transversale 30/31 des carrés A, B, C et D de la grotte Scladina. In M. OTTE, M. PATOU-MATHIS & D. BONJEAN (dir.), *Recherches aux grottes de Sclayn, vol. 2 : L'Archéologie. Études et Recherches Archéologiques de l'Université de Liège*, 79: 25-37.
- BERTRAN P. (dir.), 2004. *Dépôts de pente continentaux. Dynamique et faciès*, Paris, Quaternaire, hors-série, 1, 259 p.
- BERTRAN P., 2005. Stratigraphie du site des Peyrugues (Lot), une coupe de référence pour le dernier pléniglaciaire en Aquitaine. *Quaternaire*, 16: 25-44.
- BERTRAN P., 2006. *Dépôts de versant et application au Paléolithique. Processus de formation des sites dans les porches de grottes et d'abris en Aquitaine*. Bordeaux, Thèse inédite d'Habilitation à Diriger des Travaux, Université de Bordeaux 1, 70 p.
- BERTRAN P., BEAUVAL C., BOULOGNE S., BRENET M., CHRZAVZEZ J., CLAUD E., COSTAMAGNO S., LAROU LANDIE V., LENOBLE A., MALAURENT P., MASSON B., MALLYE J.-B., SIN P., THIÉBAUT C. & VALLIN L., 2009. Dynamique sédimentaire et taphonomie des abris-sous-roche et des porches de grotte en milieu périglaciaire. Le programme Gavarnie. *Les Nouvelles de l'archéologie*, 118: 11-16.
- BERTRAN P., CLAUD E., DETRAIN L., LENOBLE A., MASSON B. & VALLIN L., 2006. Composition granulométrique des assemblages lithiques, application à l'étude taphonomique des sites paléolithiques. *Paléo*, 18: 7-36.
- BERTRAN P. & COUTARD J.-P., 2004. Solifluxion. In P. BERTRAN (dir.), *Dépôts de pente continentaux. Dynamique et faciès*, Paris, Quaternaire, hors-série, 1: 84-109.
- BERTRAN P., FRANCOU B. & TEXIER J.-P., 2004. Ébouilisation, éboulement. In P. BERTRAN (dir.), *Dépôts de pente continentaux. Dynamique et faciès*, Paris, Quaternaire, hors-série, 1: 29-43.
- BERTRAN P., HÉTU B., TEXIER J.-P. & VAN STEIJN H., 1997. Fabric characteristics of subaerial slope deposits. *Sedimentology*, 44: 1-16.
- BERTRAN P., LENOBLE A., TODISCO D., DESROSIERS P. M. & SORENSSEN M., 2012. Particle size distribution of lithic assemblages and taphonomy of Paleolithic sites. *Journal of Archaeological Science*, 39: 3148-3166.
- BERTRAN P. & TEXIER J.-P., 1995. Fabric Analysis: Application to Paleolithic Sites. *Journal of Archaeological Science*, 22: 521-535.
- BERTRAN P. & TEXIER J.-P., 1997. Géoarchéologie des versants. Les dépôts de pente. In J.-P. BRAVARD & M. PRESTREAU (eds.), *Dynamique du paysage*, Documents d'Archéologie en Rhône-Alpes: 59-86.
- BONJEAN D., 1998^a. La stratigraphie. In M. OTTE, M. PATOU-MATHIS & D. BONJEAN (dir.), *Recherches aux grottes de Sclayn, vol. 2 : L'Archéologie. Études et Recherches Archéologiques de l'Université de Liège*, 79: 15-23.
- BONJEAN D., 1998^b. Chronologie à la grotte Scladina. In M. OTTE, M. PATOU-MATHIS & D. BONJEAN (dir.), *Recherches aux grottes de Sclayn, vol. 2 : L'Archéologie. Études et Recherches Archéologiques de l'Université de Liège*, 79: 45-57.
- BONJEAN D., ABRAMS G., DI MODICA K. & OTTE M., 2009. La microstratigraphie, une clé de lecture des remaniements sédimentaires successifs. Le cas de l'industrie moustérienne 1A de Scladina. *Notae Praehistoricae*, 29: 139-147.
- BONJEAN D., LOODTS I. & LÓPEZ BAYÓN I., 2002. La doline de Scladina (Sclayn, Andenne, province de Namur). Un second complexe sédimentaire. *Notae Praehistoricae*, 22: 15-19.
- BONJEAN D., TOUSSAINT M. & OTTE M., 1996. Scladina (Sclayn, Belgique): l'homme de néandertal retrouvé! *Notae Praehistoricae*, 16: 37-46.
- BONJEAN D., TOUSSAINT M. & OTTE M., 1997. Grotte Scladina (Sclayn, Belgique) : bilan des découvertes néandertaliennes et analyse du contexte.

- In J. PLUMIER (dir.), *Actes de la cinquième journée d'Archéologie Namuroise*, Namur, Facultés universitaires Notre-Dame de la Paix, 22 février 1997, Ministère de la Région wallonne, Direction générale de l'Aménagement du Territoire, du Logement et du Patrimoine, Direction de Namur, Service des Fouilles: 19-27.
- DEBLAERE C. & GULLENTOPS F., 1986. Lithostratigraphie de la grotte Scladina. *Bulletin de l'Association française pour l'étude du Quaternaire*, 2^e série, 25-26: 178-181.
- DRAILY C., PIRSON S. & TOUSSAINT M. (dir.), 2011. *La grotte Walou à Trooz (Belgique). Fouilles de 1996 à 2004, vol. 2: Les sciences de la vie et les datations*. Namur, Service public de Wallonie, IPW, Études et Documents, Archéologie, 21, 241 p.
- FERRIER C., 2002. Les dépôts d'entrée de grotte. In J.-C. MISKOVSKY (ed.), *Géologie de la préhistoire*, Paris, Association pour l'étude de l'environnement géologique de la préhistoire: 189-205.
- GOLDBERG P. & SHERWOOD S. C., 2006. Deciphering Human Prehistory Through the Geoarcheological Study of Cave Sediments. *Evolutionary Anthropology*, 15: 20-36.
- GULLENTOPS F. & DEBLAERE C., 1992. Érosion et remplissage de la grotte Scladina. In M. OTTE (ed.), *Recherches aux grottes de Sclayn, vol. 1: Le Contexte*. Études et Recherches Archéologiques de l'Université de Liège, 27: 9-31.
- HAESAERTS P., 1983. Stratigraphic distribution of periglacial features indicative of permafrost in the Upper Pleistocene loesses of Belgium. In T. L. PEWE & J. BROWN (eds.) *Permafrost Fourth International Conference, proceedings. Fairbanks, Alaska, July 17-22, 1983*. Washington, D.C., National Academy Press: 421-426.
- HAESAERTS P., 1992. Les dépôts pléistocènes de la terrasse de la grotte Scladina à Sclayn (province de Namur, Belgique). In M. OTTE (ed.), *Recherches aux grottes de Sclayn, vol. 1: Le Contexte*. Études et Recherches Archéologiques de l'Université de Liège, 27: 33-55.
- HAESAERTS P. & VAN VLIET-LANOË B., 1981. Phénomènes périglaciaires et sols fossiles observés à Maisières-Canal, à Harmignies et à Rocourt. *Biuletyn Peryglacjalny*, 28: 291-324.
- LENOBLE A., 2005. *Ruissellement et formation des sites préhistoriques. Référentiel actualiste et exemples d'application au fossile*. Oxford, British Archaeological Reports, International Series, 1363, 216 p.
- LENOBLE A., BERTRAN P., BOULOGNE S., MASSON B. & VALLIN, L., 2009. Évolution des niveaux archéologiques en contexte périglaciaire: apport de l'expérience Gavarnie. *Les Nouvelles de l'archéologie*, 118: 16-20.
- LENOBLE A., BERTRAN P. & LACRAMPE F., 2008. Solifluction-induced modifications of archaeological levels: simulation based on experimental data from a modern periglacial slope and application to French Palaeolithic sites. *Journal of Archaeological Science*, 35: 99-110.
- LENOBLE A. & BORDES J.-G., 2001. Une expérience de piétinement et de résidualisation par ruissellement. In L. BOURGUIGNON, I. ORTEGA & M.-C. FRÈRE-SAUTOT (eds.), *Préhistoire et approche expérimentale*. Montagnac, Éditions Monique Mergoil: 295-311.
- OTTE M., LÉOTARD J.-M., SCHNEIDER A.-M., GAUTIER A., GILOT E. & AITKEN M., 1983. Fouilles aux grottes de Sclayn (Namur). *Helinium*, 23: 112-142.
- OTTE M., SLOOTMAEKERS R., 1982. Fouilles aux grottes de Sclayn (1981). *Notae Praehistoricae*, 2-1982: 23-31.
- PATOU-MATHIS M., 1998. Les espèces chassées et consommées par l'homme en couche 5. In M. OTTE, M. PATOU-MATHIS & D. BONJEAN (dir.), *Recherches aux grottes de Sclayn, vol. 2: L'Archéologie*. Études et Recherches Archéologiques de l'Université de Liège, 79: 297-310.
- PIRSON S., 2007. *Contribution à l'étude des dépôts d'entrée de grotte en Belgique au Pléistocène supérieur. Stratigraphie, sédimentogenèse et paléoenvironnement*. Unpublished PhD thesis, University of Liège & Royal Belgian Institute of Natural Sciences, 2 vol., 435 p. & 5 annexes.
- PIRSON S., BONJEAN D., DI MODICA K. & TOUSSAINT M., 2005. Révision des couches 4 de la grotte Scladina (comm. d'Andenne, prov. de Namur) et implications pour les restes néandertaliens: premier bilan. *Notae Praehistoricae*, 25: 61-69.
- PIRSON S., COURT-PICON M., HAESAERTS P., BONJEAN D. & DAMBLON F., 2008. New data on geology, anthracology and palynology from the Scladina Cave pleistocene sequence: preliminary results. In F. DAMBLON, S. PIRSON & P. GERRIENNE (eds.), *Hautrage (Lower Cretaceous) and Sclayn (Upper Pleistocene). Field Trip Guidebook*.



Charcoal and microcharcoal: continental and marine records. IVth International Meeting of Anthracology, Brussels, Royal Belgian Institute of Natural Sciences, 8-13 September 2008. Brussels, Royal Belgian Institute of Natural Sciences, Memoirs of the Geological Survey of Belgium, 55: 71-93.

PIRSON S., DRAILY C., COURT-PICON M., HAESAERTS P., DAMBLON F., DEBENHAM N. & TOUSSAINT M., 2007. La grotte Walou (province de Liège, Belgique): une séquence stratigraphique de référence pour le Pléistocène supérieur dans le karst belge. In J. EVIN (ed.), *Un siècle de construction du discours scientifique en préhistoire.* Actes du XXVIe Congrès préhistorique de France. Avignon, 21-25 septembre 2004, vol. 3, Paris, Société préhistorique française: 295-306.

PIRSON S., DRAILY C. & TOUSSAINT M. (dir.), 2011. *La grotte Walou à Trooz (Belgique). Fouilles de 1996 à 2004, vol. 1: Les sciences de la terre.* Namur, Service public de Wallonie, IPW, Études et Documents, Archéologie, 20, 208 p.

PIRSON S., HAESAERTS P., COURT-PICON M., DAMBLON F., TOUSSAINT M., DEBENHAM N. C. & DRAILY C., 2006. Belgian cave entrance and rockshelter sequences as palaeoenvironmental data recorders: the example of Walou cave. *Geologica Belgica*, 9: 275-286.

SIMONET P., 1992. Les associations de grands mammifères du gisement de la grotte Scladina à Sclayn (Namur, Belgique). In M. OTTE (ed.), *Recherches aux grottes de Sclayn, vol. 1: Le Contexte.* Études et Recherches Archéologiques de l'Université de Liège, 27: 127-151.

TEXIER J.-P., 2000. À propos des processus de formation des sites préhistoriques. *Paléo*, 12: 379-386.

TEXIER J.-P., 2001. Sédimentogenèse des sites préhistoriques et représentativité des datations numériques. In J.-N. BARRANDON, P. GUIBERT & V. MICHEL (eds.), *Datation.* XXIe rencontres internationales d'archéologie et d'histoire d'Antibes, Éditions de l'Association pour la promotion et la diffusion des connaissances archéologiques: 159-175.

TOUSSAINT M. & PIRSON S., 2006. Neandertal Studies in Belgium: 2000-2005. *Periodicum*

Biologorum, 108, 3: 373-387.

TOUSSAINT M. & PIRSON S., 2007. Aperçu historique des recherches concernant l'homme préhistorique dans le karst belge aux XIXe et XXe siècles: archéologie, géologie, paléanthropologie, paléontologie, datations. In J. EVIN (ed.), *Un siècle de construction du discours scientifique en préhistoire.* Actes du XXVIe Congrès préhistorique de France. Avignon, 21-25 septembre 2004, vol. 3, Paris, Société préhistorique française: 117-142.

TOUSSAINT M., BONJEAN D. & OTTE M., 1994. Découverte de fossiles humains du Paléolithique moyen à la grotte Scladina à Andenne. In M.-H. CORBIAU & J. PLUMIER (eds), *Actes de la deuxième Journée d'Archéologie Namuroise.* Namur, Facultés universitaires Notre-Dame de la Paix, 26 février 1994, Ministère de la Région wallonne, Direction générale de l'Aménagement du Territoire et du Logement, Direction de Namur, Service des Fouilles: 19-33.

TOUSSAINT M., SEMAL P. & PIRSON S., 2011. Les Néandertaliens du bassin mosan belge: bilan 2006-2011. In M. TOUSSAINT, K. DI MODICA & S. PIRSON (sc. dir.), *Le Paléolithique moyen en Belgique. Mélanges Marguerite Ullrich-Closset.* Bulletin de la Société royale belge d'Études Géologiques et Archéologiques *Les Chercheurs de la Wallonie*, hors-série, 4 & Études et Recherches Archéologiques de l'Université de Liège, 128: 149-196.

TUCKER M. E., 1991 (2nd edition). *Sedimentary Petrology. An introduction to the origin of sedimentary rocks.* Oxford, Blackwell Sciences, 260 p.

VAN VLIET-LANOË B., 1987. Dynamique périglaciaire actuelle et passée. Apport de l'étude micromorphologique et de l'expérimentation. *Bulletin de l'Association française pour l'étude du Quaternaire*, 1987-3: 113-132.

VAN VLIET-LANOË B., 1988. *Le rôle de la glace de ségrégation dans les formations superficielles de l'Europe de l'ouest. Processus et héritages.* Paris, Thèse de doctorat d'état inédite, mention géographie. Université de Paris I – Sorbonne, Centre de Géomorphologie du Centre national de la recherche scientifique, 2 vol., 378 p. & 667 p.

Chapter 4

THE PALAEOENVIRONMENTAL CONTEXT AND CHRONOSTRATIGRAPHIC FRAMEWORK OF THE SCLADINA CAVE SEDIMENTARY SEQUENCE (UNITS 5 TO 3-SUP)

Stéphane PIRSON, Mona COURT-PICON,
Freddy DAMBLON, Sanda BAILESCU,
Dominique BONJEAN, & Paul HAESAERTS

*Michel Toussaint & Dominique Bonjean (eds.), 2014.
The Scladina I-4A Juvenile Neandertal (Andenne, Belgium),
Palaeoanthropology and Context
Études et Recherches Archéologiques de l'Université de Liège, 134: 69–92.*

1. Introduction

Since the first professional excavations in 1978 (see Chapter 2), numerous studies regarding palaeoenvironment and chronostratigraphy have occurred at Scladina Cave. This chapter presents a synthesis of these analyses, focusing on the layers concerning the Neandertal child (Scladina I-4A) problem, i.e., layers from sedimentary units 5 to 3-SUP (see Chapter 3). Several analyses are still in progress or will start in the very near future (e.g., palynology, heavy mineralogy, and dating); therefore, the results delineated below solely represent the progress of current scientific endeavours at Scladina Cave.

Most of the available data were obtained before the stratigraphic reappraisal began in 2003 (PIRSON et al., 2005; PIRSON, 2007; see Chapter 3). In the former stratigraphic record, the deposits that are addressed in this chapter were divided into 4 distinct layers (layers 5, 4B, 4A, and 3; Figure 1a). Since the stratigraphic revision, the same deposits now encompass more than 25 layers, which are grouped into 8 main units (units 5, 4B, 4A-AP, 4A-IP, 4A-CHE, 4A-POC, 3-INF, and 3-SUP; Figure 1b). This situation limits the possibility for detailed comparisons between the 2 data sets (see Chapter 3). In order to avoid confusion, whether the data is from the former stratigraphic record (e.g., 'former Layer 4A') or from the current one (e.g., 'Layer 4A-KG') will be systematically specified.

An attempt at integrating all the disciplines involved in palaeoenvironment and chronostratigraphy is presented below, first for the palaeoenvironmental context and then for the chronostratigraphic framework.

2. Palaeoenvironmental context

The most numerous results dealing with the palaeoenvironment of the Scladina

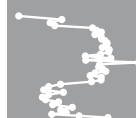
Cave sequence come from palaeobotany and palaeozoology.

Palynology was the subject of several papers in the 1980s-1990s (Schneider in OTTE et al., 1983; BASTIN & SCHNEIDER, 1984; BASTIN et al., 1986; SCHNEIDER, 1986^a, 1986^b; BASTIN, 1990, 1992). Y. QUINIF (2006) recently published some of B. Bastin's unpublished data. Finally, M. Court-Picon and F. Damblon undertook new palynological studies within the framework of the Scladina stratigraphic reappraisal (PIRSON, 2007; PIRSON et al., 2008), complemented by some anthracological data obtained by F. Damblon (PIRSON, 2007; PIRSON et al., 2008).

A few papers also deal with small mammal remains (Cordy in BASTIN et al., 1986; CORDY, 1988, 1992) and macrofauna (Gautier in OTTE et al., 1983; CORDY, 1984, 1988; Cordy in BASTIN et al., 1986; SIMONET, 1992; PATOU-MATHIS, 1998^a; LAMARQUE, 2003). These faunal results only refer to the former stratigraphic record; the study of the material unearthed after the stratigraphic reappraisal is still in progress. Macrofaunal data are complemented by archaeozoological data (PATOU-MATHIS, 1998^b; PATOU-MATHIS & LÓPEZ-BAYÓN, 1998; ABRAMS et al., 2010, 2014).

A synthesis of the palaeontological data was presented in the first monograph for Scladina Cave (CORDY & BASTIN, 1992).

Geologic inquiry also yields information about the climatic changes in the Scladina sequence. The first palaeoenvironmental interpretations that were deduced from stratigraphy and sedimentology gave very little reliable data. While HAESAERTS (1992) remained very careful, insisting on the lack of reference for cave entrance sequences in Belgium, the palaeoenvironmental reconstruction of GULLENTOPS & DEBLAERE (1992) was based on a model of sedimentogenesis in cave entrances which is no longer valid (see PIRSON, 2007). In 1999, sampling for a magnetic susceptibility study of sediment from Scladina took place. It yielded interesting



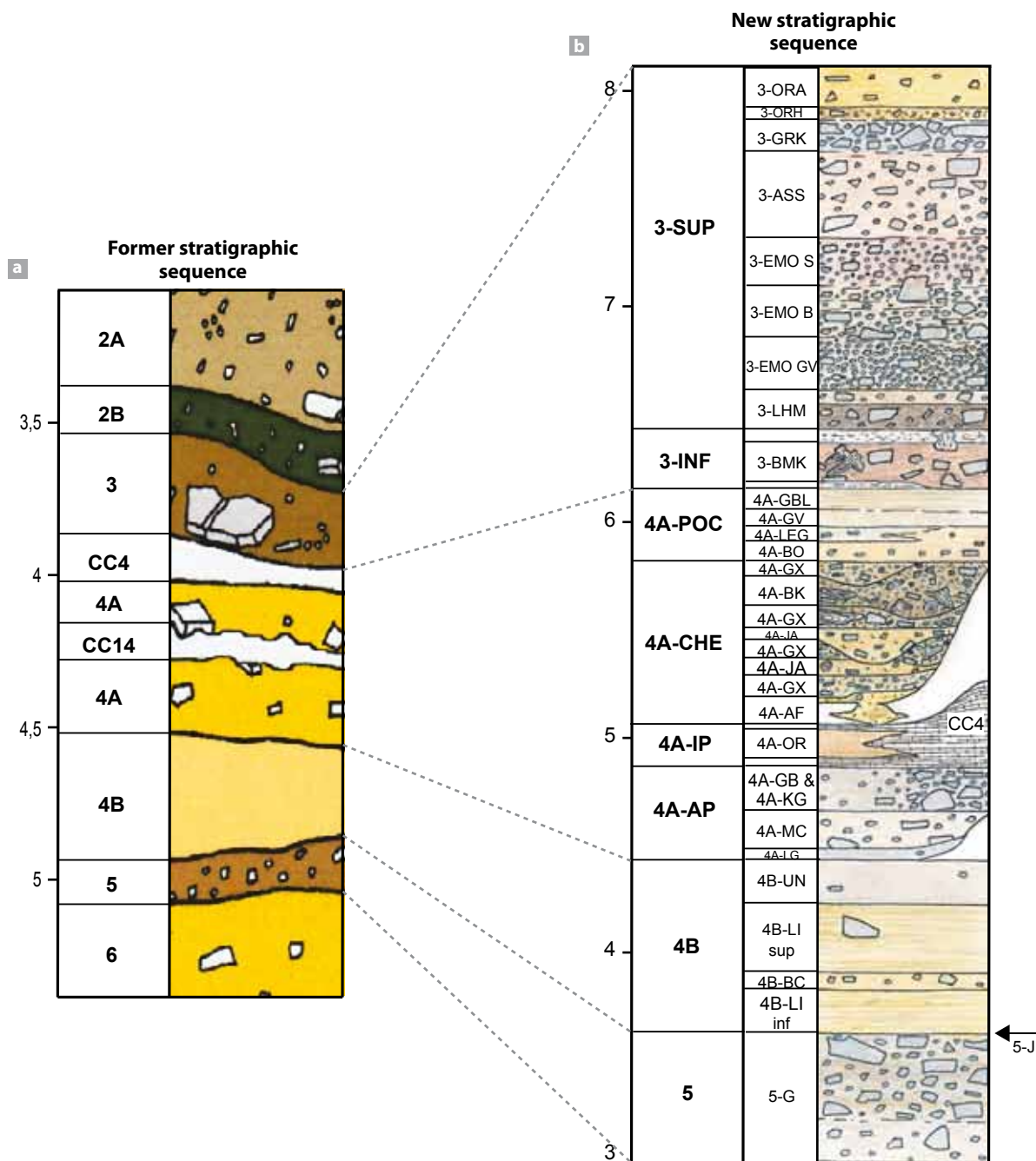


Figure 1: The former stratigraphic sequence of Scladina Cave (a; after BONJEAN, 1998) compared with the new stratigraphic sequence of Scladina Cave (b; after PIRSON, 2007).

palaeoenvironmental information (ELLWOOD et al., 2004; Figure 2), which was overall in excellent agreement with palaeontological data. Finally, quite recently, a detailed study of the sedimentary and post-sedimentary processes in the Scladina sequence allowed a set of well-documented climate changes to be evidenced (PIRSON, 2007; PIRSON et al., 2008).

All the available palaeoenvironmental information for units 5 to 3-SUP is presented below, from the oldest to the youngest (see Figure 3).

2.1. Unit 5

Unit 5 is comprised of 2 distinct layers: 5-G and 5-J (see Chapter 3; Figure 1b).

The presence of a linear fabric (*sensu* BERTRAN (dir.), 2004) affecting limestone fragments in Layer 5-G suggests the influence of solifluction (PIRSON, 2007), which is a slow downslope displacement of sediments involving 2 processes linked with ground ice formation (frost-creep and gelifluction; BERTRAN (dir.), 2004). This sedimentary process is typical of periglacial environments and therefore has a clear climatic signature.

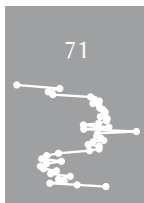
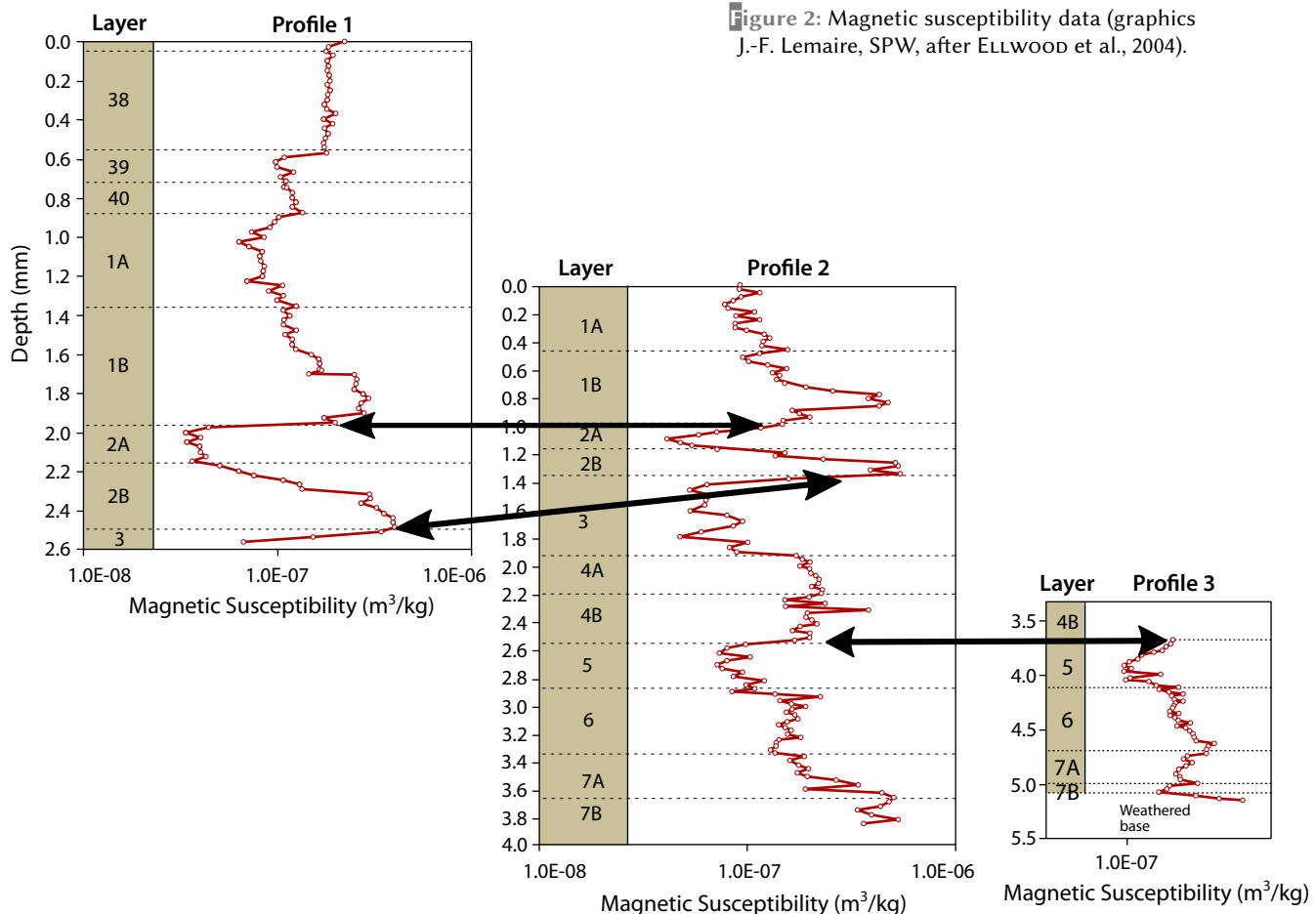
A cold climate is further attested by the presence of a thick (4-10 mm) platy structure that developed in Unit 6A, Layer 5-G being the upper part of the cryosol (see Chapter 3). This kind of feature indicates deep frost (VAN VLIET-LANOË, 1988). In Middle Belgium loess sequences, a thick platy structure is regularly observed and is interpreted as evidence for the continuous growth of ice lenses (i.e., during several years) in the upper part of permafrost (HAESAERTS & VAN VLIET-LANOË, 1981; HAESAERTS, 1983; VAN-VLIET-LANOË, 1988).

The new palynological study (Court-Picon & Damblon in PIRSON, 2007; PIRSON et al., 2008) obtained from Layer 5-G suggests cold steppic conditions with a relatively open

landscape (15-20% AP) in which tree genera indicate boreal environment (*Pinus*, *Juniperus*, *Betula*). Very low frequencies of *Quercus* are also recorded.

Comparing these new results with those available in the literature is possible because the now-understood Unit 5 is not very thick and contains only a few layers. Therefore, the equivalence between Unit 5 and former Layer 5 is well controlled and easily translatable.

Palaeontological data (palynology, small mammals, and macrofauna) from former Layer 5 suggest the existence of a cooling by a decrease of the tree cover compared to the underlying former Layer 6. Small mammals evidence the return of arctic taxa (CORDY, 1992). In the upper half of former Layer 5, palynology indicates steppic conditions (<10% AP; BASTIN, 1992); however, small mammals and large herbivores show the persistence of forest taxa (up to 25%: CORDY, 1992; SIMONET, 1992) and the bottom of former Layer 5 still yields 50% AP, including some mesophilous trees (BASTIN, 1992) that could be related to the low *Quercus* content from the new palynological data.



The magnetic susceptibility signal also suggests the existence of a cooling in former Layer 5 (ELLWOOD et al., 2004; Figure 2).

2.2. Unit 4B

Unit 4B is composed of 2 main layers: 4B-LI and 4B-UN (Figure 1a). Locally, other layers have been recognized; some are interbedded with 4B-LI, while Layer 4B-UF corresponds to a lateral variation of 4B-UN (see Chapter 3).

Depositional and post-depositional processes identified in Unit 4B (PIRSON, 2007; see Chapter 3) do not yield any climatic information; the fall of large stone slabs, run-off, settling, and dessication cracks are ubiquitous processes (BERTRAN (dir.), 2004).

On the other hand, new palynological data from Unit 4B indicates arid open steppic conditions (Court-Picon & Damblon in PIRSON, 2007; PIRSON et al., 2008). The 6 samples from layers 4B-LI and 4B-BC are largely dominated by steppic plants (<5% AP); the trees are mainly represented by *Pinus* and *Juniperus*. The top of Unit 4B, only documented by a single sample from Layer 4B-UN, shows a slight rise of the conifers (ca. 20%), almost exclusively *Juniperus*. Spores of algae increase in frequency. Thus, Layer 4B-UN could represent the beginning of the major climatic improvement recorded in Sedimentary Complex 4A (§ 2.3).

The connection between these new geological and palynological data and the data from the literature is globally possible. The palynological signal from former Layer 4B (BASTIN, 1992) is very close to what was recently obtained from Unit 4B (5-10% AP, *Pinus* dominating the trees). Small mammals indicate a similar trend on the cave terrace (Layer V gris), with the disappearance of temperate forest taxa, insectivores, and bats, and the strong return of the collared lemming (CORDY, 1992). On the contrary, the magnetic susceptibility signal indicates different conditions: a climatic improvement in both former layers 4B and 4A (ELLWOOD et al., 2004). New analyses should be undertaken in order to better understand this apparent contradiction.

Large mammals from former Layer 4B are difficult to use for climatic reconstruction because they were originally mixed and studied together with the objects from former Layer 4A, creating the 'former Layer 4' assemblage (SIMONET, 1992). The probable equivalent of former Layer 4B on the terrace (Layer V gris) is deprived of any faunal remains (SIMONET, 1992). In addition, former Layer 4B, excavated inside

the cave after Simonet's study (i.e., between 1991 and 2003), as well as the different layers from the newly defined Unit 4B (layers 4B-UN, 4B-LI, etc.) that were excavated after the stratigraphic reappraisal (i.e., since 2003), are both extremely poor in macrofaunal remains. Therefore, it is probable that most of the large mammal remains labelled 'former Layer 4' come from former Layer 4A (cf. § 2.3.2).

2.3. Sedimentary Complex 4A

The correlation of both old and new data is much more delicate for Sedimentary Complex 4A. While the former stratigraphic system included only 1 layer (i.e., Layer 4A; Figure 1a), the stratigraphic reappraisal demonstrated a much greater complexity: 4 major units, encompassing more than 10 layers (Figure 1b; PIRSON et al., 2005; PIRSON, 2007; see Chapter 3). Strong lithological and geometrical variations have been identified, including the presence of an important gully structure. Given this context, former and new palaeoenvironmental results will be presented separately.

2.3.1. New results

2.3.1.1. Unit 4A-AP

Unit 4A-AP is comprised of 3 distinct layers, including (from bottom to top): 4A-LG, 4A-MC, and 4A-KG (Figure 1b). A fourth layer, 4A-GB, corresponds to a possible lateral equivalent of 4A-KG (see Chapter 3).

The sedimentary processes recognized in Unit 4A-AP (debris flow and/or run-off: PIRSON, 2007; see Chapter 3) do not allow the identification of any specific climatic condition.

A single sample (from Layer 4A-KG) has been studied in the framework of the new palynological analyses (Court-Picon & Damblon in PIRSON, 2007; PIRSON et al., 2008). The amount of trees, especially *Pinus* and *Juniperus*, is much higher than in underlying layers (ca. 65%), while various malacophyll temperate taxa appear (*Quercus* and *Ulmus*). The presence of charcoal remains of *Quercus*, *Populus*, and *Prunus* in Layer 4A-KG (PIRSON et al., 2008) confirms the local presence of mesophilous taxa. Algae levels peak in this layer. All of this suggests a clear climatic improvement in Layer 4A-KG, which could correspond to the beginning of the major climatic improvement recorded in the overlying Unit 4A-IP.

2.3.1.2. Unit 4A-IP

Unit 4A-IP contains 2 major lithologies. The first is a thick stalagmitic floor labelled CC4 that was identified during the early stages of excavation (e.g., BASTIN et al., 1986; GULLENTOPS & DEBLAERE, 1992). The second lithology is comprised of some silty deposits locally interbedded inside Speleothem CC4 (Figure 1b). These silty deposits are grouped into 3 distinct layers that have been distinguished in different areas of the cave (4A-OR, 4A-SGR, and 4A-YS; see Chapter 3).

Stalagmitic floors are classically used in palaeoenvironmental reconstructions of caves. They indicate climatic improvements (e.g., QUINIF et al., 1994). Given the important thickness of CC4 and its large spatial distribution in the cave, this stalagmitic floor probably indicates a major climatic improvement. The silty deposits interbedded in CC4 (Layer 4A-OR and lateral equivalents) were laid down by run-off processes (PIRSON, 2007) and therefore do not directly record any climatic information.

The existence of a strong climatic improvement in CC4 is further supported by a recent palynological study (Court-Picon & Damblon in PIRSON, 2007; PIRSON et al., 2008). Unit 4A-IP is represented by several pollen spectra from Stalagmitic Floor CC4 and from Layer 4A-OR.

The spectra from CC4 clearly point to forest conditions (50 to 80% AP) with relatively high

percentages of various temperate malacophyll trees like *Ulmus*, *Quercus*, *Fraxinus*, and *Carpinus* coexisting with *Pinus* and *Picea*. The presence of sclerophyllous liana *Hedera* (up to 10%) is worth mentioning. The analyses have also provided evidence for a mass of woody microremains from vessels and tracheids. High amounts of monolet fern spores were also identified and are most probably linked to the increase of humidity around the cave. The whole pollen assemblage in CC4 points to a transition from temperate to boreal environmental conditions. The general trend shows a decrease of temperate taxa, suggesting a katathermal phase of a strong climatic improvement. This has to be determined with regard to other data.

On the contrary, the pollen spectra from Layer 4A-OR yielded much less tree pollen (ca. 25–35%), which is only boreal (*Pinus*, *Juniperus*, and *Betula*). Almost no temperate taxa were identified. They seem to correspond to a forest-steppe or even to cold steppic conditions. Further investigation is necessary to understand the apparent contradiction between CC4 and 4A-OR pollen assemblages. Nevertheless, a set of charcoal remains from malacophyll temperate taxa is preserved in Layer 4A-OR (*Quercus*, *Fraxinus*, and a Malaceae; F. Damblon in PIRSON, 2007; PIRSON et al., 2008), in good agreement with the pollen record of CC4. This demonstrates the local presence of malacophilous taxa during Unit 4A-IP.

Figure 3 (next two pages): Scladina Cave's stratigraphic log including a synthesis of the palaeoenvironmental and chronostratigraphical data.

Green amphibole: the percentage of green amphibole in the silt fraction (in green: values calculated from the data of GULLENTOPS & DEBLAERE (1992); in orange: data from PIRSON (2007)).

Dates: synthesis of all the reliable dates available for Scladina sequence.

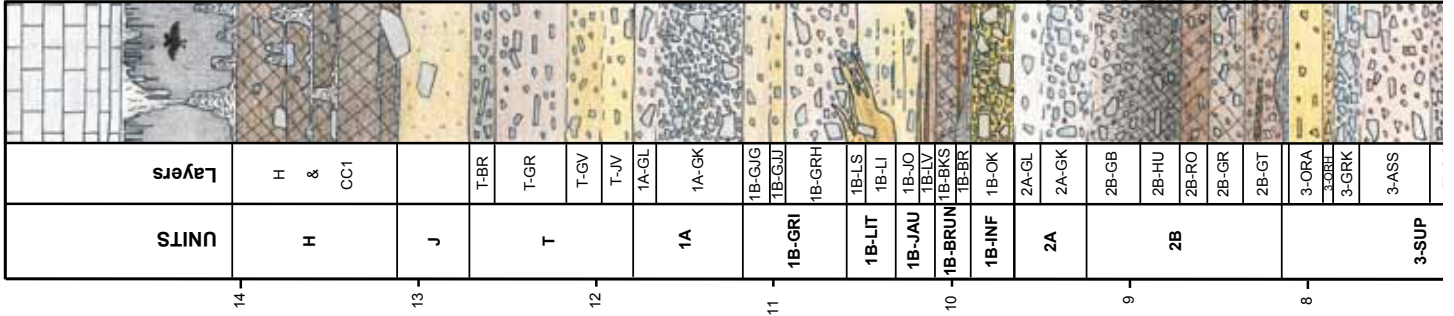
- black: already published ^{14}C date on bone;
- *black italic*: ^{14}C date on calcite (in situ speleothem, reworked speleothem or concretion);
- **black bold**: ^{14}C date on teeth obtained in Groningen, accurately positioned in the new stratigraphic system;
- blue: U/Th date on in situ speleothem;
- *blue italic*: U/Th date on reworked fragments of speleothem or on calcite concretions;
- **blue bold**: U/Th date (gamma spectrometry) obtained on the Neandertal mandible;
- red: thermoluminescence date on sediment;
- *red italic*: thermoluminescence date on in situ speleothem;
- **red bold**: thermoluminescence date on burnt flint (TL) and on sediment (IRSL);
- green: coupled U/Th–ESR dates on bone.
- () = problematic date. When an age interval is given (for CC4), the concerned total number of dates is indicated by a numeral surrounded by a circle.

Chronostratigraphy: suggested chronostratigraphic interpretation of the Scladina sequence based upon all the available analyses.

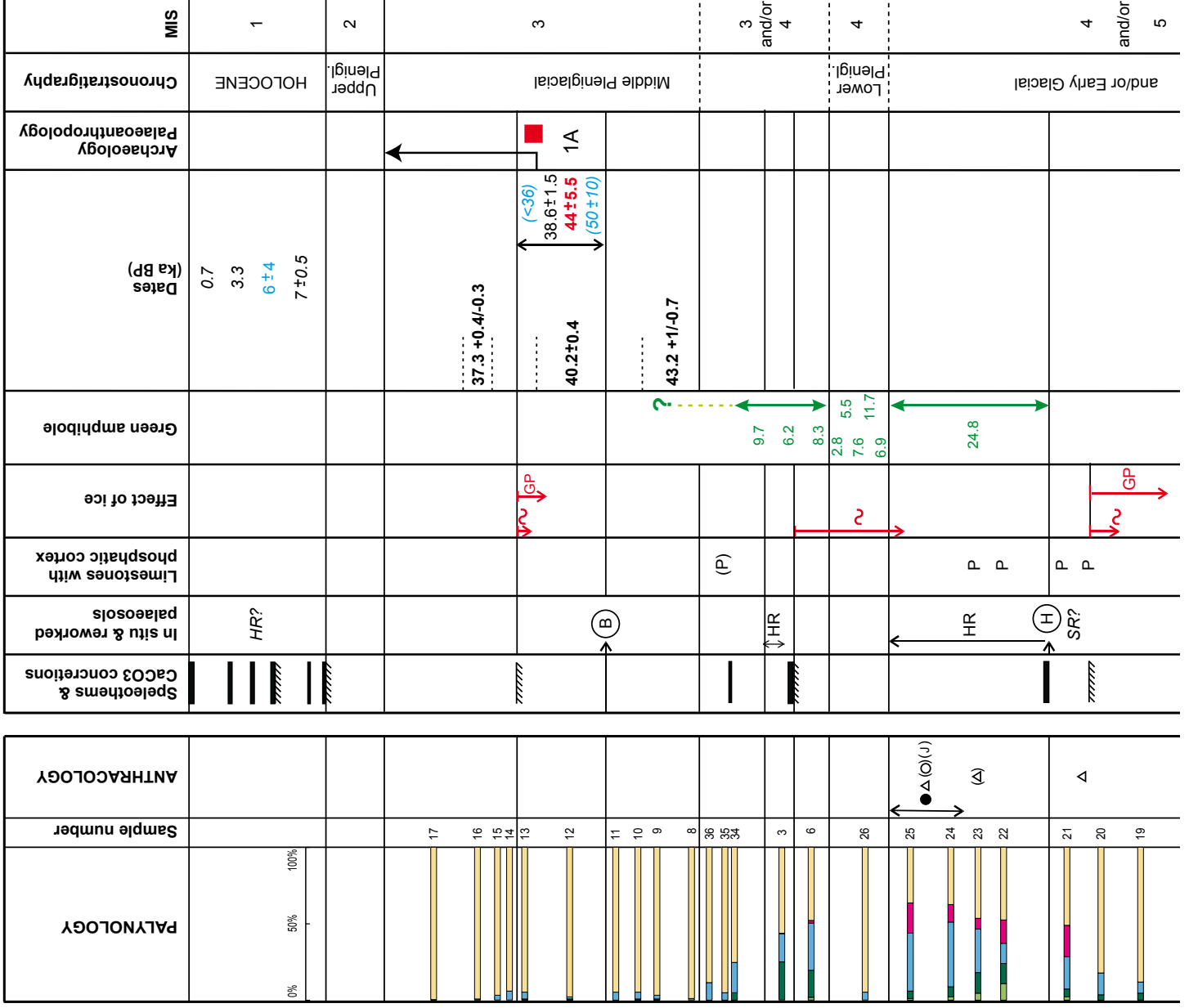
MIS: suggestion of correlation with the marine oxygen isotopic stages.



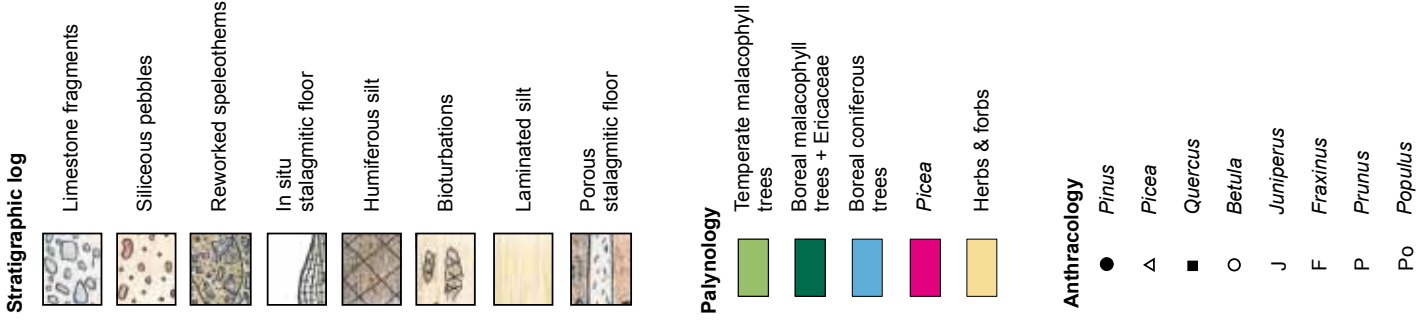
LITHOSTRATIGRAPHY

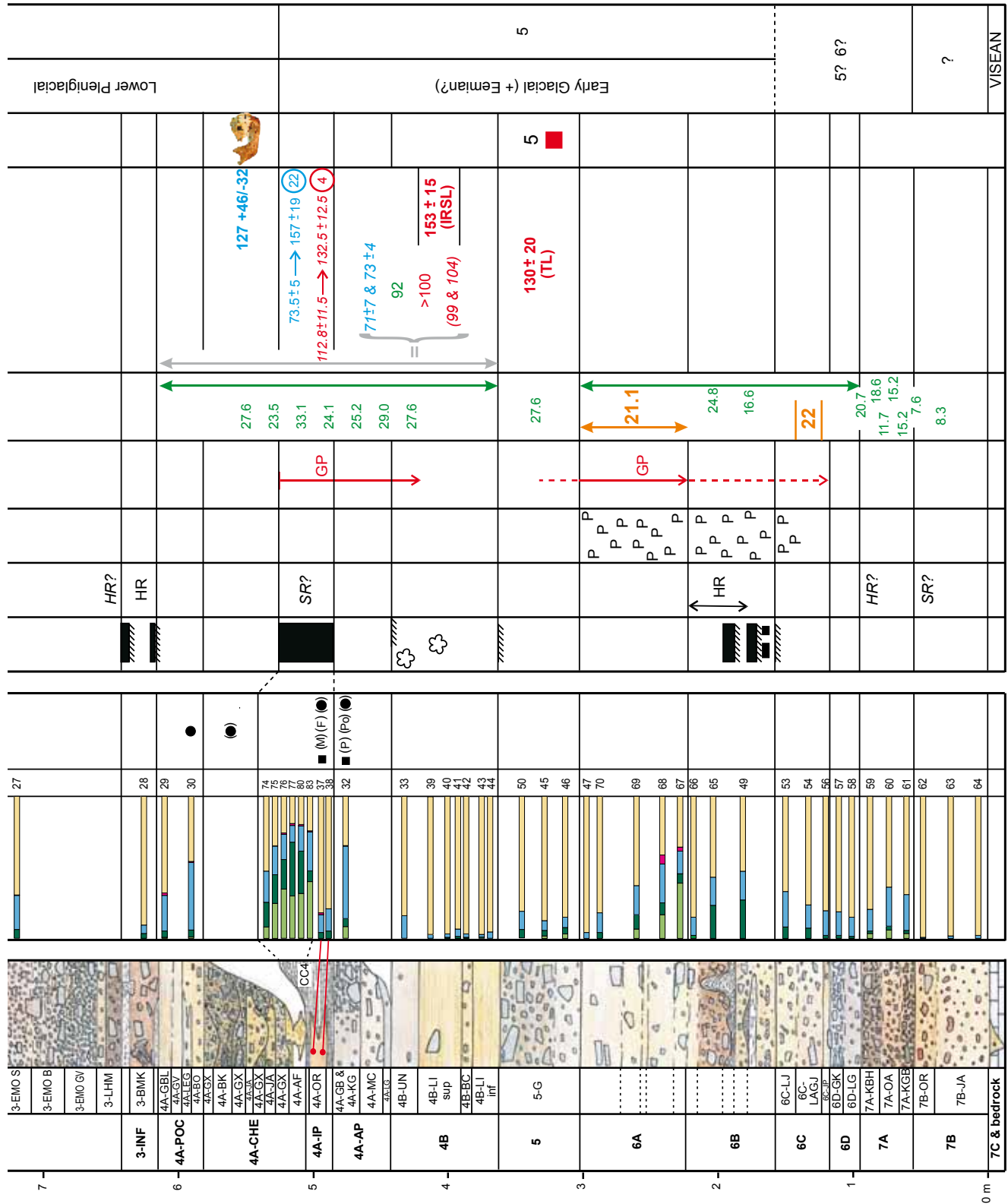


PALAEOENVIRONMENT & CHRONOSTRATIGRAPHY



GRAPHIC SYMBOLS





M Malacae
() < 10 fragments

Speleothems & CaCO₃ concretions

- In situ speleothem
- Sediment cemented by CaCO₃
- CaCO₃ concretion

In situ & reworked palaeosol

- In situ humiferous soil on the cave terrace
- In situ brown soil on the cave terrace
- Reworked humiferous soil
- Reworked soil
- Possible reworked humiferous soil
- Possible reworked soil

Effect of ice

- Deep frost
- Cryoturbations

Archaeology & palaeoanthropology

- Main Middle Palaeolithic assemblages
- Neanderthal remains

The Scladina I-4A Juvenile Neanderthal

2.3.1.3. Interface between units 4A-IP and 4A-CHE

The sediment from units 4A-IP and 4A-AP, as well as the sediment from the top of Unit 4B (Layer 4B-UN), are both affected by a thick platy structure (4–6 mm), indicating a deep frost episode (cf. § 2.1 & Figure 3).

2.3.1.4. Unit 4A-CHE

Unit 4A-CHE consists of a series of cut-and-filled layers in a complicated gully structure (Figure 1b) that has eroded the underlying layers down to the top of Unit 6A. The sediment from Unit 4A-CHE is very heterogeneous; several lithologies have been recognised (see Chapter 3). No climatic information is directly recorded in this complicated unit. Nevertheless, the existence of a cryosol at the interface between units 4A-IP and 4A-CHE, as well as some specific sedimentary features (PIRSON, 2007; see Chapter 3), suggest that this gully could correspond to the degradation of a deep frozen soil (melting structure).

No palynological data is available from this unit. The presence of some fragments of *Pinus* charcoal in 4A-CHE (F. Damblon in PIRSON, 2007; PIRSON et al., 2008) does not have any firm significance given the very erosive character of this unit, which reworked the underlying deposits where *Pinus* charcoal have been recognised (PIRSON, 2007; see Chapter 3).

2.3.1.5. Unit 4A-POC

Unit 4A-POC is comprised of 4 distinct layers, including (from bottom to top): 4A-BO, 4A-LEG, 4A-GV, and 4A-GBL (Figure 1b; see also Chapter 3).

Once again, the sedimentary dynamics of the deposits from 4A-POC are dominated by run-off processes and do not allow the identification of any specific climatic conditions. The few palynological spectra obtained from this unit suggest boreal conditions, underlined by steppic herbs and large amount of *Pinus* (30–50% AP), complemented by scattered pollen of malacophyll trees, mainly *Betula* (Court-Picon & Damblon in PIRSON, 2007; PIRSON et al., 2008). Monolete spores of ferns suggest local humidity around the cave. Local presence of *Pinus* is demonstrated by anthracology (PIRSON et al., 2008).

2.3.2. Former results

The sediments from the upper part of former Layer 4 (generally labelled 4A or V ocre: GULLENTOPS & DEBLAERE, 1992; HAESAERTS, 1992; BONJEAN, 1998) yielded palynological data that indicated forest conditions (60–95% AP) dominated by *Corylus* and *Pinus* but with high values for mesophilous trees (e.g., *Tilia*, *Quercus*, and *Ulmus*), as well as high amounts of ferns (BASTIN, 1992). These pollen assemblages from former layers 4A and V ocre are compatible with those from the palynological study of sedimentary Unit 4A-AP.

Pollen assemblages from Stalagmitic Floor CC4 (and its lateral equivalent CC14; see Chapter 3) indicate temperate forest conditions: 65–90% AP, most of the time dominated by *Corylus* and *Pinus* but including locally high percentages of *Ulmus* (up to 60%) or *Carpinus* (up to 20%), together with low values of *Tilia*, *Quercus*, *Fraxinus*, *Picea*, *Hedera*, or *Ilex* (BASTIN, 1992). Monoletes ferns are also well represented in this part of former Layer 4. The palaeoenvironmental conditions are therefore very similar to those deduced from the new palynological and anthracological analyses from CC4 (see § 2.3.1.2).

Small mammals from former Layer 4A also record a rather temperate environment: a strong presence of temperate forest taxa (up to 60%) and temperate open taxa, an important return of chiroptera and insectivores, as well as the disappearance of arctic taxa (CORDY, 1992).

The available data from the large mammals of former Layer 4A were studied together with those from 4B (“Layer 4” of SIMONET, 1992). However, as 4B is extremely poor in macrofaunal remains (see § 2.2), the presence of more than 75% forest taxa (with 50% being *Dama dama*) amongst the large herbivores from the “Layer 4” assemblage (SIMONET, 1992) is probably related to the temperate conditions of 4A.

The magnetic susceptibility signal suggests the presence of a climatic improvement in both former layers 4B and 4A (ELLWOOD et al., 2004; see § 2.2).

2.4. Sedimentary Complex 3

As for former Layer 4A, palaeoenvironmental results from former Layer 3 are delicate to accurately position in the new stratigraphic record.

From a single layer in the former stratigraphic record, this part of the sequence now includes 2 major units encompassing about 10 layers, several of which are likely lateral equivalents (Figure 1b; see also Chapter 3). Former and new results will therefore be presented separately.

2.4.1. New results

2.4.1.1. Unit 3-INF

Unit 3-INF is very poorly exposed at the site and is therefore still not well understood. It is characterized by dark brownish sediment, suggesting the reworking of humic material from the cave terrace (PIRSON, 2007; see Chapter 3). This unit could therefore record a reworked interstadial palaeosol, and thus a climatic improvement. The local presence of an unsound stalagmitic floor both at the bottom and the top of this unit supports this hypothesis. However, from a palynological point of view, the only available spectrum indicates a relatively open environment (10–30% AP). The identified trees are almost exclusively boreal taxa (*Pinus*, *Juniperus*, and *Betula*).

2.4.1.2. Unit 3-SUP

The bottom of this unit (Layer 3-LHM) is again composed of dark brownish sediments suggesting the reworking of humic material, possibly a palaeosol (PIRSON, 2007). These deposits are probably related to those from Unit 3-INF.

The major part of Unit 3-SUP is characterized by an episode of torrential flow and run-off (layers 3-EMO and 3-ASS). It was overlain by a debris flow (Layer 3-GRK). No climatic signature is recorded in these deposits (PIRSON, 2007; see Chapter 3). The 3 available pollen spectra from this part of the sequence suggest a steppic environment with some boreal trees (10–30% AP, with *Pinus*, *Juniperus*, and *Betula*; Court-Picon & Damblon in PIRSON, 2007; PIRSON et al., 2008).

A marked cooling is then recorded at the interface between 3-GRK and 3-ORH, with the presence of a thick platy structure and small cryoturbations (PIRSON, 2007).

On top of Unit 3-SUP (layers 3-ORH and 3-ORA), conditions seem to have started to change. A climatic improvement, continuing in Unit 2B, is recorded by studies under several disciplines (geology, palynology, and anthracology; PIRSON, 2007; PIRSON et al., 2008; Figure 3).

2.4.2. Former results

Palaeontological investigation has yielded some palaeoenvironmental indicators for former Layer 3. Palynology recorded a decrease in trees, although they still remained well represented (50–60% AP); *Pinus* or *Corylus* are the dominant taxa, with local occurrence of *Tilia* (up to 10%) and high amounts of monolet fern spores (BASTIN, 1992). Small mammals also indicate rather contrasting conditions (CORDY, 1992). Herbivores are represented by 40% forest taxa, including 10% *Dama dama* (SIMONET, 1992). All in all, the published palaeontological data from former Layer 3 suggests a contrasting environment, with a mixture of taxa from temperate forest and colder environments.

The magnetic susceptibility signal, while rather irregular, suggests a global cooling event when compared to underlying former Layer 4A (ELLWOOD et al., 2004; Figure 2).

As mentioned above, these former data are difficult to interpret because how they correspond with the different layers of the newly defined units 3-INF and 3-SUP is unknown. Depositional mixing between different layers that have distinct palaeoenvironmental signatures is likely.

2.5. Palaeoenvironmental synthesis

All the available palaeoenvironmental data are summarized in Figure 3. Despite the problems due to the difference between former and current stratigraphic records, the overall convergence of the palaeoenvironment results from all the available disciplines is worth mentioning, as already emphasized by J.-M. CORDY & B. BASTIN (1992). Consistency also appears at a single-discipline level, as illustrated by the reproducibility of the palynological results from distinct sedimentary profiles or from distinct analysts, i.e., former results from B. BASTIN (1992) and new results from F. Damblon and M. Court-Picon (in PIRSON et al., 2008). The viability of the existence of these recorded climatic fluctuations is thus strengthened.

The results recently obtained in the fields of geology and palynology allow the construction of a consistent palaeoenvironmental framework for the new Scladina stratigraphic sequence. Palynology appears to be more complete, as most of the sedimentary processes do not exhibit any climatic signals. However, the understanding of sedimentary dynamics helps interpreting the



palaeobotanical results while post-depositional processes provide information about climatic events for periods without sediment accumulation (e.g., frost action or the formation of authigenic phosphates). These 2 approaches therefore appear as highly complementary. The available anthracological data supplements and strengthens the palynological results, demonstrating the local (or at least regional) presence of some of the tree taxa.

Despite the specific character of stratigraphic records in caves, which often involves a highly discontinuous sedimentation rate, these concordant palaeoenvironmental results further demonstrate the high potential of Belgian cave entrance sedimentary sequences as recorders of Quaternary climatic changes, as already stated for the Walou Cave sequence (PIRSON et al., 2006).

3. Chronostratigraphic framework

3.1. Former chronostratigraphic interpretations

Several chronostratigraphic interpretations of the Scladina sequence are available in the literature, reflecting different steps in the evolution of this type of research. They are mainly based on 3 distinct elements: palaeontology, radiometric dates, and magnetic susceptibility.

A few scientists have based their chronostratigraphic framework upon palaeontology through the classical climatostratigraphical approach (e.g., BASTIN, 1992; CORDY, 1992; CORDY & BASTIN, 1992; SIMONET, 1992; BONJEAN, 1998). The most important scheme, on which almost all the others are referring to, is that of BASTIN (1992). This scientist considered that the stratigraphic sequences of Scladina Cave and underlying Sous-Saint-Paul Cave are in continuity, with the exception of a small hiatus. He recorded palynological data from the top of the sedimentary sequence of Sous-Saint-Paul Cave (Layer VIII) that he interpreted as a “true signature of the beginning of the Eemian [...] and not any other interglacial” (BASTIN, 1992: 62¹). Therefore, all the subsequent climatic fluctuations were interpreted by reference to this system: the end of Eemian in former Layer 7A, after a small hiatus; Saint Germain I in former Layer 6; and Saint Germain II in former Layer 4A. However, this system is no longer valid (PIRSON,

2007; PIRSON et al., 2008). The succession of taxa that Bastin recorded in Layer VIII is indeed typical of the beginning of an interglacial (or an interstadial of an early glacial) but not only from the Eemian (e.g., TZEDAKIS, 1993; REILLE et al., 1998; DE BEAULIEU et al., 2006). In addition, several arguments suggest that the sedimentary filling of the 2 caves (Scladina and Sous-Saint-Paul) is separated by an important hiatus (HAESAERTS, 1992; PIRSON, 2007).

Dating specialists who have provided data for the Scladina sequence rarely risk interpreting their own results in terms of chronostratigraphy. They deliver raw data, sometimes carefully suggesting some scenarios, and frequently warn against the problems inherent in the different dating methods. For instance, M. GEWELT et al. (1992) restricted themselves to merely indicate the divergence between the palynological interpretation and the radiometric results, without taking sides, or even inferring that palynology-based interpretation is more valid. The high imprecision of most of the available dates in the sequence, especially for the lower half, does not allow for a reliable and accurate chronostratigraphic framework.

The chronostratigraphic interpretation based upon the magnetic susceptibility signal, proposed by ELLWOOD et al. (2004), does not appear convincing. These researchers consider that the sedimentary filling of Scladina Cave is characterized by a rather slow sedimentation rate comparable to that of marine sediments, and stated that this sedimentation rate is constant, the sequence thus being deprived of any important hiatuses. Following these principles, they consider the magnetic susceptibility curve as representative of a continuous succession of climate changes. Then, they position the available dates on this curve and extrapolate the age of the identified climatic events. This way of understanding sedimentogenesis in cave entrances is in total contradiction with recent studies of cave sedimentary processes (e.g., CAMPY & CHALINE, 1993; FERRIER, 2002; BERTRAN, 2006; TEXIER, 2007). The inadequacy of the slow continuous sedimentation rate model is even more obvious when looking at the recent reappraisal of the filling history of Scladina Cave (PIRSON, 2007; see Chapter 3).

The major conclusion is that the arguments employed so far that place the whole Scladina sequence in Upper Pleistocene are not reliable. Bastin's palynological demonstration situating the Eemian is no longer valid. Other palaeontological disciplines yield interesting palaeoenvironmental

¹ “véritable signature du début de l'Eemien (...) à l'exclusion de tout autre interglaciaire”

indications (§ 2), but do not provide any accurate chronostratigraphic information. The dates from the lower part of the sequence (units 7B to 3) do not provide the answer either, as they are compatible with the positioning of part of the sequence in the late Middle Pleistocene. In fact, given the available data from the literature, nothing firmly excludes part of the Scladina sequence from the Middle Pleistocene.

3.2. Scladina sequence chronostratigraphic framework: current status

As a consequence of the problems stated above, the chronostratigraphic framework of the Scladina sequence had to be reconsidered (PIRSON, 2007; PIRSON et al., 2008). Several analyses are still in progress in order to test and refine the new chronostratigraphical scheme, which remains rather inaccurate in the present state of research. The following data, integrating both former and new data in the light of the new stratigraphic framework, must therefore be considered as a preliminary synthesis.

3.2.1. Dates

3.2.1.1. Published dates

The Scladina sequence is the most dated Belgian prehistoric site, with more than 60 dates including ca. 40 reliable results. A synthesis of these results is available elsewhere (BONJEAN, 1998; PIRSON, 2007). All the reliable dates are presented in Figure 3. They can be divided into 2 groups: units 5 to 4A-POC in the lower part of the sequence, and units 1B-GR to H in the upper part. The other dates were considered as aberrant by their authors (e.g., OTTE et al., 1983; GEWELT et al., 1992) and have therefore been discarded here.

In the lower part of the sequence, despite the numerous results, very few layers provided radiometric data. Most of the available dates come from Sedimentary Complex 4 and particularly from Stalagmitic Floor CC4. All these dates are rather inaccurate (Figure 3). Standard deviations frequently reach 20 ka and are often coupled with a strong variability of dates for single events, or for single objects (e.g., a single stalagmitic floor sample provided several dates with an important scattering; GEWELT et al., 1992; BONJEAN, 1998). Another problem is the lack of a precise

stratigraphic position for the dated samples in comparison with the new stratigraphic record (see Chapter 3). Therefore, because of all these problems, the available dates cannot be used to either build an accurate chronological framework or to test and refine the chronostratigraphic framework deduced from the other disciplines. They can support several distinct hypotheses: from a strict radiometric point of view and taking the standard deviations into account, the dates obtained from the top of Sous-Saint-Paul sequence, from Unit 5, and from Sedimentary Complex 4 (including the date obtained directly on the Neandertal mandible) are overlapping. Stalagmitic Floor CC4 could, according to the numerous dates (synthesis in BONJEAN, 1998 and PIRSON, 2007; see also Figure 3), either record all MIS 5, only MIS 5a and/or MIS 5c, or even late MIS 6. The thermoluminescence date obtained on burnt flint from Unit 5 (130 ± 20 ka BP; HUXTABLE & AITKEN, 1992) as well as the gamma spectrometry date performed on the Neandertal mandible ($127 +46/-32$ kaBP; Falguères & Yokoyama in TOUSSAINT et al., 1998) are also compatible with several scenarios from MIS 6 to MIS 5, or even MIS 4 for the hominid mandible taking 2σ into account. Finally, the dates obtained from the top of Sous-Saint-Paul sequence, which should be older than Scladina sequence (see § 3.2.2), do not increase the precision, as they provided a similar chronological interval ranging from late Middle Pleistocene to early Upper Pleistocene: 130 ± 18 kaBP from Layer XII at the bottom of the sequence; 177 ± 17 to 93 ± 4 kaBP from Layer VIII at the top of the sequence (GEWELT et al., 1992).

In the upper part of the Scladina sequence, the published dates from former Layer 1A are neither particularly accurate nor precisely positioned in the new stratigraphic record. The few dates available for Unit H (Figure 3), either radiocarbon dates on calcite or U/Th date on an in situ speleothem, clearly point to a Holocene age, which is further supported by other data (§ 3.2.5).

3.2.1.2. New dates

Luminescence dating

In July 2006, a sample for luminescence dating was collected from Layer 4B-LI. The IRSL signal from coarse-grained alkali feldspars (40–60 microns) was used for dating the depositional age of this layer. The IRSL technique already tested on Middle Pleistocene loess sequences of Romania



(BALESCU et al., 2003) and NW France (BALESCU, 2004; BALESCU & TUFFREAU, 2004) was applied. The optical signal was recorded using a Corning 7-59/Schott BG39 blue transmitting filter combination (300-500 nm). The equivalent doses (ED) were determined using the additive gamma dose method on multigrain aliquots. The feldspars were stored for 1 year after laboratory irradiation in order to avoid the effect of short-term fading. Preheating at 160°C for 9 hours was done prior to taking IRSL measurements. The ED value is estimated at 420 ± 29 Gy. The external and internal contributions to the dose rate were estimated from the concentrations of U, Th, and K measured by neutron activation. The total dose rate for this sample is 3.24 ± 0.26 Gy/ka (see BALESCU et al., 2003 for further methodological details). The apparent IRSL age obtained is 129 ± 13 ka BP. A correction for long-term fading (MEJDAHL, 1988) has been applied using the apparent mean life ($t_2 = 516$ ka) estimated on infinitely old alkali feldspars from a Tertiary or Early Quaternary (?) deposit lying on top of the plateau, nearby the cave. It yielded a corrected IRSL age of 153 ± 15 ka BP (see BALESCU et al., 1997 for further details on the correction protocol).

This IRSL result suggests a MIS 6 age for Unit 4B-LI, consistent with the high green amphibole content of the layer (see § 3.2.4.1). This loess was thus deposited during MIS 6 outside or near the entrance of the cave. However, it was later reworked over a short distance within the cave, probably under very dim light conditions; therefore, the estimation of the age of the deposition of Layer 4B-LI is not possible to obtain from the IRSL result alone, it needs the integration of the results from other disciplines (see § 3.2.4.1).

Radiocarbon dating

In November 2006, new ^{14}C dates were obtained from the upper part of the sequence (PIRSON, 2007; PIRSON et al., 2008). They considerably improve the chronology. In particular, 3 new ^{14}C dates obtained in layers 1B-GRH (GrA-32581: 43,150 +950/-700 BP), 1A-GK (GrA-32635: 40,210 +400/-350 BP), and T-GV (GrA-32633: 37,300 +400/-300 BP) lead to define a rather accurate

chronostratigraphic framework for this part of the stratigraphy, which can be attributed to MIS 3. Some already published dates (GEWELT et al., 1992; BONJEAN, 1998) are compatible with these new results, although they are less accurate. This allows the age of Middle Palaeolithic material from former Layer 1A to be refined to between 40 and 37 kaBP (ABRAMS et al., 2010; BONJEAN et al., 2011).

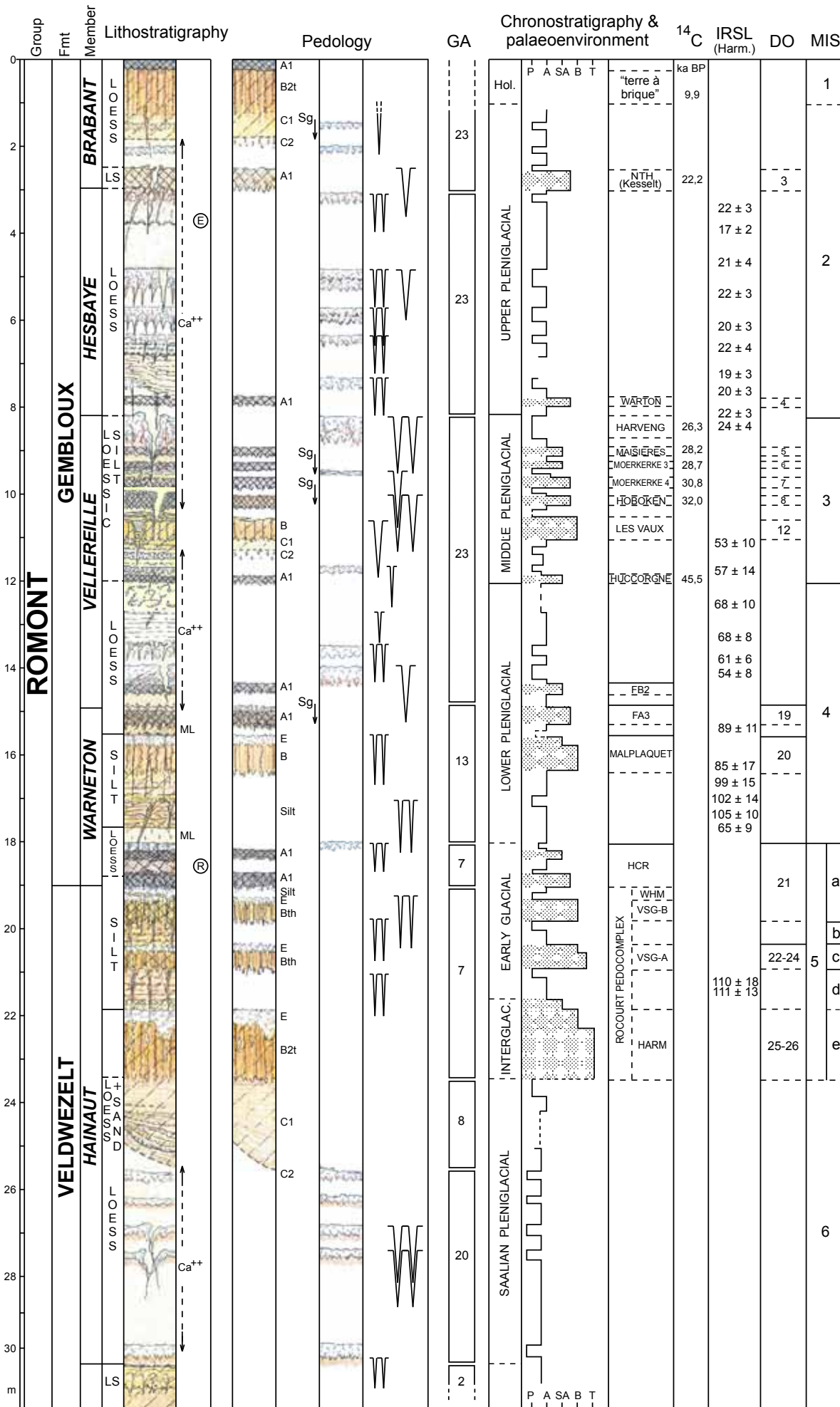
3.2.2. Biostratigraphy

The ursids are the dominant taxa in the faunal collections from the Caves of Sclayn. The only bears recognized so far in the Scladina deposits are *Ursus spelaeus* and *Ursus arctos* (SIMONET, 1992; PATOU-MATHIS, 1998^a). From a biostratigraphical point of view, the presence of *U. spelaeus* indicates that the Scladina sequence could span between the end of Middle Pleistocene and Upper Pleistocene (e.g., ARGANT & PHILIPPE, 2002), which remains rather inaccurate. However, SIMONET (1992) did not study Unit 7B, and in Unit 7A the bear remains were too poor to “carry out a fruitful study²” (SIMONET, 1992: 132).

On the other hand, in the sequence from Sous-Saint-Paul Cave (SIMONET, 1992; NIEUWLAET, 2007; GOUBEL, 2011), the ursid remains showed features from both *Ursus spelaeus* and *Ursus deningeri*. The transition between these 2 species is known to be gradual, following a mosaic-like evolutionary path (ARGANT & PHILIPPE, 2002; M. Germonpré, pers. comm.). Therefore, interpreting this information is difficult. Regardless, this tends to confirm the existence of a major hiatus between the Sous-Scladina and Scladina sequences (i.e., between Sous-Saint-Paul Layer VIII and Scladina former Layer VII/7A). In Belgium, very few data are available on bear evolution. Moreover, the sequences, which are accurately dated from the end of Middle Pleistocene and from the beginning of Upper Pleistocene, are very rare. In La Belle-Roche Cave, *Ursus deningeri* is present but in much older deposits (at least 500 ka; CORDY et al., 1992, 1993; see also PIRSON & DI MODICA, 2011). In the sequence of Walou Cave,

²“réaliser une étude fructueuse”

Figure 4 (facing page): The Middle Belgium loess reference sequence. Sg = segregation ice; GA = % of green amphibole in the silty fraction (values = average % from Table 1); P = polar; A = arctic; SA = sub-arctic; B = boreal; T = temperate; NTH = Nagelbeek tongued horizon; HCR = Humiferous Complex of Remicourt; WHM = Whitish horizon of Momalle; VSG-B and VSG-A = Villers-Saint-Ghislain B and A Soils; HARM = Harmignies Soil; IRSL: infrared optically stimulated luminescence (Harmignies, after FRECHEN et al., 2001); DO = Dansgaard-Oeschger events; MIS = marine oxygen isotopic stages.



in the deposits attributed to the end of MIS 6 and to MIS 5 (PIRSON et al., 2006; PIRSON, 2011), bear species were confined to *Ursus spelaeus* (DE WILDE, 2011).

The other species found in Scladina, including small mammals, have not yet been studied from a strict biostratigraphical point of view.

3.2.3. Archaeostratigraphy

Archaeological data does not greatly aid in the chronostratigraphic problem of the Scladina sequence. Still, some information can be gathered.

In former layers 5 and 1A, Mousterian lithic material has been unearthed (e.g., OTTE et al. (dir.), 1998; LOODTS & BONJEAN, 2004; DI MODICA, 2010; BONJEAN et al., 2011; see also Chapter 2). Recently, Mousterian artefacts were found in Layer 1A-GL and in Unit T. By comparison with the rare reliable chronological data that are available for the end of Middle Palaeolithic in Belgium (TOUSSAINT, 1988; OTTE et al., 1998; FLAS, 2006; PIRSON et al., 2006; TOUSSAINT et al., 2010; PIRSON, 2011; PIRSON et al., 2012), and if the dated material from Unit T is not reworked, the deposits from Unit T downwards should be older than ca. 40-35 kaBP.

The top of the Scladina sequence has yielded some rare Upper Palaeolithic remains in secondary position (OTTE, 1998), as well as anatomically modern human bones suggesting a multiple burial that is Holocene in age (OTTE et al., 1983: 141).

3.2.4. Comparison with the loess sequence

The data gathered within the last 60 years about Upper Pleistocene in the Middle Belgium loess belt has led to the construction of a well-documented pedostratigraphic sequence (e.g., HAESAERTS et al., 1999, 2011^a; HAESAERTS, 2004; PIRSON, 2007; PIRSON et al., 2009). This loess sequence is actually the most complete record for Upper Pleistocene

in Belgium and therefore acts as a reference sequence. It is presented in Figure 4.

In Belgium, the non-carbonated fine fraction from cave entrance deposits is almost entirely made of silt with a loessic origin (EK et al., 1974; CHEN et al., 1988; PIRSON, 1999; PIRSON & DRAILY, 2011). This is also true for Scladina deposits (GULLENTOPS & DEBLAERE, 1992; HAESAERTS, 1992; PIRSON, 2007) and allows detailed correlations between these karstic sequences and the loess reference sequences from Middle Belgium (PIRSON et al., 2006; PIRSON, 2007, 2011). In the case of Scladina Cave, the most useful tool for comparison with the loess sequence is the mineralogical signature of the silt fraction. A few other data (lithological and pedological markers) complete the system.

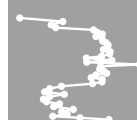
3.2.4.1. Heavy mineralogy

In the loess sequences from middle Belgium and northwestern France, one of the most useful minerals for chronostratigraphic reconstructions is green amphibole (e.g., JUVIGNÉ, 1978; BAILESCU, 1988; MEIJS, 2002). The available green amphibole (GA) data for Middle and Upper Pleistocene are rather numerous (e.g., GULLENTOPS, 1954; JUVIGNÉ, 1978; BAILESCU & HAESAERTS, 1984; BAILESCU, 1986, 1988; MEIJS, 2002; BAILESCU, 2004; BAILESCU & TUFFREAU, 2004). The integration of all the GA data, which can be accurately positioned in the detailed loess reference sequence of Middle Belgium (see PIRSON, 2007), led to the synthesis presented in Table 1.

Several researchers have studied the heavy mineralogy of the silt fraction at Scladina (GULLENTOPS & DEBLAERE, 1992; BAILESCU in HAESAERTS, 1992; BAILESCU in PIRSON, 2007; PIRSON, 2007). The comparison between the GA distributions in Scladina (Figure 3) and in the Belgian loess belt (Figure 4 & Table 1) indicates that with a GA fraction of 12 to 33%, former layers 7A to 2B carry the signature of either late Saalian or Weichselian loess (MIS 6 or MIS 4-2; HAESAERTS,

Table 1 (facing page): Synthesis of the green amphibole data from the Middle Belgian loess belt (after PIRSON, 2007; data from GULLENTOPS, 1954; JUVIGNÉ, 1978; BAILESCU, 1988; MEIJS, 2002). The lithostratigraphic divisions are based on the new lithostratigraphic scale of Middle Belgium Loess (from HAESAERTS et al., 2011^a). MIS = marine oxygen isotopic stages; A-loess to E-loess: nomenclature of Pleistocene loess following MEIJS (2002); NTH = Nagelbeek tongued horizon; HCR = Humiferous Complex of Remicourt; N1 to N5 = 5 'Nassboden' (tundra gleys) in the lower MIS 6 loess (lower B-loess); Harveng, Les Vaux, Huccorgne, Malplaquet, Rocourt pedocomplex, Hees pedocomplex, Montenaken pedocomplex, and Pottenberg pedocomplex: major pedological units (see MEIJS, 2002 and HAESAERTS et al., 2011^a). Mean values: average GA values (in %) calculated from the available data from the literature; N = number of samples; Range of % = minimal and maximal values.

Chronostratigraphy		MIS	Lithostratigraphy		Mean values	N	Range of %		
HOLOCENE		1	GEMBLOUX FORMATION	Brabant Member	Luvisol	23	14	16.2 to 34	
U P P E R P L E I S T O C E N E	Upper Pleniglacial	2			Hesbaye Member				Decalcified A-loess
									Calcareous A-loess
	Middle Pleniglacial	3			Vellereille Member				NTH
				Harveng					
	Lower Pleniglacial	4		Warneton Member	Les Vaux	23	11	16 to 35	
					Huccorgne				
					A-loess				
					FA3				
	Early Glacial	5a to 5d		Hainaut Member (top)	Malplaquet	7	6	5 to 8	
			A-loess						
M I D D L E P L E I S T O C E N E	Eemian	5e	VELDWEZELT FORMATION	Humic complex of Remicourt (CHR)	7	23	3.1 to 18		
				Rocourt pedocomplex					
	6		Hainaut Member (bottom)	Upper B-loess	8	8	4.2 to 11		
				N5					
				Lower B-loess					
				N4					
				Lower B-loess					
				N3					
				Lower B-loess					
				N2					
Lower B-loess									
7		Vlijtingen Member	N1	2	8	0.7 to 2.7			
			Lower B-loess						
8		Riemst Member	Hees pedocomplex	1	3	0.4 to 0.9			
			C-loess						
9		Op de Schans Member	Humic complex	0.4	1	0.4			
			Montenaken pedocomplex						
10			D-loess						
			Pottenberg pedocomplex						
11			E-loess						
12									



1992; PIRSON, 2007). The attribution of this part of the sequence to MIS 7 can be discarded because GA content is too high. In addition, the presence of low GA values in the overlying deposits (Unit 2A) as well as interglacial or early glacial conditions in former layers 6 and 4A (§ 2) rule out the Weichselian hypothesis. The silts with high GA values from Scladina sedimentary units 7A to 2B must therefore result from the reworking of late Saalian loess (MIS 6), which is corroborated by the IRSL date from Layer 4B-LI (see § 3.2.1.2). The late MIS 6 loesses, which have low GA content, are thus absent in Scladina, as in some loess sections from northwestern France (Cagny-la-Garenne, Sourdon or Sangatte: BALESU, 1986). In this context, temperate conditions recorded in units 6B-6A and in former Layer 6 (PIRSON et al., 2008; see also § 3.2.5) point to a MIS 5 age and indicate that from Unit 6B upward, the sequence can be positioned in Upper Pleistocene. Units 7A to 6C, with rather high GA concentrations (12–22%), should be positioned either in MIS 6 or in MIS 5. This data set indicates that most of the Scladina stratigraphic sequence belongs to the Upper Pleistocene. The part of the sequence that could belong to Middle Pleistocene amounts to units 7B to 6C. The GA values from former Layer 7B must be considered with caution because of the probable mixing between loess and the alluvial sediments reworked from the plateau.

The decrease of GA in former Layer 2A (ca. 3–12%) suggests, together with other data (§ 3.2.4.2), a new allochthonous loessic input in the sequence. Compared to the Belgian loess sequence, this silt with low GA content observed above silt with high GA content must correspond to loess from either late MIS 6 or early MIS 4, or even late MIS 6 loess reworked during MIS 5. This, combined with its stratigraphic position above sediments with an interglacial or early glacial signature, suggests an early MIS 4 age. However, no important allochthonous loessic inputs are recorded in early MIS 4 in the Belgian loess-belt, and very few GA data are available in this part of the loess sequence. Therefore, further analyses are required.

3.2.4.2. Lithological markers

Two aeolian inputs attributable to the Upper Pleistocene could be recorded as reworked loessic material in the Scladina sequence. Unit 2A probably records the first allochthonous Upper

Pleistocene loessic deposit in the sequence; several arguments led to the proposition of the positioning of Unit 2A in Weichselian Lower Pleniglacial (PIRSON, 2007; PIRSON et al., 2008). The second allochthonous loessic input is represented by the deposits from Unit J. Given their position in the stratigraphic sequence of Scladina, as well as the comparison with other sequences either in a loessic context (e.g., HAESAERTS et al., 1997; HAESAERTS, 2004) or in a cave entrance context (Walou Cave: PIRSON et al., 2006; *Trou Al'Wesse*: PIRSON, 1999; Abri supérieur of Goyet: TOUSSAINT et al., 1999), they are interpreted, in the current state of research, as probably resulting from the reworking of Weichselian Upper Pleniglacial loess (MIS 2; PIRSON, 2007).

3.2.4.3. Pedological markers

The highly humiferous sediment from Unit 2B has been interpreted as the result of the reworking of an important humiferous palaeosol, suggesting a strong interstadial (PIRSON, 2007; PIRSON et al., 2008). This hypothesis is further supported by palynological and anthracological data (PIRSON et al., 2008), as well as by magnetic susceptibility data (ELLWOOD et al., 2004). The stratigraphic position of Unit 2B and the correlation with the loess reference sequence indicate that this unit could correspond to the Humiferous Complex of Remicourt, a key marker of the Belgian loess belt (HAESAERTS et al., 1999, 2011^a, 2011^b). In this case, Unit 2B would belong to the end of Weichselian Early Glacial (Figure 4). The GA content from Unit 2A is consistent with this attribution (compare Figure 3, Figure 4 & Table 1). The high GA values from Unit 2B are not a problem since the humic soil could have been developing on OIS 6 colluvial material (as already suggested by the GA distribution in underlying units). If the presence of the Rocourt Tephra in Unit 2B was confirmed (although it is still hypothetical; PIRSON, 2007), the correlation between Unit 2B and the Humiferous Complex of Remicourt would be demonstrated, as this tephra is classically found in this humic complex in the Belgian loess belt (e.g., GULLENTOPS, 1954; HAESAERTS et al., 1997; JUVIGNÉ et al., 2008; POUCLÉ et al., 2008; PIRSON & JUVIGNÉ, 2011).

The important climatic improvement recorded in Unit 1B-BRUN could be positioned at the bottom of Weichselian Lower Pleniglacial. It would then be an equivalent to the Malplaquet soil of the loess

reference sequence, correlated by HAESAERTS (2004) with the Dansgaard-Oeschger event 20 (DO 20) from the Greenland ice records (DANSGAARD et al., 1993; GROOTES et al., 1993). Weak GA values observed in former Layer 1B (6–10%; Figure 3) are consistent with this hypothesis, with this mineral becoming much more abundant in the major loessic input from Velereille Member (16–35%, with a mean value of ca. 23%; Figure 4 & Table 1).

On the cave terrace, below the cave porch, an in situ brown soil has been observed on top of former Layer 1B (HAESAERTS, 1992). Given its nature and stratigraphic position, it could correspond to Les Vaux soil described in the Middle Belgian loess reference sequence in Harmignies (HAESAERTS & VAN VLIET, 1974) and Remicourt (HAESAERTS et al., 1997) from the Weichselian Middle Pleniglacial (Figure 4). As far as its facies and stratigraphic position are concerned, Les Vaux soil exhibits close similarities with the Bohunice soil described in Moravia (VALOCH, 1976) and the Willendorf Interstadial described in Austria (HAESAERTS, 1990; HAESAERTS & TEYSSANDIER, 2003). These pedological markers represent a single interstadial event dated between ca. 42,000 and ca. 40,000 BP in the Middle Danube Basin. This correlation is further supported by the new radiocarbon dates bracketing the top of 1B-GRI between 43 and 40 kaBP. The existence of an equivalent to the Les Vaux soil has also been proposed for 2 other Belgian cave entrance sequences: Walou Cave (PIRSON et al., 2006; PIRSON, 2011) and the Trou de l'Abîme in Couvin (TOUSSAINT et al., 2010), which both yielded Neandertal remains. In these 2 caves, the correlation with the Les Vaux soil is also supported by new radiocarbon data. According to HAESAERTS (2004), Les Vaux soil can be correlated with the DO 12 from the Greenland records.

3.2.5. Climastratigraphy

The palaeoenvironmental data from the Scladina sequence has been presented for units 5 to 3-SUP in § 2; this is not the place to present a synthesis of the whole sequence (see PIRSON, 2007; PIRSON et al., 2008). Figure 3 shows a summary of Scladina palaeoclimatic record.

No chronostratigraphical information can be directly drawn from this data set. Nevertheless, it evidences a succession of climatic events that cannot be positioned anywhere in the Pleistocene. The significance of some of the climatic changes

recorded in Scladina still has to be completed by further analyses, specifically through palynological analyses from speleothems.

Palaeozoological and palaeobotanical data clearly show the existence of major climatic improvements in former layers 6 and 4A and in new units 6B/6A and 4A-AP/4A-IP. A wooded temperate to boreal environment is thus attested by data from palynology (mesophilous taxa including *Quercus* and *Ulmus*: BASTIN, 1992; § 3), large herbivores (important presence of forested taxa, notably *Dama dama*: SIMONET, 1992) and small mammals (*Apodemus*, *Clethrionomys*, and Chiroptera: CORDY, 1992). These elements suggest the attribution of units 6B, 6A, 4A-AP, and 4A-IP (especially Speleothem CC4) to an interstadial of an early glacial or even to an interglacial without establishing whether or not they belong to either MIS 5 or another interglacial complex from the Middle Pleistocene. The chronostratigraphic interpretation can be refined if this information is compared to the heavy mineralogy data from the silt fraction (§ 3.2.4.1); units 6B/6A and 4A-AP/4A-IP could then be attributed to either the Eemian or Weichselian Early Glacial. However, it is not possible in the present state of research to precise the attribution of these 2 major climatic improvements inside MIS 5. Furthermore, the beginning and the end of MIS 5 are difficult to position in the Scladina sequence. The beginning of MIS 5 (stage 5e, Eemian) could be either missing or recorded in units 6B/6A. As for the end of MIS 5, the best current hypothesis positions Unit 2A in the Weichselian Lower Pleniglacial (MIS 4), with Unit 2B recording the end of MIS 5a.

Because of its low GA content, the major climatic improvement of Unit 1B-BRUN could belong to the Weichselian early Lower Pleniglacial (§ 3.2.4.3). The brown soil evidenced on the terrace seems to correspond to Les Vaux soil, which is further supported by the new radiocarbon dates (§ 3.2.4.3). The rest of the sequence records cold, stepic conditions. The stratigraphic position of these deposits, between Les Vaux soil and the Weichselian Upper Pleniglacial (Unit J), indicate that they belong to the Weichselian Middle Pleniglacial.

Finally, the Holocene age of Unit H is demonstrated by its stratigraphic position on top of the sequence, by some dates (§ 3.2.1), by palynology (BASTIN, 1992), as well as by geology (stalagmitic floors and important biological activity in the sediments; PIRSON, 2007).



3.3. Chronostratigraphic synthesis

All of the results that contribute to the chronostratigraphic framework of the Scladina sequence have been reconsidered; henceforth, most of the Scladina deposits can confidently be positioned in the Upper Pleistocene. The most accurate and reliable information comes from the combination of climatostratigraphy and the correlation with the Middle Belgium loess sequence. Data from other disciplines are compatible with this chronostratigraphic scheme.

However, the chronostratigraphic framework currently remains rather inaccurate. Several hypotheses can be considered, for instance those concerning the location of the beginning and end of MIS 5. The most reliable framework in the present state of research is presented in Figure 3. Considering all disciplinary approaches, the 2 units that indicate temperate forest conditions (i.e., Stalagmitic Floor CC4 in Unit 4A-IP and units 6B/6A) must be situated inside MIS 5. Whether they represent MIS 5e and 5c, or MIS 5c and 5a, or some other combination is still unknown.

4. Conclusions and prospects

The new palaeoenvironmental results from the Scladina Cave sequence, obtained from the reappraised stratigraphic record, indicate a very good concordance between palynology, anthracology, and geology. Furthermore, these new results correlate with the data from literature based on the former stratigraphic record. The reproducibility of the results and therefore the viability of the recorded climatic fluctuations are thus strengthened.

With the high complexity of the climatic signal recorded in Scladina, the site appears to be an exceptional reference for the Upper Pleistocene in Belgium, together with the Walou Cave sequence (PIRSON et al. (dir.), 2011; DRAILY et al. (dir.), 2011). Apart from a few rare loess sequences from Middle Belgium (e.g., HAESAERTS, 2004; PIRSON et al., 2009), no other sedimentary record in Belgium is as complex. These results demonstrate that rapid climatic events can be recorded in cave entrance sequences in Belgium.

However, the lack of precision of the Scladina chronostratigraphic framework is a concern when positioning fluctuations in the sequence inside the climatically complex Upper Pleistocene (e.g., DANSGAARD et al., 1993; GROOTES et al., 1993).

A better knowledge of the chronostratigraphic framework is therefore necessary. Several analyses in progress should improve the chronostratigraphic framework. Locating the Rocourt Tephra is essential; this tephra is a very good chronostratigraphical marker in Belgium (JUVIGNÉ et al., 2008; POUCKET et al., 2008) and has been proven to be very useful in cave sequences (PIRSON et al., 2006; PIRSON & JUVIGNÉ, 2011). New dating in carefully selected layers, especially in the lower part of the sequence (notably U/Th dates on speleothems), is another key point. New heavy mineral analyses will also be very useful, since very good results have recently been obtained for the Upper Pleistocene in several key loess sequences from Middle Belgium (SPAGNA et al., in preparation).

Other analyses that aim to refine the palaeoenvironmental data from Scladina Cave are also in progress. One of the priorities is the obtention of complementary palynological data, notably from speleothems other than CC4 (mainly those from Unit 6B), in order to try to determine their palaeoenvironmental signature and thus refine the climatostratigraphic signal. Analysis of the faunal material recently excavated in the new stratigraphic record would also contribute to improve the climatostratigraphical data.

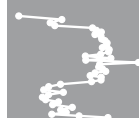
Acknowledgements

The authors are very grateful indeed to Rhylan McMillan for his valuable help in translating the manuscript into correct English. We especially thank Michel Toussaint (Service public de Wallonie), Grégory Abrams, and Kévin Di Modica (Archéologie Andennaise) for their constant support and many discussions about Scladina, as well as to Mietje Germonpré (Royal Belgian Institute of Natural Sciences) for a discussion about biostratigraphy. We also gratefully acknowledge Joël Éloy (Association wallonne d'Études mégalithiques) and Eric Dermience (Royal Belgian Institute of Natural Sciences) for their technical assistance. This work was made possible by funding to SP through an Action 2 project from the Belgian Science Policy.

References

ABRAMS G., BELLO S. M., DI MODICA K., PIRSON S. & BONJEAN D., 2014. When Neanderthals used cave bear (*Ursus spelaeus*) remains: Bone

- retouchers from unit 5 of Scladina Cave (Belgium). *Quaternary International*, 326-327: 274-287.
- ABRAMS G., BONJEAN D., DI MODICA K., PIRSON S., OTTE M. & PATOU-MATHIS M., 2010. Les os brûlés de l'ensemble sédimentaire 1A de *Scladina* (Andenne, Belgique) : apports naturels ou restes de foyer(s) néandertalien(s) ? *Notae Praehistoricae*, 30: 5-13.
- ARGANT A. & PHILIPPE M., 2002. Les ours et leur évolution. In T. TILLET & L. R. BINFORD (dir.), *L'ours et l'homme*. Actes du colloque d'Auberives-en-Royans, 1997. Études et Recherches Archéologiques de l'Université de Liège, 100: 17-26.
- BALESCU S., 1986. La minéralogie des loess du Nord de la France et la position stratigraphique des paléosols intraloessiques. In A. TUFFREAU & J. SOMMÉ (eds.), *Chronostratigraphie et faciès culturels du Paléolithique inférieur et moyen dans l'Europe du Nord-Ouest*. Actes du Colloque international organisé à Lille (4-6 septembre 1984), 22^e Congrès Préhistorique de France (Supplément au Bulletin de l'AfeQ), Paris, Société Préhistorique Française et Association française pour l'étude du Quaternaire, 26 : 165-170.
- BALESCU S., 1988. *Apports de la thermoluminescence à la stratigraphie et à la sédimentologie des loess saaliens du NW de l'Europe*, PhD thesis, Université libre de Bruxelles, 2 vol., 199 p. & 144 p.
- BALESCU S., 2004. *Datation par luminescence des sédiments quaternaires et exploration des champs d'application de la méthode (archives paléoclimatiques, paléorivages, géoarchéologie et risques naturels)*. Habilitation thesis, Université des Sciences et Technologies de Lille, 191 p.
- BALESCU S. & HAESAERTS P., 1984. The Sangatte raised beach and the age of the opening of the Strait of Dover. *Geologie en Mijnbouw*, 63: 355-362.
- BALESCU S., LAMOTHE M. & LAUTRIDOU J.-P., 1997. Luminescence evidence for two Middle Pleistocene interglacial events at Tourville, north-western France. *Boreas*, 26: 61-72.
- BALESCU S., LAMOTHE M., MERCIER N., HUOT S., BALTEANU D., BILLARD A. & HUS J., 2003. Luminescence chronology of Pleistocene loess deposits from Romania: testing methods of age correction for anomalous fading in alkali feldspars. *Quaternary Science Reviews*, 22/10-13: 967-973.
- BALESCU S. & TUFFREAU A., 2004. La phase ancienne du Paléolithique moyen dans la France septentrionale (stades isotopiques 8 à 6) : apports de la datation par luminescence des séquences loessiques. *Archaeological almanac*, 16: 5-22.
- BASTIN B., 1990. L'analyse pollinique des concrétions stalagmitiques: méthodologie et résultats en provenance des grottes belges. *Karstologia Mémoire*, 2: 3-10.
- BASTIN B., 1992. Analyse pollinique des sédiments détritiques, des coprolithes et des concrétions stalagmitiques du site préhistorique de la grotte Scladina (province de Namur, Belgique). In M. OTTE (ed.), *Recherches aux grottes de Sclayn, vol. 1: Le Contexte*. Études et Recherches Archéologiques de l'Université de Liège, 27: 59-77.
- BASTIN B., CORDY J.-M., GEWELT M. & OTTE M., 1986. Fluctuations climatiques enregistrées depuis 125.000 ans dans les couches de remplissage de la grotte Scladina (province de Namur, Belgique). *Bulletin de l'Association française pour l'étude du Quaternaire*, 2^e série, 25-26: 168-177.
- BASTIN B. & SCHNEIDER A.-M., 1984. Palynologie. In C. EK & K.-H. PFEFFER (eds.), *Le karst belge*. Karstphänomene in Nordrhein-Westfalen, Cologne, Kölner Geographische Arbeiten, 45: 87-93.
- DE BEAULIEU J.-L., ANDRIEU-PONEL V., CHEDDADI R., GUITER F., RAVAZZI C., REILLE M. & ROSSI S., 2006. Apport des longues séquences lacustres à la connaissance des variations des climats et des paysages pléistocènes. *Comptes Rendus Palevol*, 5: 65-72.
- BERTRAN P. (dir.), 2004. *Dépôts de pente continentaux. Dynamique et faciès*, Paris, Quaternaire, hors-série, 1, 259 p.
- BERTRAN P., 2006. *Dépôts de versant et application au Paléolithique. Processus de formation des sites dans les porches de grottes et d'abris en Aquitaine*. Bordeaux, Thèse inédite d'Habilitation à Diriger des Travaux, Université de Bordeaux 1, 70 p.
- BONJEAN D., 1998. Chronologie à la grotte Scladina. In M. OTTE, M. PATOU-MATHIS & D. BONJEAN (dir.), *Recherches aux grottes de Sclayn, vol. 2: L'Archéologie*. Études et Recherches Archéologiques de l'Université de Liège, 79: 45-57.
- BONJEAN D., DI MODICA K., ABRAMS G., PIRSON S. & OTTE M., 2011. La grotte Scladina : bilan 1971-2011. In M. TOUSSAINT, K. DI MODICA & S. PIRSON (sc. dir.), *Le Paléolithique moyen en Belgique. Mélanges Marguerite Ulrix-Closset*. Bulletin de la Société royale belge d'Études



Géologiques et Archéologiques *Les Chercheurs de la Wallonie*, hors-série, 4 & Études et Recherches Archéologiques de l'Université de Liège, 128: 323-334.

CAMPY M. & CHALINE J., 1993. Missing Records and Depositional Breaks in French Late Pleistocene Cave Sediments, *Quaternary Research*, 40: 318-331.

CHEN Z., EK C. & LACROIX D., 1988. Sédimentologie de quelques loess de la grotte Walou, à Trooz. *Bulletin de la Société royale belge d'Études Géologiques et Archéologiques Les Chercheurs de la Wallonie*, 28: 6679.

CORDY J.-M., 1984. Évolution des faunes quaternaires en Belgique. In D. CAHEN & P. HAESAERTS (eds.), *Peuples chasseurs de la Belgique préhistorique dans leur cadre naturel*, Bruxelles: 67-77.

CORDY J.-M., 1988. Apport de la paléozoologie à la paléocologie et à la chronostratigraphie en Europe du nord-occidental. In H. LAVILLE (ed.), *L'Homme de Néandertal, vol. 2: L'Environnement*. Études et Recherches Archéologiques de l'Université de Liège, 29: 55-64.

CORDY J.-M., 1992. Bio- et chronostratigraphie des dépôts quaternaires de la grotte Scladina (province de Namur, Belgique) à partir des micromammifères. In M. OTTE (ed.), *Recherches aux grottes de Sclayn, vol. 1: Le Contexte*. Études et Recherches Archéologiques de l'Université de Liège, 27: 79-125.

CORDY J.-M. & BASTIN B., 1992. Synthèse des études paléontologiques réalisées dans les dépôts de la grotte Scladina (Sclayn, province de Namur). In M. OTTE (ed.), *Recherches aux grottes de Sclayn, vol. 1: Le Contexte*. Études et Recherches Archéologiques de l'Université de Liège, 27: 153-156.

CORDY J.-M., BASTIN B., EK C., GEERAERTS R., OZER A., QUINIF Y., THOREZ J. & ULRIX-CLOSSET M., 1992. La Belle-Roche (Sprimont, Belgium): the Oldest Archaeological Site in the Benelux. A report on a Field Trip. In M. TOUSSAINT (ed.), *Cinq millions d'années, l'aventure humaine*. Études et Recherches Archéologiques de l'Université de Liège, 56: 287-301.

CORDY J.-M., BASTIN B., FAIRON-DEMARET M., EK C., GEERAERTS R., GROESSENS-VAN DYCK M.-C., OZER A., PEUCHOT R., QUINIF Y., THOREZ J. & ULRIX-CLOSSET M., 1993. La grotte de la Belle Roche (Sprimont, Province de Liège) : un gisement

paléontologique et archéologique d'exception au Benelux. *Académie royale de Belgique. Bulletin de la Classe des Sciences, 6^e série*, 4: 165-186.

DANSGAARD W., JOHNSEN S. J., CLAUSEN H. B., DAHL-JENSEN D., GUNDESTRUP N. S., HAMMER C. U., HVIDBERG C. S., STEFFENSEN J. P., SVEINBJÖRNSDÓTTIR A. E., JOUZEL J. & BOND G., 1993. Evidence for general instability of past climate from a 250-kyr ice-core record. *Nature*, 364: 218-220.

DE WILDE B., 2011. Les macromammifères pléistocènes de la grotte Walou. In C. DRAILY, S. PIRSON & M. TOUSSAINT (dir.), *La grotte Walou à Trooz (Belgique). Fouilles de 1996 à 2004, vol. 2: Les sciences de la vie et les datations*. Namur, Service public de Wallonie, IPW, Études et Documents, Archéologie, 21: 14-27.

DI MODICA K., 2010. *Les productions lithiques du Paléolithique moyen de Belgique: variabilité des systèmes d'acquisition et des technologies en réponse à une mosaïque d'environnements contrastés*. Unpublished PhD thesis. Université de Liège, Faculté de Philosophie et Lettres & Museum National d'Histoire Naturelle, Département de Préhistoire, 787 p.

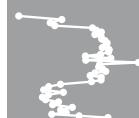
DRAILY C., PIRSON S. & TOUSSAINT M. (dir.), 2011. *La grotte Walou à Trooz (Belgique). Fouilles de 1996 à 2004, vol. 2: Les sciences de la vie et les datations*. Namur, Service public de Wallonie, IPW, Études et Documents, Archéologie, 21, 241 p.

EK C., ALEXANDRE-PYRE S. & JUVIGNÉ E., 1974. Étude sédimentologique dans la grotte de Remouchamps. In M. DEWEZ, H. BRABANT, J. BOUCHUD, M. CALLUT, F. DAMBLON, M. DEGERBOL, C. EK, H. FRÈRE & E. GILOT (eds.), *Nouvelles recherches à la Grotte de Remouchamps*. Bulletin de la Société royale belge d'Anthropologie et de Préhistoire, 85: 16-41.

ELLWOOD B. B., HARROLD F. B., BENOIST S. L., THACKER P. T., OTTE M., BONJEAN D., LONG G. J., SHAHIN A. M., HERMANN R. P. & GRANDJEAN F., 2004. Magnetic susceptibility applied as an age-depth-climate relative dating technique using sediments from Scladina Cave, a Late Pleistocene cave site in Belgium. *Journal of Archaeological Science*, 31: 283-293.

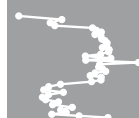
FERRIER C., 2002. Les dépôts d'entrée de grotte. In J.-C. MISKOVSKY (ed.), *Géologie de la préhistoire*, Paris, Association pour l'étude de l'environnement géologique de la préhistoire: 189-205.

- FLAS D., 2006. La transition du Paléolithique moyen au supérieur dans la plaine septentrionale de l'Europe. Les problématiques du Licombien-Ranisien-Jerzmanowicien. Unpublished PhD thesis, Université de Liège, 2 vol., 370 p. & 315 pl.
- FRECHEN M., VAN VLIET-LANOË B. & VAN DEN HAUTE P., 2001. The Upper Pleistocene loess record at Harmignies/Belgium – high resolution terrestrial archive of climate forcing. *Palaeogeography, Palaeoclimatology, Palaeoecology*, 173: 175–195.
- GEWELT M., SCHWARCZ H. P. & SZABO B. J., 1992. Datations $^{230}\text{Th}/^{234}\text{U}$ et ^{14}C de concrétions stalagmitiques de la grotte Scladina. In M. OTTE (ed.), *Recherches aux grottes de Sclayn, vol. 1: Le Contexte*. Études et Recherches Archéologiques de l'Université de Liège, 27: 159–172.
- GOUBEL H., 2011. *Analyse des contours dentaires des ursidés pléistocènes et actuels: caractérisation et étude des causes de la variabilité morphologique des dents jugales*. Unpublished PhD thesis, Université de Lille 1, 391 p.
- GROOTES P. M., STUIVER M., WHITE W. C., JOHNSEN S. J. & JOUZEL J., 1993. Comparison of oxygen isotope records from the GISP2 and GRIP Greenland ice cores. *Nature*, 366: 552–554.
- GULLENTOPS F., 1954. *Contributions à la chronologie du Pléistocène et des formes du relief en Belgique*, Louvain, Mémoires de l'Institut géologique de l'Université de Louvain, 18: 125–252.
- GULLENTOPS F. & DEBLAERE C., 1992. Érosion et remplissage de la grotte Scladina. In M. OTTE (ed.), *Recherches aux grottes de Sclayn, vol. 1: Le Contexte*. Études et Recherches Archéologiques de l'Université de Liège, 27: 9–31.
- HAESAERTS P., 1983. Stratigraphic distribution of periglacial features indicative of permafrost in the Upper Pleistocene loesses of Belgium. In T. L. PEWE & J. BROWN (eds.) *Permafrost Fourth International Conference, proceedings. Fairbanks, Alaska, July 17–22, 1983*. Washington, D.C., National Academy Press: 421–426.
- HAESAERTS P., 1990. Évolution de l'environnement et du climat au cours de l'interpléni-glaciaire en Basse Autriche et en Moravie. In J. K. KOZŁOWSKI (ed.), *Feuilles de pierre. Les industries à pointes foliacées du Paléolithique supérieur européen*. Études et Recherches Archéologiques de l'Université de Liège, 42: 523–538.
- HAESAERTS P., 1992. Les dépôts pléistocènes de la terrasse de la grotte Scladina à Sclayn (province de Namur, Belgique). In M. OTTE (ed.), *Recherches aux grottes de Sclayn, vol. 1: Le Contexte*. Études et Recherches Archéologiques de l'Université de Liège, 27: 33–55.
- HAESAERTS P., 2004. Maisières-Canal (2000-2002): cadre stratigraphique. In R. MILLER, P. HAESAERTS & M. OTTE (eds.), *L'atelier de taille aurignacien de Maisières-Canal (Belgique)*. Études et Recherches Archéologiques de l'Université de Liège, 110: 13–26.
- HAESAERTS P., DI MODICA K. & PIRSON S., 2011^b. Le gisement paléolithique de la Sablière Gritten à Rocourt (province de Liège). In M. TOUSSAINT, K. DI MODICA & S. PIRSON (sc. dir.), *Le Paléolithique moyen en Belgique. Mélanges Marguerite Ulrix-Closset*. Bulletin de la Société royale belge d'Études Géologiques et Archéologiques *Les Chercheurs de la Wallonie*, hors-série, 4 & Études et Recherches Archéologiques de l'Université de Liège, 128: 359–374.
- HAESAERTS P., MESTDAGH H. & BOSQUET D., 1997. La séquence loessique de Remicourt (Hesbaye, Belgique). *Notae Praehistoricae*, 17: 45–52.
- HAESAERTS P., MESTDAGH H. & BOSQUET D., 1999. The sequence of Remicourt (Hesbaye, Belgium): new insights on the pedo- and chronostratigraphy of the Rocourt Soil. *Geologica Belgica*, 2: 5–27.
- HAESAERTS P., PIRSON S. & MEIJS E. P. M., 2011^a. New proposal for the Quaternary lithostratigraphic units (Belgium). Aeolian sediments. *National Commission for Stratigraphy, Subcommission Quaternary* (<http://www2.ulg.ac.be/geolsed/GB/SCQ.htm>): 1–7.
- HAESAERTS P. & TEYSSANDIER N., 2003. The early Upper Paleolithic occupations of Willendorf II (Lower Austria): a contribution to the chronostratigraphic and cultural context of the beginning of the Upper Paleolithic in Central Europe. In J. ZILHÃO & F. D'ERRICO (eds.), *The Chronology of the Aurignacian and of the Transitional Technocomplexes. Dating, Stratigraphies, Cultural Implications*. Proceedings of Symposium 6.I of the XIVth Congress of the UISPP, University of Liège, Belgium, September 2–8, 2001, Lisboa, Trabalhos de Arqueologia, 33: 133–151.
- HAESAERTS P. & VAN VLIET B., 1974. Compte rendu de l'excursion du 25 mai 1974 consacrée à



- la stratigraphie des limons aux environs de Mons. *Annales de la Société géologique de Belgique*, 97: 547-560.
- HAESAERTS P. & VAN VLIET-LANOË B., 1981. Phénomènes périglaciaires et sols fossiles observés à Maisières-Canal, à Harmignies et à Rocourt. *Biuletyn Peryglacjalny*, 28: 291-324.
- HUXTABLE J. & AITKEN M. J., 1992. Thermoluminescence dating of burned flint and stalagmitic calcite from grottes de Sclayn (Namur). In M. OTTE (ed.), *Recherches aux grottes de Sclayn, vol. 1: Le Contexte*. Études et Recherches Archéologiques de l'Université de Liège, 27: 175-178.
- JUVIGNÉ É., 1978. Les minéraux denses transparents des loess de Belgique. *Zeitschrift für Geomorphologie*, 22: 68-88.
- JUVIGNÉ É., TALLIER E., HAESAERTS P. & PIRSON S., 2008. Un nouveau stratotype du Téphra de Rocourt dans la carrière de Romont (Eben/Bassenge, Belgique). *Quaternaire*, 19: 133-139.
- LAMARQUE F., 2003. Les ours spéléens de la grotte de Scladina (Namur, Belgique): essai d'explication du déséquilibre entre la conservation des dents et des os de la couche 1A. In M. PATOU-MATHIS & H. BOCHERENS (eds.), *Le rôle de l'environnement dans les comportements des chasseurs-cueilleurs préhistoriques*. Actes du XIVème Congrès de l'Union Internationale des Sciences Préhistoriques et Protohistoriques, Section 3: Paléoécologie. Colloque C3.1., Université de Liège, Belgique, 2-8 septembre 2001, Oxford, *British Archaeological Reports, International Series*, 1105: 111-119.
- LOODTS I. & BONJEAN D., 2004. La grotte Scladina à Sclayn (Andenne, Belgique). Le niveau d'occupation moustérien 1A. Actes du XIVème Congrès UISPP, Université de Liège, Belgique, 2-8 septembre 2001, Section 5, Le Paléolithique moyen. Oxford, *British Archaeological Reports, International Series*, 1239: 47-55.
- MEIJS E. P. M., 2002. Loess stratigraphy in Dutch and Belgian Limburg. *Eiszeitalter und Gegenwart*, 51: 114-130.
- MEJDAHL V., 1988. Long-term stability of the TL signal in alkali feldspars. *Quaternary Science Reviews*, 7: 357-360.
- NIEUWLAET P., 2007. *De ursiden van de diepere lagen van het terras van de grot Scladina te Sclayn, België: osteometrie, tafonomie en paleo-ecologie*. Unpublished master thesis, Universiteit Gent, 163 p.
- OTTE M., 1998. Le Paléolithique supérieur. In M. OTTE, M. PATOU-MATHIS & D. BONJEAN (dir.), *Recherches aux grottes de Sclayn, vol. 2: L'Archéologie*. Études et Recherches Archéologiques de l'Université de Liège, 79: 63-68.
- OTTE M., COLLIN F., MILLER R. & ENGESSER K., 1998. Nouvelles datations du Trou Al'Wesse dans son contexte régional. *Notae Praehistoricae*, 18: 45-50.
- OTTE M., LÉOTARD J.-M., SCHNEIDER A.-M., GAUTIER A., GILOT E. & AITKEN M., 1983. Fouilles aux grottes de Sclayn (Namur). *Helinium*, 23: 112-142.
- OTTE M., PATOU-MATHIS M. & BONJEAN D. (dir.), 1998. *Recherches aux grottes de Sclayn, vol. 2: L'Archéologie*. Études et Recherches Archéologiques de l'Université de Liège, 79, 437 p.
- PATOU-MATHIS M., 1998^a. Origine et histoire de l'assemblage osseux de la couche 5. Comparaison avec la couche 4 sus-jacente, non-anthropique. In M. OTTE, M. PATOU-MATHIS & D. BONJEAN (dir.), *Recherches aux grottes de Sclayn, vol. 2: L'Archéologie*. Études et Recherches Archéologiques de l'Université de Liège, 79: 281-295.
- PATOU-MATHIS M., 1998^b. Les espèces chassées et consommées par l'homme en couche 5. In M. OTTE, M. PATOU-MATHIS & D. BONJEAN (dir.), *Recherches aux grottes de Sclayn, vol. 2: L'Archéologie*. Études et Recherches Archéologiques de l'Université de Liège, 79: 297-310.
- PATOU-MATHIS M. & LÓPEZ-BAYÓN I., 1998. Analyse spatiale des ossements de la couche 5. In M. OTTE, M. PATOU-MATHIS & D. BONJEAN (dir.), *Recherches aux grottes de Sclayn, vol. 2: L'Archéologie*. Études et Recherches Archéologiques de l'Université de Liège, 79: 377-395.
- PIRSON S., 1999. Étude sédimentologique préliminaire au Trou Al'Wesse (Modave, Belgique). *Bulletin de la Société royale belge d'Études Géologiques et Archéologiques Les Chercheurs de la Wallonie*, 39: 115-162.
- PIRSON S., 2007. *Contribution à l'étude des dépôts d'entrée de grotte en Belgique au Pléistocène supérieur. Stratigraphie, sédimentogenèse et paléoenvironnement*. Unpublished PhD thesis, University of Liège & Royal Belgian Institute of Natural Sciences, 2 vol., 435 p. & 5 annexes.
- PIRSON S., 2011. Contextes paléoenvironnemental et chronostratigraphique du remplissage de

- la grotte Walou: apport de la géologie et comparaison avec les autres disciplines. In S. PIRSON, C. DRAILY & M. TOUSSAINT (dir.), *La grotte Walou à Trooz (Belgique). Fouilles de 1996 à 2004, vol. 1: Les sciences de la terre*. Namur, Service public de Wallonie, IPW, Études et Documents, Archéologie, 20: 170–201.
- PIRSON S., BONJEAN D., DI MODICA K. & TOUSSAINT M., 2005. Révision des couches 4 de la grotte *Scladina* (comm. d'Andenne, prov. de Namur) et implications pour les restes néandertaliens : premier bilan. *Notae Praehistoricae*, 25: 61–69.
- PIRSON S., COURT-PICON M., HAESAERTS P., BONJEAN D. & DAMBLON F., 2008. New data on geology, anthracology and palynology from the *Scladina* Cave pleistocene sequence: preliminary results. In F. DAMBLON, S. PIRSON & P. GERRIENNE (eds.), *Hautrage (Lower Cretaceous) and Sclayn (Upper Pleistocene). Field Trip Guidebook. Charcoal and microcharcoal: continental and marine records*. IVth International Meeting of Anthracology, Brussels, Royal Belgian Institute of Natural Sciences, 8-13 September 2008. Brussels, Royal Belgian Institute of Natural Sciences, *Memoirs of the Geological Survey of Belgium*, 55: 71–93.
- PIRSON S. & DI MODICA K., 2011. Position chronostratigraphique des productions lithiques du Paléolithique ancien en Belgique : un état de la question. In M. TOUSSAINT, K. DI MODICA & S. PIRSON (sc. dir.), *Le Paléolithique moyen en Belgique. Mélanges Marguerite Ulrix-Closset*. Bulletin de la Société royale belge d'Études Géologiques et Archéologiques *Les Chercheurs de la Wallonie*, hors-série, 4 & Études et Recherches Archéologiques de l'Université de Liège, 128: 105–148.
- PIRSON S. & DRAILY C., 2011. Lithostratigraphie et genèse des dépôts de la grotte Walou. In S. PIRSON, C. DRAILY & M. TOUSSAINT (dir.), *La grotte Walou à Trooz (Belgique). Fouilles de 1996 à 2004, vol. 1: Les sciences de la terre*. Namur, Service public de Wallonie, IPW, Études et Documents, Archéologie, 20: 72–131.
- PIRSON S., DRAILY C. & TOUSSAINT M. (dir.), 2011. *La grotte Walou à Trooz (Belgique). Fouilles de 1996 à 2004, vol. 1: Les sciences de la terre*. Namur, Service public de Wallonie, IPW, Études et Documents, Archéologie, 20, 208 p.
- PIRSON S., FLAS D., ABRAMS G., BONJEAN D., COURT-PICON M., DI MODICA K., DRAILY C., DAMBLON F., HAESAERTS P., MILLER R., ROUGIER H., TOUSSAINT M. & SEMAL P., 2012. Chronostratigraphic context of the Middle to Upper Palaeolithic transition: Recent data from Belgium. *Quaternary International*, 259: 78–94.
- PIRSON S., HAESAERTS P., COURT-PICON M., DAMBLON F., TOUSSAINT M., DEBENHAM N. C. & DRAILY C., 2006. Belgian cave entrance and rock-shelter sequences as palaeoenvironmental data recorders: the example of Walou cave. *Geologica Belgica*, 9: 275–286.
- PIRSON S., HAESAERTS P. & DI MODICA K., 2009. Cadre chronostratigraphique des principaux gisements du Paléolithique moyen du bassin de la Haine: un état de la question. In K. DI MODICA & C. JUNGELS (dir.), *Paléolithique moyen en Wallonie. La collection Louis Éloy*. Bruxelles, Collections du Patrimoine culturel de la Communauté française, 2: 58–77.
- PIRSON S. & JUVIGNÉ É., 2011. Bilan sur l'étude des téphras à la grotte Walou. In S. PIRSON, C. DRAILY & M. TOUSSAINT (dir.), *La grotte Walou à Trooz (Belgique). Fouilles de 1996 à 2004, vol. 1: Les sciences de la terre*. Namur, Service public de Wallonie, IPW, Études et Documents, Archéologie, 20: 134–167.
- POUCLET A., JUVIGNÉ É. & PIRSON S., 2008. The Rocourt Tephra, a widespread 90-74 ka stratigraphic marker in Belgium. *Quaternary Research*, 70: 105–120.
- QUINIF Y., 2006. Complex stratigraphic sequences in belgian caves. Correlation with climatic changes during the Middle, the Upper Pleistocene and the Holocene. *Geologica Belgica*, 9: 231–244.
- QUINIF Y., GENTY D. & MAIRE R., 1994. Les spéléothèmes: un outil performant pour les études paléoclimatiques. *Bulletin de la Société géologique de France*, 165: 603–612.
- REILLE M., ANDRIEU V., DE BEAULIEU J.-L., GUENET P. & GOEURY C., 1998. A long pollen record from Lac du Bouchet, Massif Central, France: for the period ca. 325 to 100 ka BP (OIS 9c to OIS 5e). *Quaternary Science Reviews*, 17: 1107–1123.
- SCHNEIDER A.-M., 1986^a. Résultats palynologiques à la grotte de Sclayn (Belgique). Contribution à l'étude du dernier interglaciaire. *Revue d'Archéométrie*, 10: 39–42.
- SCHNEIDER A.-M., 1986^b. Contribution à l'étude du dernier interglaciaire : résultats palynologiques à la grotte de Sclayn (Belgique). *Revue de Paléobiologie*, 5: 57–70.



- SIMONET P., 1992. Les associations de grands mammifères du gisement de la grotte Scladina à Sclayn (Namur, Belgique). In M. OTTE (ed.), *Recherches aux grottes de Sclayn, vol. 1 : Le Contexte*. Études et Recherches Archéologiques de l'Université de Liège, 27: 127-151.
- TEXIER J.-P., 2007. Anciennes et nouvelles lectures géologiques de sites paléolithiques de référence du Périgord : évolution des concepts. In J. EVIN (ed.), *Un siècle de construction du discours scientifique en préhistoire*. Actes du XXVI^e Congrès préhistorique de France. Avignon, 21-25 septembre 2004. Volume 2, Société préhistorique française: 47-53.
- TOUSSAINT M., 1988. Fouilles 1978-1981 au Trou du Diable à Hastière-Lavaux, province de Namur, Belgique. *Helinium*, XXVIII: 35-43.
- TOUSSAINT M., OLEJNICZAK A. J., EL ZAATARI S., CATTELAÏN P., FLAS D., LETOURNEUX C. & PIRSON S., 2010. The Neandertal lower right deciduous second molar from Trou de l'Abîme at Couvin, Belgium. *Journal of Human Evolution*, 58: 56-67.
- TOUSSAINT M., OTTE M., BONJEAN D., BOCHERENS H., FALGUÈRES C. & YOKOYAMA Y., 1998. Les restes humains néandertaliens immatures de la couche 4A de la grotte Scladina (Andenne, Belgique). *Comptes rendus de l'Académie des Sciences de Paris, Sciences de la terre et des planètes*, 326: 737-742.
- TOUSSAINT M., PIRSON S., LÓPEZ BAYÓN I., BECKER A., LACROIX P. & LAMBERMONT S., 1999. Bilan préliminaire de trois années de fouilles à l'Abri Supérieur de Goyet (Gesves, province de Namur). *Notae Praehistoricae*, 19: 39-47.
- TZEDAKIS P. C., 1993. Long-term tree populations in northwest Greece through multiple Quaternary climatic cycles. *Nature*, 364: 437-440.
- VALOCH K., 1976. *Die altsteinzeitliche Fundstelle in Brno-Bohunice*, Brno. Studie Archeologickeho ustavu Ceskoslovenske Akademie ved v Brne, 4, 120 p.
- VAN VLIET-LANOË B., 1988. *Le rôle de la glace de ségrégation dans les formations superficielles de l'Europe de l'ouest. Processus et héritages*. Paris, unpublished habilitation thesis, mention géographie. Université de Paris I - Sorbonne, Centre de Géomorphologie du Centre national de la recherche scientifique), 2 vol., 378 & 667 p.

Chapter 5

Stéphane PIRSON, Dominique BONJEAN
& Michel TOUSSAINT

STRATIGRAPHIC ORIGIN OF THE JUVENILE NEANDERTAL REMAINS FROM SCLADINA CAVE: RE-EVALUATION AND CONSEQUENCES FOR THEIR PALAEOENVIRONMENTAL AND CHRONOSTRATIGRAPHIC CONTEXTS

*Michel Toussaint & Dominique Bonjean (eds.), 2014.
The Scladina I-4A Juvenile Neandertal (Andenne, Belgium),
Palaeoanthropology and Context
Études et Recherches Archéologiques de l'Université de Liège, 134: 93–124.*

1. Introduction

The 19¹ remains of the Neandertal child, Scladina I-4A, that have been discovered so far were all unearthed before the recent stratigraphic reappraisal of the cave's sedimentary sequence (see Chapter 3). In the former stratigraphic system, most of the remains were attributed to Layer 4A, more specifically to the part of former Layer 4A situated between stalagmitic floors CC14 and CC4 (BONJEAN, 1998; TOUSSAINT et al., 1998; Chapter 3; Figure 1; Appendix A). Three of the discovered teeth (which all belong to the same individual) were originally attributed to former Layer 3 (OTTE et al., 1993; TOUSSAINT et al., 1994), but former Layer 4A as their origin was soon suggested as a possibility (BONJEAN et al., 1996, 1997).

The progress of excavation during the last decade provided access to new locations in the cave. Throughout this process, careful examination of the numerous available sedimentary profiles was undertaken (PIRSON, 2007). This allowed the highly complex stratigraphy to be deciphered more accurately, leading to a better understanding of the succession of the cave's different lithostratigraphic units. Former Layer 4A is one of the former layers that underwent the most important organisational changes following the stratigraphic reappraisal. Instead of one single layer (as it was previously thought to be), about 20 layers have now been recognised, which are now classified as Sedimentary Complex 4A (Chapter 3; PIRSON et al., 2005; PIRSON, 2007). Furthermore, Stalagmitic Floor CC14 was proven to be a lateral equivalent of Speleothem CC4.

¹ A 20th fossil, from Square B37 and initially labelled Scla 4A-10, was later discarded from the Neandertal remains during taphonomic and anthropological studies. Re-examination of the excavation documents led to the conclusion that this tooth came from a bioturbated context.

The newly defined layers of Sedimentary Complex 4A are grouped into 4 distinct units, each including several layers (Figure 2). These 4 units are, from bottom to top:

- Unit 4A-AP, the lowermost unit, including all the layers within the complex that are older than CC4;
- Unit 4A-IP, including Stalagmitic Floor CC4 and the layers that are contemporaneous with the formation of CC4;
- Unit 4A-CHE, which includes the layers that developed inside a large gully structure that eroded underlying layers, including CC4;
- Unit 4A-POC, the uppermost unit, superimposing both units 4A-IP and 4A-CHE.

The stratigraphic re-evaluation made reconsidering the exact position of the Scladina Neandertal child remains necessary. This reappraisal, only possible because of the rigorous excavation methods used at the site, is the subject of this chapter. Some of the arguments that will be presented have already been published (PIRSON et al., 2005; PIRSON, 2007), but they will be fully examined in the present work.

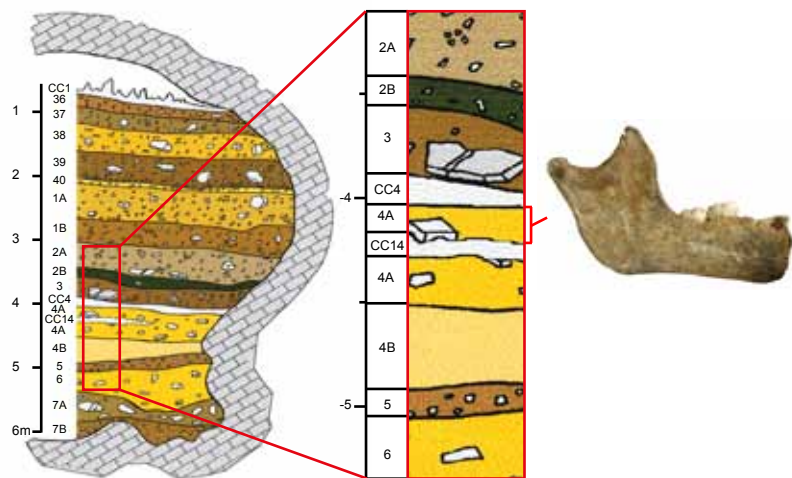


Figure 1: Position of most of the Scladina Neandertal remains in the former stratigraphic record (CC = calcitic crust). Modified after BONJEAN, 1998.



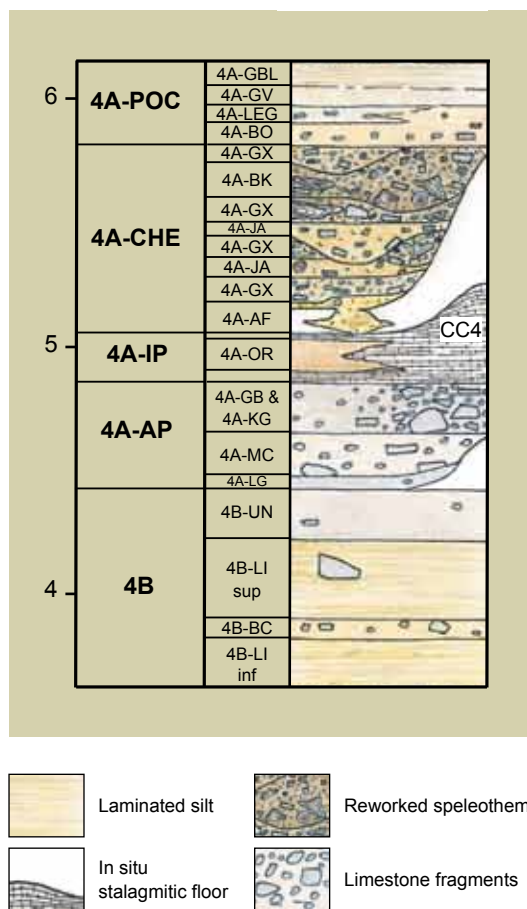
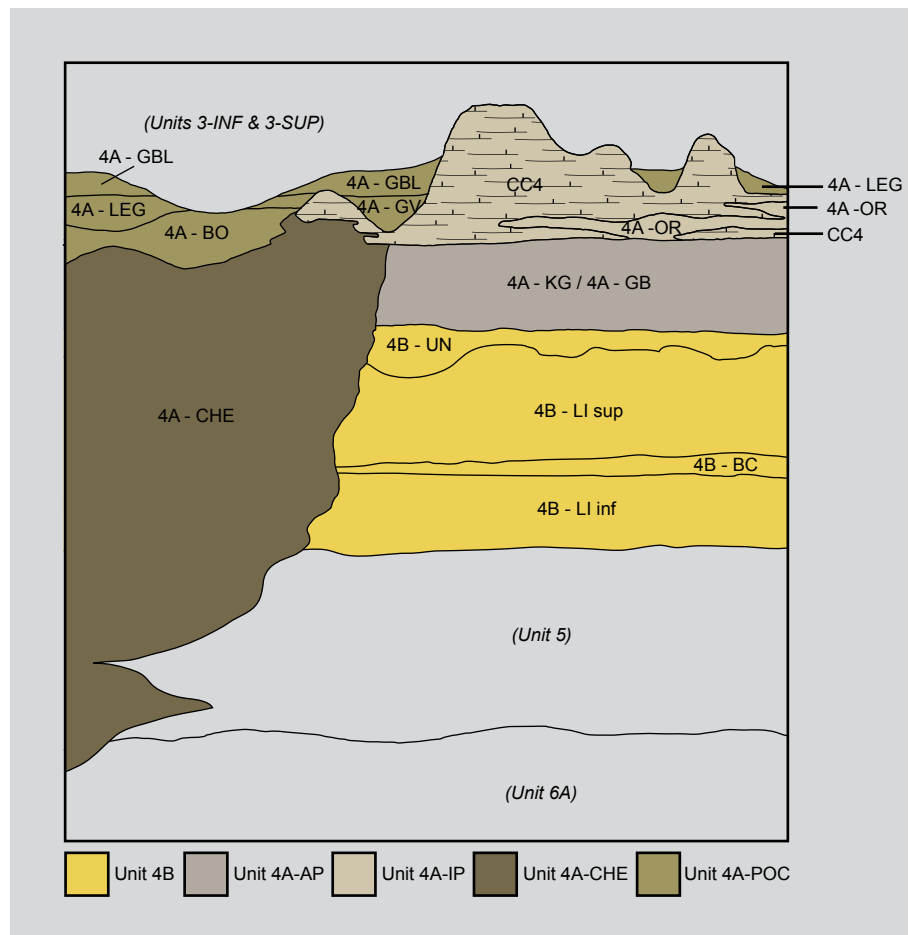
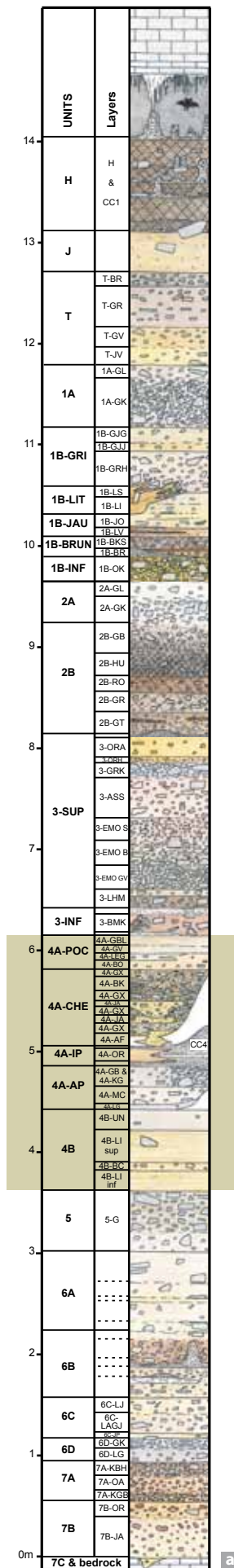


Figure 2: The new stratigraphic record. a. Details of the lithostratigraphic sequence of Sedimentary Complex 4A and Unit 4B in the framework of the global stratigraphy of the site. b. Sketch showing the stratigraphic relationships between the four units defined in the Sedimentary Complex 4A.

Anthropological number	Nature	Square	x (cm)	y (cm)	z (cm)	Former Layer	New stratigraphic record		Unearthed	Identified
							Unit	Layer		
Scla 4A-1	right half of the mandible	D 29	41	13	-484.5	4A	4A-CHE	4A-GX	16/07/1993	20/07/1993
Scla 4A-9	left half of the mandible	C 28	98	75	-478.6	4A	4A-CHE (4A-POC)	4A-JA (?)	12/07/1996	12/07/1996
Scla 4A-2	small part of right maxilla	D 30	/	/	-477 to -479	4A	4A-POC (4A-CHE)	?	18/02/1992	October 1993
Scla 4A-4	permanent maxillary right first molar	C 30	12	50	-466	4A	4A-POC	4A-BO	14/12/1993	14/12/1993
Scla 4A-3	permanent maxillary right second molar	C 30	/	/	-464 to -470	4A	4A-CHE or 4A-POC	?	15/10/1992	October 1993
Scla 4A-8	permanent maxillary right third molar	C 32	20 to 80	10 to 30	-460 to -462	4A	4A-POC (4A-CHE)	4A-LEG (4A-JA)	14/07/1995	14/07/1995
Scla 4A-13	deciduous mandibular right second molar	E 38	88	57	-481	4A	4A-POC	4A-LEG	13/11/2001	13/11/2001
Scla 4A-19 (= Scla 3-4)	permanent mandibular left lateral incisor	D 34	/	/	-460 to -471,5	3 or 4A	4A-POC or 3-INF (3-SUP)	?	08/03/1995	10/04/1995
Scla 4A-18 (= Scla 3-3)	permanent maxillary left canine	F 26	/	/	-461 to -471	3 or 4A	4A-POC (4A-IP, 4A-CHE, 3-INF)	?	19/11/1991	October 1993
Scla 4A-7	deciduous maxillary right first molar	F 27	/	/	-471 to -481	4A	4A-CHE or 4A-POC (4A-IP, 3-INF)	?	12/11/1991	October 1993
Scla 4A-12	permanent mandibular right canine	F 27	/	/	-449 to -461	4A	4A-POC or 3-INF (4A-IP, 4A-CHE, 3-SUP)	?	28/03/1990	July 2001
Scla 4A-17 (= Scla 3-2)	permanent maxillary left lateral incisor	F 27	/	/	-458 to -470	3 or 4A	4A-POC (4A-IP, 4A-CHE, 3-INF)	?	17/10/1991	October 1993
Scla 4A-5	deciduous maxillary right second molar	G 27	/	/	-447 to -462	4A	4A-POC or 3-INF (4A-IP, 4A-CHE, 3-SUP)	?	13/03/1990	October 1993
Scla 4A-6	mandibular right first premolar	G 27	/	/	-463 to -477	4A	4A-CHE or 4A-POC (4A-IP, 3-INF)	?	04/07/1990	October 1993
Scla 4A-11	permanent maxillary right central incisor	G 27	/	/	-447 to -462	4A	4A-POC or 3-INF (4A-IP, 4A-CHE, 3-SUP)	?	13/03/1990	May 2000
Scla 4A-14	permanent maxillary right lateral incisor	H 27	/	/	-445 to -454	4A	4A-POC or 3-INF (4A-IP, 4A-CHE, 3-SUP)	?	22/02/1990	14/12/2004
Scla 4A-15	permanent mandibular right central incisor	H 27	/	/	-445 to -454	4A	4A-POC or 3-INF (4A-IP, 4A-CHE, 3-SUP)	?	22/02/1990	14/12/2004
Scla 4A-16	permanent maxillary right canine	H 27	/	/	-454 to -463	4A	4A-POC (4A-IP, 4A-CHE, 3-INF)	?	23/02/1990	16/12/2004
Scla 4A-20	permanent mandibular right lateral incisor	F35-37	/	/	-350 to -500	/	4A-POC or 3-INF (3-SUP)	?	12/07/2006	12/07/2006

Table 1: List of the 19 Neandertal remains discovered so far in Scladina Cave.

	Fossil positioned in a specific layer from the new stratigraphic record	
	Fossil positioned either in 4A-CHE or in 4A-POC	
	Fossil with a possible origin from several units	Unit or layer xxx = most probable
	Fossil found after the collapse of a profile	(Unit or layer xxx) = possible but low probability

2. Methods

Several methods have been used in order to determine the exact stratigraphic origin of the hominin remains. They include:

- 3-dimensional positioning of each fossil. This is only possible for 5 out of the 19 remains, because during the early stage of excavation only the objects from former Layer 5 were recorded in 3-dimensions (see Chapter 2). From 1991 onwards, in some areas of the cave, objects from other layers (former layers 1B, 2B, 3, and 4A) were recorded 3-dimensionally in situations where the faunal material was very abundant. However, the Neandertal remains that were unearthed before the 16th of July 1993 (the date that the hemimandible, Scla 4A-1, was discovered) were only recognised later by reanalysing the faunal collections. The coordinates only included 2 pieces of location data: the square (without relative x-y values) and a range of altitudes that are more or less accurate (Table 1);
- projection of the each fossil's 3-dimensional location onto the nearest sedimentary profile(s);
- analysis of some unpublished stratigraphic drawings of the Neandertal remains' immediate surroundings;
- analysis of the field notes (sedimentological descriptions, altitudes of the layer boundaries for each square, maps of the excavated remains, etc.);
- analysis of numerous pictures (photographs and slides) including general views, details of the concerned square in horizontal view,



as well as pictures of sedimentary profiles; in some cases, some pictures were taken before, during, and after the discoveries of the fossils. These arguments will be presented for each individual fossil (§3) in order to compare the location data recorded during the excavation of each fossil to the new stratigraphic record. In the discussion (§4), other arguments linked with the sedimentary dynamics or with the anthropological or taphonomic studies will also be considered in order to refine the interpretations presented in this chapter.

Reappraisal of the stratigraphic position of the juvenile 3. Neandertal fossils

3.1. The right half of the mandible (Scla 4A-1)

The right half of the mandible was unearthed during excavation on the 16th of July 1993 in Square D29 (Figures 3 & 4), and was formally identified as being Neandertal a few days later in the laboratory (BONJEAN et al., 2009^a). It was attributed in the field to former Layer 4A. Its 3-dimensional coordinates in Square D29 are: $x = 41$ cm, $y = 13$ cm, and $z = -484.5$ cm (Table 1).

3.1.1. Available arguments

In this area of the cave, the transition between former Layer 3 (brownish stony silt with numerous bones) and former Layer 4A (yellowish silt with some bones and calcite fragments) is very well defined. In Square D29, former Layer 4A was excavated between -471 and -510 cm.

Closest sedimentary profile

Among the available sedimentary profiles studied in the framework of the stratigraphic reappraisal, the profile that is the closest to fossil Scla 4A-1 is Cross-Section 30/31. However, it is still 187 cm away. Given the stratigraphic context (and the presence of the gully in Unit 4A-CHE), the use of such a distant projection must be approached carefully. The orthogonal projection of the fossil onto this sedimentary profile points to Unit 4A-IP, and more specifically to Layer 4A-OR (Figure 5). Laterally, both south and north of where the object projects onto the sedimentary profile the layers change drastically. Toward the south, about 60 cm away from the projection, Unit 4A-CHE

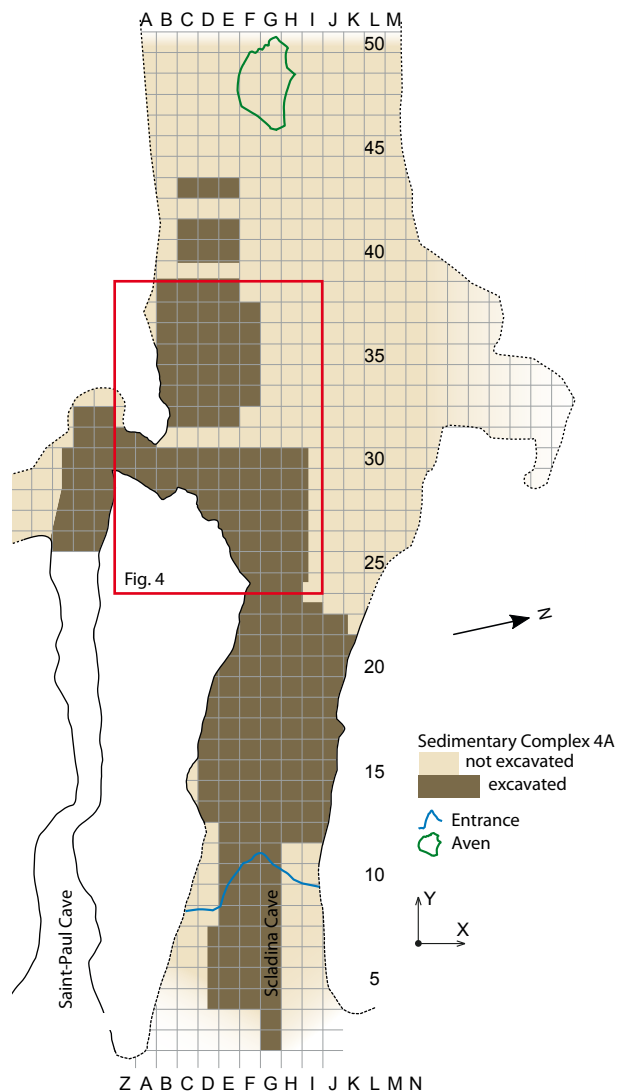
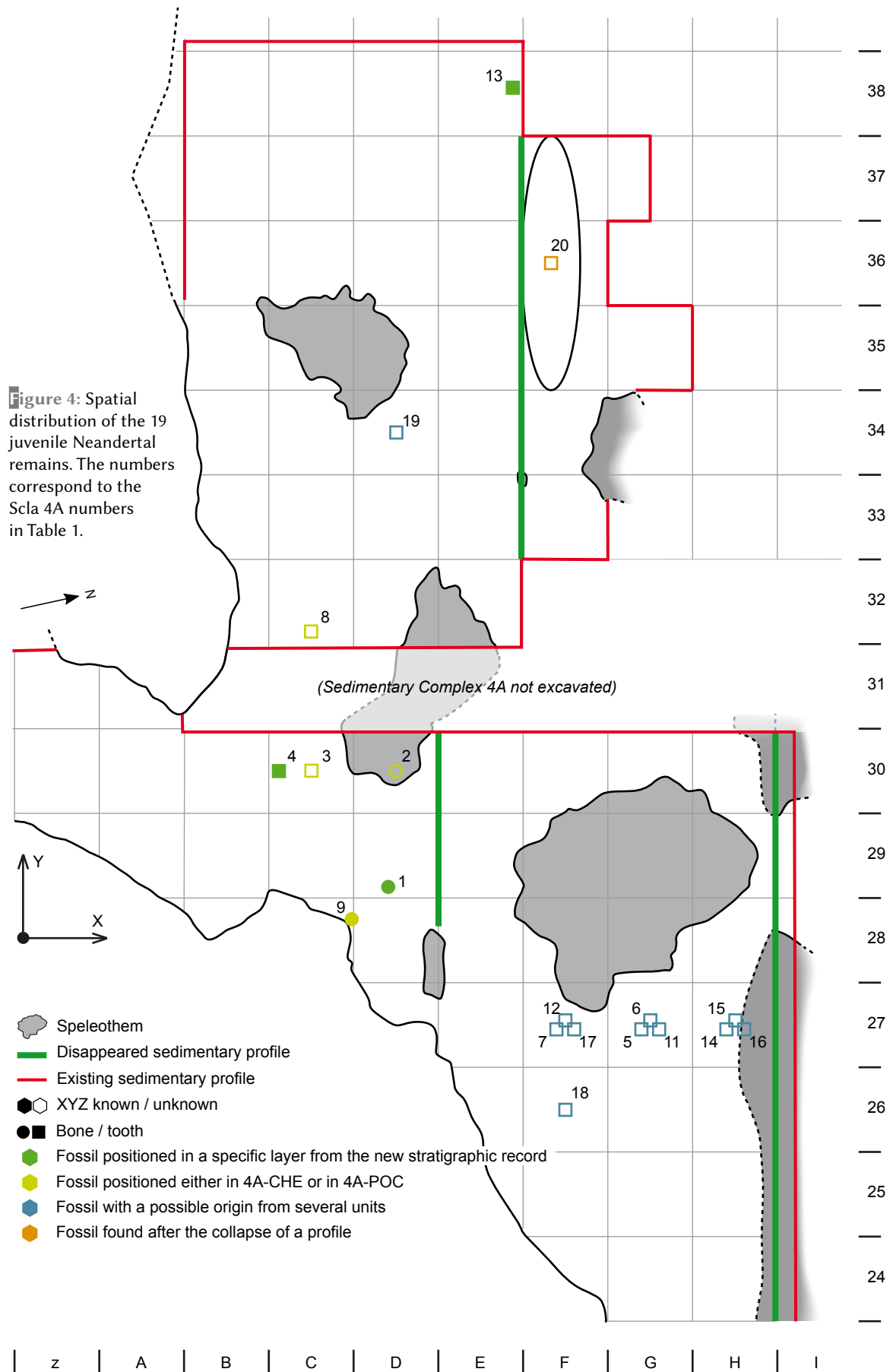


Figure 3: Plan of the cave with location of Figure 4. In dark brown, squares where Sedimentary Complex 4A has already been excavated.

is visible. Toward the north, the gully is farther away, but about 60 cm away from the projection, Unit 4A-POC is present. Consequently, on the basis of the orthogonal projection alone, the possible stratigraphic position of the fossil Scla 4A-1 remains uncertain; it could be from units 4A-IP, 4A-CHE, or 4A-POC.

Sedimentary Profile E/D in 28-29-30 (Figure 6), perpendicular to Profile 30/31, is closer (~60 cm). However, it was drawn before the stratigraphic reappraisal (BONJEAN et al., 1997). The projection of the fossil on this profile points to former Layer 4A7; following the reinterpretation of this profile using photographs and the course of the gully (Figure 9), this former layer is probably part of Unit 4A-CHE gully structure.



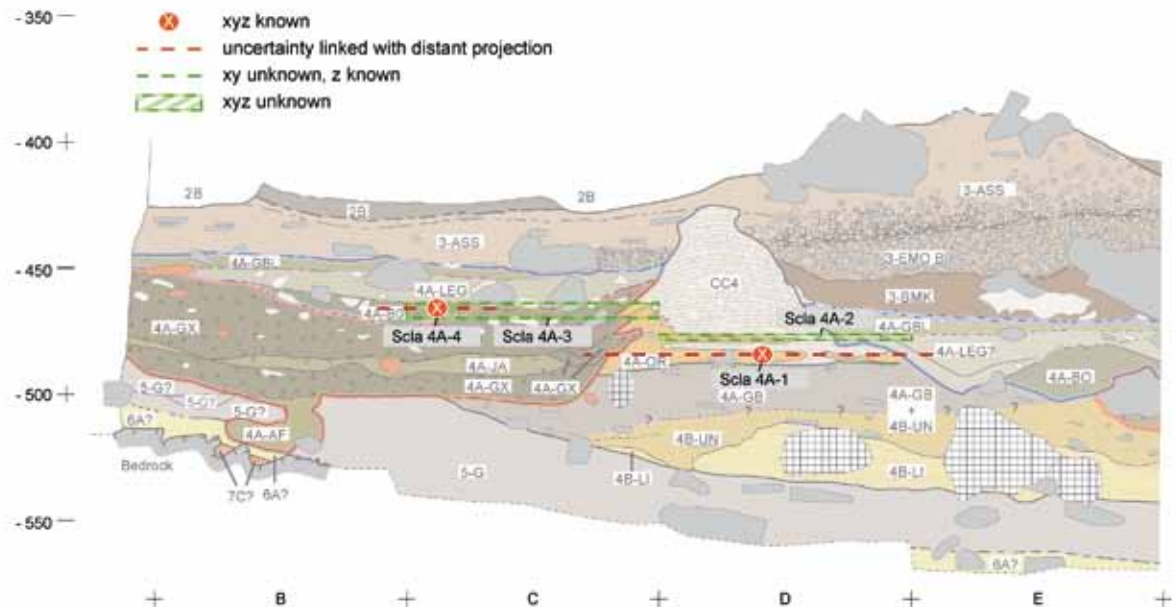


Figure 5: Orthogonal projections of the Neandertal remains Scla 4A-1 to 4 on Cross-Section 30/31 B-E (the complete section, from B to H, is presented in Chapter 3).

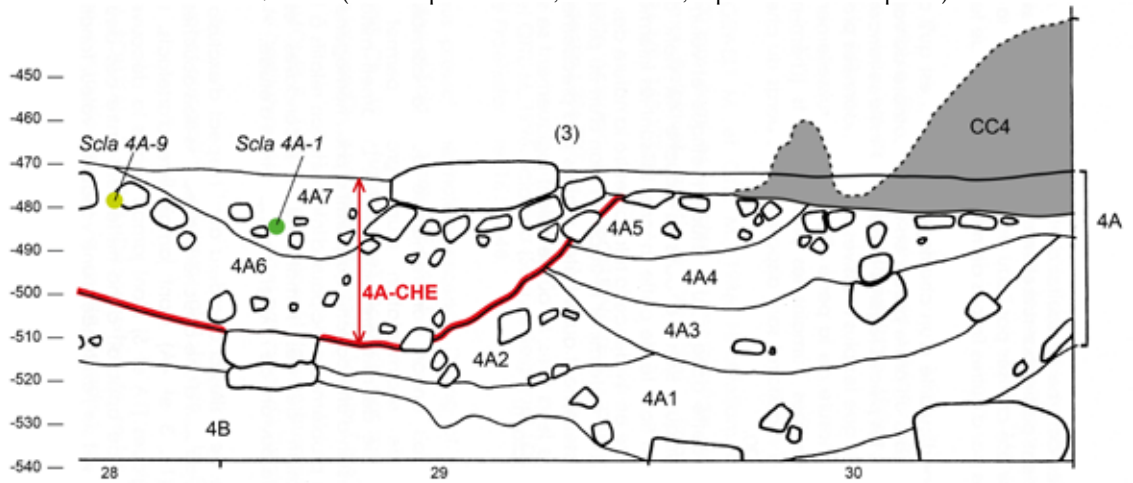


Figure 6: Orthogonal projections of the Neandertal remains Scla 4A-1 and 9 on Cross-Section E/D (modified after BONJEAN et al., 1997). This profile is a sketch drawn long before the stratigraphic reappraisal, and the exact correlations with the new stratigraphic record are difficult to make. The two CC4 stalagmites are not in the same plan than the section but about 25 cm behind (in E).

Pictures

The examination of the numerous pictures taken during the discovery of the fossil facilitated a major observation: fossil Scla 4A-1 was surrounded by speleothem fragments (Figure 7). This allows units 4A-IP and 4A-AP to be discarded as candidates, and units 4A-CHE or 4A-POC to become the likely origin for this fossil.

Some of the pictures show Square D29 shortly after the discovery of the right half of the mandible. A blue cast of the fossil is seen placed in its exact discovery position (Figure 8). These pictures permit observations of the underlying sediment on a horizontal surface, but also observations of two surrounding vertical profiles, which are within close proximity to the object (13 and 41 cm, respectively). The lithofacies 4A-JA and

4A-GX, typical of the gully from Unit 4A-CHE, are recognisable in these images. In this situation, the right half of the mandible is from 4A-GX.

Another interesting aspect of these pictures is that they allow the course of the gully to be reconstructed in this area of the cave, especially when considering the observed structures and stratigraphic sequence documented on Profile 30/31 (Figures 5 & 9).

3.1.2. Synthesis

Observations of sedimentary profiles 30/31 and E/D, when combined with the numerous available pictures, allowed for a 3-dimensional reconstruction of the area to be created. This also allowed the course and the extent of the left branch of the gully to be reconstructed (Figure 9).



Figure 7: Pictures of the right half of the mandible (Scla 4A-1), represented by a blue cast in the discovery position: left, vertical view of Square D29; right, Sedimentary Profile 29/28 in D. Numerous speleothem fragments (in white) are recognisable around the fossil.

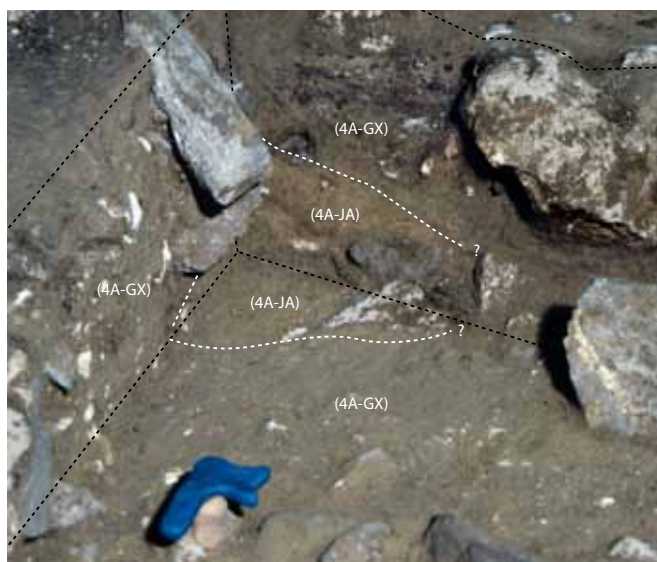


Figure 8: Pictures of the right half of the mandible (Scla 4A-1), represented by a blue cast in the discovery position: left, general view of Square D29; right, detail of the angle between profiles 29/28 and D/C. The greyish and yellowish facies are probably related to lithofacies 4A-GX and 4A-JA, respectively.

On these grounds, the stratigraphic context of the right half of the Scladina Child’s mandible can accurately be established as one of the 4A-GX lithofacies in Unit 4A-CHE. Some pictures show that at this particular location, this Lithofacies 4A-GX superimposes one of the Lithofacies 4A-JA. Since the fossil must be from the left branch of the gully, it is confirmed to be from the upper Lithofacies 4A-GX in the gully structure seen on Sedimentary Profile 30/31 (Tables 1 & 2). This

complements the results of the projection of the fossil onto Profile 30/31.

3.2. The left half of the mandible (Scla 4A-9)

The left half of the mandible (Scla 4A-9) was found and recognised in situ on the 12th of July 1996 in Square C28 (Figure 4), during the excavation of a



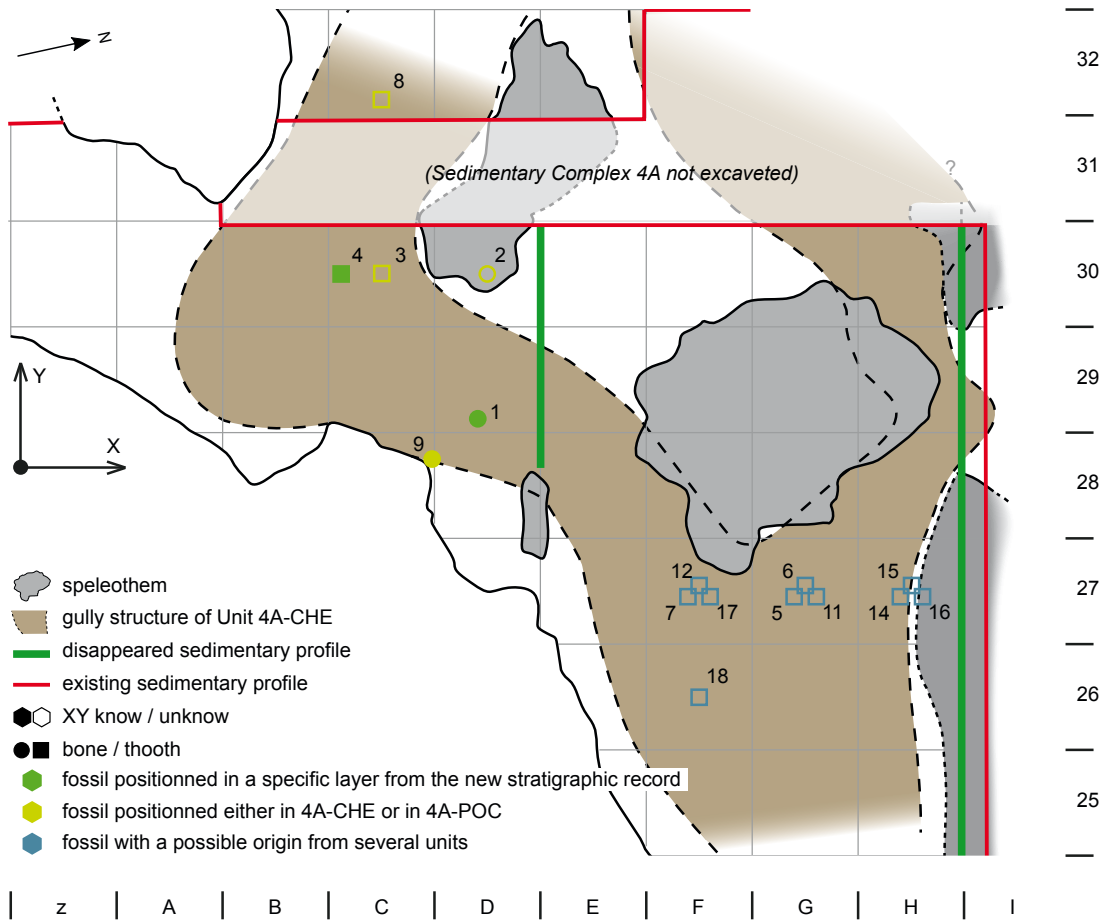


Figure 9: Course and extent of the gully structure of Unit 4A-CHE, reconstructed according to direct observation on sedimentary profiles, analysis of pictures and analysis of field notes.

- speleothem
- gully structure of Unit 4A-CHE
- disappeared sedimentary profile
- existing sedimentary profile
- XY know / unknown
- bone / tooth
- fossil positioned in a specific layer from the new stratigraphic record
- fossil positioned either in 4A-CHE or in 4A-POC
- fossil with a possible origin from several units



Figure 10: Small sedimentary profiles threatened by the collapse of large stone slabs from the wall. The symbol positions the location where the left half of the mandible has been found during the rescue excavation of this area.

Fossil n°	4A-IP	4A-CHE	4A-POC	3-INF	3-SUP
Scla 4A-1		v			
Scla 4A-9		v	(v)		
Scla 4A-2		(v)	v		
Scla 4A-4			v		
Scla 4A-3		v	v		
Scla 4A-8		(v)	v		
Scla 4A-13			v		
Scla 4A-19			v	v	(v)
Scla 4A-18	(v)	(v)	v	(v)	
Scla 4A-7	(v)	v	v	(v)	
Scla 4A-12	(v)	(v)	v	v	(v)
Scla 4A-17	(v)	(v)	v	(v)	
Scla 4A-5	(v)	(v)	v	v	(v)
Scla 4A-6	(v)	v	v	(v)	
Scla 4A-11	(v)	(v)	v	v	(v)
Scla 4A-14	(v)	(v)	v	v	(v)
Scla 4A-15	(v)	(v)	v	v	(v)
Scla 4A-16	(v)	(v)	v	(v)	
Scla 4A-20			v	v	(v)
v	0	5	17	7	0
(v)	10	10	1	5	7

- Fossil positioned in a specific layer from the new stratigraphic record
- Fossil positioned either in 4A-CHE or in 4A-POC
- Fossil with a possible origin from several units
- Fossil found after the collapse of a profile

Table 2: Possible stratigraphic origin of the 19 Scladina Neandertal juvenile remains. v = most probable candidate(s); (v) = unlikely candidate, but possible; (empty cell) = impossible.

small area threatened by the collapse of a stone slab from the wall (Figure 10). This fossil was attributed to former Layer 4A in the field. Its coordinates in Square C28 are: $x = 98$ cm, $y = 75$ cm, and $z = -478.6$ cm (Table 1).

3.2.1. Available arguments

Closest sedimentary profile

The closest profile is Cross-Section 30/31, which is more than 2 m away. From such a long distance, any projection is difficult to use, especially with the complex geometries linked with the unit 4A-CHE gully. From an altimetric point of view, on the basis of the comparison with Profile 30/31, the fossil could have originated from units 4A-IP, 4A-CHE, or 4A-POC.

Pictures

Many pictures of both horizontal and vertical views of the area around where the left hemimandible was discovered are available. About 10 cm under the fossil on a small sedimentary profile, an equivalent of Layer 4B-LI (Unit 4B) is visible (Figure 11); the upper limit of this layer is eroded by what seems to be a 4A-JA lithofacies (Unit 4A-CHE). The left half of the mandible is pictured in a yellowish sediment (Figure 11) that contains laterally some speleothem fragments. This sediment closely resembles the appearance of a 4A-JA lithofacies from Unit 4A-CHE.

3.2.2. Synthesis

From an altimetric point of view, comparing the depth of the fossil with the stratigraphic context

of the area and with Sedimentary Profile 30/31, the left half of the mandible could originate from units 4A-IP, 4A-CHE, or 4A-POC. The presence of calcite fragments allows Unit 4A-IP to be discarded. The possible candidates are thus units 4A-CHE or 4A-POC; on the basis of the photographic analysis, fossil Scla 4A-9 is probably from a facies of Unit 4A-CHE, likely 4A-JA (Tables 1 & 2).

3.3. The right maxilla fragment (Scla 4A-2)

The small part of the right maxilla was unearthed from Square D30 on the 17th of February 1992 (Figure 4). It was not assigned any 3-dimensional coordinates. This fossil was not identified until October 1993 during a re-analysis of the faunal collection. Its coordinates are thus inaccurate: x and y unknown, and $z = -477$ to -479 cm (Table 1). It was attributed to the top of former Layer 4A.

3.3.1. Available arguments

Closest sedimentary profile

The nearest useable sedimentary profile is transversal Cross-Section 30/31. The distance between the fossil and the profile is less than 1 m, although the exact distance remains unknown in the absence of x and y coordinates. When projecting the objects onto Profile 30/31 with its range of possible altitudes (-477 to -479 cm), 2 scenarios seem possible (Figure 5). If the fossil was lying in the southern half of the square (towards C), the projection points to Layer 4A-OR (Unit 4A-IP); however, the course of the gully in this area (cf. §3.1) indicates that an origin from lithofacies



Figure 11: Left half of the mandible (Scla 4A-9) in its discovery position on Profile D/C 28. The finely laminated yellowish sediment at the bottom of the picture on the right corresponds to Layer 4B-LI.



4A-GX (Unit 4A-CHE) is also possible. If the fossil was found in the northern half of the square (towards E), layers 4A-GBL or 4A-LEG (Unit 4A-POC) seem like more likely candidates. Based on these observations, the right maxilla fragment could come from units 4A-IP, 4A-CHE, or 4A-POC.

At the time of the discovery, the large stalagmite situated in Square D30 was attributed to Speleothem CC14, and overlying Unit 4A-POC was attributed to former Layer 4A. As the fossil was found close to the boundary between former layers 3 and 4A, and as the bottom of the stalagmite was not yet reached by the excavation at that time, an attribution to Unit 4A-IP can be excluded. The hypothesis of an attribution to Unit 4A-POC is the most probable, given the extent of the layer in the square. However, an origin from the top of Unit 4A-CHE cannot be totally ruled out.

Pictures

No pictures exist of the right maxilla fragment in situ. However, the numerous pictures of the area near its place of discovery (squares C29, C30, D29, and D30) allow observations to be made regarding the exact course of the Unit 4A-CHE gully (left branch; cf §3.1). This can help to evaluate the importance of Unit 4A-CHE in Square D30, showing that most of the square was not affected by the gully structure (Figure 9).

3.3.2. Synthesis

The projection of the fossil onto Sedimentary Profile 30/31, the available pictures, and the position of Unit 4A-CHE in the area all indicate that most of Square D30 was outside the influence of the gully. Positioning the right maxilla fragment in Unit 4A-POC seems the best hypothesis, but an origin from the top of Unit 4A-CHE cannot be totally ruled out (Tables 1 & 2).

3.4. The permanent maxillary right first molar (Scla 4A-4)

3.4.1. Available arguments

The Scla 4A-4 molar was identified during excavation on the 14th of December 1993, in Square C30 (Figure 4). It was attributed to former Layer 4A in the field. Its 3-dimensional coordinates in Square C30 are: $x = 12$ cm, $y = 50$ cm, and $z = -466$ cm (Table 1).

Closest sedimentary profile

The nearest cross-section is Profile 30/31, which is 50 cm away. The projection of the molar onto this profile points to the bottom of Unit 4A-POC (Layer 4A-BO; Figure 5). Given the stratigraphic context and because the tooth is 50 cm away from the profile, the object may have come from the top of Unit 4A-CHE.

Pictures

Numerous pictures of the molar were taken in situ (Figure 12). They show that the fossil was unearthed from beige-orange sediment rich in small calcite fragments. The presence of calcite fragments suggests either Unit 4A-CHE or Unit 4A-POC. The comparison between the lithofacies on the pictures and the lithofacies of the layers on Sedimentary Profile 30/31 (still visible), together with the well-known stratigraphic relationships between the layers in this part of the sequence, indicate that the tooth Scla 4A-4 was found in Layer 4A-BO (Unit 4A-POC).

3.4.2. Synthesis

The pictures of tooth Scla 4A-4 in situ clearly show the lithofacies in which the tooth was found. This beige-orange sediment corresponds to Unit 4A-POC, and more specifically to Layer 4A-BO (Tables 1 & 2). These arguments allow this molar to be precisely and accurately positioned in the new stratigraphic record.

3.5. The permanent maxillary right second molar (Scla 4A-3)

The molar Scla 4A-3 was collected during sieving on the 15th of October 1992, from Square C30 (Figure 4). It was identified as a Neandertal tooth in the laboratory in October 1993. Its 3-dimensional coordinates are rather inaccurate: x and y are unknown, and $z = -464$ to -470 cm (Table 1). In the field, the tooth was exhumed from the boundary between former layers 4A and 3; the fossil was therefore attributed to the top of former Layer 4A.

3.5.1. Available arguments

Closest sedimentary profile

The closest cross-section is Profile 30/31. As this tooth was found during sieving, the exact distance between the fossil and the profile is unknown

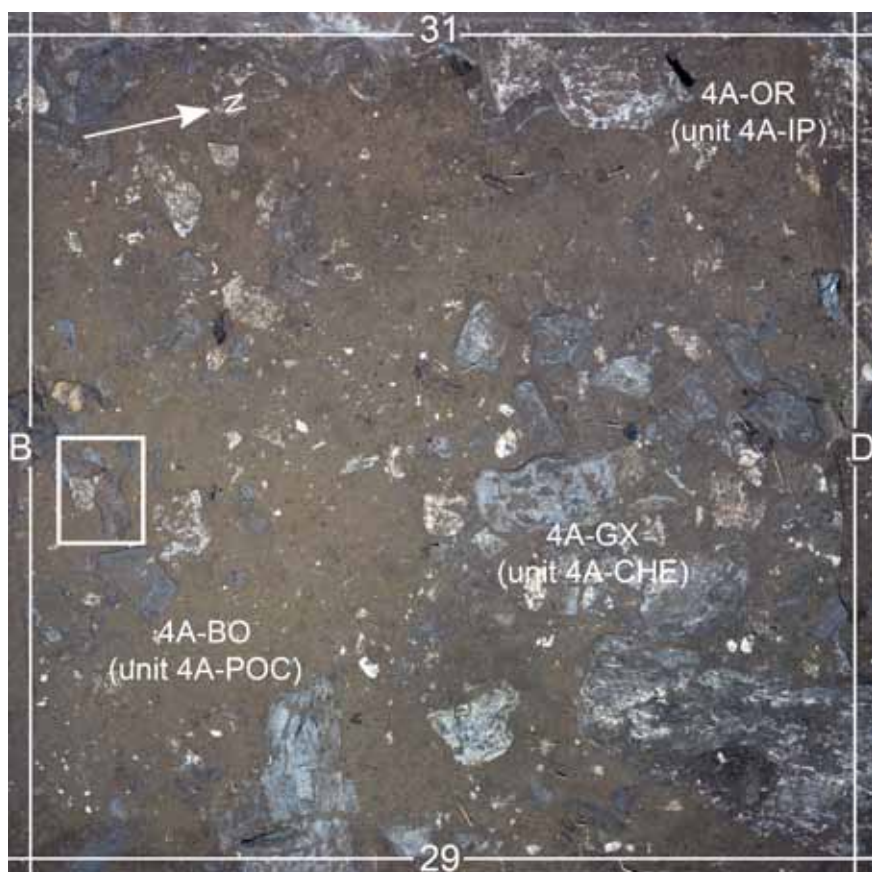


Figure 12: The permanent maxillary right first molar (Scla 4A-4) in situ in Square C30.

(but is a maximum of 1 m). The projection of this tooth onto Profile 30/31 suggests its origin as the top of Unit 4A-CHE or the bottom of Unit 4A-POC (Figure 5). If this molar was unearthed in the northern part of the square, it could also have been exhumed from Layer 4A-OR (Unit 4A-IP).

Pictures

No pictures of this tooth were taken in situ, as its discovery precedes the identification of the Neandertal child at Scladina. However, numerous pictures of the square were taken during the next stage of excavation, when the permanent maxillary right first molar (Scla 4A-4) was found (Figure 12). These pictures show the nature of the sediment that molar Scla 4A-4 was found in. The same sediment covered almost the entirety of Square C30: a silt rich in limestone and calcite fragments, attributable to units 4A-CHE or 4A-POC. Only a narrow band of sediment (10 cm wide and 40 cm long) situated in the northern part of the square contains no calcite fragments; this sediment corresponds to Layer 4A-OR (Unit 4A-IP).

Field notes

The information collected in the field clearly indicates that the narrow band of Unit 4A-IP in the northern part of Square C30 contains no bone or tooth remains. This situation suggests eliminating Unit 4A-IP from the possible candidates for the sedimentary context of Scla 4A-3.

3.5.2. Synthesis

The stratigraphic context of molar Scla 4A-3, deduced from the study of both the very close Sedimentary Profile 30/31 and the sediments visible in the pictures that show the discovery of molar Scla 4A-4 (found immediately after Scla 4A-3), suggests that this tooth likely originates either from Unit 4A-CHE (facies 4A-GX) or from Unit 4A-POC (Table 1 & 2). An origin from Layer 4A-OR (Unit 4A-IP) can be discarded, as this unit is very poorly represented in this square and contains no remains.



3.6. The crown of the permanent maxillary right third molar (Scla 4A-8)

The molar Scla 4A-8 was unearthed on the 14th of July 1995 in Square C32 (Figure 4). It was identified immediately after, during sieving. The field observations made during the discovery restrict the range of the object's x and y coordinates. Its 3-dimensional coordinates in Square C32 are thus: x = 20 to 80 cm, y = 10 to 30 cm, and z = -460 to -462 cm (Table 1). It was attributed to the top of former Layer 4A.

3.6.1. Available arguments

Closest sedimentary profile

The nearest profile is Cross-Section 32/31 (Figure 13). It is a maximum of 30 cm away from where the molar crown was discovered. The projection onto the northern half of Square C32 (towards D) points to Layer 3-LHM (Unit 3-INF), while the projection onto the southern half of the square (towards B) points to Layer 4A-LEG (Unit 4A-POC) or, less likely, to the upper 4A-JA facies (Unit 4A-CHE). However, an attribution to Layer 3-LHM (Unit 3-INF) can be ruled out because the sediment of this layer is brownish and could not have been confused with former Layer 4A; besides, according to the data collected in the field, former Layer 3 was completely excavated in this square by the 25th of March 1995.

Position in comparison with Speleothem CC4

The depth of Speleothem CC4 in Square D32 (-480 cm at the deepest) confirms that the molar Scla 4A-8 (z = -460 to -462 cm) must be from above the bottom of Speleothem CC4.

Field notes

An examination of the spatial distribution maps of the remains shows that the map concerning the tooth Scla 4A-8, at a depth of ~-460 cm, indicates the presence of calcite fragments. Therefore, the object must originate from units 4A-POC, 4A-CHE, or 3-INF, all of which contain calcite fragments.

3.6.2. Synthesis

The combination of all the available arguments suggest that the tooth originates from Unit 4A-POC, and more likely from Layer 4A-LEG, considering the position of the tooth in comparison with the Profile 32/31 (Tables 1-2). However, an origin from the top of Unit 4A-CHE (Facies 4A-JA) cannot be totally ruled out.

3.7. The deciduous mandibular right second molar (Scla 4A-13)

The Scla 4A-13 deciduous molar was found on the 13th of November 2001 in Square E38 (Figure 4).

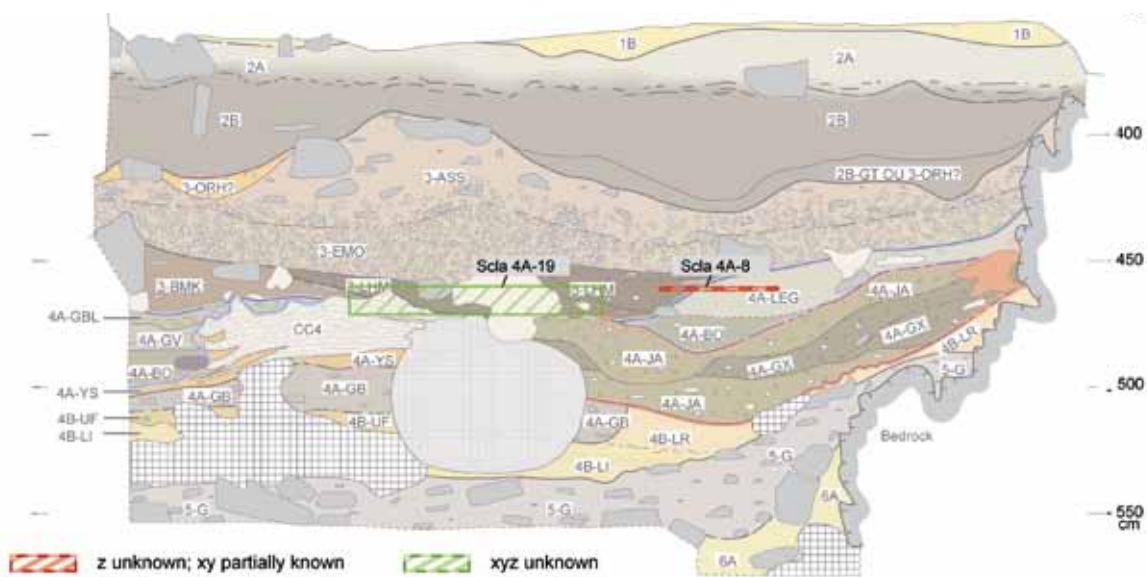


Figure 13: Orthogonal projections of the Neandertal remains Scla 4A-8 (C32) and 19 (D34) on Cross-Section 32/31.



Figure 14: The deciduous mandibular right second molar (Scla 4A-13) in situ in Square E38. Left, angle between profiles E/F and 38/39; right, close up of the tooth surrounded by an orange-brown and grey sediment corresponding to Layer 4A-LEG.



It was identified in situ. Its 3-dimensional coordinates in Square E38 are: $x = 88$ cm, $y = 57$ cm, and $z = -481$ cm (Table 1). It was attributed to former Layer 4A in the field.

3.7.1. Available arguments

Closest sedimentary profile

Sedimentary profiles E/F 38 and E 38/39 are the closest to where the molar was found (12 and 43 cm, respectively). The projection of the molar clearly shows that it is from Unit 4A-POC, and more precisely from layers 4A-BO or 4A-LEG.

Pictures

Several pictures of the area are available, including pictures with the tooth in situ. They show the junction between sedimentary profiles E/F and 38/39 (Figure 14). In these pictures, the molar can be positioned in comparison with the large speleothem fragment present at the corner of the two profiles. The tooth appears to be from sediment with grey and orange-brown lenses, corresponding to Layer 4A-LEG (Unit 4A-POC).

3.7.2. Synthesis

All the arguments, especially the pictures of the tooth in situ, demonstrate that the fossil Scla 4A-13 is from Unit 4A-POC, and more specifically from Layer 4A-LEG (Tables 1 & 2).

3.8. The permanent mandibular left lateral incisor (Scla 4A-19)

The tooth Scla 4A-19 was found during sieving on the 8th of March 1995. It is from Square D34 (Figure 4). It was attributed to former Layer 3, at the boundary with former Layer 4A. However, as it came from the last stage of excavation in former Layer 3, it is quite possible that a small part of the top of former Layer 4A was also accidentally excavated during the process.

The 3-dimensional coordinates are not accurate given the conditions of the object's discovery: the x and y values are unknown, and $z = -460$ to -471.5 cm (Table 1).

3.8.1. Available arguments

Closest sedimentary profile

The 2 available sedimentary profiles for provenancing this incisor are rather far away. The first one is Profile E/F 34, which is 1 to 2 m away (the absence of x - y coordinates prevents an accurate measurement). The projection (Figure 15) suggests a possible origin in Layer 4A-LEG (Unit 4A-POC), Layer 3-BMK (Unit 3-INF), or less likely from layers 4A-BO (Unit 4A-POC), 3-ASS, or 3-EMO (Unit 3-SUP).

The second profile is Cross-Section D 32/31 (Figure 13). It is even farther away from the fossil than E/F 34 at between 2 and 3 m, preventing any reliable projections. Regardless, the projection



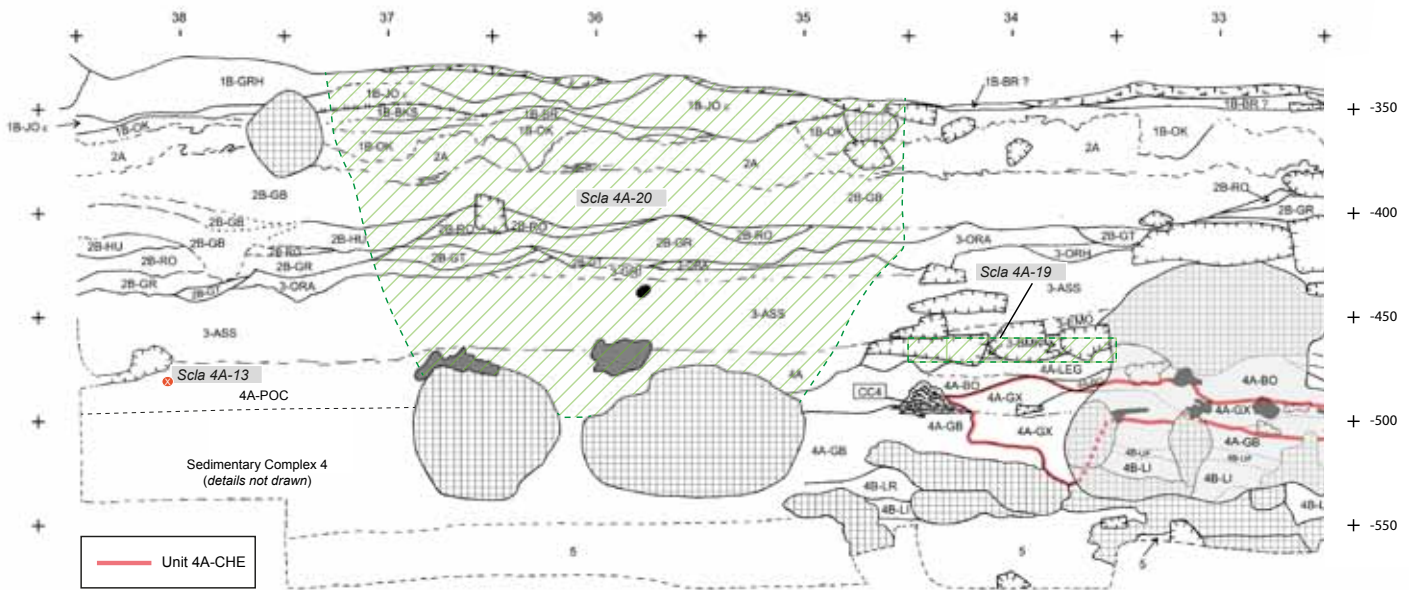


Figure 15: Orthogonal projections of the Neandertal teeth Scla 4A-13 (E38) and Scla 4A-19 (D34) on Sedimentary Profile E/F (after PIRSON, 2007). The area of this profile affected by the collapse (squares 35–37) that led to the discovery of the permanent mandibular right lateral incisor (Scla 4A-20) is also shown.

suggests Unit 3-INF (layers 3-LHM or 3-BMK), Unit 4A-POC (Layer 4A-GBL), or Unit 4A-IP (Speleothem CC4). However, taking the apparent dip observed on Profile E/F into account, an attribution to Unit 4A-IP seems unlikely and can be ruled out.

Position in comparison with Speleothem CC4

Near Square D34, Stalagmitic Floor CC4 has been observed at several locations in situ (Figure 4). In D34, Speleothem CC4 was reached during the stage of excavation following the discovery of the tooth (at an altitude of around –480 cm), which automatically implies that this fossil came from a layer overlying CC4. Units 4A-CHE and 4A-IP can therefore be discarded as candidates.

3.8.2. Synthesis

All the available arguments indicate that tooth Scla 4A-19 was excavated from a layer overlying Speleothem CC4 (i.e., postdating Unit 4A-IP). The available sedimentary profiles are too far away to allow any firm attribution to be made. Given the stratigraphic context, however, several units are possible candidates: units 4A-POC, 3-INF, or, less likely, Unit 3-SUP (Tables 1 & 2).

The fact that tooth Scla 4A-19 came from above Speleothem CC4 could explain that this fossil was attributed in the field to former Layer 3. At this

time, Speleothem CC4 was understood to seal former Layer 4A. Therefore, it was thought that an object from any sediment above CC4 had to belong to former Layer 3. In the new stratigraphic record Unit 4A-POC is understood to superimpose Speleothem CC4, so the fossil could either belong to 4A-POC or to former Layer 3 (i.e., to one of the layers of Unit 3-INF or to layers 3-ASS or 3-EMO of Unit 3-SUP).

3.9. The 10 teeth from squares F26, F27, G27, and H27

The squares F26, F27, G27, and H27 yielded 10 teeth belonging to the Scladina Neandertal child between the 22nd of February 1990 and the 19th of November 1991: Scla 4A-5, -6, -7, -11, -12, -14, -15, -16, -17, and -18 (Figure 4). These teeth were all collected before the identification of Neandertal remains in July 1993. At this time, the excavation in former Layer 4A was conducted by square metres and by ~10 cm thick levels (see Chapter 2). Their x and y coordinates inside the square are therefore unknown, while the z coordinate corresponds to an altitude range of between 9 and 15 cm (with extreme z values of –445 and –481 cm for all the 10 teeth; Table 1).

Eight of these teeth were attributed in the field to former Layer 4A. The 2 others (Scla 4A-17 and -18) were initially attributed to the bottom of

former Layer 3 and published as such (e.g., OTTE et al., 1993; TOUSSAINT et al., 1994). Soon after, these teeth were suggested to belong to former Layer 4A (BONJEAN et al., 1996, 1997; PIRSON et al., 2005). The situation will be re-examined here.

3.9.1. Available arguments

Each of the squares F26, F27, G27, and H27 include at least some of the Unit 4A-CHE gully structure (Figure 9). This probably explains why Speleothem CC4 is mainly absent from these squares. However, in the absence of x-y coordinates for the 10 teeth, and as the exact course of the gully in this area remains unknown, it cannot be excluded that some of the fossils may be from an area unaffected by the gully. In such a context, all the available arguments have been used in order to try to limit the uncertainty of the stratigraphic location for each of the 10 Neandertal teeth.

Position in comparison with Speleothem CC4

In the 4 squares listed above, Stalagmitic Floor CC4 (Unit 4A-IP) is only present in the north-western quarter of Square F27 and in the northern border of Square H27. However, it has been regularly observed in the surrounding area to the west and to the north (Figure 4). Because of the apparent dips observable on Sedimentary Profile H/I (Figure 16), and more specifically the apparent dip of the planar boundary between units 4A-AP and 4A-IP,

extrapolating the position of the bottom of Unit 4A-IP is possible in the squares where the speleothem was not observed. Most of the time, the bottom of Unit 4A-IP corresponds to the bottom of Speleothem CC4.

On Sedimentary Profile H/I, the apparent dip of the planar limit at the bottom of Unit 4A-IP has a value of about 4° (~ 7 cm/m) between metres 23 and 28, then tends to be almost horizontal between metres 29 and 30. This value (7 cm/m) corresponds to the planar limit's average apparent dip because the bottom of Unit 4A-IP regularly deviates from this mean value by only a few centimetres. The maximum observed deviation on Profile H/I is close to 10 cm, but most of the time the deviation is less than 5 cm. This extrapolation has to be used carefully, given the important lateral variations regularly observed in the cave; however, it remains one of the main arguments for the reattribution of these 10 teeth to the new stratigraphic record.

Based on this extrapolation, the estimated depth of the bottom of Unit 4A-IP in the squares F26 and F-G-H27 is indicated on Figure 17 (values between brackets). The implications for the 10 teeth are listed below, square by square:

- F26: the extrapolated bottom of Unit 4A-IP is at -473 cm. The tooth Scla 4A-18, with an altitude value of between -461 and -471 cm, would thus be situated above this limit;
- F27: the extrapolated bottom of Unit 4A-IP is at -480 cm and the measured depth of the portion of the in situ Speleothem CC4 is at -482 cm.

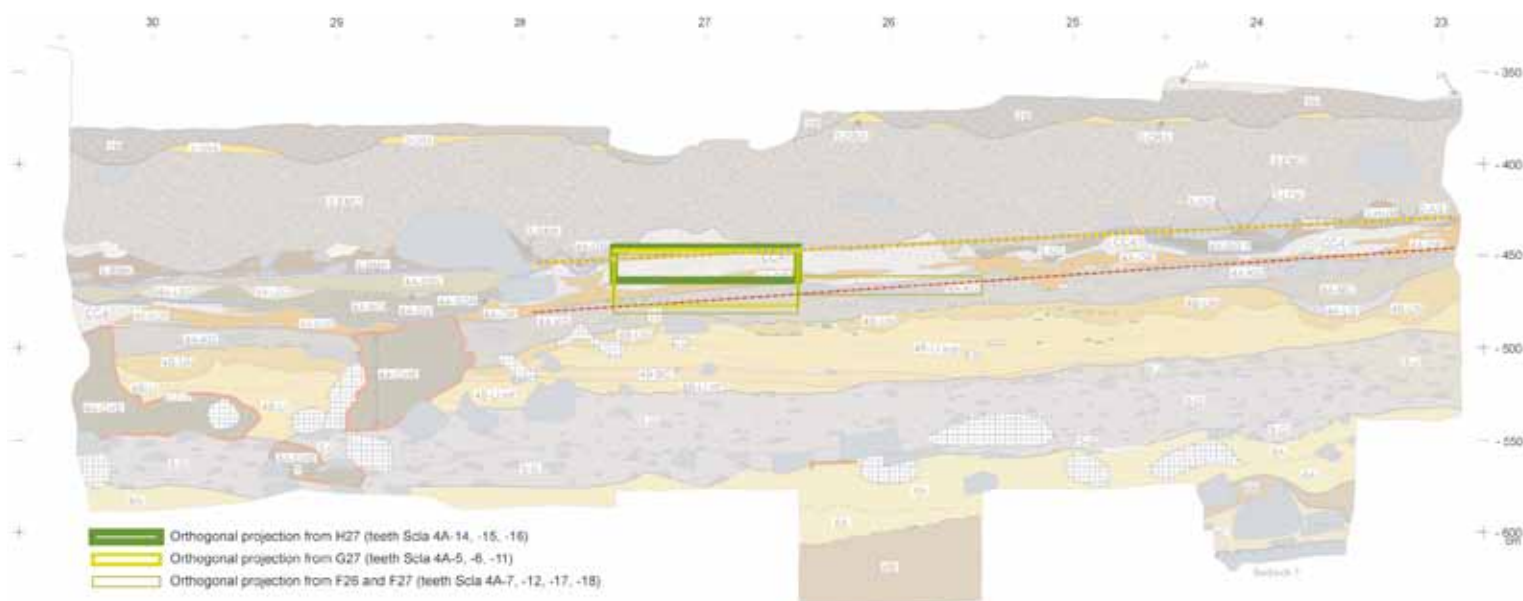


Figure 16: Orthogonal projections (rectangles) of the 10 Neandertal teeth from squares F26 and FGH-27 on Sedimentary Profile H/I. The apparent dips of the bottom of Unit 4A-IP (red; ~ 7 cm/m) and Layer 3-EMO (yellow; ~ 5 cm/m) are also shown.



- This reinforces the reliability of these extrapolations. The teeth Scla 4A-12 ($z = -449$ to -461 cm) and Scla 4A-17 ($z = -458$ to -470 cm) are clearly situated higher; the tooth Scla 4A-7 ($z = -471$ to -481 cm) is situated slightly above or immediately below the bottom of Unit 4A-IP;
- G27: the extrapolated bottom of Unit 4A-IP is at -477 cm. The teeth Scla 4A-5 and -11 ($z = -447$ to -462 cm) would thus be situated above this limit; the tooth Scla 4A-6 ($z = -463$ to -477 cm) would also be above this limit or at the boundary between units 4A-AP and 4A-IP;
 - H27: the extrapolated bottom of Unit 4A-IP is at -475 cm. This value is comparable to what was observed on Sedimentary Profile H/I 27 (-465 to -473), which again reinforces the reliability of these extrapolations. The teeth Scla 4A-14 and Scla 4A-15 ($z = -445$ to -454 cm), as well as Scla 4A-16 ($z = -454$ to -463 cm) are thus situated above the bottom of Unit 4A-IP.

As a result, 8 out of 10 teeth are clearly situated above the lower limit of Unit 4A-IP, which means that they are contemporaneous with or were deposited after Unit 4A-IP. The 2 remaining teeth are also probably above this limit, even if a position immediately below cannot be totally ruled out by this analysis.

Position in comparison with Unit 4A-CHE

Unit 4A-CHE is a gully structure that developed downwards from the top of Unit 4A-IP into subjacent layers. Most of the time, Unit 4A-CHE extends below the bottom limit of Unit 4A-IP, despite it being younger (Figure 2). However, the top of Unit 4A-CHE is sometimes situated higher than the bottom of Unit 4A-IP (e.g., on profiles 30/31 in C or 32/31 in B-C-D; Figures 5 & 13).

In this context, the 8 teeth situated above the bottom of Unit 4A-IP are most likely not from 4A-CHE, but this latter hypothesis cannot be totally ruled out. The 2 other teeth, Scla 4A-7 ($z = -471$ to -481 cm) and Scla 4A-6 ($z = -463$ to -477 cm), might originate from below Unit 4A-IP (extrapolated bottom of Unit 4A-IP at -480 and -475 cm, respectively); they could therefore belong to Unit 4A-CHE.

Unit 4A-IP vs. Unit 4A-CHE

Often where the 4A-CHE gully is present Unit 4A-IP has been completely eroded. As the squares F26, F27, G27, and H27 are most probably affected by the Unit 4A-CHE gully, Unit 4A-IP has probably been eroded from most of these squares. As a result, an origin of the teeth in Unit 4A-IP

itself seems unlikely. However, Unit 4A-IP was present on a small portion of F27 and H27 where Speleothem CC4 was recorded (Figure 9); small parts of the other squares were also potentially not affected by Unit 4A-CHE. In such conditions, an origin from Unit 4A-IP cannot be totally ruled out; however, it is unlikely.

Position in comparison with units 3-SUP and 3-INF

Given the local stratigraphic context deduced from sedimentary profiles H/I and 30/31, as well as from field data, the 10 teeth are not from a layer that superimposes Layer 3-EMO (Unit 3-SUP).

Concerning Unit 3-SUP itself and its main Layer 3-EMO, the same method as for Speleothem CC4 was applied: the apparent dip of the lower boundary of Layer 3-EMO observable on Sedimentary Profile H/I was used (Figure 16). This dip has a value of between 3 – 3.5° (~ 5 to 6 cm/m) when viewed on this profile. On Sedimentary Profile 30/31, the altitude of Layer 3-EMO varies between -470 cm in column F and -441 cm in column H due to the presence of a small gully in column F (Figure 18). In such a stratigraphic context, the use of average dip is difficult. Therefore, only the minimum dip will be taken into account (5 cm/m). Furthermore, the minimum dip will be applied to the lowest point of Layer 3-EMO on Profile 30/31, at the bottom of the small gully (-470 cm), in order to take the probable meandering course of this gully into account when going updip from metre 30 to metres 26–27. As a result, the extrapolated depth of the lower limit of Layer 3-EMO for squares F–G–H 26–27 will represent the lowest possible values for this limit.

Following this reasoning, the lowest possible depth of the bottom of Layer 3-EMO (Unit 3-SUP) ranges from -450 cm to -445 cm for metre 26, and from -455 cm to -450 cm for metre 27 (Figure 17). When comparing these values with the depth range of each Neandertal tooth, it appears that the tooth from Square F26 (Scla 4A-18; $z = -461$ to -471 cm) is clearly below Layer 3-EMO and thus cannot be from this layer. The same goes for 4 teeth from metre 27 (Scla 4A-6, -7, -16, -17). The lowest value of the depth range of the 5 remaining teeth (Scla 4A-5, -11, -12, -14, -15) is close to the limit: between -445 and -449 cm. Therefore, for these 5 teeth, Layer 3-EMO cannot be totally ruled out as their sedimentary context (Table 2).

The same method was applied to Unit 3-INF and indicated that the 10 teeth could be from this unit, even if it seems unlikely for 5 of them.

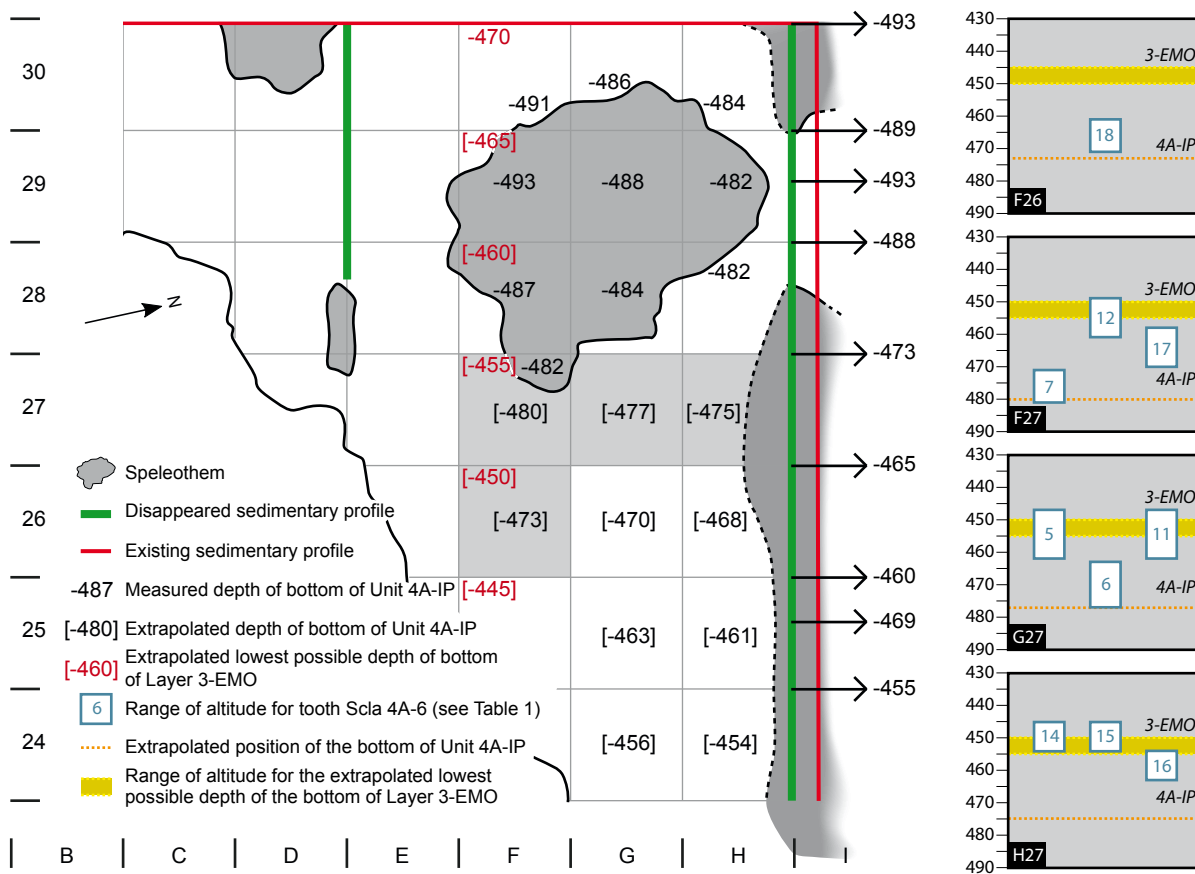


Figure 17: The extrapolated depth (see text) of the bottom of Unit 4A-IP as well as the extrapolated lowest possible depth of the bottom of Layer 3-EMO. These extrapolated depths helped reconstruct the stratigraphic position of the 10 teeth from squares FGH 27 and F26 relatively to 3-EMO and 4A-IP (see boxes at the right).

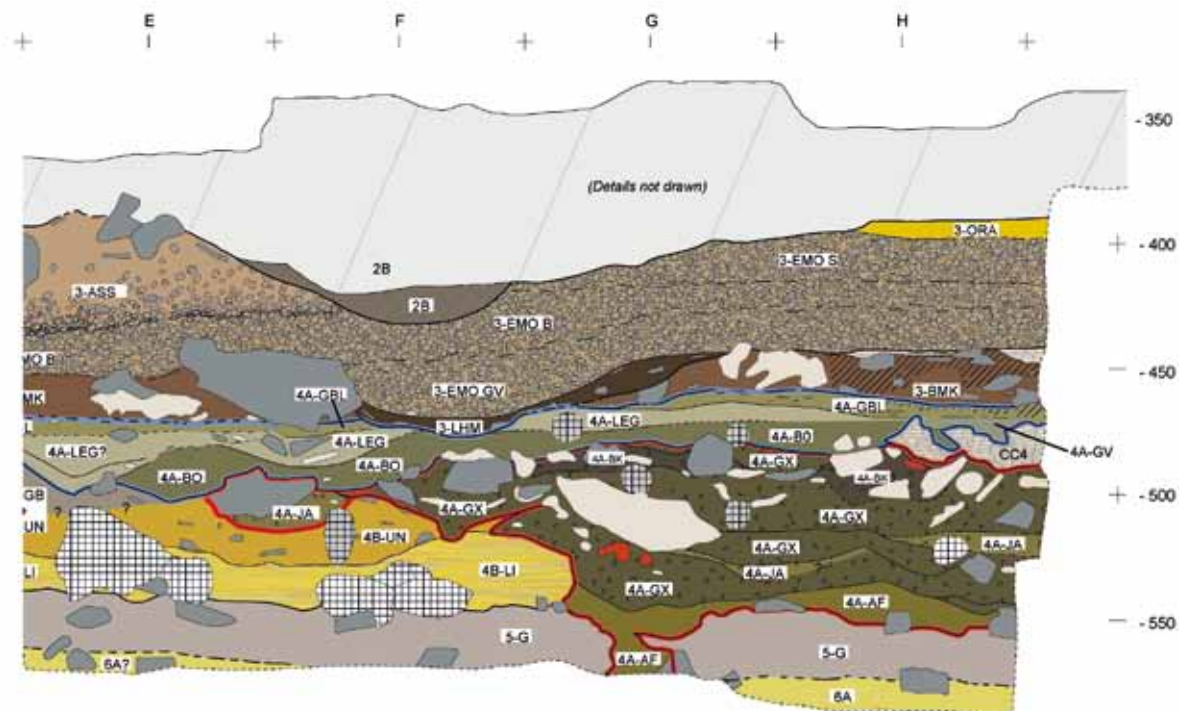


Figure 18: Sedimentary Profile 30/31 showing the concave aspect of the bottom of Layer 3-EMO (gully; the complete section, from B to H, is presented in Chapter 3).



Closest sedimentary profile

The nearest cross-section is the longitudinal Sedimentary Profile H/I. However, the orthogonal projections are not useful for several reasons: the complexity of the attitude of structures in this area, especially with the gully of Unit 4A-CHE; the concave shape of the lower limit of Speleothem CC4 on the transverse axis (Figure 17); and the irregular lower boundary of Layer 3-EMO (Unit 3-SUP) due to small gullies. The projections will therefore not be taken into account. For information only, the projection of the fossils from Square H27 (which are less than 1 m away) point to the following layers (Figure 16): Speleothem CC4 (Unit 4A-IP) or Layer 4A-OR (Unit 4A-IP) in the case of tooth Scla 4A-16; Speleothem CC4 (Unit 4A-IP) or Layer 3-EMO (Unit 3-SUP) in the case of teeth Scla 4A-14 and -15. The projections of the teeth from squares F26, F27, and G27 (Figure 16) point to Layer 4A-KG (Unit 4A-AP), Layer 4A-OR or CC4 speleothem (Unit 4A-IP), or Layer 3-EMO (Unit 3-SUP).

3.9.2. Synthesis

The 10 teeth found in squares F26, F27, G27, and H27 are the first human remains discovered at Scladina. They were unearthed between 1990 and 1991, i.e., before the identification of the Neandertal child. For these reasons, the available data is less numerous and less precise. The stratigraphic context of the objects is therefore much more difficult to establish.

The main arguments concern the stratigraphic sequence in the area, deduced from the reference sections H/I and 30/31, and the comparison between the altitude of the teeth and the altitude of the lower limit of units 4A-IP, 3-INF, and 3-EMO. A first limitation of using these arguments is the lack of precision of the altitude values given to the teeth, as they were found during sieving. A second limitation is that the altitude of units 4A-IP, 3-INF, and 3-EMO can only be obtained following an extrapolation based on an average longitudinal dip determined on the reference Sedimentary Profile H/I. Caution is therefore particularly advised here.

Taking all of this into account, suggesting that the teeth are from units 4A-IP, 4A-CHE, 4A-POC, 3-INF, and/or 3-SUP is possible, with a different combination of potential units for each tooth (see Tables 1 & 2 for the details). An origin from Unit 3-SUP or Unit 4A-IP is unlikely in all cases. Among 4A-CHE, 4A-POC, and 3-INF, the best hypothesis

would be an origin from Unit 4A-POC because it is the common possibility between all the 10 teeth.

3.10. The permanent mandibular right lateral incisor (Scla 4A-20)

The tooth Scla 4A-20 was discovered on the 12th of July 2006 during the sieving of sediment from a collapse of Sedimentary Profile E/F 35-37 (Figure 4), in an area bioturbated by 2 large badger burrows (Figures 15 & 19). The 3-dimensional coordinates of this incisor are therefore unknown (Table 1).

3.10.1. Available arguments

Closest sedimentary profile

Two sedimentary profiles influence the interpretation of this tooth's context: Profile E/F (Figure 15) and Profile F/G. The careful examination of the collapse area in 2006 indicates that only some units have been affected by this collapse: Sedimentary Complex 1B, as well as units 2A, 2B, 3-SUP, 3-INF, and 4A-POC (Figure 15). An origin from a unit older than Unit 4A-POC can therefore be discarded, allowing units 4A-AP and 4A-IP to be excluded. In addition, Unit 4A-CHE can also be ruled out because this unit does not exist in the area affected by the profile collapse (E/F 35-37) and is only visible between metres 34 and 32 on Profile E/F.

3.10.2. Synthesis

The units affected by the collapse of the Sedimentary Profile E/F in 2006 allow the sedimentary context of the tooth Scla 4A-20 to be restricted to a small number of candidates: Sedimentary Complex 1B, as well as units 2A, 2B, 3-SUP, 3-INF, and 4A-POC. An origin from Unit 4A-CHE is not possible because the unit is absent from the squares affected by the collapse. Given the available data on the stratigraphic origin of the other Neandertal child remains, an origin from units 4A-POC or 3-INF seems the most likely, but an origin from Unit 3-SUP (mainly Layer 3-ASS) cannot be ruled out (Tables 1 & 2).

4. Discussion

4.1. Where did the Scladina Child remains come from? A summary of the stratigraphic origin of the Neandertal remains

The re-examination of all the available arguments allowed all of the Neandertal remains

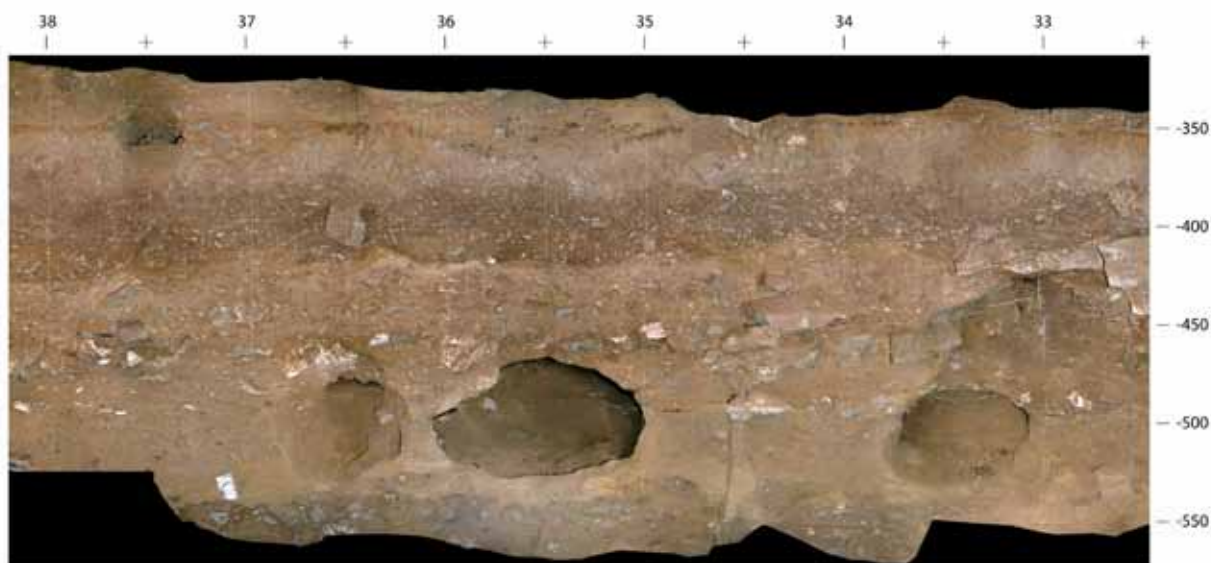


Figure 19: Sedimentary Profile E/F showing the two large badger burrows responsible for the accidental collapse of a portion of the profile (35-37; Figure 15). The sieving of sediments from this collapsed area led to the discovery of the permanent mandibular right lateral incisor (Scla 4A-20). This figure corresponds to the assemblage of several pictures; some errors are thus expected (photographs: Archéologie Andennaise; photomontage: K. Di Modica).

to be organised into the new stratigraphic record, sometimes with accuracy, sometimes with a rather high uncertainty (Tables 1 & 2; Figure 20).

Most of the time, the comparison between the 3-dimensional coordinates of the Neandertal remains and the available sedimentary profiles was insufficient for positioning the fossils with accuracy through orthogonal projections. This is due to the high complexity of this part of the stratigraphic sequence, particularly the presence of the Unit 4A-CHE gully. On the other hand, the comparison of these projections with the analysis of the available pictures often turned out to be a determining factor, especially thanks to the presence of speleothem fragments in units 4A-CHE and 4A-POC. The altitude of the Neandertal remains, when compared with the major stratigraphic marker represented by Speleothem CC4, is also an argument that is important for most of the fossils.

When taking all the arguments into account, 3 of the 19 remains could be positioned with absolute certainty in a specific layer from the new stratigraphic record. These fossils belong to 2 distinct units postdating the Speleothem CC4: units 4A-CHE and 4A-POC. The first of these fossils is the right half of the mandible (Scla 4A-1). It is from the top of Unit 4A-CHE, and more specifically from the uppermost 4A-GX lithofacies. This unit corresponds to a large gully, which suggests that the right half of the mandible is in secondary spatial position. The 2 other fossils

(Scla 4A-4 and -13) are teeth from Unit 4A-POC: the first is from Layer 4A-BO, the other is from Layer 4A-LEG. These 2 teeth are likely in tertiary spatial position because they belong to the same individual as the right half of the mandible (see Chapters 10, 12 & 13), which was exhumed from an older unit (Unit 4A-CHE, which immediately predates Unit 4A-POC). Therefore, these 2 teeth underwent a reworking phase from the top of Unit 4A-CHE.

Four other fossils are either from Unit 4A-CHE or from Unit 4A-POC: the fragment of right maxilla (Scla 4A-2), the left half of the mandible (Scla 4A-9), and 2 additional teeth (Scla 4A-3 and -8). Therefore, despite the possibility of an origin from 2 distinct units, the stratigraphic context of these 4 fossils is similar to that of the first 3.

Eleven other teeth (Scla 4A-5, -6, -7, -11, -12, -14, -15, -16, -17, -18, and -19) could originate from several units. All in all, 5 units are possible candidates: 4A-IP, 4A-CHE, 4A-POC, 3-INF, and 3-SUP (Table 1).

- Unit 4A-POC is systematically present as a possible candidate for each fossil, each time either as the most probable (3 out of 11) or as one of the most probable (8 out of 11).
- Unit 3-INF is also systematically a possible candidate for each of the 11 fossils; it is one of the most probable candidates in 6 cases and an unlikely candidate in 5 cases.
- Unit 4A-CHE is a candidate for 10 fossils out of 11; it is one of the most probable candidates in



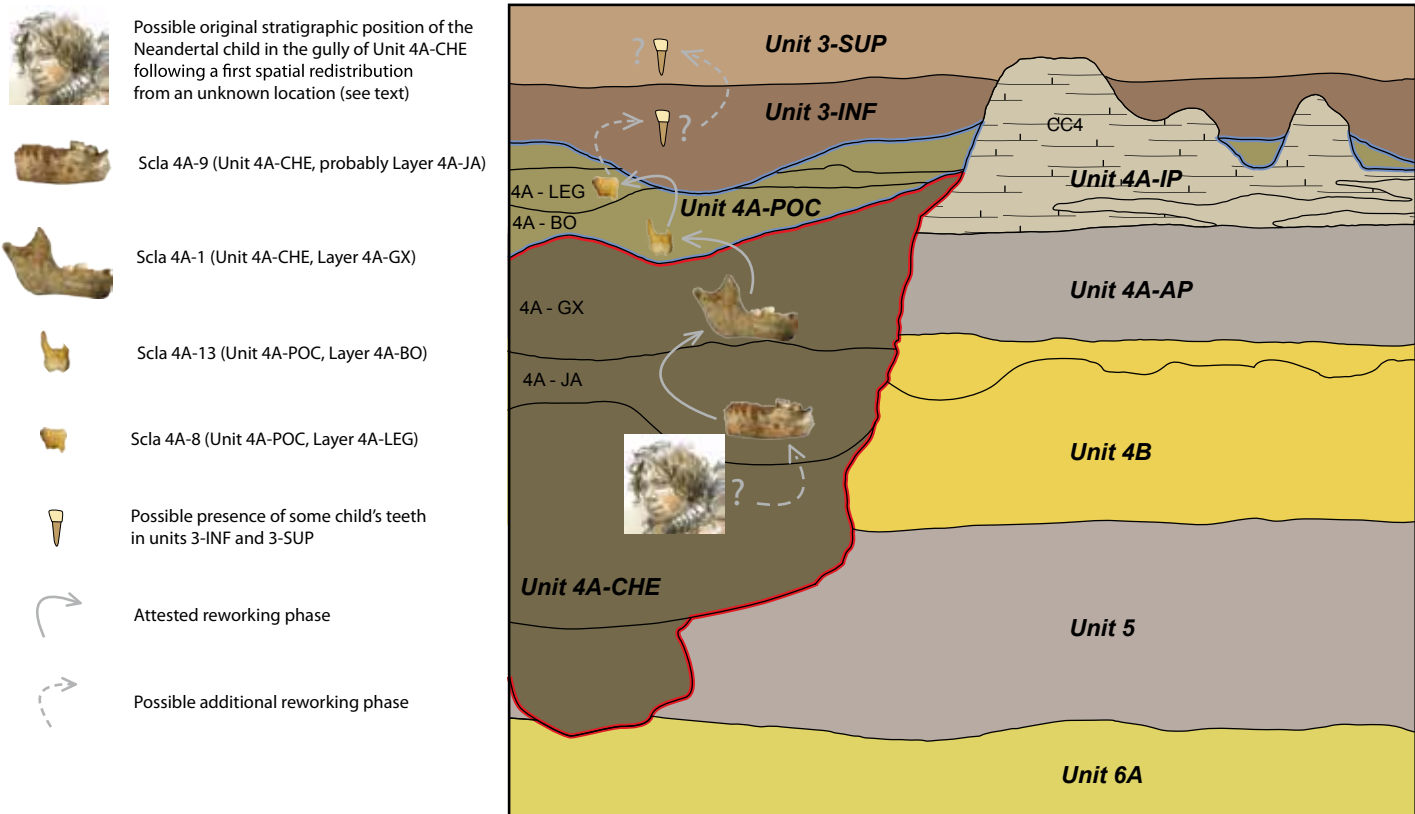


Figure 20: Sketch evoking the complex depositional history of the Neandertal child remains. This is illustrated through 4 remains: the 3 fossils that could be positioned with certainty in a specific layer from the new stratigraphic record (Scla 4A-1, -4, and -13), and the left half of the mandible (Scla 4A-9).

only 2 cases, being an unlikely candidate in the 8 other cases. In each situation, only the top of this unit is concerned.

- Unit 4A-IP is candidate for 10 fossils out of 11 but it is always as an unlikely candidate.
- Unit 3-SUP, and in particular Layer 3-EMO, is only candidate in 6 cases out of 11. It is always an unlikely candidate.

The last fossil, the tooth Scla 4A-20, is in a similar situation as the 11 above mentioned teeth, despite having been found after the collapse of Sedimentary Profile E/F 35-37. When taking into account both the stratigraphic context of all the other Neandertal remains and the layers affected by the collapse, an origin from units 4A-POC or 3-INF seems to be the best hypothesis, while an origin from Unit 3-SUP (mainly Layer 3-ASS) is unlikely.

The anthropological study of the Neandertal remains has clearly demonstrated that all the 19 fossils are from a single individual (Chapters 10, 12 & 13). These 19 objects were therefore initially deposited within the same stratigraphic unit. Two distinct stratigraphic units yielded 7 fossils out of 19: units 4A-POC and 4A-CHE. The best hypothesis would suppose that the other 12 remains also come from one of these 2 units. This hypothesis

is strengthened by the fact that Unit 4A-POC is the only unit systematically represented as one of the most probable, if not the most probable, candidates for these 12 remains.

An origin from units 3-INF or 3-SUP is a possibility for 11 fossils out of 19. This would not drastically change the outcome of the analysis. These 2 units have an erosive lower boundary on Unit 4A-POC, and the concerned fossils could originate from the reworking of material from 4A-POC. In this situation, a second and possibly a third reworking phase would have to be considered. However, this is unlikely as several successive reworking phases would have diagenetically altered the Neandertal remains, and the taphonomic study highlighted their relative unaltered state. The remains were said to have a low degree of abrasion of edges for the 3 osseous fragments, and an exceptional state of preservation of the 16 isolated teeth of the Neandertal child, with little alteration (see Chapters 7, 10 & 13). In such conditions, an origin of some fossils from Layer 3-EMO (Unit 3-SUP), laid down through high energy dynamics (torrential flow; see Chapter 3), seems very unlikely.

In fact, only an origin from Unit 4A-IP would really change the situation, as some fossils would

then be from a unit older than 4A-CHE, implying that all of the Neandertal remains were originally located in that unit. However, each time the origin from Unit 4A-IP is considered (10 isolated teeth out of the 19 remains) Unit 4A-POC is a much more probable candidate. In addition, Unit 4A-IP is almost completely deprived of any bone remains.

When taking all the elements into account, Unit 4A-POC is the most probable sedimentary context for the isolated teeth. This interpretation is strengthened by the taphonomic study, which indicates that Unit 4A-POC yielded the most animal teeth that have the strongest taphonomic correlation with the isolated Neandertal teeth (see Chapter 7). On the other hand, the 3 bone fragments offer the strongest taphonomic similarities with animal bone remains from Unit 4A-CHE. This appears to be very consistent as the right half of the Neandertal mandible is effectively from Unit 4A-CHE, while Unit 4A-CHE is the most probable context for the left half of the mandible. Regarding the small fragment of the Neandertal maxilla, it most probably came from Unit 4A-POC, but an origin from Unit 4A-CHE is not impossible.

4.2. Implications for the depositional history and the origin of the Neandertal remains

Stating that the Neandertal remains were originally deposited in Unit 4A-CHE and were subsequently reworked into one (or several) younger unit(s) is reasonable considering the data provided. Because of the sedimentary depositional dynamics of Unit 4A-CHE, all the Neandertal remains are in secondary spatial position.

The secondary spatial position of the Neandertal fossils, as well as associated high energy sedimentary dynamics, were already suggested before the stratigraphic reappraisal because of several arguments: the presence of broken speleothem fragments, the occurrence of bones and limestone blocks in a very oblique or vertical positions, a large longitudinal dispersion (several metres) of the anthropological remains, and the variable depths of the different Neandertal remains (BONJEAN et al., 1996, 1997; TOUSSAINT et al., 1998). The integration of these elements led researchers to suggest that a thick mud flow² transported the remains. The occurrence of cut-and-fill structures was also recorded on a sedimentary profile

² “*coulée boueuse épaisse*”

(Profile D/E 28-30; BONJEAN et al., 1997; see Figure 6). However, before the stratigraphic reappraisal, the mud flow event was thought to have deposited the entire former Layer 4A.

The new stratigraphic record, when combined with the reappraisal of the stratigraphic position of the Neandertal remains presented in this chapter, indicates a much more complex situation.

It is now well established that the Neandertal remains were disturbed by an event that created an important erosional structure in the form of a large and deep gully (Unit 4A-CHE). On its course, this gully eroded Speleothem CC4 and underlying layers down to Unit 6A (see Chapter 3). In such a context, is it possible to establish the primary stratigraphic position of the Neandertal child osseous fragments and teeth?

Given the sedimentary dynamics of Unit 4A-CHE, the remains could have been buried long before the gully episode and then reworked from their initial sedimentary context(s) by the gully during its initial high-energy stages. The hypothesis of the child being contemporary with Stalagmitic Floor CC4 (Unit 4A-IP) or with the underlying units (Unit 4A-AP or even units 4B, 5 or 6A) is conceivable, as the gully reworked all of these units. A much older origin cannot be totally ruled out either, especially if one takes into account an origin from another area of the cave, or even from outside the cave. However, there is no evidence that the remains were reworked into the 4A-CHE gully from another, previously deposited context. On the contrary, all the available data points to Unit 4A-CHE being the original sedimentary context of the Neandertal remains:

- The oldest stratigraphic unit that have yielded some of the Neandertal remains is Unit 4A-CHE; none were found in any subjacent layers.
- All of the Neandertal remains possibly unearthed from 4A-CHE are always from the top of the unit, suggesting that these objects were incorporated during the last stages of the gully’s formation; if they were reworked by the gully from a subjacent unit, they would probably be at least partly incorporated during the initial, high-energy stages of the gully structure.
- Their spatial distribution, restricted to the course of the 4A-CHE gully, suggests they are strictly associated with this structure, even if they were later slightly reworked from the top of Unit 4A-CHE in the low-energy Unit 4A-POC, probably through run-off.



- The results of the taphonomy study (see Chapter 7) do not suggest any high energy reworking; the relative unaltered state of the fossils discovered so far, notably the good preservation state of the tooth roots (see Chapter 16), suggests they were not strongly reworked.
- When all of the physical taphonomic attributes are combined, bones and teeth from units 4A-CHE and 4A-POC yield the strongest correlation to the Neandertal child (see Chapter 7); this suggests that the child remains are part of the objects deposited during the gully event.
- The right hemimandible was unearthed from Unit 4A-CHE, while the left hemimandible is likely also from 4A-CHE, but from another layer within the unit; the fact that they have been differentially fossilized suggests that the Neandertal remains were not yet completely fossilized or recrystallised when they were incorporated into different layers within Unit 4A-CHE (see Chapter 7), which strengthens the hypothesis of sedimentary Unit 4A-CHE being the primary sedimentary context of the child.

After the spatial redistribution of the Neandertal child remains through the gully episode, they were later affected by at least one reworking phase, some of the remains initially present in Unit 4A-CHE being reworked in Unit 4A-POC. If some of the teeth were really excavated from units 3-INF and/or 3-SUP, however unlikely it may be, a second or a third reworking phase would have to be considered.

In this context of complex subsequent redistribution and reworking phases, the important spatial distribution of the remains along the longitudinal axis of the cave makes particular sense.

In the present stage of research, the exact primary spatial position of the Neandertal fossils is still unknown. As the oldest stratigraphic unit that yielded some fossils is Unit 4A-CHE, its attitude gives some indications: the direction of the redistribution of the Neandertal remains is from the entrance to the back of the cave.

Whether the process that brought the Neandertal child remains into the cave was anthropogenic, biological (bioturbation or carnivore activity), or sedimentary, is still unknown. If the influence of the gully is proven to be the cause of the spatial redistribution of the fossils, there is still no evidence to suggest that the event which created this gully is related to the process

that first brought the child remains into Scladina Cave. In the present state of research, however, no arguments support either the hypothesis that the child was brought into the cave by an animal, or that it was brought in by anthropological activity, for instance in the form of a burial that was later reworked by the gully.

4.3. Implications for the chronostratigraphic context of the Neandertal remains

The review of the Scladina sequence led to a better understanding of the stratigraphic context of the Neandertal remains, and therefore determined the relative chronology of the events, including the relative antiquity of the child.

In the present state of understanding, the minimum age of the Neandertal child corresponds to the time the objects were deposited. Therefore, the hominin remains are, at the youngest, contemporary with the deposition of sediment in the 4A-CHE gully and thus postdate Stalagmitic Floor CC4. The proposed chronostratigraphic positioning for Unit 4A-CHE, however, is not that accurate; following the arguments developed in Chapter 4, it would span between MIS 5b (if the end of CC4 coincides with the end of MIS 5c) and early MIS 4 (if the end of CC4 coincides with the end of MIS 5a). The best hypothesis is nevertheless an age somewhere inside MIS 5b or MIS 5a, as Unit 2B best corresponds to the end of MIS 5a (see Chapter 4 & Appendix B).

However, as the bones are in secondary spatial position in the gully, the age of the deposit must theoretically be distinguished from the age of the hominin remains. That means that the maximum age of the child cannot be firmly established by stratigraphy. Despite the wide time span involved when taking 2σ into account, the direct dating by gamma spectrometry ($127^{+46/-32}$ ka BP; Yokoyama & Falguères in TOUSSAINT et al., 1998) offers a useful maximum age for the fossils.

It has nevertheless been shown that the best hypothesis is that the Neandertal child is contemporaneous with Unit 4A-CHE (§4.2). If this is correct, then the age of the Scladina Neandertal remains would correspond to the age of the 4A-CHE gully structure. Therefore, in the present stage of research, the best two hypotheses are positioning the Scladina Neandertal remains in either MIS 5b or in the beginning of the second part of MIS 5a (see Appendix B).

4.4. Implications for the palaeoenvironmental context of the Neandertal remains

Despite the good palaeoenvironmental data from Scladina (see Chapter 4), direct consequences for the Neandertal child must be considered with caution, as these hominin remains were found in secondary position. If the contemporaneity of the Neandertal remains with Unit 4A-CHE is correct, this would point to a relative cold and open environment, as the gully of Unit 4A-CHE is interpreted as a melting gully related to the degradation of a deep frozen soil (see Chapter 4).

5. Conclusions and prospects

Among the 19 juvenile Neandertal remains unearthed to date, 7 could be repositioned with accuracy inside the new stratigraphic record based on several arguments, including: their spatial distribution, projections on the closest sedimentary profiles, study of photographs taken in the field, and their position in relation to Speleothem CC4. Each of these 7 fossils is either from Unit 4A-CHE gully or from the directly overlying deposits (Unit 4A-POC). Three of these 7 fossils were even repositioned into a specific layer with certainty.

The results of the re-evaluation of the 12 other remains are still uncertain, as several sedimentary units are still possible candidates. However, an attribution to units 4A-POC and 4A-CHE is most likely when taking all elements into account, i.e., the most probable candidates combined with the results of the taphonomic study and with the fact that all the remains belong to a single individual.

All the Neandertal remains discovered so far are in secondary spatial position. A first spatial redistribution phase is linked with the development of the large gully of Unit 4A-CHE, while during the deposition of Unit 4A-POC some of the fossils were reworked from the top of Unit 4A-CHE. At least two spatial redistribution phases are therefore attested. The fact that the Scladina Child remains were displaced has been acknowledged since the first in situ discovery in 1993. Due to recently establishing a higher resolution stratigraphic sequence, a better understanding of the sedimentary dynamics, and a more accurate positioning of the Neandertal remains in the new stratigraphic record, part of their complex history is now better understood; this process led to a clarification of the remains' mode of deposition and

a better explanation of their spatial distribution. However, as they are in a secondary spatial position, neither their initial spatial origin nor the exact process that first brought the remains into the cave could be determined. Given the course of the gully from Unit 4A-CHE, the fossils must be from somewhere closer to the entrance of the cave.

The relative age of the child is difficult to establish because all the discovered fossils were spatially redistributed and the chronostratigraphic context of the sequence is not accurately understood. Their good state of preservation, however, does not suggest the strong reworking of material under high-energy circumstances. This, together with several other arguments, suggests that the Neandertal child is probably contemporaneous with their deposition in the Unit 4A-CHE gully. If this is correct, the age of the child would be close to the age of Unit 4A-CHE. Given that units 6B to 2B are positioned in MIS 5, and that the palaeoenvironmental interpretation of the genesis of Unit 4A-CHE points to cold conditions (melting gully), the most probable chronostratigraphic positioning of Unit 4A-CHE is one of the cold phases at the end of the Weichselian Early Glacial. Therefore, the two best hypotheses in the present stage of research would place the Scladina Neandertal remains in either MIS 5b or in the intra-MIS 5a cold episode. Compared with the Greenland reference sequence, this points to either GS 22 or the cold episode in the beginning of the second half of GI 21, which are respectively dated to approximately 87,000 BP and 80,000 BP according to the NorthGRIP chronology (NORTHGRIP-MEMBERS, 2004).

The prospects about the Scladina Neandertal child are promising. Thanks to the use of an excavation method adapted to the high complexity of the stratigraphic context of Sedimentary Complex 4A (see Chapter 2; BONJEAN, 2009; BONJEAN et al., 2009^b), future fieldwork should make it possible to test several hypotheses, even if no new Neandertal remains are discovered. The origin of the 4A-CHE gully, its flow direction, and its spatial extent could notably be improved, leading to better deciphering the origin of the hominin remains. On the other hand, additional remains of the child will also possibly be discovered in the areas where the gully has not been excavated yet. This would allow testing the hypothesis – however unlikely – of the possible presence of new remains of the child in pre-gully deposits, possibly even in the form of a burial cut and partially reworked by the gully of Unit 4A-CHE.



Acknowledgements

The authors gratefully acknowledge Rhylan McMillan (Vancouver Island University) for his valuable help in translating the manuscript into correct English. We are also very grateful to Joël Éloy (Association wallonne d'Études mégalithiques) for designing the figures and Jean-François Lemaire (Service public de Wallonie) for his technical assistance. We especially thank Rhylan McMillan (Vancouver Island University), Paul Spagna (Royal Belgian Institute of Natural Sciences), as well as Kévin Di Modica and Grégory Abrams (Archéologie Andennaise) for many fruitful discussions and constructive comments on the manuscript.

References

BONJEAN D., 1998. La stratigraphie. In M. OTTE, M. PATOU-MATHIS & D. BONJEAN (dir.), *Recherches aux grottes de Sclayn, vol. 2 : L'Archéologie*. Études et Recherches Archéologiques de l'Université de Liège, 79: 15-23.

BONJEAN D., 2009. L'archéologie de terrain aujourd'hui: la fouille *made in* Scladina. In K. DI MODICA & C. JUNGELS (dir.), *Paléolithique moyen en Wallonie. La collection Louis Éloy*. Bruxelles, Collections du Patrimoine culturel de la Communauté française, 2: 28-32.

BONJEAN D., ABRAMS G., DI MODICA K. & OTTE M., 2009^b. La microstratigraphie, une clé de lecture des remaniements sédimentaires successifs. Le cas de l'industrie moustérienne 1A de *Scladina*. *Notae Praehistoricae*, 29: 139-147.

BONJEAN D., MASY P. & TOUSSAINT M., 2009^a. L'enfant néandertalien de Sclayn. Petite histoire d'une découverte exceptionnelle. *Notae Praehistoricae*, 29: 49-51.

BONJEAN D., TOUSSAINT M. & OTTE M., 1996. Scladina (Sclayn, Belgique): l'homme de néandertal retrouvé! *Notae Praehistoricae*, 16: 37-46.

BONJEAN D., TOUSSAINT M. & OTTE M., 1997. Grotte Scladina (Sclayn, Belgique): bilan des découvertes néandertaliennes et analyse du contexte.

In J. PLUMIER (dir.), *Actes de la cinquième journée d'Archéologie Namuroise*, Namur, Facultés universitaires Notre-Dame de la Paix, 22 février 1997, Ministère de la Région wallonne, Direction générale de l'Aménagement du Territoire, du Logement et du Patrimoine, Direction de Namur, Service des Fouilles: 19-27.

NORTHGRIP-MEMBERS, 2004. High-resolution record of Northern Hemisphere climate extending into the last interglacial period. *Nature*, 431: 147-151.

OTTE M., TOUSSAINT M. & BONJEAN D., 1993. Découverte de restes humains immatures dans les niveaux moustériens de la grotte Scladina à Andenne (Belgique). *Bulletins et Mémoires de la Société d'Anthropologie de Paris*, nouvelle série, t. 5, 1-2: 327-332.

PIRSON S., 2007. *Contribution à l'étude des dépôts d'entrée de grotte en Belgique au Pléistocène supérieur. Stratigraphie, sédimentogenèse et paléoenvironnement*. Unpublished PhD thesis, University of Liège & Royal Belgian Institute of Natural Sciences, 2 vol., 435 p. & 5 annexes.

PIRSON S., BONJEAN D., DI MODICA K. & TOUSSAINT M., 2005. Révision des couches 4 de la grotte *Scladina* (comm. d'Andenne, prov. de Namur) et implications pour les restes néandertaliens: premier bilan. *Notae Praehistoricae*, 25: 61-69.

TOUSSAINT M., BONJEAN D. & OTTE M., 1994. Découverte de fossiles humains du Paléolithique moyen à la grotte Scladina à Andenne. In M.-H. CORBIAU & J. PLUMIER (eds.), *Actes de la deuxième Journée d'Archéologie Namuroise*. Namur, Facultés universitaires Notre-Dame de la Paix, 26 février 1994, Ministère de la Région wallonne, Direction générale de l'Aménagement du Territoire et du Logement, Direction de Namur, Service des Fouilles: 19-33.

TOUSSAINT M., OTTE M., BONJEAN D., BOCHERENS H., FALGUÈRES C. & YOKOYAMA Y., 1998. Les restes humains néandertaliens immatures de la couche 4A de la grotte Scladina (Andenne, Belgique). *Comptes rendus de l'Académie des Sciences de Paris*, Sciences de la terre et des planètes, 326: 737-742.

Appendix A

Evolution of the understanding of the stratigraphic position of the Scladina I-4A Neandertal remains

The understanding of the stratigraphic position of Scladina I-4A, exhumed from Sedimentary Complex 4A, can be summarized in four phases, reflecting both the establishment of the stratigraphic sequence and the growing importance of multidisciplinary research at Scladina Cave.

1. Phase 1 (until 1994)

The initial phase started at the beginning of excavations in 1978 and ended with the first identification of Neandertal remains around 1993/1994.

The archaeologists in charge of excavation completed the first descriptions of the Scladina Cave stratigraphic sequence (Otte et al., 1983; see Chapter 3). It was soon complemented by the work of geologists P. Haesaerts (1992) on the cave terrace and F. Gullentops and his student C. Deblaere inside the cave (Deblaere & Gullentops, 1986; Gullentops & Deblaere, 1992). During this period, the stratigraphic interpretation of about 10 sedimentary profiles within the cave led to the definition of a synthetic sequence (Otte et al., 1983; Deblaere & Gullentops, 1986; Gullentops & Deblaere, 1992), comprised of some 20 main layers that are quite thick and mainly arranged subhorizontally on transverse sections, while the longitudinal sections yielded concordant layers, gently dipping towards the back of the cave.

In the stratigraphic system defined inside the cave at the time, the part related to the Neandertal juvenile included the following succession, from bottom to top:

Layer 4B
Layer 4A
Speleothem CC4
Layer 3

In such a context, two remains found in situ (Scla 4A-1 and -4) and two that were rediscovered in the collections (Scla 4A-2 and -3) were attributed to former Layer 4A (Otte et al., 1993). However, two other teeth found in the collections (Scla 3-2 and -3) were originally attributed to the lower part of former Layer 3 (Otte et al., 1993; Toussaint et al., 1994). Three additional teeth (Scla 4A-5 to -7), also attributed to former Layer 4A, were identified in October 1993 after the information provided in the above-mentioned papers was already delivered. They were published for the first time at a later date (Toussaint et al., 1998).

2. Phase 2 (1995-2003)

Additional Neandertal remains were found in former Layer 4A in situ (Scla 4A-8, -9, and -13) and in the collections (Scla 4A-11, -12, and -14 to -16)¹. A third tooth was found in former Layer 3 in 1995 (Scla 3-4). However, the possibility was suggested that the three teeth attributed to former Layer 3 might be from former Layer 4A, given the fact that the limit between these layers was not always precisely identified during excavation in the 1990s (Bonjean et al., 1996: 42, 1997: 22; Toussaint et al., 2001: 27). After a careful anatomical study, the three teeth originally assigned

¹ A tooth found in July 1998 in Square B37 was initially labelled Scla 4A-10 (Pirson et al., 2005). It was later discarded from the Neandertal remains during taphonomic and anthropological studies. It came from a bioturbated context.



to former Layer 3 were reattributed to former Layer 4A (Toussaint & Pirson, 2006) and renamed following the Scla 4A- nomenclature, becoming Scla 4A-17 to -19 (Pirson et al., 2005).

Another change of the stratigraphic position of the Neandertal remains concerns the identification of a stalagmitic floor inside former Layer 4A, called Speleothem CC14. The succession of layers then became:

Layer 4B
Layer 4A (lower)
Lower Speleothem CC14
Layer 4A (upper)
Upper Speleothem CC4
Layer 3

The Neandertal remains were found in the upper part of former Layer 4A, situated between stalagmitic floors CC14 and CC4 (Bonjean et al., 1996; Bonjean, 1998).

The secondary spatial position of the anthropological remains, deduced from their wide horizontal dispersion combined with the presence of broken stalagmites and the occurrence of bones and limestone fragments in very oblique or vertical positions, was interpreted as resulting from a thick mudflow (Bonjean et al., 1996, 1997). A sedimentological study of a profile located near the Neandertal remains suggested the colluvial nature of Layer 4A (Benabdelhadi, 1998). However, Layer 4A was still understood as a single, subhorizontal layer (Benabdelhadi, 1998; Bonjean, 1998) despite the observation of cut-and-filled gullies on a small sedimentary profile not far from the Neandertal remains (Bonjean et al., 1997).

3. Phase 3 (after 2003)

Between 2003 and 2007, the detailed stratigraphic recording of around 70 sedimentary profiles took place in the context of a PhD study (Pirson, 2007), leading to the definition of about 120 layers grouped into 30 distinct stratigraphic units. A continuous geological survey of the archaeological excavation also took place on a regular basis and is currently still on-going. This approach allowed a great variety of lithofacies as well as numerous depositional and post-depositional processes to be observed (Chapter 3). Complex geometries were also identified. During this period an additional tooth was found (Scla 4A-20), on 12 July 2006.

Following this stratigraphic reappraisal, former Layer 4A became 'Sedimentary Complex 4A', comprised of about 20 layers grouped into 4 units (Pirson et al., 2005; Pirson, 2007). From bottom to top these were:

- **Unit 4A-AP**, the lowermost unit, including all the layers within the complex that are older than Speleothem CC4 (= pre-floor layers);
- **Unit 4A-IP**, including Stalagmitic Floor CC4 and the layers that are contemporaneous with the formation of CC4 (= syn-floor layers);
- **Unit 4A-CHE**, which includes the layers that developed inside a large gully structure that eroded underlying layers, including CC4 (= post-floor and syn-gully layers); and
- **Unit 4A-POC**, the uppermost unit, superimposing both units 4A-IP and 4A-CHE (= post-gully layers).

A key element was the identification of the important gully structure of Unit 4A-CHE in the upper part of Sedimentary Complex 4, which locally reworked Speleothem CC4 and eroded

underlying layers down to Unit 5, sometimes even down to Unit 6A. Furthermore, *Speleothem* CC14 was proven to be a lateral equivalent of CC4.

This new stratigraphic record is important for understanding the Neandertal fossils. In a first attempt of reinterpreting the stratigraphic position of the child remains, 6 out of the 19 fossils were positioned in Unit 4A-CHE and/or Unit 4A-POC (Pirson, 2007), or their former equivalents (“couches 4A-chenal” in Pirson et al., 2005). At this time, the attribution of the 13 other remains was unclear within Complex 4A. The depositional history and origin of the Neandertal remains were also briefly discussed in connection with the gully (Pirson et al., 2005).

4. Phase 4

More recently, during the preparation of this monograph, all the available arguments were re-examined in order to try to refine the stratigraphic position of the Neandertal remains. They are discussed in Chapter 5.

Appendix B

Evolution of the chronostratigraphic interpretation of the Neandertal remains

In the first few years after the discovery of the Neandertal remains, the chronostratigraphic interpretation of the Scladina sequence referenced the results presented in the first monograph that dealt with contextual data (see Otte (ed.), 1992). More specifically, former Layer 4A was dated to approximately 70,000-80,000 BP and the Saint-Germain II episode according to climatostratigraphy based on palaeontological data, even if TL and U/Th dates obtained on *Speleothem* CC4 (supposed at that time to be younger than the Neandertal remains) were older, with a mean of approximately 110,000-114,000 BP. In this context, the Neandertal remains were dated to around 70,000-80,000 BP (Otte et al., 1993; Toussaint et al., 1994).

A few years later, two distinct scenarios suggested different ages for the Neandertal remains: a young age (72,000-85,000 BP) based on palaeontological climatostratigraphy, and an older age (between 100,000 and 120,000 BP) based on the acquired numerical ages, either U/Th or TL dates on calcite, or TL dates on sediment (Bonjean, 1995; Bonjean et al., 1996, 1997). At the same time, direct gamma spectrometry dating was performed on the mandible (Yokoyama & Falguères in Toussaint et al., 1998; see Chapter 6). The result (127 +46/-32 ka BP) was the most reliable information available for estimating the age of the Neandertal remains, even if has a large range. Based on this, the remains were positioned somewhere between MIS 6 and MIS 4 taking the standard deviation into account. This high uncertainty did not help resolve the discrepancy between the youngest and the oldest chronological scenarios.

Following the stratigraphic reappraisal of the Scladina sequence (2003-2007), the stratigraphic position of the Neandertal remains was re-evaluated. This clarified the relative chronology of the events inside Sedimentary Complex 4A, including the relative age of the child (Pirson et al., 2005; Pirson, 2007). Two scenarios were possible. In the first one, the Neandertal remains were contemporaneous with the age of the oldest Neandertal-bearing deposit, the gully sequence in Unit 4A-CHE. This was the scenario that prescribed the youngest age to the Neandertal juvenile. In the new stratigraphic situation, the child would then postdate *Speleothem* CC4, which yielded a variety of dates that were mainly related to MIS 5. The second scenario considered that the Neandertal remains were reworked from older deposits eroded by the gully. In such



a situation, a maximum age could not be suggested on the basis of stratigraphy. The available direct gamma spectrometry dating was again the most reliable information available about the age of the Neandertal child, which positions the child between MIS 6 and MIS 4.

During the preparation of this monograph, all the available information was re-examined, leading to the present interpretation that is summarised in Chapter 5. Several observations made during the taphonomical study of the Neandertal remains are very important (Chapter 7), especially the conclusion that the Neandertal remains are contemporaneous with the gully of Unit 4A-CHE. Due to the reappraisal of the palaeoenvironmental data and chronostratigraphy of the Scladina sequence (Pirson, 2007; Pirson et al., 2008; see Chapter 4), a reconsideration of the age of the gully episode was possible, with major implications for the antiquity of the Scladina Neandertal juvenile. The main results are summarised below.

The new palaeoenvironmental framework is mainly based on new results from palynology, anthracology, and climatic signals recorded in the sediments themselves through the observation of sedimentary dynamics and post-depositional processes. These results correlate with the data from literature based on the former stratigraphic record (e.g., Cordy & Bastin, 1992). Overall, the palaeoenvironmental results from all the available disciplines agree. The data for Unit 4A-CHE indicates cold conditions, as the gully is interpreted as a result of the degradation of a deep frozen soil (melting structure).

The chronostratigraphic framework of the entire Scladina sequence was also reconsidered, based on all the available data sets: numerical dates (luminescence, radiocarbon), biostratigraphy, archaeostratigraphy, comparison with the loess reference sequence from Middle Belgium (heavy mineralogy, lithological, and pedological markers), and climatostratigraphy. This reappraisal concludes that most of the Scladina deposits can confidently be positioned in the Upper Pleistocene. However, the chronostratigraphic framework of Scladina is still quite imprecise. Several situations still need more attention, such as the location of the beginning and end of MIS 5 in the sequence. Interpreting the age of the Unit 4A-CHE gully relies on the integration of climatostratigraphy and heavy mineralogy, especially comparing green amphibole content with data from the loess reference sequence (see Chapter 4). The main arguments are:

- in the lower half of the sequence, from units 7A to 2B, strong green amphibole values (ca. 20%) were recorded, suggesting the reworking of either MIS 6 loess or MIS 4-2 loess;
- between units 7A to 2B, two units (Unit 6B, former Layer 6; Unit 4A-IP, former Layer 4A) indicate temperate forest conditions, compatible with an interglacial or an early glacial interstadial, notably through palynological and macrofaunal data as well as the presence of major stalagmitic floors;
- combining the first two arguments allows the reworking of MIS 4-2 loess to be discarded as a hypothesis and supports the reworking of MIS 6 loess during MIS 5 in the sequence from Unit 6B to Unit 4A-IP. The available U/Th and TL dates obtained on Speleothem CC4 (Unit 4A-IP) are in agreement with the MIS 5 interpretation. As Unit 6B was a strong climatic improvement in MIS 5, Unit 4A-IP (and Speleothem CC4) must be positioned in either MIS 5c and/or MIS 5a; and
- higher up in the sequence, Unit 2A is interpreted as the first allochthonous loess input of MIS 4, and Unit 2B is best interpreted as representing the end of MIS 5a (see Chapter 4).

Following these arguments, and integrating them in the complexity of the Scladina sequence, there are several possible interpretations for the chronostratigraphic positioning of the cold episode represented by Unit 4A-CHE (see Chapter 4) and the associated Neandertal remains, the most probable being the following (Figure 21):

- if CC4 corresponds to MIS 5c temperate conditions, 4A-CHE would belong to MIS 5b colder conditions (GS 22 of the Greenland record, between GI 22 and GI 21, around 87,000 BP; NorthGRIP-Members, 2004) and by comparison with the loess sequence, 4A-CHE would then be an equivalent of the cold episode separating the last two pedogeneses of the Rocourt pedocomplex, i.e. Villers-Saint-Ghislain-A (VSG-A) and VSG-B (cf. Pirson et al., 2009; Haesaerts et al., 2011). The Scladina Child would then be contemporaneous with the Remicourt lithic assemblage (Bosquet et al., 2011; Pirson & Di Modica, 2011);
- if CC4 corresponds to the ‘warmer’ first half of MIS 5a, 4A-CHE would belong to the intra-MIS 5a cooling (intra-GI 21, around 80,000 BP); by comparison with the loess sequence, 4A-CHE would then correspond to the cold episode situated between the VSG-B Soil of the Rocourt pedocomplex and the Humic Complex of Remicourt (cf. Pirson et al., 2009; Haesaerts et al., 2011); and
- if the end of CC4 coincides with the end of MIS 5a, 4A-CHE would belong to one of the cold phases inside the first half of MIS 4. In this latest hypothesis, Unit 2B would not belong to MIS 5a but to one of the interstadials during the first part of MIS 4 (GI 19 or 20), which is not the best current hypothesis.

Since the part of Scladina sequence from Unit 6B to Unit 2B is best attributed to MIS 5, the best two hypotheses for the chronostratigraphic positioning of the gully from Unit 4A-CHE are to place this unit in either MIS 5b or MIS 5a. Therefore, the Scladina Child would have lived either some 87,000 years ago or some 80,000 years ago (Figure 21). These two chronostratigraphic hypotheses for the Neandertal juvenile are consistent with the morphometrical studies of the fossils (see Chapters 13, 15 & 16).

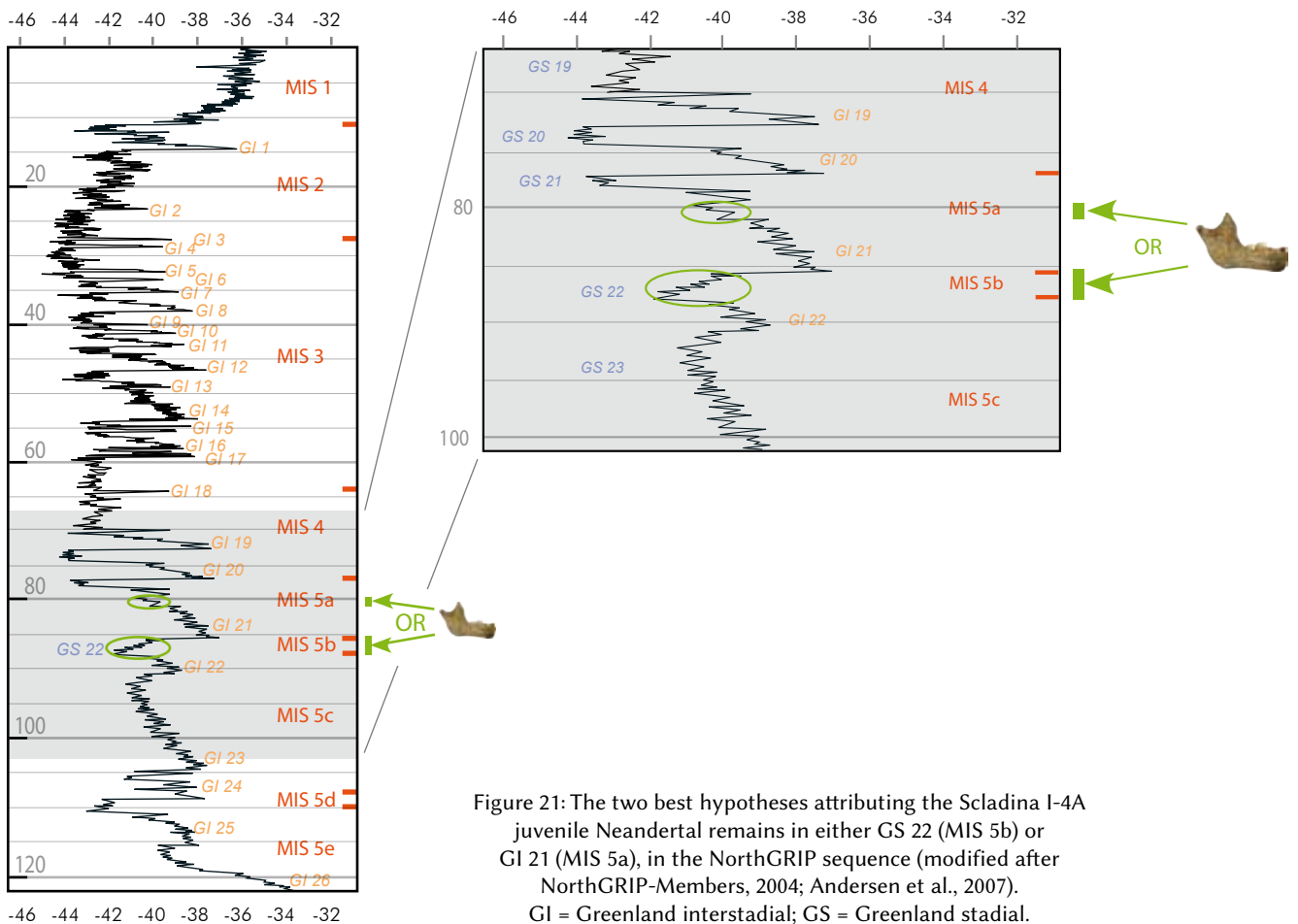


Figure 21: The two best hypotheses attributing the Scladina I-4A juvenile Neandertal remains in either GS 22 (MIS 5b) or GI 21 (MIS 5a), in the NorthGRIP sequence (modified after NorthGRIP-Members, 2004; Andersen et al., 2007). GI = Greenland interstadial; GS = Greenland stadial.



References

- Andersen K. K., Bigler M., Clausen H. B., Dahl-Jensen D., Johnsen S. J., Rasmussen S. O., Seierstad I., Steffensen J. P., Svensson A., Vinther B. M., Davies S. M., Muscheler R., Parrenin F. & Röthlisberger R., 2007. A 60 000 year Greenland stratigraphic ice core chronology, *Climate of the Past Discussions*, 3: 1235-1260.
- Benabdelhadi M., 1998. Étude sédimentologique de la coupe transversale 30/31 des carrés A, B, C et D de la grotte Scladina. In M. Otte, M. Patou-Mathis & D. Bonjean (dir.), *Recherches aux grottes de Sclayn, vol. 2 : L'Archéologie*. Études et Recherches Archéologiques de l'Université de Liège, 79: 25-37.
- Bonjean D., 1995. Dans la foulée de l'Homme de Néandertal : Sclayn 1994. Résultats scientifiques préliminaires et diffusion médiatique. In J. Plumier & M.-H. Corbiau (eds.), *Actes de la Troisième Journée d'Archéologie Namuroise*. Namur, Facultés universitaires Notre-Dame de la Paix, 26 février 1994, Ministère de la Région wallonne, Direction générale de l'Aménagement du Territoire, du Logement et du Patrimoine, Direction de Namur, Service des Fouilles: 45-48.
- Bonjean D., 1998. La stratigraphie. In M. Otte, M. Patou-Mathis & D. Bonjean (dir.), *Recherches aux grottes de Sclayn, vol. 2 : L'Archéologie*. Études et Recherches Archéologiques de l'Université de Liège, 79: 15-23.
- Bonjean D., Toussaint M. & Otte M., 1996. Scladina (Sclayn, Belgique): l'homme de néandertal retrouvé! *Notae Praehistoricae*, 16: 37-46.
- Bonjean D., Toussaint M. & Otte M., 1997. Grotte Scladina (Sclayn, Belgique) : bilan des découvertes néandertaliennes et analyse du contexte. In J. Plumier (dir.), *Actes de la cinquième journée d'Archéologie Namuroise*, Namur, Facultés universitaires Notre-Dame de la Paix, 22 février 1997, Ministère de la Région wallonne, Direction générale de l'Aménagement du Territoire, du Logement et du Patrimoine, Direction de Namur, Service des Fouilles: 19-27.
- Bosquet D., Haesaerts P., Damblon F., Jardón Giner P. & Ryssaert C., 2011. Le gisement paléolithique de Remicourt-En Bia Flo I. In M. Toussaint, K. Di Modica & S. Pirson (sc. dir.), *Le Paléolithique moyen en Belgique. Mélanges Marguerite Ulrix-Closset*. Bulletin de la Société royale belge d'Études Géologiques et Archéologiques *Les Chercheurs de la Wallonie*, hors-série, 4 & Études et Recherches Archéologiques de l'Université de Liège, 128: 375-384.
- Cordy J.-M. & Bastin B., 1992. Synthèse des études paléontologiques réalisées dans les dépôts de la grotte Scladina (Sclayn, Province de Namur). In M. Otte (ed.), *Recherches aux grottes de Sclayn, vol. 1 : Le Contexte*. Études et Recherches Archéologiques de l'Université de Liège, 27: 153-156.
- Deblaere C. & Gullentops F., 1986. Lithostratigraphie de la grotte Scladina. *Bulletin de l'Association française pour l'étude du Quaternaire*, 2^e série, 25-26: 178-181.
- Gullentops F. & Deblaere C., 1992. Érosion et remplissage de la grotte Scladina. In M. Otte (ed.), *Recherches aux grottes de Sclayn, vol. 1 : Le Contexte*. Études et Recherches Archéologiques de l'Université de Liège, 27: 9-31.
- Haesaerts P., 1992. Les dépôts pléistocènes de la terrasse de la grotte Scladina à Sclayn (province de Namur, Belgique). In M. Otte (ed.), *Recherches aux grottes de Sclayn, vol. 1 : Le Contexte*. Études et Recherches Archéologiques de l'Université de Liège, 27: 33-55.

Haesaerts P., Di Modica K. & Pirson S., 2011. Le gisement paléolithique de la Sablière Gritten à Rocourt (province de Liège). In M. Toussaint, K. Di Modica & S. Pirson (sc. dir.), *Le Paléolithique moyen en Belgique. Mélanges Marguerite Ullrich-Closset*. Bulletin de la Société royale belge d'Études Géologiques et Archéologiques *Les Chercheurs de la Wallonie*, hors-série, 4 & Études et Recherches Archéologiques de l'Université de Liège, 128: 359-374.

NorthGRIP-Members, 2004. High-resolution record of Northern Hemisphere climate extending into the last interglacial period. *Nature*, 431: 147-151.

Otte M. (ed.), 1992. *Recherches aux grottes de Sclayn, vol. 1 : Le Contexte*. Études et Recherches Archéologiques de l'Université de Liège, 27, 182 p.

Otte M., Léotard J.-M., Schneider A.-M., Gautier A., Gilot E. & Aitken M., 1983. Fouilles aux grottes de Sclayn (Namur). *Helinium*, 23: 112-142.

Otte M., Toussaint M. & Bonjean D., 1993. Découverte de restes humains immatures dans les niveaux moustériens de la grotte Scladina à Andenne (Belgique). *Bulletins et Mémoires de la Société d'Anthropologie de Paris*, nouvelle série, t. 5, 1-2: 327-332.

Pirson S., 2007. *Contribution à l'étude des dépôts d'entrée de grotte en Belgique au Pléistocène supérieur. Stratigraphie, sédimentogenèse et paléoenvironnement*. Unpublished PhD thesis, University of Liège & Royal Belgian Institute of Natural Sciences, 2 vol., 435 p. & 5 annexes.

Pirson S., Bonjean D., Di Modica K. & Toussaint M., 2005. Révision des couches 4 de la grotte *Scladina* (comm. d'Andenne, prov. de Namur) et implications pour les restes néandertaliens: premier bilan. *Notae Praehistoricae*, 25: 61-69.

Pirson S., Court-Picon M., Haesaerts P., Bonjean D. & Damblon F., 2008. New data on geology, anthracology and palynology from the Scladina Cave pleistocene sequence: preliminary results. In F. Damblon, S. Pirson & P. Gerienne (eds.), *Hautrage (Lower Cretaceous) and Sclayn (Upper Pleistocene). Field Trip Guidebook. Charcoal and microcharcoal: continental and marine records*. IVth International Meeting of Anthracology, Brussels, Royal Belgian Institute of Natural Sciences, 8-13 September 2008. Brussels, Royal Belgian Institute of Natural Sciences, *Memoirs of the Geological Survey of Belgium*, 55: 71-93.

Pirson S. & Di Modica K., 2011. Position chronostratigraphique des productions lithiques du Paléolithique ancien en Belgique : un état de la question. In M. Toussaint, K. Di Modica & S. Pirson (sc. dir.), *Le Paléolithique moyen en Belgique. Mélanges Marguerite Ullrich-Closset*. Bulletin de la Société royale belge d'Études Géologiques et Archéologiques *Les Chercheurs de la Wallonie*, hors-série, 4 & Études et Recherches Archéologiques de l'Université de Liège, 128: 105-148.

Pirson S., Haesaerts P. & Di Modica K., 2009. Cadre chronostratigraphique des principaux gisements du Paléolithique moyen du bassin de la Haine: un état de la question. In K. Di Modica & C. Jungels (dir.), *Paléolithique moyen en Wallonie. La collection Louis Éloy*. Bruxelles, Collections du Patrimoine culturel de la Communauté française, 2: 58-77.

Toussaint M., Bonjean D. & Otte M., 1994. Découverte de fossiles humains du Paléolithique moyen à la grotte Scladina à Andenne. In M.-H. Corbiau & J. Plumier (eds.), *Actes de la deuxième Journée d'Archéologie Namuroise*. Namur, Facultés universitaires Notre-Dame de la Paix, 26 février 1994, Ministère de la Région wallonne, Direction générale de l'Aménagement du Territoire et du Logement, Direction de Namur, Service des Fouilles: 19-33.



Toussaint M., Otte M., Bonjean D., Bocherens H., Falguères C. & Yokoyama Y., 1998. Les restes humains néandertaliens immatures de la couche 4A de la grotte Scladina (Andenne, Belgique). *Comptes rendus de l'Académie des Sciences de Paris, Sciences de la terre et des planètes*, 326: 737-742.

Toussaint M. & Pirson S., 2006. Neandertal Studies in Belgium: 2000-2005. *Periodicum Biologorum*, 108, 3: 373-387.

Toussaint M., Pirson S. & Bocherens H., 2001. Neandertals from Belgium – Les Néandertaliens de Belgique. *Anthropologica et Præhistorica*, 112: 21-38.

1. Introduction

During the early 1980s, developments in the field of gamma-ray spectrometry allowed the observation of long half-life natural radionuclides such as uranium (^{238}U , ^{234}U), thorium (^{230}Th) and protactinium (^{231}Pa ; YOKOYAMA & NGUYEN, 1980). This new technique does not require prior chemical treatment of the sample, which is highly advantageous for studying rare and valuable objects. This technique was applied for the first time in the field of prehistory on the fossilized human remains from Caune de l'Arago (YOKOYAMA & NGUYEN, 1981). Later, other human fossils were dated with this method. These include crania, notably that of Biache-Saint-Vaast; numerous mandibles, such as Fate in Italy and Atapuerca in Spain; long bones, such as the femur from the Venosa site in Italy; and an ilium from the Prince Cave, also in Italy, Qafzeh 6 skull, Israel and recently Ngandong calvaria, Indonesia (YOKOYAMA et al., 1988, 1997, 2008; YOKOYAMA, 1989).

This paper presents the results obtained in 1994 from non-destructive gamma-ray spectrometry applied to a the right hemimandible Scla 4A-1 of the Neandertal child found during the 1993 archaeological excavations at Scladina Cave.

2. Methods

The gamma-ray spectrometry method is based on radioactive disequilibrium of uranium series. During permineralization at the beginning of the fossilization process, bones readily absorb dissolved trace elements, such as uranium, from groundwater. As a consequence, fossilized bones may contain a variable amount of uranium (from 1 to 300 ppm). However, during the early phase of fossilization, bones do not take up uranium descendants such as thorium (^{230}Th) and protactinium

(^{231}Pa), since these nuclides are insoluble in water. As time passes, these two nuclides grow from their parents decay respectively ^{234}U and ^{235}U . Measuring the $^{230}\text{Th}/^{234}\text{U}$ (or $^{231}\text{Pa}/^{235}\text{U}$) ratio therefore yields the date of the sample. Details about these methods (U-Th and U-Pa) have been well described (KU, 1976, IVANOVICH et al., 1992, BOURDON et al., 2003). Gamma-ray spectrometry is not only applicable to bones and teeth, but also to antlers, reindeer palms, mammoth ivory, shells, and corals.

The Scladina sample was placed on a low background, high purity ORTEC germanium detector (GeHP) connected to a computer controlled by a microanalyzer. The detector had a relative effectiveness of 25% and a resolution of 0.7 keV at 63 keV. ^{234}U and ^{230}Th activities were determined from gamma rays directly emitted by these nuclides at 53.3 keV and 120.9 keV for ^{234}U , and at 67.7 keV for ^{230}Th . ^{238}U was determined from its direct daughter, ^{234}Th , at 63.3, 92.4, and 92.8 keV. Determination of ^{231}Pa activity is obtained from those of its daughters, ^{227}Th , ^{223}Ra , and ^{219}Rn .

3. Results and discussion

The Neandertal remains were found in Sedimentary Complex 4A. The mandible weighs 30.18 g and was counted during 91 effective days because the level of uranium in the mandible is low (Table 1) and did not allow the calculation of a date from the $^{231}\text{Pa}/^{235}\text{U}$ ratio. The age obtained via the $^{230}\text{Th}/^{234}\text{U}$ ratio presents an important error range due to the measurement difficulty of ^{234}U which is superimposed with ^{214}Pb at 53.2 KeV. The low level of ^{232}Th in the sample (the $^{230}\text{Th}/^{232}\text{Th}$ ratio is equal to 22) indicates correcting the age on the basis of exogenous thorium is not necessary. The age obtained reveals that the child lived at least 100,000 years ago.



U content (ppm)	2.6 ± 0.26
²³⁴ U / ²³⁸ U	2.2 ± 0.35
²³⁰ Th / ²³⁴ U	0.75 ± 0.12
²³⁰ Th / ²³² Th	22 ± 2.2
Age EU (ka)	127 +46 / -32 ka BP

Table 1. Measured uranium content, isotopic ratios, and age of the Scladina mandible within 1 standard deviation of the mean.

Acknowledgements

The authors wish to express their gratitude to Rhylan McMillan (Vancouver Island University) as well as Jean-François Lemaire, Service de l'Archéologie en province de Liège du Service public de Wallonie, for improving the English text.

References

BOURDON B., HENDERSON G. M., LUNDSTROM C. C., TURNER S. P. (eds.), 2003. *Uranium-Series Geochemistry*. Reviews in Mineralogy and Geochemistry, 52, 656 p.

IVANOVICH M., LATHAM A. G. & KU T. L., 1992. Uranium-series disequilibrium applications in geochronology. In M. IVANOVICH & R. S. HARMON (eds.), *Uranium Series Disequilibrium; Applications to Earth, Marine and Environmental Sciences*. Oxford, Clarendon Press: 62-94.

KU T. L., 1976. The uranium-series methods of age determination. *Annual Review of Earth and Planetary Sciences*, 4, New York, Pergamon Press: 347-379.

YOKOYAMA Y., 1989. Direct gamma-ray spectrometric dating of anteneandertalian and neandertalian human remains. In G. GIACOBINI (ed.), *Proceedings of the 2nd International Congress of Human Palaeontology*, Milan, Jaca Book: 387-390.

YOKOYAMA Y., FALGUÈRES C. & BIBRON R., 1988. Direct dating of neandertalian remains and animal bones by the non destructive gamma-ray spectrometry: comparison with other methods. In H. P. SCHWARCZ (ed.), *L'Homme de Néandertal, vol. 1: La Chronologie*. Études et Recherches Archéologiques de l'Université de Liège, 28: 135-141.

YOKOYAMA Y., FALGUÈRES C. & DE LUMLEY M. A., 1997. Datation directe d'un crâne Proto-Cro-Magnon de Qafzeh par la spectrométrie gamma non destructive. *Comptes rendus de l'Académie des Sciences de Paris*, 324: 773-779.

YOKOYAMA Y., FALGUÈRES C., SÉMAH F., JACOB T. & GRÜN R., 2008. Gamma-Ray spectrometric dating of late Homo erectus skulls from Ngandong and Sambungmacan, Central Java, Indonesia. *Journal of Human Evolution*, 55: 274-277.

YOKOYAMA Y. & NGUYEN H. V., 1980. Direct and non destructive dating of marine sediments, manganese nodules, and corals by high resolution gamma-ray spectrometry. In E. D. GOLDBERG, Y. HORIBE & K. SARUHASHI (eds.), *Isotope Marine Chemistry*, Tokyo, Uchida Rokakuho: 259-289.

YOKOYAMA Y. & NGUYEN H. V., 1981. Datation directe de l'Homme de Tautavel par la spectrométrie gamma non destructive, du crâne humain fossile Arago XXI. *Comptes rendus de l'Académie des Sciences de Paris*, 292, série III: 741-744.

Chapter 7

TAPHONOMY OF THE JUVENILE NEANDERTAL REMAINS FROM SEDIMENTARY COMPLEX 4A, SCLADINA CAVE

Dominique BONJEAN, Grégory ABRAMS, Élise DELAUNOIS, Kévin DI MODICA, Rhylan McMILLAN, Stéphane PIRSON, Cheryl A. ROY, & Michel TOUSSAINT

Michel Toussaint & Dominique Bonjean (eds.), 2014. The Scladina I-4A Juvenile Neandertal (Andenne, Belgium), Palaeoanthropology and Context

Études et Recherches Archéologiques de l'Université de Liège, 134: 127-154.

1. Introduction

When hominid remains are discovered, such as the Neandertal specimen Scladina I-4A, many different questions arise. These include: What was the cause of death? How did the deceased individual, or parts of their body or skeleton, enter the site? What happened to the fossils between their deposition and the archaeological excavation that unearthed them?

All these questions, and numerous related others, are on the topic of 'taphonomy' (EFREMOV, 1940), i.e. the study of the processes an organism is subject to between its death and its discovery (GRUPE, 2007), including effects induced by the passage of an individual from a living community to a fossil one (DENYS, 2002). Numerous applications of this discipline for palaeontology and palaeoanthropology have been developed for over half a century (see, for instance, among thousands of contributions: DART, 1957; BEHRENSMEYER, 1978; BEHRENSMEYER & HILL, 1980; SHIPMAN, 1981; BRAIN, 1981; BINFORD, 1981; BEHRENSMEYER & KIDWELL, 1985; BLUMENSCHINE, 1986; VILLA & MAHIEU, 1991; WHITE, 1992; BOULESTIN, 1999; MARTIN, 1999; BEHRENSMEYER et al., 2000; LYMAN, 2001; PICKERING et al., 2007; KROVITZ & SHIPMAN, 2007).

However, as far as European Pleistocene hominid remains are concerned, only a limited number of them have been the subjects of taphonomic studies. Some works focus on cut marks (e.g. LE MORT, 1988; 1989). Others are about cannibalism, for instance at Krapina (PATOUMATHIS, 1997; FRAYER et al., 2006; ULLRICH, 2006), or Moula-Guercy (DEFLEUR et al., 1999). Others try to apply various aspects of taphonomy to studied bones, for example at Atapuerca-Sima de los Huesos (ANDREWS & FERNÁNDEZ-JALVO, 1997), Le Moustier 1 (ULLRICH, 2005), Rochers-de-Villeneuve

(BEAUVAL et al., 2005), and Oliveira Cave (TRINKAUS et al., 2007).

At Scladina, the 19 fossils (3 bone fragments and 16 isolated teeth) from Sedimentary Complex 4A that belong to the 8-year-old juvenile Neandertal exhibit a particular set of various characteristics. Among these attributes is a planimetric dispersal within an elliptical area of around 13 m long by 6 m wide, a stratigraphic dispersal within different layers/units of Sedimentary Complex 4A, colour differences between bones and between isolated teeth, the presence of manganese coatings on some bones, the fact that most fossils were scattered in the axial part of the cave while some others were discovered nearly against the south wall, and the relative completeness of the mandible when the two parts are refitted juxtaposed against the relative incompleteness of the maxilla.

This wide variety of information (detailed and analysed below) immediately indicates a complex depositional history. Therefore, this chapter tries to decipher, at least in part, these events. To do this, the following approaches were taken into consideration:

- the examination of the fossils for evidence of different surface modifications and, when applicable, their description;
- the analysis of the spatial and stratigraphic distribution of the isolated teeth and fragments of bones;
- the comparison of these observations to those from the analysis of faunal remains;
- the integration of all these approaches in order to build a model of successive chronological phases in relation to death (necrology), pre-burial processes (biostratinomy), burial processes, post-depositional processes (diagenesis), and archaeological or palaeontological excavation.



2. Material and methods

2.1. Stratigraphic context of the Neandertal fossils from Scladina Cave

Although the main stratigraphic units of Scladina were identified during the initial excavation (e.g. DEBLAERE & GULLENTOPS, 1986; GULLENTOPS & DEBLAERE, 1992; HAESAERTS, 1992), the real stratigraphic complexity of the site was observed and recorded during the research for a PhD in geology (PIRSON, 2007). This revision identified 30 sedimentary units comprised of more than 120 layers. Also, numerous sedimentary processes were recognised, including run-off, debris flow, torrential flow, and decantation. Post-depositional phenomena, such as bioturbation, the precipitation of manganese, and cryoturbation were also recorded. All of these processes have an impact on the preservation of both hominid and faunal remains.

The stratigraphic revision of former Layer 4A, which yielded the hominid remains, demonstrated that 4A is clearly much more sedimentologically complicated than previously considered (PIRSON et al., 2005, 2008; PIRSON, 2007; see Chapter 5). Therefore, former Layer 4A was renamed Sedimentary Complex 4A, and is now comprised

of approximately 20 layers situated around Speleothem CC4. They are organized into 4 units (Figure 1):

- underlying Speleothem CC4, Unit 4A-AP contains layers 4A-LG, 4A-MC, 4A-GB, and 4A-KG;
- Speleothem CC4 and the layers interstratified with CC4 are grouped into Unit 4A-IP. Locally, CC4 is divided into 2-3 distinct generations that are separated by lenses of sediment. The layers interstratified with CC4, with which they are contemporary, are layers 4A-OR, 4A-SGR, and 4A-YS;
- a unit composed of several discontinuous lithofacies and corresponding with the filling of an important gully is called Unit 4A-CHE. This gully cross-cuts the layers of units 4A-AP and 4A-IP, as well as Speleothem CC4. These lithofacies contain many limestone fragments, as well as calcite fragments eroded from Stalagmitic Floor CC4;
- layers that were deposited after the gully, overlying both units 4A-IP and 4A-CHE, constitute Unit 4A-POC, which is divided into 4 layers: 4A-BO, 4A-LEG, 4A-GV, and 4A-GBL.

According to what is currently understood from a chronostratigraphic perspective, the entire Sedimentary Complex 4A appears to have been deposited during the Weichselian Early Glacial (for details, see Chapters 4 & 5).

Following the stratigraphic revision, the increased number of identified layers caused the excavations at Scladina to become much more precise. The stratigraphic contexts of bones and artefacts are therefore now better understood (for excavation methodology see BONJEAN et al., 2009; see Chapter 2).

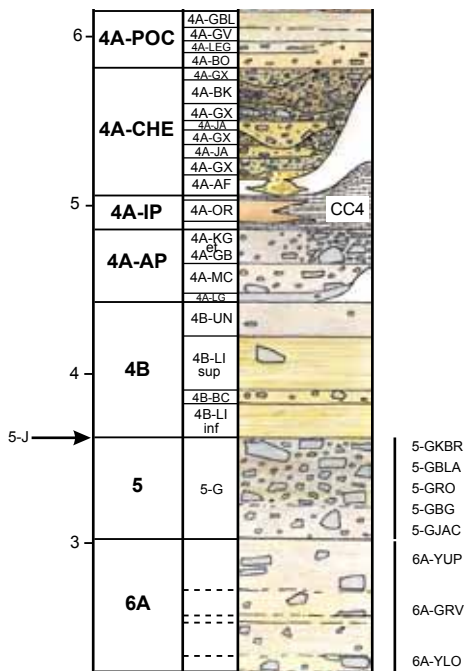


Figure 1: Stratigraphic log of units 6A to 4A-POC that contained the faunal remains used in this study (from PIRSON, 2007).

2.2. Taphonomy of the Neandertal child

The Scladina Neandertal fossils have been examined under a hand lens and, in some cases, a stereomicroscope in order to check for the presence or absence of numerous classic taphonomic criteria. These observations are related to surface colour, coloration at breakage sites, surface condition/lustre (polished, glossy, porous, etc.), weathering traces, adhered matrix, types of fracturing, degree of fragmentation, abrasion of fracture edges, peeling, trampling, burning, precipitation of manganese and iron hydroxides, tool-induced marks, carnivore and rodent tooth marks, (micro)

mammal gnawing, insect action, pathological markers, excavation damage, preparation damage, and sampling damage (POTTER & ROSSMAN, 1979; BINFORD, 1981; HILL, 1982; ORTNER & PUTSCHAR, 1985; BEHRENSMEYER et al., 1986; NOE-NYGAARD, 1989; WHITE & TOTH, 1989; HAGLUND, 1992, 1997; WHITE, 1992: 129; ANDREWS & FERNÁNDEZ JALVO, 1997; LÓPEZ-GONZÁLEZ et al., 2006).

When possible, the features were then classified according to the different chronological phases of the taphonomic process that they were related to:

1. antemortem trauma, which precedes the study area of taphonomy *sensu stricto*, is by definition characterized by the survival of the victim. Therefore, these traces show clear signs of healing as well as associated breaks consistent with fresh or ‘green’ bone fractures;
2. perimortem trauma, i.e. damage to bone that occurs just before, during, or shortly after death, which exhibits no evidence of healing; the associated breaks are similar to antemortem fractures, as both occur on fresh or ‘green’ bones (WAKELY, 1997; CRAIG et al., 2005; KNÜSEL, 2005). Perimortem traces can, theoretically, be divided into three types: (a) trauma occurring shortly before death but not a direct cause of death (e.g. “perimortem injury that occurred before death,” see WALKER, 2001: 577); (b) trauma responsible for the death, i.e., lethal perimortem damage (fractures indicating violence, arrowhead wounds, carnivore predation activity, etc.; see CRAIG et al., 2005; KNÜSEL, 2005); (c) anthropogenic traces occurring shortly after death (e.g., “perimortem injury that occurred after death” as defined by WALKER, 2001: 577) or scavenger damage which can sometimes be distinguished from perimortem damage occurring just before death by other clues, such as the location and symmetry of the marks, which do not allow assumption that these marks could have been inflicted on a living person/animal. However, in many cases, it is impossible to distinguish between these three types of traces, as the persistence of collagen allows bone to respond to trauma in a similarly elastic manner in the three types (WALKER, 2001; ROGERS, 2004; CRAIG et al., 2005);
3. postmortem damage exhibits no signs of healing and is mainly due to site formation

processes, occurring more or less long after death. Postmortem damage consists of “stage 2, dry bone breakage” and “stage 3, post-fossilization breakage” of KROVITZ & SHIPMAN (2007). Such damage is inferred from numerous taphonomic markers;

4. recovery and post-recovery damage induced by archaeological activity, either from excavation (e.g., metal tool damage), preparation (WHITE & TOTH, 1989; WHITE, 1992: 129), sampling (DNA, biogeochemistry, dating), or museum curation.

2.3. Taphonomy of the faunal remains

Since 2005, the archaeologists at Scladina have undertaken a systematic examination of the main taphonomic signatures of the faunal remains from the cave. Six main attributes were used including: the general colour of the fossils, the number of fractures, the degree of abrasion of fractured edges, the condition and lustre of the cortical surface (original, polished, cracked), and the precipitation of both metallic oxides (mainly iron and manganese) and carbonates (DELAUNOIS, 2010; DELAUNOIS et al., 2012).

This analysis showed that the majority of the faunal remains from the same sedimentary layer exhibited a similar state of preservation. Between the objects from different layers, a logical variation of the intensity of taphonomic properties was observed. When combined, the various physical attributes observed on the bones of each layer provide a unique taphonomic signature that can be used as a dynamic tool in the field during excavation, as well as in the laboratory, to evaluate the integrity of a group of objects. The results of the use of this tool may have large implications on the understanding of the contemporaneity of faunal remains and their attribution to a specific type of environment (DELAUNOIS et al., 2012).

The results of the taphonomic analysis described above show the potential for the use of this method when analysing the Neandertal child, especially because the 2 hemimandibles have different taphonomic signatures (e.g. colour, surface cracking). Verification of whether or not the variation of the taphonomic characteristics was unique to the Neandertal child or if they were also exhibited on faunal remains from the same sedimentary complex was important.

Secondary to this, the results of this study will also have stratigraphic, and therefore chronological, implications. Because the Neandertal remains



were excavated before the stratigraphic revision (started in 2003; PIRSON, 2007), the objects were attributed to the entirety of the 4A stratigraphic complex (BONJEAN et al., 1997; PIRSON et al., 2005). Later, with the help of the new stratigraphic framework, some of the objects were reattributed to more precise contexts, including the gully, Unit 4A-CHE (at least 1 hemimandible), or to Unit 4A-POC (post-gully; see Chapter 5). The affirmation of this reattribution by a method other than stratigraphic observation was relevant. To do this, the taphonomic properties examined

on faunal remains were compared to the ones on the Neandertal remains in order to observe if commonalities exist. This comparison determined whether or not the hominid and faunal remains were altered in the same way, which is possibly linked to similar biostratigraphic and diagenetic processes, and thus their deposition in the same sedimentary environment. Therefore, the layers that provided most of the animal remains that are taphonomically similar to the child could become potential candidates to have contained the Neandertal remains before they were reworked into the gully (Unit 4A-CHE).

The fauna that constituted the comparative material used in the analysis came mainly from recent excavations (2003–2010) that respected microstratigraphy. Only 1 cave bear (*Ursus spelaeus*) phalanx that was exhumed in 1996 was added to this collection, due to the pertinence of its taphonomic criteria when compared to those of the child. The collection is composed of 597 bones that belong to various mammalian species, but mainly to cave bear. The chosen anatomic segments were variable, and therefore represented objects with different densities. These segments include cranial elements, sterna, vertebrae, and both upper and lower limb bones.

The 597 bones are from 4 different zones within the cave (Figure 2), which are all situated on the periphery of the area that yielded the hominid remains. One of them is a zone between metres 24 and 30 adjacent to the concentration of the 10 isolated teeth of the child. The 3 other zones are deeper in the cave, from metres 32 to 43, and surround the area where the other 4 isolated teeth were exhumed.

The faunal remains originate from 16 different layers within 7 sedimentary units:

- 6A (6A-YLO, 6A-GRV, 6A-YUP)¹;
- 5 (5-GJAC, 5-GBG, 5-GRO, 5-GBLA, 5-GKBR)¹;
- 4B (4B-LI, 4B-UN);
- 4A-AP (4A-KG);
- 4A-IP (4A-OR);
- 4A-CHE;
- 4A-POC (4A-BO, 4A-LEG, 4A-GBL).

In addition to this, a complimentary study was undertaken due to the fact that most of the Neandertal fossils from Scladina are isolated teeth. Therefore, a comparison of the Neandertal teeth to

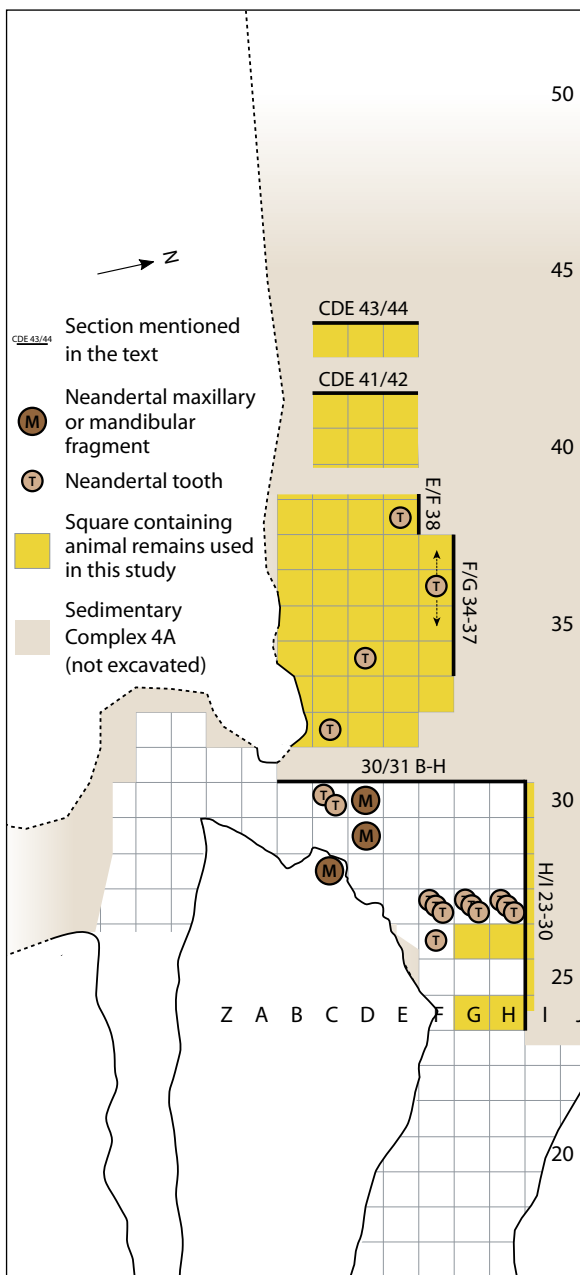


Figure 2: Spatial distribution of the hominid and animal remains compared in the study.

¹ In this paper, these lithologies will be considered as layers. The stratigraphic study of this part of the sequence, still in progress, will have to confirm if those lithologies are real layers or rather lateral variations of facies.

the isolated incisors of cave bear from the same sedimentary units was appropriate. However, the excavations after the stratigraphic revision have yielded only 52 *Ursus spelaeus* teeth. To increase the sample size, 248 other cave bear incisors were selected from 32 m² of former Layer 4A. These 248 objects were all reattributed to their original sedimentary units (4A-AP, 4A-CHE, 4A-POC), which was made possible thanks to several observations recorded during excavation of this specific area. Stalagmitic Floor CC4 was excavated when in situ on a surface of 6 m² (F, G, and H from metres 28 to 29). The altitudes of the teeth were recorded which facilitated clarification of whether they were excavated from below the stalagmitic floor (Unit 4A-AP) or from above it (Unit 4A-POC). Unit 4A-CHE was also localized in squares G30 and H30 through stratigraphic observation of the adjacent profiles 30/31 and H/I.

3. Results

3.1. Taphonomy of the Scladina Neandertal fossils

The three osseous fragments of the Scladina Juvenile, including the Scla 4A-1 and Scla 4A-9 hemimandibles, and the small part of the right maxilla (Scla 4A-2), as well as the child's isolated teeth are all fossilized to some degree (the extent of fossilization is presently under investigation; Figure 3).

3.1.1. Left hemimandible Scla 4A-9

Scla 4A-9 (Figure 4) consists of the very anterior part of the right body, the symphysis, and the essentially complete left body, but the ramus is not present. It weighs 31.69 g.

Figure 3: The 19 juvenile Neandertal fossils (scale 1:1):

- 4A-1, right hemimandible;
- 4A-2, right maxillary fragment;
- 4A-3, permanent maxillary right second molar (M²);
- 4A-4, permanent maxillary right first molar (M¹);
- 4A-5, deciduous maxillary right second molar (dm²);
- 4A-6, mandibular right first premolar (P₃);
- 4A-7, deciduous maxillary right first molar (dm¹);
- 4A-8, permanent maxillary right third molar (M³);
- 4A-9, left hemimandible;
- 4A-11, permanent maxillary right central incisor (I¹);
- 4A-12, permanent mandibular right canine (C);
- 4A-13, deciduous mandibular right second molar (dm₂);
- 4A-14, permanent maxillary right lateral incisor (I²);
- 4A-15, permanent mandibular right central incisor (I₁);
- 4A-16, permanent maxillary right canine (C');
- 4A-17, permanent maxillary left lateral incisor (I²);
- 4A-18, permanent maxillary left canine (C');
- 4A-19, permanent mandibular left lateral incisor (I₂);
- 4A-20, permanent mandibular right lateral incisor (I₂).

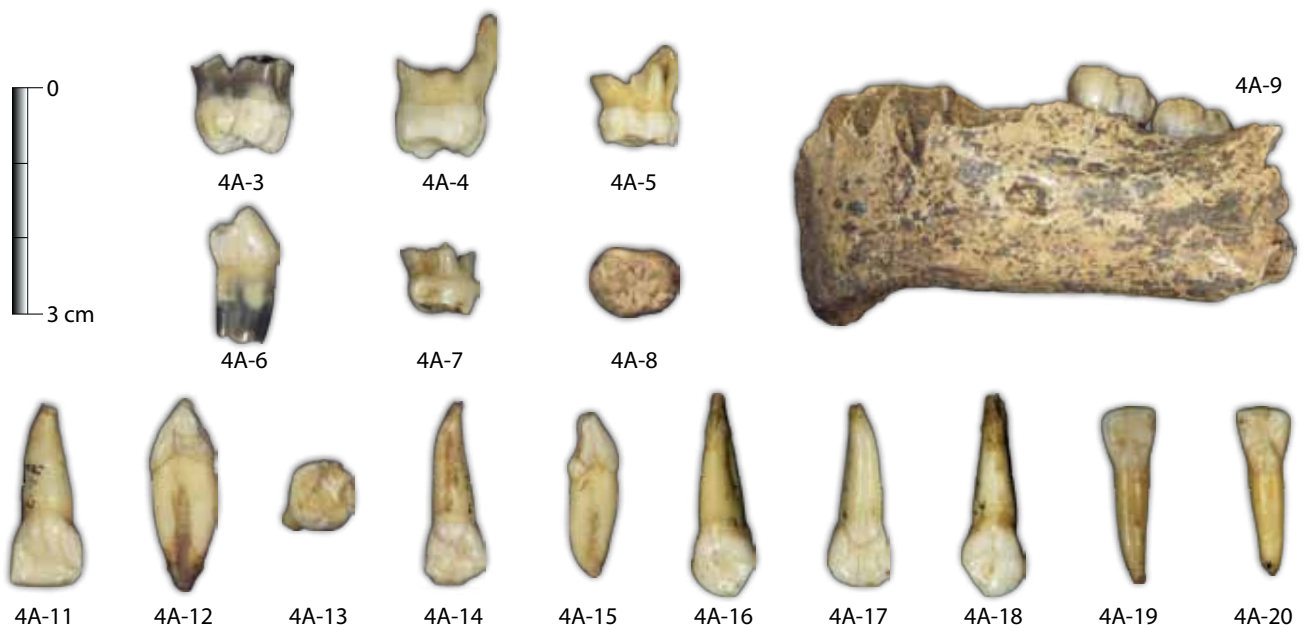




Figure 4: The left hemimandible Scla 4A-9, labiobuccal (above) and lingual (below) surfaces (scale 1:1).

The main colour of the fossil is orange (dull yellow orange, 10 YR 7/4 and light yellow orange, 10 YR 8/3 and 8/4). Its surface is slightly polished.

Numerous thin cracks (Figure 5), visible to the naked eye, are present and correspond to stage 1 of BEHRENSMEYER (1978); no flaking is associated with them. The fractures are nearly parallel to the inferior margin of the body and present on both faces, although mainly the lingual one. There are also some subvertical cracks.

Small stains of manganese are present (generally no more than a few millimetres in diameter, but sometimes connected) on both the lingual and buccal faces of the fossil (Figure 6). The area covered by manganese is at stage 2 of LÓPEZ-GONZÁLEZ et al. (2006), which is to say between 10% and 50%. The colour of the coating is intense dark dun (intensity 2) on the buccal surface and in the posterior lingual part of the hemimandible, but darker (intensity 2 to 3) in the mesial lingual area. In most cases, manganese covers the fractures. Some stains of manganese are also present inside the fracture that separated the mandible in two, as well as inside the dental alveoli. Manganese is never precipitated in dendritic form on the Neandertal fossils. All the manganese is clearly superimposed over previously existing features on the bone's surfaces, such as the fractures.

The anterior break of this fossil, which can be refitted almost perfectly with the anterior break of the right hemimandible (Scla 4A-1), is transversal

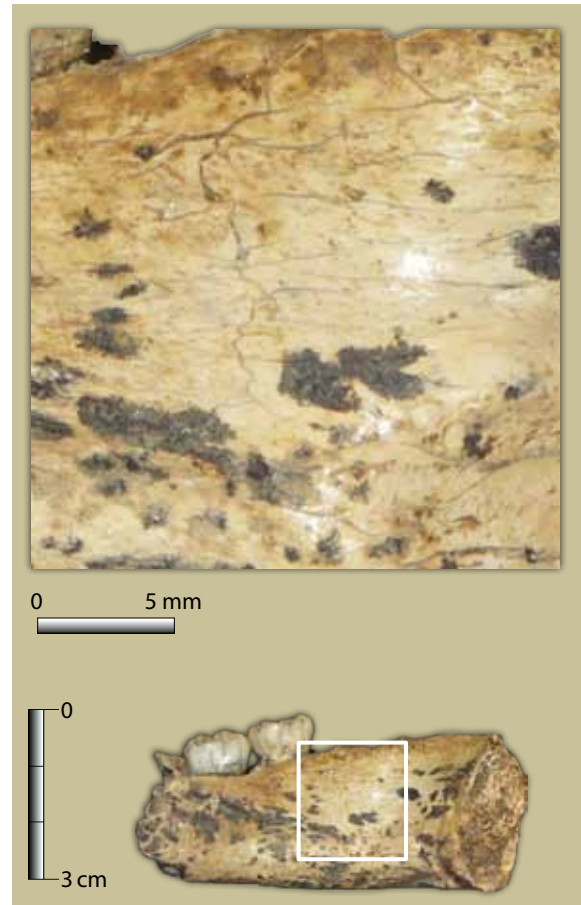


Figure 5: Cracks on Scla 4A-9.



Figure 6: The manganese deposits on Scla 4A-9.

and nearly vertical in the superior half of the body, curving distally in its inferior part. The edges of the break are sharp on the buccal surface. On the lingual surface, adjacent to the anterior fracture, a small area of 'peeling' was observed (Figure 7), which is a pattern related to fractures that have occurred in fresh, fibrous osseous material (WHITE, 1992: 140-143). Some small manganese stains are present on the peeled surfaces.

The facial portion of the canine dental alveolus is largely missing. The anterior wall of the dental alveoli of the four incisors and the buccal face of the P₄ are also eroded.

The posterior break is affected by some recent small fractures, which were the result of the excavation of the object.

Some other excavation damage was detected on the lingual surface, below the second molar and third molar crypts: metal scraper marks made by the excavator who unearthed the fossil (Figure 8). Contrary to the thin cracks discussed earlier, these marks were made after manganese had already precipitated onto the object. Several other thin marks are present on the fossil, for instance a curved one on the facial surface which is inferiorly concave, under M₁ and under the dental alveolus of P₄.

Neither rodent nor carnivore marks, such as scoring and furrowing from gnawing/chewing, pits, or punctures are observed on 4A-9. Also, no cut marks are present.

No real curatorial damage has occurred, and no moulding or casting methods have been used, no sampling for DNA or isotopic analysis has been done. In fact, a replica of this left hemimandible was made with a medical scanner and stereo-lithography. It was then replicated using classical moulding methods to produce further copies.

3.1.2. Right hemimandible Scla 4A-1

The Scla 4A-1 (Figure 9) hemimandible consists of the right body and ramus. The bone is highly lustrous, likely due to fossilization. However, that characteristic may be slightly accentuated by the presence of wax residue from when both Scla 4A-1 and Scla 4A-2 were moulded.

The general colour of the fossil is greyish-green. The two main components are light grey (2.5 Y 8/2) and pale yellow (2.5 Y 8/3) with traces of grey (7.5 Y 6/1 and 5/1) and pale green. Cracks, mainly parallel to the body, are present but not as visible as on Scla 4A-9 (Figure 10); they are at the very beginning of BEHRENSMEYER (1978)

Figure 7: The peeling adjacent to the anterior fracture of Scla 4A-9.

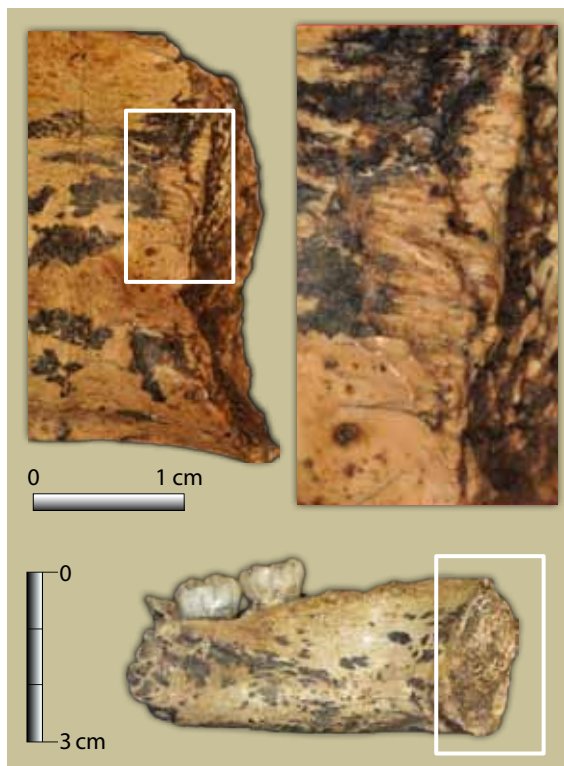


Figure 8: Excavation damage on Scla 4A-9.





Figure 9: The right hemimandible Scla 4A-1, buccal (left) and lingual (right) surfaces (scale 1:1).



Figure 10: Thin horizontal cracks on Scla 4A-1, represented by thin red lines.

stage 1. The external wall of the M₁ dental alveolus exhibits a wider subvertical crack.

A few subtle manganese stains are present. Neither rodent nor carnivore marks, such as scores, furrows, pits, or punctures are observed on Scla 4A-1.

The anterior break corresponds to that of Scla 4A-9: vertical in its upper part, then distally oblique (Figure 11).

The gonion is eroded (Figure 12). On the bone's buccal surface a network of surface cracks is present in a star-shaped form (Figure 13). No trace

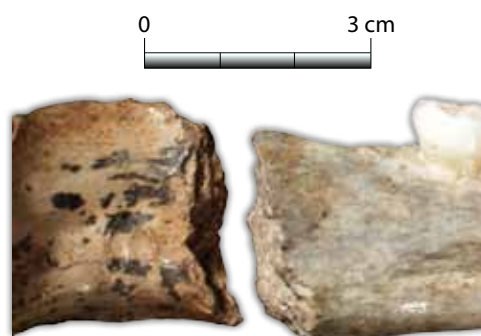


Figure 11: Fig 11. Side-by-side comparison of the anterior break that separates Scla 4A-1 and 4A-9.

of applied pressure is visible. The cracks appear to be the possible result of cortex rupturing that originated from inside the bone. This rupture could have been produced by an expansion of the bone from freezing (gélifraction, *GUADELLI & OZOUF, 1994*). The condyle is damaged; its lingual part is eroded and its buccal one is missing at least 4 mm of osseous material. The posterior border is also heavily worn.

A straight, thin groove that at first glance is very similar to an anthropogenic cut mark,

is present on the lingual surface of Scla 4A-1 (Figure 14). However, the position is unusual for cut marks and it is the only similar trace observed on the three bones of the juvenile, so this mark was probably caused by some sedimentary process.

The facial surfaces of some dental alveoli, mainly of P₃, are heavily abraded.

A small splinter from the upper part of the anterior border of the right ramus was detached during the excavation process and later refitted (Figure 15).



Figure 12: The eroded gonion of Scla 4A-1.



Figure 13: The star-shaped fracture of Scla 4A-1.

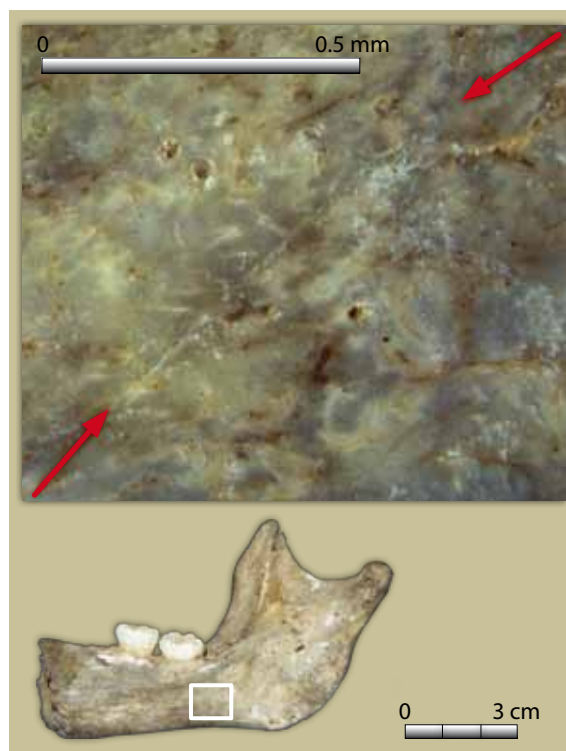


Figure 14: The straight thin groove that was likely caused by sedimentary processes (between the red arrows).





Figure 15: The splinter broken off from Scla 4A-1 during excavation.

Figure 17: The crenulated margin of Scla 4A-2, especially above the canine dental alveolus.



Figure 16: The maxilla Scla 4A-2, labiobuccal (above) and lingual (below) surfaces (scale 1:1).

Contrary to Scla 4A-9, a mould was prepared in order to obtain casts of this fossil and some tiny traces of white silicone are still present on it.

3.1.3. Maxilla Scla 4A-2

This fossil (Figure 16) is a part of the right maxilla, comprised of just the partial alveolar processes, from the complete I¹ crypt to the middle of the M¹ crypt. The maxilla is broken mesially, distally, and superiorly. On the bone's inferior component, the mesial breakage extends along part of the intermaxillary suture for a few millimetres in front of the incisive canal and then curves distally on the superior part. The distal fracture is vertical but irregular and located in the middle of the socket of the first molar. The floor of the nasal cavity constitutes the superior part of the fossil medially, and the floor of the maxillary sinus laterally.

Currently, the superior margin of the fossil is somewhat crenulated, especially above the canine alveolus (Figure 17).

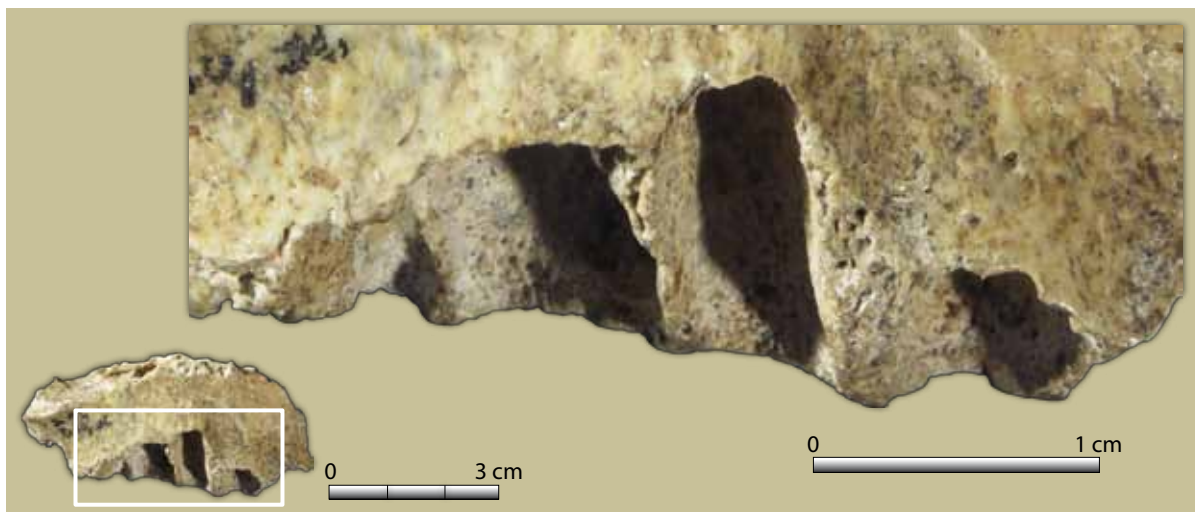




Figure 18: The thin cracks of Scla 4A-2.

The general colour of Scla 4A-2 is greyish-green, relatively similar to that of the right hemimandible Scla 4A-1. The main colours are pale yellow (2.5 Y 8/3 and 8/4) with traces of greyish yellow (2.5 Y 7/2) on the lingual surface and bright yellowish brown (10 YR 7/6) on the buccal surface.

Some thin cracks are present but not as visible as those on Scla 4A-9. There are also some rare manganese stains that are as subtle as the ones on Scla 4A-1 (Figure 18).

The facial walls of the alveoli of both incisors and the anterior part of dm^2 and M^1 are heavily worn; those of the C^1 and the P^4 are also significantly altered.

As for Scla 4A-1, a mould was prepared in order to cast the fossil and some tiny traces of white silicone are still present.

3.1.4. Isolated teeth

All of the teeth (see Figure 3) from the mandible and the maxilla that were found scattered throughout the sediment were disarticulated postmortem. The alveoli of the permanent teeth are still open and not resorbed at all. Such a situation is expected as the juvenile died at only 8 years of age (see Chapters 8 & 16). Only antemortem trauma could have made the child lose a permanent tooth and

have a resorbed alveolus, which was not the case for this individual.

Most of the teeth are nearly complete and very well preserved. The roots of the deciduous teeth have started to resorb. The roots of the permanent maxillary right second molar (Scla 4A-3) are not fully developed. The apices of some incisors are not completely closed (Scla 4A-16). Only two incisors (Scla 4A-20 & Scla 4A-11) have broken roots, which occurred after they were lost postmortem.

The 16 isolated teeth of the Neandertal child are exceptionally well preserved with little alteration. 15 of the teeth exhibit crowns with light grey enamel (2.5 Y 8/1 and 8/2) comparable to the original colour of in vivo teeth. Their roots exhibit a white-yellow colour (yellow 2.5 Y 8/6, pale yellow 5 Y 8/3 and 8/4, light grey 7.5 Y 7/2) with the exception of 2 not fully developed roots that exhibit a darker, greyish colour (black 10 YR 2/1 and brownish grey 10 YR 4/1). On Scla 4A-3 the dark colour covers the entire root while on Scla 4A-6 only the apical part of the root is covered (Figure 3).

The 16th isolated tooth, the crown of the permanent maxillary right third molar (Scla 4A-8), exhibits a dull yellow orange tint (10 YR 6/4), probably due to the fact that it was not yet erupted and still inside the hemimandible (Scla 4A-9) at the time of death. Because of its unique colour in comparison to the other 15, Scla 4A-8 was excluded from this study. The crown of the permanent mandibular right third molar is still included in the right hemimandible Scla 4A-1. This crown is visible within the alveolus and has the same colour as Scla 4A-8.

Four other in situ erupted teeth were within the alveoli of the 2 hemimandibles at the time of discovery. The original colour of the enamel of the M_1 and M_2 of hemimandible Scla 4A-1 is very similar to the 15 isolated teeth that were previously described. However, the colour of the permanent mandibular left first and second molars, still in situ in the hemimandible Scla 4A-9, is completely different. Their crowns exhibit dull yellow orange enamel (10 YR 7/4) and are full of microcracks, in which a blue-black substance has precipitated (possibly manganese). If a definite sedimentary context gives the bones and teeth within it a homogeneous taphonomic signature (as proposed in the introduction), Scla 4A-9 was not present



within the same sediment as Scla 4A-1 during its diagenesis.

3.2. Planimetry and stratigraphy of the juvenile Neandertal

The remains of the Scladina Neandertal child were spread throughout different layers of Sedimentary Complex 4A over quite a large horizontal area. The understanding of the stratigraphic (see Chapter 3) and planimetric context of the isolated teeth and fragments of mandible and maxilla is therefore very important in deciphering their unique taphonomic histories.

3.2.1. Stratigraphy

Current stratigraphic information indicates that the Neandertal remains came from layers that were deposited after the Stalagmitic Floor CC4 (units 4A-CHE and 4A-POC). The remains were at least in secondary position, either brought from outside the cave or reworked by the erosion of one or more sedimentary layers that were already present within the cave. Unit 4A-CHE has reworked sediment from at least 12 different layers from sedimentary units 6A, 5, 4B, and Complex 4A.

3.2.2. Spatial distribution

Currently, the excavated area of the Complex 4A is approximately 6 m wide by 40 m long (see Figure 2). No Neandertal remains have been discovered on the terrace or within the first 15 metres of the cave (i.e. before and including metre 25). The fossils were found beyond this area, from metre 26 to 38. The child's remains were distributed within the second half of the cave, along a narrow band included within a rectangle that is 6 m wide by 13 m long and sub-parallel to the cave's axis. That region dips gently towards the back of the cave, and seems to correspond to the course of the 4A-CHE gully. Inside the band, the fossils were organized in 3 groups:

- first, 10 teeth were concentrated on a small surface of 4 m² (F26, F27, G27, and H27), and are spread perpendicular to the long axis of the cave;
- second, the 2 mandibular fragments, the fragment of maxilla, and 2 isolated teeth were grouped in a rectangle that is 2.5 m × 2 m and in contact with the left wall of the cave (C28, C30, D29, and D30);

- third, 4 isolated teeth were found further in the cave, spread in 3 squares (C32, D34, E38), and in a zone from F35 to F37.

3.3. Comparative taphonomic study: the rest of the faunal remains

Six physical taphonomic criteria were selected for the study of the 597 faunal remains: colour, number of fractures, abrasion of fracture edges, bone surface state, the precipitation of manganese, and the precipitation of carbonate. The analysis of those attributes is synthesized in Table 1, where the Neandertal remains are indicated by a black triangle.

3.3.1. Colour

The analysis of bones has continuously indicated a distinctive dominant colour of objects from the same sedimentary layer, which is sometimes accompanied by variations of intensity. The objective of this study was to observe and record faunal remains from units 6A, 5, 4B, 4A-AP, 4A-IP, 4A-CHE, and 4A-POC that exhibit the typical colour of the Neandertal hemimandibles and maxilla. Therefore, all of the other colours not relevant to the Neandertal child, yet observed on the faunal remains, are not differentiated in Table 1 and are presented as 'other colour'.

The colours represented on the Neandertal fossils are extremely rare amongst the studied faunal remains. Only 16 bones (2.8%) could be used as comparisons for this study.

The greyish-green colour of the hemimandible Scla 4A-1 and the maxilla Scla 4A-2 (Figure 19) is totally absent in the material from units 6A and 5. Layer 4B-UN has yielded 2 bones that exhibit similar colouration: 1 metatarsal (Figure 19-a) and 1 cranial fragment (Figure 19-g). The most frequent similarities have been recorded in Complex 4A with 5 remains that have colours very similar to those of the Neandertal fossils: 1 pisiform from Layer 4A-KG (Figure 19-c); 1 fragment of a radius (Figure 19-h), 1 diaphyseal fragment (Figure 19-b), and 1 rib fragment (Figure 19-e) from Unit 4A-CHE; and 1 diaphyseal fragment from Layer 4A-GBL (Figure 19-i).

The orange colour, exhibited on hemimandible Scla 4A-9, is absent from the remains of Unit 6A. Higher in the stratigraphic sequence, the colour is present on 10 remains (Figure 20). They are distributed in layers 5-GRO (pisiform,

Taphonomic criteria		Stratigraphical distribution of the studied faunal remains																							
		Layers cross-cut by the gully																		Gully					
		6A-						5-						4B-						4A-					
Number of fossils	Colour	Fractures	Abrasion	Lustre	Manganese	Calcite	YLO	GRV	YUP	GJAC	GBG	GRO	GBLA	GKBR	LI	UN	KG	OR	CHE	BO	LEG	GBL			
							11	29	39	15	9	7	30	19	9	39	91	11	213	33	7	35			
							0%	0%	0%	0%	0%	0%	0%	0%	0%	5%	1%	0%	1.5%	0%	0%	0%			
	greyish-green						0%	0%	0%	0%	0%	0%	0%	0%	0%	0%	3%	9%	1%	3%	0%	0%			
	orange						0%	0%	0%	0%	1.4%	3%	0%	0%	0%	0%	3%	9%	1%	3%	0%	0%			
	other						100%	100%	100%	100%	86%	97%	100%	100%	100%	95%	96%	91%	97.5%	97%	100%	97%			
	none						36%	10%	27%	22%	29%	33%	21%	56%	29%	42%	27%	38%	9%	9%	0%	0%			
	1						10%	38%	7%	67%	43%	10%	11%	22%	16%	12%	0%	18%	21%	86%	17%				
	2						27%	45%	13%	11%	14%	40%	26%	22%	37%	14%	18%	13%	9%	9%	14%	31%			
	>2						27%	7%	53%	0%	14%	17%	42%	0%	18%	32%	55%	31%	61%	61%	0%	41%			
	none						18%	10%	0%	0%	0%	0%	0%	0%	11%	0%	13%	8%	0%	0%	0%	0%			
	low						64%	21%	7%	22%	29%	13%	37%	33%	33%	47.5%	66%	48%	27%	27%	14%	40%			
	medium						9%	31%	53%	78%	57%	57%	63%	56%	34%	19%	45%	33%	64%	43%	43%	57%			
	high						9%	38%	40%	0%	14%	30%	0%	0%	18.5%	2%	10%	11%	9%	9%	43%	3%			
	high						0%	0%	0%	0%	0%	0%	0%	0%	0%	0%	0%	0%	0.9%	0%	0%	2.8%			
	matte						100%	100%	100%	100%	100%	100%	100%	100%	100%	100%	100%	100%	99.1%	100%	100%	97.2%			
	none/very few spots						0%	7%	0%	0%	0%	0%	0%	0%	0%	13%	1%	0%	26%	3%	71%	17%			
	regular spots						0%	3%	0%	0%	0%	0%	5%	15%	5%	84%	27%	29%	64%	29%	29%	34%			
	large spots						100%	76%	100%	100%	86%	97%	95%	48%	71%	13%	73%	38%	12%	0%	0%	23%			
	total cover						0%	14%	0%	0%	14%	3%	0%	37%	11%	2%	0%	7%	21%	0%	0%	26%			
	none						100%	100%	100%	100%	100%	100%	100%	100%	100%	100%	99%	91%	95.3%	100%	57%	100%			
	present						0%	0%	0%	0%	0%	0%	0%	0%	0%	0%	1%	9%	4.7%	0%	43%	0%			

Table 1: Table of the taphonomic results. Six taphonomic criteria have been taken into account. The Neanderthal fossils are marked by a black triangle. Important criteria are highlighted in grey.





Figure 19: The greyish-green colour of the right hemimandible Scla 4A-1 (f) and the maxilla Scla 4A-2 (d) among 7 faunal remains (scale 1:1).

	Taxon	Segment	Inventory N°	Figure
4A-GBL	?	Splinter	Sc 2006-341-1	19-i
4A-CHE	Unidentified Herbivore	Rib fragment	Sc 2007-668-2	19-e
4A-CHE	?	Diaphysis fragment	Sc 2007-122-3	19-b
4A-CHE	<i>Rupicapra rupicapra</i>	Proximal radius fragment	Sc 2004-678-1	19-h
4A-KG	<i>Ursus spelaeus</i>	Pisiform	Sc 2006-416-2	19-c
4B-UN	<i>Ursus spelaeus</i>	Juvenile cranium fragment	Sc 2006-477-3	19-g
4B-UN	<i>Ursus spelaeus</i>	3rd metatarsal	Sc 2004-185-1	19-a

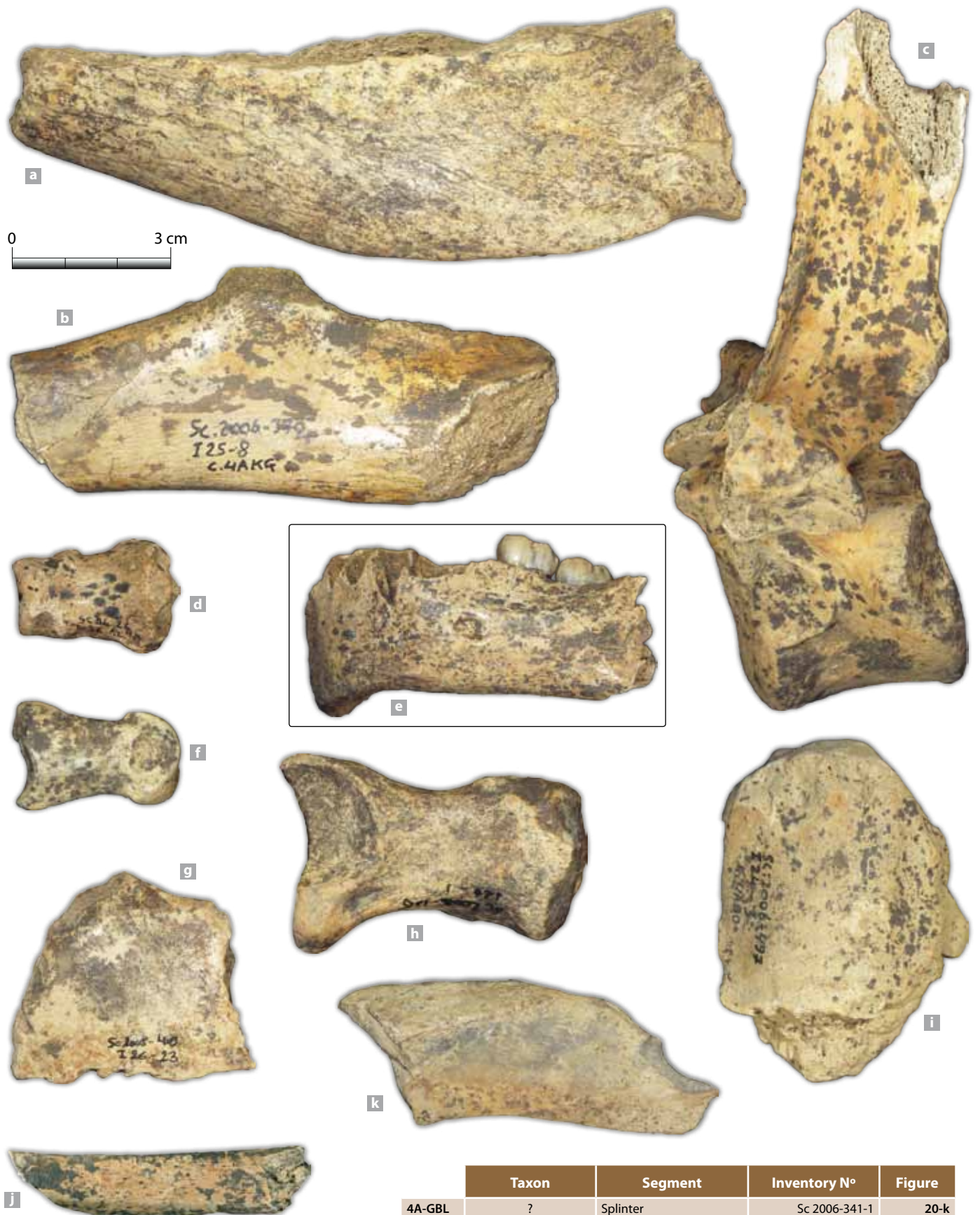


Figure 20: The orange colour of the hemimandible Scla 4A-9 (e) among 10 faunal remains (scale 1:1).

	Taxon	Segment	Inventory N°	Figure
4A-GBL	?	Splinter	Sc 2006-341-1	20-k
4A-BO	<i>Ursus spelaeus</i>	Patella	Sc 2006-497-3	20-i
4A-CHE	<i>Ursus spelaeus</i>	2nd phalanx	Sc 1996-26-12	20-d
4A-CHE	?	Hemimandible fragment	Sc 2006-510-1	20-a
4A-OR	<i>Dama dama</i>	2nd phalanx	Sc 2006-330-1	20-f
4A-KG	<i>Ursus spelaeus</i>	Ulnar fragment	Sc 2006-370-8	20-b
4A-KG	?	Rib fragment	Sc 2006-506-4	20-j
4A-KG	<i>Ursus spelaeus</i>	Thoracic vertebra	Sc 2006-511-1	20-c
5-GBLA	<i>Ursus spelaeus</i>	Cranium fragment	Sc 2008-409-23	20-g
5-GRO	<i>Ursus spelaeus</i>	Pisiform	Sc 2008-156-1	20-h

Figure 20-h), 5-GBLA (cranial fragment, Figure 20-g), 4A-KG (thoracic vertebra, Figure 20-c; rib fragment, Figure 20-j; ulnar fragment, Figure 20-b), 4A-OR (phalanx, Figure 20-f), 4A-CHE (hemimandible fragment, Figure 20-a; phalanx, Figure 20-d), 4A-BO (patella, Figure 20-i), and 4A-GBL (diaphyseal fragment, Figure 20-k). However, of these bones, 4 are more similar than the rest. These bones are from layers 4A-KG (thoracic vertebra, Figure 20-c), 4A-OR (phalanx, Figure 20-f), and 4A-CHE (hemimandible fragment, Figure 20-a; phalanx, Figure 20-d). One of the last two bones listed from 4A-CHE (above) is a 2nd phalanx of *Ursus spelaeus* (Sc 1996-26-12; Figure 20-d) that has a nearly identical colour to the Neandertal hemimandible Scla 4A-9 and was found approximately 20 cm from Scla 4A-9. The phalanx was exhumed in 1996 before the stratigraphic revision; but by observing numerous pictures, it has been clearly attributed to 4A-CHE.

The rarity of comparable objects has negative implications on the viability of a statistical approach to this study. Regardless, nearly perfect matches based on colour have been made between the Neandertal fossils and faunal remains which permitted the determination that

the hominid fossils are most similar to objects from Sedimentary Complex 4A.

Among the 597 osseous remains, only one diaphyseal fragment (Sc 2006-341-1) from Layer 4A-GBL exhibits the two different colours discussed previously on the same object. The cortical surface is light orange in colour (Figure 21), which is similar to hemimandible Scla 4A-9. A band on the middle part of the cortex is greyish-green in colour and highly lustrous, which is very similar to hemimandible Scla 4A-1. This greyish-green area appears to be superimposed over the orange, which is possibly due to the object being subjected to multiple sedimentary environments. The specific mechanism(s) that would cause a single object to exhibit two different colours and lustres inside Unit 4A-POC are currently unknown and could be the subject of a future analysis.

3.3.2. Number of fractures

The depositional mode of sediment has unavoidable impacts on the preservation state of material within it. Therefore, Layer 4B-LI, constituted by alternating lithofacies of silt and clay caused by decantation (low energy) contains the highest



Figure 21: The doubly coloured splinter (below, scale 1:1, and above right, enlarged) Sc 2006-341-1 and its comparison with the hemimandible Scla 4A-1 (above left) and Scla 4A-9 (below right).

frequency of intact bones (56%). The stratigraphic distribution of the objects according to the number of fractures per bone demonstrates an increased amount of alteration as they were reworked upwards through the sedimentary sequence from Layer 4A-KG to Unit 4A-CHE. For example, the number of completely intact bones differs between the two layers: 42% intact bones in 4A-KG, compared to 38% in 4A-CHE. This observation is accompanied by only 12% of the bones from 4A-KG exhibiting 1 fracture, compared to 18% in 4A-CHE.

The number of fractures per object varies between the 3 osseous fragments of the Neandertal child: Scla 4A-1 has 1 fracture, Scla 4A-9 has 2 fractures, and Scla 4A-2 has at least 3 fractures. Therefore, their dispersion in the 3 categories allows them to be attributed to any of the studied layers since they are comparable to every object which renders this method as not useful for this study.

3.3.3. Abrasion of fracture edges

The low degree of edge abrasion ('low' category; Table 1) that categorizes the 3 osseous fragments of the Neandertal child is a characteristic that is also present on a large number of faunal remains, constituting the major tendency for 5 faunal assemblages: 6A-YLO, 6A-YUP, 4B-UN, 4A-KG, and 4A-CHE. The remains from the other studied layers show a globally higher degree of abrasion and, therefore, are not comparable to the Neandertal child.

3.3.4. The state of the cortex

Climatic agents affect bones that are shallowly buried or in direct contact with the atmosphere. This effect is also known as "weathering" (BEHRENSMEYER, 1978). The process begins by longitudinal followed by transversal cracking, the intensity of which varies based on the bone density, the age of the individual, the fragmentation of the bone before the weathering began, the degree of fossilization, etc. (GUADELLI & OZOUF, 1994; GUADELLI, 2008; MALLYE et al., 2009). In some extreme cases, lengthy exposure of bones to these processes can lead to the formation of long rectangular prism-shaped fragments (state 4) that can eventually lead to the complete fragmentation of the object. Furthermore, during a prolonged exposure to the sun the bone cortex can become white to greyish-white (Figure 22).

Some of these attributes were observed in the material studied; however, they were only minimally visible on the Neandertal remains. Among the hominid bones, only the left hemimandible Scla 4A-9 has cortex cracking comparable to weathering stage 1 (BEHRENSMEYER, 1978), which includes longitudinal cracking parallel to the fibrous bone structure, accompanied by thin transversal cracking. Scla 4A-1 and Scla 4A-2 exhibit very light superficial cracking that is between stages 0 and 1 of BEHRENSMEYER (1978). Nearly all the faunal remains of Scladina are also between these two stages of weathering. This attribute is not useful for this study and is not included in Table 1.

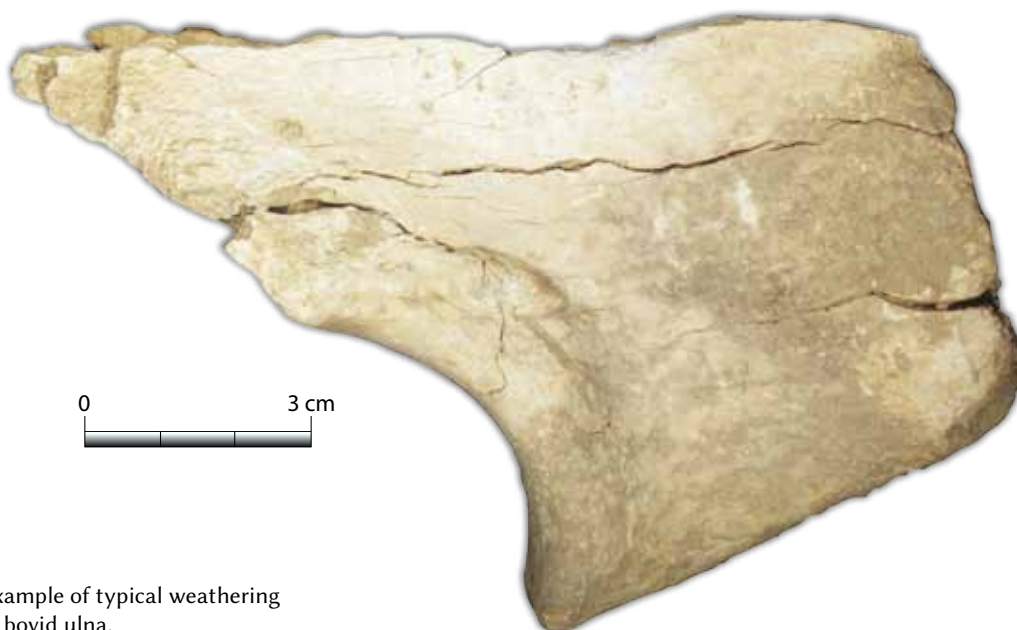


Figure 22: An example of typical weathering marks on a large bovid ulna.



Furthermore, the fossils Scla 4A-1 and Scla 4A-2 both have very highly lustrous surfaces. This is a very rare trait for bones used in this study and is only visible on 3 bones (0.5%). This characteristic can be the result of chemical processes as well as physical processes, such as run-off. A highly lustrous surface is often accompanied with slightly dulled fractured edges (LENOBLE, 2005: 106) and this characteristic is also exhibited on these 2 Neandertal remains. Unfortunately, these 2 fossils were traditionally cast which possibly artificially changed the lustre of the objects.

3.3.5. Manganese deposits

The origin of the manganese in the sediment must be assessed carefully and may possibly result from the percolation of rainwater through the limestone; from the deterioration of organic material in the sediment; and from bacterial or fungal activity, the intensity of which is dependant on the hygro-thermic conditions as well as pH (MARÍN ARROYO et al., 2008). The precipitation of manganese on objects must be used with care in the determination of the homogeneity of the collection. In some layers, large spots of manganese covering the faunal material from sedimentary units 6A, 5, and 4B constitute a viable taphonomic characteristic of the bones from those units. However, the Neandertal remains do not exhibit this trait.

On the contrary, in Layer 4A-KG, manganese variably affects bones. This variable effect is directly linked with the unit's relationship to Speleothem CC4. Often, the remains directly beneath CC4 do not have any trace of manganese while those not protected by the speleothem are affected by manganese. The 91 bones and fragments from 4A-KG of this study do not show any manganese (1%) or exhibit regular spots (84%), large spots (13%), or are sometimes completely covered (2%). This observation allows for the interpretation that the precipitation of manganese occurred after the formation of the speleothem.

The hemimandible Scla 4A-9 has regular spots of manganese (Figures 6 & 20). Through the stratigraphic sequence, bones that exhibit the same trait are very rare or absent in the 8 layers of units 6A and 5. However, the regular spots are frequently found on the faunal remains from units 4A-CHE and 4A-POC. The largest number are found in Layer 4A-KG (Table 1; 84%), which authorises a strong comparison to Scla 4A-9. The spots were determined to be manganese by SEM (scanning electron microscopy), coupled to EDS (Energy-dispersive X-ray Spectroscopy) which was done (by Christian Burlet, Geological Survey of Belgium, Royal Belgian Institute of Natural Sciences) on the 2nd phalanx of *Ursus spelaeus* (Sc 1996-26-12; Figure 20-d) from Unit 4A-CHE.

The fossils Scla 4A-1 and Scla 4A-2 have tiny dark grey spots (Figure 23) that could correspond to the remnants of precipitated manganese. This attribute is strongly associated with the highly lustrous cortical surfaces commented on previously. That peculiar combination is extremely rare and is evident on only 3 faunal remains from units 4A-CHE and 4A-POC (Sc 2004-678-1, Figure 19-h; Sc 2007-668-2, Figure 19-e; Sc 2006-341-1, Figure 19-i).

3.3.6. Carbonate deposits

Although the deposition of carbonates on bone is very rare among the studied faunal remains (15 out of 597 pieces, or 2.5%), their presence is very stratigraphically significant. Only layers that are superimposed by a stalagmitic floor (e.g. 4A-KG, 4A-OR, both covered by Speleothem CC4) and layers that reworked them (e.g. layers within units 4A-CHE and 4A-POC) have yielded some remains that are partially covered by carbonates. This observation, however, has little statistical value and, because there are no carbonate deposits on the Neandertal remains, is not useful for this study.

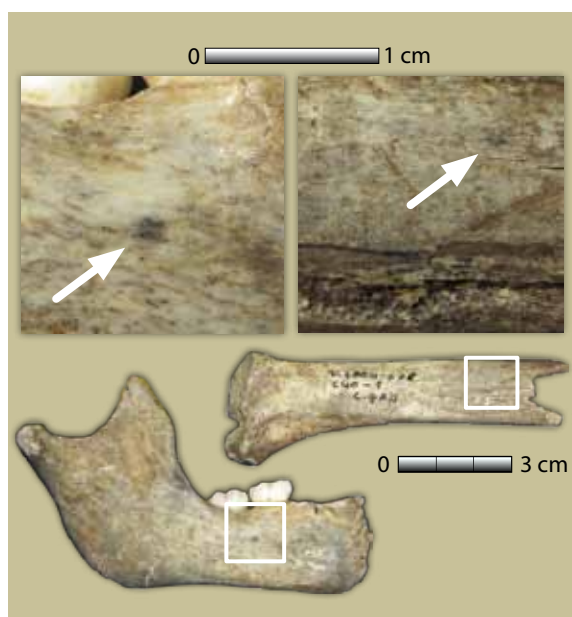


Figure 23: The tiny light grey spots on Scla 4A-1 (left) compared with the *Ursus spelaeus* proximal radius fragment Sc 2004-678-1 (right).

3.4. Comparative study between the isolated teeth of the Neandertal child and *Ursus* from Sedimentary Complex 4A

Fifteen isolated teeth from the Neandertal child have a crown with light grey enamel as well as a white-yellow root. This colour combination, corresponding to the original colour of a tooth in vivo, characterizes 30.6% (92 out of 300) of the bear teeth from Sedimentary Complex 4A. However, this combination is nearly absent from the teeth collected from Unit 5.

Within Complex 4A, a second study on the same 300 *Ursus spelaeus* incisors was conducted to determine if the unique colour combination was typical of a specific sedimentary unit or units. Of the sample, 52 teeth were excavated through

microstratigraphy and 248 were attributed to units 4A-AP, 4A-CHE, or 4A-POC.

The results of the study of the bear teeth indicate that 66.3% of the teeth with this colour combination originate from Unit 4A-POC (61 out of 92 pieces), 16.3% from Unit 4A-CHE (15 out of 92 pieces), and 17.4% from Unit 4A-AP (16 out of 92 pieces). The fact that most of the teeth with the same characteristics as the Neandertal child teeth came from 4A-POC is demonstrated by the comparison of the inferior Neandertal incisor Scla 4A-19 to 26 *Ursus spelaeus* teeth that were excavated from the same square (D34) and Unit 4A-POC (Figure 24).

This step of the analysis attributes the isolated teeth of the Neandertal child to Unit 4A-POC; however, this suggestion must be considered with prudence.



Figure 24: In Unit 4A-POC, Square D34, the 26 *Ursus spelaeus* teeth and fragments of teeth show the same stage of abrasion and the original colour as the permanent mandibular left central incisor Scla 4A-19 (center) of the child.



3.5. Synthesis

The state of preservation of the Neandertal fossils is exceptional and only a small number of similarities are found among the faunal remains from the sedimentary units analysed in this study. However, this comparative taphonomic analysis provides evidence for 7 main taphonomic characteristics (Table 2):

- 1 the greyish-green and orange colours of the Neandertal mandibular fragments have been observed on 9 remains from layers 5-GRO and 5-GBLA (Unit 5), Layer 4B-UN (Unit 4B), Layer 4A-KG (Unit 4A-AP), Layer 4A-OR (Unit 4A-IP), Layer 4A-GBL (Unit 4A-POC), as well as from layers of Unit 4A-CHE;
- 2 the small degree of abrasion observed on the hominid remains is primarily present on the fauna from layers 6A-YLO and 6A-YUP (Unit 6A), Layer 4B-UN (Unit 4B), Layer 4A-KG (Unit 4A-AP), as well as from Unit 4A-CHE;
- 3 the highly lustrous surface is only present on 3 remains from Layer 4A-GBL (Unit 4A-POC) as well as Unit 4A-CHE;
- 4 the manganese spots typical of Scla 4A-9 are present on the fauna from Layer 4A-KG (Unit 4A-AP), Layer 4A-OR (Unit 4A-IP), layers 4A-BO, 4A-LEG and 4A-GBL (Unit 4A-POC), as well as the layers from Unit 4A-CHE;
- 5 the tiny dark grey remnants of spots are present only on 3 remains from Layer 4A-GBL (Unit 4A-POC) as well as those from Unit 4A-CHE;

- 6 the large spots of manganese are frequent on remains from the units 6A, 5, and 4B, and the Neandertal does not exhibit these;
- 7 the original colour recorded on the enamel and roots of the teeth are mainly present in the layers of the Unit 4A-POC.

Finally, when integrating all the taphonomic characteristics, the faunal remains from the units within the Complex 4A share the most similarities with the Neandertal remains (Table 2). Beyond this, when all of the physical taphonomic attributes are combined, sedimentary units 4A-CHE and 4A-POC have yielded most of the bones and teeth that have the strongest correlation to the Neandertal child. This correlation is in harmony with a stratigraphic analysis (see Chapter 5) that attributed, when possible, some of the bone fragments to the Unit 4A-CHE and some of the isolated teeth to Unit 4A-POC. Among the layers that were deposited before the gully, the objects from Layer 4A-KG have the most taphonomic similarities to the Neandertal child.

Discussion: how to interpret the presence of the Scladina

4. Neandertal remains

4.1. Highly preserved hominid remains

The cause of death of the Scladina Child is still unknown. No antemortem or perimortem traces, such as pathological stigma, wounds due to human actions, or carnivore predation are present on the remains.

Some observable postmortem traces are present on the fossils. The cortices of the three

Stratigraphic distribution of the taphonomic criteria observed on faunal remains		Layers cross-cut by the gully												Gully	Superimposing		
		6A-			5-						4B-		4A-AP		4A-CHE	4A-POC	
Bone		YLO	GRV	YUP	GJAC	GBG	GRO	GBLA	GKBR	LI	UN	KG	OR	CHE	BO	LEG	GBL
Colour	greyish-green																
	orange																
Abrasion	low																
Lustre	high																
Manganese	very few spots																
	regular spots																
Isolated teeth																	
Colour	original																

Table 2: Synthesis of the stratigraphic distribution of faunal remains that exhibit the same taphonomic properties as the Neandertal child remains (grey backgrounds). Note that the majority are from Sedimentary Complex 4A (4A-POC and 4A-CHE; black borders).

osseous elements of the child exhibit thin cracks that are the first effects of weathering. Only the left hemimandible Scla 4A-9 has sufficient cracking to be attributed to stage 1 of BEHRENSMEYER (1978). Weathering can equally affect objects in direct contact with the atmosphere as well as those shallowly buried. However, the remains of the Neandertal child do not exhibit evidence of long exposure to the sun, as they have not been bleached white. If the bones experienced any exposure to the atmosphere, that exposure was necessarily short and may have occurred within the protective environment of the cave.

The break under the alveolus of the right inferior canine, which has separated the two hemimandibles, is a 'green bone' fracture (Figure 11). The presence of a small area of peeling on Scla 4A-9, on the inner side of the break between the two parts of the mandible, is an additional indicator that the breakage occurred on wet or fresh bone (stage 1 of KROVITZ & SHIPMAN, 2007), so probably not long after death.

The only possible cut mark observed on Scla 4A-1 is questionable because the position of the mark is quite unusual. Removing the tongue should have created other marks, which are not present. This mark is very close to trampling marks (BEHRENSMEYER et al., 1986; DOMÍNGUEZ-RODRIGO et al., 2009), which could have been made during the reworking of the right hemimandible by sedimentary processes.

4.2. No fossil in primary spatial position

The mode of the first incorporation of the child in the sediments is currently unknown. The fossils are not in primary spatial position. Since the child died, most teeth were lost postmortem, possibly when the bones were on the surface. The spatial distribution of the remains as well as post-depositional rounding of the right condyle and the absence of the left ramus are all indications of displacement after deposition.

The study of the stratigraphic data that are available for the osseous Neandertal remains further suggests their attribution to the gully of Unit 4A-CHE. The sediment that filled the gully most likely originated from the terrace and the entrance to the cave. The presence of numerous calcite fragments throughout the sediment of the gully is explained by the dismantling of Speleothem CC4 during the event that formed the gully. Therefore, the depositional dynamics had to be high energy enough to destroy the

stalagmitic floor, unavoidably affecting the sediment and objects in its path. The reworking and incorporation of the formerly deposited sediment of at least units 6A, 5, 4B, 4A-AP, and 4A-IP provide an explanation for the taphonomic heterogeneity of 4A-CHE.

At the time the child was deposited, at least 20 m separated the entrance (estimated to have been at metre 5) from the location at which the closest fossil was found (metre 26). The spatial distribution of the child's remains does not reflect one reworking event but several successive events of varying intensities. The absence of hominid remains in the first 25 m from the edge of the terrace is possibly explained by an important erosional event, resulting in the 4A-CHE gully, that reworked the layer within or on which the child was deposited. A unique, high-energy erosional event across a large surface does not seem to be a likely candidate for explaining the stratigraphic distribution of the remains into 2 distinct sedimentary units (4A-CHE and 4A-POC) and their spatial distribution into the 3 separate areas of concentration. Furthermore, a powerful erosional event over the long distance of 25 m would unavoidably damage material within it; however, the Neandertal remains are well preserved. The isolated teeth are nearly unaltered, the 2 hemimandibles can be almost perfectly refitted, and on both the hemimandible and the maxilla the main evidence of erosion is only on the alveolar margins. This observation suggests the remains were successively reworked a small distance from their original location by low energy processes. The economical hypothesis is the Neandertal remains were reworked several times from a zone at the entrance of the cave (between the porch and metre 25) and were then buried relatively quickly deeper into the cave.

4.3. The taphonomic message

The taphonomic study of the Neandertal child's remains and their comparison to faunal remains provided information as to whether the hominid fossils were deposited before (e.g. in units 6A, 5, 4B, 4A-AP or 4A-IP) or contemporaneously with the gully.

No evidence permits the attestation of the presence of the fossils in the cave before the event(s) that created the gully.

The taphonomic incompatibility of the fossils with sedimentary units 6A, 5, and 4B is clear when large spots of manganese are observed in high frequency on the objects. This argument is



based on the hypothesis that this type of deposit cannot be easily removed.

The differential alteration between the 2 hemimandibles seems to refute Layer 4A-KG as the origin of the objects even though the bone colour and the peculiar deposition of regular spots of manganese are similar between objects from this layer and Scla 4A-9. In fact, Layer 4A-KG and its numerous fossils were protected for several thousands of years by Speleothem CC4, as the thickness of CC4 often reaches 30 cm and can support stalagmites up to 1 m high. The resulting lengthy interment of bones within Layer 4A-KG should have resulted in an intense and uniform alteration of all the osseous elements of the Neandertal child, as has been observed for nearly all the cave bear remains exhumed from it.

The differential alteration of the 2 hemimandibles seems to be a consequence of their interment in different sediments from the beginning of the process and for a long period of time afterward. After this process is complete, a total and radical change of colour is difficult to imagine; the current understanding is only fracturing, surface alteration, and abrasion of edges can be superimposed over the background colour. That hypothesis is based on the concept that the colour exhibited by the fossil and its manganese staining, initially acquired in its primary sedimentary context, are not easily removed, which is reinforced by all the observations made on all the bones throughout the stratigraphy of Scladina since 2005.

According to the evidence provided above, the Neandertal remains were not yet fossilized when they were distributed into the different sedimentary contexts from which they were collected. This scenario would relatively date the fossils to approximately contemporaneous with the event that created the gully.

4.4. The sequence of events

The taphonomic observations do not provide a complete explanation as to why the Neandertal remains were discovered in Scladina. Beyond the fact the objects themselves were not anthropogenically altered, the reworked sedimentary environment in which the fossils were found has erased any potential evidence of anthropogenic structures (e.g. those caused by ritual activity, burials, etc.). However, the fresh state of preservation of the remains when they entered the cave, their spatial and stratigraphic distribution, and their differential alteration all authorize the

proposition of a sequence of events. The proposition is the partial or complete body of the child entered the cave when the bones were not yet fossilized. Sedimentary processes linked to the gully most likely caused the separation of the 2 hemimandibles, as the causal fracture exhibits the characteristic peeling of green bones. The low degree of weathering augments this hypothesis; the remains did not have a long direct exposure to the atmosphere nor were they shallowly buried for a long period of time. No proof that the gully-creating mechanisms were what brought the maxilla and mandible into the cave has been discovered; however, the processes that created the gully are known to be responsible for the initial reworking of the bones, likely for fracturing them, and for their dispersal into different layers within Unit 4A-CHE and in superimposing layers in Unit 4A-POC. The child's remains were distributed in several different sedimentary layers that have differentially altered the bones. A proposed succession of events follows.

Stage 0: Layer 4A-KG was deposited. During its deposition, numerous cave bear remains were incorporated in the sediment. They were altered throughout the formation of Speleothem CC4 (directly superimposing 4A-KG) and in the process their colour changed. Evidence for their alteration at this time was provided by the taphonomic study of the remains from the gully (4A-CHE); in fact, numerous bones exhibiting the characteristic colour of remains from 4A-KG were found in Unit 4A-CHE, suggesting that 4A-KG was heavily reworked by the processes that formed the gully.

As of now, according to what has been observed, both stratigraphy and taphonomy do not suggest that the Neandertal remains were present in the cave at that stage.

After the formation of Speleothem CC4, a cryosol developed that is evidence of a phase of deep-freezing, and affected the sediment below the speleothem, including 4A-OR, 4A-KG, and up to the summit of 4B-LI (see Chapter 3).

Stage 1: The processes of the gully caused an important erosional event that included the partial destruction of Speleothem CC4. This event was probably linked to the degradation of the cryosol. This erosional event was followed by phases of erosion and/or sedimentation producing the several layers that constitute Unit 4A-CHE. These layers appear to be responsible

for the reworking of the Neandertal remains in the cave. The fossils are well preserved (e.g. there is low abrasion on the fractured edges of the bones) which demonstrates that some of the phases of erosion and/or sedimentation were low energy, although some must have been high energy in order to have fragmented some of Speleothem CC4. The fact that excavation has yet to yield any postcranial elements of the child does not preclude their presence within the cave.

The processes that formed the gully probably broke the mandible while it was still fresh (hence the green bone fracture and peeling). At this time, the possibility exists that the teeth were already disarticulated from both the mandible and the maxilla. Regardless, the cranium and mandible were not on the surface for a long period of time (limited effects of weathering and no evidence of necrophagy). This disarticulation logically occurred in the first 25 metres of the cave, due to the gully's course (see Chapters 3 & 5).

Some erosion/sedimentation phases of the gully (Unit 4A-CHE) could have successively reworked the bone fragments and some isolated teeth:

- a phase of sedimentation transported and deposited hemimandible Scla 4A-1 in Square D29 in one of the 4A-GX lithofacies and maybe also the fragment of maxilla Scla 4A-2 in Square D30;
- a similar process could have deposited the hemimandible Scla 4A-9 in one of the 4A-JA lithofacies, but its stratigraphic context is less secure (see Chapter 5).

Stage 2: After 4A-CHE was deposited, the layers of Unit 4A-POC covered it. Where 4A-CHE is not present 4A-POC directly superimposed Speleothem CC4. Some isolated teeth were reworked from 4A-CHE into 4A-POC:

- a depositional event that is attributable to Layer 4A-BO transported and deposited the tooth Scla 4A-4 (and maybe also Scla 4A-3) in Square C30;
- another event, probably related to 4A-POC (see Chapter 5), transported and deposited 10 teeth in squares F26, F27, G27, and H27, closer to the cave entrance than the bones;
- one or several events distributed 4 teeth in squares C32, D34, E38, further in the cave and in a zone between F35 and F37; one tooth was related to Layer 4A-LEG (E38,

see Chapter 5), the others were probably from 4A-POC.

Except for the sedimentation phase that deposited Layer 4A-BO, which is the first in the sequence of Unit 4A-POC, the establishment of a chronological order for the several phases of reworking (stated above) that redistributed the 16 isolated teeth is nearly impossible.

The taphonomic study does not allow for the temporal evaluation of the separation between the reworking phenomena of the gully (Unit 4A-CHE; stage 1) and those of 4A-POC (stage 2). No variability of preservation is observed between the molars still articulated with hemimandible Scla 4A-1 (deposited in the gully; stage 1) and the 15 isolated teeth (mostly attributed to Unit 4A-POC; stage 2). Even though some information suggests that these objects remained in their respective sedimentary contexts for at least 85,000 years (see Chapter 5), all of these 15 teeth have maintained their original colour.

Stage 3: From this time, the fossils that were deposited within at least 4 different sedimentary environments (2 different layers of 4A-CHE and at least 2 layers of 4A-POC) were affected by differential alteration and generated the taphonomic variability recorded in this study.

The different sedimentation phases of 4A-CHE seem to have incorporated a large quantity of remains (mainly *Ursus spelaeus*) by the erosion of previously deposited layers. So those bones, already fossilized at the time of their reworking, exhibited their specific taphonomic signature. The best example of this is the taphonomic variability of the fauna inside the gully. On the contrary, the 2 Neandertal hemimandibles, which exhibit 2 different taphonomic signatures, appear to not have been fossilized at the time that they were reworked, suggesting their possible contemporaneity to the deposition of 4A-CHE. After the breakage and reworking of the mandible, and deposition of the various elements in different sediments, the still fresh bone fragments obtained the typical taphonomic signatures of their respective sedimentary contexts.

Based on this proposed scenario, the age of the Neandertal remains is the same as the gully (4A-CHE), which was deposited during the Weichselian Early Glacial and most likely during the second part (see Chapter 5).



5. Conclusions

Although detailed taphonomic descriptions of hominid remains are frequent in the palaeoanthropological literature, few, if any, are compared to stratigraphically contemporaneous fauna. This comparison is only possible if all of the remains are precisely excavated by stratigraphy at the scale of individual sedimentary layers, rather than just the sedimentary unit or complex. This type of study was possible at Scladina because the excavation has been conducted with rigorous stratigraphic control for approximately the last decade. Since then, 1,500 faunal remains have been exhumed, some of which have provided interesting comparisons to the hominid remains. The observation of the taphonomic attributes that are associated to sedimentary dynamics has allowed for the construction of several stages of a complicated depositional history of the Neandertal child, from the first reworking of the hominid remains in the cave until their discovery by archaeologists.

Only a small part of the maxilla has been found so far. This fossil, however, articulates perfectly with the right hemimandible. As no traces of carnivore damage were present on the fossils to support the idea that only the mandible with a small part of the cranium was brought into the cave, the suggestion that at least the entire skull, if not the whole individual, was present seems reasonable. This infers that the possibility still exists for other stimulating palaeoanthropological discoveries to be made at Scladina.

Since the hominid remains were discovered on both sides of the transversal berm B-H 31 (Figure 2) that separates the excavation zones, the presence of other cranial elements or dentition in the berm, which was left for stratigraphic reference, remains a possibility. However, leaving this berm of sediment unexcavated is strategic because the profiles provided by the berm are the only ones still present that document the dimensions of the gully (4A-CHE) in which the Neandertal remains were found. Without these sections, the depositional dynamics of this structure could not be as well understood.

However, stratigraphic analysis allowed the tracking of the gully and the retention of information about where the gully and the layers of Unit 4A-POC are still present in the cave. The gully is divided into two branches, separated by Speleothem CC4 (see Chapter 5, Figure 9). According to the studied sections, the area where the gully was most erosive is localized around

Section 30/31 between G and H, where the gully contacts Unit 6A. This northern branch of the gully has not yet been fully excavated beyond metre 30, and has only been reached on the longitudinal Section F/G 32 to 34 (Figure 2), where the erosion of previously deposited sediment and the frequency of reworked stalagmite fragments are high. The southern branch of the gully appears less erosive on sections 30/31 and 32/31 in B-C-D. Deeper in the cave the erosive capability of this left branch of the gully on previously deposited layers decreases (e.g. transversal Profile 41/42 between C and E). This decrease is also exhibited on Section 43/44 between C and E.

All in all, if any other hominid remains are yet to be unearthed, they will most likely be found in the unexcavated zone towards the northern part of the cave (currently located beyond the longitudinal profiles E/F 38 and F/G from 32 to 37) in sedimentary units 4A-CHE, 4A-POC, and 3-INF (see Chapter 5).

6. Annexes

The bones and teeth of the Scladina Child were sampled for different analyses, sometimes several times (see Chapters 8, 17 & 19). The alterations caused by these analyses are now part of the general conservation state of these fossils. The following list denotes the impacts of these alterations.

6.1. Moulding

Most of the fossils were moulded using silicon rubber by Michel Toussaint:

- Scla 4A-1, right hemimandible, 1993;
- Scla 4A-2, maxilla, 1994;
- all isolated teeth except Scla 4A-20.

Because of its fragility, the left part of the mandible (Scla 4A-9) was not moulded using the classic rubber technique but by creating a replica from micro-CT data.

6.2. Palaeodiet (C/N)

The right partial maxilla (Scla 4A-2) was sampled in 1996 by Hervé Bocherens, at Paris Jussieu (see Chapter 17).

6.3. DNA

The superior right M¹ (Scla 4A-4) had its buccal roots destroyed during sampling for DNA analysis

in Munich by Svante Pääbo, in 1993. The test was not successful.

In 2001, a sample was taken from the root and the pulpar chamber of Scla 4A-13, the deciduous inferior right M₂, for mitochondrial DNA analysis (see Chapter 19).

In 2007, Johannes Krause, Ludovic Orlando (visitor), and Svante Pääbo at the Max Planck Institute in Leipzig attempted to get a sample for nuclear DNA using the interior of the superior right M¹ (Scla 4A-4) after it was cut for histological analysis (see 6.4). This attempt was not successful.

6.4. Histology

A histological thin section of the superior right M¹ (Scla 4A-4) was prepared in 2006 by Tanya Smith at the Max Planck Institute for Evolutionary Anthropology (Leipzig, Germany) to estimate the biological age of the Scladina Child. The tooth was sectioned with an annular saw and then embedded in methylmethacrylate resin. The tooth was then restored; less than 1.5 mm of the specimen's mesial-distal thickness is missing. In 2007, two other teeth (Scla 4A-6 and Scla 4A-11) were brought to the European Synchrotron Radiation Facility (ESRF) in Grenoble (France), in order to confirm results on the long-period lines periodicity obtained from the physical section of the molar. This technique facilitates non-destructive analysis of the dental microstructure loss (see details in Chapter 8).

6.5. Strontium

Sampling for strontium analysis is limited to a vertical, millimetre scale groove on the crown and one similar groove on the root of the selected teeth. These grooves are nearly invisible to the naked eye. Fourteen teeth have been affected by this procedure: Scla 4A-3, 4, 5, 6, 7, 8, 11, 12, 13, 14, 16, 18, 19, and 20. The sampling was done at the Max Planck Institute for Evolutionary Anthropology, Leipzig (Germany), under the control of Mike Richards and Christine Verna.

Acknowledgements

The authors would like to express their deepest gratitude to Joël Éloy, Association d'Études mégalithiques (AWEM) for the photographs of the Neandertal remains.

References

- ANDREWS P. & FERNÁNDEZ JALVO Y., 1997. Surface modifications of the Sima de los Huesos fossil humans. *Journal of Human Evolution*, 33: 191-217.
- BEAUVAL C., MAUREILLE B., LACRAMPE-CUYAUBÈRE F., SERRE D., PERESSINOTTO D., BORDES J.-G., COCHARD D., COUCHOUD I., DUBRASQUET D., LAROULANDIE V., LENOBLE A., MALLYE J.-B., PASTY S., PRIMAULT J., ROHLAND N., PÄÄBO S. & TRINKAUS E., 2005. A late Neandertal femur from Les Rochers-de-Villeneuve, France. *Proceedings of the National Academy of Sciences of the United States of America*, 102, 20: 7085-7090.
- BEHRENSMEYER A. K., 1978. Taphonomic and ecologic information from bone weathering. *Paleobiology*, 4, 2: 150-162.
- BEHRENSMEYER A. K., GORDON K. D. & YANAGI G. T., 1986. Trampling as a cause of bone surface damage and pseudo-cutmarks. *Nature*, 319: 768-771.
- BEHRENSMEYER A. K. & HILL A. P., 1980. *Fossils in the making. Vertebrate taphonomy and Paleocology*, University of Chicago Press, Prehistoric Archeology and Ecology Series, 345 p.
- BEHRENSMEYER A. K. & KIDWELL S. M., 1985. Taphonomy's contributions to paleobiology. *Paleobiology*, 11: 105-119.
- BEHRENSMEYER A. K., KIDWELL S. M. & GASTALDO R. A., 2000. Taphonomy and paleobiology. *Paleobiology*, 26, 4: 103-147.
- BINFORD L. R., 1981. *Bones. Ancient men and modern myths*. Orlando, Academic Press, 320 p.
- BLUMENSCHINE R. J., 1986. *Early Hominid Scavenging Opportunities: Implications of Carcass Availability in the Serengeti and Ngorongoro Ecosystems*. Oxford, British Archaeological Reports, International Series, 283: 163 p.
- BONJEAN D., ABRAMS G., DI MODICA K. & OTTE M., 2009. La microstratigraphie, une clé de lecture des remaniements sédimentaires successifs. Le cas de l'industrie moustérienne 1A de Scladina. *Notae Praehistoricae*, 29: 139-147.
- BONJEAN D., TOUSSAINT M. & OTTE M., 1997. Grotte Scladina (Sclayn, Belgique): bilan des découvertes néandertaliennes et analyse du contexte. In J. PLUMIER (dir.), *Actes de la cinquième Journée d'Archéologie Namuroise*, Namur, Facultés universitaires Notre-Dame de la Paix, 22 février 1997,



Ministère de la Région wallonne, Direction générale de l'Aménagement du Territoire, du Logement et du Patrimoine, Direction de Namur, Service des Fouilles: 19-27.

BOULESTIN B., 1999. *Approche taphonomique des restes humains. Le cas des Mésolithiques de la grotte des Perrats et le problème du cannibalisme en préhistoire récente européenne*. Oxford, British Archaeological Reports, International Series, 776, 276 p., 4 tables, 65 figures, 50 plates.

BRAIN C. K., 1981. *The Hunters or the Hunted? An Introduction to African Cave Taphonomy*. The University of Chicago Press, Chicago & London, 365 p.

CRAIG C. R., KNÜSEL C. J. & CARR G. C., 2005. Fragmentation, mutilation and dismemberment: an interpretation of human remains on Iron Age Sites. In M. K. PEARSON & I. J. N. THORPE (eds.), *Warfare, Violence and Slavery in Prehistory*, Oxford, British Archaeological Reports, International Series, 1374: 165-180.

DART R. A., 1957. *The Osteodontokeratic Culture of Australopithecus Prometheus*. Pretoria, Transvaal Museum. Memoir N° 10, 105 p.

DEBLAERE C. & GULLENTOPS F., 1986. *Lithostratigraphie de la grotte Scladina*. Bulletin de l'Association française pour l'étude du Quaternaire, 2^e série, 25-26: 178-181.

DEFLEUR A., WHITE T., VALENSI P., SLIMAK L. & CRÉGUT-BONNOURE E., 1999. Neanderthal Cannibalism at Moula-Guercy, Ardèche, France. *Science*, 286, 5437: 128-131.

DELAUNOIS É., 2010. *L'altération différentielle des vestiges en archéologie paléolithique. Contribution à l'établissement d'une clé de contrôle stratigraphique et d'homogénéité des collections. L'exemple des couches 4A de Scladina (Namur, Belgique)*. Unpublished master thesis. Université de Liège, 2 vol., 95 & 110 p.

DELAUNOIS É., ABRAMS G., BONJEAN D., DI MODICA K. & PIRSON S., 2012. Altération différentielle des ossements de l'ensemble sédimentaire 4A de la grotte Scladina (Andenne, Belgique). *Notae Praehistoricae*, 32: 5-18.

DENYS C., 2002. Taphonomy and experimentation. *Archaeometry*, 44: 469-484.

DOMÍNGUEZ-RODRIGO M., DE JUANA S., GALÁN A. B. & RODRÍGUEZ M., 2009. A new protocol to differentiate trampling marks from butchery cut marks. *Journal of Archaeological Science*, 36: 2643-2654.

EFREMOV I. A., 1940. Taphonomy: new branch of paleontology. *Pan-American Geologist*, 74: 81-93.

FRAYER D. W., ORSCHIEDT J., COOK J., RUSSELL M.D. & RADOVČIĆ J., 2006. Krapina 3: Cut Marks and Ritual Behavior. *Periodicum Biologorum*, 108, 4: 519-524.

GRUPE G., 2007. Taphonomy and Diagenetic Processes. In W. HENKE & I. TATTERSALL (eds), *Handbook of Paleoanthropology, vol. I, Principles, methods and Approaches*, Berlin Heidelberg New-York, Springer-Verlag: 241-259.

GUADELLI J.-L., 2008. La gélifraction des restes fauniques. Expérimentation et transfert au fossile. *Annales de Paléontologie*, 94: 121-165.

GUADELLI J.-L. & OZOUF J.-C., 1994. Études expérimentales de l'action du gel sur les restes fauniques. Premiers résultats. In M. PATOU-MATHIS (ed.), *Outillage peu élaboré en os et en bois de Cervidés IV: taphonomie/bone modification*. Artefacts, 9: 47-56.

GULLENTOPS F. & DEBLAERE C., 1992. Érosion et remplissage de la grotte Scladina. In OTTE M. (ed.), *Recherches aux grottes de Sclayn, vol. 1: Le Contexte*. Études et Recherches Archéologiques de l'Université de Liège, 27: 9-31.

HAESAERTS P., 1992. Les dépôts pléistocènes de la terrasse de la grotte Scladina à Sclayn (province de Namur, Belgique). In OTTE M. (ed.), *Recherches aux grottes de Sclayn, vol. 1: Le Contexte*. Études et Recherches Archéologiques de l'Université de Liège, 27: 33-55.

HAGLUND W. D., 1992. Contributions of Rodents to Postmortem Artifacts of Bone and Soft Tissue. *Journal of Forensic Sciences*, 37, 6: 1459-1465.

HAGLUND W. D., 1997. Rodents and Human Remains. In W. D. HAGLUND, M. H. SORG (dir.), *Forensic Taphonomy. The Postmortem Fate of Human Remains*. Boca Raton (Florida): CRC Press: 405-414.

HILL C. A., 1982. Origin of black deposits in caves. *National Speleological Society Bulletin*, 44: 15-19.

KNÜSEL C. J., 2005. The physical evidence of warfare-subtle stigma? In M. K. PEARSON & I. J. N. THORPE (eds.), *Warfare, Violence and Slavery in Prehistory*, Oxford, British Archaeological Reports, International Series, 1374: 49-65.

KROVITZ G. E. & SHIPMAN P., 2007. Taphonomy of Immature Hominid Skulls and the Taung, Mojokerto, and Herto Specimens. In

- T. R. PICKERING, K. SCICK & N. TOTH (eds.), *Breathing Life into Fossils: Taphonomic Studies in Honor of C. K. (Bob) Brain*. Gosport, Stone Age Institute Press, 2: 207–232.
- LE MORT F., 1988. Le décharnement du cadavre chez les Néandertaliens: quelques exemples. In O. BAR-YOSEF (ed.), *L'Homme de Néandertal, vol. 5. La Pensée. Études et Recherches Archéologiques de l'Université de Liège*, 32: 43–55.
- LE MORT F., 1989. Traces de décharnement sur les ossements néandertaliens de Combe-Grenal (Dordogne). *Bulletin de la Société Préhistorique Française*, 86, 3: 79–87.
- LENOBLE A., 2005. *Ruissellement et formation des sites préhistoriques: référentiel actualistes et exemples d'application au fossile*, Oxford, British Archaeological Reports, International Series, 1363, 222 p.
- LÓPEZ-GONZÁLEZ F., GRANDAL-D'ANGLADE A. & VIDAL-ROMANI J. R., 2006. Deciphering bone depositional sequences in caves through the study of manganese coatings. *Journal of Archaeological Sciences*, 33: 707–717.
- LYMAN L. R., 2001. *Vertebrate taphonomy*. Cambridge manuals in archaeology, 524 p.
- MALLYE J.-B., COSTAMAGNO S., LAROULANDIE V. & BEAUVAL C., 2009. Impacts des processus périglaciaires sur la préservation des ossements. *Les Nouvelles de l'archéologie*, 118: 26–31.
- MARÍN ARROYO A. B., LANDETE RUIZ M. D., VIDAL BERNABEU G., SEVA ROMÁN R., GONZÁLEZ MORALES M. R. & STRAUS L. G., 2008. Archaeological implications of human-derived manganese coatings: a study of blackened bones in El Mirón Cave, Cantabrian Spain. *Journal of Archaeological Science*, 35: 801–813.
- MARTIN R. E., 1999. *Taphonomy. A process approach*. Cambridge University Press, 508 p.
- NOE-NYGAARD N., 1989. Man-made trace fossils on bones. *Human Evolution*, 4: 461–491.
- ORTNER D. J. & PUTSCHAR W. G., 1985. *Identification of Pathological Conditions in Human Skeletal Remains*. Smithsonian Contributions to Anthropology, 28, Washington, Smithsonian Institution Press, 488 p.
- PATOU-MATHIS M., 1997. Analyses taphonomiques et paléontologiques du matériel osseux de Krapina (Croatie): nouvelles données sur la faune et les restes humains. *Préhistoire Européenne*, 10: 63–90.
- PICKERING T., SCHICK K. & TOTH N. (eds.), 2007. *Breathing Life into Fossils: Taphonomic Studies in Honor of C. K. (Bob) Brain*. Gosport, Stone Age Institute Press, 2, 296 p.
- PIRSON S., 2007. *Contribution à l'étude des dépôts d'entrée de grotte en Belgique au Pléistocène supérieur. Stratigraphie, sédimentogenèse et paléoenvironnement*. Unpublished PhD thesis, University of Liège & Royal Belgian Institute of Natural Sciences, 2 vol., 435 p. & 5 annexes.
- PIRSON S., BONJEAN D., DI MODICA K. & TOUSSAINT M., 2005. Révision des couches 4 de la grotte Scladina (comm. d'Andenne, prov. de Namur) et implications pour les restes néandertaliens: premier bilan. *Notae Praehistoricae*, 25: 61–69.
- PIRSON S., COURT-PICON M., HAESAERTS P., BONJEAN D. & DAMBLON F., 2008. New data on geology, anthracology and palynology from the Scladina Cave pleistocene sequence: preliminary results. In F. DAMBLON, S. PIRSON & P. GERRIENNE (eds.), *Hautrage (Lower Cretaceous) and Sclayn (Upper Pleistocene). Field Trip Guidebook. Charcoal and microcharcoal: continental and marine records*. IVth International Meeting of Anthracology, Brussels, Royal Belgian Institute of Natural Sciences, 8–13 September 2008. Brussels, Royal Belgian Institute of Natural Sciences, Memoirs of the Geological Survey of Belgium, 55: 71–93.
- POTTER R. M. & ROSSMAN G. R., 1979. Mineralogy of manganese dendrites and coatings. *American Mineralogist*, 64: 26–30.
- ROGERS T., 2004. Recognizing inter-personal violence: a forensic perspective. In M. ROKSANDIC (ed.), *Violent Interactions in the Mesolithic*. Oxford, British Archaeological Reports, International Series, 1237: 9–21.
- SHIPMAN P., 1981. *Life History of a Fossil. An Introduction to Taphonomy and Paleoecology*. Cambridge, Harvard University Press, 221 p.
- TRINKAUS E., MAKI J. & ZILHÃO J., 2007. Middle Paleolithic Human Remains from the Gruta da Oliveira (Torres Novas), Portugal. *American Journal of Physical Anthropology*, 134: 263–273.
- ULLRICH H., 2005. Cut Marks and other Bone Modifications on Le Moustier 1 Remains. In H. ULLRICH (ed.), *The Neandertal Adolescent Le*



Moustier 1. New Aspects, New Results. Staatliche Museen zu Berlin — Preußischer Kulturbesitz, Berliner Beiträge zur Vor- und Frühgeschichte, Neue Folge, Band 12: 293–307.

ULLRICH H., 2006. Krapina — A Mortuary Practice Site with Cannibalistic Rites. *Periodicum Biologorum*, 108, 4: 503–517.

VILLA P. & MAHIEU E. 1991. Breakage Patterns of Human Long Bones. *Journal of Human Evolution*, 21, 1: 7–48.

WAKELY J., 1997. Identification and analysis of Violent and Non-violent Head Injuries in

Osteo-archaeological material. In J. CARMAN (ed.) *Material Harm, archaeological studies of war and violence*, Glasgow, Cruithne Press: 24–45.

WALKER P. L., 2001. A Bioarchaeological Perspective on the History of Violence. *Annual Review of Anthropology*, 30: 573–596.

WHITE T. D., 1992. *Prehistoric cannibalism at Mancos 5mTURM-2346*. New Jersey, Princeton University Press, 462 p.

WHITE T. D. & TOTTH N., 1989. Engis: Preparation Damage, not Ancient Cutmarks. *American Journal of Physical Anthropology*, 78: 361–367.

Chapter 8

DENTAL DEVELOPMENT IN AND AGE AT DEATH OF THE SCLADINA I-4A JUVENILE NEANDERTAL

Tanya M. SMITH, Donald J. REID, Anthony J. OLEJNICZAK, Paul T. TAFFOREAU, Jean-Jacques HUBLIN & Michel TOUSSAINT

Michel Toussaint & Dominique Bonjean (eds.), 2014. The Scladina I-4A Juvenile Neandertal (Andenne, Belgium), Palaeoanthropology and Context Études et Recherches Archéologiques de l'Université de Liège, 134: 155-166.

1. Introduction

1.1. Dental microstructure and age at death estimation

Dental development in humans and apes begins prior to birth and continues throughout adolescence. Like many biological systems, tooth formation is characterized by a circadian (daily) rhythm (reviewed in SMITH, 2006). Teeth grow in a layered fashion through the addition of incremental features (that may be understood by analogy with tree rings), as well as by the progressive activation of secretory cells (reviewed in BOYDE, 1989). Developmental rate

and time are permanently recorded by these incremental lines in the enamel and dentine, which remain unchanged for millions of years.

Enamel is secreted by cells known as ameloblasts, which differentiate at the enamel-dentine junction and migrate outward towards what becomes the surface of the crown. The tracks left by these individual cells are known as enamel prisms. The prisms show cross-striations that result from the circadian rhythm of enamel secretion (BROMAGE, 1991; SMITH, 2006). The successive positions of the advancing front of forming enamel are preserved as long-period incremental structures termed Retzius lines (Figure 1), which contact the enamel surface and form perikymata (Figure 2). Cross-striations and Retzius lines are also frequently referred to as short- and long-period structures due to their respective 24-hour and greater than 24-hour rhythms (6-12 days in hominins). An important relationship exists between these lines, as the long-period line periodicity (repeat interval or number of days between long-period lines), may only be determined by counting cross-striations between Retzius lines internally. This value is the same for all teeth in an individual's dentition, although it may vary among individuals (FITZGERALD, 1998).

Dentine is produced by cells known as odontoblasts that rhythmically produce daily incremental lines known as von Ebner's lines (equivalent to cross-striations), long-period structures known as Andresen lines (equivalent to Retzius lines), and periradicular bands (equivalent to perikymata; Figures 1 & 2; reviewed in DEAN, 1995 and SMITH, 2008). Counts and measurements of these

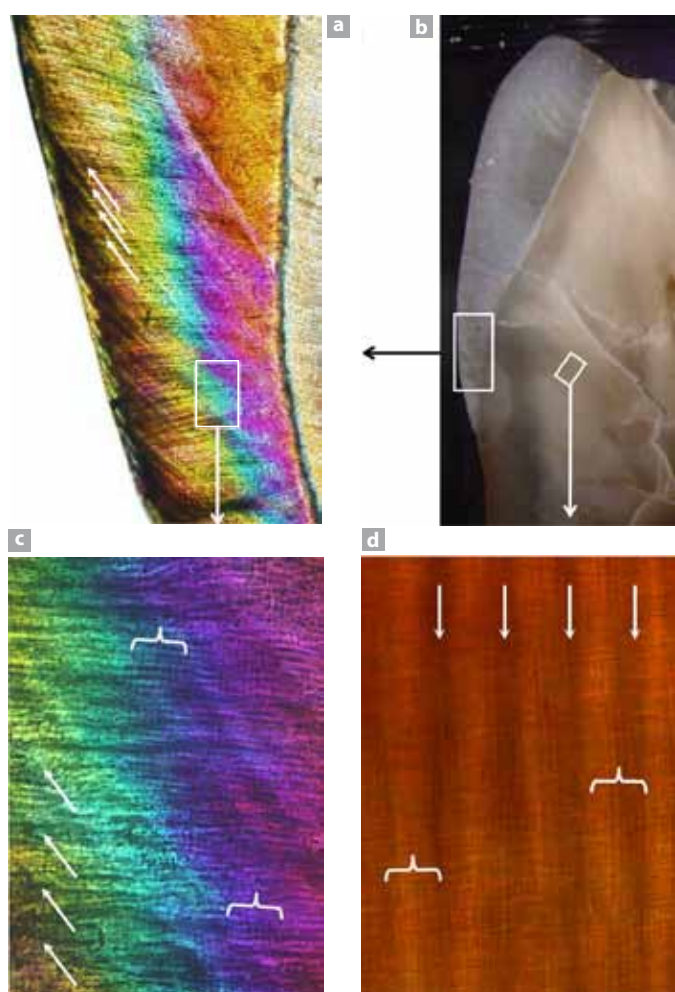


Figure 1: Incremental features found in enamel and dentine. a) Long-period Retzius lines in enamel (arrowed); b) overview of Scladina permanent maxillary right first molar (Scla 4A-4) showing the position of higher magnification images in a) and d); c) Retzius lines (arrowed) and short-period cross-striations in enamel (light and dark bands indicated by brackets); d) Long-period Andresen lines (arrowed) and short-period von Ebner's lines in dentine (light and dark bands indicated by brackets).



Figure 2: Long-period incremental growth lines (indicated by fine dotted lines) on the surface of the mandibular first premolar (Scla 4A-6). a) tooth crown: perikymata, and b) tooth root: periradicular bands.



short- and long-period lines provide information on the rate and duration of enamel and dentine secretion, which may be combined to accurately determine the total crown formation time, and the rate and duration of crown and root extension (e.g., SMITH et al., 2006^a). Furthermore, the age at death in developing dentitions may be precisely determined by identifying the birth line (neonatal line), and adding subsequent crown and root formation time to yield the age.

1.2. Tooth growth and age at death in fossil hominins

In the past few decades, several studies have used information from incremental features preserved in dental tissues to determine age at death, as well as to infer patterns of life history (development scheduling and the timing of reproductive events) in juvenile fossil hominins (e.g., BROMAGE & DEAN, 1985; DEAN et al., 1993, 2001; SMITH et al., 2007^{a,b}, 2010). Dental microstructure research on juvenile Neandertals has focused on individuals from Devil's Tower, Gibraltar (DEAN et al., 1986; STRINGER et al., 1990; STRINGER & DEAN, 1997; SMITH et al., 2010); Hortus, France (RAMIREZ ROZZI, 2005); Le Moustier, France (SMITH et al., 2010); Obi-Rakhmat Grotto, Uzbekistan (SMITH et al., 2010, 2011); Engis, Belgium (SMITH et al., 2010); Krapina, Croatia (SMITH et al., 2010) and an infant from Dederiyeh, Syria (SASAKI et al., 2003). These studies were concerned primarily with determining the age at death from counts of incremental features in the dental enamel.

Other studies have been conducted on the number and spacing of long-period growth lines (perikymata/Retzius lines) in diverse samples of Neandertals and Middle Stone Age and Upper Palaeolithic Modern Humans (MANN et al., 1991; RAMIREZ ROZZI, 1993; MANN & VANDERMEERSCH,

1997; RAMIREZ ROZZI & BERMEDEZ DE CASTRO, 2004; GUATELLI-STEINBERG et al., 2005, 2007^{a, b}; SMITH et al., 2006^b; GUATELLI-STEINBERG & REID, 2008; REID et al., 2008), in addition to the study of Neandertal internal enamel development in single permanent molars from Tabun, Israel (DEAN et al., 2001; DEAN, 2007^a); La Chaise, France (MACCHIARELLI et al., 2006); and Lakonis, Greece (SMITH et al., 2009). Research on relative dental development in Neandertals has been conducted by WOLPOFF (1979), TOMPKINS (1996), THOMPSON & NELSON (2000), and GRANAT & HEIM (2003). Most of these studies have suggested that Neandertals show more rapid dental development than modern humans, although Neandertals appear to overlap with the lower end, or shorter-forming portion, of the human range. This distinction is of particular importance for studies that use modern human developmental profiles to assign ages to juvenile Neandertals (e.g., MANN & VANDERMEERSCH, 1997; TILLIER, 2000; COQUEUGNIOT & HUBLIN, 2007; but see SHACKELFORD et al., 2012).

This study aims to assess crown and root formation time of the juvenile Neandertal Scladina I-4A, as well as the age at death. Surface manifestations of long-period incremental features on tooth crowns and roots were quantified, the degree of root formation was assessed, and a first molar tooth was sectioned to determine the long-period line periodicity and to register chronological and developmental time. In addition, a sequence of developmental stress across the dentition was mapped, which allowed registry of teeth forming at the same time, and the estimation of the age at death. These data were compared with data on incremental development in modern humans from northern England and southern Africa, as well as a large sample of Neandertals (REID & DEAN, 2006; SMITH et al., 2007^b; GUATELLI-STEINBERG & REID, 2008; REID et al., 2008).

2. Material and methods

2.1. Preparation

The dental material from the Scladina Juvenile recovered over the past two decades provides an exceptional opportunity to examine isolated but associated teeth, which are described in detail in this volume. For this study, all permanent right tooth types of the Scladina Juvenile were examined, save for the mandibular first premolar, which has yet to be recovered. The first stage in the analysis involved photographic documentation with stereomicroscopy, followed by micro-computed tomographic (micro-CT) scanning with the Skyscan 1076 at Antwerp University (Belgium) and Skyscan 1172 (for selected additional scans) at the Max Planck Institute for Evolutionary Anthropology (Germany). Micro-CT scanning ensured that the entire sample would be accurately preserved digitally, and that the teeth would be available for non-destructive study of enamel thickness (OLEJNICZAK et al., 2008; SMITH et al., 2012). High resolution peels and molds of all available permanent teeth were made with Struers' Repliset and Coltene President impression materials, and casts were subsequently prepared with Epo-Tek 301 epoxy resin. The casts were lightly gold coated with a sputter coater for enhanced stereomicroscopic visualization.

In order to determine the long-period line periodicity, a histological thin section of the permanent maxillary right first molar (Scla 4A-4) was prepared. To approximate a plane of section passing through the tips of the mesial dentine horns, a virtual 3D model was generated with Vox Blast Software (Vaytek, Inc.; Figure 3), the dentine horn tips were located, and a virtual plane of section was cut through the mesial cusp tips and dentine horns. The virtual model was used to orient the tooth prior to sectioning, which facilitated the production of a physical section plane that was similar to

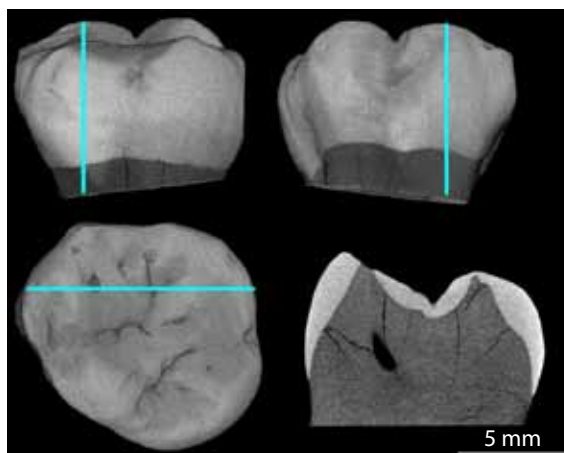


Figure 3: Virtual model of permanent maxillary right first molar crown (Scla 4A-4) with the orientation used to produce the least oblique virtual section and to orient the tooth prior to physical sectioning.

the 'ideal' virtual plane (Figure 4). In order to stabilize the tooth during sectioning, it was first embedded in methylmethacrylate resin, and then cut with a Logitech annular saw (Figure 5). The thin section was mounted to a microscope slide according to procedures described in REID et al. (1998). This involved a temporary bond with dental sticky wax, lapping one face with 1 micron alumina, bonding the lapped face with UV-curing resin under pressure, lapping the other face down to approximately 120 microns, and covering the section with a coverslip and DPX mounting media. The remaining tooth was then removed from the methylacrylate resin with dichloromethane and restored to its original appearance with temporary dental restoratives and dental sticky wax (Figure 6). After the two cuts to remove the section for histological preparation, it was estimated that less than 1.5 mm of the specimen's mesial-distal thickness was lost.

Two teeth (Scla 4A-6, Scla 4A-11) were brought to the European Synchrotron Radiation Facility in Grenoble, France in order to confirm results on

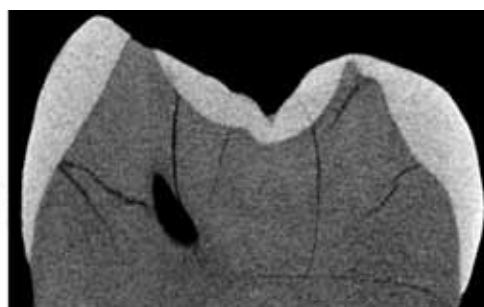


Figure 4: Histological section of the permanent maxillary right first molar crown (Scla 4A-4) (left) compared to the virtual (target) plane of section (right).



the long-period lines periodicity obtained from the physical section of the molar. In order to assess internal features non-destructively, small portions of the mid-lateral enamel of the maxillary right central incisor were scanned using an isotropic 0.7 µm voxel size with propagation phase contrast X-ray synchrotron micro-CT performed on the beamline ID 19 (Figure 7). This technique facilitates non-destructive resolution of dental microstructure (invisible with conventional

micro-CT) at the sub-micron level (TAFFOREAU, 2004; TAFFOREAU et al., 2006), including the long-period line periodicity (SMITH et al., 2007^a, 2010; SMITH & TAFFOREAU, 2008; TAFFOREAU & SMITH, 2008).

These scans were performed with a monochromatic beam at an energy of 52 keV using a multilayer monochromator. The propagation phase effect used to reveal dental microstructure was created with a sample-to-detector distance of

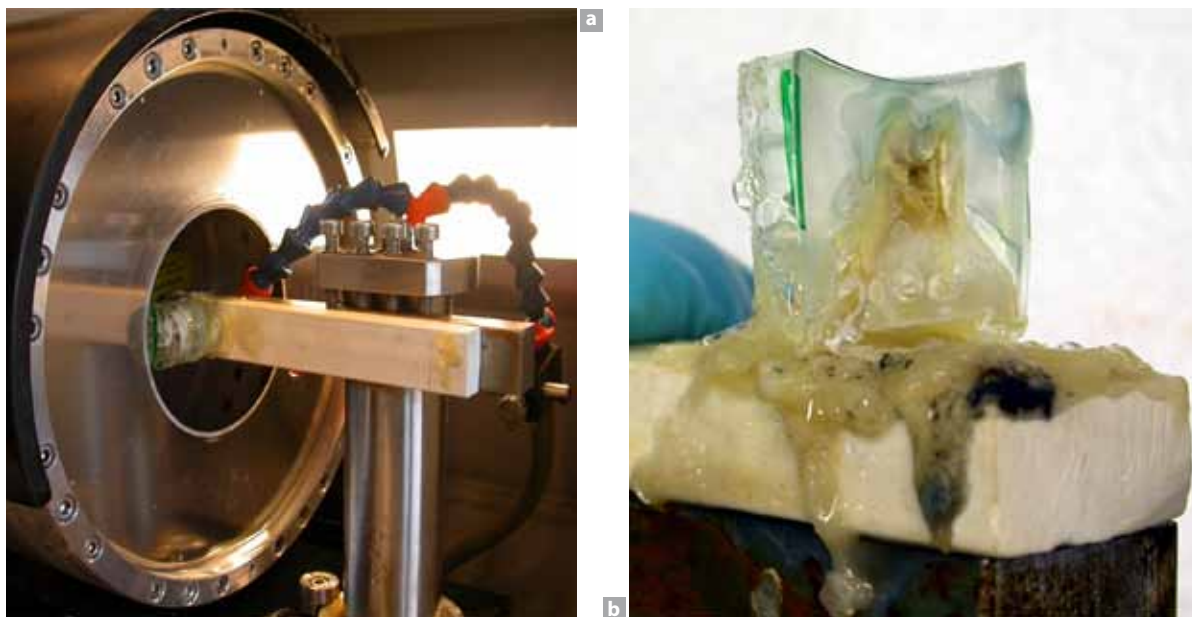


Figure 5: a) The embedded permanent maxillary right first molar (Scla 4A-4) on the annular saw, and b) after the section has been cut.

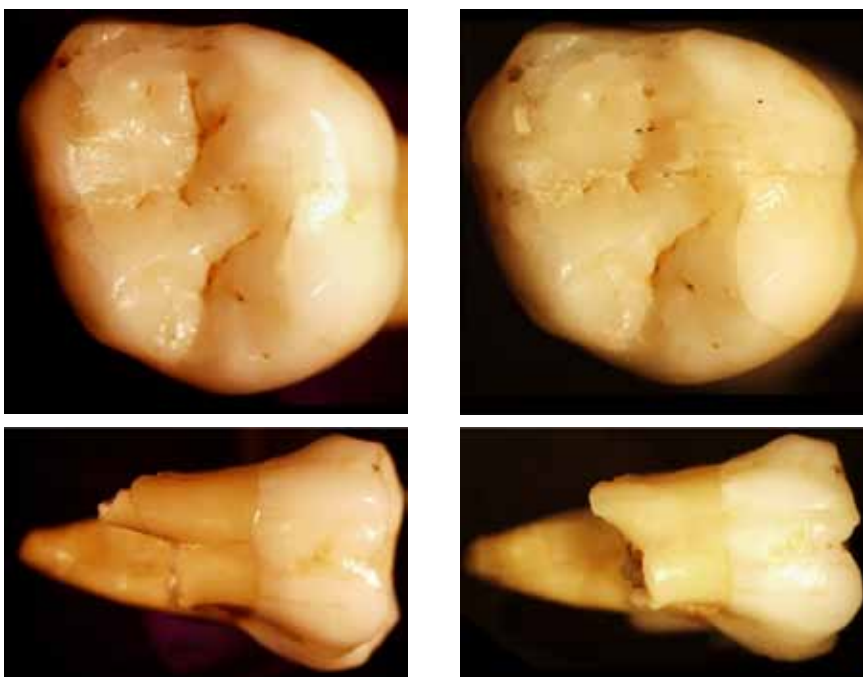


Figure 6: Comparison of the Scladina molar (Scla 4A-4) before (left) and after (right) reconstruction. The small amount of missing root on the right was removed for ancient DNA analysis prior to reconstruction. (Note the orientation and scale is slightly different in the panels.)

150 mm. Strong ring artefacts due to the multi-layer and detector were corrected using four processing steps: conditional flatfield correction, residual horizontal line removal, subtraction of a filtered average of all scan projections (general ring correction), and finally a correction of residual rings on reconstructed slices (adapted from TAFFOREAU, 2004). Virtual histological slices were prepared using average projections on a virtual thickness of 100 slices (70 μm) after precise alignment along incremental features, following the protocol described in TAFFOREAU et al. (2007) and TAFFOREAU & SMITH (2008).

2.2. Developmental analysis

Crown formation time was determined from the mesiopalatal cusp (protocone) of the permanent maxillary right first molar according to the procedure described in BOYDE (1963, 1990). The neonatal line was identified, and daily cross-striations were counted and/or measured along a prism track from the neonatal line to an accentuated line to yield formation time in days (Figure 8). The accentuated line was tracked down toward the enamel-dentine junction, and the count was continued along a prism to the next accentuated line. This process was repeated until the enamel cervix was reached. It was not possible to determine formation times for cuspal and imbricational regions of the crown (e.g., REID et al., 1998; SMITH, 2008) due to the degree of attrition, which prohibited identification of the beginning of imbricational enamel formation. A particularly marked accentuated line was estimated to have been formed at approximately 435 days of age and matched in the mesiobuccal cusp; 47 Retzius lines were counted after this line to yield the age at mesiobuccal cusp completion. It was not possible to identify a neonatal line in this cusp due to heavy attrition that had worn the enamel away (Figure 4).

Crown formation times for unworn/lightly worn teeth were determined by summing an estimate of cuspal formation time with the total number of perikymata times the periodicity. Cuspal formation time was calculated by two different methods and an average value was determined; a minimum estimate was calculated as cuspal thickness divided by the modern human mean cuspal daily secretion rate: 3.80 $\mu\text{m}/\text{day}$ for anterior teeth (SCHWARTZ et al., 2001) and 4.11 $\mu\text{m}/\text{day}$ for postcanine teeth (SMITH et al., 2007^b). Linear cuspal enamel thickness was determined from micro-CT slices; measurements were made

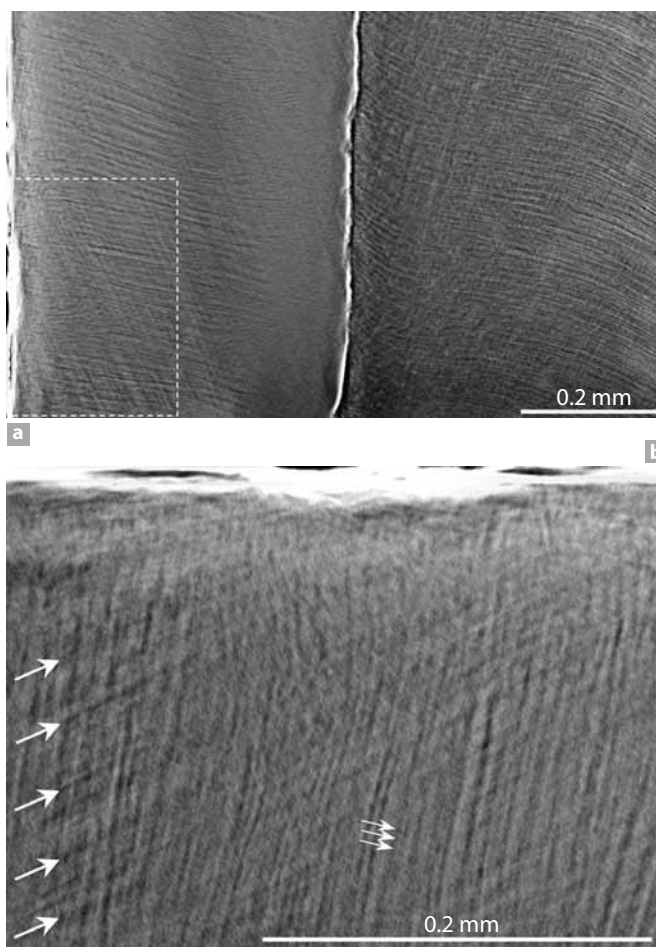


Figure 7: Scladina permanent maxillary right central incisor (Scla 4A-11) scanned with phase-contrast X-ray synchrotron microtomography. a) Overview of enamel (left) and dentine (right), showing an area (dotted box) enlarged in b). b) Developmental features revealed with non-destructive synchrotron imaging: Retzius lines (large arrows) and daily cross-striations (small arrows).

from the tip of the dentine horn to the approximate position of the first perikymata at the cusp surface. A maximum cuspal formation time estimate was calculated with regression equations for anterior and posterior modern human teeth (DEAN et al., 2001; SCHWARTZ & DEAN, 2001).

Developmental stress in the enamel and dentine of the first molar was mapped, registered to hypoplasias on anterior teeth, and subsequent long-period lines were counted on tooth crowns and roots. Crown initiation ages were determined by subtracting coronal developmental time prior to the known age stress events. Crown completion ages were determined by adding coronal developmental time after the known age stress events. This individual's age at death was determined by adding the time of formation of the first premolar



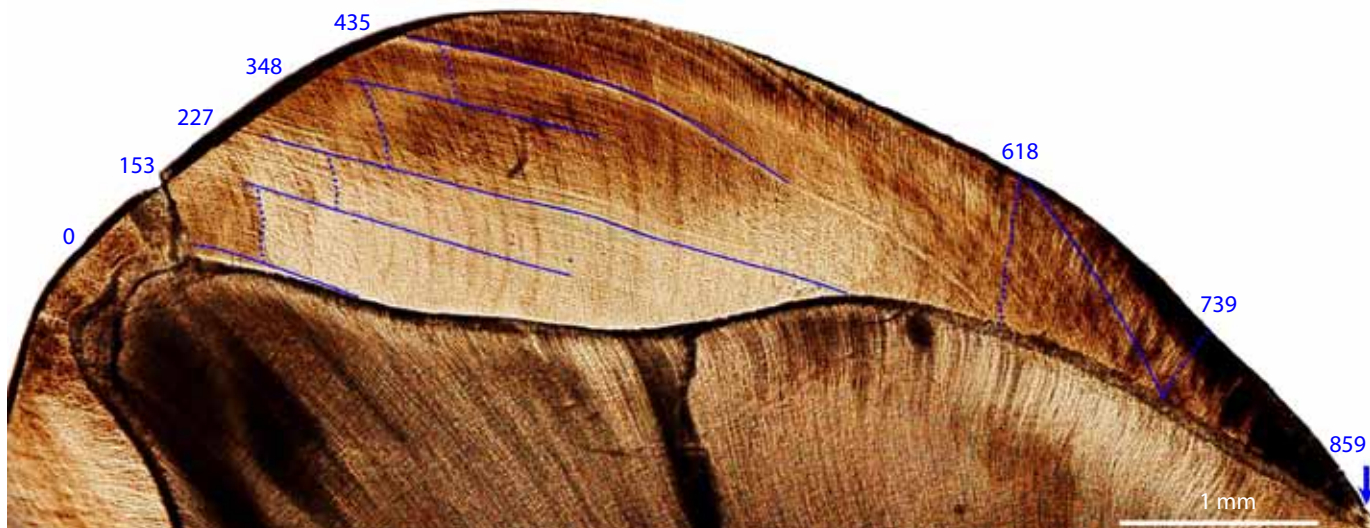


Figure 8: Permanent maxillary right first molar (Scla 4A-4) reconstruction of protocone crown formation time. The neonatal line is indicated by the first blue line on the lower left (0), with subsequent calculated time indicated for a series of stress events as 153 days, 227 days, 348 days, and 435 days postnatal age. The stress event at 435 days (1.19 years) was the most marked until the later stressors at 875 and 1779 days of age (not shown here). The crown was completed at 859 days of age (2.35 years).

after the final registered stress event. The permanent maxillary right third molar initiation age was determined by subtracting the estimated time of crown formation time from the age at death.

For root development, root length was first assessed from casts and photographs of the original teeth, and corrections were made for minor amounts of missing root. Long-period lines (periradicular bands: SMITH et al., 2007^b) were counted from the enamel cervix to the developing edge where possible on peels, casts, and original specimens using 50× or greater magnification. The number of lines was multiplied by the periodicity to determine the formation time in days. The overall rate of root extension was determined by division of the root length (in microns) by the time of formation (in days).

3. Results

The developmental variables for each tooth in the Scladina Juvenile's dentition are given in Table 1. The long-period line periodicity was 8 days in this individual, which was determined in both the histological section of the permanent maxillary right first molar and the virtual section of the permanent maxillary right central incisor imaged with phase contrast synchrotron microtomography. The permanent maxillary right first molar showed a neonatal (birth) line 13 days after mesiopalatal cusp initiation (Figure 7), which

allowed subsequent developmental time to be registered to chronological age. Crown formation time of the mesiopalatal cusp was approximately 872 days, and ages at cuspal crown completion were 2.35 years and 2.22 years for the mesiopalatal and mesiobuccal cusps, respectively. A chronology of developmental stress was identified in the enamel and dentine of the first molar at approximately 435, 875, and 1779 days of age, which was matched across anterior teeth (Figure 9). The final known-age developmental stress (at 1779 days of age) in the developing mandibular first premolar was used to establish that the individual was approximately 8 years old at death (~2939 days). Registry of developmental stress across the dentition allows the establishment of a developmental chronology (Figure 10), including ages at crown initiation and completion (see Table S2 in SMITH et al., 2007^b). Root extension rates for various teeth are given in Table 2. Anterior tooth root formation rates were found to be considerably higher than posterior rates.

4. Discussion

Crown formation times in the Scladina Juvenile permanent maxillary right first molar cusps are less than modern human first molar mean formation times (SMITH et al., 2007^{b,c}, 2010), but are similar to chimpanzee times (SMITH et al., 2007^d). In the case of Neandertal molars,

	Row	Tooth	Cusp	Thick (um)	Min (days)	Max (days)	Pkg	Imb (days)	Total (days)
Scla 4A-11	Maxillary	I1	—	worn	n/a	n/a	~121	968	n/a
Scla 4A-14		I2	—	~800	211	281	~120	960	1206
Scla 4A-16		C	—	~825	217	288	~131	1048	1301
Scla 4A-2/P4 (unerupted)		P4	ling	995	242	327	n/a	n/a	n/a
			buc	775	189	265	n/a	n/a	n/a
Scla 4A-4		M1	mp	worn	n/a	n/a	n/a	n/a	872
			mb	worn	n/a	n/a	n/a	n/a	811*
Scla 4A-3		M2	mp	1260	307	396	77	616	967
			mb	1155	281	369	78	624	949
			dp	1220	297	386	74	592	933
			db	1300	316	405	71	568	929
Scla 4A-8		M3	mp	1265	308	397	54+	432	784+
			mb	1405	342	430	58+	464	850+
			mp	1260	307	396	48+	384	735+
			db	1315	320	409	45+	360	724+
Scla 4A-15	Mandibular	I1	—	worn	n/a	n/a	~95	760	n/a
Scla 4A-20		I2	—	worn	n/a	n/a	~101	808	n/a
Scla 4A-12		C	—	~660	174	239	~140	1120	1326
Scla 4A-6		P3	—	830	202	281	94	752	994
Scla 4A-1/P4 (unerupted)		P4	ling	890	217	298	n/a	n/a	n/a
			buc	915	223	305	n/a	n/a	n/a
Scla 4A-1/M1		M1	ml	worn	n/a	n/a	n/a	n/a	n/a
			mb	worn	n/a	n/a	n/a	n/a	n/a
Scla 4A-1/M2		M2	ml	965	235	319	n/a	n/a	n/a
			mb	1060	258	345	n/a	n/a	n/a
	dl		885	215	297	n/a	n/a	n/a	
	db		1535	373	459	n/a	n/a	n/a	
Scla 4A-1/M3 (unerupted)	M3	ml	905	220	303	n/a	n/a	n/a	
		mb	905	220	303	n/a	n/a	n/a	
		dl	1100	268	355	n/a	n/a	n/a	
		db	1655	403	484	n/a	n/a	n/a	

Table 1: Developmental variables for the Scladina juvenile tooth crowns. **Tooth** = central incisor (I1), lateral incisor (I2), canine (C), first premolar (P3), second premolar (P4), and first, second and third molars (M1, M2, & M3). For maxillary molar cusps (**Cusp**): ‘mb’ = mesiobuccal cusp (paracone), ‘mp’ = mesiopalatal cusp (protocone), ‘db’ = distobuccal cusp (metacone), ‘dp’ = distopalatal cusp (hypocone). For mandibular molar cusps: ‘mb’ = mesiobuccal cusp (protoconid), ‘ml’ = mesiolingual cusp (metaconid), ‘db’ = distobuccal cusp (hypoconid), ‘dl’ = distolingual cusp (entoconid). **Thick** = linear enamel thickness (in microns) taken from micro-CT slices. Slight estimations were made for light wear, as indicated by ‘~’. **Min** = cusp time derived from cuspal enamel thickness divided by 3.80 and 4.11 microns/day for anterior and posterior teeth respectively. **Max** = cuspal time derived from the use of regression equations (DEAN et al., 2001; SCHWARTZ & DEAN, 2001). **Pkg** = perikymata, the number of long-period lines on the enamel surface counted from casts of the original teeth. Slight estimations were made for light wear, as indicated by ‘~’. **Imb** = total number of perikymata multiplied by 8. **Total** = crown formation time; mean cuspal enamel formation time plus the imbricational formation time. ‘*’ Assumes an equal amount of prenatal formation as the permanent maxillary first molar mp cusp. ‘worn’ indicates that data are not available due to heavy attrition.

relatively short formation times may be explained in part by differences in cuspal enamel, which is approximately 60–90% thinner than in modern humans (SMITH et al., 2007^b, 2010). Molar cuspal enamel formation times are likely to be shorter than in modern humans, as overall daily secretion rates do not vary between Neandertals and modern humans (DEAN et al., 2001; MACCHIARELLI et al., 2006; SMITH et al., 2009). Furthermore, coronal extension rates for first molar cusps were outside the range of modern human values, and were more similar to chimpanzee values (SMITH et al., 2007^b, 2010). A similar pattern of thinner

cuspal enamel and faster coronal extension was also found in a Neandertal third molar from Greece (SMITH et al., 2009).

When the rest of the dentition is examined, it appears that certain Neandertal anterior teeth form over a greater period of time than modern human populations (e.g., permanent maxillary lateral incisor), however this is not the case for other anterior teeth (e.g., permanent mandibular canine) or the first premolar, which appear to form over shorter periods of time than modern human populations (SMITH et al., 2007^b, 2010; REID et al., 2008). Although similarities in perikymata



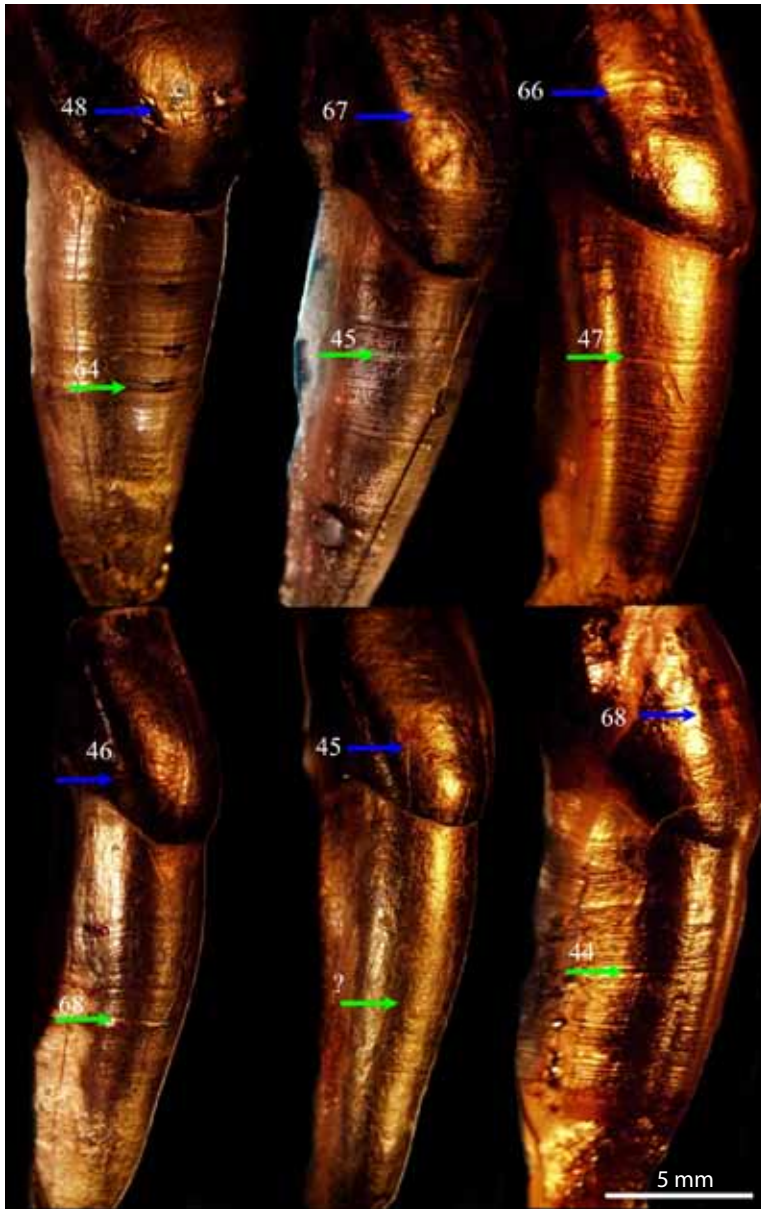


Figure 9: Developmental stress matched across the anterior dentition. From left to right (maxillary above, mandibular below) central incisor, lateral incisor, canine. The first stress event (blue arrow) was identified in the histological section of the permanent maxillary first molar at 875 days of age, with the number of subsequent perikymata after this event indicated on each tooth. The number of periradicular bands between the cervix and subsequent stress event (green arrow) is indicated, with 113 lines between events (904 days). Thus this second event occurred at 1779 days of age. Modified from SMITH et al. (2007^b).

numbers between Neandertals and modern humans have been noted (GUATELLI-STEINBERG & REID, 2008), this study suggests that certain Neandertal teeth are characterized by shorter periods of overall crown formation, due to thinner cuspal enamel and greater rates of crown extension. SMITH et al. (2007^b, 2010) suggested that

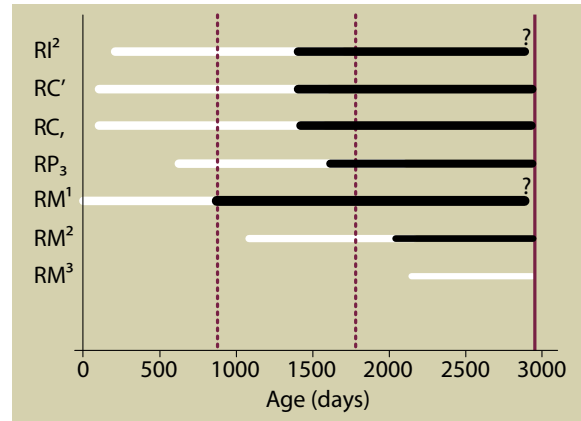


Figure 10: Developmental chronology of the Scladina Juvenile. Horizontal lines indicate crown formation (white) and root formation (black). The position of two stress events used to register teeth (see Figure 9) is indicated (dotted vertical lines), as well as death (solid vertical line). Given that the permanent maxillary lateral incisor and first molar had completed root formation prior to death, it was not possible to determine the end of root formation (indicated by '?'). Modified from SMITH et al. (2007^b).

anterior tooth formation times in Neandertals may also relate to their absolutely larger crowns.

Due to the lack of comparative hominoid root formation data, it is difficult to interpret root extension rates in the Scladina individual. This is further complicated by the fact that root extension rates vary within teeth and among tooth positions. Limited data on modern humans suggests that the first few millimetres of root formation takes place at ~3–4 microns/day (DEAN & BEYNON, 1991; SMITH et al., 2007^a), although the first few millimetres of human first molars may form at ~4–7 microns/day on average (MACCHIARELLI et

Tooth	Length	Rate
RI ¹	5.94	11.6
RI ²	2.63	7.3
RC' (partial)	3.63	9.6
RC' (complete)	17.66	11.5
RM ¹	13.59	*6.5
RM ²	5.83	6.4
RI ₁	5.88	10.8
RI ₂	6.03	11.1
RC, (partial)	4.04	11.5
RC, (complete)	16.38	10.8
RP ₃	10.41	7.8

Table 2: Cumulative mean root extension rates for the Scladina individual's dentition. **Tooth** = right (R), central incisor (I1), lateral incisor (I2), canine (C), first premolar (P3), and first and second molars (M1 – palatal root, M2 – mesiobuccal root). **Length** is in mm, and **Rate** is in microns/day. Rates are for the length of root specified, measured from the enamel cervix apically. "*" Minimum rate: based on assumption that UM1 root completed formation at death.

Tooth	Scladina	Mean Pkg	Min	Max	N
Rl ¹	~121	138	121	161	10
Rl ²	~120	143	133	156	9
RC	~131	138	114	157	14
RM ²		96	77	117	11
Rl ₁	~95	134	118	158	5
Rl ₂	~101	147	110	177	8
RC ₁	~140	159	135	198	10
RP ₃		109	88	130	5

Table 3: Comparison of perikymata number in the Scladina dentition with other Neandertals. **Tooth** = right dentition (R), central incisor (I1), lateral incisor (I2), canine (C), first premolar (P3) buccal cusp, and second molar (M2) mesiobuccal cusp. Slight estimations were made for light wear, as indicated by '~'. Mean pkg (**Mean Pkg**), minimum (**Min**), maximum (**Max**), and sample sizes are derived from Neandertal data in GUATELLI-STEINBERG & REID (2008).

al., 2006; DEAN, 2007^b). Chimpanzee first molar roots may show similar or slightly faster rates of extension (SMITH et al., 2007^d). The minimum average root extension rate estimated for the Scladina permanent maxillary first molar palatal root (6.5 microns/day) is greater than similar data on modern human permanent mandibular first molars (6.1 microns/day; DEAN, 2007^b) or the La Chaise permanent mandibular molar (6.3 microns/day; MACCHIARELLI et al., 2006). Moreover, because the root had completed formation prior to death, it is quite likely that the average extension rate in the Scladina permanent maxillary first molar was greater than 6.5 microns/day. This may have led to an earlier age of M1 eruption, although it was not possible to determine this conclusively.

Perikymata numbers in the Scladina Juvenile fall either near the low end of values reported for other Neandertals, or below this range in the case of the permanent maxillary and mandibular lateral incisors and the permanent mandibular central incisor (Table 3). Comparisons of canine size between the Scladina Juvenile and the Obi-Rakhmat individual may indicate that sex differences influence Neandertal variation (Figure 11). Modern human females tend to show slightly younger ages of tooth initiation, eruption and completion (e.g., SMITH, 1991; LIVERSIDGE, 2003), in addition to shorter canine crown formation times than males (SCHWARTZ & DEAN, 2001). Although it is tempting to suggest that the Scladina individual is a female (TOUSSAINT, Chapter 9), potentially leading to some degree of advanced dental development, confirmation of this awaits recovery of associated postcranial material.

When the tooth calcification stages and eruption status of the Scladina Juvenile are compared modern human (SMITH, 1991; LIVERSIDGE, 2003; SMITH et al., 2010), it is clear that this individual is several years younger than a modern human juvenile at the same developmental stage. For example, the second molar is beyond clinical (gingival) occlusion; second molar eruption occurs on average at 10–13 years of age in global human populations. Advanced molar formation has previously been noted in Neandertals (WOLPOFF, 1979; TOMPKINS, 1996). While early third molar initiation ages have been reported for modern humans of southern African origin (LIVERSIDGE, 2008), we conclude that age at death in Neandertals should not be assessed by comparison with modern human standards, particularly those derived from European or North American populations. The recovery of postcranial material from the Scladina Juvenile would be a welcome complement to this study, particularly given debates over differences in relative skeletal versus dental ages of other well-preserved hominins (e.g. Devil's Tower, Le Moustier 1, Narikotome).

Acknowledgements

We are grateful to Nora De Clerck, Heiko Temming, Andreas Winzer, and the ID 19 beam-line staff for technical support. This research was supported by the Max Planck Society, EU FP6 Marie Curie Actions MRTN-CT-2005-019564, the University of Liège, the city of Andenne, the Direction de l'Archéologie of the Service public de Wallonie in Belgium, the European Synchrotron Radiation Facility, and Harvard University.

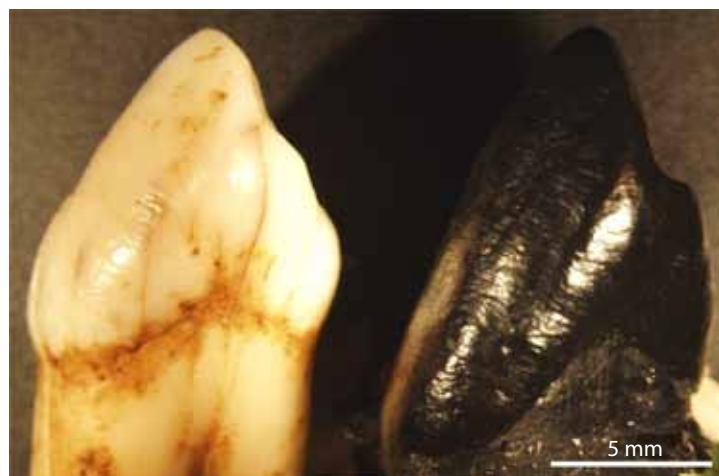


Figure 11: Permanent maxillary canine size variation in Neandertals from Scladina (Scla 4A-18; left) and Obi Rakhmat Grotto (right, cast of original).



References

- BOYDE A., 1963. Estimation of age at death of young human skeletal remains from incremental lines in the dental enamel. *Third International Meeting in Forensic Immunology, Medicine, Pathology, and Toxicology*, London, April 1963: 16–24.
- BOYDE A., 1989. Enamel. In A. OKSCHE & L. VOLLRATH (eds.), *Handbook of Microscopic Anatomy*, V, 6: Teeth. Berlin, Springer-Verlag: 309–473.
- BOYDE A., 1990. Developmental interpretations of dental microstructure. In C. J. DEROUSSEAU (ed.), *Primate Life History and Evolution*. New York, Wiley-Liss: 229–267.
- BROMAGE T. G., 1991. Enamel incremental periodicity in the pig-tailed macaque: a polychrome fluorescent labeling study of dental hard tissues. *American Journal of Physical Anthropology*, 86: 205–214.
- BROMAGE T. G. & DEAN M. C., 1985. Re-evaluation of the age at death of immature fossil hominids. *Nature*, 317: 525–527.
- COQUEUGNIOT H. & HUBLIN J.-J., 2007. Endocranial volume and brain growth in immature Neandertals. *Periodicum Biologorum*, 109: 379–385.
- DEAN M. C., 1995. The nature and periodicity of incremental lines in primate dentine and their relationship to periradicular bands in OH 16 (*Homo habilis*). In J. MOGGI CECCHI (ed.), *Aspects of Dental Biology: Paleontology, Anthropology and Evolution*. Florence, International Institute for the Study of Man: 239–265.
- DEAN M. C., 2007^a. Dental development and life history in primates and a comparison of cuspal enamel growth trajectories in a specimen of *Homo erectus* from Java (Sangiran S7-37), a Neandertal (Tabun C1), and an early *Homo sapiens* specimen (Skhul II), from Israel. In M. FAERMAN, L. K. HORWITZ, T. KAHANA & U. ZILBERMAN (eds.), *Faces from the past: diachronic patterns in the biology of human populations from the eastern Mediterranean*. Oxford, British Archaeological Reports, International Series, 1603: 21–27.
- DEAN M. C., 2007^b. A radiographic and histological study of modern human lower first permanent molar root growth during the supraosseous eruptive phase. *Journal of Human Evolution*, 53: 635–646.
- DEAN M. C. & BEYNON A. D., 1991. Histological reconstruction of crown formation times and initial root formation times in a modern human child. *American Journal of Physical Anthropology*, 86: 215–228.
- DEAN M. C., BEYNON A. D., THACKERAY J. F. & MACHO G. A., 1993. Histological reconstruction of dental development and age at death of a juvenile *Paranthropus robustus* specimen, SK 63, from Swartkrans, South Africa. *American Journal of Physical Anthropology*, 91: 401–419.
- DEAN M. C., LEAKEY M. G., REID D. J., SCHRENK F., SCHWARTZ G. T., STRINGER C. B. & WALKER A., 2001. Growth processes in teeth distinguish modern humans from *Homo erectus* and earlier hominins. *Nature*, 414: 628–631.
- DEAN M. C., STRINGER C. B. & BROMAGE T. G., 1986. Age at death of the Neanderthal child from Devil's Tower, Gibraltar and the implications for studies of general growth and development in Neanderthals. *American Journal of Physical Anthropology*, 70: 301–309.
- FITZGERALD C. M., 1998. Do enamel microstructures have regular time dependency? Conclusions from the literature and a large-scale study. *Journal of Human Evolution*, 35: 371–386.
- GRANAT J. & HEIM J.-L., 2003. Nouvelle méthode d'estimation de l'âge dentaire des Néandertaliens. *L'Anthropologie*, 107: 171–202.
- GUATELLI-STEINBERG D. & REID D. J., 2008. What molars contribute to an emerging understanding of lateral enamel formation in Neandertals vs. modern humans. *Journal of Human Evolution*, 54: 236–250.
- GUATELLI-STEINBERG D., REID D. J., BISHOP T. A. & LARSEN C. S., 2005. Anterior tooth growth periods in Neandertals were comparable to those of modern humans. *Proceedings of the National Academy Science of the United States of America*, 102, 40: 14197–14202.
- GUATELLI-STEINBERG D., REID D. J. & BISHOP T. A., 2007^a. Did the lateral enamel of Neandertal anterior teeth grow differently from that of modern humans? *Journal of Human Evolution*, 52: 72–84.
- GUATELLI-STEINBERG D., REID D. J., BISHOP T. A. & LARSEN C. S., 2007^b. Imbricational enamel formation in Neandertals and recent modern humans. In S. E. BAILEY & J.-J. HUBLIN (eds.), *Dental Perspectives on Human Evolution: State of the Art Research in Dental Paleoanthropology*.

- Dordrecht, Springer: 211-227.
- LIVERSIDGE H. M., 2003. Variation in modern human dental development. In J. L. THOMPSON, G. E. KROVITZ & A. J. NELSON (eds.), *Patterns of Growth and Development in the Genus Homo*, Cambridge University Press: 73-113.
- LIVERSIDGE H. M., 2008. Timing of human mandibular third molar formation. *Annals of Human Biology*, 35: 294-321.
- MACCHIARELLI R., BONDIOLI L., DEBÉNATH A., MAZURIER A., TOURNÉPICHE J.-F., BIRCH W. & DEAN C., 2006. How Neandertal molar teeth grew. *Nature*, 444: 748-751.
- MANN A. E., MONGE J. M. & LAMPL M., 1991. Investigation into the relationship between perikymata counts and crown formation times. *American Journal of Physical Anthropology*, 86: 175-188.
- MANN A. & VANDERMEERSCH B., 1997. An adolescent female Neandertal mandible from Montgaudier Cave, Charente, France. *American Journal of Physical Anthropology*, 103: 507-527.
- OLEJNICZAK A. J., SMITH T. M., FEENEY R. N. M., MACCHIARELLI R., MAZURIER A., BONDIOLI L., ROSAS A., FORTEA J., DE LA RASILLA M., GARCÍA-TABERNEIRO A., RADOVČIĆ J., SKINNER M. M., TOUSSAINT M. & HUBLIN J.-J., 2008. Dental tissue proportions and enamel thickness in Neandertal and modern human molars. *Journal of Human Evolution*, 55: 12-23.
- RAMIREZ ROZZI F. V., 1993. Microstructure and development of the enamel tooth of the Neandertal from Zafarraya, Spain. *Comptes Rendus de l'Académie des Sciences de Paris*, 316: 1635-1642.
- RAMIREZ ROZZI F. V., 2005. Age at death of the Neandertal child from Hortus. *Bulletins et Mémoires de la Société d'Anthropologie de Paris*, 17: 47-55.
- RAMIREZ ROZZI F. V. & BERMUDEZ DE CASTRO J. M., 2004. Surprisingly rapid growth in Neandertals. *Nature*, 428: 936-939.
- REID D. J. & DEAN M. C., 2006. Variation in modern human enamel formation times. *Journal of Human Evolution*, 50: 329-346.
- REID D. J., GUATELLI-STEINBERG D. & WALTON P., 2008. Variation in modern human premolar enamel formation times: Implications for Neandertals. *Journal of Human Evolution*, 54: 225-235.
- REID D. J., SCHWARTZ G. T., DEAN C. & CHANDRASEKERA M. S., 1998. A histological reconstruction of dental development in the common chimpanzee, *Pan troglodytes*. *Journal of Human Evolution*, 35: 427-448.
- SASAKI C., SUZUKI K., MISHIMA H. & KOZAWA Y., 2003. Age determination of the Dederiyeh 1 Neandertal child using enamel cross-striations. In T. AKAZAWA & S. MUHESEN (eds.), *Neandertal Burials: Excavations of the Dederiyeh Cave, Afrin, Syria*. Kyoto, International Research Center for Japanese Studies: 263-267.
- SCHWARTZ G. T. & DEAN C., 2001. Ontogeny of canine dimorphism in extant hominoids. *American Journal of Physical Anthropology*, 115: 269-283.
- SCHWARTZ G. T., REID D. J. & DEAN C., 2001. Developmental aspects of sexual dimorphism in hominoid canines. *International Journal of Primatology*, 22: 837-860.
- SHACKELFORD L. L., STINESPRING HARRIS A. E. & KONIGSBERG L. W., 2012. Estimating the distribution of probable age-at-death from dental remains of immature human fossils. *American Journal of Physical Anthropology*, 147: 227-253.
- SMITH B. H., 1991. Standards of human tooth formation and dental age assessment. In M. S. KELLEY & C. S. LARSEN (eds.), *Advances in Dental Anthropology*. New-York, Wiley-Liss: 143-168.
- SMITH T. M., 2006. Experimental determination of the periodicity of incremental features in enamel. *Journal of Anatomy*, 208: 99-114.
- SMITH T. M., 2008. Incremental dental development: methods and applications in hominoid evolutionary studies. *Journal of Human Evolution*, 54: 205-224.
- SMITH T. M., HARVATI K., OLEJNICZAK A. J., REID D. J., HUBLIN J.-J. & PANAGOPOULOU E., 2009. Brief communication: Dental development and enamel thickness in the Lakonis Neandertal molar. *American Journal of Physical Anthropology*, 138: 112-118.
- SMITH T. M., OLEJNICZAK A. J., TAFFOREAU P. T., REID D. J., GRINE F. E. & HUBLIN J.-J., 2006^b. Molar crown thickness, volume, and development in South African Middle Stone Age humans. *South African Journal of Science*, 102: 513-517.
- SMITH T. M., OLEJNICZAK A. J., ZERMENO J. P., TAFFOREAU P. T., SKINNER M. M., HOFFMANN A., RADOVČIĆ J., TOUSSAINT M., KRUSZYNSKI R., MENTER C., MOGGI-CECCHI J., GLASMACHER U. A.,



- KULLMER O., SCHRENK F., STRINGER C. B. & HUBLIN J.-J., 2012. Variation in enamel thickness within the genus *Homo*. *Journal of Human Evolution*, 62: 395–411.
- SMITH T. M., REID D. J., DEAN M. C., OLEJNICZAK A. J., FERRELL R. J. & MARTIN L. B., 2007^b. New perspectives on chimpanzee and human dental development. In S. E. BAILEY & J.-J. HUBLIN (eds.), *Dental Perspectives on Human Evolution: State of the Art Research in Dental Paleoanthropology*. Dordrecht, Springer: 177–192.
- SMITH T. M., REID D. J., DEAN M. C., OLEJNICZAK A. J. & MARTIN L. B., 2007^d. Molar development in common chimpanzees (*Pan troglodytes*). *Journal of Human Evolution*, 52: 201–216.
- SMITH T. M., REID D. J., OLEJNICZAK A. J., BAILEY S., GLANTZ M., VIOLA B. & HUBLIN J.-J., 2011. Dental development and age at death of a Middle Paleolithic juvenile hominin from Obi-Rakhmat Grotto, Uzbekistan. In S. CONDEMI & G. C. WENIGER, (eds.), *Continuity and Discontinuity of the Peopling of Europe. One Hundred Fifty Years of Neanderthal Study*. Dordrecht, Springer: 155–164.
- SMITH T. M., REID D. J. & SIRIANNI J. E., 2006^a. The accuracy of histological assessments of dental development and age at death. *Journal of Anatomy*, 208: 125–138.
- SMITH T. M. & TAFFOREAU P. T., 2008. New visions of dental tissue research: tooth development, chemistry, and structure. *Evolutionary Anthropology*, 17: 213–226.
- SMITH T. M., TAFFOREAU P. T., REID D. J., GRÜN R., EGGINS S., BOUTAKIOUT M. & HUBLIN J.-J., 2007^a. Earliest evidence of modern human life history in North African early *Homo sapiens*. *Proceedings of the National Academy Science of the United States of America*, 104, 15: 6128–6133.
- SMITH T. M., TAFFOREAU P. T., REID D. J., POUÉCH J., LAZZARI V., ZERMENO J. P., GUATELLI-STEINBERG D., OLEJNICZAK A. J., HOFFMAN A., RADOVČIĆ J., MASROUR M., TOUSSAINT M., STRINGER C. B. & HUBLIN J.-J., 2010. Dental evidence for ontogenetic differences between modern humans and Neanderthals. *Proceedings of the National Academy of Sciences of the United States of America*, 107, 49: 20923–20928.
- SMITH T. M., TOUSSAINT M., REID D. J., OLEJNICZAK A. J. & HUBLIN J.-J., 2007^c. Rapid dental development in a Middle Paleolithic Belgian Neanderthal. *Proceedings of the National Academy Science of the United States of America*, 104, 51: 20220–20225.
- STRINGER C. B. & DEAN M. C., 1997. Age at death of Gibraltar 2 — a reply. *Journal of Human Evolution*, 32: 471–472.
- STRINGER C. B., DEAN M. C. & MARTIN R. D., 1990. A comparative study of cranial and dental development within a recent British sample and among Neandertals. In C. J. DEROUSSEAU (ed.), *Primate Life History and Evolution*. Wiley-Liss, New York: 115–152.
- TAFFOREAU P. T., 2004. *Phylogenetic and functional aspects of tooth enamel microstructure and three-dimensional structure of modern and fossil primate molars: contributions of X-ray synchrotron microtomography*. PhD Thesis, Université de Montpellier II.
- TAFFOREAU P. T., BENTALEB I., JAEGER J.-J. & MARTIN C., 2007. Nature of laminations and mineralization in rhinoceros enamel using histology and X-ray synchrotron microtomography: potential implications for palaeoenvironmental isotopic studies. *Palaeogeography, Palaeoclimatology, Palaeoecology*, 246: 206–227.
- TAFFOREAU P. T., BOISTEL R., BOLLER E., BRAVIN A., BRUNET M., CHAIMANEE Y., CLOETENS P., FEIST M., HOSZOWSKA J., JAEGER J.-J., KAY R. F., LAZZARI V., MARIVAUX L., NEL A., NEMOZ C., THIBAUT X., VIGNAUD P. & ZABLER S., 2006. Applications of X-ray synchrotron microtomography for non-destructive 3D studies of paleontological specimens. *Applied Physics A*, 83, 2: 195–202.
- TAFFOREAU P. T. & SMITH T. M., 2008. Nondestructive imaging of hominoid dental microstructure using phase contrast X-ray synchrotron microtomography. *Journal of Human Evolution*, 54: 272–278.
- THOMPSON J. L. & NELSON A. J., 2000. The place of Neandertals in the evolution of hominid patterns of growth and development. *Journal of Human Evolution*, 38: 475–495.
- TILLIER A.-M., 2000. Palaeoauxology applied to Neanderthals. Brno, *Anthropologie*, 38: 109–120.
- TOMPKINS R. L. 1996. Relative dental development of Upper Pleistocene hominids compared to human population variation. *American Journal of Physical Anthropology*, 99: 103–118.
- WOLPOFF M. H., 1979. The Krapina dental remains. *American Journal of Physical Anthropology*, 50: 67–114.

Michel TOUSSAINT

*Michel Toussaint & Dominique Bonjean (eds.), 2014.
The Scladina I-4A Juvenile Neandertal (Andenne, Belgium),
Palaeoanthropology and Context
Études et Recherches Archéologiques de l'Université de Liège, 134: 167-178.*

1. Introduction

Sexual dimorphism is obvious in living and extinct primates, including human species (BRACE, 1973; FRAYER & WOLPOFF, 1985; OXNARD, 1987). It is acknowledged that males are, on average, taller in stature than females, possess stronger bones, bigger teeth, and greater strength and muscularity. Throughout human evolution, there is also ample evidence of reduction in sexual dimorphism.

Consequently, the interpretation of the morphology and morphometry of any human remain, either modern or ancient, should include as accurate an estimation of the sex as possible. As with the determination of age at death, the identification of the sex of fossil remains has implications in fields as varied as taxonomy, palaeodemography, palaeopathology, behaviour and phylogeny.

Numerous sexing techniques have been developed for adult modern human bones. They are based either on morphological traits, or on metric differences (FEREMBACH et al., 1980; KROGMAN & IŞCAN, 1986; BASS, 1986). Nearly all categories of bones have been taken into account.

Morphological male or female traits may sometimes be differentiated by shape, for instance the prominent aspect of the male chin against the female rounded one (FEREMBACH et al., 1980; BASS, 1986), the development of the glabella and inion, or the morphology of postcranial features such as the distal humerus (ROGERS, 1999). However, the accuracy of assessment using cranial and long bone characteristics is never as good as that using pelvic bones, which have a higher prediction accuracy in this regard, over 95% (KROGMAN & IŞCAN, 1986; BRUZEK, 2002). Many discriminant functions have been increasingly utilized for sex diagnosis over the last half century (among the first to develop them were: GILES & ELLIOT, 1963; GILES, 1964; HOWELLS, 1965; KAJANOJA, 1966; BOULINIER, 1968). They were developed through

the use of modern *Homo sapiens sapiens* skeletal collections of known ancestry, sex and age such as the Hamann-Todd and Terry Collections. These functions should be applied only to bones closely related to the series for which they were developed.

Estimating the sex of juvenile and subadult skeletal remains is more difficult. Most techniques in current use derive from adult-centric ones, so the question often arises of whether juvenile bones, including those from the pelvis, can be accurately sexed using these criteria (BASS, 1986; MAJO, 1992). In fact, due to limited sexual dimorphism before puberty, no really reliable sex diagnosis techniques are applicable for juveniles (HENRY-GAMBIER et al., 2007).

In the case of fossilized specimens, the attribution of sex using modern standards is even more difficult. This probably results from the use of the general level of robusticity as a sexual indicator (TRINKAUS, 1983). Under such conditions, robust females are often classified as males while slender males might be mistaken for females. As for discriminant function analyses, these modern standards are almost inapplicable to fossils.

With Neandertal juvenile cranial remains, such as those from Scladina, the three problems referred to above are combined: the remains belonged to sub-adults; traits commonly used for sexing modern humans are not accurate enough for fossils; and, finally, mandibles and maxillae are not the most accurate bones to use in determining sex.

As a consequence of all these problems, some palaeoanthropologists with an interest in Neandertals simply do not try to assess the sex of the fossils they study, especially if the skeletal remains do not include the pelvic bones (MADRE-DUPOUY, 1992: 247-249; VERNA, 2006: 109). The assessment of sex is even more problematic with fossils of juveniles (HEIM, 1982; TEILHOL, 2001). In the context of the analysis of the Scladina I-4A

remains it is important to re-emphasize this difficulty (HEIM, 1981-1982: 462) as the remains are from a juvenile represented by an isolated mandible and portions of the maxilla. Obviously, such precautions are wise. Nevertheless, other experts do prefer to discuss and assess the identification of the sex of their cranial and mandibular specimens, even when they are well aware that it is often a quite delicate process (THOMA, 1975; MANN & VANDERMEERSCH, 1997; QUAM et al., 2001; THOMPSON & NELSON, 2005). This is exactly the approach taken in the present chapter. Even though the determination of the sex of the *Scladina* remains may finally prove to be a tricky objective, trying to discuss such a nightmarish issue is not without interest.

However, as the *Scladina* fossil remains are juvenile and comprised of just a mandible, a small piece of maxilla and a few teeth, only a few criteria could be taken into account. Metrical traits which should still increase during the end of the growth were only used when it was possible to get comparative data from other juvenile Neandertals.

2. Methods

Since the beginning of Neandertal palaeo-anthropological research, attempts have been made to determine the sex of the remains palaeontologists were studying. For example, as early as 1887, Fraipont classified Spy 1 as female and Spy 2 as male (FRAIPONT & LOHEST, 1887: 707-709). Two decades later, BOULE (1911-1913) considered La Chapelle-aux-Saints male. Henri-Martin suggested that the partial skeleton from La Quina 5 was female, then expressed reservations on his determination (MARTIN, 1923); nevertheless, most palaeoanthropologists think the fossil is really female (e.g. VANDERMEERSCH, 1965; HEIM, 1976; TRINKAUS, 1980; but see VERNA, 2006 for a critical discussion).

In fact, determination of sex of Neandertal bones is always difficult. More than half a century ago, GENOVES (1954) drew palaeoanthropologists' attention to the fact that the sex of some fossils had already changed up to five times since their discovery!

Regardless of the above reservations, the current – if debated – state of the art in Neandertal estimation of sex is summarized in some papers and books.

In regards to cranial remains, Smith pointed out that the morphological and metrical features

that have to be taken into account are the same as for modern humans (SMITH, 1980: 364), only with varying degrees of differences. Smith focused primarily on the shape of the supraorbital torus, the morphology of the mastoid process and its surrounding area as well as the robustness of the nuchal plane. The sexual value of the overall dimensions of the Neandertal skull has also been emphasized (HEIM, 1981-1982); and indeed, cranial capacity is generally acknowledged as a reliable indicator when sexing adult and subadult Neandertals (THOMA 1975; HOLLOWAY, 1985; THOMPSON & NELSON, 2005).

Some features of the mandible are also seen as useful in sexing Neandertals (SMITH, 1976: 183-187; WOLPOFF, 1976; HEIM, 1981-1982), in particular the height and thickness of the symphysis, the height at the condyle as well as the condylar breadth.

Other authors emphasize the importance of the dimensions of teeth in the attribution of sex (OXNARD, 1987). On the contrary, WOLPOFF (1979) concluded his study of the Krapina remains by stating that the dentition was by no means a reliable indicator of sex with that sample, as both large and small teeth may be found in the same dentition. However, it has recently been noted (MANN & VANDERMEERSCH, 1997: 524) that the sample of teeth from Krapina is at the upper end of the Neandertal range as far as size is concerned. Therefore Krapina might not represent the best series for studying the importance of tooth size in evaluating sexual dimorphism in Neandertals. So, recent papers resort to Oxnard's tooth dimensions as a sex indicator for Neandertals (QUAM et al., 2001; THOMPSON & NELSON, 2005).

According to TRINKAUS (1983: 43), Neandertal pelvic morphology provides the most secure criteria for the determination of sex although a variety of other morphological features can also be used.

Trinkaus also notes that “it is possible to use [...] appendicular dimensions to assign sex to Neandertal specimens” but not without difficulties such as an overlap in size between males and females (TRINKAUS, 1983: 44; see also TRINKAUS, 1980). For instance, amongst the numerous dimensions of postcranial bones that have been used to indicate the sex of modern humans (KROGMAN & IŞCAN, 1986; BASS, 1986), the vertical diameter of the femoral head is supposed to be able to distinguish male and female Neandertals quite well (TRINKAUS, 1980, 1983; THOMPSON & NELSON, 2005).

In conclusion of this quick overview, it seems clear that only specifically designed techniques,

which do not presuppose that modern morphological features are valid for determining the sex of Neandertal remains, should be applied. Since both taxa bear obvious differences in robustness, some of their anatomical features may not have the same sexual meaning. As for the estimation of the sex of the *Scladina* remains, only a few mandibular and dental criteria could be used. They are discussed below.

2.1. Measurements

2.1.1. Teeth

2.1.1.1. Crowns

In his monograph dealing with the pattern of sexual dimorphism in human evolution, OXNARD (1987) developed a technique which cleverly avoids the pitfall of applying modern humans measurements to fossil taxa. He analysed a number of dental samples of extinct hominins, including Neandertals. He noticed statistically significant bimodal distributions in the BL or MD diameters of some categories of fossil teeth whose gender had not been estimated from the morphology of the hip bone. He interpreted these bimodal distributions in the size of the teeth as evidence of sexual dimorphism.

In practice, most researchers who referred to Oxnard's approach (MANN and VANDERMEERSCH, 1997; QUAM et al., 2001; THOMPSON & NELSON, 2005) made use of the permanent mandibular canine breadth, as it is acknowledged that the size distribution of the canines shows the greatest differences between males and females in recent human populations.

Indeed, in Oxnard's Neandertal sample, the range of permanent mandibular canine breadth, both sexes included, exhibit a clear bimodal pattern. The smaller values, presumably female, range from 7.5 to 9.0 mm, with an average of 8.5 mm (OXNARD, 1987: 81), while the larger values, probably male, range from approximately 9.4 to 10.5 mm, with an average of 10.0 mm.

More recently, BERMÚDEZ DE CASTRO et al. (1993; BERMÚDEZ DE CASTRO & NICOLÁS, 1997) assessed the sexual dimorphism of the Atapuerca-Sima del Huesos Neandertal sample from the crown area.

2.1.1.2. Tooth roots

In modern humans, sexual dimorphism is greater in root length than in crown diameters

(GARN et al., 1978, 1979), and males have longer roots than females (JAKOBSSON & LIND, 1973). The role of sex chromosomes in root length also seems to be important (LÄHDESMÄKI, 2006; LÄHDESMÄKI & ALVESALO, 2007; LE CABEC et al., this volume, Chapter 16).

2.1.2. Mandibular corpus

Usually adult male cranial and postcranial remains are bigger and more robust than those of females. It is reasonable to suppose that this is also true for juveniles and conclude that, at an equal age, the smallest specimens are female and the biggest male.

According to SMITH (1976: 185) the height of the symphysis might be indicative of sexual differences. This trait has to be very cautiously used as there are important differences between this measurement depending on who took it. For SMITH (1976), the symphyseal height of the Krapina C mandible is 29.6 mm but only 23.7 mm for MINUGH-PURVIS (1988); Krapina E has a symphysis height of 34.8 mm for Smith but 34.5 or only 31.4 mm for Minugh-Purvis. For Smith, the height at the condyle and the condylar breadth also exhibit sexual dimorphism. Other mandibular dimensions are also used insofar as they reflect the size of the mandible with small ones reasonably supposed to be female.

If these measurements really exhibit sexual differences, the mandible of *Scladina* must not, however, be compared with adult specimens but with other immature Neandertals and Early Moderns aged over 8 years.

2.2. Morphological features

2.2.1. Teeth

2.2.1.1. External morphology

According to some authors (SCOTT 1977; SCOTT & TURNER, 1997: 106) the presence of a distal accessory ridge on permanent maxillary and mandibular canines is one of the most sexually dimorphic, albeit moderately, dental traits in modern humans. In fact, although more pronounced expressions of this trait have a higher frequency in males than in females, they are present in both sexes. In the case of Neandertals, it has been shown that this feature is present on around two thirds of the canines (BAILEY, 2006) but its significance in the attribution of sex is unknown and, therefore, reference



to it when assessing the sex of the mandible of *Sceladina* is unwise.

2.2.1.2. Internal morphology

Secondary dentine deposition could be related to sexual dimorphism; males would have thicker radicular dentine than females (SCHWARTZ & DEAN, 2005). A large root pulp volume is also considered a female trait, though little is known about the variability of sexual dimorphism in dental root dimensions of fossil populations, which calls for some caution in this regard (LE CABEC et al. this volume, Chapter 16).

2.2.2. Mandibular features

2.2.2.1. Development of the *incisura submentalis*

A decade ago, LOTH & HENNEBERG (1997) suggested that the development of the *incisura submentalis* at the base of the symphysis is usable as a reliable morphological indicator of sex in both modern and Palaeolithic mandibles. According to them, males would tend to exhibit a stronger and more frequent expression of this character than females. However, the validity of this criteria has not yet been rigorously tested.

2.2.2.2. Morphology of the chin

In modern humans, one of the classic traits used for sexing mandibles is the robust and square shape of the chin in males versus the small and rounded aspect with a point in the middle in females (FEREMBACH et al., 1980; BASS, 1986). Such a feature is totally inadequate for Neandertals as the structure of this region is very different (WEIDENREICH, 1936).

2.2.2.3. Mandibular ramus posterior flexure

According to LOTH & HENNEBERG (1996, 1998), the angulation of the posterior border of the mandibular ramus differs between modern males and females. In females it would be straight, whereas it would be angled at the level of the occlusal surface of the molar in males. The accuracy of the method would be of 94.2% on combined American and African subjects. However, blind tests conducted by other researchers to assess the precision of this method as an indicator of

sex provided a much lower overall probability of accuracy than that initially reported by Loth and Henneberg: below 70% or even much less (KOSKI, 1996; DONNELLY et al., 1998; HAUN, 2000; HILL, 2000; KEMKES-GROTTENTHALER et al., 2002; BALCI et al., 2005). LOTH & HENNEBERG (1997) also stated that the same differences in ramus shape are present on fossil material, notably on Neandertals, *Homo erectus* and australopithecines. Indeed, the Neandertal adolescent mandible of Le Moustier 1 might, at first glance, provide an argument in favour of Loth and Henneberg's technique. The distinctive flexure of the posterior border of the ramus is present, suggesting that the fossil is likely male and is in accordance with other sex indicators, e.g. cranial capacity, dental metrics and femoral head diameter (THOMPSON & NELSON, 2005). On the contrary, a test conducted on three Neandertal and three Early Modern Human mandibles whose sex had already been estimated from the associated os coxae – the bones that exhibit most sexual dimorphism in adults – produced results which drastically contrasted with those published by Loth and Henneberg (COQUEUGNIOT et al., 2000). The three Neandertal mandibles turned out to be male according to the hip bone but female according to the posterior flexure of the mandibular ramus, while two of the three Early Modern Human mandibles also provided opposite sexual diagnoses. Therefore, it seems that the potential usefulness of the presence or absence of a distinctive flexure on the posterior margin of the mandibular ramus in the determination of sex for fossil hominids could have been largely overestimated.

2.2.2.4. Gonial Eversion

Traditionally, gonial eversion of the mandible is cited as an adult male sex indicator (ASCÁDI & NEMÉSKERI, 1970; FEREMBACH et al., 1980). However, it has recently been proven that this criteria has 'a lower probability of determining sex than could be predicted by chance' and is consequently not a reliable indicator of sex (LOTH & HENNEBERG, 2000: 86; see also KEMKES-GROTTENTHALER et al., 2002 and OETTLÉ et al., 2009). Furthermore, it is well known that most Neandertal gonions are inwardly inflected (BILLY & VALLOIS, 1977: 420), even those that are clearly male, such as La Ferrassie 1. Therefore, this trait is inapplicable to this taxon.

3. Results

3.1. Teeth

3.1.1. Crowns

The breadth of the Scladina permanent mandibular right canine (Scla 4A-12) is 8.75 mm. By comparison with Oxnard's Neandertal bimodal distributions – 7.5 to 9.0 mm for probable females and 9.4 to 10.5 mm for probable males – such a dimension supports the hypothesis that the fossil might be female (Figure 1). This diameter is also below the average for the permanent mandibular canines of European Neandertal as computed by TRINKAUS (1983: 167), both sexes included: 9.2 mm \pm 0.8 (n = 29). The breadth of the permanent maxillary lateral incisors also has a bimodal distribution and the two specimens from Scladina (Scla 4A-14 and 17) also fit within the upper part of the female range (Figure 1).

However, compared to the crown area of the Atapuerca-SH sample (BERMÚDEZ DE CASTRO & NICOLÁS, 1997: 348), the Scla 4A-12 permanent mandibular canine is in an intermediate position (69.2) between the upper range of specimens referred to as females and the lower range of supposed males.

Using the crown area, the Scla 4A-6 permanent mandibular first premolar is also in the area where it is difficult to distinguish between males and females of Atapuerca-Sima del Huesos.

Table 1 presents MD and BL diameters and the calculated means of other permanent teeth, especially incisors and permanent maxillary canines, which are supposed to present significant sexual dimorphism according to OXNARD (1987). With regard to these dimensions, the Scladina fossils are either at the upper part of the female distribution – for instance breadth of the permanent mandibular central incisor Scla 4A-15 – or undetermined.

3.1.2. Roots

The short roots of these teeth would suggest that the Scladina Child may have been female (LE CABEC et al., this volume, Chapter 16).

In addition, the pulp cavity volumes of all the investigated Scladina teeth are among the largest of the Neandertal teeth, which would be another argument to suggest a female attribution (LE CABEC et al., this volume, Chapter 16).

3.2. Mandible corpus dimensions

Table 2 lists corpus dimensions of the Scladina mandible as well as comparable measurements from other immature Neandertals and Early Moderns aged from about 8 to 16 years.

The Scladina symphyseal height is 27.75 mm. The range of Neandertal females close in age extend from 22.0 mm in Montgaudier to 28.1 mm in Petit-Puymoyen, while the male range seems to

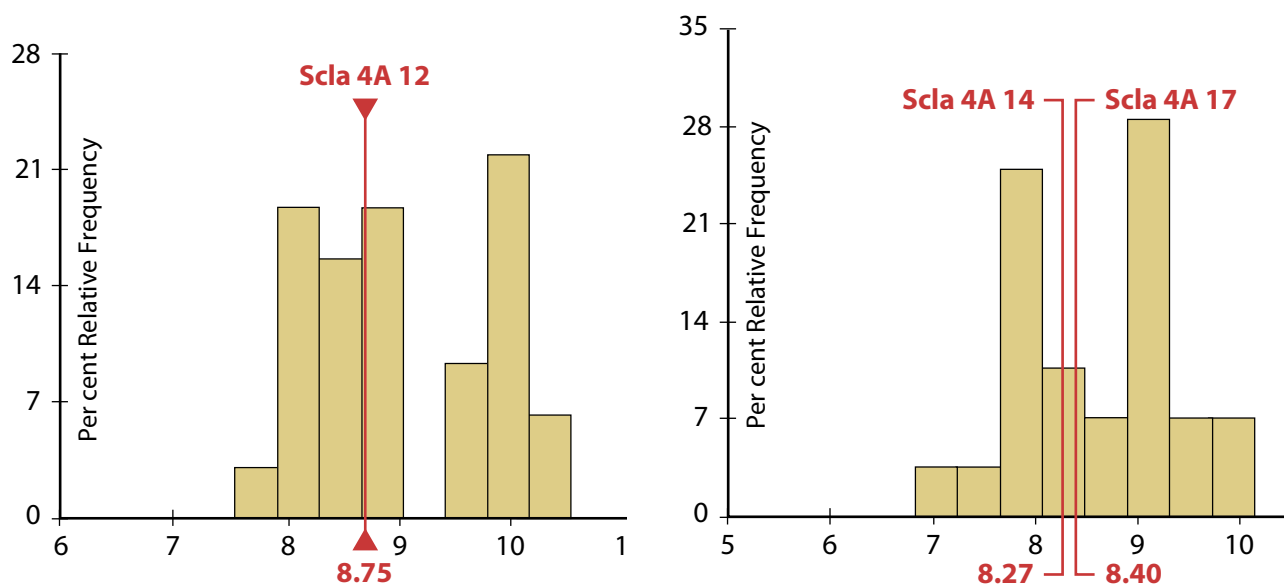


Figure 1: Left, permanent mandibular canine breadth (after OXNARD, 1987: 72); right, permanent maxillary lateral incisors breadth (after OXNARD, 1987: 74).



Permanent Tooth	Oxnard (1987)							Scladina			
	Measurement	Mode	Female	Transition	Male	Female mean	Male mean	Inventory number	Side	Dimension (mm)	Diagnosis
Mandibular central incisor	breadth	bimodal				7.0	8.0	Scla 4A-15	right	6.79	(female)
Mandibular lateral incisor	length	bimodal				6.2	7.5	Scla 4A-20	right	7.03	undetermined
Mandibular canine	breadth	bimodal	7.5–9.0	9.0–9.4	9.4–10.5	8.5	10.0	Scla 4A-12	right	8.75	female
Maxillary lateral incisor	length					7.2	8.4	Scla 4A-14	right	8.21	undetermined
								Scla 4A-17	left	8.38	undetermined
Maxillary lateral incisor	breadth	bimodal	6.9–8.5	8.5–8.9	8.9–10.25	8.0	9.2	Scla 4A-14	right	8.27	female
								Scla 4A-17	left	8.4	female
Maxillary canine	length					8.2	9.0	Scla 4A-18	left	8.6	undetermined
								Scla 4A-16	right	9.05	undetermined
Maxillary canine	breadth	bimodal	8.0–9.4	9.4–9.9	9.9–11.3	9.0	10.3	Scla 4A-18	left	9.95	undetermined
								Scla 4A-16	right	9.65	undetermined
Maxillary second molar	length					10.0	11.3	Scla 4A-3	right	10.21	(female)
Maxillary third molar	length	bimodal	8.2–8.7	8.7–9.9	9.9–11.4	8.8	10.1	Scla 4A-8	right	9.55	undetermined

Table 1: Ranges and means of some Neandertal teeth (OXNARD, 1987: 72, 74, 77, 81) compared with the Scladina teeth.

extend from 28.6 in Atapuerca–Sima del Huesos AT-607 Preneandertal to 30.6 mm in Valdegoba. According to its height, Scladina might be female, but that dimension is very close to the higher range of females, so near the interval where male and female dimensions overlap.

As far as symphyseal thickness is concerned, the Scladina jaw is quite small in comparison with other immature specimens of comparable age. In fact, only the Montgaudier and Petit-Puymoyen mandibles are slightly thinner. If all the sexual determinations of the fossils listed in Table 2 are correct, Scladina, with a symphyseal thickness of 12.36 mm, is clearly in the range of perceived Neandertal females of similar age. These values range from 11.8 mm at Montgaudier to 13.6 mm at Hortus 2-3 and might be extended to 14 mm if the Malarnaud mandible was proven to be female. Males are obviously thicker, 15 mm at Le Moustier 1 and 15.5 mm at Valdegoba.

Other measurements of the Scladina corpus thickness provide the same kind of results. Corpus thickness at the level of the canine, the first and second premolars as well as at the first molar is quite small; only the female mandible of Montgaudier has smaller dimensions. All males have much higher measurements than Scladina. Height measurements are less conclusive but Scladina always yields small or middle size results.

In conclusion, as far as corpus dimensions are concerned, the Scladina mandible is relatively small compared with a sample of other Neandertal mandibles of comparable ages at death. Such observations could tentatively indicate that the fossil is female.

3.3. Morphological mandibular features

The *incisura submentalis* of the Scladina mandible is only minimally expressed. According to LOTH & HENNEBERG’s observations (1997), this might suggest that the fossil belonged to a female.

The other possible morphological indicators of the sex of mandibles are not usable in the case of Scladina as it has been shown that they are not really reliable, especially for Neandertals.

4. Discussion

Oxnard’s technique is a valuable alternative in the analysis of Neandertal teeth as it avoids the problems encountered through the application of methods elaborated for the analyses of modern humans. (MADRE-DUPOUY, 1992). Based on Oxnard’s data, some of the teeth from Scladina fit within the female range, particularly the permanent mandibular canine which is one of the most informative teeth for the determination of sex. The dimensions of other teeth fall into the range of overlap between males and females. In addition, the MD and BL diameters of the Scladina teeth are almost always below the mean of supposed male Neandertals which might substantiate a female designation.

However, it seems important to ask oneself if the bimodal aspect of the curves of Oxnard is not, at least partially, an illusion. Can we really consider Neandertals as a homogeneous population? They were scattered over a wide geographic area (most of Europe and the Middle East) for hundreds of

Specimen	Taxon	Age at death (years)	Possible sex	Symphysis			Canine		P3		P4		M1		Reference
				Height	Thickness	Index (Th/H)	Height	Thickness	Height	Thickness	Height	Thickness	Height	Thickness	
Scladina 4A-9 (left)	Neandertal	8 (histology); 10–11 (anthropo)		27.75	12.36	44.5	26.32	13.1	13.2	(24.1)	13.2	(23.0)	14.2	MT, present paper	
Scladina 4A-1 (right)	Neandertal	8 (histology); 10–11 (anthropo)						(13.45)	(24.5)	23.9	13.1	22.2	14.0	MT, present paper	
Hortus 2-3	Neandertal	9	(Female)	25.0	13.6	54.4								DE LUMLEY-WOODYEAR, 1973: 345	
Montgaudier	Neandertal	12.5–14.5	Female	22.0	11.8	53.6	24.9	12.15	23.3	23.3	13.45	22.45	13.55	MAANN & VANDERMEERSCH, 1997	
Malarnaud 1	Neandertal	15	Female	25	14	56	24.4	14.9	20.9	20.9		21.5	16.1	MINUGH-PURVIS, 1988: 179, 185, 188; HEIM & GRANAT, 1995	
Petit-Puymoyen 1	Neandertal	16–17	Female	28.1	12.2	43.4	28.9		28.3	29.1		28.0		MINUGH-PURVIS, 1988: 179, 185	
Krapina E	Early Neandertal	15–17	Female	31.4	13.5 (14.1)		23.7	15.0	25.7	26.8	14.4	25.9	16.5	MINUGH-PURVIS, 1988: 179; 185, 188	
Valdegoba	Neandertal	13–14	Male	30.6	15.5	50.6		17.0	(16.9)		(16.6)		(16.6)	QUAM et al., 2001	
Le Moustier 1	Neandertal	15.5	Male	30.0	15.0	50.0	27.5	15.0	27.3	25.4	15.2	27.2	16.6	MINUGH-PURVIS, 1988: 179, 185, 188; THOMPSON & NELSON, 2005	
Atapuerca SH AT-607 (XXIII)	pre-Neandertal	Adolescent	Male	28.6	14.7	51.4					15.2 (P4/M1)			ROSAS, 1995	
Teshik-Tash 1	Neandertal	8.5–11		27.0	13.7	50.7	26.4	17.0	26.5	25.1	15.1	21.2	15.8	MINUGH-PURVIS, 1988: 179, 185, 187	
Zaskalnaya VI	Neandertal	9–10		30.0	13.4	44.7	19.8	14.0	(18.0)	21.4	13.6	20.7	13.8	MINUGH-PURVIS, 1988: 184, 187	
Sipka 1	Neandertal	9–10.5		28.4	14.0	49.3								MINUGH-PURVIS, 1988: 179	
Fate 2	Neandertal	9–10					(20.5)	(17.2)	(22.0)			18.5	14.0	GIACOBINI et al., 1984 & MT	
Krapina B (52)	Early Neandertal	9.5		26.0	(12.0)	(46.2)	(29.0)	15.6			17.9	23.5		MINUGH-PURVIS, 1988: 179; 184, 187	
Krapina C (53)	Early Neandertal	11		23.7	13.6	57.4	(26.0)	17.4		22.1	17.5	21.0	17.1	MINUGH-PURVIS, 1988: 179; 184, 187	
Ehringsdorf 7	Early Neandertal	12		28.3	15.3	54.1	25.6	15.6	(17.0)			20.8	(15.0)	MINUGH-PURVIS, 1988: 179	
Modern <i>Homo sapiens sapiens</i>		8–11		22.0–27.2	11.7–14.7		20.7–28.4	11.1–14.7	22.2–28.6	19.2–26.6	11.5–18.8	15.0–23.8	12.3–15.4	MINUGH-PURVIS, 1988: 179, 184, 185, 187, 188	
Modern <i>Homo sapiens sapiens</i>		10–12		21.3–30.4	12.0–16.9		24.8–28.8	10.3–14.9	18.9–27.8	19.8–27.0	11.4–14.1	15.2–25.2	13.7–17.3	MINUGH-PURVIS, 1988: 179, 184, 185, 187, 188	
Modern <i>Homo sapiens sapiens</i>		13–17		24.5–35.0	10.8–15.3		23.3–33.1	9.9–13.3	21.4–32.9	20.5–31.3	10.4–14.5	20.8–29.9	12.1–17.5	MINUGH-PURVIS, 1988: 179, 184, 185, 187, 188	

Table 2: Height, thickness and index of robusticity (thickness/height × 100) of mandibles at the symphysis, C, P₃, P₄s and M₁s.

millennia! If the Oxnard method was applied to a more limited region, such as the Belgian Meuse Basin as well as to fossils of the same period (for instance the OIS 3 Neandertals), the method might gain more credibility. Unfortunately, the extremely small samples of Neandertal teeth which can be employed in relatively small geographical areas make this attempt difficult.

MANN & VANDERMEERSCH (1997) also emphasize another problem with Oxnard's analysis. Indeed, Oxnard presents only some graphs and a summary table that identifies teeth with significant sexual dimorphism, but unfortunately, without providing numerical data to support his observations, which must therefore remain provisional.

In conclusion, even if the results of Oxnard are interesting and are increasingly used by scholars, they should only be accepted as presumption and not as unquestionable evidence. Only when they are in accordance with other kinds of results can they be trusted.

In this regard, it is interesting to note that the tooth roots in Scladina are very short and that their pulp cavities are very large. Most of the root dimensions of Scladina fall within the lower end of the Neandertal variation (LE CABEC et al., this volume, Chapter 16). These arguments support the hypothesis that Scladina would be female.

The measurements of the mandible are often used for sexing. The smallest, such as those of Montgaudier, are seen as females and the largest, such as Le Moustier 1, as males (MANN & VANDERMEERSCH, 1997). Obviously, this technique is size dependent. If fossil mandibles do exhibit sexual dimorphism, then the small size of the Scladina mandible suggests the specimen is female. However, the validity of this technique would be enhanced if a bimodal distribution was obtained from samples whose sex was previously determined using the pelvis.

The reliability of the shape of the *incisura submentalis* as a sex indicator is unknown, contrary to, for instance, the mandibular ramus posterior flexure.

To conclude this short discussion, it seems clear that the indications useful in determining the sex of a Neandertal mandible, especially a juvenile one, are indeed tenuous. We therefore have to admit that, as cautiously pointed out by HEIM (1981-1982: 462, 465) a third of a century ago, the sexual determination of an isolated mandible is often unfounded.

5. Conclusion

In view of the above-mentioned difficulties, it is clear that sexual determination of isolated Neandertal fossils, e.g. mandibles, should, in the future, be envisaged through approaches other than those exclusively based on morphology or morphometry. In this regard, nuclear DNA is sometimes able to provide good results (GREEN et al., 2006). Unfortunately, DNA is not always preserved, or not well preserved enough, especially in the case of very old fossils (over a hundred millenia) and discoveries from more than a few years. This reliable technique is therefore not applicable very often. Other methods such as the identification of the male form of the TRAP protein could help resolve this complication (NIELSEN-MARCH et al., 2009).

In the meantime, hopefully other fragments of the Scladina Child will be discovered in the years to come, possibly even some pelvic fragments, which are more diagnostic for determination of sex, although less reliable in the case of juveniles.

In conclusion and to refer to the question expressed in the title of this chapter, and even if it is tempting to suggest that the Scladina Child might be female, it is obvious that accurate sexing of this fossil is probably closer to a dream than to an objective achievement.

Acknowledgements

The author would like to thank Adeline Le Cabec, Max Planck Institute for Evolutionary Anthropology, Leipzig, Germany, and European Synchrotron Radiation Facility, Grenoble, France, for her valuable comments on the tooth roots. He also wishes to thank Cheryl Roy (Vancouver Island University) for her valuable comments and her help editing the English version of this chapter.

References

- ASCÁDI G. & NEMÉSKERI J., 1970. *History of Human life Span and Mortality*. Budapest, Akadémiai Kiadó, 346 p.
- BAILEY S.E., 2006. Beyond Shovel-Shaped Incisors: Neandertal Dental Morphology in a Comparative Context. *Periodicum Biologorum*, 108, 3: 253-267.

- BALCI Y., YAVUZ M. F. & CAĞDIR S., 2005. Predictive accuracy of sexing the mandible by ramus flexure. *Homo – Journal of Comparative Human Biology*, 55: 229–237.
- BASS W. M., 1986 (1971). *Human Osteology: a Laboratory and Field Manual on the Human Skeleton*. Columbia, Missouri Archaeological Society, 288 p.
- BERMÚDEZ DE CASTRO J. M., DURAND A. & IPIÑA S. L., 1993. Sexual dimorphism in the human dental sample from the SH site (Sierra de Atapuerca Spain): a statistical approach. *Journal of Human Evolution*, 24: 43–56.
- BERMÚDEZ DE CASTRO J. M. & NICOLÁS M. E., 1997. Palaeodemography of the Atapuerca-SH Middle Pleistocene hominid sample. *Journal of Human Evolution*, 33: 333–355.
- BILLY G. & VALLOIS H. V., 1977. La mandibule pré-rissienne de Montmaurin. *L'Anthropologie*, 81: 273–311 & 411–458.
- BOULE M., 1911–1913. *L'homme fossile de La Chapelle-aux-Saints*. Extraits des Annales de Paléontologie, 278 p.
- BOULINIER G., 1968. La détermination du sexe des crânes humains à l'aide des fonctions discriminantes. *Bulletins et Mémoires de la Société d'Anthropologie de Paris*, 3, XII^e série: 301–316.
- BRACE C. L., 1973. Sexual dimorphism and human evolution. *Yearbook of Physical Anthropology*, 16: 31–49.
- BRUZEK J., 2002. A method for visual determination of sex, using the human hip bone. *American Journal of Physical Anthropology*, 117: 157–168.
- COQUEUGNIOT H., TILLIER A.-M. & BRUZEK J., 2000. Mandibular ramus posterior flexure: a sex indicator in *Homo sapiens* fossil hominids? *International Journal of Osteoarchaeology*, 10, 6: 426–431.
- DE LUMLEY-WOODYEAR M.-A., 1973. *Anté-neandertaliens et Néandertaliens du bassin méditerranéen occidental européen*. Marseille, Études Quaternaires, 2, 626 p.
- DONNELLY S. M., HENS S. M., ROGERS N. L. & SCHNEIDER K. L., 1998. Technical note: a blind test of mandibular ramus flexure as a morphological indicator of sexual dimorphism in the human skeleton. *American Journal of Physical Anthropology*, 107: 363–366.
- FEREMBACH D., SCHWIDETZKY I. & STLOUKAL M., 1980. Recommendations for Age and Sex Diagnosis of Skeletons. *Journal of Human Evolution*, 9: 517–549.
- FRAIPONT J. & LOHEST M., 1887. La race humaine de Néanderthal ou de Canstadt en Belgique. Recherches ethnographiques sur des ossements humains découverts dans les dépôts quaternaires d'une grotte à Spy et détermination de leur âge géologique. Gand, *Archives de Biologie*, 7 (1886): 587–757, 4 pl. h.t.
- FRAYER D. & WOLPOFF M. H., 1985. Sexual Dimorphism. *Annual Review of Anthropology*, 14: 429–473.
- GARN S. M., COLE P. E. & VAN ALSTINE W. L., 1979. Sex discriminatory effectiveness using combinations of root lengths and crown diameters. *American Journal of Physical Anthropology*, 50: 115–117.
- GARN S. M., VAN ALSTINE W. L. JR & COLE P. E., 1978. Root-length and crown-size correlations in the mandible. *Journal of Dental Research*, 57: 114.
- GENOVES S., 1954. The problem of the sex of certain fossil Hominids with special reference to the neandertal skeleton from Spy. *Journal of the Royal Anthropological Institute*, 84: 131–144.
- GIACOBINI G., DE LUMLEY M.-A., YOKOYAMA Y. & NGUYEN H.-V., 1984. Neanderthal Child and Adult Remains from a Mousterian Deposit in Northern Italy (Caverna Delle Fate, Finale Ligure). *Journal of Human Evolution*, 13: 687–707.
- GILES E., 1964. Sex discrimination by discriminant function analysis of the mandible. *American Journal of Physical Anthropology*, 22: 129–135.
- GILES E. & ELLIOT O., 1963. Sex discrimination by discriminant function analysis of crania. *American Journal of Physical Anthropology*, 21: 53–58.
- GREEN R. E., KRAUSE J., PTAK S. E., BRIGGS A. D., RONAN M. T., SIMONS J. F., DU L., EGHOLM M., ROTHBERG J. M., PAUNOVIĆ M. & PÄÄBO S., 2006. Analysis of one million base pairs of Neanderthal DNA, *Nature*, 444, 16: 330–336.
- HAUN S. J., 2000. Brief communication: a study of the predictive accuracy of mandibular ramus flexure as a singular morphologic indicator of sex in an archaeological sample. *American Journal of Physical Anthropology*, 111: 429–432.



- HEIM J.-L., 1976. *Les Hommes Fossiles de La Ferrassie. Tome 1: Le Gisement. Les Squelettes adultes (Crâne et Squelette du Tronc)*. Archives de l'Institut de Paléontologie humaine, 35. Paris, Masson, 331 p.
- HEIM J.-L., 1981-1982. Le dimorphisme sexuel du crâne des hommes de Neandertal (suite). *L'Anthropologie*, 85/86, 3: 451-469.
- HEIM J.-L., 1982. *Les enfants néandertaliens de La Ferrassie. Étude anthropologique et analyse ontogénique des hommes de Néandertal*. Paris, Masson, Fondation Singer Polignac, 169 p.
- HEIM J.-L. & GRANAT J., 1995. La mandibule de l'enfant néandertalien de Malarnaud (Ariège). Une nouvelle approche anthropologique par la radiographie et la tomodensitométrie. *Anthropologie et Préhistoire*, 106: 75-96.
- HENRY-GAMBIER D., BRUZEK J., SCHMITT A., HOUËT F. & MURAIL P., 2007. Changement de paradigme dans la détermination du sexe et de l'âge au décès des sujets adultes à partir du squelette: application aux fossiles du Paléolithique supérieur d'Europe. *Un siècle de discours scientifique en préhistoire, vol. III: "Aux conceptions d'aujourd'hui"*. XXV^e congrès préhistorique de France, Avignon 21-25 septembre 2004: 515-525.
- HILL C. A., 2000. Technical note: Evaluating mandibular ramus flexure as a morphological indicator of sex. *American Journal of Physical Anthropology*, 111: 573-578.
- HOLLOWAY R. L., 1985. The poor brain of *Homo sapiens neanderthalensis*: see what you please... In E. DELSON (ed.), *Ancestors: The hard evidence*, New York: 319-324.
- HOWELLS W. W., 1965. Détermination du sexe du bassin par fonction discriminante: étude du matériel du Docteur Gaillard. *Bulletins et Mémoires de la Société d'Anthropologie de Paris*, 7, XI^e série, 1964: 95-105.
- JAKOBSSON R. & LIND V., 1973. Variation in root length of the permanent maxillary central incisor. *Scandinavian Journal of Dental Research*, 81: 335-338.
- KAJANOJA P., 1966. Sex determination of Finnish crania by discriminant function analysis. *American Journal of Physical Anthropology*, 24: 29-33.
- KEMKES-GROTTENTHALER A., LÖBIG F. & STOCK F., 2002. Mandibular ramus flexure ang gonial eversion as morphologic indicators of sex. *Homo — Journal of Comparative Human Biology*, 53, 2: 97-115.
- KOSKI K., 1996. Mandibular ramus flexure — indicator of sexual dimorphism? *American Journal of Physical Anthropology*, 101: 545-546.
- KROGMAN W. M. & İŞCAN M. Y., 1986. *The human skeleton in forensic medicine*. Springfield, Charles C. Thomas, second edition, 551 p.
- LÄHDESMÄKI R., 2006. *Sex chromosomes in human tooth root growth Department of Oral Development and Orthodontics*. University of Oulu, Finland, 65 p.
- LÄHDESMÄKI R. & ALVESALO L., 2007. Root lengths in the permanent teeth of Klinefelter (47,XXY) men. *Archives of Oral Biology*, 52: 822-827.
- LOTH S. R. & HENNEBERG M., 1996. Mandibular ramus flexure: a new morphologic indicator of sexual dimorphism in the human skeleton. *American Journal of Physical Anthropology*, 99: 473-485.
- LOTH S. R. & HENNEBERG M., 1997. Ramus flexure and symphyseal base shape: sexually dimorphic morphology in the premodern hominid mandible. *American Journal of Physical Anthropology*, Abstract: 157-158.
- LOTH S. R. & HENNEBERG M., 1998. Mandibular ramus flexure is a good indicator of sexual dimorphism. *American Journal of Physical Anthropology*, 105: 91-92.
- LOTH S. R. & HENNEBERG M., 2000. Gonial eversion: facial architecture, not sex. *Homo — Journal of Comparative Human Biology*, 51, 1: 81-89.
- MADRE-DUPOUY M., 1992. *L'enfant du Roc de Marsal. Étude analytique et comparative*. Paris, Éditions du Centre national de la recherche scientifique, Cahiers de Paléanthropologie, 300 p.
- MAJO T., 1992. Ontogenèse de l'os coxal et détermination sexuelle: l'importance de l'ilium. *Bulletins et Mémoires de la Société d'Anthropologie de Paris*, 4: 53-65.
- MANN A. & VANDERMEERSCH B., 1997. An Adolescent Female Neandertal Mandible from Montgaudier Cave, Charente, France. *American Journal of Physical Anthropology*, 103: 507-527.

- MARTIN H., 1923. *Recherches sur l'Évolution du Moustérien dans le Gisement de La Quina. Tome 3. L'Homme fossile de La Quina*. Archives de Morphologie générale et expérimentale, 15. Paris, Doin, 264 p.
- MINUGH-PURVIS N., 1988. *Patterns of craniofacial growth and development in Upper Pleistocene Hominids*. PhD thesis, Philadelphia, University of Pennsylvania, 657 p.
- NIELSEN-MARSH C., STEGEMANN C., HOFFMAN R. SMITH T. M., FEENEY R., TOUSSAINT M., HARVATI K., PANAGOPOULOU E., HUBLIN J.-J. & RICHARDS M. P., 2009. Extraction and sequencing of human and Neanderthal mature enamel proteins using MALDI-TOF/TOF MS. *Journal of Archaeological Science*, 36: 1758-1763.
- OETTLÉ A. C., PRETORIUS E. & STEYN M., 2009. Geometric morphometric analysis of the use of mandibular gonial eversion in sex determination. *Homo – Journal of Comparative Human Biology*, 60: 29-43.
- OXNARD C. E., 1987. *Fossils, teeth and sex. New Perspectives on Human Evolution*. Seattle & London, University of Washington Press, 281 p.
- QUAM R. M., ARSUAGA J.-L., BERMÚDEZ DE CASTRO J.-M., DÍEZ J. C., LORENZO C., CARRETERO J. M., GARCÍA N. & ORTEGA A. I., 2001. Human remains from Valdegoba Cave (Huérmeces, Burgos, Spain). *Journal of Human Evolution*, 41: 385-435.
- ROGERS T. L., 1999. A Visual method of Determining the Sex of Skeletal Remains Using the Distal Humerus. *Journal of Forensic Sciences*, 44, 1: 57-60.
- ROSAS A., 1995. Seventeen new mandibular specimens from the Atapuerca/Ibeas Middle Pleistocene Hominids sample (1985-1992). *Journal of Human Evolution*, 28: 533-559.
- SCHWARTZ G. T. & DEAN M. C., 2005. Sexual dimorphism in modern human permanent teeth. *American Journal of Physical Anthropology*, 128: 312-317.
- SCOTT G. R., 1977. Classification, sex dimorphism, association and population variation of the canine distal accessory ridge. *Human Biology*, 49: 453-469.
- SCOTT G. R. & TURNER C. G. II, 1997. *The anthropology of modern human teeth. Dental morphology and its variations in recent human populations*. Cambridge University Press, 382 p.
- SMITH F. H., 1976. *The Neanderthal remains from Krapina. A descriptive and comparative study*. Report of Investigations, 15, Knoxville, Department of Anthropology, University of Tennessee, 359 p.
- SMITH F. H., 1980. Sexual differences in European Neanderthal crania with special reference to the Krapina remains. *Journal of Human Evolution*, 9: 359-375.
- TEILHOL V., 2001. *Contribution à l'étude individuelle des ossements d'enfants de La Chaise de Vouthon (Charente, France): Approche paléodémographique, paléoethnologique, aspect morphologique et étude métrique. Place phylogénique des enfants de La Chaise*. Unpublished PhD thesis, Université de Perpignan, Centre Européen de Recherche Préhistorique de Tautavel, 2 vol., 160 p. & annexes.
- THOMA A., 1975. Were the Spy Fossils Evolutionary Intermediates between Classic Neanderthal and Modern man? *Journal of Human Evolution*, 4: 387-410.
- THOMPSON J. I. & NELSON A. J., 2005. Estimated Age at death and sex of Le Moustier 1. In H. ULRICH (ed.), *The Neanderthal Adolescent Le Moustier 1. New aspects, new results*. Berlin, Staatliche Museum zu Berlin, Berliner Beiträge zur Vor- und Frühgeschichte, 12: 208-222.
- TRINKAUS E., 1980. Sexual differences in Neanderthal limb bones. *Journal of Human Evolution*, 9: 377-397.
- TRINKAUS E., 1983. *The Shanidar Neanderthals*. New York, Academic Press, 502 p.
- VANDERMEERSCH B., 1965. Position stratigraphique et chronologique relative des restes humains du paléolithique moyen du Sud-Ouest de la France. *Annales de Paléontologie (Vertébrés)*, 51: 69-126.
- VERNA C., 2006. *Les restes humains moustériens de la Station Amont de La Quina – (Charente, France). Contexte archéologique et constitution de l'assemblage. Étude morphologique et métrique des restes crânio-faciaux. Apport à l'étude de la variation néandertalienne*. Unpublished PhD thesis, Anthropologie biologique, Université de Bordeaux 1, 629 p.
- WEIDENREICH F., 1936. *The mandibles of Sinanthropus Pekinensis: a comparative study*. Palaeontologia Sinica, Series D, vol. VII, fasc. 3, Peiping, Geological Survey of China, 132 p., 15 pl.



WOLPOFF M. H., 1976. Some aspects of the evolution of early hominid sexual dimorphism. *Current Anthropology*, 17: 574-606.

WOLPOFF M. H., 1979. The Krapina dental remains. *American Journal of Physical Anthropology*, 50: 67-114.

Michel TOUSSAINT

Michel Toussaint & Dominique Bonjean (eds.), 2014. The Scladina I-4A Juvenile Neandertal (Andenne, Belgium), Palaeoanthropology and Context Études et Recherches Archéologiques de l'Université de Liège, 134: 179-214.

1. Introduction

Mandibles are among the most frequently studied bones within the corpus of hominin fossils. These studies mainly concern patterns of growth and development as well as phylogenetic relationships. Regarding Neandertals, one of the limitations in these studies is the relatively small number of available immature mandibles in each age group and at every stage of their evolution, at least from MIS 8 – and from MIS 12 or even 13 for the first appearance of some Neandertal features – to MIS 3. In addition, most of the known specimens are incomplete or at worst very fragmentary. As a result (MANN & VANDERMEERSCH, 1997), fossils originating from sites all over Europe and the Near-East must be used in order to have a graduated series of Neandertal specimens from infancy to adulthood, which may unfortunately introduce bias that complicates the decoding of the influence of other features. Furthermore, it has to be considered that the determination of the age of Neandertal fossils can vary depending on the methods used as most of them are conventional methods of anthropology originally designed for modern populations applied to Neandertals, sometimes with some random corrections. Newer determinations, like on Scla 4A-1 & 9, are sometimes based on the most recent histological techniques. Another problem that can be encountered is the difficulty of taking into account differences related to sexual dimorphism, which is very difficult to evaluate on fossils and particularly on isolated specimens not associated with innominate bones, as is the case for Scla 4A-1 & 9.

Despite such challenges, the Scla 4A-1 & 9 hemimandibles (Figure 1), the two parts of the Scladina I-4A specimen, are of great interest.

The first quality of the specimen is that it is one of the most well-preserved Eurasian Neandertal juvenile mandibles and by far the most complete from the Meuse Basin. In fact, although about 25% of the entire Neandertal remains are

immature individuals (TILLIER, 1995; MANN & VANDERMEERSCH, 1997), most of them are more or less fragmentary, which further accentuates the interest of this mandible.

A second essential interest of the specimen is its biological age since immature fossil bones, notably mandibles and maxillae, are uncommon in the European Neandertal age group represented on Scladina I-4A (MINUGH-PURVIS, 1988).

Finally, a third major interest of the mandible is its antiquity which likely corresponds to MIS 5 b-a – or less probably to the very beginning of MIS 4 – a period in which Neandertal fossils are rare in northwestern Europe. In this regard, most of the Belgian Neandertals belong to MIS 3, i.e. Spy, Couvin, Walou and Goyet. In fact, at the scale of the Belgian Meuse Basin, six complete and partial mandibles have been found since the beginning of palaeoanthropological research, at the end of the third decade of the 19th century



Figure 1: Scladina mandible (Scla4A-1 & 9) without the refitted teeth found isolated in the cave sediments (photograph Joël Éloy, AWEM).





Figure 2: Scla 4A-1 right hemimandible: a. superior view; b. inferior view (photographs Joël Éloy, AWEM).

(TOUSSAINT, 2001; TOUSSAINT et al., 2011). Four of these belong to adults, i.e. the famous La Naulette specimen (DUPONT, 1866; LEGUEBE & TOUSSAINT, 1988), two from Spy (FRAIPONT & LOHEST, 1887; THOMA, 1975) and one from Goyet (ROUGIER et al., 2009). The two remaining mandibles belong to children: the partial Spy VI (CREVECOEUR et al., 2010) and Scladina I-4A (TOUSSAINT et al., 1998). This information also means that one or more mandibles, nearly complete or fragmented, have been found in half of the Mosan Neandertal fossil sites. It is also of importance to note that by adding the teeth of Engis (TILLIER, 1983^a), Couvin (TOUSSAINT et al., 2010) and Walou (TOUSSAINT, 2011), as well as the maxillary molar, now lost, found at Fonds de Forêt (TWIESELDMANN, 1961), all regional Mosan Neandertal sites have yielded mandibular remains. At Fonds de Forêt however, it is not possible to be certain that the lost molar is really from the same taxon as the partial femur found on this site.

The Scla 4A-1 & 9 mandible examined here was never before completely analysed and only briefly described in preliminary papers (especially TOUSSAINT et al., 1998).

2. Discovery and preservation —

The Scla 4A-1 & 9 mandible was found in two major pieces, with, in addition, a set of teeth discovered separately and found scattered in the sediments of different layers of Sedimentary Complex 4A (see Chapter 5). Altogether, the different bones and teeth belonging to the

mandible were found in an elliptical area of about 13 m in length and 5 m wide. They were discovered in the stratigraphical units 4A-CHE and 4A-POC, at least in secondary position.

The largest portion of the mandible, referred to as Scla 4A-1 (Figure 2), was found on July 16, 1993 in Square D29. Although not immediately authenticated as a Neandertal in the field (BONJEAN et al., 2009), its position was precisely recorded in situ as is the case for thousands of bones found in Scladina Cave. The fossil consists of the biggest part of a right hemimandible including the ramus and much of the corpus of which the anterior part, that is to say the area before the middle of the socket of the canine, is missing. Four permanent teeth are present, i.e. the completely erupted M_1 , the nearly erupted M_2 , the germ of M_3 , partially visible in occlusal view in its already open socket, as well as the unerupted P_4 , which had to be studied using X-rays and micro-CT. The bone is dense. No indications of pathology are present. A small splinter belonging to the upper part of the anterior border of the right ramus was detached during the excavation process and was latter refitted. This right hemimandible is fossilized. Its surface is slightly polished; but, this may have been accentuated by the wax used in moulding the fossil. The main colours are grey and pale yellow. Small and thin cracks, mainly parallel to the longitudinal axis of the body, are present (beginning of stage 1 of BEHRENSMEYER, 1978). No manganese coating was present. No rodent or carnivore marks were observed. The anterior break corresponds to that of Scla 4A-9: vertical in its two upper thirds, then slightly distally oblique. The gonion is eroded. The internal part of the condyle is eroded while the external one is partially missing.

The second portion of the mandible, Scla 4A-9 (Figure 3), was found 3 years after the first part, on July 12, 1996 in Square C28, at a horizontal distance of about 1 m from Scla 4A-1. The fossil, immediately identified as human, is represented by the anterior part of the right corpus (missing on Scla 4A-1), the symphysis and the left corpus. The left ramus is missing. Three permanent left teeth are present, i.e. the completely erupted M_1 , the nearly erupted M_2 , and the unerupted P_4 . The fossil exhibits numerous thin cracks, mainly horizontal but also vertical. Manganese coats both sides, generally as small stains, but sometimes fused; in most cases, a manganese coating covers the cracks. Excavation damage, i.e. marks



Figure 3: Scla 4A-9 left hemimandible: a. superior view; b. inferior view (photographs Joël Éloy, AWEM).

of an metal scraper used by the excavator, is also present, mainly on the inner face. Scla 4A-9 is not as heavy as 4A-1. The color is different from the other side of the mandible: its main colours are dull yellow orange and light yellow orange.

Both Scla 4A-1 and 4A-9 can be perfectly refitted. The mandible, taken as a whole, is nearly undistorted and fairly well preserved. The right part (Scla 4A-1) articulates with the maxillary fragment Scla 4A-2. Some isolated teeth were refitted on both parts of the mandible (see Chapter 13).

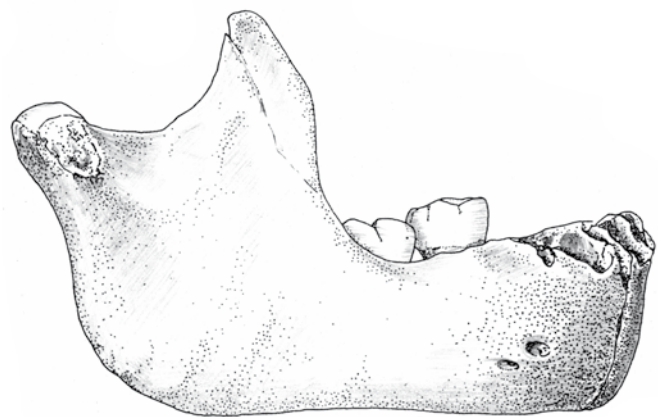


Figure 4: Scladina mandible (Scla 4A-1 & 9) viewed from the right side showing the receding symphyseal region (photograph Joël Éloy, AWEM; drawing Sylviane Lambermont, AWEM).

3. Age and sex

Initially estimated at around 10-11 years using conventional methods (OTTE et al., 1993; TOUSSAINT et al., 1998), the subject's age has been determined more precisely to 8 years thanks to a histological study (SMITH et al., 2007; see also Chapter 8). The sex of an isolated fossil mandible, especially one belonging to a juvenile, is virtually impossible to determine with certainty. In the case of Scladina I-4A, however, various features of the teeth and the mandible might suggest a female (see Chapter 9).

4. Mandibular morphology

4.1. Symphyseal region

4.1.1. Description

4.1.1.1. Anterior face

Viewed from the side with the fossil resting on its base, the anterior profile of the symphyseal region (Scla 4A-9) leans slightly backward (Figure 4). In fact, when the mandible lies on its inferior border, its anterior face is entirely hidden in superior view (Figure 5). By contrast, this face is perceptible in modern juveniles due to a prominent mental protuberance.

The anterior face of the symphyseal region (Figure 6) only shows a very slight depression which could suggest the presence of a faint *incurvatio mandibulae anterior*. The Scla 4A-9 *mentum osseum* rank is only 2 according to DOBSON & TRINKAUS' (2002) terminology. The outline of a non-projecting *tuber symphyseos*, or symphyseal



Figure 5: Scladina mandible (Scla 4A-1 & 9) in superior view (photograph Joël Éloy, AWEM; drawing: Sylviane Lambermont, AWEM).



Figure 6: Scladina mandible (Scla 4A-1 & 9), anterior face of the symphyseal region (photograph Joël Éloy, AWEM).

tubercle, can be observed along the midline approximately a third of the way up from the base; but, the specimen lacks the lateral tubercles (*tubercula lateralia*) and, therefore, there is no clearly defined modern human-like protruding mentum osseum or “chin”. Between

both anterior walls of the central incisors, on Scla 4A-9, is a faint vertical ridge which corresponds to the symphysis.

4.1.1.2. Posterior surface of the symphysis

The superior third of the posterior surface (Figure 7) of the Scla 4A-9 symphysis recedes obliquely backwards, producing a relatively well expressed alveolar plane (*planum alveolare*). This inclined area is delineated superiorly by the alveolar posterior border of the sockets of the incisives and canines and inferiorly by the superior transverse torus (Figures 8 & 9). This thickening (*torus transverses superior* or *margo terminalis*) extends laterally to about the level of the P₃, then becomes indistinguishable. Both the *planum* and the torus are vertically divided by a thin groove which is the remnant of the fusion of both hemimandibles (*crista interincisiva interna*). The *planum* itself is slightly concave, which could correspond to very weak *fossae subincisivae internae*.

In the upper part of the *planum* is one vascular foramen on each side of the sagittal suture. The left one has a diameter of around 0.75 mm and is at 4 mm from the suture and at around 3 mm below the alveolar border. The right one is slightly below, at around 3.5 mm from the alveolar border, and at 4.7 mm from the suture; its diameter is about 0.5 mm.

The well marked genioglossal fossa (*fossula supraspinata*) is overhung by and just below the superior transverse torus. This fossa opens slightly below the mid-level of the mandible and is transversally oval. Its depth is 1.4 mm. A genial canal (*foramen supraspinosum*) is present at the deepest part of the fossa. One small adjacent foramen is present in both lateral parts of the fossa, 5 mm from the genial canal and around 1 mm below the level of its centre.

The genioglossal fossa is bounded below by the inferior transverse torus (*torus transverses inferior* of Holl), which is a thickening of the posterior part of the base of the mandible. In inferior view, the inferior transverse torus appears to be less developed in its postero-central part, a few millimeters on each side of the vertical axis of the symphysis. Laterally, the torus bulges forming two excrescences, the ‘transverse rolls’ (“*éminences arrondies*”, parts of the “*bourrelet transversal*” of PIVETEAU, 1963: 302), and extends, although increasingly less marked, to the level of the P₃-P₄ septum.

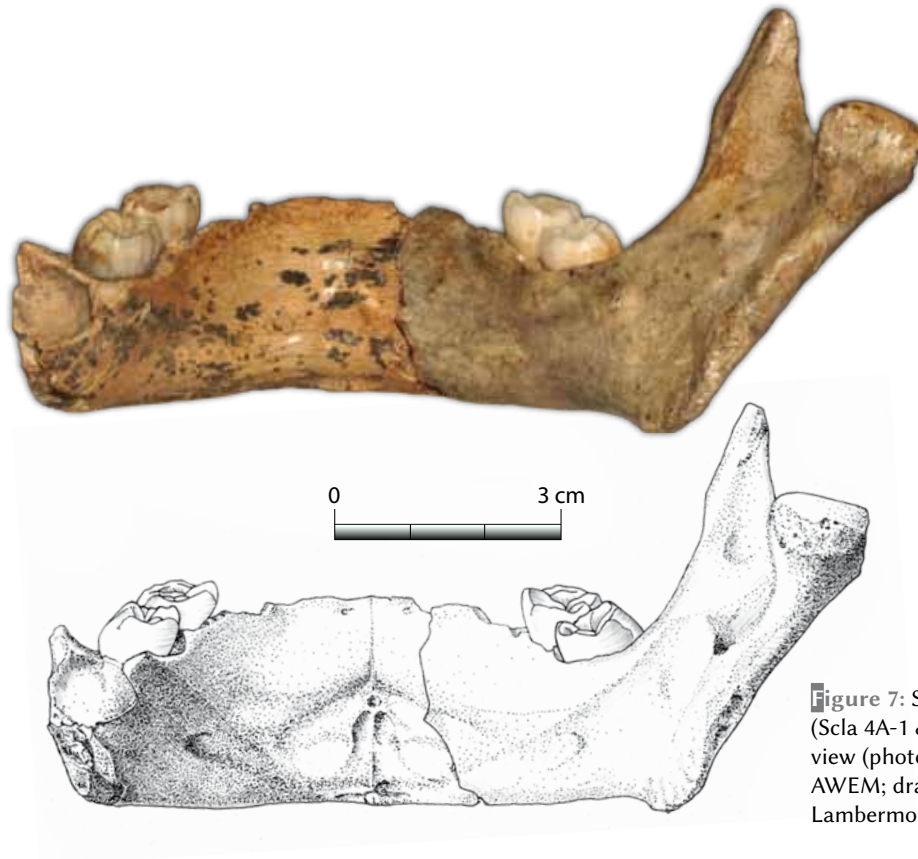


Figure 7: Scladina mandible (Scla 4A-1 & 9), posterior view (photograph Joël Éloy, AWEM; drawing Sylviane Lambermont, AWEM).

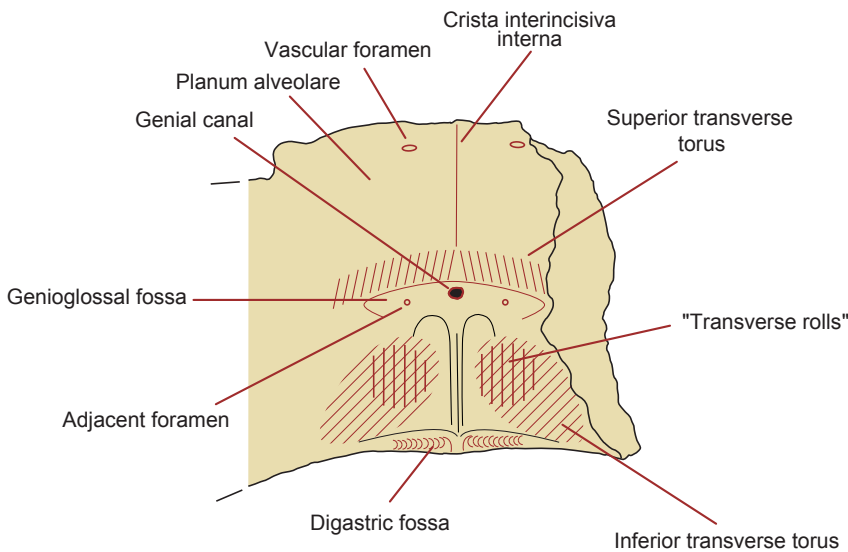


Figure 8: Scladina hemimandible (Scla 4A-9), posterior surface of the symphysis (graphics Sylviane Lambermont, AWEM).

The lower part of the genioglossal fossa is vertically divided by three parallel sagittal ridges which join just below the genial canal: a sagittal one, and two lateral curved ones. These three crests are the mental spine (*spina mentalis* of WEIDENREICH, 1936: 45). The two small vertical areas between the three crests are slightly depressed. The two lateral spines end at the superior inner part of the excrescences (“bour-relets transversaux”) while the central mental

spine goes down between the excrescences and continues between the digastric fossae as a series of very fine accessory crests which form the interdigastric spine.

4.1.1.3. Alveolar border

In the occlusal view, the alveoli of the incisors and, to a lesser extent, of the canines, as well as the teeth themselves, tend to be placed in a

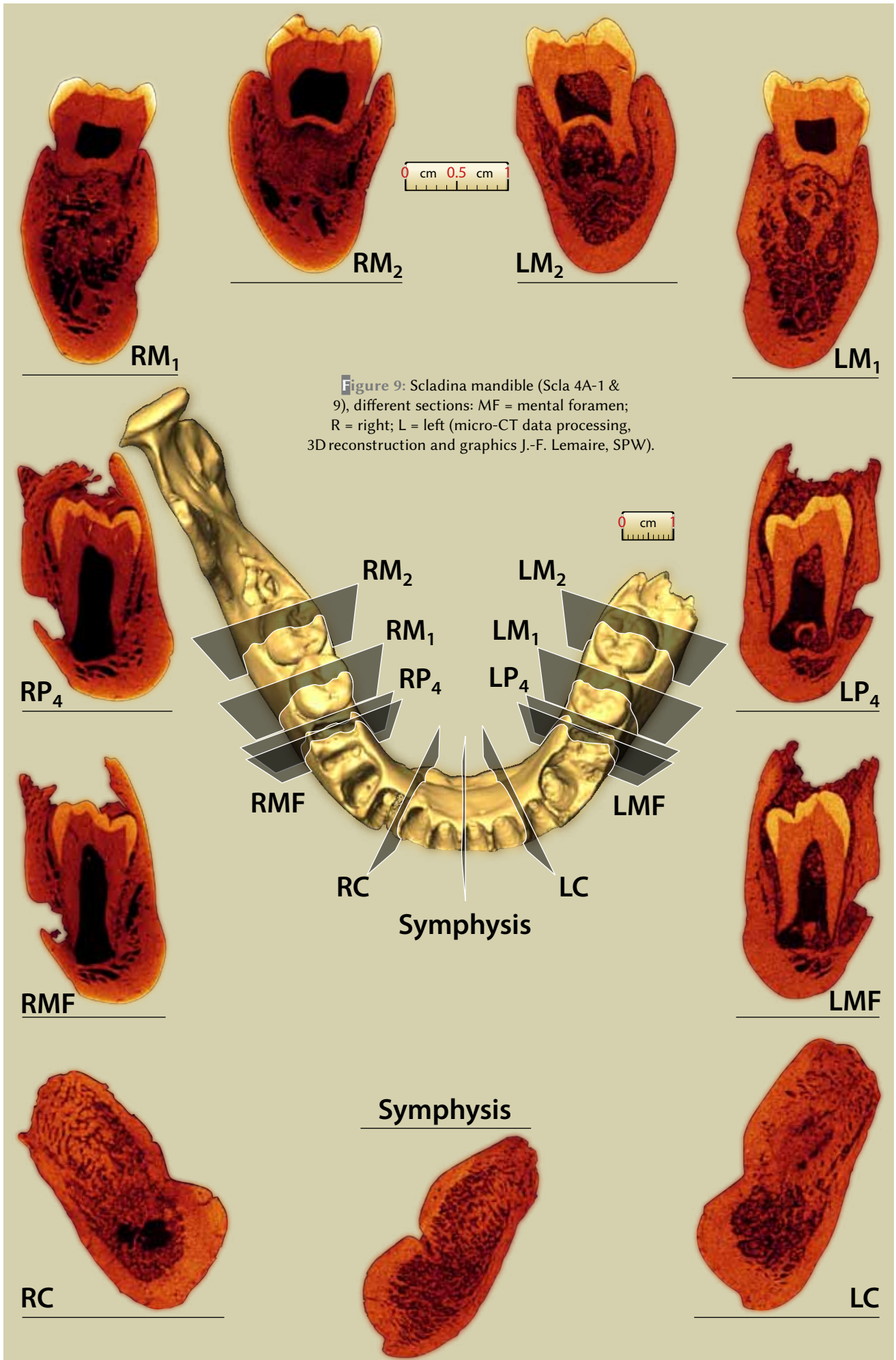


Figure 9: Scladina mandible (Scla 4A-1 & 9), different sections: MF = mental foramen; R = right; L = left (micro-CT data processing, 3D reconstruction and graphics J.-F. Lemaire, SPW).

frontal alignment, although slightly arched from side to side. In other words, the main axis of the central incisors is antero-posterior, the axis of the lateral incisors is nearly antero-posteriorly orientated while that of the canines is slightly laterally turned.

In superior view, the width of the central incisor alveolus is 4.7 mm and that of the lateral ones 5.5 mm. The antero-posterior diameters of these teeth cannot be measured precisely as the anterior walls of the upper part of the corresponding sockets are strongly eroded. Nevertheless, the sockets of the lateral incisors are slightly longer than those of the central ones. The mesiodistal diameter of the left canine socket is around 6.8 mm.

4.1.1.4. Inferior border

On the inferior part of the symphyseal region, the digastric fossae, attachment sites for the digastric muscles, are well marked (Figure 10). They face inferiorly and slightly downwards, are oval in shape, and are separated from each other by the interdigastric spine, an extension of the mental

spine. The dimensions of the digastric fossae are around 14.5 mm × around 7.5 mm on both sides.

On the basal symphysis, there is a slight arch corresponding to a very weak *incisura submentalis*. As already pointed out, conspicuous arches are usually associated with developed anterior marginal tubercles (ROSAS, 1995: 552; QUAM et al., 2001: 397; DAURA et al., 2005: 63). The fact that the *incisura submentalis* appears to be weakly expressed correlates well with the weakness of the corresponding anterior marginal tubercles.

4.1.2. Taxonomy

Some important features observed on the symphysis of the mandible (Scla 4A-9) are archaic/plesiomorphic as on the other immature Neandertal mandibles (TILLIER, 1983^b: 143; TILLIER, 1991: 109):

- on the anterior face, the absence of a modern chin with all its components (RAK et al., 2002);
- on the posterior face of the symphysis, a distinct *planum alveolare* (TILLIER, 1979; HUBLIN & TILLIER, 1981; RIGHTMIRE, 1990; QUAM et al.,

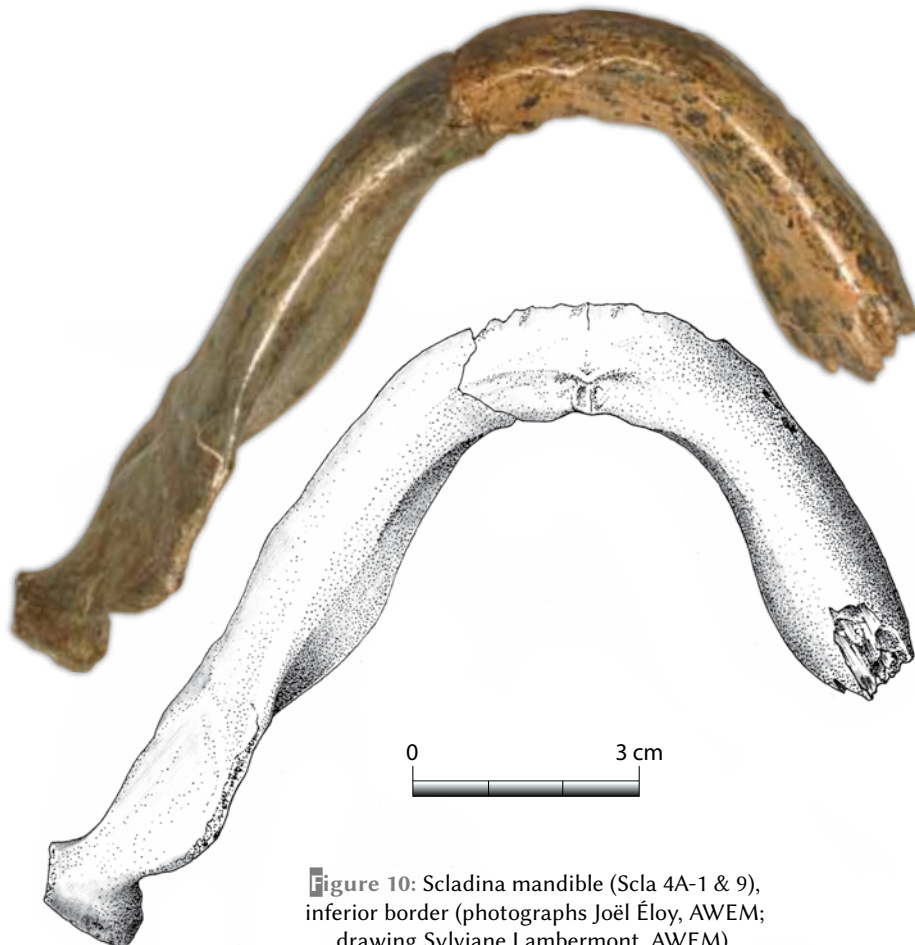


Figure 10: Scladina mandible (Scla 4A-1 & 9), inferior border (photographs Joël Éloy, AWEM; drawing Sylviane Lambermont, AWEM).



- 2001: 400, 429; DAURA et al., 2005: 62), a superior transverse torus (HUBLIN & TILLIER, 1981) and a genioglossal fossa (*fossula supraspinata*; TILLIER, 1979; HUBLIN & TILLIER, 1981; TILLIER, 1986: 214);
- on the inferior border, a nearly inferior orientation of the digastric fossae (TILLIER, 1984; RIGHTMIRE, 1990; HEIM & GRANAT, 1995; DAURA et al., 2005), whereas modern humans usually have more posteriorly-facing fossae.

Frontal alignment of the anterior alveoli and teeth is common, but not constant, among Neandertals, including juveniles (VANDERMEERSCH, 1981: 152; TILLIER, 1986: 209, 213; 1991: 110). However, the morphologically modern immature Qafzeh 11 mandible in a Mousterian context (TILLIER, 2002; DAURA et al., 2005) shows a frontal alignment. So, the taxonomic inferences which could be drawn on this feature are likely not really founded and this feature cannot be considered as derived (HEIM & GRANAT, 1995: 85).

4.2. Mandibular body

4.2.1. Height and thickness

The height of the mandibular body (or lateral corpus or horizontal ramus) decreases and is progressively thickened from the front to the rear. This characteristic is often seen as modern (VANDERMEERSCH, 1981: 147–148), but the analysis of a modern collection (Place Saint-Lambert in Liège; personal observation) suggests that it has little taxonomic value in juveniles as all combinations of these two measurements are present.

4.2.2. Description

4.2.2.1. External aspect

On both sides, the lateral prominence (*protuberantia lateralis*) is at the level of M_2 , but has only vague outlines (Figures 11–13). Other reliefs are very poorly expressed and difficult to individualize as the outer face is smooth. The weakly discernible superior lateral torus (*torus lateralis superior*, WEIDENREICH, 1936: 24, or *torus marginalis superior*, ROSAS, 1995), the upper anterior branch of the lateral prominence, makes its way towards the upper part of the mental foramen. Above the lateral prominence and the superior lateral torus is the extramolar sulcus (*sulcus extramolaris*, KEITER, 1935; WEIDENREICH, 1936: 24). Below the superior lateral torus, the *sulcus intertoralis* (WEIDENREICH, 1936: 24) is not really present, just as a very shallow depression barely palpable below and behind the foramina, especially on the left side (Scla 4A-9). The weak marginal rim (*torus marginalis inferior*; WEIDENREICH, 1936: 24) blends into the inferior border of the corpus.

The anterior marginal tubercle (*tuberculum marginale anterius*) is only weakly expressed; on the right side (Scla 4A-1), it is along the external edge of the basal border, at the level of P_4 , below the posterior part of the biggest mental foramen and below the bridge of bone between both foramina.

The left mental foramen (Scla 4A-9; Figure 14a) is located at the level of the still included P_4 and has the aspect of a postero-inferior irregular oval depression in which two foramen open, one inferiorly and slightly inferiorly and the second anteriorly. The longitudinal diameter of the depression is about 5.5 mm and its height nearly 4.1 mm.

The right foramen (Scla 4A-1; Figure 14b) is duplicated. The main aperture, 4.4 mm long and 2.7 mm high, is at the level of the embedded P_4 and



Figure 11: Scla 4A-1 right hemimandible, external aspect (photograph Joël Éloy, AWEM).



Figure 12: Scla 4A-9 left hemimandible, external aspect (photograph Joël Éloy, AWEM).

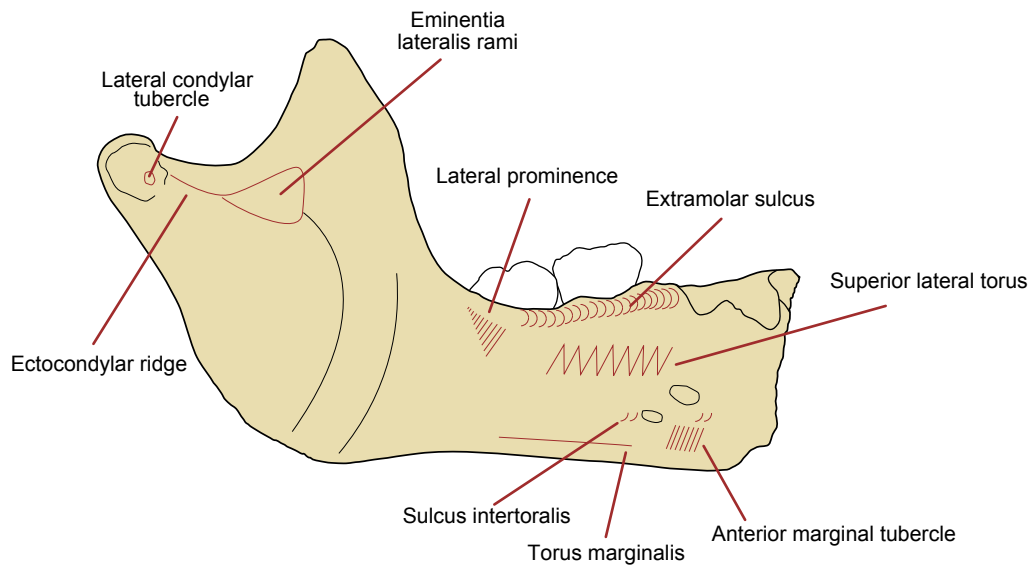


Figure 13: Scladina right hemimandible (Scla 4A-1), external aspect of the body (graphics Sylviane Lambermont, AWEM).

is posteriorly orientated. The accessory foramen (3.8×2.0 mm) is behind and slightly below the main one, at which it is internally connected but externally separated by a bony bridge of ± 2.8 mm; this foramen just at the level of the septum between P_4 and M_1 , and is posteriorly orientated. A bridging of the mental foramen has been reported on other Neandertals: adults as the Regourdou right ramus (PIVETEAU, 1963-1966); adolescents or young adults such as Cova del Gegant (DAURA et al., 2005) or juveniles such as Combe-Grenal (GARRALDA & VANDERMEERSCH, 2000).

The left mental foramen and the main right one are on the lower half of the mandibular body, but just below the middle of the body height. The

small right foramen is near the limit between the middle and lower third of the ramus. Different methods are used to assess this low position. The Virchow index compares the distance from the center of the aperture to the basal border (A) with the corpus height (B) at that level ($I = 100 \times A / B$). Some other authors compare the distance from the mental foramen to the basal border and to the alveolar border (ROSAS, 1995: 552-553). Table 1 provides all these measurements for Scla 4A-1 and 4A-9 as well as for some other (pre-) Neandertal and modern mandibles. It confirms that on both sides of the Scladina I-4A mandible, the main mental foramen is located in the upper part of the lower half of the corpus.



Figure 14: Scladina mandible, mental foramen: a. left (Scla 4A-9); b. right (Scla 4A-1; photographs Joël Éloy, AWEM).



Specimen	Age at death			Mental foramen				Reference
	Classic	Histology or Granat's technique	Class	Height of corpus	Height from basal margin	Height to alveolar margin	Virchow index	
Scla 4A-9 (left)	10-11 yrs	8 yrs	S3	24.5	11.0	13.5	44.9	Present author (M. T.)
Scla 4A-1 (right)				23.9	10.3	13.6	43.1	Present author (M. T.)
Ehringsdorf 6 (F, 109/69; right)	adult			27	15	12	55.5	VLČEK, 1993: 128, 130, 136
Ehringsdorf 6 (F, 109/69; left)				27	13.5	13.5	50	VLČEK, 1993: 128, 130, 136
La Naulette	adult			25	12		48	LEGUEBE & TOUSSAINT, 1988
Mauer	adult			34	18		53	BILLY & VALLOIS, 1977
Montmaurin	adult			29	15		51.7	BILLY & VALLOIS, 1977
Bañolas (right)	adult						61.5	DE LUMLEY-WOODYEAR, 1973
Bañolas (left)	adult						61.6	DE LUMLEY-WOODYEAR, 1973
Arago 2	adult						39.6	DE LUMLEY-WOODYEAR, 1973
Spy 1	adult			33	15		45.5	BILLY & VALLOIS, 1977
La Ferrassie 1	adult			35	14		40	BILLY & VALLOIS, 1977
Krapina H	adult			35	14		40	BILLY & VALLOIS, 1977
La Quina H9	adult						48.4	DE LUMLEY-WOODYEAR, 1973
Regourdou (sup. foram.)	adult						48.4	DE LUMLEY-WOODYEAR, 1973
Regourdou (inf. foram.)							33.4	DE LUMLEY-WOODYEAR, 1973
Circé II (sup. foram.)	adult						48.5	SERGI & ASCENZI, 1955
Circé II (inf. foram.)							34.2	SERGI & ASCENZI, 1955
Circé III (sup. foram.)	adult						35.1	SERGI & ASCENZI, 1955
Circé III (inf. foram.)							32.4	SERGI & ASCENZI, 1955
Cova del Gegant	15 yrs or adult			(31.0)	11.1	(17.0)	35.8	DAURA et al, 2005: 63
Atapuerca AT-1	adult			30.2	12.1	17	40.1	ROSAS, 1997: 322, 324
Atapuerca AT-2	adolescent			26.5	9.6	15	36.2	ROSAS, 1997: 324
Atapuerca AT-3	immature			27.8	10.9	17.7	39.2	ROSAS, 1997: 324
Atapuerca AT-172	immature			28	11.8	17.1	42.1	ROSAS, 1997: 324
Atapuerca AT-250	senile			31	11.5	19.8	37.1	ROSAS, 1997: 324
Atapuerca AT-300	adult			34.3	12.5	22.5	36.4	ROSAS, 1997: 324
Atapuerca AT-505	adult			26.7	10.4	16.9	38.9	ROSAS, 1997: 324
Atapuerca AT-605	adult			37.1	16.3	19.8	43.9	ROSAS, 1997: 324
Atapuerca AT-607	adolescent			27.1	11.9	13.8	43.9	ROSAS, 1997: 324
Atapuerca AT-888				42	13.3	21.7	31.7	ROSAS, 1997: 324
Atapuerca AT-950				43.6	11.8	17.8	27.1	ROSAS, 1997: 324
Roc de Marsal (left)	± 3 yrs	2 yrs 5 months	S1	17.6	(7.6)	10	(43.2)	MADRE-DUPOUY, 1992
Roc de Marsal (left)					(9.8)	7.8	(55.7)	MADRE-DUPOUY, 1992
Roc de Marsal (right)				17.4	(7.9)	9.5	(45.4)	MADRE-DUPOUY, 1992
Roc de Marsal (right)					(8.3)	9.1	(47.7)	MADRE-DUPOUY, 1992
Archi 1	5-6 yrs (or 3)	2.5 yrs	S1	21.3	6.8	11.2	31.9	ARNAUD, 2014
Combe-Grenal	6-7 yrs	4.5 yrs	S3	26.9	10.5	16.4	39.0	GENET-VARCIN, 1982
Fate 2	9-10 yrs		S3	19.9	(9)		45.2	GIACOBINI et al., 1984 and M. T.
Hortus 2-3	9 yrs		S3	25.5	7.8	(17.7)	30.9	DE LUMLEY-WOODYEAR, 1973
Malarnaud 1	12 yrs	11 yrs 2 months	(S4)	24	(11.2)		46.9	HEIM & GRANAT, 1995
Montgaudier 1	12.5-14.5		S4	23.3	8 (lowest foram.)	13.1 (highest foram.)	34.3	MANN & VANDERMEERSCH, 1997
Valdegoba VB1	13-14 yrs		S4			11.7		QUAM et al., 2001: 402, 404
Petit-Puymoyen 1	16-17 yrs	14 yrs 4 months	S4	28.2	10.5	17.7	37.2	Present author (M. T.)
Neandertal	juveniles		S1-S4	23.3 ± 4.5 (n= 13)	10.1 ± 3 (n= 13)	11.5 ± 1.8 (n= 13)		ARNAUD, 2014
MHSS	juveniles		S1	18.2 ± 1.9 (n= 14)	7.4 ± 0.6 n= 14)	9.9 ± 1.8 (n= 14)		ARNAUD, 2014
MHSS	juveniles		S2	21.9 ± 2.2 (n= 16)	9.7 ± 1.6 (n= 16)	11.1 ± 1.2 (n= 16)		ARNAUD, 2014
MHSS	juveniles		S3	25.4 ± 4.7 (n= 13)	11.0 ± 2 (n= 13)	13.3 ± 2.8 (n= 13)		ARNAUD, 2014
MHSS (Virchow)	adult						42-58	BILLY & VALLOIS, 1977
MHSS (Schultz)	adult						36-65	BILLY & VALLOIS, 1977

Table 1: Position of the mental foramen of Scladina I-4A and comparisons (heights in mm; for age classes, see § 5.1).



Figure 15: Scladina right hemimandible (Scla 4A-1), internal aspect (photograph Joël Éloy, AWEM).



Figure 16: Scladina left hemimandible (Scla 4A-9), internal aspect (photograph Joël Éloy, AWEM).

4.2.2.2. Internal aspect

This area is well preserved on both sides of the mandible (Figures 15–17).

The mylohyoid line (*linea mylohyoidea*) extends from the anterior part of the M_3 where

it is close to the alveolar margin. This line is then diagonally inclined. On both sides, it merges with the surrounding surface of bone below the P_3 – P_4 septum, about 5 mm behind and slightly above the “*éminences arrondies*” (see 4.1.1.2.) and around 15 mm below the alveolar margin.

There is no *torus mandibularis* as can be seen on some adult Neandertals, such as Regourdou (PIVETEAU, 1964: 161).

The *planum subalveolaris* (also called *fossa sublingualis* and *fossa subalveolaris anterior*; see WEIDENREICH, 1936: 49) exhibits a triangular shape and is flat and smooth.

The submandibular/sublingual fossa (also known as *fossa subalveolaris posterior* by WEIDENREICH, 1936: 48, *fossa submaxillaris* by WEIDENREICH 1936: 48 or *fovea submaxillare*) is relatively deep and antero-posteriorly elongated, parallel to the inferior rim.

4.2.2.3. Inferior border

In lateral view, the base of the right hemimandible Scla 4A-1 only touches the basal plane on two points, below the very posterior part of the right P_3 and at the gonial angle. The *incisura praeangularis*, or pregonial notch, of Scla 4A-1 between these two points, is very long, i.e. 52 mm. The depth of this notch is low but regularly increases up to the middle of M_2 , at the level of which the deepest point of the incisura is located, then rapidly decreases posteriorly.

The anterior marginal tubercles which are above the limit between the submental incisure of the anterior face of the symphysis and the long *incisura praeangularis* are extremely weak.

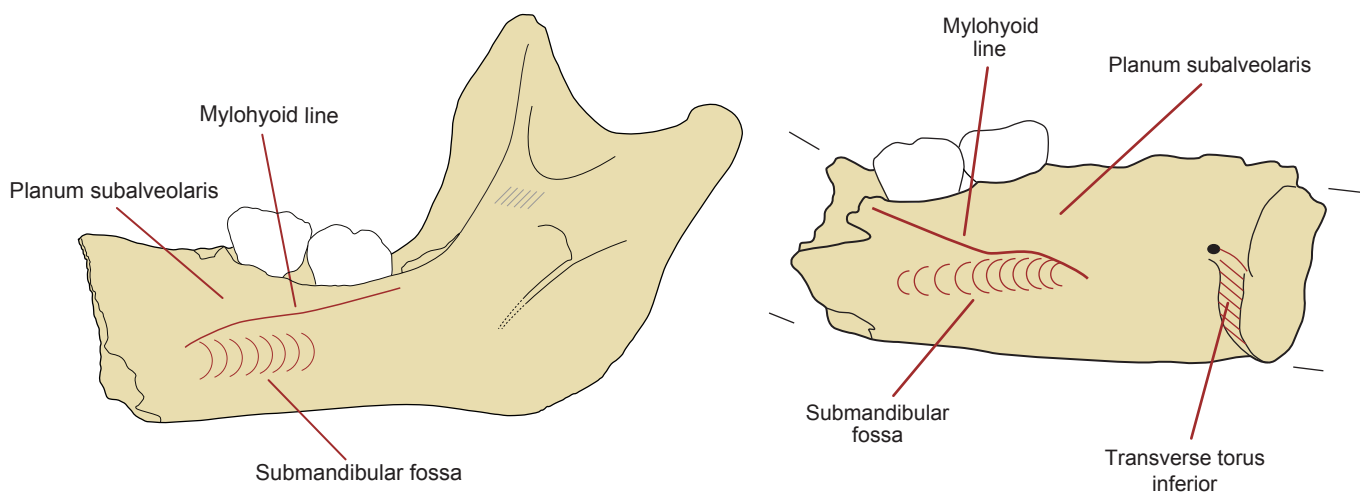


Figure 17: Scladina mandible, internal aspect of the right (Scla 4A-1) and left (Scla 4A-9) bodies (graphics Sylviane Lambermont, AWEM).

In basal view and on both sides, the lower margin of the body is slightly lingually concave from the gonion to the interdental septum P_4/P_3 where it turns strongly medially at the posterior limit of the digastric fossa. The margin expands from a thin rear edge behind unerupted M_3 to a progressively thicker one from M_2 to P_4 and even more in the symphyseal region. So, this structure decreases continuously and regularly from the symphysis to the ramus.

4.2.2.4. Superior border

The superior border of the Scladina mandible does not have any retromolar space on the right side (Scla 4A-1) on which the corresponding area is well preserved; apparently the same is true on the left side (Scla 4A-9) where this area is only partially preserved. It has been shown that the retromolar space only develops near the end of the growth period (TILLIER, 1988) while the Scladina Child is around eight years old (SMITH et al., 2007).

In the superior view, the root sockets of the left and right P_3 and of both dm_2 s can be observed. The sockets of the P_3 are slightly buccoanteriorly orientated. The upper parts of the septa between the first P_3 s and the dm_2 s exhibit marks of remodelling inherent to the exfoliation of the dm_2 s and root resorption, a result of the beginning eruption of the still embedded P_4 . Both P_3 sockets are not bifurcated. The sockets of the dm_2 s show two roots, mesial and distal, with bony septa – also with marks of remodelling – separating them.

4.2.3. Taxonomy

4.2.3.1. Mental foramen

A frequent suggestion is that a distal mental foramen position, under M_1 , is a derived feature of the European Classic Neandertals (STRINGER et al., 1984; TILLIER, 1988: 127; ROSAS, 2001: 81; CONDEMI, 2005). However, the mental foramen of more than half of the European Classic Neandertal specimens is mesial of the M_1 , i.e. below P_4/M_1 or below P_4 (TRINKAUS, 1993), while mental foramina placed below the M_1 are present in other non-classical Neandertal fossils (Atapuerca 1, Arago 2 and 13) as well as in modern human samples (usually in a small percentage, but sometimes up to 12,7%). Therefore, it is inappropriate to use this trait as a Neandertal derived characteristic.

On Scladina I-4A, the mental foramina are under P_4 on the right side as well as under P_4 and under the septum P_4/M_1 on the left side.

4.2.3.2. High placement and diagonal disposition of the mylohyoid line

A high placement of the mylohyoid line at the level of M_3 and a diagonal, or inclined, trajectory have both been suggested to be derived Neandertal characteristics (ROSAS, 2001: 81; see also DAURA et al., 2005: 65) while in modern humans, the trajectory of the line is more parallel to the alveolar border. On both sides of the Scladina mandible, the mylohyoid line is close to the alveolar margin at the level of the non-erupted M_3 and is diagonally inclined in front of this tooth.

4.2.3.3. Retromolar space

The retromolar space is often included in the list of Neandertal autapomorphies (STRINGER et al., 1984; TILLIER, 1988; CONDEMI, 2001; ROSAS, 2001, etc.). However, such a view has been challenged (FRANCISCUS & TRINKAUS, 1995). According to RAK (1998^b: 362), the space itself is not an autapomorphy but, rather, a result of the anterior position of M_3 .

In fact (TILLIER, 1986: 213-214; 1988: 129), the presence of a retromolar space is linked to a complete permanent dentition including the erupted M_3 . The space is due to the anterior projection of the lower facial area (TILLIER, 1986: 213). So none of the Neandertal mandibles with only deciduous teeth erupted, such as Pech de l'Azé, Roc de Marsal, Archi, etc., has a retromolar space. The same absence occurs on mandibles with only an erupted M_1 such as Fate II, or with erupted M_1 and M_2 , such as Scladina I-4A.

4.2.3.4. Basal border

From the inferior view, the basal border thickness regularly decreases from the symphysis to the gonion and this is sometimes considered as a derived characteristic of European Neandertals (PIVETEAU, 1957, 1963; ROSAS, 2001: 81). Scla 4A-1 exhibits this feature.

4.2.3.5. Submandibular fossa

A highly excavated submandibular fossa could be another derived characteristic of European Neandertals (CREED-MILES et al., 1996; ROSAS,

2001: 81). Both submandibular fossae Scla 4A-1 and 4A-9 are relatively deep and antero-posteriorly elongated, parallel to the inferior rim.

4.3. Ramus

Only the right ramus and gonial region are preserved on Scla 4A-1. These areas are totally missing on the left Scla 4A-9 hemimandible. The ramus is in the same plane as the corpus.

4.3.1. Dimensions

The ramus has a minimum width of 35.1 mm., a high value compared to other Neandertals of similar age.

4.3.2. Description

4.3.2.1. Internal surface

Upper and anterior reliefs of the ramus

The reliefs of the upper part of the internal (orlingual) surface of the right ramus are differently marked (Figure 18). The *crista endocoronoidea*, or endocoronoid crest, coursing nearly vertically along the inner side of the coronoid process is well expressed. The *crista endocondyloidea*, running antero-inferiorly from the internal border of

the condyloid process (VON LENHOSSÉK, 1920; WEIDENREICH, 1936: 50; 68), is well developed in its inferior part but is strongly attenuated near the condyle. Both cristae delineate a distinct *planum triangulare*, which is slightly concave in its anterior part, but the depth of which is increased by the relief of the surrounding *crista endocoronoidea*. The *planum triangulare* is, by contrast, often nearly flat on some other Neandertals mandibles, for instance Regourdou and La Ferrassie 1.

At the junction of the *crista endocoronoidea* and the *crista endocondyloidea*, just before the *foramen mandibulare*, is a clear eminence, the *torus triangularis* (WEIDENREICH, 1936: 49; 50; 68).

In front of the medial part of the condyle, the *fovea subcondylea* is nearly imperceptible.

From the *torus triangularis*, one rounded crest, which prolongs the endocoronoid crest, runs down antero-inferiorly to join the *linea mylohyoidea* (see Figure 18) and is known as the *crista pharyngea* (WEIDENREICH, 1936: 68).

Mandibular foramen

The right mandibular foramen of Scladina I-4A, i.e. the aperture of the mandibular canal, points posteriorly and superiorly (Figures 18 & 19). There is a clearly defined *lingula*, but it does not project strongly. The specimen exhibits a narrow V-shaped notch in its postero-inferior margin, the mylohyoid notch; the specimen does not have a

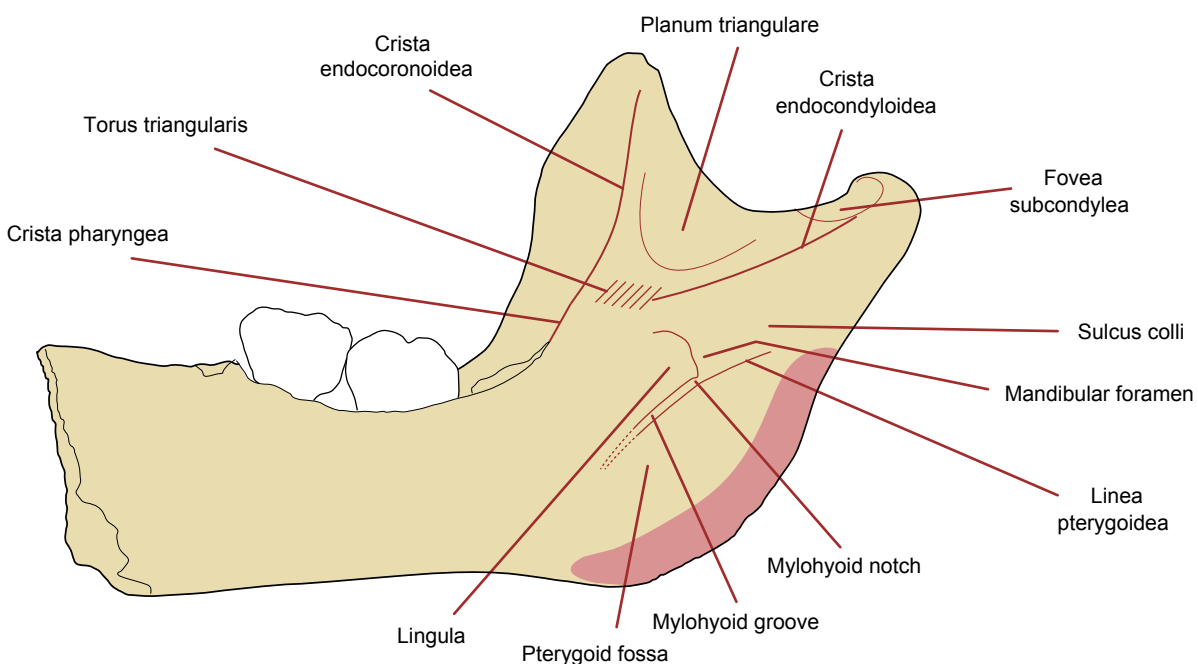


Figure 18: Scladina right hemimandible (Scla 4A-1), internal aspect of the ramus (graphics Sylviane Lambermont, AWEM).



Figure 19: Scladina mandible, right mandibular foramen (Scla 4A-1; photograph Joël Éloy, AWEM).

lingular bridging (RICHARDS et al., 2003: 63). So, the Scladina I-4A foramen does not exhibit the specific form described as ‘Horizontal-Oval’. In this H-O type, the inferior rim of the foramen does not dip but extends straight across the foramen; in addition, the *lingula* blends into the inferior rim of the mandibular foramen and extends over the foramen (see also COQUEUGNIOT, 1999).

A small vascular foramen is present 5.5 mm above the upper part of the mandibular foramen.

Mylohyoid groove

The mylohyoid groove descends antero-obliquely directly from the mylohyoid notch. The groove is not bridged but continuous, like in the Regourdou mandible. This sulcus is shallow and not perfectly rectilinear but very slightly concave postero-inferiorly. The sulcus disappears just behind the level of the distal end of the crown of the still included third molar, at about 8 mm from the inferior border of the mandible.

Pterygoid fossa

The internal side of the inferior half of the right Scla 4A-1 ramus exhibits a well demarcated subcircular and deeply excavated pterygoid fossa, the depth

of which is emphasized by the internal inflection of the gonial region. The fossa has a diameter of almost 2 cm. Moving forward, it merges into the submandibular fossa which is distinct thanks to a blunt rise.

Sulcus colli and tubercles of the posterior border of the ramus

Behind and below the inferior part of the *crista endocondyloidea* is the well marked sulcus colli. The crest which composes the anterior part of the inferior border of this sulcus and continues as the posterior, albeit low, border of the mylohyoid groove can be called *linea pterygoidea* (WEINDENREICH, 1936: 70; RICHARDS et al., 2003:20). The length of the sulcus colli is just above 15 mm at its axis, which is long when the immature state of the fossil is taken into account. The maximum width is 5.5 mm. The anterior part of the sulcus is relatively deep while its posterior component is shallow.

Considerable controversy exists in the naming of the tubercles of the postero-medial part of the mandibular ramus, (Figures 20 & 21; see RAK et al., 1994, 1996; CREED-MILES et al., 1996; RICHARDS et al., 2003).

A small tubercle is present at the postero-inferior end of the sulcus colli, near and on the posterior border of the ramus of Scla 4A-1. It is the *tuberculum sulcis colli* (tsc) of RICHARDS et al. (2003: 10), and serves as the attachment for the sphenomandibular ligament. In RAK et al.’s (1996) terminology, based on WEIDENREICH (1936), this feature would be the *tuberculum pterygoideum inferius* (tpi), even if tpi and tsc are not identical (see RICHARDS et al., 2003: 55).

A strongly developed tubercle occurs in the upper area of attachment of the *pterygoideus medialis* muscle, a few mm below the *tuberculum sulcis colli*. This structure is the medial pterygoid tubercle (m.p.t.) of RAK et al., 1994, 1996). In reference to SCHUMACHER’S (1959, 1961, 1962) numbering system for tendons of the *pterygoideus medialis* muscle, this fits with septum 6 but also, slightly below, the less marked septum 4.

At the internal part of the Scla 4A-1 gonion are the scallop tubercles (ANTÓN, 1996: 395, 401) which correspond to Schumacher’s septa 2’ 2’’ 2’’’ of the *pterygoideus medialis* muscle. These three septa are well separated by shallow depressions.

As far as size is concerned, the septa 6 and in a lesser extent 4 are the most hypertrophied while the *tuberculum sulcis colli* and septa 2’, 2’’ and 2’’’ are less developed.

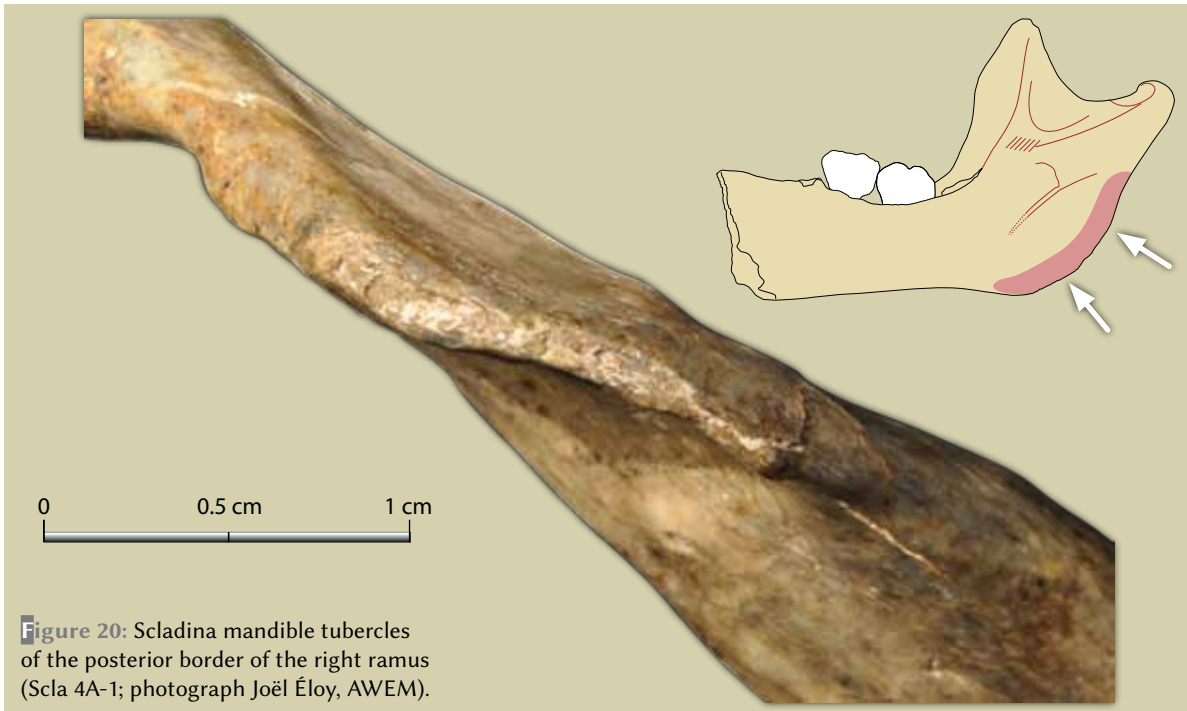


Figure 20: Scladina mandible tubercles of the posterior border of the right ramus (Scla 4A-1; photograph Joël Éloy, AWEM).

4.3.2.2. Anterior border

In side view, the outline of the anterior margin of the ascending ramus is sinuous: nearly straight in its anteriorly oblique upper third, and anteriorly concave in its lower part. The ramus displays rather shallow pre-angular notch (RAK, 1998^b: 360). This depression, when present in Neandertals like Regourdou or La Ferrassie, is not well defined. By contrast, an often well marked pre-angular notch is found in early *Homo sapiens* as well as in modern human mandibles.

In upper as well as in side views, the anterior border does not exhibit a retromolar space.

Behind the still included M_3 , the socket from which being already largely opened, is a triangular area. The buccal border of this area is the buccinator crest. This crest is well marked in adult Neandertals such as Regourdou or Spy I. At the mesial end of this area is the opening of Robinson's canal (see HEIM & GRANAT, 1995).

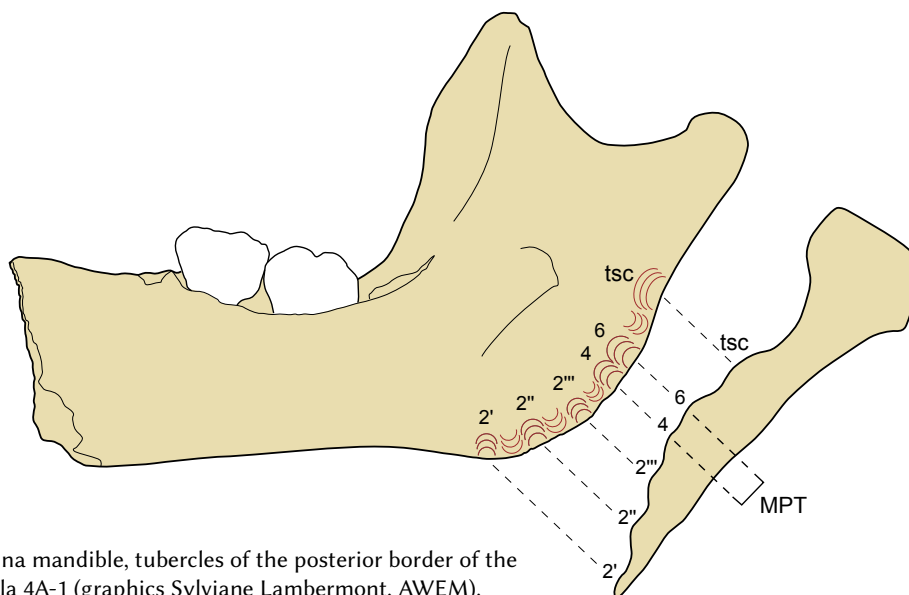


Figure 21: Scladina mandible, tubercles of the posterior border of the right ramus of Scla 4A-1 (graphics Sylviane Lambermont, AWEM).

4.3.2.3. Posterior border

In posterior view, the posterior border of the ramus is slightly medially convex in its inferior two thirds because of the inward inflection of the gonial area. The border thickens from the gonion to the condyle, being 3.37 mm at septum 2^o and 5.37 mm just above the *tuberculum sulcus colli*.

In side view, the posterior border is sinuous. It is posteriorly concave below the condyle until the inferior border of the sulcus colli, then posteriorly convex.

4.3.2.4. Inferior border and outline of the gonial region

The gonion of the Scadina mandible is only preserved on the right side (Scla 4A-1) which is slightly abraded. In side view, the gonion does not exhibit a sharp angle nor the typical Neandertal truncated outline in its uppermost segment, such as the one of Saint-Césaire. Nevertheless, this trait is present on Scla 4A-1, as pointed out by HEIM & GRANAT (1995: 88), but strongly attenuated as its gonion profile shows a regular slightly rounded outline with a large radius of curvature.

The Scla 4A-1 gonial region is inwardly inflected. So, no lateral flaring of this area is present. Such an internal inflection is common on adult Neandertals (BILLY & VALLOIS, 1977: 420), for instance Saint-Césaire, Regourdou, La Chapelle-aux-Saints, La Ferrassie 1, La Quina 5 and 9, or Malarnaud.

4.3.2.5. External surface

A clear tubercle can be observed at the external (or lateral) border of the neck of the Scla 4A-1 condyle (Figures 13 & 22). It is the lateral condylar tubercle (LCT; STEFAN & TRINKAUS, 1998; JABBOUR et al., 2002) or *tuberculum subcondyloideum laterale* (WEIDENREICH, 1936: 66) which is the attachment area for the *temporomandibular ligament*. In fact, only the base – well marked as a break in the general curvature of the area – of this eminence is preserved. Nevertheless, using JABBOUR et al.'s criteria (2002: 148), a score of at least 2 and probably 3 – which would mean a large tubercle – can be proposed, as it seems to project beyond the missing part of the articular surface.

From the lateral condylar tubercle a blunt ridge begins, the *crista ectocondyloidea* (VON LENHOSSÉK, 1920; WEIDENREICH, 1936) or



Figure 22: Scladina right hemimandible (Scla 4A-1), lateral surface of the ramus (photograph Joël Éloy, AWEM).

ectocondylar ridge (Figure 13) which goes down anteriorly and obliquely to the middle of the surface of the ramus where it blends with a large raised and blunt swelling, the *eminencia lateralis rami* (WEIDENREICH, 1936: 65). The small fossa present between the posterior part of the mandibular notch and the ectocondylar ridge houses the deep masseter muscle (ANTÓN, 1996).

The *eminencia* extends down to the middle region of the lateral surface of the ramus as a vertical, but anteriorly and convexly curved blunt line (Figure 13). In front of this curve, and parallel to it in the inferior part, is a second nearly vertical blunt curve. Both curves are related to the masseter insertions.

The lateral surface of the coronoid process and of all the ramus displays a narrow and shallow vertical depression between the anterior border of the ramus, the *eminencia lateralis* and both convex curved lines.

4.3.2.6. Superior border

Coronoid process (processus coronoideus)

The moderately sharp but eroded tip of the right coronoid process as well as the anterior border of the ramus were damaged during the excavation: an elongated splinter 34 mm long and 7.5 mm in maximum width was pulled off and later refitted.

The process is sub-triangular in shape. In a lateral view, this process is much larger than the condylar process. When Scla 4A-1 lies on its inferior border, the coronoid process is about 12 mm higher than the condyle.

Mandibular notch (incisura mandibulae)

In lateral view, the high configuration of the coronoid process gives the outline of the mandibular notch or mandibular incisure an asymmetrical appearance. The notch is also quite shallow. Its deepest point is in the middle third of the distance from the coronoid process to the condyle and is just behind the middle of its arch. The lowest point on the incisure is about 3 mm below the condylion when the mandible rests on its base. This is also about 16.5 mm from the posterior ramal margin at the same level below the condyle. This distance is nearly 47% of the minimum ramus breadth (STEFAN & TRINKAUS, 1998: 300, 304).

The length of the notch (condylion-coronion) is 30.3 mm and its maximum depth (perpendicular to the length) is 9.6 mm; the index is 31.6. The length from the coronion to the juncture between the crest of the mandibular notch and Scladina I-4A's very well marked anterior border of the articular surface of the condyle, is 26.5 mm.

Mandibular condyle or condylar process (Processus condylaris)

Only the right mandibular condyle, or condylar process, is preserved (Figure 23), however damaged postmortem: the internal part of the condyle is nearly complete, but abraded, while the lateral part is partially missing, having been strongly eroded. The surface of the condyle is also superficially abraded in its posterior part. In fact, only the central part of the articular surface and the central part of the anterior border of the condyle are completely preserved.

Based on the present state of preservation, the maximum length of the condyle is about 15.7 mm, divided in 9.2 mm for the preserved mesial part and 6.5 mm for the lateral part; adding at least 1.5 mm for the lateral missing part and about 0.5 mm for the eroded internal part, the real maximum length seems to be at least 17.7 mm. The preserved part of the articular surface of the condyle is 13.2 mm. The preserved antero-posterior diameter is 8.18 mm, but due to some erosion this region was at least 8.3 mm.

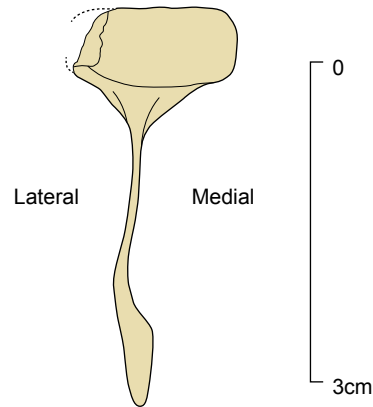


Figure 23: Scladina right hemimandible (Scla 4A-1), condyle in superior view (graphics Sylviane Lambermont, AWEM).

Approximately half of the Scla 4A-1 condyle is, in superior view (Figure 23), located outside the plane defining the ramus or more precisely by the intersection between the condyle and the posterior part of the upper edge of the mandibular notch. In other words, the condyle occupies a medial position with regards to the crest that defines the mandibular notch (CMN). This corresponds to score IV of JABBOUR et al. (2002).

Viewed from the top, the main axis of the condyle is directed towards the back and inside forming an open angle with the crest of the mandibular notch.

4.3.3. Taxonomy

4.3.3.1. Corpus and ramus in the same plane

The alignment of the corpus and the ramus in the same plane is seen to be a derived characteristic of the Neandertal lineage (ROSAS, 2001: 81, 88). This is the situation observed on the right Scla 4A-1 hemimandible.

4.3.3.2. Relationship between the mandibular condyle and the crest of the mandibular notch

The relationship between the mandibular condyle (condyloid process) and the crest of the mandibular notch has long been considered of primary importance in the discussion of Neandertal facial morphology as well as taxonomy.

In modern humans, the condyle has been described as projecting, at least for its main part,



inside the ramus, and more precisely inside the virtual posterior extension of the crest of the mandibular notch (for instance BOULE, 1911-1913; BILLY & VALLOIS, 1977: 426; VANDERMEERSCH, 1981: 154). On the contrary, the argument that with Neandertals an important part of the condyle, often half of it or even more, is located outside the plane defining the ascending ramus (laterally expanded condyle) has been presented. In other words, the crest of the mandibular notch is often seen as intersecting the anterior margin of the condyle in an approximate medial position. This feature has been interpreted as a Neandertal lineage apomorphy (RAK & KIMBEL, 1995; RAK, 1998^{a,b}; ROSAS, 2001: 81; RAK et al., 2002).

However, a more statistical analysis has argued that the central position of the crest is not autapomorphic in Neandertals (JABBOUR et al., 2002), which was confirmed some years later (WOLPOFF & FRAYER, 2005). Indeed, some modern humans have a crest that shows the so-called 'Neandertal' morphology while a few Neandertals exhibit the lateral 'modern' position (La Quina 9, Zaffaraya 2; see WOLPOFF & FRAYER, 2005: 249). Nevertheless, on average, the Neandertal crest is significantly placed in a less lateral position than in modern humans (JABBOUR et al., 2002).

On Scladina I-4A, approximately half of the only preserved condyloid process is located outside the plane defining the ramus. So, in this regard, the mandible shows the more common, but not autapomorphic, Neandertal disposition.

4.3.3.3. H-O shape of the mandibular foramen

The H-O variety was first pointed out by GORJANOVIĆ-KRAMBERGER (1906) in his original description of the Krapina fossils. Later, KALLAY (1955, 1970), designated this variant the horizontal-oval (H-O) type. The horizontal-oval (H-O) shape was seen as an autapomorphy of the Neandertals (STRINGER et al., 1984: 55), as the correlated lingular/mylohyoid bridging (CREED-MILES et al., 1996: 152; TRINKAUS, 2006: 601).

In fact only about half of the Neandertals (43% in SMITH, 1976: 170; 46.2% in SMITH, 1978: 526; 52.6% in FRAYER, 1992: 31) exhibit the HO morphology which, in addition, is present in one fifth of the early Upper Palaeolithic Modern Humans (18.2% in FRAYER, 1992). and even in very small percentages in Late Upper Palaeolithic, Mesolithic and Medieval humans. In the Krapina sample, this

feature is found in 56% of the specimens (SMITH, 1976: 170). Mandibles exhibiting the H-O mandibular foramina pattern include, among others, La Ferrassie I, Tabun II or Kebara 2, Krapina J or 59, etc. While other specimens, such as Regourdou and Fate II, whose mandibular foramen are close to Scladina I-4A, Amud 1, La Chapelle-aux-Saints or the pre-Neandertal juvenile Atapuerca SH AT-6O6 do not exhibit this shape.

In conclusion, it seems wise not to include the H-O variety of the mandibular foramen in the list of Neandertal autapomorphies even if this configuration is a common feature in that taxon.

The Scla 4A-1 hemimandible does not exhibit this particular form. On the contrary, the foramen exhibits a narrow V-shaped notch in its postero-inferior margin.

4.3.3.4. Truncated gonion

The gonion of the Neandertal mandible often exhibits a distinctive truncated morphology (BOULE, 1911-13; WEIDENREICH, 1936: 73; PATTE, 1955: 245-246; HEIM 1976: 263; BILLY & VALLOIS, 1977: 419). In this configuration, the gonial angle is formed by an oblique, but quite rectilinear, border or third "arista" (CREED-MILES et al., 1996: 152; ROSAS 2001: 78), between the basal border of the corpus and the posterior margin of the ramus. This is, for instance, the case at La Chapelle-aux-Saints (BOULE, 1911-13), La Ferrassie 1 (HEIM, 1976) and Malarnaud (HEIM & GRANAT, 1995) or Saint-Césaire. This trait, which is referred to as a truncated gonion or a truncated gonial area, is sometimes interpreted as derived (CREED-MILES et al., 1996: 151-152; ROSAS, 2001). However, according to ROSAS (2001: 87), such a configuration is only found in 70% of the Neandertals as well as in Arago XIII and Mauer.

In contrast, the gonion is well-developed in modern humans and in the Sima de los Huesos (SH) pre-Neandertal sample. In detail, the posterior margin of the ramus and the inferior margin of the corpus of recent *Homo sapiens* connect as a marked angle or a curve with a small radius. The SH gonial profile defines a gradual arc connecting the posterior border of the ramus with the basal border whereas the Neandertal pattern is foreshadowed in some fossils such as the AT-605 mandible. On the mandible of Montmaurin (BILLY & VALLOIS 1977: 419), the gonial area forms a regular rounded arc with an important curvature of the radius.

The gonion of the Scadina mandible is only preserved on the right side (Scla 4A-1) and is slightly abraded. In side view, it does not exhibit the modern pattern with a sharp angle or an arc with a small radius. In contrast, the Scla 4A-1 gonial profile shows a regular and slightly rounded outline with a large radial curvature like other Neandertal mandibles such as La Quina 5 (VERNA, 2006). However, the gonial area of Scla 4A-1 does not present the typical Neandertal truncated outline in its extreme expression; nevertheless, this trait is present but attenuated.

4.3.3.5. Curve of the mandibular notch

According to RAK (1998^b) and RAK et al. (2002), the Neandertal curve of the mandibular notch is characteristic and corresponds to a derived condition, being apomorphic or synapomorphic. And indeed, the outline of the Neandertal's mandibular notch is seen as asymmetric and shallow with a posterior position for its deepest point. By contrast, in modern humans the deepest point would be near the midpoint between the coronoid and the condylar processes and the shape of the notch is symmetric. Scla 4A-1 is closed to this so-called Neandertal shape.

However, such a view has been challenged and is no longer seen as a Neandertal autapomorphy

(STEFAN & TRINKAUS, 1998: 330; WOLPOFF & FRAYER, 2005) as the shape of the mandibular notch exhibits tremendous variability within human samples, Neandertals included (WEIDENREICH, 1936; PIVETEAU, 1963-66; HEIM, 1976; BILLY & VALLOIS, 1977).

4.3.3.6. Deeply excavated pterygoid fossa

A deeply excavated pterygoid fossa is a classical trait in Neandertals and is considered as derived by some authors (CREED-MILES et al., 1996: 152; ROSAS, 2001: 81). The internal right Scla 4A-1 ramus exhibits such a well demarcated pterygoid fossa. However, it should be pointed out that, up to now, this feature has not been discussed in the same critical way as some other so-called Neandertal apomorphies.

4.3.3.7. Highly excavated submandibular fossa

A highly excavated submandibular fossa is also interpreted as a derived feature by some researchers (CREED-MILES et al., 1996; ROSAS, 2001: 81). On Scla 4A-1, this fossa is quite deep on both sides.

Character	Archaic feature	Possible Neandertal derived	Frequent in Neandertals but not derived	Scladina	Reference
Absence of modern chin	x			yes	RAK et al., 2002
Planum alveolare and genioglossal fossa	x			yes	TILLIER, 1979
Inferior orientation of digastric fossae	x			yes	TILLIER, 1984
Frontal alignment of anterior alveoli and teeth			x	yes	TILLIER, 1986
Posterior position of mental foramen below M ₁			x	no (P ₄)	STRINGER et al., 1984; ROSAS, 2001
Inclination of the mylohyoid line close to alveolar margin at M3 level		x		yes	ROSAS, 2001
Highly excavated submandibular fossa		x		yes	CREED-MILES et al., 1996; ROSAS, 2001
Thin basal border of the body, decreasing from symphysis to ramus		x		yes	PIVETEAU, 1957, 1964: 163
Developed retromolar space			x	no	COON, 1962; HOWELLS, 1975; STRINGER et al., 1984; RAK, 1998 ^b
Deeply excavated pterygoid fossa		x		yes	CREED-MILES et al., 1996
Corpus and ramus in same plane		x		yes	ROSAS, 2001
Truncated gonial area		x		slight	BOULE, 1911-13; BILLY & VALLOIS, 1977; ROSAS, 2001
Horizontal-Oval (HO) mandibular foramen			x	no	STRINGER et al., 1984;
Laterally expanded condyle with regards to the ramus plane			x	yes	RAK & KIMBEL, 1995; JABBOUR et al., 2002
Curve of the mandibular notch			x	yes	RAK, 1998 ^b ; STEFAN & TRINKAUS, 1998

Table 2: Some features of the Scladina mandible (Scla4A-1 & 9) compared with Neandertal characteristics.



Corpus	Value
Infradentale-pogonion angle on resting plane (Scla 4A-9)	(98°)
Infradentale-gnathion angle on resting plane (Scla 4A-9)	(73°)
Height of the symphysis (Scla 4A-9)	27.75
Thickness at symphysis (Scla 4A-9)	12.36
Index of robustness at the symphysis (Scla 4A-9)	44.5
Height of the body at the canine (Scla 4A-9)	26.32
Thickness of the body at the canine (Scla 4A-9)	13.1
Index of robustness at the canine (Scla 4A-9)	49.8
Height of the body at the C-P ₃ border (Scla 4A-9)	26.55
Thickness of the body at the C-P ₃ border (Scla 4A-9)	13.1
Index of robustness at the C-P ₃ border (Scla 4A-9)	49.3
Height of the body at the P ₃ (Scla 4A-1)	(24.5)
Thickness of the body at the P ₃ (Scla 4A-1)	12.8
Index of robustness at the P ₃ (Scla 4A-1)	52.2
Height of the body at the P ₃ -P ₄ border (Scla 4A-1)	(24.35)
Thickness of the body at the P ₃ -P ₄ border (Scla 4A-1)	13.2
Index of robustness at the P ₃ -P ₄ border (Scla 4A-1)	54.2
Height of the body at the P ₄ (Scla 4A-1)	23.9
Thickness of the body at the P ₄ (Scla 4A-1)	13.1
Index of robustness at the P ₄ (Scla 4A-1)	54.8
Height of the body at the P ₄ -M ₁ border (Scla 4A-1)	23.5
Thickness of the body at the P ₄ -M ₁ border (Scla 4A-1)	13.4
Index of robustness at the P ₄ -M ₁ border (Scla 4A-1)	57.0
Height of the body at the M ₁ (Scla 4A-1)	22.2
Thickness of the body at the M ₁ (Scla 4A-1)	14.0
Index of robustness at the M ₁ (Scla 4A-1)	63.0
Height of the body at the M ₁ -M ₂ border (Scla 4A-1)	20.55
Thickness of the body at the M ₁ -M ₂ border (Scla 4A-1)	14.45
Index of robustness at the P ₄ -M ₁ border (Scla 4A-1)	70.3
Height of the body at the M ₂ (Scla 4A-1)	20.3
Thickness of the body at the M ₂ (Scla 4A-1)	15.8
Index of robustness at the M ₂ (Scla 4A-1)	77.8

Ramus	Value
Angle of the ramus	118.5°
Minimum breadth	35.1
Maximum breadth	38.1
Height of the coronoid process (perpendicular to resting plane)	56.0
Height of the coronoid process (projection)	54.0
Length of the mandibular notch	30.3
Maximum depth of the mandibular notch	9.6
Index of the mandibular notch	31.6
Height of the condyle (perpendicular to resting plane)	43.0
Height of the condyle (projection)	41.6
Length of the ramus	45.5
Minimum height of the ramus (perpendicular to resting plane)	40.2
Minimum height of the ramus (projection)	38.2

Mandible	Value
Maximum mandibular length (Martin 68-1)	(85.0)
Corpus length (Martin 68)	(± 70)
Bicondylar breadth (Martin 65)	(± 140)
Bigonial breadth (Martin 66)	(± 80)

Table 3: Principal measurements (mm and °) of the Scladina mandible (Scla 4A-1 & 9).

Table 4: Dimensions and comparisons (mm and °) of the right ramus of the Scladina mandible (Scla 4A-1).

4.3.3.8. Basal border

A continuous and regular decrease of the basal border from the symphysis to the ramus is considered to be a derived characteristic (PIVETEAU, 1964: 163; ROSAS, 2001: 81). The Scladina I-4A mandible corresponds to this pattern.

4.4. Discussion

Table 2 summarizes the main anatomical features developed in the paragraphs concerning the taxonomy of the symphysis (4.1.2), the mandibular body (4.2.3) and the ramus (4.3.3). The few characters of the Neandertals mentioned therein are considered archaic, Neandertal derived or simply as frequent characters in this taxon. It should be noted that in many cases features initially regarded as derived are contradicted by scholars when they are the subject of detailed studies. In the present state of research, it is possible, on Scladina I-4A, to consider as possibly derived the inclination of the mylohyoid line close to alveolar margin at M₃ level, the highly excavated submandibular fossa, the decreasing of the basal border thickness from symphysis to ramus, the deeply excavated pterygoid fossa, the corpus and ramus in same plane, and the tendency to have a truncated gonial area. Other characters present on Scladina I-4A are common among Neandertals, but not exclusive of this taxon, notably (Table 2): frontal alignment of anterior alveoli and teeth, horizontal-oval (HO) mandibular foramen, laterally expanded condyle

		Ramus minimum breadth			
Scla 4A-1 values	8 years	35,1			

		Mean	n	St. dev.	Ref
EN (Early Neandertals)	adult	39.15	6 (r)	2.93	1
LN (Late Neandertals)	adult	40.55	10 (r)	3.09	1
Neandertals (EN + LN)	adult	40.03	16 (r)	3.01	1
NE	juvenile	28.5	11	3.47	5
MPMH (Middle Palaeolithic Modern Humans)	adult	36.66	3 (r + l)		1
UPMH (Upper Palaeolithic Modern Humans)	adult	39.69	11	3.12	1
MHSS (Modern Human <i>sapiens sapiens</i>)	S1	22.4	15	1.6	
MHSS	S2	23.8	4	4.2	2
MHSS	S3 (7-10 years)	27.4	12	1.9	2
MHSS	adult	33.99	1107	3.19	1

with regards to the ramus plane, and curve of the mandibular notch. It also appears that the absence of modern chin of the Scladina mandible, the *planum alveolare* and genioglossal fossa, as well as the inferior orientation of digastric fossae are archaic traits. The absence of retromolar space results from the young age of the subject (8 years old), as is also the case in other juvenile Neandertals. This could also be the case for the position of the mental foramen below P₄ and not M₁, although some adults Neandertals also do not have that posterior location.

In conclusion, what characterizes a Neandertal mandible like Scla 4A-1/9 lies less in one or another derived or supposed derived trait than in the unique combination of a set of traits that, taken together, correspond to the general pattern of Neandertals.

5. Morphometry

5.1. Material and Methods

This section statistically compares the Scladina mandible to samples of subadult Neandertals, subadult modern humans (Neolithic/Middle Ages/submodern Modern; MHSS), Early (EN) and Late (LN) adult Neandertals and adult MHSS.

As in Chapter 12, which discusses the maxilla, all individuals are attributed to age classes that are based on dental eruption:

- S1: deciduous dentition only;
- S2: deciduous dentition and M₁ fully erupted;
- S3: mixed dentition with the M₁ and at least another fully erupted permanent tooth (but usually not the M₂);
- S4: permanent dentition only, with the M₂ fully erupted, but not the M₃.

The reported measurements of the Scladina mandible and comparison fossils are those commonly used in anthropology. These include angles such as that of the symphysis as well as measurements of the thickness and height of the various parts of the mandible. These values are presented in Tables 3 to 5.

Measurements of the Scladina mandible were repeatedly taken by the author himself and later averaged. Measurements of the comparison samples were collected from the literature, with the exception of some of Fate 2 and Krapina that were also taken by the author.

Significant differences may exist between values of the same dimensions obtained by various authors. For example, the measurements of the Malarnaud 1 mandible as published by MINUGH-PURVIS (1988) and HEIM & GRANAT (1995) show significant differences, such as a thickness of 12.8 mm at the symphysis according to Minugh-Purvis but 14 mm for Heim & Granat. The same fossil has a canine height of 18.2 mm for MINUGH-PURVIS (1988) and 24.4 mm for ARNAUD (2014). Another problem is that researchers sometimes propose different values for the same dimension, either

Ramus height M 70				Ramus projection height M-70a				Coronion height M 70-1 (projection)				Ramus minimum height M 70-2				Mandibular angle M 79			
45,5				41,6				54.0				40,2				116			
Mean	n	St. dev.	Ref	Mean	n	St. dev.	Ref	Mean	n	St. dev.	Ref	Mean	n	St. dev.	Ref	Mean	n	St. dev.	Ref
66.04	4 (r)	3.23	1	60.37	4 (r & l)	4.38	1	66.33	3 (r)	4.86	1	49.47	3 (r)	5.76	1	113.5	4	6.61	1
67.68	5 (r & l)	5.77	1	64.69	8 (r & l)	6.47	1	74.02	4 (r & l)	3.02	1	55.42	6 (r)	7.27	1	107.3	6	3.56	1
64.98	6 (r)	3.63	1	63.25	12 (r & l)	6.03	1	69.61	5 (r)	6.33	1	53.44	9(r)	7.09	1	109.8	10	5.63	1
41.4	6	10.01	5													120.7	10	7.79	5
71.33	1 (r)		1	70.5	1 (r)		1	71.5	1(r)		1								
63.95	9 (r & l)	6.25	1	57.4	5 (r)	4.17	1	62.0	6(r)	6.67	1					116.68	19	5.65	1
																134.6	20	6.25	3
45.4	12	4.3	2									36.4	12	3.1	2	137			4
57.06	879	4.89	1					57.74	626	4.97	1					122.19	1037	6.42	



Specimen	Age at death			Sex	Length			Breadth						I dent/ pog angle	
	Classic	Histology or Granat's technique	Class		Max	Cor- pus	di1-dm2 projec- tion	Bicon- dylar	Bigonial	Bicanine	Bi dm1/ P3	Bi dm2/ P4	Bi M1		Bi M2
Scla 4A-1 & 9	10–11 yrs		S3		(86.0)	(± 70)		(± 140)	(± 80)						
Scla 4A-9 (left)	10–11 yrs	8 yrs		F											(98°)
Scla 4A-1 (right)	10–11 yrs														
Molare 1	3–4 yrs		S1							(33)	(46)	(60)			(90°)
Dederiyeh 1	± 2 yrs		S1							30.7					98°
Dederiyeh 2	± 2 yrs		S1							31					
Barakai	± 3 yrs		S1		78.1	55.9	26					50			84°
Archi 1	5–6 yrs or 3 yrs	2.5 yrs	S1				27.8			35.8	43.3	49.5			93°
Gibraltar 2 (Devil's Tower)	± 3 yrs		S1		72		25.6	(105)		(33.9)	45.8	53.4			93°
Roc de Marsal	± 3 yrs	G/H: 2 yrs 5 months	S1		(70)	(56)	28.4	(95)	(72)	30.6	42.3	51.1			93°
Pech de l'Azé 1	2 yrs	G/H: 18.5 months	S1		67	49	(26.2)	(89)	(79)	30.5	(41.1)	(49.3)			92.3°
Krapina A (51)	5–6 yrs		S2												
La Chaise 13 (S5)	4–5 yrs	2.5 yrs	S2				27.8			(31)	42.5	(52)			83°
Zaskalnaya VI	9–10 yrs		S3					109	66						
Combe-Grenal	6–7 yrs	4.5 yrs	S3												
Krapina B (52)	9.5 yrs		S3												106.5°
Teshik Tash 1	8.5– 11 yrs	7.5 yrs ± 6 months	S3		95	71		122	83		46.5	54			90°
Sipka 1	8–10 yrs		S3												
Fate 2	9–10 yrs		S3												(90°)
Hortus 2-3	9 yrs		S3	F											87°
Malarnaud 1	12 yrs	11 yrs 2 months	S4	F	87			114	80.5						90.5°
Petit-Puy- moyen 1	16–17 yrs	14 yrs 4 months	S4	F											
Ehringsdorf 7 (G, 1010/69)	10.5– 12 yrs		S4		104	84		(126)	82	(35)	(49)		(71)	(81)	92°
Montgaudier 1	12.5– 14.5 yrs		S4	F											
Krapina C (53)	11 yrs		S4												96.5°
Krapina E-55	15–17 yrs		S4	F											95°
Le Moustier 1	15.5 yrs ± 1.25		S4	M											88°
Valdegoba VB1	13–14 yrs		S4	M											
Atapuerca SH AT-607 (XXIII)	adoles- cent		S4	M											

Table 5: Dimensions (mm and °) of the symphysis and corpus of the Scladina mandible (Scla 4A-1 & 9) compared to other juvenile Neandertal specimens. H = height, T = thickness, I = index.

by mistake or by having measured it at different times. So for Krapina E-55, MINUGH-PURVIS (1988) gives 31.4 mm for the height at the symphysis (p. 179) contra 34.5 mm (p. 185), or 13.5 mm (p. 188) and 14.1 mm (p. 179) for the thickness at

the symphysis. In view of such discrepancies, the choice of a particular value of a precise measurement of a fossil can, at least when the differences are significant, influence statistical analysis and inferences drawn from them. Ideally, to avoid

I dent/ gna angle	Symphysis			Canine			Mental foramen			P ₃ (m1-m2)			P ₄ (m2)			M ₁			Reference	
	H	T	I	H	T	I	H	T	I	H	T	I	H	T	I	H	T	I		
(73°)	27.75	12.36	44.5	26.32	13.1	49.8	23.9				13.2		(24.1)	13.2	(54.8)	(23.0)	14.2	(61.7)	Present Author (M. T.)	
					(13.45)		24.5				(24.5)	12.8		23.9	13.1	54.8	22.2	14.0	63.1	Present Author (M. T.)
79°	25.7	14	54.5								20.9	12.2	58.4							MALLEGNI & RONCHITELLI, 1987
75°	21.6	10.6	49.1								16	11.6	72.5							DODO et al., 2002
74°	20.3	10.5	51.7								15.2	10.3	67.8							ISHIDA & KONDO, 2002
	24.1	12.5	51.9				19.2	13.5	70.3	20.1	14.2	70.6								FAERMAN et al., 1994
78°	22	13.5	61.4							20	11.8	59.0	18.4 (r)	13.4 (r)	72.8					ASCENZI & SEGRE, 1971; TILLIER, 1983 ^b ; MALLEGNI & TRINKAUS, 1997; ARNAUD, 2014
79°	21.2	12.6	59.4							22.8	13.6	59.6								TILLIER, 1983 ^b
74°	20.2	12.6	62.4				17.6 (r)	12.9 (r)		17.2	13.2	76.7								MADRE-DUPOUY, 1992: 103; TILLIER, 1983 ^b
	17.8	10	56.2							14.2	11.5	81.0								MADRE-DUPOUY, 1992: 103; TILLIER, 1983 ^b
		11.5		22.5	12.6	56.0					12.3			12.6						SMITH, 1976; MINUGH-PURVIS, 1988
85°	22.1	12.8	59.9	21	12.1	57.6				20.5	12.5	60.9	17	12.5	73.5	16.4	12.5	76.2		TILLIER & GENET-VARCIN, 1980; TILLIER, 1982; MINUGH-PURVIS, 1988
	30	13.4	44.7	19.8	14	70.7				(18)	14	77.8	21.4	13.6	63.5	20.7	13.8	66.7		MINUGH PURVIS, 1988
	26.2	13.4	51.1				26.9	13.8		26.9	13.8	51.3								GENET-VARCIN, 1982
	26	(12.0)	46.1	(29.0)	15.6	53.8					16.7			17.9		23.5				SMITH, 1976; MINUGH-PURVIS, 1988
75°	27.0	13.7	50.7	26.4	17.0	64.4	26	15	57.7	26.5	16.6	62.6	25.1	15.1	60.1	21.2	15.8	74.5		ULLRICH, 1955; MADRE-DUPOUY, 1992; MINUGH-PURVIS, 1988
	30.0	14.0	46.7																	HEIM & GRANAT, 1995; MADRE-DUPOUY, 1992
(78°)				(20.5)	12.2	59.5	19.9	12.7		22	(12.5)					18.5	14.0	75.7		GIACOBINI et al., 1984 and M. T.
79°	25.0	13.6	54.4				25.5	15.0	58.8											DE LUMLEY-WOODEYER, 1973
	25	14	56	24.4	14.9	61.1	24	14		20.9			20.9			21.5	17.5	81.4		HEIM & GRANAT, 1995; ARNAUD, 2014; MINUGH-PURVIS, 1988
	28.1	12.2	43.4	28.9			27	13	48.1	28.3			29.1			28.0				GABIS, 1956; MINUGH-PURVIS, 1988: 179, 185
73°	28.3	15.3	54.1	25.6	15.6	60.9					(17.0)					20.8	(15.0)	72.1		VLČEK, 1993; MINUGH-PURVIS, 1988
	22.0	11.8	53.6	24.9	12.15	48.8	(23.3)	(13.5)	(53.3)	23.3	13.7	58.8	23.3	13.45	57.7	22.45	13.55	60.3		MANN & VANDERMEERSCH, 1997; ARNAUD, 2014
	23.7	13.6	57.4	(26.0)	17.4	66.9	23.3	16.2	69.5		17.9		22.1	17.5	79.2	21.0	17.1	81.4		SMITH, 1976; MINUGH-PURVIS, 1988
	31.4	14.1	44.9	23.7	15.0	63.3	28.1	15.2	54.1	25.7	14.8	57.6	26.8	14.4	53.7	25.9	16.5	63.7		SMITH, 1976; MINUGH-PURVIS, 1988
82°	30.0	15.0	50.0	27.5	15.0	54.5				27.3	14.2	52.0	25.4	15.2	59.8	27.2	16.6	61.0		MINUGH-PURVIS, 1988; THOMPSON & BILSBOROUGH, 2005; VLČEK, 1993
	30.6	15.5	50.6		17.0						(16.9)			(16.6)			(16.6)			QUAM et al., 2001: 403–404
	28.6	14.7	51.4				27.1	15.2						15.2						ROSAS, 1995

these problems, each author should individually measure all the fossils they compare. This is obviously almost impossible, mainly for financial reasons and sometimes due to restricted access to fossils. Researchers therefore need to be critical

about the measurements they use, especially by trying to validate them from good quality casts and photos. However, the relative inaccuracy of anthropological measurements is likely not sufficient enough to influence general trends,



although the relatively small size of most juvenile mandible comparison samples is often an additional problem.

Univariate analyses using the methods developed by F. HOUËT (2001) were carried out to compare the measurements of the Scladina

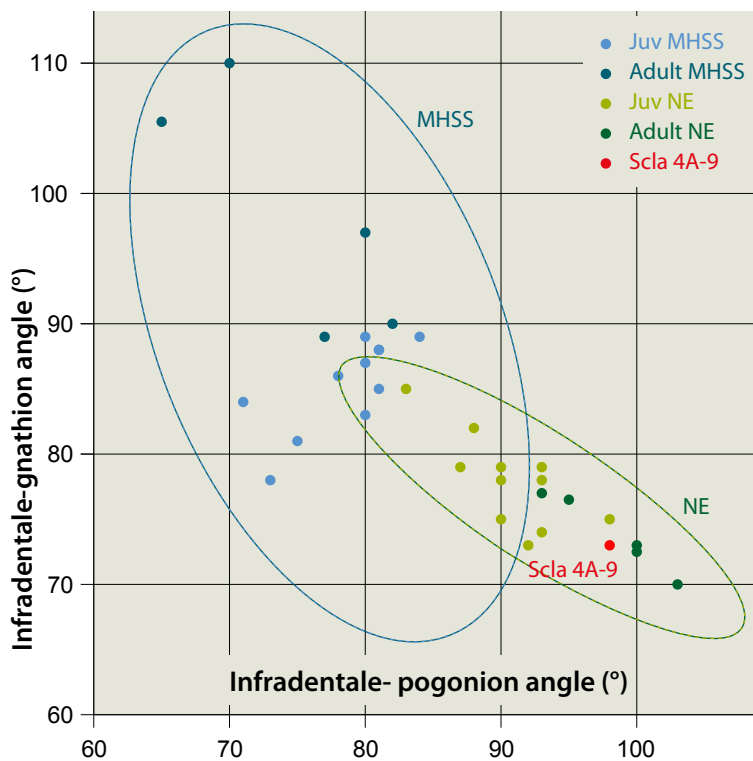


Figure 24: Bivariate analysis of the infradentale-pogonion and infradentale-gnathion angles of the Scladina symphysis (Scla 4A-9) with 95% equiprobable ellipses of Neandertals (adults and juveniles) and MHSS (adults and juveniles).

mandible with the above mentioned samples. These analyses include:

- Probabilistic distances (DP) to compare the measurements of a fossil to parameters of a reference population, according to the formula $DP = \text{student law} (\text{Abs} (x-m) / s; n-1; 2)$;
- ECRA (“écart centré réduit ajusté” of HOUËT, 2001) = $(x-m) / \text{inverse student law} (0.05; n-1) * s$.

In both formulas, x = individual value, m = sample mean, s = standard deviation, n = number of fossils. In the tables corresponding to each specimen, the numbers in brown indicate values of DP and ECRA that diverge significantly from the estimated variation of the reference population ($DP > 0.05$ or < -0.05 ; $ECRA > 1$ or < -1).

The bivariate comparisons used the well-known technique of equiprobable ellipses (DEFRISE-GUSSENHOVEN, 1955); 95% confidence ellipses were plotted using the statistical software package PAST (PALaeontological STATistics, version 1.77, 2008; HAMMER et al., 2001).

5.2. Results

The mental angle – infradentale-pogonion angle on resting plane – cannot be estimated with precision on Scla 4A-9 due to the erosion of the anterior borders of the alveoli of the central incisors. The value appears to be close to 100°. After extensive testing, we chose the approximate value of 98°. For the same reason, the infradentale-gnathion angle on resting plane (Martin 79-1a) is equally inaccurate: we estimate 73°. Both angles are not significantly different from those of juvenile and adult immature Neandertals, both using DP probabilistic distance and ECRA (Table 6). In contrast, the infradentale-pogonion angle departs significantly from immature and adult MHSS. Regarding

Scla 4A-9	infradentale-pogonion	98°
	infradentale-gnathion	73°

Comparison Samples	Angle	n	mean	St dev	DP	ECRA
Immature NE S1–S4	intra-pog	17	91.8°	5.47	0.274	0.535
	intra-gna	12	77.6°	3.58	0.225	-0.584
Immature NE S1–S2	intra-pog	8	90.7°	5.01	0.188	0.616
	intra-gna	7	77.7°	3.9	0.274	-0.493
Immature NE S3–S4	intra-pog	9	92.8°	5.96	0.408	0.378
	intra-gna	5	77.4°	3.5	0.277	-0.453
Immature MHSS S1	intra-pog	17	78.7°	3.64	0.000	2.501
	intra-gna	11	85.3°	3.52	0.006	-1.568
Adult Neandertal	intra-pog	15	97.8°	6.27	0.975	0.015
	intra-gna	5	73.9°	2.88	0.770	-0.113
Adult Palaeo MHSS (= UPMH)	intra-pog	14	74.6°	7.67	0.009	1.412
	intra-gna	5	98.3°	9.3	0.053	-0.980
Adult Meso MHSS	intra-pog	24	76°	4.68	0.000	2.272

Table 6: Infradentale-pogonion angle and infradental-gnathion angle of the Scladina symphysis (Scla 4A-1 & 9) compared to those of immature and adult Neandertals and MHSS, with DP and ECRA.

Scla 4A-9	Symphysis	Height	27.75
		Thickness	12.36
		Index	44.5

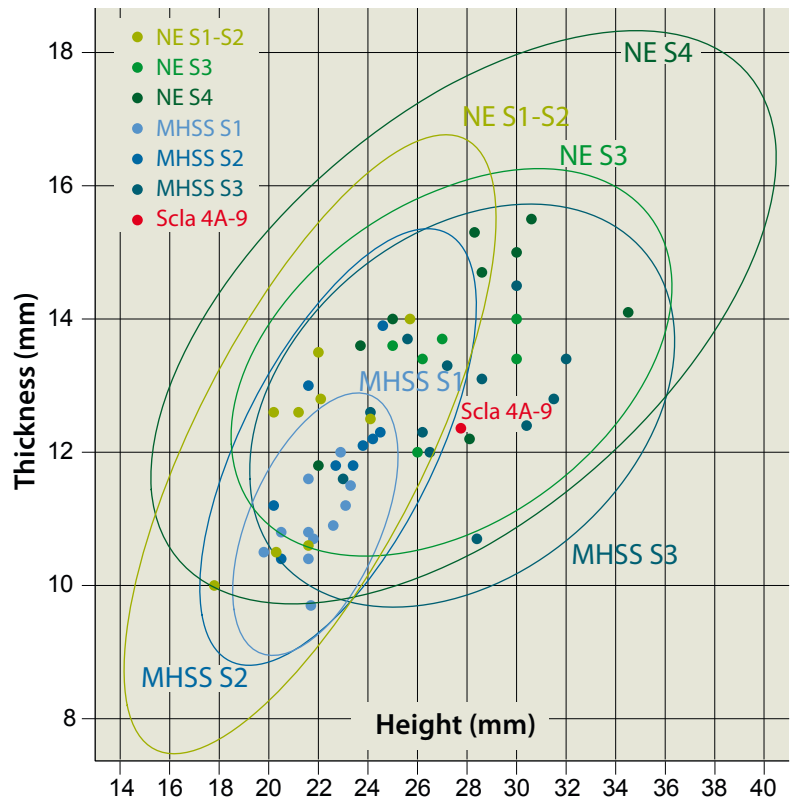
Comparison Samples	Measurement	n	mean	St dev	DP	ECRA
Immature NE S1–S4	Height	24	25.4	4.08	0.57	0.278
	Thickness	25	13.1	1.46	0.617	-0.246
	Index	24	52.3	5.49	0.191	-0.652
Immature NE S1–S2	Height	9	21.7	2.28	0.029	1.151
	Thickness	10	12.1	1.34	0.85	0.086
	Index	9	56.05	4.61	0.042	-1.049
Immature NE S3	Height	6	27.4	2.14	0.876	0.064
	Thickness	6	13.3	0.69	0.231	-0.53
	Index	6	48.9	3.69	0.328	-0.422
Immature NE S4	Height	9	27.9	3.82	0.97	-0.017
	Thickness	9	14	1.3	0.243	-0.547
	Index	9	50.8	5.51	0.316	-0.464
Immature MHSS S1	Height	11	21.8	1.07	0.000	2.496
	Thickness	11	10.9	0.64	0.046	1.024
	Index	11	49.9	2.72	0.096	-0.825
Immature MHSS S2	Height	9	22.8	1.69	0.019	1.27
	Thickness	9	12	0.99	0.726	0.158
	Index	9	52.9	3.55	0.054	-0.977
Immature MHSS S3	Height	11	27.8	2.86	0.986	-0.008
	Thickness	11	12.7	1.0	0.741	-0.153
	Index	11	46.0	5.0	0.83	-0.099
Immature MHSS S1–S3	Height	32	24.3	3.38	0.315	0.50
	Thickness	32	11.9	1.16	0.694	0.194
	Index	32	49.3	4.75	0.361	-0.454
Adult Early Neandertals	Height	11	34.71	5.53	0.237	-0.565
	Thickness	9	15.23	1.6	0.111	-0.778
	Index	9	43.69	6.78	0.863	0.077
Adult Late Neandertals	Height	14	35.34	4.15	0.09	-0.847
	Thickness	14	15.4	1.27	0.032	-1.108
	Index	12	45.12	6.18	0.972	-0.016

Table 7: Height and thickness (mm) of the Scladina symphysis (Scla 4A-9) compared to those of immature and adult Neandertals and MHSS, with DP and ECRA.

Figure 25: Bivariate analysis of the height and thickness of the Scladina symphysis (Scla 4A-9) with 95% equiprobable ellipses of juveniles Neandertals and MHSS.

Neandertals, the infradentale-pogonion angle changes from 90.7° in the immature class S1-S2 to 92.8° in immature S3-S4 and to 97.8° in adults, indicating a more recessed mandible as the individual ages. In the bivariate graph of Figure 24, the infradentale-pogonion angle and the infradentale-gnathion angle of the Scladina mandible are compared to two samples: Neandertals (immature and adult) and MHSS (immature and adult). Scla 4A-9 is situated outside the area of the graph where the two ellipses slightly overlap, in an area where only Neandertals are present.

The symphyseal height of Scla 4A-9 departs significantly from the average of the comparison samples in the case of immature Neandertals of classes S1-S2 and modern humans (MHSS) of age classes S1 and S2, both using DP probabilistic distance and ECRA (Table 7). In contrast, the symphyseal thickness of the Scladina mandible only departs from immature MHSS of class S1 and from adult late Neandertals. In the bivariate graph of Figure 25, symphyseal height and thickness of the mandible are compared to three age



Scla 4A-9	Canine	Height	26.32
		Thickness	13.1
		Index	49.8

Comparison Samples	Value	n	mean	St. dev.	DP	ECRA
Immature NE S2-S4	Height	13	24.6	3.03	0.581	0.261
	Thickness	13	14.6	1.91	0.447	-0.36
	Index	12	58.9	6.1	0.164	-0.678
Immature NE S2 & S3	Height	6	23.2	3.69	0.436	0.329
	Thickness	6	13.9	2.01	0.707	-0.155
	Index	6	60.3	6.22	0.152	-0.657
Immature NE S4	Height	7	25.8	1.81	0.784	0.117
	Thickness	7	15.3	1.71	0.246	-0.526
	Index	6	59.2	6.52	0.209	-0.561
Immature MHSS S1	Height	12	19.6	1.35	0.000	2.262
	Thickness	12	9.6	0.71	0.000	2.24
	Index	12	48.5	3.67	0.73	0.161
Immature MHSS S2	Height	13	20.9	1.85	0.013	1.345
	Thickness	13	10.3	1.08	0.024	1.19
	Index	13	49.2	3.2	0.854	0.086
Immature MHSS S3	Height	14	23.5	3.87	0.479	0.337
	Thickness	14	10.9	1.18	0.085	0.863
	Index	14	47.3	4.6	0.596	0.252
Immature MHSS S1-S3	Height	39	21.4	3.07	0.117	0.792
	Thickness	39	10.3	1.14	0.019	1.213
	Index	39	48.32	3.88	0.705	0.188
Adult Early Neandertals	Height	8	32.54	4.24	0.186	-0.62
	Thickness	8	15.71	1.36	0.096	-0.812
	Index	8	49.2	6.7	0.931	0.038
Adult Late Neandertals	Height	10	33.75	2.35	0.012	-1.398
	Thickness	9	14.96	1.17	0.151	-0.689
	Index	8	44.01	3.71	0.163	0.66

Table 8: Height and thickness (mm) of the Scladina mandible (Scla 4A-9) at the level of the left canine compared to those of immature and adult Neandertals and immature MHSS, with DP and ECRA.

samples of immature Neandertals and immature MHSS. Scla 4A-9 is situated in the central area where the ellipses of the two oldest immature Neandertal groups (NE S3 & NE S4) and the MHSS S3 immature groups overlap, but only just over the NE S1-S2 and MHSS S2 groups. Even if the symphyseal thickness mean is slightly higher in Neandertal age groups than in corresponding MHSS age groups, symphyseal dimensions do not provide clear taxonomic indications in the case of the Scladina specimen.

At the level of the canine, the height and thickness of the left hemimandible (Scla 4A-9) do not depart significantly from the average of the juvenile Neandertal comparison samples nor from immature modern human (MHSS) from age class S3, both using DP probabilistic distance and ECRA (Table 8). In contrast, both the height and thickness of the Scladina mandible at the canine significantly depart from immature MHSS of classes S1 and S2. The height of the mandible also significantly departs from adult Late Neandertals. The bivariate graph of Figure 26 compares the height and thickness of the Scladina mandible at the canine to juvenile Neandertals as a whole and also to three age groups of immature MHSS. Scla 4A-9 is situated close to the centre of the ellipse of immature Neandertals and inside the ellipses of the MHSS S3 immature group, but just at the limit of the MHSS S2 group and outside the MHSS S1 group.

At the level of the P₃, the height and thickness of the right hemimandible Scla 4A-1 do not depart significantly from the average of the three juvenile Neandertal comparison samples nor from immature modern humans (MHSS) from age class S3, both using DP probabilistic distance and ECRA (Table 9). In contrast, both the height and thickness of the mandible at the P₃ significantly depart from immature MHSS of class S1. Concerning immature MHSS of class S2, Scladina is only significantly different in terms of the thickness.

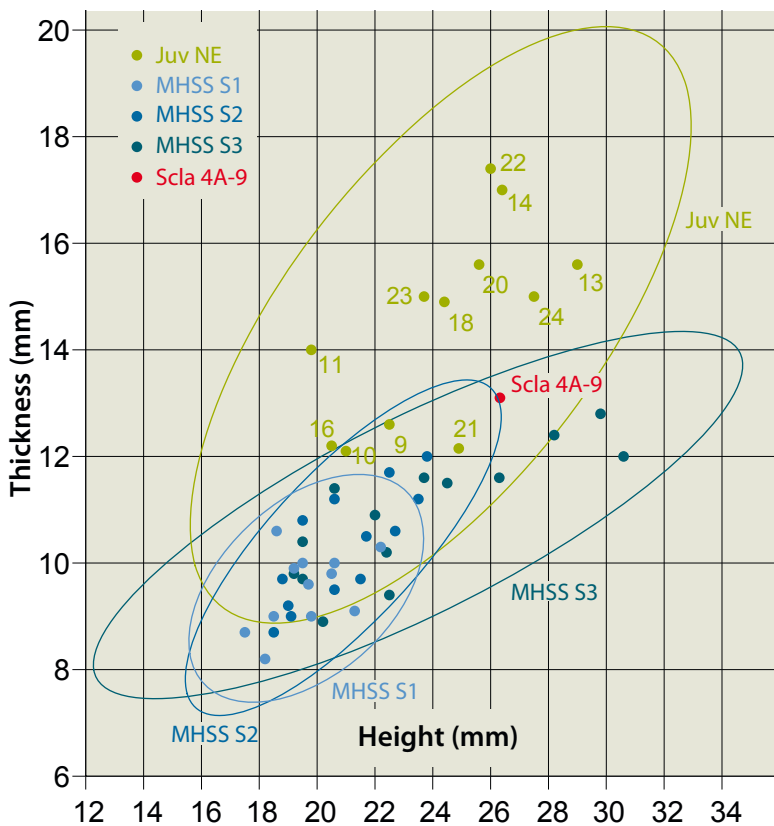


Figure 26: Bivariate analysis of the height and thickness (mm) of the Scla 4A-9 hemimandible at the level of the canine with 95% equiprobable ellipses of juvenile Neandertals and juvenile MHSS.

Table 9: Height and thickness (mm) of the Scladina right hemimandible (Scla 4A-1) at the level of the right P₃ compared to those of immature Neandertals and MHSS as well as of adult Neandertals, with DP and ECRA.

Scla 4A-1	First premolar	Height	(24.5)
		Thickness	12.8
		Index	52.2

The height of the mandible also significantly departs from adult Late Neandertals. In the bivariate graph of Figure 27, the height and thickness of the mandible are compared to two age samples of Neandertals (NE S1-S2 & NE S3-S4) and three age groups of immature MHSS. Scla 4A-1 is situated in the central area of the graph where the ellipses of the two immature Neandertal groups and the MHSS S2 and S3 immature groups overlap, but far outside the MHSS S1 group. So, as for symphyseal dimensions, dimensions at the P₃ do not provide clear taxonomic indications in the case of the Scladina specimen.

The height at the M₁ of Scla 4A-1 and 9 only departs significantly from the average of the immature modern human (MHSS) of age classes S1 and S2 as well as from adult late Neandertals and adult MHSS, using DP probabilistic distance and ECRA (Table 10). In contrast, the thickness at the M₁ only departs from adult MHSS. In the bivariate graph of Figure 28, the height and thickness at the M₁ are compared to samples of immature MHSS taken as a whole – but with different symbols according to the age classes – and to juvenile Neandertals also taken as a whole (due to their small number). Both Scladina hemimandibles are situated in the central area where the ellipses of the immature Neandertal and MHSS S1-S3 groups overlap, but in an area where only specimens of age group S3 MHSS are present, over the specimens of MHSS groups S1 and S2.

The minimum breadth of the Scla 4A-1 ramus only departs significantly from immature modern humans (MHSS) of age classes S1 and S3 (class S2 does not contain enough fossils to provide reliable results), using DP probabilistic distance and ECRA (Table 11). In contrast, the Scladina I-4A mandible minimum breadth fits well within the variability of both immature and adult Neandertals and, despite the young age of eight years, within that of adult Upper Palaeolithic and modern humans (MHSS).

Samples		n	mean	St dev	DP	ECRA
Immature NE S1–S4	Height	18	21.4	4.32	0.483	0.34
	Thickness	21	13.8	2.12	0.642	-0.226
	Index	16	63.9	9.2	0.223	-0.597
Immature NE S1	Height	8	18.3	3.07	0.083	0.854
	Thickness	8	12.3	1.28	0.708	0.165
	Index	8	68.1	8.5	0.104	-0.791
Immature NE S2–S3	Height	5	22.7	3.93	0.671	0.165
	Thickness	7	14	1.95	0.561	-0.251
	Index	5	61.8	9.9	0.387	-0.349
Immature NE S4	Height	5	25.1	3.01	0.852	-0.072
	Thickness	6	15.7	1.73	0.155	-0.652
	Index	3	56.1	3.6	0.392	-0.252
Immature MHSS S1	Height	10	19.6	1.96	0.034	1.105
	Thickness	10	9.6	0.73	0.002	1.938
	Index	10	49.4	5.6	0.629	0.221
Immature MHSS S2	Height	13	22.9	2.76	0.573	0.266
	Thickness	13	10.8	0.85	0.037	1.08
	Index	13	47.5	7.4	0.537	0.292
Immature MHSS S3	Height	12	24.9	3.55	0.912	-0.051
	Thickness	12	11.6	0.97	0.242	0.562
	Index	12	46.9	7.8	0.511	0.309
Immature MHSS S1–S3	Height	35	22.7	3.45	0.605	0.257
	Thickness	35	10.7	1.18	0.084	0.876
	Index	35	47.8	6.96	0.531	0.311
Adult Early Neandertals	Height	7	32.2	4.71	0.153	-0.668
	Thickness	8	15.66	1.5	0.098	-0.806
	Index	7	49.55	5.24	0.631	0.207
Adult Late Neandertals	Height	11	33.42	1.92	0.001	-2.085
	Thickness	9	14.77	1.23	0.148	-0.695
	Index	9	44.56	3.86	0.083	0.858

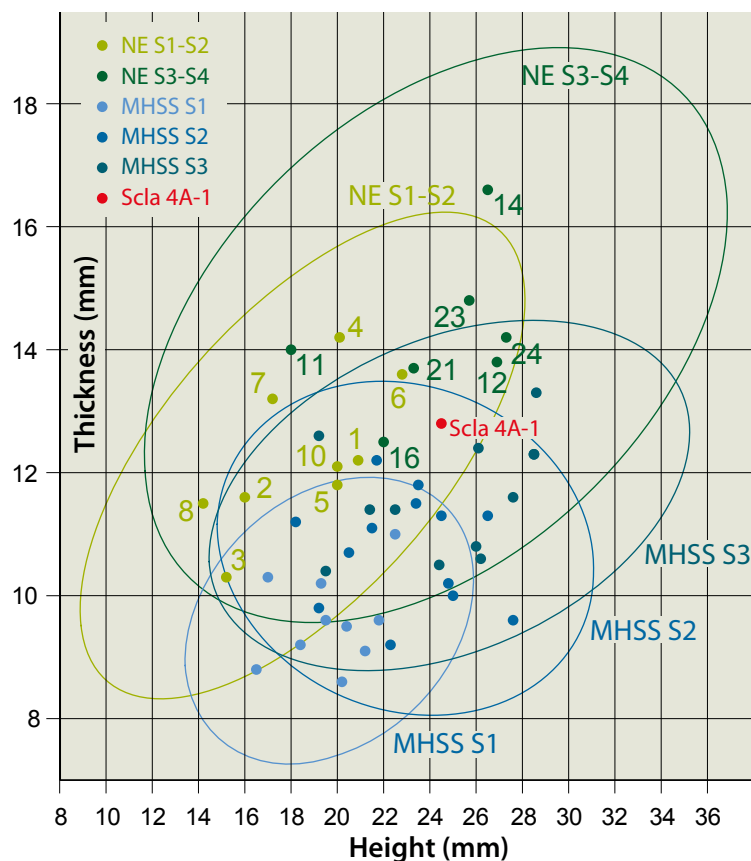


Figure 27: Bivariate analysis of the height and thickness (mm) of the Scla 4A-1 right hemimandible at the level of the P₃ with 95% equiprobable ellipses of juvenile Neandertals and MHSS.



Scla 4A-9/M ₁			Scla 4A-1/M ₁	Scla 4A-1/M ₁			vs Scla 4A-9		vs Scla 4A-1	
Height	23	Height		22.2	DP	ECRA	DP	ECRA		
Thickness	14.2	Thickness		14	DP	ECRA	DP	ECRA		
Index	61.6	Index	63.1	DP	ECRA	DP	ECRA	DP	ECRA	
Comparison Samples		n	mean	St dev						
Immature NE (S1-S4)	Height	11	23.7	3.79		0.857	-0.083	0.701	-0.178	
	Thickness	10	15.8	1.31		0.253	-0.540	0.203	-0.607	
	Index	10	70.1	10.9		0.456	-0.345	0.537	-0.284	
Immature MHSS (S1)	Height	11	16.7	2.1		0.013	1.346	0.026	1.175	
	Thickness	11	13.4	1.1		0.484	0.326	0.597	0.245	
	Index	11	80.2	5.7		0.009	-1.465	0.013	-1.346	
Immature MHSS (S2)	Height	10	17.7	1.81		0.017	1.294	0.035	1.099	
	Thickness	10	14.3	0.96		0.919	-0.046	0.762	-0.138	
	Index	10	81.5	6.6		0.015	-1.333	0.021	-1.232	
Immature MHSS (S3)	Height	12	23.5	3.1		0.875	-0.073	0.683	-0.191	
	Thickness	12	14.4	0.9		0.828	-0.101	0.665	-0.202	
	Index	12	62.0	8.8		0.965	-0.021	0.903	0.057	
Immature MHSS (S1-S3)	Height	33	19.5	3.9		0.376	0.441	0.494	0.340	
	Thickness	33	14.0	1.0		0.843	0.098	1	0.000	
	Index	33	73.9	11.6		0.297	-0.521	0.359	-0.457	
Adult Early Neandertals	Height	11	30.52	4.26		0.108	-0.792	0.079	-0.877	
	Thickness	10	15.49	1.04		0.246	-0.548	0.186	-0.633	
	Index	9	52.07	7.69		0.250	0.537	0.189	0.622	
Adult Late Neandertals	Height	11	33.1	1.8		0.000	-2.518	0	-2.718	
	Thickness	9	14.71	1.49		0.741	-0.148	0.646	-0.207	
	Index	9	44.6	3.53		0.001	2.088	0.001	2.273	
Adult MHSS	Height	490	30.67	3.31		0.021	-1.179	0.011	-1.302	
	Thickness	200	11.8	1.18		0.043	1.031	0.064	-0.945	

Table 10: Height and thickness (mm) of the Scladina mandible (Scla 4A-1 & 9) at the level of the M₁ compared to those of immature and adult Neandertals and MHSS with DP and ECRA.

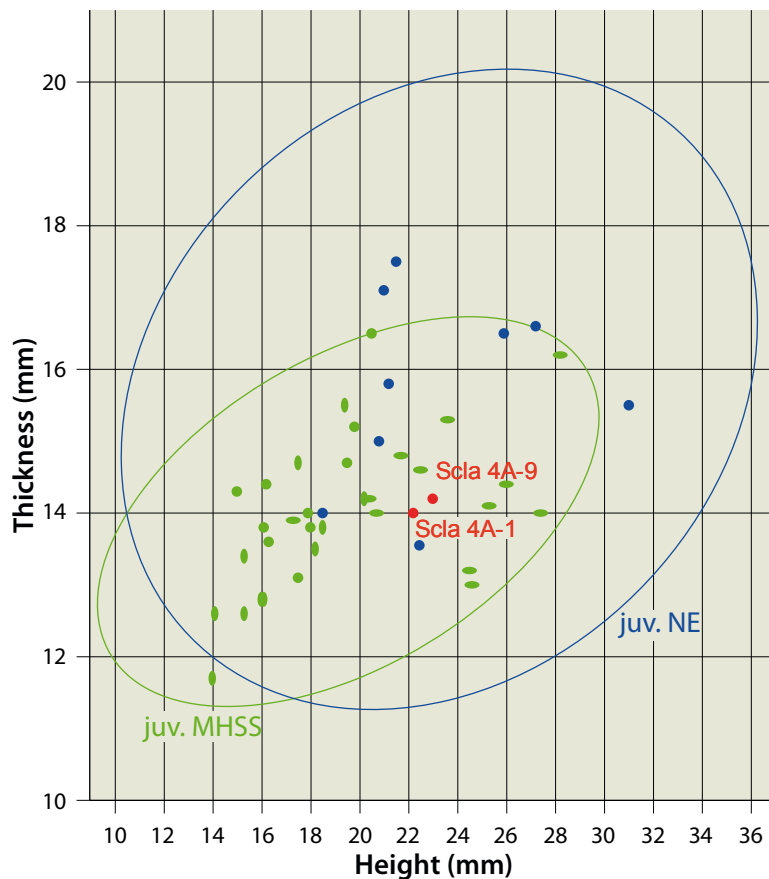


Figure 28: Bivariate analysis of the height and thickness (mm) of the Scladina mandible (Scla 4A-1 & 9) at the level of the M₁ with 95% equiprobable ellipses of juvenile Neandertals and MHSS.

- juvenile MHSS S1
- juvenile MHSS S2
- juvenile MHSS S3
- juvenile NE
- Scla 4A-1 & 9

Scla 4A-1	Ramus minimum breadth	35.1
------------------	-----------------------	------

Comparison Samples		n		Mean	Stand. dev.	DP	ECRA
NE (Neandertal)	juvenile (S1-S4)	11		28.5	3.47	0.086	0.854
MHSS (Spitalfields)	2-5 years (S1)	15		22.4	1.6	0.000	3.701
MHSS (Hasanlu-Tapeh)	S2	4		23.8	4.2	0.074	0.845
MHSS	7-10 years (S3)	12		27.4	1.9	0.002	1.841
EN	adult	6	r	39.15	2.93	0.225	-0.538
LN	adult	10	r	40.55	3.09	0.112	-0.78
N (EN + LN)	adult	16	r	40.03	3.01	0.122	-0.768
UPMH	adult	11		39.69	3.12	0.172	-0.66
MHSS	adult	1107		33.99	3.19	0.728	0.177
Belgian MHSS	adult	11		33.3	3.45	0.613	0.234
Belgian MHSS	S3	8		27.3	3.59	0.066	0.919

Table 11: Ramus minimum breadth of the Scladina right hemimandible (Scla 4A-1) compared to that of immature and adult Neandertals and MHSS with DP and ECRA.

Scla 4A-1	Ramus height	45.5
------------------	--------------	------

Comparison Samples		n		Mean	Stand. dev.	DP	ECRA
NE	S1-S4	6		41.4	10.01	0.699	0.159
MHSS	7-10 years (S3)	12		45.4	4.3	0.982	0.011
Belgian MHSS	S3	8		45.2	4.1	0.944	0.031
EN	adult	4	r	66.04	3.23	0.008	-1.998
LN	adult	5	r&l	67.68	5.77	0.018	-1.385
NE (EN + LN)	adult	6	r	64.98	3.63	0.003	-2.088
UPMH	adult	9	r&l	63.95	6.25	0.018	-1.28
MHSS	adult	879		57.06	4.89	0.018	-1.204
Belgian MHSS	adult	11		56.04	4.21	0.031	-1.124

Table 12: Ramus height of the Scladina right hemimandible (Scla 4A-1) compared to that of immature and adult Neandertals and MHSS with DP and ECRA.

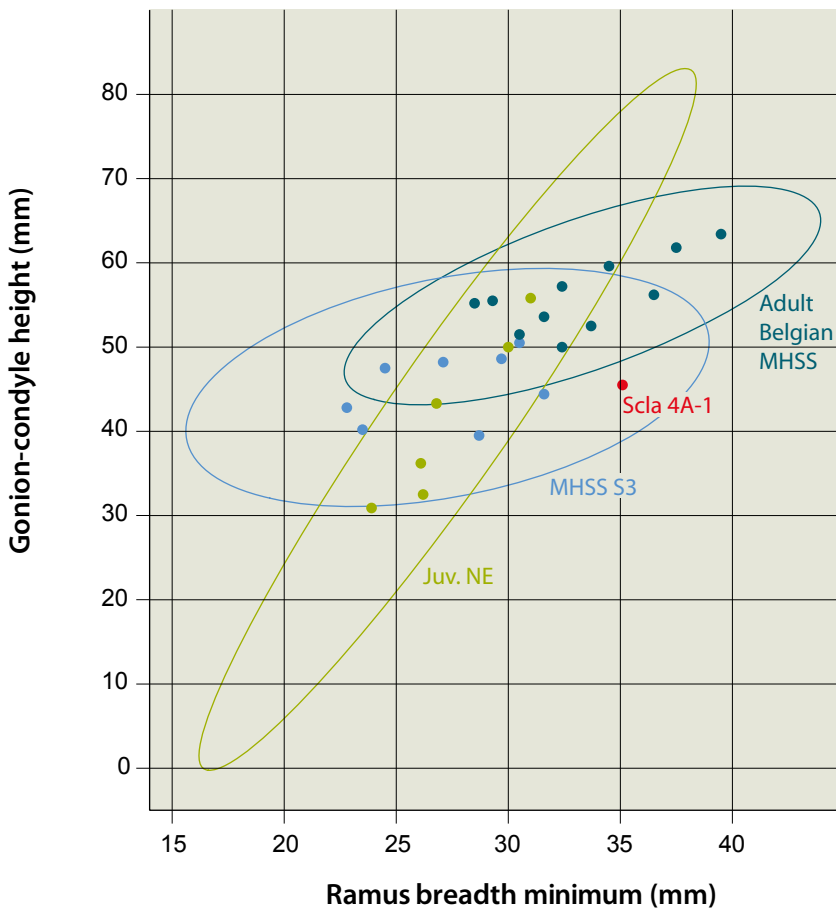


Figure 29: Bivariate analysis of the minimum breadth (mm) of the right ramus and the gonion-condyle height. The hemimandible Scla 4A-1, compared to immature Neandertals as well as to some Belgian immature and adult MHSS.

- Juvenile NE
- MHSS S3
- Adult Belgian MHSS
- Scla 4A-1



The gonion-condyle height (M 70) along the posterior border of the ramus of Scla 4A-1 does not significantly differ from the average of immature Neandertals or of immature modern human (MHSS) of age class S3 (Table 12). In contrast, it significantly differs from all Neandertal and MHSS adults.

In the bivariate graph of Figure 29 the minimum breadth of the ramus and the gonion-condyle height of the mandible are compared to immature Neandertals as well as to some Belgian immature and adult MHSS. Scla 4A-1 is situated outside the area of adult MHSS but also outside

the too small sample of juvenile Neandertals and, in contrast, in the area of juvenile MHSS of age class S3.

The mandibular angle of Scla 4A-1 (116°) only departs significantly from immature modern humans (MHSS) of age class S1 (Table 13). Clearly, the ramus is less inclined on the corpus than in modern children (see GIACOBINI et al., 1984).

5.3. Discussion

In the previous section, some dimensions of the Scladina mandible were statistically compared

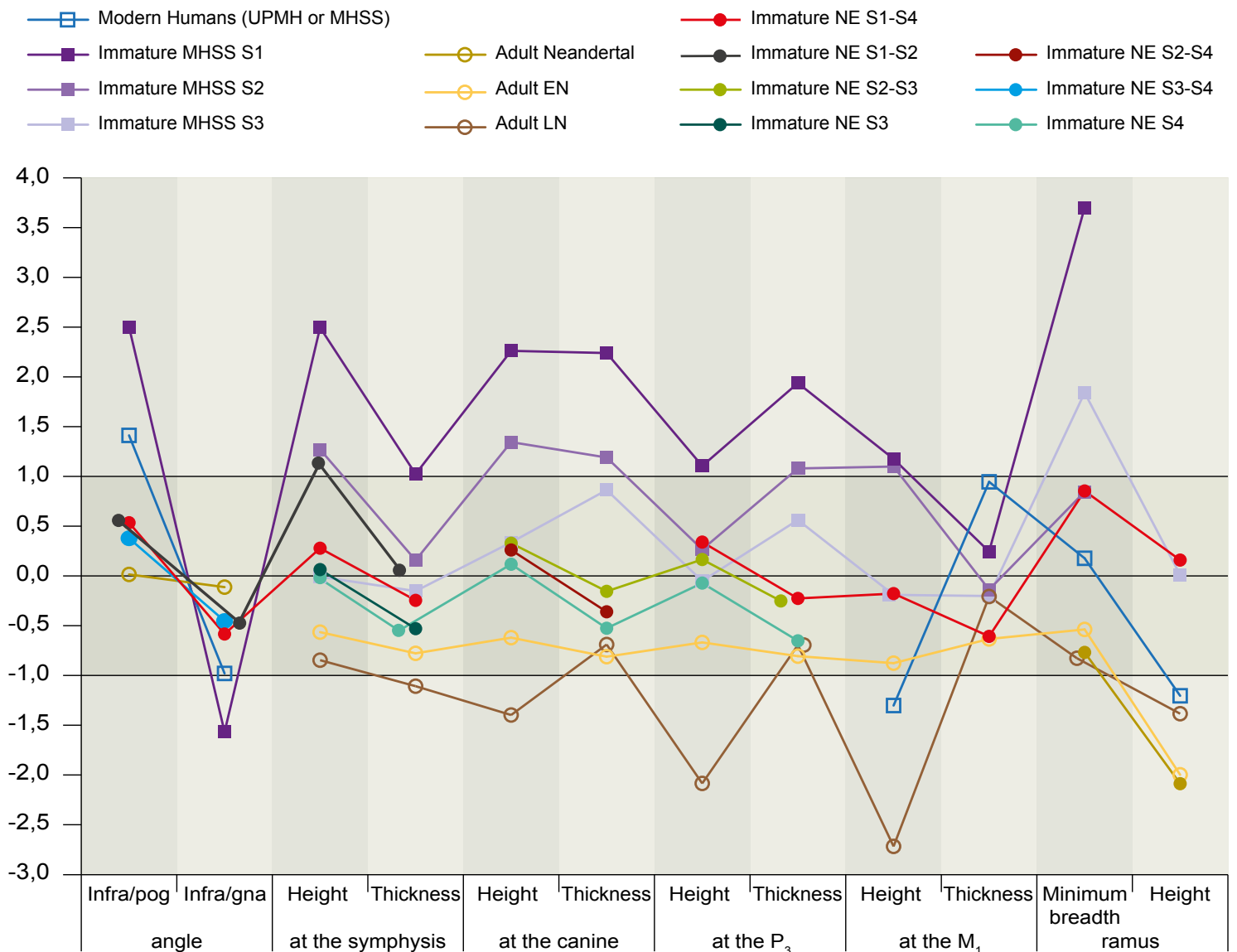


Figure 30: ECRA of the symphysis angles as well as of the height and thickness of the Scladina mandible.

Scla 4A-1		Mandibular angle (°)	116			
Comparison Samples		n	Mean	St. Dev	DP	ECRA
EN (Early Neandertals)	adult	4	113.5	6.61	0.73	0.119
LN (Late Neandertals)	adult	6	107.3	3.56	0.058	0.951
Neandertals (EN + LN)	adult	10	109.8	5.63	0.299	0.487
NE	juvenile	10	120.7	7.79	0.561	-0.267
UPMH	adult	19	116.68	5.65	0.906	-0.057
MHSS	juvenile S1	20	134.6	6.25	0.008	-1.422
MHSS	adult	1037	122.19	6.42	0.335	-0.491

Table 13: Mandibular angle of the right hemimandible (Scla 4A-1) compared to those of immature and adult Neandertals and MHSS with DP and ECRA.

to different immature and adult Neandertal and MHSS samples. In Figure 30, we analyse all ECRA dimensions as a series. It shows that the Scladina I-4A mandible differs from immature MHSS of classes S1 and frequently S2 as well as, often, from adult modern humans (UPMH or MHSS). The Scladina mandible fits perfectly with immature NE S2-S3-S4, including the angles at the symphysis, which clearly mark the difference with MHSS. It differs more from adult Late Neandertals than from adult Early Neandertals, which could be linked to the approximate age of the fossil at 80,000, which relates to either MIS 5b or 5a (see Chapter 5: § 4.3).

6. Conclusion

The anatomical observations and morphometric analysis in this chapter highlight a range of features found on immature and adult Neandertals.

In terms of morphology, the Scladina mandible combines some features generally considered as derived — such as, among others (Table 2), the highly excavated submandibular fossa or the deeply excavated pterygoid fossa — and some features not unanimously accepted as derived, but frequent among Neandertals, for instance the laterally expanded condyle. In fact, what characterizes a Neandertal mandible, both adult and juvenile, lies less in supposed derived traits and more in the unique combination of a set of traits that, taken individually, are not typical of this taxon. In this regard, the Scladina mandible matches the general pattern of Neandertals.

Statistically, the Scladina mandible is close to immature Neandertals, particularly those who were about the same age at death. Compared to adult Neandertals, it seems closer to Early Neandertals than to Late Neandertals.

Acknowledgements

The author gratefully acknowledges Joël Éloy (Association wallonne d'Études mégalithiques, AWEM) for the photographs of the Neandertal remains, for designing the equiprobable ellipse figures, and for his technical assistance, Sylviane Lambermont (AWEM) for the line drawings and Jean-François Lemaire (SPW) for Figure 9.

References

- ANTÓN S. C., 1996. Tendon-associated bone features of the masticatory system in Neanderthals. *Journal of Human Evolution*, 31: 391-408.
- ARNAUD J., 2014. La mandibule d'Archi 1: Étude morphologique et morphométrique détaillée d'un néandertalien immature. *Bulletin et Mémoires de la Société anthropologique de Paris*, 14 p. doi 10.1007/s13219-014-0096-z.
- ASCENZI A. & SEGRE A., 1971. A New Neandertal Child Mandible from a Upper Pleistocene Site in Southern Italy. *Nature*, 233: 280-283.
- BEHRENSMEYER A. K., 1978. Taphonomic and ecologic information from bone weathering. *Paleobiology*, 4, 2: 150-162.
- BILLY G. & VALLOIS H. V., 1977. La mandibule pré-rissienne de Montmaurin. *L'Anthropologie*, 81: 273-311 & 411-458.
- BONJEAN D., MASY P. & TOUSSAINT M., 2009. L'enfant néandertalien de Sclayn. Petite histoire d'une découverte exceptionnelle. *Notae Praehistoricae*, 19: 49-51.
- BOULE M., 1911-1913. *L'homme fossile de La Chapelle-aux-Saints*. Annales de Paléontologie, 278 p.



- CONDEMI S., 2001. *Les Néandertaliens de La Chaise (abri Bourgeois-Delaunay)*. Paris, Éditions du Comité des travaux historiques et scientifiques. Documents préhistoriques, 15, 178 p.
- CONDEMI S., 2005. Continuité et/ou discontinuité des premiers peuplements européens. In N. MOLINES, M.-H. MONCEL & J.-L. MONNIER (eds.), *Les premiers peuplements en Europe : données récentes sur les modalités de peuplement et sur le cadre chronostratigraphique, géologique et paléogéographique des industries du Paléolithique ancien et moyen en Europe*. Oxford, British Archaeological Reports, International Series, 1364: 9-15.
- COON C. S., 1962. *The origin of races*. New-York, Knopf.
- COQUEUGNIOT H., 1999. *Le crâne d'Homo sapiens en Eurasie: croissance et variation depuis 100 000 ans*. Oxford, British Archaeological Reports, International Series, 822, 197 p.
- CREED-MILES M., ROSAS A. & KRUSZYNSKI R., 1996. Issues in the identification of Neandertal derivative traits at early post-natal stages. *Journal of Human Evolution*, 30: 147-153.
- CREVECOEUR I., BAYLE P., ROUGIER H., MAUREILLE B., HIGHAM T. F. G., VAN DER PLICHT J., DE CLERCK N. & SEMAL P., 2010. The Spy VI child: A newly discovered Neandertal infant. *Journal of Human Evolution*, 59: 641-656.
- DAURA J., SANZ M., SUBIRÁ M. E., QUAM R., FULLOLA J. M. & ARSUGA J. L., 2005. A Neandertal mandible from the Cova del Gegant (Sitges, Barcelona, Spain). *Journal of Human Evolution*, 49: 56-70.
- DEFRISE-GUSSENHOVEN, E., 1955. Ellipses équi-probables et taux d'éloignement en biométrie. *Bulletin de l'Institut Royal des Sciences Naturelles de Belgique*, 26: 1-31.
- DE LUMLEY-WOODYEAR M.-A., 1973. *Anté-néandertaliens et Néandertaliens du bassin méditerranéen occidental européen*. Marseille, Université de Provence, Études Quaternaires, 2, 626 p.
- DOBSON S. D. & TRINKAUS E., 2002. Cross-sectional geometry and morphology of the mandibular symphysis in Middle and Late Pleistocene *Homo*. *Journal of Human Evolution*, 43: 67-87.
- DODO Y., KONDO O. & NARA T., 2002. The Skull of the Neanderthal Child of Burial No.1. In T. AKAZAWA & S. MULHESEN (eds.), *Neanderthal Burials. Excavations of the Dederiyeh Cave, Afrin, Syria*. Kyoto, International Research Center for Japanese Studies: 93-137.
- DUPONT E., 1866. Étude sur les fouilles scientifiques exécutées pendant l'hiver de 1865-1866 dans les cavernes des bords de la Lesse. *Bulletins de l'Académie royale des Sciences, des Lettres et des Beaux-Arts de Belgique*, 2^e série, XXII: 31-54.
- FAERMAN M., ZILBERMAN U., SMITH P. & KHARITONOV V., 1994. A Neanderthal infant from the Barakai Cave, Western Caucasus. *Journal of Human Evolution*, 27: 405-415.
- FRAIPONT J. & LOHEST M., 1887. La race humaine de Néanderthal ou de Canstadt en Belgique. Recherches ethnographiques sur des ossements humains découverts dans les dépôts quaternaires d'une grotte à Spy et détermination de leur âge géologique. Gand, *Archives de Biologie*, 7 (1886): 587-757, 4 pl. h.t.
- FRANCISCUS R. G. & TRINKAUS E., 1995. Determinants of retromolar space presence in Pleistocene *Homo* mandibles. *Journal of Human Evolution*, 28: 577-595.
- FRAYER D. W., 1992. Evolution at the European edge: Neanderthal and Upper Paleolithic relationships. *Préhistoire européenne*, 2: 9-69.
- GABIS R., 1956. Étude de la mandibule humaine de la station moustérienne de Petit-Puymoyen (Charente). *Bulletin de la Société géologique de France*, 6^e série, tome VI: 1021-1028.
- GARRALDA M. D. & VANDERMEERSCH B., 2000. Les Néandertaliens de la grotte de Combe-Grenal (Domme, France). *Paleo*, 12: 213-259.
- GENET-VARCIN E., 1982. Vestiges humains du Würmien inférieur de Combe-Grenal, commune de Domme (Dordogne). *Annales de Paléontologie*, 68, 2: 133-169.
- GIACOBINI G., DE LUMLEY M.-A., YOKOYAMA Y. & NGUYEN H.-V., 1984. Neanderthal Child and Adult Remains from a Mousterian Deposit in Northern Italy (Caverna Delle Fate, Finale Ligure). *Journal of Human Evolution*, 13: 687-707.
- GORJANOVIĆ-KRAMBERGER D., 1906. Der diluviale Mensch von Krapina in Kroatien. Ein Beitrag zur Paläoanthropologie. In O. WALKHOFF (ed.), *Studien über die Entwicklungsmechanik des Primatenskelletes*, vol. II. Wiesbaden, C. W. Kreidel: 59-277.

- HAMMER O., HARPER D.A.T. & RYAN P. D., 2001. PAST: PAleontological STatistics software package for education and data analysis. Available at: Palaeontol. Electr. 4 http://palaeo-electronica.org/2001_1/past/issue1_01.htm.
- HEIM J.-L., 1976. *Les Hommes Fossiles de La Ferrassie. Tome 1: Le Gisement. Les Squelettes adultes (Crâne et Squelette du Tronc)*. Paris, Masson, Archives de l'Institut de Paléontologie humaine, 35, 331 p.
- HEIM J.-L. & GRANAT J., 1995. La mandibule de l'enfant néandertalien de Malarnaud (Ariège). Une nouvelle approche anthropologique par la radiographie et la tomodynamométrie. *Anthropologie et Préhistoire*, 106: 75-96.
- HOUËT F., 2001. Limites de variation, distance (position) et écart réduit ajusté. *Paléo*, 13: 195-200.
- HOWELLS W.W., 1975. Neanderthal man: facts and figures. In R. H. TUTTLE (ed.), *Palaeoanthropology, morphology and paleoecology*. Paris, Mouton: 389-407.
- HUBLIN J.-J. & TILLIER A.-M., 1981. The Mousterian Juvenile Mandible from Irhoud (Morocco). A Phylogenetic Interpretation. In C. B. STRINGER (ed.), *Aspects of Human Evolution*. Symposia of the Society for the Study of Human Biology, 21, London, Taylor & Francis Ltd.: 167-185.
- ISHIDA H. & KONDO O., 2002. The Skull of the Neanderthal Child of Burial No.2. In T. AKAZAWA & S. MULHESEN (eds.), *Neanderthal Burials. Excavations of the Dederiyeh Cave, Afrin, Syria*. Kyoto, International Research Center for Japanese Studies: 271-297.
- JABBOUR R. S., RICHARDS G. D. & ANDERSON J. Y., 2002. Mandibular Condyle Traits in Neanderthals and Other *Homo*: a Comparative, Correlative, and Ontogenetic Study. *American Journal of Physical Anthropology*, 119: 144-155.
- KALLAY J., 1955. Lage und Form des Foramen mandibulare beim Krapina-menschen. *Österreichischen Zeitschrift für Stomatologie*, 10: 523-526.
- KALLAY J., 1970. Komparative napomene o čeljustima Krapinskih praljudi s obzirom na Položaj među hominidima. In M. MALEZ (ed.), *Krapina 1899-1969*. Zagreb, Jugoslavenska Akademija znanosti i umjetnosti: 153-164.
- KEITER F., 1935. Unterkiefer aus Australien und Neuguinea aus dem Nachlasse Rudolf Pöchs. *Zeitschrift für Morphologie und Anthropologie*, 33: 190-226.
- LEGUEBE A. & TOUSSAINT M., 1988. *La mandibule et le cubitus de La Naulette, morphologie et morphométrie*. Paris, Éditions du Centre national de la recherche scientifique, Cahiers de Paléanthropologie, 125 p., 8 pl.
- MADRE-DUPOUY M., 1992. *L'enfant du Roc de Marsal. Étude analytique et comparative*. Paris, Éditions du Centre national de la recherche scientifique, Cahiers de Paléanthropologie, 300 p.
- MALLEGNI F. & RONCHITELLI A., 1987. Découverte d'une mandibule néandertalienne à l'abri du Molare près de Scario (Salerno-Italie) : observations stratigraphiques et paléontologiques. Étude anthropologique. *L'Anthropologie*, 91: 163-174.
- MALLEGNI F. & TRINKAUS E., 1997. A reconsideration of the Archi 1 Neanderthal mandible. *Journal of Human Evolution*, 33: 651-668.
- MANN A. & VANDERMEERSCH B., 1997. An Adolescent Female Neanderthal Mandible from Montgaudier Cave, Charente, France. *American Journal of Physical Anthropology*, 103: 507-527.
- MINUGH-PURVIS N., 1988. *Patterns of craniofacial growth and development in Upper Pleistocene Hominids*. PhD thesis, Philadelphia, University of Pennsylvania, 657 p.
- OTTE M., TOUSSAINT M. & BONJEAN D., 1993. Découverte de restes humains immatures dans les niveaux moustériens de la grotte Scladina à Andenne (Belgique). *Bulletins et Mémoires de la Société d'Anthropologie de Paris*, nouvelle série, t. 5, 1-2: 327-332.
- PATTE E., 1955. *Les Néandertaliens. Anatomie, physiologie, comparaisons*. Paris, Masson, 559 p.
- PIVETEAU J., 1957. *Traité de Paléontologie. VII: Primates, Paléontologie humaine*. Paris, Masson, 657 p.
- PIVETEAU J., 1963; 1964; 1966. La grotte du Regourdou (Dordogne). Paléontologie humaine. *Annale de Paléontologie (Vertébrés)*, XLIX: 285-304; L: 155-194; LII, fasc. 2: 163-194.
- QUAM R. M., ARSUAGA J.-L., BERMÚDEZ DE CASTRO J.-M., DíEZ J. C., LORENZO C., CARRETERO J. M., GARCÍA N. & ORTEGA A. I., 2001. Human remains from Valdegoba Cave (Huérmeces, Burgos, Spain). *Journal of Human Evolution*, 41: 385-435.



- RAK Y., 1998^a. The derived mandible of *Homo neanderthalensis*. *American Journal of Physical Anthropology*, Suppl., abstract, 27: 183.
- RAK Y., 1998^b. Does any Mousterian cave present evidence of two hominid species? In T. AKAZAWA, K. AOKI & O. BAR-YOSEF (eds.), *Neandertals and modern human in western Asia*. New York, Plenum Press: 353-366.
- RAK Y., GINZBURG A. & GEFFEN E., 2002. Does *Homo neanderthalensis* Play a Role in Modern Human Ancestry? The Mandibular Evidence. *American Journal of Physical Anthropology*, 119: 199-204.
- RAK Y. & KIMBEL W. H., 1995. Diagnostic Neandertal characters in the Amud 7 infant. *American Journal of Physical Anthropology*, Suppl., abstract, 20: 177-178.
- RAK Y., KIMBEL W. H. & HOVERS E., 1994. A Neandertal infant from Amud Cave, Israel. *Journal of Human Evolution*, 26: 313-324.
- RAK J., KIMBEL W. H. & HOVERS E., 1996. On Neandertal autapomorphies discernible in Neandertal infants: a response to Creed-Miles et al., 1996, *Journal of Human Evolution*, 30: 155-158.
- RICHARDS G. D., JABBOUR R. S., ANDERSON J. Y., 2003. *Medial Mandibular Ramus. Ontogenetic, idiosyncratic, and geographic variation in recent Homo, great apes, and fossil hominids*. Oxford, British Archaeological Reports, International Series, 1138, 113 p.
- RIGHTMIRE G. P., 1990. *The Evolution of Homo erectus*. New York, Cambridge University Press, 260 p.
- ROSAS A., 1995. Seventeen new mandibular specimens from the Atapuerca/Ibeas Middle Pleistocene Hominids sample (1985-1992). *Journal of Human Evolution*, 28: 533-559.
- ROSAS A., 1997. A gradient of size and shape for the Atapuerca sample and Middle Pleistocene hominid variability. *Journal of Human Evolution*, 33: 319-331.
- ROSAS A., 2001. Occurrence of Neandertal Features in Mandibles from the Atapuerca-SH Site. *American Journal of Physical Anthropology*, 114 : 74-91.
- ROUGIER H., CREVECOEUR I., SEMAL P. & TOUSSAINT M., 2009. Des Néandertaliens dans la troisième caverne de Goyet. In K. DI MODICA & C. JUNGELS (dir.), *Paléolithique moyen en Wallonie. La collection Louis Éloy*. Bruxelles, Collections du Patrimoine culturel de la Communauté française, 2: 173.
- SCHUMACHER G. H., 1959. Die Kaumuskulatur von menschlichen Früh- und Neugeborenen. *Zeitschrift für Anatomie und Entwicklungsgeschichte*, 121: 304-321.
- SCHUMACHER G. H., 1961. *Funktionelle Morphologie der Kaumuskulatur*. Jena, VEB Gustav Fischer Verlag, 262 p.
- SCHUMACHER G. H., 1962. Struktur- und Funktionswandel der Kaumuskulatur nach der Geburt. *Fortschritte der Kieferorthopädie*, 23: 135-166.
- SERGI S. & ASCENZI A., 1955. La mandibola neandertaliana Circeo III. *Rivista di Antropologia*, XLII: 337-403, 20 pl.
- SMITH F. H., 1976. *The Neandertal Remains of Krapina: a descriptive and comparative Study*. Report of Investigations, 15, Knoxville, Department of Anthropology, University of Tennessee, 359 p.
- SMITH F. H., 1978. Evolutionary Significance of the Mandibular Foramen Area in Neandertals. *American Journal of Physical Anthropology*, 48: 523-532.
- SMITH T. M., TOUSSAINT M., REID D. J., OLEJNICZAK A. J. & HUBLIN J.-J., 2007. Rapid dental development in a Middle Paleolithic Belgian Neandertal. *Proceedings of the National Academy of Sciences of the United States of America*, 104, 51: 20220-20225.
- STEFAN V. H. & TRINKAUS E., 1998. La Quina 9 and Neandertal Mandibular Variability. *Bulletins et Mémoires de la Société d'Anthropologie de Paris*, nouvelle série, t. 10, 3-4: 293-324.
- STRINGER C. B., HUBLIN J.-J. & VANDERMEERSCH B., 1984. The origin of anatomically modern humans in Western Europe. In F. H. SMITH & F. SPENCER (eds.), *The Origins of Modern Humans: A World Survey of the Fossil Evidence*. New-York, Alan R. Liss: 51-135.
- THOMA A., 1975. Were the Spy Fossils Evolutionary Intermediates between Classic Neandertal and Modern Man? *Journal of Human Evolution*, 4: 387-410.
- THOMPSON J. L. & BILSBOROUGH A., 2005. The Skull of Le Moustier 1. In H. ULLRICH (ed.), *The*

- Neandertal Adolescent Le Moustier 1, New Aspects, New Results*. Berlin, Staatliche Museum zu Berlin: 79-94.
- TILLIER A.-M., 1979. Restes crâniens de l'enfant moustérien Homo 4 de Qafzeh (Israël). La mandibule et les maxillaires. *Paléorient*, 5: 67-85.
- TILLIER A.-M., 1982. Les enfants néanderthaliens de Devil's Tower (Gibraltar). *Zeitschrift für Morphologie und Anthropologie*, 73: 125-148.
- TILLIER A.-M., 1983^a. Le crâne d'enfant d'Engis 2: un exemple de distribution des caractères juvéniles, primitifs et néanderthaliens. *Bulletin de la Société royale belge d'Anthropologie et de Préhistoire*, 94: 51-75.
- TILLIER A.-M., 1983^b. L'enfant néanderthalien du Roc de Marsal (campagne du Bugue, Dordogne). Le squelette facial. *L'Anthropologie*, 69: 137-149.
- TILLIER A.-M., 1984. L'enfant Homo 11 de Qafzeh (Israël) et son apport à la compréhension des modalités de la croissance des squelettes moustériens. *Paléorient*, 10: 7-48.
- TILLIER A.-M., 1986. Quelques aspects de l'ontogénèse du squelette crânien des Néanderthaliens. In V. V. NOVOTNY & A. MIZEROVA (eds.), *Fossil Man. New Facts – New Ideas*. Papers in honour of Jan Jelinek's life anniversary. *Anthropos*, 23: 207-216.
- TILLIER A.-M., 1988. À propos de séquences phylogénique et ontogénique chez les Néanderthaliens. In E. TRINKAUS (ed.), *L'Homme de Néandertal, vol. 3. L'Anatomie*. Études et Recherches Archéologiques de l'Université de Liège, 30: 125-135.
- TILLIER A.-M., 1991. La mandibule et les dents. In O. BAR OSEF & B. VANDERMEERSCH (eds.), *Le squelette moustérien de Kébara 2*. Paris, Éditions du Centre national de la recherche scientifique, Cahiers de Paléanthropologie: 97-111, 7 fig. h.t.
- TILLIER A.-M., 1995. Neanderthal ontogeny: a new source for critical analysis. Brno, *Anthropologie*, XXXIII, 1-2: 63-68.
- TILLIER A.-M., 2002. *Les enfants moustériens de Qafzeh. Interprétation phylogénétique et paléoaurologique*. Paris, Éditions du Centre national de la recherche scientifique, Cahiers de Paléanthropologie, 239 p.
- TILLIER A.-M. & GENET-VERCIN E., 1980. La plus ancienne mandibule d'enfant découverte en France dans le gisement de La Chaise de Vouthon (Abri Suard). *Zeitschrift für Morphologie und Anthropologie*, 71, 2: 196-214.
- TOUSSAINT M., 2001. *Les hommes fossiles en Wallonie. De Philippe-Charles Schmerling à Julien Fraipont, l'émergence de la paléanthropologie*. Carnet du Patrimoine, 33, Namur, Ministère de la Région wallonne: 60 p.
- TOUSSAINT M., 2011. Une prémolaire néanderthalienne dans la couche CI-8 (anciennement C sup et C8) de la grotte Walou. In C. DRAILY, S. PIRSON & M. TOUSSAINT (dir.), *La grotte Walou à Trooz (Belgique). Fouilles de 1996 à 2004, vol. 2: Les sciences de la vie et les datations*. Namur, Service public de Wallonie, Études et documents, Archéologie, 21: 148-163.
- TOUSSAINT M., OLEJNICZAK A. J., EL ZAATARI S., CATTELAÏN P., FLAS D., LETOURNEUX C. & PIRSON S., 2010. The Neandertal lower right deciduous second molar from Trou de l'Abîme at Couvin, Belgium, *Journal of Human Evolution*, 58: 56-67.
- TOUSSAINT M., OTTE M., BONJEAN D., BOCHERENS H., FALGUÈRES C. & YOKOYAMA Y., 1998. Les restes humains néanderthaliens immatures de la couche 4A de la grotte Scladina (Andenne, Belgique). *Comptes rendus de l'Académie des Sciences de Paris, Sciences de la terre et des planètes*, 326: 737-742.
- TOUSSAINT M., SEMAL P. & PIRSON S., 2011. Les Néanderthaliens du bassin mosan belge: bilan 2006-2011. In M. TOUSSAINT, K. DI MODICA & S. PIRSON (sc. dir.), *Le Paléolithique moyen en Belgique. Mélanges Marguerite Ulrix-Closset*. Bulletin de la Société royale belge d'Études Géologiques et Archéologiques *Les Chercheurs de la Wallonie*, hors-série, 4 & Études et Recherches Archéologiques de l'Université de Liège, 128: 149-196.
- TRINKAUS E., 1993. Variability in the position of the mandibular mental foramen and the identification of Neandertal apomorphies. Roma, *Rivista di Anthropologia*, 71: 259-274.
- TRINKAUS E., 2006. Modern Human versus Neandertal Evolutionary Distinctiveness. *Current Anthropology*, 47: 597-620.
- TWIESSELMANN F., 1961. *Le fémur néanderthalien de Fond-de-Forêt (province de Liège)*. Bruxelles, Mémoires de l'Institut royal des Sciences naturelles de Belgique, 148, 164 p.



ULLRICH H., 1955. Paläolitische Menschenreste aus der Sowjet union II: Das Kinderskelett aus der Grotte Teschik-Tasch. *Zeitschrift für Morphologie und Anthropologie*, 47, 1: 99-112.

VANDERMEERSCH B., 1981. *Les hommes fossiles de Qafzeh (Israël)*. Paris, Éditions du Centre national de la recherche scientifique, Cahiers de Paléontologie, Paléoanthropologie, 319 p., 12 pl.

VERNA C., 2006. *Les restes humains moustériens de la Station Amont de La Quina - (Charente, France). Contexte archéologique et constitution de l'assemblage. Étude morphologique et métrique des restes crânio-faciaux. Apport à l'étude de la variation néandertalienne*. Unpublished PhD thesis, anthropologie biologique, Université de Bordeaux 1, 629 p.

VLČEK E., 1993. *Fossile Menschenfunde von Weimar-Ehringsdorf*. Stuttgart, Konrad Theiss Verlag, Thüringisches Landesamt für Archäologische Denkmalpflege Weimar, 22 p., 88 pl.

VON LENHOSSÉK M., 1920. Das innere Relief des Unterkieferastes. *Archiv für Anthropologie*, neue Folge, 18, 48: 49-59.

WEIDENREICH F., 1936. *The mandibles of Sinanthropus Pekinensis: a comparative study*. Palaeontologia Sinica, Series D, vol. VII, fasc. 3, Peiping, Geological Survey of China, 132 p., 15 pl.

WOLPOFF M. H. & FRAYER D., 2005. Unique Ramus Anatomy for Neandertals? *American Journal of Physical Anthropology*, 128: 245-251.

Chapter 11

3-D GEOMETRIC MORPHOMETRIC ANALYSIS OF THE SCLADINA NEANDERTAL CHILD'S MANDIBLE IN A DEVELOPMENTAL CONTEXT

Katerina HARVATI & Michel TOUSSAINT

*Michel Toussaint & Dominique Bonjean (eds.), 2014.
The Scladina I-4A Juvenile Neandertal (Andenne, Belgium),
Palaeoanthropology and Context*

Études et Recherches Archéologiques de l'Université de Liège, 134: 215-222.

1. Introduction

The Scladina specimen represents a subadult individual of an Early Neandertal, dated to the OIS 5. Age at death is estimated at close to 8 years (TOUSSAINT & PIRSON 2006; SMITH et al., 2007 & Chapter 8). Morphology, both metric and non-metric, closely aligns the child with Neandertals, as does the mtDNA sequences recovered from the specimen (ORLANDO et al., 2006). In this study we analyze the three-dimensional shape of the Scladina I-4A juvenile mandible and place it within a comparative developmental context of both modern human and Neandertal samples.

2. Materials and methods

The fossil sample used in this study comprised seven adult and six subadult Neandertal mandibles. When the original fossil specimens were not available for study, we measured high quality casts from the collections of the Division of Anthropology (American Museum of Natural

History, New York), the Department of Human Evolution (Max Planck Institute for Evolutionary Anthropology, Leipzig) and the Institut de Paléontologie Humaine (Paris). We also used a recent human comparative sample of thirty two adult and thirteen subadult South African Khoisan as well as ten adult Greenland and Alaskan Inuit mandibular specimens (Table 1). The subadult specimens, both Neandertal and modern human, were subdivided into six categories based on stage of dental eruption: 1. neonate–2 years old; 2. 2–5 years old; 3. 5–8 years old; 4. 8–10 years old; 5. 10–15 years old; and 6. 15–20 years old. This was done because of the uncertainty inherent in the aging of individuals based on dental eruption stages, and due to the paucity of fossil juvenile remains. The age categories were displayed in the principal component plots by their number (Figure 2). Although the human mandible is sexually dimorphic (HRDLÍČKA, 1940^{a,b}; HUMPHREY et al., 1999), sexually dimorphic patterns differ regionally in modern humans (HUMPHREY et al., 1999) and probably also across taxa. In addition, sex assignment is very difficult in subadults.

Figure 1: The Scladina mandible, surface rendering of a reconstruction so that the two parts are in contact.

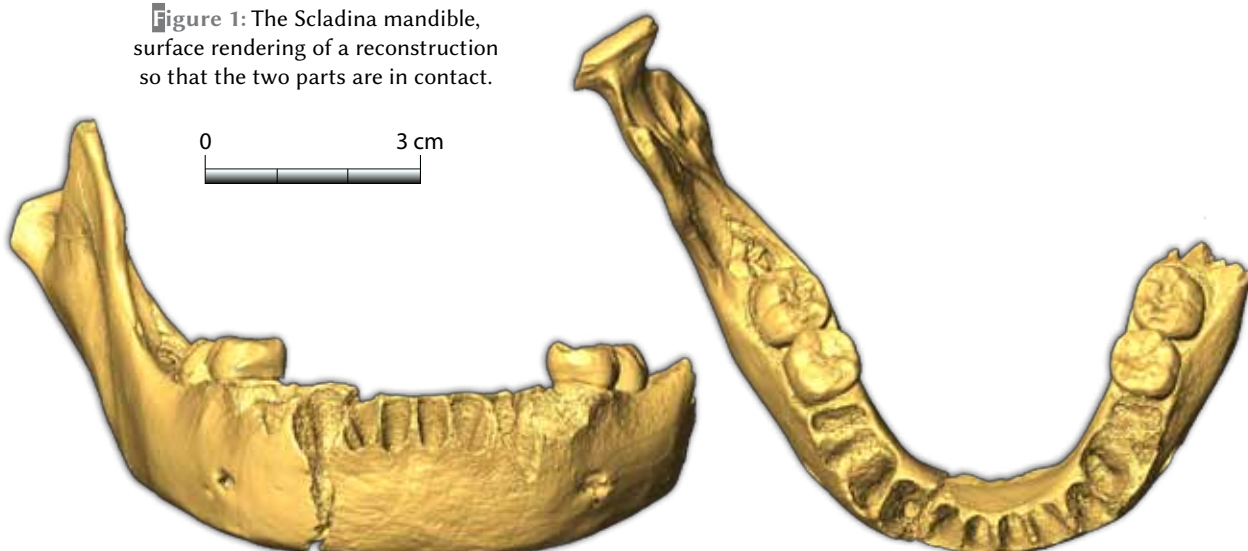


Table 1: 70 mandibles constitute the basis of this comparative study.

Modern humans	
Khoisan adults	32 (SAM, UCT)
Khoisan subadults	13 (SAM, UCT)
Inuit adults	10 (AMNH)
Fossils	
Neandertal adults (7)	Krapina J, La Ferrassie 1, La Quina 9, Montmaurin, Regourdou, Tabun 1, Zafarraya
Neandertal subadults (6)	Gibraltar 2, Le Moustier, Pech de l'Azé, Roc de Marsal, Scladina I-4A, Teshik-Tash
<i>H. heidelbergensis</i> (2)	Mauer, Sima 5

Because no sex information was available for most of our samples, males and females were pooled in the analysis, and sexual dimorphism was not examined in this study.

A surface rendering of the Scladina specimen was measured using the software Amira (Figure 1), while the comparative sample was measured directly with a Microscribe 3D-X (Immersion Corp.) portable digitizer. Fifteen osteometric landmarks, defined as homologous points that can be reliably and repeatedly located and which represented the midline and left side of the mandible were used (Table 2 and Figure 2; see also NICHOLSON & HARVATI, 2006). All data were collected by one observer (KH). This type of morphometric analysis does not accommodate missing data. Therefore some data reconstruction was undertaken. Landmarks on specimens with minimal damage were estimated during data collection, using anatomical clues from the

preserved surrounding areas. Bilateral landmarks missing on the left side were estimated from the preserved homologues on the right side by mirroring-imaging, using reflected relabeling (HARVATI, 2003). This procedure exploits the Procrustes geometry to reflect the paired landmarks without having to specify a mirroring plane. During reflected relabeling, specimens with a missing landmark on one side were least-squared superimposed with their reflections. The coordinates for the missing landmark were then substituted from the fitted homologous points in the preserved side. The level of error that is introduced by this procedure has been shown to be minimal (HARVATI, 2003).

The landmark coordinates were processed according to geometric morphometric methods. Specimen configurations were superimposed using Procrustes Generalized Analysis (GPA) using the Morpheus software package

Landmark	Definition
1. Gonion	The point along the rounded posterioinferior corner of the mandible where the line bisecting the angle between the body and the ramus would meet
2. Posterior ramus	The point at the posterior margin of the ramus at the level of the M ₃
3. Condyle tip	The most superior point on the mandibular condyle
4. Condylion mediale	The most medial point on the mandibular condyle
5. Condylion laterale	The most lateral point on the mandibular condyle
6. Root of sigmoid process	The point where the mandibular notch intersects the condyle
7. Mandibular notch	The most inferior point on the mandibular notch
8. Coronion	The most superior point on the coronoid process
9. Anterior ramus	The point at the anterior margin of the ramus at the level of the M ₃
10. M ₃	The point on the alveolar bone just posterior to the midline of the third molar
11. Mental foramen	The point in the middle of the mental foramen
12. Canine	The point on the alveolar margin between the canine and the first premolar
13. Gnathion	The most inferior midline point on the symphysis
14. Infradentale	The midline point at the superior tip of the septum between the mandibular central incisors
15. Mandibular orale	The most superior midline point on the lingual side of the mandible between the two central incisors

Table 2: Landmarks used and their definitions. The first 12 landmarks were collected on the left side. Adapted from NICHOLSON & HARVATI, 2006.

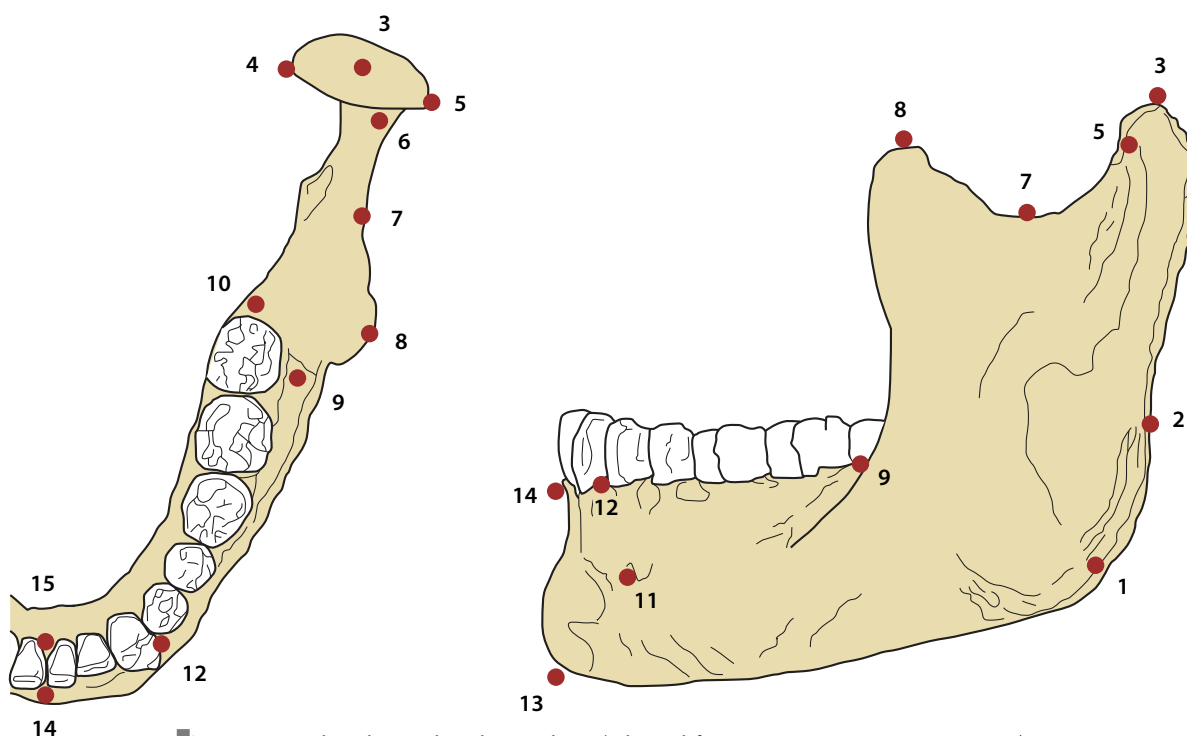


Figure 2: Landmarks used in this analysis (adapted from NICHOLSON & HARVATI, 2006). Landmark numbers correspond to those listed in Table 2.

(SLICE, 1998). This procedure translates the landmark configurations to common origin, scales them to unit centroid size (the square root of the sum of squared distances of all landmarks to the centroid of the object, the measure of size used here), and rotates them according to a best-fit criteria. During GPS centroid size is removed.

To explore the relationship of Scladina to the Neandertal and modern human comparative samples, a principal components analysis (PCA) was conducted using the superimposed coordinates as variables (shape space). Additionally, and in order to analyze the growth trajectories of Neandertals and modern humans, we conducted a PCA using the superimposed coordinates and the logarithm of centroid size (logCS) as variables (size-shape space), as outlined by MITTEROECKER et al. (2004). In such an analysis of size-shape space, data logCS has the greatest variance of any other variable, and thus the first principal component reflects differences in size and can be interpreted as a temporal pattern of shape change. Higher size-shape principal components in turn can be interpreted as spatial patterning of shape changes reflecting taxonomic differentiation along a growth trajectory. Because biological interpretations can sometimes be affected by the projection of a higher-dimension space onto two dimensions,

we examined the first three principal components following MITTEROECKER et al. (2004).

The GPS, size-shape principal components analysis, and visualization of shape differences along size-shape principal components were conducted using Morphologika 2 (O'HIGGINS & JONES, 2006). The three-dimensional plots of principal components 1, 2 and 3 were made using the SAS software package (SAS Institute, 1999-2001).

3. Results

The results of the principal components analyses are shown in Figures 3-6.

Shape-space analysis: Neandertal and modern human adults were separated along principal component 1 (26.1% of the total variance), although there was some overlap along this axis (Figure 3). PC 1 also separated subadults (both modern and Neandertal) from modern human, but not Neandertal adults. PC 2 separated Neandertal and Khoisan adults from modern human and some Neandertal subadults. Inuit adults for the most part overlapped with Khoisan subadults along that axis. Scladina fell with Neandertals on the positive ends of both PC 1 and 2. The two *H. heidelbergensis* specimens clustered with Neandertals, but fell near the zone of overlap with modern humans along PC 1.



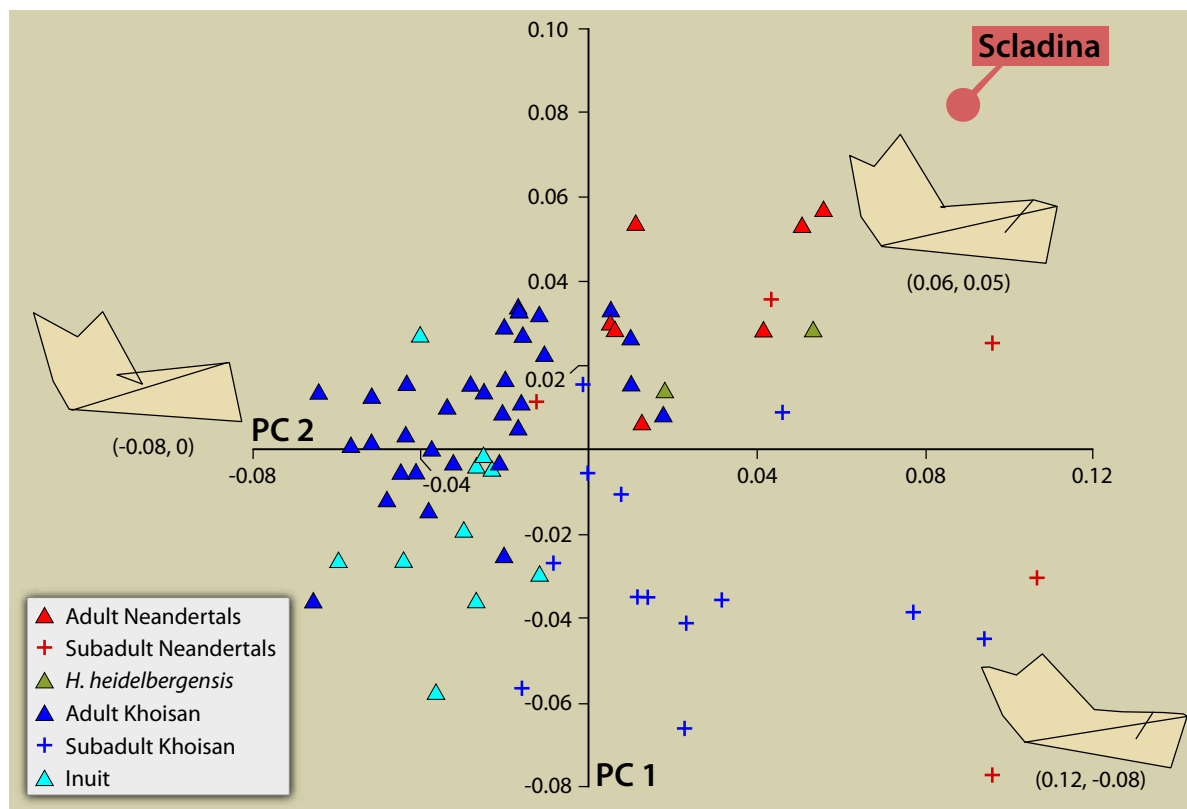


Figure 3: Shape-space analysis. Principal components 1 (x-axis) and 2 (y-axis). Shape differences shown between Neandertals (positive ends of PC1 and 2), juvenile *Homo sapiens* (positive end of PC1, negative end of PC2) and adult *Homo sapiens* (negative end of PC1).

Shape differences along PC 1 included on the Neandertal/subadult (positive) end: a short condyle, an infero-posteriorly inclined symphysis, an anteriorly placed distal end of the toothrow, a medially placed gonion, lateral position of the condyle relative to the mandibular notch, and a posterior and lateral position of the mental foramen. Shape changes along PC 2, on the other hand, included on the juvenile/Inuit (positive) end: a more posteriorly sloping ramus and posterior position of the condyle, short ramus and corpus height (as reflected at the level of the canine), anteriorly placed distal end of the toothrow, and more medial and anterior position of the canine.

PC 1 was weakly correlated with centroid size when the entire sample was considered ($r^2 = 0.07$, $p = 0.04$), but the correlation was much stronger when *Homo sapiens* and *Homo neanderthalensis* were examined separately (Neandertals: $r^2 = 0.56$, $p = 0.003$; *Homo sapiens*: $r^2 = 0.44$, $p < 0.0001$). When plotted against centroid size (Figure 4, left panel), Neandertals, adults and subadults, were clearly more similar in their PC 1 scores to Khoisan subadults but were well separated from modern human adults. While the subadults had a similar

starting point, the trajectory of Neandertals with increasing size (and time) along PC1 was very different from that of modern humans. PC 2 was also mildly correlated with centroid size when the entire sample was analyzed either in its entirety ($r^2 = 0.16$, $p = 0.0005$) or separately (Neandertals: $r^2 = 0.29$, $p = 0.06$; *Homo sapiens*: $r^2 = 0.07$, $p < 0.04$). Figure 4 (right panel) also shows Neandertals and modern humans have a similar starting point on PC 2 and this time follow a similar trajectory with increasing size, though the Neandertal trajectory is longer than that of modern humans.

Form-space analysis: The results of the shape-space analysis were confirmed with a form (or size-shape) -space analysis. Here principal component 1 accounted for 78.9% of the total variance (Figure 5) and very closely reflected differences in size (Figure 5). PC 1, therefore, can be interpreted as a temporal axis with younger individuals placed on the negative side and older ones on the positive end of the axis. PC 2 accounted for 5.6% of the total variance and showed spatial patterning. This information can be interpreted as reflecting taxonomic differences between Neandertal and modern human

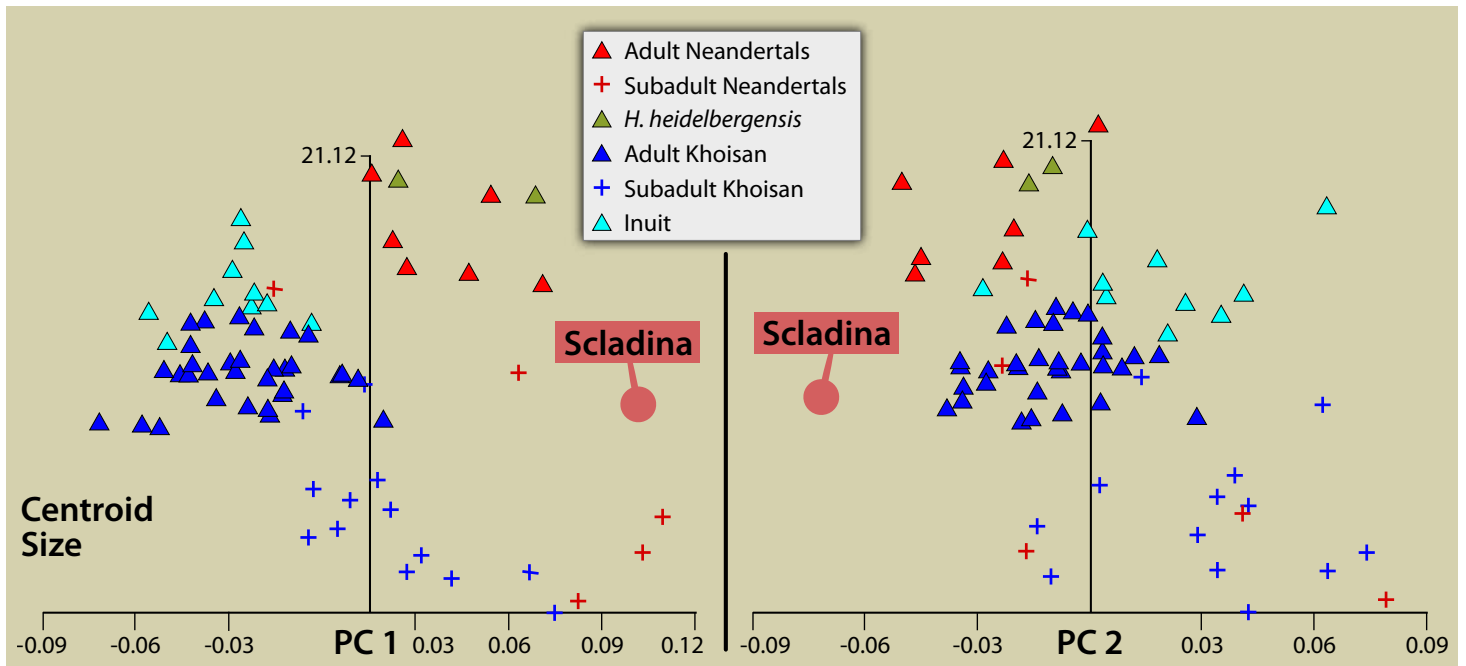


Figure 4: Shape-space analysis. Principal component 1 (left panel) and 2 (right panel) plotted against centroid size.

mandibular shape. Neandertals, both subadults and adults, and *H. heidelbergensis* clustered on the positive side of PC 2, with modern human adults and subadults on the negative side. While there was no overlap among adults, some Neandertal subadults fell at the edge of the modern human range of variation: Le Pech de l’Azé fell very close to a Khoisan child of similar chronological age; the Le Moustier adolescent fell within the range of modern adults on PC 2. Nonetheless, the Scladina individual was well on the positive end of PC 2, at the edge of the adult Neandertal range on that axis (Figure 5).

Although Neandertal and modern human subadults are closer to each other than the adults are, the principal shape differences distinguishing the taxa are already seen in young individuals (age category 2 [2-5 years] being the smallest one included in this analysis). Scladina, at the dental stage 4, is already characterized by the taxonomic features that differentiate Neandertals from modern humans. This finding is consistent with previous results that the anatomical features that distinguish Neandertals from modern humans appear either prenatally or early postnatally (PONCE DE LEÓN & ZOLLIKOFER

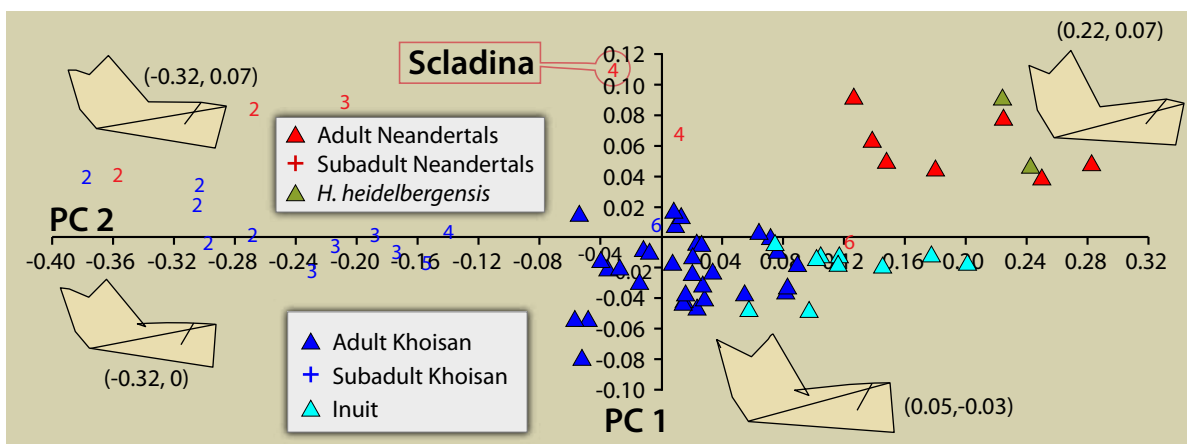


Figure 5: Size-shape space principal components analysis. PC1 (x-axis) plotted against PC 2 (y-axis). Shape differences along PC1 and 2 are shown. Age categories as follows: 1: Neonate-2 years old; 2: 2-5 years old; 3: 5-8 years old; 4: 8-10 years old; 5: 10-15 years old; 6: 15-20 years old.

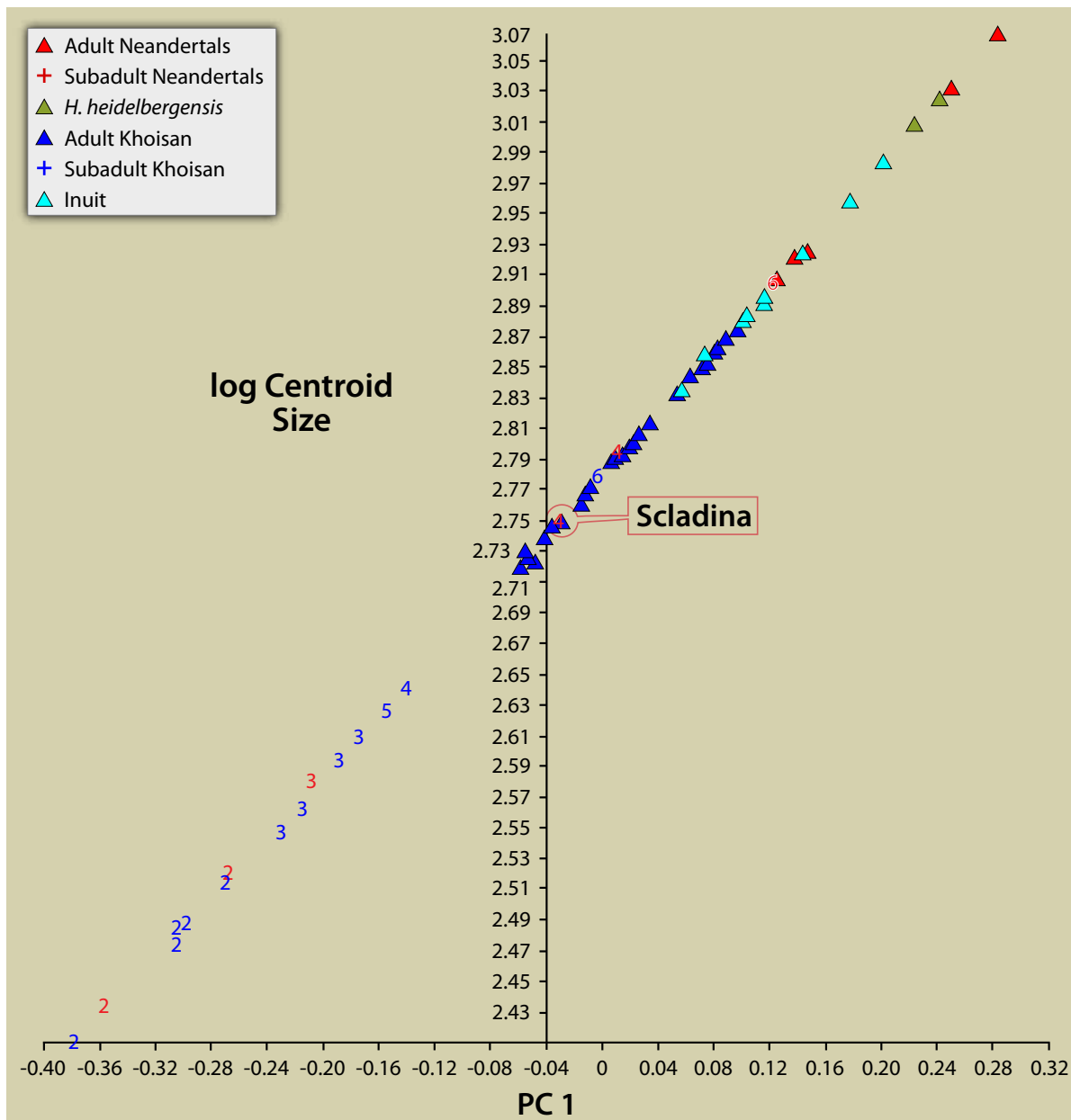


Figure 6: PC 1 plotted against log centroid size. Age categories as follows: 1: Neonate-2 years old; 2: 2-5 years old; 3: 5-8 years old; 4: 8-10 years old; 5: 10-15 years old; 6: 15-20 years old.

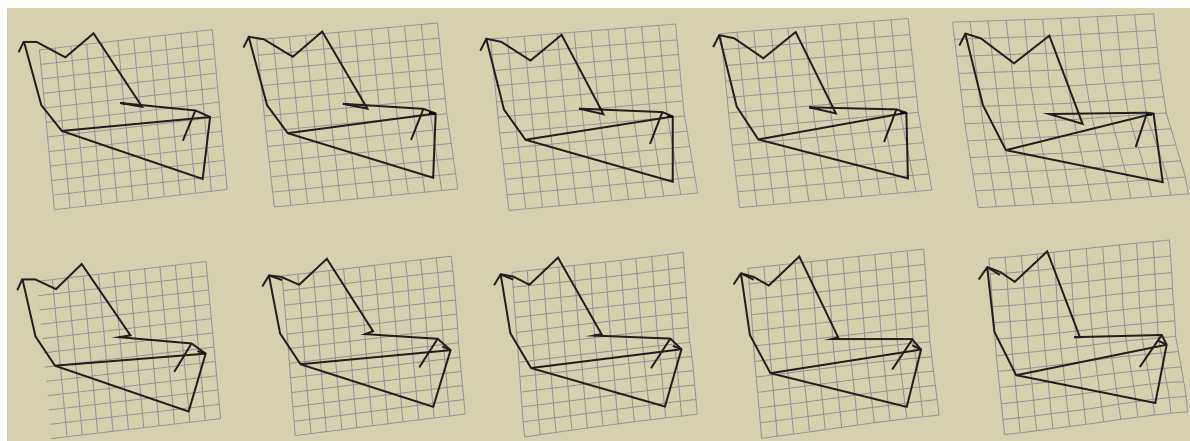


Figure 7: The modern human (above) and Neandertal (below) growth trajectories along PC 1:

2001, 2006; BASTIR et al. 2007). The Neandertal growth trajectory is longer along PC 1 and overlaps partially only with some of the larger individuals from the Inuit sample. Neandertal subadults, particularly those in the later stages (4-6), are more advanced along PC 1 than modern human children of similar dental stage (Figure 5). Scladina, with a dental stage of 4, overlaps on PC 1 with modern Khoisan adults, while Le Moustier (dental stage 6) overlaps with some of the larger Inuit adults.

The modern human trajectory along PC 1 (Figure 7) can be described as showing growth in both the vertical and anterior dimension, with an increase in the ramal height, a change in the orientation between the ramus and the body, and an increase in the antero-posterior length of the body being the dominant features. The Neandertal trajectory is similar in the vertical component of growth and is also characterized by a change in the relative position and orientation of the ramus and body, though not by a pronounced antero-posterior direction of growth (Figure 7).

4. Discussion and conclusions

This study shows that the Scladina mandible, although quite young in chronological age and relatively old in geological age, is already characterized by the features that distinguish Neandertals from modern humans as reflected by our data. The data also found that Neandertal juveniles show some of the crucial features differentiating Neandertal from modern human adults at an early age. Nonetheless both groups are characterized by considerable shape change throughout ontogeny. These results are consistent with previous work indicating that both prenatal development and postnatal growth are important in determining the adult Neandertal and modern human mandibular shape (BASTIR et al., 2007). The Neandertal growth trajectory was found to be longer than that of modern humans, reaching a larger adult form, though the inclusion of a large-bodied modern human group (Inuit) resulted in more overlap in size than previously reported (BASTIR et al., 2007). Neandertal juveniles appeared to be more advanced than modern human juveniles of similar dental stage, though this was more apparent in the later stages of growth.

Acknowledgements

We are grateful to all curators in various institutions in Europe, Africa and Israel for allowing us to study the fossil and recent human collections in their care. We also thank Jean-Jacques Hublin and Philipp Gunz. This is NYCEP morphometric contribution N° 36. Funding for this research was provided by the Max Planck Society, the Wenner-Gren Foundation and the EVAN Marie Curie Research Training Network MRTN-CT-019564.

References

- BASTIR M., O'HIGGINS P. & ROSAS A. 2007. Facial ontogeny in Neanderthals and modern humans. *Proceedings of the Royal Society B: Biological Sciences*, 274: 1125-1132.
- HARVATI K., 2003. The Neanderthal taxonomic position: models of intra- and inter-specific craniofacial variation. *Journal of Human evolution*, 44: 107-132.
- HRDLIČKA A., 1940^a. Lower jaw. The gonial angle, I. The bigonial breadth, II. *American Journal of Physical Anthropology*, 27: 281-308.
- HRDLIČKA A. 1940^b. Lower jaw further studies. *American Journal of Physical Anthropology*, 27: 383-467.
- HUMPHREY L. T., DEAN M. C. & STRINGER C. B., 1999. Morphological variation in great ape and modern human mandibles. *Journal of Anatomy*, 195: 491-513.
- MITTEROECKER P., GUNZ P., BERNHARD M., SCHAEFER K. & BOOKSTEIN F. L., 2004. Comparison of cranial ontogenetic trajectories among great apes and humans. *Journal of Human Evolution*, 46: 679-698.
- NICHOLSON E. & HARVATI K., 2006. Quantitative Analysis of Human Mandibular Shape Using 3-D Geometric Morphometrics. *American Journal of Physical Anthropology*, 131: 368-383.
- O'HIGGINS P. & JONES N., 2006. *Tools for statistical shape analysis*. Hull York Medical School. <http://www.york.ac.uk/res/fme/resources/software.htm>.
- ORLANDO L., DARLU P., TOUSSAINT M., BONJEAN D., OTTE M. & HÄNNI C., 2006. Revisiting Neandertal diversity with a 100,000 year old mtDNA sequence. *Current Biology*, 16: R400-R402.
- PONCE DE LEÓN M. S. & ZOLLIKOFER C. P. E., 2001. Neanderthal cranial ontogeny and its implications for late hominid diversity. *Nature*, 412: 534-538.



PONCE DE LEÓN, M. S. & ZOLLIKOFER C. P. E., 2006. Neanderthals and modern humans – chimps and bonobos: Similarities and differences in development and evolution. In K. HARVATI & T. HARRISON (eds.), *Neanderthals Revisited: New Approaches and Perspectives*. Dordrecht, Springer: 89-111.

SLICE D. E., 1998. *Morpheus et al.*: software for morphometric research. Revision 01-30-98. Department of Ecology and Evolution, State

University of New York, Stony Brook.

SMITH T. M., TOUSSAINT M., REID D. J., OLEJNICZAK A. J. & HUBLIN J.-J., 2007. Rapid dental development in a Middle Paleolithic Belgian Neanderthal. *Proceedings of the National Academy of Sciences of the United States of America*, 104, 51: 20220-20225.

TOUSSAINT M. & PIRSON S., 2006. Neandertal Studies in Belgium: 2000-2005. *Periodicum Biologorum*, 108, 3: 373-387.

Christine VERNA & Michel TOUSSAINT

*Michel Toussaint & Dominique Bonjean (eds.), 2014.
The Scladina I-4A Juvenile Neandertal (Andenne, Belgium),
Palaeoanthropology and Context*

Études et Recherches Archéologiques de l'Université de Liège, 134: 223-232.

1. Introduction

After the initial discovery of the right hemimandible Scla 4A-1, in July 1993, sorting of the faunal collections found previously at Scladina in the same stratigraphic unit was undertaken. During this laboratory work, which mainly took place in the second part of 1993, several human teeth and a right partial maxilla were identified. The teeth had been discovered a few years earlier, from 1990 until 1992, and the maxilla in February 1992, but none of these fossils had been recognized as human and more specifically as Neandertal at that time. The partial maxilla comes from Square D30 and was first attributed to former Layer 4A; however, according to the recent and more precise analysis of the stratigraphy of the cave (Chapter 3), it would seem to originate from Unit 4A-POC, even if an origin from the top of Unit 4A-CHE cannot be entirely ruled out (Chapter 5).

Below we provide a description of the partial maxilla and compare its morphology to samples of subadult Neandertals as well as Early Modern Humans associated with Middle and Upper Palaeolithic industries. Each individual is attributed to a dental development stage based on dental eruption as follows: S1: deciduous dentition only; S2: deciduous dentition and M1 fully erupted; S3: mixed dentition with the M1 and at least another fully erupted permanent tooth (but usually not the M2); S4: permanent dentition only, with the M2 fully erupted, but not the M3. The Scladina Child belongs to the S3 stage.

Maxillas, in particular immature ones, are fragile skeletal elements and are therefore relatively scarce in the fossil record. In addition, individuals from age class S1 are far more abundant than those from the other age classes, which considerably limits our comparison of Scladina to children of similar age. Our Neandertal samples include nine individuals distributed as follows: four from dental stage S1 (Engis 2, Roc de Marsal, Subalyuk 2, Devil's Tower), two S2 individuals (La

Quina 18; Krapina 46), three S3 (Kůlna, Krapina 47, Teshik-Tash) and two S4 (Krapina 48, 49). The Pleistocene Modern Human sample includes the Middle Palaeolithic individuals Qafzeh 4, Qafzeh 11 and Mugharet-el-Aliya as well as eight individuals associated with Upper Palaeolithic industries (UPMH). Five of these belong to the S1 age class (Le Figuier, Grotte des Enfants 1 and 2, La Madeleine, Le Placard 31); one to S2 (Saint-Germain-la-Rivière 7); one to either the S2 or S3 age classes (Le Placard 33) and one to S4 (Cova del Parpalló). All data were gathered from the study of the original specimen except for Teshik-Tash and Cova del Parpalló for which the data were recorded from casts.

2. State of preservation

The Scla 4A-2 maxilla is a single fragment from the right mid-facial region that retains part of the alveolar and palatine processes and a small part of the body (Figure 1). The fragment is 50 mm in length and 25 mm in both height and width. The bone is broken along a subhorizontal section at the level of the floor of the nasal fossa, so that the frontal process, the upper part of the body and the zygomatic process are all missing. A small part of the nasal floor is preserved and, laterally, parts of the floor of the maxillary sinus are revealed by the breakage.

Medially, the bone is preserved up to the sagittal midline in its lower part and retains the interdental wall between the permanent maxillary incisor sockets as well as a portion of the contact surface with the left maxilla (Figures 1e & 3a). However, the breakage runs laterally upwards so that the inferior margin of the piriform aperture is missing except for a very small portion at the level of the interalveolar septum between the two central incisors.

The fragment extends laterally from the midline to the mesial part of both the distobuccal





Figure 1: Scla 4A-2 right maxilla at 1:1 scale. (a) external (antero-lateral), (b) internal, (c) superior, (d) inferior, (e) medial and (f) posterior views. Photographs Joël Éloy, AWEM.

and lingual roots of the M^1 . The alveoli of the right incisors, canine and dm^1 are well preserved, with their medial side almost intact whereas the lateral one is eroded (I^1 , I^2) or largely destroyed (C, dm^1). Only a small part of the palatine process is preserved. It extends backward for about 30 mm from the *orale* and does not reach the transverse suture.

Six right teeth, found isolated in former Layer 4 (see Chapter 5 for more details about the stratigraphic origin of the fossils), can be refitted in the maxilla (see Chapter 13): both permanent incisors (Scla 4A-11 & 14), the permanent canine (Scla 4A-16), both deciduous molars (Scla 4A-7 & 5), and the first permanent molar (Scla 4A-4). In addition, the unerupted Scla 4A-2/ P^4 is visible in the bottom of the dm^2 socket. The second maxillary molar (Scla 4A-3) and the third molar germ (Scla 4A-8) have also been found.

3. Morphology

3.1. Antero-lateral view: external face of the body

Anteriorly, the very small preserved portion of the inferior margin of the piriform aperture, above the I^1 - I^2 interdental septum (ca. 6.5 mm long), shows two crests separated by a prenasal

groove (*fossa intranasalis*). In addition, the presence of a *fossa intranasalis* suggests a pattern similar to the FRANCISCUS (2003) nasal margin category 5 (spinal crest fused to the lateral one and partially fused to the turbinal) or 6 (partial fusion of the spinal and turbinal crests). We shall recall here that 67% of Neandertals show configuration 5 ($n = 21$), whereas only 3% of Upper Palaeolithic Modern Humans and none of the specimens from Qafzeh and Skhul (FRANCISCUS, 2003) present this pattern. Note also that configuration 6 is very rare and was never observed in these Pleistocene samples. Group differences are even more marked when only subadult individuals are considered (see Table 1).

Based on the preserved portion of the nasolacrimal clivus, the subnasal height (M48-1, MARTIN, 1928) would be higher than 18 mm and may be estimated at close to 19.5 mm. This value is higher than all Neandertals belonging to age class S1 (Table 2; Figure 2a) but very close to Engis 2 (19.3 mm). It falls well within the range of the class 3 Neandertals, being higher than Teshik-Tash but lower than Kùlna and Krapina 47, and is much lower than the older Krapina 49 individual. When compared to Pleistocene Modern Humans the subnasal height of Scladina is higher than Qafzeh 10 (age class S2) and above all Upper Palaeolithic individuals from all age classes, falling well outside their range of variation ($m = 12.5$;

sd = 1.4; m+2sd = 15.3). Finally, the value measured on Scla 4A-2 is also well above the mean obtained by MINUGH-PURVIS (1993) for samples of modern humans of similar ages (mid- and late-childhood, m = 14.8 and 14.5 respectively) and at the upper limit of the variation of a sample of 10-12 dental development ages (range = 11-19, m = 14.9, n = 7). Therefore, the subnasal height of Scladina is rather high and consistent with the range of variation of Neandertals, who have a high nasoalveolar region when compared to recent humans (MAUREILLE, 1994). Although MINUGH-PURVIS (1988) suggested that this high subnasal height seen in adult Neandertals would not develop before late childhood, our data (Table 2) as well as other studies (e.g. MADRE-DUPOUY, 1992; KROVITZ, 2003) show that young Neandertals (age class S1) already have a higher subnasal height than Upper Palaeolithic and modern children of similar ages. This might not be the case when compared to earlier modern humans (associated with Middle Palaeolithic or Middle Stone Age industries) but insufficient data are available in the fossil record.

The nasoalveolar clivus is a rather flat surface, only slightly superio-inferiorly concave, and marked by the *jugum* of the two incisors. Laterally, the vertical canine *jugum* is visible, although partially destroyed. Behind it, above the molar sockets, the body takes a quite strong lateral orientation upwards. Although not enough is preserved to assess the infra-orbital topography, this lateral projection of the body above the post-canine dental alveoli makes it unlikely that this piece could have exhibited any strong *incurvatio inframalaris sagittalis* or *incurvatio horizontalis* as described in the 'flexion' type infraorbital surface of SERGI (1948). Furthermore, the preserved morphology shows that the root of the zygomatic process, i.e. the zygomaticoalveolar crest, emerges at the level of m²/M¹, at a location more posterior than Subalyuk 2 and La Quina 18, similar to the younger individual Roc-de-Marsal, but more anterior than all the other S2-S3 individuals (Table 1). The emergence of the crest is overall slightly more anterior in the UPMH sample (Table 1), being most often located at the m² in the

	Specimen	Age class	Internal nasal floor pattern	Nasal margin configuration	Zygoalveolar crest placement
	Scladina	S3	bilevel	5/6?	m2M1
	Devil's Tower ⁽¹⁾ (Gibraltar)	S1	bilevel	–	–
	Engis 2 (Belgium)	S1	bilevel	5	–
	Roc de Marsal 1 (France)	S1	bilevel	5	m2M1
NEAND	Subalyuk 2 (Hungary)	S1	bilevel	5	m1m2
	La Quina 18 (France)	S2	bilevel	5	m1m2/m2r
	Krapina 46 (Croatia)	S2	–	–	M1
	Kůlna (Czech Republic)	S3	–	5	M1
	Krapina 47 (Croatia)	S3	sloped	3	M1
	Teshik-Tash ⁽¹⁾ (Uzbekistan)	S3	–	–	M1
	Krapina 48 (Croatia)	S4	level	–	–
	Krapina 49 (Croatia)	S4	sloped	2	–
	Qafzeh 4 (Israel)	S2	–	4	M1
MPMH	Qafzeh 11 ⁽¹⁾ (Israel)	S2	level	4	
	Mugharet-el-Aliya ^(1,2) (Morocco)	S3	sloped	3/7	
	Arene Candide 6 ⁽¹⁾ (Italy)	S1	bilevel	3,7	
	Lagar Velho ⁽¹⁾ (Portugal)	S1	sloped/bilevel?	7	
	Le Figuiier (France)	S1	level	3	m2
	Grotte des Enfants 1 (Italy)	S1	level	1	m2
	Grotte des Enfants 2 (Italy)	S1	level	1	m2
UPMH	La Madeleine (France)	S1	((level	3	
	Le Placard 31 (France)	S1	level	–	m2M1
	Saint-Germain-la-Rivière 7 (France)	S2	–	–	m2M1
	Le Placard 33 (France)	S2/3	level	–	m2M1
	Cova del Parpalló ⁽¹⁾ (Spain)	S4	level	1	M1

Table 1: Morphological features. Internasal floor pattern and nasal margin configuration following the categories defined by FRANCISCUS (2003). **NEAND:** Neandertals; **MPMH:** Middle Palaeolithic Modern Humans; **UPMH:** Upper Palaeolithic Modern Humans. Otherwise indicated, all data were recorded by the authors on the original specimens. ⁽¹⁾ data collected on a cast; ⁽¹⁾ data from Franciscus, 2003; ⁽²⁾ data from MINUGH-PURVIS, 1993. See the text for the definition of the age classes.



	Taxon	Age Class	Subnasal Height	LA1	LA2	LP1	LP2
Scladina I-4A	NEAN	S3	19.5	12.7	17.1	22.7	17.2
Dederiyeh 2 ⁽¹⁾	NEAN	S1	16.4				
Engis 2	NEAN	S1	19.3	12.1	18.7		
Roc de Marsal	NEAN	S1	15.0	14.0	20.8	18.0	17.6
Subalyuk 2	NEAN	S1	15.9	9.7	16.8	23.6	18.0
Kůlna	NEAN	S3	24.8	10.9	16.17		13.3
La Quina 18 L	NEAN	S2				21.6	16.6
Krapina 47 L	NEAN	S3	22.9	15.5	20.6		
Teshik-Tash ^(c)	NEAN	S3	18.3	15.3	21.0	22.1	15.3
Krapina 49 L	NEAN	S4	27.4	16.6	20.7		
Qafzeh 4 R	MPMH	S2				20.1	15.0
Qafzeh 10 ⁽²⁾	MPMH	S2	18.6				
Arene Candide 5B ⁽³⁾	UPMH	S1	14.6				
Arene Candide 11 ⁽³⁾	UPMH	S1	13.4				
Le Figuiet L	UPMH	S1	11.4	11.3	17.1	21.4	16.6
Grotte des Enfants 2	UPMH	S1	11.3	10.5	16.0		15.6
Grotte des Enfants 1	UPMH	S1	11.4	10.5	15.5		
La Madeleine	UPMH	S1	13.6	10.6	15.7	21.5	
Le Placard 61401-31 R	UPMH	S1		11.8	17.7		
Le Placard 61401-33 R	UPMH	S2/S3		13.6	19.3		15.2
Saint-Germain-Rivière 7 R	UPMH	S2				20.2	15.6
Sungir 4 ⁽⁴⁾	UPMH	S3	11.0				
Cova del Parpalló 1 ^(c)	UPMH	S4	13.5	13.6	18.2	17.2	11.9

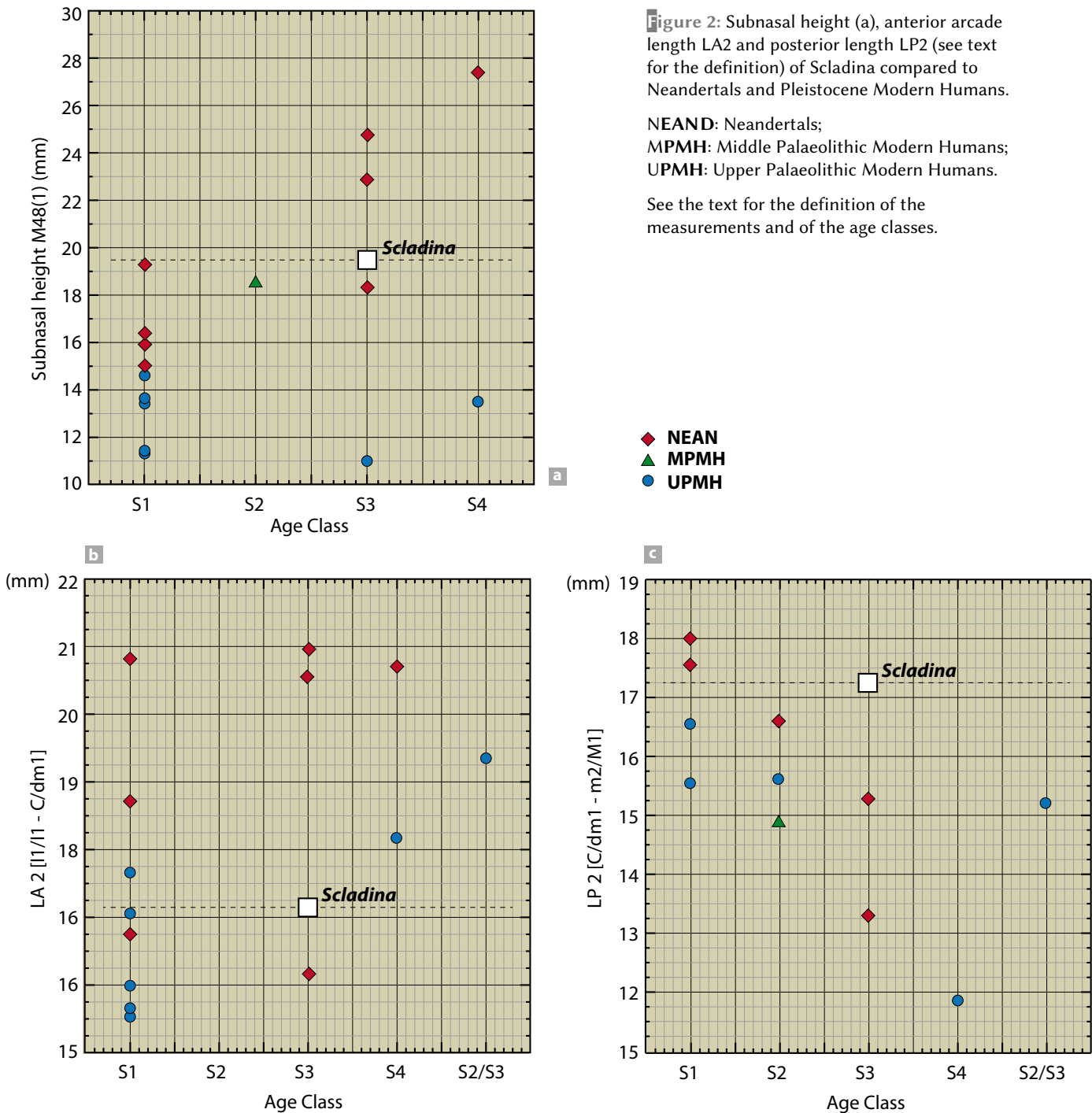
Table 2: Subnasal height and arcade length measurements. **NEAND:** Neandertals; **MPMH:** Middle Palaeolithic Modern Humans; **UPMH:** Upper Palaeolithic Modern Humans. Otherwise indicated, all data were recorded by the authors on the original specimens. ^(c) data collected on a cast; ⁽¹⁾ data from DODO et al., 2002; ISHIDA & KONDO, 2002; ⁽²⁾ data from TILLIER, 2002; ⁽³⁾ data from HENRY-GAMBIER, 2001; ⁽⁴⁾ data from MINUGH-PURVIS, 1993. See the text for the definition of the age classes.

S1 age class, m^2/M^1 in the S2/S3 classes, reaching the M^1 only in the single individual belonging to age class S4. According to MINUGH-PURVIS (1993), the root of the zygomatic process emerges at the level of m^2/M^1 in 56% of 9 modern children aged 7 to 8 years, and above the M^1 in 44% of them. However, it emerges at or posterior to the M^1 in 100% of the individuals over 8 years of age. It has been shown that in adult Neandertals the root of the zygomatic process emerges more posteriorly relative to the dentition than in recent humans (RAK, 1986; TRINKAUS, 1987; MAUREILLE, 1994). Indeed, the zygomaticoalveolar crest emerges at the level of M^2 or M^2/M^3 on all but one adult Neandertals ($n = 9$, VERNA, 2006), whereas it is anterior to the M^2 on 90% of the recent humans ($n = 159$; MAUREILLE, 1994). This posterior placement of the zygomaticoalveolar crest has been linked to the mid-facial prognathism and topography characterizing Neandertals (RAK, 1986; TRINKAUS, 1987). It has also been suggested that allometric relationships between infraorbital surface topography and infraorbital size could

explain the Neandertal infraorbital surface topography (MADDUX & FRANCISCUS, 2009), although not entirely (FREIDLIN et al., 2012). The Scladina pattern appears rather anterior when compared to similarly aged Neandertals, which might then reflect a rather low mid-facial prognathism and/or a relationship with size factors (i.e. an infraorbital region not as large as other Neandertals). Not enough of the mid-facial region is however preserved to test this hypothesis.

3.2. Superior view: floors of nasal fossa and maxillary sinus

As stated above, an anterior portion of the nasal floor (ca. 28 mm in length and 16 mm in width) is preserved. Medially, a very small part of the incisive crest is visible at the level of the incisive canal opening as well as tiny parts of the nasal crest behind that opening. Below that opening, in medial view, the incisive canal runs down vertically and emerges on the palatine process (see



below). Postero-laterally, on the preserved portion of the floor of the maxillary sinus, two small holes (ca. 3 mm) reveal the two root apices of the still imbedded P⁴ (Figure 3a).

Despite the absence of the nasal spine region, the preserved morphology allows us to assess the internal configuration of the nasal floor, following the criteria of FRANCISCUS (2003). The Scladina nasal floor shows a bilevel configuration, a pattern also shown by five out of eight subadult Neandertals (S2-S4) but only one or two UPMH

(Table 1). According to FRANCISCUS's (2003) data, this bilevel pattern is also found in 87% of adult Neandertals (n = 15) but only one of seven MPMH (Near East and North Africa) and none of the adult UPMH (n = 30).

Furthermore, we can observe the premaxillary suture (*sutura premaxillaris*; see MAUREILLE & BRAGA, 2002) in the anterior part of the nasal floor (Figures 3a & 4). The suture runs medio-laterally across the entire portion of the nasal floor that is preserved, following a rectilinear path.



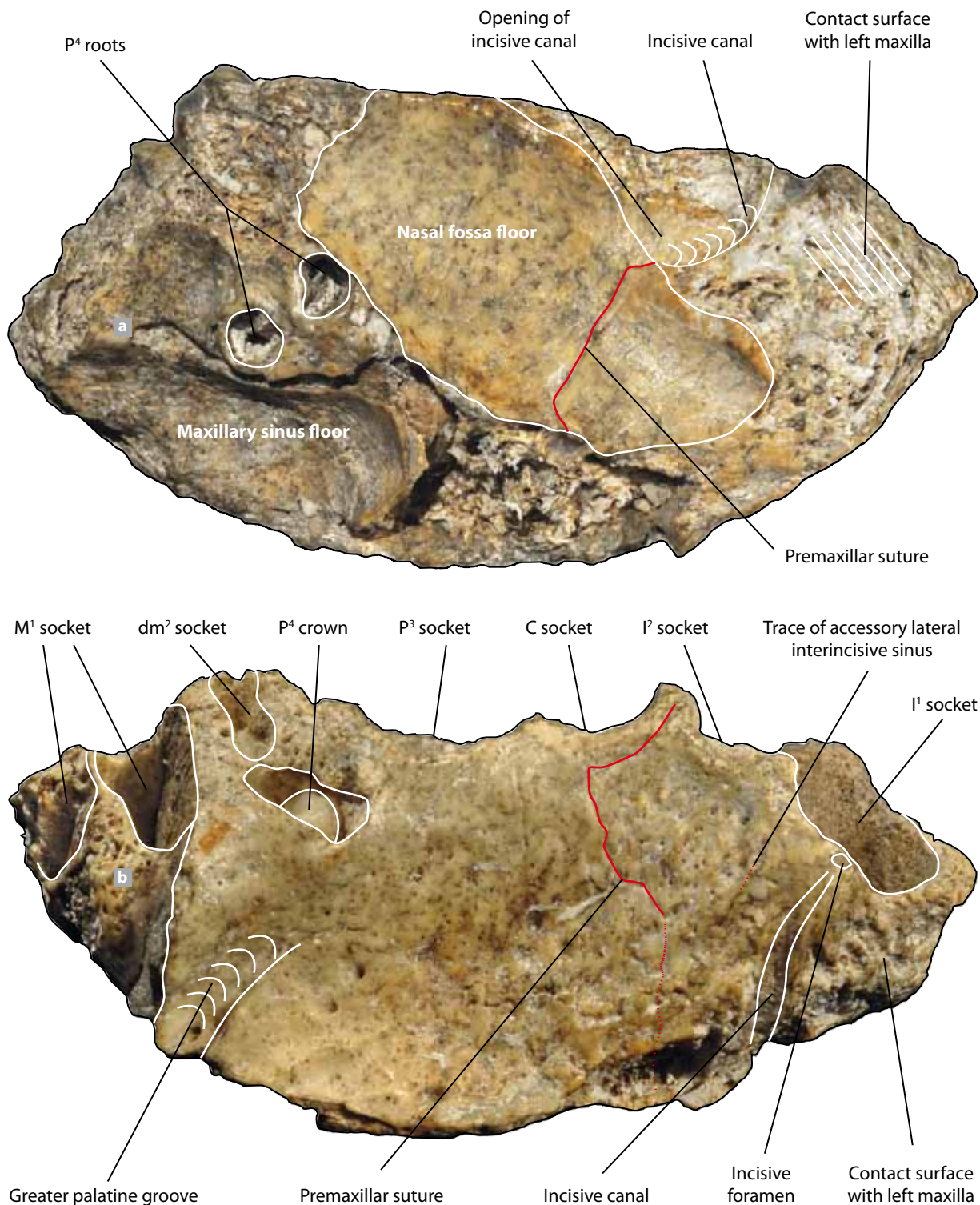


Figure 3: Superior (a) and inferior (b) views of the Scladina maxilla with main anatomical details underlined (photographs Joël Éloy, graphics Sylviane Lambermont, AWEM).

3.3. Inferior view: alveolar and palatine process

The palatine process is insufficiently preserved to allow any of the standard measurements of the

palatal and dental arch. In order to compare the dental arch size of Scladina to that of other Upper Pleistocene individuals we took several linear measurements of the arcade length. We measured these on the inner side of the alveolar process and

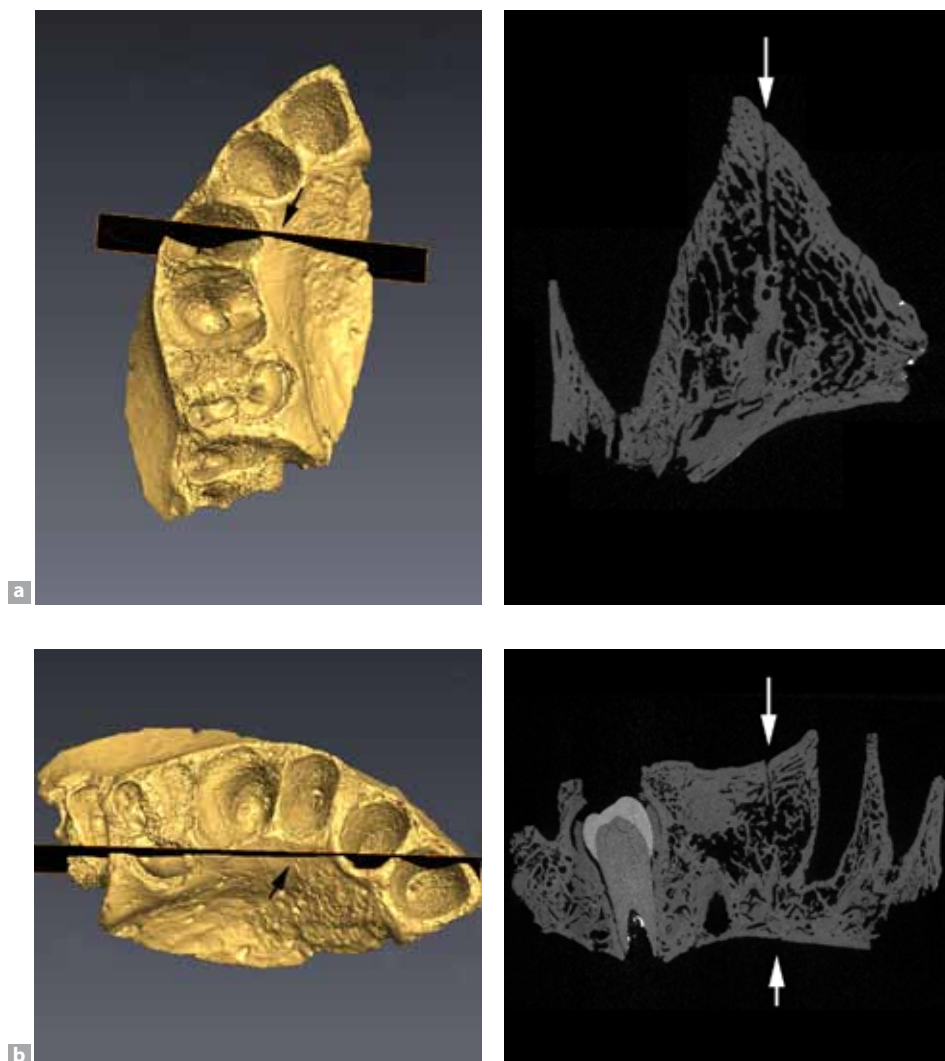


Figure 4: micro-CT scans data showing the premaxillary suture (as indicated by the arrows).

the landmarks selected were the lowest and most medial points on the interalveolar septum. Two lengths (LA 1 and LA2) provide an estimate of the anterior length of the arcade: LA1 = distance I^1/I^1 (or i^1/i^1) to I^2/C (or i^2/dc); LA2 = distance I^1/I^1 (or i^1/i^1) to C/P^3 (or dc/dm^1). In addition, two measurements were taken for the posterior part of the arcade: LP1 = distance I^2/C (or i^2/dc) - m^2/M^1 (P^4/M^1); LP2 = distance C/P^3 (c/m^1) - m^2/M^1 (P^4/M^1).

The distance from the midline (I^1/I^1) to the I^2/C septum of Scladina (LA1 = 17.1 mm) falls well within the range of variation of both Neandertal and UPMH samples, even though it is rather high when compared to the UPMH and rather small when compared to other Neandertals (Table 2). Indeed, it falls within the range of variation of the younger S1 Neandertals (with I^1 and I^2 not yet erupted), and close to Engis 2. Although it is

higher than Kůlna, it falls well below other S3 and S4 individuals (Krapina 47, 49 and Teshik-Tash). The same distance to the P^3 - dm^1 septum (LA2) is also rather low, falling in the lower part of the Neandertal range (all age classes pooled) and well within the UPMH range (Table 2 & Figure 2b). The distance I^2/C - m^2/M^1 (LP1) is by contrast among the highest values of our comparative samples, being higher than all Neandertals but one (Subalyuk 2), Qafzeh 4 (MPMH) and above all UPMH individuals (Table 2). The same is true when only the first two cheek teeth are considered, i.e. the distance LP2 between C/P^3 (or c/dm^1) and P^4/M^1 (or dm^2/M^1). Overall, Scladina falls among the highest Neandertal values, above Qafzeh 4 and above all UPMH individuals (Figure 2c).

On the anterior part of the alveolar process, the right wall of a unique incisive foramen can be observed behind the medial wall of the I^1 socket.



		Scla	Ded1	DevTo	Eng2	PAze	RdM	Sub2	LQ18	Kra47	Kûlna	TTash
NEAND	Age class	S3	S1	S1	S1	S1	S1	S1	S2	S3	S3	S3
	Origin of the data	(1)	(2)	(3)	(1)	(3)	(1)(3)	(1)	(1)	(3)	(1)	(3)
	Premaxillary suture above <i>crista conchalis</i>	x		x	Yes		Yes	Yes		x	x	
	Premax. suture below <i>crista conchalis</i>	x		x	Yes		Yes	Yes		x	x	
	Premax. suture on the floor of nasal fossae	Yes		No	Yes		Yes	Yes		x	Trace	
	Premax. suture on palatal face	Yes	Yes	No	Yes	Yes	Yes	Yes	Yes	No	No	Yes
	Lateral secondary interincisive sinus	Trace	Yes	No	Yes	Yes	Yes	Yes	Trace	x	No	
	Medial secondary interincisive sinus	Trace?	Yes	No	Yes	Yes	Yes	Yes	x	x	No	

		Qafz4	GE1	GE2	Le Figuier	Plac31	Plac33	StGer7
MPMH & UPMH	Age class	S2	S1	S1	S1	S1	S2/3	S2
	Origin of the data	(1)	(1)	(1)	(1)	(1)	(1)	(1)
	Premaxillary suture above <i>crista conchalis</i>	No	Yes	Yes		Yes	x	
	Premax. suture below <i>crista conchalis</i>	x		Yes		Yes	x	
	Premax. suture on the floor of nasal fossae	x	(No)	Yes		Yes	Yes	(Yes)
	Premax. suture on palatal face	Trace	Yes	Yes	Yes	Yes	Yes	
	Lateral secondary interincisive sinus	Yes	Yes	Yes	Yes	x	No	
	Medial secondary interincisive sinus	Yes	x	No	No	No	No	

Table 3: Expression of the premaxillary suture in the fossil specimens. **NEAND:** Neandertals; **MPMH:** Middle Palaeolithic Modern Humans; **UPMH:** Upper Palaeolithic Modern Humans. Origin of the data: ⁽¹⁾ This Study; ⁽²⁾ DODO et al., 2002; ⁽³⁾ MAUREILLE & BAR, 1999. See the text for the definition of the age classes. **Scla** = Scladina; **Ded1** = Dederiyeh; **DevTo** = Devil's Tower; **Eng2** = Engis 2; **PAze** = Pech de l'Azé (PATTE, 1957); **RdM** = Roc de Marsal; **Sub2** = Subalyuk 2; **LQ18** = La Quina 18; **Kra47** = Krapina 47; **TTash** = Teshik-Tash; **Qafz4** = Qafzeh 4; **GE** = Grotte des Enfants; **Plac** = Le Placard; **StGer7** = Saint-Germain-Rivière 7.

All Neandertals show a unique incisive foramen, whereas among recent humans there is more variation, sometimes with additional openings. A deep, larger palatine groove emerges distally at the level of the dm^2/M^1 septum.

The premaxillary suture (*sutura premaxillaris*) can be observed on the palatine process (Figures 3b & Figure 4). It runs first distally from the I²-C interalveolar septum along the canine alveolar edge, and turns then medially and slightly anteriorly. As described above, this suture is also visible on the nasal floor (but its possible presence on the lateral wall of the nasal fossa cannot be confirmed). In addition, slight traces of the secondary interincisive sinus are visible behind the I1-I2 interdental septum. Finally, slight traces close to the incisive canal might reflect the presence of a medial interincisive sinus (see MAUREILLE & BAR, 1999) but the traces are not clear enough to assert it. The premaxillary suture is well observed on the micro-CT data (Figure 4), which show that the suture is not restricted to the surface of the palatal face but runs upwards inside the bone. Micro-CT data also show that the lateral interincisive sinus is open in its medial part.

A similar pattern, with an open premaxillary suture on the palatal face as well as on the nasal

floor is observed on all the younger Neandertals from the S1 dental development with the exception of Devil's Tower. The suture is also visible on the palatal face of La Quina 18 and Teshik-Tash, but is closed on Krapina 47 and Kûlna (Table 3). The premaxillary suture is also most often visible on the palatal face and nasal floor of the UPMH individuals, showing no difference in expression with Neandertals (but the data set is limited). It has been suggested that the closure of the premaxillary suture is delayed on Neandertals compared to recent humans (MAUREILLE, 1994; COQUEUGNIOT, 1998; MAUREILLE & BAR, 1999; MAUREILLE & BRAGA, 2002). The premaxillary suture on Scladina is still open on part of its path, adding to the evidence provided by MAUREILLE & BAR (1999) on younger individuals. A delayed closure of the suture might have allowed a longer growth period of the Neandertal midface. In addition, MAUREILLE & BAR (1999) have stressed that the presence of two interincisive sinuses is much more frequent than in recent humans, possibly because of their larger incisor size. Our data suggest that UPMH show most often only one sinus in a pattern similar to recent humans (Table 3). More data are however needed on Pleistocene Early Modern Humans.

4. Conclusions

The maxilla of Scladina is a rather small fragment retaining only parts of the right body, palatine and alveolar processes. Its high subnasal height (estimated) and the bilevel configuration of its internal nasal floor are consistent with the Neandertal group. The location of the zygoalveolar crest is however not as posterior as similarly aged Neandertals. In addition, the anterior part of its dental arcade is rather short when compared to other Neandertals, which is consistent with the rather low cervical area of the anterior teeth (see Chapter 13) which fall in the lower part of the Neandertal range. Finally, the premaxillary suture is visible on the palatal face and on the nasal floor and still open on a large part of its path as shown by the Ct-scan data. This adds to previous studies suggesting a delayed closure of the premaxillary suture on Neandertals compared to recent humans.

Acknowledgements

We would like to thank the following people and institutions who provided research access to the original fossil remains included in the comparative samples C. Schwab and M.-S. Larguèze, Musée d'Archéologie nationale, Saint-Germain-en-Laye (France); J.-J. Cleyet-Merle, Musée national de Préhistoire, Les Eyzies-de-Tayac (France); I. Pap, Hungarian Natural History Museum, Budapest (Hungary); K. Valoch, P. Neruda, Anthropos Institute of the Moravian Museum; Prof. H. de Lumley, A. Vialet and S. Renault from the Institut de Paléontologie Humaine (Paris); Ph. Menecier, A. Fort and L. Huet from the Musée de l'Homme, Paris (France); E. Poty, University of Liège; J. Radovčić, Croatian Natural History Museum (Zagreb).

The authors are also grateful to Sylviane Lambermont and Joël Éloy, graphic artists at the Association wallonne d'Études mégalithiques as well as Jean-François Lemaire, Service de l'Archéologie en province de Liège du Service public de Wallonie, for all the figures. For taking the time to improve the English text, Jean-François Lemaire again and Rebecca Miller, University of Liège.

References

COQUEUGNIOT H., 1998. *Variabilité morphologique de la tête osseuse au cours de l'ontogenèse. L'exemple des enfants de l'espèce Homo*

sapiens. Unpublished PhD thesis, Université Bordeaux 1, 334 p.

DODO Y., KONDO O. & NARA T., 2002. The Skull of the Neandertal Child of Burial No.1. In T. AKAZAWA & S. MUHESEN (eds.), *Neandertal Burials: Excavations of the Dederiyeh Cave, Afrin, Syria*. Kyoto, International Research Center for Japanese Studies. Roma, L'Erma di Bretschneider: 93-137.

FRANCISCUS R. G., 2003. Internal nasal floor configuration in *Homo* with special reference to the evolution of Neandertal facial form. *Journal of Human Evolution*, 44: 701-729.

FREIDLIN S. E., GUNZ P., JANKOVIĆ I., HARVATI K. & HUBLIN J.-J., 2012. A comprehensive morphometric analysis of the frontal and zygomatic bone of the Zuttiyeh fossil from Israel. *Journal of Human Evolution*, 62: 225-241.

GOWER C. G., 1923. A contribution to the morphology of the apertura piriformis. *American Journal of Physical Anthropology*, 6: 27-36.

HENRY-GAMBIER D., 2001. *Les Enfants de Grimaldi (Grotte des Enfants, Site des Baoussé-Roussé, Italie)*, *Anthropologie et Paléontologie Funéraire (avec les contributions de M.-A. Courty, É. Crubézy, B. Kervazo)*. Paris, Éditions du Comité des travaux historiques et scientifiques & Éditions de la Réunion des Musées Nationaux, 14, 177 p.

ISHIDA H. & KONDO O., 2002. The Skull of the neandertal Child of Burial No.2. In T. AKAZAWA & S. MUHESEN (eds.), *Neandertal Burials: Excavations of the Dederiyeh Cave, Afrin, Syria*. Kyoto, International Research Center for Japanese Studies. Roma, L'Erma di Bretschneider: 271-297.

KROVITZ G. E., 2003. *Shape and growth differences between Neandertals and modern humans: Grounds for a species-level distinction?* In J. L. THOMPSON, G. KROVITZ & A. J. NELSON (eds.), *Growth and Development in the Genus Homo*. Cambridge University Press: 320-342.

MADDUX S. D. & FRANCISCUS R. G., 2009. Allometric scaling of infraorbital surface topography in *Homo*. *Journal of Human Evolution*, 56: 161-174.

MADRE-DUPOUY M., 1992. *L'Enfant du Roc de Marsal*. Paris, Éditions du Centre national de la recherche scientifique, Cahiers de Paléanthropologie, 299 p.



- MARTIN R., 1928 (2nd ed.). *Lehrbuch der Anthropologie in systematischer Darstellung*, II, Jena, Fischer, 3 vols.
- MAUREILLE B., 1994. *La face chez Homo erectus et Homo sapiens : recherche sur la variabilité morphologique et métrique*. Unpublished PhD thesis, Université de Bordeaux 1, 486 p.
- MAUREILLE B. & BAR D., 1999. The premaxilla in Neandertal and early modern children: ontogeny and morphology. *Journal of Human Evolution*, 37: 137-152.
- MAUREILLE B. & BRAGA J., 2002. Between the incisive Bone and Premaxilla. From African apes to *Homo sapiens*. In N. MINUGH-PURVIS & K. J. McNAMARA (eds.), *Human evolution through developmental change*. Baltimore, Johns Hopkins University Press: 464-478.
- MINUGH-PURVIS N., 1988. *Patterns of craniofacial growth and development in Upper Pleistocene Hominids*. Unpublished PhD thesis. University of Pennsylvania, 657 p.
- MINUGH-PURVIS N., 1993. Reexamination of the Immature Hominid maxilla From Tangier, Morocco. *American Journal of Physical Anthropology*, 92: 449-461.
- PATTE E., 1957. *L'enfant néanderthalien du Pech de l'Azé*. Paris, Masson & Cie, 230 p.
- SERGI S., 1948. Sulla morfologia della facies anterior corporis maxillae nei paleantropi di Saccopastore e del Monte Circeo. *Rendiconto della Reale Accademia Nazionale dei Lincei, classe de Scienze Fisiche, Matematiche e Naturali, ser. 8*: 387-394.
- RAK Y., 1986. The Neanderthal: a new look at an old face. *Journal of Human Evolution*, 15: 151-164.
- TILLIER A.-M., 2002. *Les Enfants Moustériens de Qafzeh. Interprétation Phylogénétique et Paléoaurologique*. Paris, Éditions du Centre national de la recherche scientifique, Cahiers de Paléoanthropologie, 239 p.
- TRINKAUS E., 1987. The Neandertal face: evolutionary and functional perspectives on a recent hominid face. *Journal of Human Evolution*, 16: 429-443.
- VERNA C., 2006. *Les restes humains moustériens de la Station Amont de La Quina - (Charente, France). Contexte archéologique et constitution de l'assemblage. Étude morphologique et métrique des restes crânio-faciaux. Apport à l'étude de la variation néandertalienne*. Unpublished PhD thesis, Université de Bordeaux 1, 629 p.

Chapter 13

THE DENTITION OF THE SCLADINA I-4A JUVENILE NEANDERTAL

Michel TOUSSAINT

Michel Toussaint & Dominique Bonjean (eds.), 2014.
The Scladina I-4A Juvenile Neandertal (Andenne, Belgium),
Palaeoanthropology and Context
Études et Recherches Archéologiques de l'Université de Liège, 134: 233-306.

1. Introduction

Teeth found in cave sediments are usually well preserved and represent the most frequent hominin fossils.

Beginning with the first detailed studies of Neandertal remains these fossils always interested palaeontologists who have been describing them in more or less details. This was for instance the case with the remains from Spy (FRAIPONT & LOHEST, 1887) and La Chapelle-aux-Saints (BOULE, 1911-1913) as well as in some overviews (PATTE, 1959-1961).

Even if Neandertal teeth contain much morphological information, for a long time they were not widely used for taxonomic and phylogenetic purposes, mainly because this taxon and anatomically modern humans, notably Upper Palaeolithics, share numerous non-metric features (BAILEY & HUBLIN, 2006). It is true that some traits are sometimes mistakenly viewed as typical of Neandertals (e.g. shovelling). It has, however, been shown that Neandertals exhibit a specific dental pattern characterized by the high frequency of some traits and their combination, not only when the entire dentition is taken into consideration but also isolated teeth (BAILEY, 2002^a, 2006^a).

The purpose of this chapter is to provide a description of the 24 Scladina teeth, belonging to a rare example of juvenile western European Neandertal which is dated, probably from MIS 5b or MIS 5a. The choice was made to seek the associations of morphological features which, mainly based on the work of S. Bailey, distinguish the teeth of Neandertals from other taxa. More specific aspects of the teeth, such as enamel thickness, enamel dentine junction, and root morphology are analysed in other chapters (respectively Chapters 14, 15 & 16).

2. Materials and methods

Table 1 presents all 24 teeth recovered from former units 4A and 3 of Scladina Cave, either found isolated or within the mandible and

maxilla (erupted or completely embedded). After analysis, it is absolutely certain that all the teeth found in the former Layer 4A belong to the same juvenile individual, as has been thought since the first palaeoanthropological discoveries (OTTE et al. 1993; TOUSSAINT et al., 1998). It was also understood that the three teeth first assigned to the base of Layer 3 actually belonged to the same child as the fossils found in former Layer 4A. This observation also confirmed the secondary position at least of all the Neandertal remains already put

Teeth inventory number	Anatomical Tooth Identification	Status	Refitting
Scla 4A-1/M ₁	mandibular right first molar	in situ: erupted	
Scla 4A-1/M ₂	mandibular right second molar	in situ: erupted	
Scla 4A-1/M ₃	mandibular right third molar (crown)	in situ: unerupted	
Scla 4A-1/P ₂	mandibular right second premolar	in situ: unerupted	
Scla 4A-2/P ²	maxillary right second premolar	in situ: unerupted	
Scla 4A-3	maxillary right second molar	isolated	fits in 4A-4
Scla 4A-4	maxillary right first molar	isolated	fits in 4A-2
Scla 4A-5	deciduous maxillary right second molar	isolated	fits in 4A-2
Scla 4A-6	mandibular right first premolar	isolated	fits in 4A-1
Scla4A-7	deciduous maxillary right first molar	isolated	fits in 4A-2
Scla 4A-8	maxillary right third molar	isolated	fits with 4A-3
Scla 4A-9/M ₁	mandibular left first molar	in situ: erupted	
Scla 4A-9/M ₂	mandibular left second molar	in situ: erupted	
Scla 4A-9/P ₂	mandibular left second premolar	in situ: unerupted	
Scla 4A-11	maxillary right central incisor	isolated	fits in 4A-2
Scla 4A-12	mandibular right canine	isolated	fits in 4A-1 & 9
Scla 4A-13	deciduous mandibular right second molar	isolated	fits in 4A-1
Scla 4A-14	maxillary right lateral incisor	isolated	fits in 4A-2
Scla 4A-15	mandibular right central incisor	isolated	fits in 4A-9
Scla 4A-16	maxillary right canine	isolated	fits in 4A-2
Scla 4A-17	maxillary left lateral incisor	isolated	
Scla 4A-18	maxillary left canine	isolated	
Scla 4A-19	mandibular left lateral incisor	isolated	fits in 4A-9
Scla 4A-20	mandibular right lateral incisor	isolated	fits in 4A-9

Table 1: List of all the Scladina juvenile teeth. **In situ** = tooth still attached to the mandible or maxilla, either erupted or unerupted; **isolated** = the tooth was found isolated in sediments. Except when noted as deciduous, all teeth are to be considered as permanent.



in evidence by their planimetric distribution (see Chapters 5 & 7).

Small variations in the identification occurred in the preliminary articles published about the remains of the Scladina Juvenile; they are presented in Table 2. This chapter provides the final determinations based on a detailed study of each tooth.

The descriptions of the 24 Scladina teeth focus on diagnostic morphological features of Neandertal teeth, in accordance with recent dental anthropological studies (notably by BAILEY 2002^a, 2002^b, 2004^a, 2004^b, 2006^a, 2006^b; BAILEY & LYNCH, 2005; BAILEY & HUBLIN, 2006; BAILEY et al., 2011). The terminology used for cusp identification follows that of classic procedures (see e.g. HILLSON, 1996; SCOTT & TURNER, 1997). Occlusal wear has been scored according to MOLNAR (1971). Non-metric data were collected following the worldwide international standard for morphological study, the Arizona State University Dental Anthropology System, or ASUDAS, developed to reduce subjectivity in tooth description. These non-metric traits are scored by using a set of plaques and descriptions of the corresponding variations (TURNER et al., 1991; SCOTT & TURNER, 1997) that were

developed for modern humans. On hominin fossils, it sometimes appears that trait expressions may exceed the grades found in modern humans; in Scladina for instance, the labial face of the permanent maxillary central incisor is, mesiodistally, more convex than in the ASUDAS UI-1 curvature, grade 4. The micro-CT data used for this study were recorded at the University of Antwerp and at the Max Planck Institute in Leipzig.

All teeth were compared to a sample of similar specimens from different periods: Early Neandertals (EN), Late Neandertals (LN), Middle Palaeolithic Modern Humans (MPMH), Upper Palaeolithic Modern Humans (UPMH) as well as Middle Ages/submodern Modern *Homo sapiens sapiens* (MHSS) from the city of Liège (Belgium). The first four groups are mainly part of the file prepared by C. VERNA (2006) in her PhD thesis and developed thereafter as well as some data collected by the present author. The modern group consists of personal measurements by the author.

Univariate analyses using the method developed by F. HOUËT (2001) were carried out to compare the MD (mesiodistal) and BL (buccolingual) measurements of the Scladina teeth with the above mentioned samples:

Tooth Inventory Number	OTTE et al., 1993	TOUSSAINT et al., 1998	SEMAL et al., 2005	PIRSON et al., 2005	TOUSSAINT et al., 2011	Present chapter	Conclusion
Scla 4A-1	Right hemimandible	Right hemimandible	Right hemimandible	Right hemimandible	Right hemimandible	Right hemimandible	identical
Scla 4A-2	Right maxilla fragment	Right maxilla fragment	Right maxilla	Right maxilla fragment	Right maxilla fragment	Right maxilla fragment	identical
Scla 4A-3	RM ²	RM ²	RM ²	RM ²	RM ²	RM ²	identical
Scla 4A-4	RM ¹	RM ¹	RM ¹	RM ¹	RM ¹	RM ¹	identical
Scla 4A-5		Rdm ²	Rdm ²	Rdm ²	Rdm ²	Rdm ²	identical
Scla 4A-6		RP ₁		RP ₁	RP ₁	RP ₁	identical
Scla 4A-7		Rdm ¹	Rdm ¹	Rdm ¹	Rdm ¹	Rdm ¹	identical
Scla 4A-8		M3 (unspecified)	LM ₃	LM ₃	LM ₃	RM ³	different
Scla 4A-9		Left hemimandible	Left hemimandible	Left hemimandible	Left hemimandible	Left hemimandible	identical
Scla 4A-10				LC,			declassified
Scla 4A-11			RI ¹	RI ¹	RI ¹	RI ¹	identical
Scla 4A-12			R ^C	R ^C	R ^C	R ^C	identical
Scla 4A-13				Rdm ₂	Rdm ₂	Rdm ₂	identical
Scla 4A-14			RI ²	RI ²	RI ²	RI ²	identical
Scla 4A-15			RI ₂	RI ₂	RI ₂	RI ₁	different
Scla 4A-16			R ^C	R ^C	R ^C	R ^C	identical
Scla 4A-17 (= Scla 3-2)	LI ²		LI ²	LI ²	LI ²	LI ²	identical
Scla 4A-18 (= Scla 3-3)	LC		LC	LC	LC	LC	identical
Scla 4A-19 (= Scla 3-4)				Permanent mandibular I (unspecified)	Permanent mandibular I (unspecified)	LI ₂	more precise
Scla 4A-20						RI ₂	

Table 2: Variations in the identification of the teeth of the Scladina Child (I = incisor; C = canine; P = premolar; M & m = molar; d = deciduous; R = right; L = left; subscript number or ⁻ = mandibular tooth; superscript number or ₋ = maxillary tooth).

– Probabilistic distances (DP) compare the measurement of a fossil to parameters of a reference population, according to the formula $DP = \text{student law} (Abs (x-m) / s; n-1; 2)$;

– ECRA (“*écart centré réduit ajusté*” of HOVĚT, 2001) = $(x-m) / \text{inverse student law} (0.05; n-1) * s$.

In both formulas, x = individual value, m = sample mean, s = standard deviation, n = number of fossils. In tables corresponding to each tooth, numbers in brown indicate values of DP and ECRA that diverge significantly from the estimated variation of the reference population ($DP > 0.05$ or < -0.05 ; $ECRA > 1$ or < -1).

Bivariate biometric comparisons were conducted from the mesiodistal and buccolingual diameters of the crown to try to clarify the taxonomic position of the Scladina teeth. The bivariate comparisons made use of the well-known technique of equiprobable ellipses (DEFRISE-GUSSENHOVEN, 1955); 95% confidence ellipses were plotted using the statistical software package PAST (PALaeontological STATistics, version 1.77, 2008; HAMMER et al., 2001).

Above each tooth description, the following information is given:

- the anatomical identification of the fossil;
- the identification number given during the palaeoanthropological study;
- the identification number given either on the field at the time of discovery or later during laboratory sorting of the palaeontological material found in the cave, without any reference to the human or non-human nature of the fossil;
- the date of the discovery;
- the date the fossil was identified as human (sometimes this is a precise date, sometimes only a year and a month);
- the excavation square of the discovery;
- the position of the fossil in the first stratigraphical interpretation;
- the new stratigraphical position: most probable unit (and sometimes layer); in brackets, potential unit (see Chapter 5 for more details).

3. Description of the Scladina I-4A teeth _____

3.1. Permanent maxillary right central incisor, RI¹

Palaeoanthropological identification: Scla 4A-11

Field identification: Sc 1990-81-47

Date of discovery: 13 March 1990

Date of identification: May 2000

Square: G27

Stratigraphic position:

- **Former stratigraphy:** 4A
- **New stratigraphy:** units 4A-POC or 3-INF (units 4A-IP, 4A-CHE, 3-SUP)

3.1.1. Description (Figure 1)

This permanent maxillary central incisor fits perfectly in the corresponding tooth socket of the Scla 4A-2 right maxillary fragment, found in Square D30, former Layer 4A, at a distance of more than 4 m.

The crown is completely formed and the root fully occluded but its tip is broken. The crown and the root exhibit numerous microfissures, along their length and perpendicular to it. No pathological conditions are noted.

The incisal rim of the crown presents minor transversal occlusal wear, without significant dentine exposure (grade 2, according to MOLNAR, 1971). The rounded occluso-distal angle is only slightly concerned by the occlusal wear. The incisal plane of wear slants slightly towards the lingual surface.

The lingual surface of the crown is shovel-shaped (ASUDAS, grade 3). Both mesial and distal marginal ridges are well marked but do not contact the cingulum. They circumscribe a shallow area, the lingual fossa. A large but shallow interruption groove dissects the distal marginal ridge from the cingulum, without reaching the cervix. Two extensions of the *tuberculum*, or lingual tubercles (*tuberculum dentale*), are present but lack free apices. The height of both tubercles is 6.6 mm, from the cervix, while the height of the crown is 10.5 mm on the lingual face. First observed on the outer enamel surface (OES), all these features are also visible, and even more marked, on the enamel dentine junction surface (EDJ).

When viewed from the occlusal aspect, the labial face is mesiodistally strongly convex (more than in the ASUDAS UI-1 curvature, grade 4). This face also exhibits an irregular superior-inferior convexity, from the cervical line to the incisal edge. In detail, as seen in mesial or distal views, the labial face is convex near the cervix, then becomes oblique in the inferior half adjacent to the incisal edge. Double shovelling is not present as the labial surface is smooth (ASUDAS, grade 0).

Both side edges of the crown asymmetrically diverge from the cervix: the distal edge is more rounded and lower than the mesial one, and the



Permanent Maxillary Right Central Incisor Scla 4A-11

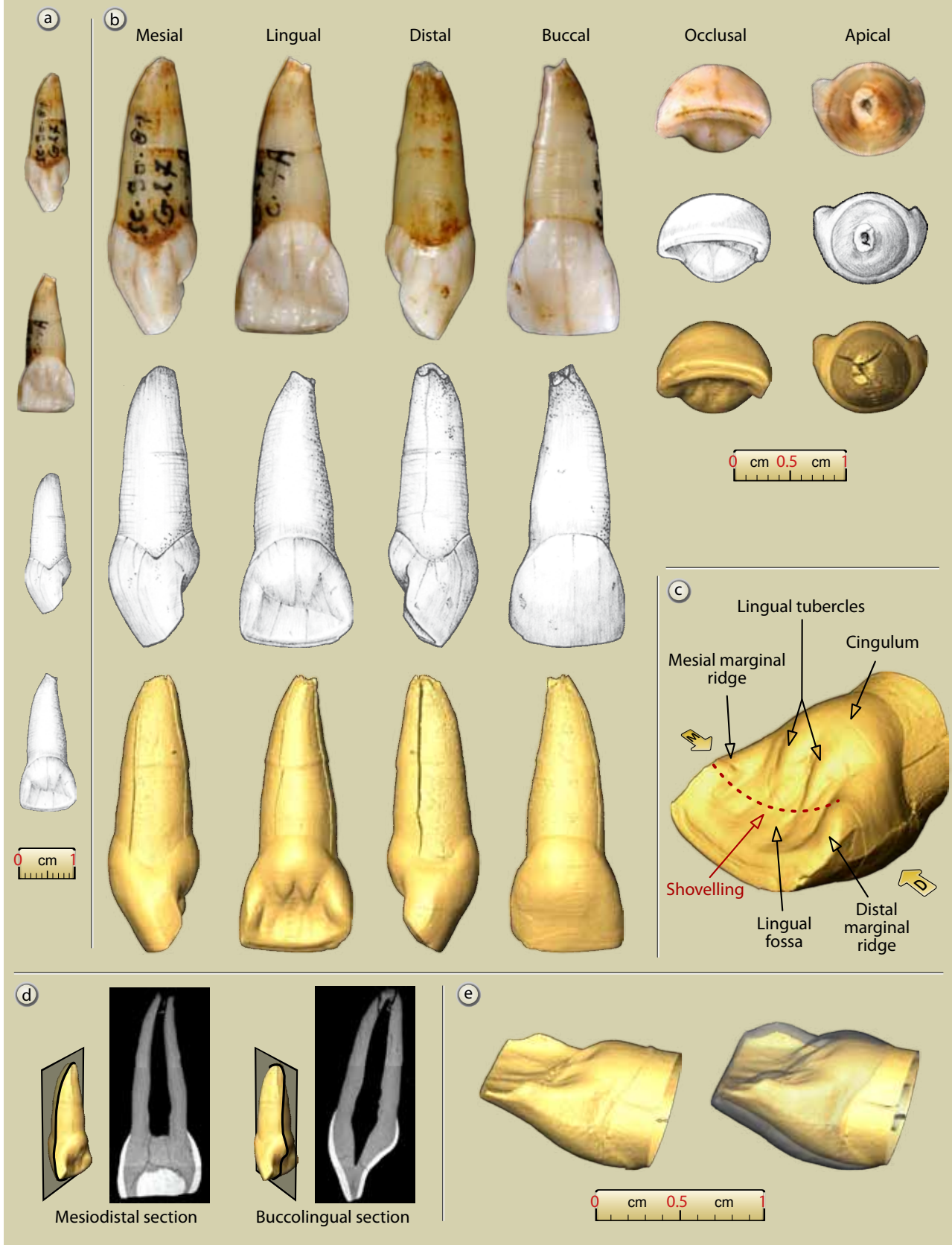


Figure 1: Scla 4A-11 permanent maxillary right central incisor: a. mesial and lingual views (1:1 scale); b. photographs, drawings and 3D reconstructions of the six faces of the incisor (2:1 scale); c. 3D reconstruction with main anatomical features; d. internal sections; e. 3D lingual views at the EDJ without and with enamel (micro-CT data processing and graphics J.-F. Lemaire, SPW; pencil drawings S. Lambermont, AWEM; photographs J. Eloy, AWEM).

mesioincisal corner is sharp. The incisal ridge, which is slightly convex downward, slightly slopes from the mesial up to the distal sides.

On the mesial and distal marginal ridges, near the cervical rim, are interproximal wear facets indicating that the tooth was functional. The mesial facet is flat and is vertically elongated with rounded upper angles. It has no subvertical grooves. Its height is 4.4 mm and its width 2.5 mm. The distal facet is smaller and narrower with a rounded upper extremity; height: 3.6 mm and width: 1.7 mm. There are no subvertical grooves.

As usual on incisors, the V-convexity of the enamel line is more marked on the mesial face than on the distal one.

The lingual length of the root is about 14 mm in its actual state of preservation, but as the tip is damaged, at least 1.3 mm has to be added to get the original length which is then 15.3 mm or slightly more. The section of the root is rounded. The apical third of the root is anteriorly convex, when viewed from the side. No longitudinal root groove is present.

3.1.2. Taxonomy

Neandertal maxillary central incisors exhibit a distinctive combination of features which makes them particularly useful for distinguishing between Neandertals and modern humans (CRUMMETT, 1995; BAILEY & HUBLIN, 2006; BAILEY, 2006^a): strong expression of lingual marginal ridges and associated marked shovelling, labial convexity, developed lingual tubercles, and superior-inferior convexity of the crown and root when viewed from the side. All these features can be found, in moderate degrees, in Early Modern Humans, but it is the high frequency of the combination of all of them and of their marked expression that make Neandertals distinctive (Table 3).

The permanent Scla 4A-11 maxillary right central incisor of Scladina exhibits the distinctive combination of features of Neandertals.

3.1.3. Morphometric analysis

Measurements of Scla 4A-11 are as follows:

MD: 9.90 mm

BL: 7.98 mm

MD at the cervix: 6.95 mm

BL at the cervix: 6.95 mm

Length of the root: 15.3 mm in its current state of preservation

Total length of the tooth: 24.67 mm in its current state of preservation

Using BAILEY (2006^b)'s data, the length of the Scla 4A-11 root (± 15.3 mm) fits just between the ranges of variation of Neandertals (15.7–19.7 mm) and modern humans (11.7–15.2 mm). More recent results (LE CABEC et al., Chapter 16) confirm that Scladina has comparatively very short incisor roots compared to those of the other MIS 5 Neandertals. On the other hand, Scladina displays the largest pulp cavities.

The MD and BL diameters of Scla 4A-11 depart significantly from the average of the different comparison samples only in the case of modern humans (MHSS), both in the case of the DP probabilistic distance and ECRA (Table 4). MD and BL diameters of the crown are, in the bivariate graph of Figure 2, compared to the ellipses (95%) of Early and Late Neandertals as well as of MPMH, UPMH and MHSS. Partial overlap of the equiprobable ellipses indicate that the dimensions of the crown of the central incisor crowns permanent only provide limited taxonomic indications. And indeed, in the case of Scla 4A-11, the tooth is located in the central area where the four ellipses of fossils remains overlap, but outside the 95% ellipse of MHSS.

Permanent Maxillary Central Incisors	Modality	Neandertals	Early Modern Afro-Asians	Early Modern Europeans	Scla 4A-11
Lingual marginal ridges/shovelling	presence (grade 2 or above)	(92)-100%	33.3%	50%	yes
	strong expression (grade 4 or above)	> 50%	no	no	grade 3
Labial convexity	presence	> 95%	50%	18.8%	yes
	expression	grade 4 or above: 71%	weak (\leq grade 3)	weak (\leq grade 3)	> grade 4
Lingual tubercles(s)	presence	100%	50%	58.3%	yes
	strong expression	yes	weak	weak	moderate
Double shovelling	presence	4,30%	no	no	no
	expression	weak (grade 1)			

Table 3: Distinctive anatomical features on permanent maxillary central incisors of Neandertals, Early Modern Humans (after BAILEY, 2006^a) and Scla 4A-11.



Table 4: Scla 4A-11 (permanent maxillary right central incisor): MD and BL dimensions compared to those of Early and Late Neandertals as well as MPMH, UPMH and MHSS, with DP and ECRA.

Scladina		Diameter	Value			
RI ¹ (Scla 4A-11)		MD	9.9			
		BL	7.98			
Comparison Samples	N	Diameter	Mean	Stand. Dev.	DP	ECRA
EN right & left	21	MD	9.871	0.846	0.973	0.016
	22	BL	8.795	0.527	0.137	-0.744
LN right & left	27	MD	9.235	0.626	0.298	0.517
	32	BL	8.050	0.489	0.887	-0.070
MPMH right & left	11	MD	9.809	0.763	0.908	0.053
	9	BL	8.156	0.482	0.725	-0.158
UPMH right & left	36	MD	8.739	1.040	0.272	0.550
	37	BL	7.532	0.420	0.293	0.526
MHSS right & left	92	MD	8.136	0.642	0.007	1.384
	92	BL	6.888	0.473	0.023	1.163

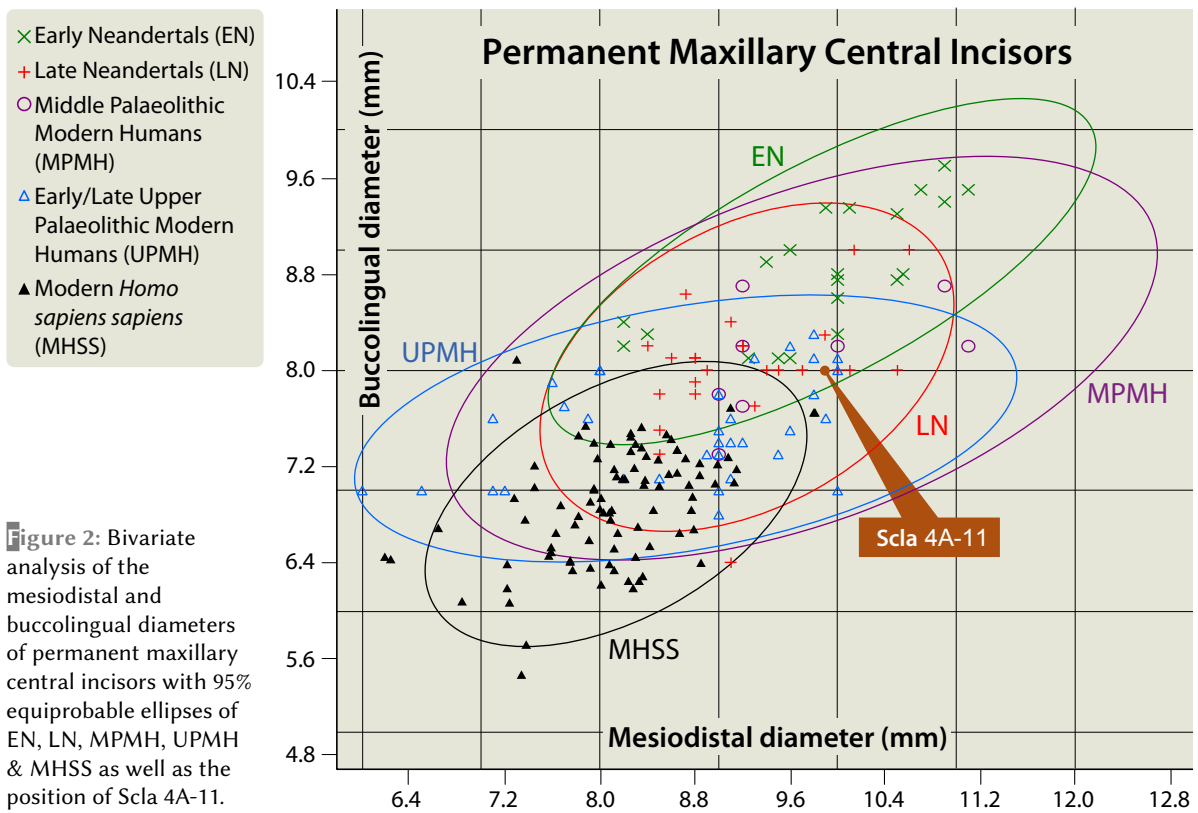


Figure 2: Bivariate analysis of the mesiodistal and buccolingual diameters of permanent maxillary central incisors with 95% equiprobable ellipses of EN, LN, MPMH, UPMH & MHSS as well as the position of Scla 4A-11.

3.2. Permanent maxillary lateral incisors, I²

3.2.1. Description

Permanent maxillary left lateral incisor, LI² (Figure 3)

- Palaeoanthropological identification: Scla 4A-17 (= Scla 3-2)
- Field identification: Sc 1991-526-1
- Date of discovery: 17 October 1991
- Date of identification: October 1993
- Square: F27
- Stratigraphic position:

- Former stratigraphy: 3, then 4A
- New stratigraphy: Unit 4A-POC (units 4A-IP, 4A-CHE, 3-INF)

The crown and the root are completely formed and erupted. The specimen is well preserved. However, it is labiolingually cracked in two nearly equal parts along its longitudinal axis. It exhibits secondary longitudinal and transversal cracks on the crown. No pathological conditions are noted.

The incisal rim is slightly worn, a bit rounded antero-posteriorly, but without exposing the dentine (stage 2 of MOLNAR, 1971). The tooth was functional.

Permanent Maxillary Left Lateral Incisor Scla 4A-17

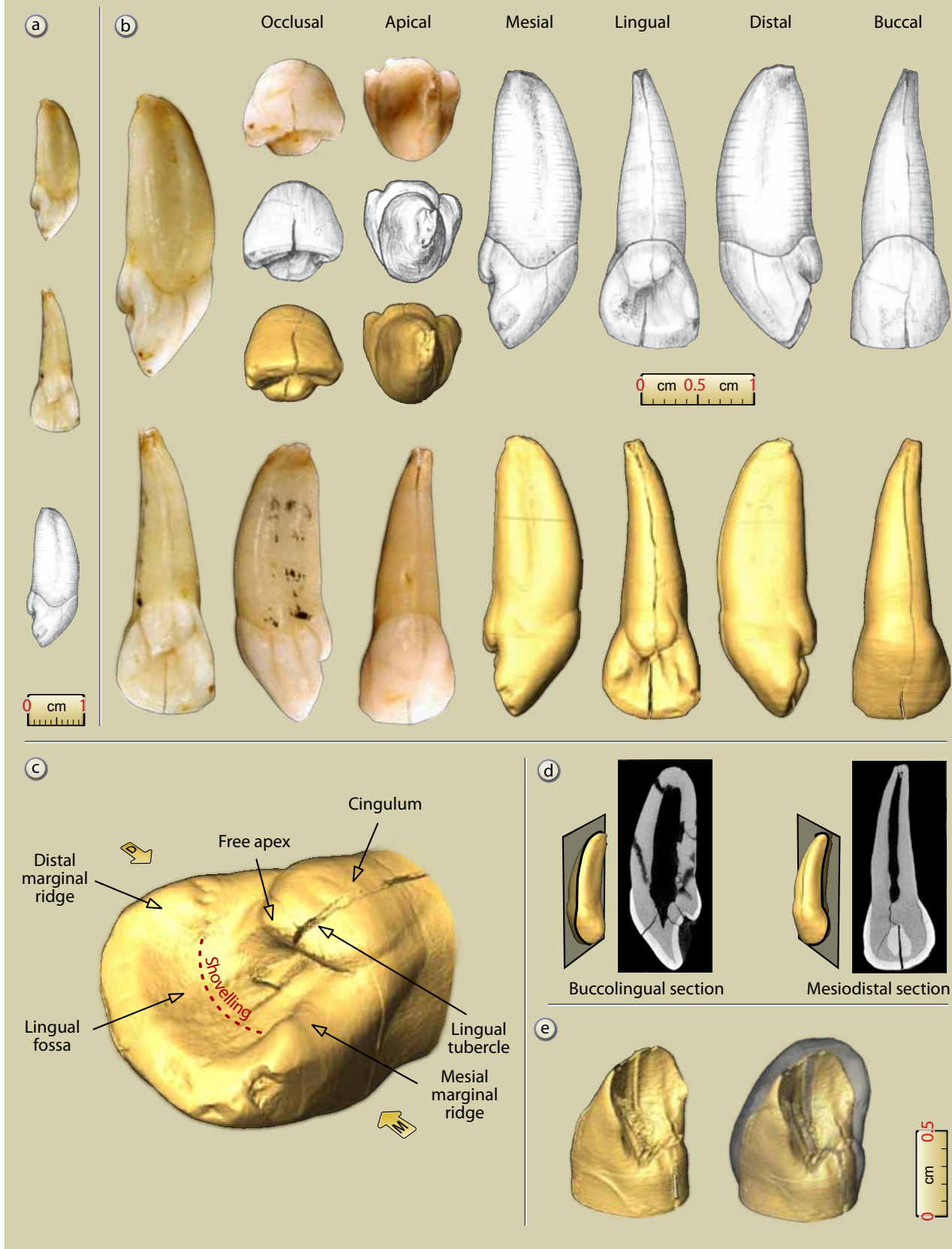


Figure 3: Scla 4A-17 permanent maxillary left lateral incisor: a. mesial and lingual views (1:1 scale); b. photographs, drawings and 3D reconstructions of the six faces of the incisor (2:1 scale); c. 3D reconstruction with main anatomical features; d. internal sections; e. 3D lingual views at the EDJ without and with enamel (micro-CT data processing and graphics J.-F. Lemaire, SPW; pencil drawings S. Lambermont, AWEM; photographs J. Eloy, AWEM).



The labial surface of the crown is mesiodistally convex, as in ASUDAS, grade 4. In mesial view, this face is strongly convex in its cervical part, then becomes nearly flat in the direction of the incisal edge. In anterior view, the labial surface is smooth, without double shovelling (ASUDAS, grade 0). Both side edges of the crown asymmetrically diverge from the cervix: the distal edge is more rounded and lower than the mesial one, and the incisal ridge, which is slightly convex downward, rises slightly distally.

The lingual surface of the crown is shovel-shaped, as in ASUDAS, grade 4. Both mesial and distal marginal ridges are well developed. They circumscribe a fairly deep lingual fossa.

The lingual tubercle, the striking feature of the moderate cingulum, is better marked than on the central maxillary incisor Scla 4A-11. It looks like a marked cuspule with a free apex (grade 6 in TURNER et al., 1991: 16, and even more pronounced than on ASU UC DAR, grade 5). In lingual view, the lower part of the tubercle is vertically divided by a slight groove. Two interruption grooves dissect the tubercle from both the distal and the mesial marginal ridges. Both go up to the cervix but none of them are expressed on the root. The shape of the lingual tubercle is slightly asymmetric when viewed from the lingual side. Distally, it is closer to the incisal edge than it is mesially, so that its free border looks obliquely truncated. In its mesial part, the lingual fossa also exhibits two blunt vertical crests. The usual mamelons of the incisal edge have been worn away.

The maximum height of the tubercle from the cervix is around 4.7 mm, while the total height of the crown is 10.2 mm.

On the mesial and distal faces, the enamel line dips inferiorly, forming a rounded V-shape with its tip in the direction of the incisal rim. As usual on incisors, canines, and premolars, this V-shaped convexity is better marked on the mesial face than on the distal one.

An interproximal wear facet for the central maxillary incisor is present. It is flat, vertically elongated, and nearly vertically divided in two. It does not exhibit subvertical grooves. Its width is 1.5 mm. The tooth does not have a distal interproximal wear facet.

The length of the root is about 14.7 mm on its lingual border and 15.1 on its labial one. The section of the root is irregularly elliptical with flattened sides and an anterior-posterior long axis; two shallow longitudinal root grooves run on the

mesial and distal sides of the root, the mesial one being a bit more pronounced.

When viewed from the side, the root is anteriorly convex and this convexity is in continuity with that of the crown. So, the complete profile of the tooth, crown and root included, is globally convex. In labial or lingual views, the tip of the root bends distally.

Permanent maxillary right lateral incisor, RI² (Figure 4)

Palaeoanthropological identification: Scla 4A-14

Field identification: Sc-1990-37-1

Date of discovery: 22 February 1990

Date of identification: 14 December 2004

Square: H27

Stratigraphic position:

— **Former stratigraphy:** 4A

— **New stratigraphy:** units 4A-POC or 3-INF (units 4A-IP, 4A-CHE, 3-SUP)

This specimen fits well in the corresponding socket of the Scla 4A-2 right maxilla, found in Square D30, at a distance of more than 5 m. No pathological conditions are noted.

The morphology of this tooth is similar to the corresponding permanent maxillary left lateral incisor Scla 4A-17.

The crown and the root are completely formed and erupted. The specimen is well preserved, though it exhibits longitudinal and transversal cracks on the crown and a marked longitudinal crack on the buccal face of the root.

The incisal rim is slightly worn, a bit rounded, but does not expose the dentine (stage 2 of MOLNAR, 1971). In addition, two small chips of enamel are missing from the buccal face of the incisal rim, one at the mesial angle and another one 2 mm off the distal angle. The tooth was functional.

The labial face of the crown is extremely close to that of its antimere: mesiodistally convex (ASUDAS, grade 4), strongly convex in mesial view near the cervix, smooth without double shovelling, distal angle more rounded than the mesial one, and the incisal edge distally. Like its antimere, the lingual surface of the crown exhibits marked shovelling (as in ASUDAS, grade 4), both marginal and distal developed ridges, a deep lingual fossa, a moderate cingulum with an asymmetric lingual tubercle forming a free apex (grade 6 in TURNER et al., 1991: 16), two interruption grooves, a *tuberculum* extension, two blunt vertical crests between

Permanent Maxillary Right Lateral Incisor Scla 4A-14

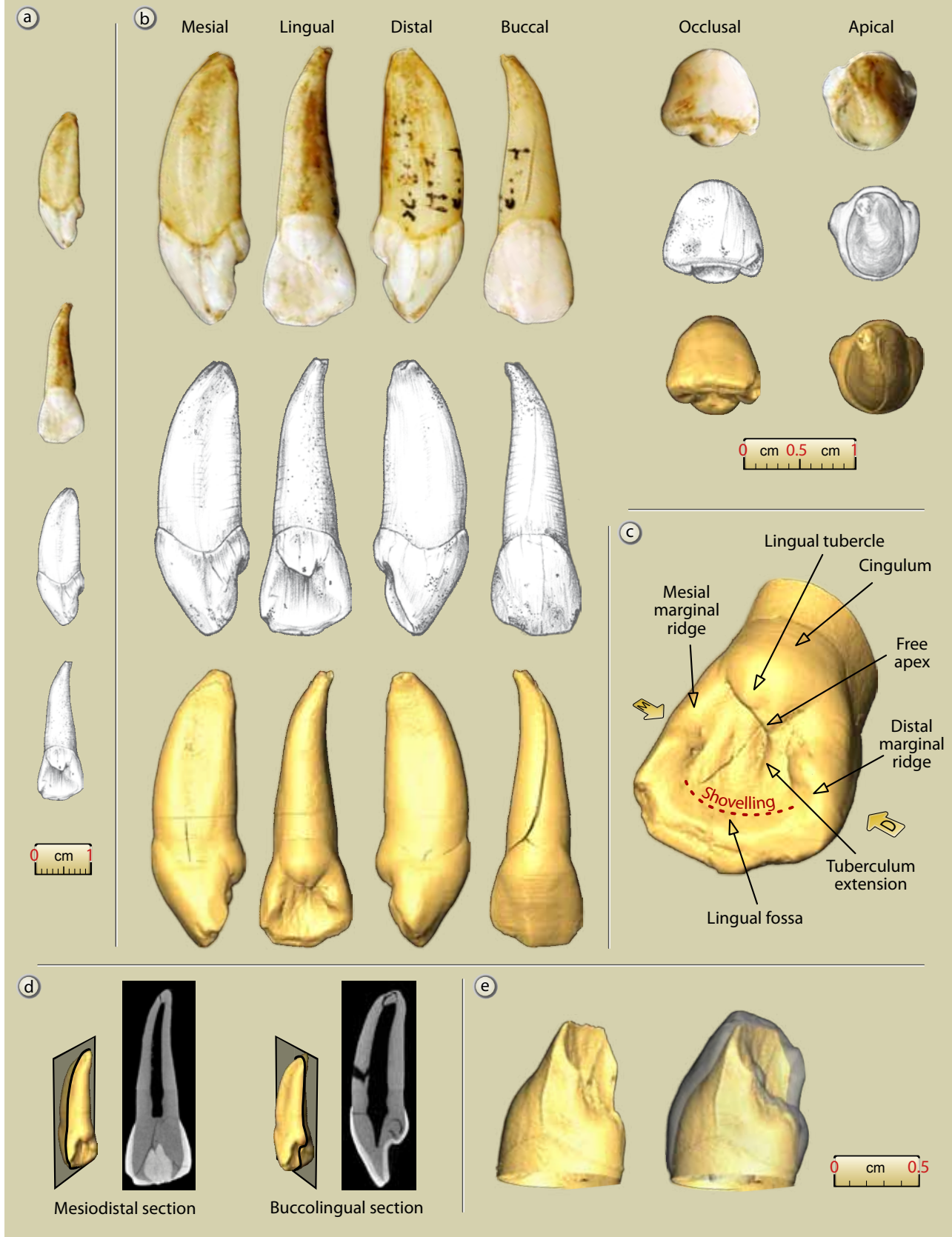


Figure 4: Scla 4A-14 permanent maxillary right lateral incisor: a. mesial and lingual views (1:1 scale); b. photographs, drawings and 3D reconstructions of the six faces of the incisor (2:1 scale); c. 3D reconstruction with main anatomical features; d. internal sections; e. 3D lingual views at the EDJ without and with enamel (micro-CT data processing and graphics J.-F. Lemaire, SPW; pencil drawings S. Lambermont, AWEM; photographs J. Eloy, AWEM).



the mesial marginal ridge, and the *tuberculum* extension.

The mamelons of the incisal edge have been worn away.

The maximum height of the tubercle from the cervix is around 4.75 mm, while the total height of the crown is 10.05 mm.

The rounded V-shape of the enamel-cement junction convexity is better marked on the mesial face than on the distal one.

The interproximal wear facet for the central maxillary incisor is flat, vertically elongated, and with subvertical grooves. Its height is 3.6 mm and its width 1.8 mm. The tooth does not have a distal interproximal wear facet.

The length of the root is about 14.8 mm on its lingual border and 14.9 mm on the labial one. The section of the root is irregularly elliptical with flattened sides and an anterior-posterior long axis; two shallow longitudinal grooves run on the mesial and distal sides of the root, the mesial one being a bit more pronounced.

When viewed from the side, the root is anteriorly convex and this convexity is in the continuity of that of the crown. So, the complete profile of the tooth, crown and root included, is generally convex. In labial or lingual views, the tip of the root is tilted distally.

3.2.2. Taxonomy

The Neandertal permanent maxillary lateral incisors exhibit a morphology which is very close to that of the permanent maxillary central incisors and allow them to be distinguished from anatomically modern humans (CRUMMETT, 1995; BAILEY, 2006^a): marked expression of lingual marginal ridges with associated shovel shape, labial convexity, developed lingual tubercle (*tuberculum dentale*), and superior-inferior convexity of the crown and root when viewed from the side (Table 5). Compared with the central incisors, the main differences are slightly smaller dimensions.

Both Scla 4A-14 and Scla 4A-17 present the typical features of Neandertal permanent maxillary lateral incisors.

3.2.3. Morphometric analysis

Measurements of the permanent maxillary lateral incisors are as follows:

Scla 4A-14, RI²

- MD diameter: 8.21 mm
- BL diameter: 8.27 mm
- MD at the cervix: 5.70 mm
- BL at the cervix: 7.38 mm
- Length of the tooth: 24.55 mm

Scla 4A-17, LI²

- MD: 8.38 mm
- BL: 8.40 mm
- MD at the cervix: 5.96 mm
- BL at the cervix: 7.65 mm
- Length of the tooth: 24.45 mm

The MD and BL diameters of Scla 4A-14 and 4A-17 depart significantly from the average of the different comparison samples only in the case of modern humans, both in the case of the DP probabilistic distance and ECRA. In addition, the BL diameter also departs from UPMH (Table 6). The MD and BL diameters of the crown are also, in the bivariate graph of Figure 5, compared to the ellipses (95%) of Early and Late Neandertals as well as of MPMH, UPMH and MHSS. Scla 4A-14 and 4A-17 are situated in the area where EN, LN and MPMH ellipses overlap, just slightly outside the ellipse of UPMH and clearly outside that of modern humans (MHSS). These observations indicate that the size of the upper lateral incisors distinguish Neandertals and recent MHSS (Semal, 1988: 49); however, these dimensions do not provide clear taxonomic indications within fossil taxa (especially between EN, LN, MPMH)..

Permanent Maxillary Lateral Incisors	Modality	Non-Neandertal Archaics	Neandertals	Early Modern Afro-Asians	Early Modern Europeans	Scla 4A-17	Scla 4A-14
Lingual marginal ridges/shovelling	presence (grade 2 or above)	100%	100%	83.3%	43%	yes	yes
	strong expression (grade 4 or above)		81%			grade 4	grade 4
Lingual tubercles	presence	100%	96%	66.70%	0%	yes	yes
	strong expression		cusplike: 62%	0%	0%	cusplike grade >5	cusplike grade 6
Double shovelling	presence	100%	3.7%	0%	12.50%	no	no
	expression		weak				

Table 5: Distinctive anatomical features on permanent maxillary lateral incisors of Non-Neandertal Archaics, Neandertals, Early Modern Humans (after BAILEY, 2006^a) and Scla 4A-14 & 17.

Table 6: Scla 4A-14 & 17 (permanent maxillary right and left second incisors): MD and BL dimensions compared to those of Early and Late Neandertals as well as MPMH, UPMH and MHSS, with DP and ECRA.

Scladina		N	Diameter	Value			vs Scla 4A-14		vs Scla 4A-17	
I ²	Scla 4A-14		MD	8.21						
			BL	8.27						
	Scla 4A-17		MD	8.38						
			BL	8.4						
Comparison Samples	N	Diameter	Mean	Stand. Dev.	DP	ECRA	DP	ECRA		
LN left & right	22	MD	7.713	0.7448	0.512	0.321	0.381	0.431		
	29	BL	8.145	0.5669	0.827	0.108	0.656	0.220		
EN left & right	21	MD	8.242	0.5566	0.955	-0.028	0.807	0.119		
	21	BL	8.752	0.8600	0.581	-0.269	0.687	-0.196		
MPMH left & right	12	MD	7.841	0.6515	0.583	0.257	0.426	0.376		
	12	BL	7.516	0.5874	0.226	0.583	0.161	0.684		
UPMH left & right	28	MD	6.896	0.9547	0.180	0.671	0.132	0.758		
	31	BL	6.851	0.5265	0.011	1.320	0.006	1.441		
MHSS	88	MD	6.302	0.652	0.004	1.472	0.002	1.603		
	88	BL	6.027	0.477	0.000	2.366	0.000	2.503		

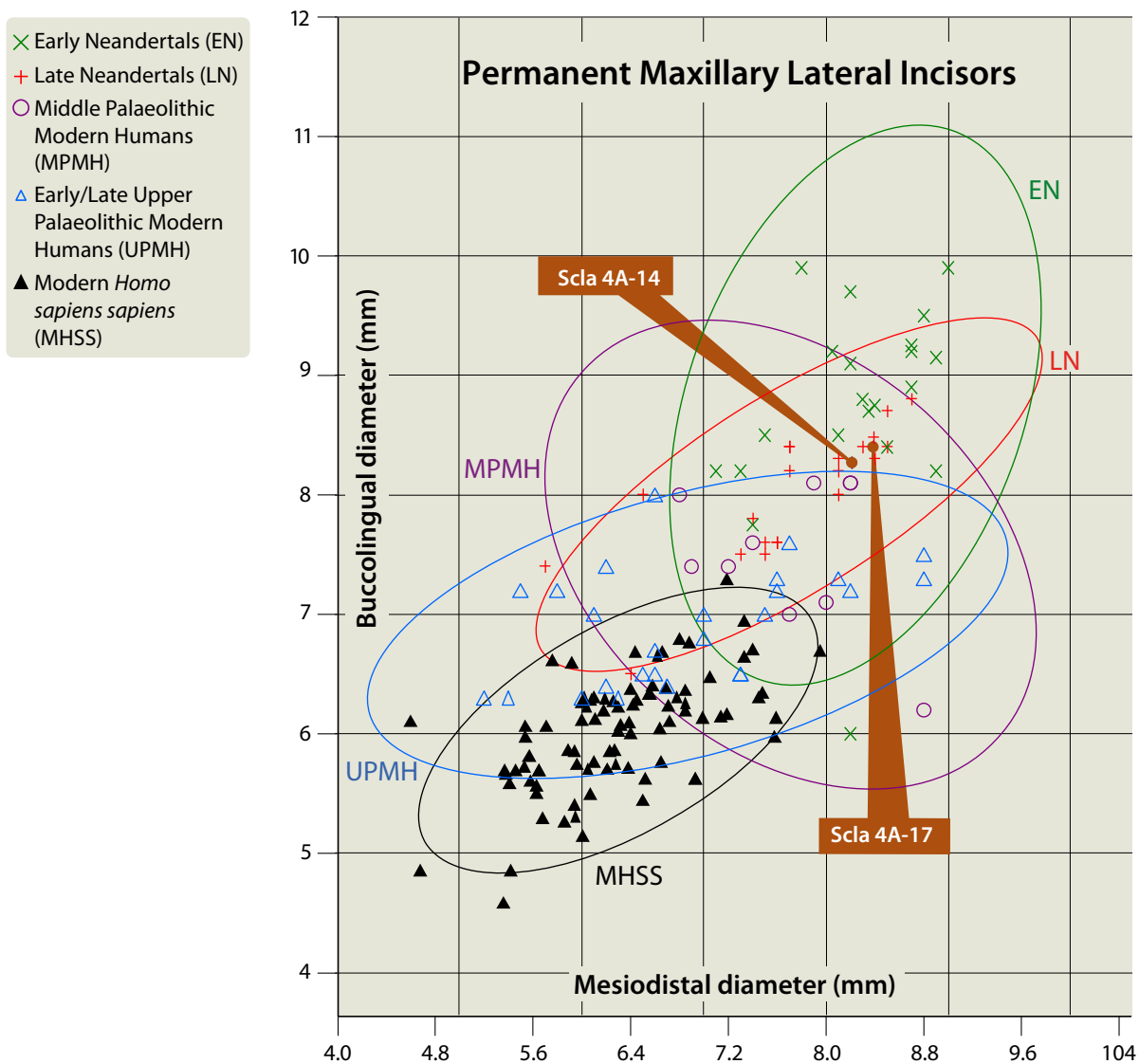


Figure 5: Bivariate analysis of the mesiodistal and buccolingual diameters of permanent maxillary lateral incisors with 95% equiprobable ellipses of EN, LN, MPMH, UPMH & MHSS as well as the position of Scla 4A-14 & 17.



3.3. Permanent mandibular right central incisor, RI₁

Field identification: Sc 1990-37-25

Palaeoanthropological identification: Scla 4A-15

Date of discovery: 22 February 1990

Date of identification: 14 December 2004

Square: H27

Stratigraphic position:

- **Former stratigraphy:** 4A
- **New stratigraphy:** units 4A POC or 3-INF (units 4A-IP, 4A-CHE, 3-SUP)

3.3.1. Description (Figure 6)

This permanent mandibular right central incisor was first identified as a lateral incisor. However, the discovery in 2006 of another right mandibular incisor, Scla 4A-20, larger than Scla 4A-15, led us to realize that Scla 4A-15 was in fact a central incisor (see Table 2).

This tooth fits well in the corresponding tooth socket of the Scla 4A-1 mandibular fragment, found in Square D29, former Layer 4A, at a distance of nearly 5 m.

The crown and root of this incisor are completely formed. The crown exhibits numerous vertical cracks, but also some oblique ones. The root has some vertical cracks too. No pathological conditions have been noted.

The incisal rim of the crown exhibits minor occlusal wear which has produced a transversal occlusal narrow strip, but without dentine exposure (grade 2 of MOLNAR, 1971, tending towards grade 3). The incisal plane of wear slightly slants mesiodistally, as well as slightly lingually. No mamelons are still present. The tooth was clearly in functional occlusion.

Both mesial and distal marginal ridges are very weakly expressed, mainly on the upper half of the lingual surface. The lingual surface of the crown is not strongly shovel-shaped (ASUDA, grade 2). The cingulum is moderately expressed and lacking a free apex. It blends into a median ridge which is weakly developed. A weak interruption groove separates the cingulum from the distal edge of the crown.

The height of the crown is 9.2 mm on the lingual face while the total length of the tooth is 22.15 mm.

One third of the way down from the occlusal surface the labial face exhibits a moderate degree of transversal convexity, as in ASUDAS, grade

3. In mesial view, this labial face is convex in its third portion that is close the cervix, then becomes nearly flat in the direction of the incisal edge. In anterior view, the labial surface is smooth, without double-shovelling. Both lateral sides diverge from the cervix. The angle between incisal edge and mesial edge is sharp, while the angle between incisal edge and distal edge is nearly right.

The two interproximal wear facets of Scla 4A-15 are well marked. Both are vertically orientated and nearly flat.

On the mesial and distal faces, the enamel line dips inferiorly, forming a V-shape with its tip pointing towards the incisal rim. As usual, this V convexity is better marked on the mesial face than on the distal one.

The root is mesiodistally compressed, with its labial component slightly broader than the lingual one, forming an elliptical cross-section. There are wide and shallow longitudinal developmental grooves on both the mesial and distal faces. When viewed from the side, the labial root outline is slightly convex from cervix to apex. The upper two thirds of the lingual outline are vertical and the lower third is strongly convex. The apex is fully closed. In lingual and labial views, the root is gently inclined distally, except for the tip of the apex which is inclined mesially. The length of the root is 13.5 mm.

3.3.2. Taxonomy

Neandertal mandibular central incisors tend to be unremarkable and are therefore not very useful to establish taxonomical relationships (BAILEY, 2006^a). Indeed, they exhibit a combination of features also present in other Non-Neandertal Archaics (BAILEY, 2006^a; BAILEY & HUBLIN, 2006): trace to moderate shovelling, median ridge moderately or strongly developed, and occasionally a cingulum shelf. In addition, the Neandertal mandibular incisor crowns, relative to the crowns of their posterior teeth, seem to be significantly larger than those of Early Modern Humans (STEFAN & TRINKAUS, 1998). It has also been suggested that Neandertals have significantly longer mandibular incisor roots relatively to Early Modern Europeans (BAILEY, 2006^b, but see Chapter 16 for a critical discussion of this aspect).

The Scladina Scla 4A-15 first right mandibular incisor possesses the features of a Neandertal mandibular incisor.

Permanent Mandibular Right Central Incisor Scla 4A-15

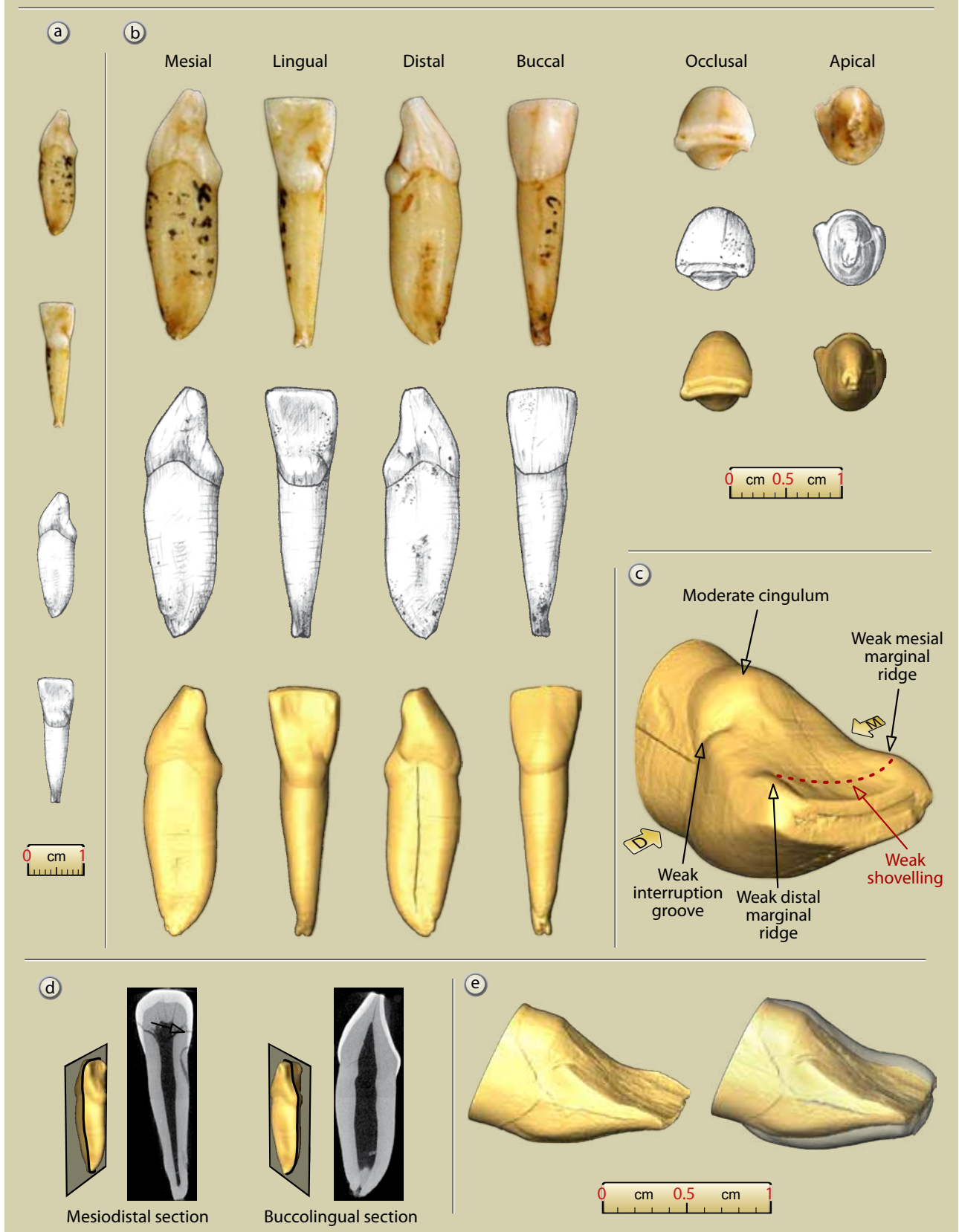


Figure 6: Scla 4A-15 permanent mandibular right central incisor: a. mesial and lingual views (1:1 scale); b. photographs, drawings and 3D reconstructions of the six faces of the incisor (2:1 scale) c. 3D reconstruction with main anatomical features; d. internal sections; e. 3D lingual views at the EDJ without and with enamel (micro-CT data processing and graphics J.-F. Lemaire, SPW; pencil drawings S. Lambermont, AWEM; photographs J. Eloy, AWEM).



3.3.3. Morphometric analysis

Measurements of Scla 4A-15 are as follows:

- MD: 6.27 mm
- BL: 6.79 mm
- MD at the cervix: 4.30 mm
- BL at the cervix: 6.21
- Length of the tooth: 22.08 mm

The MD diameter of Scla 4A-15 departs significantly from the average of the different comparison samples only in the case of modern humans (MHSS), both in the case of the DP probabilistic distance and ECRA. The same applies for the BL diameter (Table 7). In addition, MD and BL diameters of the crown are, in the bivariate graph of Figure 7, compared to the ellipses (95%) of Early and Late Neandertals as well as of UPMH

Scladina	Diameter	Value
Rl ₁ (Scla 4A-15)	MD	6.27
	BL	6.79

Comparison Samples	N	Diameter	Mean	Stand. Dev.	DP	ECRA
EN right & left	16	MD	5.759	0.446	0.270	0.537
	16	BL	7.619	0.405	0.059	-0.960
LN right & left	23	MD	5.500	0.462	0.110	0.804
	25	BL	7.112	0.406	0.436	-0.384
MPMH right & left	6	MD	5.717	0.941	0.582	0.229
	9	BL	6.878	0.429	0.843	-0.089
UPMH right & left	27	MD	4.997	0.916	0.176	0.676
	28	BL	6.216	0.482	0.244	0.581
MHSS right & left	94	MD	5.058	0.392	0.003	1.556
	94	BL	5.712	0.372	0.005	1.460

Table 7: Scla 4A-15 (permanent mandibular right central incisor): MD and BL dimensions compared to those of Early and Late Neandertals as well as MPMH, UPMH and MHSS, with DP and ECRA.

- × Early Neandertals (EN)
- + Late Neandertals (LN)
- Middle Palaeolithic Modern Humans (MPMH)
- △ Early/Late Upper Palaeolithic Modern Humans (UPMH)
- ▲ Modern *Homo sapiens sapiens* (MHSS)

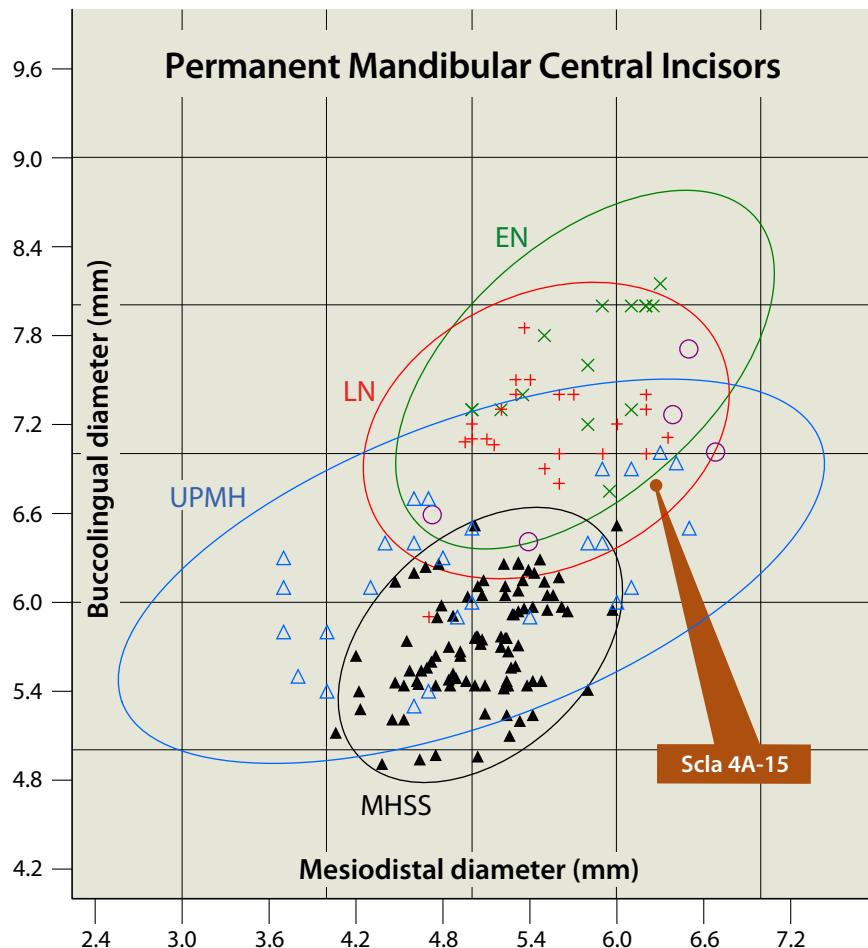


Figure 7: Bivariate analysis of the mesiodistal and buccolingual diameters of permanent mandibular central incisors with 95% equiprobable ellipses of EN, LN, UPMH & MHSS as well as the position of some MPMH and Scla 4A-15.

and MHSS. Scla 4A-15 is situated in the area where EN, LN and UPMH ellipses (95%) overlap, however close the upper limit of the MD diameter. Scla 4A-15 is clearly outside the 95% ellipse of modern humans. As for the permanent maxillary incisors, this indicates that the dimensions of the crown of the mandibular central incisor do not always provide many clear taxonomic indications as far as fossil taxa are concerned.

3.4. Permanent mandibular lateral incisors, I_2

3.4.1. Description

Permanent mandibular right lateral incisor, RI_2 (Figure 8)

Palaeoanthropological identification: Scla 4A-20

Field identification: Sc 2006-81-1

Date of discovery: 12 July 2006

Date of identification: 12 July 2006

Square: F35-F37

Stratigraphic position:

- **Former stratigraphy:** unknown (collapse of a sedimentary profile)
- **New stratigraphy:** units 4A-POC or 3-INF (Unit 3-SUP)

This permanent tooth was found isolated in collapsed sediments after a section fell down during the night of 26–27 April 2006 in squares F35 to F37. Only later, on July 12, during the sieving of these sediments, the tooth was recognized as human and identified. According to the morphology of the area of collapse, where badger dens cross-cut portions of the cave's sediment, it seems that it comes from the Sedimentary Complex 4A, possibly Unit 4A-POC (or maybe 3-INF; see Chapter 5 for more details).

This mandibular lateral incisor fits relatively well in the corresponding tooth socket of the Scla 4A-1 mandibular fragment, found in Square D29, former Layer 4A, at a distance between 6 and 9 m.

The crown is completely formed and fully occluded. The root apex was broken postmortem. The crown exhibits numerous vertical cracks, but also some oblique ones. No pathological conditions have been noted.

The incisal rim of the crown exhibits minor occlusal wear which has produced a transversal, occlusal, narrow strip, without dentine exposure (grade 2, according to MOLNAR, 1971). No mamelons are present. The tooth was in functional occlusion.

Both mesial and distal marginal ridges are moderately expressed, mainly on the upper half of the lingual face. There are traces of shovelling, as in ASUDAS UI1, grade 2. The cingulum is more developed than that of the I1 Scla 4A-15. It lacks a free apex, but blends into the central ridge which is weakly developed.

The height of the tubercle is 3.95 mm from the cervix, while the height of the crown is 9.20 mm on the lingual face.

At one third of the way down from the occlusal surface, the labial face is moderately and mesio-distally convex, as in ASUDAS, grade 3. In mesial view, this face also exhibits an irregular superior-inferior convexity, from the incisal edge to the cervical line. In anterior view, the labial surface is smooth, without double shovelling. Both lateral sides asymmetrically diverge from the cervix. The angle between incisal edge and mesial edge is sharp, while the angle between incisal edge and distal edge is much more rounded.

Interproximal wear facets for the adjacent teeth are present. Both are vertically elongated and nearly flat.

On the mesial and distal faces, the crown-root junction line is V-shaped with its tip pointing towards the incisal rim. This V-convexity is better marked on the mesial face.

The lingual length of the root is about 13.9 mm in its actual state of preservation, but as it is broken, a few millimetres has to be added to obtain the original length which was obviously over 15.0 mm (15.23 in Table 2a of Chapter 16). The root is mesio-distally compressed, with its labial component slightly broader than the lingual one. There are wide and shallow longitudinal developmental grooves on both mesial and distal faces. When viewed from the side, the anterior root outline is slightly convex from cervix to apex.

Permanent mandibular left lateral incisor, LI_2 (Figure 9)

Palaeoanthropological identification:

Scla 4A-19 (= Scla 3-4)

Field identification: Sc 1995-108-197-1

Date of discovery: 08 March 1995

Date of identification: 10 April 1995

Square: D34

Stratigraphic position:

- **Former stratigraphy:** 3, then 4A
- **New stratigraphy:** units 4A-POC or 3-INF (Unit 3-SUP)



Permanent Mandibular Right Lateral Incisor Scla 4A-20

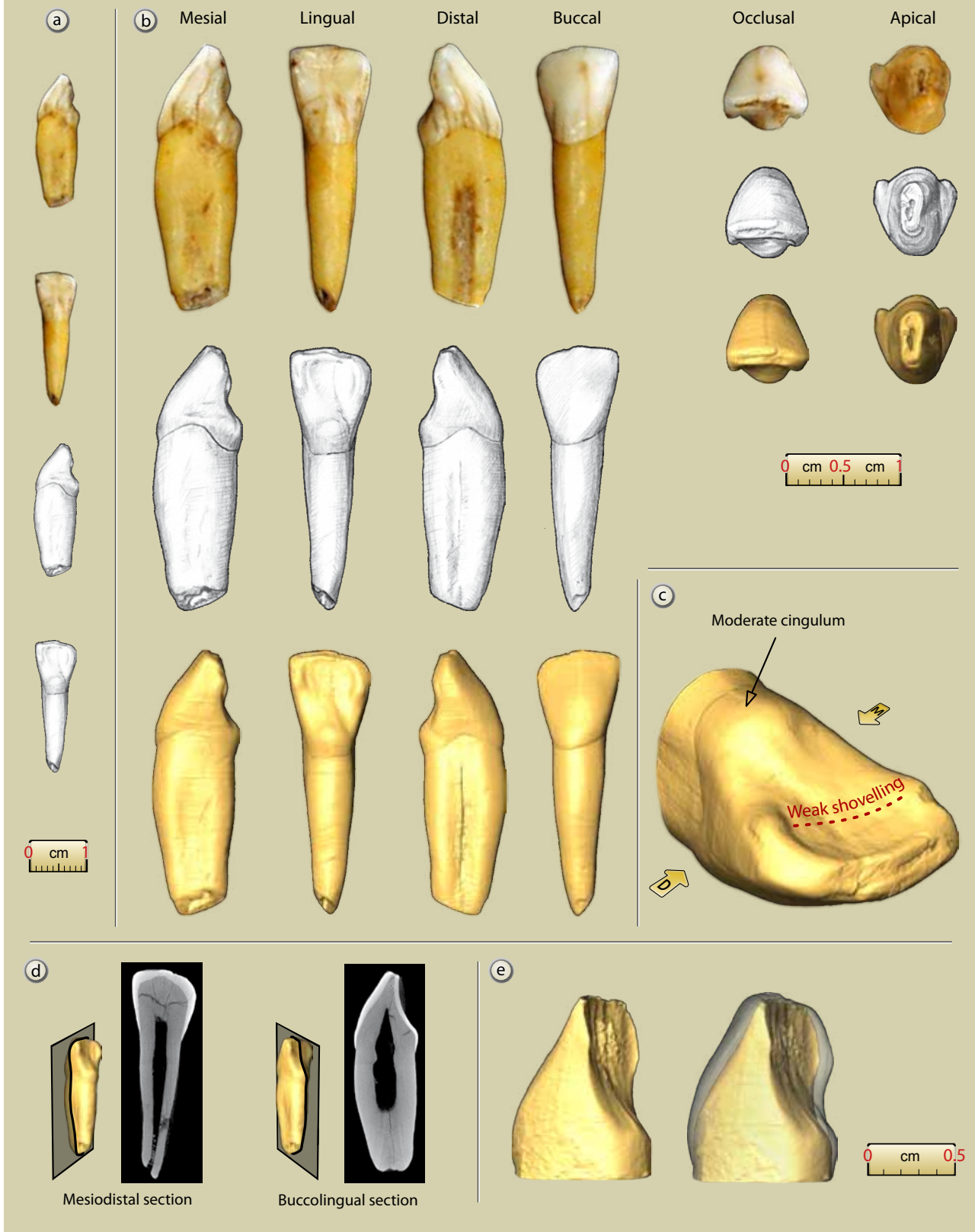


Figure 8: Scla 4A-20 permanent mandibular right lateral incisor: a. mesial and lingual views (1:1 scale); b. photographs, drawings and 3D reconstructions of the six faces of the incisor (2:1 scale); c. 3D reconstruction with main anatomical features; d. internal sections; e. 3D lingual views at the EDJ without and with enamel (micro-CT data processing and graphics J.-F. Lemaire, SPW; pencil drawings S. Lambermont, AWEM; photographs J. Eloy, AWEM).

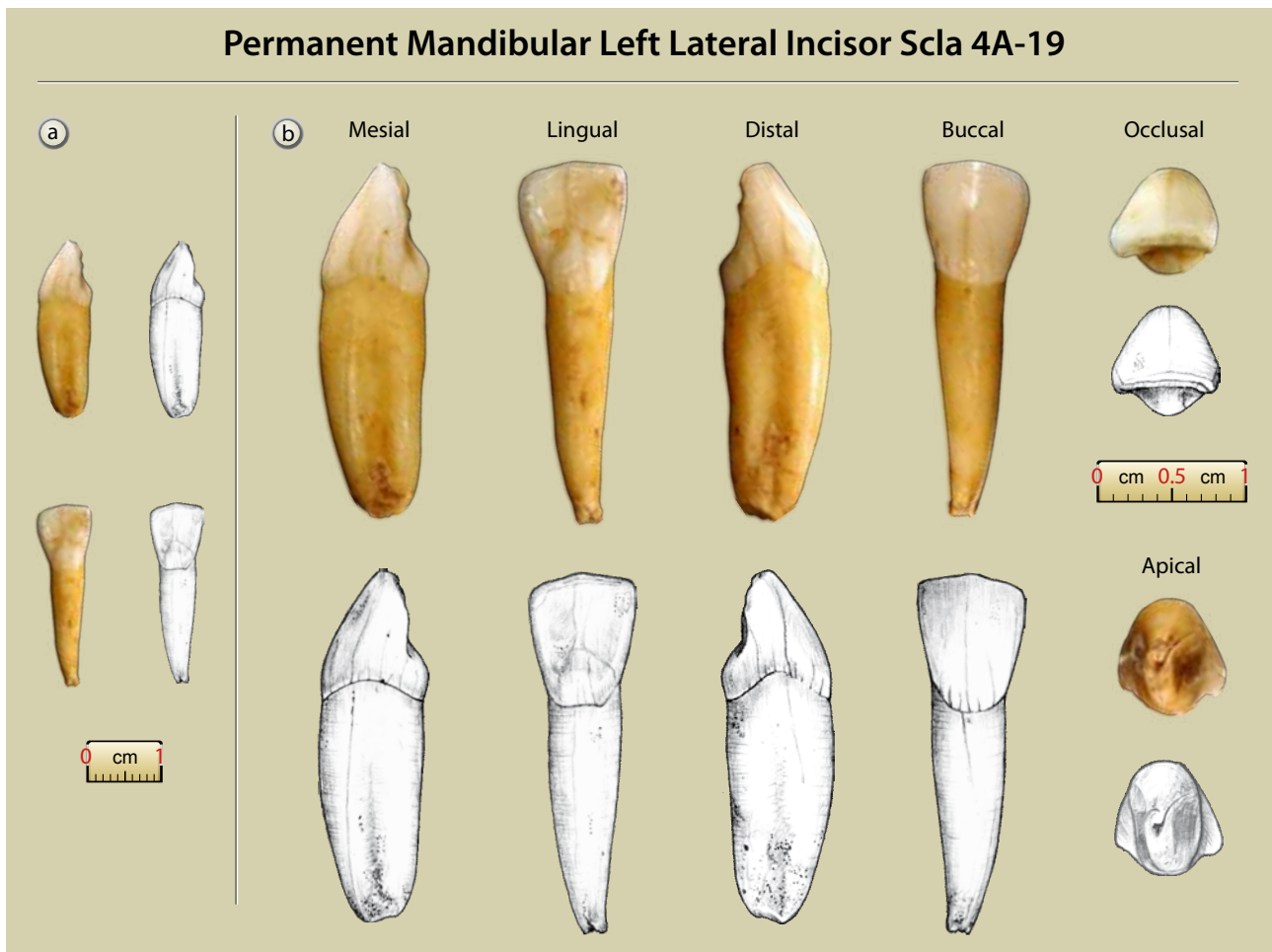


Figure 9: Scla 4A-19 permanent mandibular left lateral incisor: a. mesial and lingual views (1:1 scale); b. photographs and drawings of the six faces of the tooth (2:1 scale) (pencil drawings S. Lambermont, AWEM; photographs J. Eloy, AWEM).

This incisor fits relatively well in the corresponding tooth socket of the Scla 4A-9 mandibular fragment, found in Square C28, at a distance of over 6 m.

The crown is completely formed and fully occluded. The root apex is slightly damaged. The crown and root exhibit some cracks, mainly vertical. No pathological conditions have been noted.

The incisal rim of the crown exhibits minor occlusal wear which produced a transversal narrow strip, with very little dentine exposure (grade 2, according to MOLNAR, 1971). No mamelons are present. The tooth was in functional occlusion.

Both mesial and distal marginal ridges are moderately expressed and mainly on the upper half of the lingual face. There are small traces of shovelling, slightly less than in Scla 4A-20 (ASUDAS UI1, grade 1). The cingulum lacks a free apex, but blends into the central ridge which is weakly developed.

The height of the tubercle is 4.1 mm from the cervix, while the height of the crown is 9.03 mm on the lingual face.

One third of the way down from the occlusal surface the labial face is moderately and mesio-distally convex, as in ASUDAS, grade 3. In mesial view, this face also exhibits an irregular superior-inferior convexity, from the incisal edge to the cervical line. In anterior view, the labial surface is smooth, without double shovelling. Both lateral sides asymmetrically diverge from the cervix. The angle between the incisal and mesial edges is sharp, while the angle between the incisal and distal edges is nearly right but rounded.

An interproximal wear facet for the adjacent left central incisor is present. It is vertically elongated and nearly flat.

On the mesial and distal faces the crown-root junction line is V-shaped with its tip pointing towards the incisal rim. This V-convexity is better marked on the mesial face.



The lingual length of the root is about 15.0 mm. The root is mesiodistally compressed with its labial component slightly broader than the lingual one. There are wide and shallow longitudinal developmental grooves on both the mesial and distal faces. When viewed from the side, the anterior root outline is slightly convex from the cervix to the apex.

3.4.2. Taxonomy

Neandertal mandibular lateral incisors, like the central ones, are not very useful to establish taxonomical relationships (BAILEY, 2006^a). They exhibit a combination of features also present in other Non-Neandertal Archaics (BAILEY, 2006^a ; BAILEY & HUBLIN, 2006): trace to moderate shovelling, median ridge moderately or strongly developed, and occasionally a cingulum shelf. They also appear to be distinctive in their relative size, being significantly larger relatively to the posterior teeth than those of Early Modern Humans.

The two Scladina second mandibular incisors exhibit these features.

3.4.3. Morphometric analysis

Measurements of the permanent mandibular lateral incisors are as follows:

Scla 4A-20, RI₂

- MD: 7.03 mm
- BL: 7.28 mm
- MD at the cervix: 4.50 mm
- BL at the cervix: 6.79 mm
- Length of the tooth in its actual state of preservation: 22.63 mm

Scla 4A-19, LI₂

- MD: 7.20 mm
- BL: 7.35 mm
- MD at the cervix: 4.67 mm
- BL at the cervix: 6.89 mm
- Length of the tooth: 23.72 mm

The MD and BL diameters of Scla 4A-19 and 4A-20 only depart significantly from the average of the different comparison samples in the case of modern humans, both in the case of the DP probabilistic distance and ECRA (Table 8). In addition, the MD and BL diameters of the two crowns are, in Figure 10, compared to the ellipses (95%) of Early and Late Neandertals as well as of MPMH, UPMH and MHSS. Both Scla 4A-19 & 20 are situated in the area where EN, LN, MPMH and UPMH ellipses (95%) overlap. They are outside the 95% ellipse of modern humans. As for the other permanent maxillary and mandibular incisors, this indicates that the dimensions of the crown of the permanent mandibular lateral incisor provide only limited taxonomic indications.

3.5. Permanent maxillary canines, C³

3.5.1. Description

Permanent maxillary right canine, RC³ (Figure 11)

- Palaeoanthropological identification:** Scla 4A-16
- Field identification:** Sc 1990-49-1
- Date of discovery:** 23 February 1990
- Date of identification:** 16 December 2004
- Square:** H27
- Stratigraphic position:**
 - Former stratigraphy: 4A

Scladina	N	Diameter	Value
I ₂	Scla 4A-19	MD	7.2
		BL	7.35
	Scla 4A-20	MD	7.03
		BL	7.28

Table 8: Scla 4A-19 & 20 (permanent mandibular left and right lateral incisors): MD and BL dimensions compared to those of Early and Late Neandertals as well as MPMH, UPMH and MHSS, with DP and ECRA.

Comparison Samples	N	Diameter	Mean	Stand. Dev.	vs Scla 4A-19		vs Scla 4A-20	
					DP	ECRA	DP	ECRA
EN right & left	21	MD	6.702	0.572	0.394	0.417	0.573	0.275
	21	BL	7.986	0.472	0.193	-0.646	0.150	-0.717
LN right & left	28	MD	6.454	0.485	0.136	0.749	0.246	0.578
	34	BL	7.705	0.527	0.505	-0.331	0.426	-0.396
MPMH right & left	12	MD	6.617	0.598	0.350	0.443	0.504	0.314
	10	BL	7.400	0.693	0.944	-0.032	0.866	-0.077
UPMH right & left	29	MD	5.956	0.813	0.137	0.747	0.197	0.645
	31	BL	6.799	0.491	0.271	0.549	0.335	0.480
MHSS right & left	102	MD	5.692	0.425	0.001	1.790	0.002	1.588
	102	BL	6.113	0.385	0.002	1.618	0.003	1.526

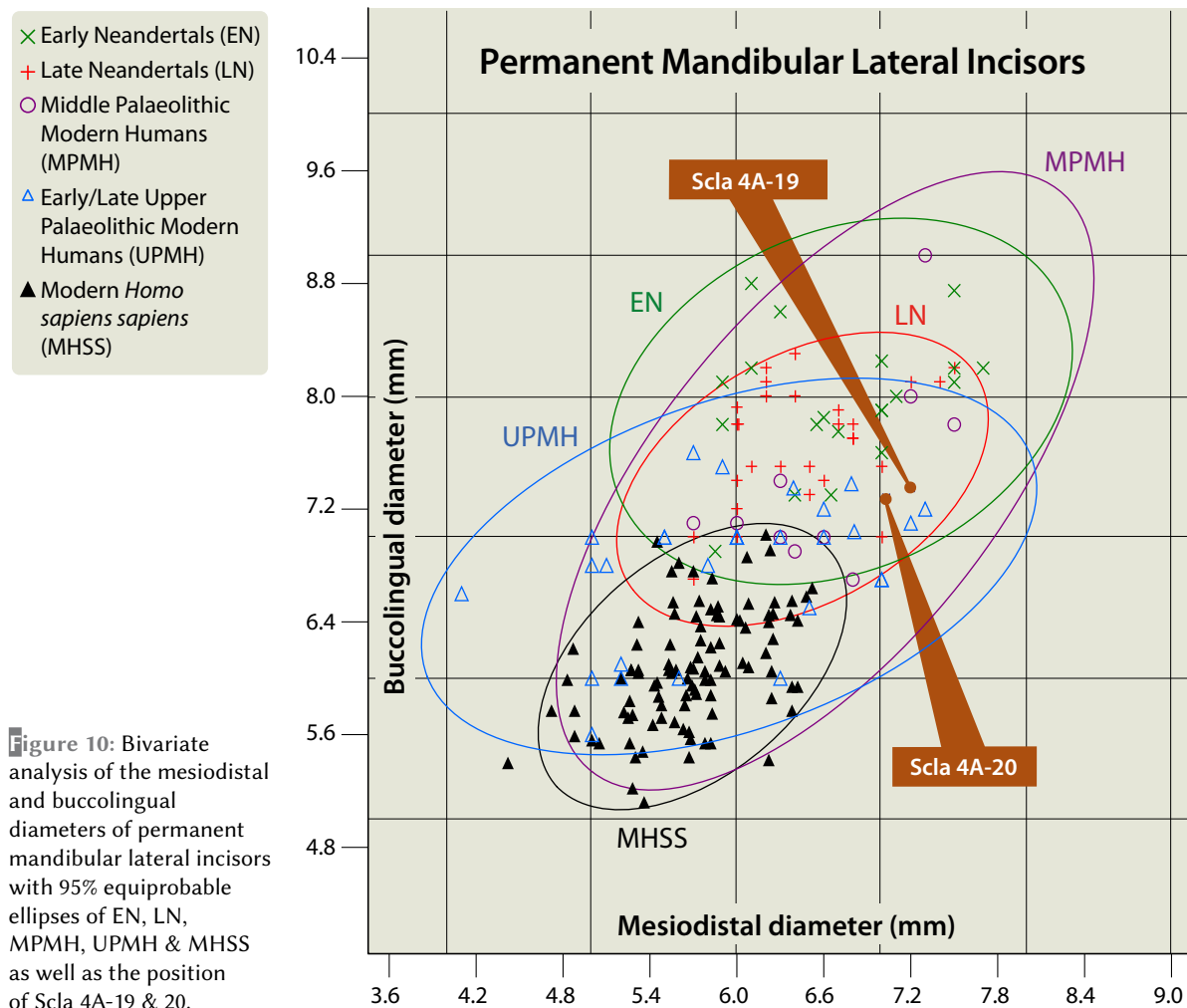


Figure 10: Bivariate analysis of the mesiodistal and buccolingual diameters of permanent mandibular lateral incisors with 95% equiprobable ellipses of EN, LN, MPMH, UPMH & MHSS as well as the position of Scla 4A-19 & 20.

— **New stratigraphy:** Unit 4A-POC
(units 4A-IP, 4A-CHE, 3-INF)

The tooth is in good condition. The tip of the apex is slightly open (1.9×1.2 mm), so the root is not fully formed. As usual with Scladina teeth, this fossil exhibits cracks on the crown, mainly vertical ones. It fits well in the corresponding socket of the Scla 4A-2 right maxilla, found in Square D30, former Layer 4A, at a distance over 4 m. No pathological conditions have been noted.

The incisal edge and its main cusp are mostly unworn, with a very superficial and small wear facet on its tip (MOLNAR, 1971, stage 2, but very close to 1).

On the buccal surface, some very weak double shovelling can be seen in contrasting light, especially on the distal side of the crown (grade 1 of ASUDAS). Occlusally viewed, the labial face is, mesiodistally, strongly convex, more than in ASUDAS UI1, grade 4. When viewed from the

mesial and distal sides this face also exhibits an irregular superoinferior convexity, from the cervical line to the incisal edge, though the convexity is much stronger near the cervix, as is also the case for the permanent maxillary incisors.

In buccal and lingual views, the crown is asymmetrical; it is divergent in its cervical half; in its lower half, the mesial part of the incisal edge is rounded while the distal edge is mesially oblique but nearly straight.

The mesial and distal marginal ridges are well expressed. Therefore, traces of shovelling are clear (grade 2 of ASUDAS). The canine mesial ridge does not form a Bushmen canine.

There is a quite prominent lingual tubercle (*tuberculum dentale*). In its lower half, it is divided into two parts by a vertical groove. The mesial part forms a separate cusplet with a small but distinct free apex (smaller but close to DAR UC grade 5). The distal part goes down to the lingual surface, forming a *tuberculum* extension (medial ridge).



Permanent Maxillary Right Canine Scla 4A-16

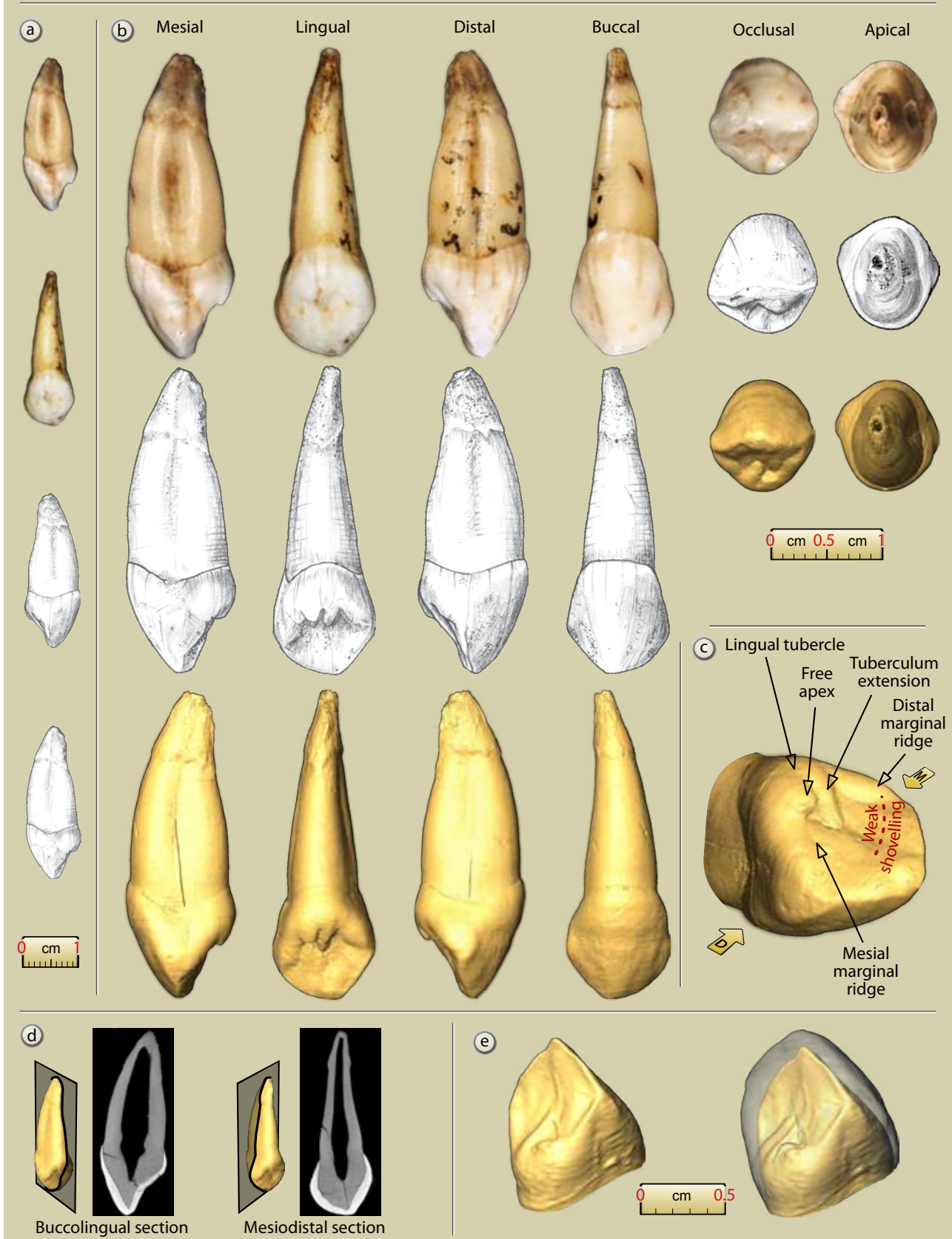


Figure 11: Scla 4A-16 permanent maxillary right canine: a. mesial and lingual views (1:1 scale); b. photographs, drawings and 3D reconstructions of the six faces of the tooth (2:1 scale); c. 3D reconstruction with main anatomical features; d. internal sections; e. 3D lingual views at the EDJ without and with enamel (micro-CT data processing and graphics J.-F. Lemaire, SPW; pencil drawings S. Lambermont, AWEM; photographs J. Eloy, AWEM).

On both sides, the lingual tubercle is distinct from the marginal ridges but without marked grooves.

No distal accessory ridge is present.

On the mesial and distal faces, the enamel line dips inferiorly, forming a rounded V-shape with its tip in the direction of the incisal rim; the incisal curve of the cervical margin is deeper on the mesial face than on the distal one.

There is a rounded interproximal wear facet for the adjacent permanent maxillary lateral incisor that is extremely faint and small, but no distal interproximal wear facet.

The root is mesiodistally compressed and ovoid in its transverse section, and broader labially. It has well marked mesial and distal longitudinal grooves. There is a rough thickening of the apical part of the root surface. In mesial or distal view, the anterior border of the root is convex, as is also the crown; so, the profile of the tooth, crown and root included, is generally convex. The length of the root, measured from the lingual aspect, is 17.1 mm. As the tip of the apex is not completely formed, at least 0.5 mm should be added in order to obtain the fully developed root length.

*Permanent maxillary left canine,
LC' (Figure 12)*

Palaeoanthropological identification:

Scla 4A-18 (Scla 3.3)

Field identification: Sc 1991-590-1

Date of discovery: 19 November 1991

Date of identification: October 1993

Square: F26

Stratigraphic position:

- **Former stratigraphy:** 3, then 4A
- **New stratigraphy:** Unit 4A-POC (units 4A-IP, 4A-CHE, 3-INF)

The tooth is in good condition. The tip of the apex is still slightly open (2×1.4 mm), so the root is not fully formed. The fossil exhibits cracks on the crown and root, in particular, a strong vertical one on the buccal side, but also oblique and sub-horizontal ones. No pathological conditions have been noted.

The morphology of this permanent maxillary left canine is quite similar to that of its antimere, Scla 4A-16.

The incisal edge and its central cusp are mostly unworn. In contrasting light, some very weak double shovelling can be seen on the distal side of the crown (grade 1 of ASUDAS).

The labial face is mesiodistally (over ASUDAS UI1, grade 4) and superoinferiorly (mainly near the cervix) strongly convex.

In buccal and lingual views, the outline of the crown is slightly narrower than that of its antimere and even looks slightly more asymmetrical; it is divergent in its upper half while in its lower half, the mesial part of the incisal edge is more rounded. The mesial and distal marginal ridges are well expressed, with clear traces of shovelling (grade 2 of ASUDAS). The lingual tubercle, divided in two in its lower part, exhibits a separate cusplet in its mesial part (Dar UC grade 4-5) while its distal part goes down to the lingual surface, forming a *tuberculum* extension (medial ridge).

No distal accessory ridge is present. There are no interproximal wear facets for the adjacent teeth.

As its antimere, the root is mesiodistally compressed and ovoid in its transverse section, and broader labially. It has well marked mesial and distal longitudinal grooves. There is also a rough thickening of the apical part of the root surface. In mesial or distal view, the anterior border of the root is convex, as is also the crown; so, the profile of the tooth, crown and root included, is generally convex. The length of the root, measured from the lingual aspect, is 17.5 mm. As the tip of the apex is not completely formed, at least 0.5 mm should be added in order to estimate the fully developed root length.

3.5.2. Taxonomy

Neandertal permanent maxillary canines are usually quite robust. They tend to reflect the lingual morphology of the permanent maxillary incisors, especially in the lingual surface of the crown (BAILEY, 2006^a). Their main features are (Table 9):

- moderate to strong convexity in both mesiodistal and inferosuperior directions;
- trace of shovelling (at least grade 2 of ASUDAS) or semi shovelling (grade 3) are extremely frequent (96%);
- high frequency (84%) of lingual tubercle, sometimes strongly developed;
- moderately high frequency (two thirds) of distal accessory ridge;
- presence of Bushmen canine (43%);
- a third of the permanent maxillary canines exhibit double shovelling, but only weakly (grade 1).



Permanent Maxillary Left Canine Scla 4A-18

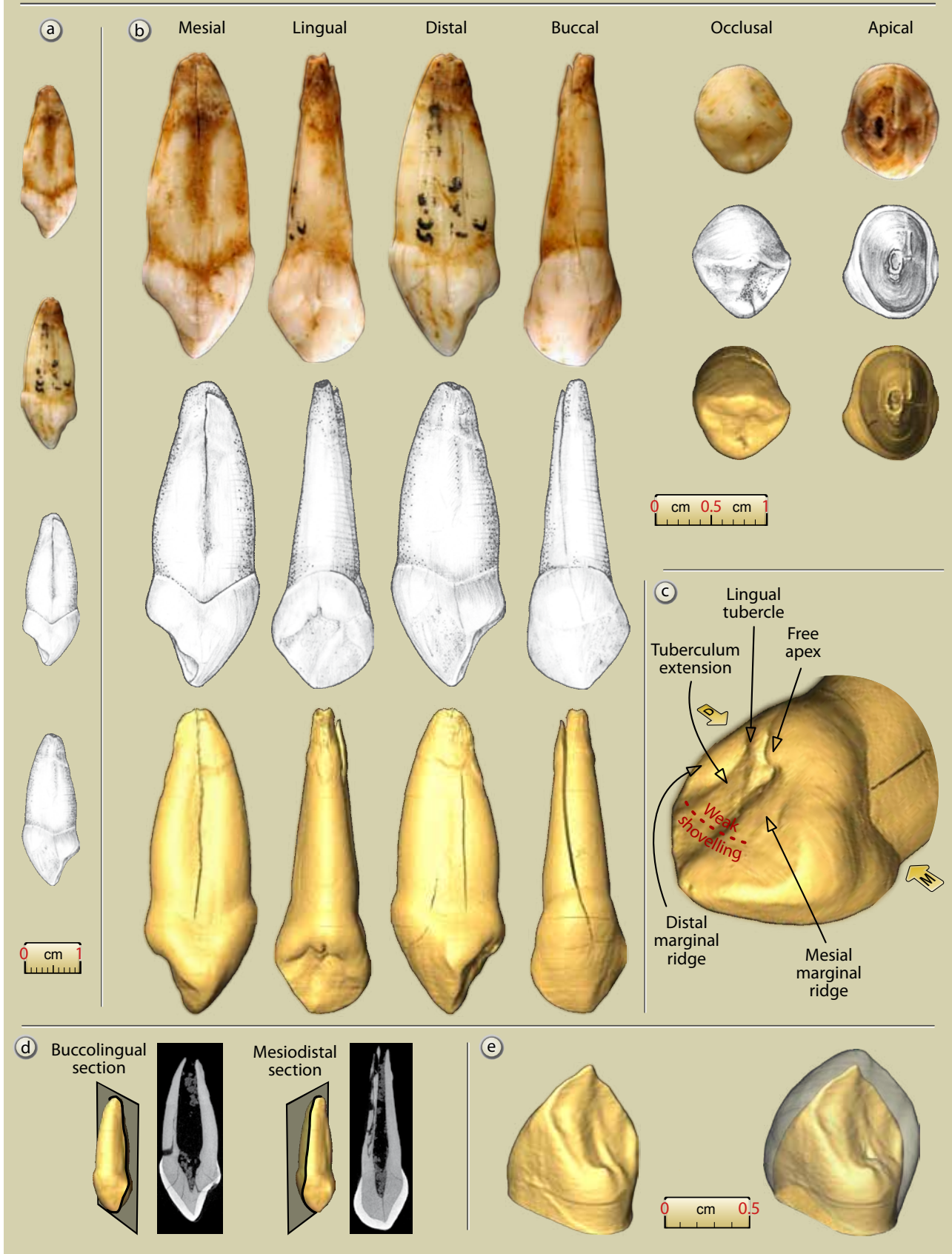


Figure 12: Scla 4A-18 permanent maxillary left canine: a. mesial and distal views (1:1 scale); b. photographs, drawings and 3D reconstructions of the six faces of the tooth (2:1 scale); c. 3D reconstruction with main anatomical features; d. internal sections; e. 3D lingual views at the EDJ without and with enamel (micro-CT data processing and graphics J.-F. Lemaire, SPW; pencil drawings S. Lambermont, AWEM; photographs J. Eloy, AWEM).

Permanent Maxillary Canines	Modality	Non-Neandertal Archaics	Neandertals	Early Modern Afro-Asians	Early Modern Europeans	Scla 4A-16	Scla 4A-18
Lingual marginal ridges/showelling	presence (grade 2 or above)	100%	95.8%	100%	50%	yes	yes
	expression		42% (grade 3 or above)	max grade 2	max grade 2	grade 2	grade 2
Double shovelling	presence	0%	0–33.0%	12.5%	12.5%	yes	yes
	expression		grade 1	grade 1	(grade 1)	grade 1	grade 1
Lingual tubercles(s)	presence	100%	84%	20%	50%	yes	yes
	strong expression (tubercle form > grade 4)		32%	relatively weak	relatively weak	grade 5	grade 4–5
Canine mesial ridge (Bushman canine)	presence	—	42.9%	0%	14.3%	no	no
Distal accessory ridge	presence	—	66.7%	100%	100%	no	no
	large expression (> grade 3)		20%	50%	50%		

Table 9: Distinctive anatomical features on permanent maxillary canines of Non-Neandertal Archaics, Neandertals, Early Modern Humans (after BAILEY, 2006*) and Scla 4A-16 & 18.

Both maxillary canines from Scladina exhibit most of these features: convexity in both inferosuperior and mesiodistal directions, trace of shovelling, weak double shovelling and developed lingual tubercle. Conversely, neither distal accessory ridge nor Bushmen canine are present.

3.5.3. Morphometric analysis

Measurements of the permanent maxillary canines are as follows:

Scla 4A-16, RC'

- MD: 9.05 mm
- BL: 9.65 mm
- MD at the cervix: 6.16 mm
- BL at the cervix: 8.67 mm
- Length of the tooth: 27.31 mm

Scla 4A-18, LC'

- MD: 8.60 mm
- BL: 9.95 mm
- MD at the cervix: 6.10 mm
- BL at the cervix: 9.02 mm
- Length of the tooth: 27.30 mm

The MD and BL diameters of Scla 4A-16 and 18 depart significantly from the average of the recent humans (MHSS), both in regard to the DP probabilistic distance and ECRA. Also, the MD diameter of Scla 4A-16 departs significantly from the average of the UPMH comparative sample (Table 10). The MD and BL diameters of the Scla 4A-16 and 18 permanent maxillary canine crowns are, in Figure 13, compared to the ellipses (95%) of Early and Late Neandertals as well as of MPMH, UPMH, and MHSS. Both Scla 4A-16 and 18 are situated in

Scladina	N	Diameter	Value
C'	Scla 4A-16	MD	9.05
		BL	9.65
	Scla 4A-18	MD	8.6
		BL	9.95

Comparison Samples	N	Diameter	Mean	Stand. Dev.	vs Scla 4A-16		vs Scla 4A-18	
					DP	ECRA	DP	ECRA
EN right & left	22	MD	8.716	0.870	0.705	0.185	0.895	-0.064
	24	BL	10.035	0.743	0.609	-0.251	0.909	-0.056
LN right & left	24	MD	8.169	0.713	0.229	0.597	0.552	0.292
	29	BL	9.551	0.729	0.893	0.066	0.588	0.267
MPMH right & left	14	MD	8.643	0.573	0.490	0.329	0.942	-0.035
	13	BL	9.315	0.749	0.663	0.205	0.414	0.389
UPMH right & left	36	MD	7.886	0.457	0.016	1.253	0.128	0.769
	33	BL	8.827	0.822	0.324	0.492	0.181	0.671
MHSS right & left	91	MD	7.299	0.468	0.000	1.882	0.007	1.399
	92	BL	7.898	0.637	0.007	1.385	0.002	1.622

Table 10: Scla 4A-16 & 18 (permanent maxillary canines): MD and BL dimensions compared to those of Early and Late Neandertals as well as MPMH, UPMH and MHSS, with DP and ECRA.



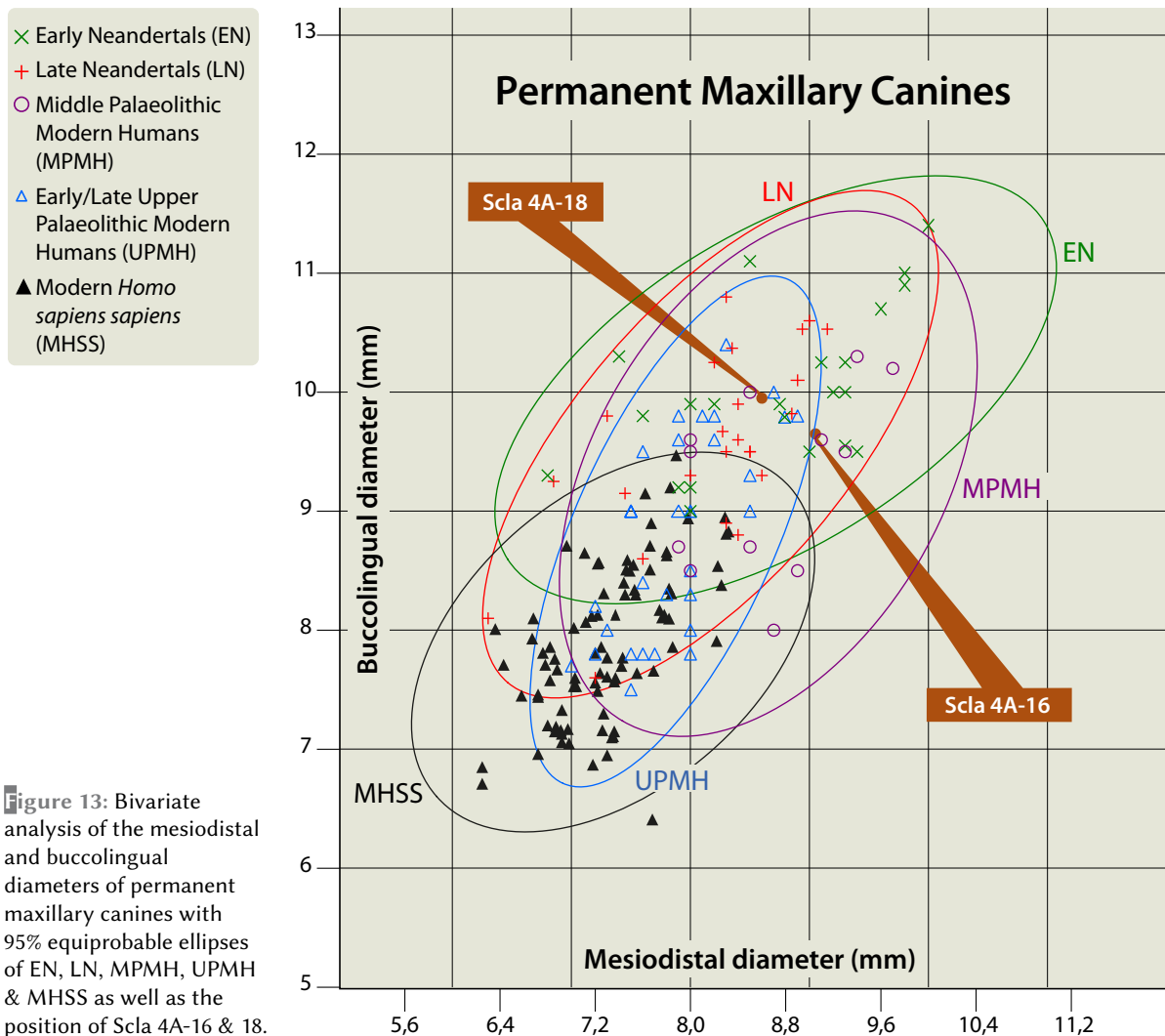


Figure 13: Bivariate analysis of the mesiodistal and buccolingual diameters of permanent maxillary canines with 95% equiprobable ellipses of EN, LN, MPMH, UPMH & MHSS as well as the position of Scla 4A-16 & 18.

the area where EN, LN, MPMH and UPMH ellipses overlap. They are outside the ellipse of modern humans. Like for most other permanent anterior teeth, this indicates that the dimensions of the permanent maxillary canine crowns often allow to separate fossils from MHSS but do not provide clear taxonomic indications within fossil taxa.

3.6. Permanent mandibular right canine, RC,

- Palaeoanthropological identification:** Scla 4A-12
- Field identification:** Sc 1990-90-1
- Date of discovery:** 28 March 1990
- Date of identification:** July 2001
- Square:** F27
- Stratigraphic position:**
 - **Former stratigraphy:** 4A
 - **New stratigraphy:** units 4A-POC or 3-INF (units 4A-IP, 4A-CHE, 3-SUP)

3.6.1. Description (Figure 14)

The specimen is very well preserved. The root is complete with the tip of the apex still very slightly open (1.1 mm). It exhibits some cracks on the crown and root, mainly vertical ones. No pathological conditions have been noted. It fits well in the corresponding socket divided between Scla 4A-1 (right part of the mandible) and Scla 4A-9 (left part). Scla 4A-1 was found in Square D29 at a distance of over 2 m from the tooth, and Scla 4A-9 was found in Square C28, at a distance over 2 m.

The central cusp and the incisal edge are slightly worn. There is a very small wear facet present on the tip and a transversely elongated but narrow wear facet on the mesial part of the incisal edge (MOLNAR, 1971, stage 2).

When viewed from the occlusal aspect, the buccal face is mesiodistally strongly convex (over ASUDAS, grade 4). When viewed from the mesial and distal sides, that face also exhibits a

Permanent Mandibular Right Canine Scla 4A-12

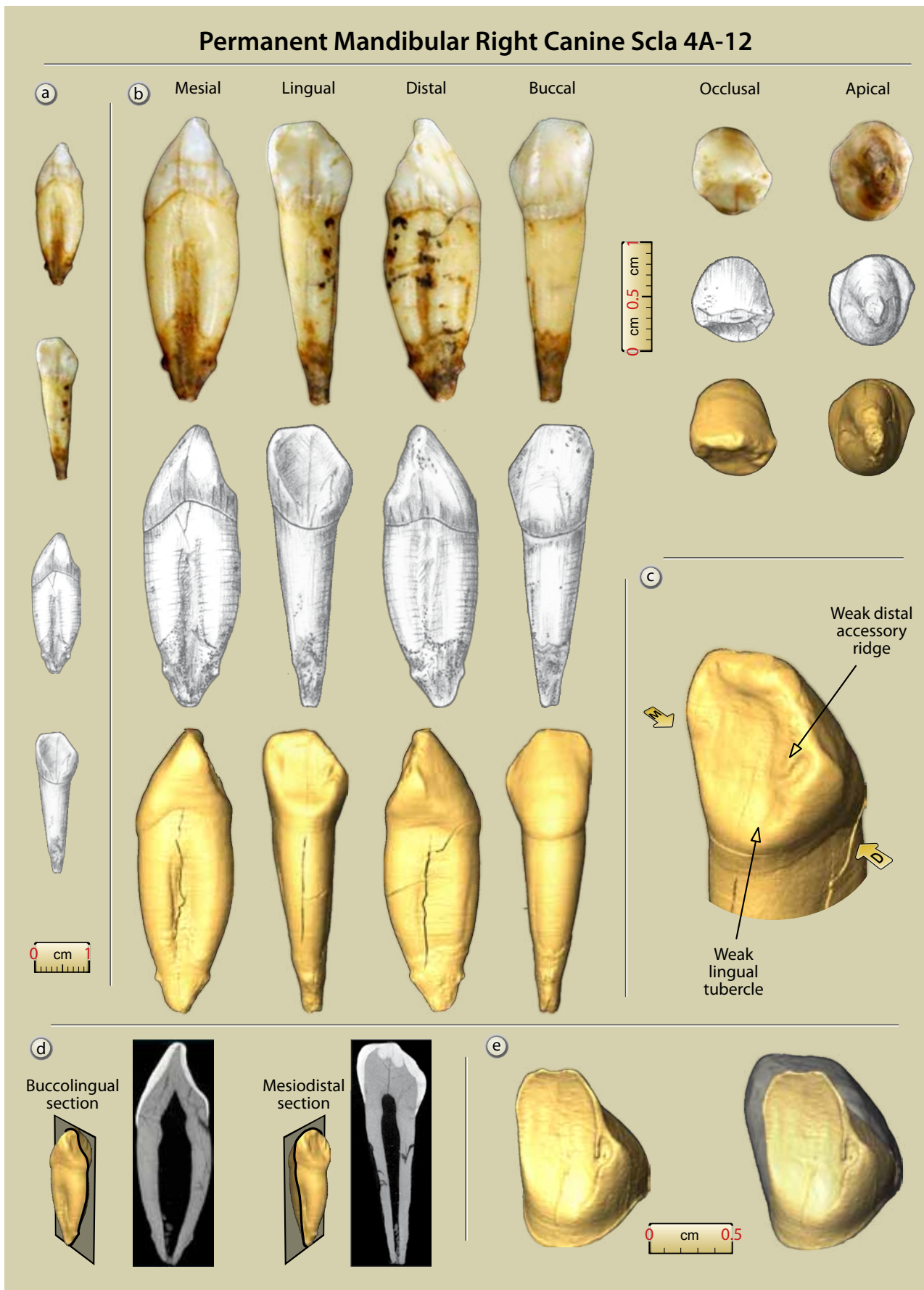


Figure 14: Scla 4A-12 permanent mandibular right canine: a. mesial and lingual views (1:1 scale); b. photographs, drawings and 3D reconstructions of the six faces of the tooth (2:1 scale); c. 3D reconstruction with main anatomical features; d. internal sections; e. 3D lingual views at the EDJ without and with enamel (micro-CT data processing and graphics J.-F. Lemaire, SPW; pencil drawings S. Lambermont, AWEM; photographs J. Eloy, AWEM).



slight irregular superoinferior convexity, from the cervical line to the incisal edge, with a stronger convexity near the cervix.

In lingual view, the crown is asymmetrical: the mesial half of the incisal edge is nearly horizontal, like in incisors, while its lateral part is running down distally.

The distal marginal ridge is slightly expressed, and the mesial one even less. There is no clear shovelling (grade 1 of ASUDAS). A faint distal accessory ridge is present (DAR LC grade 1-2).

The lingual tubercle is very weak, much less marked than in the permanent maxillary canine. It has no separate cusplet.

The rounded V-shape of the incisal rim is deeper on the mesial face than on the distal one.

A flat interproximal wear facet for the second right mandibular incisor is present. It is roughly rounded.

The root is mesiodistally compressed and has well marked mesial, and to a lesser extent, distal, longitudinal grooves. Its section is elliptical. In proximal view, the anterior border of the root is convex, but less so than on the permanent maxillary canines. There is a slight thickening on the apical part of the root.

The length of the root, measured from the lingual aspect, is 16.5 mm.

3.6.2. Taxonomy

Like the permanent mandibular incisors, the permanent mandibular canines are not really useful indicators of taxonomic and biological distance. Neandertal permanent mandibular canines tend to reflect the permanent maxillary canines morphology (BAILEY, 2006^a). They are, however, less robust. The frequency of the distal accessory ridge is 50% in Non-Neandertal

Archais, nearly 85% in Neandertals, 100% in Early Modern Afro-Asians and 28.6% in Early Modern Europeans. The Scla 4A-12 permanent mandibular canine exhibits a very faint distal accessory ridge.

3.6.3. Morphometric analysis

Measurements of the permanent mandibular right canine are as follows:

- MD: 7.80 mm
- BL: 8.75 mm
- MD at cervix: 5.60 mm
- BL at cervix: 8.46
- Length of the tooth: 25.89 mm

The MD and BL diameters of Scla 4A-12 depart significantly only from the average of the recent humans (MHSS) comparison sample, in regard to both the DP probabilistic distance and ECRA. (Table 11). The MD and BL diameters of the Scla 4A-12 crown are, in Figure 15, compared to the ellipses (95%) of Early and Late Neandertals as well as of UPMH and MHSS. Scla 4A-12 is situated in the area where EN, LN and UPMH ellipses overlap. The fossil is outside the 95% ellipse of modern humans. Like for most other permanent anterior teeth, this indicates that the dimensions of the permanent mandibular canines often allow to separate fossils from MHSS but do not provide clear taxonomic indications within fossil taxa.

3.7. Maxillary right second premolar, RP⁴

Palaeoanthropological identification:

Scla 4A-2/P⁴

Field identification: Sc 1992-1283-96-1

Table 11: Scla 4A-12 (permanent mandibular right canine): MD and BL dimensions compared to those of Early and Late Neandertals as well as MPMH, UPMH and MHSS, with DP and ECRA.

Scladina	Diameter	Value
RC, (Scla 4A-12)	MD	7.8
	BL	8.75

Comparison Samples	N	Diameter	Mean	Stand. Dev.	DP	ECRA
EN right & left	25	MD	7.830	0.586	0.960	-0.025
	24	BL	9.119	0.714	0.611	-0.250
LN right & left	40	MD	7.662	0.386	0.722	0.177
	43	BL	8.899	0.878	0.866	-0.084
MPMH right & left	10	MD	7.890	0.886	0.921	-0.045
	11	BL	8.400	0.844	0.687	0.186
UPMH right & left	33	MD	7.065	0.636	0.256	0.567
	34	BL	8.440	0.695	0.658	0.220
MHSS right & left	99	MD	6.427	0.467	0.004	1.482
	99	BL	7.291	0.542	0.008	1.357

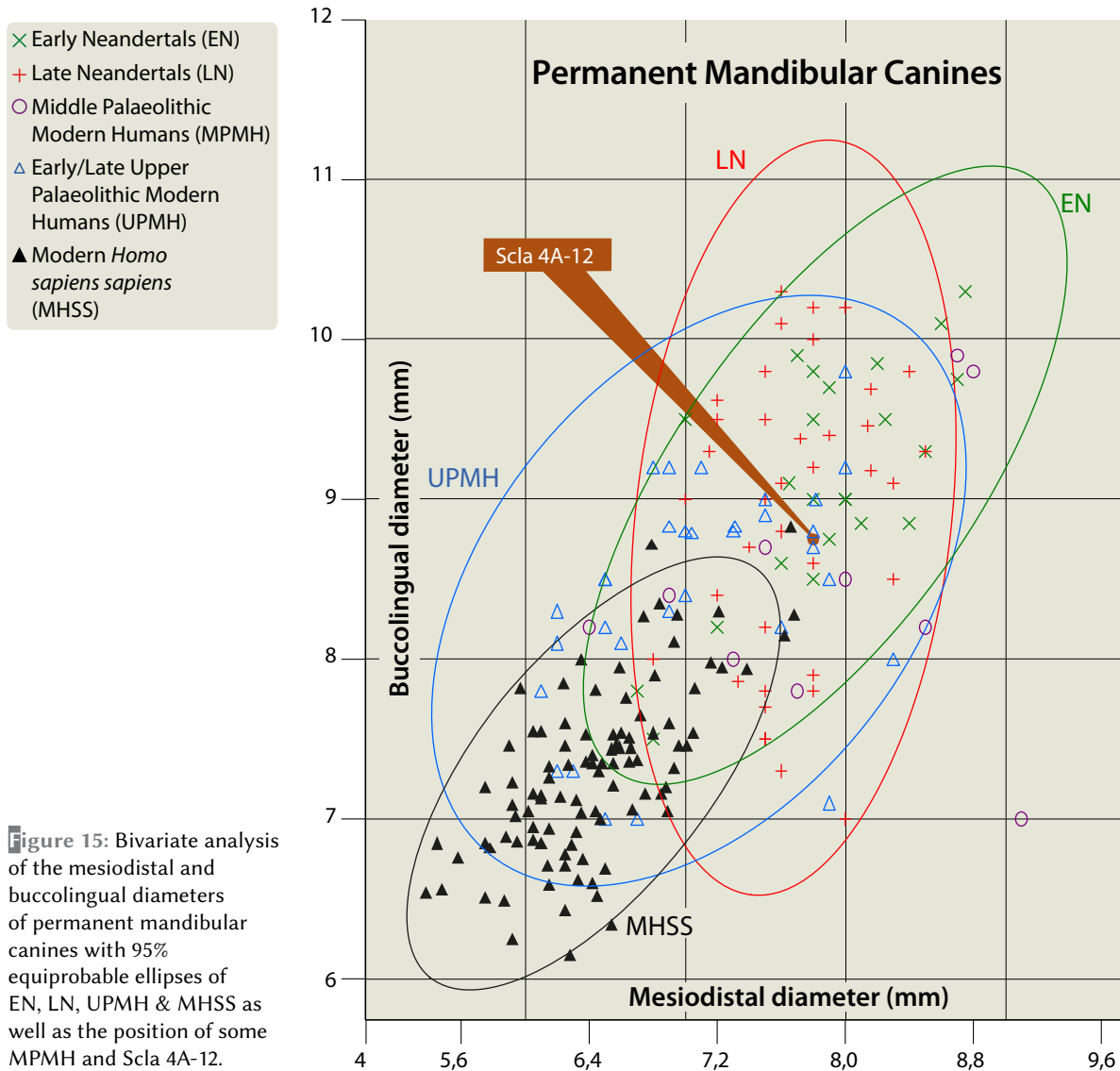


Figure 15: Bivariate analysis of the mesiodistal and buccolingual diameters of permanent mandibular canines with 95% equiprobable ellipses of EN, LN, UPMH & MHSS as well as the position of some MPMH and Scla 4A-12.

Date of discovery: 18 February 1992

Date of identification: October 1993

Square: D30

Stratigraphic position:

– **Former stratigraphy:** 4A

– **New stratigraphy:** Unit 4A-POC (Unit 4A-CHE)

3.7.1. Description (Figure 16)

This tooth is unerupted in the Scla 4A-2 right part of the maxilla. Its crown is completely formed and unworn; a small part of the crown can be seen from the bottom of the crypt of the second deciduous molar. About half of the root is formed.

The crown has two primary cusps, the protocone (lingual cusp or cusp 1) and the paracone (cusp 2). The paracone is nearly as high as the protocone, as usual in UP⁴s. The occlusal morphology of the fossil tends to be complex. The essential crests of

both cusps are well developed and present slight bifurcations. Mesial and distal accessory ridges, visible on the outer enamel surface (OES) and even more clearly on the enamel–dentine junction (EDJ), are present on the slopes of the protocone and paracone. The mesiodistal groove exhibits two pits: a small mesial fossa and a bigger distal fossa. An accessory cusplet with its own crenulation is present on the distal border of the occlusal surface. In mesial and distal views, the buccal face of the tooth is more convex than the lingual face.

The uncompleted root has a distal groove which produces a strong C-shaped cross-section.

3.7.2. Taxonomy

The morphology of the occlusal surface of Neandertal upper P⁴s is somewhat complex (BAILEY, 2002^b, 2006^a). They frequently present accessory cusplets, more frequently distal than



Maxillary Right Second Premolar Scla 4A-2/P⁴

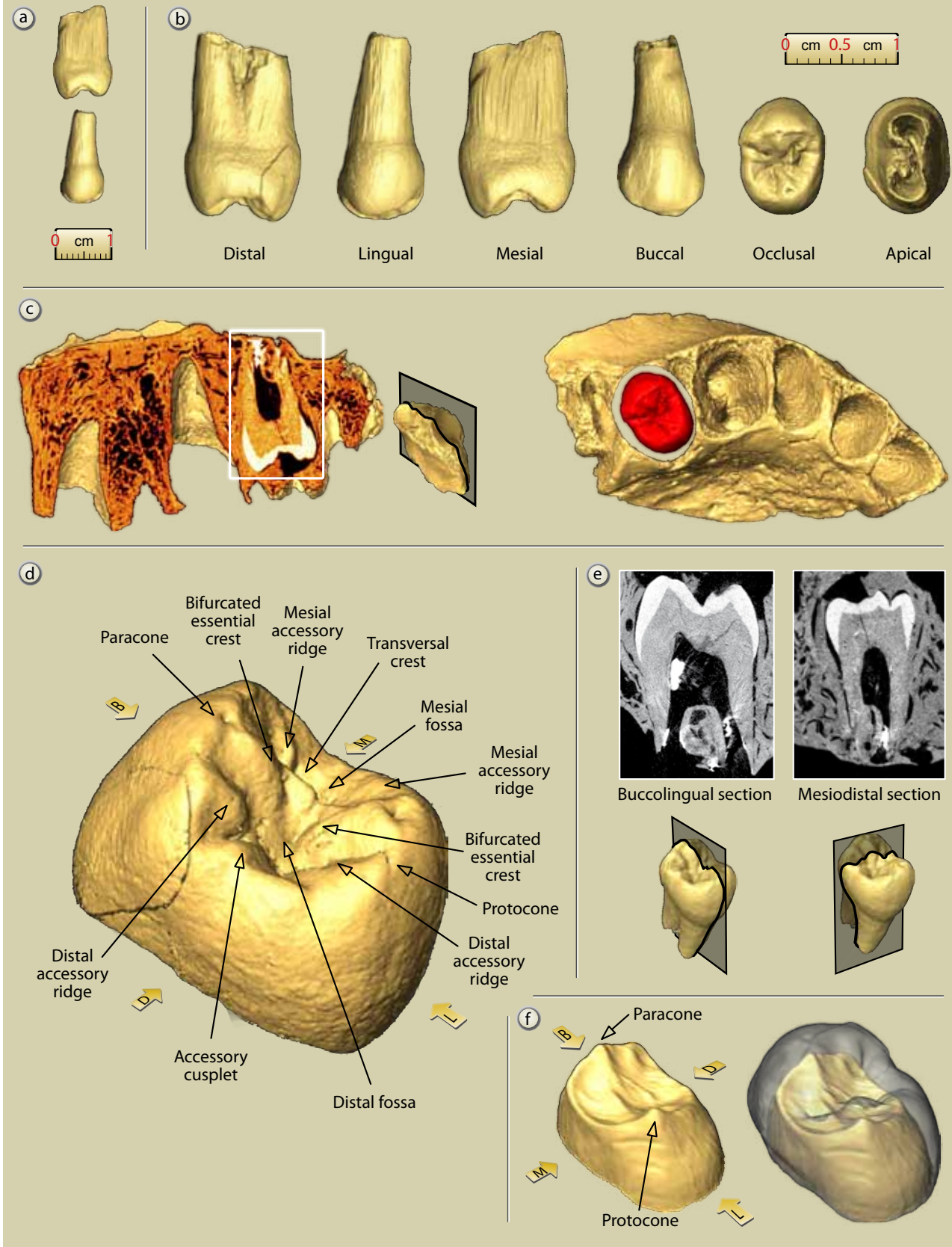


Figure 16: Scla 4A-2/P⁴ unerupted maxillary right second premolar: a. mesial and lingual views (1:1 scale); b. 3D reconstructions of the six faces of the tooth (2:1 scale); c. section showing the unerupted premolar in situ; d. 3D reconstruction with main anatomical features; e. internal sections; f. 3D lingual views at the EDJ without and with enamel (micro-CT data processing and graphics J.-F. Lemaire, SPW; pencil drawings S. Lambermont, AWEM; photographs J. Eloy, AWEM).

Maxillary Second Premolars	Non-Neandertal Archaics	Neandertals	Early Modern Afro-Asians	Early Modern Europeans	Scla 4A-2/P ⁴
Mesial/distal accessory ridges	50%	77.8%	40%	33.3%	mesial and distal
Accessory cusps	50%	47.6%	12.5%	33.3%	yes
Bifurcated buccal essential crest	50%	70%	0%	0%	yes

Table 12: Distinctive anatomical features on maxillary second premolars of Non-Neandertal Archaics, Neandertals, Early Modern Humans (after BAILEY, 2006^a) and Scla 4A-2/P⁴.

mesial. Both primary cusps have a developed essential crest which is often bifurcated. Mesial and distal accessory ridges are frequent but more often buccally than lingually (Table 12). Scla 4A-2/P⁴ associates all the typical Neandertal features.

3.7.3. Morphometric analysis

Measurements of the maxillary right second premolar are as follows:

MD: 7.65 mm

BL: 10.38 mm

The MD and BL diameters of Scla 4A-2/P⁴ depart significantly from the average of the recent humans (MHSS) comparative sample, both in the case of the DP probabilistic distance and ECRA (Table 13). The MD and BL diameters of the Scla 4A-12 crown are, in Figure 17, compared to the means of Early and Late Neandertals as well as of UPMH and MHSS. Scla 4A-12 is situated in the area where EN, LN and UPMH ellipses (95%) overlap. The fossil is outside the 95% ellipse of modern humans. Like for the incisors and canines, this indicates that the dimensions of the P⁴ crowns do not provide clear taxonomic indications within fossil taxa but sometimes allow to distinguish between the latter and MHSS.

Table 13: Scla 4A-2/P⁴ (maxillary right second premolar): MD and BL dimensions compared to those of Early and Late Neandertals as well as MPMH, UPMH and MHSS, with DP and ECRA.

Scladina	Diameter	Value
RP ⁴ (Scla 4A-2/P ⁴)	MD	7.65
	BL	10.38

Comparison Samples	N	Diameter	Mean	Stand. Dev.	DP	ECRA
EN left & right	21	MD	7.624	0.795	0.974	0.016
	20	BL	10.513	0.626	0.835	-0.101
LN left & right	31	MD	6.958	0.510	0.185	0.665
	31	BL	10.104	0.622	0.661	0.217
MPMH right & left	11	MD	7.073	0.476	0.253	0.545
	10	BL	10.150	0.826	0.787	0.123
UPMH right & left	36	MD	6.811	0.683	0.227	0.605
	40	BL	9.660	0.630	0.260	0.565
MHSS right & left	200	MD	6.464	0.452	0.009	1.330
	200	BL	8.907	0.563	0.010	1.326

3.8. Mandibular right first premolar, RP₃

Palaeoanthropological identification: Scla 4A-6

Field identification: Sc 1990-132-41

Date of discovery: 04 July 1990

Date of identification: October 1993

Square: G27

Stratigraphic position:

- **Former stratigraphy:** 4A
- **New stratigraphy:** units 4A-CHE or 4A-POC (units 4A-IP, 3-INF)

3.8.1. Description (Figure 18)

Found isolated, this mandibular right first premolar fits well in the corresponding tooth socket of the Scla 4A-1 right mandible, found in Square D29, former Layer 4A, at a distance over 3 m.

The tooth is not fully erupted. Approximately two thirds of the root are formed. The tooth is well preserved, though the crown and the root exhibit numerous microfissures, mainly along their length. The lower two fifths of the root are dark brown. No pathological conditions have been noted.

The crown of the Scla 4A-6 premolar shows a sub-triangular outline in occlusal view. It tends to be asymmetrically shaped, with an inclination of



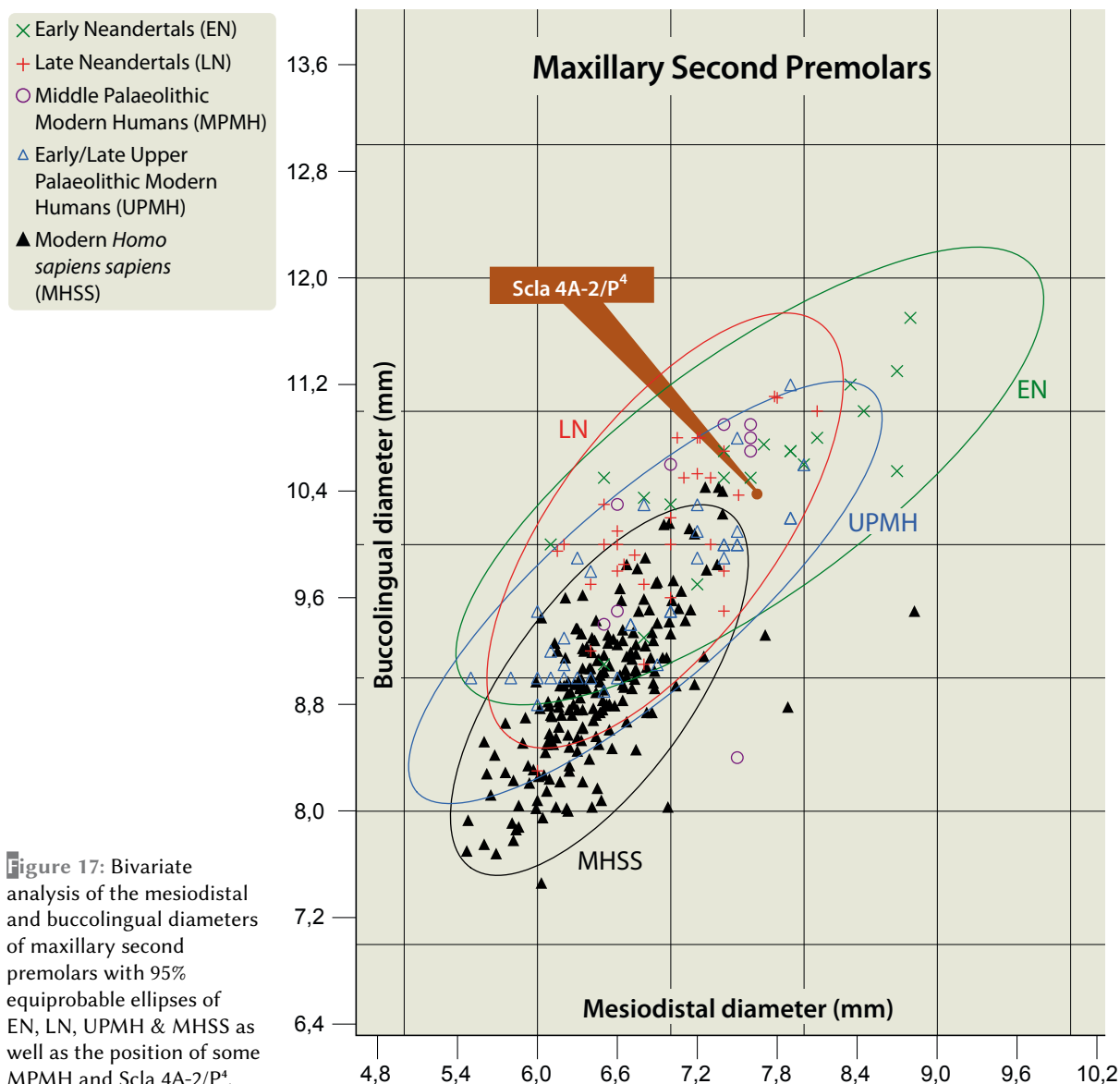


Figure 17: Bivariate analysis of the mesiodistal and buccolingual diameters of maxillary second premolars with 95% equiprobable ellipses of EN, LN, UPMH & MHSS as well as the position of some MPMH and Scla 4A-2/P⁴.

its mesiolingual border. Its occlusal morphology is quite complex.

As usual in mandibular first premolars, the buccal cusp, or protoconid, is significantly higher than the lingual part of the crown, while the buccal cusp of the second premolar is usually just slightly higher than the lingual cusp. The mandibular right first premolar exhibits a double lingual cusp composed of two not very well separated parts. One of these, the metaconid, is slightly mesially placed. A small accessory cusplet (distolingual accessory cusp) is on the crest lingually limiting the distal fossa; it is much smaller and more distally placed than the metaconid (ASUDAS LP1 cusp, grade 3; TURNER et al., 1991: 21).

A mesiodistal groove, or central groove, separates the buccal and lingual cusps. An essential

crest runs down the buccal cusp into this groove and fuses with the essential crest running down the metaconid, forming a continuous buccolingual ridge, the transverse crest. So, the central groove is divided into two depressions, the mesial and distal fossae, limited by distal and mesial marginal ridges. From the distal part of the protoconid, a distal accessory ridge descends to the center of the distal fossa. No mesial accessory ridge is present. All these features, visible on the outer enamel surface (OES), are even better marked on the enamel dentine junction surface (EDJ). The mesiolingual groove is short and only very weakly marked.

In proximal and distal views, the buccal face is convex near the cervix and nearly flat but oblique anterosuperiorly, in its upper two thirds.

Mandibular Right First Premolar Scla 4A-6

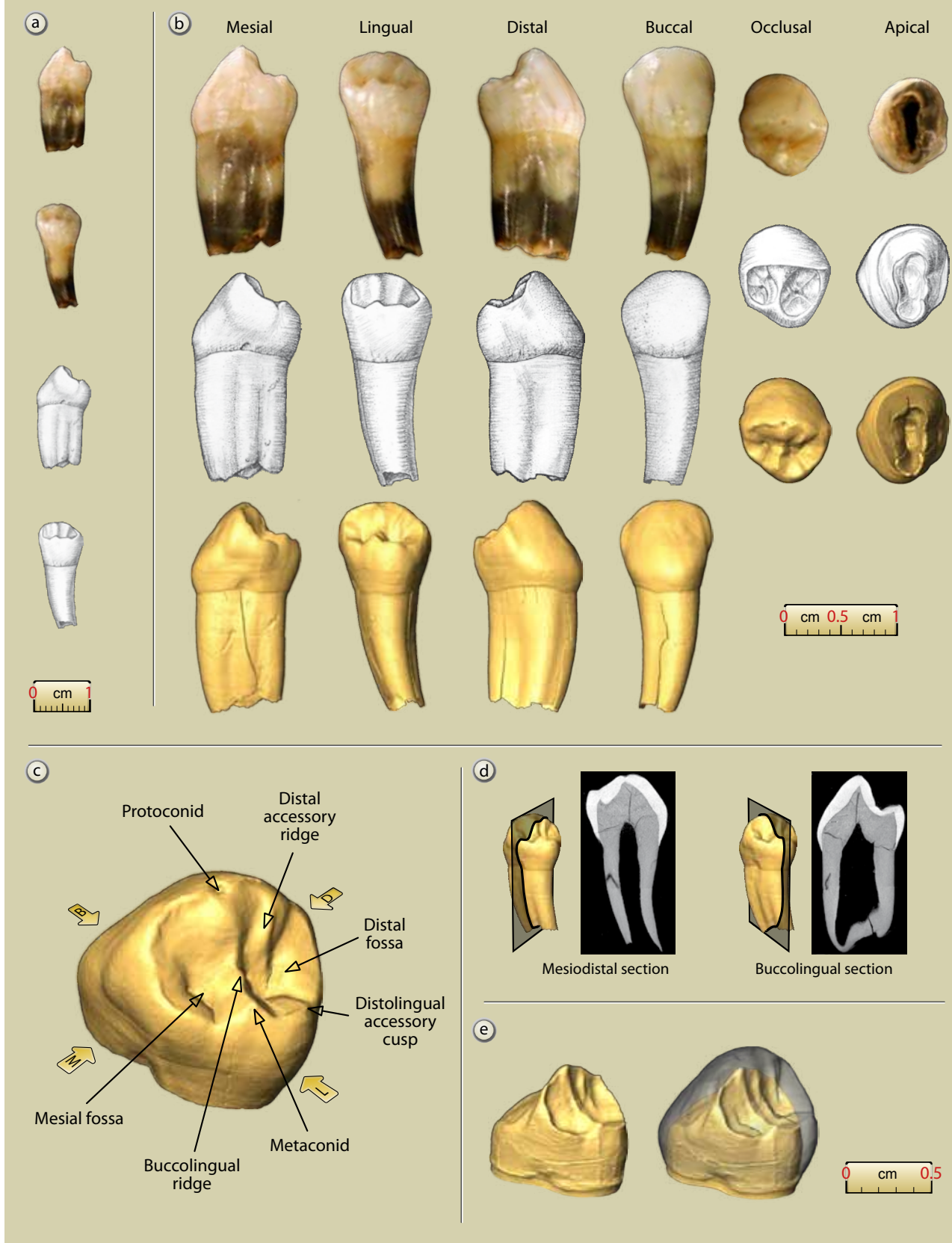


Figure 18: Scla 4A-6 mandibular right first premolar: a. mesial and lingual views (1:1 scale); b. photographs, drawings and 3D reconstructions of the six faces of the tooth (2:1 scale); c. 3D reconstruction with main anatomical features; d. internal sections; e. 3D lingual views at the EDJ without and with enamel (micro-CT data processing and graphics J.-F. Lemaire, SPW; pencil drawings S. Lambermont, AWEM; photographs J. Eloy, AWEM).



The crown is unworn, or nearly so (MOLNAR, 1971, stage 2). There are no interproximal wear facets.

The tooth is single-rooted, at least in its already formed part. The root deflects distally. Its length below the cervix is 10.6 mm on its buccal side and 9.6 mm on its lingual side. This premolar exhibits one distal and two mesial developmental grooves, showing the limits of the radicals. The section of the cervix is elliptical.

3.8.2. Taxonomy

The occlusal morphology of Neandertal first mandibular premolars tend to be complex (BAILEY, 2006^a). It exhibits some traits that, while sometimes present in modern human, make it distinctive because of their higher frequency and their combination (Table 14; BAILEY, 2002^a, 2002^b, 2006^a):

- complex occlusal morphology with a triangular outline and a tendency to be asymmetrically shaped;
- well developed and continuous essential/transverse crest;
- higher frequency of the distal accessory ridge (90%) than in modern human;
- higher frequency of the mesial lingual groove than in modern human;
- frequent presence of a distal accessory cusplet co-occurring with the metaconid.

The Scla 4A-6 premolar presents a combination of most of these traits.

3.8.3. Morphometric analysis

Measurements of the Scla 4A-6 mandibular right first premolar are as follows:

MD diameter: 8.12 mm
 BL diameter: 9.38 mm
 MD diameter at the cervix: 5.50 mm
 BL diameter at the cervix: 7.76 mm
 Length of the tooth: 18.30 mm

The MD and BL diameters of Scla 4A-6 departs significantly only from the average of the recent humans (MHSS) comparative sample, both in regard to the DP probabilistic distance and ECRA. The BL diameter of Scla 4A-6 also departs significantly from the average of the UPMH sample (Table 15). The MD and BL diameters of the crown of Scla 4A-6 are, in Figure 19, compared to the ellipses (95%) of Early and Late Neandertals as well as of MPMH, UPMH and MHSS. Scla 4A-6 is situated in the area where EN, LN and UPMH ellipses (95%) overlap, and at the limit of the UPMH ellipse. In addition, the fossil is outside the 95% ellipse of modern humans. As with all incisors, canines and the maxillary second premolar, this indicates that the dimensions of the crown of the mandibular first premolar do not provide clear taxonomic indications except that they allow to distinguish fossils taxa from MHSS.

3.9. Mandibular second premolars, P₄

3.9.1. Description

Both right and left portions of the Scladina Child mandible, namely Scla 4A-1 and Scla 4A-9, have an unerupted second premolar.

These two teeth have been extracted from a 3D computerized model reconstructed from micro-CT scans of the fossils recorded at the University of Antwerp and the Max Planck Institute in Leipzig, with the Amira® software package. These 3D reconstructions were then reproduced as physical objects via stereolithography.

Mandibular First Premolars	Non-Neandertal Archaics	Neandertals	Early Modern Afro-Asians	Early Modern Europeans	Scla 4A-6
Asymmetry/triangular outline	66.7%	94.4% (well marked in 39%)	75%	56.3%	yes
Distal accessory ridge	75%	90%	50%	100%	yes
Mesial accessory ridge	0%	23.5%	0%	12.5%	no
Accessory lingual cusp	25%	20.6%	16.7%	7.1%	distolingual accessory cusp. grade 3
Transverse crest	50%	96.7%	75%	81.3%	yes
Mesial lingual groove	66.7%	64%	25%	50%	very weak

Table 14: Distinctive anatomical features on mandibular first premolars of Non-Neandertal Archaics, Neandertals, Early Modern Humans (after BAILEY, 2006^a) and Scla 4A-6.

Scladina		Diameter	Value
RP ₃ (Scla 4A-6)		MD	8.12
		BL	9.38

Comparison Samples	N	Diameter	Mean	Stand. Dev.	DP	ECRA
EN right & left	23	MD	7.878	0.753	0.751	0.155
	21	BL	9.057	0.724	0.661	0.214
LN right & left	42	MD	7.536	0.488	0.238	0.592
	41	BL	8.994	0.698	0.583	0.274
MPMH right & left	8	MD	7.888	0.426	0.602	0.231
	8	BL	8.888	0.599	0.438	0.348
UPMH right & left	39	MD	7.058	0.536	0.055	0.979
	39	BL	8.322	0.416	0.015	1.254
MHSS right & left	82	MD	6.578	0.423	0.000	1.830
	82	BL	7.330	0.483	0.000	2.132

Table 15: Scla 4A-6 (mandibular right first premolar): MD and BL dimensions compared to those of Early and Late Neandertals as well as MPMH, UPMH and MHSS, with DP and ECRA.

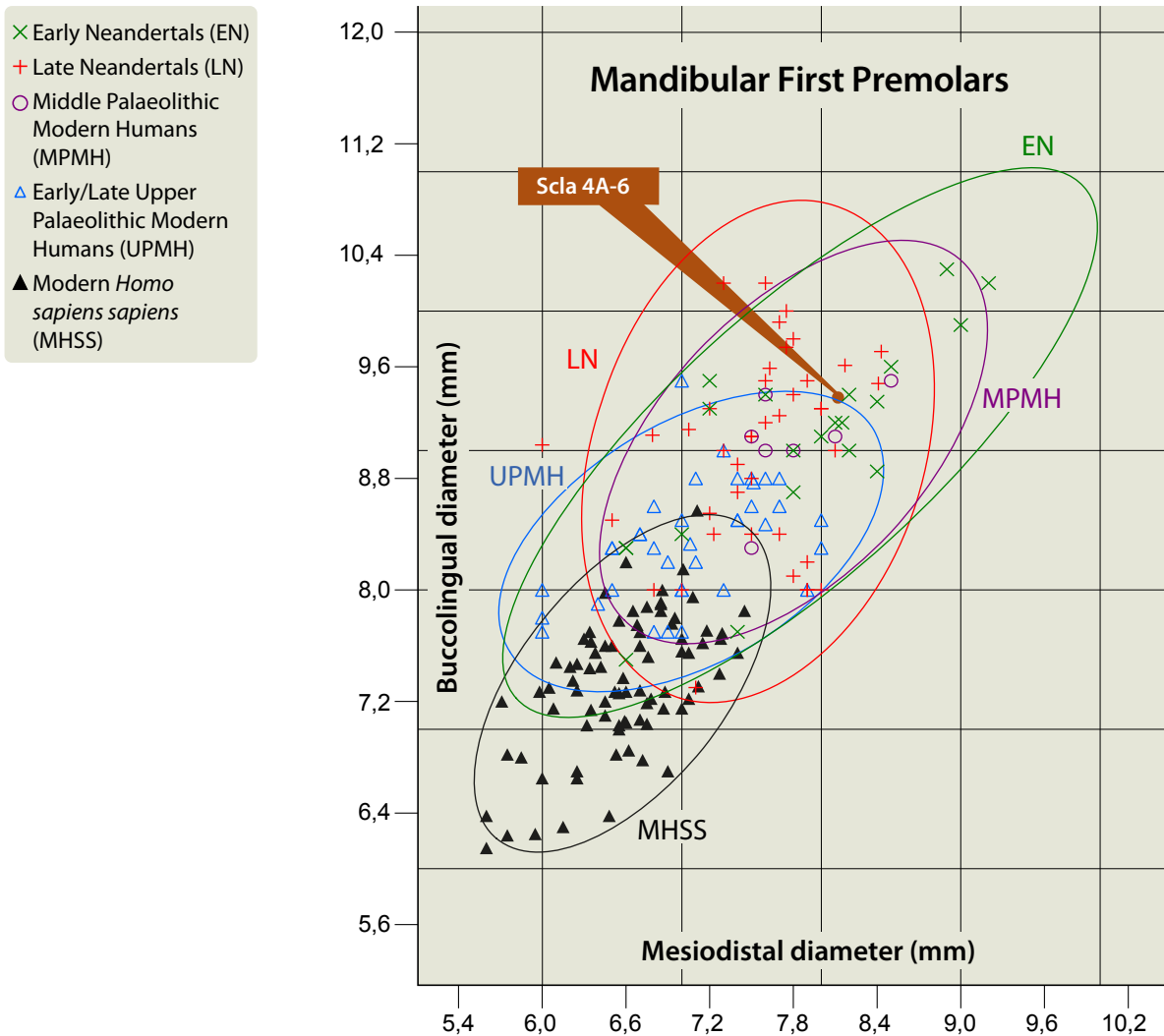


Figure 19: Bivariate analysis of the mesiodistal and buccolingual diameters of mandibular first premolars with 95% equiprobable ellipses of EN, LN, MPMH, UPMH & MHSS as well as the position of Scla 4A-6.



*Mandibular left second premolar, LP₄ (Figure 20)***Palaeoanthropological****identification:** Scla 4A-9/P₄**Field identification:** Sc 1996-203-1**Date of discovery:** 12 July 1996**Date of identification:** 12 July 1996**Square:** C28**Stratigraphic position:**

- **Former stratigraphy:** 4A
- **New stratigraphy:** Unit 4A-CHE (Unit 4A-POC), Layer 4A-JA (?)

This tooth is included in the Scla 4A-9 left part of the mandible. Its crown is completely formed and unworn. Its root is not complete; about two thirds are formed (Figure 20).

The crown is asymmetrical in occlusal view, with an inclination of the mesiolingual border and a truncated mesiolingual lobe. So its outline is somewhat triangular. Its occlusal topography is complex.

The metaconid is well developed, just a little lower than the protoconid. It is mesially placed and more strongly developed than the metaconid of the mandibular right first premolar Scla 4A-6.

A continuous and strong transversal crest, visible on the OES and even more clearly on the EDJ, connects the protoconid and metaconid. Because of the mesial position of the metaconid, this crest is also mesially disposed and the mesial fovea is much smaller than the distal one.

The protoconid does not have any mesial accessory ridge. However, it exhibits a central ridge which descends from the apex of the cusp and, after a few millimetres, divides itself into two branches, one forming the continuous transverse ridge already mentioned and another, very faint, descending to the distal fovea. Slightly more distal is the DAR (distal accessory ridge).

In mesial and distal views, the buccal face of the tooth is very convex.

The P₄ has two accessory lingual cusps. The first one is on the distolingual angle of the occlusal surface and the second one on the distal marginal ridge. They are well separated by shallow grooves going down to the center of the distal fovea.

The uncompleted root has a mesiolingual groove which produces a C-shaped root morphology or Tomes' root morphology (HILLSON, 1996: 41, 44). This vertical groove is shallow in its cervical third, but becomes increasingly deeper as it reaches the end of the root. The lingual part of the root is the largest.

*Mandibular right second premolar, RP₄ (Figure 21)***Palaeoanthropological****identification:** Scla 4A-1/P₄**Field identification:** Sc 1993-148-185**Date of discovery:** 16 July 1993**Date of identification:** 20 July 1993**Square:** D29**Stratigraphic position:**

- **Former stratigraphy:** 4A
- **New stratigraphy:** Unit 4A-CHE, Layer 4A-GX

This tooth is totally unerupted. It is embedded within the Scla 4A-1 right part of the mandible. However it is possible to see a very small part of its crown by looking carefully through the bottom of the alveolus of the right second deciduous molar.

Its crown is completely formed but unworn and its root is not complete, like that of its antimere.

The morphology of this tooth is quite similar to the corresponding mandibular left first premolar unerupted in the Scla 4A-9 left part of the mandible.

The crown exhibits a somewhat triangular outline. It is asymmetrical in occlusal view, with an inclination of the mesiolingual border.

The metaconid is well developed, just a little lower than the protoconid, and is mesially disposed. A continuous and strong transversal crest connects the protoconid and metaconid. This crest is also mesially disposed and the mesial fovea is much smaller than the distal fovea.

The protoconid does not have any mesial accessory ridge. As in the left P₄, it exhibits a central ridge descending from the apex of the protoconid which divides itself into two branches, one forming the transverse ridge already mentioned. A distal accessory ridge is also present.

In lateral view, the buccal face of the tooth is irregularly convex.

This right P₄, like the left one, has two accessory distolingual cusps and they are at the same position. The first lies at the distolingual angle of the occlusal surface and the second on the distal marginal ridge. They are well separated by shallow grooves going down to the center of the distal fovea.

As for the left P₄, the incomplete root of the right P₄ has a mesiolingual vertical groove which produces a C-shaped root morphology or Tomes' root morphology. The lingual component of the root is also the largest.

Mandibular Left second Premolar Scla 4A-9/P₄

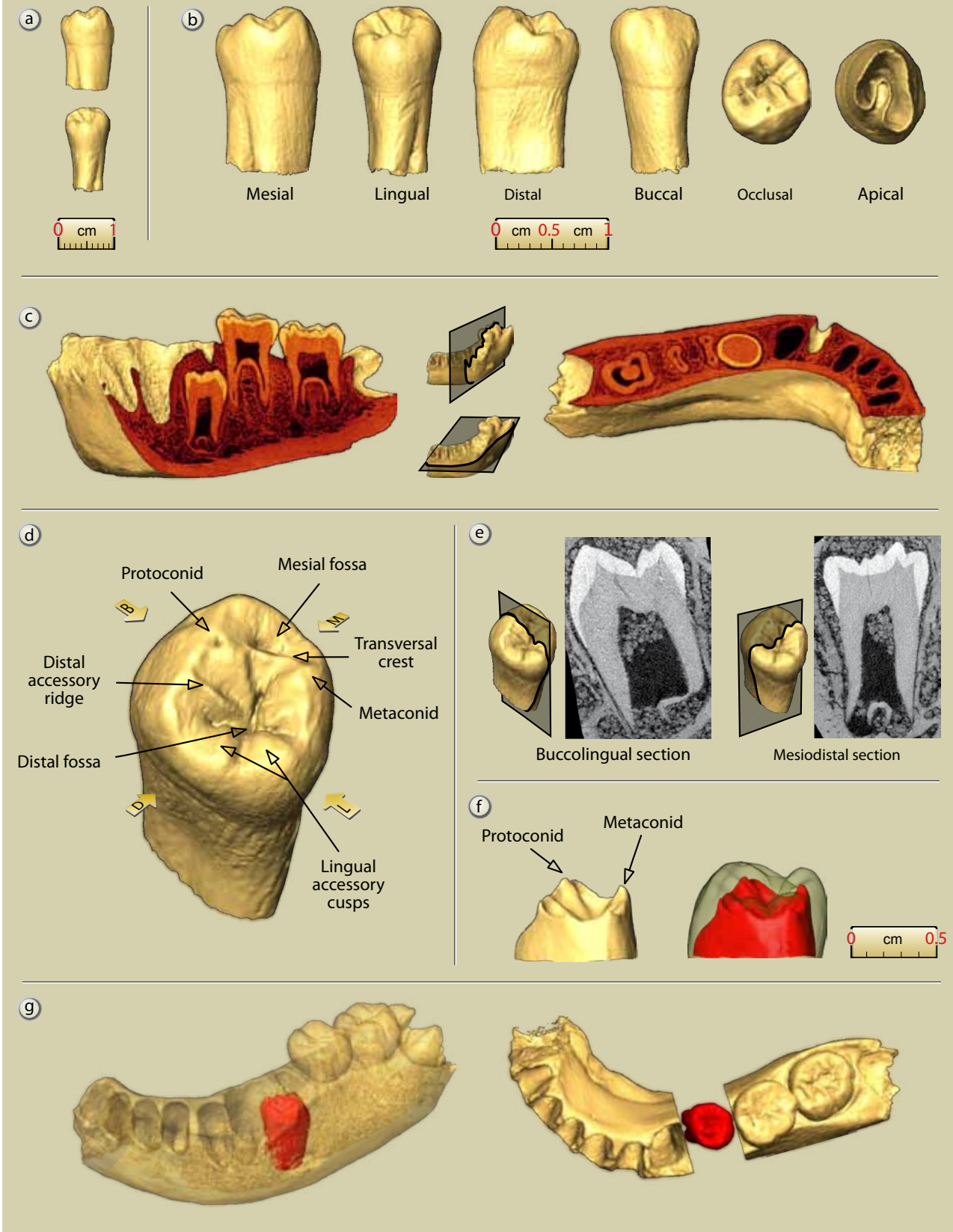


Figure 20: Scla 4A-9/P₄ unerupted mandibular left second premolar: a. mesial and lingual views (1:1 scale); b. 3D reconstructions of the six faces of the tooth (2:1 scale); c. section showing the unerupted premolar in situ; d. 3D reconstruction with main anatomical features; e. internal sections; f. 3D lingual views at the EDJ without and with enamel; g. other views of the location of the unerupted premolar (micro-CT data processing and graphics J.-F. Lemaire, SPW; pencil drawings S. Lambermont, AWEM; photographs J. Eloy, AWEM).



Mandibular Right Second Premolar Scla 4A-1/P₄

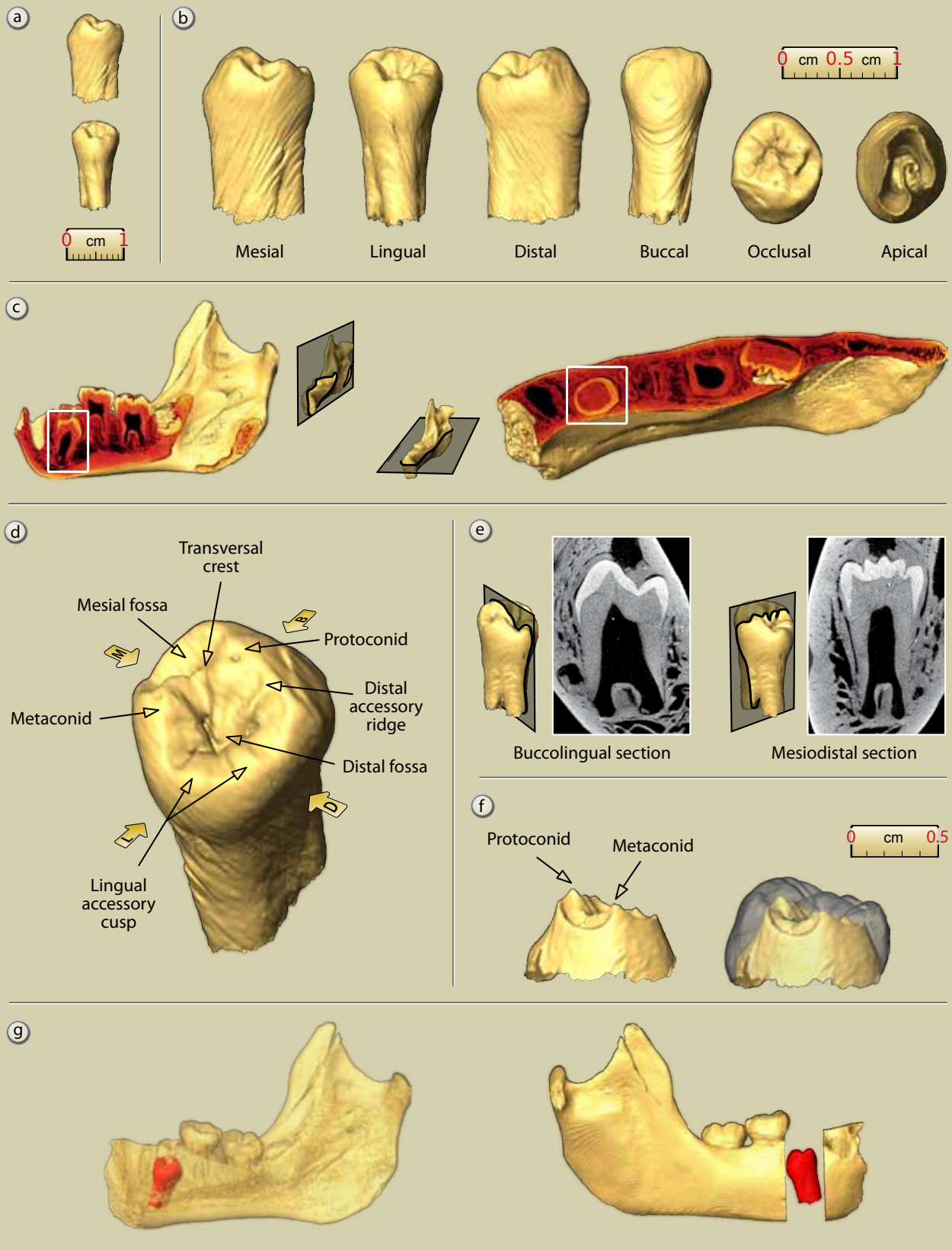


Figure 21: Scla 4A-1/P₄, unerupted mandibular right second premolar: a. mesial and lingual views (1:1 scale); b. 3D reconstructions of the six faces of the tooth (2:1 scale); c. section showing the unerupted premolar in situ; d. 3D reconstruction with main anatomical features; e. internal sections; f. 3D lingual views at the EDJ without and with enamel; g. other views of the location of the unerupted premolar (micro-CT data processing and graphics J.-F. Lemaire, SPW; pencil drawings S. Lambermont, AWEM; photographs J. Eloy, AWEM).

Mandibular Second Premolars	Non-Neandertal Archaics	Neandertals	Early Modern Afro-Asians	Early Modern Europeans	Scla 4A-1/P ₄	Scla 4A-9/P ₄
Asymmetry/triangular outline	16.7%	93.5%	33.3%	33.3%	yes	yes
Mesial position of the metaconid	100%	96.9%	50%	73.3%	yes	yes
Transverse crest (continue)	33.3%	93.5%	16.7%	23.5%	yes	yes
Distal accessory ridge	100%	87.5%	66.7%	25%	yes	yes
Mesial accessory ridge	20%	12.5%	66.7%	0%	-	-
Accessory lingual cusps	80%	90.6%	66.7%	50%	yes	yes
Mesial lingual groove	0%	8%	0%	0%	-	-

Table 16: Distinctive anatomical features on mandibular second premolars of Non-Neandertal Archaics, Neandertals, Early Modern Humans (after BAILEY, 2006^a) and Scla 4A-1/P₄ & Scla 4A-9/P₄.

3.9.2. Taxonomy

Some P₄ crown traits are particularly useful to distinguish Neandertal P₄s from those of modern humans and *Homo erectus* (Table 16; BAILEY, 2002^a, 2002^b, 2005, 2006^a):

- distinctive complex crown outline in occlusal view, with marked asymmetry of the lingual contour, caused by the truncation of its mesiolingual lobe ($\pm 90\%$ of Neandertal P₄s, against a third or less in Archaic *Homo erectus*, *Homo sapiens* and modern humans);
- mesially placed metaconid which is also large and well developed;
- strong and continuous transverse crest (over 90% of Neandertal P₄s).
- extra lingual cusps (present on $\pm 90\%$ of Neandertal P₄s);
- distal accessory ridges, whose frequency in Neandertals and *Homo erectus* ($\geq 90\%$) is higher than in modern humans (two thirds or less).

In fact, each of these traits may be present in anatomically modern populations but it is the frequency with which they occur together within a single tooth which is taxonomically diagnostic and distinguishes Neandertals from contemporary humans and *Homo erectus*. In detail (BAILEY, 2002^a: 154), 59% of Neandertals exhibit the first three traits together and 35% two of these traits, whereas 94% of Neandertals present at least two of these three features in combination; only 2.4% of the modern humans do.

The two Scladina P₄s both present the asymmetry of the lingual contour when viewed occlusally, a mesially positioned metaconid, multiple lingual cusps as well as a marked transverse crest.

3.9.3. Morphometric analysis

Measurements of the mandibular second premolars are as follows:

Scla 4A-1/P₄

MD = 8.0 mm
BL = 9.68 mm

Scla 4A-9/P₄

MD = 8.1 mm
BL = 9.3 mm

The MD and BL diameters of both mandibular second premolars depart significantly from the average of the recent humans (MHSS) comparative sample, in regards to the DP probabilistic distance and ECRA. The BL diameter of both teeth also departs significantly from the average of the UPMH sample (Table 17). The MD and BL diameters of the crown of both mandibular second premolars are, in Figure 22, compared to the means of Early and Late Neandertals as well as of MPMH, UPMH and MHSS. They are situated in the area where EN, LN, MPMH and UPMH ellipses (95%) overlap. In addition, the fossil is outside the 95% ellipse of Modern Humans. As with all incisors, canines and other premolars, this indicates that the dimensions of the crown of the mandibular second premolar do not always provide clear taxonomic indications within fossil taxa but often allow to separate the latter from MHSS.

3.10. Permanent maxillary right first molar, RM¹

Palaeoanthropological identification: Scla 4A-4

Field identification: Sc 1993-330-127

Date of discovery: 14 December 1993

Date of identification: 14 December 1993

Square: C30



Scladina	N	Diameter	Value	vs Scla 4A-1/P ₄		vs Scla 4A-9/P ₄		
P ₄	Scla 4A-1/P ₄	MD	8.0					
		BL	9.68					
	Scla 4A-9/P ₄	MD	8.1					
		BL	9.3					
Comparison Samples	N	Diameter	Mean	Stand. Dev.	DP	ECRA	DP	ECRA
EN right & left	24	MD	7.729	0.692	0.699	0.189	0.597	0.259
	23	BL	9.348	0.501	0.515	0.319	0.925	-0.046
LN right & left	47	MD	7.371	0.637	0.329	0.491	0.258	0.569
	47	BL	9.019	0.748	0.381	0.439	0.709	0.187
MPMH right & left	9	MD	7.611	0.535	0.488	0.315	0.387	0.396
	9	BL	8.989	0.655	0.322	0.458	0.647	0.206
UPMH right & left	39	MD	7.312	0.577	0.240	0.589	0.18	0.675
	40	BL	8.649	0.486	0.040	1.050	0.188	0.663
HSS right & left	90	MD	6.896	0.426	0.011	1.305	0.006	1.423
	90	BL	7.973	0.484	0.001	1.774	0.007	1.379

Table 17: Scla 4A-1/P₄ & Scla 4A-9/P₄ (mandibular second premolars): MD and BL dimensions compared to those of Early and Late Neandertals as well as MPMH, UPMH and MHSS, with DP and ECRA.

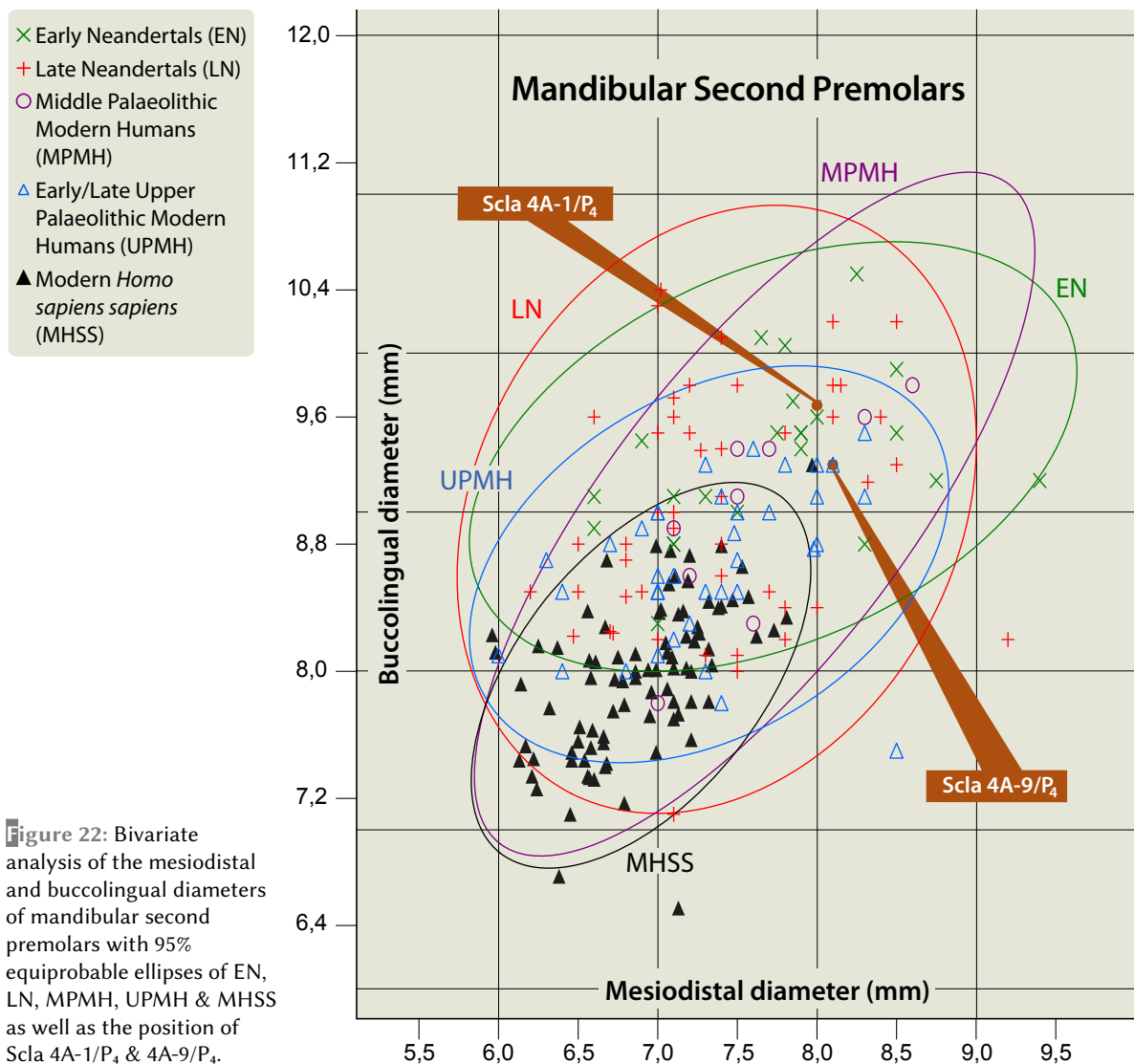


Figure 22: Bivariate analysis of the mesiodistal and buccolingual diameters of mandibular second premolars with 95% equiprobable ellipses of EN, LN, MPMH, UPMH & MHSS as well as the position of Scla 4A-1/P₄ & 4A-9/P₄.

Stratigraphic position:

- **Former stratigraphy:** 4A
- **New stratigraphy:** Unit 4A-POC, Layer 4A-BO

3.10.1. Description (Figure 23)

Immediately recognized as human in the field, this permanent maxillary first right molar fits perfectly into the corresponding socket of the Scla 4A-2 right maxilla fragment found in adjacent Square D30, at a distance of about 1 m.

The tooth is completely formed and was functional, as attested by the slight wear of the cuspids (grade 2 of MOLNAR, 1971). The crown and roots, with closed apices, were well preserved at the time of discovery of the fossil. The buccal roots were later sampled for C/N and DNA analysis. On the Scla 4A-2 maxilla, the alveoli of the buccomesial root is well preserved and that of the buccodistal root is partially preserved, from which the shapes of the roots can also be studied. Later, in 2007, a histological section was obtained from the molar, in order to study the age at death of the specimen (SMITH et al., 2007 & Chapter 7). The two resulting portions of the tooth were subsequently glued together to the approximate original dimensions and coloured with a dental restorative (temporary resin acrylic) and dental sticky wax.

No pathological conditions have been noted. The right M¹ has four main cusps: protocone>paracone>hypocone>metacone.

In occlusal view, the Scla 4A-4 crown exhibits a skewed rhomboidal surface. The cusps also appear to be internally compressed. The tooth is crenulated with essential crests running down from the cusps into the depressed occlusal surface. The paracone (cusp 2) draws a sharp, but truncated, angle. The hypocone (cusp 4) is large, projecting lingually and rounded. The metacone (cusp 3) is quite small, rounded and shifted internally. A tiny distal accessory cusp lies between the hypocone and the metacone on the distal marginal ridge (ASUDAS UM cusp 5, grade 2/3). The two buccal cusps (paracone and metacone) are more mesially placed than the lingual cusps (protocone and hypocone).

In side view, the protocone (cusp 1) has tiny subvertical smooth grooves at the limit of its mesial and lingual surfaces; these represent an extremely subtle manifestation of the tubercle of Carabelli (ASUDAS, grade 1). A small cusp is present on the buccal surface of the paracone: a very weak parastyle (grade 2 in the ASUDAS

scoring system). On the lingual face of the crown a well marked groove separates the protocone and the hypocone. Another groove separates the paracone and the metacone on the occlusal half of the buccal surface of the crown. Between the hypocone and metacone, on the distal surface of the tooth, the cervical enamel line forms a faint enamel extension directed apically which deviates by nearly 1 mm from the horizontal axis of the cervical enamel line.

On the mesial face of the crown is a large (5 mm) horizontal interproximal wear facet; its height is 2.3 mm. This facet slightly affects the outline of the crown. On the distal face of the crown, no interproximal wear facet is present for the second molar, which is normal as the second molar was not completely erupted.

The lingual root forms a cone flattened in the buccolingual direction. It diverges at first from the vertical axis of the crown then bends slightly to become again almost vertical. Its apex is fully closed. Both the buccal and lingual faces of that lingual root have a shallow vertical groove. The length of the root is 13.6 mm, measured on the lingual face from the middle of the cervix. The two buccal roots (now broken) join near the cervical line, only separated by a shallow vertical groove. The mesiobuccal root is wider than the distobuccal one. They diverge at around 5 mm of the cervix. The distobuccal root has a length of 12.4 mm and is slightly curved distally. The mesiobuccal root is 10.5 mm and is nearly straight.

3.10.2. Taxonomy

In occlusal view, Neandertal maxillary first molars exhibit a few interesting features (Table 18) which, however, fall within the range of anatomically modern *Homo sapiens* (amHS; BAILEY, 2002^b, 2004^a, 2006^{a, b}).

The crowns are usually strongly skewed, compared with the maxillary molars of contemporary modern humans, with a large hypocone projecting lingually. Their shape is therefore rhomboidal. The Neandertal M¹ is somewhat crenulated and has usually four main cusps as well as accessory cusps and crests. The buccal cusps (paracone and metacone) are more mesially placed than the lingual cusps (protocone and hypocone). The Neandertal metacone is also shifted lingually. Cusp 5 is present in two thirds of the M¹. Carabelli's cusp is frequently present and often well developed. The cusps are more internally compressed than in modern humans, their



Permanent Maxillary Right First Molar Scla 4A-4

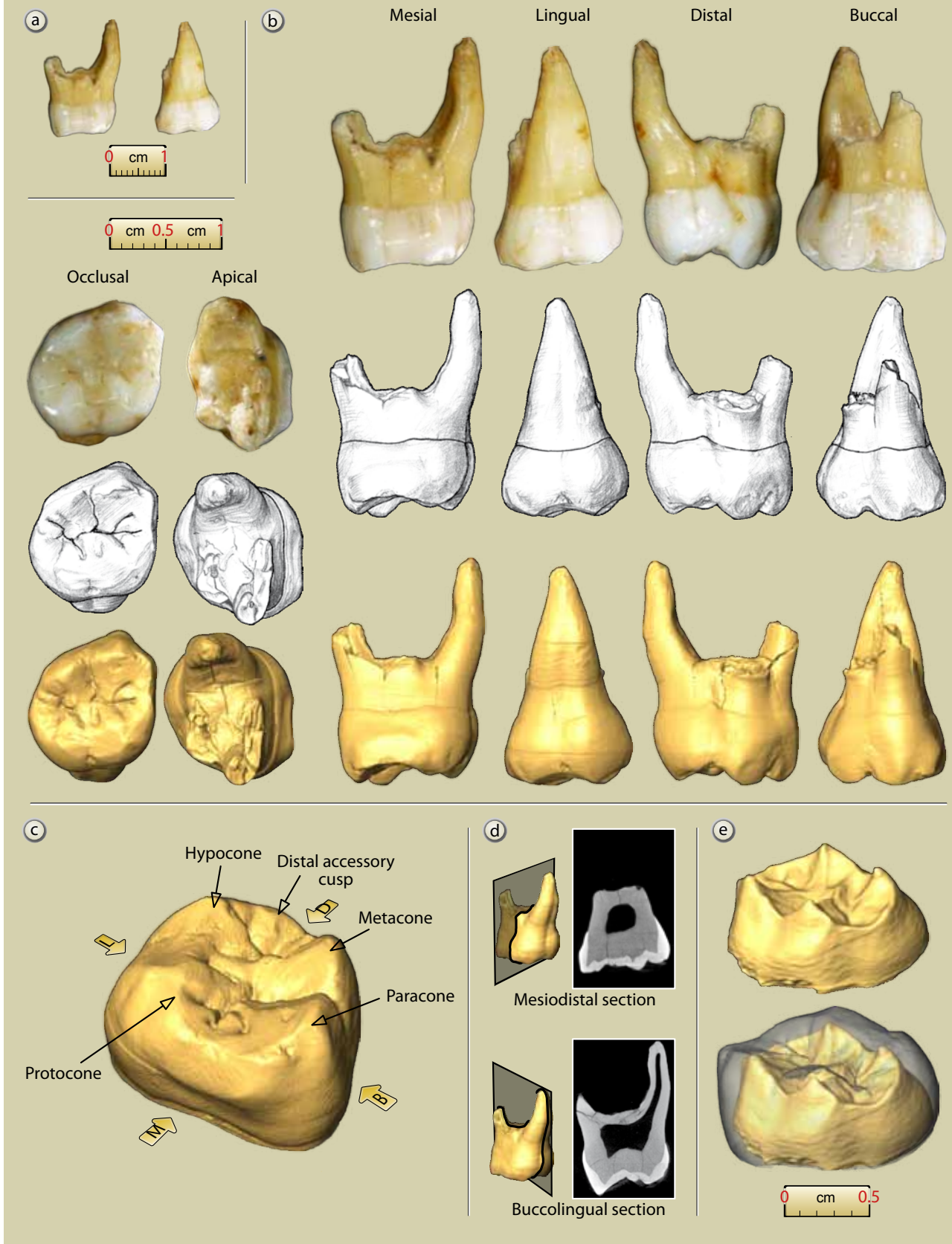


Figure 23: Scla 4A-4 permanent maxillary right first molar: a. mesial and lingual views (1:1 scale); b. photographs, drawings and 3D reconstructions of the six faces of the tooth (2:1 scale); c. 3D reconstruction with main anatomical features; d. internal sections; e. 3D lingual views at the EDJ without and with enamel (micro-CT data processing and graphics J.-F. Lemaire, SPW; pencil drawings S. Lambermont, AWEM; photographs J. Eloy, AWEM).

Permanent Maxillary First Molars	Non-Neandertal Archaics	Neandertals	Early Modern Afro-Asians	Early Modern Europeans	Scla 4A-4
Distal accessory cusplet	25%	63.6%	40%	52.9%	yes (tiny)
Carabelli's trait	75%	68%	33.3%	40.0%	yes (tiny)
Mesial accessory cusps	0%	40%	0%	22.2%	yes
Hypocone reduction	0%	0%	0%	0%	no

Table 18: Distinctive anatomical features on permanent maxillary first molars of Non-Neandertal Archaics, Neandertals, Early Modern Humans (after BAILEY, 2006^a) and Scla 4A-4.

apices being orientated more towards the occlusal basin as well as closer; therefore, the occlusal polygon, drawn by joining the apices of the four main cusps, is smaller than in other human groups (BAILEY, 2004^a: 194). The metacone is relatively reduced and internally oriented.

The Scla 4A-4 first maxillary molar presents all these Neandertal traits. It is skewed, the buccal cusps are mesially placed, the cusps are internally compressed, there is a large hypocone.

3.10.3. Morphometric analysis

Measurements of the Scla 4A-4 permanent maxillary first molar are as follows:

MD: 10.57 mm

BL: 11.92 mm

Length of the tooth: (21.0 mm)

MD at the cervix: 7.80 mm

BL at the cervix: 11.0 mm

The MD and BL diameters of Scla 4A-4 do not depart significantly from the average of any of the five comparison samples (EN, LN, MPMH, UPMH & MHSS), both in regard to the DP probabilistic distance and ECRA (Table 19). When both diameters are situated on equiprobable ellipses

(95%) they are in an area where of all these taxa overlap (Figure 24). Like for all incisors, canines and premolars, this indicates that the dimensions of the crown of the permanent maxillary first molar do not provide taxonomic indications in the case of Scladina.

3.11. Permanent maxillary right second molar, RM²

Palaeoanthropological identification: Scla 4A-3

Field identification: Sc 1992-411-107-1

Date of discovery: 15 October 1992

Date of identification: October 1993

Square: C30

Stratigraphic position:

– **Former stratigraphy:** 4A

– **New stratigraphy:** units 4A-CHE or 4A-POC

3.11.1. Description (Figure 25)

Like the permanent maxillary right first molar, the permanent maxillary right second molar of the Scladina Juvenile was lost postmortem.

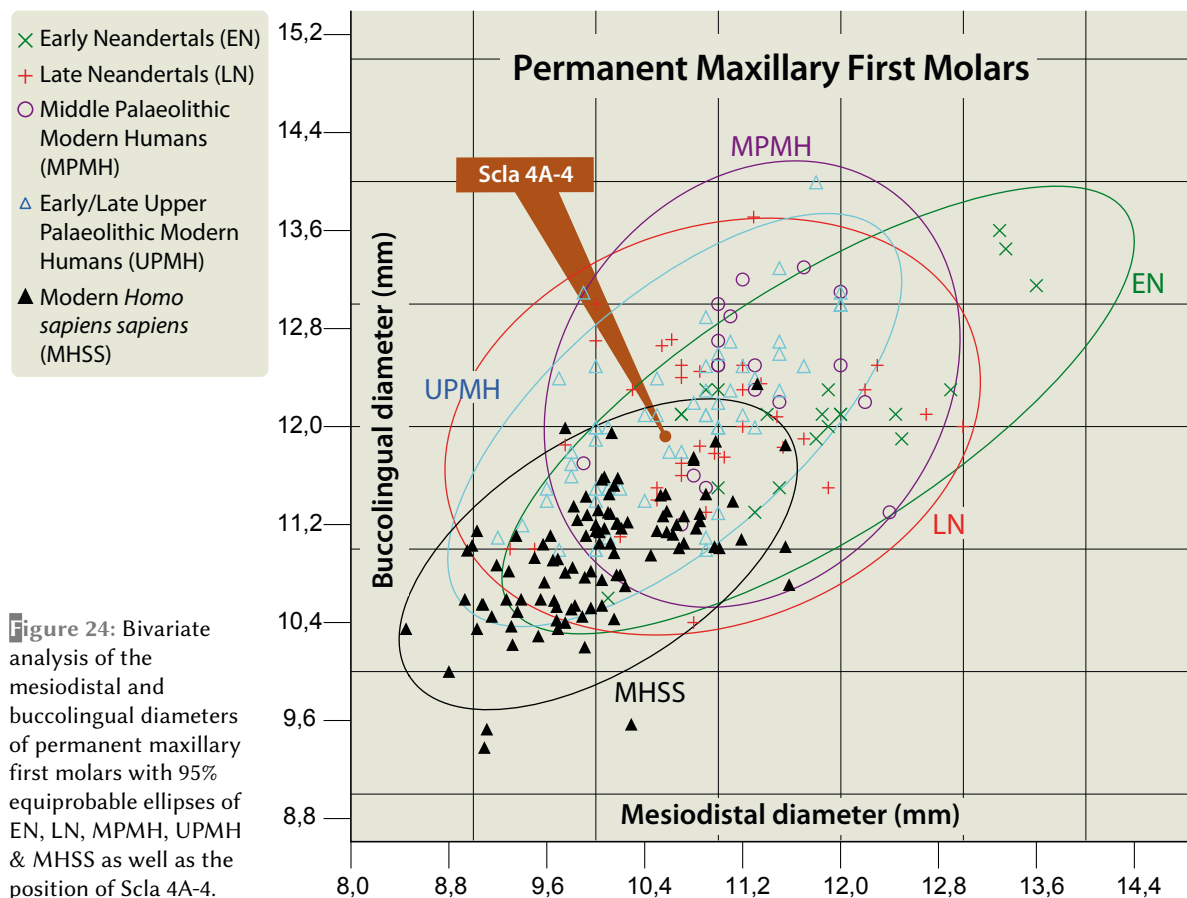
The fossil is well preserved, despite the presence of numerous vertical cracks. The crown is

Table 19: Scla 4A-4 (permanent maxillary right first molar): MD and BL dimensions compared to those of Early and Late Neandertals as well as MPMH, UPMH and MHSS, with DP and ECRA.

Scladina	Diameter	Value
RM ¹ (Scla 4A-4)	MD	10.57
	BL	11.92

Comparison Samples	N	Diameter	Mean	Stand. Dev.	DP	ECRA
EN right & left	21	MD	11.817	0.949	0.204	-0.630
	21	BVL	12.133	0.671	0.754	-0.152
LN right & left	36	MD	11.008	0.884	0.623	-0.244
	37	BL	12.052	0.667	0.845	-0.097
MPMH right & left	19	MD	11.268	0.594	0.255	-0.559
	18	BL	12.344	0.655	0.526	-0.307
UPMH right & left	59	MD	10.644	0.731	0.920	-0.051
	60	BL	12.038	0.668	0.860	-0.089
MHSS right & left	102	MD	10.020	0.651	0.401	0.425
	103	BL	10.988	0.593	0.119	0.793





not completely erupted and is nearly unworn (grade 1 of MOLNAR, 1971). About half of each root is formed (max length: 7 mm). No pathological condition has been observed.

In occlusal view, this M² exhibits a skewed rhomboidal shape. Its occlusal surface is very complex. It is a crenulated tooth characterized by four main cusps and some accessory cusps, fissures, and crests. Its shape is slightly different from that of the Scla 4A-4 M¹ as its distal outline is not as rounded but is more transversal due to a slightly more important metacone (cusp 3). In occlusal view, the protocone (cusp 1) exhibits an essential crest descending from its tip (Figure 25c: no. 1). Three other essential crests (no. 2-4) are present on the mesial marginal ridge: the most lingual one (no. 2) originates from the slope of the protocone and the most buccal one (no. 4) emanates from the mesial accessory tubercle. The paracone (cusp 2) has two essential crests (no. 5-6). The metacone has three crests, an essential one on its tip and an accessory one on each side descending from very small accessory cusps (no. 7-9). It is separated from the hypocone

(cusp 4) by a quite deep groove which runs mesio-lingually. The metacone (cusp 3) is slightly more developed than on the M¹ (ASUDAS, grade 5). The distolingual corner of the tooth exhibits two cusplets: the hypocone itself and a more distal cusp 5 (metaconule). Two other small accessory cusps are between the protocone and the hypocone: one on the middle of the lingual border of the occlusal surface and another one more internal (no. 10).

In mesiolingual view, the protocone (cusp 1) has tiny subvertical smooth grooves on the limit of its mesial and lingual surfaces; it is a slightly individualized expression of the tubercle of Carabelli (ASUDAS, grade 1). The paracone (cusp 2) does not have a parastyle.

Scla 4A-3 has three roots. The lingual root is oval in shape; its length is 5.6 mm; its opening, whose main axis is mesiolingual to distobuccal, is 5.5 × 3.7 mm. The mesiobuccal and distobuccal roots are fused near the cervix but can be distinguished as they are separated by a buccal groove. Their irregular opening is 7.5 mm buccolingually and 6.4 mm mesiodistally.

Permanent Maxillary Right Second Molar Scla 4A-3

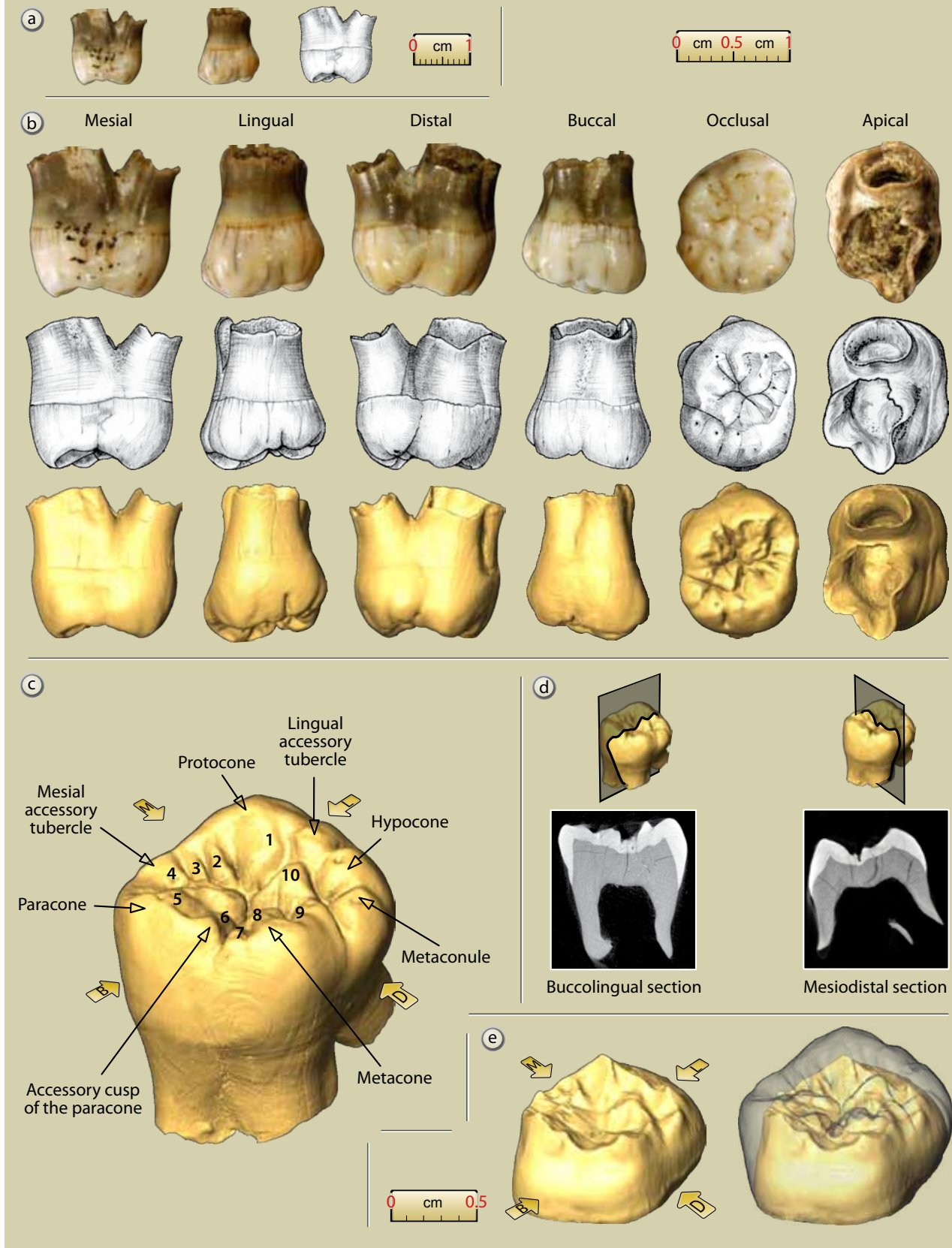


Figure 25: Scla 4A-3 permanent maxillary right second molar: a. mesial and lingual views (1:1 scale); b. photographs, drawings and 3D reconstructions of the six faces of the tooth (2:1 scale); c. 3D reconstruction with main anatomical features; d. internal sections; e. 3D lingual views at the EDJ without and with enamel (micro-CT data processing and graphics J.-F. Lemaire, SPW; pencil drawings S. Lambermont, AWEM; photographs J. Eloy, AWEM).



3.11.2. Taxonomy

The morphology of the Neandertal M² is complex (Table 20; BAILEY, 2002^a, 2002^b, 2004, 2006^a). The Neandertal M² possesses four developed main cusps; indeed, the hypocone is usually well developed. Cusp 5 is frequent (two thirds), as is Carabelli’s trait (50%). There are accessory cusps deriving from the mesial marginal ridge (100%). The Scla 4A-3 second maxillary molar presents all these Neandertal traits.

3.11.3. Morphometric analysis

Measurements of the Scla 4A-3 permanent maxillary second molar are as follows:

- MD: 10.21 mm
- BL: 12.60 mm
- MD at the cervix: 8.9 mm
- BL at the cervix: 12.4 mm
- Length of the tooth: 13.1 mm

The MD diameter of Scla 4A-3 does not depart significantly from the average of any of the five comparative samples (EN, LN, MPMH, UPMH & MHSS), both in regard to the DP probabilistic distance and ECRA. On the contrary, Scla 4A-3 departs from the MHSS sample as far as the BL diameter is concerned

(Table 21). When both diameters of Scla 4A-3 are situated on equiprobable ellipses (95%) they are in an area where all these taxa overlap, even if close to the upper limit of the BL diameter of MHSS (Figure 26). Like for all incisors, canines, premolars and M¹, this indicates that the dimensions of the crown of the permanent maxillary second molar provide only limited taxonomic indications.

3.12. Permanent maxillary right third molar, RM³

Palaeoanthropological identification: Scla 4A-8
Field identification: Sc 1995-286-7-1
Date of discovery: 14 July 1995
Date of identification: 14 July 1995
Square: C32
Stratigraphic position:
 – Former stratigraphy: 4A
 – New stratigraphy: Unit 4A-POC (Unit 4A-CHE), Layer 4A-LEG (Layer 4A-JA)

3.12.1. Description (Figure 27)

The germ of this permanent maxillary right third molar was immediately recognized as human on the day of the discovery. When the child was alive

Permanent Maxillary Second Molars	Non-Neandertal Archaics	Neandertals	Early Modern Afro-Asians	Early Modern Europeans	Scla 4A-3
Distal accessory cusplet (5)	100%	68.2%	50%	38.9%	yes
Carabelli's trait	66.7%	50%	14.3%	15.8%	yes
Mesial accessory cusps	100%	100%	50%	12.5%	yes
Hypocone reduction	0%	6%	0%	15%	no

Table 20: Distinctive anatomical features on permanent maxillary second molars of Non-Neandertal Archaics, Neandertals, Early Modern Humans (after BAILEY, 2006^a) and Scla 4A-3.

Table 21: Scla 4A-3 (permanent maxillary right second molar): MD and BL dimensions compared to those of Early and Late Neandertals as well as MPMH, UPMH and MHSS, with DP and ECRA.

Scladina	Diameter	Value
RM ² (Scla 4A-3)	MD	10.21
	BL	12.6

Comparison Samples	N	Diameter	Mean	Stand. Dev.	DP	ECRA
EN right & left	26	MD	10.979	1.096	0.490	-0.341
	26	BL	12.444	0.830	0.853	0.091
LN right & left	30	MD	10.521	0.830	0.711	-0.183
	30	BL	12.474	0.981	0.898	0.063
MPMH right & left	13	MD	10.454	1.074	0.824	-0.104
	12	BL	12.242	0.502	0.490	0.324
UPMH right & left	56	MD	10.154	0.838	0.947	0.034
	56	BL	12.175	0.866	0.626	0.245
MHSS right & left	100	MD	9.202	0.678	0.141	0.749
	100	BL	11.148	0.671	0.033	1.091

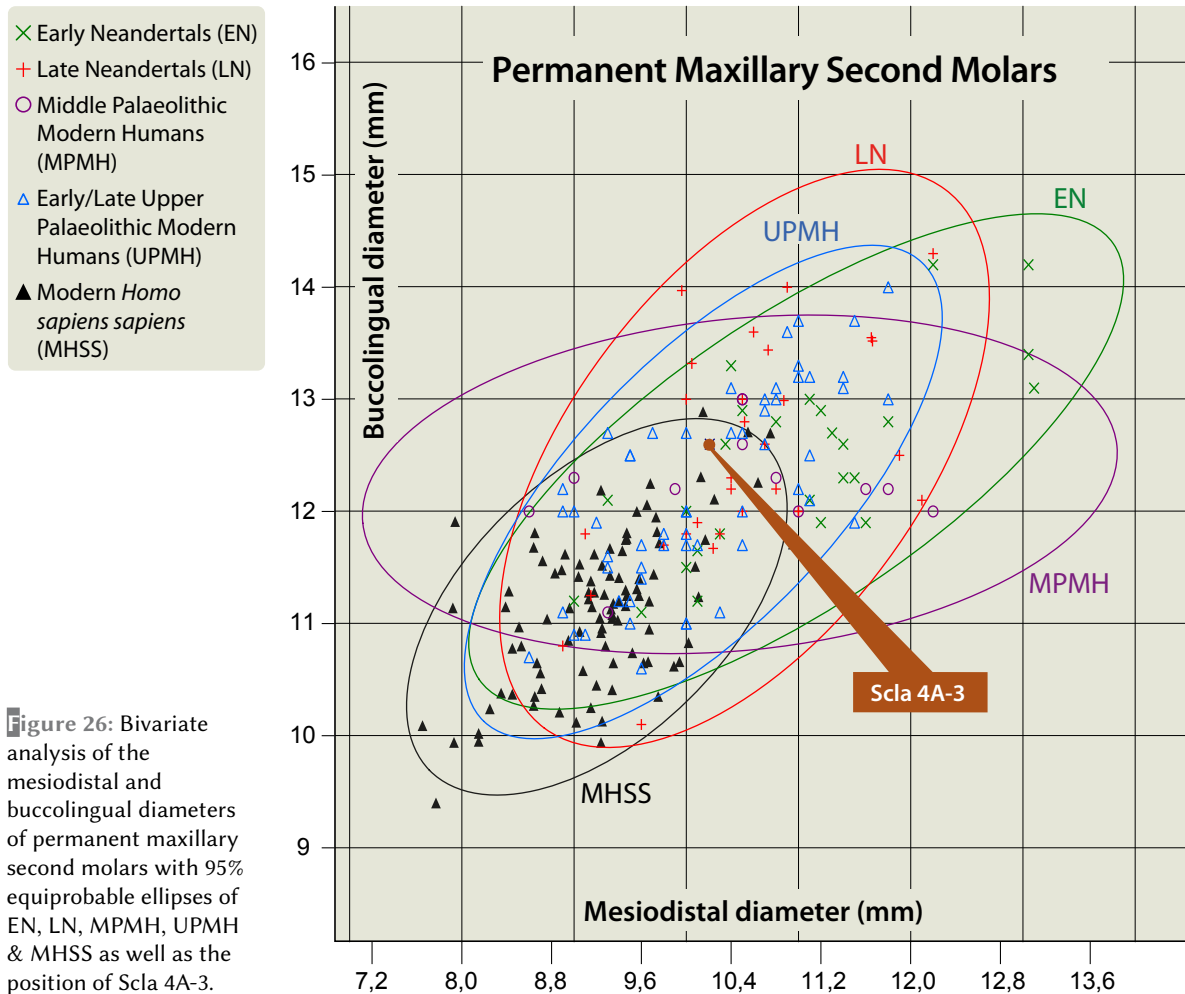


Figure 26: Bivariate analysis of the mesiodistal and buccolingual diameters of permanent maxillary second molars with 95% equiprobable ellipses of EN, LN, MPMH, UPMH & MHSS as well as the position of Scla 4A-3.

the tooth was still in its crypt; it was lost post-mortem. The crown is nearly completely formed and is unworn. It is well preserved, despite numerous vertical cracks. No root is yet formed. No pathological conditions are noted.

In occlusal view, this M^3 exhibits a complex morphology around a central fovea. The crown is crenulated and characterized by numerous cusps, fissure, and crests. It is skewed and has a rhomboidal shape. The protocone and the paracone are the highest cusps.

The paracone (cusp 2) exhibits three crests: mesial (Figure 27c: no. 1), essential (no. 2) and distal (no. 3). A faint groove on its buccal surface corresponds to stage 1 of the parastyle ASU UM plaque of ASUDAS.

The protocone (cusp 1) has 2 crests, essential (no. 6), and distal (no. 7). Lingually to the distal crest of the protocone and distally to the protocone itself is a small rounded independent cusplet. Two ridges originate from the mesial marginal ridge: a small buccal one (no. 4) which joins the

essential ridge of the paracone and a central one (no. 5) descending from a very faint mesial accessory tubercle (SCOTT & TURNER, 1997: 46).

The distal marginal ridge exhibits three small, low cusplets. The one at the limit of the lingual and distal faces seems to correspond to a reduced hypocone. The more distal one could be cusp 5 (metaconule; ASUDAS, grade 3) and the more buccal one a reduced metacone.

3.12.2. Taxonomy

The Neandertal M^3 presents a complex occlusal morphology with a hypocone that is often reduced (two thirds) or nearly absent (Table 22; BAILEY, 2006^a). Frequently, the mesial marginal ridge has accessory cusps (two thirds). Cusp 5 may also be present (one third). Carabelli's trait is less frequent (14%) than on M^1 and M^2 . Scla 4A-8 has a complex morphology, notably a reduced hypocone, a cusp 5 and an accessory cusp on its mesial marginal ridge.



Permanent Maxillary Right Third Molar Scla 4A-8

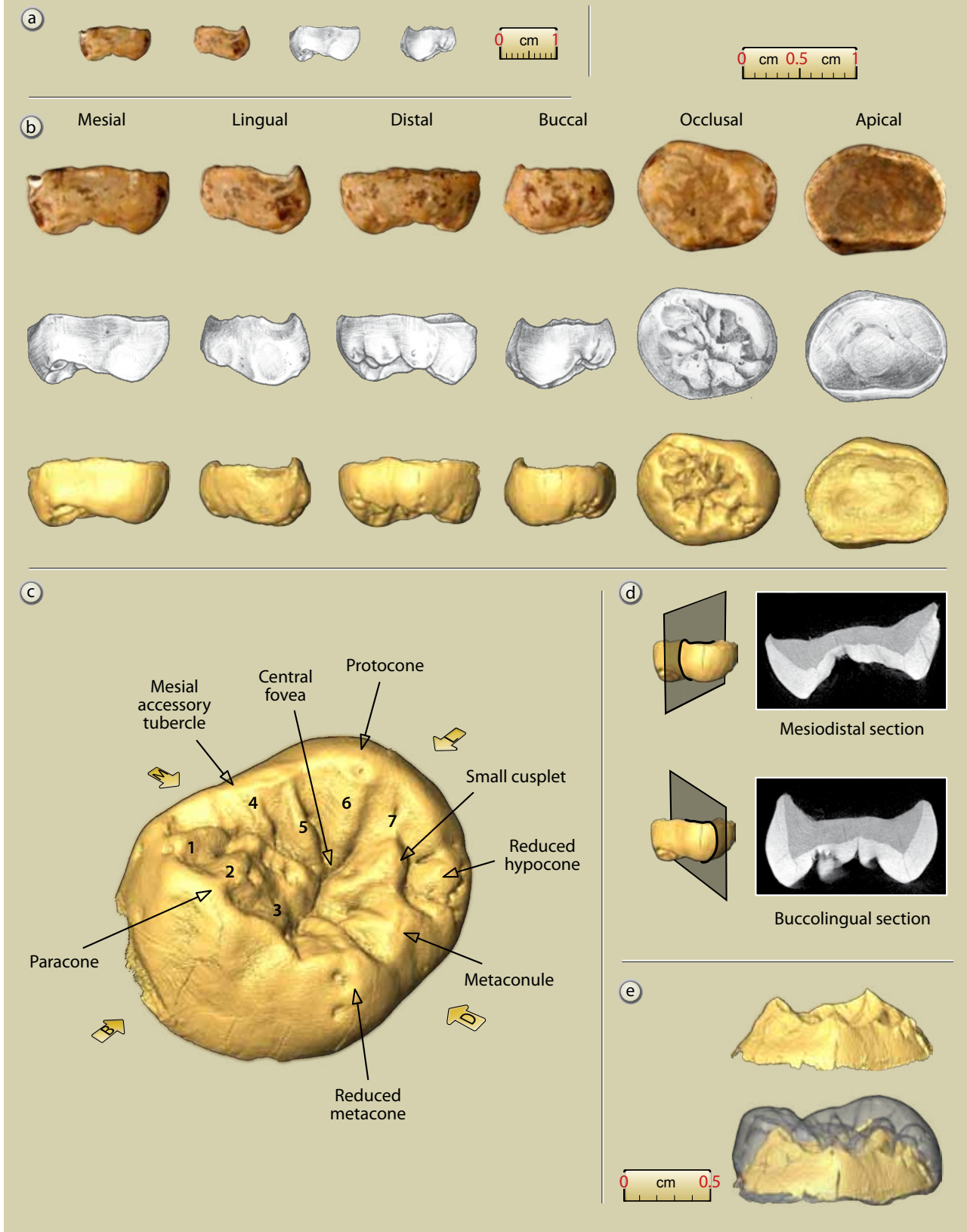


Figure 27: Scla 4A-8 permanent maxillary right third molar: a. mesial and lingual views (1:1 scale) ; b. photographs, drawings and 3D reconstructions of the six faces of the tooth (2:1 scale); c. 3D reconstruction with main anatomical features; d. internal sections; e. 3D lingual views at the EDJ without and with enamel (micro-CT data processing and graphics J.-F. Lemaire, SPW; pencil drawings S. Lambermont, AWEM; photographs J. Eloy, AWEM).

Permanent Maxillary Third Molars	Non-Neandertal Archaics	Neandertals	Early Modern Afro-Asians	Early Modern Europeans	Scla 4A-8
Distal accessory cusplet	100%	35.3%	33.3%	28.6%	yes
Carabelli's trait	0%	14.3%	0%	25.0%	yes
Mesial accessory cusps	-	70%	100%	27.5%	yes
Hypocone reduction	0%	68.4%	25.0%	57.1%	yes

Table 22: Distinctive anatomical features on permanent maxillary third molars of Non-Neandertal Archaics, Neandertals, Early Modern Humans (after BAILEY, 2006^a) and Scla 4A-8.

3.12.3. Morphometric analysis

Measurements of the Scla 4A-8 permanent maxillary right second molar are as follows:

MD: 9.55 mm
BL: 12.20 mm

The MD and BL diameters of Scla 4A-8 do not depart significantly from the average of any of the five comparison samples (EN, LN, MPMH, UPMH & MHSS), both in regard to the DP probabilistic distance and ECRA (Table 23). When both diameters are situated on equiprobable ellipses (95%) they are in an area where all these five taxa overlap (Figure 28). Like for all incisors, canines, premolars and UM¹ and UM², this indicates that the dimensions of the crown of the permanent maxillary third molar do not frequently provide clear taxonomic indications.

3.13. Deciduous maxillary right first molar, Rdm¹

Palaeoanthropological identification: Scla 4A-7
Field identification: Sc 1991-574-11
Date of discovery: 12 November 1991
Date of identification: October 1993
Square: F27

Stratigraphic position:

- **Former stratigraphy:** 4A
- **New stratigraphy:** Units 4A-CHE or 4A-POC (units 4A-IP, 3-INF)

3.13.1 Description (Figure 29)

This deciduous upper molar consists of a complete crown with roots affected by partial resorption, but preserved for slightly more than the cervical third. The crown is quite heavily worn (MOLNAR, 1971, stage 4); its wear is very close to that of the right dm¹ of La Quina 18 (Figure 30) and, to a lesser extent, of the left dm¹ of La Quina 18. The enamel is vertically cracked over all its surfaces. No pathological conditions are noted.

The wear of the occlusal surface makes an accurate description difficult. Four cusps (paracone, protocone, hypocone and metacone) are present. The surface is crossed by some bridges of enamel, one joining the protocone and the metacone and another the protocone and hypocone. Between these bridges are six dentine areas of varying dimension. The cusp tips are internally compressed. The paracone is the biggest and the highest cusp.

The tooth exhibits a strong cingulum bulge near the crown base and, on its buccal face,

Scladina		Diameter	Value			
RM ³ (Scla 4A-8)		MD	9.55			
		BL	12.2			
Comparison Samples	N	Diameter	Mean	Stand. Dev.	DP	ECRA
EN right & left	21	MD	10.069	0.773	0.510	-0.322
	19	BL	12.121	0.868	0.929	0.043
LN right & left	22	MD	9.437	0.594	0.851	0.092
	21	BL	12.026	1.224	0.888	0.068
MPMH right & left	10	MD	9.440	0.631	0.865	0.077
	9	BL	12.089	0.891	0.904	0.054
UPMH right & left	36	MD	9.312	0.936	0.801	0.125
	37	BL	11.581	1.141	0.591	0.268
MHSS right & left	91	MD	8.616	0.659	0.160	0.714
	91	BL	10.693	0.818	0.069	0.928

Table 23: Scla 4A-8 (permanent maxillary right third molar): MD and BL dimensions compared to those of Early and Late Neandertals as well as MPMH, UPMH and MHSS, with DP and ECRA.



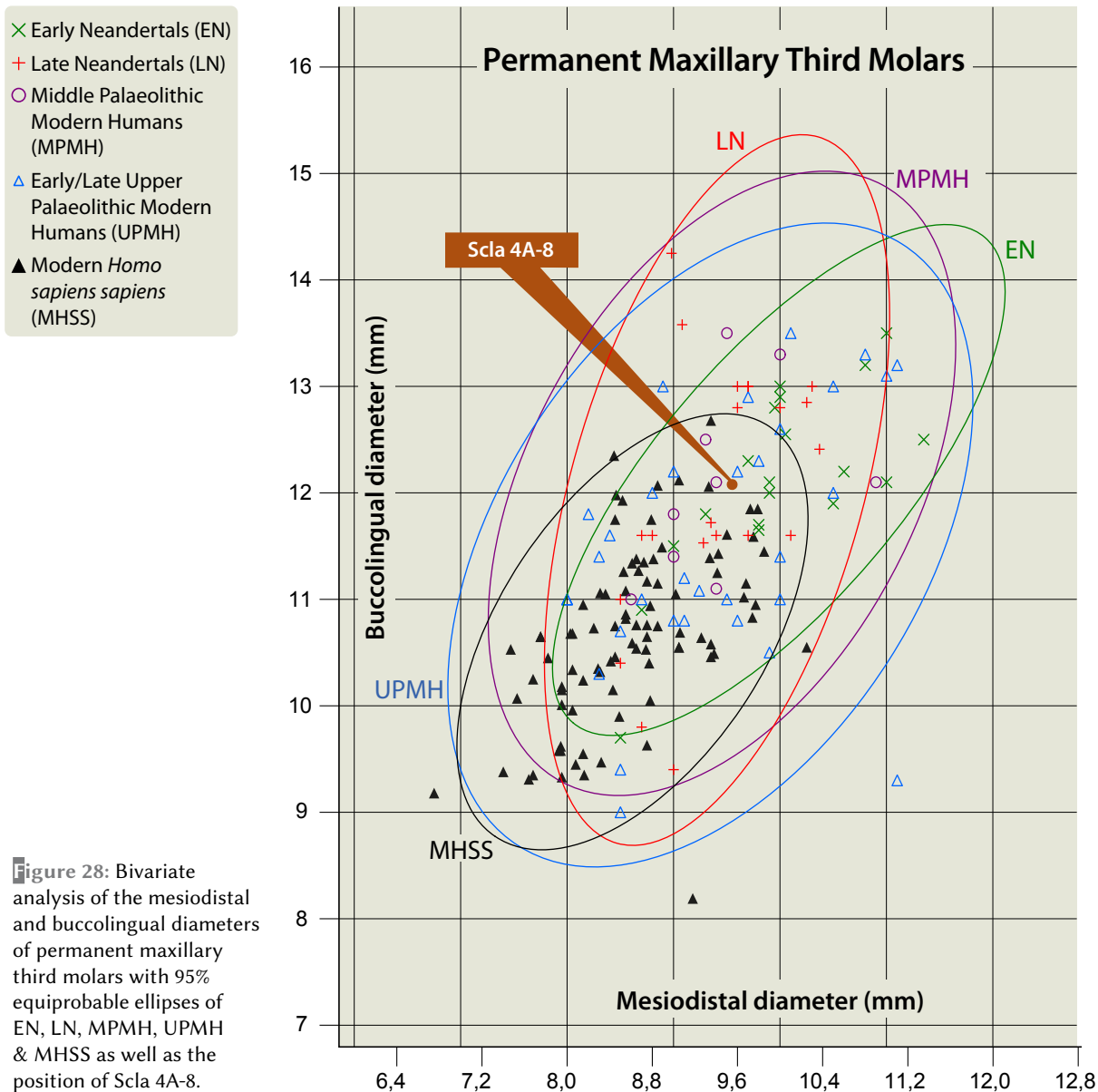


Figure 28: Bivariate analysis of the mesiodistal and buccolingual diameters of permanent maxillary third molars with 95% equiprobable ellipses of EN, LN, MPMH, UPMH & MHSS as well as the position of Scla 4A-8.

3.13.2. Taxonomy

a pronounced mesiobuccal cingulum projection at the base of the paracone: the paramolar tubercle (*tuberculum molare* or parastyle). The protocone does not exhibit a Carabelli trait.

Interproximal wear facets are present on both the mesial and distal surfaces. In occlusal view, they affect the outline of the crown. The mesial side has a slight ripple parallel to its lower edge, highlighted by a breaking of the edge of the buccal side. There seems to have been two successive facets, one for the deciduous canine and the other for the permanent canine that is superimposed over the first.

Most Neandertal dm's have four cusps (Châteauneuf, Subalyuk, Shanidar 7, Grotte du Renne 34, Gibraltar II). Early Modern Middle Palaeolithic Humans are variable: four at Skhul I but three at Qafzeh 4 (BAILEY & HUBLIN, 2006; TILLIER, 1979). Upper Palaeolithic and MHSS dm's have usually two or three cusps; these teeth are more premolar-like than those of Neandertals. It has been reported (BAILEY & HUBLIN, 2006) that the presence of Carabelli's structure would be diagnostic as such a trait would be absent in MHSS dm's. Scla 4A-7 has four cusps but no Carabelli trait.

Deciduous Maxillary Right First Molar Scla 4A-7

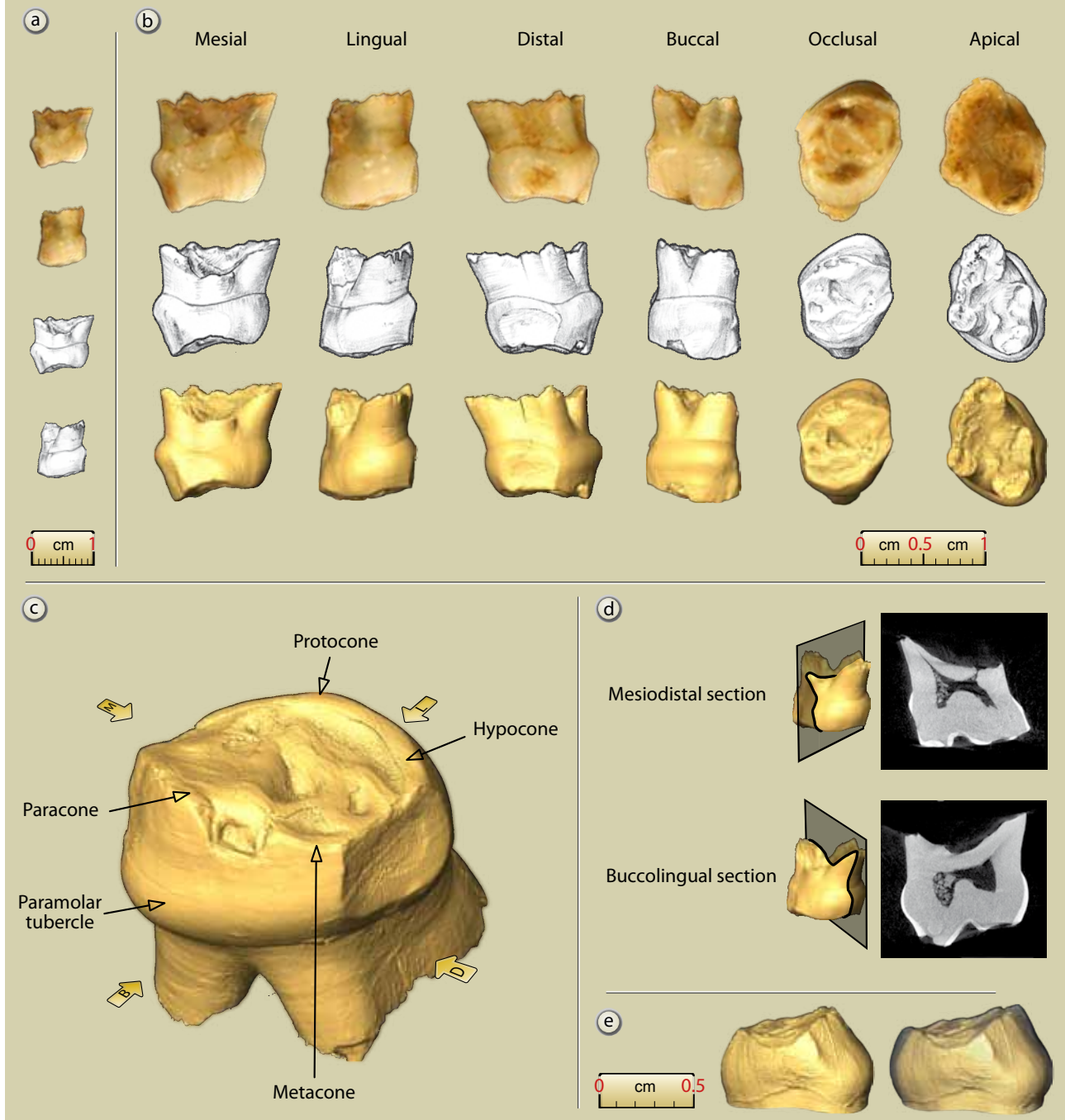


Figure 29: Scla 4A-7 deciduous maxillary right first molar: a. mesial and lingual views (1:1 scale); b. photographs, drawings and 3D reconstructions of the six faces of the tooth (2:1 scale); c. 3D reconstruction with main anatomical features; d. internal sections; e. 3D lingual views at the EDJ without and with enamel (micro-CT data processing and graphics J.-F. Lemaire, SPW; pencil drawings S. Lambermont, AWEM; photographs J. Eloy, AWEM).

Figure 30. Comparison of the wear of maxillary right dm^1 , dm^2 and M^1 of Scladina I-4A (below) and La Quina 18 (above): original specimens.



3.13.3. Morphometric analysis

Measurements of the Scla 4A-7 deciduous maxillary right first molar are as follows:

- MD: 7.52 mm
- BL: 9.29 mm
- MD at the cervix: 6.33 mm
- BL at the cervix: 8.65 mm

The MD diameter of Scla 4A-7 departs significantly from the average of the MPMH comparative sample, only in regard to the DP probabilistic distance, but the samples are very small. The BL diameter does not depart from any of the comparative samples (Table 24). When both diameters of Scla 4A-7 are situated on equiprobable ellipses (95%) they are in an area where Neandertals, Upper Palaeolithic Modern Humans (UPMH) and MHSS overlap

Scladina	Diameter	Value
Rdm ¹ (Scla 4A-7)	MD	7.52
	BL	9.29

Table 24: Scla 4A-7 (deciduous maxillary right first molar): MD and BL dimensions compared to those of Neandertals as well as MPMH, UPMH and MHSS, with DP and ECRA.

Comparison Samples	N	Diameter	Mean	Stand. Dev.	DP	ECRA
Neandertals	17	MD	7.84	0.43	0.468	-0.351
	17	BL	9.14	0.4	0.713	0.177
MPMH	4	MD	8.6	0.23	0.018	-1.475
	4	BL	9.16	0.51	0.815	0.004
UPMH	17	MD	7.37	0.6	0.806	0.118
	16	BL	9.15	0.77	0.858	0.085
MHSS	99	MD	7.1	0.61	0.493	0.347
	100	BL	8.55	0.56	0.189	0.666

- + Neandertals (NE)
- Middle Palaeolithic Modern Humans (MPMH)
- △ Early/Late Upper Palaeolithic Modern Humans (UPMH)
- ▲ Modern *Homo sapiens sapiens* (MHSS)

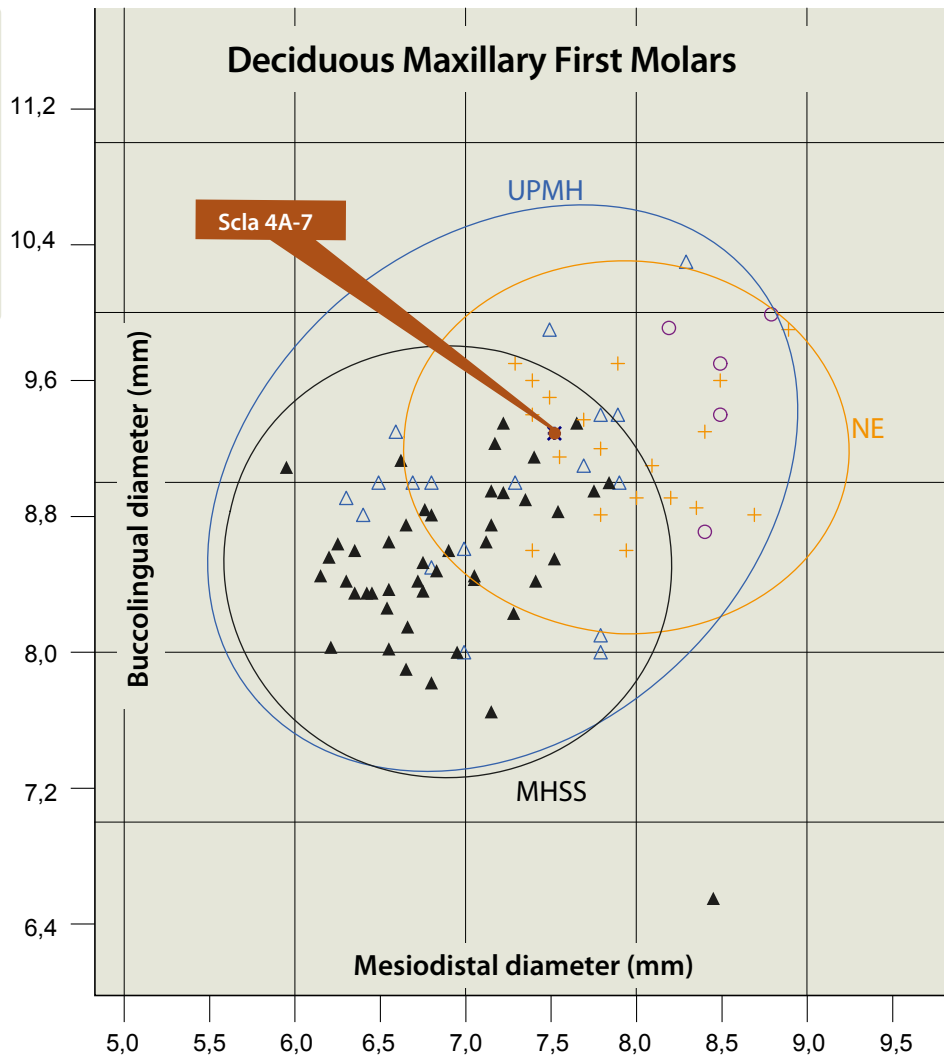


Figure 31: Bivariate analysis of the mesiodistal and buccolingual diameters of deciduous maxillary first molars with 95% equiprobable ellipses of NE, UPMH & MHSS as well as the position of Scla 4A-7.

(Figure 31). This indicates that the dimensions of the crown of the deciduous maxillary first molar do not provide clear taxonomic indications.

3.14. Deciduous maxillary right second molar, Rdm²

Palaeoanthropological identification: Scla 4A-5

Field identification: Sc 1990-81-46

Date of discovery: 13 March 1990

Date of identification: October 1993

Square: G27

Stratigraphic position:

- **Former stratigraphy:** 4A
- **New stratigraphy:** units 4A-POC or 3-INF (units 4A-IP, 4A-CHE, 3-SUP)

3.14.1. Description (Figure 32)

This tooth consists of a complete crown. The mesiobuccal root is complete, but the lingual and distobuccal roots are incomplete, due to the beginning of resorption. The enamel is vertically cracked over all its surfaces. No pathological conditions are noted.

The occlusal outline of the tooth, which has four large main cusps, is rhomboidal; the distal cusps (especially the metacone) are placed lingually relatively to the mesial cusps (paracone and protocone). The crown is slightly worn (MOLNAR, 1971, stage 2-3), which prevents a detailed description of the details of the occlusal basin.

The protocone is the largest cusp. It does not have Carabelli's cusp. A well-developed *crista obliqua* connects the protocone and metacone. Another crest connects the metacone and the mesial part of the hypocone. The hypocone is larger than the metacone.

The lingual surfaces exhibit a vertical groove between the protocone and the hypocone. On the buccal surface is a similar, but incomplete, groove separating the paracone and the metacone.

There is a large distal interproximal wear facet in the middle of the distal face of the crown: 3.9 mm in width × 2.25 mm in height. A small mesial interproximal wear facet occurs on the lingual part of the mesial face of the crown.

The tooth has three divergent roots, the buccal-distal and the lingual ones being incomplete, due to the erupting P⁴. The section of the lingual root is slightly C-shaped while the sections of both the buccal roots are 8-shaped.

3.14.2. Taxonomy

The dental morphology of the Neandertal second deciduous maxillary molar is similar to that of the permanent M¹ (TILLIER, 1979; BAILEY & HUBLIN, 2006), i.e. four main cusps, metacone mesially and lingually orientated, hypocone larger than metacone and sometimes a large Carabelli's cusp. The Scla 4A-5 deciduous molar is similar to this Neandertal pattern, except for the absence of Carabelli's structure.

3.14.3. Metrics

Measurements of the Scla 4A-5 deciduous maxillary right second molar are as follows:

MD: 8.83 mm

BL: 10.29 mm

MD at the cervix: 7.3 mm

BL at the cervix: 9.4 mm

Length of the tooth: 13.6 mm

The MD and BL diameters of Scla 4A-5 do not depart significantly from the average of any of the five comparative samples (Neandertals, MPMH, UPMH & MHSS), in regard to both the DP probabilistic distance and ECRA (Table 25). When both MD and BL crown diameters of Scla 4A-5 are situated on equiprobable ellipses (95%) they are in an area where Neandertals, Upper Palaeolithic Modern Humans and MHSS overlap (Figure 33). This indicates that the dimensions of the crown of the deciduous maxillary second molar do not often provide clear taxonomic indications, especially in the case of Scla 4A-5.

3.15. Permanent mandibular first molars, M₁

3.15.1. Description

Permanent mandibular right first molar, RM₁, (Figure 34)

Palaeoanthropological identification:

Scla 4A-1/M₁ (as part of the right hemimandible)

Field identification: Sc 1993-148-185

Date of discovery: 16 July 1993

Date of identification: 20 July 1993

Square: D29

Stratigraphic position:

- **Former stratigraphy:** 4A
- **New stratigraphy:** Unit 4A-CHE, Layer 4A-GX



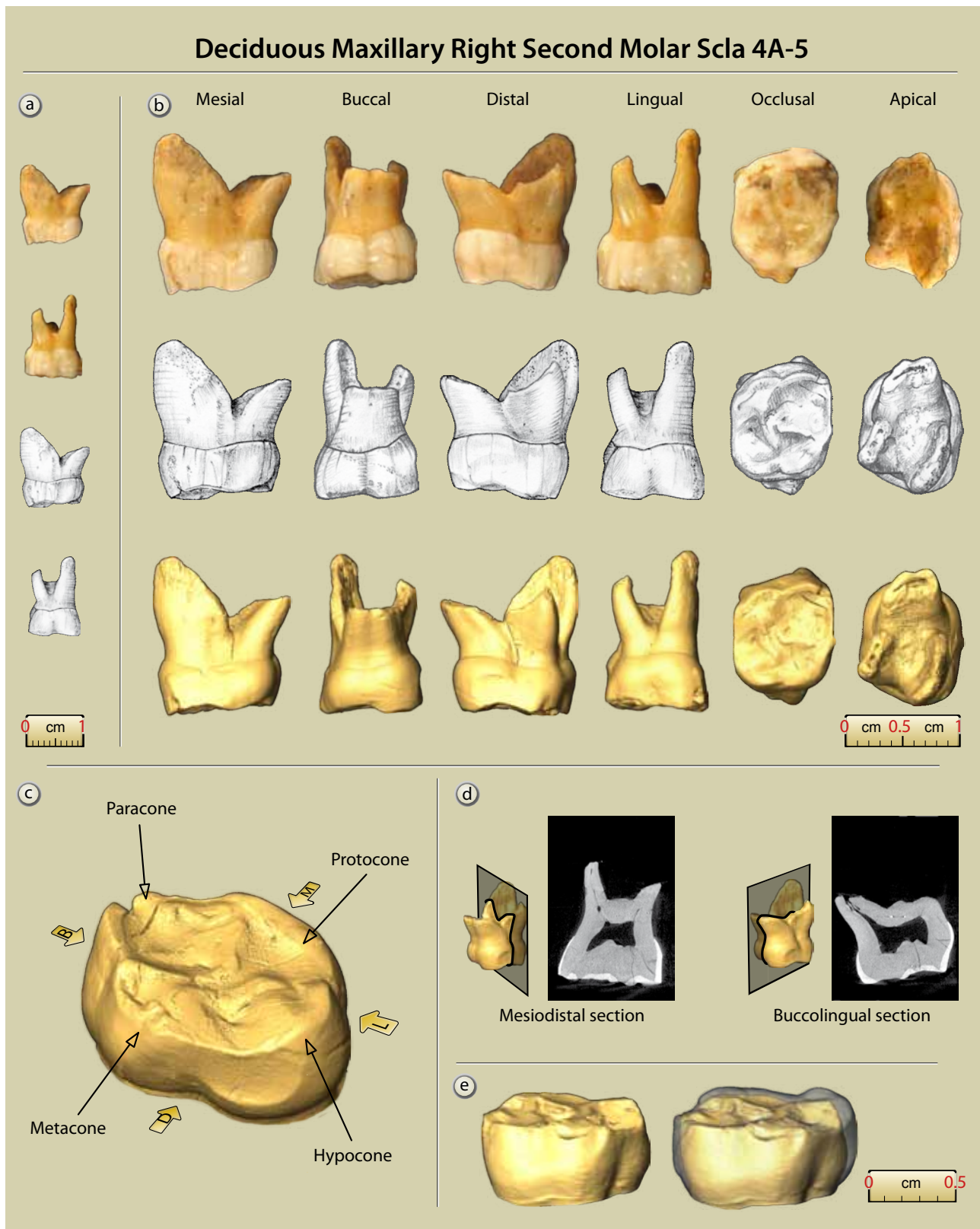


Figure 32: Scla 4A-5 deciduous maxillary right second molar: a. mesial and lingual views (1:1 scale); b. photographs, drawings and 3D reconstructions of the six faces of the tooth (2:1 scale); c. 3D reconstruction with main anatomical features; d. internal sections; e. 3D lingual views at the EDJ without and with enamel (micro-CT data processing and graphics J.-F. Lemaire, SPW; pencil drawings S. Lambermont, AWEM; photographs J. Eloy, AWEM).

Scladina	Diameter	Value
Rdm ² (Scla 4A-5)	MD	8.83
	BL	10.29

Table 25: Scla 4A-5 (deciduous maxillary right second molar): MD and BL dimensions compared to those of Neandertals as well as MPMH, UPMH and MHSS, with DP and ECRA.

Comparison Samples	N	Diameter	Mean	Stand. Dev.	DP	ECRA
Neandertals	17	MD	9.43	0.67	0.383	-0.422
	17	BL	10.26	0.58	0.959	0.024
MPMH	5	MD	9.58	0.36	0.105	-0.750
	5	BL	10.81	0.65	0.468	-0.288
UPMH	17	MD	9.14	0.73	0.676	-0.200
	16	BL	10.21	0.55	0.886	0.068
MHSS	47	MD	8.64	0.422	0.654	0.224
	47	BL	9.54	0.497	0.138	0.750

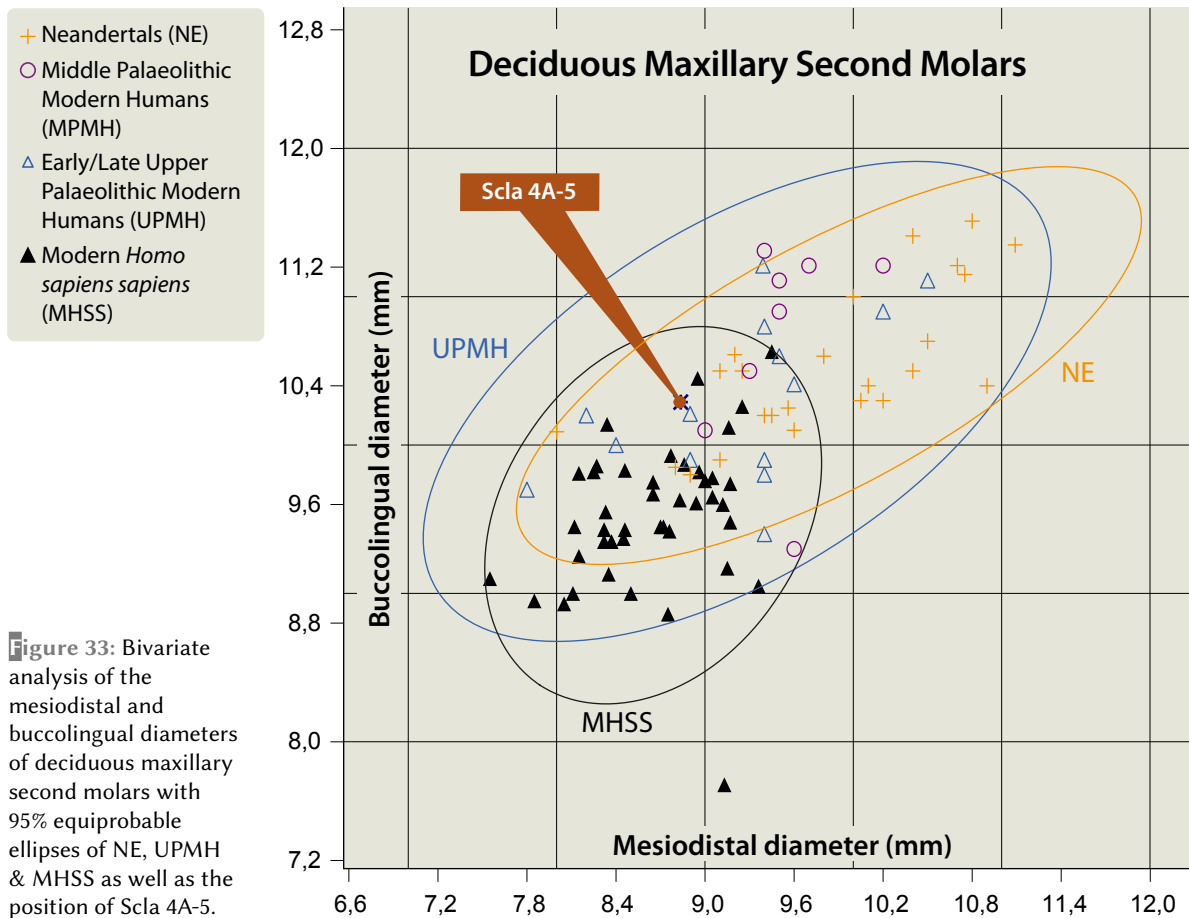


Figure 33: Bivariate analysis of the mesiodistal and buccolingual diameters of deciduous maxillary second molars with 95% equiprobable ellipses of NE, UPMH & MHSS as well as the position of Scla 4A-5.

This tooth, in situ in the Scla 4A-1 right half of the mandible, is completely erupted. Its crown was functional. Its roots are also completely formed with closed apices. No pathological conditions are noted. It is well preserved, except for vertically, and some horizontally, orientated microfractures on the crown.

The occlusal surface presents five cusps, arranged in a Y5 pattern. The protoconid (cusp 1, mesiobuccal) is the largest, followed by the

metaconid (cusp 2, mesiolingual) and entoconid (cusp 4, distolingual), then the hypoconid (cusp 3, centrobuccal), and the hypoconulid (cusp 5, distobuccal), which is the smallest (ASUDAS, grade 4). There is neither cusp 6 (*tuberculum sextum*/entoconulid) nor cusp 7 (*tuberculum intermedium*/metaconulid). Wear degree is nearly at stage 3 of MOLNAR (1971) with only extremely small dentine patches.



Permanent Mandibular Right First Molar Scla 4A-1/M₁

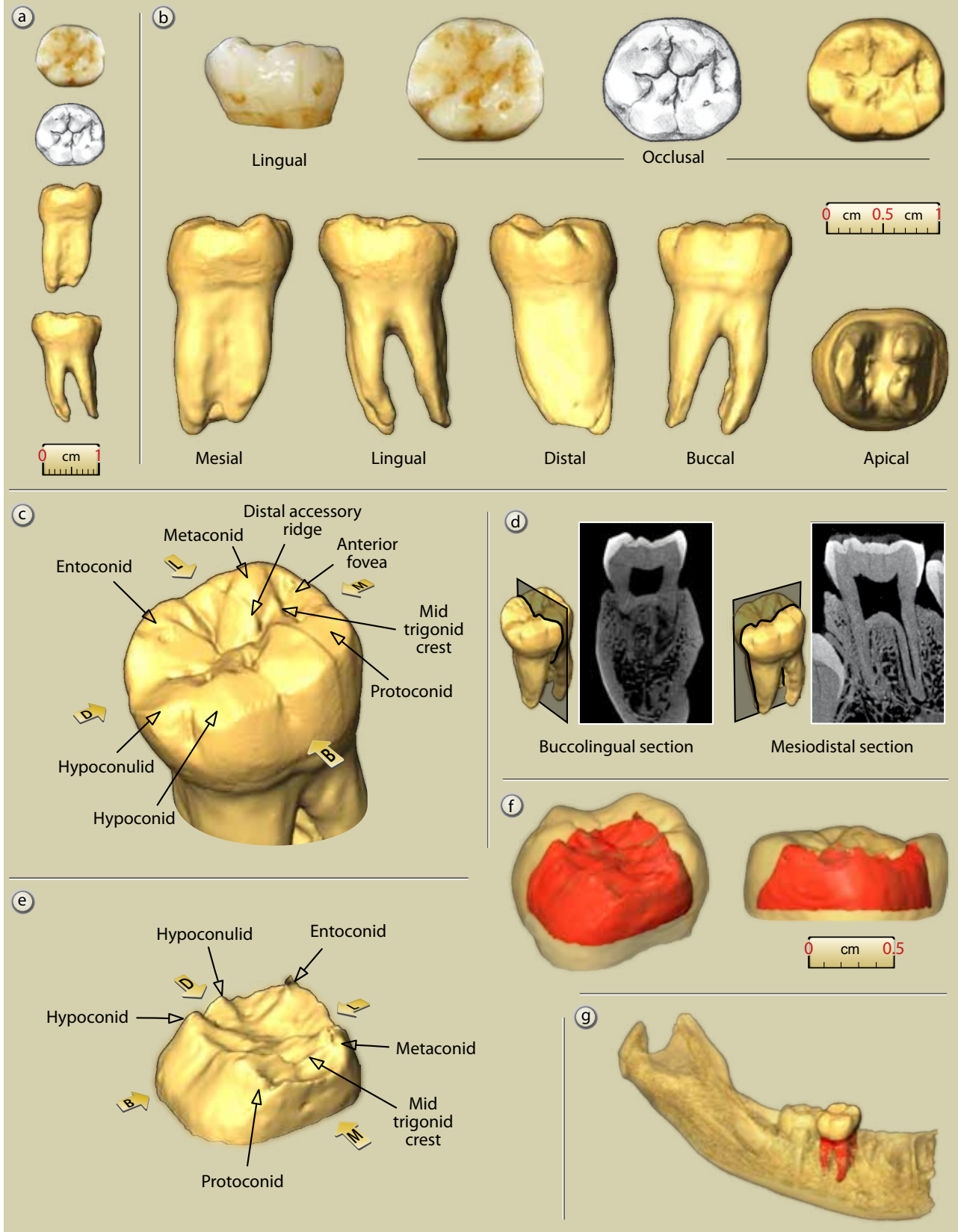


Figure 34: Scla 4A-1/M₁, permanent mandibular right first molar: a. occlusal, mesial and lingual views (1:1 scale); b. lingual and occlusal faces, photographs; occlusal face, drawing; 3D reconstruction of the six faces of the tooth (2:1 scale); c. 3D reconstruction with main anatomical features; d. internal sections; e. 3D reconstruction with main anatomical features at the EDJ; f. 3D views at the EDJ with enamel; g. position of the tooth (micro-CT data processing and graphics J.-F. Lemaire, SPW; pencil drawings S. Lambermont, AWEM; photographs J. Eloy, AWEM).

The mesial marginal ridge, delineating the mesial edge of the occlusal surface, exhibits a concave profile in anterior view. It does not have any clear mesial marginal accessory tubercle, just a tiny undulation in its center. Behind the mesial marginal ridge, the anterior fovea is transversal, wide and quite deep (ASUDAS, Anterior fovea LM₁, grade 4).

On the outer enamel surface (OES), the mid-trigonid crest (MTC; BAILEY, 2002^{a, b}) is continuous but is reduced at the level of the sagittal sulcus (BAILEY et al., 2011). Its distal slope is marked by an oblique groove toward the lingual side, corresponding to the front part of the sagittal sulcus. The MTC is formed by the junction of the essential/middle ridge of the protoconid and the mesial accessory ridge of the metaconid (see SKINNER et al., 2008). On the EDJ (enamel-dentine junction) surface, the MTC is also continuous but reduced at the sagittal sulcus; it has the same origin as the OES, i.e. on the middle lobe segment of the protoconid and the mesial lobe segment of the metaconid.

The protoconid exhibits a short and low distal accessory ridge on the OES and more clearly on the EDJ. It joins the mesial part of the essential crest of the metaconid, forming a faint and interrupted bridge.

The essential crest of the metaconid does not exhibit any clear angulation, or deflection, in its course towards the central occlusal fossa; so there is no real deflecting wrinkle (TURNER et al., 1991). The distal part of this essential crest of the metaconid joins, on the OES, that of the hypoconid, creating a Y pattern.

The protoconid lacks a true protostylid (as defined by the ASUDAS; TURNER et al., 1991: 24).

The hypoconid is well defined and separated from the adjacent protoconid and hypoconulid by marked grooves, both on the OES and the EDJ. The hypoconulid, which has one essential crest or wrinkle, is well separated from the entoconid on the OES and more strongly on the EDJ.

A mesial interproximal wear facet, measuring 2.6 mm in height × 3.2 mm in width, is present on the buccal half of the mesial face of the crown. Its inferior border is slightly concave; the angles between inferior and lateral borders are rounded. It does not have any subvertical grooves. In occlusal view, this facet slightly alters the outline of the crown. As the adjacent right M₂ was not at its final level at death, and as far as the 3D reconstruction visually allowed, there is no real distal interproximal facet. The cervix of Scla 4A-1/M₁ slightly dips in the middle of both the buccal and lingual sides.

This M₁ does not exhibit any degree of taurodontism. The mesial root is flattened, 8-shaped in cross-section, slopes distally, and curves behind its apex, where it is divided in two (bifurcated apically). Its mesial face exhibits a vertical groove. The distal root is also flattened, but C-shaped, and slopes distally but with a weaker groove and without apical division. The three apices are all closed.

Permanent mandibular left first molar, LM₁ (Figure 35)

Palaeoanthropological identification:

Scla 4A-9/M₁ (as part of the left hemimandible)

Field identification: Sc 1996-203-1

Date of discovery: 12 July 1996

Date of identification: 12 July 1996

Square: C28

— **Stratigraphic position:**

Former stratigraphy: 4A

— **New stratigraphy:** Unit 4A-CHE

(Unit 4A-POC), Layer 4A-JA (?)

The morphology of this permanent mandibular left first molar is very close to that of the corresponding right molar.

The tooth is in situ in the Scla 4A-9 left half of the mandible. It is completely erupted and has a functional crown. Its roots are also completely formed with closed apices. No pathological conditions are noted. It is well preserved, except for vertically, and some horizontally, orientated microfractures on the crown. Black spots of manganese are present, mainly on the occlusal surface.

Like its antimere, the occlusal surface has five cusps, arranged in an Y5 pattern. The protoconid (cusp 1) is the largest, followed by the metaconid (cusp 2) and entoconid (cusp 4), then the hypoconid (cusp 3), and the hypoconulid (cusp 5), which is the smallest (ASUDAS, grade 5). There is no cusp 6 (*tuberculum sextum*/entoconulid) or cusp 7 (*tuberculum intermedium*/metaconulid). Wear degree is at stage 3 of MOLNAR (1971) with only small dentine patches.

As in the right M₁, the mesial accessory crest of the metaconid and the essential crest of the protoconid form the MTC which is, on the OES, continuous but reduced at the sagittal sulcus (BAILEY, 2002^b, grade 2). On the EDJ surface, the MTC is nearly continuous. The essential crest of the metaconid does not present deflection. It joins the essential crest of the hypoconid, so that the



Permanent Mandibular Left First Molar Scla 4A-9/M₁

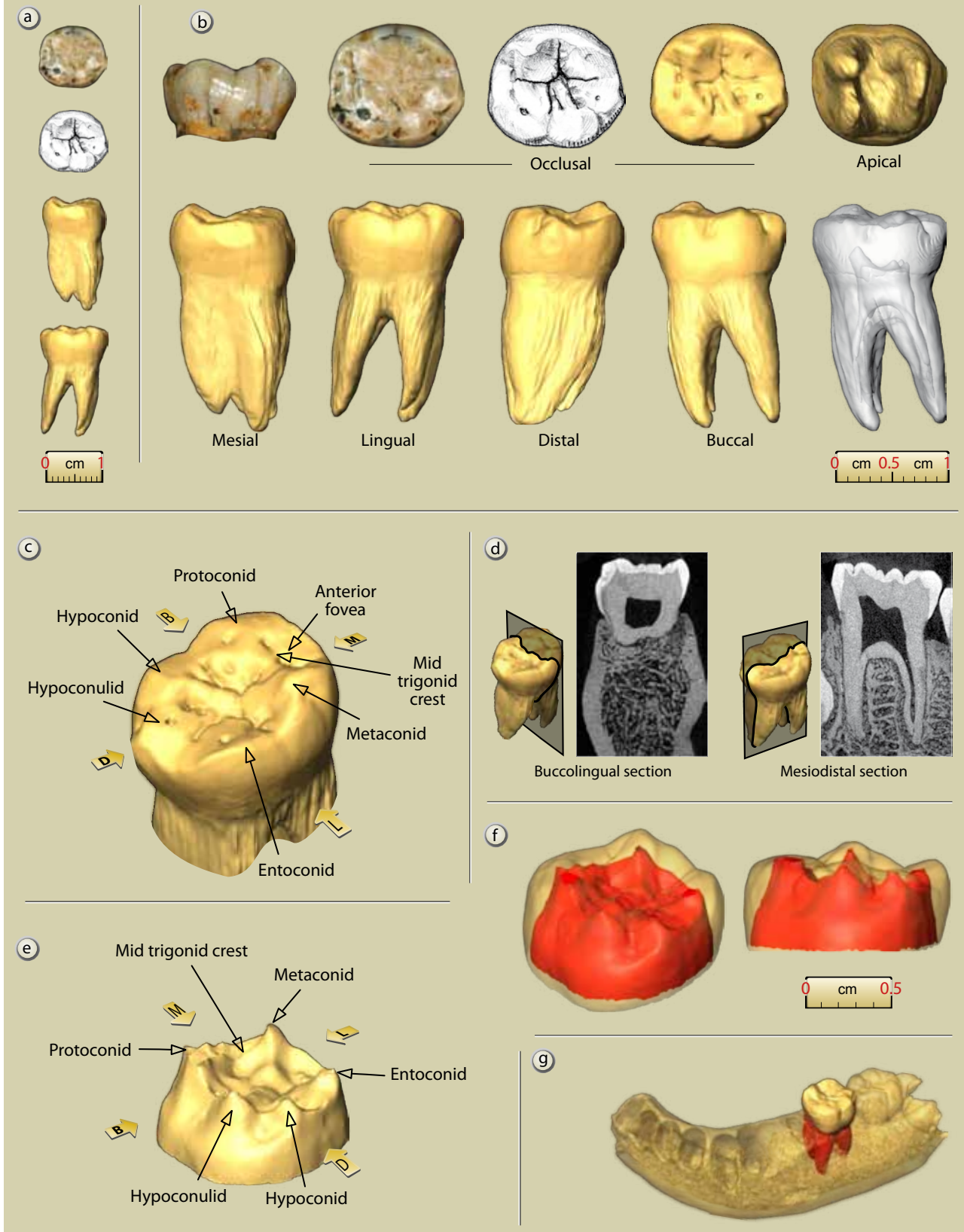


Figure 35: Scla 4A-9/M₁, permanent mandibular left first molar: a. occlusal, mesial and lingual views (1:1 scale); b. lingual and occlusal faces, photographs; occlusal face, drawing; 3D reconstruction of the six faces of the tooth (2:1 scale); c. 3D reconstruction with main anatomical features; d. internal sections; e. 3D reconstruction with main anatomical features at the EDJ; f. 3D views at the EDJ with enamel; g. position of the tooth (micro-CT data processing and graphics J.-F. Lemaire, SPW ; pencil drawings S. Lambermont, AWEM; photographs J. Eloy, AWEM).

Permanent Mandibular First Molars	Non-Neandertal Archaics	Neandertals	Early Modern Afro-Asians	Early Modern Europeans	Scla 4A-9/M ₁	Scla 4A-1/M ₁
Four cusps	0%	2%	0%	2.9%	no (5 cusps)	no (5 cusps)
Fissure pattern: Y	100%	97.3%	100%	92.9%	yes	yes
Anterior fovea	83.3%	88.6%	83.3%	52.6%	yes	yes
Mid-trigonid crest	71.4%	93.5%	20%	0%	yes	yes
Distal trigonid-crest	0%	3%	0%	4%	weak	weak
Deflecting wrinkle	0%	3.8%	75%	15.8%	no	no
Cusp 6	0%	36.4%	0%	18.2%	no	no
Cusp 7	0%	36.1%	50%	6.9%	no	no

Table 26: Distinctive anatomical features on permanent mandibular first molars of Non-Neandertal Archaics, Neandertals, Early Modern Humans (after BAILEY, 2006^a) and Scla 4A-9/M₁ & Scla 4A-1/M₁.

tooth has a Y pattern. No well defined distal trigonid crest is present.

A mesial interproximal wear facet can be observed, on the buccal half of the mesial face of the crown, like on the right M₁. Its general shape is similar but it can be divided into two parts, with a small superior subfacet on the buccal side. It does not have subvertical grooves. In occlusal view, the outline of the crown is only slightly affected. There is no clear distal interproximal facet.

In buccal view, there is a strong but short groove separating the protoconid and the hypoconid and a furrow between the hypoconid and hypoconulid. Like its antimere, the cervix of Scla 4A-9/M₁ slightly dips in the middle of both the buccal and lingual sides.

The left M₁ does not exhibit any degree of taurodontism. Its roots are very close to those of the right M₁. They are flattened and slope distally; the mesial one is 8-shaped and curves behind its apex, where it is divided in two. It exhibits a vertical groove. The distal root is C-shaped. The three apices are closed.

3.15.2 Taxonomy

Overall, the morphology of the Neandertal M₁s tend to be complex (BAILEY, 2002^b and Table 26, from BAILEY, 2006^a):

- Neandertal M₁s nearly always (98%) possess more than four cusps, like *Homo erectus* and Archaic *Homo sapiens*. A few Upper Palaeolithic amHS and contemporary humans may have, however in very low frequency, four cusps;
- Neandertal M₁s exhibit high frequencies of the Y-pattern but this feature is not specific to this taxon insofar as other human fossils and modern humans have almost similar percentages;

- some Neandertal M₁s exhibit an entoconulid (cusp 6) and a metaconulid (cusp 7), but in relatively low frequencies (BAILEY, 2002^b: 91, 93), which is within the ranges of contemporary amHS;
- Neandertal M₁s tend to possess a deep and wide anterior fovea (BAILEY, 2002^b), much outside the range of Early Modern Europeans, while *Homo erectus* and Archaic *Homo sapiens* are closer to Neandertals;
- The M₁s exhibit a well-developed bridge of enamel, the mid-trigonid crest (MTC), which joins the protoconid and metaconid, bordering distally the anterior fovea (BAILEY, 2002^b: 91–94; BAILEY & HUBLIN, 2006: 19). The Neandertal MTC is continuous. It is the most notable feature differentiating Neandertals from contemporary humans.

The first two mandibular molars of Scladina exhibit a deep and wide anterior fovea and a MTC, two typical characters of the Neandertal M₁ pattern. They also possess five cusps and an Y5 pattern, like numerous other Neandertal molars.

3.15.3. Metrics

Measurements of the Scla 4A-1/M₁ and Scl 4A-9/M₁ molars are as follows:

Scla 4A-1

MD: 11.70 mm

BL: 10.48 mm

Scla 4A-9

MD: 11.64 mm

BL: 10.68 mm

The MD and BL diameters of Scla 4A-1/M₁ and 4A-9/M₁ do not depart significantly from the average of any of the five comparison samples (EN,



LN, MPMH, UPMH & MHSS), in regard to both the DP probabilistic distance and ECRA (Table 27). When both MD and BL crown diameters of the permanent mandibular first molars are situated

on equiprobable ellipses (95%) they are in an area where Early and Late Neandertals, Middle Palaeolithic and Upper Palaeolithic Modern Humans as well as MHSS overlap (Figure 36).

Scladina	N	Diameter	Value
M ₁	Scla 4A-1/M ₁	MD	11.7
		BL	10.48
	Scla 4A-9/M ₁	MD	11.64
		BL	10.68

Table 27: Scla 4A-1/M₁ & 4A-9/M₁ (permanent mandibular first molars): MD and BL dimensions compared to those of Early and Late Neandertals as well as MPMH, UPMH and MHSS, with DP and ECRA.

Comparison Samples	N	Diameter	Mean	Stand. Dev.	vs Scla 4A-1/M ₁		vs Scla 4A-9/M ₁	
					DP	ECRA	DP	ECRA
EN right and left	28	MD	11.902	0.864	0.817	-0.114	0.764	-0.148
	27	BL	11.165	0.731	0.358	-0.456	0.513	-0.323
LN right and left	58	MD	11.291	0.632	0.520	0.323	0.583	0.276
	58	BL	10.783	0.567	0.595	-0.267	0.857	-0.091
MPMH right and left	14	MD	11.707	0.812	0.993	-0.004	0.935	-0.038
	13	BL	11.385	0.954	0.362	-0.435	0.474	-0.339
UPMH right and left	60	MD	11.512	0.826	0.821	0.114	0.877	0.077
	62	BL	10.995	0.522	0.328	-0.493	0.549	-0.302
MHSS	102	MD	10.813	0.679	0.194	0.659	0.226	0.614
	103	BL	10.125	0.458	0.440	0.390	0.229	0.610

- × Early Neandertals (EN)
- + Late Neandertals (LN)
- Middle Palaeolithic Modern Humans (MPMH)
- △ Early/Late Upper Palaeolithic Modern Humans (UPMH)
- ▲ Modern *Homo sapiens sapiens* (MHSS)

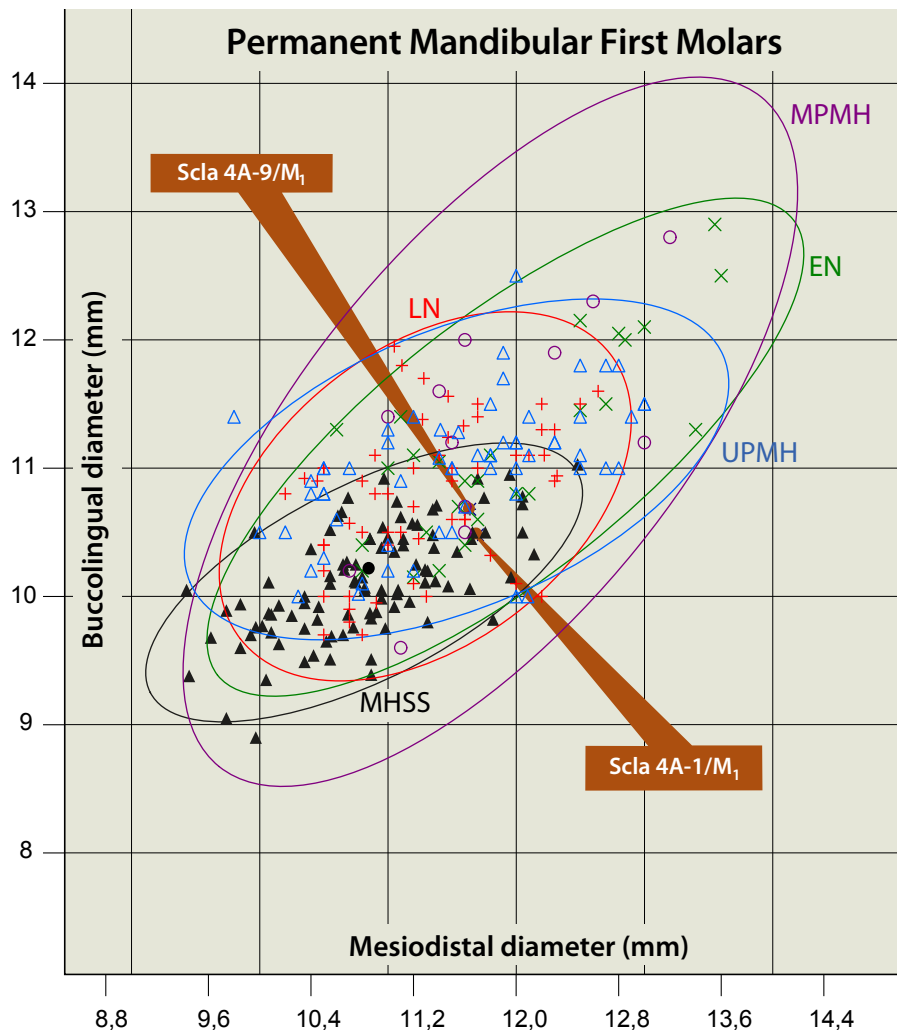


Figure 36: Bivariate analysis of the mesiodistal and buccolingual diameters of permanent mandibular first molars with 95% equiprobable ellipses of EN, LN, MPMH, UPMH & MHSS as well as the position of Scla 4A-1/M₁ & 4A-9/M₁.

3.16. Permanent mandibular second molars, M_2

3.16.1. Description

Permanent mandibular right second molar, RM_2 (Figure 37)

Palaeoanthropological identification:

Scla 4A-1/ M_2 (as part of the right hemimandible)

Field identification: Sc 1993-148-185

Date of discovery: 16 July 1993

Date of identification: 20 July 1993

Square: D29

Stratigraphic position:

– **Former stratigraphy:** 4A

– **New stratigraphy:** Unit 4A-CHE, Layer 4A-GX

This tooth, embedded within the Scla 4A-1 right half of the mandible, is almost completely erupted. Its crown was not yet really functional. The M_2 shows only very superficial wear of the cusp tips' enamel (MOLNAR, 1971, stade 2). Only two thirds of its roots are formed. No pathological conditions are noted. It is well preserved, except for rare, vertically orientated microfractures on the crown.

The occlusal surface presents five cusps. The protoconid is the largest, then the metaconid, followed by the hypoconid and entoconid, and finally the hypoconulid, the smallest (ASUDAS, grade 4). There is no cusp 6 (*tuberculum sextum*) or cusp 7 (*tuberculum intermedium*/metaconulid).

The mesial marginal ridge does not present any clear marginal accessory tubercle. The anterior fovea is transversal, deep and wide (ASUDAS LM_1 , grade 4).

The MTC is formed by the junction of the essential/middle ridge of the protoconid and the mesial accessory ridge of the metaconid (see SKINNER et al., 2008). This bridge is interrupted in its upper half by two grooves. The most lingual (Figure 37c: no. 1) of these grooves corresponds to the central groove (sagittal sulcus) which also runs across the anterior fovea. The most buccal groove (no. 2) of the mid-trigonid crest slopes inward to the central fovea, so that the centre of the MTC nearly forms a distinct cuspule (no. 3). On the EDJ, however, the MTC is more continuous but concave at the level of the sagittal sulcus. In mesial view, the MTC is higher than the mesial marginal ridge.

As on the first molar, the protoconid exhibits a distal, but better marked, accessory ridge (no. 4) on the OES and the EDJ. It joins the central part of the essential ridge (no. 5) of the metaconid,

forming a bridge, interrupted at the level of the sagittal sulcus, that can be regarded as a distal trigonid crest. The distal part of the essential crest of the metaconid joins, on the OES, the essential crest of the hypoconid, creating a Y5 pattern. There is no deflecting wrinkle of the essential crest of the metaconid. A weak protostylid is visible on the buccal surface of the protoconid (ASUDAS, grade 1).

The entoconid presents an essential crest that bifurcates mid-way to the occlusal basin, with a distal branch (no. 7) joining the sagittal fissure and a mesial one (no. 6) joining the transverse sulcus between the metaconid and entoconid. The hypoconid has a small mesial accessory ridge and a long essential crest joining the distal part of the essential crest of the metaconid. The hypoconulid is grade 3 of ASUDAS; it has an essential crest and, mainly on the EDJ, a faint accessory crest on its buccal part. In buccal view, there is a strong but short furrow between the protoconid and the hypoconid. A furrow also appears between the hypoconid and hypoconulid.

Neither mesial nor distal interproximal facets are present.

Both roots are flattened, and slope slightly distally. In cross-section, the mesial root is 8-shaped while the distal root is C-shaped.

Permanent mandibular left second molar, LM_2 (Figure 38)

Palaeoanthropological identification:

Scla 4A-9/ M_2 , (as part of the left hemimandible)

Field identification: Sc 1996-203-1

Date of discovery: 12 July 1996

Date of identification: 12 July 1996

Square: C28

Stratigraphic position:

– **Former stratigraphy:** 4A

– **New stratigraphy:** Unit 4A-CHE (Unit 4A-POC), Layer 4A-JA (?)

In situ in the Scla 4A-9 left hemimandible, this tooth has a general morphology which is quite similar to its Scla 4A-1/ M_2 antimer.

It is not completely erupted, but somewhat more so than Scla 4A-1/ M_1 . The crown is at least partly functional with superficial wear of the enamel of the tips of the cusps (MOLNAR, 1971, stade 2). The roots are incompletely formed: only two thirds are formed. No pathological conditions are noted. Numerous microfractures, mainly vertically orientated, can be observed on the crown.



Permanent Mandibular Right Second Molar Scla 4A-1/M₂

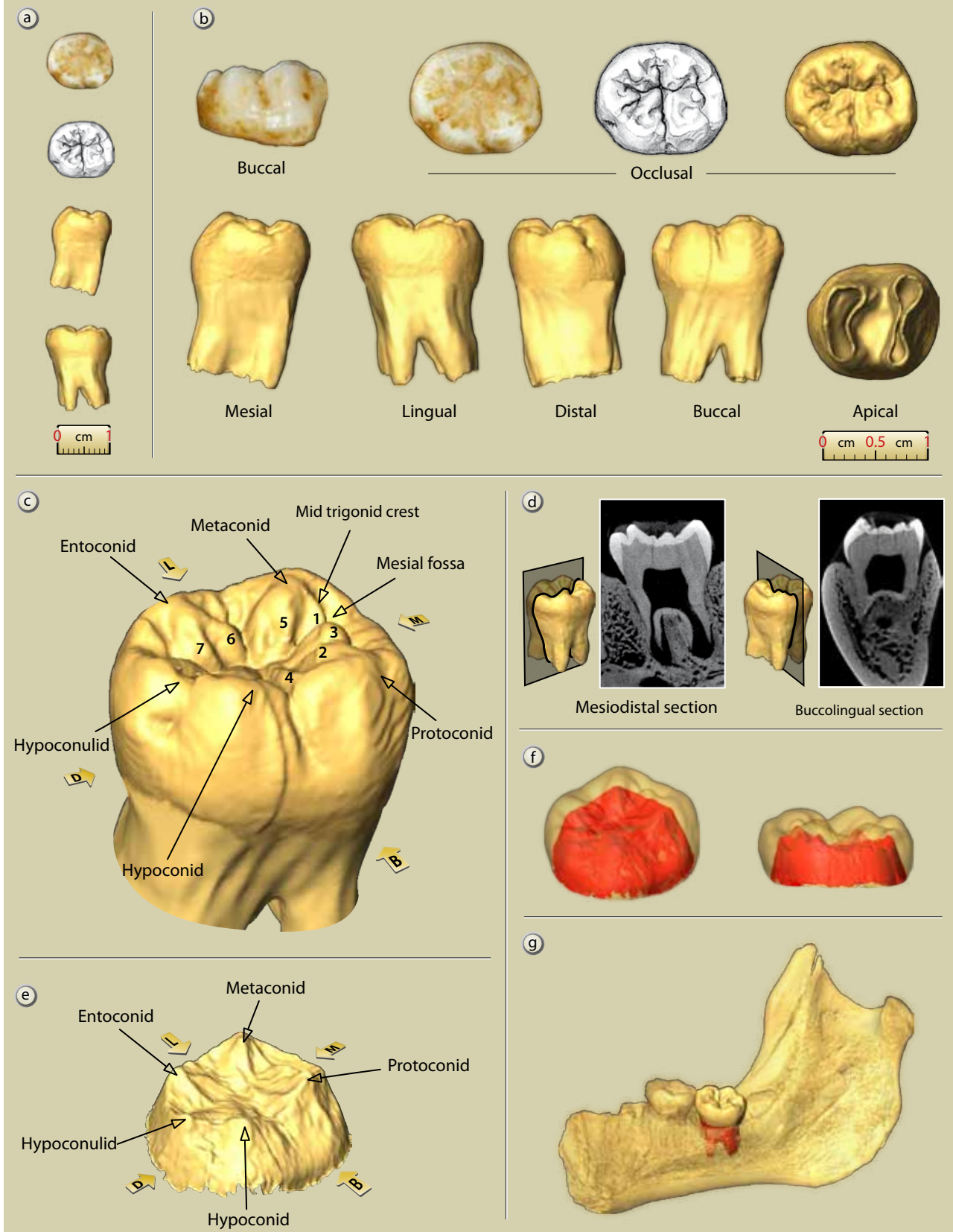


Figure 37: Scla 4A-1/M₂ permanent mandibular right second molar: a. occlusal, mesial and lingual views (1:1 scale); b. buccal and occlusal faces, photographs; occlusal face, drawing; 3D reconstruction of the six faces of the tooth (2:1 scale); c. 3D reconstruction with main anatomical features; d. internal sections; e. 3D reconstruction with main anatomical features at the EDJ; f. 3D views at the EDJ with enamel; g. position of the tooth (micro-CT data processing and graphics J.-F. Lemaire, SPW; pencil drawings S. Lambermont, AWEM; photographs J. Eloy, AWEM).

Permanent Mandibular Left Second Molar Scla 4A-9/M₂

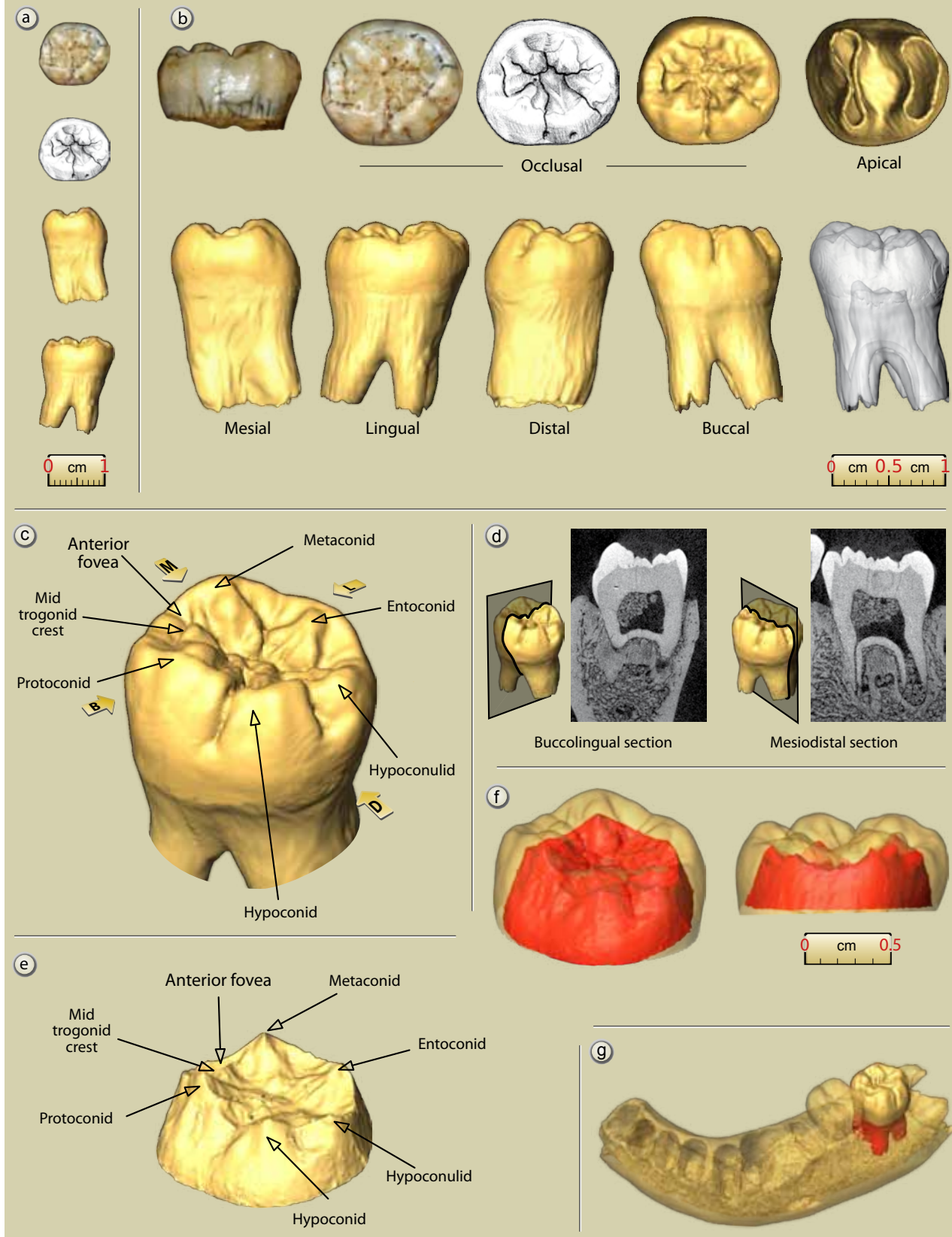


Figure 38: Scla 4A-9/M₂ permanent mandibular left second molar: a. occlusal, mesial and lingual views (1:1 scale); b. lingual and occlusal faces, photographs; occlusal face, drawing; 3D reconstruction of the six faces of the tooth (2:1 scale); c. 3D reconstruction with main anatomical features; d. internal sections; e. 3D reconstruction with main anatomical features at the EDJ; f. 3D views at the EDJ with enamel; g. position of the tooth (micro-CT data processing and graphics J.-F. Lemaire, SPW; pencil drawings S. Lambermont, AWEM; photographs J. Eloy, AWEM).



The occlusal surface presents five cusps, arranged in a Y5 fissure pattern in the central fossa but with only narrow contact between metaconid and hypoconid. The protoconid (cusp 1) is the largest, then the metaconid, following by the hypoconid and entoconid, then the hypoconulid (cusp 5), the smallest (ASUDAS, grade 3). There is no cusp 6 or cusp 7.

The anterior fovea is transversal, deep and wide. The mesial accessory crest (ridge) of the metaconid runs buccally to form a bridge of enamel, the mid-trigonid crest, or MTC, with the mesial crest of the protoconid. This bridge is continuous but interrupted, in its upper half, by two grooves, notably the sagittal sulcus (BAILEY, 2002^b, grade 2), like its antimeres, so that the centre of the MTC nearly forms a distinct cusplet. In mesial view, the MTC is higher than the mesial marginal ridge. There is no deflecting wrinkle, or angulation of the essential crest of the metaconid.

Just behind the essential crest of the protoconid, the distal accessory ridge of this cusp runs buccolingually, forming a low distal trigonid crest with the anterior part of the essential crest of the metaconid. The distal part of the essential crest of the metaconid joins, on the OES, the essential crest of the hypoconid, creating a Y5 pattern.

A weak protostylid is present on the buccal surface of the protoconid; it is a bit more marked than on its antimeres.

The essential crest of the entoconid, mid-way to the occlusal basin, is divided in four crenulations, therefore being more complex than its antimeres. The hypoconid has a bifurcated essential crest as well as small mesial and distal accessory ridges. The hypoconulid is grade 5 of ASUDAS; it has an essential crest and a long buccal accessory crest. In buccal view, there is a distinct but short furrow between the protoconid and hypoconid. A large furrow also appears between the hypoconid and hypoconulid. Between entoconid and hypoconulid is a weak posterior fovea but better marked than on its antimeres.

Neither mesial nor distal interproximal wear facets are present. Both roots are flattened, and slope slightly distally. In cross-section, the mesial root is 8-shaped while the distal root is C-shaped.

3.16.2. Taxonomy

The Neandertal permanent mandibular second molar is generally similar to the M_1 in its morphology (Table 28; BAILEY, 2002^a, 2006^a; BAILEY & HUBLIN, 2006):

- rarely four cusps (2.7% in BAILEY, 2002^a; 0% in BAILEY, 2006^a and Table 28), but often at least five cusps;
- large anterior fovea;
- mid-trigonid crest (\pm 95%), rare on the M_2 of anatomically modern Humans;
- Y pattern much more frequent than in European amHS;
- No deflecting wrinkle.

Although each of these individual features may be present in anatomically modern humans, their frequent association is characteristic of Neandertals. Both M_2 s exhibit a typical Neandertal combination of traits: five cusps, large anterior fovea, MTC, Y pattern, and absence of deflecting wrinkle.

3.16.3. Metrics

Measurements of the permanent mandibular second molars are as follows:

Scla 4A-1/ M_2

MD: 11.97 mm

BL: 10.68 mm

Scla 4A-9/ M_2

MD: 12.2 mm

BL: 10.80 mm

Only the MD diameter of Scla 4A-9/ M_2 departs significantly from the average of one of the five comparative samples (MHSS), both in regard to the DP probabilistic distance and ECRA (Table 29). When both MD and BL crown diameters of the permanent mandibular second molars are situated on equiprobable ellipses, (95%), they are in an area where Early and Late Neandertals, Middle Palaeolithic and Upper Palaeolithic Modern Humans as well as MHSS overlap (Figure 39).

3.17. Permanent mandibular right third molar, RM_3

Palaeoanthropological identification:

Scla 4A-1/ M_3 , as part of the right hemimandible

Field identification: Sc 1993-148-185

Date of discovery: 16 July 1993

Date of identification: 20 July 1993

Square: D29

Stratigraphic position:

- Former stratigraphy: 4A

Permanent Mandibular Second Molars	Non-Neandertal Archaics	Neandertals	Early Modern Afro-Asians	Early Modern Europeans	Scla 4A-9/M ₂	Scla 4A-1/M ₂
Four cusps	0%	0%	10%	35%	no (5 main cusps)	no (5 main cusps)
Fissure pattern: Y	70%	75%	100%	44.4%	yes	yes
Anterior fovea	75%	88.5%	20%	50%	yes	yes
Mid-trigonid crest	71.4%	96.2%	0%	4.2%	yes	yes
Distal trigonid-crest	0%	13.8%	0%	0%	very weak	very weak
Deflecting wrinkle	0%	0%	0%	0%	no	no
Cusp 6	0%	50%	0%	23.5%	no	no
Cusp 7	12.5%	20%	10%	8.3%	no	no

Table 28: Distinctive anatomical features on permanent mandibular second molars of Non-Neandertal Archaics, Neandertals, Early Modern Humans (after BAILEY, 2006^a) and Scla 4A-9/M₂ & Scla 4A-1/M₂.

Scladina	N	Diameter	Value
M ₂	Scla 4A-1/M ₂	MD	11.97
		BL	10.68
	Scla 4A-9/M ₂	MD	12.2
		BL	10.8

Table 29: Scla 4A-1/M₂ & 4A-9/M₂ (permanent mandibular second molars): MD and BL dimensions compared to those of Early and Late Neandertals as well as MPMH, UPMH and MHSS, with DP and ECRA.

Comparison Samples	N	Diameter	Mean	Stand. dev.	vs Scla 4A-1/M ₂		vs Scla 4A-9/M ₂	
					DP	ECRA	DP	ECRA
EN right & left	24	MD	12.242	0.826	0.745	-0.159	0.960	-0.024
	23	BL	11.320	0.571	0.275	-0.540	0.373	-0.439
LN right & left	57	MD	11.612	0.732	0.627	0.244	0.425	0.401
	59	BL	10.963	0.732	0.700	-0.193	0.824	-0.112
MPMH right & left	12	MD	11.083	0.816	0.300	0.494	0.198	0.622
	13	BL	11.169	0.670	0.479	-0.335	0.592	-0.253
UPMH right & left	53	MD	11.201	0.848	0.369	0.452	0.244	0.587
	67	BL	11.009	0.734	0.656	-0.224	0.777	-0.142
MHSS right & left	92	MD	10.637	0.765	0.085	0.878	0.044	1.029
	92	BL	9.835	0.633	0.186	0.671	0.131	0.767

– **New stratigraphy:** Unit 4A-CHE, Layer 4A-GX

3.17.1. Description (Figure 40)

This crown, unerupted in the Scla 4A-1 right hemimandible, is well preserved and, of course, not functional. The following description of this tooth is therefore based on micro-CT data and stereolithographic models. Its roots are not formed. No pathological conditions are noted.

The occlusal surface is complex. It presents seven cusps, both on the OES and on the EDJ: protoconid > metaconid > hypoconid > entoconid > hypoconulid as well as two very small cusps between the hypoconulid and the entoconid (one of them is the *tuberculum sextum*/entoconulid or cusp 6).

The mesial marginal ridge does not present any marginal accessory tubercle but exhibits some

anteroposterior crenulations. The anterior fovea is transversal, deep and wide.

The mesial accessory ridge (Figure 40d: no. 1) of the metaconid and the mesial accessory ridge (no. 2) of the protoconid join to form a bridge of enamel, the mid-trigonid crest (MTC), interrupted in its upper part at the level of the sagittal sulcus.

The distal ridge (no. 3) of the metaconid joins the essential ridge (no. 4) of the protoconid to form the distal trigonid crest which is much lower than the MTC and is interrupted by the sagittal sulcus. Between the mesial and distal ridge of the metaconid is a short central ridge (no. 5). Other salient features are: a distal ridge (no. 6) on the protoconid; the bifurcation (no. 7-8) of the essential/central ridge of the entoconid; an essential ridge on both the hypoconid (no. 9) and the hypoconulid (no. 10); a small essential ridge on the two small cusps (no. 11-12) between the entoconid and hypoconulid.



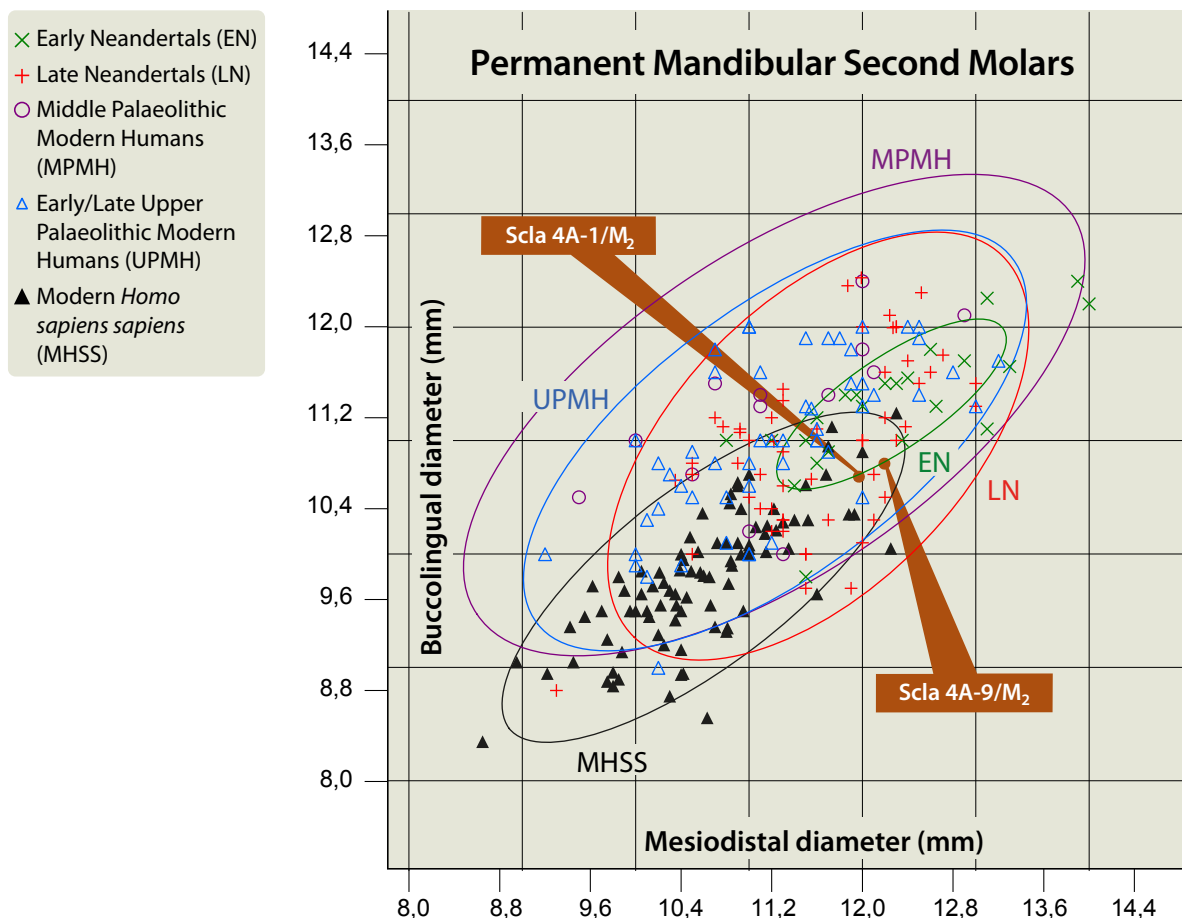


Figure 39: Bivariate analysis of the mesiodistal and buccolingual diameters of permanent mandibular second molars with 95% equiprobable ellipses of EN, LN, MPMH, UPMH & MHSS as well as the position of Scla 4A-1/M₂ & 4A-9/M₂.

A vertical depression on the anterior part of the buccal surface of the protoconid corresponds to a weak protostylid. In buccal view, two vertical grooves separate the hypoconid of the adjacent cusps 1 and 5.

3.17.2. Taxonomy (Table 30)

The Neandertal M₃ usually has five or more cusps, with a *tuberculum sextum* (cusp 6) in half of the cases. That tooth has very frequently (over 90%) a mid-trigonid crest (MTC) and a large anterior fovea. The distal trigonid crest is occasionally present (10.5%). Some deflecting wrinkles occur ($\pm 7\%$).

Hence the M₃ is probably the most informative permanent mandibular molar in distinguishing Neandertals from recent and Early Modern Humans (BAILEY, 2006^a). For instance, Early Modern Human M₃s often have four cusps and no MTC.

The Scladina right M₃ presents most of the Neandertal traits: seven cusps, large anterior fovea, MTC, weak distal trigonid crest and *tuberculum sextum*.

3.17.3. Metrics

Measurements of the permanent mandibular third molar are as follows:

MD: 11.5 mm

BL: 11.4 mm

The BL diameter of this tooth departs significantly from the five comparative samples only in the case of MHSS, both in regard to the DP probabilistic distance and ECRA (Table 31). When both MD and BL crown diameters of Scla 4A-1/M₃ are situated on equiprobable ellipses (95%) they are in an area where Early and Late Neandertals, Middle Palaeolithic and Upper Palaeolithic Modern Humans as well as MHSS overlap, but very close to the upper limit of BL diameter of MHSS (Figure 41).

Permanent Mandibular Right Third Molar Scla 4A-1/M₃

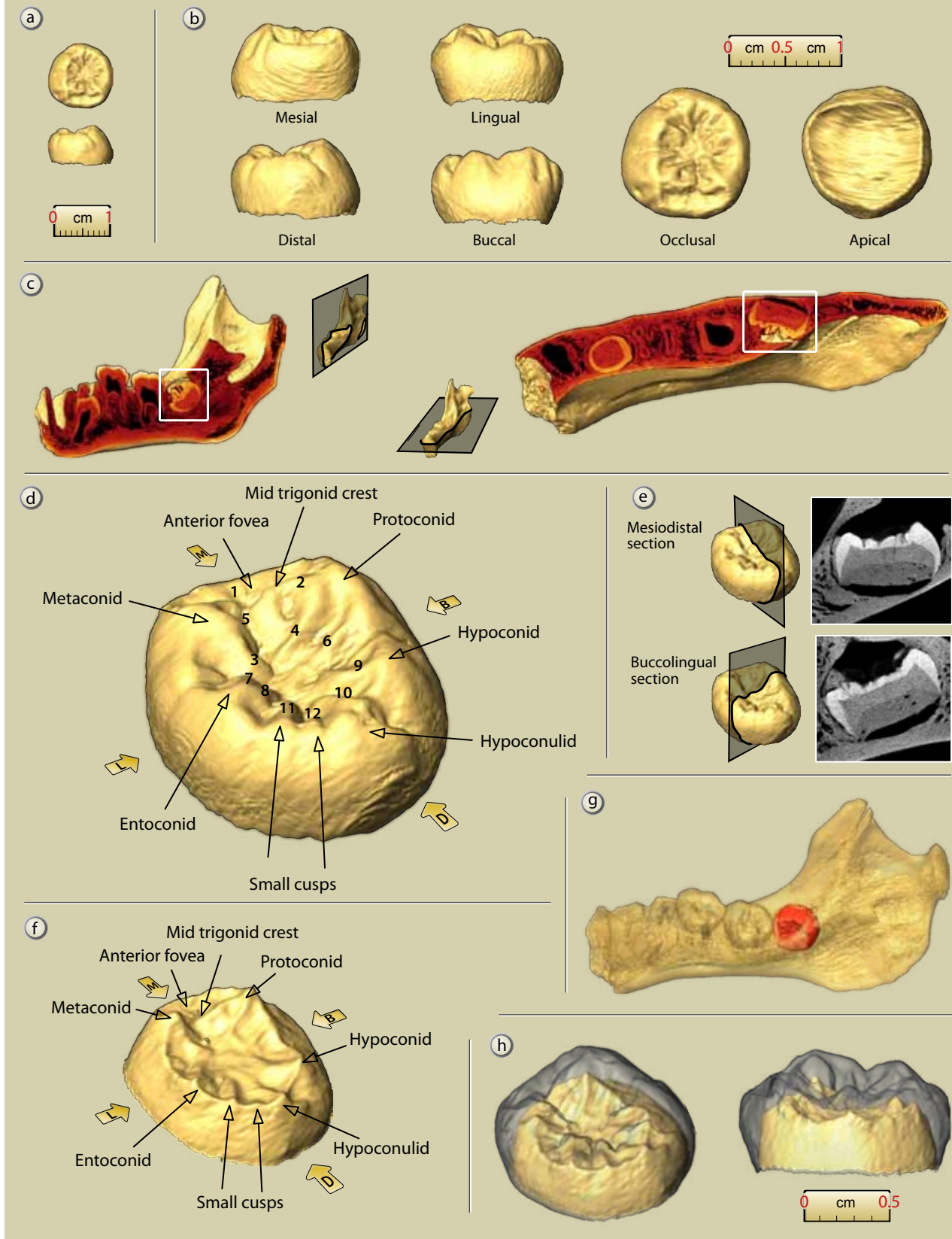


Figure 40: Scla 4A-1/M₃, permanent mandibular right third molar: a. occlusal and distal views (1:1 scale); b. 3D reconstruction of the six faces of the tooth (2:1 scale); c. views of the position of the unerupted molar; d. 3D reconstruction with main anatomical features; e. internal sections; f. 3D reconstruction with main anatomical features at the EDJ; g. position of the tooth; h. 3D views at the EDJ with enamel; (micro-CT data processing and graphics J.-F. Lemaire, SPW; pencil drawings S. Lambermont, AWEM; photographs J. Eloy, AWEM).



Table 30: Distinctive anatomical features on permanent mandibular third molars of Non-Neandertal Archaics, Neandertals, Early Modern Humans (after BAILEY, 2006^a) and Scla 4A-1/M₃.

Permanent Mandibular Third Molars	Non-Neandertal Archaics	Neandertals	Early Modern Afro-Asians	Early Modern Europeans	Scla 4A-1/M ₃
Four cusps	0%	0%	28.6%	31.6%	no (7 cusps)
Fissure pattern: Y	0%	41.2%	50%	55.6%	no
Anterior fovea	75%	92.9%	0%	46.7%	yes
Mid-trigonid crest	50%	93.3%	0%	0%	yes
Distal trigonid-crest	0%	10.5%	0%	0%	yes (weak)
Deflecting wrinkle	0%	6.7%	0%	0%	no
Cusp 6	66.7%	50%	40%	41.2%	yes
Cusp 7	0%	40%	0%	16.7%	no

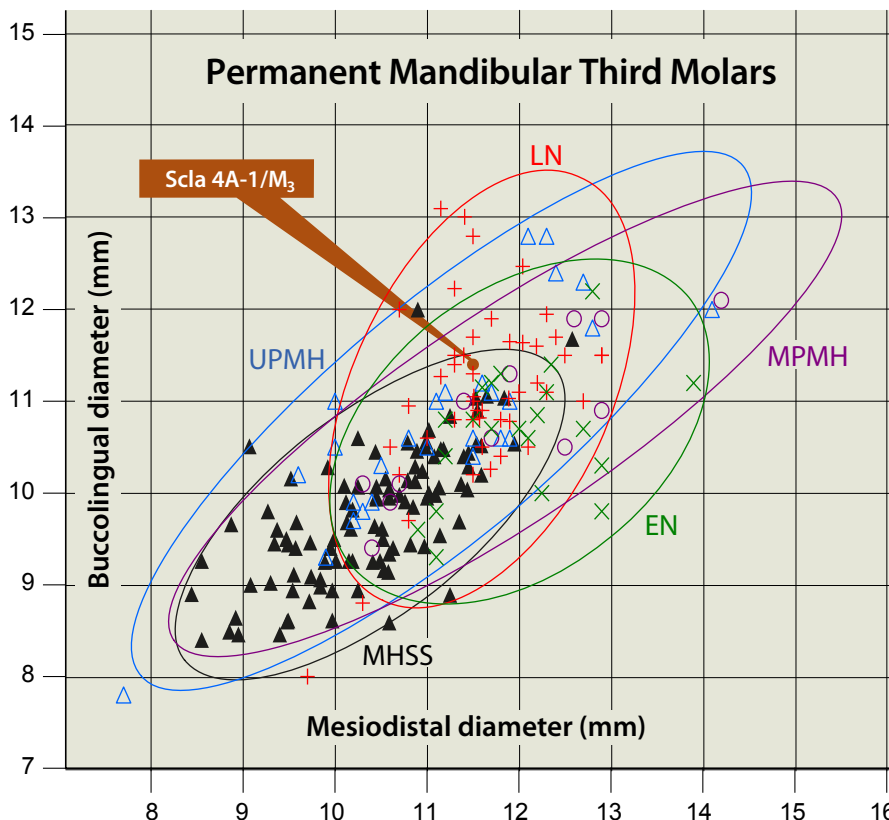
Scladina	Diameter	Mean
RM ₃ (Scla 4A-1/M ₃)	MD	11.5
	BL	11.4

Table 31: Scla 4A-1/M₃ (permanent mandibular right third molar): MD and BL dimensions compared to those of Early and Late Neandertals as well as MPMH, UPMH and MHSS, with DP and ECRA.

Comparison Samples	N	Diameter	Mean	Stand. Dev.	DP	ECRA
EN right & left	23	MD	12.033	0.745	0.482	-0.345
	22	BL	10.673	0.675	0.294	0.518
LN right & left	47	MD	11.596	0.649	0.884	-0.073
	49	BL	11.117	0.918	0.759	0.154
MPMH right & left	11	MD	11.627	1.013	0.903	-0.056
	11	BL	10.691	0.804	0.399	0.396
UPMH right & left	25	MD	11.016	1.166	0.682	0.201
	26	BL	10.746	1.105	0.559	0.287
MHSS right & left	104	MD	10.436	0.924	0.252	0.581
	104	BL	9.796	0.761	0.037	1.063

- × Early Neandertals (EN)
- + Late Neandertals (LN)
- Middle Palaeolithic Modern Humans (MPMH)
- △ Early/Late Upper Palaeolithic Modern Humans (UPMH)
- ▲ Modern *Homo sapiens sapiens* (MHSS)

Figure 41: Bivariate analysis of the mesiodistal and buccolingual diameters of permanent mandibular third molars with 95% equiprobable ellipses of EN, LN, MPMH, UPMH & MHSS as well as the position of Scla 4A-1/M₃.



Deciduous Mandibular Right Second Molar Scla 4A-13

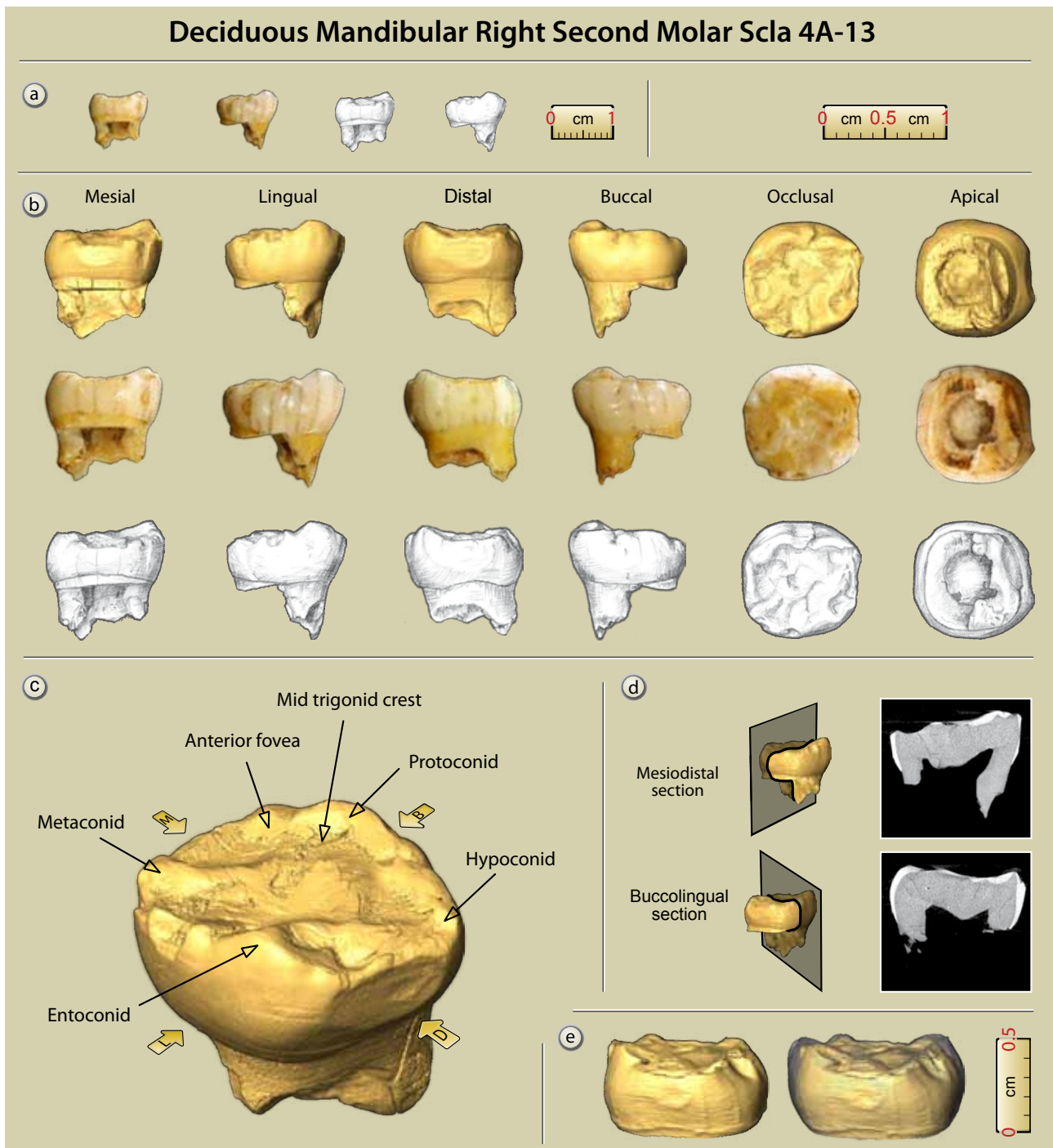


Figure 42: Scla 4A-13 deciduous mandibular right second molar: a. mesial and lingual views (1:1 scale); b. photographs, drawings and 3D reconstructions of the six faces of the tooth (2:1 scale); c. 3D reconstruction with main anatomical features; d. internal sections; e. 3D lingual views at the EDJ without and with enamel (micro-CT data processing and graphics J.-F. Lemaire, SPW; pencil drawings S. Lambermont, AWEM; photographs J. Eloy, AWEM).

3.18. Deciduous mandibular right second molar, Rdm₂

Palaeoanthropological identification: Scla 4A-13

Field identification: Sc 2001-262-44

Date of discovery: 13 November 2001

Date of identification: 13 November 2001

Square: E38

Stratigraphic position:

– Former stratigraphy: 4A

– New stratigraphy: Unit 4A-POC; Layer 4A-LEG

3.18.1. Description (Figure 42)

The deciduous mandibular right second molar has a fully formed crown. Only a small part (3.8 mm) of its roots is preserved, the rest being reduced by



the emergence of the right second premolar which is still unerupted in the mandible. The tooth was still in situ in the Scla 4A-1 right hemimandible when the child was alive, but was lost post-mortem. It was found in Square E38, at a distance of 9.5 m from the mandible.

The mesial half of the root was removed in 2001 for DNA analysis, which provided interesting results (ORLANDO et al., 2006 & Chapter 17).

The crown is worn. In fact, all the cusps are blunt and large areas of dentine are exposed. The wear is close to stage 4-5 of MOLNAR (1971). The four lateral faces of the crown are affected by some vertical cracks. No pathological conditions are noted.

Due to the strong level of wear, the morphology of the crown cannot be described in detail. Nevertheless, the four major cusps are present as well as some additional small cusps. So it seems that the crown did present a complex occlusal morphology before being worn.

The occlusal plane is nearly horizontal, with just the entoconid slightly higher. Only the bottom of the anterior fovea is preserved. The mid-trigonid crest (MTC) is present but blunt. Between the blunt metaconid and the entoconid there is a small cuspid; in lingual view, it is separated from the metaconid by a distinct fissure, so it could be a trace of cusp 7 (*tuberculum intermedium*). Behind the hypoconid, the hypoconulid (cusp 5) can be detected.

In buccal view, a small groove limited to the upper part of the crown separates the protoconid and the hypoconid.

The mesial surface exhibits a transversally elongated interproximal wear facet which modifies only slightly the outline of the tooth as seen in occlusal view. This facet has a maximal height of 1.8 mm, a buccolingual diameter of 3.3 mm, and a slightly curved inferior border. The distal surface has an interproximal wear facet (height: 2.5 mm; buccolingual diameter: 4.1 mm) related to the presence of the permanent first molar; its inferior border is slightly curved. In occlusal view, this facet does affect the outline of the crown.

3.18.2. Taxonomy

According to BAILEY & HUBLIN (2006: 505), the primary feature differentiating Neandertal deciduous mandibular molars from those of anatomically modern humans is the prominent crest that connects the mesial cusps (i.e. the mid-trigonid crest or MTC). MACCHIARELLI et al. (2006) add that such a morphology seems to be

associated with a generally more complex enamel-dentine junction. Other Neandertal features are an ovoid occlusal outline, internally compressed cusps, and a wide anterior fovea bordered by a well-defined mesial marginal ridge (BAILEY & HUBLIN, 2006). In contrast, Upper Palaeolithic dm_2 s have a rectangular occlusal outline, with more widely spaced cusps and no continuous mid-trigonid crest. It should be added that at least some immature Neandertal dm_2 s, such as those of Engis 2 and La Chaise, have a MTC which does not form a complete bridge (score 1 of BAILEY, 2002^b), like some Upper Palaeolithic dm_2 s, Isturitz for instance (BAILEY & HUBLIN, 2006). As far as morphology is concerned, the Scla 4A-13 dm_2 closely resembles those of Neandertals. It exhibits a complex occlusal morphology and possesses an ovoid outline, internally compressed cusps, and well defined marginal ridges. An MTC is present, although only preserved in its lower part.

It is well known that permanent Neandertal molars have a thinner enamel than *Homo sapiens* (MACCHIARELLI et al., 2006; OLEJNICZAK et al., 2008; BAYLE et al., 2009; SMITH et al., 2012). In addition, the analysis of the Couvin dm_2 has recently proved that deciduous Neandertal molars present thinner lateral enamel (TOUSSAINT et al., 2010; Figure 43). Scla 4A-13 exhibits the same Neandertal pattern, despite the shortcomings of the previously used methods, including at Couvin, might have amplified the real range of enamel thickness variation of this taxon, which is still poorly known (see Chapter 14).

3.18.3. Metrics

The dm_2 has a MD diameter of 9.47 mm and a BL diameter of 9.38 mm. It has been compared to five series of teeth: 1) Preneandertals/Early Neandertals; 2) Classic Neandertals; 3) Palaeolithic Modern Humans (combination of Mousterian from the Middle East and Upper Palaeolithic from Europe); 4) Belgian Neolithics; 5) Middle Ages and subactual modern humans.

The MD diameter of Scla 4A-13 departs significantly from the EN and Palaeolithic Modern Humans comparative samples only, both in regard to the DP probabilistic distance and ECRA (Table 32). The BL diameter is statistically close to all comparison samples. Due to its low MD diameter, the tooth is outside the ellipse (95%, Figure 44) of the Early Neandertals, at the limit of MHSS, and in an area where Late Neandertals and Palaeolithic *Homo sapiens* overlap.

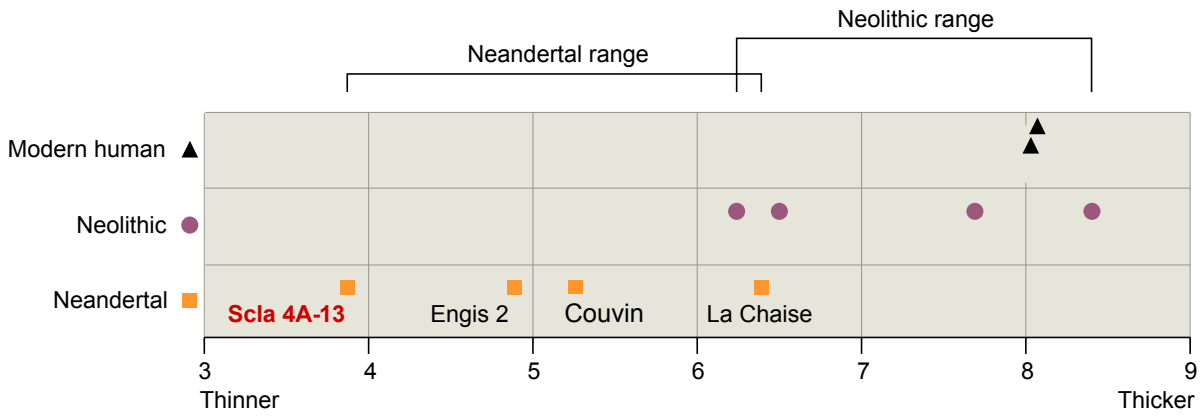


Figure 43: Plot depicting the range of lateral relative enamel thickness index values in the Neandertal, Neolithic *Homo sapiens* and Recent Modern *Homo sapiens* samples. The Scla 4A-13 deciduous molar falls clearly within the range of Neandertals (modified after TOUSSAINT et al., 2010).

Table 32: Scla 4A-13 (deciduous mandibular right second molar): MD and BL dimensions compared to those of Early and Late Neandertals as well as Palaeolithic Modern Humans (MPMH & UPMH) and two samples of Belgian MHSS, with DP and ECRA.

Scladina		Diameter	Value
Rdm ₂ (Scla 4A-13)		MD	9.47
		BL	9.38

Comparison Samples	N	Diameter	Mean	Stand. Dev.	DP	ECRA
EN	11	MD	10.764	0.486	0.024	-1.195
	11	BL	9.573	0.438	0.669	-0.198
LN	32	MD	10.266	0.579	0.179	-0.674
	32	BL	9.278	0.451	0.823	0.111
Palaeolithics modern humans (MPMH & UPMH)	19	MD	10.737	0.601	0.049	-1.003
	20	BL	9.465	0.620	0.892	-0.066
Belgian Neolithics	29	MD	10.128	0.458	0.162	-0.701
	29	BL	9.017	0.390	0.360	0.454
Belgian Modern Humans	57	MD	10.000	0.492	0.286	-0.537
	57	BL	8.660	0.478	0.138	0.752

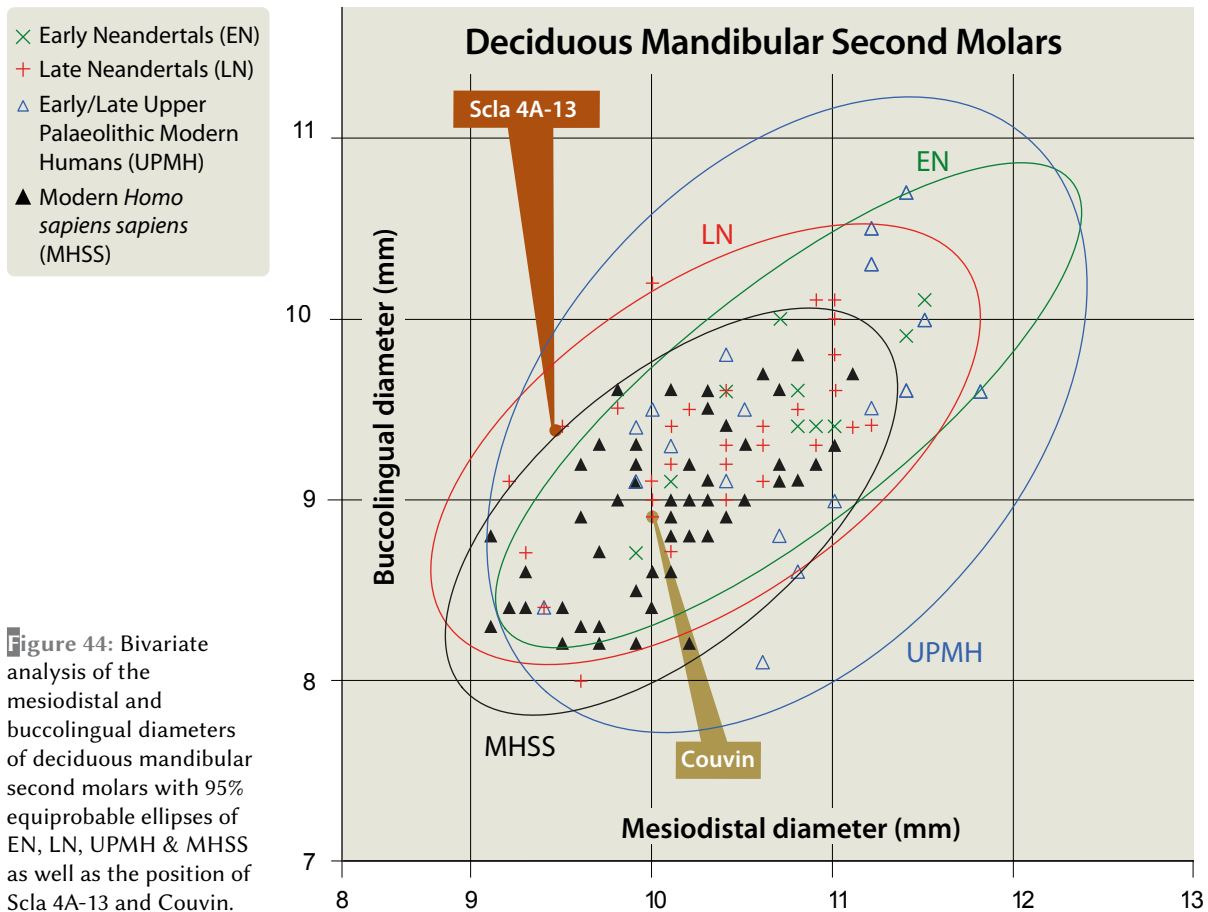


Figure 44: Bivariate analysis of the mesiodistal and buccolingual diameters of deciduous mandibular second molars with 95% equiprobable ellipses of EN, LN, UPMH & MHSS as well as the position of Scla 4A-13 and Couvin.

4. Discussion

The crowns of the 24 teeth available for the mandible and maxilla of Scladina (Figure 45) have been examined one by one in a statistical and anatomical perspective in the previous paragraphs.

It would be useful, and this is one of the purposes of this discussion, to analyse them as a series.

The ECRA of both the MD and BL diameters of all Scladina teeth are shown, in Figures 46 & 47, compared to a series of samples, i.e. Early Neandertals (EN), Late Neandertals (LN), Middle



Figure 45: Scladina mandible (Scla 4A-1 & 9) and maxilla (Scla 4A-2) with the isolated teeth refitted (photographs J. Eloy, AWEM).

Palaeolithic Modern Humans (MPMH), Early/Late Upper Palaeolithic Modern Humans (UPMH) and modern *Homo sapiens sapiens* (MHSS). It thus appears that the diameters of the Scladina tooth crowns are never different from those of Late Neandertals; only in one case (dm₂), the MD diameter departs from Early Neandertals. Scladina differs slightly from MPMH only for the MD diameter of the deciduous maxillary first molar. Compared to UPMH, significant differences were observed with the BL diameter of the permanent maxillary lateral incisors and the MD diameter of the permanent maxillary canine and with the BL diameters of the mandibular premolars. Further significant differences occur between Scladina

and MHSS; this is the case for both the MD and BL diameters of all the incisors, canines and premolars and very rarely for molars.

All these observations confirm those that were made individually for each tooth. The Scladina teeth are therefore systematically within the variability of Neandertals and present some differences with other taxa, especially with MHSS. However, on the strict basis of MD and BL diameters, it is generally not possible to classify these teeth as either Early or Late Neandertals. However, the Scladina mandible is outside the ellipse of Early Neandertals and inside that of Late Neandertals for the deciduous mandibular second molar (Figure 44; see also Figure 47).

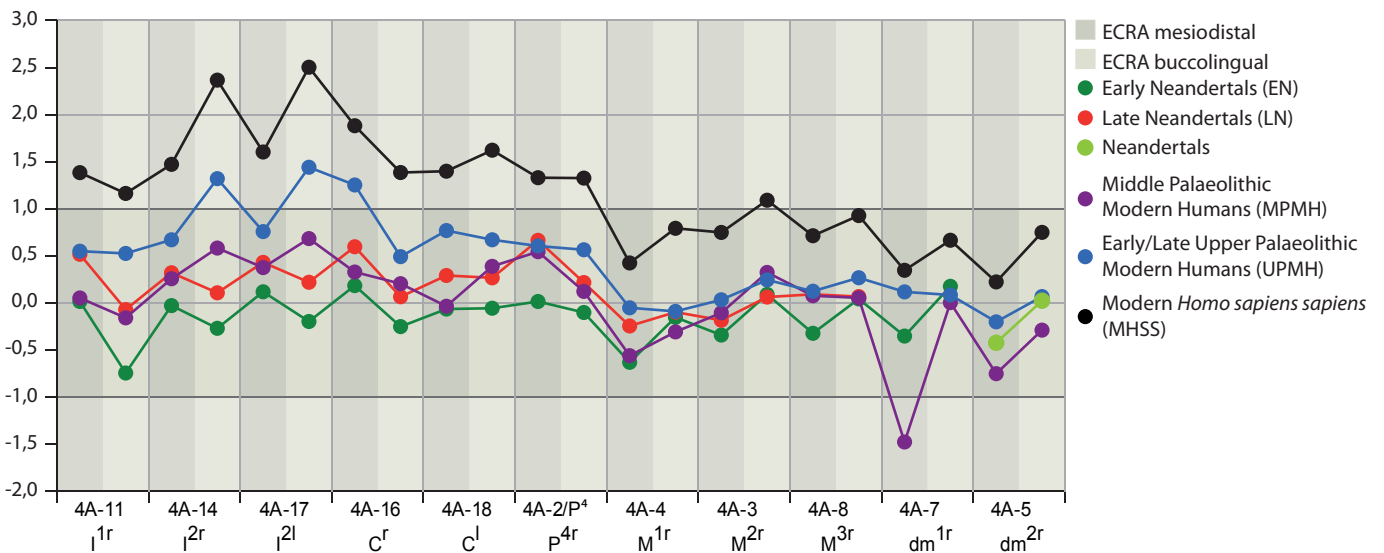


Figure 46: ECRA of both the MD and BL diameters of the maxillary Scladina teeth.

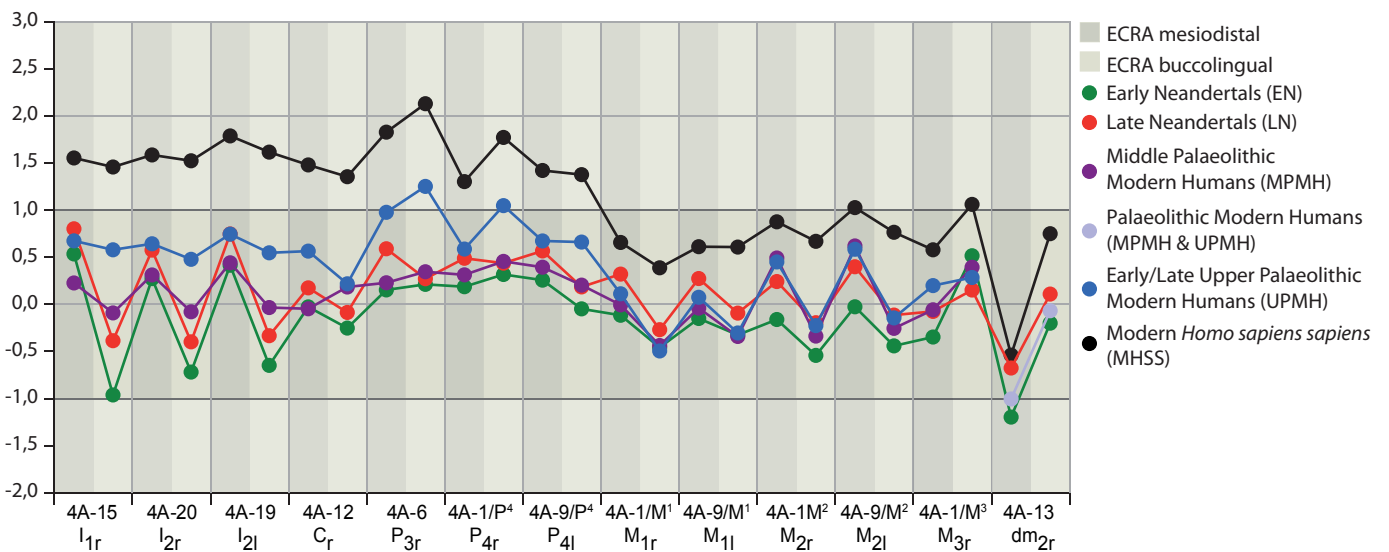


Figure 47: ECRA of both the MD and BL diameters of the mandibular Scladina teeth.



Morphologically, the Scladina teeth, like those of similar sites, do not exhibit any character which would be exclusively Neandertal. But, as mentioned previously by many scholars, for example BAILEY (2002^{a, b}; 2004^{a, b}; 2006^{a, b}), most Neandertal teeth often possess an original pattern which distinguishes them from anatomically modern humans because of the higher frequency of their features and their combination. The Scladina teeth fit very well in the general Neandertal pattern.

Regarding the taxonomic allocation of the juvenile teeth from Scladina, there is no doubt, based on descriptions and analyzes presented in this chapter, that they possess the characteristic Neandertal pattern. The question of their attribution to either an Early or a Late Neandertal is less obvious. However, some clues tend to substantiate a hypothetical allocation to an early classic form of this taxon (see Chapters 20 & 21), which is also true of some analyzes of specific aspects presented in other chapters, including the study of the enamel dentine junction (see Chapters 14 & 15).

Acknowledgements

The author wishes to express his gratitude to: Dr. Christine Verna, CNRS, France, and Max Planck Institute, Leipzig, Germany, for her data file; Sylviane Lambermont, graphic artist at the Association wallonne d'Études mégalithiques (AWEM), for her beautiful drawings of the different faces of each tooth; Joël Éloy (AWEM), for the design of the equiprobable ellipse figures and for his technical assistance; Jean-François Lemaire, Service de l'Archéologie en province de Liège of the Service public de Wallonie, for the processing of the micro-CT data and the design of most figures.

Thanks to Nora De Clerk (University of Antwerp) and Jean-Jacques Hublin (Max Planck Institute) for the microtomography.

Also, for taking the time to improve the English text, Rebecca Miller, University of Liège, as well as Cheryl Roy and Rhylan McMillan, Vancouver Island University and Jean-François Lemaire again.

References

BAILEY S.E., 2002^a. A closer look at Neandertal postcanine dental morphology: the mandibular dentition. *New Anatomist*, 269: 148-156.

BAILEY S.E., 2002^b. *Neandertal Dental Morphology: Implications for modern human origins*. PhD thesis, Arizona State University, Tempe: 238 p.

BAILEY S.E., 2004^a. A morphometric analysis of maxillary molar crowns of Middle-Late Pleistocene hominins. *Journal of Human Evolution*, 47: 183-198.

BAILEY S.E., 2004^b. Derived morphology in Neandertal maxillary molars: insights from above. *American Journal of Physical Anthropology*, 123: 57.

BAILEY S.E., 2006^a. Beyond Shovel-Shaped Incisors: Neandertal Dental Morphology in a Comparative Context. *Periodicum Biologorum*, 108, 3: 253-267.

BAILEY S.E., 2006^b. Diagnostic Dental Differences between Neandertals and Upper Paleolithic Modern Humans: getting to the root of the Matter. *Current Trends in Dental Morphology Research*: 201-209.

BAILEY S.E. & HUBLIN J.-J., 2006. Dental remains from the Grotte du Renne at Arcy-sur-Cure (Yonne). *Journal of Human Evolution*, 50: 485-508.

BAILEY S.E. & LYNCH J.M., 2005. Diagnostic Differences in Mandibular P4 Shape between Neandertals and Anatomically Modern Humans. *American Journal of Physical Anthropology*, 126: 268-277.

BAILEY S.E., SKINNER M. M. & HUBLIN J.-J., 2011. What Lies Beneath? An Evaluation of Lower Molar Trigonid Crest Patterns Based on Both Dentine and Enamel Expression, *American Journal of Physical Anthropology*, 145: 505-518.

BAYLE P., BRAGA J., MAZURIER A. & MACCHIARELLI R., 2009. Dental developmental pattern of the Neandertal child from Roc de Marsal: a high-resolution 3D analysis. *Journal of Human Evolution*, 56: 66-75.

BOULE M., 1911-1913. L'homme fossile de La Chapelle-aux-Saints. *Annales de Paléontologie*, VI: 111-172; VII: 21-56 & 85-192; VIII: 1-70.

CRUMMETT T., 1995. The three dimensions of shovel-shaping. In J. MOGGI-CECCHI (ed.), *Aspects of Dental Biology, Anthropology and Evolution*. Florence, International Institute for the Study of Man: 305-313.

DEFRISE-GUSSENHOVEN E., 1955. Ellipses équiprobables et taux d'éloignement en biométrie.

- Bulletin de l'Institut Royal des Sciences Naturelles de Belgique*, 26: 1–31.
- FRAIPONT J. & LOHEST M., 1887. La race humaine de Néanderthal ou de Canstadt en Belgique. Recherches ethnographiques sur des ossements humains découverts dans les dépôts quaternaires d'une grotte à Spy et détermination de leur âge géologique. Gand, *Archives de Biologie*, 7 (1886): 587–757, 4 pl. h.t.
- HAMMER O., HARPER D.A.T. & RYAN P. D., 2001. PAST: paleontological statistics software package for education and data analysis. Available at: Palaeontol. Electr. 4 http://palaeo-electronica.org/2001_1/past/issue1_01.htm.
- HILLSON S., 1996. *Dental Anthropology*. Cambridge University Press, 373 p.
- HOUËT F., 2001. Limites de variation, distance (position) et écart réduit ajusté. *Paléo*, 13: 195–200.
- MACCHIARELLI R., BONDIOLI L., DEBÉNATH A., MAZURIER A., TOURNÉPICHE J.-F., BIRCH W. & DEAN C., 2006. How Neanderthal molar teeth grew. *Nature*, 444: 748–751.
- MOLNAR S., 1971, Human Tooth Wear, Tooth Function and Cultural Variability. *American Journal of Physical Anthropology*, 34: 175–190.
- OLEJNICZAK A. J., SMITH T. M., FEENEY R. N. M., MACCHIARELLI R., MAZURIER A., BONDIOLI L., ROSAS A., FORTEA J., DE LA RASILLA M., GARCIA-TABERNEO A., RADOVČIĆ J., SKINNER M.M., TOUSSAINT M. & HUBLIN J.-J., 2008. Dental tissue proportions and enamel thickness in Neanderthal and modern human molars. *Journal of Human Evolution*, 55: 12–23.
- ORLANDO L., DARLU P., TOUSSAINT M., BONJEAN D., OTTE M. & HÄNNI C., 2006. Revisiting Neanderthal diversity with a 100,000 year old mtDNA sequence. *Current Biology*, 16: R400–R402.
- OTTE M., TOUSSAINT M. & BONJEAN D., 1993. Découverte de restes humains immatures dans les niveaux moustériens de la grotte Scladina à Andenne (Belgique). *Bulletins et Mémoires de la Société d'Anthropologie de Paris*, nouvelle série, t. 5, 1-2: 327–332.
- PATTE E., 1959–1961. La dentition des Néanderthaliens. *Annales de Paléontologie*, XLV: 223–238; XLVI: 197–288; XLVII: 253–303.
- PIRSON S., BONJEAN D., DI MODICA K. & TOUSSAINT M., 2005. Révision des couches 4 de la grotte Scladina (comm. d'Andenne, prov. de Namur) et implications pour les restes néandertaliens : premier bilan. *Notae praehistoricae*, 25: 61–69.
- SCOTT G.R. & TURNER C.G. II, 1997. *The Anthropology of Modern Human Teeth. Dental Morphology and its Variations in Recent Human Populations*. Cambridge University Press: 382 p.
- SEMAL P., 1988. *Evolution et variabilité des dimensions dentaires chez Homo sapiens Neanderthalensis*. Viroinval, Editions du C.E.D. Arc, 112 p.
- SEMAL P., TOUSSAINT M., MAUREILLE B., ROUGIER H., CREVECOEUR I., BALZEAU A., BOUCHNEB L., LOURYAN S. DE CLERCK N. & RAUSIN L., 2005. Numérisation des restes humains néandertaliens belges. Préservation patrimoniale et exploitation scientifique. *Notae praehistoricae*, 25: 25–38.
- SKINNER M. M., GUNZ P., WOOD B. A. & HUBLIN J.-J., 2008. Enamel-dentine junction (EDJ) morphology distinguishes the lower molars of *Australopithecus africanus* and *Paranthropus robustus*. *Journal of Human Evolution*, 55: 979–988.
- SMITH T. M., OLEJNICZAK A. J., ZERMENO J. P., TAFFOREAU P. T., SKINNER M. M., HOFFMANN A., RADOVČIĆ J., TOUSSAINT M., KRUSZYNSKI R., MENTER C., MOGGI-CECCHI J., GLASMACHER U. A., KULLMER O., SCHRENK F., STRINGER C. B. & HUBLIN J.-J., 2012. Variation in enamel thickness within the genus *Homo*. *Journal of Human Evolution*, 62: 395–411.
- SMITH T. M., TOUSSAINT M., REID D. J., OLEJNICZAK A. J. & HUBLIN J.-J., 2007. Rapid dental development in a Middle Paleolithic Belgian Neanderthal. *Proceedings of the National Academy Science of the United States of America*, 104, 51: 20220–20225.
- STEFAN V. & TRINKAUS E., 1998. Discrete trait and dental morphometric affinities of the Tabun 2 mandible. *Journal of Human Evolution*, 34: 443–468.
- TILLIER A.-M., 1979. La dentition de l'enfant moustérien Châteauneuf 2 découverte à l'abri de Hauteroche. *L'Anthropologie*, 83: 417–438.
- TOUSSAINT M., OLEJNICZAK A. J., EL ZAAATARI S., CATTELAINE P., FLAS D., LETOURNEUX C. & PIRSON S., 2010. The Neanderthal lower right deciduous second molar from Trou de l'Abîme at Couvin, Belgium, *Journal of Human Evolution*, 58: 56–67.
- TOUSSAINT M., OTTE M., BONJEAN D., BOCHERENS H., FALGUÈRES C. & YOKOYAMA Y., 1998.



Les restes humains néandertaliens immatures de la couche 4A de la grotte Scladina (Andenne, Belgique). *Comptes rendus de l'Académie des Sciences de Paris, Sciences de la terre et des planètes*, 326: 737-742.

TOUSSAINT M., SEMAL P. & PIRSON S., 2011. Les Néandertaliens du bassin mosan belge : bilan 2006-2011. In M. TOUSSAINT, K. DI MODICA & S. PIRSON (sc. dir.), *Le Paléolithique moyen en Belgique. Mélanges Marguerite Ullrix-Closset*. Bulletin de la Société royale belge d'Études Géologiques et Archéologiques *Les Chercheurs de la Wallonie*, hors-série, 4 & Études et Recherches Archéologiques de l'Université de Liège, 128: 149-196.

TURNER C.G. II, NICHOL C.R. & SCOTT G.R., 1991. Scoring Procedures for Key Morphological Traits of the Permanent Dentition: The Arizona State University Dental Anthropology System. In M. KELLEY & C. LARSEN (eds.), *Advances in Dental Anthropology*, New York, Wiley Liss: 13-31.

VERNA C., 2006. *Les restes humains moustériens de la Station Amont de La Quina - (Charente, France). Contexte archéologique et constitution de l'assemblage. Étude morphologique et métrique des restes crânio-faciaux. Apport à l'étude de la variation néandertalienne*. Unpublished PhD thesis, Université de Bordeaux 1, 629 p.

Stefano BENAZZI, Michel TOUSSAINT &
Jean-Jacques HUBLIN

Michel Toussaint & Dominique Bonjean (eds.), 2014.
*The Scladina I-4A Juvenile Neandertal (Andenne, Belgium),
Palaeoanthropology and Context*

Études et Recherches Archéologiques de l'Université de Liège, 134: 307-314.

1. Introduction

Over the past century, the enamel thickness has been extensively used for the taxonomic, phylogenetic, and dietary assessment of extant and fossil primates, and is considered an effective dental feature to distinguish between the thickly-enamelled hominin taxa and the relatively thin-enamelled extant African apes (e.g., MOLNAR & GANTT, 1977; SCHWARTZ, 2000; MARTIN et al., 2003; GRINE et al., 2005; OLEJNICZAK et al., 2007; VOGEL et al., 2008).

Even though a general overlap in enamel thickness range of variation characterizes the genus *Homo* (SMITH et al., 2012), it has been observed that recent and fossil *Homo sapiens* possess absolutely and relatively thicker enamel than *Homo neanderthalensis* (OLEJNICZAK et al., 2008; BENAZZI et al., 2011^a; SMITH et al., 2012). These findings mainly depend on differences in both dental topography and tissue proportions, since Neandertals have more complex enamel-dentine junction (EDJ) surface and larger dentine volume than *Homo sapiens*, resulting in lower average and relative enamel thickness (e.g., MACCHIARELLI et al., 2006; SMITH et al., 2007; 2012; OLEJNICZAK et al., 2008; BAYLE et al., 2009^{a,b}, 2010; BENAZZI et al., 2011^a). Nonetheless, some contributions reported a Neanderthal enamel thickness in the range of *Homo sapiens* (BENAZZI et al., 2011^{b,c}, 2013). This might be due to methodological shortcomings of previous techniques to compute the enamel thickness (BENAZZI et al., 2014). In addition, the real Neanderthal range of variation is not yet clearly understood.

With regard to the methodology, preliminary studies on the enamel thickness considered physical cross-sections of molar teeth (e.g., MOLNAR & GANTT, 1977; MARTIN, 1985; SCHWARTZ, 2000; GRINE, 2004, 2005; GRINE et al., 2005), but concerns have been raised about its destructive nature, as well as

problems related to specimen orientation and the reductive information carried by the two-dimensional (2D) enamel cap morphology when compared with the more complex three-dimensional (3D) shape of the crown (OLEJNICZAK, 2006). Therefore, non-destructive techniques based on micro-computed tomography (micro-CT) were proposed to refine the 2D enamel thickness analysis and, most importantly, to study the thicknesses of dental enamel in its full 3D form (OLEJNICZAK, 2006, followed by OLEJNICZAK et al., 2008). However, it has been recently emphasized that the suggested digital approaches have some methodological flaws and can only be applied to molar teeth, thus explaining the reason for the low number of studies on premolars and anterior teeth (FEENEY et al., 2010; SMITH et al., 2012). In a recent contribution Benazzi and colleagues (2014) addressed this issue, providing rigorous guidelines for the digital computation of 2D and 3D enamel thickness in molars, premolars, canines and incisors.

The enamel thickness variation in Neandertal teeth is difficult to assess. The 2D and mainly the 3D enamel thickness analyses require unworn or slightly worn teeth, which are much less frequent in the fossil record than worn teeth. Teeth are often affected by a certain amount of wear and there is no tool, physical or digital, that can be used confidently to restore the internal and external original shape of heavily worn crowns. This is why unworn or slightly worn teeth such as those from the Scladina dental sample are of particular value for the investigation of enamel thickness variability.

In this contribution we provide the components of 2D and 3D enamel thickness of the Scladina molars, premolars and canines using a new approach recently standardized by Benazzi and colleagues (2014). We aim to improve our understanding of the Neandertal range of variation for the enamel thickness, and then to promote the comparison of the results.



2. Materials and methods

Thirteen Neandertal teeth from Scladina, Belgium, were considered to compute the components of 2D and 3D enamel thickness. Most of the teeth are unworn or slightly worn, except for three first molars that show moderate dentine exposure (wear stage 3, based on SMITH, 1984). A list of the Scladina teeth included in the analysis, as well as their wear stage, is reported in Tables 1 & 2.

The teeth were scanned with a Skyscan 1172 micro-CT (Max Planck Institute for Evolutionary Anthropology, Leipzig, Germany) using the following scan parameters: 100kV, 100µA, with an aluminum/copper filter (0.5 mm/0.04 mm thickness). Volume data were reconstructed using isometric voxels of 13.74 µm. Each image stack was segmented using a semiautomatic threshold-based approach in Avizo 7 (Visualization Sciences Group Inc.) to separate the enamel, the dentine and the pulp chamber and to reconstruct 3D digital models from the tooth volume data.

Following guidelines underlined by BENAZZI et al. (2014), the digital models were then imported in Rapidform XOR2 (INUS Technology Incorporated, Seoul, Korea), and for each tooth class a specific protocol was used to compute both the 2D and 3D enamel thickness. As already emphasized by OLEJNICZAK and colleagues (2008), discrepancies are observed between 3D and 2D data due to the dimensional loss in the latter. Since the 3D approach registers variation in enamel thickness across the tooth crown, the 3D data are more appropriate than 2D data. However, because

the latter have been widely used to study hominoid teeth (e.g., SMITH et al., 2006; 2012), in this contribution we also provide the values of the components of 2D enamel thickness.

In molars and second premolars, the cervical line was digitized using a spline curve and the best-fit plane through the points of the curve was computed (cervical plane) to separate the crown (enamel cap and dentine core) from the root (Figures 1 & 2).

For the 3D analysis of molars and second premolars, the following measurements were obtained from the crown: the volume of the enamel cap (mm³); the volume of the dentine core (which includes the volume of the coronal pulp – mm³); the enamel-dentine junction (EDJ) surface (the interface between the enamel cap and the dentine core – mm²). These measurements were used for the computation of both the 3D average enamel thickness index (3D AET = volume of enamel divided by the EDJ surface; index in millimetres) and the 3D relative enamel thickness index (3D RET = 3D AET divided by the cubic root of dentine volume; scale-free index).

For the 2D analysis of molars and second premolars, a digital cross-section perpendicular to the cervical plane and passing through the two mesial (mesial section) dentine horn tips (paracone and protocone in permanent maxillary molars; protoconide and metaconide in permanent mandibular molars/second premolars) was created. Then, a line was digitized to join the most buccal and lingual apical extension of enamel (Figures 1 & 2). The following measurements were recorded from the sections: the area of the enamel

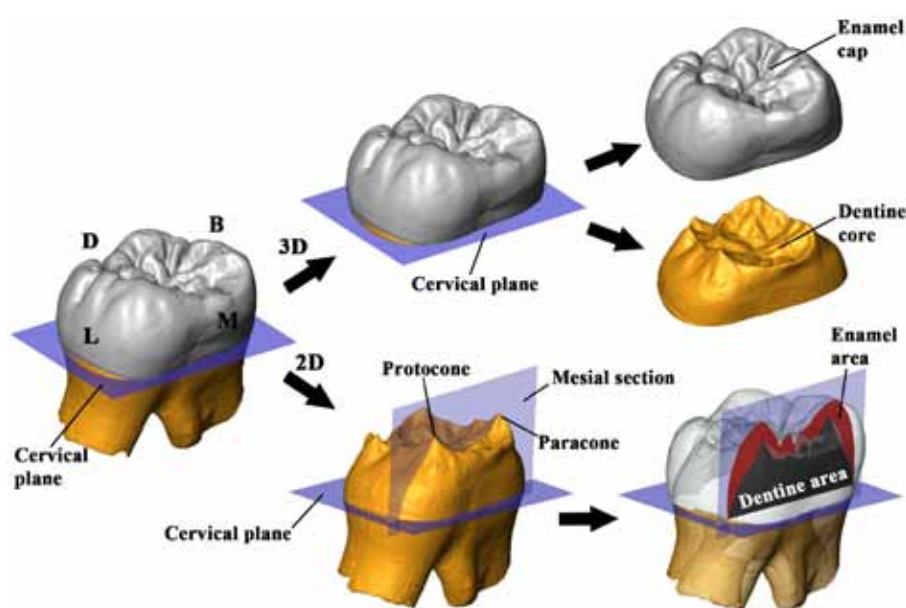


Figure 1: On the left, a best-fit plane (cervical plane) was computed on the cervical line of Scla 4A-3 permanent maxillary right second molar (RM²). For 2D enamel thickness, the mesial section is perpendicular to the cervical plane and passes through the mesial (paracone and protocone) dentine horn tips. In the 3D enamel thickness, the crown is separated from the root based on the cervical plane to identify the enamel cap and the dentine core of the crown. B = buccal; D = distal; L = lingual; M = mesial.

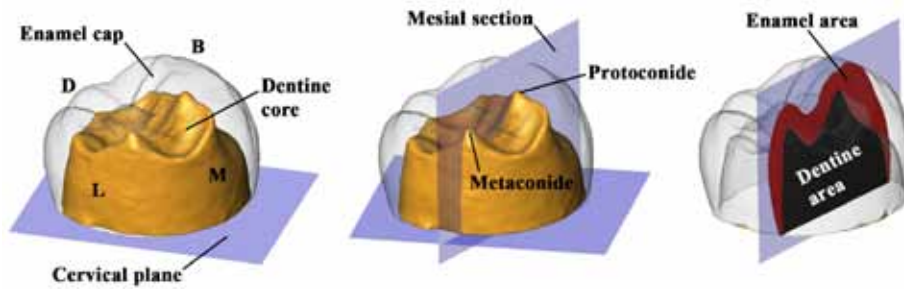


Figure 2: On the left, a best-fit plane (cervical plane) was computed on the cervical line of Scla 4A-9/P₄ mandibular left second premolar to separate the crown from the root; the enamel cap, the dentine core, and the interface between them (enamel-dentine junction (EDJ) surface) were used for the computation of the 3D enamel thickness indices. For 2D enamel thickness, the mesial section is perpendicular to the cervical plane and passes through the mesial (protoconide and metaconide) dentine horn tips.

cap (mm²); the area of the coronal dentine (mm²), which includes the coronal pulp; the length of the EDJ (the linear interface between the enamel area and the dentine area – mm); the 2D average enamel thickness index (2D AET = the area of the enamel cap divided by the length of the EDJ; index in millimetres); the 2D relative enamel thickness index (2D RET = 2D AET divided by the square root of the coronal dentine area; scale-free index).

In the 3D analysis of first premolars and canines the coronal dentine was separated from the root dentine based on the curve digitized on the cervical line. The smooth surface interpolating the curve was then used to seal the digital model of the dentine core (Figures 3 & 4).

In the 2D analysis of first premolars, a virtual section of the tooth perpendicular to the best-fit plane of the cervical line (cervical plane) and passing through the main dentine horn tips (protoconide and metaconide in mandibular first premolars; paracone and protocone in maxillary first premolars) was created (Figure 3). Instead, each canine was oriented in its anatomical position to visualize the buccal and lingual sides. A virtual section was created passing through two

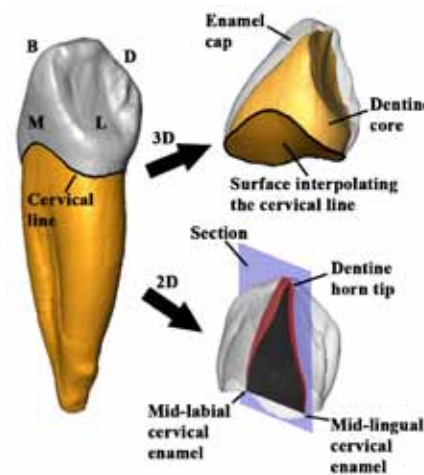


Figure 4: On the left, a spline curve (black) was digitized on the cervical line of Scla 4A-12 permanent mandibular right canine (RC₁). For 3D enamel thickness, the coronal dentine was separated from the root dentine based on the cervical line, which was then interpolated by a smooth surface to seal the bottom of the dentine core. For 2D enamel thickness, the cross-section passes through two points digitized on the mid-labial and mid-lingual cervical enamel, respectively, and one point digitized on the dentine horn tip. B = buccal; D = distal; L = lingual; M = mesial.

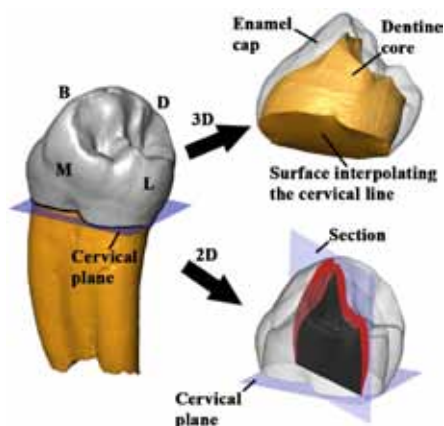


Figure 3: On the left, a spline curve (black) was digitized on the cervical line of Scla 4A-6 mandibular right first premolar (RP₃). For the 2D enamel thickness, the best-fit plane of the curve was computed (cervical plane), and a mesial section perpendicular to this plane and passing through the mesial (protoconide and metaconide) dentine horn tips was created. For the 3D enamel thickness, the coronal dentine was separated from the root dentine based on the cervical line, which was then interpolated by a smooth surface to seal the bottom of the dentine core. B = buccal; D = distal; L = lingual; M = mesial.



points digitized on the mid-labial and mid-lingual cervical enamel, respectively, and the dentine horn tip (Figure 4). In both first premolars and canines, a line was then digitized to join the most buccal and lingual apical extension of enamel. The computation of the AET and RET indices (both in 2D and 3D) follows indications mentioned above.

Comparative data for 2D and 3D enamel thickness for Neandertals and *Homo sapiens* were sourced from SMITH et al. (2006; 2012) and OLEJNICZAK et al. (2008). When possible, for 2D data standardized score (Z-scores) values were computed to establish whether the values obtained for the Scladina teeth were closest to either the Neandertal or *Homo sapiens* group mean. However, since the comparative data were obtained using approaches that have been recently refined by BENAZZI et al. (2014), who recognized shortcomings in the protocol of tooth orientation, we emphasize that the comparison should be considered tentative at best.

3. Results

The values of the components of 2D and 3D enamel thickness, as well as the AET and RET indices for the 13 Scladina Neandertal teeth are shown in Tables 1 & 2. Results obtained for the first molars should be considered with caution, because tooth wear (wear stage 3 based on SMITH, 1984) affects much more the enamel than the dentine, so that the computed AET and RET indices are certainly lower than the indices we would have computed for the unworn teeth. While in some cases 2D and 3D indices supply

similar results, in other circumstances differences between the two approaches are quite noticeable (e.g., Scla 4A-1/P₄, Scla 4A-2/P³, Scla 4A-9/P₄, Scla 4A-16 RC¹). Interestingly, it seems that the discrepancy between 2D and 3D data increases in premolars and anterior teeth when compared with molars, but this tendency might be biased by the small sample size. In any case, as mentioned above, 3D data (Table 2) are more suitable than 2D data (Table 1).

Based on 3D data of the unworn/slightly worn teeth (Table 2), premolars have generally larger RET index than molars (premolars = 20.89±2.45; molars = 18.61±0.69), but the condition is reversed for the AET index (premolars = 1.08±0.11; molars = 1.20±0.04). The canines show the lowest values, both for AET (0.77±0.11) and RET (13.44±1.03) indices, having absolutely and relatively little enamel surrounding a large bulk of dentine. Similar results are observed in the 2D data, at least for the AET indices (molars = 1.16±0.08; premolars = 1.0±0.06; canines = 0.69±0.1) and the canine RET indices (canines = 10.43±0.7) (Table 1). However, a reverse condition, when compared with 3D data, characterizes the mean 2D RET indices computed for molars (19.44±1.74) and premolars (17.58±1.59). Therefore, results obtained for canines and molars are more consistent between 2D and 3D analysis than results obtained for premolars.

When the Scladina molars are compared with AET and RET mean values (both 2D and 3D) computed for Neandertals and *Homo sapiens*, results are ambiguous. When the three most worn first molars are excluded (their low indices ally them with Neandertal but might well be an artefact

Scladina specimens	Tooth class	Enamel area (mm ²)	Coronal area (mm ²)	EDJ length (mm)	AET (mm)	RET (scale-free)	Wear stage ^a
Scla 4A-1/P ₄	RP ₄	17.75	31.09	17.51	1.01	18.18	1
Scla 4A-1/M ₁	RM ₁	15.58	37.16	18.01	0.86	14.19	3
Scla 4A-1/M ₂	RM ₂	19.92	36.78	18.78	1.06	17.49	1
Scla 4A-1/M ₃	RM ₃	19.74	32.10	17.10	1.15	20.38	unworn
Scla 4A-2/P ³	RP ³	19.98	38.03	19.16	1.04	16.91	unworn
Scla 4A-3	RM ²	22.14	38.11	19.33	1.15	18.56	unworn
Scla 4A-4	RM ¹	17.19	39.41	19.00	0.90	14.41	3
Scla 4A-6	RP ₃	16.14	33.81	17.59	0.92	15.78	unworn
Scla 4A-9/P ₄	LP ₄	17.48	28.58	16.81	1.04	19.45	1
Scla 4A-9/M ₁	LM ₁	15.08	39.57	18.16	0.83	13.20	3
Scla 4A-9/M ₂	LM ₂	22.81	35.12	18.03	1.26	21.34	unworn
Scla 4A-12	RC ₁	12.53	38.38	20.35	0.62	9.94	1
Scla 4A-16	RC ¹	16.83	47.95	22.24	0.76	10.93	unworn

Table 1: Values of the components of two-dimensional (2D) enamel thickness measurements in the Scladina teeth (^abased on SMITH (1984); EDJ = enamel dentine junction; AET = average enamel thickness; RET = relative enamel thickness).

Scladina specimens	Tooth class	Enamel volume (mm ³)	Coronal dentine + pulp volume (mm ³)	EDJ surface (mm ²)	AET (mm)	RET (scale-free)	Wear stage ^a
Scla 4A-1/P ₄	RP ₄	134.54	131.12	116.88	1.15	22.66	1
Scla 4A-1/M ₁	RM ₁	198.26	285.73	202.97	0.98	14.83	3
Scla 4A-1/M ₂	RM ₂	229.69	275.63	197.00	1.17	17.92	1
Scla 4A-1/M ₃	RM ₃	209.91	230.14	175.59	1.20	19.51	unworn
Scla 4A-2/P ³	RP ³	142.53	149.72	128.98	1.11	20.81	unworn
Scla 4A-3	RM ²	228.29	264.81	194.67	1.17	18.26	unworn
Scla 4A-4	RM ¹	219.65	286.69	201.23	1.09	16.55	3
Scla 4A-6	RP ₃	120.58	144.40	131.68	0.92	17.45	unworn
Scla 4A-9/ P ₄	LP ₄	132.99	127.69	116.65	1.14	22.64	1
Scla 4A-9/ M ₁	LM ₁	194.59	300.40	209.21	0.93	13.89	3
Scla 4A-9/ M ₂	LM ₂	257.35	297.81	205.66	1.25	18.74	unworn
Scla 4A-12	RC ₁	99.56	160.67	144.11	0.69	12.71	1
Scla 4A-16	RC	145.16	215.02	170.99	0.85	14.17	unworn

Table 2: Values of the components of three-dimensional (3D) enamel thickness measurements in the Scladina teeth (^abased on SMITH (1984); EDJ = enamel dentine junction; AET = average enamel thickness; RET = relative enamel thickness).

Tooth class	Sample	N	AET			RET		
			Mean (SD)	Min–Max	Z–score	Mean (SD)	Min–Max	Z–score
M ¹	N	3 ^a	1.05 (0.13)	0.93–1.19		15.37 (1.57)	13.8–16.93	
	FHS	4 ^b	1.28	1.08–1.58		18.2	15.7–20.9	
	RHS	37 ^c	1.22 (0.12)	0.98–1.5		18.75 (2.08)	13.95–23.86	
	Scla 4A-4		0.90		N=–1.15 RHS=–2.67	14.41		N=–0.61 RHS=–2.09
M ²	N	5 ^a	1.21 (0.08)	1.13–1.29		18.18 (2.05)	15.65–20.85	
	FHS	1 ^b	1.31			19.8		
	RHS	25 ^c	1.40 (0.17)	1.13–1.76		21.59 (3.13)	16.49–28.03	
	Scla 4A-3		1.15		N=–0.75 RHS=–1.47	18.56		N=0.19 RHS=–0.97
M ₁	N	12 ^a	1.01 (0.07)	0.93–1.18		16.06 (1.64)	13.77–20.46	
	FHS	6 ^b	1.19	0.96–1.47		18.0	15.2–23.3	
	RHS	55 ^c	1.07 (0.13)	0.8–1.4		16.99 (2.29)	11.76–22.62	
	Scla 4A-1/M ₁		0.86		N=–2.14 RHS=–1.62	14.19		N=–1.14 RHS=–1.22
M ₂	N	6 ^a	1.02 (0.08)	0.94–1.14		15.63 (0.87)	14.21–16.8	
	FHS	4 ^b	1.28	1.17–1.41		18.3	16.3–20.2	
	RHS	45 ^c	1.19 (0.14)	0.94–1.55		20.51 (2.93)	14.85–27.66	
	Scla 4A-1/M ₂		1.06		N=0.5 RHS=–0.93	17.49		N=2.14 RHS=–1.03
M ₃	N	8 ^a	0.99 (0.06)	0.92–1.1		16.55 (1.28)	14.3–18.34	
	FHS	2 ^b	1.28	1.15–1.41		20.5	19.2–21.9	
	RHS	44 ^c	1.24 (0.15)	0.98–1.67		21.63 (2.99)	17.22–31.84	
	Scla 4A-1/M ₃		1.15		N=2.67 RHS=–0.6	20.38		N=2.99 RHS=–0.42

Table 3: Two-dimensional (2D) enamel thickness in the Scladina molar sample, compared with mean value indices computed in Neandertal (N), fossil *Homo sapiens* (FHS) and recent *Homo sapiens* (RHS); when possible, standard deviation (SD), minimum-maximum values and standardized Z-scores are provided. Data from ^aOLEJNICZAK et al. (2008), ^bSMITH et al. (2012), ^cSMITH et al. (2006).

of tooth wear), the Scladina teeth (particularly for the RET index) generally fall on the higher end or even outside the Neandertal range of variation, often in between the currently known Neandertal and *Homo sapiens* mean values (Tables 3 & 4).

The paucity of comparative data for premolars and canines (SMITH et al., 2012), which are only in 2D, and the incompleteness of statistic information given (e.g., standard deviation and range values are not provided), limit us in the



Tooth class	Sample	n	AET		RET	
			Mean (SD)	Min–Max	Mean (SD)	Min–Max
M ¹	N	1	1.07		15.13	
	RHS	6	1.13		17.05	
	Scla 4A-4		1.09		16.55	
M ²	N	4	1.07 (0.08)	0.97–1.14	15.33 (1.83)	13.65–17.56
	RHS	6	1.46		23.36	
	Scla 4A-3		1.17		18.26	
M ₁	N	9	1.17 (0.23)	0.97–1.63	16.77 (3.8)	13.03–24.02
	RHS	1	1.05		15.87	
	Scla 4A-1/M ₁		0.98		14.83	
M ₂	N	4	0.99 (0.11)	0.89–1.13	13.63 (0.47)	13.13–14.18
	RHS	9	1.46		23.44	
	Scla 4A-1/M ₂		1.17		17.92	
M ₃	N	6	1.06 (0.20)	0.82–1.3	15.43 (2.82)	12.74–19.67
	RHS	9	1.45		23.79	
	Scla 4A-1/M ₃		1.20		19.51	

Table 4: Three-dimensional (3D) enamel thickness in the Scladina molar sample, compared with mean value indices computed in Neandertal (N) and recent *Homo sapiens* (RHS); when possible, standard deviation (SD) and minimum-maximum values are provided (data from OLEJNICZAK et al., 2008).

Tooth class	Taxon	n	AET (mean)	RET (mean)
RC	FHS	2	0.87	12.71
	RHS	22	0.91	14.43
	Scla 4A-16		0.76	10.93
RC ₁	FHS	4	0.77	10.65
	RHS	20	0.81	12.91
	Scla 4A-12		0.62	9.94
RP ³	FHS	1	1.26	18.74
	RHS	19	1.1	17.69
	Scla 4A-2/P ³		1.04	16.91
RP ₃	FHS	3	1.04	15.81
	RHS	17	1.01	17.78
	Scla 4A-6		0.92	15.78
LP ₄	FHS	2	1.08	16.17
	RHS	17	1.20	21.19
	Scla 4A-1/P ₄		1.01	18.18
	Scla 4A-9/P ₄		1.04	19.45

Table 5: Two-dimensional (2D) enamel thickness in the Scladina canine and premolar sample, compared with mean value indices computed in fossil *Homo sapiens* (FHS) and recent *Homo sapiens* (RHS); data from SMITH et al. (2012).

discussion of the results obtained for the Scladina enamel thickness. However, we can summarize our findings as follows: the low AET values of the Scladina premolars and canines find more correspondence with Neandertal than *Homo sapiens* mean values (Table 5). Similarly, the low RET index of the canines is in agreement with values observed in Neandertal, while results computed for the premolars are more ambiguous, but this is certainly due to the extremely small Neandertal comparative sample size.

4. Discussion and conclusions

As absence of wear is an essential precondition to compute the values for 2D and 3D enamel thickness, the unworn/slightly worn Scladina teeth represent a valuable sample for the advancement of our knowledge on Neandertal’s enamel thickness variability.

It is generally accepted that Neandertals had a lower average and relative enamel thicknesses than *Homo sapiens*, (e.g. MACCHIARELLI et al., 2006; SMITH et al., 2007, 2012; OLEJNICZAK et al., 2008; BAYLE et al., 2009^{a,b}, 2010), but shortcomings observed in previous methods might have contributed to the confusing result and misrepresent the real range of enamel thickness variation. Results obtained for the Scladina teeth point out that indeed Neandertals have lower AET and RET indices than *Homo sapiens*, but they also suggest that the discrepancy observed in previous studies between the two groups (e.g. SMITH et al., 2006, 2012; OLEJNICZAK et al., 2008) has been overemphasized, as recently observed by Benazzi and colleagues (2011^c, 2013^a). This does not mean that Neandertals and *Homo sapiens* overlap in AET and RET indices, but it suggests that the Neandertal range of variation is still unknown. This issue could be solved using rigorous and consistent methodological protocols in large *Homo sapiens* (recent and fossil) and Neandertal dental samples.

This contribution is one of the few providing 2D enamel thickness for premolars and canines

(see also FEENEY et al., 2010; SMITH et al., 2012), and the first providing 3D enamel thickness for these dental classes. With regard to the 3D data, our results suggest that molars, premolars and canines (and presumably incisors) have a different and peculiar trend, with premolars having a generally larger RET index than molars, and canines showing the lowest values. Moreover, our results confirm that Neandertal canines have lower AET and RET indices than *Homo sapiens* canines, as previously suggested by 2D data (SMITH et al., 2012).

We are confident that the values of the components of 2D and 3D enamel thickness measurements reported in this paragraph for the Scladina teeth (Tables 1 & 2), coupled with a thorough explanation of the method, will be useful to favor future comparative studies between Neandertal and *Homo sapiens*, making scholars aware of the importance to increase the sample size to evaluate the enamel thickness range of variation of these two human groups.

Acknowledgements

This research was supported by the Max Planck Society.

References

- BAYLE P., BRAGA J., MAZURIER A. & MACCHIARELLI R., 2009^a. Dental developmental pattern of the Neandertal child from Roc de Marsal: a high-resolution 3D analysis. *Journal of Human Evolution*, 56: 66–75.
- BAYLE P., BRAGA J., MAZURIER A. & MACCHIARELLI R., 2009^b. Brief communication: high-resolution assessment of the dental developmental pattern and characterization of tooth tissue proportions in the late Upper Paleolithic child from La Madeleine, France. *American Journal of Physical Anthropology*, 138: 493–498.
- BAYLE P., MACCHIARELLI R., TRINKAUS E., DUARTE C., MAZURIER A. & ZILHÃO J., 2010. Dental maturational sequence and dental tissue proportions in the early Upper Paleolithic child from Abrigo do Lagar Velho, Portugal. *Proceedings of the National Academy Science of the United States of America*, 107, 4: 1338–1342.
- BENAZZI S., BAILEY S. E. & MALLEGNI F., 2013. A morphometric analysis of the Neandertal upper second molar Leuca I. *American Journal of Physical Anthropology*, 152: 300–305.
- BENAZZI S., DOUKA K., FORNAI C., BAUER C. C., KULLMER O., SVOBODA J., PAPI I., MALLEGNI F., BAYLE P., COQUERELLE M., CONDEMI S., RONCHITELLI A., HARVATI K. & WEBER G. W., 2011^a. Early dispersal of modern humans in Europe and implications for Neandertal behaviour. *Nature*, 479: 525–528.
- BENAZZI S., FORNAI C., BAYLE P., COQUERELLE M., KULLMER O., MALLEGNI F. & WEBER G. W., 2011^b. Comparison of dental measurement systems for taxonomic assignment of Neandertal and modern human lower second deciduous molars. *Journal of Human Evolution*, 61: 320–326.
- BENAZZI S., PANETTA D., TOUSSAINT M., GRUPPIONI G. & HUBLIN J.-J., 2014. Guidelines for the digital computation of 2D and 3D enamel thickness. *American Journal of Physical Anthropology*, 153: 305–313.
- BENAZZI S., VIOLA B., KULLMER O., FIORENZA L., HARVATI K., PAUL T., GRUPPIONI G., WEBER G. W. & MALLEGNI F., 2011^c. A reassessment of the Neandertal teeth from Taddeo cave (southern Italy). *Journal of Human Evolution*, 61: 377–387.
- FEENEY R. N. M., ZERMENO J. P., REID D. J., NAKASHIMA S., SANO H., BAHAR A., HUBLIN J.-J. & SMITH T. M., 2010. Enamel thickness in Asian human canines and premolars. *Anthropological Science*, 118: 191–198.
- GRINE F. E., 2004. Geographic variation in tooth enamel thickness does not support Neandertal involvement in the ancestry of modern Europeans. *South African Journal of Science*, 100: 389–394.
- GRINE F. E., 2005. Enamel thickness of deciduous and permanent molars in modern *Homo sapiens*. *American Journal of Physical Anthropology*, 126: 14–31.
- GRINE F. E., SPENCER M. A., DEMES B., SMITH H. F., STRAIT D. S. & CONSTANT D. A., 2005. Molar enamel thickness in the chacma baboon, *Papio ursinus* (KERR, 1792). *American Journal of Physical Anthropology*, 128: 812–822.
- MACCHIARELLI R., BONDIOLI L., DEBÉNATH A., MAZURIER A., TOURNEPICHE J.-F., BIRCH W. & DEAN C., 2006. How Neandertal molar teeth grew. *Nature*, 444: 748–751.
- MARTIN L. B., 1985. Significance of enamel thickness in hominoid evolution. *Nature*, 314: 260–263.



- MARTIN L. B., OLEJNICZAK A. J. & MAAS M. C., 2003. Enamel thickness and microstructure in pitheciin primates, with comments on dietary adaptations of the middle Miocene hominoid Kenyapithecus. *Journal of Human Evolution*, 45: 351–367.
- MOLNAR S. & GANTT D. G., 1977. Functional implications of primate enamel thickness. *American Journal of Physical Anthropology*, 46: 447–454.
- OLEJNICZAK A. J., 2006. *Micro-Computed Tomography of Primate Molars*. Unpublished PhD thesis. Stony Brook University.
- OLEJNICZAK A. J., GILBERT C. C., MARTIN L. B., SMITH T. M., ULHAAS L. & GRINE F. E., 2007. Morphology of the enamel-dentine junction in sections of anthropoid primate maxillary molars. *Journal of Human Evolution*, 53: 292–301.
- OLEJNICZAK A. J., SMITH T. M., FEENEY R. N. M., MACCHIARELLI R., MAZURIER A., BONDIOLI L., ROSAS A., FORTEA J., DE LA RASILLA M., GARCIA-TABERNEO A., RADOVČIĆ J., SKINNER M. M., TOUSSAINT M. & HUBLIN J.-J., 2008. Dental tissue proportions and enamel thickness in Neandertal and modern human molars. *Journal of Human Evolution*, 55: 12–23.
- SCHWARTZ G. T., 2000. Taxonomic and functional aspects of the patterning of enamel thickness distribution in extant large-bodied hominoids. *American Journal of Physical Anthropology*, 111: 221–244.
- SMITH B. H., 1984. Patterns of molar wear in hunter-gatherers and agriculturalists. *American Journal of Physical Anthropology*, 63: 39–56.
- SMITH T. M., OLEJNICZAK A. J., REID D. J., FERRELL R. J. & HUBLIN J.-J., 2006. Modern human molar enamel thickness and enamel-dentine junction shape. *Archives of Oral Biology*, 51: 974–995.
- SMITH T. M., OLEJNICZAK A. J., ZERMENO J. P., TAFFOREAU P. T., SKINNER M. M., HOFFMANN A., RADOVČIĆ J., TOUSSAINT M., KRUSZYNSKI R., MENTER C., MOGGI-CECCHI J., GLASMACHER U. A., KULLMER O., SCHRENK F., STRINGER C. B. & HUBLIN J.-J., 2012. Variation in enamel thickness within the genus Homo. *Journal of Human Evolution*, 62: 395–411.
- SMITH T. M., TOUSSAINT M., REID D. J., OLEJNICZAK A. J. & HUBLIN J.-J., 2007. Rapid dental development in a Middle Paleolithic Belgian Neandertal. *Proceedings of the National Academy Science of the United States of America*, 104, 51: 20220–20225.
- VOGEL E. R., VAN WOERDEN J. T., LUCAS P. W., UTAMI ATMOKO S. S., VAN SCHAİK C. P. & DOMINY N. J., 2008. Functional ecology and evolution of hominoid molar enamel thickness: Pan troglodytes schweinfurthii and Pongo pygmaeus wurmbii. *Journal of Human Evolution*, 55: 60–74.

Chapter 15

INTERSPECIFIC AND INTRASPECIFIC TAXONOMIC AFFINITY BASED ON PERMANENT MANDIBULAR MOLAR ENAMEL- DENTINE JUNCTION MORPHOLOGY OF THE SCLADINA I-4A JUVENILE

Dorien DE VRIES, Jean-Jacques HUBLIN,
Michel TOUSSAINT & Matthew M. SKINNER

*Michel Toussaint & Dominique Bonjean (eds.), 2014.
The Scladina I-4A Juvenile Neandertal (Andenne, Belgium),
Palaeoanthropology and Context*

Études et Recherches Archéologiques de l'Université de Liège, 134: 315-324.

1. Introduction

Dental crown morphology is often used to assess the taxonomic affinity and phylogenetic relationship of individual specimens. In a number of studies molar crown morphology has been found to discriminate between extant hominoid species and sub-species (JOHANSON, 1974; UCHIDA, 1992, 1996; PILBROW, 2003, 2006) and extinct hominoid taxa (WEIDENREICH, 1937; ROBINSON, 1956; SPERBER, 1974; WOOD & ABBOTT, 1983; SUWA, 1996; BAILEY, 2002, 2006; IRISH & GAUTELLI-STEINBERG, 2003; GRINE, 2004; HLUSKO, 2004; GUATELLI-STEINBERG & IRISH, 2005). However, the effects of dental attrition on the outer enamel surface can decrease the taxonomic information of external crown morphology and necessitate the use of less comprehensive measures of tooth crown shape (e.g. linear crown measurements).

Recently, it has been demonstrated that the internal structure of the tooth crown, and in particular the enamel-dentine junction (EDJ), retains considerable taxonomic information in variably worn fossil teeth (e.g. CORRUCINI, 1987, 1998; OLEJNICZAK et al., 2004, 2007; MACCHIARELLI et al., 2006; SUWA et al., 2007; SKINNER et al., 2008) and is able to discriminate chimpanzee species and sub-species (SKINNER et al., 2009). In particular, this is because the EDJ retains valuable information on vertical crown components, such as relative/absolute dentine horn height and crown height, which have been lost in the external crown morphology of worn teeth. The EDJ can therefore be used to assess the taxonomic and phylogenetic position of individual specimens, populations, and species.

In this contribution we address three questions: 1) is the EDJ morphology of the mandibular molars consistent with the classification of Scladina I-4A as a Neandertal, 2) are there consistent differences in EDJ morphology between Early and Classic Neandertals, and 3) is the morphology of the EDJ of the Scladina specimen consistent with other

Neandertals of a similar geochronological age. We use micro-computed tomography to image the EDJ; geometric morphometric analysis to capture the shape of the EDJ; and multivariate analyses to compare the EDJ morphologies among the different taxa.

2. Materials and methods

The materials used for this study are outlined in Table 1. The comparative sample consists of a large number of Neandertal specimens ($n = 47$), fossil *Homo sapiens* ($n = 19$), and recent *Homo sapiens* ($n = 55$). Specimens that exhibited an abnormal morphology were excluded from the comparative sample. In the case of antimeres being present for a specimen the side that was better preserved was used in the analysis. The references cited in Table 1 were used to establish the taxonomy and tooth position of each specimen. Additionally, the tooth position of all specimens, based on EDJ shape, was evaluated. Specimens whose classification was inconsistent were excluded from the comparative sample. If specimens were consistently classified to a molar position that was different than previously published, the specimen was reclassified based on the EDJ results (and listed with a '4' in the 'Tooth' column in Table 1).

Geometric morphometric analysis

The molars of our comparative sample were subjected to micro-CT scanning using both industrial and desktop micro-CT systems with resultant voxel resolutions ranging from 14 to 70 μm . The image stack of each scan was filtered using a three-dimensional median and mean-of-least variance filter to facilitate segmentation (using Avizo 6.3) into enamel and dentine components. The enamel-dentine junction was exported as a ply surface model for the collection of landmarks



Specimen (n = 121)	Tooth	Side	Basis	Molar ref	Source
<i>Homo neanderthalensis</i> (n = 47)					
Abri Suard 5	1	L	1	—	TNT
Abri Suard 14_7	1	R	2	1	TNT
Abri Suard 43	3	R	3	1	TNT
Abri Suard 36	2	L	1	—	TNT
	3	L	1	—	TNT
Abri Suard 49	1	R	3	1	TNT
Combe-Grenal I	1	R	1	—	MNP
Combe-Grenal IV	1	L	1	—	MNP
Combe-Grenal XII	3	L	3	2	MNP
El Sidron SD540	2	L	2	3	MNCN
El Sidron SD755	2	R	4	—	MNCN
El Sidron SD780	1	L	2	3	MNCN
El Sidron SD1135	3	R	1	—	MNCN
Krapina 52	1	L	1	—	CMNH
Krapina 53	1	R	1	—	CMNH
	2	R	1	—	CMNH
	3	R	1	—	CMNH
Krapina 54	1	L	1	—	CMNH
	2	L	1	—	CMNH
Krapina 55	1	L	1	—	CMNH
	2	L	1	—	CMNH
Krapina 57	2	R	1	—	CMNH
	3	R	1	—	CMNH
Krapina 59	2	R	1	—	CMNH
Krapina D1	2	R	2	4	CMNH
Krapina D6	2	L	2	4	CMNH
Krapina D9	2	L	3	4	CMNH
Krapina D79	1	R	2	4	CMNH
Krapina D80	2	R	3	4	CMNH
Krapina D81	1	L	2	4	CMNH
Krapina D86	2	L	3	4	CMNH
Krapina D104	3	R	3	4	CMNH
Krapina D105	2	L	3	4	CMNH
Krapina D106	3	L	2	4	CMNH
Krapina D107	2	L	2	4	CMNH
Lakonis	3	L	3	5	EPSNE
La Quina H9	2	L	1	—	TNT
	3	L	1	—	TNT
Le Moustier	1	L	1	—	NMP
	2	L	1	—	NMP
	3	L	1	—	NMP
Le Regourdou	2	L	1	—	MAA
	3	L	1	—	MAA
Roc de Marsal	1	R	1	—	MNP
Saint-Césaire 1	3	R	1	—	MAN
Vindija 11_39	2	R	1	—	CNHM
	3	R	1	—	CNHM
Pleistocene <i>Homo sapiens</i> (n = 19)					
Dar es Soltane 2 H4	2	L	1	—	INSAP
	3	L	1	—	INSAP
El Harhoura	2	R	1	—	INSAP
	3	R	1	—	INSAP
Equus Cave H3	3	R	4	—	MM
Irhoud 3	1	L	1	—	UM
	2	L	1	—	UM
	3	L	1	—	UM
Oberkassel D999.02	2	L	1	—	LVRB
	3	L	1	—	LVRB
Qafzeh 9	1	L	1	—	SSM
	2	L	1	—	SSM

	3	L	1	—	SSM
Qafzeh 10	2	L	1	—	TAU
Qafzeh 11	2	L	1	—	TAU
Qafzeh 15	1	L	1	—	TAU
	2	L	1	—	TAU
Temara mandible	2	L	1	—	INSAP
	3	L	1	—	INSAP
Recent <i>Homo sapiens</i> (n = 55)					
Belgian A31	1	R	1	—	RBINS
Belgian A32	1	R	1	—	RBINS
Belgian 13e	2	R	1	—	RBINS
Belgian 76a	2	L	1	—	RBINS
Belgian 89a	1	L	1	—	RBINS
Belgian 93a	1	L	1	—	RBINS
Belgian 129a	1	L	1	—	RBINS
MPI M3	1	L	1	—	MPI-EA
MPI M5	1	L	1	—	MPI-EA
MPI M71	3	L	1	—	MPI-EA
MPI M131	3	R	1	—	MPI-EA
MPI M132	3	L	1	—	MPI-EA
MPI M133	3	L	1	—	MPI-EA
MPI M135	3	L	1	—	MPI-EA
MPI M146	2	L	1	—	MPI-EA
MPI M162	2	R	1	—	MPI-EA
MPI M190	2	L	1	—	MPI-EA
MPI M213	3	L	1	—	MPI-EA
Romanian R123	1	L	1	—	IA
Romanian R167_175	1	L	1	—	IA
Romanian R258_144	1	L	1	—	IA
Romanian R488_274	1	L	1	—	IA
Romanian R605_1185	1	L	1	—	IA
	3	R	1	—	IA
Romanian R1101_1498	1	R	1	—	IA
	3	L	1	—	IA
Romanian R1160_440	1	L	1	—	IA
Romanian R1586_2425	3	L	1	—	IA
Romanian R1620_2480	3	R	1	—	IA
Romanian R1719_1237	3	L	1	—	IA
Romanian R1989_1382	1	L	1	—	IA
	2	L	1	—	IA
Romanian R2070_1423	2	R	1	—	IA
Romanian R2525_1641	2	L	1	—	IA
Romanian R2602_1673	1	L	1	—	IA
NMNH SI12	1	R	4	—	NMNH
NMNH SI13	1	L	4	—	NMNH
NMNH SI15	1	R	4	—	NMNH
NMNH SI34	1	L	4	—	NMNH
NMNH SI36	1	L	4	—	NMNH
NMNH SI37	1	L	4	—	NMNH
NMNH SI38	1	L	4	—	NMNH
NMNH SI40	1	L	4	—	NMNH
NMNH SI42	1	R	4	—	NMNH
NMNH SI44	1	R	4	—	NMNH
NMNH SI45	1	R	4	—	NMNH
NMNH SI46	1	R	4	—	NMNH
NMNH SI47	1	R	4	—	NMNH
NMNH SI48	1	R	4	—	NMNH
ULAC 58	1	L	1	—	ULAC
	3	L	1	—	ULAC
ULAC 179	3	R	1	—	ULAC
ULAC 536	3	L	1	—	ULAC
ULAC 790	3	L	1	—	ULAC
ULAC 797	1	R	1	—	ULAC

Table 1 (facing page): Comparative sample, showing for each specimen the tooth position and side, basis of tooth position certainty, tooth position reference, and source of specimen.

Basis: 1 – specimen is in jaw; 2 – associated dentition; 3 – estimate based on morphology; 4 – classified through geometric morphometric analysis in this study. **Molar references:** 1. TEILHOL, 2001; 2. GARRALDA & VANDERMEERSCH, 2000; 3. ROSAS, 2009; 4. RADOVČIĆ et al., 1988; 5. HARVATI et al., 2003. **Source:** CMNH – Croatian Museum of Natural History; EPSNE – Ephorate of Palaeoanthropology & Speleology of Southern Greece; GPIH - Geologisch-Paläontologisches Institut der Universität Heidelberg; IA – Francisc J. Rainer Institute of Anthropology; INSAP – Institut National des Sciences de l’Archéologie et du Patrimoine; LVRB – Landschaftsverband Rheinland – LandesMuseum Bonn; MA – Le Musée d’Agoulême, France; MAA – Musée d’Art et d’Archéologie du Périgord; MAN – Musée d’Archéologie nationale de Saint-Germain-en-Laye; MM – McGregor Museum, Kimberley; MNCN – Museo Nacional de Ciencias Naturales; MNP – Musée National de Préhistoire, France; MPI-EVA – Max Planck Institute for Evolutionary Anthropology; MVFB – Museum für Vor- und Frühgeschichte Berlin; NMNH – National Museum of Natural History; RBINS – Royal Belgian Institute of Natural Sciences; SMF – Senckenberg Forschungsinstitute und Naturmuseum; SSM – Sackler School of Medicine; TAU – Tel Aviv University; TNT – The Neanderthal Tools project of the Neanderthal Studies Professional Online Service (NESPOS); ULAC – Universität Leipzig, Institut für Anatomie, Lehrsammlung Anatomie; UM – University Mohammed V-Agdal, Rabat.

in Avizo 6.3. Worn teeth of which small portions of the dentine horns were incomplete were reconstructed in Geomagic Studio 10. Molars that showed evidence of significant damage, missing areas, or an abnormal (i.e. pathological) morphology were excluded from this study.

Three sets of landmarks were collected on each EDJ surface (Figure 1): 1) the CEJ RIDGE, capturing the shape of the cementum-enamel junction of the tooth crown starting at the mesiobuccal corner moving lingually; 2) the EDJ MAIN, placed on the dentine horn tips of the protoconid, metaconid, entoconid, and hypoconid, respectively; and 3) the EDJ RIDGE, capturing the EDJ ridge that connects

the dentine horns starting at the protoconid and moving lingually.

For each specimen a single set of homologous landmarks was created in Mathematica v8.0 following methods outlined in SKINNER (2008) and SKINNER & GUNZ (2010). Briefly, a smooth curve was interpolated for both the CEJ and EDJ RIDGE landmark sets using a cubic-spline function. On each curve a fixed number of equidistantly-spaced landmarks was placed (30 for the CEJ RIDGE and 60 for the EDJ RIDGE, see Figure 1). The EDJ MAIN landmarks were treated as landmarks, whereas the former ridge landmarks were treated as semi-landmarks. Semi-landmarks were subjected to sliding (described in GUNZ et al., 2005) and, finally, the landmark set of each specimen were converted to shape coordinates by generalized least squares Procrustes superimposition (GOWER, 1975; RÖHLF & SLICE, 1990).

A principal component analysis (PCA) of the shape coordinates was used to assess the shape variation of the different groups at each molar position (see Figure 2). A canonical variate analysis (CVA) was used to find the axes that best separate groups, illustrating the minor but consistent differences in EDJ morphology between groups. As classification based on a CVA can differ for the same specimen depending on the number of PCs used, we report the cross-validated classification results of each specimen using each of 5-20 PCs. PCA, CVA, and classification were all carried out in R and groups were assigned equal prior probabilities.

Intraspecific temporal variation in EDJ morphology of the Neandertal sample was assessed by splitting the sample into Early Neandertals and Classic Neandertals; early being all specimens dated to >100,000 years and classic being all specimens dated to <100,000 years. This date was

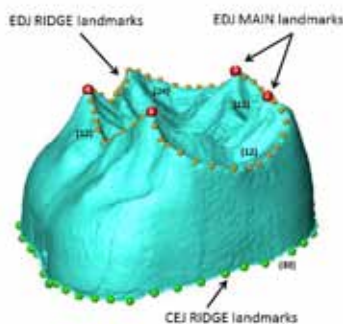


Figure 1: The three landmark sets illustrated on the EDJ surface of the Scladina permanent mandibular right second molar Scla 4A-1/M₂. The EDJ MAIN landmarks are pictured as red dots, located on the top of the four main dentine horns (numbers showing the order of collection). The EDJ RIDGE landmarks start at the protoconid (MAIN landmark number 1), the CEJ RIDGE starts at the mesiobuccal corner. The EDJ and CEJ ridges consist of an arbitrary number of landmarks, which are later replaced by a fixed number of equally spaced semi-landmarks in Mathematica. The number in brackets refers to the number of semi-landmarks after the derivation of homologous landmarks in Mathematica, the landmarks shown here are the original landmarks.



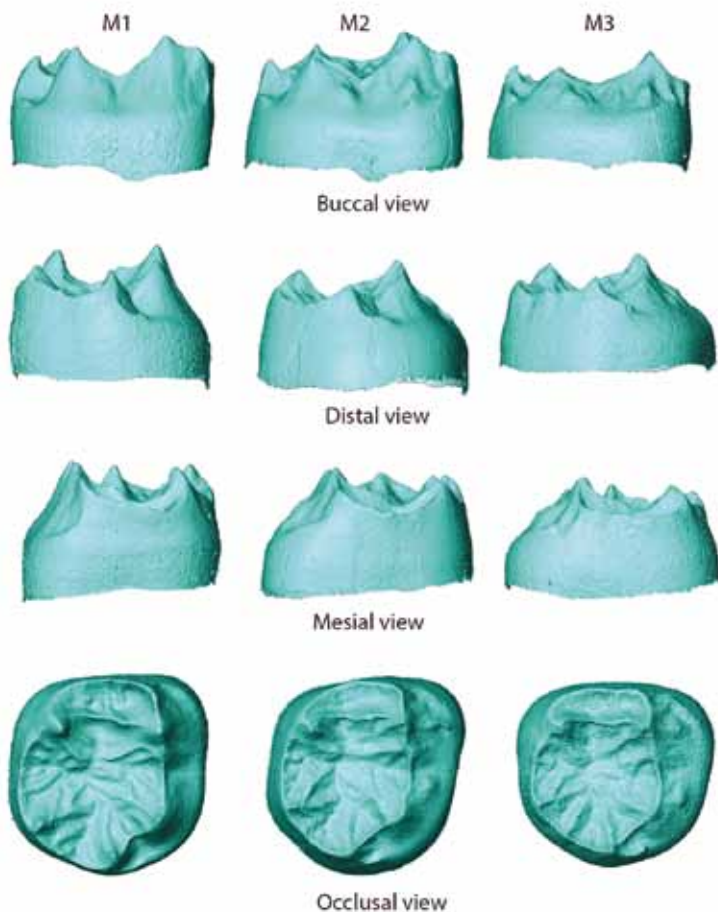


Figure 2: Scladina EDJ morphology of permanent mandibular right molars (Scla 4A-1/M₁, M₂ & M₃) in buccal, distal, mesial, and occlusal view.

chosen based on previous studies assessing the morphological transitions inherent to an accretion of Classic Neandertal morphology (e.g. DEAN et al., 1998; HUBLIN, 1998, 2009; HARVATI et al., 2010).

We used a Mann-Whitney U Test to determine if tooth size (measured as the natural log of centroid size) differed significantly between groups. The Neandertal and Pleistocene Modern Human groups did not differ significantly in log centroid size ($p = 0.161$ for the M₁, $p = 0.754$ for M₂, and $p = 0.934$ for M₃). When the Neandertal group was split into Early and Classic Neandertal groups, the log centroid size of these groups also did not differ significantly ($p = 0.721$ for M₁, $p = 0.639$ for M₂, and $p = 0.598$). Therefore, we restrict the results presented here to those in *shape* space only, excluding log centroid size as part of the CVA. However, we examined the results in *form* space (see GUNZ et al., 2012) and the results were broadly similar.

3. Results

3.1. Classification of Scladina among Late Pleistocene *Homo* (Table 2)

Based on the geometric morphometric analysis of the EDJ of the permanent mandibular molars, the Scladina specimen (Figure 3) classifies consistently as a Neandertal. The M₁ and M₂ are classified as Neandertal 100% of the time. The M₃ classifies as a Neandertal 56% of the time and as a Recent Modern Human 44% of the time (in *form* space 69% and 31%, respectively).

3.2. Temporal variation in Neandertal molar EDJ morphology (Table 3)

The Neandertal sample was divided into Early and Classic Neandertals, based on their geochronological age. The majority of the Neandertal specimens were classified correctly into Early and Classic Neandertals according to their geochronological age (Table 3). These results indicate that there are subtle but consistent differences in Early and Classic Neandertal permanent mandibular molar EDJ morphology. A small number of specimens did not classify as expected and classified inconsistently with their geochronological

Hs = recent *Homo sapiens*, **Hsp** = Pleistocene *Homo sapiens*, **Hn** = *Homo neanderthalensis*, **Hne** = Early Neandertal, **Hnc** = Classic Neandertal.

M ₁	Accuracy	M ₂	Accuracy	M ₃	Accuracy
Hs (32)	97%	Hs (8)	88%	Hs (15)	93%
Hsp (3)	100%	Hsp (9)	100%	Hsp (7)	100%
Hn (14)	100%	Hn (18)	100%	Hn (14)	100%

Table 2: Classification accuracy of Late Pleistocene *Homo* shown as the percentage of correctly classified specimens for each group. A specimen was considered classified correctly when at least 75% of analyses (using each of 5-20 PCs) classified the specimen correctly.

M ₁	Accuracy	M ₂	Accuracy	M ₃	Accuracy
Hs (32)	97%	Hs (8)	100%	Hs (15)	93%
Hsp (3)	100%	Hsp (9)	100%	Hsp (7)	100%
Hne (9)	89%	Hne (13)	92%	Hne (6)	67%
Hnc (5)	100%	Hnc (6)	100%	Hnc (8)	100%

Table 3: Classification accuracy when Early and Classic Neandertals are treated as two separate groups, shown as the percentage of correctly classified specimens for each group. A specimen was considered classified correctly when at least 75% of analyses (using each of 5-20 PCs) classified the specimen correctly.

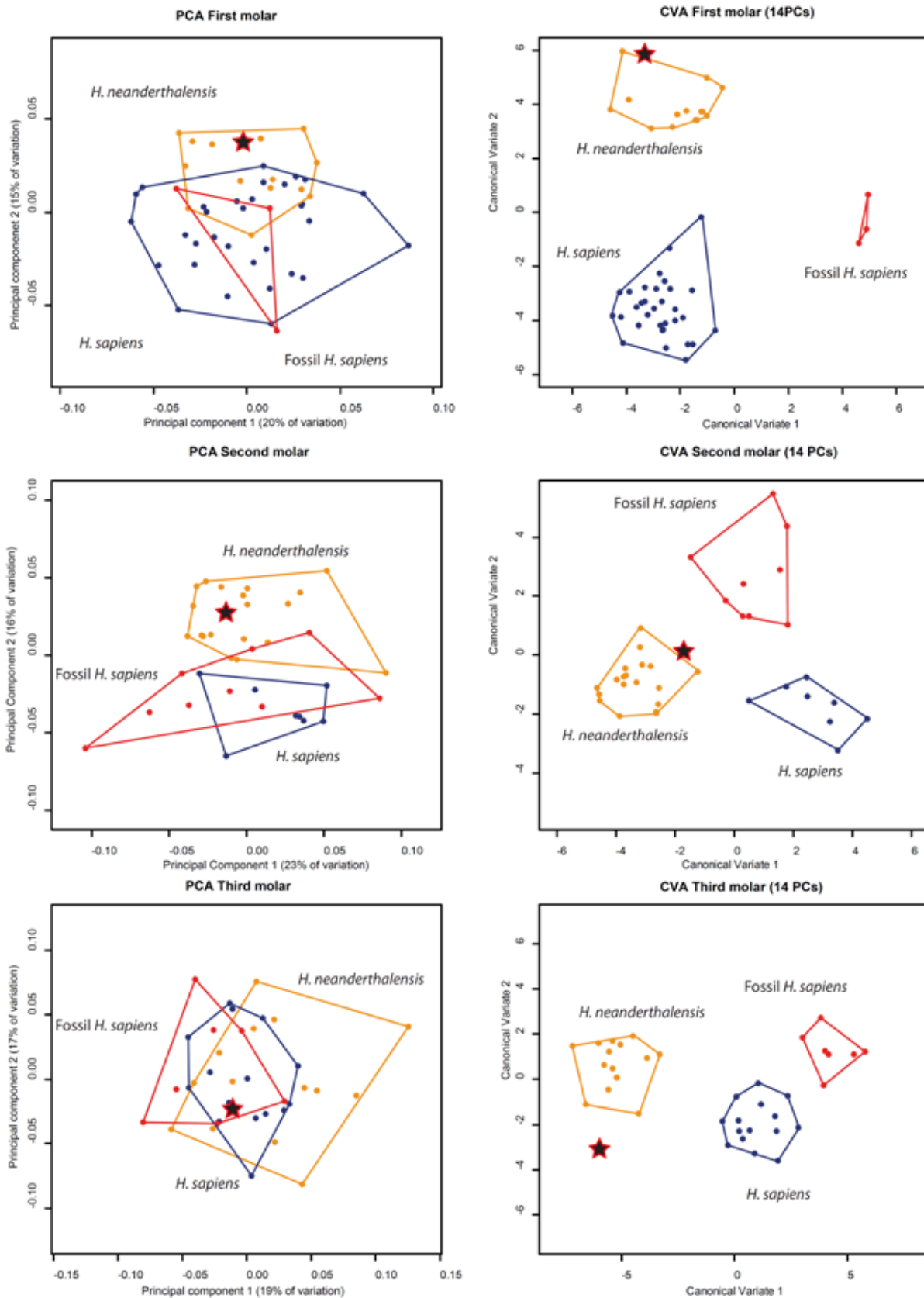


Figure 3: Principal component analysis and canonical variate analysis of EDJ shape in modern humans, Pleistocene Modern Humans and Neandertals for each mandibular molar.

age (i.e., Abri Suard 14-7 LRM₁; Krapina D1 LRM₂; Abri Suard 43 LRM₃, and Abri Suard 36 LLM₃; see Appendix 1). For the assessment of the

classification of the Scladina specimens as Early or Classic Neandertals, these specimens were removed from the analysis.



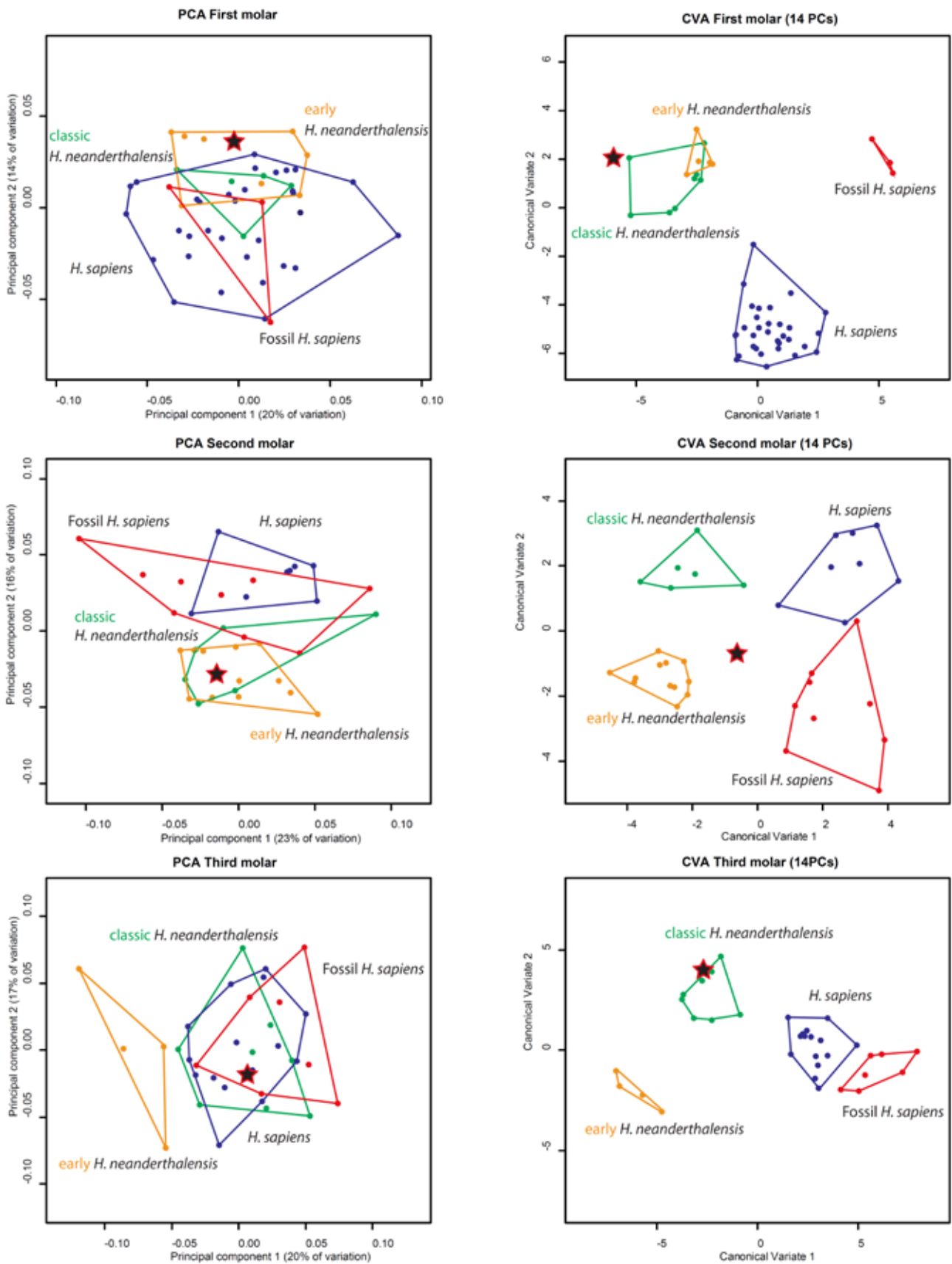


Figure 4: Principal component analysis and canonical variate analysis of EDJ shape for each mandibular molar and dividing the Neanderthal sample into Early and Classic groups.

3.3. Comparison of Scladina I-4A with Early and Classic Neandertal morphotypes

In order to evaluate the affinity of Scladina with respect to Early and Classic Neandertal samples we excluded the ambiguously classified Neandertal specimens (see above). The M_1 of Scladina is classified as a Classic Neandertal (100%), the M_2 is classified as a Classic Neandertal 69% of the time, 19% as an Early Neandertal and the remaining times as a Pleistocene Modern Human (Figure 4). The M_3 is classified as a Classic Neandertal 63% of the time and as a Recent Modern Human 37% of the time (see Appendix 1).

The mean shape models of the different groups illustrate the subtle differences in Early and Classic Neandertal morphology (Figure 5). The Early morphology of the M_1 is characterised by a taller and more distally placed protoconid and a cervix that does not undulate in the occlusal-apical plane. The Classic morphology of the M_1 is characterised by a shorter and more mesially placed protoconid, and a cervix that dips in the middle of the lingual and buccal sides. Scladina shares with the classic morphotype the height of the protoconid and the dipping of the cervix along the lingual and buccal sides. For the M_2 and M_3 the differences in morphology between Early and Classic Neandertals are even more subtle. The Early morphotype of the M_2 is characterized by the more centrally placed entoconid, which Scladina shares. The Early morphotype of the M_3 is characterized by a slightly taller and more distally placed protoconid, a more distal location of both the hypoconid and entoconid, and a more mesially placed hypoconulid and distal ridge. The classic morphotype of the M_3 is characterized by a slightly shorter and more mesially placed protoconid, a more mesial location of both the hypoconid and the entoconid, and a more distally located hypoconulid and distal ridge. Scladina shares with the Early Neandertals the more mesially placed distal ridge, a protoconid height similar to that of the Classic Neandertals, but a protoconid position similar to Classic Neandertals.

4. Discussion

Dating of Scladina has been problematic because of the complicated stratigraphy of the Sedimentary Complex 4 (TOUSSAINT & PIRSON, 2006), and has been estimated to 127 +46/-32ka by gamma spectrometry dating (TOUSSAINT et al.,

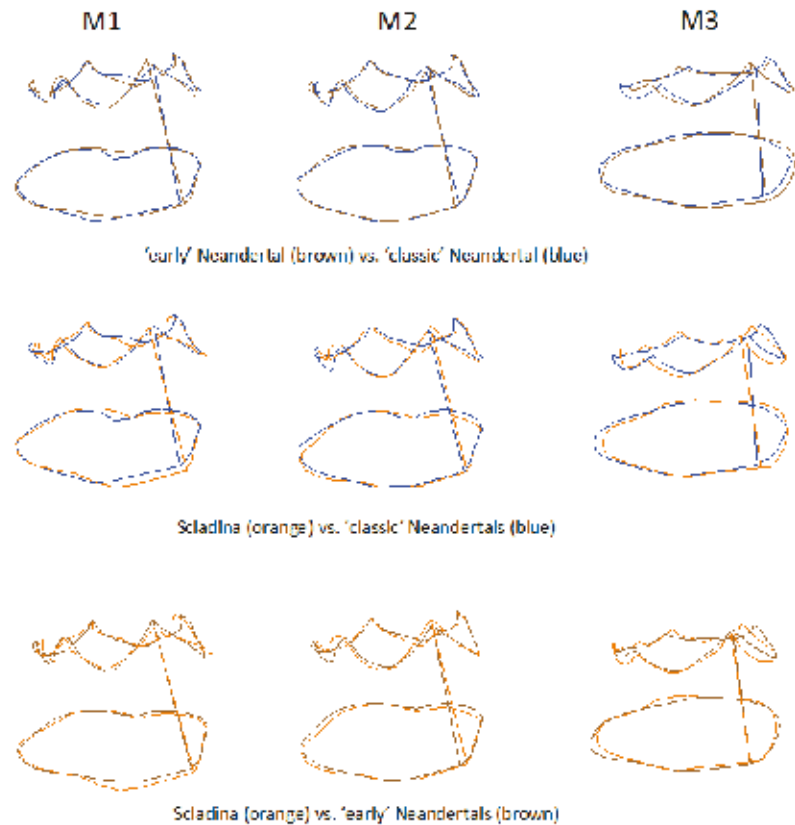


Figure 5: EDJ mean shape comparison between Scladina, Early Neandertals, and Classic Neandertals, shown from buccal side.

1998). However, it has recently been suggested that the best hypothesis would be to position the Scladina Neandertal remains in MIS 5b or MIS 5a (see Chapter 5). Each of the studied Scladina teeth is classified as a Classic Neandertal the majority of the time. As the date of Scladina is close to the cut-off point used in this study, 100ka, it is interesting to see that the EDJ morphology of Scladina aligns itself stronger with the Classic Neandertal sample than to the Early Neandertal sample.

The M_3 exhibits a greater variation in its morphology within species and greater overlap between species. This makes the M_3 less reliable when used in taxonomic classification studies as its results are less consistent compared to the classification results of M_1 or M_2 . Therefore, the classification results of the Scladina M_3 as a modern human do not alter the taxonomic position of Scladina and can be attributed to the nature of the M_3 morphology in general.

The ambiguous classification of some Neandertal specimens compared to their geochronological age illustrates the continuous variation in morphology rather than the dichotomous distinction between two groups that has been tested here. This is illustrated by the oldest Neandertal specimens of our comparative sample, the Abri Suard individuals, not classifying consistently as Early Neandertals.



This demonstrates that as well as having a continuous variation instead of two separate groups, the temporal extremities of both the Early and Classic Neandertals exhibit significant variation as well. However, this study has shown that within the Neandertal continuum the differences in EDJ morphology are consistent enough to successfully distinguish between Early and Classic Neandertals.

5. Conclusion

This study confirms the Neandertal affinity of the Scladina specimen based on its EDJ morphology. The intraspecific taxonomic position of Scladina shows to be closer to that of the Classic Neandertal sample such as the El Sidron and Combe-Grenal specimens than to the Early Neandertal sample such as the Krapina and Abri Suard specimens. Furthermore, this study illustrates the presence of subtle yet consistent differences in EDJ morphology between the Early Neandertals and Classic Neandertals.

Acknowledgements

For access to specimens we thank the following institutions and individuals: Department of Archaeology, Belgrade University and the National Museum (Dušan Mihailović, Bojana Mihailović), Croatian National History Museum and the Croatian Academy of Science and Arts (Jakov Radovčić, Dejana Brajković); Francisc J. Rainer Institute of Anthropology (Andrei Dorian Soficaru); Geologisch-Paläontologisches Institut der Universität Heidelberg (Ullrich A. Glasmacher); Institut National des Sciences de l'Archéologie et du Patrimoine (A. Ben-Ncer, M. A. El Hajraoui, F. Z. Sbihi-Alaoui); Musée Archéologique de Rabat (S. Raoui); Iziko South African Museum (access to specimen from Fred Grine, scanning by Paul Tafforeau); Musée d'Archéologie Nationale de Saint-Germain-en-Laye (Patrick Périn); Musée d'Angoulême (Jean-François Tournepiche); Musée d'Art et d'Archéologie du Périgord (Véronique Merlin-Langlade); Musée National de Préhistoire, Les Eyzies-de-Tayac (Jean-Jacques Cleyet-Merle); Museo Nacional de Ciencias Naturales (Antonio Rosas); Museum für Vor- und Frühgeschichte Berlin (Almut Hoffmann); National Museum of Natural History (David Hunt); Rockefeller Museum Jerusalem (Alegre Savariago and Ibrahim Fawzi); Royal Belgian Institute of Natural Sciences; Sackler School of Medicine (Israel Hershkovitz, Yoel Rak, Alon Barash); Senckenberg Forschungsinstitut und

Naturmuseum (Ottmar Kullmer and Friedemann Schrenk); TNT/NESPOS (Roberto Macchiarelli); Michel Toussaint; Universität Leipzig; Institut für Anatomie, Lehrsammlung Anatomie (Christine Feja) and Jean-Jacques Hublin's private collection; University Mohammed V-Agdal (Mohamed Boutakiout). For technical assistance we thank Adeline Le Cabec, Collin Moore, Robin Feeney, Tanya Smith, Kornelius Kupczik, and Simon Neubauer. For scanning assistance we thank Heiko Temming and Patrick Schoenfeld.

References

- BAILEY S. E., 2002. A closer look at Neanderthal postcanine dental morphology: the mandibular dentition. *The Anatomical Record, The New Anatomist*, 269: 263–299.
- BAILEY S. E., 2006. Beyond shovel-shaped incisors: Neandertal dental morphology in a comparative context. *Periodicum Biologorum*, 108: 253–267.
- CORRUCINI R. S., 1987. The Dentinoenamel junction in primates. *International Journal of Primatology*, 8: 99–114.
- CORRUCCINI R. S. 1998. The dentino-enamel junction in primate mandibular molars. In J. R. LUKACS (ed.), *Human dental development, morphology, and pathology: a tribute to Albert A. Dahlberg*. Portland, University of Oregon, Anthropological Papers: 1–16.
- DEAN D., HUBLIN J.-J., HOLLOWAY R. & ZIEGLER R., 1998. On the phylogenetic position of the pre-Neanderthal specimen from Reilingen, Germany. *Journal of Human Evolution*, 34: 485–508.
- GARRALDA M.-D., VANDERMEERSCH B., 2000. The Neanderthals from Combe-Grenal cave (Domme, Dordogne, France). *Paleo*, 12: 213–259.
- GOWER J. C., 1975. Generalized Procrustes analysis. *Psychometrika*, 40: 33–51.
- GRINE F. E., 2004. Description and preliminary analysis of new hominid craniodental remains from the Swartkrans Formation. In C. K. BRAIN (ed.), *Swartkrans: A Cave's Chronicle of Early Man*. Pretoria, Transvaal Museum: 75–116.
- GUATELLI-STEINBERG D. & IRISH J. D., 2005. Early hominin variability in first molar dental trait frequencies. *American Journal of Physical Anthropology*, 128: 477–484.
- GUNZ P., MITTEROECKER P. & BOOKSTEIN F. L., 2005. Semilandmarks in three dimensions. In D. E. SLICE (ed.), *Modern Morphometrics in Physical Anthropology*. New York, Kluwer Academic/Plenum Publishers: 73–98.
- GUNZ P., RAMSIER M., KUHRIG M., HUBLIN J.-J. & SPOOR F., 2012. The mammalian bony labyrinth reconsidered,

- introducing a comprehensive geometric morphometric approach. *Journal of Anatomy*, 220: 529–543.
- HARVATI K., HUBLIN J.-J. & GUNZ P., 2010. Evolution of middle-late Pleistocene human cranio-facial form: A 3-D approach. *Journal of Human Evolution*, 59, 5: 445–464.
- HARVATI K., PANAGOPOULOU E. & KARKANAS P., 2003. First Neanderthal remains from Greece: the evidence from Lakonis. *Journal of Human Evolution*, 45: 465–473.
- HLUSKO L. J., 2004. Protostylid variation in *Australopithecus*. *Journal of Human Evolution*, 46: 579–594.
- HUBLIN J.-J., 1998. Climatic changes, paleogeography and the evolution of Neanderthals. In K. AOKI & O. BAR-YOSEF (eds.), *Neanderthals and Modern Humans in Western Asia*. Plenum Press, New York: 295–310.
- HUBLIN J.-J. 2009. The origin of Neandertals. *Proceedings of the National Academy of Sciences of the United States of America*, 106, 38: 16022–16027.
- IRISH J. & GUATELLI-STEINBERG D., 2003. Ancient teeth and modern human origins: an expanded comparison of African Plio-Pleistocene and recent world dental samples. *Journal of Human Evolution*, 45: 113–144.
- JOHANSON D. C., 1974. *An odontological study of the chimpanzee with some implications for hominoid evolution*. Unpublished PhD thesis, University of Chicago.
- MACCHIARELLI R., BONDIOLI L., DEBÉNATH A., MAZURIER A., TOURNÉPICHE J.-F., BIRCH W & DEAN C., 2006. How Neanderthal molar teeth grew. *Nature*, 444: 748–751.
- OLEJNICZAK A. J., GIBLERT C. C., MARTIN L. B., SMITH T. M., ULHAAS L. & GRINE F. E., 2007. Morphology of the enamel-dentine junction in sections of anthropoid primate maxillary molars. *Journal of Human Evolution*, 53: 292–301.
- OLEJNICZAK A. J., MARTIN L. B. & ULHAAS L., 2004. Quantification of dentine shape in anthropoid primates. *Annals of Anatomy*, 186: 479–485.
- PILBROW V., 2003. *Dental variation in African apes with implications for understanding patterns of variation in species in fossil apes*. Unpublished PhD thesis, New York University.
- PILBROW V., 2006. Population systematics of chimpanzees using molar morphometrics. *Journal of Human Evolution*, 51: 646–662.
- RADOVČIĆ J., POMTYKALO D. & WOLPOFF M. H., 1988. *The Krapina Hominids: an illustrated catalog of skeletal collection*. Zagreb, Mladost Publishing House.
- ROBINSON J. T., 1956. *The Dentition of the Australopithecinae*. Pretoria, Transvaal Museum. Memoir No 9, 179 p.
- ROHLF F. J. & SLICE D., 1990. Extensions of the Procrustes method for the optimal superimposition of landmarks. *Systematic Zoology*, 39: 40–59.
- SKINNER M. M., 2008. *Enamel-dentine junction morphology in extant hominoid and fossil hominin lower molars*. Unpublished PhD thesis, George Washington University.
- SKINNER M. M., GUNZ P., WOOD B. A., BOESCH C. & HUBLIN J.-J., 2010. Discrimination of extant *Pan* species and subspecies using the enamel-dentine junction morphology of lower molars. *American Journal of Physical Anthropology*, 140: 234–243.
- SKINNER M. M., GUNZ P., WOOD B. A. & HUBLIN J.-J., 2008. Enamel-dentine junction (EDJ) morphology distinguishes the lower molars of *Australopithecus africanus* and *Paranthropus robustus*. *Journal of Human Evolution*, 55: 979–988.
- SKINNER M. M., WOOD B. A. & HUBLIN J.-J., 2009. Protostylid expression at the enamel-dentine junction and enamel surface of mandibular molars of *Paranthropus robustus* and *Australopithecus africanus*. *Journal of Human Evolution*, 56: 76–85.
- SPERBER G., 1974. *Morphology of the cheek teeth of early South African hominids*. Unpublished PhD thesis, University of Witwatersrand.
- SUWA G., 1996. Serial allocations of isolated mandibular molars of unknown taxonomic affinities from the Shungura and Usno formations, Ethiopia, a combined method approach. *Human Evolution*, 11: 269–282.
- SUWA G., KONO R. T., KATOH S., ASFAW B. & BEYENE Y., 2007. A new species of great ape from the late Miocene epoch in Ethiopia. *Nature*, 448: 921–924.
- TEILHOL V., 2001. *Contribution à l'étude individuelle des ossements d'enfants de la Chaise de Vouthon (Charente, France): approche paléodémographique, paléoethnologique, aspect morphologique et étude métrique. Place phylogénique des enfants de la Chaise*. Unpublished PhD thesis, University of Perpignan.
- TOUSSAINT M., OTTE M., BONJEAN D., BOCHERENS H., FALGUÈRES C. & YOKOYAMA Y., 1998. Les restes humains neandertaliens immatures de la couche 4A de la grotte Scladina (Andenne, Belgique). *Comptes rendus de l'Académie des Sciences de Paris, Sciences de la terre et des planètes*, 326: 737–742.
- TOUSSAINT M. & PIRSON S., 2006. Neandertal Studies in Belgium: 2000–2005. *Periodicum Biologorum*, 108, 3: 373–387.
- UCHIDA A., 1992. *Intra-species variation among the great apes: implications for taxonomy of fossil hominoids*. Unpublished PhD thesis, Cambridge, Harvard University.
- UCHIDA, A., 1996. *Craniodental Variation among the Great Apes*. Peabody Museum. Bulletin 4, Cambridge, Harvard University Press.



WEIDENREICH F., 1937. The dentition of *Sinanthropus pekinensis*: a comparative odontography of the hominids. *Palaeontologia Sinica*, Series D, 1: 1–180.

WOOD B. A. & ABBOTT S. A., 1983. Analysis of dental morphology of Plio-Pleistocene hominids. I. Mandibular molars: crown area measurements and morphological traits. *Journal of Anatomy*, 136: 197–210.

Specimen	Tooth	Date	Expected	Early Hn	Classic Hn	Hs	Fossil Hs
Lakonis_LLM3	LM3	<38–44ka	Classic	0	16	0	0
Le Moustier LLM1	LM1	40ka	Classic	0	16	0	0
Le Moustier LLM2	LM2	40ka	Classic	0	16	0	0
Le Moustier LLM3	LM3	40ka	Classic	0	16	0	0
Saint-Césaire LRM3	LM3	40ka	Classic	0	16	0	0
Vindija 11_39 LRM2	LM2	45–35ka	Classic	0	16	0	0
Vindija 11_39 LRM3	LM3	45–35ka	Classic	4	12	0	0
El Sidron SD1135 LRM3	LM3	49–39ka	Classic	0	15	1	0
El Sidron SD540 LLM2	LM2	49–39ka	Classic	0	16	0	0
El Sidron SD755 LRM2	LM2	49–39ka	Classic	0	16	0	0
El Sidron SD780_LLM1	LM1	49–39ka	Classic	2	14	0	0
Combe-Grenal I LRM1	LM1	70ka	Classic	0	16	0	0
Combe-Grenal XII LLM3	LM3	70ka	Classic	0	16	0	0
Combe-Grenal IV LLM1	LM1	70ka	Classic	0	16	0	0
Le Regourdou LLM2	LM2	70ka	Classic	0	16	0	0
Le Regourdou LLM3	LM3	70ka	Classic	0	16	0	0
La Quina H9 LLM2	LM2	71–60ka	Classic	0	16	0	0
La Quina H9 LLM3	LM3	71–60ka	Classic	0	16	0	0
Roc de Marsal LRM1	LM1	90–60ka	Classic	0	16	0	0
Scladina 4A–1 LRM1	LM1	100ka	?	0	16	0	0
Scladina 4A–1 LRM2	LM2	100ka	?	3	11	0	2
Scladina 4A–1 LRM3	LM3	100ka	?	0	10	6	0
Krapina 52 LLM1	LM1	130ka	Early	16	0	0	0
Krapina 53 LRM1	LM1	130ka	Early	16	0	0	0
Krapina 53 LRM2	LM2	130ka	Early	16	0	0	0
Krapina 53 LRM3	LM3	130ka	Early	16	0	0	0
Krapina 54 LLM1	LM1	130ka	Early	16	0	0	0
Krapina 54 LLM2	LM2	130ka	Early	16	0	0	0
Krapina 55 LLM1	LM1	130ka	Early	15	0	0	1
Krapina 55 LLM2	LM2	130ka	Early	16	0	0	0
Krapina 57 LRM3	LM3	130ka	Early	16	0	0	0
Krapina 79 LRM1	LM1	130ka	Early	16	0	0	0
Krapina 81 LLM1	LM1	130ka	Early	15	1	0	0
Krapina D1 LRM2	LM2	130ka	Early	10	6	0	0
Krapina D104 LRM3	LM3	130ka	Early	16	0	0	0
Krapina D105 LLM2	LM2	130ka	Early	16	0	0	0
Krapina D106 LLM3	LM3	130ka	Early	16	0	0	0
Krapina D107 LLM2	LM2	130ka	Early	16	0	0	0
Krapina D6 LLM2	LM2	130ka	Early	16	0	0	0
Krapina D80 LRM2	LM2	130ka	Early	14	2	0	0
Krapina D86 LLM2	LM2	130ka	Early	16	0	0	0
Krapina D9 LLM2	LM2	130ka	Early	16	0	0	0
Krapina 57 LRM2	LM2	130ka	Early	16	0	0	0
Krapina 59 LRM2	LM2	130ka	Early	16	0	0	0
Abri Suard 14 7 LRM1	LM1	185–101ka	Early	9	7	0	0
Abri Suard 36 LLM3	LM3	185–101ka	Early	11	5	0	0
Abri Suard 36 LLM2	LM2	185–101ka	Early	16	0	0	0
Abri Suard 43 LRM3	LM3	185–101ka	Early	6	10	0	0
Abri Suard 49 LRM1	LM1	185–101ka	Early	15	1	0	0
Abri Suard 5 LLM1	LM1	185–101ka	Early	14	2	0	0

Appendix 1: Classification results for the complete Neandertal sample using PC 5–20. Specimens that have been highlighted in grey have been removed from the sample as they were classified ambiguously. Early Hn = Early *Homo neanderthalensis*, Classic Hn = Classic *Homo neanderthalensis*, Hs = *Homo sapiens*, Fossil Hs = Fossil *Homo sapiens*.

Chapter 16

MICRO-COMPUTED TOMOGRAPHIC QUANTIFICATION OF TOOTH ROOT SIZE AND TISSUE PROPORTIONS IN THE SCLADINA I-4A JUVENILE, A SHORT-ROOTED NEANDERTAL

Adeline LE CABEC, Christine VERNA,
Michel TOUSSAINT, Jean-Jacques HUBLIN &
Kornelius KUPCZIK

*Michel Toussaint & Dominique Bonjean (eds.), 2014.
The Scladina I-4A Juvenile Neandertal (Andenne, Belgium),
Palaeoanthropology and Context*

Études et Recherches Archéologiques de l'Université de Liège, 134: 325-350.

1. Introduction

Scladina Cave (Belgium) has yielded the dentition of an eight-year-old juvenile Neandertal (TOUSSAINT et al., 1998 & Chapter 1; SMITH et al., 2007 & Chapter 8). A direct date of 127 +46/-32 ka BP was obtained on the mandible by gamma-ray spectrometry (TOUSSAINT et al., 1998; YOKOYAMA & FALGUÈRES, Chapter 6), which points to a wide chronological range, between MIS 6 and 4. A recent reassessment of the stratigraphy of the site attributes the Neandertal remains to a secondary deposit (mainly in units 4A-CHE and 4A-POC, see Chapters 3 & 5 for description). The general chronostratigraphic framework of the sequence (PIRSON et al., 2005, 2008; this volume, Chapter 4) however supports an attribution of the fossil to the second half of MIS 5 (PIRSON et al., this volume, Chapter 5). On a regional scale, and because of excessively rigorous climatic conditions, it seems currently granted that the territory encompassing present-day Belgium and the surrounding areas of northwest Europe was deserted by human populations during the second half of MIS 4 (CORDY, 1984, 1988; HAESAERTS, 1984; TOUSSAINT et al., 2001; VAN PEER, 2001; PIRSON & DI MODICA, 2011: 135). This is especially true for the calcareous areas where all the Neandertal remains of the Mosan Basin have been recovered. Except for the La Naulette mandible and for the mandible and the fragment of maxilla of Scladina which are more ancient, all the Mosan Neandertals are attributed to MIS 3, as for the eponymous site of Neandertal. This is well established for Spy (SEMAL et al., 2009), Couvin (TOUSSAINT et al., 2010), Walou (PIRSON et al., 2011; TOUSSAINT, 2011) and Goyet (ROUGIER et al., 2009). So there is a clear distinction between fossils dated to MIS 5-MIS 4 (for this later time period, no Neandertal remains have ever been found in Belgium) and those attributed to MIS 3. This is the reason why, in this chapter, we chose to compare Scladina primarily with MIS 5 Neandertals.

Although the dental development of the Scladina specimen is well documented (SMITH et al., 2007; SMITH et al., 2010 & Chapter 8), its dental morphology has not yet been described in detail before the present monograph (Chapters 13 to 16 & 18). However, it has to be noted that Scladina has already been included in two large-scale studies focusing on the root morphology of Neandertals (see KUPCZIK & HUBLIN, 2010 for the molar root morphology; LE CABEC et al., 2013 for the incisors and canines).

Several studies using innovative techniques of investigation (e.g. tomographic imaging and synchrotron virtual histology) have emphasized that tooth roots can yield valuable information regarding taxonomy (WOOD et al., 1988; BRUNET et al., 2002; BAILEY, 2005; KUPCZIK & HUBLIN, 2010; EMONET et al., 2012), life history (SMITH et al., 2007; SMITH et al., 2010), diet (SPENCER, 2003; KUPCZIK & DEAN, 2008; KUPCZIK & HUBLIN, 2010), tooth use (LE CABEC et al., 2013) and facial biomechanics (SMITH, 1983). In this context, recent studies have shown that tooth root form can distinguish Neandertals from anatomically modern humans (BAILEY, 2005; KUPCZIK & HUBLIN, 2010; LE CABEC et al., 2013).

Here we document and compare the permanent incisors, canines and first molars' root morphology of the Scladina Juvenile to European MIS 5 Neandertals from Krapina, Abri Bourgeois-Delaunay and Regourdou. MIS 5 Neandertals lie at the end of step 3 of the accretion model (DEAN et al., 1998; HUBLIN, 1998). Although steps 1 and 2 of the accretion model show some of the facial features characterizing the Neandertal lineage, the derived Neandertal facial morphology is fully achieved in step 4 specimens (DEAN et al., 1998; HARVATI et al., 2010). The interpretation of the Neandertal crown and root morphology is very likely influenced by the geographic and chronologic distribution of the fossil record, in which the later stage of the evolution of the lineage, MIS 4-3 Neandertals, is better represented than



earlier phases. Such a discontinuous fossil record often prevents an assessment of the intra- and interpopulational variability that is crucial for our understanding of the evolutionary history of the lineage.

The Krapina Neandertals are known for having very large crown dimensions compared to other European Neandertals, especially regarding their anterior teeth (BROSE & WOLPOFF, 1971; SMITH, 1976^a; BRACE, 1979; WOLPOFF, 1979; MANN & VANDERMEERSCH, 1997; WOLPOFF, 1999). The same observation was made for the Abri Bourgeois-Delaunay sample by GENET-VARCIN (1975^{a, b}) and CONDEMI (2001). Moreover, Krapina is also the most extensively studied MIS 5 Neandertal sample and because of its large dental sample size may bias characterizations of MIS 5 Neandertal dental morphology (SMITH, 1976^a; SMITH, 1976^b; WOLPOFF, 1979; FOX & FRAYER, 1997; LEE, 2006; SCHWARTZ & TATTERSALL, 2006; OLEJNICZAK et al., 2008). Regourdou 1 was shown to have rather small crowns in comparison to MIS 4-3 Neandertals (MAUREILLE et al., 2001).

We used micro-computed tomography (micro-CT) to image and quantify internal tooth root tissues proportions of Scladina and the comparative MIS 5 Neandertal specimens. This technique has the particular advantage that it allows the virtual extraction of teeth still embedded in their jaws, and to access internal dental structures such as the pulp cavity. In addition to the focus on the Scladina Juvenile, this will allow us to question whether variation in Krapina can reliably represent MIS 5 Neandertal dental variability and whether the other three MIS 5 Neandertals samples can be accommodated within the variation represented by Krapina.

2. Material and methods

2.1. Sample

The external and the cross-sectional root morphology of the teeth of the Scladina Juvenile will be described for all the teeth present in the individual (for an extensive inventory of the teeth, see Chapter 1, Table 1 & Chapter 13). Further quantitative analyses will be restricted to the permanent incisors, canines and first molars, which have completed their roots.

In the metric study, the total sample includes 68 isolated and in situ permanent mandibular and maxillary central and lateral incisors, canines and first molars from Scladina and comparative MIS 5 Neandertals (Table 1). The selection of the teeth was based on preservation and formation of the roots. However, when a small portion of the root tip was missing for some anterior teeth, and given the small sample sizes available for study, these teeth were nonetheless included in the samples. The amount of root missing has been estimated following the protocol described in LE CABEC et al. (2013), which modeled the missing part as an elliptic cone and proved to be of good accuracy (Tables 1, 2a & 2b). The comparative Neandertal sample from the Croatian site of Krapina includes 43 teeth. These dental remains have been directly dated by ESR to ca. 130±10 ka BP (RINK et al., 1995). The second Neandertal sample includes a complete adult mandible (BD1) and nine non-associated isolated teeth (CONDEMI, 2001) discovered at the French site of La Chaise-Abri Bourgeois-Delaunay (DEBÉNATH, 1977), and which are attributed to the MIS 5e (CONDEMI, 2001). In addition, we analyzed four teeth preserved in situ in the adult mandible of Regourdou 1 (Montignac,

For Tables 1 to 6, abbreviations for permanent teeth are: **I₁** (mandibular central incisor), **I₂** (mandibular lateral incisor), **C**, (mandibular canine), **M₁** (mandibular first molar), **I¹** (maxillary central incisor), **I²** (maxillary lateral incisor), **C¹** (maxillary canine), **M¹** (maxillary first molar).

Tooth type	Krapina (Krp)	Abri Bourgeois-Delaunay (BD)	Scladina (Scla)	Regourdou 1 (Reg)
I ₁	55 (Mandible E), 58 (Mandible H), 59 (Mandible J)	BD1, BD20, BD21	Scla 4A-15	Right I ^{1*}
I ₂	53 (Mandible C), 54 (Mandible D), 55, 58, 59	BD1	Scla 4A-20*	Right I ^{2*}
C	54, 55, 58, 59	BD1, BD13	Scla 4A-12	Right C
M ₁	53, 54, 55, 58, 57, 59, D80, D82	BD1, BDJ4C9	Scla 4A-9/M ₁	Left M ₁
I ¹	49 (Maxilla E), 50 (Maxilla F), D123*, D126*, D157, D158	BD12	Scla 4A-11*	–
I ²	49, 50, D122*, D125, D127, D156, D159, D160	BD10	Scla 4A-14	–
C ¹	D36, D37, D56, D76, 49, 50*	BD11, BD15, BD16	Scla 4A-16*	–
M ¹	45 (Maxilla A), 48 (Maxilla D), D164	–	Scla 4A-4	–

Table 1: Samples of permanent teeth of MIS 5 Neandertals. ‘*’ denotes specimens in which a small part of the root tip is broken. Values used in the statistics of Tables 2a & 2b include an estimation of the missing part of the root following the protocol described in LE CABEC et al. (2013, S.I.1 and S.I.2).

From LE CABEC et al. (2013, S.I.1 and S.I.2).

Specimen	Tooth type	Side	Cause	rMD [mm]	rLL [mm]	rAv. [mm]	hMd [mm]	hLL [mm]	hAv. [mm]	RL meas. [mm]	Msg RL [mm]	%age Mis RL	Total estim. RL [mm]
Regourdou 1	I ₁	R	t	0.43	1.18	0.81	0.26	1.11	0.69	15.72	0.69	4.18	16.41
Regourdou 1	I ₂	R	t	1.12	2.09	1.6	0.78	1.05	0.92	16.88	0.92	5.14	17.80
Scla 4A-20	I ₂	R	t	1.13	2.05	1.6	0.51	2.14	1.33	13.9	1.33	8.70	15.23
Scla 4A-11	I ¹	R	t	1	1.07	1.0	1.24	1.45	1.35	13.97	1.35	8.78	15.32
Krp D123	I ¹	L	t	1.32	1.69	1.5	1.36	2.64	2.00	17.57	2.00	10.22	19.57
Krp D126	I ¹	R	t/d	1.03	1.43	1.2	1.31	1.39	1.35	15.24	1.35	8.14	16.59
Krp D122	I ²	L	d	0.72	1.8	1.3	0.69	1.42	1.06	16.36	1.06	6.06	17.42
Krp 50 [Max. F]	C'	R	t	1.68	1.79	1.7	1.81	2.29	2.05	20.99	2.05	8.90	23.04
Scla 4A-16	C'	R	d	0.5	0.83	0.7	0.37	0.7	0.54	17.15	0.54	3.03	17.69

Table 2a: Root length estimation for missing root apical portions in damaged or developmentally incomplete specimens (incisors and canines). We scored the reason why the root is incomplete as 't' for taphonomical break, 'd' for developmentally incomplete, 't/d' when the reason is uncertain between taphonomy and development. 'rMD' stands for the mesiodistal radius of the elliptic cone, 'rLL' for its labiolingual radius, 'rAv.' for the average of both radii; 'hMD' and 'hLL' for the height of the cone measured in the mesiodistal and in the labiolingual plane respectively and 'hAv.' for the average of both heights. 'hMd', 'hLL' and 'hAv.' are italicized since they are used for further computations. 'RL meas.' stands for the measured root length [incomplete], 'Total estim. RL' is the reconstructed root length summing the average height and the measured root length, and '%age Mis RL' is the percentage of the total root length (bold in the table) represented by the portion of root that has been reconstructed. We notice that for Regourdou 1 I1, it is highly likely that the missing part of the root is actually some broken hypertrophic cementum.

France). This specimen is attributed to the second half of MIS 5 (MAUREILLE & TILLIER, 2008; TURQ et al., 2008; VANDERMEERSCH et al., 2008).

2.2. Micro-CT image acquisition and 3D model generation.

Isolated and in situ teeth were subjected to micro-CT at the Max Planck Institute for Evolutionary Anthropology (Leipzig, Germany) on a Skyscan 1172 micro-CT scanner or a BIR ARCTIS 225/300 industrial micro-CT scanner, with an isotropic voxel-size ranging from 25.5 to 34.8 μm . Data for BDJ4C9 were acquired at the European Synchrotron Radiation Facility (Beamline ID 17, Grenoble, France) and downloaded from the NESPOS website.

In order to facilitate the dental tissue segmentation in Avizo 6.1. (Mercury Systems), the reconstructed micro-CT slices were filtered using a median filter followed by a mean-of-least-variance filter (each with a kernel size of three). Dental tissues (enamel, dentine and pulp) were semi-automatically segmented using thresholding and manual editing, as well as the cracks in the enamel and dentine when they appeared clearly on the scans, to avoid any overestimation of root volume and surface area.

On several teeth from Krapina (Krp D36, D56 and D76) and Abri Bourgeois-Delaunay (BD11, BD15 and BD16), hypertrophic cementum has been successfully segmented as a separate material (see Figures 1, 3 & 5 in LE CABEC et al., 2013 for more details). As visible on the micro-CT

From LE CABEC et al. (2013, S.I.1 and S.I.2).

Specimen	Tooth type	RSA meas. [mm ²]	Misg RSA [mm ²]	%age Misg RSA	Total estim RSA [mm ²]	RV meas. [mm ³]	Misg RV [mm ³]	%age Misg RV	Total estim. RV [mm ³]
Regourdou 1	I ₁	257.47	2.47	0.95	259.93	251.96	0.36	0.14	252.32
Regourdou 1	I ₂	319.84	8.78	2.67	328.62	355.33	2.24	0.63	357.57
Scla 4A-20	I ₂	230.23	9.98	4.16	240.21	255.68	3.21	1.24	258.89
Scla 4A-11	I ¹	239.46	5.52	2.25	244.98	327.83	1.51	0.46	329.34
Krp D123	I ¹	357.72	11.81	3.20	369.53	576.45	4.67	0.80	581.12
Krp D126	I ¹	281.84	7.01	2.43	288.85	387.65	2.08	0.53	389.74
Krp D122	I ²	360.61	6.04	1.65	366.65	510.62	1.43	0.28	512.06
Krp 50 [Max. F]	C'	430.75	14.64	3.29	445.39	617.58	6.46	1.03	624.03
Scla 4A-16	C'	309.50	1.73	0.56	311.23	406.63	0.23	0.06	406.87

Table 2b: Root surface area and volume estimations for missing root apical portions in damaged or developmentally incomplete specimens (incisors and canines). 'RSA meas.' stands for the measured root surface area (bolded), and 'RV meas.' for the measured root volume (bolded). Further abbreviations follow the pattern used in Table 2a above.



scans, most of the Bourgeois-Delaunay teeth involved in this study, were affected by a taphonomic demineralization on an even thickness of the root involving both dentine and hypertrophic cementum when present. These demineralized tissues were attributed to their respective non-affected dental materials.

Following this segmentation process, 3D surface models of the teeth were generated using a constrained smoothing algorithm in Avizo. Each tooth was then virtually divided into crown and root(s), by cutting the 3D models at the cervical plane defined by a best-fit plane between landmarks set on the uppermost enamel margins on the labial/buccal and lingual sides of the cemento-enamel junction (Figure 1a).

2.3. Metric study of root and crown size.

2.3.1. Quantification of tooth crown size

Given the effects of both occlusal/incisal and interproximal wear on mesiodistal diameters, we used the dental crowns' breadths (bucco/labiolingual) to account for crown size. Maximum buccolingual crown diameter (Cr) was measured following the definition of Martin (M81(1) in BRÄUER, 1988) as the maximal distance between the buccal and the lingual aspect of the teeth, measured perpendicularly to the mesiodistal diameter of the tooth (Figure 1b). The Scladina and the Bourgeois-Delaunay crown data were directly measured on the specimens using a caliper. Data for the Krapina sample and for Regourdou 1 were collected from the literature (see Appendix 1 in WOLPOFF, 1979; MAUREILLE et al., 2001). Since no information was found in the literature on the dental dimensions of Krapina 59 (except for the permanent mandibular left central incisor), the buccolingual crown diameter was measured on the 3D models as described above.

2.3.2. Quantification of tooth root size

In all the four dental samples under study, root measurements were performed on the segmented roots on the 3D models in Avizo (mandibular first

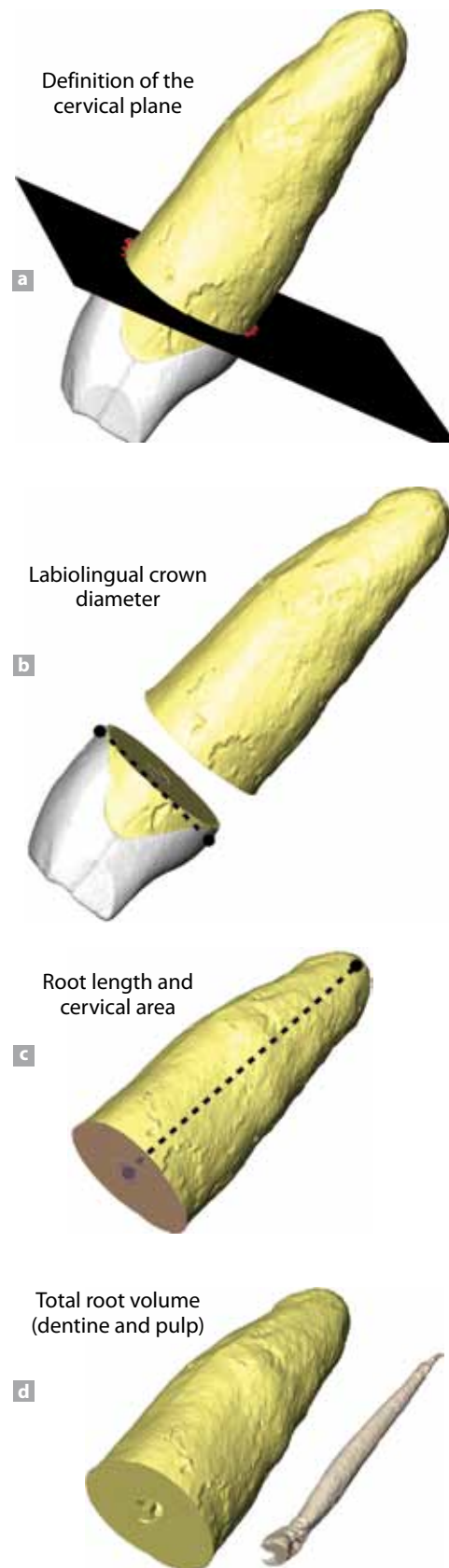


Figure 1: Crown and root measurements used in this study (modified after Figure 2 in LE CABEC et al., 2013). After defining the cervical plane based on a best fit plane (a), the tooth is virtually cut into a root and a crown (b), which allows measurement of the maximum labiolingual crown diameter (b), the cervical area (in light purple) and the root length from the center of the cervical plane to the root apex (c). The total root volume includes dentine and pulp (d).

molar root data from KUPCZIK & HUBLIN, 2010; incisor and canine data from LE CABEC et al., 2013; regarding the specimens with incompletely preserved root tips, see Tables 2a & 2b for the estimation of the missing root part). Root length (RL) was measured from the center of the pulp cavity at the cervical plane to the root apex for single rooted-teeth (Figure 1c), on the lingual root of the maxillary molars and on the distal root of the mandibular molars. In addition, within the most complete mandibular dentitions, we computed the relative differences in root length of the incisors and canine compared to the root length of M_1 as follows: $p(x) = -100 + ([RL(x) * 100] / RL(M_1))$, with $p(x)$ for this relative difference for each tooth type, RL for root length, and x for I_1 , I_2 and C . The cervical surface area (CA) has been computed as the area of the section of the tooth at the cervical plane previously defined (Figure 1c). The root surface area (RSA) as the surface area of the radicular dentine, the total root volume (RV), and the volume of radicular pulp (RPV) were measured as well (Figure 1d). The hypertrophic cementum was included in the total root volume.

2.3.3. Relationship between crown size and root size

For each tooth type within each of our four subsamples, we estimated the proportion of crown size to root length by the ratio: $(Cr * 100) / RL$. This will allow us to discuss the relationship between crown size and root size in our samples.

2.4. Statistical analyses

Descriptive statistics (sample size, mean, standard deviation, range and coefficient of variation) were computed for the crown and root variables. For all measurements and for each tooth type, adjusted z-scores (MAUREILLE et al., 2001) were performed (abbreviated as 'Azs', $\alpha = 0.05$) to test whether Scladina can be statistically accommodated within the variability of the Krapina sample. $Azs < -1$ and $Azs > 1$ mean that the specimen studied (here, Scladina) is excluded from the range of variation of the comparative sample (Krapina, in this study) while $-1 < Azs < 0$ and $0 < Azs < 1$ place the specimen in the lower or upper half of the variation of the comparative sample, respectively. Azs close to 0 corresponds to a specimen whose dimensions are very similar to the mean of the comparative sample. Statistical analyses and graphs were

performed using R 2.15.0 (R Development Core Team, 2012).

3. Results

3.1. Description of the external and cross-sectional root morphology in the Scladina I-4A mixed dentition

Overall, the roots of Scladina are well preserved. Table 3 lists the cross-sections and a general description of the external root morphology of all the Scladina teeth that have been scanned. The permanent anterior tooth roots show a labial convexity, typical in Neandertals. This is illustrated in Figure 2 (from LE CABEC et al., 2013), showing that the root shape of the Scladina I^2 falls in the middle of Neandertal variability. The fully formed molar roots are divergent and do not show the typical Neandertal taurodontic morphology.

3.2. Crown and root size metrics


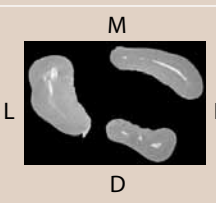

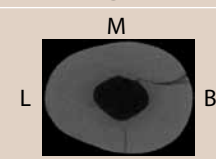
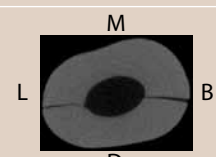
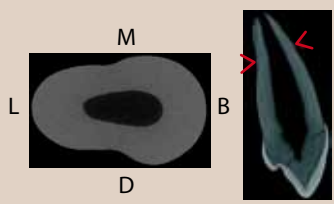
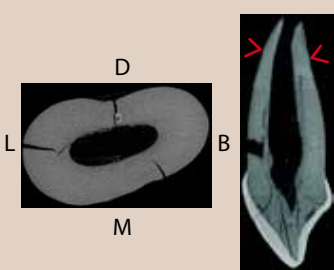
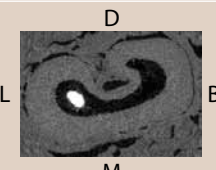
3.2.1. Overall variability in crown and root size

The surface models of a selection of teeth illustrating the variation in tooth morphology in the samples are presented in Figure 3. For the Krapina and Bourgeois-Delaunay subsamples, the coefficient of variation of the buccolingual crown diameter (ranging from 3.84% to 7.39% for Krapina, and from 0.63% to 3.78% for Bourgeois-Delaunay, Table 4) is much lower than that of the root measurements (RL, RSA, CA and RV) for all tooth types (varying from 4.23% to 22.31% for Krapina, and from 0.38% to 12.42% for Bourgeois-Delaunay, Tables 5-8). The root pulp volume is the most variable dental parameter for all tooth types (CV ranging from 19.01% to 78.55% for Krapina, and from 22.61% to 33.06% in Bourgeois-Delaunay, Table 9).

3.2.2. Tooth crown size

The tooth crown size descriptive statistics are presented in Table 4. The adjusted z-scores show that the buccolingual crown diameters of the Scladina teeth consistently fall within the lower half of the Krapina variation, the M^1 being very close to the Krapina mean (Figure 4). The incisors of Scladina have crowns strictly smaller than the incisors from Bourgeois-Delaunay, and from



Tooth	Specimen ID	Root complete?	#R	External root morphology
dm ¹ (R)	Scla 4A-7		3 (supposedly)	More than the cervical third of the roots is preserved. For all roots: root resorption. Eight-shaped L root and circular MB root. Picture taken at the 2/3 of what is left of the roots.
dm ² (R)	Scla 4A-5		3	3 divergent roots. The furcation occurs at the cervical quarter of the divergent roots. One C-shaped L root, one DB and one MB eight-shaped roots. Slightly more apical location of the root furcation between the L and the DB roots. MB root complete, L and DB root tips broken. Picture taken below at half root.
I ¹ (R)	Scla 4A-11		1	The root tip is broken (estimation at 8.78% of the total root length). Circular root cross-section.
I ² (R)	Scla 4A-14		1	The root is complete. More elliptical in root cross-section. The root tip bends distally.
I ² (L)	Scla 4A-17		1	The root is complete. More elliptical in root cross-section. The root tip bends distally.
C ['] (R)	Scla 4A-16		1	The root is not fully formed, a small portion of the root tip remains to develop. Irregular circular root cross-section (broader labially). Conspicuous thickening with a rough aspect of the apical third of the root surface (red lines). This is possibly related with deposition of secondary cementum around the apex, suggesting a case of hypercementosis. This is however very surprising considering the young age of the Scladina Juvenile, and the fact that the canine apex is not fully closed yet.
C ['] (L)	Scla 4A-18		1	The root is not fully formed, a small portion of the root tip remains to develop. Irregular circular root cross-section. Conspicuous thickening with a rough aspect of the apical third of the root surface (red lines). This is possibly related with deposition of secondary cementum around the apex, suggesting a case of hypercementosis. This is however very surprising considering the young age of the Scladina Juvenile, and the fact that the canine apex is not fully closed yet.
P ⁴ (R)	Scla 4A-2/P ⁴		1	About half of the root is formed. C-shaped cross-section, strong invagination on the distal side.

Maxillary dentition

Table 3 (continues on the next pages): Description of the external root morphology in the Scladina mixed dentition. **Specimen ID:** identity of the specimen described; **#R:** number of roots; (R) stands for right and (L) for left, dm_x and dm^x stand for mandibular and maxillary deciduous molars. P₃, P₄ and P³, P⁴ stand for the mandibular and maxillary first and second premolars; M for mesial, L for lingual, B for buccal/labial; D for distal; MB for mesiobuccal; MD for mesiodistal. It has to be noted that Scla 4A-19 (left I₂) has not been scanned.

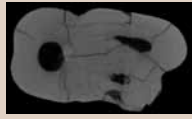

	Tooth	Specimen ID	Root complete?	#R	External root morphology
Maxillary dentition	M ¹ (R)	Scla 4A-4	<div style="text-align: center;">M</div>  <div style="text-align: center;">D</div>	3	<p>Only the L root is preserved, while the MB and DB roots are broken at the level of the bifurcation, at the cervical third of the roots. From the L, one can suppose that the roots were fully formed with closed apices.</p> <p>The mesiobuccal root appears to be wider buccolingually than the distobuccal root.</p> <p>Picture taken just above the point of root furcation.</p>
	M ² (R)	Scla 4A-3	<div style="text-align: center;">M</div>  <div style="text-align: center;">D</div>	3?	<p>About half of the roots is formed; the furcation point would be at the cervical third of the fully formed root. The DB and MB roots are not separated yet, and the DB root seems to be larger and more flattened mesiodistally than the MB root.</p>
	M ³ (R)	Scla 4A-8		—	No root formed yet (crown almost complete).

Table 3 (continued): Description of the external root morphology in the Scladina mixed dentition.

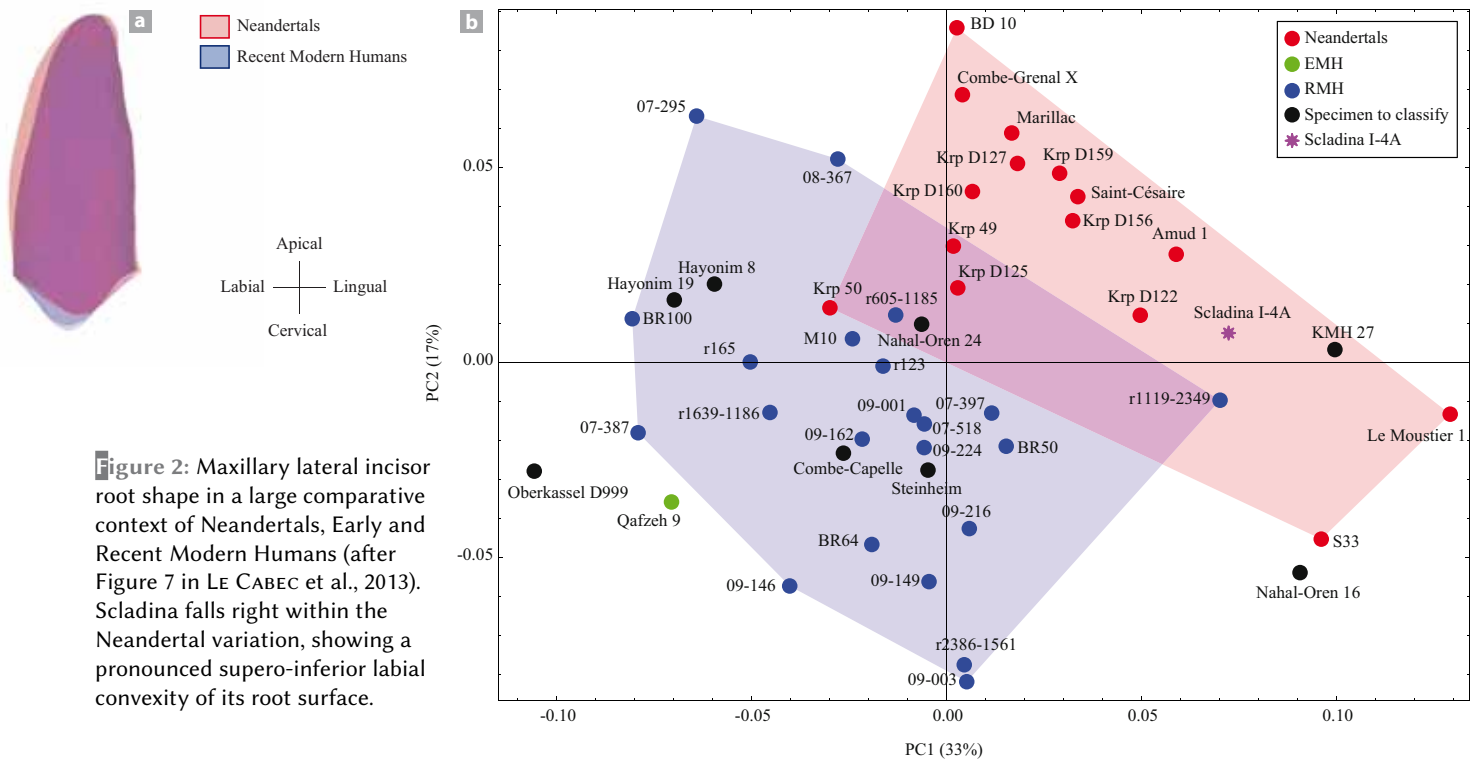


Figure 2: Maxillary lateral incisor root shape in a large comparative context of Neandertals, Early and Recent Modern Humans (after Figure 7 in LE CABEC et al., 2013). Scladina falls right within the Neandertal variation, showing a pronounced supero-inferior labial convexity of its root surface.

the mandibular canine and incisors of Regourdou 1. The Scladina mandibular canine crown size falls in between the values of the two Bourgeois-Delaunay canines. In contrast, regarding the maxillary canine and M₁, Scladina has clearly larger crowns than the Bourgeois-Delaunay teeth, and the same applies for the M₁ compared to Regourdou 1 (Table 4).

The crown size of the I¹ and I₂ of Bourgeois-Delaunay are very close to the Krapina mean, while the I² falls within the lower end of the Krapina variation (Table 4). The variability of the

I₁ from Bourgeois-Delaunay is equivalent to the one described in Krapina. In contrast, the M₁ and both the maxillary and mandibular canine crowns are strictly smaller than the ones of Krapina.

Regarding the Regourdou 1 mandible, its central incisor and first molar have a labiolingual crown diameter falling below the lower half of the Krapina range of variation (Table 4). The lateral incisor is included in the lower half of the Krapina variability. In contrast, the mandibular canine crown is larger than any value reported for the Krapina sample.



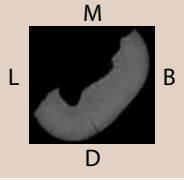
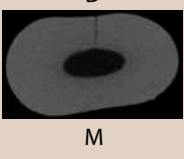
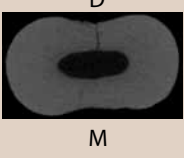
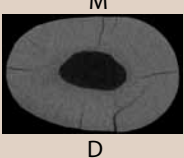
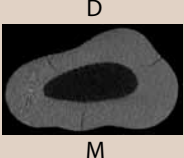
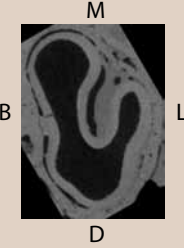



	Tooth	Specimen ID	Root complete?	#R	External root morphology
Mandibular dentition	dm ₂ (R)	Scla 4A-13		2	Supposedly 2 roots, one M and one D. The roots are broken very close to the cervix. Only the very cervical part of the distal root is preserved.
	I ₁ (R)	Scla 4A-15		1	Root apex is fully closed. Root mesiodistally compressed resulting in an elliptical root cross-section. Supero-inferior labial convexity of the root surface. Picture taken at mid-root.
	I ₂ (R)	Scla 4A-20		1	Root tip is broken (estimation at 8.70% of the total root length). Root mesiodistally compressed resulting in an elliptical root cross-section. Supero-inferior labial convexity of the root surface. Sagittal groove on the distal aspect of the root. Picture taken at mid-root.
	C ₁ (R)	Scla 4A-12		1	The root is complete. A slight thickening is observed at the apical root third, and the same hypothesis can be made as for the maxillary canines. Elliptical root cross-section. Midline groove on the mesial aspect and to a lesser extent on the distal aspect of the root.
	P ₃ (R)	Scla 4A-6		1	About two thirds of the root are formed. The mesiodistally compressed root is bent distally and exhibits a single central groove on its distal aspect and two grooves on the mesial aspect. The cervix is elliptical in cross-section. Picture taken at mid-root.
	P ₄ (R)	Scla 4A-1/P ₄		1	About two thirds of the root are formed. Strong mesiolingual invagination (Tomes' root morphology described in HILLSON, 1996). The lingual component of the root is the largest. Since the root formation is not complete, it cannot be ascertained whether the root would have been completely bifurcated more apically. Picture taken towards the end of the formed root.
	P ₄ (L)	Scla 4A-9/P ₄		1	About two thirds of the root are formed. Strong mesiolingual invagination (Tomes' root morphology described in HILLSON, 1996). The lingual component of the root is the largest. Since the root formation is not complete, it cannot be ascertained whether the root would have been completely bifurcated more apically. Picture taken towards the end of the formed root.
	M ₁ (R)	Scla 4A-1/M ₁		2	Fully formed roots with closed apices. In cross-section, the mesial root is 8-shaped while the distal root is C-shaped. The mesial root is bifurcated apically. Picture taken towards the end of the roots.
	M ₁ (L)	Scla 4A-9/M ₁		2	Fully formed roots with closed apices. In cross-section, the mesial root is 8-shaped while the distal root is C-shaped. The mesial root is bifurcated apically. Picture taken towards the apical third of the roots.

Table 3 (continued): Description of the external root morphology in the Scladina mixed dentition.

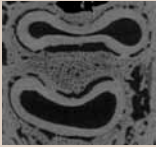

	Tooth	Specimen ID	Root complete?	#R	External root morphology
Mandibular dentition	M ₂ (R)	Scla 4A-1/M ₂	L  M D B	2	About two thirds of the roots are formed. The point of root furcation is below the cervical third of the total root size. In cross-section, the mesial root is 8-shaped while the distal root is C-shaped Picture taken towards the end of the formed root.
	M ₂ (L)	Scla 4A-9/M ₂	L  D B M	2	About two thirds of the roots are formed. The point of root furcation is below the cervical third of the total root size. In cross-section, the mesial root is 8-shaped while the distal root is C-shaped Picture taken towards the end of the formed root.
	M ₃ (R)	Scla 4A-1/M ₃	—	—	No root formed yet (crown about complete).

Table 3 (continued): Description of the external root morphology in the Scladina mixed dentition.

3.2.3. Tooth root size

The root length (RL), surface area (RSA) and total volume (RV) of the Scladina teeth are included in the lower half of the Krapina variation (I₂ and M₁) or strictly smaller (I₁, I² and C') than in the Krapina teeth (Figures 3 & 5 and see adjusted z-scores in Figure 4). However, the root length of the M¹ is very close to the Krapina mean. The cervical area (CA) of all the Scladina teeth falls within the lower half of the Krapina variability. Regourdou 1 and Bourgeois-Delaunay have strictly larger roots (for RL, CA, RSA and RV) than Scladina (Figure 5 & Tables 5-8).

Among the 28 root measurements of Bourgeois-Delaunay (RL, RSA, CA, RV, excluding RPV), 24 fall in the lower half of the Krapina range of variation, whereas only the I¹ root length is superior to the Krapina upper end. The root length of the I₁ and the cervical area of the I¹ and C' are above the Krapina range (Tables 5 & 7).

For Regourdou 1, all the root measurements of the I₁, except the root pulp volume, are strictly inferior to the Krapina range. Overall, the I₂, C, and M₁ of Regourdou 1 are included within the lower half of the Krapina variability. It has to be noted that the root length of its M₁ falls in the upper half of the Krapina range of variation (Tables 5-8).

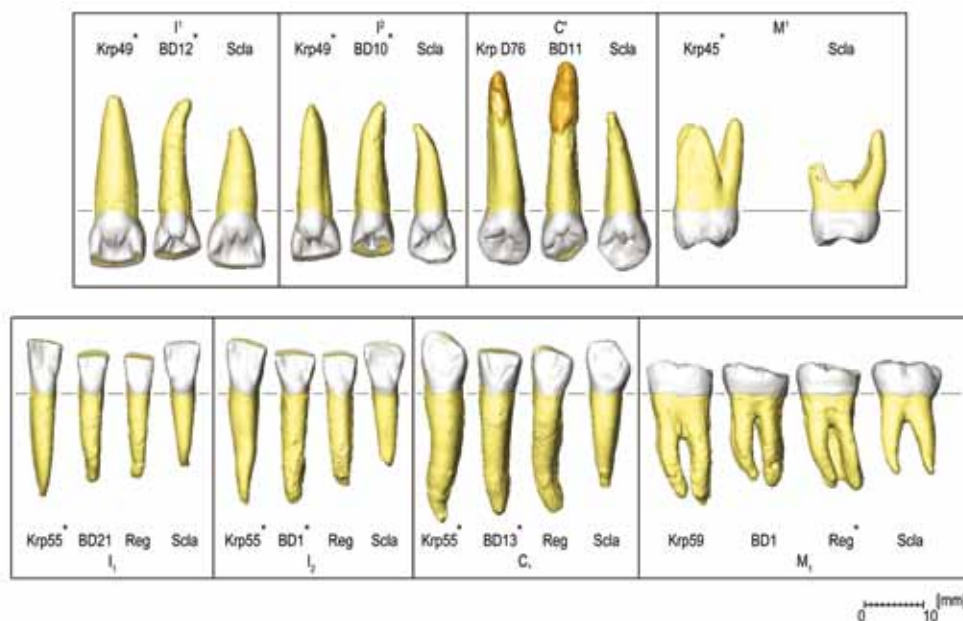


Figure 3: 3D surface models of selected right teeth for each tooth type from Scladina (Scla), Krapina (Krp), Abri Bourgeois-Delaunay (BD) and Regourdou (Reg). Note the presence of hypercementosis on the permanent maxillary canines root apex (shown in light brown). Several specimens were mirrored for illustrative purposes (indicated by an asterisk).



	Maxillary Dentition				Mandibular Dentition			
	I ¹	I ²	C'	M ¹	I ₁	I ₂	C _r	M ₁
Krapina	N=6 8.90 ± 0.66 [8.10–9.50] (7.39)	N=8 8.99 ± 0.35 [8.40–9.50] (3.84)	N=6 10.20 ± 0.68 [9.50–11.10] (6.66)	N=3 11.90 ± 0.53 [11.30–12.30] (4.45)	N=3 7.57 ± 0.38 [7.30–8.00] (5.00)	N=5 7.94 ± 0.57 [7.30–8.75] (7.22)	N=4 9.11 ± 0.37 [8.75–9.50] (4.02)	N=8 11.42 ± 0.62 [10.70–12.15] (5.40)
Abri Bourgeois-Delaunay	N=1 8.40	N=1 8.50	N=3 9.23 ± 0.06 [9.20–9.30] (0.63)	—	N=3 7.63 ± 0.29 [7.30–7.80] (3.78)	N=1 7.90	N=2 7.90; 9.10	N=2 10.50; 10.66
Regourdou 1	—	—	—	—	N=1 7.00	N=1 7.90	N=1 9.60	N=1 10.40
Scladina I-4A	N=1 7.98	N=1 8.27	N=1 9.65	N=1 11.92	N=1 6.79	N=1 7.28	N=1 8.75	N=1 10.68

Table 4: Descriptive statistics for the labiolingual crown diameter (in mm).

	Maxillary Dentition				Mandibular Dentition			
	I ¹	I ²	C'	M ¹	I ₁	I ₂	C _r	M ₁
Krapina	N=6 18.75 ± 1.28 [16.59–19.58] (6.85)	N=8 19.11 ± 0.83 [17.42–19.97] (4.33)	N=6 23.01 ± 1.07 [20.94–23.81] (4.63)	N=3 13.58 ± 1.32 [12.07–14.51] (9.72)	N=3 19.89 ± 0.84 [19.36–20.86] (4.23)	N=5 19.72 ± 1.78 [17.70–21.63] (9.05)	N=4 23.93 ± 2.16 [21.04–25.64] (9.04)	N=8 16.43 ± 1.48 [14.47–18.45] (9.00)
Abri Bourgeois-Delaunay	N=1 19.79	N=1 18.72	N=3 25.05 ± 0.10 [24.98–25.16] (0.38)	—	N=3 17.56 ± 1.58 [16.46–19.37] (9.00)	N=1 19.44	N=2 21.78; 22.22	N=2 13.33; 15.67
Regourdou 1	—	—	—	—	N=1 16.41	N=1 17.80	N=1 22.95	N=1 17.00
Scladina I-4A	N=1 15.32	N=1 15.15	N=1 17.69	N=1 13.65	N=1 13.80	N=1 15.23	N=1 16.51	N=1 13.41

Table 5: Descriptive statistics for the root length (in mm).

	Maxillary Dentition				Mandibular Dentition			
	I ¹	I ²	C'	M ¹	I ₁	I ₂	C _r	M ₁
Krapina	N=6 355.95 ± 47.04 [288.85–409.32] (13.22)	N=8 376.03 ± 25.06 [337.81–409.22] (6.66)	N=6 473.00 ± 43.06 [414.18–539.41] (9.10)	N=3 —	N=3 337.36 ± 19.60 [320.50–358.86] (5.81)	N=5 360.49 ± 48.09 [279.72–403.59] (13.34)	N=4 508.51 ± 93.07 [393.47–619.68] (18.30)	N=8 615.61 ± 76.35 [491.46–691.67] (12.40)
Abri Bourgeois-Delaunay	N=1 356.45	N=1 371.10	N=3 492.02 ± 14.02 [481.21–507.86] (2.85)	—	N=3 331.55 ± 26.65 [305.10–358.40] (8.04)	N=1 383.05	N=2 427.08; 462.15	N=2 457.84; 555.37
Regourdou 1	—	—	—	—	N=1 259.93	N=1 328.62	N=1 468.91	N=1 569.38
Scladina I-4A	N=1 244.98	N=1 252.79	N=1 311.23	N=1 —	N=1 195.57	N=1 240.21	N=1 302.09	N=1 446.07

Table 6: Descriptive statistics for the root surface area (in mm²).

	Maxillary Dentition				Mandibular Dentition			
	I ¹	I ²	C'	M ¹	I ₁	I ₂	C _r	M ₁
Krapina	N=6 47.74 ± 9.42 [36.53–59.07] (19.74)	N=8 41.89 ± 4.98 [35.13–49.56] (11.89)	N=6 49.15 ± 5.29 [44.64–55.84] (10.76)	N=3 —	N=3 25.91 ± 1.48 [24.87–27.61] (5.72)	N=5 30.14 ± 3.91 [25.13–35.72] (13.00)	N=4 45.55 ± 3.16 [41.54–48.54] (6.94)	N=8 95.01 ± 11.95 [77.99–111.53] (12.58)
Abri Bourgeois-Delaunay	N=1 33.15	N=1 36.06	N=3 41.59 ± 2.59 [40.00–44.57] (6.22)	—	N=3 27.00 ± 2.70 [25.30–30.12] (10.01)	N=1 26.99	N=2 35.20; 43.77	N=2 77.70; 78.79
Regourdou 1	—	—	—	—	N=1 23.03	N=1 28.60	N=1 44.03	N=1 85.70
Scladina I-4A	N=1 37.19	N=1 33.35	N=1 43.34	N=1 —	N=1 20.99	N=1 24.83	N=1 40.07	N=1 76.08

Table 7: Descriptive statistics for the cervical surface area (in mm²).

	Maxillary Dentition				Mandibular Dentition			
	I ¹	I ²	C'	M ¹	I ₁	I ₂	C _r	M ₁
Krapina	N=6 549.58 ± 122.61 [389.74–693.61] (22.31)	N=8 528.47 ± 72.18 [431.09–633.22] (13.66)	N=6 690.61 ± 74.58 [617.91–817.26] (10.80)	N=3 —	N=3 371.65 ± 26.36 [341.36–389.32] (7.09)	N=5 430.65 ± 70.13 [313.68–491.84] (16.29)	N=4 740.28 ± 157.65 [524.13–902.34] (21.30)	N=8 832.07 ± 148.43 [582.45–999.90] (17.84)
Abri Bourgeois-Delaunay	N=1 473.62	N=1 504.64	N=3 680.57 ± 46.81 [650.64–734.51] (6.88)	—	N=3 371.12 ± 46.10 [331.53–421.73] (12.42)	N=1 455.70	N=2 568.60; 656.03	N=2 561.68; 691.22
Regourdou 1	—	—	—	—	N=1 252.32	N=1 357.57	N=1 619.29	N=1 774.13
Scladina I-4A	N=1 329.34	N=1 310.68	N=1 406.87	N=1 —	N=1 200.08	N=1 258.89	N=1 387.93	N=1 513.92

Table 8: Descriptive statistics for the root volume (in mm³).

	Maxillary Dentition				Mandibular Dentition			
	I ¹	I ²	C'	M ¹	I ₁	I ₂	C _r	M ₁
Krapina	N=6 48.86 ± 24.17 [18.88–85.97] (49.48)	N=8 31.81 ± 21.82 [12.41–81.67] (68.60)	N=6 42.67 ± 8.11 [27.27–49.49] (19.01)	N=3 —	N=3 13.86 ± 8.69 [7.47–23.75] (62.70)	N=5 27.07 ± 21.27 [8.02–63.03] (78.55)	N=4 41.77 ± 22.10 [17.19–70.75] (52.91)	N=8 75.19 ± 42.75 [44.51–167.45] (56.86)
Abri Bourgeois-Delaunay	N=1 19.40	N=1 11.36	N=3 24.66 ± 5.58 [18.26–28.49] (22.61)	—	N=3 8.40 ± 2.78 [6.42–11.57] (33.06)	N=1 16.62	N=2 13.77; 19.37	N=2 38.09; 102.17
Regourdou 1	—	—	—	—	N=1 12.53	N=1 16.41	N=1 34.30	N=1 67.88
Scladina I-4A	N=1 44.32	N=1 43.33	N=1 66.34	N=1 —	N=1 20.32	N=1 29.60	N=1 55.85	N=1 64.83

Table 9: Descriptive statistics for the root pulp volume (in mm³).

By contrast, for most of the tooth types (except M₁ and I¹), the radicular pulp volumes (RPV) of the Scladina teeth are systematically higher than the Krapina means (Figure 4 & Table 9). The maxillary canine even has a RPV strictly superior to Krapina. Volumetric proportions of root dentine and pulp reveal a consistent pattern for all tooth types. Scladina has a larger proportion of pulp despite its short roots (Figure 6; Tables 8 & 9). However, the I₂ and M₁ of Krp 53 and the I² of Krp D122 have extremely large pulp cavities, exceeding the corresponding Scladina teeth by 1.4%, 4.1% and 2.0% respectively (Figure 6). Regourdou 1 has radicular dentine to pulp proportions similar to Bourgeois-Delaunay for the incisors, and to Krapina for the canine and first molar (Figure 6).

The intra-individual comparison in relative differences in root lengths has yielded an interesting and consistent pattern (Figure 7 & Table 5). Compared to the M₁ root length, one observes relatively longer mandibular anterior tooth roots in our Krapina individuals (Krp 54, 55, 58 and 59; 27.89% on average), Bourgeois-Delaunay (BD1; 28.89%) and Scladina (13.19%). The root length increases gradually from I₁ to mandibular canine although both incisors have a similar root length.

Regourdou 1 follows the same pattern, except that its I₁ root is shorter than its M₁ roots.

3.2.4. Relationship between crown size and root size

Figure 8 presents the ratio between the buccolingual crown diameter and the root length for each tooth type in our four subsamples. Scladina shows consistently the highest value for each tooth type, meaning that these teeth display large crowns in proportion to their short roots. Crown size and root size proportionally contribute with the same amount to the tooth size (percentages around 50% in Figure 8) in the Scladina incisors and canines. However, the first molars have markedly short roots for the size of their crown (percentages about 80–90% in Figure 8). Overall, Bourgeois-Delaunay shows relatively small crowns for large roots, although it has to be noted that the M₁ has a proportionally shorter palatal root. Regourdou 1 follows the same pattern as Bourgeois-Delaunay, although its roots are shorter. Finally, Krapina shows for all tooth types a very large variability that encompasses all the previously described



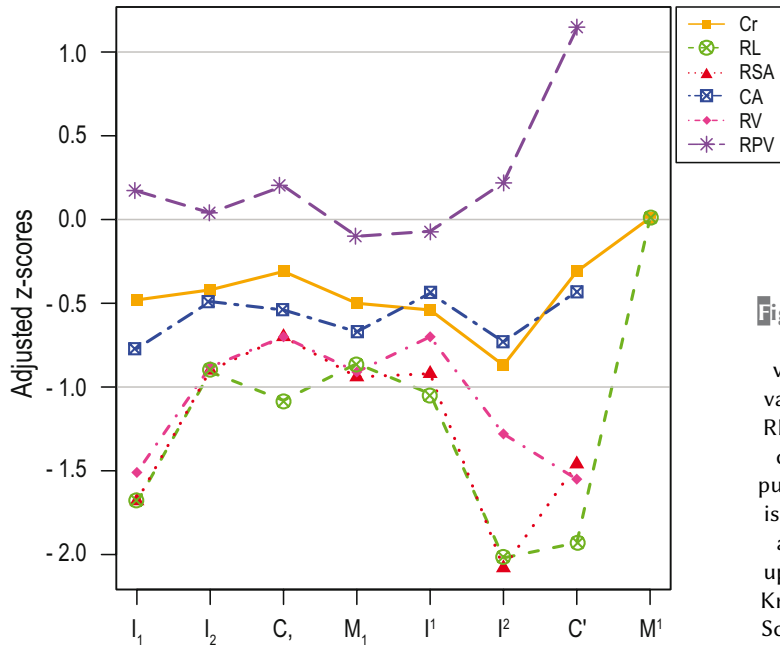


Figure 4: Adjusted z-scores (Azs) comparing how Scladina fits into the Krapina variability using six tooth crown and root variables (Cr: labiolingual crown diameter; RL: root length; RSA: root surface area; CA: cervical area; RV: root volume; RPV: root pulp volume). For Azs close to zero, Scladina is similar to the Krapina mean; for $0 < Azs < 1$ and $-1 < Azs < 0$, Scladina falls within the upper and the lower half of the variation of Krapina, respectively; for $-1 < Azs$ and $Azs > 1$, Scladina is outside of the Krapina variation.

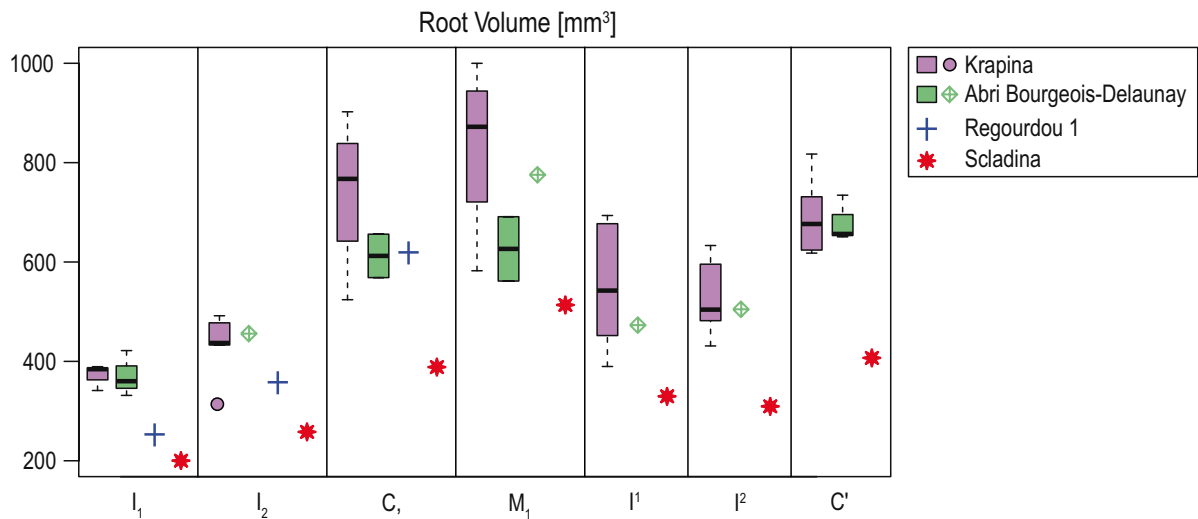


Figure 5: Total root volume [mm³] of the mandibular and maxillary permanent incisors, canines and first molars of Bourgeois-Delaunay, Krapina, Regourdou 1 and Scladina (minimum, first quartile, median, third quartile, and maximum; outliers are denoted by circles).

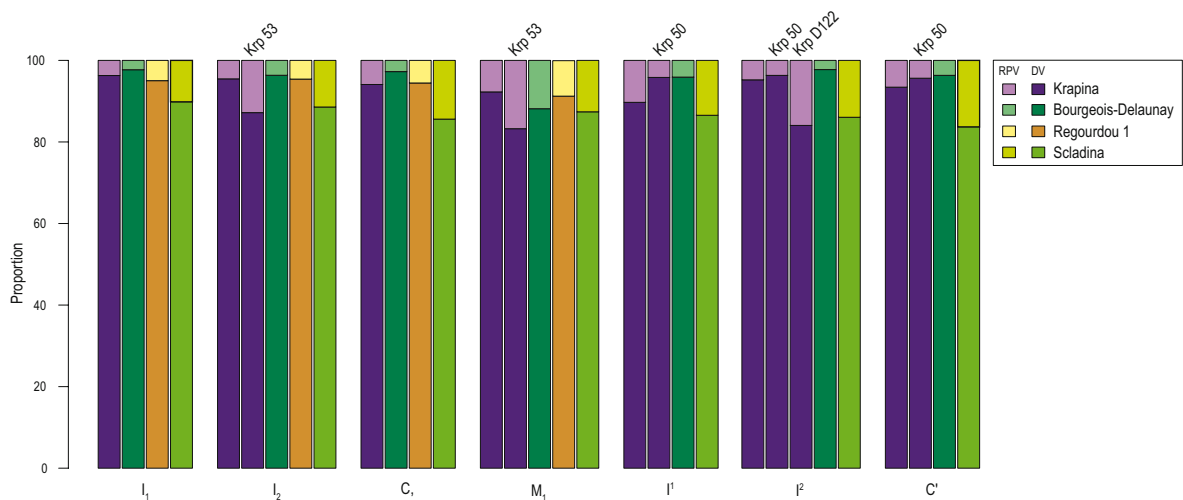


Figure 6: Proportions of tooth root dentine (DV) and pulp (RPV) volumes. The proportions of individuals of similar age as Scladina are represented separately.

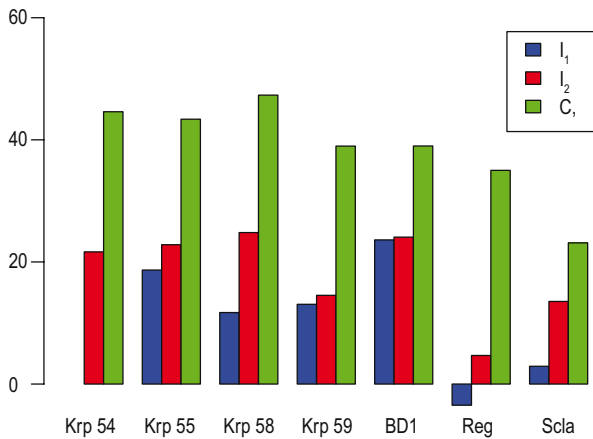


Figure 7: Intra-individual proportions in root length of I₁, I₂ and C, compared to M₁ for individuals with most complete mandibular dentitions. This percentage is calculated as follows: $p(x) = -100 + ([RL(x) * 100] / RL(M_1))$, with RL for root length, and x for I₁, I₂ and C.

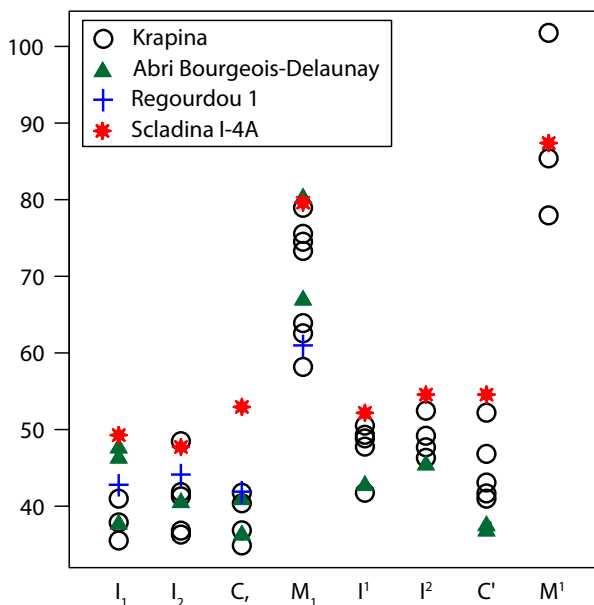


Figure 8: Proportion of the maximum buccolingual crown diameter (Cr, in mm) to the root length (RL, in mm) computed as: $(Cr * 100) / RL$.

patterns. About half of the Krapina sample has relatively shorter roots for the size of its crowns, while the other half has relatively longer roots for its crown size.

To summarize, our results show that overall root size is much more variable than crown size. The measurements of the Scladina maxillary and mandibular teeth fall within the lower half of the Krapina range of variation or are excluded from their variation. Only the Scladina pulp volumes are among the largest measured in our sample. The Krapina sample has the largest crown and

root dimensions of the four samples (Tables 4–9). The Bourgeois-Delaunay and Regourdou 1 teeth are smaller than those from Krapina but the Bourgeois-Delaunay remains are always included in the lower half of the Krapina range of variation.

4. Discussion

This study aimed to document the tooth root morphology of the permanent mandibular and maxillary incisors, canines and first molars of the Scladina Juvenile. After a description of the external morphology of all the roots of the Scladina mixed dentition, the root morphology of its permanent teeth was further investigated using micro-computed tomography and in the comparative context of other MIS 5 Neandertals from Krapina, Abri Bourgeois-Delaunay and Regourdou. Our results show that Scladina has comparatively very short tooth roots while the size of its crowns is similar to those of the other Neandertals. Scladina also displays the largest pulp cavities among all samples studied.

4.1. Taxonomical interest of root dimensions: the case of Scladina I-4A, a short-rooted MIS 5 Neandertal

The root length of I¹, I₁, C' and P⁴ has been proposed to taxonomically discriminate Neandertals from anatomically modern humans (BAILEY, 2005; BAILEY & HUBLIN, 2006). However, in view of our results, we recommend a cautious taxonomical diagnosis of Neandertal fossil teeth, based solely on tooth root metrics (see LE CABEC et al., 2013 for examples on taxonomically debated specimens). Indeed, the root lengths of all the corresponding Scladina teeth (except for the premolars which were not studied here due to incompleteness of their roots) are outside the Neandertal range of variation provided in BAILEY (2005), but fall within the Upper Palaeolithic range of variation sampled in her study. The Scladina dental dimensions are very small compared to other MIS 5 Neandertals sampled in this study. Such interpopulational or interindividual differences also exist for MIS 3 Neandertals specimens. The Spanish Sima de Las Palomas Neandertals (WALKER et al., 2008) have shorter anterior tooth roots than more northern Neandertals, but they are still longer than those of Scladina, except for an I² (SP48) and a C' (SP26).



The first molars of Scladina also have short and overall small roots compared to our MIS 5 Neandertals. They do not display any degree of taurodontism, typical root morphology very frequently seen in Neandertals.

The case of Scladina thus extends the range of variability in tooth root dimensions in Neandertals, and requires a careful assessment of taxonomical identity using root length including both Early and Late Neandertals from different geographic origins.

4.2. In light of this study, is Krapina representative of the MIS 5 Neandertal dental variation?

Both Krapina and Bourgeois-Delaunay are known to have large-crowned teeth (WOLPOFF, 1979; CONDEMI, 2001). Our results extend these previous studies by including the external (root length, surface area, and volume) and internal (root pulp volume) tooth root measurements.

On the one hand, crown size seems to be stable overall in MIS 5 Neandertals ($CV < 7.5\%$, Table 4), with Scladina, Regourdou 1 and Bourgeois-Delaunay falling in the majority of cases within the lower half of the Krapina variation. On the other hand, root dimensions are much more variable (on average 11.15% for Bourgeois-Delaunay and 19.83% for Krapina), especially root pulp volumes. This could be explained by the fact that crown development is said to be under strong genetic control, whereas root development is more influenced by environmental factors (KOVACS, 1967). Krapina was found to have the largest crown and root dimensions of our Neandertal samples, while the Bourgeois-Delaunay teeth are slightly smaller. The latter, however, consistently fall within the lower half of the Krapina range of variation. These two samples thus represent populations with both robust crown and root dimensions.

Overall, Regourdou 1 is smaller than Bourgeois-Delaunay and Krapina, for both crown and root dimensions. While Scladina has crowns of comparable size with the other MIS 5 Neandertals, its roots are markedly short. Moreover, one can notice that variation in relative incisors root dimensions (Figure 7) does not appear to be related to geography as suggested by the large-rooted Krapina and Bourgeois-Delaunay (central Europe and southwestern Europe) in contrast to the relatively smaller Scladina and Regourdou 1 (northern Europe and southwestern Europe).

In addition, a comparison of the crown dimensions of the four MIS 5 samples with published values for the MIS 5e skulls of Saccopastore 1 and 2 (Italy) indicates a marked variability among Early Neandertals. For example, the buccolingual crown diameters of the maxillary canine and first molars of Saccopastore 1 and 2 reported in CONDEMI (1992) are smaller and consistently excluded from the variation we observed in the Neandertals from Krapina, Bourgeois-Delaunay and Scladina (see also STRINGER, 1982 for a comparison between Saccopastore and Krapina). However, no information is currently available in the literature regarding the dimensions of the maxillary tooth roots of those Italian specimens. Future studies involving micro-CT data are needed to document the root morphology in the Saccopastore specimens.

Although Krapina is often used because of its large sample size, it is not representative of the MIS 5 Neandertal variability, this population being exceptionally robust. Scladina and Regourdou 1 are good examples of small-rooted contemporaneous Neandertals.

4.3. What about crown to root size proportions?

The analysis of the proportion of crown size to root size reveals that Krapina has relatively large roots for the size of its crowns and the same applies to Bourgeois-Delaunay and Regourdou 1, although to a lesser extent. Conversely, Scladina has relatively short roots for his/her crowns (Figure 8). This raises the question whether one can estimate tooth root size from its crown size. In other words does a tooth with a large crown have associated big root(s)? The case of Scladina suggests that there would be no predictive relationship between crown size and root size. Interestingly, Smith and Paquette (PAQUETTE, 1985; SMITH & PAQUETTE, 1989) concluded that there was a positive correlation between crown and root size in the Krapina anterior teeth, that is, large-crowned teeth have large roots. Conversely, LE CABEC et al. (2013) cannot find any significant correlation in a geographically and chronologically broad sample of Neandertal anterior teeth. Smith and Paquette (PAQUETTE, 1985; SMITH & PAQUETTE, 1989) have also shown that the ratio of the crown labiolingual diameter to the root length still distinguishes Neandertals from extant humans. This discordance may stem from the fact that these authors

took into account the crown diameters and the corresponding root diameters, whereas LE CABEC et al. (2013) tested the correlation between the root length and the labiolingual crown diameter. KUPCZIK & HUBLIN (2010) have reported that mandibular molar root surface area correlates significantly with cervical plane area and enamel-dentine junction area in both Neandertals and modern humans. There are indications of a low correlation between crown and root size in Recent Modern Humans (GARN et al., 1978^a; GARN et al., 1978^b; SMITH et al., 1986; OZAKI et al., 1988; SMITH et al., 1989; KUPCZIK, 2003; KUPCZIK et al., 2009). As pointed out by SPENCER (2003) on platyrrhine seed-eaters, crown and root size may not covary the same way in all taxa. Moreover, as shown by the divergence between Smith and Paquette's findings and the LE CABEC et al. (2013) study, results may depend on the measurements selected (e.g. root length vs. crown diameters, root diameters vs. crown diameters, root surface area vs. enamel-dentine junction area). However, the case of Scladina with its short roots for its relatively large crowns questions the relation of crown size to root size in Neandertals.

4.4. What can be discussed about sexual dimorphism?

Clinical studies on Recent Modern Humans have shown that sexual dimorphism is greater in root length than in crown diameters (GARN et al., 1978^c; GARN et al., 1979), males having longer roots than females (JAKOBSSON & LIND, 1973). Furthermore, studies of genetic disorders support the role of sex chromosomes in root length (ALVESALO et al., 1991; LÄHDESMÄKI, 2006; LÄHDESMÄKI & ALVESALO, 2007). In the light of these clinical studies, the short roots of Scladina would suggest that this individual may have been female. Toussaint (Chapter 9) highlights the small mandibular corpus dimensions of Scladina, in comparison with other Neandertals of the same age group, and he further suggests that Scladina could have been female. The pulp cavity volumes of all the investigated Scladina teeth are among the largest of the teeth measured in this study. It has been proposed that secondary dentine deposition would be related to sexual dimorphism, with males having thicker radicular dentine than females (SCHWARTZ & DEAN, 2005). In addition to the short roots, this would be a second argument to suggest that this individual may have been female.

4.5. How influential can the young age of Scladina be on its roots dimensions?

ZILBERMAN & SMITH (2001) further suggested that sexual dimorphism combined with ageing would affect the progressive closing of the pulp cavity throughout life. Having significantly smaller total root volumes than the three other samples, the Scladina teeth therefore display thinner dentine walls of their large pulp cavities. A possible explanation for this may be the young age of the Scladina individual, estimated at eight years old (SMITH et al., 2007). It has to be reminded that contrary to bone which is subject to remodeling throughout life, the teeth initiate and complete their mineralization while they erupt, to reach functional emergence, and they do not remodel afterwards. They can be subject to various pathologies or traumatic events, the roots can resorb, and the only way of healing or changing the shape of a tooth is to secrete hypertrophic cementum (see LE CABEC et al., 2013 for a discussion in the functional context of the Neandertal dentition). Among our Krapina sample, Krp53 (Mandible C), whose age at death is estimated at 11 years old (WOLPOFF, 1979), also shows outlier values for the pulp volume of its lateral incisor and first molar. The permanent maxillary lateral incisor Krp D122 estimated to belong to a 13 years old individual also shows a large pulp volume (Figure 6). Several studies have shown that apposition of secondary dentine on the walls of the pulp chamber increases with age (GUSTAFSON, 1950; PHILIPPAS, 1961; PHILIPPAS & APPLEBAUM, 1967; WOODS et al., 1990; PAEWINSKY et al., 2005). Furthermore, secondary dentine is commonly thought to be deposited throughout life to compensate for occlusal wear (also referred to as tertiary dentine or irregular dentine, e.g. KUTTLER, 1959), leading to a progressive retraction of the pulp (e.g. BROESTE et al., 1944; PEDERSEN, 1949; SICHER & DUBRUL, 1970; BARRETT, 1977). The filling of the pulp cavity occurs then from the cervix to the apex whereas wear erodes the coronal dentine core (BERRY & POOLE, 1976; BARRETT, 1977). No systematic clear-cut identification of secondary dentine apposition in the pulp cavity could be made from our micro-CT data, as the two types of dentine have a very similar density. Yet, in some cases, a slight difference in gray-values delineates the secondary dentine evenly deposited on the walls of the pulp cavity, in some of the older specimens from Krapina (e.g. permanent mandibular right canine in Krp59, estimated age



at death of 20 years following WOLPOFF, 1979) and Bourgeois-Delaunay (e.g. BD15, see Figure 1E in LE CABEC et al., 2013). Then, only the use of appropriate filters (as described in the Materials and Methods section and Figure 1E in LE CABEC et al., 2013) could reveal the border between these two materials. Combined observations of photographs and of our micro-CT data reveal that the reparative secondary dentine was sometimes exposed by severe attrition, e.g. on the permanent mandibular left central incisors of Krp58 and Krp59. Therefore, differences in individual age could account for the difference in pulp volume observed between Scladina and Krapina.

4.6. How reliable is it to discuss about sexual dimorphism and age in fossils?

Although it is impossible to discern the relative importance of age and sex in the conformation of the Scladina roots, its large pulp cavities are likely accounted for by its young age whereas its short roots and thin root dentine walls of the pulp cavities point that it could be a female individual. However, sexual dimorphism in root length and root pulp volume cannot account alone for the difference between Scladina on one hand, and Regourdou 1, Krapina and Bourgeois-Delaunay on the other hand. As the two last samples contain isolated, non-associated teeth, especially for the larger Krapina sample, it is likely that males and females are sampled in this archeological population. WOLPOFF (1979) and BERMÚDEZ DE CASTRO et al. (1993) highlight a low sexual dimorphism in the dental remains from Krapina. Only mandibular corpus variation accurately estimates the sex of the extremes, such as Krp 58 and Krp 59 being likely males. This means that, although the level of sexual dimorphism in Krapina is low, this population likely includes females and is overall larger in dental dimensions than Scladina, Regourdou 1 and Bourgeois-Delaunay. The sex-ratio being unknown in our samples, any more developed discussion regarding sexual dimorphism would be speculative.

4.7. Dental development

The short roots of Scladina could be attributable to variation in particular dental developmental parameters.

Most of the developmental studies have focused on enamel growth involving enamel secretion and extension rates, and crown formation time. Although it has been argued that the duration of tooth development might have been similar in Neandertals and modern humans (GUATELLI-STEINBERG et al., 2005), microstructural studies on large samples, including Scladina in particular, have shown significant developmental differences between Neandertals and modern humans (RAMIREZ ROZZI & BERMÚDEZ DE CASTRO, 2004; SMITH et al., 2007; SMITH, 2008; SMITH et al., 2010). SMITH et al. (2010) conclude that the faster dental development in Neandertals does not seem to be related to ontogenetic stage, geological age or geography, albeit Scladina and Engis 2, both from Belgian sites, show a particularly rapid dental growth that is also faster than other Neandertals for the molars, while some of their incisors are slower. Moreover, BAYLE et al. (2009^a; 2009^b) also noted a specific pattern of dental maturation in the Roc-de-Marsal child where incisors are delayed and the first molars advanced compared to a sample of modern humans. In addition to its peculiar timing of dental development, the pattern of dental maturation can be affected by the small dimensions of the Scladina's roots, that is, incisors and molars could show intra-individual differences in their relative sequence of eruption.

In contrast, very little is known about root formation. According to MACCHIARELLI et al. (2006) a late peak in root extension rate occurs in molars and this distinguishes Neandertals from anatomically modern humans. Smith et al. (Chapter 8) provide values for root extension rate, especially for the first molar of Scladina. A finer overview of the phenomenon would require a larger amount of comparative data. But since crown extension rates are much faster in Neandertals than in Recent Modern Humans (SMITH et al., 2007; SMITH et al., 2010), one could speculate that the same applies to root extension rates.

To conclude, one can speculate that the short roots of Scladina could result from a shorter period of dental development combined with an individual faster rate of root extension. Further research may investigate in more detail how the absolutely and relatively short incisor roots and contrasted overall rapid dental development in Scladina might have implications in understanding the relative differences in intra-individual dental maturation sequences within Neandertals.

4.8. Scladina I-4A in a broader comparative context

Compared to a larger sample of Neandertals, Early and Recent Modern Humans (see KUPCZIK & HUBLIN, 2010 for the first molars; see LE CABEC et al., 2013 for the anterior teeth), Scladina has among the smallest roots documented.

For the anterior dentition, the Scladina root metrics fall in the area of overlap of Neandertals and the Recent Modern Humans, or even strictly

in the modern human distribution. Figures 9–14 illustrate the position of Scladina among temporally and geographically broad comparative samples: this Neandertal has the shortest roots among all Neandertals ranging from MIS 7 to 3. However, when all root and crown metrics are combined into PCA and CVA analyses, the results of the cross-validation tests show that all maxillary anterior teeth classify correctly as Neandertals, as for the I₁, while the I₂ and C, classify among Early Modern Humans (EMH,

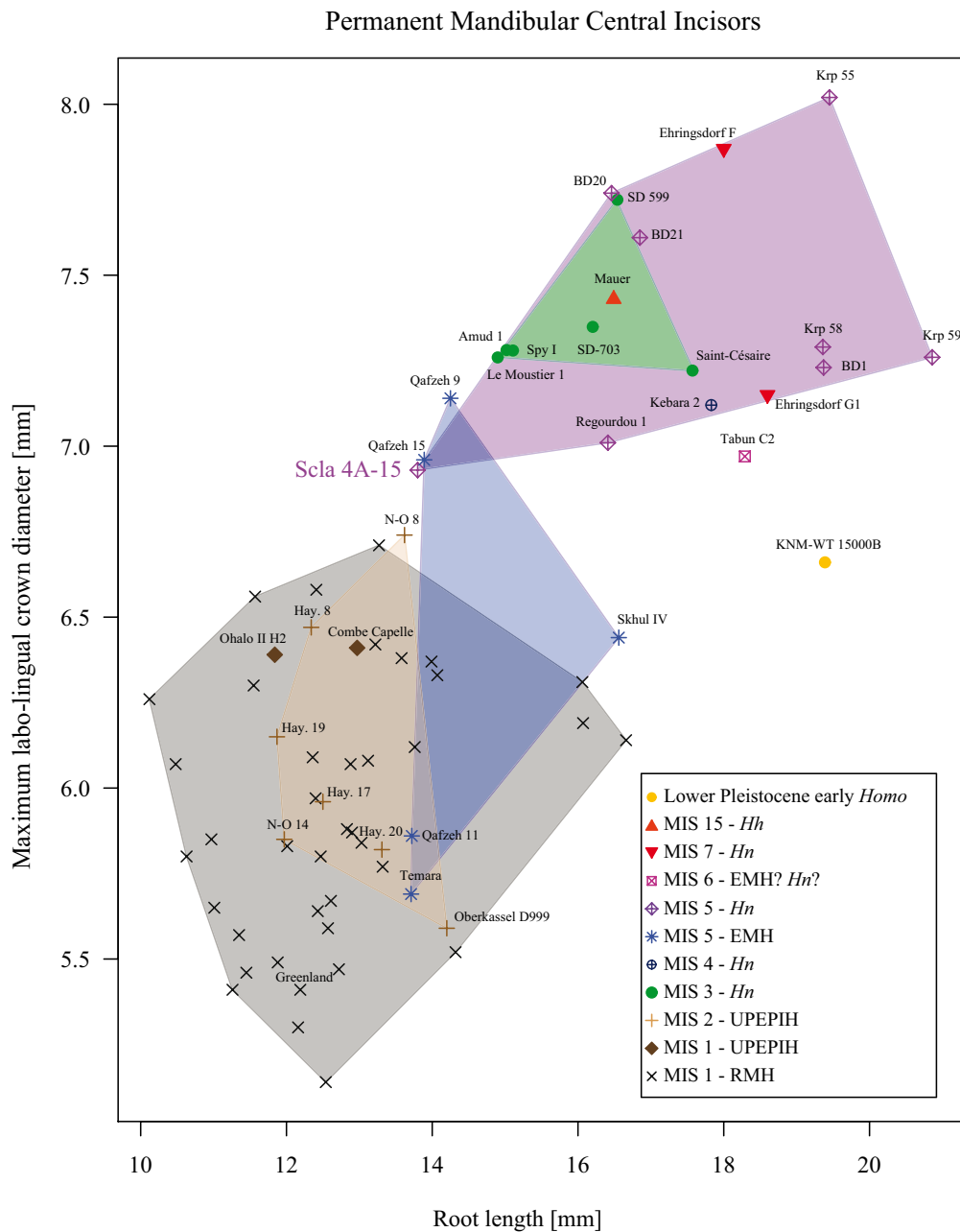


Figure 9: Scla 4A-15 in the broader context of permanent mandibular central incisors. The observed pattern suggests a chronological trend in our crown and root size data. A gradient is clearly visible, from the older specimens (at the right) toward the more gracile Recent Modern Humans (at the very left). Note the smaller variability of MIS 3 Neandertals (this is possibly due to small sample size). Adapted from LE CABEC et al., 2013.



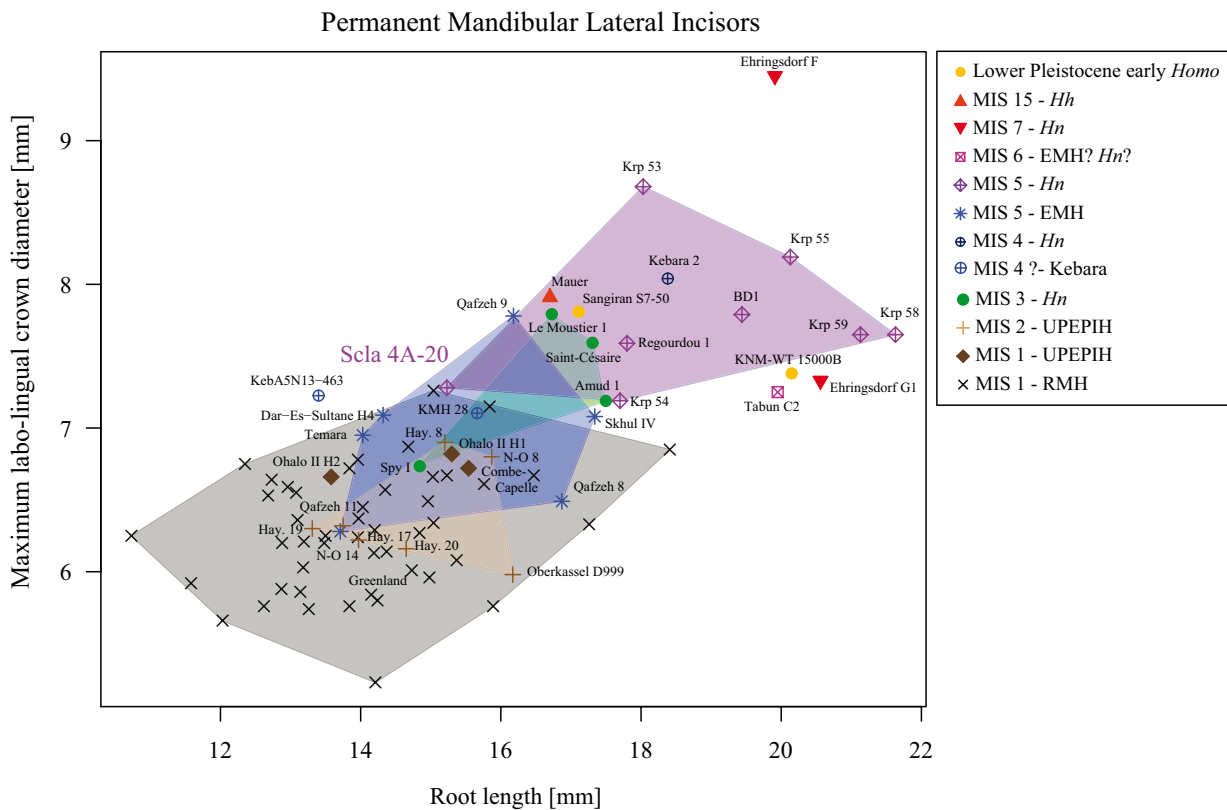


Figure 10: Scla 4A-20 in the broader context of permanent mandibular lateral incisors. Same possible gradient in size and chronological trend as in Figure 9.

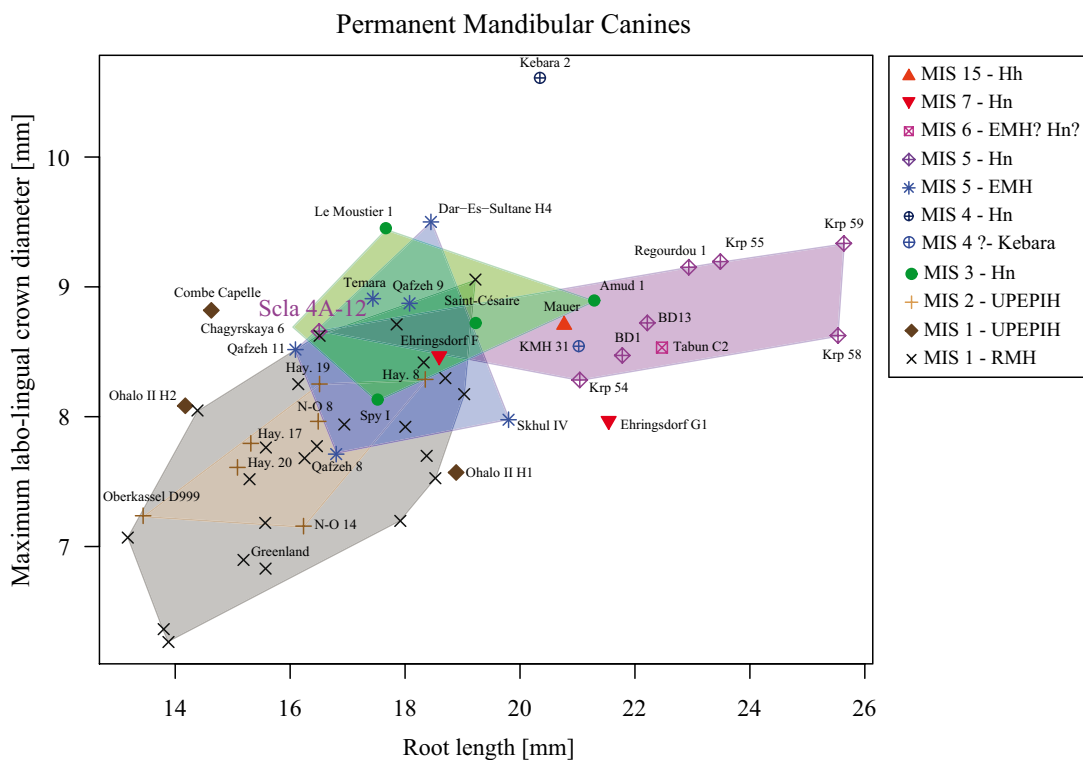


Figure 11: Scla 4A-12 in the broader context of permanent mandibular canines. Same possible gradient in size and chronological trend as in Figure 9.

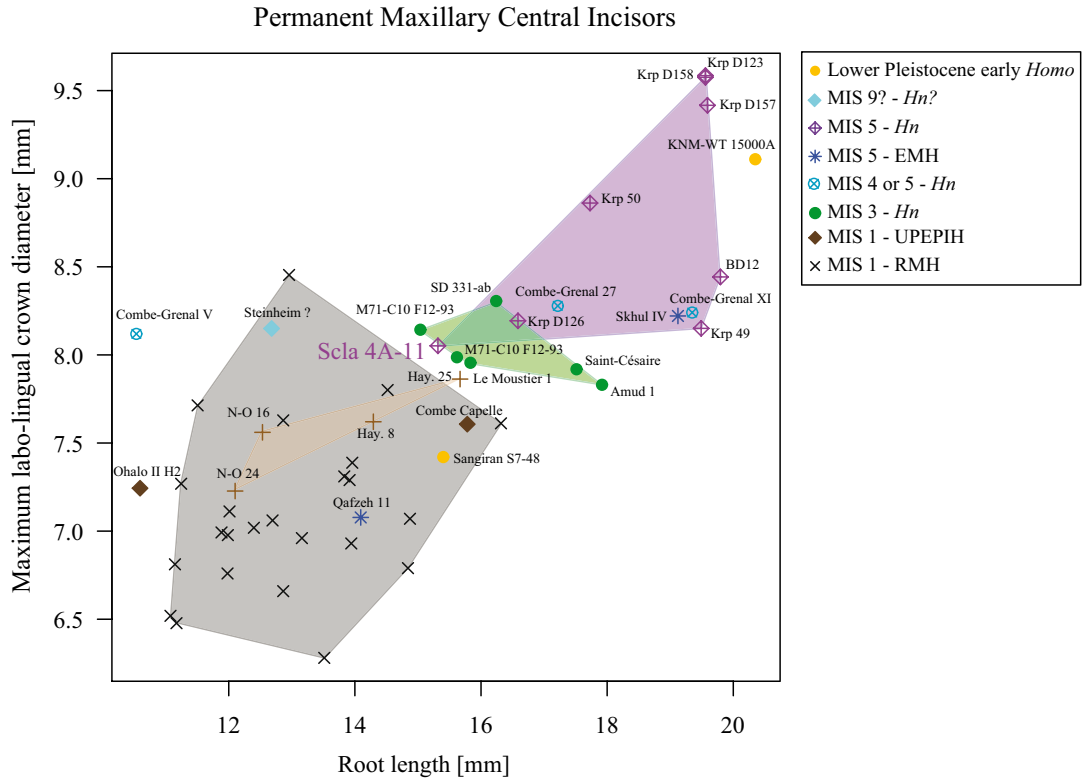


Figure 12: Scla 4A-11 in the broader context of permanent maxillary central incisors. Same possible gradient in size and chronological trend as in Figure 9.

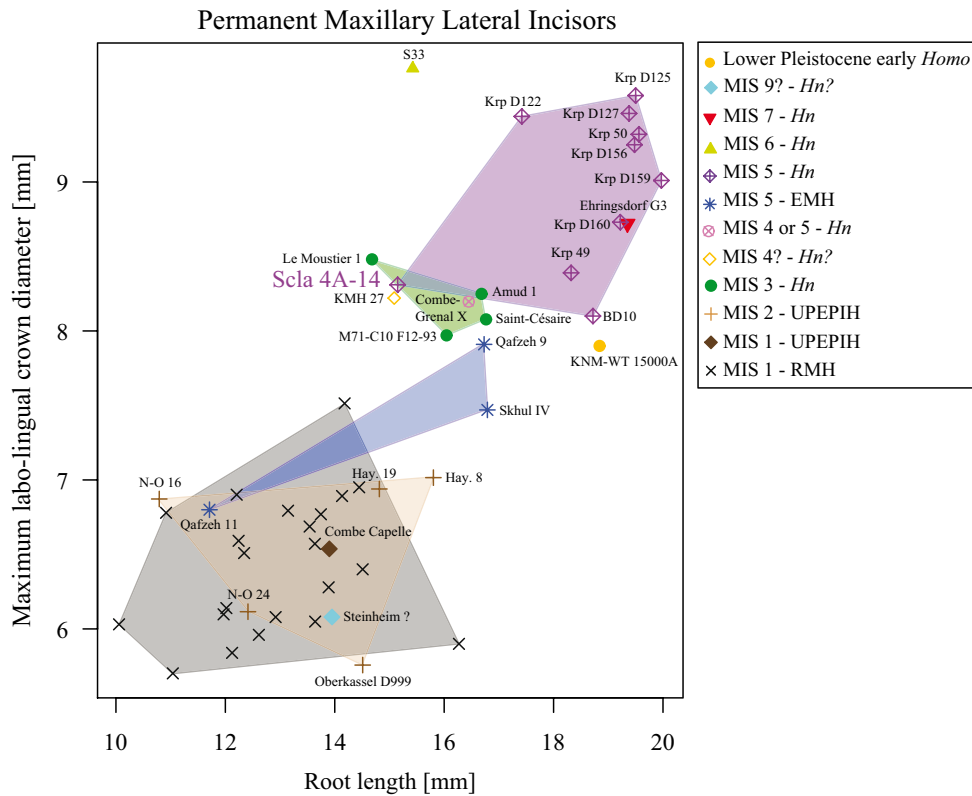


Figure 13: Scla 4A-14 in the broader context of permanent maxillary lateral incisors. Same possible gradient in size and chronological trend as in Figure 9.



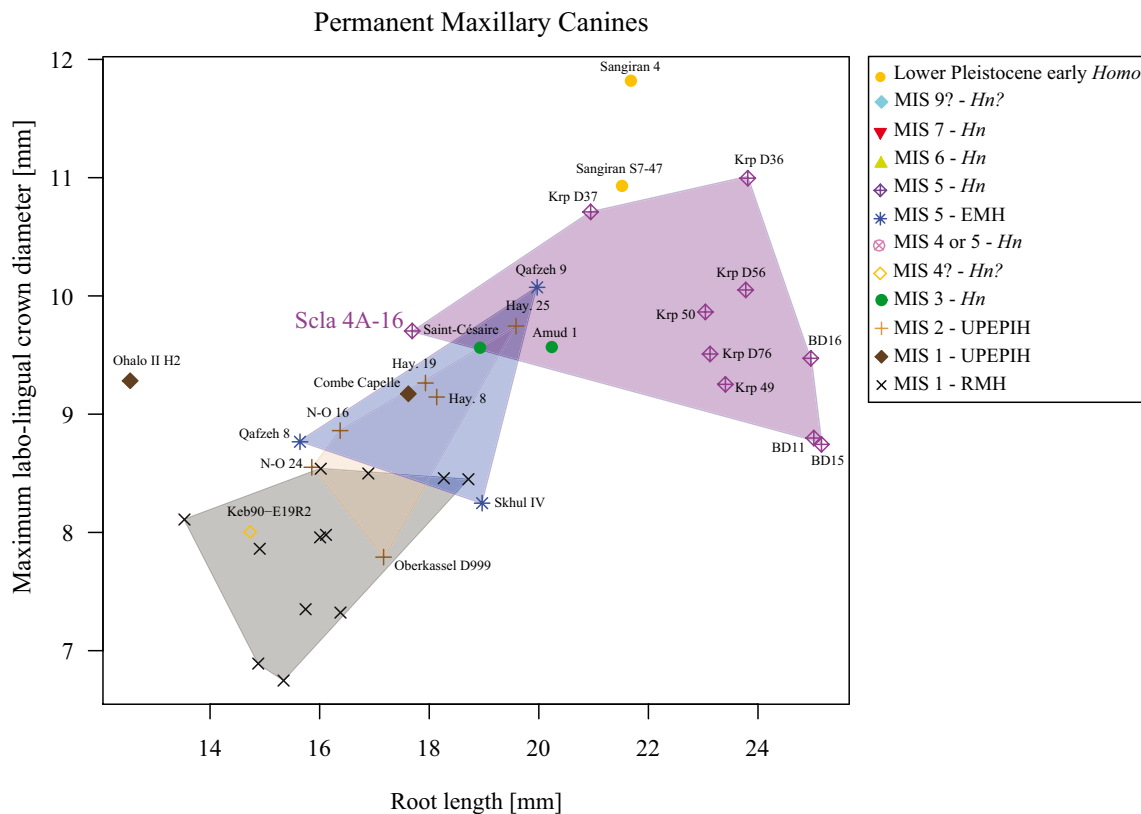


Figure 14: Scla 4A-16 in the broader context of permanent maxillary canines. Same possible gradient in size and chronological trend as in Figure 9.

see Figure 6 and supplementary information Figure 1 in LE CABEC et al., 2013). This later result can be easily explained, since most of the classification is driven by size, the smaller Neandertals will have a higher probability to be classified as EMH. LE CABEC et al. (2013) have demonstrated that long roots in Neandertals likely result from the retention of an ancestral condition. The EMH are not yet as specialized as the Recent Modern Humans, whence their overlapping position between Neandertals and extant humans. As pointed out earlier with Sima de las Palomas and, here with Scladina, Neandertals have a broader variability in root dimensions than previously thought, although they remain overall significantly larger than extant humans. The shape of the anterior roots of the Scladina Juvenile (see Figure 2, after LE CABEC et al., 2013, see this publication for details) are typically Neandertal, involving a supero-inferior labial convexity of the root surfaces.

The lack of any degree of taurodontism in the mandibular first molars of Scladina could be taxonomically misleading (Figure 15). KUPCZIK

& HUBLIN (2010) provide a larger comparative context for the M₁. The root pulp volume of the Scladina M₁ falls within the lower half of the Neandertal descriptive statistics reported (mean ± standard deviation). Regarding root length, surface and volume, the Scladina M₁ falls below the distribution reported, but should be equal or close to the minimal values. All the Scladina M₁ root dimensions fall within the Recent Modern Human variation described by KUPCZIK & HUBLIN (2010).

To summarize, our results highlight the very small root dimensions of the Scladina Juvenile. Krapina shows a large intra-population variability and has the largest dental dimensions. Specimens from Abri Bourgeois-Delaunay fall in the Krapina variability and also exceed Scladina in root dimensions. The same is true for the Regourdou 1 specimen which has relatively small teeth. In addition, the relatively small teeth of Regourdou 1 and the short roots of Scladina go against the assumption that Krapina can reliably be taken as representative of the dental variation of MIS 5 Neandertals.

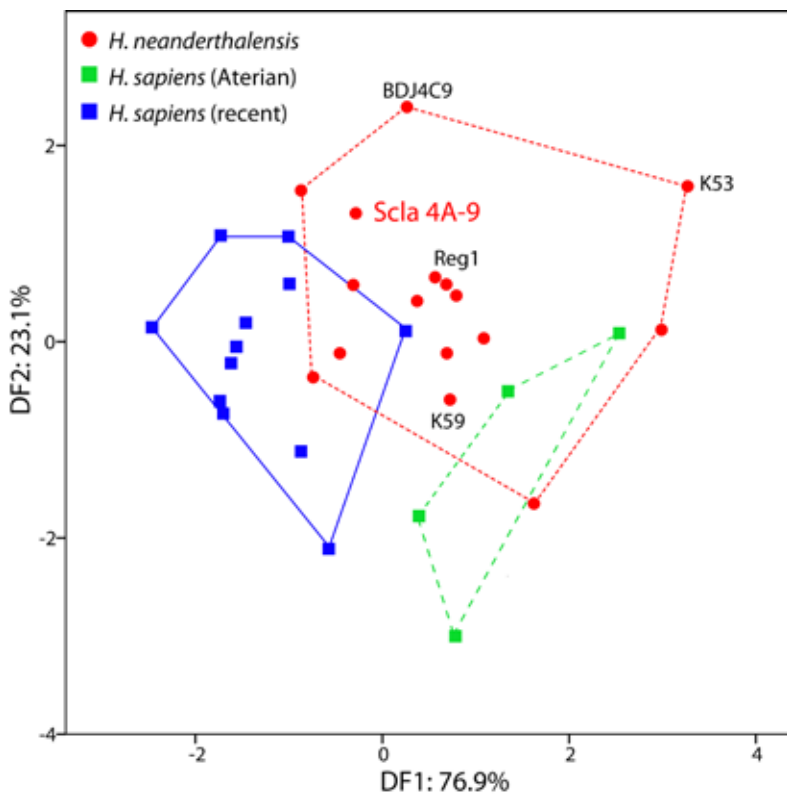


Figure 15: Molar root morphology and taurodontism. Plot of the first two principal components calculated from the covariance matrix of five linearised root variables (root length, cervical plane area, pulp volume, root stem volume, root apex volume) in the first mandibular molar (modified after KUPCZIK & HUBLIN, 2010).

5. Conclusion

Using micro-computed tomography, the present study documents the external and cross-sectional root morphology in all teeth of the Scladina Child. Moreover, we compare the Scladina crown and root, external and internal dimensions, to a sample of MIS 5 Neandertal teeth from central Europe (Krapina) and southwestern France (Bourgeois-Delaunay and Regourdou 1). While the crown and root dimensions of Bourgeois-Delaunay and Regourdou 1 are well within the range of the Krapina sample, the teeth of the Scladina Juvenile have relatively short tooth roots with large pulp cavities. These differences in root form among MIS 5 Neandertals may be due to geographic variability, sexual dimorphism, individual variability in dental development, and age modifications of the dental tissues. Furthermore, our results suggest that taxonomical diagnosis based on root metrics alone has to be considered carefully, as shown by the outlier short-rooted Scladina.

Acknowledgements

We would like to thank Dominique Bonjean, archeologist in charge of the excavations at the

Scladina Cave and his team; the curators in charge of the fossil material: Jean-François Tournepicche (*Musée d'Angoulême*, France), Véronique Merlin-Anglade (*Musée d'Art et Archéologie de la ville de Périgueux*) and Jakov Radović (*Croatian Natural History Museum*, Zagreb); Andreas Winzer, Heiko Temming, Matthew Skinner, Robin Feeney and Tanya Smith for micro-CT scanning expertise; Rico Tilgner for advice and expertise in image processing and software expertise; Philipp Gunz for discussion and advice in statistical analyses; Matthew Skinner for constructive comments on an earlier version of this manuscript; the staff of the ID 17 beamline at the ESRF (Grenoble, France) and NESPOS for the data of BDJ4C9.

References

- ALVESALO L., TAMMISALO E. & TOWNSEND G., 1991. Upper central incisor and canine tooth crown size in 47,XXY males. *Journal of Dental Research*, 70: 1057–1060.
- BAILEY S. E., 2005. Diagnostic dental differences between Neandertals and Upper Paleolithic modern humans: getting to the root of the matter. In E. ZADZINSKA (ed.), *Current trends in dental morphology research*. Łódź (Poland), Univeristy of Łódź Press: 201–210.



- BAILEY S. E. & HUBLIN J.-J., 2006. Dental remains from the Grotte du Renne at Arcy-sur-Cure (Yonne). *Journal of Human Evolution*, 50: 485-508.
- BARRETT M. J., 1977. Masticatory and non-masticatory uses of teeth. In R. V. S. WRIGHT (ed.), *Stone tools as cultural markers: change, evolution and complexity*, Canberra, Institute of Aboriginal Studies, Humanities Press Incorporated: 18-23.
- BAYLE P., BRAGA J., MAZURIER A. & MACCHIARELLI R., 2009^a. Brief communication: High-resolution assessment of the dental developmental pattern and characterization of tooth tissue proportions in the late upper paleolithic child from La Madeleine, France. *American Journal of Physical Anthropology*, 138: 493-498.
- BAYLE P., BRAGA J., MAZURIER A. & MACCHIARELLI R., 2009^b. Dental developmental pattern of the Neandertal child from Roc de Marsal: a high-resolution 3D analysis. *Journal of Human Evolution*, 56: 66-75.
- BERMÚDEZ DE CASTRO J. M., DURAND A. I. & IPIÑA S. L., 1993. Sexual dimorphism in the human dental sample from the SH site (Sierra de Atapuerca, Spain): a statistical approach. *Journal of Human Evolution*, 24: 43-56.
- BERRY D. C. & POOLE D. F., 1976. Attrition: possible mechanisms of compensation. *Journal of Oral Rehabilitation*, 3: 201-206.
- BRACE C. L., 1979. Krapina, "Classic" Neandertals, and the evolution of the European face. *Journal of Human Evolution*, 8: 527-550.
- BRÄUER G. O., 1988. Osteometrie. In R. MARTIN & R. KNUSSMANN (eds.), *Anthropologie: Handbuch der Vergleichenden Biologie Des Menschen. Band 1: Wesen und Methoden der Anthropologie. Teil 1: Wissenschaftstheorie, Geschichte, Morphologische Methoden*. Stuttgart, Gustav Fischer: 160-232.
- BROESTE K., FISCHER-MOLLER K. & PEDERSEN P. O., 1944. The medieval Norsemen at Gardar. *Meddelelser om Grønland*. Copenhagen, C. A. Reitzel: 40-62.
- BROSE D. S. & WOLPOFF M. H., 1971. Early Upper Paleolithic Man and Late Middle Paleolithic Tools. *American Journal of Physical Anthropology*, 73: 1156-1194.
- BRUNET M., GUY F., PILBEAM D., MACKAYE H. T., LIKIUS A., AHOUNTA D., BEAUVILAIN A., BLONDEL C., BOCHERENS H., BOISSERIE J.-R., DE BONIS L., COPPENS Y., DEJAX J., DENYS C., DURINGER P., EISENMANN V., FANONE G., FRONTY P., GERAADS D., LEHMANN T., LIHOREAU F., LOUCHART A., MAHAMAT A., MERCERON G., MOUCHELIN G., OTERO O., CAMPOMANES P. P., DE LEON M. P., RAGE J.-C., SAPANET M., SCHUSTER M., SUDRE J., TASSY P., VALENTIN X., VIGNAUD P., VIRIOT L., ZAZZO A. & ZOLLIKOFER C., 2002. A new hominid from the Upper Miocene of Chad, Central Africa. *Nature*, 418: 145-151.
- CONDEMI S., 1992. *Les hommes fossiles de Saccopastore et leurs relations phylogénétiques*. Paris, Éditions du Centre national de la recherche scientifique, Cahiers de Paléanthropologie, 174 p.
- CONDEMI S., 2001. Les Dents. In S. CONDEMI (ed.), *Les Néandertaliens de La Chaise (Abri Bourgeois-Delaunay)*. Paris, Editions du Comité des travaux historiques et scientifiques, Collection Documents préhistoriques, 15: 107-134.
- CORDY J.-M., 1984. Évolution des faunes quaternaires en Belgique. In D. CAHEN & P. HAESAERTS (eds.), *Peuples chasseurs de la Belgique préhistorique dans leur cadre naturel*. Bruxelles, Patrimoine de l'Institut royal des Sciences naturelles de Belgique: 67-77.
- CORDY J.-M., 1988. Apport de la paléozoologie à la paléoécologie et à la chronostratigraphie en Europe du Nord-occidental. In H. LAVILLE (ed.), *L'Homme de Néandertal, vol. 2: L'Environnement*. Études et Recherches Archéologiques de l'Université de Liège, 29: 55-64.
- DEAN D., HUBLIN J.-J., HOLLOWAY R. & ZIEGLER R., 1998. On the phylogenetic position of the pre-Neandertal specimen from Reilingen, Germany. *Journal of Human Evolution*, 34: 485-508.
- DEBÉNATH A., 1977. The latest finds of Antewürmian human remains in Charente (France). *Journal of Human Evolution*, 6: 297-302.
- EMONET E.-G., TAFFOREAU P. T., CHAIMANEE Y., GUY F., DE BONIS L., KOUFOS G. & JAEGER J.-J., 2012. Three-dimensional analysis of mandibular dental root morphology in hominoids. *Journal of Human Evolution*, 62: 146-154.
- FOX C. L. & FRAYER D. W., 1997. Non-dietary Marks in the Anterior Dentition of the Krapina Neandertals. *International Journal of Osteoarchaeology*, 7: 133-149.
- GARN S. M., COLE P. E. & VAN ALSTINE W. L., 1979. Sex discriminatory effectiveness using combinations of root lengths and crown diameters.

- American Journal of Physical Anthropology*, 50: 115–117.
- GARN S. M., VAN ALSTINE W. L. JR & COLE P. E., 1978^a. Root-length and crown-size correlations in the mandible. *Journal of Dental Research*, 57: 114.
- GARN S. M., VAN ALSTINE W. L. JR & COLE P. E., 1978^b. Relationship between root lengths and crown diameters of corresponding teeth. *Journal of Dental Research*, 57: 636.
- GARN S. M., VAN ALSTINE W. L. JR & COLE P. E., 1978^c. Intraindividual root-length correlations. *Journal of Dental Research*, 57: 270.
- GENET-VARCIN E., 1975^a. Étude de dents humaines isolées provenant des grottes de la Chaise de Vouthon (Charente) (Incisives Supérieures). *Bulletins et Memoires de la Société d'Anthropologie de Paris*, 2: 129–141.
- GENET-VARCIN E., 1975^b. Études de dents humaines isolées provenant des grottes de la Chaise Vouthon (Charente) (Canines Supérieures). *Bulletins et Mémoires de la Société d'Anthropologie de Paris*, 2: 277–286.
- GUATELLI-STEINBERG D., REID D. J., BISHOP T. A. & LARSEN C. S., 2005. Anterior tooth growth periods in Neandertals were comparable to those of modern humans. *Proceedings of the National Academy of Sciences of the United States of America*, 102, 40: 14197–14202.
- GUSTAFSON G., 1950. Age determination on teeth. *Journal of the American Dental Association*, 41: 45–54.
- HAESAERTS P., 1984. Le Quaternaire: problèmes, méthodologie et cadre stratigraphique. In D. CAHEN & P. HAESAERTS (eds.), *Peuples chasseurs de la Belgique préhistorique dans leur cadre naturel*, Bruxelles, Patrimoine de l'Institut royal des Sciences naturelles de Belgique: 17–25.
- HARVATI K., HUBLIN J.-J. & GUNZ P., 2010. Evolution of middle-late Pleistocene human cranio-facial form: A 3-D approach. *Journal of Human Evolution*, 59: 445–464.
- HILLSON S., 1996. *Dental Anthropology*. Cambridge University Press, 373 p.
- HUBLIN J.-J., 1998. Climatic changes, Paleogeography, and the evolution of the Neandertals. In T. AKAZAWA, K. AOKI & O. BAR-YOSEF (eds.), *Neandertals and Modern Humans in Western Asia*. New York, Plenum Press: 295–310.
- JAKOBSSON R. & LIND V., 1973. Variation in root length of the permanent maxillary central incisor. *Scandinavian Journal of Dental Research*, 81: 335–338.
- KOVACS I., 1967. Contribution to the Ontogenetic Morphology of Roots of Human Teeth. *Journal of Dental Research*, 46: 865–874.
- KUPCZIK K., 2003. *Tooth root morphology in primates and carnivores*. PhD thesis, University College London, 307 p.
- KUPCZIK K. & DEAN M. C., 2008. Comparative observations on the tooth root morphology of *Gigantopithecus blacki*. *Journal of Human Evolution*, 54: 196–204.
- KUPCZIK K. & HUBLIN J.-J., 2010. Mandibular molar root morphology in Neandertals and Late Pleistocene and recent *Homo sapiens*. *Journal of Human Evolution*, 59: 525–541.
- KUPCZIK K., OLEJNICZAK A. J., SKINNER M. M. & HUBLIN J.-J., 2009. Molar crown and root size relationship in anthropoid primates. *Front Oral Biology*, 13: 16–22.
- KUTTLER Y., 1959. Classification of dentine into primary, secondary, and tertiary. *Oral Surgery, Oral Medicine, Oral Pathology*, 12: 996–1001.
- LÄHDESMÄKI R., 2006. *Sex chromosomes in human tooth root growth Department of Oral Development and Orthodontics*. University of Oulu, Finland, 65 p.
- LÄHDESMÄKI R. & ALVESALO L., 2007. Root lengths in the permanent teeth of Klinefelter (47,XXY) men. *Archives of Oral Biology*, 52: 822–827.
- LE CABEC A., GUNZ P., KUPCZIK K., BRAGA J. & HUBLIN J.-J., 2013. Anterior Tooth Root Morphology and Size in Neandertals: Taxonomic and Functional Implications. *Journal of Human Evolution*, 64: 169–193.
- LEE S., 2006. Patterns of Dental Sexual Dimorphism in Krapina and Predmosti: A New Approach. *Periodicum Biologorum*, 108: 417–424.
- MACCHIARELLI R., BONDIOLI L., DEBÉNATH A., MAZURIER A., TOURNEPICHE J.-F., BIRCH W. & DEAN M. C., 2006. How Neandertal molar teeth grew. *Nature*, 444: 748–751.
- MANN A. & VANDERMEERSCH B., 1997. An adolescent female Neandertal mandible from Montgaudier Cave, Charente, France. *American Journal of Physical Anthropology*, 103: 507–527.



- MAUREILLE B., ROUGIER H., HOUËT F. & VANDERMEERSCH B., 2001. Les dents inférieures du Néandertalien Regourdou 1 (site de Regourdou, commune de Montignac, Dordogne): Analyses métriques et comparatives. *Paléo*, 13: 183-200.
- MAUREILLE B. & TILLIER A.-M., 2008. Répartition géographique et chronologique des sépultures néandertaliennes. In B. VANDERMEERSCH (ed.), *Première humanité. Gestes funéraires des néandertaliens*. Paris, Éditions de la Réunion des musées nationaux: 67-74.
- OLEJNICZAK A. J., SMITH T. M., FEENEY R. N. M., MACCHIARELLI R., MAZURIER A., BONDIOLI L., ROSAS A., FORTEA J., DE LA RASILLA M., GARCIA-TABERNEIRO A., RADOVČIĆ J., SKINNER M. M., TOUSSAINT M. & HUBLIN J.-J., 2008. Dental tissue proportions and enamel thickness in Neandertal and modern human molars. *Journal of Human Evolution*, 55: 12-23.
- OZAKI T., SATAKE T. & KANAZAWA E., 1988. Morphological significance of root length variability in comparison with other crown dimensions. II – Correlation between crown and root measurements. *Journal of Nihon University School of Dentistry*, 30: 11-21.
- PAEWINSKY E., PFEIFFER H. & BRINKMANN B., 2005. Quantification of secondary dentine formation from orthopantomograms – A contribution to forensic age estimation methods in adults. *International Journal of Legal Medicine*, 119: 27-30.
- PAQUETTE S. P., 1985. *Patterns of Variation in the Permanent Maxillary Anterior Tooth Roots: A Different Approach to the Problem of Anterior Dental Reduction During the Transition from Archaic to Modern Homo sapiens*. University of Tennessee, Knoxville, 133 p.
- PEDERSEN P. O., 1949. *The East Greenland Eskimo dentition. Numerical Variations and Anatomy. A Contribution to Comparative Ethnic Odontology*. Copenhagen, Meddelelser om Grønland, 142, 3, 256 p.
- PHILIPPAS G. G., 1961. Influence of Occlusal Wear and Age on Formation of Dentin and Size of Pulp Chamber. *Journal of Dental Research*, 40: 1186-1198.
- PHILIPPAS G. G. & APPLEBAUM E., 1967. Age Changes in the Permanent Upper Lateral Incisor. *Journal of Dental Research*, 46: 1002-1009.
- PIRSON S., BONJEAN D., DI MODICA K. & TOUSSAINT M., 2005. Révision des couches 4 de la grotte Scladina (comm. d'Andenne, prov. de Namur) et implications pour les restes néandertaliens : premier bilan. *Notae Praehistoricae*, 25: 61-69.
- PIRSON S., COURT-PICON M., HAESAERTS P., BONJEAN D. & DAMBLON F., 2008. New data on geology, anthracology and palynology from the Scladina Cave pleistocene sequence: preliminary results. In F. DAMBLON, S. PIRSON & P. GERRIENNE (eds.), *Hautrage (Lower Cretaceous) and Sclayn (Upper Pleistocene). Field Trip Guidebook. Charcoal and microcharcoal: continental and marine records*. IVth International Meeting of Anthracology, Brussels, Royal Belgian Institute of Natural Sciences, 8-13 September 2008. Brussels, Royal Belgian Institute of Natural Sciences, Memoirs of the Geological Survey of Belgium, 55: 71-93.
- PIRSON S. & DI MODICA K., 2011. Position chronostratigraphique des productions lithiques du Paléolithique ancien en Belgique : état de la question. In M. TOUSSAINT, K. DI MODICA & S. PIRSON (sc. dir.), *Le Paléolithique moyen en Belgique. Mélanges Marguerite Ulrix-Closset*. Bulletin de la Société royale belge d'Études Géologiques et Archéologiques *Les Chercheurs de la Wallonie*, hors-série, 4 & Études et Recherches Archéologiques de l'Université de Liège, 128: 105-148.
- PIRSON S., DRAILY C., BOVY B., CORNET Y., COURT-PICON M., DAMBLON F., DEBENHAM N., DEMOULIN A., DE WILDE B., HAESAERTS P., JUVIGNÉ É., LA GRAPPE P., PARFITT A., PIROUELLE F., RENSON V., STEWART J. R., UDRESCU M., VAN NEER W., WOUTERS W. & TOUSSAINT M., 2011. Contexte chronostratigraphique et paléoenvironnemental de la séquence de la grotte Walou : synthèse et perspectives. In C. DRAILY, S. PIRSON & M. TOUSSAINT (dir.), *La grotte Walou à Trooz (Belgique). Fouilles de 1996 à 2004, vol. 2 : Les sciences de la vie et les datations*. Namur, Service public de Wallonie, IPW, Études et documents, Archéologie, 21: 214-233.
- RAMIREZ ROZZI F. V. & BERMÚDEZ DE CASTRO J. M., 2004. Surprisingly rapid growth in Neandertals. *Nature*, 428: 936-939.
- R DEVELOPMENT CORE TEAM, 2012. R: A Language and Environment for Statistical Computing. R 2.15.0 ed. R Foundation for Statistical Computing, Vienna, Austria.

- RINK W. J., SCHWARCZ H. P., SMITH F. H. & RADOVČIĆ J., 1995. ESR dates for Krapina hominids. *Nature*, 378: 150.
- ROUGIER H., CREVECOEUR I., SEMAL P. & TOUSSAINT M., 2009. Des Néandertaliens dans la troisième caverne de Goyet. In K. DI MODICA & C. JUNGELS (dir.), *Paléolithique moyen en Wallonie. La collection Louis Éloy*. Bruxelles, Collections du Patrimoine culturel de la Communauté française, 2: 173.
- SCHWARTZ G. T. & DEAN M. C., 2005. Sexual dimorphism in modern human permanent teeth. *American Journal of Physical Anthropology*, 128: 312-317.
- SCHWARTZ J. H. & TATTERSALL I., 2006. Morphology, Variability, and Systematics: Lessons from Krapina. *Periodicum Biologorum*, 108: 389-401.
- SEMAL P., ROUGIER H., CREVECOEUR I., JUNGELS C., FLAS D., HAUZEUR A., MAUREILLE B., GERMONPRÉ M., BOCHERENS H., PIRSON S., CAMMAERT L., DE CLERCK N., HAMBÜCKEN A., HIGHAM T. F. G., TOUSSAINT M. & VAN DER PLICHT J., 2009. New Data on the Late Neandertals: Direct Dating of the Belgian Spy Fossils. *American Journal of Physical Anthropology*, 138: 421-428.
- SICHER H. & DUBRUL E. L., 1970 (5th ed.). *Oral anatomy*, St. Louis, Courtesy of C.V. Mosby, 502 p.
- SMITH F. H., 1976^a. *The Neandertal remains from Krapina: a descriptive and comparative study*. Knoxville, University of Tennessee, Report of Investigations, 15, 359 p.
- SMITH F. H., 1976^b. On Anterior Tooth Wear at Krapina and Ochoz. *Current Anthropology*, 17: 167-168.
- SMITH F. H., 1983. Behavioral interpretation of changes in craniofacial morphology across the archaic/modern *Homo sapiens* transition. In E. TRINKAUS (ed.), *The Mousterian Legacy: Human Biocultural Change in the Upper Pleistocene*. Oxford, British Archaeological Reports, International Series, 164: 141-163.
- SMITH F. H. & PAQUETTE S. P., 1989. The adaptive basis of Neandertal facial form, with some thoughts on the nature of modern human origins. In E. TRINKAUS (ed.), *The emergence of modern humans*. Cambridge University Press: 181-210.
- SMITH P., WAX Y. & ADLER F., 1989. Population variation in tooth, jaw, and root size: A radiographic study of two populations in a high-attrition environment. *American Journal of Physical Anthropology*, 79: 197-206.
- SMITH P., WAX Y., ADLER F., SILBERMAN U. & HEINIC G., 1986. Post-pleistocene changes in tooth root and jaw relationships. *American Journal of Physical Anthropology*, 70: 339-348.
- SMITH T. M., 2008. Incremental dental development: Methods and applications in hominoid evolutionary studies. *Journal of Human Evolution*, 54: 205-224.
- SMITH T. M., TAFFOREAU P. T., REID D. J., POUECH J., LAZZARI V., ZERMENO J. P., GUATELLI-STEINBERG D., OLEJNICZAK A. J., HOFFMAN A., RADOVČIĆ J., MAKAREMI M., TOUSSAINT M., STRINGER C. B. & HUBLIN J.-J., 2010. Dental evidence for ontogenetic differences between modern humans and Neandertals. *Proceedings of the National Academy of Sciences of the United States of America*, 107, 49: 20923-20928.
- SMITH T. M., TOUSSAINT M., REID D. J., OLEJNICZAK A. J. & HUBLIN J.-J., 2007. Rapid dental development in a Middle Paleolithic Belgian Neandertal. *Proceedings of the National Academy of Sciences of the United States of America*, 104, 51: 20220-20225.
- SPENCER M. A., 2003. Tooth-root form and function in platyrrhine seed-eaters. *American Journal of Physical Anthropology*, 122: 325-335.
- STRINGER C. B., 1982. Towards a solution to the Neandertal problem. *Journal of Human Evolution*, 11: 431-438.
- TOUSSAINT M., 2011. Une prémolaire néandertalienne dans la couche CI-8 (anciennement C sup et C8) de la grotte Walou. In C. DRAILY, S. PIRSON & M. TOUSSAINT (dir.), *La grotte Walou à Trooz (Belgique). Fouilles de 1996 à 2004, vol. 2: Les sciences de la vie et les datations*. Namur, Service public de Wallonie, IPW, Études et documents, Archéologie, 21: 148-163.
- TOUSSAINT M., OLEJNICZAK A. J., EL ZAATARI S., CATTELAÏN P., FLAS D., LETOURNEUX C. & PIRSON S., 2010. The Neandertal lower right deciduous second molar from Trou de l'Abîme at Couvin, Belgium. *Journal of Human Evolution*, 58: 56-67.



- TOUSSAINT M., OTTE M., BONJEAN D., BOCHERENS H., FALGUÈRES C. & YOKOYAMA Y., 1998. Les restes humains néandertaliens immatures de la couche 4A de la grotte Scladina (Andenne, Belgique). *Comptes rendus de l'Académie des Sciences de Paris, Sciences de la terre et des planètes*, 326: 737-742.
- TOUSSAINT M., PIRSON S. & BOCHERENS H., 2001. Neandertals from Belgium. *Anthropologica et Praehistorica*, 112: 21-38.
- TURQ A., JAUBERT J., MAUREILLE B. & LAVILLE D., 2008. Le cas des sépultures néandertaliennes sur Sud-Ouest: et si on les vieillissait ? In B. VANDERMEERSCH, J.-J. CLEYET-MERLE, J. JAUBERT, B. MAUREILLE & A. TURQ (eds.), *Première humanité, gestes funéraires des Néandertaliens*. Catalogue d'exposition, Musée National de Préhistoire, Les Eyzies-de-Tayac. Paris, Réunion des Musées Nationaux: 40-41.
- VANDERMEERSCH B., CLEYET-MERLE J.-J., JAUBERT J., MAUREILLE B. & TURQ A., 2008. *Première humanité. Gestes funéraires des néandertaliens*. Paris, Éditions de la Réunion des musées nationaux, 143 p.
- VAN PEER P., 2001. A Status Report on the Lower and Middle Palaeolithic of Belgium. *Anthropologica et Praehistorica*, 112: 11-19.
- WALKER M. J., GIBERT J., LOPEZ M. V., LOMBARDI A. V., PÉREZ-PÉREZ A., ZAPATA J., ORTEGA J., HIGHAM T. F. G., PIKE A., SCHWENNINGER J.-L., ZILHÃO J. & TRINKAUS E., 2008. Late Neandertals in Southeastern Iberia: Sima de las Palomas del Cabezo Gordo, Murcia, Spain. *Proceedings of the National Academy of Sciences of the United States of America*, 105, 52: 20631-20636.
- WOLPOFF M. H., 1979. The Krapina dental remains. *American Journal of Physical Anthropology*, 50: 67-113.
- WOLPOFF M. H., 1999. *Paleoanthropology*. McGraw-Hill Humanities, Social Sciences & World Languages.
- WOOD B. A., ABBOTT S. A. & UYTTERSCHAUT H., 1988. Analysis of the dental morphology of Plio-Pleistocene hominids. IV. Mandibular postcanine root morphology. *Journal of Anatomy*, 156: 107-139.
- WOODS M. A., ROBINSON Q. C. & HARRIS E. F., 1990. Age-Progressive Changes in Pulp Widths and Root Lengths During Adulthood: A Study of American Blacks and Whites. *Gerodontology*, 9: 41-50.
- ZILBERMAN U. & SMITH P., 2001. Sex- and Age-related Differences in Primary and Secondary Dentin Formation. *Advances in Dental Research*, 15: 42-45.

Hervé BOCHERENS

*Michel Toussaint & Dominique Bonjean (eds.), 2014.
The Scladina I-4A Juvenile Neandertal (Andenne, Belgium),
Palaeoanthropology and Context
Études et Recherches Archéologiques de l'Université de Liège, 134: 351-362.*

1. Introduction

Reconstruction of the habitat and diet of fossil hominids is essential to understand their evolution. In prehistoric sites, zooarchaeological analysis of faunal remains yields information about possible prey species and how they were acquired and processed. In the case of the Neandertal child found in former Layer 4A from Scladina Cave, this approach is not really helpful since the hominid bones are found without an archaeological context. In such a case, retrieving palaeoenvironmental and palaeodietary information directly from the skeletal remains of the Neandertal is almost the only way to proceed. Such approaches are used since a few decades, particularly the isotopic tracking of diet in fossil mammals.

Carbon and nitrogen atoms present in the skeletal tissues of a vertebrate are ultimately derived from the food intake and their isotopic signature is linked to that of the diet consumed during their synthesis. When a biogenic fraction can be purified from fossilized skeletal tissues, this fraction contains invaluable palaeobiological information about extinct organisms. In the case of a fossilized Neandertal skull and the faunal elements associated, it is possible to reconstruct some characteristics of the environment around the site at the time of life of this individual, and to replace this individual within his trophic system. A first article was published ten years ago on the first isotopic results obtained on the fossil material from former Layer 4 of Scladina Cave, and this led to some palaeodietary reconstruction of the Neandertal specimen (BOCHERENS et al., 1999). Since then, new reference work on isotopic tracking in terrestrial ecosystems allows more detailed reconstructions (e.g. DRUCKER et al., 2008, DRUCKER & BOCHERENS, 2009). In addition, a reappraisal of the stratigraphy of Scladina Cave permits the consideration of more faunal elements than previously thought in the comparative analysis (e.g. PIRSON et al., 2005). Finally, new isotopic

data, especially on the mineral fraction of tooth enamel, provides additional insight on the palaeoecology of some species that lived at the time of the Neandertal child (this work).

Principles of isotopic tracking of Pleistocene terrestrial palaeoecosystems in Europe with fossil mammal bone and tooth: collagen, and bioapatite

Bones and teeth are composed of both organic and mineral fractions, which are synthesized during the lifetime of a vertebrate. The organic fraction of bone and dentine is mainly formed of a protein, collagen, which contains carbon (around 40%) and nitrogen (around 15%), while the mineral fraction, a calcium phosphate (apatite) with many impurities, includes 3 to 5% carbonate. The crystal size of apatite is much larger in enamel than in bone and dentine, making these last two tissues more prone to diagenetic alteration. The isotopic signatures of nitrogen are measured in the organic fraction (collagen), while the isotopic signatures of carbon can be measured in the organic (collagen) and the mineral (carbonate) phases.

All the carbon of an organism comes from its dietary intake, in the form of proteins, carbohydrates and lipids. Some of these nutrients are incorporated directly by the organism and sequestered in different tissues, while other molecules are synthesized by the organism from dietary nutrients. Due to these different biochemical characteristics and isotopic fractionations, the average carbon isotopic abundance of a vertebrate is close to that of its average diet, but those recorded in a given tissue or molecule exhibit specific differences (e.g., DENIRO & EPSTEIN, 1978, 1981; HOBSON et al., 1996). The $\delta^{13}\text{C}$ values of collagen are typically 5‰ more positive than those of the average diet, while the $\delta^{13}\text{C}$ values of the carbonate fraction of bone



and tooth mineral fraction is 9 to 14‰ more positive than that of the average diet (e.g., LEE-THORP et al., 1989; CERLING & HARRIS, 1999; BOCHERENS & MARIOTTI, 2002). Therefore, the $\delta^{13}\text{C}$ values of collagen and carbonate apatite are typically used to track the type of plant food consumed by herbivores and the type of plants at the base of the food web to which predators belong.

The carbon isotopic abundances discriminate between different types of plants, principally between marine and terrestrial plants. Terrestrial plants in cold and temperate climates use the same photosynthetic pathway ('C₃-plants') (EHLERINGER et al., 1997). In such environments, an isotopic distinction can be seen between plants growing under a closed canopy and those at the top of the canopy or growing in an open environment (e.g., reviews in BROADMEADOW & GRIFFITHS, 1993; HEATON, 1999). Since herbivore teeth and bones record the carbon isotopic abundances of their plant food, it is possible to identify which kind of plant was consumed by an herbivore, and therefore to determine in which type of environment it lived (e.g., BOCHERENS et al., 2005^a; DRUCKER, 2007; DRUCKER et al., 2008; DRUCKER & BOCHERENS, 2009).

Nitrogen is incorporated through dietary intake in the organic molecules of an organism's tissues. Contrary to carbon, the isotopic signature of nitrogen is significantly enriched in vertebrate tissues relatively to its average diet, typically by 3 to 5‰ (review in BOCHERENS & MARIOTTI, 2002). Therefore, the nitrogen isotopic signature of a given individual depends on the isotopic signature at the base of the foodweb to which it belongs (i.e. in the plants), and on the position of the specimen within the foodweb (herbivore or predator).

3. Material

The material of this analysis is mainly from the first excavations (1981–1990) at Scladina Cave, long before the important stratigraphic revision (2007). At the time, the research was concerned with approximately the first 20 m of the cave and the stratigraphy seemed much more simple, with a single 'Layer 4' superimposed over 'Layer 5'. Deeper in the cave, the stratigraphic reappraisal revealed the existence of numerous layers corresponding to the former layers 4 and 5 found at the entrance. Unfortunately, the reattribution of the exhumed material to either one or several layers of the new stratigraphic record

is impossible. In this chapter, the material stated to be from 'former Layer 4' and 'former Layer 5' must be understood as being from sedimentary complexes 4 and 5 (see Chapter 3).

The present study is based on the carbon and nitrogen isotopic analyses previously published for bones and teeth from former Layer 4 in Scladina Cave, including a bone sample from the Neandertal child (BOCHERENS et al., 1999). Since this publication, it has been shown that the stratigraphical origin of the Neandertal is more uncertain than previously believed, since the pieces that could be precisely located in the stratigraphy come from a channel deposit that cuts through former layers 4 and 5 (PIRSON et al., 2005). As an initial position in former Layer 5 cannot be ruled out for the Neandertal individual, 30 faunal specimens from this layer and from the coeval former Layer Vb were also analyzed. This material belongs to horse *Equus caballus*, red deer *Cervus elaphus*, reindeer *Rangifer tarandus*, chamois *Rupicapra rupicapra*, woolly rhinoceros *Coelodonta antiquitatis*, mammoth *Mammuthus primigenius*, cave bear *Ursus spelaeus*, brown bear *Ursus arctos* and wolf *Canis lupus*.

In former layers 5 and Vb, not all the specimens yielded well-preserved collagen. To compensate this lack of isotopic information for some species, some tooth enamel of identified taxa was analyzed for the carbon isotopic signature of the carbonate fraction. Moreover, additional samples from former layers 4 (3 teeth of horse and fallow deer *Dama dama*) and 1A in Scladina (8 teeth of mammoth, woolly rhinoceros, giant deer *Megaloceros giganteus*, and horse), as well as 10 Holocene horse and red deer bone samples from Bercy, a Neolithic site in forested context (Paris, France, around 5000 years BP; BOCHERENS et al., 1997^a & 1997^b), and 6 modern red deer bone samples from Bialowieza forest (Poland) were analyzed using the same method to provide a reference dataset for large herbivores feeding under a closed canopy or in an open environment.

4. Methods

Prior to collagen extraction of fossil bone, an elemental analysis of nitrogen in whole bone powder was performed to screen out samples without collagen preserved (BOCHERENS et al., 2005^b). Samples with more than 0.4% N, i.e. at least one tenth of their original collagen, have been treated for collagen extraction by the

HCl demineralization protocol (BOCHERENS et al., 1997^a). Briefly, around 300 mg of bone powder is decalcified in 1 M HCl for 20 min at room temperature, and filtered through a 5 µm filter. The insoluble residue is soaked in 0.125 N NaOH for 20 hours at room temperature. The rinsed residue is heated in closed tubes at 100°C for 17 h in a 10⁻² M HCl solution, in order to gelatinize the collagen. After filtration through a 5 µm filter, the filtrate containing gelatine is freeze-dried. Yield is expressed as the amount of freeze-dried gelatine relative to the dry weight of bone (in mg.g⁻¹). In most of the cases, the NaOH step was not used, following BOCHERENS et al. (1999), due to excessive loss in collagen, since tests have demonstrated that samples from Scladina Cave could be treated that way without any significant influence on the collagen isotopic compositions (BOCHERENS et al., 1999). Determination of stable carbon and nitrogen isotope ratios was performed on a Carlo-Erba NA1500 CHN-elemental analyzer coupled to an isotopic ratio mass spectrometer (Fisons Optima) at the department of Earth Sciences in University Paris 6 (France), following BOCHERENS et al. (1997^a). During the process, the amounts of C and N were measured. Isotopic abundances measured this way are relative abundances: enrichments or depletions of heavy isotopic varieties (¹³C, ¹⁵N) are expressed *versus* international standards. The isotope ratios are expressed for carbon as δ¹³C *versus* V-PDB (a marine carbonate) and for nitrogen as δ¹⁵N *versus* atmospheric N₂: $\delta X = (R_{\text{sample}}/R_{\text{standard}} - 1) \times 1000$, where X stands for ¹³C or ¹⁵N and R stands for ¹³C/¹²C or ¹⁵N/¹⁴N, respectively. The precision is 0.1‰ for δ¹³C and 0.2‰ for δ¹⁵N.

Some tooth samples were used for carbon isotopic measurement of their enamel carbonate fraction. Enamel was physically separated from dentine and crushed to a fine powder with mortar and pestle. Enamel fragments corresponding to the whole tooth crown were used in order to average possible seasonal variations within the tooth, such as those observed by FRICKE & O'NEIL (1996) and SHARP & CERLING (1998). It was subsequently pre-treated according to BOCHERENS et al. (1991): powdered enamel was soaked in 2-3% NaOCl for 20 hours at 20 °C to oxidize organic residues, rinsed with distilled water, then treated with 1M acetic acid-Ca acetate buffer (pH = 4.75) for 20 hrs at 20 °C to remove exogenous carbonate. Carbon dioxide was produced from the treated powders by dissolution in 100% H₃PO₄ at 50 °C for 5 hours on around 15 mg of powder. Carbon

dioxide was collected and purified by cryogenic distillation in a vacuum line, and carbon isotope compositions were measured on a VG Optima gas source mass spectrometer. The isotopic ratios are expressed as δ¹³C values with an analytical precision better than 0.1‰ (BOCHERENS et al., 1996).

5. Results and discussion

The results of whole bone nitrogen analysis, collagen extraction and isotopic analysis, and carbon isotopic analysis of the carbonate fraction of enamel bioapatite for specimens from former layers 5 and Vb are given in Table 1. The result of collagen and bioapatite δ¹³C values of large herbivores used in the palaeoecological reconstruction are given in Table 2.

5.1. Reliability of the isotopic results

All the collagen samples considered in the palaeobiological interpretation meet the requirements for reliability, i.e. a C/N ratio ranging from 2.9 to 3.6 (DENIRO, 1985), %N are higher than 8% (AMBROSE, 1990). Moreover, predictable biogenic isotopic patterns, such as more positive δ¹⁵N values in carnivore dentine than in the bone of the same individual (BOCHERENS, 2000), are indeed observed for samples from former Layer 5 in Scladina Cave (Table 1).

The reliability of the bioapatite results can be assessed by comparing the δ¹³C values of collagen and bioapatite when both types of analyses could be performed on the same individual, since these two isotopic signatures are offset by a more or less constant value in large herbivores (LEE-THORP et al., 1989; BOCHERENS & MARIOTTI, 1992; BOCHERENS, 2000). The observed values range from 7.3 to 11.3, which is within the range seen in modern herbivores.

5.2. Palaeoecology of mammal fauna from former layers 4A and 5 in Scladina Cave

Most palaeoecological studies using bone and tooth isotopic tracking in Europe have considered the steppe-tundra environment and the Holocene interglacial, but almost nothing has been published so far on older interglacial periods, such as the Eemian. In Sedimentary Complex 4 and Sedimentary Unit 5 (see Chapter 3) from



Analysis #	Species	Piece	Layer	Excavation #	%N _{bone}	Yield mg.g ⁻¹	%C _{coll}	%N _{coll}	C/N _{coll}	δ ¹³ C _{coll}	δ ¹⁵ N _{coll}	δ ¹³ C _{bioap}
SC14700	<i>Equus ferus</i>	maxillary tooth	5	SC84 215 (G17)	0.2							-12.8
SC14800	<i>Equus ferus</i>	carpal or tarsal bone	5	SC75 (D15)	0.3							
SC15000	<i>Cervus elaphus</i>	phalanx II	Vb	SC82 93	1.2	25.6	37.4	13.7	3.2	-21.4	3.6	
SC15100	<i>Cervus elaphus</i>	mandibular dp4 dental bud	Vb	SC84 109 (E13)	0.7	14.4	36.9	13.3	3.2	-24.9	10.5	-16.3
SC15200	<i>Cervus elaphus</i>	maxillary molar	Vb	SC84 55 (F22)	0.3							-14.2
SC16600	<i>Rangifer tarandus</i>	mandibular tooth	Vb	SC82 396	0.9	21.7	40.3	14.7	3.2	-20.1	8.1	
SC23900	<i>Rangifer tarandus</i>	maxillary third premolar	Vb	SC81 78	0.7	22.4	36.7	13.4	3.2	-23.4	7.6	
SC24000	<i>Rangifer tarandus</i>	maxillary second premolar	Vb	no number	0.6	23.3	38.1	13.9	3.2	-23.0	7.3	
SC21700	<i>Rupicapra rupicapra</i>	left humerus (distal end, subadult)	5	SC86 c13.12	0.2							
SC21800	<i>Rupicapra rupicapra</i>	left humerus (distal end, adult)	5	SC84 G19 93	0.3							
SC21900	<i>Rupicapra rupicapra</i>	left humerus (distal end, adult)	5	SC84 D16/68	0.1							
SC22000	<i>Rupicapra rupicapra</i>	phalanx I	5	SC84 E18.5	0.5	11.4	34.2	12.9	3.1	-20.4	4.9	
SC22100	<i>Rupicapra rupicapra</i>	phalanx I	5	SC85 - 75	1.2	32.4	38.2	14.1	3.2	-19.9	1.9	
SC22200	<i>Rupicapra rupicapra</i>	phalanx I	5	SC86 H123	0.2							
SC22300	<i>Rupicapra rupicapra</i>	phalanx I	5	SC86 H 193 15	0.7	12.9	34.0	13.2	3.0	-20.3	4.5	
SC16300	<i>Coelodonta antiquitatis</i>	mandibular fourth premolar	5	SC84 325 (G16)	0.1							-12.7
SC16400	<i>Coelodonta antiquitatis</i>	mandibular fourth premolar	5	SC84 296 (H19)	0.4							-11.8
SC16500	<i>Mammuthus primigenius</i>	tooth fragment	5	SC82 347	0.2							-12.4
SC15300	<i>Ursus spelaeus</i>	phalanx II	5	SC85 53 (D17)	0.2							
SC15400	<i>Ursus spelaeus</i>	phalanx I	5	SC85 316 (F20)	1.2	17.8	35.8	12.9	3.2	-22.8	7.6	
SC15500	<i>Ursus spelaeus</i>	phalanx I	5	SC85 104 (G22)	0.2							
SC15700	<i>Ursus spelaeus</i>	phalanx	5	SC84 70 (G20)	2.1	107.7	40.6	14.7	3.2	-21.8	5.4	
SC15800	<i>Ursus spelaeus</i>	phalanx II	5	SC82 93	1.6	22.5	36.8	13.2	3.3	-21.5	6.1	
SC17100	<i>Ursus arctos</i>	carpal or tarsal bone	Vb	SC85 119 (G20)	1.4	22.2	27.2	10.4	3.1	-19.7	4.0	
SC16800*	<i>Canis lupus</i>	maxillary	Vb	SC83 22 (F19)	0.3	9.3	32.8	11.5	3.3	-19.6	11.1	
SC16820*	<i>Canis lupus</i>	maxillary fourth premolar	Vb	SC83 22 (F19)	1.1	21.9	39.9	14.5	3.2	-19.9	13.2	
SC16840*	<i>Canis lupus</i>	maxillary first molar	Vb	SC83 22 (F19)	1.0	15.3	39.1	14.5	3.2	-19.8	13.1	
SC16700	<i>Canis lupus</i>	maxillary canine	Vb	SC84 276 (G17)	0.8	18.5	38.5	14.5	3.1	-19.6	11.9	
SC16750	<i>Canis lupus</i>	mandibular canine	Vb	SC83 153 (G14)	0.7	9.5	38.7	14.1	3.2	-19.9	13.4	

Table 1: Bone nitrogen analysis, collagen extraction, isotopic, and carbon isotopic analysis of the carbonate fraction of enamel bioapatite for animal specimens from former layers 5 and Vb of Scladina. The 3 sample numbers followed by “*” are from the same excavation number.

Scladina Cave, the faunal assemblages are ‘mixed’, including taxa traditionally associated to forested landscape (e.g. red deer, fallow deer), taxa usually associated to open environments (e.g. horse) and taxa associated to cold environments (e.g. woolly mammoth, woolly rhinoceros, reindeer). Such mixed assemblages could reflect real biological communities containing large mammal species exhibiting different ecological needs during younger time periods, meaning that their ecological specificity has changed through time for species still extant, or it could be the consequence of a postmortem mixture due to taphonomic processes? The carbon isotopic signatures of the mammal bones and teeth from former layers 4 and 5 in Scladina Cave provide a clear answer: some members of species that are classically associated to open or cold environments, such as horse or reindeer, exhibit in this case a carbon isotopic signature that indicates a dense forest habitat (Figure 1). For instance, two horses from former Layer 4A and two reindeer from former Layer Vb have δ¹³C values indicative of dense forest conditions. In the case of horses, the reconstructed δ¹³C values of the ecosystem ranges from values found

in typical steppe-tundra environment, as in former Layer 1A in Scladina or Kent’s Cavern to values measured on Holocene samples from forested context in France (Figure 1). In general, the range of δ¹³C values is quite large when samples from former layers 4 and 5 in Scladina Cave are considered, and some taxa such as horse and cervids exhibit no clear partitioning according to open and close habitat. It is not clear if the variation in δ¹³C values, and hence of habitat, corresponds to stratigraphical differences within former layers 4 and 5 (PIRSON et al., 2005). In any case, the ecological selectivity of ungulates was different around 100,000 years ago than in more recent periods, suggesting either that the landscape had no analog with more recent plant formations, or that some change occurred in the species ecological flexibility through time. A possible reduction of ecological flexibility could be linked to a reduction of genetic diversity through time, as suggested for different mammal species during the Pleistocene by ancient DNA investigations (e.g., ORLANDO et al., 2002; SHAPIRO et al., 2004; BARNES et al., 2007; HOFREITER, 2007). The carbon isotopic results show that large herbivores were

Analysis #	Species	Piece	Site-layer	$\delta^{13}\text{C}_{\text{coll}}$	$\delta^{13}\text{C}_{\text{bioap}}$	$\Delta^{13}\text{C}_{\text{bioap-coll}}$	$\delta^{13}\text{C}_{\text{ecosystem}}$ from collagen	$\delta^{13}\text{C}_{\text{ecosystem}}$ from bioapatite	$\delta^{13}\text{C}_{\text{ecosystem}}$ summary	Reference
6138?	<i>Mammuthus primigenius</i>	molar	Kent's Cavern	nd	-10.3	nd	nd	-24.3	-24.3	BOCHERENS et al. (1995)
SC600E	<i>Mammuthus primigenius</i>	molar	Scladina-1A	-20.9	-12.3	8.6	-25.9	-26.3	-25.9	This work
SC700E	<i>Mammuthus primigenius</i>	molar	Scladina-1A	-21.5	-12.0	9.5	-26.5	-26.0	-26.5	This work
SC16500E	<i>Mammuthus primigenius</i>	molar	Scladina-5	nd	-12.4	nd	nd	-26.4	-26.4	This work
61369	<i>Coelodonta antiquitatis</i>	tooth	Kent's Cavern	-20.2	-8.9	11.3	-25.2	-22.9	-25.2	BOCHERENS et al. (1995)
61377	<i>Coelodonta antiquitatis</i>	tooth	Kent's Cavern	-20.8	-11.0	9.8	-25.8	-25.0	-25.8	BOCHERENS et al. (1995)
61381	<i>Coelodonta antiquitatis</i>	tooth	Kent's Cavern	-21	-10.8	10.2	-26.0	-24.8	-26.0	BOCHERENS et al. (1995)
4/3470	<i>Coelodonta antiquitatis</i>	tooth	Kent's Cavern	-20.2	-10.2	10.0	-25.2	-24.2	-25.2	BOCHERENS et al. (1995)
61387	<i>Coelodonta antiquitatis</i>	tooth	Kent's Cavern	-20.2	-10.7	9.5	-25.2	-24.7	-25.2	BOCHERENS et al. (1995)
60/2104	<i>Coelodonta antiquitatis</i>	tooth	Kent's Cavern	-21	-12.0	9.0	-26.0	-26.0	-26.0	BOCHERENS et al. (1995)
SC1100E	<i>Coelodonta antiquitatis</i>	mandibular 2nd premolar	Scladina-1A	-20	-10.0	10.0	-25.0	-24.0	-25.0	This work
SC1200E	<i>Coelodonta antiquitatis</i>	mandibular 2nd premolar	Scladina-1A	-21.1	-10.9	10.2	-26.1	-24.9	-26.1	This work
SC16300E	<i>Coelodonta antiquitatis</i>	mandibular 4th premolar	Scladina-5	nd	-12.7	nd	nd	-26.7	-26.7	This work
SC16400E	<i>Coelodonta antiquitatis</i>	mandibular 4th premolar	Scladina-5	nd	-11.8	nd	nd	-26.8	-25.8	This work
61351	<i>Equus ferus</i>	tooth	Kent's Cavern	-21.2	-10.2	11.0	-26.2	-24.2	-26.2	BOCHERENS et al. (1995)
61370	<i>Equus ferus</i>	tooth	Kent's Cavern	nd	-11.6	nd	nd	-25.6	-25.7	BOCHERENS et al. (1995)
61375	<i>Equus ferus</i>	tooth	Kent's Cavern	-21.6	-10.9	10.7	-26.6	-24.9	-26.6	BOCHERENS et al. (1995)
61376	<i>Equus ferus</i>	tooth	Kent's Cavern	nd	-11.5	nd	nd	-25.5	-25.6	BOCHERENS et al. (1995)
61376	<i>Equus ferus</i>	tooth	Kent's Cavern	nd	-12	nd	nd	-26.0	-26.1	BOCHERENS et al. (1995)
61378	<i>Equus ferus</i>	tooth	Kent's Cavern	-21.6	-10.5	11.1	-26.6	-24.5	-26.6	BOCHERENS et al. (1995)
61386	<i>Equus ferus</i>	tooth	Kent's Cavern	-21	-11.5	9.5	-26.0	-25.5	-26.0	BOCHERENS et al. (1995)
61387	<i>Equus ferus</i>	tooth	Kent's Cavern	nd	-11.3	nd	nd	-25.3	-25.4	BOCHERENS et al. (1995)
	<i>Equus ferus</i>	tooth	Kent's Cavern	-21.6	-11.2	10.4	-26.6	-25.2	-26.6	BOCHERENS et al. (1995)
SC4100E	<i>Equus ferus</i>	maxillary tooth	Scladina-1A	-21.7	-12.6	9.1	-26.7	-26.6	-26.7	This work
SC4200E	<i>Equus ferus</i>	maxillary tooth	Scladina-1A	-21.9	-12.2	9.7	-26.9	-26.2	-26.9	This work
SC4300E	<i>Equus ferus</i>	maxillary tooth	Scladina-1A	-21.5	-13.0	8.6	-26.5	-27.0	-26.5	This work
SC14300E	<i>Equus ferus</i>	maxillary tooth	Scladina-4A	-20.5	-12.4	8.1	-25.5	-26.4	-25.5	This work
SC14400E	<i>Equus ferus</i>	maxillary tooth	Scladina-4A	-23.1	-15.8	7.3	-28.1	-29.8	-28.1	This work
SC14500E	<i>Equus ferus</i>	tooth	Scladina-4A	-21.1	nd	nd	-26.1	nd	-26.1	This work
SC14600E	<i>Equus ferus</i>	bone	Scladina-4	-25.1	nd	nd	-30.1	nd	-30.1	This work
SC14700E	<i>Equus ferus</i>	tooth	Scladina-5	nd	-12.8	nd	nd	-26.8	-26.9	This work
B6700	<i>Equus ferus</i>	mandibule	Bercy	nd	-15.2	nd	nd	-29.2	-29.3	This work
B6800	<i>Equus ferus</i>	femur	Bercy	-23.1	-14.9	8.2	-28.1	-28.9	-28.1	This work
B6900	<i>Equus ferus</i>	coxal bone	Bercy	nd	-14.8	nd	nd	-28.8	-28.9	This work
SC4500E	<i>Bos or Bison</i>	tooth	Scladina-1A	-20.5	-11.6	8.9	-25.5	-25.6	-25.5	This work
SC4700E	<i>Bos or Bison</i>	tooth	Scladina-1A	-20.5	-9.8	10.7	-25.5	-23.8	-25.5	This work
SC13100	<i>Dama dama</i>	bone	Scladina-4	-23.3	nd	nd	-28.3	nd	-28.3	This work
SC13200	<i>Dama dama</i>	bone	Scladina-4	-22.3	nd	nd	-27.3	nd	-27.3	This work
SC13500E	<i>Dama dama</i>	tooth	Scladina-4	-24.6	-16.1	8.5	-29.6	-30.1	-29.6	This work
SC19100	<i>Dama dama</i>	bone	Scladina-4	-23.9	nd	nd	-28.9	nd	-28.9	This work
SC19200	<i>Dama dama</i>	bone	Scladina-4	-21.8	nd	nd	-26.8	nd	-26.8	This work
SC19300	<i>Dama dama</i>	bone	Scladina-4	-23.1	nd	nd	-28.1	nd	-28.1	This work
SC19400	<i>Dama dama</i>	bone	Scladina-4	-22.9	nd	nd	-27.9	nd	-27.9	This work
SC19600	<i>Dama dama</i>	bone	Scladina-4	-22.4	nd	nd	-27.4	nd	-27.4	This work
	<i>Cervus elaphus</i>	bone	Scladina-1A	-19.9	nd	nd	-24.9	nd	-24.9	This work
SC15100	<i>Cervus elaphus</i>	bone	Scladina-Vb	-21.4	nd	nd	-26.4	nd	-26.4	This work
SC15100E	<i>Cervus elaphus</i>	decidua 4th premolar	Scladina-Vb	-24.9	-16.3	8.6	-29.9	-30.3	-29.9	This work
SC15200E	<i>Cervus elaphus</i>	tooth	Scladina-Vb	nd	-14.2	nd	nd	-28.2	-28.2	This work
B2601	<i>Cervus elaphus</i>	humerus	Bercy	-23	-14.6	8.4	-28.0	-28.6	-28.0	This work
B5000	<i>Cervus elaphus</i>	radius	Bercy	-23.3	nd	nd	-28.3	nd	-28.3	This work
B5400	<i>Cervus elaphus</i>	métapode	Bercy	-21.6	-13.8	7.8	-26.6	-27.8	-26.6	This work
B5200	<i>Cervus elaphus</i>	radius	Bercy	-23.5	-14.8	8.7	-28.5	-28.8	-28.5	This work
B5100	<i>Cervus elaphus</i>	radius	Bercy	-22.3	-14.4	7.9	-27.3	-28.4	-27.3	This work
B5300	<i>Cervus elaphus</i>	humerus	Bercy	-22.5	-15	7.5	-27.5	-29.0	-27.5	This work
B4800	<i>Cervus elaphus</i>	tibia	Bercy	-21.4	nd	nd	-26.4	nd	-26.4	This work
SC16600	<i>Rangifer tarandus</i>	tooth	Scladina-Vb	-20.1	nd	nd	-25.1	nd	-25.1	This work
SC23800	<i>Rangifer tarandus</i>	tooth	Scladina-Vb	-20.9	nd	nd	-25.9	nd	-25.9	This work
SC23900	<i>Rangifer tarandus</i>	tooth	Scladina-Vb	-23.4	nd	nd	-28.4	nd	-28.4	This work
SC24000	<i>Rangifer tarandus</i>	tooth	Scladina-Vb	-23	nd	nd	-28.0	nd	-28.0	This work
SC22000	<i>Rupicapra rupicapra</i>	bone	Scladina-5	-20.4	nd	nd	-25.4	nd	-25.4	This work
SC22100	<i>Rupicapra rupicapra</i>	bone	Scladina-5	-19.9	nd	nd	-24.9	nd	-24.9	This work
SC22300	<i>Rupicapra rupicapra</i>	bone	Scladina-5	-20.3	nd	nd	-25.3	nd	-25.3	This work

Table 2: Collagen and bioapatite $\delta^{13}\text{C}$ values of large herbivores from Scladina and other northwestern European Palaeolithic sites used in the palaeoecological reconstruction.

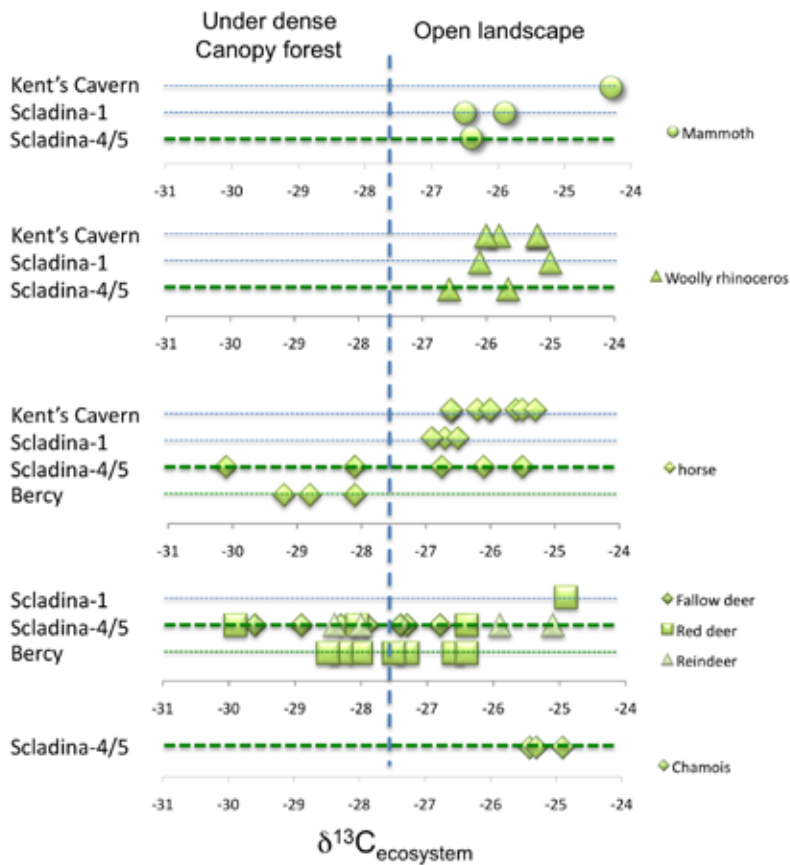


Figure 1: Reconstruction of vegetation type based on $\delta^{13}\text{C}$ of collagen and bioapatite.

living either in dense forest or open environments around Scladina Cave during the time of deposition of former layers 4 and 5, and the position of the Neandertal individual within this landscape can also be determined using its stable isotopic signatures.

5.3. Trophic position of the Neandertal child

The determination of the trophic position of the Neandertal child (Figure 2) using its $\delta^{13}\text{C}$ and $\delta^{15}\text{N}$ values requires a comparison with similar data from coeval fauna, with the possibility to quantify the contribution of different prey specimen in favorable cases (e.g., DRUCKER & HENRY-GAMBIER, 2005; BOCHERENS et al., 2005⁶). Unfortunately two difficulties arise in the case of the Neandertal from former Layer 4A in Scladina: the uncertain stratigraphical origin of the human specimen and the large isotopic variations observed in the coeval fauna. Therefore it is only possible to derive broad trophic conclusions from the collagen isotopic signatures, which are nonetheless very interesting.

A comparison of $\delta^{13}\text{C}$ and $\delta^{15}\text{N}$ values of the Neandertal collagen with fauna from former Layer

4 and fauna from former Layer 5 is presented in Figure 3. It appears clearly that the Neandertal isotopic data plot in the same part of the graph as animal predators such as cave lion, hyaena and wolf. The diet of this human was therefore meat oriented, and clearly different from the diet of cave bears or brown bears, both bear species exhibiting lower $\delta^{15}\text{N}$ values that point to a mainly vegetarian diet. The $\delta^{13}\text{C}$ value of the Neandertal collagen is rather high and indicates that the consumed prey were herbivores dwelling in open environments and not in dense forests. For instance, species such as horse, reindeer, red deer and chamois have $\delta^{13}\text{C}$ values consistent with the possible prey of this Neandertal. No collagen could be extracted from woolly rhinoceros, but the $\delta^{13}\text{C}$ values measured on the carbonate fraction of tooth enamel indicate that this species would have also yielded collagen isotopic values consistent with those of possible preys of the Neandertal. Interestingly, chamois bones from former Layer 5 present abundant anthropic activity traces such as butchery marks (PATOU-MATHIS, 1998) and their $\delta^{13}\text{C}$ values indicate an open environment habitat consistent

Figure 2: Hervé Bocherens samples the maxillary fragment Scla 4A-2 in preparation for stable isotopic analysis (SC18800) at the University of Paris Jussieu (1996).



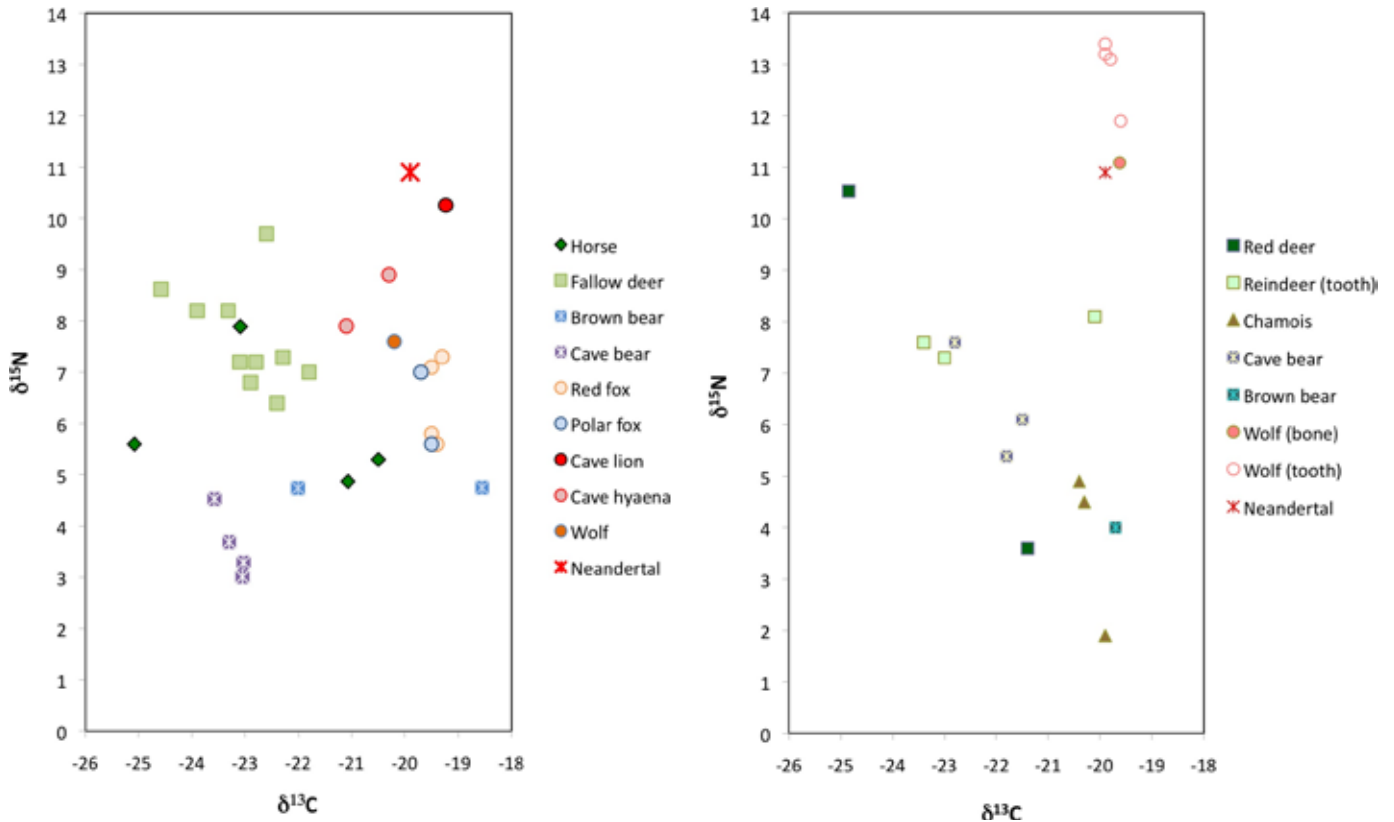


Figure 3: Comparison of isotopic values of bone collagen from Scladina I-4A with fauna from former Layer 4 (left) and from former Layer 5 (right).

with the $\delta^{13}\text{C}$ values of Neandertal prey. When compared to those of predators, the $\delta^{13}\text{C}$ and $\delta^{15}\text{N}$ values of Neandertal are most similar to those of one wolf from former Layer 5 and of one cave lion from former Layer 4, and quite different from those of foxes from former Layer 4 (Figure 3).

In conclusion, it is possible to state that the Neandertal child was predominantly a meat eater and consumed mainly prey living in open environment and not in dense forest. It is however not possible to tell if this choice was due to the lack of forest animals when the Neandertal was living, or if dense forest herbivores were present but not hunted, due to the uncertainty on the stratigraphical origin of the human specimen.

5.4. Comparison with other European Neandertals

It is difficult to compare directly the isotopic results obtained on collagen from Neandertal bones coming from different regions and different periods due to local and chronological variations in carbon and nitrogen isotopic signatures of plants (e.g., FIZET et al., 1995; DRUCKER et al., 2003; DRUCKER & BOCHERENS, 2004). However, the increasing number of isotopic published results

on Neandertals makes it tempting to investigate possible patterns that could yield hypotheses on Neandertal ecology that may be tested further. A first step is to sort out the data that may not be usable for such a purpose.

Since the initial publication of the isotopic results of the Neandertal child from former Layer 4A in Scladina (BOCHERENS et al., 1999), a number of other Neandertal specimens have been investigated using the isotopic approach. These include samples from Belgium (BOCHERENS et al., 2001), France (BOCHERENS et al., 2005^c; BEAUVAL et al., 2006; RICHARDS et al., 2008), Germany (RICHARDS & SCHMITZ, 2008), and Croatia (RICHARDS et al., 2000 & Table 3). Unfortunately, not all of these data can be used for reconstruction of Neandertal trophic ecology. Indeed, a significant proportion of these results do not comply with the preservation criteria retained for biogenic collagen, or the isotopic data on coeval fauna required for a valid palaeo-trophic interpretation are missing. For instance, the isotopic data measured on collagen from sample 27801 from Les Pradelles and both Neandertal samples from Vindija have been shown some years after their original publication to be likely altered (BOCHERENS et al., 2005^c; HIGHAM et al., 2006). The isotopic data from Feldhofer Neandertals are



No analysis (excavation)	Site	Age	Piece	yield (mg/g)	%C	%N	C/N	$\delta^{13}\text{C}$	$\delta^{15}\text{N}$	References
RPB7000	La Roche-à-Pierrot (Saint-Césaire, Charentes-Maritimes, France)	36,000 BP (TL of layer)	fibula	26.0	40.8	14.2	3.3	-19.8	11.4	BOCHERENS et al. (2005)
MT200 (SPY OMO 1)	Spy (Betche-al-Roche Cave (Belgium))	31,810±250 BP	scapula	123.9	41.5	14.4	3.4	-19.8	11.0	BOCHERENS et al. (2001); SEMAL et al. (2009)
Nea1	Kleine Feldhofer Grotte (Germany)	39,900±620 BP	right humerus	?	?	?	?	-21.6	7.9	RICHARDS & SCHMITZ (2008)
NN1	Kleine Feldhofer Grotte (Germany)	39,240±670 BP	right humerus	?	?	?	?	-21.5	9.0	RICHARDS & SCHMITZ (2008)
S-EVA-2152.1	Jonzac, level 7 (Charentes-maritimes, France)	40-55,000 BP	tooth	2.0	33.5	12.1	3.2	-19.7	11.2	RICHARDS et al. (2008)
64801	Les Pradelles (Marillac-le-Franc, Charente, France)	>48,000 BP	skull fragment	82.4	38.8	13.7	3.3	-19.1	11.6	FIZET et al. (2005)
M300 (M70 c10 F10-41)	Les Pradelles (Marillac-le-Franc, Charente, France)	>48,000 BP	skull fragment	107.4	41.1	14.7	3.3	-19.1	11.5	BOCHERENS et al. (2005)
M400 (H1)	Les Pradelles (Marillac-le-Franc, Charente, France)	>48,000 BP	mandible	41.5	37.6	13.1	3.3	-19.5	11.4	BOCHERENS et al. (2005)
OxA-15257	Rochers-de-Villeneuve (Vienne, France)	45,200±1100 BP	femur	37.2	39.4	14.1	3.3	-19.0	11.6	BEAUVAl et al. (2006)
SC18800 (Scla 4A-2)	Scladina Cave (Sclayn, Belgium)	OIS5b	skull fragment	62.0	38.7	14.1	3.2	-19.9	10.9	BOCHERENS et al. (2001)
Excluded because of identification problems										
MT500 (Scla 1B 4, former Layer IV)	Scladina Cave (Sclayn, Belgium)	neolithic?	phalanx	n.d.	39.9	14.7	3.2	-21.2	11.8	BOCHERENS et al. (2001)
Excluded because of preservation problems										
VI-207	Vindija Cave (Croatia)	OIS3	mandible	65.0	37.1	13.5	3.2	-19.5	10.1	RICHARDS et al. (2000)
VI-208	Vindija Cave (Croatia)	OIS3	parietal	42.0	36.1	11.7	3.6	-20.5	10.8	RICHARDS et al. (2000)
27801	Les Pradelles (Marillac-le-Franc, Charente, France)	>48,000 BP	skull fragment	7.0	n.d.	n.d.	n.d.	-20.2	9.3	BOCHERENS et al. (1991)
M100 (H2)	Les Pradelles (Marillac-le-Franc, Charente, France)	>48,000 BP	skull fragment	13.4	18.9	7.0	3.2	-21.8	8.4	BOCHERENS et al. (2005)
S-EVA-2152	Jonzac, level 7 (Charentes-maritimes, France)	40-55,000 BP	tooth	1.0	30.2	9.7	3.6	-20.7	10.6	RICHARDS et al. (2008)
S-EVA-2152.2	Jonzac, level 7 (Charentes-maritimes, France)	40-55,000 BP	tooth	3.0	26.7	8.4	3.7	-21.3	10.3	RICHARDS et al. (2008)
Excluded because of ontogenic interference										
MT100 (Engis 2)	Awirs Cave (Belgium)	OIS3	skull fragment	176.4	41.7	14.4	3.4	-19.6	12.6	BOCHERENS et al. (2001)

Table 3: Isotopic results of different Neandertal specimens from Europe. The human phalanx (MT 500) most probably of Neolithic age was originally thought to be from a Neandertal from former Layer IV in Scladina (BOCHERENS et al., 2001).

considered reliable by their authors (RICHARDS & SCHMITZ, 2008) although no actual chemical criteria are given, such as carbon and nitrogen content and C/N ratios. One juvenile specimen, the child from Engis, is also kept apart. Indeed, the age at death determined from the tooth eruption degree points to an age of 5-6 years (TILLIER, 1983; MAUREILLE & BAR, 1999) or possibly younger, between 3 and 4 years old (STRINGER et al., 1990; SKINNER, 1997). These last estimates are confirmed by a new evaluation using an improved modern reference dataset (Holly Smith, pers. com., 2007). Since it is now known that tooth development in Neandertals was faster than in modern humans (SMITH et al., 2007), this young individual died at a younger age than its tooth development indicated, at a time when the ^{15}N -enriched collagen linked to the consumption of mother milk was not eliminated from the bones (e.g. FOGEL et al., 1989; KATZENBERG et al., 1996; FULLER et al., 2006). It is therefore very likely that the high $\delta^{15}\text{N}$ values measured on this specimen are due to this very young age and not to a special diet (BOCHERENS et al., 2001).

The remaining carbon and nitrogen isotopic signatures from well-preserved collagen extracted from weaned Neandertals are plotted on Figure 3. The isotopic signatures seem to plot in 3 different areas of the graph. The majority of the specimens, including those from southwestern France and Spy, exhibit relatively high $\delta^{13}\text{C}$ and $\delta^{15}\text{N}$ values, one individual supposedly from former Layer IV in Scladina exhibits high $\delta^{15}\text{N}$ value but a rather low $\delta^{13}\text{C}$ value (see discussion below about this specimen), and both specimens from Feldhofer Cave exhibit lower $\delta^{13}\text{C}$ and $\delta^{15}\text{N}$ values (Figure 4). Interestingly, the Neandertal child from former Layer 4A clusters well with the Belgian specimen from Spy that is much younger in age, actually one of the youngest Neandertals known in Europe with a direct radiocarbon age of around 35,000 years BP (SEMAL et al., 2009), and with the slightly older specimen from Saint-Césaire in southwestern France. The older specimens from southwestern France, from Les Pradelles, Les Rochers-de-Villeneuve and Jonzac, also plot in the same range of $\delta^{15}\text{N}$ values but with slightly less negative $\delta^{13}\text{C}$ values. Quite different are the

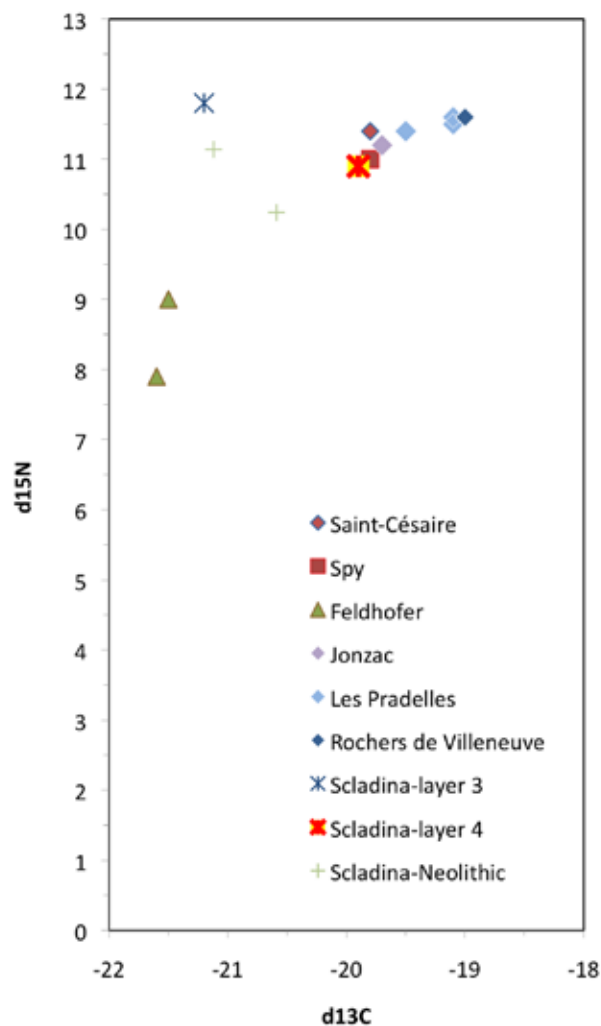


Figure 4: Comparison of carbon and nitrogen isotopic signatures of European Neandertal collagen, excluding specimen with clear signs of alteration (see text).

isotopic signatures of the Neandertal from the former Layer IV from Scladina Cave, with significantly more negative $\delta^{13}\text{C}$ values but high $\delta^{15}\text{N}$ values, and both specimens from Feldhofer Cave, with significantly lower $\delta^{15}\text{N}$ values and more negative $\delta^{13}\text{C}$ values (Figure 4).

The palaeodietary interpretation of the isotopic patterns observed in European Neandertals suggest that the child from the former Layer 4 in Scladina Cave obtained his protein supply from large herbivores living in open conditions. In the sites where a comparison could be made with coeval carnivores, it appears that these Neandertals exhibit the most positive $\delta^{15}\text{N}$ values, as in Saint-Césaire, Spy, Les Pradelles and Jonzac, pointing to the consumption of a subset of prey including predominantly species with particularly high $\delta^{15}\text{N}$ values, such as mammoth in

Saint-Césaire and Spy (BOCHERENS et al., 2001, 2005^c), large bovids in Les Pradelles (BOCHERENS, 2011), and large bovids and horse in Jonzac (RICHARDS et al., 2008). The comparison with coeval fauna shows that similar isotopic signatures do not necessarily indicate similar diets, as different prey species could be represented in different sites at different periods.

More evidence for dietary variation in Neandertals may be provided from the isotopic data of the Neandertal from former Layer IV in Scladina Cave, with a more negative $\delta^{13}\text{C}$ value suggesting an additional protein source. However this specimen is not secured in stratigraphy, and its isotopic signatures look suspiciously similar to those of two human bones from the Neolithic burial ground located on top of the Scladina Pleistocene sedimentary layers. Under these circumstances, it is preferable to consider this sample as dubious and refrain from discussing further dietary variability within Neandertals based on this single specimen.

The case of the Neandertals from Feldhofer is even more complicated. Very few faunal specimens from the same site could be analysed and their relationship with the human specimens is not clear (RICHARDS & SCHMITZ, 2008). The suggestion made by these authors that the isotopic data point to the predominant consumption of deer is not founded since the $\delta^{13}\text{C}$ of these deer are less negative than those of their presumed consumer. Some proteins with more negative $\delta^{13}\text{C}$ values need to be included, and they could be either dense forest herbivores, although they are not observed in the analyzed fauna, or freshwater fish. However, the $\delta^{15}\text{N}$ values seem rather low to be consistent with this hypothesis. A third hypothesis could be that these specimens included high proportions of plant food in their diet, as they fall close to the predicted values for such a diet (BOCHERENS, 2009). However, all this discussion is pending the assumption that no alteration occurred for these collagens, a fact that unfortunately cannot be independently assessed from the published data.

In summary, the current isotopic data available for European Neandertals point to some variability in the origin of dietary proteins, with a majority of specimens relying on open environment large herbivores, and even megaherbivores in the case of the last Neandertals from Saint-Césaire and Spy. Additional data should allow testing to see if this pattern holds and if chronological and/or geographical patterns occur.



6. Conclusion

The palaeodietary reconstruction of the Neandertal child from former Layer 4A in Scladina Cave points to the consumption of open environment herbivores, similar to the majority of European Neandertal analysed so far. However, it is not possible to tell if this selection was due to the absence of dense forest herbivores at the time when this specimen was living, or if such animals were present but not consumed.

References

- AMBROSE S. H., 1990. Preparation and characterization of bone and tooth collagen for isotopic analysis. *Journal of Archaeological Science*, 17: 431-451.
- BARNES I., SHAPIRO B., LISTER A. M., KUZNETSOVA T., SHER A., GUTHRIE D. & THOMAS M. G., 2007. Genetic structure and extinction of the woolly mammoth, *Mammuthus primigenius*. *Current Biology*, 17: R1072-R1075.
- BEAUVAL C., LACRAMPE-CUYAUBÈRE F., MAUREILLE B. & TRINKAUS E., 2006. Direct radiocarbon dating and stable isotopes of the Neandertal femur from Les Rochers-de-Villeneuve (Lussac-les-Châteaux, Vienne). *Bulletins et Mémoires de la Société d'Anthropologie de Paris*, 18: 35-42.
- BOCHERENS H., 2000. Preservation of isotopic signals (^{13}C , ^{15}N) in Pleistocene mammals. In M. A. KATZENBERG & S. H. AMBROSE (eds.), *Biogeochemical approaches to Paleodietary Analyses*. New York, Kluwer Academic/Plenum Publishers: 65-88.
- BOCHERENS H., 2009. Neanderthal dietary habits: Review of the isotopic evidence. In J.-J. HUBLIN & M. P. RICHARDS (eds.), *The Evolution of Hominid Diets: Integrating approaches to the study of Palaeolithic subsistence, Vertebrate Paleobiology & Paleoanthropology*, Springer, Dordrecht: 241-250.
- BOCHERENS H., 2011. Diet and Ecology of Neanderthals: Implications from C and N Isotopes. Insights from Bone and Tooth Biogeochemistry. In N. J. CONARD & J. RICHTER (eds.), *Neanderthal Lifeways, Subsistence and Technology, One Hundred Fifty Years of Neanderthal Study*, Vertebrate Paleobiology & Paleoanthropology Series, chapter 8, Heidelberg, New York, Springer: 73-85.
- BOCHERENS H., BILLIOU D., PATOU-MATHIS M., BONJEAN D., OTTE M. & MARIOTTI A., 1997^a. Isotopic biogeochemistry (^{13}C , ^{15}N) of fossil mammal collagen from Scladina cave (Sclayn, Belgium). *Quaternary Research*, 48: 370-380.
- BOCHERENS H., BILLIOU D., PATOU-MATHIS M., OTTE M., BONJEAN D., TOUSSAINT M. & MARIOTTI A., 1999. Palaeoenvironmental and palaeodietary implications of isotopic biogeochemistry of late interglacial Neandertal and mammal bones in Scladina Cave (Belgium). *Journal of Archaeological Science*, 26: 599-607.
- BOCHERENS H., BILLIOU D. & TRESSET A., 2005^a. Approche biogéochimique (^{13}C , ^{15}N) de l'exploitation de l'environnement par les humains. In F. GILIGNY (ed.), *Louviers "La Vilette" (Eure): Un site néolithique moyen en zone humide*, Documents Archéologiques de l'Ouest, Presses universitaires de Rennes: 265-269.
- BOCHERENS H., DRUCKER D. G., BILLIOU D. & MOUSSA I., 2005^b. Une nouvelle approche pour évaluer l'état de conservation de l'os et du collagène pour les mesures isotopiques (datation au radiocarbone, isotopes stables du carbone et de l'azote). *L'Anthropologie*, 109: 557-567.
- BOCHERENS H., DRUCKER D. G., BILLIOU D., PATOU-MATHIS M. & VANDERMEERSCH B., 2005^c. Isotopic evidence for diet and subsistence pattern of the Saint-Césaire I Neanderthal: Review and use of a multi-source mixing model. *Journal of Human Evolution*, 49: 71-87.
- BOCHERENS H., FIZET M., MARIOTTI A., BILLIOU D., BELLON G., BORE, J. P. & SIMONE S., 1991. Biogéochimie isotopique (^{13}C , ^{15}N , ^{18}O) et paléoécologie des ours Pléistocènes de la grotte d'Aldène. *Bulletin du Musée d'Anthropologie Préhistorique de Monaco*, 34: 29-49.
- BOCHERENS H., FOGEL M. L., TUROSS N. & ZEDER M., 1995. Trophic structure and climatic information from isotopic signatures in a Pleistocene cave fauna of Southern England. *Journal of Archaeological Science*, 22: 327-340.
- BOCHERENS H., KOCH P. L., MARIOTTI A., GERAADS D. & JAEGER J.-J., 1996. Isotopic biogeochemistry (^{13}C , ^{18}O) of mammal enamel from African Pleistocene hominid sites: implications for the preservation of paleoclimatic isotopic signals. *Palaios*, 11: 306-318.
- BOCHERENS H. & MARIOTTI A., 1992. Biogéochimie isotopique du carbone dans les os et les dents de

- mammifères actuels et fossiles de zones froides et tempérées. Paris, *Comptes Rendus de l'Académie des Sciences*, série II, 315: 1147–1153.
- BOCHERENS H. & MARIOTTI A., 2002. Paléoenvironnements et paléoalimentations: biogéochimie isotopique des vertébrés. In J.-C. MISKOWSKI (ed.), *Géologie de la Préhistoire*, GEOPRE, Presses Universitaires de Perpignan: 1323–1344.
- BOCHERENS H., TOUSSAINT M., BILLIOU D., PATOU-MATHIS P., BONJEAN M., OTTE M. & MARIOTTI A., 2001. New isotopic evidence for dietary habits of Neandertals from Belgium. *Journal of Human Evolution*, 40: 497–505.
- BOCHERENS H., TRESSET A., WIEDEMANN F., GILIGNY F., LAFAGE F., LANCHON Y. & MARIOTTI A., 1997^p. Bone diagenetic evolution in two French Neolithic sites. *Bulletin de la Société Géologique de France*, 168: 555–564.
- BROADMEADOW M. S. J. & GRIFFITHS H., 1993. Carbon isotope discrimination and the coupling of CO₂ fluxes within forest canopies. In J. R. EHLERINGER, A. E. HALL & G. D. FARQUHAR (eds.), *Stable isotopes and plant carbon-water relations*, San Diego, Academic Press, Incorporated: 109–129.
- CERLING T. E. & HARRIS J. M., 1999. Carbon isotope fractionation between diet and bioapatite in ungulate mammals and implications for ecological and paleoecological studies. *Oecologia*, 120: 347–363.
- DENIRO M. J., 1985. Post-mortem preservation and alteration of *in vivo* bone collagen isotope ratios in relation to palaeodietary reconstruction. *Nature*, 317: 806–809.
- DENIRO M. J. & EPSTEIN S., 1978. Influence of diet on the distribution of carbon isotopes in animals. *Geochimica et Cosmochimica Acta*, 42: 495–506.
- DENIRO M. J. & EPSTEIN S., 1981. Influence of diet on the distribution of nitrogen isotopes in animals. *Geochimica et Cosmochimica Acta*, 45: 341–351.
- DRUCKER D. G., 2007. Les cervidés durant le tardiglaciaire et l'holocène ancien en Europe occidentale: approche isotopique. In S. BEYRIES & V. VATÉ (eds.), *Les civilisations du renne d'hier et d'aujourd'hui. Approches ethnohistoriques, archéologiques et anthropologiques*, XXVII^e rencontres internationales d'archéologie et d'histoire d'Antibes, Éditions de l'Association pour la promotion et la diffusion des connaissances archéologiques, Antibes: 243–253.
- DRUCKER D. G. & BOCHERENS H., 2004. Carbon and Nitrogen stable Isotopes as Tracers of Diet Breadth Evolution during Middle and Upper Palaeolithic in Europe. *International Journal of Osteoarchaeology*, 14: 162–177.
- DRUCKER D. G. & BOCHERENS H., 2009. Carbon Stable Isotopes of Mammal Bones as Tracers of Canopy Development and Habitat Use in Temperate and Boreal Contexts. In J. D. CREIGHTON & P. J. RONEY (eds.), *Forest Canopies: Forest Production, Ecosystem Health, and Climate Conditions*, Nova Science Publishers, Incorporated: 103–109.
- DRUCKER D. G., BOCHERENS H. & BILLIOU D., 2003. Evidence for shifting environmental conditions in Southwestern France from 33,000 to 15,000 years ago derived from carbon-13 and nitrogen-15 natural abundances in collagen of large herbivores. *Earth and Planetary Science Letters*, 216: 163–173.
- DRUCKER D. G., BRIDAULT A., HOBSON K. A., SZUMA E. & BOCHERENS H., 2008. Can carbon-13 abundances in large herbivores track canopy effect in temperate and boreal ecosystems? Evidence from modern and ancient ungulates. *Palaeogeography, Palaeoclimatology, Palaeoecology*, 266: 69–82.
- DRUCKER D. G. & HENRY-GAMBIER D., 2005. Determination of the dietary habits of a Magdalenian woman from Saint-Germain-la-Rivière in southwestern France using stable isotopes. *Journal of Human Evolution*, 49: 19–35.
- DUFOUR E., BOCHERENS H. & MARIOTTI A., 1999. Palaeodietary implications of isotopic variability in Eurasian lacustrine fish. *Journal of Archaeological Science*, 26: 627–637.
- EHLERINGER J. R., CERLING T. E. & HELLIKER B. R., 1997. C₄ photosynthesis, atmospheric CO₂, and climate. *Oecologia*, 112: 285–299.
- FIZET M., MARIOTTI A., BOCHERENS H., LANGE-BADRÉ B., VANDERMEERSCH B., BOREL J. P. & BELLON G., 1995. Effect of diet, physiology and climate on carbon and nitrogen isotopes of collagen in a late Pleistocene anthropic paleoecosystem (France, Charente, Marillac). *Journal of Archaeological Science*, 22: 67–79.
- FOGEL M. L., TUROSS N. & OWSLEY D. W., 1989. Nitrogen isotope tracers of human lactation in modern and archaeological populations. *Carnegie Institution Year Book*, 88: 111–117.
- FRICKE H. C. & O'NEIL J. R., 1996. Inter- and intra-tooth variation in the oxygen isotope composition of mammalian tooth enamel: Some implications



- for paleoclimatological and paleobiological research. *Palaeogeography, Palaeoclimatology, Palaeoecology*, 126: 91-100.
- FULLER B. T., MOLLESON T. I., HARRIS D. A., GILMOUR L. T. & HEDGES R. E. M., 2006. Isotopic evidence for breastfeeding and possible adult dietary differences from Late/Sub-Roman Britain. *American Journal of Physical Anthropology*, 129: 45-54.
- HEATON T. H. E., 1999. Spatial, species, and temporal variations in the $^{13}\text{C}/^{12}\text{C}$ ratios of C3 plants: implications for palaeodiet studies. *Journal of Archaeological Science*, 26: 637-649.
- HIGHAM T. F. G., BRONK RAMSEY C., KARAVANIĆ I., SMITH F. H. & TRINKAUS E., 2006. Revised direct radiocarbon dating of the Vindija G1 Upper Paleolithic Neandertals. *Proceedings of the National Academy of Sciences of the United States of America*, 103: 553-557.
- HOBSON K. A., SCHELL D. M., RENOUG D. & NOSEWORTHY E., 1996. Stable carbon and nitrogen isotopic fractionation between diet and tissues of captive seals: implications for dietary reconstructions involving marine mammals. *Canadian Journal of Fisheries and Aquatic Sciences*, 53: 528-533.
- HOFREITER M., 2007. Pleistocene extinctions: haunting the survivors. *Current Biology*, 17: R609-R611.
- KATZENBERG M. A., HERRING D. A. & SAUNDERS S. R., 1996. Weaning and infant mortality: evaluating the skeletal evidence. *Yearbook of Physical Anthropology*, 39: 177-199.
- LEE-THORP J. A., SEALY J. C. & VAN DER MERWE N. J., 1989. Stable carbon isotope ratio differences between bone collagen and bone apatite, and their relationship to diet. *Journal of Archaeological Science*, 16: 585-599.
- MAUREILLE B. & BAR D., 1999. The premaxilla in Neandertal and early modern children: ontogeny and morphology. *Journal of Human Evolution*, 37: 137-152.
- ORLANDO L., BONJEAN D., BOCHERENS H., THENOT A., ARGANT A., OTTE M. & HÄNNI C., 2002. Ancient DNA and the population genetics of cave bears (*Ursus spelaeus*) through space and time. *Molecular Biology and Evolution*, 19: 1920-1933.
- PATOU-MATHIS M., 1998. Les espèces chassées et consommées par l'Homme en couche 5. In M. OTTE, M. PATOU-MATHIS & D. BONJEAN (dir.), *Recherches aux grottes de Sclayn, vol. 2: L'Archéologie. Études et Recherches Archéologiques de l'Université de Liège*, 79: 297-310.
- PIRSON S., BONJEAN D., DI MODICA K. & TOUSSAINT M., 2005. Révision des couches 4 de la grotte Scladina (comm. d'Andenne, prov. de Namur) et implications pour les restes néandertaliens: premier bilan. *Notae prehistoricae*, 25: 61-69.
- RICHARDS M. P., PETTITT P. B., TRINKAUS E., SMITH F. H., PAUNOVIĆ M. & KARAVANIĆ I., 2000. Neandertal diet at Vindija and Neandertal predation: The evidence from stable isotopes. *Proceedings of the National Academy of Sciences of the United States of America*, 97, 13: 7663-7666.
- RICHARDS M. P. & SCHMITZ R. W., 2008. Isotope evidence for the diet of the Neanderthal type specimen. *Antiquity*, 82: 553-559.
- RICHARDS M. P., TAYLOR G., STEELE T., MCPHERRON S. P., SORESSI M., JAUBERT J., ORSCHIEDT J., MALLYE J.-B., RENDU W. & HUBLIN J.-J., 2008. Isotopic dietary analysis of a Neanderthal and associated fauna from the site of Jonzac (Charente-Maritime), France. *Journal of Human Evolution*, 55: 179-185.
- SEMAL P., ROUGIER H., CREVECOEUR I., JUNGEL C., FLAS D., HAUZEUR A., MAUREILLE B., GERMONPRÉ M., BOCHERENS H., PIRSON S., CAMMAERT L., DE CLERCK N., HAMBUCHEN A., HIGHAM T. F. G., TOUSSAINT M. & VAN DER PLICHT J., 2009. New data on the Late Neandertals: direct dating of the Belgian Spy fossils. *American Journal of Physical Anthropology*, 138: 421-428.
- SHAPIRO B., DRUMMOND A. J. & RAMBAUT A., 2004. Rise and fall of the Beringian steppe bison. *Science*, 306, 5701: 1561-1565.
- SHARP Z. D. & CERLING T. E., 1998. Fossil isotope records of seasonal climate and ecology: Straight from the horse's mouth. *Geology*, 26: 219-222.
- SKINNER M. F., 1997. Dental wear in immature Late Pleistocene European hominines. *Journal of Archaeological Science*, 24: 677-700.
- STRINGER C. B., DEAN M. C., & MARTIN R. D., 1990. A comparative study of cranial and dental development within a recent British sample and among Neandertals. In C. J. DEROUSSEAU (ed.), *Primate Life History and Evolution*, New York, Wiley-Liss: 115-152.
- TILLIER A.-M., 1983. Le crâne d'enfant d'Engis 2: un exemple de distribution des caractères juvéniles, primitifs et néandertaliens. *Bulletin de la Société royale belge d'Anthropologie et de Préhistoire*, 94: 51-75.

Chapter 18

Sireen EL ZAATARI, Kristin L. KRUEGER & Jean-Jacques HUBLIN

DENTAL MICROWEAR TEXTURE ANALYSIS AND THE DIET OF THE SCLADINA I-4A NEANDERTAL CHILD

*Michel Toussaint & Dominique Bonjean (eds.), 2014.
The Scladina I-4A Juvenile Neandertal (Andenne, Belgium),
Palaeoanthropology and Context
Études et Recherches Archéologiques de l'Université de Liège, 134: 363-378.*

1. Introduction

Microwear texture analysis, the objective, repeatable, and three-dimensional approach to dental microwear, has proven to be a valuable method for characterizing microwear surfaces and for distinguishing dietary and non-dietary tooth use behaviors in a wide range of extant taxa, including bovids (e.g., UNGAR et al., 2007), kangaroos (PRIDEAUX et al., 2009), carnivores (e.g., UNGAR et al., 2010), non-human primates (KRUEGER et al., 2008; SCOTT et al., 2012) and Recent Modern Human groups (e.g., EL ZAATARI, 2014; KRUEGER & UNGAR, 2010; KRUEGER, 2014). In particular, this approach can provide different information depending on the tooth type examined. When applied to the anterior dentition, it has been effective in differentiating bioarchaeological human groups based on diet, non-dietary anterior tooth use, and dietary and/or abrasive loads (KRUEGER & UNGAR, 2010). On the other hand, when applied to their occlusal molar surfaces, microwear texture analysis has been useful in distinguishing recent human groups based on their diets and food preparation techniques (EL ZAATARI, 2014). The relationship between dental microwear texture signatures, diet, and behavior established among modern human populations has led to additional important insights into dietary and non-dietary tooth-use behaviors of Neandertals (KRUEGER, 2011; KRUEGER & UNGAR, 2012; EL ZAATARI et al., 2013).

The wide-scale occlusal molar microwear texture analysis of adult Neandertal specimens from numerous western Eurasian sites has revealed that not all Neandertals are top-level carnivores (EL ZAATARI et al., 2011), as they had been perceived based on stable isotope analyses (e.g., BOCHERENS et al., 1999, 2001, 2005; RICHARDS et al., 2000; BOCHERENS & DRUCKER, 2003; RICHARDS & TRINKAUS, 2009). Specifically, the microwear signatures of many of the Neandertals analyzed, especially those that lived in more open,

cold-steppe habitats, were found to be similar to recent human populations whose diets consisted almost exclusively or primarily of meat. However, some Neandertals, specifically those that lived in wooded habitats, were found to have microwear textures similar to recent hunter-gatherer groups with a mixed diet. This indicates that, at least for some Neandertals, plant foods formed an important part of the diet (EL ZAATARI et al., 2011).

Moreover, the application of anterior microwear texture analysis to adult Neandertal specimens has helped better understand non-dietary anterior tooth use behaviors among these fossil hominins (KRUEGER, 2011; KRUEGER & UNGAR, 2012). Previous examinations of the unusual and excessive anterior dental wear found on some noteworthy Neandertal specimens, such as La Ferrassie 1 and Spy 1, has been linked to their use of their dentition for non-dietary purposes (e.g., STEWART, 1959; WALLACE, 1975; SMITH, 1976; WOLPOFF, 1979). These behaviors have been described in a variety of ways, with the most cited scenario proposed from ethnographic reports of Alaskan Eskimo and Canadian and Greenland Inuit, and referred to as the 'stuff and cut' method. This scenario suggested that Neandertals would clamp a piece of meat between their anterior teeth, and slice a portion off close to their lips (BRACE, 1967, 1975; RYAN, 1980; BRACE et al., 1981). This idea has been expanded to propose other types of non-dietary anterior tooth use behaviors, such as animal hide processing, sinew thread production, weaving tasks, wood softening, and tool production and retouching (CYBULSKI, 1974; LUKACS & PASTOR, 1988; FOOTE, 1992; MAYES, 2001). The results of the microwear texture analysis of Neandertals' anterior dentition confirmed that the Neandertals did in fact use their dentition for non-dietary purposes (KRUEGER, 2011). Yet, this analysis also showed that the Neandertals' engagement in such behaviors was linked to climatic conditions, such that those that lived under cold, open steppe conditions were found to



use their anterior dentition in non-dietary behaviors much more intensely than those in the warm, woodland climates (KRUEGER, 2011).

For the current study, anterior and molar microwear textures of the Scladina Neandertal were analyzed. The examination of the microwear texture signatures of the Scladina Neandertal is an interesting addition to the present dataset of adult Neandertal specimens. Not only will it provide additional insight into the dietary and behavioral strategies of Neandertals as a whole, but it will also begin to allow the examination of sub-adult Neandertal individuals.

2. Materials

Microwear data was recovered from one permanent canine (RC₁; Scla 4A-12) and one permanent molar (RM₁; Scla 4A-1/M₁) of the Scladina Juvenile. Since it remains unclear whether permanent and deciduous dentitions have similar levels of resistance to premortem masticatory wear, permanent rather than deciduous dentitions were selected to represent the Scladina individual for this study to allow for securely comparing its microwear data to similar data available for permanent dentitions of: 1) adult individuals belonging to six recent human groups of known or inferred diet, anterior tooth use behaviors, and abrasive loads, and 2) adult Neandertal specimens (EL ZAATARI, 2014; KRUEGER, 2014; KRUEGER & UNGAR, 2010, 2012; EL ZAATARI et al., 2013).

Aleut

Study sample: The specimens were collected from the islands of Agattu, Amaknak, Kagamil, Unmak, and Unalaska, Alaska, USA (HRDLIČKA, 1945) and date to 3400-400 years BP (COLTRAIN, 2010). Anterior dental microwear data was recovered from 24 individuals and molar microwear data was recovered from 21 individuals.

Diet: The Aleutian diet consists predominantly of marine animals including sea mammals, fish, shellfish, supplemented by land resources including, foxes, birds, rodents, and tubers (HRDLIČKA, 1945; LAUGHLIN, 1963; COLTRAIN, 2010).

Abrasive loads: The Aleut are known for their extensive chewing of frozen and dried animal meat and skin (HOFFMAN, 1993). Environmental abrasives, such as sand and

grit, are hypothesized to have been a daily inclusion in their diet (MOORREES, 1957).

Non-dietary anterior tooth use behaviors: Ethnographically, the Aleut used their anterior dentition in non-dietary anterior tooth use behaviors, including hide production and wood softening (HRDLIČKA, 1945; MOORREES, 1957).

Arikara

Study sample: This sample consists of individuals from the Mobridge Site (39WWI), South Dakota, USA, and date to 400-300 years BP (JANTZ, 1973). Anterior microwear data was recovered from 18 individuals and molar microwear data was recovered from 16 individuals.

Diet: The Arikara's diet had strong emphasis on big game, supplemented by a mix of wild and cultivated plant foods including peppers, pumpkins, grapes, black cherries, beans, squash, corn, and sunflowers (HURT, 1969; MEYER, 1977; TUROSS & FOGEL, 1994; BLAKESLEE, 1994).

Abrasive loads: It has been suggested that the Arikara were subject to dietary abrasives from corn phytoliths and food processing techniques, including the use of stone mortars, as well as the frequent consumption of dried strips of game meat (LEIGH, 1925; MEYER, 1977).

Non-dietary anterior tooth use behaviors: None documented.

Ipiutak

Study sample: These specimens were recovered from the site of Point Hope, Alaska, USA, and date to 2050-1450 years BP (LARSEN & RAINEY, 1948). Anterior microwear data was recovered from 22 individuals and molar microwear data was recovered from 17 individuals.

Diet: While inhabiting the coast during the summer months, the Ipiutak's diet was based on caribou, and sea mammals, including seals and walrus (LESTER & SHAPIRO, 1968).

Abrasive loads: Point Hope is a coastal site, and environmental abrasives, such as sand, would have been included in the Ipiutak's diet.

Non-dietary anterior tooth use behaviors: Evidence suggests the Ipiutak used their anterior dentition in intense caribou hide preparation and processing (KRUEGER, 2014).

Tigara

Study sample: These specimens were recovered from the site of Point Hope, Alaska, USA, and date to 750-250 years BP (LARSEN & RAINEY, 1948). Anterior microwear data was recovered

Site	Specimen	Palaeovegetation Cover
Spy	I	Open (CORDY, 1988)
La Quina	5 20	Open (BOUCHUD, 1966; HENRI-MARTIN, 1966)
Subalyuk	1	Open (GROSS, 1956; Kordos in SCHWARTZ & TATTERSALL, 2002)
Grotte de l'Hyène (Arcy-sur-Cure)	IVb6 B9	Open (LEROI-GOURHAN, 1988)
Saint-Césaire	1	Mixed (LAVAUD-GIRARD, 1993; LEROYER & LEROI-GOURHAN, 1993; MARQUET, 1988, 1993; MISKOVSKY & LEVÉQUE, 1993; MORIN, 2004; PATOU-MATHIS, 1993)
Vindija	11.45 11.46 12.1	Mixed (MIRACLE et al., 2010)
Petit-Puymoyen	2 4	Mixed (BCEUF, 1969)
Rochelot	1098	Mixed (TOURNEPICHE & COUTURE, 1999)
La Chaise Bourgeois-Delaunay	8	Mixed (FELLAG, 1996)
Kebara	2	Mixed (EISENMANN, 1992; SPETH & TCHERNOV, 1998, 2001, 2002)
Tabun	II	Mixed (JELINEK et al., 1973)
Zafarraya	4	Wooded (BARROSO RUIZ et al., 2006)
Grotta Breuil	2	Wooded (KOTSAKIS, 1990-1991; STINER, 1994; RECCHI, 1995)
El Sidrón	SDR-005	Wooded (FORTEA et al., 2003)
Lakonis	LKH1	Wooded (PANAGOPOULOU et al., 2002-2004)
Amud	I	Wooded (RABINOVICH & HOVERS, 2004; KOLSKA HORWITZ & HONGO, 2006; BELMAKER & HOVERS, 2008)

Table 1: Neandertal specimens whose occlusal molar microwear textures were used for the comparison with those of the Scladina Child (see EL ZAATARI et al., 2011 for details on the specimens and the palaeovegetation cover reconstructions).

from 34 individuals and molar microwear data was recovered from 27 individuals.

Diet: The Tigara diet consisted predominantly of sea mammals, including whales, walrus, and seals, and was supplemented by fish, birds, berries, and other edible plants (LARSEN & RAINEY, 1948; DABBS, 2009; BRUBAKER et al., 2010).

Abrasive loads: The Tigara's food preparation techniques, which included freezing meat underground as a year-round staple (DE PONCINS, 1941; GIDDINGS, 1967), would have led to the inclusion of large amounts of environmental abrasives, such as sand, in their diet. Also, dried and frozen uncooked meat and skin -together with its attached subcutaneous fat- were often chewed for prolonged periods of time (BALIKCI, 1970).

Non-dietary anterior tooth use behaviors: Ethnographically, the Tigara used their anterior dentition in some hide processing and sinew thread production (FOOTE, 1992).

Fuegian

Study sample: The sample consists of specimens from the Yamana Tribe of the Beagle Channel Islands, Argentine Tierra del Fuego, extreme southern South America and date to AD 1880 (MANZI, 1986). Molar microwear data was recovered from 6 individuals.

Diet: The Fuegians relied on seals, sea lions,

guanaco (*Lama guanicoe*), shellfish, fish, penguin, and waterfowl for subsistence (BRIDGES, 1885; SNOW, 1861; YESNER et al., 2003).

Abrasive loads: None documented

Non-dietary anterior tooth use behaviors:

None documented

Puye Pueblo

Study sample: This sample consists of specimens from the volcanic plateau in northcentral New Mexico, USA dating to 100–330 BP (BARNES, 1994). Anterior microwear data was recovered from 18 individuals.

Diet: The Puye Pueblo diet consisted predominantly of maize, squash, and bean agriculture, supplemented by prickly pear, yucca fruit, plums, grapes, foxes, deer, rabbits, and beeweed (HEWETT, 1938; TRIERWEILER, 1990; BARNES, 1994).

Abrasive loads: Maize phytoliths and stone-on-stone grinding processes contributed dietary abrasives, and environmental abrasives, including dust and grit common to the open setting (TRIERWEILER, 1990).

Non-dietary anterior tooth use behaviors: None documented.

Neandertals

The anterior microwear textures of the Scladina Juvenile were compared to a sample of



		<i>Asfc</i>	<i>epLsar</i>	<i>Smc</i>	<i>Tfv</i>	<i>HAsfc₉</i>	<i>HAsfc₈₁</i>
SCLADINA NEANDERTAL		1.22	0.0051	0.34	10778.82	0.44	0.97
Aleut (<i>n</i> = 24)	Mean	0.93	0.0030	0.40	7434.50	0.38	0.61
	SD	0.45	0.0011	0.36	5272.19	0.07	0.12
Arikara (<i>n</i> = 18)	Mean	0.77	0.0036	0.38	1897.76	0.37	0.56
	SD	0.40	0.0016	0.22	2466.36	0.08	0.12
Ipiutak (<i>n</i> = 22)	Mean	3.43	0.0020	0.34	12143.02	0.66	1.36
	SD	3.03	0.0008	0.28	4253.49	0.31	0.80
Tigara (<i>n</i> = 34)	Mean	1.20	0.0032	0.35	7296.02	0.53	0.89
	SD	0.99	0.0015	0.12	5391.20	0.26	0.46
Puye Pueblo (<i>n</i> = 18)	Mean	1.24	0.0040	0.31	5093.03	0.48	0.75
	SD	1.01	0.0012	0.22	4183.08	0.14	0.32
Neandertals Krapina (<i>n</i> = 17)	Mean	1.27	0.0031	0.39	5810.11	0.42	0.68
	SD	0.45	0.0013	0.14	3620.88	0.08	0.16

Table 2: Raw data for the Scladina Neandertal anterior teeth microwear texture and summary statistics for the modern human and Neandertal comparative samples. Five texture variables were generated: complexity (*Asfc*), anisotropy (*epLsar*), scale of maximum complexity (*Smc*), textural fill volume (*Tfv*), and heterogeneity (*HAsfc₉* and *HAsfc₈₁*).

Neandertals from the site of Krapina (KRUEGER & UNGAR, 2012). The Krapina Neandertals date to $130,000 \pm 10,000$, and are generally attributed to MIS 5e. If accurate, this would suggest these individuals were living in a warm, wooded climate (RINK et al., 1995; SIMEK & SMITH, 1997; KARAVANIĆ, 2004). These Neandertals are noted for the presence of labial-lingual rounding (incisor beveling) on some specimens, and the cause of this has been suggested to be non-dietary anterior tooth use behaviors (WOLPOFF, 1979). Labial striations on the incisors and anterior dental microwear analyses support this hypothesis (LALUEZA-FOX & FRAYER, 1997; KRUEGER & UNGAR, 2012). Specifically, microwear textures suggest that the Krapina Neandertals were engaging in moderate non-dietary anterior tooth use behaviors that did not require a heavy anterior loading regime (KRUEGER & UNGAR, 2012).

The molar microwear data of the Scladina Juvenile was compared to those of a total of 20 adult Neandertal individuals from 16 sites (listed in Table 1) located in different parts of Europe (southern, central, northern) as well as the Levant and dating to between MIS 6 to MIS 3 (EL ZAATARI et al., 2011, 2013). An analysis of the molar microwear textures of these specimens examining the effects of time, geography, and palaeoecology on their diets showed that their diets differed significantly in response to the changes in palaeoecological conditions. Indeed, the microwear textures of these Neandertals indicate that they increased their intake of plant foods with the increase in tree cover, whereas they increased their intake of meat with the spread of cold, open steppic conditions

(EL ZAATARI et al., 2011). Thus, for the comparisons with the Scladina molar microwear texture, the Neandertal specimens were grouped into three groups based on habitat, i.e., open, mixed, and wooded habitats.

3. Methods

The microwear analyses of the Scladina teeth were conducted on high resolution dental casts. Following gentle cleaning of the dentition with cotton swabs soaked with distilled water, negative molds were first made of the Scladina teeth using Coltène President microSystem™ (Coltène®; polysiloxane vinyl) impression material and the positive casts were then poured using Epo-Tek 301 epoxy resin and hardener (Epoxy Technologies).

A Sensofar Plu white-light scanning confocal microscope (Solarius Development Inc., Sunnyvale California) with a 100× objective lens was used to scan the labial surface nearest the occlusal edge of the Scladina canine and the crushing/grinding facet 9 of the molar. Point clouds were generated for a total of four adjoining scans for each surface, with a lateral sampling interval of 0.18 μm, and a total field of view of 276 × 204 μm for each tooth. Any identifiable defects, such as adhesive or dust particles were then removed and photosimulations and 3D images were generated using the Solarmap Universal software (Solarius Development Inc., Sunnyvale, CA).

The four adjoining scans of each specimen were characterized using Toothfrax and SFrax (Surfract, www.surfract.com) scale-sensitive fractal analysis (SSFA) software packages. Five texture variables

		<i>Asfc</i>	<i>epLsar</i>	<i>Smc</i>	<i>Tfv</i>	<i>HAsfc₁</i>
SCLADINA NEANDERTAL		0.76	0.0014	1.67	9422.17	0.13
Aleut (<i>n</i> = 21)	Mean	2.59	0.0028	0.45	10383.20	0.22
	SD	1.60	0.0011	0.73	5419.60	0.14
Arikara (<i>n</i> = 16)	Mean	1.15	0.0027	0.82	5672.80	0.20
	SD	1.09	0.0015	0.97	5997.80	0.15
Ipiutak (<i>n</i> = 17)	Mean	10.03	0.0019	0.18	13984.20	0.20
	SD	7.61	0.0006	0.05	3133.60	0.13
Tigara (<i>n</i> = 27)	Mean	6.41	0.0031	0.22	12434.10	0.29
	SD	5.62	0.0016	0.07	4946.70	0.20
Fuegians (<i>n</i> = 6)	Mean	0.95	0.0044	0.40	5224.80	0.11
	SD	0.29	0.0014	0.14	3522.50	0.03
Neandertals Open (<i>n</i> = 5)	Mean	1.08	0.0023	0.30	10770.26	0.11
	SD	0.24	0.0008	0.10	1645.88	0.09
Neandertals Mixed (<i>n</i> = 10)	Mean	1.54	0.0030	0.44	10935.31	0.26
	SD	0.47	0.0010	0.57	5519.59	0.14
Neandertals Wooded (<i>n</i> = 5)	Mean	2.87	0.0023	3.72	14560.62	0.53
	SD	0.52	0.0016	4.98	2085.99	0.44

Table 3: Raw data for the Scladina Neandertal molar microwear texture and summary statistics for the modern human and Neandertal comparative samples. Five texture variables were generated: complexity (*Asfc*), anisotropy (*epLsar*), scale of maximum complexity (*Smc*), textural fill volume (*Tfv*), and heterogeneity (*HAsfc₁*).

were generated: complexity (*Asfc*), anisotropy (*epLsar*), scale of maximum complexity (*Smc*), textural fill volume (*Tfv*), and heterogeneity (*HAsfc*). These variables have been discussed in detail elsewhere (see SCOTT et al., 2005, 2006; UNGAR et al., 2007). Briefly, complexity (*Asfc*) is a measure of the change of surface roughness across different scales of observation. Anisotropy (*epLsar*) is a reflection of the concentration of wear feature orientations. Scale of maximum complexity (*Smc*) is an indicator of the size of the microwear features. Textural fill volume (*Tfv*) is a reflection of the geometrical shape and depth of wear features. Heterogeneity (*HAsfc*) reveals the variability in complexity across the surface. It should be noted that the individual heterogeneity value for the Scladina molar used in this study was calculated using the four scans for this tooth without splitting single scans into smaller sub-regions, whereas two values of heterogeneity for the Scladina canine were calculated by dividing each field of view into 3×3 (*HAsfc₃*) and 9×9 (*HAsfc₈₁*) grids. Finally, for the four scans, median values for each of the five texture variables were calculated for each tooth.

The values for the five variables for the Scladina canine were then compared to data available from maxillary central incisors of the modern comparative samples and from maxillary and mandibular incisors and canines of the Krapina Neandertals (KRUEGER & UNGAR, 2010, 2012; KRUEGER, 2014). Microwear textures have been shown to not differ significantly between these tooth types and jaws

(KRUEGER, 2011). The values for the texture variables for the Scladina molar were compared to similar data collected from molars of the modern human and Neandertal samples (EL ZAATARI, 2014; EL ZAATARI et al., 2011, 2013). The lack of significant differences in microwear patterns by molar type or position in recent hunter-gatherer groups makes it possible to include data from molars with different positions for the specimens analyzed (EL ZAATARI, 2010).

4. Results

Representative 2D photosimulations of the surfaces of the Scladina and the comparative groups' dentition are presented in Figures 1 & 2. Raw data for the Scladina Neandertal microwear textures, along with the summary statistics for the modern human and Neandertal comparative samples are presented in Tables 2 & 3. Results are illustrated in Figures 3 & 4.

4.1. Complexity

The Scladina canine complexity value is 1.22. It is nearly identical to, and intermediate between, the mean values for the Puye Pueblo and the Tigara modern human samples. This value also falls within the one standard deviation ranges of the means of the Ipiutak and Aleut. The complexity value of the Scladina canine is very close to the mean value of the Krapina Neandertal sample.



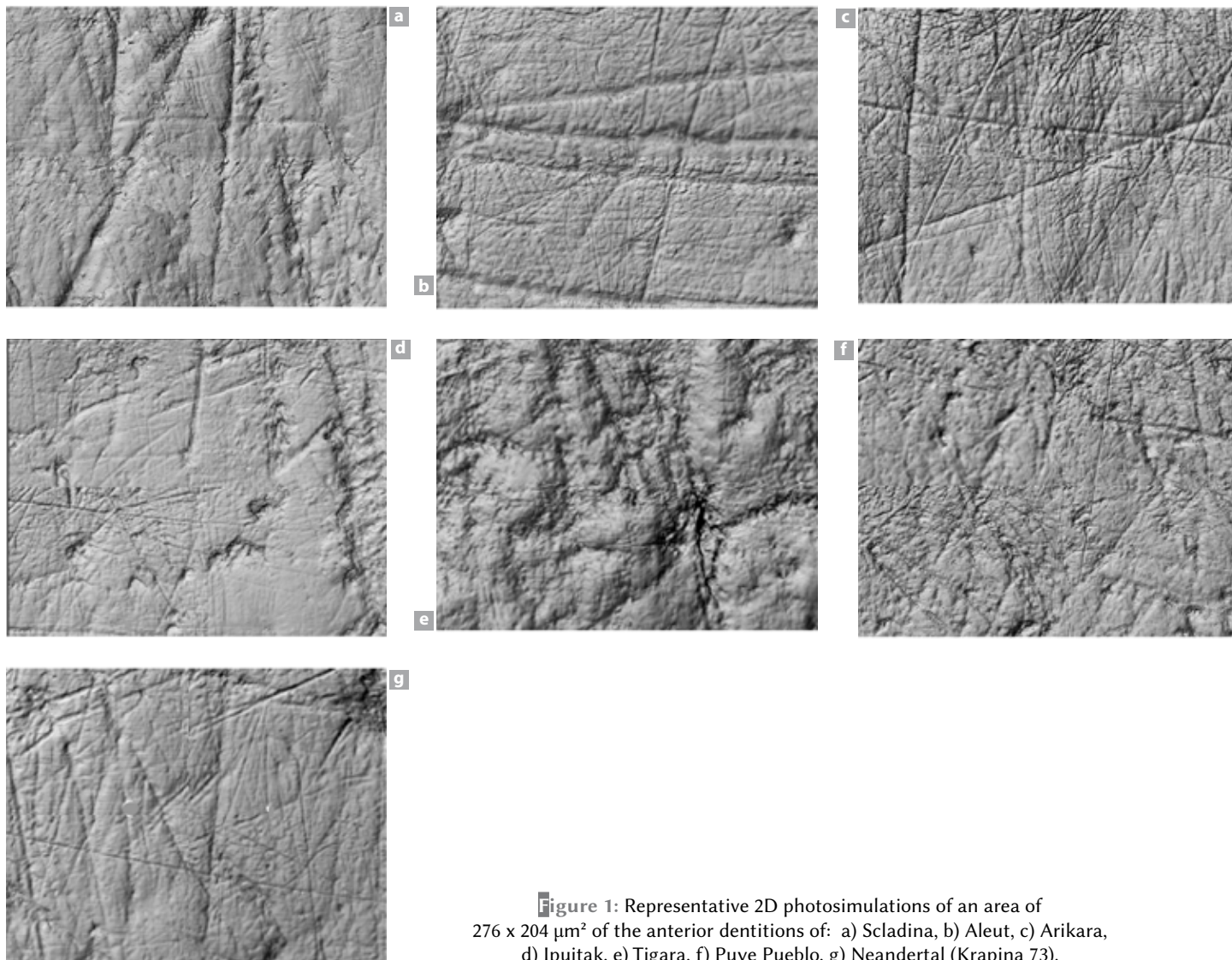


Figure 1: Representative 2D photosimulations of an area of 276 x 204 μm^2 of the anterior dentitions of: a) Scladina, b) Aleut, c) Arikara, d) Ipiutak, e) Tigara, f) Puye Pueblo, g) Neandertal (Krapina 73).

The complexity value of the Scladina molar falls within the one standard deviation ranges of the means of the Arikara, Fuegians, and Neandertals from open habitats, and outside the ranges of variation of the rest of the modern and Neandertal groups.

4.2. Anisotropy

The Scladina canine anisotropy value, which is 0.0051, is higher than the mean values for all the modern human samples as well as the sample of Krapina Neandertals. It also falls outside the ranges of all the comparative groups with the exception of the Puye Pueblo and Arikara.

The molar anisotropy value for the Scladina Juvenile falls within the one standard deviation ranges of the means of the Arikara, Ipiutak, and Tigara and outside the ranges of the Aleut and

Fuegians. From the Neandertal groups, the anisotropy value of the Scladina molar falls within the ranges of the Neandertals from open as well as those from wooded habitats.

4.3. Scale of maximum complexity

The Scladina canine *Smc* value is 0.34, and is identical to that of the Ipiutak. It is also very close to the value for the Tigara. The Scladina individual is within the range of every modern human sample and the Krapina Neandertals.

The Scladina molar has a relatively high value for the scale of maximum complexity. This value falls within the one standard deviation range of the mean of the Arikara from the recent human groups and the Neandertals from wooded habitats from the Neandertal groups analyzed.

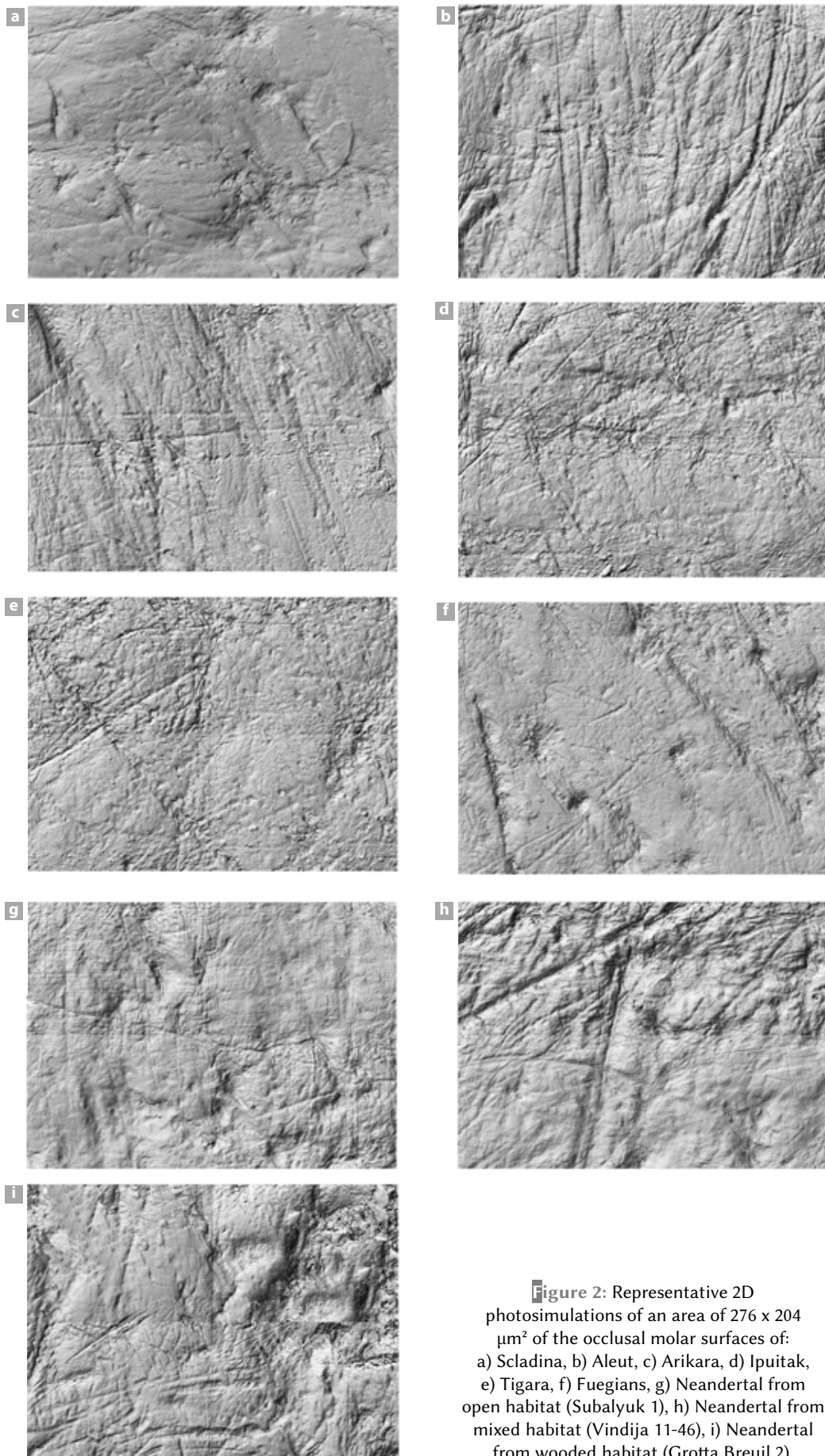


Figure 2: Representative 2D photosimulations of an area of 276 x 204 μm^2 of the occlusal molar surfaces of: a) Scladina, b) Aleut, c) Arikara, d) Ipuitak, e) Tigara, f) Fuegians, g) Neandertal from open habitat (Subalyuk 1), h) Neandertal from mixed habitat (Vindija 11-46), i) Neandertal from wooded habitat (Grotta Breuil 2).



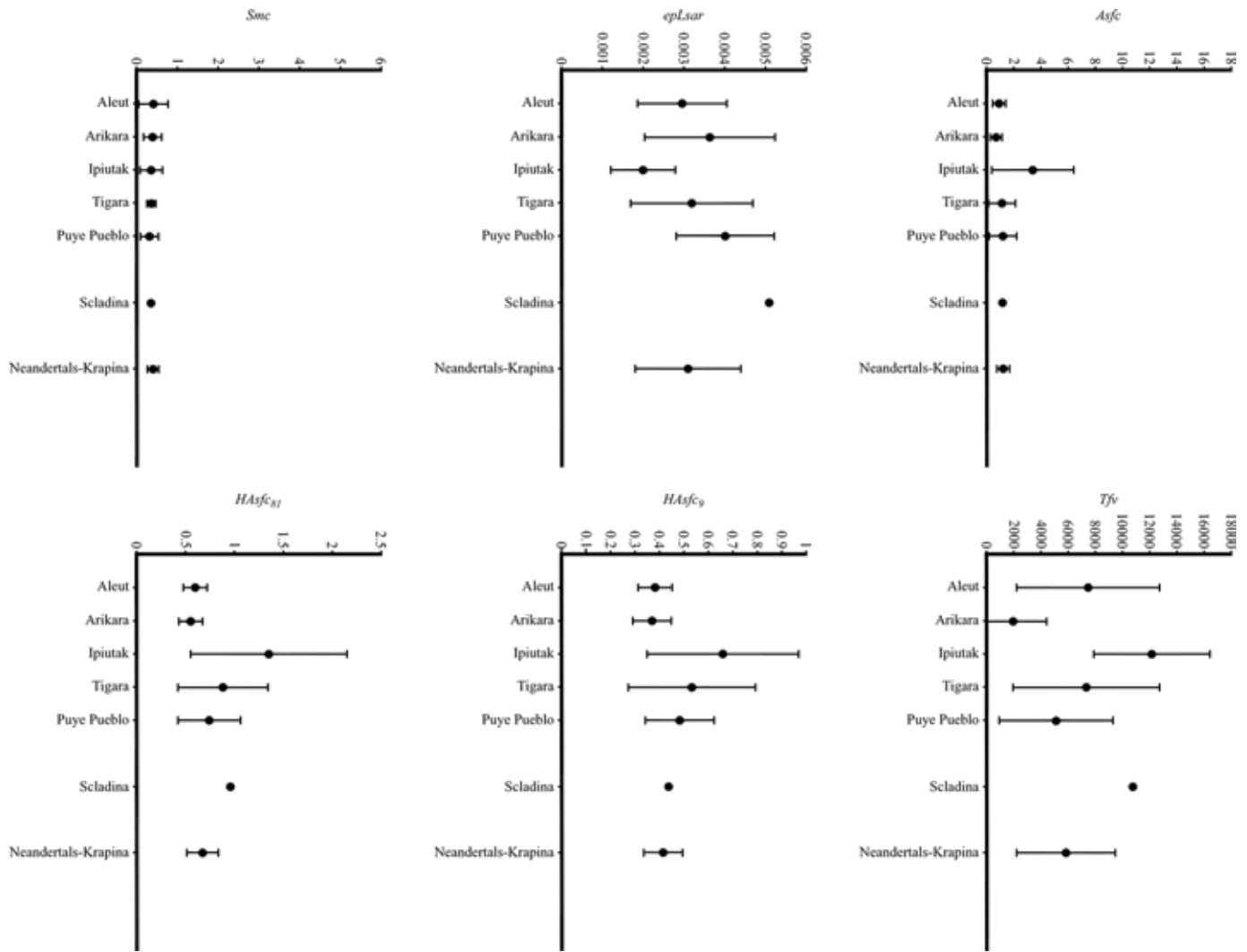


Figure 3: Plots of the means (dots) and one standard deviation ranges (bars) for the anterior dental microwear texture variables for Scladina and the modern human and Neandertal comparative groups.

4.4. Textural fill volume

The Scladina canine textural fill volume is 10,778.82. This Tfv value falls within the range of the Ipiutak, Tigara, and Aleut, i.e., all the arctic comparative samples used in this study, and outside the ranges of the Arikara and the Puye Pueblo. It is higher than the mean Krapina Neandertal value, and also falls outside the range of this sample.

The textural fill volume value for the Scladina molar falls within the ranges of one standard deviation of the means of the Aleut, Arikara, and Tigara from the recent human groups, as well as the Neandertals from open and mixed habitats, and outside the ranges of the remaining recent human groups and the Neandertals from wooded habitats.

4.5. Heterogeneity

The Scladina canine heterogeneity 3×3 and 9×9 values are 0.44 and 0.97. The 3×3 value is closest to the mean of the Puye Pueblo from the modern comparative samples. Yet, this value also falls within the ranges of the Tigara and Ipiutak from Point Hope. The Scladina canine 3×3 value is also very close to the mean of the Krapina Neandertal sample. On the other hand, the 9×9 value is closest to the mean of the Tigara sample, but it also falls within the one standard deviation ranges of the means of the Ipiutak and Puye Pueblo. The Scladina canine 9×9 value is not only considerably higher than the mean of the Krapina Neandertals, but is also above the range for this sample.

The heterogeneity value ($HAsfc'$) of the Scladina molar falls within the one standard

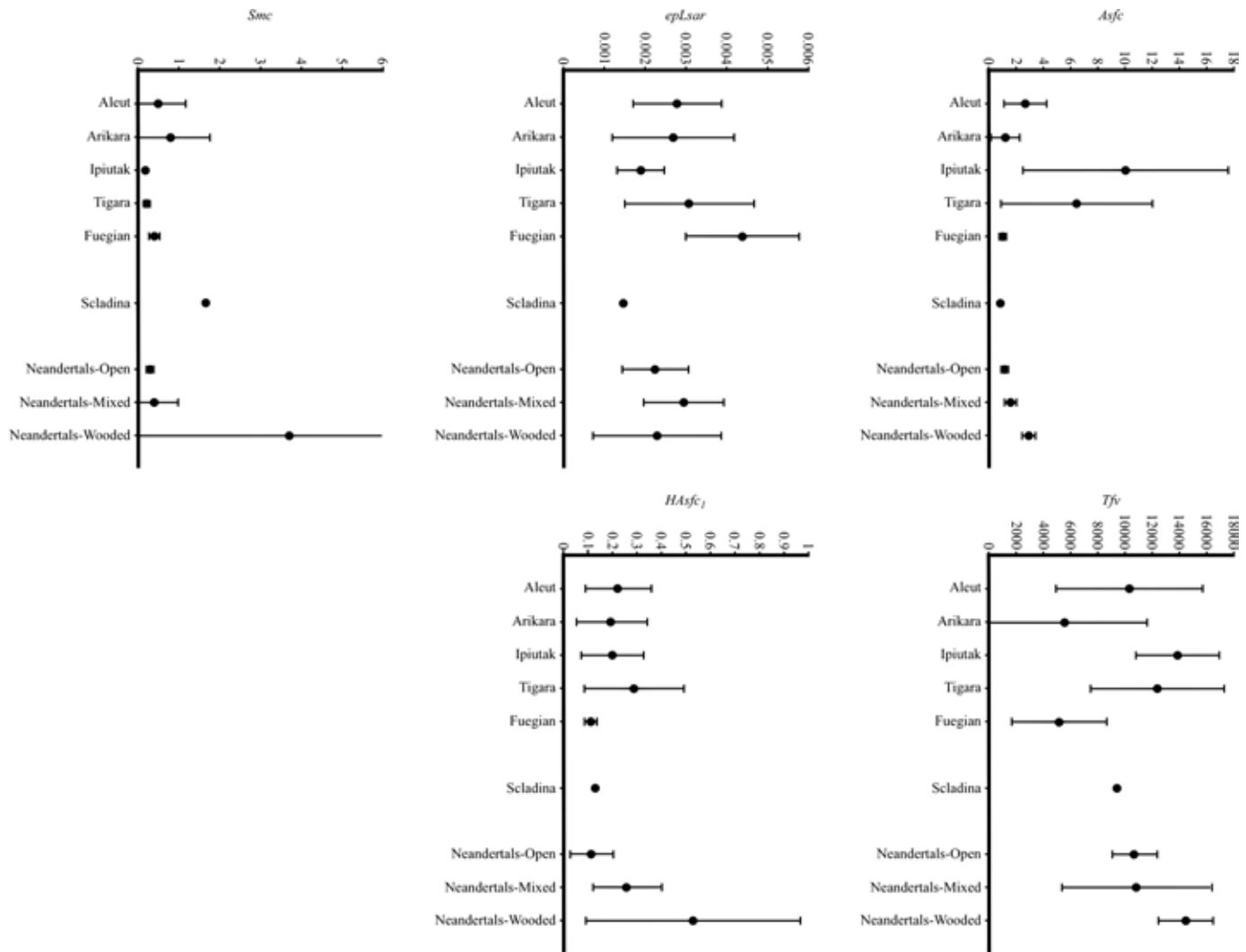


Figure 4: Plots of the means (dots) and one standard deviation ranges (bars) for the molar microwear texture variables for Scladina and the modern human and Neandertal comparative groups.

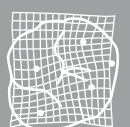
deviation of the mean ranges of all the recent human and the Neandertal groups analyzed.

5. Discussion

5.1. Anterior dental microwear textures

Microwear texture analysis of anterior dentition in bioarchaeological modern human groups with known dietary and non-dietary anterior tooth use behaviors have shown that the different microwear texture variables reflect these behaviors (KRUEGER & UNGAR, 2010; KRUEGER, 2011). The anisotropy variable has been demonstrated to be good at distinguishing non-dietary from dietary anterior tooth use behaviors (KRUEGER & UNGAR, 2010; KRUEGER, 2011). Specifically, the samples with low anisotropy values (0.0032 and lower) are those that are documented as using their anterior dentition in

non-dietary behaviors. On the other hand, those with higher values are the samples that only use their anterior dentition for dietary purposes, such as incising a food item (KRUEGER & UNGAR, 2010; KRUEGER, 2011). Textural fill volume has been associated with anterior loading regimes (KRUEGER, 2011). Those samples with high textural fill volume values indicate high anterior loading, while those with low values suggest the opposite (KRUEGER, 2011). Both Point Hope samples as well as the Aleut have high texture fill volume values. These samples are documented to have participated in high loading regimes which were related to various uses of the anterior dentition in non-dietary behaviors. Heterogeneity 3×3 and 9×9 has been linked to coarse- and fine-scale abrasive particle density and size, respectively (KRUEGER & UNGAR, 2010; KRUEGER, 2011). If the heterogeneity values are high, exposure to abrasives were also high, and vice versa. Complexity values of anterior dentition have been linked to two factors:



1) the level of abrasive exposure and 2) the level of non-dietary anterior tooth use behaviors (KRUEGER, 2011). Thus, if both factors are high or low, complexity will be high or low, respectively. If one factor is high, then complexity will be moderate. Lastly, the *Smc* variable has not been shown to be particularly useful for distinguishing samples in anterior dental microwear studies, and will not be discussed further here.

Overall, in comparison to the modern human samples, the Scladina Neandertal anterior microwear texture values for anisotropy, texture fill volume, and heterogeneity 9×9 are relatively high, while those for heterogeneity 3×3 and complexity are relatively moderate. The relatively very high Scladina Neandertal anisotropy value and its congruence only with the Puye Pueblo and Arikara, the two samples that used their anterior dentition solely for dietary purposes, strongly indicates only dietary use of the anterior dentition. Similarly, the high textural fill volume value of the Scladina Neandertal suggests that this individual participated in high anterior loading regimes, yet its relatively high anisotropy value indicates that these anterior loads were most likely associated with incising tough food items rather than non-dietary anterior tooth use behaviors. Both heterogeneity values for the Scladina individual fall within the ranges of the modern human comparative groups that were exposed to relatively high amounts of dietary and environmental abrasive loads (i.e., Puye Pueblo, and the two Point Hope samples). This suggests that the Scladina Juvenile was also exposed to a relatively high amount of environmental and/or dietary abrasive loads. The Scladina canine complexity value is relatively moderate. Yet, since other texture values do not suggest non-dietary anterior tooth use behaviors for the Scladina Neandertal, this is not a factor here. Thus, the moderate value of the Scladina Neandertal is congruent with high levels of abrasive exposure only.

In comparison to the Krapina Neandertals, the Scladina anterior dental microwear values for heterogeneity 3×3 and complexity fall within the Krapina sample's ranges for these two variables. This suggests that the Scladina Neandertal was exposed to similar amounts of dietary and/or environmental coarse abrasive loads as the Krapina Neandertals. The Scladina values for the remaining variables, i.e., anisotropy, heterogeneity 9×9 , and textural fill volume, are all higher than those of the Krapina Neandertals. This suggests that the Scladina Juvenile engaged in fewer non-dietary

tooth use behaviors and was exposed to relatively higher amounts of fine-scale abrasive loads compared to the Krapina Neandertals. It should be mentioned that the Krapina Neandertal values for these variables reflect a moderate anterior loading regime associated with moderate non-dietary anterior tooth use behaviors and an exposure to relatively low amounts of fine-scale abrasive loads (KRUEGER & UNGAR, 2012).

The results of the anterior microwear texture analysis of the Scladina Neandertal show that, while Neandertals are often associated with non-dietary anterior tooth use behaviors, most often associated with intense clamping and grasping activities, this is not always the case, at least for the Scladina individual. Several explanations can be put forth for the lack of a non-dietary anterior tooth use signal for the Scladina Neandertal. One possible explanation is that perhaps the Scladina Neandertal lived during a relatively warm period of MIS 5 which would have allowed for the release of the anterior dentition from intense non-dietary behaviors that are often affiliated with the processing of hide for protective purposes. Unfortunately, this cannot be confirmed as environmental reconstructions for the layer from which the Scladina Neandertal was recovered are unavailable (see Chapter 5). Another explanation is that the Scladina Neandertal was too young to participate in non-dietary anterior tooth behaviors. Indeed, this individual is approximately eight years old (SMITH et al., 2007), and it remains unknown when sub-adult Neandertals would have fully participated in adult activities. Thus, the anterior dental microwear analysis of the Scladina individual offers a unique look into the dietary and behavioral strategies of Neandertals, and perhaps offers a glimpse into the responsibilities of sub-adults.

5.2. Molar microwear textures

Differences in occlusal molar microwear textures of Recent Modern Human groups were found to be highly correlated with the ethnographically documented or archeologically inferred differences in the diets and food preparation techniques of these groups (EL ZAATARI, 2014). Specifically, the complexity values have been found to be positively correlated with the levels of abrasives (hard brittle items) ingested. These abrasives can either be of dietary nature or can also be extraneous particles (i.e., environmental abrasives

such as sand, grit, etc) that get attached to the food items as a result of food preparation techniques (EL ZAATARI, 2014). To this end, the two Point Hope populations, known to ingest very high amounts of environmental abrasives, have very high complexity values compared to the remaining groups. On the other hand, the anisotropy variable has been found to be linked to the level of consumption of softer, but tougher items, such that a high anisotropy value would indicate the consumption of large amounts of tough foods compared to hard foods (EL ZAATARI, 2014). The high anisotropy value of the Fuegians compared to the rest of the modern human samples analyzed illustrates the relation between the anisotropy variable and the consumption of tough foods relative to abrasive foods. Unlike the other groups, the Fuegians' based their subsistence almost exclusively on meat (a relatively tough dietary item) that was generally free of dietary and environmental abrasives. The scale of maximum complexity was found to be mostly correlated with the size of the wear causing particles (EL ZAATARI, 2014). The two Point Hope populations who ingested substantial amounts of small sand particles along with their food were found to have the lowest, as well as the least dispersed, values for scale of maximum complexity among the groups analyzed. On the other hand, the Arikara whose diet consisted of different kinds of plant food abrasives were found to have the highest scale of maximum complexity mean value and the most dispersion in individual values for this variable among the groups analyzed (EL ZAATARI, 2014). Textural fill volume values are most likely affected by two factors, the amount and size of the abrasive particles. A high textural fill volume value would indicate a large consumption of abrasive particles or a consumption of very hard abrasive particles that would cause deep features on the occlusal molar surface (EL ZAATARI, 2014). The heterogeneity variable has not been found to be a differentiating factor among the recent human populations analyzed to date (EL ZAATARI, 2014). But, studies of non-human primates have suggested this variable to be associated with the level of individual dietary variability. Ingesting different kinds of particles would increase the variability in microwear texture across the tooth surface, and thus would lead to a higher heterogeneity value (SCOTT et al., 2012).

Compared to the recent human samples, the relatively low surface complexity of the Scladina molar and its similarity to those of individuals

belonging to two of the recent human samples, the Fuegians and the Arikara, whose diets consisted of the smallest amount of abrasives among the groups analyzed, reflects a diet focused on softer foods with a low level of abrasives for the Scladina Neandertal. The low anisotropy value of the Scladina molar suggests that this juvenile's diet did not consist exclusively of tough foods. Indeed, The Scladina molar has anisotropy value that is substantially lower than the Fuegians' values, but falls within the lower range of values of the Arikara, a group that is known to have consumed substantial amounts of dried bison meat (a tough food item) along with dietary abrasives for its subsistence. The Scladina molar textural fill volume value is relatively intermediate. This most likely reflects large abrasive particles since, as illustrated by the complexity value, the diet of the Scladina Child did not consist of large amounts of abrasives. The ingestion of large size abrasive particles by the Scladina Child is also supported by its relatively large scale of maximum complexity value. This value is substantially higher than individuals from Point Hope whose diets consisted of large amounts of small extraneous grit and sand particles and similar to specimens from the Arikara group, whose diet consisted of abrasives of dietary nature. Overall, the molar microwear texture indicates that the diet of the Scladina Child consisted of a mix of soft and tough food items along with some abrasive items that were most likely dietary rather than environmental in nature. Stable isotope analyses have indicated a meat based diet for this Neandertal (BOCHERENS et al., 1999, 2001). The results of this study are in accord with this reconstruction since meat is generally a soft, but tough food item. Yet, the microwear data also reveals that the diet of the Scladina Child most likely included small amounts of abrasive plant foods as well.

The Neandertal groups from different palaeo-ecological conditions were best distinguished based on the complexity and heterogeneity variables. For the complexity variable, the low value of the Scladina Juvenile is most similar to adult Neandertals from open habitats. The Scladina heterogeneity value falls within the range of the Neandertals from open as well as wooded habitats. Yet, it is much closer to the mean of the former rather than that of the latter. Neandertals from wooded habitats were found to have a relatively wide dispersion of values most likely reflecting a high level of variation in individual dietary variability. The relatively low heterogeneity value for



the Scladina Juvenile reflects a diet consisting of low variability in food items ingested by this child. Unfortunately, palaeoenvironmental reconstructions are unavailable for the layers of the Scladina site that yielded the Neandertal juvenile (see Chapter 5). Thus, it remains unclear whether the similarity in molar microwear textures between the Scladina Juvenile and the adult Neandertals from open habitats is simply a reflection of dietary similarity in similar environmental conditions or whether it was linked to other factors such as the young age of this individual.

6. Conclusions

In this study the microwear textures of the anterior and molar dentition of the Scladina Neandertal were analyzed and compared to those of bioarchaeological human populations as well as adult Neandertals. The aim of this study was to gain insights into the diet and behavior of the Scladina Juvenile. The results of this study show that the Scladina Neandertal used his/her anterior dentition solely for dietary purposes and that this child did not practice non-dietary anterior tooth use behaviors. Concerning diet, the microwear textures of the Scladina Child show that the diet of this Neandertal can be best described as having consisted of a mix of soft and tough foods in addition to some amounts of dietary abrasives. Also, the anterior dental microwear texture results suggest that some of the foods ingested by this child required a high anterior loading regime. Synthesizing these data, perhaps the Scladina Neandertal was subsisting on dried meat. Incising such a foodstuff would require a high anterior loading regime. Once in the oral cavity, it would be tough, but as the saliva and molars break it down chemically and mechanically, respectively, it would become soft. This is just one explanation of many possible ideas, and perhaps further research can shed more light. Overall, the dental microwear analysis of the Scladina individual offered a unique look into the dietary and behavioral strategies of Neandertals, and perhaps also offered a glimpse into the diets and responsibilities of sub-adults.

Acknowledgements

We would like to thank Michel Toussaint for inviting us to participate in this volume. We are grateful for Peter Ungar for providing access to the microscope facilities at the Department of

Anthropology at the University of Arkansas at Fayetteville. This study was supported by the Max Planck Society and the National Science Foundation DDIG Program (#0925818), and Hunt Post-doctoral Fellowship (#8554).

References

- BALIKCI A., 1970. *The Netsilik Eskimo. Prospect Heights*. Natural History Press, 264 p.
- BARNES E., 1994. Puye and the Pajarito: historical background. In E. BARNES (ed.), *Developmental Defects of the Axial Skeleton in Paleopathology*. Boulder, University of Colorado Press, 298–317.
- BARROSO RUIZ C., MARCHI F., ABDESSADOK S., BAILÓN S., DESCLAUX E., GRÉGOIRE S., HERNANDEZ CARRASQUILLAS F., LACOMBAT F., LEBRETON V. & LECERVOISIER B., 2006. Contexte paléocologique, paléoclimatique et paléogéographique des Néandertaliens de la grotte du Boquete de Zafarraya. In C. BARROSO RUIZ & H. DE LUMLEY (eds.), *La grotte du Boquete de Zafarraya (Málaga, Andalousie): Junta de Andalucía, Consejería de Cultura*: 1127–1166.
- BELMAKER M. & HOVERS E., 2008. A diachronic study of the micromammal remains of Amud Cave, Israel: implications for the paleoecology of a Neanderthal site during MIS 4-3 in the Levant. *Abstracts of the 73rd Society for American Archaeology Meeting*: 75.
- BLAKESLEE D. J., 1994. The archaeological context of human skeletons in the northern and central Plains. In D. W. OWSLEY & R. L. JANTZ (eds.), *Skeletal Biology in the Great Plain: Migration, Warfare, Health and Subsistence*. Washington, DC, Smithsonian Institution Press: 9–32.
- BOCHERENS H., BILLIOU D., MARIOTTI A., PATOU-MATHIS M., OTTE M., BONJEAN D. & TOUSSAINT M., 1999. Palaeoenvironmental and palaeodietary implications of isotopic biogeochemistry of late interglacial Neandertal and mammal bones in Scladina Cave (Belgium). *Journal of Archaeological Science*, 26: 599–607.
- BOCHERENS H., BILLIOU D., MARIOTTI A., TOUSSAINT M., PATOU-MATHIS M., BONJEAN D. & OTTE M., 2001. New isotopic evidence for dietary habits of Neandertals from Belgium. *Journal of Human Evolution*, 40: 497–505.
- BOCHERENS H. & DRUCKER D. G., 2003. Reconstructing Neandertal diet from 120,000 to 30,000 BP using carbon and nitrogen isotopic abundances. In M. PATOU-MATHIS &

- H. BOCHERENS (eds.), *Le rôle de l'environnement dans les comportements des chasseurs-cueilleurs préhistoriques*. Actes du XIV^{ème} Congrès de l'Union Internationale des Sciences Préhistoriques et Protohistoriques, Section 3: Paléoécologie. Colloque C3.1., Université de Liège, Belgique, 2-8 septembre 2001, Oxford, British Archaeological Reports, International Series, 1105: 1-7.
- BOCHERENS H., DRUCKER D. G., BILLIOU D., PATOU-MATHIS M. & VANDERMEERSCH B., 2005. Isotopic evidence for diet and subsistence pattern of the Saint-Césaire I Neanderthal: review and use of a multi-source mixing model. *Journal of Human Evolution*, 49: 71-87.
- BŒUF O., 1969. Faune et nouveaux restes humains du gisement moustérien du Petit-Puyrouseau (Charente). *Mémoires de la Société Archéologique et historique de la Charente*: 53-128.
- BOUCHUD J., 1966. *Essai sur le Renne et la climatologie du Paléolithique moyen et supérieur*. Périgueux, Imprimerie Magne, 300 p.
- BRACE C. L., 1967. Environment, tooth form and size in the Pleistocene. *Journal of Dental Research*, 46: 809-816.
- BRACE C. L., 1975. Comment on: Did La Ferrassie I use his teeth as a tool? *Current Anthropology*, 16: 396-397.
- BRACE C. L., RYAN A. S. & SMITH B. H., 1981. Comment: tooth wear in La Ferrassie man. *Current Anthropology*, 22: 426-430.
- BRIDGES T., 1885. The Yahgans of Tierra del Fuego. *Journal of the Royal Anthropological Institute*, 14: 288-289.
- BRUBAKER M., BERNER J., BELL J., WARREN J. & ROLIN A., 2010. *Climate change in Point Hope, Alaska: strategies for community health*. Alaska Native Tribal Health Consortium, Center for climate and Health, 44 p.
- COLTRAIN J. B., 2010. Temporal and dietary reconstruction of past Aleut populations: stable- and radio-isotope evidence revisited. *Arctic*, 63: 391-398.
- CORDY J.-M., 1988. Apport de la paléozoologie à la paléoécologie et à la chronostratigraphie en Europe du nord-occidental. In H. LAVILLE (ed.), *L'Homme de Néandertal, vol. 2: L'Environnement*. Études et Recherches Archéologiques de l'Université de Liège, 29: 55-64.
- CYBULSKI J. S., 1974. Tooth wear and material culture: precontact patterns in the Tsimshian area, British Columbia. *Syesis*, 7: 31-35.
- DABBS G. R., 2009. *Health and nutrition at prehistoric Point Hope, Alaska: application and critique of the Western Hemisphere Health Index*. University of Arkansas, 215 p.
- DE PONCINS G., 1941. *Kabloona Reynal*. New York, Reynal & Hitchcock Incorporated, 339 p.
- EISENMANN V., 1992. Systematic and biostratigraphical interpretation of the equids from Qafzeh, Tabun, Skhul and Kebara (Acheuloyabrudian to Upper Paleolithic of Israel). *Archaeozoologica*, 1: 43-62.
- EL ZAATARI S., 2010. Occlusal microwear texture analysis and the diets of historical/prehistoric hunter-gatherers. *International Journal of Osteoarchaeology*, 20: 67-87.
- EL ZAATARI S., 2014. The diets of the Ipiutak and Tigara (Point Hope, Alaska): evidence from occlusal molar microwear texture analysis. In C. HILTON, B. AUERBACH & L. COWGILL (eds.), *The Foragers of Point Hope: the biology and archaeology of humans on the edge of the Alaskan arctic*. Cambridge University Press: 120-137.
- EL ZAATARI S., GRINE F. E., UNGAR P. S. & HUBLIN J.-J., 2011. Ecogeographic variation in Neandertal dietary habits: evidence from occlusal microwear texture analysis. *Journal of Human Evolution*, 61: 411-424.
- EL ZAATARI S., HARVATI K. & PANAGOPOULOU E., 2013. Occlusal molar microwear texture analysis: the method and its application for the dietary reconstruction of the Lakonis Neandertal. In S. VOUTSAKI & S.-M. VALAMOTI (eds.), *Subsistence, Economy and Society in the Greek World*. Louvain. Peeters Publishers: 55-63.
- FELLAG H., 1996. Étude palynologique de l'abri paléolithique Bourgeois-Delaunay (Chaise, Charente). *Quaternaire*, 7: 187-196.
- FOOTE B. A., 1992. *The Tigara Eskimos and their Environment*. North Slope Borough, Commission on Inupiat History, Language and Culture, Point Hope, AK, 190 p.
- FORTEA J., DE LA RASILLA M., MARTÍNEZ E., SÁNCHEZ-MORAL S., CAÑAVÉRAS J. C., CUEZVE S., ROSAS A., SOLER V., JULIA R., DE TORRES T., 2003. La cueva de El Sidrón (Borines, Piloña, Asturias): primeros resultados. *Estudios Geológicos*, 59: 159-179.



- GIDDINGS J. L., 1967. *Ancient Men of the Arctic*. London, Secher and Warburg, 391 p.
- GROSS H., 1956. Die Umwelt des Neandertaler. In K. TACKENBERG (ed.), *Der Neandertaler und seine Umwelt. Gedenkschrift zur Erinnerung an die Auffindung im Jahre 1856*. Bonn, Rheinisches Landesmuseum Bonn und Verein von Altertumsfreunden im Rheinlande: 68-105.
- HENRI-MARTIN G., 1966. Découverte d'un temporel humain néandertalien dans le gisement de La Quina, Charente. *Comptes rendus de l'Académie des sciences*, 262: 1937-1939.
- HEWETT E. L., 1938. *Pajarito Plateau and Its Ancient People*. Albuquerque, University of New Mexico Press, 191 p.
- HOFFMAN K. L., 1993. *Unalaska Aleut subsistence adaptations at the time of early Russian contact as represented in the Reese Bay artifact assemblage*. Fayetteville, University of Arkansas, 1122 p.
- HRDLIČKA A., 1945. *The Aleutian and Commander Islands and their Inhabitants*. Philadelphia, Wistar Institute of Anatomy and Biology, 630 p.
- HURT W. R., 1969. Seasonal economic and settlement patterns of the Arikara. *Plains Anthropology*, 14: 32-37.
- JANTZ R. L., 1973. Microevolutionary change in Arikara crania: multivariate analysis. *American Journal of Physical Anthropology*, 38: 15-26.
- JELINEK A. J., FARRAND W. R., HAAS G., HOROWITZ A. & GOLDBERG P., 1973. New excavations at the Tabun Cave, Mount Carmel, Israel 1967-1972. *Paléorient*, 1: 151-183.
- KARAVANIĆ I., 2004. The Middle Paleolithic settlement of Croatia. In N. J. CONARD (ed.), *Settlement Dynamics of the Middle Paleolithic and Middle Stone Age*, 2, Tübingen, Kerns Verlag: 185-200.
- KOLSKA HORWITZ L. & HONGO H., 2006. Putting the meat back on old bones. A reassessment of Middle Palaeolithic fauna from Amud Cave (Israel). In E. VILLA, L. GOURICHON, A. M. CHOYKE & H. BUITENHUIS (eds.), *Archaeozoology of the Near East, VIII*, Proceedings of the eighth international Symposium on the Archaeozoology of southwestern Asia and adjacent areas. Travaux de la Maison de l'Orient et de la Méditerranée, 49: 45-64.
- KOTSAKIS T., 1990-1991. Late Pleistocene fossil microvertebrates of Grotta Breuil (Monte Circeo, central Italy). *Quaternaria Nova*, I: 325-332.
- KRUEGER K. L., 2011. *Dietary and behavioral strategies of Neandertals and anatomically modern humans: evidence from anterior dental microwear texture analysis*. PhD thesis, University of Arkansas, 346 p.
- KRUEGER K. L., 2014. Contrasting dietary and behavioral strategies of the Ipiutak and Tigara: evidence from incisor microwear texture analysis. In C. HILTON, B. AUERBACH & L. COWGILL (eds.), *The Foragers of Point Hope: the biology and archaeology of humans on the edge of the Alaskan arctic*. Cambridge University Press: 99-119.
- KRUEGER K. L., SCOTT J. R., KAY R. F. & UNGAR P. S., 2008. Technical note: Dental microwear textures of "Phase I" and "Phase II" facets. *American Journal of Physical Anthropology*, 137: 485-490.
- KRUEGER K. L. & UNGAR P. S., 2010. Incisor microwear textures of five bioarcheological groups. *International Journal of Osteoarchaeology*, 20: 549-560.
- KRUEGER K. L. & UNGAR P. S., 2012. Anterior dental microwear texture analysis of the Krapina Neandertals. *Central European Journal of Geosciences*, 4: 651-662.
- LALUEZA-FOX C. & FRAYER D. W., 1997. Non-dietary marks in the anterior dentition of the Krapina Neanderthals. *International Journal of Osteoarchaeology*, 7: 133-149.
- LARSEN H. & RAINEY F. G., 1948. *Ipiutak and the Arctic Whale Hunting Culture*. New York, Anthropological Papers of the American Museum of Natural History, 42, 486 p.
- LAUGHLIN W. S., 1963. Eskimos and Aleuts: their origins and evolution. *Science*, 142: 633-645.
- LAVAUD-GIRARD F., 1993. Macrofauna from the Castelperronian Levels at Saint-Césaire, Charente-Maritime. In F. LÉVÊQUE, A. M. BACKER & M. GUILBAUD (eds.), *Context of a Late Neandertal: Implications of Multidisciplinary Research for the Transition to Upper Paleolithic Adaptations at Saint-Césaire, Charente-Maritime, France*. Madison, Prehistory Press: 71-77.
- LEIGH R. W., 1925. Dental pathology of Indian tribes of varied environmental and food conditions. *American Journal of Physical Anthropology*, 8: 179-199.
- LEROI-GOURHAN A., 1988. Le passage Moustérien-Châtelperronien à Arcy-sur-Cure. *Bulletin de la Société préhistorique française*, 85: 102-104.

- LEROYER C. & LEROI-GOURHAN A., 1993. Pollen analysis at Saint-Césaire. In F. LÉVÊQUE, A. M. BACKER & M. GUILBAUD (eds.), *Context of a Late Neandertal*. Madison, Prehistory Press: 61–70.
- LESTER C. W. & SHAPIRO H. L., 1968. Vertebral arch defects in the lumbar vertebrae of pre-historic American Eskimos. *American Journal of Physical Anthropology*, 28: 43–48.
- LUKACS J. R. & PASTOR R. F., 1988. Activity-induced patterns of dental abrasion in prehistoric Pakistan: evidence from Mehrgarh and Harappa. *American Journal of Physical Anthropology*, 76: 377–398.
- MANZI G., 1986. I Fuegini del Museo di Antropologia dell'Università di Roma “La Sapienza”: Significato di una collezione osteologica. *Museologia Scientifica* V, supplemento: 43–54.
- MARQUET J.-C., 1988. L'Homme de Néandertal et son environnement dans la moitié ouest de la France d'après les rongeurs. In H. LAVILLE (ed.), *L'Homme de Néandertal, vol. 2: L'Environnement*. Études et Recherches Archéologiques de l'Université de Liège, 29: 105–110.
- MARQUET J.-C., 1993. *Paléoenvironnement et Chronologie des Sites du Domaine Atlantique Français d'Âge Pléistocène Moyen et Supérieur d'Après l'Étude des Rongeurs*. Tours, Les Cahiers de la Claise, 2, 344 p.
- MAYES A. T., 2001. *Patterns through time: interactions between changes in subsistence and human dentition at Illinois Bluff, Jersey County, Illinois, and Spiro Mounds, Oklahoma*. University of Colorado, 428 p.
- MEYER R. W., 1977. *The Village Indians of the Upper Missouri*. Lincoln, NE, University of Nebraska Press, 354 p.
- MIRACLE P. T., LENARDIĆ J. M. & BRAJKOVIĆ D., 2010. Last glacial climates, “Refugia”, and faunal change in Southeastern Europe: Mammalian assemblages from Veternica, Velika pećina, and Vindija caves (Croatia). *Quaternary International*, 212: 137–148.
- MISKOVSKY J.-C. & LÉVÊQUE F., 1993. The sediments and stratigraphy of Saint-Césaire: contributions to the paleoclimatology of the site. In F. LÉVÊQUE, A. M. BACKER & M. GUILBAUD (eds.), *Context of a Late Neandertal: Implications of Multidisciplinary Research for the Transition to Upper Paleolithic Adaptations at Saint-Césaire, Charente-Maritime, France*. Madison, Prehistory Press: 7–14.
- MOORREES C. F. A., 1957. *The Aleut Dentition: A Correlative Study of Dental Characteristics in an Eskimoid People*. Cambridge, Harvard University Press, 196 p.
- MORIN E., 2004. *Late Pleistocene population interaction in western Europe and modern human origins: new insights based on the faunal remains from Saint-Césaire, southwestern France*. Unpublished PhD thesis, University of Michigan, 450 p.
- PANAGOPOULOU E., KARKANAS P., TSARTSIDOU G., KOTJABOPOULOU E., HARVATI K. & NTINOU M., 2002–2004. Late Pleistocene Archaeological and Fossil Human Evidence from Lakonis Cave, Southern Greece. *Journal of Field Archaeology*, 29: 323–349.
- PATOU-MATHIS M., 1993. Taphonomic and palaeoethnographic study of the fauna associated with the Neandertal of Saint-Césaire. In F. LÉVÊQUE, A. M. BACKER & M. GUILBAUD (eds.), *Context of a Late Neandertal: Implications of Multidisciplinary Research for the Transition to Upper Paleolithic Adaptations at Saint-Césaire, Charente-Maritime, France*. Madison, Prehistory Press: 79–102.
- PRIDEAUX G. J., AYLIFFE L. K., DESANTIS L. R. G., SCHUBERT B. W., MURRAY P. F., GAGAN M. K. & CERLING T. E., 2009. Extinction implications of a chenopod browse diet for a giant Pleistocene kangaroo. *Proceedings of the National Academy of Sciences of the United States of America*, 106, 28: 11646–11650.
- RABINOVICH R. & HOVERS E., 2004. Faunal analysis from Amud Cave: preliminary results and interpretations. *International Journal of Osteoarchaeology*, 14: 287–306.
- RECCHI A., 1995. Bird remains from the Upper Pleistocene sites of Grotta Breuil (M. Circeo, Latina, Italy) and Riparo Salvini (Terracina, Latina, Italy). *Quaternaria Nova*, V: 81–98.
- RICHARDS M. P., PETTITT P. B., TRINKAUS E., SMITH F. H., PAUNOVIĆ M. & KARAVANIĆ I., 2000. Neanderthal diet at Vindija and Neanderthal predation: the evidence from stable isotopes. *Proceedings of the National Academy of Sciences of the United States of America*, 97, 13: 7663–7666.
- RICHARDS M. P. & TRINKAUS E., 2009. Isotopic evidence for the diets of European Neanderthals and early modern humans. *Proceedings of the National Academy of Sciences of the United States of America*, 106, 38: 16034–16039.



- RINK W. J., SCHWARCZ H. P., LEE H. K., REES-JONES J., RABINOVICH R. & HOVERS E., 2001. Electron Spin Resonance (ESR) and Thermal Ionization Mass Spectrometric (TIMS) $^{230}\text{Th}/^{234}\text{U}$ dating of teeth in Middle Paleolithic layers at Amud Cave, Israel. *Geoarchaeology*, 16: 701-717.
- RINK W. J., SCHWARCZ H. P., SMITH F. H. & RADOVČIĆ J., 1995. ESR ages for Krapina hominids. *Nature*, 378: 24.
- RYAN A. S., 1980. Anterior dental microwear in Neanderthals. *American Journal of Physical Anthropology*, 52: 274.
- SCHWARTZ J. H. & TATTERSALL I., 2002. *The Human Fossil Record: Terminology and Craniodental Morphology of Genus Homo (Europe)*. New York, Wiley-Liss.
- SCOTT R. S., TEAFORD M. F. & UNGAR P. S., 2012. Dental Microwear Texture and Anthropoid Diets. *American Journal of Physical Anthropology*, 147: 551-579.
- SCOTT R. S., UNGAR P. S., BERGSTROM T. S., BROWN C. A., CHILDS B. E., TEAFORD M. F. & WALKER A., 2006. Dental microwear texture analysis: technical considerations. *Journal of Human Evolution*, 51: 339-349.
- SCOTT R. S., UNGAR P. S., BERGSTROM T. S., BROWN C. A., GRINE F. E., TEAFORD M. F. & WALKER A., 2005. Dental microwear texture analysis shows within-species diet variability in fossil hominins. *Nature*, 436: 693-695.
- SIMEK J. F. & SMITH F. H., 1997. Chronological changes in stone tool assemblages from Krapina (Croatia). *Journal of Human Evolution*, 32: 561-575.
- SMITH P., 1976. Dental pathology in fossil hominids: what did Neanderthals do with their teeth? *Current Anthropology*, 17: 149-151.
- SMITH T. M., TOUSSAINT M., REID D. J., OLEJNICZAK A. J. & HUBLIN J.-J., 2007. Rapid dental development in a Middle Paleolithic Belgian Neanderthal. *Proceedings of the National Academy of Sciences of the United States of America*, 104, 51: 20220-20225.
- SNOW W. P., 1861. A few remarks on the wild tribes of Tierra del Fuego from personal observation. *Transactions of the Ethnological Society*, 1: 261-267.
- SPETH J. D. & TCHERNOV E., 1998. The role of hunting and scavenging in Neandertal procurement strategies: new evidence from Kebara Cave (Israel). In T. AKAZAWA, K. AOKI & O. BAR-YOSEF (eds.), *Neandertals and Modern Humans in Western Asia*. New York, Plenum Press: 223-239.
- SPETH J. D. & TCHERNOV E., 2001. Neandertal hunting and meat-processing in the Near East: Evidence from Kebara Cave (Israel). In C. B. STANFORD & H. T. BUNN (eds.), *Meat-Eating and Human Evolution*. Oxford University Press: 52-72.
- SPETH J. D. & TCHERNOV E., 2002. Middle Paleolithic tortoise use at Kebara Cave (Israel). *Journal of Archaeological Science*, 29: 471-483.
- STEWART T. D., 1959. The restored Shanidar I skull. *The Annual Report of the Smithsonian Institution for 1958*: 473-480.
- STINER M. C., 1994. *Honor Among Thieves*. Princeton University Press, 447 p.
- TOURNEPICHE J.-F. & COUTURE C., 1999. The Hyena den of Rochelot Cave (Charente, France). *Monographien des Römisch-Germanischen Zentralmuseums*, 42: 89-101.
- TRIERWEILER W. N., 1990. *Prehistoric Tewa Economy: Modeling Subsistence Production on the Pajarito Plateau*. New York, Garland Publishing.
- TUROSS N. & FOGEL M. L., 1994. Stable isotope analysis and subsistence patterns at the Sully Site. In D. W. OWSLEY & R. L. JANTZ (eds.), *Skeletal Biology of the Great Plain: Migration, Warfare, Health and Subsistence*. Washington, DC, Smithsonian Institution Press: 283-289.
- UNGAR P. S., MERCERON G. & SCOTT R. S., 2007. Dental microwear texture analysis of Varswater bovids and early Pliocene paleoenvironments of Langebaanweg, Western Cape Province, South Africa. *Journal of Mammalian Evolution*, 14: 163-181.
- UNGAR P. S., SCOTT J. R., SCHUBERT B. W. & STYNDER D. D., 2010. Carnivoran dental microwear textures: comparability of carnassial facets and functional differentiation of postcanine teeth. *Mammalia*, 74: 219-224.
- WALLACE J. A., 1975. Did La Ferrassie I use his teeth as a tool? *Current Anthropology*, 16: 393-401.
- WOLPOFF M. H., 1979. The Krapina dental remains. *American Journal of Physical Anthropology*, 50: 67-114.
- YESNER D. R., FIGUERERO TORRES M. J., GUICHON R. A., & BORRERO L. A., 2003. Stable isotope analysis of human bone and ethnohistoric subsistence patterns in Tierra del Fuego. *Journal of Anthropological Archaeology*, 22: 279-291.

Chapter 19

NEANDERTAL EVOLUTION AND HUMAN ORIGINS: A TALE FROM THE SCLADINA I-4A CHILD

Ludovic ORLANDO & Catherine HÄNNI

*Michel Toussaint & Dominique Bonjean (eds.), 2014.
The Scladina I-4A Juvenile Neandertal (Andenne, Belgium),
Palaeoanthropology and Context
Études et Recherches Archéologiques de l'Université de Liège, 134: 379-394.*

Foreword

The following article was written soon after the publication of the first genetic analysis of the Scladina Neandertal Child (Orlando et al., 2006). By then — it was in 2006 — sequencing even short DNA pieces from ancient material represented a big challenge. It is still true to some extent as ancient DNA molecules are nowhere near the long stretches of millions of As, Cs, Gs and Ts (nucleotides) that constitute our chromosomes. Those molecules are rather extremely fragmented into 50-100 nucleotide chunks at best and are also chemically degraded, which makes their analysis particularly difficult (Paabo et al., 2004). However, the recent years have experienced a massive technological revolution. First, so-called next-generation sequencing platforms can now generate millions to billions of sequences in a cost- and time- effective manner. This, coupled with sound bioinformatic procedures, makes it possible to identify the minority of sequences that come from the Neandertal individual as opposed to the majority of those originating from environmental microbes that colonized its bones and teeth after death (Schubert et al., 2012, 2014; Der Sarkissian et al., 2014). Second, novel methods have been developed in ancient DNA research facilitating access to (Dabney et al., 2013; Meyer et al., 2014), and possibly even enriching for ancient molecules (Briggs et al., 2009; Burbano et al., 2010). This resulted in an unexpected blossoming characterization of ancient genomes (Rasmussen et al., 2010, 2011, 2014; Keller et al., 2012; Raghavan et al., 2014) that recently culminated with the characterization of the complete genome from a horse that lived 700 ka BP ago, and for Neandertals, the complete genome sequence of no more than several individuals from Croatia (Green et al., 2010), the Caucasus and the Altai (Prüfer et al., 2014). We know today the genome of Neandertals, as well as that of other archaic hominins, called Denisovans (Reich et al., 2010; Meyer et al., 2012). The sequencing of the genome of the pre-Neandertal *Homo heidelbergensis* is on its way (Meyer et al., 2014; Orlando, 2014). At the same time, our knowledge and understanding of the genetic diversity present amongst modern human populations has improved (The 1000 Genomes Project Consortium 2012). Therefore, the sequence information available now is order of magnitude greater than what we knew back in 2006. The 123 nucleotides characterized from the mitochondrial DNA of the Scladina Child represent only 0.000004% of the information present in its genome! Therefore, and not surprisingly, what we know today from our relationships with Neandertals goes well beyond the conclusions that we could draw in 2006. In particular, we know now that Neandertals and non-African modern humans share an excess of derived (non-chimp-like) mutations (Green et al., 2010; Prüfer et al., 2014). Although alternative models could explain this pattern (Yang et al., 2012; Eriksson and Manica, 2014), this probably indicates that Neandertal and modern human population outside of Africa admixed, most likely around 50 thousand years ago (Sankararaman et al., 2012). This contradicts the picture as depicted by mitochondrial DNA alone, where Neandertals and modern humans appeared as two distinct entities. This is because mitochondrial DNA can only track one single genealogy



where the genome reflects a large number of independent genealogies as recombination makes every single gene/locus independent. We can even scan our own genome for segments of Neandertal origin (Sankararaman et al., 2014; Vernot & Akey, 2014)! We also know, as hypothesized following the genetic analysis of the Scladina Child, that Neandertal populations were limited demographically and harbored only low levels of genetic diversity (Prüfer et al., 2014). Therefore, the value of the following article is mostly historical, as it ultimately illustrates that knowledge is a moving target and thereby showcases the profound changes in paradigm that we experienced over the last few years. There are still many things left to discover about our past and our relationships with Neandertals: there is no doubt that the Scladina Child, who lived in Belgium at a time when modern humans did not yet discover the European continent, could potentially help solve some of the final pieces of the puzzle!

Ludovic Orlando, April 2014.

References

- Briggs A. W., Good J. M., Green R. E., Krause J., Maricic T., Stenzel U., Lalueza-Fox C., Rudan P., Brajkovic D., Kucan Z., Gusic I., Schmitz R., Doronichev V. B., Golovanova L. V., de la Rasilla M., Fortea J., Rosas A. & Pääbo S., 2009. Targeted retrieval and analysis of five Neandertal mtDNA genomes. *Science*, 325, 5938: 318–321.
- Burbano H. A., Hodges E., Green R. E., Briggs A. W., Krause J., Meyer M., Good J. M., Maricic T., Johnson P. L., Xuan Z., Rooks M., Bhattacharjee A., Brizuela L., Albert F. W., de la Rasilla M., Fortea J., Rosas A., Lachmann M., Hannon G. J. & Pääbo S., 2010. Targeted investigation of the Neandertal genome by array-based sequence capture. *Science*, 328, 5979: 723–725.
- Dabney J., Knapp M., Glocke I., Gansauge M. T., Weihmann A., Nickel B., Valdiosera C., García N., Pääbo S., Arsuaga J. L. & Meyer M., 2013. Complete mitochondrial genome sequence of a Middle Pleistocene cave bear reconstructed from ultrashort DNA fragments. *Proceedings of the National Academy of Sciences of the United States of America*, 110, 39: 15758–15763.
- Der Sarkissian C., Ermini L., Jónsson H., Alekseev A. N., Crubezy E., Shapiro B. & Orlando L., 2014. Shotgun microbial profiling of fossil remains. *Molecular Ecology*, 23, 7: 1780–1798.
- Eriksson A. & Manica A., 2014. The Doubly-Conditioned Frequency Spectrum Does Not Distinguish between Ancient Population Structure and Hybridization. *Molecular Biology and Evolution*, doi: 10.1093/molbev/msu103.
- Green R. E., Krause J., Briggs A. W., Maricic T., Stenzel U., Kircher M., Patterson N., Li H., Zhai W., Fritz M. H., Hansen N. F., Durand E. Y., Malaspina A. S., Jensen J. D., Marques-Bonet T., Alkan C., Prüfer K., Meyer M., Burbano H. A., Good J. M., Schultz R., Aximu-Petri A., Butthof A., Höber B., Höffner B., Siegemund M., Weihmann A., Nusbaum C., Lander E. S., Russ C., Novod N., Affourtit J., Egholm M., Verna C., Rudan P., Brajkovic D., Kucan Z., Gusic I., Doronichev V. B., Golovanova L. V., Lalueza-Fox C., de la Rasilla M., Fortea J., Rosas A., Schmitz R. W., Johnson P. L., Eichler E. E., Falush D., Birney E., Mullikin J. C., Slatkin M., Nielsen R., Kelso J., Lachmann M., Reich D. & Pääbo S., 2010. A draft sequence of the Neandertal genome. *Science*, 328, 5979: 710–722.
- Keller A., Graefen A., Ball M., Matzas M., Boisguerin V., Maixner F., Leidinger P., Backes C., Khairat R., Forster M., Stade B., Franke A.,

- Mayer J., Spangler J., McLaughlin S., Shah M., Lee C., Harkins T. T., Sartori A., Moreno-Estrada A., Henn B., Sikora M., Semino O., Chiaroni J., Rootsi S., Myres N. M., Cabrera V. M., Underhill P. A., Bustamante C. D., Vigil E. E., Samadelli M., Cipollini G., Haas J., Katus H., O'Connor B. D., Carlson M. R., Meder B., Blin N., Meese E., Pusch C. M. & Zink A., 2012. New insights into the Tyrolean Iceman's origin and phenotype as inferred by whole-genome sequencing. *Nature Communications*, 3, article number 698, doi: 10.1038/ncomms1701.
- Meyer M., Fu Q., Aximu-Petri A., Glocke I., Nickel B., Arsuaga J. L., Martínez I., Gracia A., de Castro J. M., Carbonell E. & Pääbo S., 2014. A mitochondrial genome sequence of a hominin from Sima de los Huesos. *Nature*, 505: 403–406.
- Meyer M., Kircher M., Gansauge M. T., Li H., Racimo F., Mallick S., Schraiber J. G., Jay F., Prüfer K., de Filippo C., Sudmant P. H., Alkan C., Fu Q., Do R., Rohland N., Tandon A., Siebauer M., Green R. E., Bryc K., Briggs A. W., Stenzel U., Dabney J., Shendure J., Kitzman J., Hammer M. F., Shunkov M. V., Derevianko A. P., Patterson N., Andrés A. M., Eichler E. E., Slatkin M., Reich D., Kelso J. & Pääbo S., 2012. A high-coverage genome sequence from an archaic Denisovan individual. *Science*, 338, 6104: 222–226.
- Orlando L., 2014. A 400,000-year-old mitochondrial genome questions phylogenetic relationships amongst archaic hominins: Using the latest advances in ancient genomics, the mitochondrial genome sequence of a 400,000-year-old hominin has been deciphered. *Bioessays*, doi: 10.1002/bies.201400018.
- Orlando L., Darlu P., Toussaint M., Bonjean D., Otte M. & Hänni C., 2006. Revisiting Neandertal diversity with a 100,000 year old mtDNA sequence. *Current Biology*, 16: R400–R402.
- Pääbo S., Poinar H., Serre D., Jaenicke-Despres V., Hebler J., Rohland N., Kuch M., Krause J., Vigilant L. & Hofreiter M., 2004. Genetic analyses from ancient DNA. *Annual Review of Genetics*, 38: 645–679.
- Prüfer K., Racimo F., Patterson N., Jay F., Sankararaman S., Sawyer S., Heinze A., Renaud G., Sudmant P. H., de Filippo C., Li H., Mallick S., Dannemann M., Fu Q., Kircher M., Kuhlwilm M., Lachmann M., Meyer M., Ongyerth M., Siebauer M., Theunert C., Tandon A., Moorjani P., Pickrell J., Mullikin J. C., Vohr S. H., Green R. E., Hellmann I., Johnson P. L., Blanche H., Cann H., Kitzman J. O., Shendure J., Eichler E. E., Lein E. S., Bakken T. E., Golovanova L. V., Doronichev V. B., Shunkov M. V., Derevianko A. P., Viola B., Slatkin M., Reich D., Kelso J. & Pääbo S., 2014. The complete genome sequence of a Neanderthal from the Altai Mountains. *Nature*, 505: 43–49.
- Raghavan M., Skoglund P., Graf K. E., Metspalu M., Albrechtsen A., Moltke I., Rasmussen S., Stafford T. W. Jr, Orlando L., Metspalu E., Karmin M., Tambets K., Rootsi S., Mägi R., Campos P. F., Balanovska E., Balanovsky O., Khusnutdinova E., Litvinov S., Osipova L. P., Fedorova S. A., Voevoda M. I., DeGiorgio M., Sicheritz-Ponten T., Brunak S., Demeshchenko S., Kivisild T., Villems R., Nielsen R., Jakobsson M. & Willerslev E., 2014. Upper Palaeolithic Siberian genome reveals dual ancestry of Native Americans. *Nature*, 505: 87–91.
- Rasmussen M., Anzick S. L., Waters M. R., Skoglund P., DeGiorgio M., Stafford T. W. Jr, Rasmussen S., Moltke I., Albrechtsen A., Doyle S. M., Poznik G. D., Gudmundsdottir V., Yadav R., Malaspina A. S., White S. S. 5th, Allentoft M. E., Cornejo O. E., Tambets K., Eriksson A., Heintzman P. D., Karmin M., Korneliussen T. S., Meltzer D. J., Pierre T. L., Stenderup J., Saag L., Warmuth V. M., Lopes M. C., Malhi R. S., Brunak S., Sicheritz-Ponten T., Barnes I., Collins M., Orlando L., Balloux F., Manica A., Gupta R., Metspalu M., Bustamante C. D., Jakobsson M., Nielsen R. & Willerslev E., 2014. The genome of a Late Pleistocene human



- from a Clovis burial site in western Montana. *Nature*, 506: 225–229.
- Rasmussen M., Guo X., Wang Y., Lohmueller K. E., Rasmussen S., Albrechtsen A., Skotte L., Lindgreen S., Metspalu M., Jombart T., Kivisild T., Zhai W., Eriksson A., Manica A., Orlando L., De La Vega F. M., Tridico S., Metspalu E., Nielsen K., Ávila-Arcos M. C., Moreno-Mayar J. V., Muller C., Dortch J., Gilbert M. T., Lund O., Wesolowska A., Karmin M., Weinert L. A., Wang B., Li J., Tai S., Xiao F., Hanihara T., van Driem G., Jha A. R., Ricaut F. X., de Knijff P., Migliano A. B., Gallego Romero I., Kristiansen K., Lambert D. M., Brunak S., Forster P., Brinkmann B., Nehlich O., Bunce M., Richards M. P., Gupta R., Bustamante C. D., Krogh A., Foley R. A., Lahr M. M., Balloux F., Sicheritz-Pontén T., Vilems R., Nielsen R., Wang J. & Willerslev E., 2011. An Aboriginal Australian genome reveals separate human dispersals into Asia. *Science*, 334, 6052: 94–98.
- Rasmussen M., Li Y., Lindgreen S., Pedersen J. S., Albrechtsen A., Moltke I., Metspalu M., Metspalu E., Kivisild T., Gupta R., Bertalan M., Nielsen K., Gilbert M. T., Wang Y., Raghavan M., Campos P. F., Kamp H. M., Wilson A. S., Gledhill A., Tridico S., Bunce M., Lorenzen E. D., Binladen J., Guo X., Zhao J., Zhang X., Zhang H., Li Z., Chen M., Orlando L., Kristiansen K., Bak M., Tommerup N., Bendixen C., Pierre T. L., Grønnow B., Meldgaard M., Andreasen C., Fedorova S. A., Osipova L. P., Higham T. F. G., Ramsey C. B., Hansen T. V., Nielsen F. C., Crawford M. H., Brunak S., Sicheritz-Pontén T., Vilems R., Nielsen R., Krogh A., Wang J. & Willerslev E., 2010. Ancient human genome sequence of an extinct Palaeo-Eskimo. *Nature*, 463: 757–762.
- Reich D., Green R. E., Kircher M., Krause J., Patterson N., Durand E. Y., Viola B., Briggs A. W., Stenzel U., Johnson P. L., Maricic T., Good J. M., Marques-Bonet T., Alkan C., Fu Q., Mallick S., Li H., Meyer M., Eichler E. E., Stoneking M., Richards M. P., Talamo S., Shunkov M. V., Derevianko A. P., Hublin J.-J., Kelso J., Slatkin M. & Pääbo S., 2010. Genetic history of an archaic hominin group from Denisova Cave in Siberia. *Nature*, 468: 1053–1060.
- Sankararaman S., Mallick S., Dannemann M., Prüfer K., Kelso J., Pääbo S., Patterson N. & Reich D., 2014. The genomic landscape of Neanderthal ancestry in present-day humans. *Nature*, 507: 354–357.
- Sankararaman S., Patterson N., Li H., Pääbo S. & Reich D., 2012. The date of interbreeding between Neandertals and modern humans. *Public Library of Science, Genetics*, 8, 10: e1002947, doi: 10.1371/journal.pgen.1002947.
- Schubert M., Ermini L., Sarkissian C. D., Jónsson H., Ginolhac A., Schaefer R., Martin M. D., Fernández R., Kircher M., McCue M., Willerslev E. & Orlando L., 2014. Characterization of ancient and modern genomes by SNP detection and phylogenomic and metagenomic analysis using PALEOMIX. *Nature Protocols*, 9, 5: 1056–1082.
- Schubert M., Ginolhac A., Lindgreen S., Thompson J. F., Al-Rasheid K. A., Willerslev E., Krogh A. & Orlando L., 2012. Improving ancient DNA read mapping against modern reference genomes. *BioMed Central (BMC) Genomics*, 13: 178.
- The 1000 Genomes Project Consortium, 2012. An integrated map of genetic variation from 1,092 human genomes. *Nature*, 491: 56–65.
- Vernot B. & Akey J. M., 2014. Resurrecting surviving Neandertal lineages from modern human genomes. *Science*, 343, 6174: 1017–1021.
- Yang M. A., Malaspina A. S., Durand E. Y. & Slatkin M., 2012. Ancient structure in Africa unlikely to explain Neanderthal and non-African genetic similarity. *Molecular Biology and Evolution*, 29: 2987–2995.

1. Introduction

In Europe as a whole, Neandertals and modern humans have coexisted from 42-28 ka BP (MELLARS, 2006; FINLAYSON, et al., 2006). Though the coexistence took place only in some parts of the continent, it might have provided enough time for interbreeding (SMITH et al. 1999; HUBLIN, 2000). Between 1997 and 2006, sequences of mtDNA hypervariable regions (HVR) have been reported from ten Neandertal specimens dated 42-28 ka BP from Feldhofer (Germany), Mezmaiskaya (northern Caucasus), Vindija (Croatia), Engis (Belgium), La Chapelle-aux-Saints (France), Rochers-de-Villeneuve (France) and El Sidron (Spain) (KRINGS et al., 1997; KRINGS et al. 1999; OVCHINNIKOV et al., 2000; KRINGS et al., 2000; SCHMITZ et al., 2002; LALUEZA-FOX et al., 2005). Comparison with modern humans and chimpanzees revealed that Neandertal haplotypes were more similar to humans than chimpanzees but fall outside the range of modern human genetic diversity, making any suggestion that Neandertals contributed to the mitochondrial gene pool of contemporary humans through interbreeding highly unlikely (CURRAT & EXCOFFIER, 2004). Furthermore, the facts that (i) Neandertal sequences show no preferential regional affinity with Europeans and (ii) that the divergence between Neandertals and modern humans well predated the origin of the current mitochondrial diversity of modern humans have been taken as key arguments for the validity of the Rapid Replacement Model (also called 'Out of Africa').

These interpretations have been criticized though. For instance, RELETFORD (2001^{ab}) has convincingly demonstrated that the lack of regional affinity between Neandertals and modern Europeans does not preclude multiregionalism as multiregional evolution is *not* independent from regional evolution. Archaic human populations (including the European Neandertals) remained rather interconnected by gene flow across the Old World (RELETFORD, 1999). And actually, even low levels of continued gene flows result in equivalent accumulated Neandertal ancestry for any kind of modern human population according to migration matrix theory (RELETFORD, 2001^{a, b}). Another critic relied on the fact that Neandertals have been compared with current (and not ancient) modern humans, leaving open the possibility for recent elimination of Neandertal-like sequences from the modern human gene pool as a consequence of demographic events (NORDBORG,

1998) or selective sweeps (HAWKS & WOLPOFF, 2001). Methodological concerns have also been raised since the models used for reconstructing phylogenies did not take into account possible homoplastic effects occurring on numerous mutational hotspots described in mtDNA hypervariable regions. Yet a reanalysis of the sequence data under appropriate models has surprisingly suggested that Neandertals "would be more akin to modern humans than what recent claims suggest" (GUTTIEREZ et al., 2002).

Hence, at this point, it was clear that more data were needed for the debate to progress. Albeit they came from dispersed locations over the whole Neandertal geographic range (west to east from Spain to the Caucasus, and north to south from Belgium to Croatia), all the Neandertal specimens that delivered genetic information belonged to the Oxygen Isotopic Stage 3. Older Neandertal specimens would offer the opportunity to get insights into the long-time evolution of the Neandertal gene pool by comparison with other Neandertal sequences. As such, it could reveal possible drastic changes or long-time stability at the time of cohabitation and give insights into the Rapid Replacement/Multiregionalism debate. We therefore decided to retrieve the first sequence information from a Neandertal related to Oxygen Isotopic Stage 5 by analyzing the remains of the Scladina Child. It is true though two Neandertal bones predating the contact with modern humans in Europe (>50 and 100-110 ka BP from Warendorf-Neuwarendorf (Germany) and Krapina (Croatia) were already used for southern-blotting experiments (SCHOLZ et al., 2000). However, the southern hybridization approach suffers from serious flaws and has been shown to be misleading (GEIGL, 2001). Therefore, so far, the Scladina Child is the sole Neandertal specimen that has delivered authenticated DNA sequence information related to Oxygen Isotopic Stage 5 (ORLANDO et al., 2006).

2. Results

2.1. Sequence authenticity

We took advantage of previously reported Neandertal sequences to use primers that favour the amplification of Neandertal DNA. PCR was never successful when fragments larger than 173 bp were targeted as expected for ancient templates (Box 1). We amplified four fragments spanning 221 bp of the mtDNA HVR-I. Each PCR



Ancient DNA: applications, pitfalls and experimental procedure

Ancient DNA technology offers the unique opportunity to recover genetic information from the past (for the last 500,000 years at best). As such, it opens the door for an incredibly wide range of applications. Of course, the prehistoric megafauna, with its innumerable bone and tooth remains preserved in caves, has represented a precious source of DNA so far (e.g. cave bears, woolly rhinos and giant elks in HÄNNI et al., 1994; ORLANDO et al., 2003; HUGHES et al., 2006). But besides, ancient human individuals (HANDT et al., 1996) as well as plant seeds (JAENICKE-DESPRÈS et al., 2003) or pieces of wood (DEGUILLLOUX et al., 2002), microbes (DRANCOURT et al., 1998) and ancient viruses (TUMPEY et al., 2005), coprolithes (POINAR et al., 2003) and even Pleistocene sediments (WILLERSLEV et al., 2003) have also delivered nucleotidic sequences, providing valuable information as for the kinship among individuals inside necropoles (KOLMAN & TUROSS, 2000), the tempo and mode of the domestication process (ZEDER et al., 2006) or the consequences of global climate on biodiversity (eg. species richness: WILLERSLEV et al., 2004; or population diversity: VAN TUINEN et al., 2004).

However, recovering ancient DNA is by no standard a straightforward process, mainly because of the chemical nature of ancient molecules in itself. DNA decay indeed starts the very moment an organism dies. Hydrolytic reactions contribute to extensive fragmentation of the DNA backbone (in molecules barely longer than 200 nucleotides), to local loss of sequence information (eg. through base elimination, such as depurination) and even to subtle changes in sequence information (e.g. Cytosine modified in Uracile as a result of a local deamination; LINDAHL, 1993). These features considerably complicate the recovery of ancient DNA molecules and extensive laboratory work (including rigorous technical procedures as well as redundant experimental controls) is generally requested before any ancient DNA molecules can be authenticated (GILBERT et al., 2005).

Briefly, the extraction procedure is conducted in a laboratory specially devoted to ancient DNA work. It consists in an overpressurized lab where (i) work surfaces are bleached, (ii) DNA-free materials are used and (iii) no modern DNA is stored or manipulated ever. After a typical extraction procedure (sample powdering and decalcification followed by DNA purification and concentration), the total amount of ancient DNA molecules that can be retrieved is generally not sufficient for sequencing. Therefore, an amplification step by Polymerase Chain Reaction (PCR) is most of the times required. The PCR is a cycling-amplification process which restores minute traces of a chosen part of the genome into billions of copies. The specificity of the reaction is due to short oligonucleotides (DNA primers) that can act as probes for the targeted DNA locus. Whenever it is possible, the sequence of the primers is chosen to target specifically the DNA of interest. But given the very degraded nature of ancient DNA fragments, fresh DNA contaminants very often outcompete their ancient counterparts during the PCR process if primer annealing is possible. Therefore, contamination — and false positive amplification — is one of the most serious concern in palaeogenetics and scrupulous controls are requested to insure the bona-fide DNA was actually amplified (and not contaminant by-products).

Note that PCR is often problematic when dealing with ancient templates. Molecules present in the soil as well as bone constituents *per se* (such as the protein Collagen type I) are coextracted with DNA molecules and act as *Taq* polymerase inhibitors, preventing any amplification (SCHOLZ et al., 2000). Moreover, Maillard reactions may lead to covalent bond formation between DNA and sugar residues during the taphonomic process, resulting in templates unsuitable for *Taq* elongation. Lastly, artefactual mutations can be generated by PCR because some bases are turned into others in the course of the taphonomic process. The most prevalent of these DNA-damage induced errors leads to GC \Rightarrow AT mutations (HOFREITER et al., 2001^a; GILBERT et al., 2006; STILLER et al., 2006). Consequently, no aDNA sequence can be deduced from a single amplification product but must be checked through multiple amplification replications to be trusted. Moreover, the cloning (and sequencing) of each PCR product is also highly recommended to pinpoint each artefactual mutations along the sequence. All these experimental procedures were respected for determining the DNA sequence of the Scladina Child. One supplemental precaution was undertaken: the DNA extract was treated with an enzyme (namely Uracile-DNA Glycosylase, UDG) to discard all DNA substrates carrying the artefactual Uraciles (HOFREITER et al., 2001^a). Therefore, PCR products were generated starting from Uracile-free DNA templates and were highly unlikely to bear artefactual mutations.

product was cloned and the final sequence was deduced from the consensus of 61 clones. But given the age of the sample and material limitation, we managed to amplify the most 5' and 3' fragments only once; thus, the 39-first and 59-last nucleotides have been respectively deduced from the sequences of 8 and 12 clones from only one amplification product. These sites exhibit 5 substitutions never observed between the already published Neandertal sequences: 2 C \Rightarrow T, 2 G \Rightarrow A and one T \Rightarrow C. Though some polymorphism has already been observed in the same part of the HVR-I among other Neandertal sequences (eg. one A/C transversion and one C/T transition) and the DNA extract was treated with Uracil DNA-Glycosylase (to eliminate artefactual GC \rightarrow AT substitutions, Box 1), we decided to discard the sequence information present in the 39-bp and 59-bp terminal parts of the Scladina sequence, leaving 123 bp of sequence information. Therefore, the final sequence of the Scladina Child consists only on nucleotide positions that have been recovered from at least two (up to four) independent PCR products. As a consequence, the final sequence can be considered as truly authentic and none of the polymorphic sites (with regards to other Neandertal sequences) can be regarded as artefactual mutations (i.e. DNA-damage induced errors, Box 1). Notably, none of these polymorphic sites has been found in any of the coworkers (Box 2) (nor in the *Homo sapiens* sequences found in some of the amplifications), which makes it highly unlikely that the Scladina sequence – obtained through combination of four overlapping PCR fragments – results from mosaic association of PCR contaminants, as it has been already suggested for other ancient sequences (BANDELT, 2005). Likewise, sequence differences between the Scladina sequence and other Neandertal sequences are not located in any of the sites demonstrated by GILBERT et al. (2003) as being highly affected by postmortem degradation in humans.

Furthermore, we are confident that the environmental conditions in Scladina Cave are particularly prone to biomolecule preservation (and therefore to DNA preservation). Cave bear bones from the same excavation layer as the Neandertal child, or from even older layers (former Layer 5, LOREILLE et al., 2001; ORLANDO et al., 2002) already delivered authentic ancient DNA. Moreover, 70–60 ka BP old nuclear DNA sequences were successfully amplified from woolly rhinoceroses from Scladina (ORLANDO et al., 2003). Lastly, carbon and nitrogen isotopic

survey of one maxillary sample from the Scladina Neandertal has revealed an atomic C/N ratio typical of well-preserved collagen (BOCHERENS et al., 1999).

2.2. Comparison with available Neandertal sequences

The sequence of the Scladina Child has not been found among the 7161 human HVR-I sequences present in the HvrBase++. It appears more distantly related to the Cambridge Reference Sequence (1 insertion/deletion, 14 substitutions along 123 sites) than to the sequences from other Neandertal specimens (3–4 substitutions). Within the 123 bp of sequence information, only 1 substitution distinguished the previously reported Neandertal sequences. Therefore, the Scladina sequence reveals that the genetic diversity of Neandertals has been previously underestimated.

2.3. Phylogenetic analyses

Sequence comparisons were conducted with the 171 human HVR-I sequences used in GUTTIEREZ et al. (2002) as a representative subset of the overall human diversity. A supplemental dataset of 8 chimp haplotypes was used as outgroup. The selected models of molecular evolution accurately estimate nucleotide substitution parameters and takes into account rate heterogeneity among sites (Figure 1). When chimpanzee sequences are used as outgroups, all Neandertals cluster apart modern humans, in a monophyletic group with substantial bootstrap-support (67%). When chimpanzee sequences are excluded as in SCHMITZ et al. (2002), the separation between Neandertal and modern human lineages is supported by almost maximum bootstrap values (99%). Importantly, these results confirm previous claims of early divergence between Neandertal and modern human lineages and appear in sharp contrast to Gutierrez and colleagues's report of "no support for a branch separating the Neandertal cluster from the human sequences" (GUTTIEREZ et al., 2002).

2.4. Pairwise comparisons

Pairwise distances were estimated using the best phylogenetic model of nucleotide substitution and rate heterogeneity (HKY+G+I). According to the Rapid Replacement Model, the sequence from Scladina, being 70–60 ka BP closer to the MRCA



Ancient or modern human DNA? The contamination case

The study of ancient DNA in human remains is plagued by problems caused by contamination of specimens since virtually all human fossils have been handled by human beings (before any DNA extraction is started). PCR experiments have clearly shown that human mtDNA sequences can be virtually retrieved from almost every ancient animal specimen. For instance, not less than 20 different modern human signatures could be retrieved from a 30,000-year-old bear tooth (Upper Cave, Zhoukoudian, China) using human-specific PCR primers (HOFREITER et al., 2001^b). Monitoring human and dog mtDNA in dog bones and teeth from the Neolithic and medieval periods, MALMSTRÖM et al. (2005) systematically found the presence of human DNA, often at levels exceeding the amount of authentic endogenous DNA. Likewise, dot blot experiments revealed the presence of human DNA in a large diversity of animal fossils (NICHOLSON et al., 2002). Genomic data from skeletal remains of a 40,000-year-old cave bear (NOONAN et al., 2005) and a 27,000-year-old mammoth (POINAR et al., 2006) have more recently identified a significant presence of DNA of human origin.

Because the surface is the only part of the sample that is exposed to human contamination sources, it has been advocated to scrap the surface of human fossils or to bleach it with hypochlorite solution before DNA extraction to eliminate the false positive results such a contamination may lead to. Deliberate contamination of samples (by constant handling for 10 min at 30°C to maximize sweating and therefore DNA transfer) have indeed revealed low penetration of contamination sequences inside fossils (MALMSTRÖM et al., 2005). However, it is frequent to recover contaminant DNA on human samples, though scraped (KOLMAN & TUROSS, 2000) or bleached (KEMP & SMITH, 2005). Interestingly, GILBERT et al. (2005) have shown Havers canals and dental tubules offer appropriate circulation routes for exogenous DNA penetration in bones and teeth. All in all, the authenticity of ancient human sequences may be, most of the time, difficult (if possible) to demonstrate.

One way to circumvent contamination problems would be to excavate human specimens for ancient DNA analysis under strict clean and DNA-free conditions (LALUEZA-FOX et al., 2006). Similarly, choosing the most freshly excavated specimens would lower the rate of contamination with modern human DNA. This strategy was followed for the genetic analysis of the Scladina Child. A molar tooth, excavated on 13 November, 2001, was selected for ancient DNA analysis. The tooth-root was sampled in sterile conditions using a power saw. The blade was sterilized in sodium hydroxide 10%; gloves, mobcap, and disposable coat were used. The sequences of all the co-workers that had potentially been in contact with the Neandertal sample was determined in order to trace any contamination from modern humans. Despite such precautions, some modern human sequences were found in the Scladina DNA extract (such was also the case in the very first ancient DNA study on Neandertals; KRINGS et al., 1997). But as all of these could be attributed to one of the coworkers, they could not be mistaken for Neandertal sequences. Moreover, we took advantage of Neandertal specific-primers (designed according to previously reported Neandertal sequences) to favour the amplification of Neandertal DNA by PCR. This procedure allowed to recover an authentic mtDNA sequence of the Scladina Child.

between Humans and Neandertals, should exhibit fewer substitutions than younger Neandertal sequences when compared to contemporary human sequences. According to minimum estimates of the HVR-I substitution rate, at least 3.9% substitution differences are indeed expected between sequences that are 70–60 ka BP distant (EXCOFFIER & YANG, 1999). The observed pattern though, is the opposite: the pairwise distance distributions within humans, and between humans and Neandertals, become closer and overlap more extensively for younger Neandertals (age < 42 ka BP, $P < 0.001$) than for the Scladina specimen (Figure 2). The switch towards a modern

human distribution is however not due to a closer proximity of Neandertals and Europeans after contact, as Europeans do not appear more closely related to Neandertals than humans from other continents are.

3. Discussion

The sequence extracted from the Scladina Child (Figure 3) has revealed unexpected levels of genetic diversity among Neandertals. Since its publication (ORLANDO et al., 2006), this discovery has been further supported.

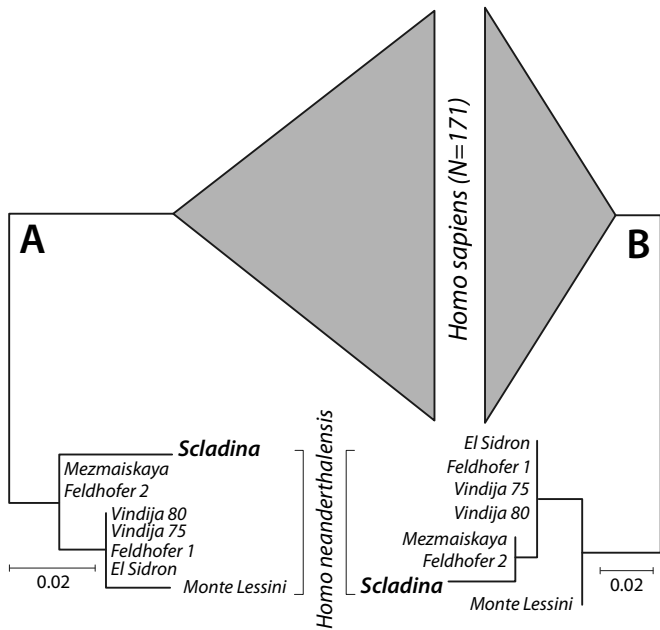


Figure 1: Phylogenetic trees showing the relationships between Neandertal and modern human lineages. (A) Rooted with 8 chimpanzee haplotypes (Maximum of Likelihood: HKY+G4). (B) Rooted according to the midpoint location (Maximum of Likelihood: HKY+G4+I). Phylogenetic trees have been reconstructed under the best model of molecular evolution (see ORLANDO et al., 2006). Note that the branching order among Neandertal lineages is still an open question and will require further information to be definitively solved.

Another Neandertal specimen (Monte Lessini, Italy, 50 ka BP) has been shown to carry another divergent mtDNA haplotype (exhibiting two supplemental polymorphic sites along

the 123 bp in common with the Scladina haplotype; CAMELLI et al., 2006). In spite of this genetic diversity, all Neandertal haplotypes cluster in a monophyletic group that diverged from the human lineage long before the coalescence time of the MRCA of all contemporary humans (Figure 1).

Pairwise mismatch distribution analyses have revealed a second unexpected pattern. Using an unbiased data set of 171 modern human sequences, pairwise distance uncorrected distributions between modern humans and between pairs of modern humans and Neandertal sequences were shown to largely overlap (GUTTIEREZ et al., 2002). This result was confirmed here using distances corrected for heterogeneity between rate of substitutions (ORLANDO et al., 2006, Figure 2). What the sequence from Scladina reveals is that this situation has been shaped between 100 and 42 ka BP (all the Neandertal sequences younger than 42 ka BP are significantly less distant to modern human than the Scladina sequence is; Figure 2).

Selective sweep as well as genetic drift could explain this pattern. The fact that human mtDNA could be subjected to selection has already been hypothesized (HEY, 1997; HEY & HARRIS, 1999). As some mtDNA lineages are preferentially associated with bioenergetic disorders, the regional variation in mtDNA sequences of extant modern humans may have been possibly shaped by natural selection (MISHMAR et al., 2003; RUIZ-PESINI et al., 2004). If more Neandertal-like haplotypes were selected among modern humans in response to similar environmental constraints (e.g. climatic conditions), the gap between modern humans and

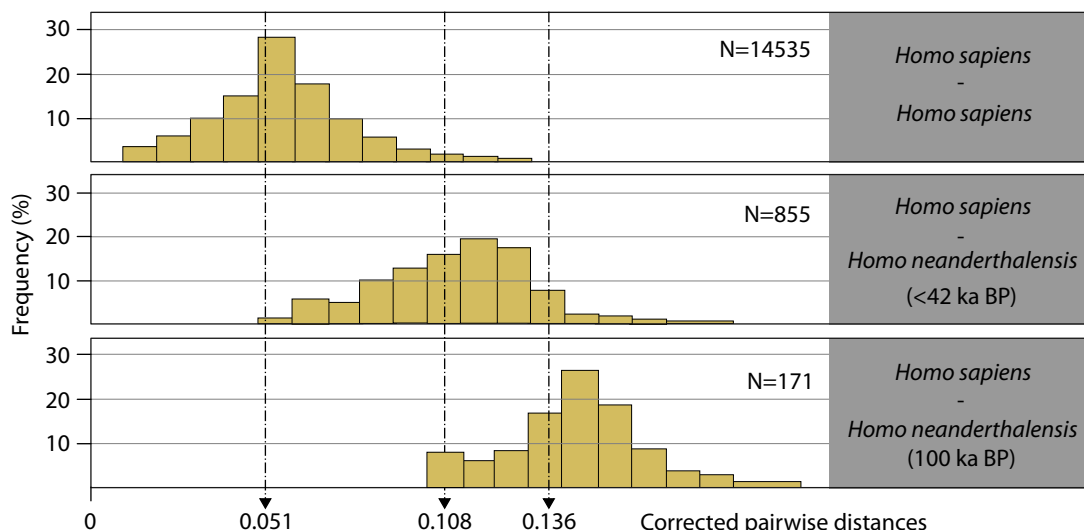


Figure 2: Pairwise mismatch distributions among modern humans or modern humans and Neandertals from different ages.





Figure 3: The sequence extracted from the Scladina Child has revealed unexpected levels of genetic diversity among Neandertals. Pictured left: at the Prehistory Service of the University of Liège, Dominique Bonjean (front) proceeds to the amputation of one root of the Scla 4A-13 molar while Ludovic Orlando prepares the tube that will collect the fragments (photographs Michel Toussaint, February 2002).

Neandertals would be reduced all the more than selection acted for a long time. Yet our data set reveals that the large majority of polymorphic sites might become homoplastic under a selective force. Indeed, only two sites have been fixed between the Neandertal and the modern human gene pools; at positions 16230 and between positions 16263 and 16264, Neandertals exhibit, respectively, A and G whereas modern humans display a gap and an A. By contrast, all polymorphic sites observed between Neandertal sequences are also polymorphic between modern humans. Any selected change on those sites might thus bring modern humans closer to Neandertals.

Genetic drift might alternatively have lead Neandertal and human mtDNA gene pools to become closer at the time Neandertals coexisted with premodern Europeans. Consider first how much the Neandertal mtDNA gene pool was diverse in the past. Now consider a putative demographic bottleneck that Neandertals experienced (for instance, following the competition with premodern humans in Europe till their extinction, or even earlier as a consequence of

the global climatic changes related to the cold Oxygen Isotopic Stage 4 – 74–60 ka BP; AMBROSE, 1998). As for any genetic drift event, less frequent haplotypes are the most probable to be lost; in populations the less frequent haplotypes are the youngest ones, because those have had less time than older ones to expand. Then, after the genetic drift event, the Neandertal haplotypes which are most likely conserved would be those that appeared first, that is the haplotypes more closely related to the MRCA between modern humans and Neandertals. After the drift, the old haplotypes are most likely to have become more frequent in Neandertal populations, which then in turn appeared genetically closer to modern human populations than older Neandertal populations. Interestingly, a recent survey of the regional distribution of SNPs within the complete human genome sequence is consistent with a demographic collapse in human demography at the time of the colonization of Europe (40 ka BP, MARTH et al., 2003).

Though interesting, these results should be taken as very preliminary. Only 2 specimens older

than 50 ka BP have delivered some genetic information so far (Scladina and Monte Lessini) and for all but one of the other specimens (Vi-80), the available genetic information is still reduced. Any inference of the long-term changes in Neandertal genetic diversity remains still very speculative and additional information is required before drawing definitive conclusions.

Perspectives: Neandertal

4. genomics

The Neandertal HVR-I sequences do suggest an early divergence of *Homo neanderthalensis* from *Homo sapiens* and suggest a rather weak (if any) admixture. But as the mtDNA is only maternally inherited, the mitochondrial evidence leave the possibility open that Neandertal father contributed to the modern nuclear gene pool. Recent technological breakthroughs have made it possible to recover nuclear DNA sequences from Neandertal specimens. Two-rounds multiplex-PCRs (Box 3) now allow the recovery of complete nuclear gene and therefore to relate genotype and phenotype for past individuals/species (RÖMPLER et al., 2006). Furthermore, metagenomic screens and high-throughput sequencing technology now make it possible to recover large amounts of genomic information (Box 3). Such genomic data will soon furnish the opportunity to test our possible Neandertal inheritance through both parental lines (GREEN et al., 2006; NOONAN et al., 2006). Moreover, comparative genomics of chimps, Neandertals and modern humans promise to provide the complete list of the functionally important genetic changes that gave rise to our species.

The first complete mtDNA genome from extinct species (two genera of New-Zealand moas) was published in 2001 (COOPER et al., 2001). In the following five years, two mammoth specimens have delivered complete mtDNA genomes (KRAUSE et al., 2005; ROGAEV et al., 2006). Now the first draft of the Neandertal genome may be achieved within the next two years (GREEN et al., 2006). Recent technological breakthroughs clearly represent the way forward and open the hunt for large scale DNA retrieval of other ancient hominids such as the late *Homo floresiensis* (BROWN et al., 2004; MORWOOD et al., 2005). By doing so, ancient DNA will place the 'Rapid Replacement' versus 'Multiregionalism' debate in a broader context than the single Neandertal-*sapiens*

admixture possibility and promises to give invaluable insights on our phylogenetic tree. Hopefully, the remains from the Scladina Child, as part of such projects, will keep on enlightening our own origins.

References

- BACHMANN L., 2001. Reply to Geigl. *American Journal of Human Genetics*, 68: 290-291.
- BANDELT H. J., 2005. Mosaics of ancient mitochondrial DNA: positive indicators of nonauthenticity. *European Journal of Human Genetics*, 13: 1106-1112.
- BOCHERENS H., BILLIOU D., PATOU-MATHIS M., OTTE M., BONJEAN D., TOUSSAINT M. & MARIOTTI A., 1999. Palaeoenvironmental and palaeodietary implications of isotopic biogeochemistry of late interglacial Neandertal and mammal bones in Scladina Cave (Belgium). *Journal of Archaeological Science*, 26: 599-607.
- BROWN P., SUTIKNA T., MORWOOD M. J., SOEJONO R. P., JATMIKO, SAPTOMO E. W. & DUE R. A., 2004. A new small-bodied hominin from the Late Pleistocene of Flores, Indonesia. *Nature*, 431: 1055-1061.
- CARAMELLI D., LALUEZA-FOX C., CONDEMI S., LONGO L., MILANI L., MANFREDINI A., DE SAINT PIERRE M., ADONI F., LARI M., GIUNTI P., RICCI S., CASOLI A., CALAFELL F., MALLEGNI F., BERTRANPETIT J., STANYON R., BERTORELLE G. & BARBUJANI G., 2006. A highly divergent mtDNA sequence in a Neandertal individual from Italy. *Current Biology*, 16: R630-R632.
- COOPER A., RAMBAUT A., MACAULAY V., WILLERSLEV E., HANSEN A. J. & STRINGER C. B., 2001. Human origins and ancient human DNA. *Science*, 292, 5522: 1655-1656. Erratum in 292: 2252.
- CURRAT M. & EXCOFFIER L., 2004. Modern humans did not admix with Neanderthals during their range expansion into Europe. *Public Library of Science, Biology*, 2: e421.
- DEGUILLOUX M. F., PEMONGE M. H. & PETIT R. J., 2002. Novel perspectives in wood certification and forensics: dry wood as a source of DNA. *Proceedings of Biological Sciences*, 269: 1039-1046.
- DRANCOURT M., ABOUDHARAM G., SIGNOLI M., DUTOUR O. & RAOULT D., 1998. Detection of 400-year-old *Yersinia pestis* DNA in human dental



Technological advances and the dawn of Neandertal genomics

What is metagenomics?

Metagenomic DNA libraries are built in a two-step procedure (i.e. insertion, transformation). First, the DNA fragments from a sample are randomly inserted into plasmids (circular DNA of bacterial origin) thanks to DNA recombining technology. Then, each modified plasmid is integrated inside a bacteria (through a process called transformation). During cell divisions, the plasmid is transmitted from mother to daughter cells in bacterial colonies, leading to a clonal amplification of the plasmid. Since the sequence of the plasmid is known, the sequence of the inserted fragment can be determined. Finally, sequence comparison with already available annotated genomes and characterized sequences allow sequence identification. In addition to bona-fide sequences, other types of sequences — mainly from environmental bacteria — are characterized through this process (NOONAN et al., 2005; NOONAN et al., 2006).

High-throughput technology: the 454 sequencing system

Recent high-throughput technological breakthroughs have made the dream of sequencing the whole Neandertal genome a realistic objective. The strategy that delivered so far the most extensive sequence information relies on the 454 Life Science system. Briefly, each DNA fragment from a sample is attached to a bead. Beads are mixed and captured in the droplets of an emulsion where PCR amplification can occur. As a result, each bead is coated with ten million copies of the initial DNA fragment and can be deposited into one of the 1,6 million wells of a fibre-optic PicoTiterPlate for massive parallel pyrosequencing (MARGULIES et al., 2005). Most strikingly, the 454 technology is able to gather 25 million bases of sequence information every four hours which outcompetes by more than 60 times the current capacity of most automatic sequencing instruments. This sequencing system has already succeeded to recover 1-million base of the Neandertal genome from a 100-mg sample (GREEN et al., 2006).

Alternative strategies

One important drawback of both metagenomic library screening and 454 sequencing system is that most of the recovered sequences are environment contaminants. A selective (rather than random) might be more preferable. Using specific human DNA probes could help for fishing Neandertal genes in metagenomic libraries before sequencing, as proposed (and tested) by Noonan and colleagues (2006). Alternatively, two-round multiplex-PCRs could help for targeting genes under selection in modern humans (RÖMPLER et al., 2006). Briefly, a first PCR amplification using large combinations of primers restores numerous DNA fragments to amplifiable levels. Each fragment separately is then amplified separately in a second step. This strategy has recently allowed the characterization of the whole mtDNA genome of the mammoth (KRAUSE et al., 2006) and of the first complete coding sequence of a nuclear gene (RÖMPLER et al., 2006).

pulp: an approach to the diagnosis of ancient septicemia. *Proceedings of the National Academy Science of the United States of America*, 95, 21: 12637-12640.

EXCOFFIER L. & YANG Z., 1999. Substitution rate variation among sites in mitochondrial hyper-variable region I of humans and chimpanzees. *Molecular Biology and Evolution*, 16: 1357-1368.

FINLAYSON C., PACHECO F. G., RODRIGUEZ-VIDAL J., FA D. A., GUTIERREZ LOPEZ J. M., SANTIAGO PEREZ A., FINLAYSON G., ALLUE E., BAENA PREYSLER J., CACERES I., CARRION J. S., FERNANDEZ JALVO Y., GLEED-OWEN C. P., JIMENEZ ESPEJO F. J., LOPEZ P., LOPEZ SAEZ J. A., RIQUELME CANTAL J. A., SANCHEZ MARCO A., GUZMAN F. G., BROWN K., FUENTES N., VALARINO C. A., VILLALPANDO A., STRINGER C. B., MARTINEZ RUIZ F. & SAKAMOTO T.,

2006. Late survival of Neanderthals at the southernmost extreme of Europe. *Nature*, 443: 850–853.
- GEIGL E. M., 2001. Inadequate use of molecular hybridization to analyze DNA in Neanderthal fossils. *American Journal Human Genetics*, 68: 287–290.
- GILBERT M. T., BANDELT H. J., HOFREITER M. & BARNES, I., 2005. Assessing ancient DNA studies. *Trends in Ecology and Evolution*, 20: 541–544.
- GILBERT M. T., BINLADEN J., MILLER W., WIUF C., WILLERSLEV E., POINAR H., CARLSON J. E., LEEBENS-MACK J. H. & SCHUSTER S. C., 2006. Recharacterization of ancient DNA miscoding lesions: insights in the era of sequencing-by-synthesis. *Nucleic Acids Research*, 35: 1–10.
- GILBERT M. T., WILLERSLEV E., HANSEN A. J., BARNES I., RUDBECK L., LYNNERUP N. & COOPER A., 2003. Distribution patterns of postmortem damage in human mitochondrial DNA. *American Journal of Human Genetics*, 72: 32–47. Erratum in 72: 779.
- GREEN R. E., KRAUSE J., PTAK S. E., BRIGGS A. W., RONAN M. T., SIMONS J. F., DU L., EGHOLM M., ROTHBERG J. M., PAUNOVIĆ M. & PÄÄBO S., 2006. Analysis of one million base pairs of Neanderthal DNA. *Nature*, 444: 330–336.
- GUTIERREZ G., SANCHEZ D. & MARI A., 2002. A reanalysis of the ancient mitochondrial DNA sequences recovered from Neanderthal bones. *Molecular Biology and Evolution*, 19: 1359–1366.
- HANDT O., KRINGS M., WARD R. H. & PÄÄBO S., 1996. The retrieval of ancient human DNA sequences. *American Journal of Human Genetics*, 59: 368–376.
- HÄNNI C., LAUDET V., STÉHÉLIN D. & TABERLET P., 1994. Tracking the origins of the cave bear (*Ursus spelaeus*) by mitochondrial DNA sequencing. *Proceedings of the National Academy of Sciences of the United States of America*, 91, 25: 12336–12340.
- HAWKS J. & WOLPOFF M. H., 2001. Paleoanthropology and the Population Genetics of Ancient Genes. *American Journal of Physical Anthropology*, 114: 269–272.
- HEY J. & HARRIS E., 1999. Population bottlenecks and patterns of human polymorphism. *Molecular Biology and Evolution*, 16: 1423–1426.
- HOFREITER M., JAENICKE V., SERRE D., VON HAESELER A. & PÄÄBO S., 2001^a. DNA sequences from multiple amplifications reveal artifacts induced by cytosine deamination in ancient DNA. *Nucleic Acids Research*, 29: 4793–4799.
- HOFREITER M., SERRE D., POINAR H. N., KUCH M. & PÄÄBO S., 2001^b. Ancient DNA. *Nature Review Genetics*, 2: 353–359.
- HUBLIN J.-J., 2000. Modern/Non Modern human interactions: a Mediterranean perspective. In O. BAR-YOSEF & D. PILBEAM (eds.), *The Geography of the Neanderthals and Modern Humans in Europe and the Greater Mediterranean*, Harvard, Peabody Museum Bulletin, 8: 157–182.
- HUGHES S., HAYDEN T. J., DOUADY C. J., TOUGARD C., GERMONPRÉ M., STUART A., LBOVA L., CARDEN R. F., HÄNNI C. & SAY L., 2006. Molecular phylogeny of the extinct giant deer, *Megaloceros giganteus*. *Molecular Phylogenetics and Evolution*, 40: 285–291.
- JAENICKE-DESPRES V., BUCKLER E. S., SMITH B. D., GILBERT M. T., COOPER A., DOEBLEY J. & PÄÄBO S., 2003. Early allelic selection in maize as revealed by ancient DNA. *Science*, 302, 5648: 1206–1208.
- KEMP B. M. & SMITH D. G., 2005. Use of bleach to eliminate contaminating DNA from the surface of bones and teeth. *Forensic Science International*, 154: 53–61.
- KOLMAN C. J. & TUROSS N., 2000. Ancient DNA analysis of human populations. *American Journal of Physical Anthropology*, 111: 5–23.
- KRAUSE J., DEAR P. H., POLLACK J. L., SLATKIN M., SPRIGGS H., BARNES I., LISTER A. M., EBERSBERGER I., PÄÄBO S. & HOFREITER M., 2006. Multiplex amplification of the mammoth mitochondrial genome and the evolution of Elephantidae. *Nature*, 439: 724–727.
- KRINGS M., CAPELLI C., TSCHENTSCHER F., GEISERT H., MEYER S., VON HAESELER A., GROSSCHMIDT K., POSSNERT G., PAUNOVIĆ M. & PÄÄBO S., 2000. A view of Neanderthal genetic diversity. *Nature Genetics*, 26: 144–146.
- KRINGS M., GEISERT H., SCHMITZ R. W., KRAINITZKI H. & PÄÄBO S., 1999. DNA sequence of the mitochondrial hypervariable region II from the Neanderthal type specimen. *Proceedings of the National Academy of Sciences of the United States of America*, 96: 5581–5585.
- KRINGS M., STONE A., SCHMITZ R. W., KRAINITZKI H., STONEKING M. & PÄÄBO S., 1997. Neanderthal DNA sequences and the origin of modern humans. *Cell*, 90: 19–30.



- LALUEZA-FOX C., KRAUSE J., CARAMELLI D., CATALANO G., MILANI L., SAMPIETRO M. L., CALAFELL F., MARTINEZ-MAZA C., BASTIR M., GARCIA-TABERNEIRO A., DE LA RASILLA M., FORTEA J., PÄÄBO S., BERTRANPETIT J. & ROSAS A., 2006. Mitochondrial DNA of an Iberian Neandertal suggests a population affinity with other European Neandertals. *Current Biology*, 16: R629–R630.
- LALUEZA-FOX C., SAMPIETRO M. L., CARAMELLI D., PUDER Y., LARI M., CALAFELL F., MARTINEZ-MAZA C., BASTIR M., FORTEA J., DE LA RASILLA M., BERTRANPETIT J. & ROSAS A., 2005. Neandertal evolutionary genetics: mitochondrial DNA data from the Iberian peninsula. *Molecular Biology and Evolution*, 22: 1077–1081.
- LINDAHL T., 1993. Instability and decay of the primary structure of DNA. *Nature*, 362 : 709–715.
- LOREILLE O., ORLANDO L., PATOU-MATHIS M., PHILIPPE M., TABERLET P. & HÄNNI C., 2001. Ancient DNA analysis reveals divergence of the cave bear, *Ursus spelaeus*, and brown bear, *Ursus arctos*, lineages. *Current Biology*, 11: R200–R203.
- MALMSTRÖM H., STORA J., DALEN L., HOLMLUND G. & GOTHERSTROM A., 2005. Extensive human DNA contamination in extracts from ancient dog bones and teeth. *Molecular Biology and Evolution*, 22: 2040–2047.
- MARGULIES M., EGHOLM M., ALTMAN W. E., ATTIYA S., BADER J. S., BEMBEN L.A., BERKA J., BRAVERMAN M. S., CHEN Y. J., CHEN Z., DEWELL S. B., DU L., FIERRO J. M., GOMES X. V., GODWIN B. C., HE W., HELGESEN S., HO C. H., IRZYK G. P., JANDO S. C., ALENQUER M. L., JARVIE T. P., JIRAGE K. B., KIM J. B., KNIGHT J. R., LANZA J. R., LEAMON J. H., LEFKOWITZ S. M., LEI M., LI J., LOHMAN K. L., LU H., MAKHIJANI V. B., MCDADE K. E., MCKENNA M. P., MYERS E. W., NICKERSON E., NOBILE J. R., PLANT R., PUC B. P., RONAN M. T., ROTH G. T., SARKIS G. J., SIMONS J. F., SIMPSON J. W., SRINIVASAN M., TARTARO K. R., TOMASZ A., VOGT K. A., VOLKMER G. A., WANG S. H., WANG Y., WEINER M. P., YU P., BEGLEY R. F. & ROTHBERG J. M., 2005. Genome sequencing in microfabricated high-density picolitre reactors. *Nature*, 437: 376–380. Erratum in 441: 120.
- MARTH G., SCHULER G., YEH R., DAVENPORT R., AGARWALA R., CHURCH D., WHEELAN S., BAKER J., WARD M., KHOLODOV M., PHAN L., CZABARKA E., MURVAI J., CUTLER D., WOODING S., ROGERS A., CHAKRAVARTI A., HARPENDING H. C., KWOK P. Y. & SHERRY S. T., 2003. Sequence variations in the public human genome data reflect a bottlenecked population history. *Proceedings of the National Academy of Sciences of the United States of America*, 100, 1: 376–381.
- MELLARS P., 2006. A new radiocarbon revolution and the dispersal of modern humans in Eurasia. *Nature*, 439: 931–935.
- MISHMAR D., RUIZ-PESINI E., GOLIK P., MACAULAY V., CLARK A. G., HOSSEINI S., BRANDON M., EASLEY K., CHEN E., BROWN M. D., SUKERNIK R. I., OLCKERS A. & WALLACE D. C., 2003. Natural selection shaped regional mtDNA variation in humans. *Proceedings of the National Academy of Sciences of the United States of America*, 100, 1: 171–176.
- MORWOOD M. J., BROWN P., JATMIKO, SUTIKNA T., SAPTOMO E. W., WESTAWAY K. E., DUE R. A., ROBERT R. G., MAEDA T., WASISTO S. & DJUBIANTONO T., 2005. Further evidence for small-bodied hominins from the Late Pleistocene of Flores, Indonesia. *Nature*, 437: 1012–1017.
- NICHOLSON G. J., TOMIUK J., CZARNETZKI A., BACHMANN L. & PUSCH C. M., 2002. Detection of bone glue treatment as a major source of contamination in ancient DNA analyses. *American Journal of Physical Anthropology*, 118: 117–120.
- NOONAN J. P., COOP G., KUDARAVALLI S., SMITH D. G., KRAUSE J., ALESSI J., CHEN F., PLATT D., PÄÄBO S., PRITCHARD J. K. & RUBIN E. M., 2006. Sequencing and analysis of Neanderthal genomic DNA. *Science*, 314, 5802: 1113–1118.
- NOONAN J. P., HOFREITER M., SMITH D., PRIEST J. R., ROHLAND N., RABEDER G., KRAUSE J., DETTER J. C., PÄÄBO S. & RUBIN E. M., 2005. Genomic sequencing of Pleistocene cave bears. *Science*, 309, 5734: 597–599.
- NORDBORG M., 1998. On the probability of Neanderthal ancestry. *American Journal of Human Genetics*, 63: 1237–1240.
- ORLANDO L., BONJEAN D., BOCHERENS H., THÉNOT A., ARGANT A., OTTE M. & HÄNNI C., 2002. Ancient DNA and the population genetics of cave bears (*Ursus spelaeus*) through space and time. *Molecular Biology and Evolution*, 19: 1920–1933.
- ORLANDO L., DARLU P., TOUSSAINT M., BONJEAN D., OTTE M. & HÄNNI C., 2006. Revisiting Neandertal diversity with a 100,000 year old mtDNA sequence. *Current Biology*, 16: R400–R402.

- ORLANDO L., LEONARD J. A., THÉNOT A., LAUDET V., GUÉRIN C. & HÄNNI C., 2003. Ancient DNA analysis reveals woolly rhino evolutionary relationships. *Molecular Phylogenetics and Evolution*, 28: 485–499.
- OVCHINNIKOV I. V., GOTHERSTROM A., ROMANOVA G. P., KHARITONOV V. M., LIDEN K. & GOODWIN W., 2000. Molecular analysis of Neanderthal DNA from the northern Caucasus. *Nature*, 404: 490–493.
- POINAR H., KUCH M., McDONALD G., MARTIN P. & PÄÄBO S., 2003. Nuclear gene sequences from a late pleistocene sloth coprolite. *Current Biology*, 13: R1150–R1152.
- POINAR H. N., SCHWARZ C., QI J., SHAPIRO B., MACPHEE R. D., BUIGUES B., TIKHONOV A., HUSON D. H., TOMSHO L. P., AUCH A., RAMPP M., MILLER W. & SCHUSTER S. C., 2006. Metagenomics to paleogenomics: large-scale sequencing of mammoth DNA. *Science*, 311, 5759: 392–394.
- RELETFORD J. H., 1999. Models, predictions, and the fossil record of modern human origins. *Evolutionary Anthropology*, 8: 7–10.
- RELETFORD J. H., 2001^a. Absence of Regional Affinities of Neanderthal DNA With Living Humans Does Not Reject Multiregional Evolution. *American Journal of Physical Anthropology*, 115: 95–98.
- RELETFORD J. H., 2001^b. Ancient DNA and the origin of modern humans. *Proceedings of the National Academy of Sciences of the United States of America*, 98, 2: 390–391.
- ROGAEV E. I., MOLIKA Y. K., MALYARCHUK B. A., KONDRASHOV F. A., DERENKO M. V., CHUMAKOV I. & GRIGORENKO A. P., 2006. Complete mitochondrial genome and phylogeny of Pleistocene mammoth *Mammuthus primigenius*. *Public Library of Science, Biology*, 4: e73.
- RÖMPLER H., ROHLAND N., LALUEZA-FOX C., WILLERSLEV E., KUZNETSOVA T., RABEDER G., BERTRANPETIT J., SCHONEBERG T. & HOFREITER M., 2006. Nuclear gene indicates coat-color polymorphism in mammoths. *Science*, 313, 5783: 62.
- RUIZ-PESINI E., MISHMAR D., BRANDON M., PROCACCIO V. & WALLACE D. C., 2004. Effects of purifying and adaptive selection on regional variation in human mtDNA. *Science*, 303, 5655: 223–226.
- SCHMITZ R. W., SERRE D., BONANI G., FEINE S., HILLGRUBER F., KRAINITZKI H., PÄÄBO S. & SMITH F. H., 2002. The Neanderthal type site revisited: interdisciplinary investigations of skeletal remains from the Neander Valley, Germany. *Proceedings of the National Academy of Sciences of the United States of America*, 99, 20: 13342–13347.
- SCHOLZ M., BACHMANN L., NICHOLSON G. J., BACHMANN J., GIDDINGS I., RUSCHOFF-THALE B., CZARNETZKI A. & PUSCH C. M., 2000. Genomic differentiation of Neanderthals and anatomically modern man allows a fossil-DNA-based classification of morphologically indistinguishable hominid bones. *American Journal of Human Genetics*, 66: 1927–1932.
- SMITH F. H., TRINKAUS E., PETTITT P. B., KARAVANIĆ I. & PAUNOVIĆ M., 1999. Direct radiocarbon dates for Vindija G₁ and Velika Pećina late Pleistocene hominid remains. *Proceedings of the National Academy of Science of the United States of America*, 96, 22: 12281–12286.
- STILLER M., GREEN R. E., RONAN M., SIMONS J. F., DU L., HE W., EGHOLM M., ROTHBERG J. M., KEATES S. G., OVODOV N. D., ANTIPINA E. E., BARYSHNIKOV G. F., KUZMIN Y. V., VASILEVSKI A. A., WUENSCHEL G. E., TERMINI J., HOFREITER M., JAENICKE-DESPRES V. & PÄÄBO S., 2006. Patterns of nucleotide misincorporations during enzymatic amplification and direct large-scale sequencing of ancient DNA. *Proceedings of the National Academy of Sciences of the United States of America*, 103, 37: 13578–13584. Erratum in: 103, 14977.
- TUMPEY T. M., BASLER C. F., AGUILAR P. V., ZENG H., SOLORZANO A., SWAYNE D. E., COX N. J., KATZ J. M., TAUBENBERGER J. K., PALESE P. & GARCIA-SASTRE A., 2005. Characterization of the reconstructed 1918 Spanish influenza pandemic virus. *Science*, 310, 5745: 77–80.
- VAN TUINEN M., RAMAKRISHNAN U. & HADLY E. A., 2004. Studying the effect of environmental change on biotic evolution: past genetic contributions, current work and future directions. *Philosophical Transactions A Mathematics Physics Engineering Sciences*, 362: 2795–2820.
- WILLERSLEV E., HANSEN A. J., BINLADEN J., BRAND T. B., GILBERT M. T., SHAPIRO B., BUNCE M., WIUF C., GILICHINSKY D. A. & COOPER A., 2003. Diverse plant and animal genetic records from



Holocene and Pleistocene sediments. *Science*, 300, 5620: 791-795.

WILLERSLEV E., HANSEN A. J., RONN R., BRAND T.B., BARNES I., WIUF C., GILICHINSKY D., MITCHELL D. & COOPER A., 2004. Long-term

persistence of bacterial DNA. *Current Biology*, 14: R9-R10.

ZEDER M. A., EMSHWILLER E., SMITH B. D. & BRADLEY D. G., 2006. Documenting domestication: the intersection of genetics and archaeology. *Trends in Genetics*, 22: 139-155.

Chapter 20

SCLADINA I-4A IN THE CHRONOLOGICAL CONTEXT OF THE NEANDERTALS FROM THE BELGIAN MEUSE VALLEY AND NORTHWEST EUROPE

Michel TOUSSAINT & Stéphane PIRSON

Michel Toussaint & Dominique Bonjean (eds.), 2014. The Scladina I-4A Juvenile Neandertal (Andenne, Belgium), Palaeoanthropology and Context Études et Recherches Archéologiques de l'Université de Liège, 134: 395-408.

1. Introduction

The anthropological discoveries made over the past quarter of a century at Scladina Cave are far from being the only Neandertal remains discovered in the Belgian Meuse River Basin.

Apart from Scladina, at least seven other sites have yielded Neandertal fossils (Figure 1; TOUSSAINT et al., 2011). Five of them were found during the 19th century, at a time when the quality of available contextual information

was far below the standards of modern prehistorical research. Most of them were assigned to simplistic stratigraphic records, without exact distribution plans or contextual analyses. These include Engis (1829-30), La Naulette (1866), Goyet (~1870), Spy (1886), and Fonds de Forêt (1895). Three of these finds (Engis, La Naulette, and Spy) have played a major role in the genesis and initial developments of palaeoanthropology and prehistory (TOUSSAINT, 1992; 2001).

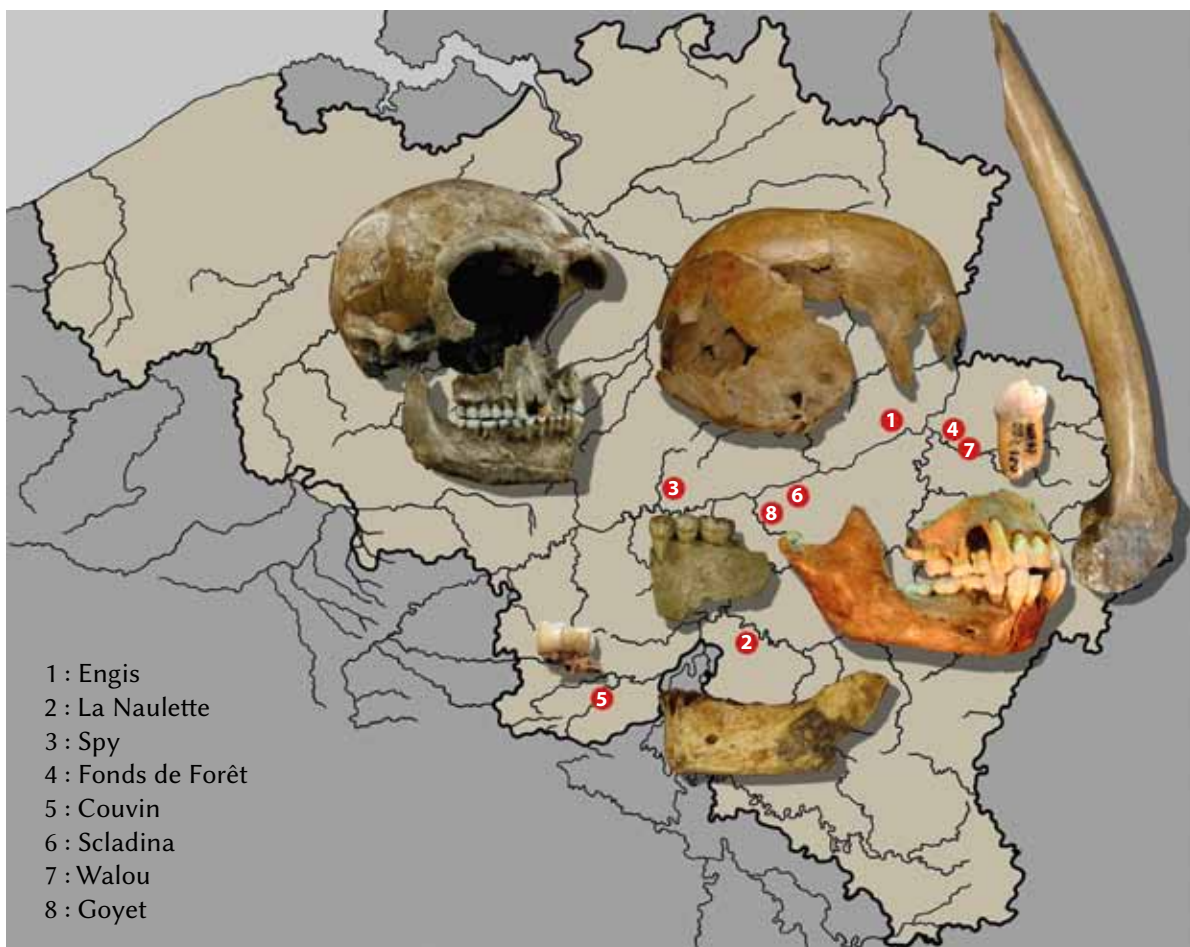


Figure 1: Location of the sites which have yielded unquestionable Neandertal remains in Belgium (graphics Semal & Toussaint, after TOUSSAINT et al., 2011).



During the last three decades of the 20th century, there was a revival of prehistoric research in karstic areas, both in terms of excavation methods and the development of multidisciplinary approaches. This was initiated during the excavation of Remouchamps Cave in 1969 and 1970 by the University of Liège, in contexts dating back to the end of the Upper Palaeolithic (DEWEZ et al., 1974; TOUSSAINT & PIRSON, 2007). In this new research context and after nine decades without the discovery of any Neandertal remains, the end of the 20th and the beginning of the 21st centuries were marked by three findings, all of them associated with more precise information due to newly developed methods. These include: an isolated deciduous tooth from Trou de l'Abîme in Couvin (1984); isolated teeth, a mandible, and a maxilla found in former Layer 4A of Scladina Cave (1990–2006), and a premolar discovered in Walou Cave in 1997.

This chapter solely provides anthropological context to the juvenile of Scladina from a chronological perspective, both in the Belgian Meuse Basin as well as neighbouring regions. It only briefly presents the contextual archaeological and anthropological data of these discoveries. These data are available in full in previous synthetic contributions (TOUSSAINT et al., 2001, 2011; TOUSSAINT & PIRSON, 2006), as well as in more specific detailed works (e.g. TOUSSAINT et al., 1998, 2010; CREVECOEUR et al., 2010) and monographs (DRAILY et al., 2011; PIRSON et al., 2011; ROUGIER & SEMAL (eds.), 2013, 2014 in press).

Methodological limits of the 2. chronological approach

The quality of available information varies greatly for the stratigraphic, archaeological, and palaeoenvironmental contexts of the Neandertal fossils found in the Meuse River Basin cave sites.

From our perspective, to optimally guarantee the accurate context of the fossils found in all these sites, the conjunction of three main pieces of information is essential:

- human remains must be taxonomically well-attributed,
- large sedimentary sequences must be established with detailed stratigraphic surveys, and
- chronostratigraphic frameworks must be accurately established.

In addition, two other kinds of information are also extremely valuable:

- direct dating of the fossils (¹⁴C AMS, gamma spectrometry), and
- typical lithic artefacts found in the same context as the remains.

In the Meuse River Basin, these criteria are rarely met. There are several possible causes for this. The first is the antiquity of most excavations. Even when new analyses were undertaken as thoroughly as possible, such as the direct dating and anthropological analyses of fossils at Spy (ROUGIER & SEMAL (eds.), 2013), the deficiencies in precise contextual data make rigorous correlations between the results of all involved disciplines difficult. The second is the lack of

Cave	Town	Date of discovery	Taxonomy	Precise stratigraphy	Palaeo-environmental data	Good chronostratigraphy	Direct dates of the fossils	Association of characteristic lithic material		
								Good	Problematic	Absence
Engis	Flémalle	1829–1830	+	–	–	–	(AMS)		+	
La Naulette	Houyet	1866	+	(+)	–	–	–			+
Goyet	Gesves	around 1870	+	–	–	–	AMS		+	
Spy	Jemeppe-sur-Sambre	1886	+	–	–	–	AMS		+	
Fonds de Forêt	Trooz	1895	+	–	–	–	–		+	
Couvin	Couvin	1984	+	+	+	(+)	–	+		
Scladina	Andenne	from 1990	+	+	+	+	^γ spectrometry			+
Walou	Trooz	1997	+	+	+	+	–	+		
Montigny-le-Tilleuls	Montigny-le-Tilleuls	1889	–	–	–	–	–		+	
Tiène des Maulins	Rochefort	2002–2008?	–	–	–	–	–			+

Table 1: Assessing the quality of data on Neandertals from the Belgian Meuse River Basin.

sites in which complex sedimentary situations are thoroughly addressed by geological analyses. The third is the scarcity of sedimentary sequences where a reliable chronostratigraphic framework exists. In most cases, the only chronological indicators are a limited number of ¹⁴C dates. However, the results have to be considered with caution due to problems inherent to that technique, such as contamination or taphonomic disturbances of the dated samples (HIGHAM, 2011). Recent radiocarbon analyses have shown that the initial ages of the fossils from Mezmaiskaya, Vindija, and Zafarraya were significantly underestimated (see HIGHAM et al., 2006; PINHASI et al., 2011; WOOD et al., 2013). To be reliable, ¹⁴C dates should be obtained through a replicable protocol, they should be numerous enough to compose a continuous sequence, and should be cross-checked with independent datasets, e.g., from climatostratigraphy, the study of tephras, or pedostratigraphic markers.

Based on this, only three Neandertal fossils (or series of fossils) from the Belgian Meuse River Basin are well positioned stratigraphically, allowing detailed chronostratigraphic and palaeoenvironmental studies (Table 1): Walou, Couvin, and Scladina. Some human remains from Spy and Goyet were directly dated with ¹⁴C AMS. The radiocarbon dates in the case of the Engis 2

skull were clearly too young. The chronological position of the two other sites is more speculative.

Chronology of the Belgian 3. Meuse River Basin Neandertals—

Despite all the problems evoked above, the Neandertal remains from the Meuse River Basin can tentatively be classified into different groups, combining the ¹⁴C chronology of the Neandertal remains themselves (AMS), the ¹⁴C chronology of the associated fauna, and, when possible, contextual data (TOUSSAINT & PIRSON, 2006; PIRSON & DI MODICA, 2011).

3.1. The La Naulette problem

In 1866, the discovery of the famous La Naulette mandible in the Lesse Valley by the geologist Édouard Dupont marked an important step in the history of palaeoanthropology. The antiquity of the fossil was confirmed by a relatively precise stratigraphic context—clearly the best for the discovery’s time period—and its probable association with large, extinct prehistoric mammals.

Dating the La Naulette mandible is challenging. The stratigraphic sequence of the cave is over 11 m high. In his second description, DUPONT (1867; Figure 2) identified three “ossiferous levels”

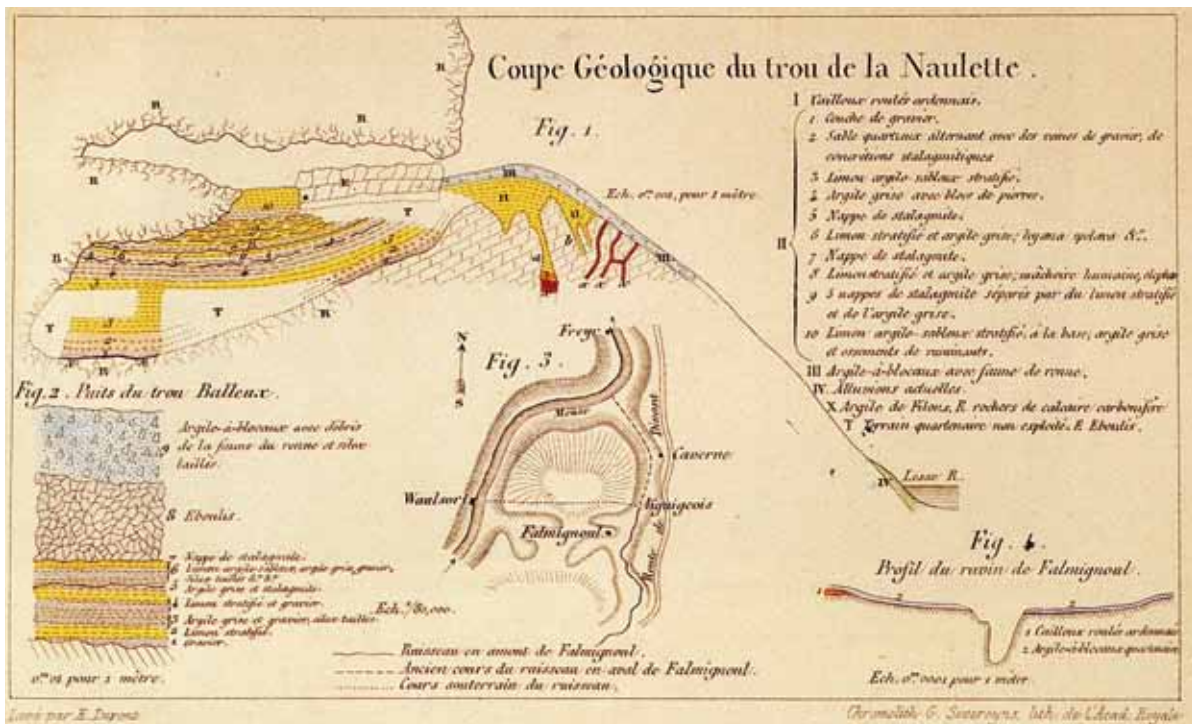


Figure 2: La Naulette: sedimentary profile, after DUPONT (1867).





Figure 3: La Naulette: ulna, mandible (lateral and superior views) and third metacarpal.

and seven “stalagmitic sheets”. Three human bones - and an isolated tooth - were found in the second ossiferous level, between the stalagmitic sheets 2 and 3, without any associated lithic material. The mandible (Figure 3) is thought to have belonged to a young female (LEGUEBE & TOUSSAINT, 1988); it is comprised of the left side of the mandibular body, the symphyseal region and the anterior part of the right side of the body. The three other remains are an ulna, a damaged third metacarpal as well as a tooth now lost. The human remains from La Naulette have never been directly dated. However, stratigraphic and palaeoanthropological evidence suggest they may be older than Classic Neandertals.

The age of the fossils is supported by the presence of five overlying stalagmitic levels, considering both their thickness and quantity. They point to interglacial or early glacial conditions, suggesting MIS 5 or some temperate phase of Middle Pleistocene. The mandible has archaic features and fits within the biometric variability of Neandertals and their pre-Neandertal ancestors. Although the ulna and metacarpal show modern morphological and metric characters, it does not change the likelihood of the mandible’s antiquity.

Two hypotheses can be proposed to explain the presence of an archaic mandible and modern-like

postcranial bones. One explanation is that Dupont may have mistakenly associated an ancient mandible with modern postcranial remains because of the absence of an accurate stratigraphic record. However, the overall accuracy and precision of his stratigraphic observations contradicts this hypothesis, especially when added to other evidence, such as the absence of modern human bones inside the main section of the cave. The second hypothesis is that all the remains are from the same layer and the same individual, suggesting they are from a very early Neandertal. Neandertal characteristics were progressively acquired mosaically, resulting in classical specimens around the Eemian interglacial (DEAN et al., 1998; CONDEMI, 2000). In some of their anatomical details, earlier fossils may be morphologically closer to anatomically modern humans than to Classic Neandertals. As a consequence, the seemingly modern features of the postcranial bones from La Naulette could be interpreted as plesiomorphies. Since 1999, a few short excavations have occurred at La Naulette, notably to look for evidence that addresses the hypotheses presented above (TOUSSAINT & PIRSON, 2002). New direct dates and some palynological analyses are being done on some of the recovered speleothems.

Regardless of these two assumptions, in the present state of research the La Naulette mandible may be the oldest human fossil from the Meuse River Basin, dating to at least MIS 5.

3.2. MIS 5 fossils

Until now, and if La Naulette is older than MIS 5 (cf. supra), only the 8-year-old Neandertal from Scladina Cave appears to belong to MIS 5 and even possibly to MIS 5a or b (see this volume, Chapter 5).

3.3. MIS 4

In the current stage of research, and if the Scladina Child does date to MIS 5b or 5a, no human remains that date to MIS 4 (\pm 78–60 ka BP) have been found. This lack of human fossils could be related to the current absence of archaeological occupations in Belgium during the second half of the Weichselian Lower Pleniglacial (second part of MIS 4), which corresponds to a major climatic deterioration, starting with the development of continuous permafrost followed by the first major Weichselian loess cover (HAESAERTS, 1984; PIRSON et al., 2009; PIRSON & DI MODICA, 2011).

3.4. MIS 3 fossils

Based on the quality of available contextual data, the Neandertal remains that date to the Weichselian Middle Pleniglacial (MIS 3) can be ordered in three sub-groups.

3.4.1. MIS 3 on the basis of good multidisciplinary context

This sub-group is comprised of the Couvin and Walou teeth, i.e., fossils unearthed in recent decades with good stratigraphical and palaeoenvironmental information, as well as ^{14}C dates for the associated fauna.

The right dm_2 (Figure 4), discovered in 1984 in front of the main entrance of Trou de l'Abîme in Couvin during a multidisciplinary program of excavation, has been determined as Neandertal due to its occlusal morphology and enamel thickness (TOUSSAINT et al., 2010). It has good stratigraphical context. A new archaeological study (FLAS, 2008) established that the associated lithic material is definitely Mousterian rather than transitional, as previously hypothesized (OTTE, 1984). However, even if the stratigraphic context is well defined, no analyses regarding the origin of the sediments or the sedimentary dynamics have taken place. The chronostratigraphic framework of the site is only known because of two ^{14}C dates ($46,820 \pm 3,290$ BP and $44,500 \pm 1,100/-800$ BP) available from faunal remains found in Layer II, from where the Neandertal tooth was exhumed. These dates are consistent with the possible presence of a palaeosol in overlying Layer III, which might be an equivalent of "Les Vaux Soil" and therefore situated between 42,000–40,000 BP at the youngest (PIRSON et al., 2009; TOUSSAINT et al., 2010). Therefore, the Couvin tooth seems to date back to approximately 45,000 BP.

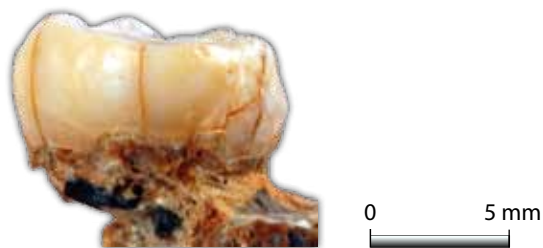


Figure 4: The Couvin mandibular deciduous right second molar (after TOUSSAINT et al., 2011).

A mandibular left first premolar (Figure 5) was found in 1997 at Walou Cave during the second multidisciplinary excavation, which took place from 1996 to 2004 (DRAILY, 2011; DRAILY et al. (dir.), 2011; PIRSON et al. (dir.), 2011). Despite being the only human remain discovered in the site (in Layer CI-8, which is dated around 40,000–38,000 BP), relatively to the recent Neandertal fossils of northwest Europe, it has the best context: an accurate stratigraphic position, a strict association with a well-characterized archaeological lithic industry (i.e., Mousterian), and a well-established chronostratigraphic framework based on tephrostratigraphy, climatostratigraphy, pedosedimentary markers, as well as several dates (^{14}C , ESR/U-Th, and TL).

3.4.2. MIS 3 on the sole basis of direct AMS radiocarbon dates

This sub-group of fossils is composed of the Spy (Figure 6) and Goyet Neandertals, respectively discovered in 1886 and ~1870, in conditions which do not correspond to current standards of archaeological fieldwork. Nevertheless, these fossils are extremely valuable for anthropological research.

In recent years, new research on the archaeology and palaeoanthropology of Spy has occurred at the Royal Belgian Institute of Natural



Figure 5: Walou: mandibular left first premolar (after TOUSSAINT et al., 2011).



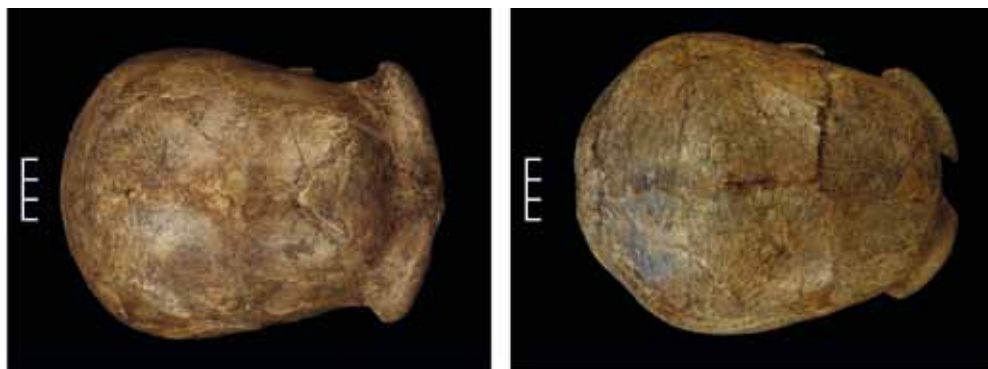


Figure 6: Spy: two skullcaps (after TOUSSAINT et al., 2011).

Sciences, which houses most of the site material (FRAIPONT & LOHEST, 1887; ROUGIER & SEMAL (eds.), 2013, 2014 in press). Concurrently, three direct AMS radiocarbon dates were performed directly on fragments of the two Neandertal adults in two different laboratories (Groningen and Oxford), which indicated that the skeletons date back to around 36,000 BP, (TOUSSAINT & PIRSON, 2006; SEMAL et al., 2009, 2013). Unfortunately, the stratigraphical, palaeoenvironmental, and archaeological context of the fossils is not precise enough. Therefore, linking the Spy fossils to the end of the Middle Palaeolithic or to the Lincombian-Ranisian-Jerzmanowician (LRJ; FLAS, 2008) transitional industry is difficult, even if the LRJ hypothesis is the most attractive.

At Goyet, a fragment of mandible (Figure 7) and numerous fragments of human bone with anthropogenic traces were recently identified in the collections of the Royal Belgian Institute of Natural Sciences in the assemblage unearthed around 1870 by É. Dupont in the third cave (ROUGIER et al., 2012, 2014). They were identified as Late Neandertals on the basis of a morphometric study supported by radiocarbon dating. The absence of a precise stratigraphic record makes it difficult to reliably associate the fossils to the lithic industry found in the cave.

3.4.3. Possible MIS 3 Neandertal remains

The third group is composed of apparently recent fossils - or sets of fossils - found during the 19th century in conditions, which, like the fossils of Spy and Goyet discussed above, do not correspond to current standards of archaeological research.

The first, Engis 2 (Figure 8), found by Ph.-Ch. Schmerling during the winter of 1829-1830 in a highly inaccurate stratigraphic position, exhibits clear Neandertal attributes (TILLIER, 1983). The recently acquired ¹⁴C dates at 26,830 ± 340 BP and 30,460 ± 210 BP seems to be too young when

compared to the regional archaeological context, probably due to sample contamination (TOUSSAINT & PIRSON, 2006). An attribution to MIS 3 is the most probable hypothesis.

The second, a femur found in 1895 in the caves of Fonds de Forêt, was shown to be Neandertal (Figure 9; TWIESELNANN, 1961); however, the conditions of its discovery do not allow it to be precisely positioned in a stratigraphical layer, so no chronological information is available. The possibly associated archaeological industry seems to be from the Middle Palaeolithic.

Other arguments often used to support the recent dates from Engis and Fonds de Forêt, are observations made by excavators of the stratigraphic proximity of the fossils and the Mousterian and early Upper Palaeolithic (e.g. ULRIX-CLOSSET, 1975, 1990). The structural complexity of cave stratigraphy highlighted in recent studies done at Walou and Scladina, with frequent erosive boundaries, large gullies and other disturbances, clearly



Figure 7: Goyet: fragment of mandible found by E. Dupont around 1870 (after ROUGIER et al., 2009).



Figure 8: Engis 2 skullcap, found by P.-C. Schmerling in the second cave of Engis during the winter 1829–1830 (from TOUSSAINT et al., 2011).

limits the scope of this argument (PIRSON, 2007; PIRSON & DI MODICA, 2011).

3.5. Other Neandertal remains?

In addition to the eight above-mentioned caves, other karstic sites of Wallonia may have also yielded Neandertal remains, but serious analysis have to be carried out before accepting or rejecting them into the collection of Neandertal sites of the Meuse River Basin. This is the case in Montignies-le-Tilleul and in Eprave.

A femur fragment and three metacarpals were discovered in 1889 in Rotches de D’Genny Cave, at Montignies-le-Tilleul, in the Sambre Valley (OTTE, 1986); their possible association with the Mousterian industry is interesting, but the absence of anthropological studies prevents further interpretation.

The oldest sediments of Tiène des Maulins Cave, in Éprave along the right bank of the Lomme River, could date back to 75,000–60,000 years ago (GROENEN, 2005; GROENEN et al., 2013), but without any association with typical Mousterian



Figure 9: Fonds de Forêt: the Neandertal femur (after TOUSSAINT et al., 2011).



lithic material (DI MODICA, 2011). Some bone and dental remains have also been attributed to the Middle Palaeolithic at this site and were interpreted as Neandertals (GROENEN, 2010). However, no detailed stratigraphic study has been conducted to confirm or refute the stratigraphic position of these remains and no anthropological study was so far made to test their current allocation as Neandertals (TOUSSAINT et al., 2011).

4. Northwest European context

In addition to the concentration of Neandertal remains in the Meuse River Basin, the northwest European regions surrounding Belgium (i.e. Great Britain, The Netherlands, north France, and northwest Germany) have also yielded some fossils. Within the context of the Scladina discoveries, those dating back to the Upper Pleistocene (MIS 5-3; Figure 10) are interesting, although they do not offer the best opportunities for dating and palaeoenvironment, similar to most of the sites of the Meuse River Basin that were excavated long ago. Middle Pleistocene remains such as Biache 1 and 2 or Boxgrove are not included here.

Found in 1856, the Neandertal type specimen site, Feldhofer Cave in Germany, is just about 100 km northeast of the Belgian sites. In fact, Feldhofer provided the only Neandertal remains of North Rhine-Westphalia that have been directly dated by ¹⁴C AMS, which produced dates of approximately 40-39 ka BP (BONANI, 2006; STREET et al., 2006). However, no rigorous in situ stratigraphic context was established due to the antiquity of the discovery. During field research in 1997 and 2000 (FEINE, 2006; SCHMITZ et al., 2006), Mousterian artefacts were found with new Neandertal remains in sediment that was anthropogenically removed, at least in part, during the time of industrial use of the quarry (HILLGRUBER, 2006). The original association of the lithic artefacts and the Neandertal fossils, either found in 1856, 1997, or 2000, cannot be demonstrated, as the new findings are from a disturbed context. The chronostratigraphical position of the fossils relies solely on direct ¹⁴C dates; the bones are positioned within disturbed sediment that has neither climatic markers nor other chronostratigraphic data from layers associated to the Neandertal remains.

In the Netherlands, no Neandertal remains have been found in situ at an archaeological site.



Figure 10: Location of the sites which have yielded Classic Neandertal remains in northwestern Europe discussed in this chapter: 1. Feldhofer Cave, the Neandertal type site; 2. North Sea, the Zeeland Ridges area; 3. Grotte du Renne at Arcy-sur-Cure, Yonne department; 4. Kent's Cavern; 5. La Cotte de Saint-Brelade, Jersey; in green, the geographical area of the eight Meuse River Basin sites (graphics Sylviane Lambermont, AWEM & J.-F. Lemaire, SPW).

The only specimen discovered is a portion of human frontal bone found in 2001 within sediments extracted from the bottom of the North Sea in the Zeeland Ridges area, 15 km off the coast (HUBLIN et al., 2009). The remains have neither context nor associated lithic material, and therefore have no chronostratigraphic data. The fossil itself has not been dated directly with ^{14}C AMS. However, the details of the supraorbital morphology and the shape of the external surface of the squama, allow the bone to be assigned to *Homo neanderthalensis*.

In the northern third of France, i.e. north of the Seine River, recent Neandertal remains have not yet been found. The northernmost French Classical Neandertals are those of the Grotte du Renne at Arcy-sur-Cure, in the Yonne department, Burgundy. They were mainly found in Châtelperronian contexts but some teeth are from Mousterian layers (LEROI-GOURHAN, 1958; BAILEY & HUBLIN, 2006).

In Great Britain, there are very few human fossils with a chronostratigraphic context that dates from MIS 5 to 3. Found in 1927 in an imprecise stratigraphic position, the Kent's Cavern-4 maxilla with deeply worn teeth was originally interpreted as modern. Its direct ^{14}C AMS date of $30,900 \pm 900$ BP (OxA-1621) is now considered contaminated and much too recent. A new reassessment of the specimen suggests that its teeth possess more modern human than Neandertal characteristics (STRINGER et al., 2007; HIGHAM et al., 2011). According to AMS radiocarbon dates obtained using ultrafiltration on animal bones and teeth found above and below the reported stratigraphic context of the object, the maxilla would be much older, with a modelled age of 44,180–41,530 cal BP (approximately between 40,000 and 37,000 BP; HIGHAM et al., 2011). Based on this data, this find would represent the oldest anatomically modern human discovered in northwest Europe, demonstrating the large and rapid dispersal of Early Modern Humans across all Europe more than 40 ka ago. However, these dates have been challenged on the grounds that the sedimentary context is not well controlled due to poorly executed excavations (WHITE & PETTITT, 2012).

A total of 13 Neandertal teeth from one individual and an occipital fragment from a juvenile human skull were recovered at the Palaeolithic site of La Cotte de Saint-Brelade, Jersey, at the beginning of the 20th century (STRINGER & CURRANT, 1986). Recent in situ research provided optically stimulated luminescence (OSL) dates

of the sediments, which could indicate that the Neandertal fossils date to between MIS 5 and 3 (BATES et al., 2013).

5. Conclusion

Eight karstic sites have yielded Neandertal remains in Belgium, which represents a unique concentration in northwest Europe. Even if several gaps remain, this allows a hypothetical chronological model for the Late Neandertals of the Meuse River Basin. Dating back to MIS 5, the Scladina Child has a special place in this scheme, as, like apparently La Naulette, they are older than the other remains. In the current state of research, the following pattern emerges as the best hypothesis for Neandertals (Figure 11):

- during MIS 5b or 5a (or less likely early MIS 4) Early Classic Neandertals, with the Scladina Juvenile, are present;
- during the second part of MIS 4 there currently is no evidence for occupation of the Belgian Meuse River Basin, deduced from the lack of human fossils and of archaeological occupations, which corresponds to a major climatic deterioration;
- at approximately 45 ka BP Late Neandertals with late Mousterian industries are present, represented by the Couvin dm₂;
- at approximately 40–38 ka BP or slightly after some Neandertals with late Mousterian industries, represented by the Walou P₃ from Layer CI-8 and consistent with the age of the youngest Mousterian assemblage from Scladina Cave, i.e., Unit 1A (40–37 ka BP) are present;
- at approximately 36 ka BP Neandertals still are present at Spy where the associated lithic industry is imprecise: possibly transitional LRJ, or even late Mousterian; and
- at approximately 33 ka BP probably only modern humans are present, since after then the only known dated industries are Aurignacian, e.g., Maisières-Canal and Spy (SEMAL et al., 2009; PIRSON et al., 2012) and the only proven fossil humans associated with those industries in northwest Europe are *Homo sapiens sapiens*, represented mainly by isolated teeth (BAILEY et al., 2009).

Such a model is obviously not precise enough. Firstly, it is based on too few sites: just eight,



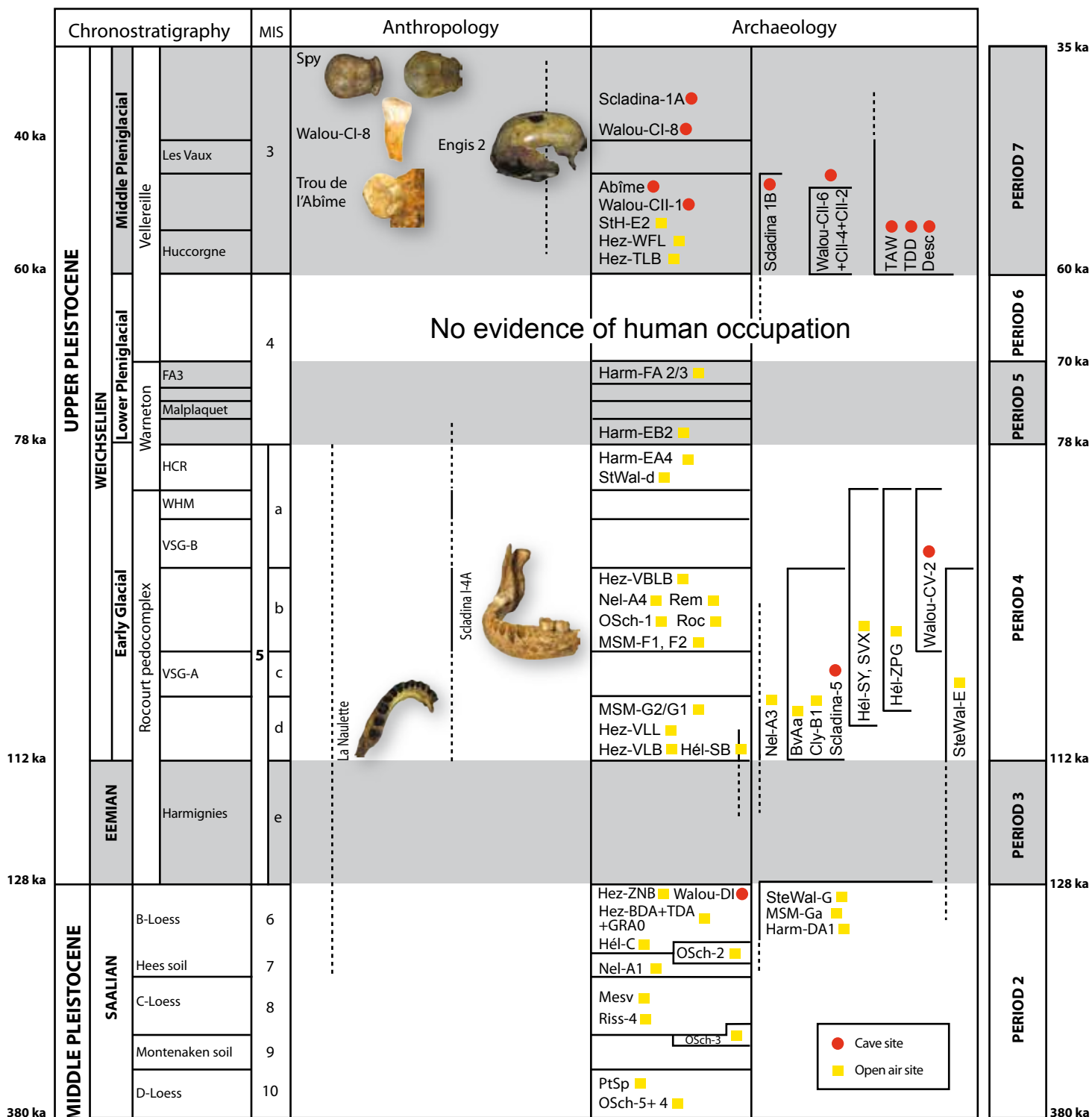


Figure 11: Hypothetical chronology of the Meuse River Basin Neandertals (modified from Pirson & Di Modica, 2011). **Chronostratigraphy:** FA3 = Harmignies FA3 soil; HCR = Humiferous Complex of Remicourt; VSG-A = Villers-Saint-Ghislain A soil; VSG-B = Villers-Saint-Ghislain B soil; WHM = Whitish Horizon of Momalle.

Archaeology: Abîme = Trou de l'Abîme; BvAa = Bos van Aa; Cly-B1 = Le Clypot-B1; Desc = Grotte Descy; Harm = Harmignies; Hël = Hêlin; Hez = Hezerwater; Mesv = Mesvin (Mesvin IV, Petit-Spiennes III); MSM = Mont-Saint-Martin; Nel = Nelissen; OSch = Op de Schans; PtSp = Petit-Spiennes; Rem = Remicourt; Riss-4 = Le Rissori-4; Roc = Rocourt; Scladina = Scladina Cave; StH-E2 = Station de l'Hermitage-E2; StWal = Sainte-Walburge; TAW = Trou Al'Wesse; TDD = Trou du Diable; Walou = Walou Cave.

The letters and numbers following the abbreviations refer either to a specific stratigraphic layer or to a different concentration.

with only three found within modern multi-disciplinary excavations and only two others having delivered direct reliable ^{14}C AMS dating of Neandertal remains. It does not provide a reliable date for the La Naulette mandible and for the Fonds de Forêt and Engis fossils. Secondly, this model does not explain precisely what happened in Belgium between 36 and 33 ka BP, so the question of the possible overlap and contacts between Neandertals and Early Modern Humans in the Meuse River Basin cannot be properly addressed in terms of chronology.

Acknowledgements

The authors wish to express their gratitude to Sylviane Lambermont (AWEM), Jean-François Lemaire (SPW), and Joël Éloy (AWEM), graphic artists. They also wish to thank Rhylan McMillan (Vancouver Island University) for his valuable comments and his help editing the English version of this chapter.

References

- BAILEY S. E. & HUBLIN J.-J., 2006. Dental remains from the Grotte du Renne at Arcy-sur-Cure (Yonne). *Journal of Human Evolution*, 50: 485–508.
- BAILEY S. E., WEAVER T. D. & HUBLIN J.-J., 2009. Who made the Aurignacian and other early Upper Paleolithic industries? *Journal of Human Evolution*, 57: 11–26.
- BATES M., POPE M., SHAW A., SCOTT B. & SCHWENNINGER J.-L., 2013. Late Neanderthal occupation in North-West Europe: rediscovery, investigation and dating of a last glacial sediment sequence at the site of La Cotte de Saint Brelade, Jersey. *Journal of Quaternary Science*, 316: 14–26.
- BONANI G., 2006. Accelerator Mass Spectrometry (AMS) radiocarbon dating of Middle and Upper Palaeolithic samples from the Neander Valley, Germany. In R. W. SCHMITZ (ed.), *Neanderthal 1856-2006*. Rheinische Ausgrabungen, 58, Mainz am Rhein, Philipp von Zabern: 335–336.
- CONDEMI S., 2000. The Neanderthals: *Homo Neanderthalensis* or *Homo sapiens Neanderthalensis*? Is there a contradiction between the paleogenetic and the paleoanthropological data? In J. ORSCHIEDT & G.-C. WENIGER (eds.), *Neanderthals and Modern Humans – Discussing the transition. Central and Eastern Europe from 50.000-30.000 B.P.*, Neanderthal Museum: 287–295.
- CREVECOEUR I., BAYLE P., ROUGIER H., MAUREILLE B., HIGHAM T. F. G., VAN DER PLICHT J., DE CLERCK N. & SEMAL P., 2010. The Spy VI child: A newly discovered Neandertal infant. *Journal of Human Evolution*, 59: 641–656.
- DEAN D., HUBLIN J.-J., HOLLOWAY R. & ZIEGLER R., 1998. On the phylogenetic position of the pre-Neandertal specimen from Reilingen, Germany. *Journal of Human Evolution*, 34: 485–508.
- DEWEZ M., ALEXANDRE-PYRE S., BRABANT H., BOUCHUD J., CALLUT M., DAMBLON F., DEGERBØL M., EK C., FRÈRE H., GILOT E., GLIBERT M. & JUVIGNÉ É., 1974. Nouvelles recherches à la grotte de Remouchamps. *Bulletin de la Société royale d'Anthropologie et Préhistoire*, 85: 5–161.
- DI MODICA K., 2011. La documentation du Paléolithique moyen en Belgique aujourd'hui, état de la question. In M. TOUSSAINT, K. DI MODICA & S. PIRSON (sc. dir.), *Le Paléolithique moyen en Belgique. Mélanges Marguerite Ulrix-Closset*. Bulletin de la Société royale belge d'Études Géologiques et Archéologiques *Les Chercheurs de la Wallonie*, hors-série, 4 & Études et Recherches Archéologiques de l'Université de Liège, 128: 75–104.
- DRAILY C., 2011. *La grotte Walou à Trooz (Belgique). Fouilles de 1996 à 2004, vol. 3: L'Archéologie*, Namur, Service public de Wallonie, IPW, Études et Documents, Archéologie, 22, 332 p.
- DRAILY C., PIRSON S. & TOUSSAINT M. (dir.), 2011. *La grotte Walou à Trooz (Belgique). Fouilles de 1996 à 2004, vol. 2: Les sciences de la vie et les datations*. Namur, Service public de Wallonie, IPW, Études et documents, Archéologie, 21, 241 p.
- DUPONT E., 1867. Étude sur cinq cavernes explorées dans la vallée de la Lesse et le ravin de Falmignoul pendant l'été de 1866. *Bulletins de l'Académie royale des Sciences, des Lettres et des Beaux-Arts de Belgique*, 2^e série, XXIII: 244–265.
- FEINE S., 2006. The sediments containing finds from the caves Feldhofer Kirche and Keine Feldhofer Grotte in the Neander Valley. Analysis of the secondary stratification using GoCAD. In R. W. SCHMITZ (ed.), *Neanderthal 1856-2006*. Rheinische Ausgrabungen, 58, Mainz am Rhein, Philipp von Zabern: 61–72.
- FLAS D., 2008. *La transition du Paléolithique moyen au supérieur dans la plaine septentrionale*



de l'Europe. *Anthropologica et Praehistorica*, 119, 254 p.

FRAIPONT J. & LOHEST M., 1887. La race humaine de Néanderthal ou de Canstadt en Belgique. Recherches ethnographiques sur des ossements humains découverts dans les dépôts quaternaires d'une grotte à Spy et détermination de leur âge géologique. Gand, *Archives de Biologie*, 7 (1886): 587-757, 4 pl. h.t.

GROENEN M., 2005. Interprétation des datations absolues aurignaciennes et moustériennes pour la grotte-abri du Tiène des Maulins. *Notae Praehistoricae*, 25: 71-79.

GROENEN M., 2010. Rochefort/Éprave: campagne de fouille 2008 dans la grotte-abri du Tiène des Maulins. *Chronique de l'Archéologie wallonne*, Éditions du Service public de Wallonie, Direction générale opérationnelle de l'Aménagement du Territoire, du Logement, du Patrimoine et de l'Énergie, Département du patrimoine, 17: 183-185.

GROENEN M., SMOLDEREN A., DUVIGNEAUD P.-H. & SEGATO T., 2013. Les structures de combustion du Tiène des Maulins (province de Namur, Belgique). Regards croisés. In M. Groenen (ed.), *Expressions esthétiques et comportements techniques au Paléolithique*. Actes du XVI Congrès de l'UISPP, vol. 3: Actes des sessions 36 et 37, Oxford, British Archaeological Reports, International Series, 2496: 97-132.

HAESAERTS P., 1984. Aspects de l'évolution du paysage et de l'environnement en Belgique au Quaternaire. In D. CAHEN & P. HAESAERTS (eds.), *Peuples chasseurs de la Belgique préhistorique dans leur cadre naturel*. Patrimoine de l'Institut royal des Sciences naturelles de Belgique, Bruxelles: 27-39.

HIGHAM T. F. G., 2011. European Middle and Upper Palaeolithic radiocarbon dates are often older than they look: problems with previous dates and some remedies. *Antiquity*, 85: 235-249.

HIGHAM T. F. G., BRONK RAMSEY C., KARAVANIĆ I., SMITH F. H. & TRINKAUS E., 2006. Revised direct radiocarbon dating of the Vindija G1 Upper Paleolithic Neandertals. *Proceedings of the National Academy of Sciences of the United States of America*, 103, 3: 553-557.

HIGHAM T. F. G., COMPTON T., STRINGER C. B., JACOBI R., SHAPIRO B., TRINKAUS E., CHANDLER B., GRÖNING F., COLLINS C., HILLSON S., O'HIGGINS

P., FITZGERALD C. & FAGAN M., 2011. The Earliest Evidence for Anatomically Modern Humans in Northwestern Europe. *Nature*, 479: 521-524.

HILLGRUBER K. F., 2006. The Middle Palaeolithic Stone artefacts from the site in the Neander Valley. In R. W. SCHMITZ (ed.), *Neanderthal 1856-2006*. Rheinische Ausgrabungen, 58, Mainz am Rhein, Philipp von Zabern: 111-144.

HUBLIN J.-J., WESTON D., GUNZ P., RICHARDS M. P., ROEBROEKS W., GLIMMERVEEN J. & ANTHONIS D., 2009. Out of the North Sea: the Zeeland Ridges Neandertal. *Journal of Human Evolution*, 57: 777-785.

LEGUEBE A. & TOUSSAINT M., 1988. *La mandibule et le cubitus de la Naulette. Morphologie et morphométrie*. Paris, Éditions du Centre national de la recherche scientifique, Cahiers de Paléoanthropologie, 125 p.

LEROI-GOURHAN A., 1958. Étude des restes humains fossiles provenant des grottes d'Arcy-sur-Cure. *Annales de Paléontologie*, 84: 87-147.

OTTE M., 1984. Le Paléolithique supérieur en Belgique. In D. CAHEN & P. HAESAERTS (eds.), *Peuples chasseurs de la Belgique préhistorique dans leur cadre naturel*. Patrimoine de l'Institut royal des Sciences naturelles de Belgique, Bruxelles: 157-179.

OTTE M., 1986. L'occupation préhistorique à la grotte de Montignies-le-Tilleul (Hainaut). *Bulletin de la Société royale belge d'Anthropologie et de Préhistoire*, 97: 183-188.

PINHASI R., HIGHAM T. F. G., GOLOVANOVA L. V. & DORONICHEV V. B., 2011. Revised age of late Neanderthal occupation and the end of the Middle Paleolithic in the northern Caucasus. *Proceedings of the National Academy of Sciences of the United States of America*, 108, 21: 8611-8616.

PIRSON S., 2007. *Contribution à l'étude des dépôts d'entrée de grotte en Belgique au Pléistocène supérieur. Stratigraphie, sédimentogenèse et paléoenvironnement*. Unpublished PhD thesis, University of Liège & Royal Belgian Institute of Natural Sciences, 2 vol., 435 p. & 5 annexes.

PIRSON S., CATTELAÏN P., EL ZAATARI S., FLAS R., LETOURNEUX C., MILLER R., OLEJNICZAK A. J., OTTE M. & TOUSSAINT M., 2009. Le Trou de l'Abîme à Couvin. Bilan des recherches de laboratoire avant la reprise de nouvelles fouilles en septembre 2009. *Notae Praehistoricae*, 29: 59-75.

- PIRSON S. & DI MODICA K., 2011. Position chronostratigraphique des productions du Paléolithique ancien en Belgique. In M. TOUSSAINT, K. DI MODICA & S. PIRSON (sc. dir.), *Le Paléolithique moyen en Belgique. Mélanges Marguerite Ulrix-Closset*. Bulletin de la Société royale belge d'Études Géologiques et Archéologiques *Les Chercheurs de la Wallonie*, hors-série, 4 & Études et Recherches Archéologiques de l'Université de Liège, 128: 105-148.
- PIRSON S., DRAILY C. & TOUSSAINT M. (dir.), 2011. *La grotte Walou à Trooz (Belgique). Fouilles de 1996 à 2004, vol. 1: Les sciences de la terre*. Namur, Service public de Wallonie, IPW, Études et documents, Archéologie, 20, 208 p.
- PIRSON S., FLAS D., ABRAMS G., BONJEAN D., COURT-PICON M., DI MODICA K., DRAILY C., DAMBLON F., HAESAERTS P., MILLER R., ROUGIER H., TOUSSAINT M. & SEMAL P., 2012. Chronostratigraphic context of the Middle to Upper Palaeolithic transition: Recent data from Belgium, *Quaternary International*, 259: 78-94.
- ROUGIER H., CREVECOEUR I., BEAUVAL C., BOCHERENS H., FLAS D., GERMONPRÉ M., SEMAL P. & VAN DER PLICHT J., 2012. New data from an old Site: Neandertals at Goyet (Belgium) and their mortuary behavior. *American Journal of Physical Anthropology*, 147, supplement 54: 252-253.
- ROUGIER H., CREVECOEUR I., BEAUVAL C., FLAS D., BOCHERENS H., WIßING C., GERMONPRÉ M., SEMAL P. & VAN DER PLICHT J., 2014. New fossils at the «Troisième Caverne» of Goyet (Belgium) and the mortuary practices of Late Neandertals. *Middle Palaeolithic in North-West Europe. Multidisciplinary approaches*. Book of Abstracts, Namur, March 20th-21st: 35.
- ROUGIER H., CREVECOEUR I., SEMAL P. & TOUSSAINT M., 2009. Des Néandertaliens dans la troisième caverne de Goyet. In K. DI MODICA & C. JUNGELS (dir.), *Paléolithique moyen en Wallonie. La collection Louis Éloy*. Bruxelles, Collections du Patrimoine culturel de la Communauté française, 2: 173.
- ROUGIER H. & SEMAL P. (eds.), 2013. *Spy Cave, 125 years of multidisciplinary research at the Betche aux Rotches (Jemeppe-sur-Sambre, Province of Namur, Belgium)*, vol. 1, Anthropologica et Praehistorica, 123, 380 p.
- ROUGIER H. & SEMAL P. (eds.), 2014. *Spy Cave, 125 years of multidisciplinary research at the Betche aux Rotches (Jemeppe-sur-Sambre, Province of Namur, Belgium)*, vol. 2, Anthropologica et Praehistorica, 124, in press.
- SCHMITZ R. W., 2006. The rediscovery of the sediments from the Neanderthal type specimen's site. In R. W. SCHMITZ (ed.), *Neanderthal 1856-2006*. Rheinische Ausgrabungen, 58, Mainz am Rhein, Philipp von Zabern: 55-60.
- SEMAL P., HAUZEUR A., ROUGIER H., CREVECOEUR I., GERMONPRÉ M., PIRSON S., HAESAERTS P., JUNGELS C., FLAS D., TOUSSAINT M., MAUREILLE B., BOCHERENS H., HIGHAM T. F. G. & VAN DER PLICHT J., 2013. Radiocarbon dating on human remains and associated archaeological materials. In H. ROUGIER & P. SEMAL (eds.), *Spy Cave, 125 years of multidisciplinary research at the Betche aux Rotches (Jemeppe-sur-Sambre, Province of Namur, Belgium)*, vol. 1, Chapter XVI, Anthropologica et Praehistorica, 123: 331-356.
- SEMAL P., ROUGIER H., CREVECOEUR I., JUNGELS C., FLAS D., HAUZEUR A., MAUREILLE B., GERMONPRÉ M., BOCHERENS H., PIRSON S., CAMMAERT L., DE CLERCK N., HAMBUCKEN A., HIGHAM T. F. G., TOUSSAINT M. & VAN DER PLICHT J., 2009. New Data on the Late Neandertals: Direct Dating of the Belgian Spy Fossils. *American Journal of Physical Anthropology*, 138: 421-428.
- STREET M., TERBERGER T. & ORSCHIEDT J., 2006. A critical review of the German Paleolithic hominin record. *Journal of Human Evolution*, 51: 551-579.
- STRINGER C. B. & CURRANT A. P., 1986. Hominid specimens from La Cotte de St. Brelade. In La Cotte de St. Brelade 1961-1978. Excavations by C. B. M. MCBURNEY, P. CALLOW, J. M. CORNFORD (eds.). Norwich, Geo Books: 155-158.
- STRINGER C. B., JACOBI R. & HIGHAM T. F. G., 2007. New research on the Kent's Cavern 4 maxilla, its context and dating. In C. B. STRINGER & S. BELLO (eds.), *First Workshop of AHOB2: Ancien Human Occupation of Britain and its European Context*. London, October 10-11th 2007: 27-29.
- TILLIER A.-M., 1983. Le crâne d'enfant d'En-gis 2: un exemple de distribution des caractères juvéniles, primitifs et néandertaliens. *Bulletin de la Société royale belge d'Anthropologie et de Préhistoire*, 94: 51-75.
- TOUSSAINT M., 1992. The Role of Wallonia in the History of Palaeo-anthropology. In M. TOUSSAINT (ed.), *Cinq millions d'années, l'aventure humaine*. Études et Recherches Archéologiques de l'Université de Liège, 56: 27-41.



- TOUSSAINT M., 2001. *Les hommes fossiles en Wallonie. De Philippe-Charles Schmerling à Julien Fraipont, l'émergence de la paléanthropologie*. Carnet du Patrimoine, 33, Namur, Éditions du Ministère de la Région Wallonne, 60 p.
- TOUSSAINT M., OLEJNICZAK A. J., EL ZAATARI S., CATTELAÏN P., FLAS D., LETOURNEUX C. & PIRSON S., 2010. The Neandertal lower right deciduous second molar from Trou de l'Abîme at Couvin, Belgium. *Journal of Human Evolution*, 58: 56-67.
- TOUSSAINT M., OTTE M., BONJEAN D., BOCHERENS H., FALGUÈRES C. & YOKOYAMA Y., 1998. Les restes humains néandertaliens immatures de la couche 4A de la grotte Scladina (Andenne, Belgique). *Comptes rendus de l'Académie des Sciences de Paris, Sciences de la terre et des planètes*, 326: 737-742.
- TOUSSAINT M. & PIRSON S., 2002. Houyet/Hulsonniaux : La Naulette, les fossiles humains les plus anciens de Belgique ? *Chronique de l'Archéologie wallonne*, 10: 230-234.
- TOUSSAINT M. & PIRSON S., 2006. Neandertal Studies in Belgium: 2000-2005. *Periodicum Biologorum*, 108, 3: 373-387.
- TOUSSAINT M. & PIRSON S., 2007. Aperçu historique des recherches concernant l'homme préhistorique dans le karst belge au XIX^e et XX^e siècles : archéologie, géologie, paléanthropologie, paléontologie, datations. XXVI^e congrès préhistorique de France, Avignon 21-25 septembre 2004. *Un siècle de construction du discours scientifique en Préhistoire*, vol. II: 117-142.
- TOUSSAINT M., PIRSON S. & BOCHERENS H., 2001. Neandertals from Belgium. *Anthropologica et Præhistorica*, 112: 21-38.
- TOUSSAINT M., SEMAL P. & PIRSON S., 2011. Les Néandertaliens du bassin mosan belge : bilan 2006-2011. In M. TOUSSAINT, K. DI MODICA & S. PIRSON (sc. dir.), *Le Paléolithique moyen en Belgique. Mélanges Marguerite Ulix-Closset*. Bulletin de la Société royale belge d'Études Géologiques et Archéologiques *Les Chercheurs de la Wallonie*, hors-série, 4 & Études et Recherches Archéologiques de l'Université de Liège, 128: 149-196.
- TWIESELDMANN F., 1961. *Le fémur néandertalien de Fond-de-Forêt (province de Liège)*. Institut royal des Sciences naturelles de Belgique, mémoire n° 148, Bruxelles, 164 p.
- ULRIX-CLOSSET M., 1975. *Le Paléolithique moyen dans le Bassin mosan en Belgique*. Wetteren, Universa, 221 p.
- ULRIX-CLOSSET M., 1990. Le paléolithique moyen récent en Belgique. Actes du Colloque international de Nemours, 1988 : Paléolithique moyen récent et Paléolithique supérieur ancien en Europe. Ruptures et transitions : examen critique des documents archéologiques, *Mémoires du Musée de Préhistoire d'Ile-de-France*, 3: 135-143.
- WHITE M. J. & PETTITT P. B., 2012. Ancient digs and modern myths. The context and age of the Kent's Cavern 4 maxilla and the spread of Homo sapiens in Europe. *European Journal of Archaeology*, 15: 1-30.
- WOOD R. E., BARROSO-RUIZ C., CAPARRÓS M., JORDÁ PARDO J., GALVÁN SANTOS B. & HIGHAM T. F. G., 2013. Radiocarbon dating casts doubt on the late chronology of the Middle to Upper Palaeolithic transition in southern Iberia. *Proceedings of the National Academy of Sciences of the United States of America*, www.pnas.org/cgi/doi/10.1073/pnas.1207656110.

Michel TOUSSAINT, Dominique BONJEAN & Stéphane PIRSON

Michel Toussaint & Dominique Bonjean (eds.), 2014. The Scladina I-4A Juvenile Neandertal (Andenne, Belgium), Palaeoanthropology and Context

Études et Recherches Archéologiques de l'Université de Liège, 134: 409-418.

1. Introduction

▲ total of 19 Neandertal remains – bones and —teeth – have been discovered at Scladina Cave. They consist of the mandible and a fragment of the maxilla of an eight-year-old child (Figure 1). Most of these fossils (11 teeth and the fragment of the right maxilla) were discovered between 1990 and 1992 but not identified until after the discovery of Scla 4A-1, the right hemimandible, in July 1993 (BONJEAN et al., 2009).

Many papers have been devoted to these remains. Some are just preliminary presentations (e.g. OTTE et al., 1993; TOUSSAINT et al., 1998), while others are detailed studies of specific subjects (e.g. SMITH et al., 2007). Various contributions, often derived from PhD theses or post-doctoral research, include the Scladina fossils in aspects of general Neandertal studies, for example the enamel-dentine junction (SKINNER et al., 2010) or tooth root size (LE CABEC et al., 2013). Although of great interest, these works divide the information into a large number of contributions, with only little confrontation between all involved disciplines and subdisciplines.

0 3 cm



Figure 1: The Scladina I-4A juvenile Neandertal remains.

Conversaly, this monograph combines most of the information obtained for the juvenile Neandertal remains from Scladina, in topics ranging from their stratigraphic position, their chronology, their taphonomy, their age at death, their morphology, their DNA, and their isotopes of carbon and nitrogen. In this context, this chapter summarizes key aspects of this monograph from a multidisciplinary perspective and discusses the future of Neandertal research in the region.

2. Main interdisciplinary results of the research at Scladina

2.1. Context

2.1.1. Stratigraphic position of the Neandertal remains

■ In the years following the discovery of the — Scladina Child, the stratigraphy related to these remains was understood as the following sequence, from bottom to top: Layer 4B, Layer 4A, Stalagmitic Floor CC4, and Layer 3. A few years later, the identification of a stalagmitic floor inside Layer 4A, called CC14, led to the definition of a new stratigraphic succession: Layer 4B, Layer 4A (lower), lower Stalagmitic Floor CC14, Layer 4A (upper), upper Stalagmitic Floor CC4, and Layer 3. Most of the remains were attributed to the upper part of Layer 4A at that time, situated between stalagmitic floors CC14 and CC4 (BONJEAN et al., 1996; BONJEAN, 1998), while some teeth, originally attributed to Layer 3, were reattributed to Layer 4A.

In the context of a PhD thesis (PIRSON, 2007), detailed stratigraphic observations took place of almost all the available sedimentary profiles within Scladina, allowing about 120 layers to be defined and grouped into 30 distinct stratigraphic units. Following this stratigraphic reappraisal, former Layer 4A became ‘Sedimentary Complex 4A’, including about 20 layers grouped into 4 units (Chapter 3). These include, from bottom to top:



- Unit 4A-AP, the lowermost unit, including the layers within the complex that are older than Stalagmitic Floor CC4 (i.e. pre-floor layers);
- Unit 4A-IP, including stalagmitic floor CC4 (which is in fact an equivalent of CC14) and the layers that are contemporaneous with the formation of CC4 (i.e. syn-floor layers);
- Unit 4A-CHE, which includes the layers that developed inside a large gully structure that eroded underlying layers, including CC4 (i.e. post-floor and syn-gully layers);
- Unit 4A-POC, the uppermost unit, superimposing both units 4A-IP and 4A-CHE (i.e. post-gully layers).

For this monograph, all available arguments were re-examined in order to refine the stratigraphic position of the Neandertal remains discovered in former Layer 4A (Chapter 5). These arguments include the 3-dimensional coordinates, the analysis of sedimentary profiles, the projection of the remains onto the nearest profiles, the analysis of field notes, the analysis of pictures, etc.

Based on this, out of the 19 juvenile Neandertal remains unearthed to date, seven were accurately and precisely repositioned inside the new stratigraphic record (see Chapters 3 & 5). Each of these seven fossils is either from the gully in Unit 4A-CHE or from the directly superimposing deposits (Unit 4A-POC). Three of these seven fossils were repositioned with a high degree of certainty into a specific layer:

- the right half of the mandible (Scla 4A-1) is from the top of Unit 4A-CHE, and more specifically from the uppermost 4A-GX lithofacies;
- two teeth are from Unit 4A-POC, including Scla 4A-4 from Layer 4A-BO and Scla 4A-13 from Layer 4A-LEG.

The stratigraphic provenance of the 12 other remains is still uncertain, as several units are possible candidates (4A-IP, 4A-CHE, 4A-POC, 3-INF, and, less likely, 3-SUP). However, an attribution to Unit 4A-POC is most probable when considering the results of the taphonomic study (Chapter 7) as well as the palaeoanthropological analysis, which indicates that the remains are from a single individual.

Given the sedimentary depositional dynamics of Unit 4A-CHE, all remains unearthed from there are at least in secondary spatial position. Some remains were subsequently reworked into at least one superimposing unit (Unit 4A-POC). These reworked remains are therefore in tertiary spatial

position. The spatial distribution of the fossils along the longitudinal axis of the cave is logical within this framework. In the present state of research, the primary spatial position of the child is still unknown.

Because the Neandertal remains were redeposited through an episode of gully formation, questioning the relationship between the age of the remains and this structure is important: were the remains reworked from a much older unit, or are they contemporaneous with the gully's formation? This issue is addressed in the next section.

2.1.2. Chronostratigraphy: integrating the disciplines

Several observations made during the taphonomical study of the Neandertal remains (Chapter 7) led to the conclusion that the Neandertal remains are contemporaneous with the gully of Unit 4A-CHE. They include:

- when combining all of the physical taphonomic attributes, animal bones and teeth from units 4A-CHE and 4A-POC have the strongest correlation to the Neandertal child, which suggests that the remains were deposited during the gully event;
- the mandible was a 'green bone' when it was broken into two parts;
- the two halves of the mandible differ in colour and have different taphonomical properties, indicating that they were embedded in different sediment before the majority of their taphonomic alteration began. This suggests that the Neandertal remains were not (at least not completely) fossilized when they were incorporated into different layers within Unit 4A-CHE.

These are fully compatible with the following stratigraphic arguments:

- the oldest stratigraphic unit that has yielded Neandertal remains is Unit 4A-CHE;
- all of the Neandertal remains assigned to 4A-CHE are from the top of the unit, suggesting that these objects were incorporated during the last stages of the gully's formation;
- their spatial distribution, restricted to the course of the 4A-CHE gully, suggests they are strictly associated with this structure, even if they were later reworked from the top of Unit 4A-CHE into the low energy Unit 4A-POC, probably through run-off.

Along with the reappraisal of the stratigraphic sequence, the palaeoenvironmental data and chronostratigraphy of the Scladina sequence were also re-examined (PIRSON, 2007; see Chapter 4). The new palaeoenvironmental framework is mainly based on new results from palynology, anthracology, as well as climatic signals recorded in the sediments themselves through the observation of sedimentary dynamics and post-depositional processes. These results correlate with the data from literature that was based on the former stratigraphic record (e.g., CORDY & BASTIN, 1992). Overall, the palaeoenvironment results from all the available disciplines are in agreement. The data for Unit 4A-CHE indicates cold conditions, which is logical considering that the gully is interpreted as a result of the degradation of a deep frozen soil (melting structure).

The chronostratigraphic framework of the entire Scladina sequence was also reconsidered, based on all the available data sets: numerical dates (luminescence, radiocarbon), biostratigraphy, archaeostratigraphy, comparison with the loess reference sequence from Middle Belgium (heavy mineralogy, lithological, and pedological markers), and climatostratigraphy. This reappraisal concludes that most of the Scladina deposits can confidently be positioned in the Upper Pleistocene. However, the chronostratigraphic framework of Scladina is still quite imprecise. Several situations still need more attention, such as the location of the beginning and end of MIS 5 in the sequence. Interpreting the age of the Unit 4A-CHE gully relies on the integration of climatostratigraphy and heavy mineralogy, especially the green amphibole contents when compared with the data from the loess reference sequence (see Chapter 4). The main arguments are:

- in the lower half of the sequence, from units 7A to 2B, strong green amphibole values (ca. 20%) were recorded, suggesting the reworking of either MIS 6 loess or MIS 4-2 loess;
- between units 7A to 2B, two units (Unit 6B, former Layer 6; Unit 4A-IP, former Layer 4A) indicate temperate forest conditions, compatible with an interglacial or an early glacial interstadial, notably through palynological and macrofaunal data as well as the presence of major stalagmitic floors;
- combining the first two arguments allows the reworking of MIS 4-2 loess to be discarded as a hypothesis and supports the reworking of MIS 6 loess during MIS 5, in the sequence from Unit 6B to Unit 4A-IP. The available

- U/Th and TL dates obtained on speleothem CC4 (Unit 4A-IP) are in agreement with the MIS 5 interpretation. With a strong climatic improvement evidenced in MIS 5 (Unit 6B), Unit 4A-IP (and Speleothem CC4) must be positioned in either MIS 5c and/or MIS 5a;
- higher up in the sequence, Unit 2A is interpreted as the first allochthonous loess input of MIS 4, and Unit 2B is best interpreted as representing the end of MIS 5a (see Chapter 4).

Following these arguments, and combining them with the complexity of the Scladina sequence, there are several possible interpretations for the chronostratigraphic positioning of the cold episode represented by Unit 4A-CHE and the associated Neandertal remains, the most probable being the following:

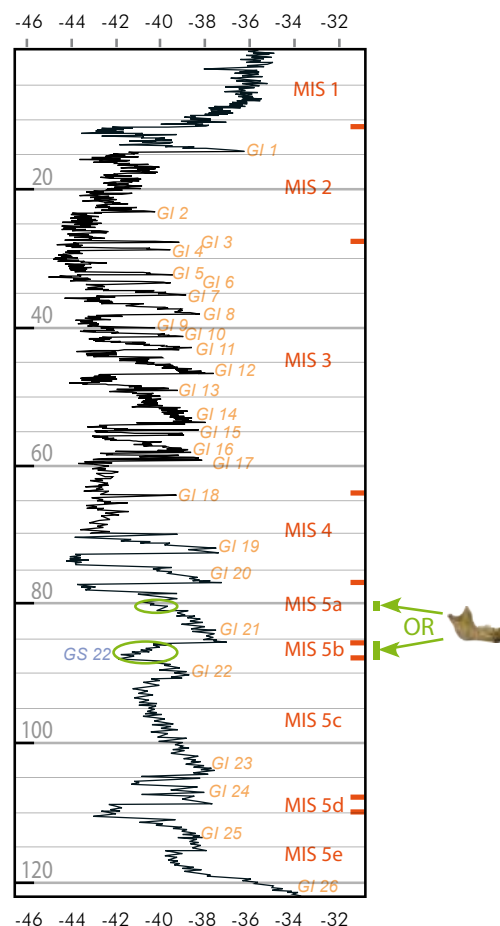


Figure 2: The two best hypotheses attributing the Scladina I-4A juvenile Neandertal remains in either GS 22 (MIS 5b) or GI 21 (MIS 5a), in the NorthGRIP sequence (modified after NORTHGRIP-MEMBERS, 2004; ANDERSEN et al., 2007). GI = Greenland interstadial; GS = Greenland stadial.



- if CC4 corresponds to MIS 5c temperate conditions, 4A-CHE would be part of MIS 5b colder conditions (GS 22 of the Greenland record, between GI 22 and GI 21, around 87,000 BP; NORTHGRIP-MEMBERS, 2004); in this case, the Scladina Child would be contemporaneous with the Remicourt lithic assemblage (BOSQUET et al., 2011; PIRSON & DI MODICA, 2011);
- if CC4 corresponds to the ‘warmer’ first half of MIS 5a, 4A-CHE would belong to the intra-MIS 5a cooling (intra-GI 21, ~80,000 BP);

The best hypothesis attributes the whole sequence from Unit 6B to Unit 2B to part of MIS 5; the gully from Unit 4A-CHE is placed in either MIS 5b or MIS 5a. Therefore, the Scladina Child would have lived either ~87,000 years ago, or ~80,000 years ago (Figure 2). This chronostratigraphic hypothesis is consistent with the morphometrical and the diet studies of the fossils (see below, § 2.2.2. & 2.2.5).

2.2. Palaeoanthropology

2.2.1. Morphology

The morphology of the Scladina juvenile mandible exhibits a general pattern that is quite characteristic of Neandertals. Indeed, the fossil shows a typical association of some characters either derived Neandertal or, without being derived, frequent on this taxon; all of these characters fit well with the collection of Neandertal mandibles of similar ages (Chapter 10). Statistically, comparative analysis of the shape of the mandible in the context of ontogenetic and adult variation of Neandertals and modern humans (Chapters 10 & 11) shows that the fossil has features that distinguish Neandertals from modern humans.

The Scla 4A-2 maxilla is a small fragment of the right midfacial region that is comprised of part of the alveolar and palatine processes, as well as a small part of the body (Chapter 12). The fossil is consistent with Neandertal maxillae with regards to the bilevel configuration of its internal nasal floor and its rather high estimated subnasal height. The anterior part of its dental arcade does not seem very large and the location of its zygoalveolar crest is not as posterior when compared to other similarly aged Neandertals.

The crowns of the 24 teeth from the mandible and maxilla have been examined from anatomical and statistical perspectives (Chapter 13). Regarding the taxonomic allocation, the teeth fit very well in the characteristic Neandertal pattern,

even if, as for the teeth from similar sites, they do not exhibit characteristics that are exclusively Neandertal. Mesiodistal and buccolingual diameters of all crowns were compared to samples of Early and Late Neandertals (EN and LN), Middle Palaeolithic Modern Humans (MPMH), Upper Palaeolithic Modern Humans (UPMH), and Modern *Homo sapiens sapiens* (MHSS) using univariate methods, i.e. probabilistic distances (DP), *écart centré réduit ajusté* (ECRA), as well as bivariate equiprobable ellipses. Regardless of the method, significant differences between Scladina and MHSS are present. Slight differences exist for the UPMH comparison sample. By contrast, the Scladina teeth crowns are never different from those of Late Neandertals and rarely from Early Neandertals and MPMH.

The analysis of the Scladina teeth enamel thickness (Chapter 14) confirms, using 3D μ CT data, that Neandertals have lower average enamel thickness and relative enamel thickness indices than *Homo sapiens*, and that molars, premolars, canines, and possibly also incisors, have a different trend, with premolars having generally larger relative enamel thickness index than molars, while the canines have the lowest values. Tooth root morphology has been shown to taxonomically differentiate Neandertals from modern humans, for both anterior (incisors and canines) and posterior (molars) teeth (Chapter 16). Compared to MIS 5 Neandertals, Scladina I-4A has the shortest root dimensions relative to its crown sizes. Scladina has also an anterior tooth root shape similar to other Neandertals. Moreover, the molar roots are lacking any degree of taurodontism.

2.2.2. Scladina, Early or Classic Neandertal?

Following the accretion model, the Neandertal evolution comprises four Neandertal ‘stages’ (DEAN et al., 1998; HUBLIN, 1998): stage 1 or “Early-Pre-Neandertals”, before and during MIS 12, with fossils such as Arago and Mauer; stage 2 or “Pre-Neandertals” from MIS 11 to 9 with Atapuerca (Sima de los Huesos) or Steinheim (no specimens are placed in MIS 8 according to the accretion model; DEAN et al., 1998); stage 3 or “Early Neandertals” during MIS 7-5 with, for instance, Ehringsdorf, La Chaise, or Lazaret; stage 4 or “Classic Neandertals”, during MIS 4 and 3 with Feldhofer, Spy, La Chapelle-aux-Saints, La Ferrassie, Le Moustier, La Quina, etc. The morphological division between stage 4 and stage 3 of

the evolution of Neandertals is the least clear, as some late 'Early Neandertals' of MIS 5, such as Saccopastore or La Chaise, Abri Bourgeois-Delaunay, exhibit intermediate conditions between Early and Classic Neandertals (DEAN et al, 1998).

CONDEMI (2000)'s views are not so different, especially regarding MIS 5 to 3: "Proto-Neandertals" during stage 5, which correspond to the "intermediate condition" of the accretion model, and "Classic Neandertals" dating back to stage 4 and stage 3 (see also CONDEMI, 2005).

For SERANGELI & BOLUS (2008), "Early Neandertals" are younger than 200,000 BP but pre-Weichselian, while "Classic Neandertals" appear in the largest number during the Weichselian, ca. 115,000 years ago, which is near the beginning of MIS 5.

In the context of these models, what is the place of the Scladina I-4A juvenile specimen in Neandertal evolution? The morphology of the incisors and canines, as well as the occlusal surface of the premolars and molars, present some combinations of features that give them a general Neandertal appearance (Chapter 13). Metrically, MD and BL diameters of the Scladina teeth correspond quite well to Early and Classic/Late Neandertals of the accretion model. For some attributes, they are not closely related to Early Neandertals but correspond well to Late Neandertals instead. Intraspecific temporal variation in enamel-dentine junction (EDJ) morphology confirms the intraspecific taxonomic position of Scladina, which is closer to that of the Classic Neandertals than to the Early Neandertal sample (Chapter 15). In addition, the tooth root size is most comparable with the Neandertals of MIS 5, with the exception of MIS 5e (Chapter 16). In addition, using ECRA, the mandible seems closer to EN than LN. Therefore, the best hypothesis is to consider Scladina as a "Classic Neandertal", but with subdividing a continuum, these fossils can be considered an "old Classic Neandertal" – "Proto-Neandertal" from Conde mi's perspective and "intermediate condition" of Dean et al.'s view – particularly when compared to Late Neandertals, such as Spy. The morphology of the Scladina teeth seems consistent with the best chronostratigraphic hypothesis for the fossils, i.e. MIS 5b or 5a.

2.2.3. Age at death

The final estimation of the dental age of the Scladina Juvenile, proposed in Chapter 8 (see also SMITH et al., 2007), was performed using a histological method that potentially offers the most

reliable and accurate results. Based on this, the Scladina Child appears to have died at 8 years old.

However, summarizing the estimation of the age at death previously obtained at Scladina by conventional anthropological methods – the study of tooth maturation, mainly the beginning of calcification; calcification scoring dental; tooth emergence; growth of the roots; and root completion – and then comparing these results to those of histology is very useful.

Based on this, a preliminary report concluded that "[i]f the criteria of age linked to dental eruption and to the formation of molar roots observed in modern humans are applied to Neandertals, the Child of Sclayn [...] would have been at least 12-13 years old. The persistence of deciduous molars could however indicate a younger age, probably not more than about ten years" (TOUSSAINT et al., 1998: 740). More recently another perspective was used: "[d]ental age determination compared with cutting teeth and molar root formation in modern humans suggest that the child died at age 12, yet the persistence of deciduous molars is consistent with a younger age, but probably not less than 10" (TOUSSAINT & PIRSON, 2006: 382-383).

In two methodological studies, GRANAT & HEIM (2001, 2003) developed a new model for dental maturation that estimates the age at death of Neandertals without referring to the classic modern populations dental growth tables. Several postulates forced the authors to mention a 'suspected age', i.e. an age relative to the onset of maturation that is considered identical in both Neandertals and modern humans, rather than an absolute age. Among these postulates is the age of only the central deciduous incisors as estimated from modern populations' dental growth tables, as well as the notion that the deciduous teeth, incisors, canines, and first molars of Neandertals begin calcifying at the same time. They proposed two methods, one using two mathematical formulas and the second using a graph; both of them yield the age of a Neandertal from the degree of maturation of his/her deciduous and permanent teeth, but the graphical approach is clearly more approximate. Although it has been nearly 15 years since it was established, the palaeo-anthropological community only minimally uses this new approach. Comparing results from these methods with results obtained by histological determination of the individual's age offers a valid test of their applicability. Individually, the teeth of Scladina provide an age range from 7 years 8 months to 10 years 6 months, with most of them ranging between 8 years 3 months and 8



years 9 months. The average is therefore 8 years and almost 6 months. Histological techniques and Granat and Heim's method yield similar results for the Scladina Child: only 6% older for Granat's technique compared to 25% older when the minimal average age of 10 obtained through traditional methods are taken into account. Despite its lack of acceptance in the anthropological community, Granat and Heim's technique provides an interesting perspective, although it slightly overestimates the age.

2.2.4. Sex

Numerous sex determination techniques, based either on morphological traits or on metric differences, have been developed for adult bones, but they were mainly developed from modern human skeletons of known age and sex. Regarding juveniles, there are no really precise sex diagnosis techniques.

At Scladina, these problems exist: the remains belonged to an 8-year-old child, traits commonly used for sexing modern humans are not accurate enough for Neandertals, and mandibles and maxillae are not the most accurate bones to use for determining sex.

The dental technique developed by OXNARD (1987) avoids the pitfall of applying modern human measurements to other taxa by using the bimodal appearance of some dimensions of the crowns of teeth, as it is largely acknowledged that the size distribution of some teeth, particularly the canines, show the greatest differences between males and females. On this basis, the Scladina Juvenile may have been female (Chapter 9).

Other evidence from the histological study and the study of tooth roots align with the same interpretation. Based on the Scladina teeth, perikymata numbers fall either near the low end or below the values reported for other Neandertals, which, based on comparisons with other fossils, may provide another argument for the determination of Scladina as a female (Chapter 9). The Scladina tooth roots are very short and fall within the lower end of the Neandertal variation. In addition, the pulp cavities are very large. Both arguments support the hypothesis that the Scladina Child is female (Chapter 16).

The dimensions of the mandibular body are relatively small when compared with other Neandertal mandibles of similar ages at death. Even if this is body size dependent, it could tentatively support the hypothesis that the fossil is female (Chapter 9).

Although none of these indices are determinant, and even if it is extremely difficult to estimate the sex of the Scladina Juvenile, the conjunction of the various analyses presented in this monograph suggests a female trend.

2.2.5. Diet and environment

At Scladina, both techniques used for the reconstruction of the child's diet, carbon/nitrogen isotopic signatures (Chapter 17) and tooth microwear patterns (Chapter 18), indicate that the child mainly ate meat. However, the microwear data also reveals that the diet of the child most likely included small amounts of abrasive plant foods.

In this regard, and throughout Europe, it seems that the Neandertal diet may significantly differ in response to the changes in palaeoecological context, with increased consumption of plant foods with the expansion of tree cover and the use of meat in cold, open, steppic conditions (EL ZAATARI et al., 2011; see also Chapter 18). Scladina microwear texture is within the range of Neandertals who lived in both open and wooded habitats, but appears closer to the former group, which is somewhat expected in the context of a cold episode from the second half of Weichselian Early Glacial. To complete this information, studying starch grains and phytoliths in calculus on teeth could confirm the consumption of a variety of plant foods, such as with the Spy I and II specimens (HENRY et al., 2011). However, the Scladina teeth are not clearly encrusted with visible deposits of calculus, possibly because of the individual's young age.

Some perspectives for the Neandertal research in the 3. Belgian Meuse River Basin

3.1. Scladina

At Scladina, the study of Neandertal remains still offers interesting prospects, both in the field and laboratory.

In the cave, Sedimentary Complex 4A, which yielded the Neandertal remains, is far from being completely excavated (see Chapter 7). In addition, the Middle Palaeolithic context situated near the top of the cave in former Layer 1B is not all excavated and has already yielded some human remains. Their analyses have not yet been completed.

The origin of the Neandertal remains and how they became interred in Sedimentary Complex 4A

is also unknown, so excavation will undoubtedly continue.

The re-examination of the available sedimentary profiles at the cave entrance is also promising in terms of providing new results.

During the final stages of preparing this monograph, the remains of the child were shown to date from the end of Weichselian Early Glacial (most probably MIS 5b or 5a). This is a significant improvement over the previously assumed age, which ranged from MIS 6 to MIS 4. However, new palaeoenvironmental research to be undertaken in parallel with the ongoing excavations will confirm or deny the new MIS 5b-5a interpretation.

Analysis of the fossils will undoubtedly continue. Ongoing research on the potential use of strontium as a marker of Neandertal movement between different ecological niches is a good example (VERNA et al., 2014). Hopefully the current edition of the monograph will inspire researchers to continue analysing the Scladina remains, incorporating them in different aspects of Neandertal research.

3.2. Other sites

The chronology of Neandertals in the Meuse River Basin, although relatively well established, still lacks precision (Chapter 20). This will likely be improved in the future by using new radiocarbon dates, especially when these methods better control the effects of pollutants (glue, varnish), which have made some dates, such as Engis 2, appear too young. Improvements in ^{14}C dating methods may eventually allow the acquisition of dates for fossils that are older than what can be currently dated.

New discoveries of Neandertal remains are likely to continue, even from museums and private collections as recently demonstrated with the examples of Spy and Goyet. At Spy Cave, the careful analyses of many skeletal remains collected by François Twiesselmann's team in the 1950s from the debris accumulated on the slope between the cave and the Orneau River (ROUGIER et al., 2004), as well as the purchase of a private collection of material from the site (SEMAL et al., 2009), led to the discovery of various previously unidentified Neandertal remains. These findings have also triggered a new comprehensive analysis of anthropological and archaeological material discovered at Spy since 1886, which led to the publication of a large monograph (ROUGIER & SEMAL (eds.), 2013, 2014 in press). In the caves of Goyet, the excavations of 1998 on the terrace and in the main cave did not yield palaeolithic

human remains (TOUSSAINT et al., 1999); most of the sediments were removed by E. Dupont in the 1870s and his many successors without the use of detailed stratigraphic records. In contrast, since 2004 numerous human remains from the Upper and Middle Palaeolithic were discovered in the collections of the Royal Belgian Institute of Natural Sciences. Although retrieved by Dupont nearly a century and a half ago, they had never been analysed in detail (ROUGIER et al., 2014).

Most of the caves where Neandertal remains have been discovered no longer have any significant amount of in situ sediments, making new anthropological discoveries and the acquisition of geological and palaeoenvironmental data next to impossible. This is the case at Engis and Spy, where only the sieving of debris from old excavations on the slope in front of the cave at Spy and at the bottom of a small quarry dug adjacent to the cave at Engis may yield finds. At Fonds de Forêt, the excavations completed ten years ago (before the installation of fences to protect bats) yielded only contaminated or sterile sediment (TOUSSAINT & PIRSON, 2004). At Couvin, after the 1984 excavations (CATTELAINE & OTTE, 1985), research undertaken between 2009 and 2012 discovered in situ sediment, including some Middle Palaeolithic artefacts, although the area was quite limited and no new human remains were discovered (MILLER et al., 2014). In Walou Cave, most of the sediment was excavated during two excavation campaigns: 1985 to 1990 (DEWEZ dir, 2008) and 1996 to 2004 (DRAILY, 2011; DRAILY et al. (dir.), 2011; PIRSON et al. (dir.), 2011). In Goyet, as the terrace and the third cave were carefully excavated by E. Dupont and his successors, secondary sites on a nearby cliff, including an intact entrance recently found below the upper rock shelter, provide the best possibility.

Except Scladina, La Naulette provides the best opportunity for new in situ anthropological discoveries out of the sites that have already yielded Neandertal remains, even if the dating of the fossils is very imprecise. The human remains from La Naulette could be the oldest from the Meuse Basin. During some short field campaigns that have been conducted since 1999 (TOUSSAINT et al., 2000), backfill obstructing the cave was removed. In situ sections left by E. Dupont in 1866-67 were partially recovered. The continuation of this field program aims to excavate the in situ sediment, study palaeoenvironmental deposits, and hopefully find new human remains.

At Montignies-le-Tilleul and Le Tiène des Maulins, two other karstic sites which supposedly



have already yielded Neandertal remains (OTTE, 1986; GROENEN, 2005), numerous analysis have to be carried out before deciding whether or not to add them to the list of Neandertal sites in Belgium (see Chapter 20).

Due to the limited number of opportunities for new anthropological discoveries in the currently available karst sites, new multidisciplinary excavations are absolutely necessary for finding well-contextualized fossils, ideally in unexcavated sites or in caves where human remains have not yet been found. Ongoing research at Trou Al'Wesse, in Petit-Modave in the Hoyoux Valley, could become particularly interesting; excavations undertaken in the 21st century at the site (MILLER et al., 2007), which was only partially excavated during the 19th century, provided Mesolithic, Aurignacian and Middle Palaeolithic layers.

However, due to the relatively limited palaeoanthropological potential of the ongoing excavations in Middle Palaeolithic karstic sites an intensive survey program is needed to expand our knowledge of regional Neandertals. Such a program would require a lot of work before providing results, as, so far, all the regional Neandertal remains were discovered in large sites, and most of these sites, such as Engis, Spy, Goyet, or Fonds de Forêt, are highly visible on the landscape and were identified long ago, especially because speleology was very extensive in the region. In this context, finding intact sites like Walou and Scladina in the 20th century is extremely rare. Their discovery shows the extreme importance of developing contacts with speleologists.

When a new cave or rock shelter is discovered with archaeological and anthropological potential, research there must be undertaken from a multidisciplinary perspective. A Quaternary geologist should be present from the beginning of excavations, together with palaeontologists, prehistorians, palaeoanthropologists, and experts in many other disciplines. The importance of understanding the stratigraphic details and the sedimentary depositional phenomena is critical to any palaeoenvironmental, palaeontological, or archaeological interpretation of a karstic site.

In laboratories, the prospect of regional Neandertal anthropology remains large, as well as throughout all of Eurasia, especially with the constant development of new investigation techniques, such as 3D reconstruction with computer tomography, isotopic biogeochemistry ($^{13}\text{C}/^{15}\text{N}$, Sr, Ba, etc.), histology, and DNA extraction (especially nuclear DNA). Scladina will be very important for

developing these future methods due to the relatively large number of fossils discovered at the site and the opportunity for future geological and palaeoenvironmental studies to be done.

Acknowledgements

The authors wish to express their gratitude to Rhylan McMillan (Vancouver Island University) for his valuable comments and his help editing the English version of this chapter.

References

- ANDERSEN K. K., BIGLER M., CLAUSEN H. B., DAHL-JENSEN D., JOHNSEN S. J., RASMUSSEN S. O., SEIERSTAD I., STEFFENSEN J. P., SVENSSON A., VINTHER B. M., DAVIES S. M., MUSCHELER R., PARRENIN F. & RÖTHLISBERGER R., 2007. A 60 000 year Greenland stratigraphic ice core chronology, *Climate of the Past Discussions*, 3: 1235-1260.
- BONJEAN D., 1998. La stratigraphie. In M. OTTE, M. PATOU-MATHIS & D. BONJEAN (dir.), *Recherches aux grottes de Sclayn, vol. 2 : L'Archéologie. Études et Recherches archéologiques de l'Université de Liège*, 79: 15-23.
- BONJEAN D., MASY P. & TOUSSAINT M., 2009. L'enfant néandertalien de Sclayn. Petite histoire d'une découverte exceptionnelle. *Notae Praehistoricae*, 29: 49-51.
- BONJEAN D., TOUSSAINT M. & OTTE M., 1996. Scladina (Sclayn, Belgique) : l'Homme de Néandertal retrouvé! *Notae Praehistoricae*, 16: 37-46.
- BOSQUET D., HAESAERTS P., DAMBLON F., JARDÓN GINER P. & RYSSAERT C., 2011. Le gisement paléolithique de Remicourt-En Bia Flo I. In M. TOUSSAINT, K. DI MODICA & S. PIRSON (sc. dir.), *Le Paléolithique moyen en Belgique. Mélanges Marguerite Ulrix-Closset*. Bulletin de la Société royale belge d'Études Géologiques et Archéologiques *Les Chercheurs de la Wallonie*, hors-série, 4 & Études et Recherches Archéologiques de l'Université de Liège, 128: 375-384.
- CATTELAINE P. & OTTE M., 1985. Sondage 1984 au « Trou de l'Abîme » à Couvin : état des recherches. *Helinium*, 25: 123-130.
- CONDEMI S., 2000. The Neanderthals: *Homo Neanderthalensis* or *Homo sapiens Neanderthalensis*? Is there a contradiction between the paleogenetic and the paleoanthropological data? In J. ORSCHIEDT & G.-C. WENIGER (eds.), *Neanderthals and Modern Humans –Discussing*

- the transition. *Central and Eastern Europe from 50.000–30.000 B.P.* Neanderthal Museum: 287–295.
- CONDEMI S., 2005. Continuité et/ou discontinuité des premiers peuplements européens. In N. MOLINES, M.-H. MONCEEL & J.-L. MONNIER (dir.), *Données récentes sur les premiers peuplements en Europe*, Oxford, British Archaeological Reports, International Series, 1364: 9–15.
- CORDY J.-M. & BASTIN B., 1992. Synthèse des études paléontologiques réalisées dans les dépôts de la grotte Scladina (Sclayn, Province de Namur). In M. OTTE (ed.), *Recherches aux grottes de Sclayn, vol. 1: Le Contexte*. Études et Recherches Archéologiques de l'Université de Liège, 27: 153–156.
- DEAN D., HUBLIN J.-J., HOLLOWAY R. & ZIEGLER R., 1998. On the phylogenetic position of the pre-Neandertal specimen from Reilingen, Germany, *Journal of Human Evolution*, 34: 485–508.
- DEWEZ M. dir, 2008. Recherches à la grotte Walou à Trooz (Belgique). Second rapport de fouille, Oxford, British Archaeological Report, International Series, 1789, 88 p.
- DRAILY C., 2011. *La grotte Walou à Trooz (Belgique). Fouilles de 1996 à 2004, vol. 3: L'Archéologie*, Namur, Service public de Wallonie, IPW, Études et Documents, Archéologie, 22, 332 p.
- DRAILY C., PIRSON S. & TOUSSAINT M. (dir), 2011. *La grotte Walou à Trooz (Belgique). Fouilles de 1996 à 2004, vol. 2: Les sciences de la vie et les datations*. Namur, Service public de Wallonie, IPW, Études et documents, Archéologie, 21, 241 p.
- EL ZAATARI S., GRINE F. E., UNGAR P. S. & HUBLIN J.-J., 2011. Ecogeographic variation in Neandertal dietary habits: evidence from occlusal microwear texture analysis. *Journal of Human Evolution*, 61: 411–424.
- GRANAT J. & HEIM J.-L., 2001. Croissance dentaire chez l'homme de Néandertal – Élaboration d'une nouvelle méthode d'estimation de l'âge dentaire. *Biométrie humaine et Anthropologie*, 19: 205–215.
- GRANAT J. & HEIM J.-L., 2003. Nouvelle méthode d'estimation de l'âge dentaire des Néandertaliens. *L'Anthropologie*, 107: 171–202.
- GROENEN M., 2005. Interprétation des datations absolues aurignaciennes et moustériennes pour la grotte-abri du Tiène des Maulins. *Notae Praehistoricae*, 25: 71–79.
- HENRY A. G., BROOKS A. S. & PIPERNO D. R., 2011. Microfossils in calculus demonstrate the consumption of plants and cooked foods in Neandertal diets (Shanidar III, Iraq; Spy I and II, Belgium). *Proceedings of the National Academy of Sciences of the United States of America*, 108, 2: 486–491.
- HUBLIN J.-J., 1998. Climatic changes, paleogeography and the evolution of the Neandertals. In T. AKAZAWA, K. AOKI & O. BAR-YOSEF (eds.), *Neandertals and Modern Humans in Western Asia*, Plenum Press, New York and London: 295–310.
- LE CABEC A., GUNZ P., KUPCZIK K., BRAGA J. & HUBLIN J.-J., 2013. Anterior Tooth Root Morphology and Size in Neandertals: Taxonomic and Functional Implications. *Journal of Human Evolution*, 64: 169–193.
- MILLER R., CATTELAINE P., OTTE M., FLAS D., PIRSON S. & TOUSSAINT M., 2014. Couvin/Couvin : Trou de l'Abîme. *Chronique de l'Archéologie wallonne*, Éditions du Service public de Wallonie, Direction générale opérationnelle de l'aménagement du territoire, du logement, du patrimoine et de l'énergie, Département du patrimoine, 21: 251.
- MILLER R., STEWART J. & OTTE M., 2007. Résultats préliminaires de l'étude de la séquence paléolithique au Trou Al'Wesse (comm. de Modave). *Notae Praehistoricae*, 27: 41–49.
- NORTHGRIP-MEMBERS, 2004. High-resolution record of Northern Hemisphere climate extending into the last interglacial period. *Nature*, 431: 147–151.
- OTTE M., 1986. L'occupation préhistorique à la grotte de Montignies-le-Tilleul (Hainaut). *Bulletin de la Société royale belge d'Anthropologie et de Préhistoire*, 97: 183–188.
- OTTE M., TOUSSAINT M. & BONJEAN D., 1993. Découverte de restes humains immatures dans les niveaux moustériens de la grotte Scladina à Andenne (Belgique). *Bulletins et Mémoires de la Société d'Anthropologie de Paris*, nouvelle série, t. 5, 1-2: 327–332.
- OXNARD C. E., 1987. *Fossils, teeth and sex. New Perspectives on Human Evolution*. Seattle & London, University of Washington Press, 281 p.
- PIRSON S., 2007. *Contribution à l'étude des dépôts d'entrée de grotte en Belgique au Pléistocène supérieur. Stratigraphie, sédimentogenèse et paléoenvironnement*. Unpublished PhD thesis, University of Liège & Royal Belgian Institute of Natural Sciences, 2 vol., 435 p. & 5 annexes.



- PIRSON S. & DI MODICA K., 2011. Position chronostratigraphique des productions lithiques du Paléolithique ancien en Belgique : un état de la question. In M. TOUSSAINT, K. DI MODICA & S. PIRSON (sc. dir.), *Le Paléolithique moyen en Belgique. Mélanges Marguerite Ulrix-Closset*. Bulletin de la Société royale belge d'Études Géologiques et Archéologiques *Les Chercheurs de la Wallonie*, hors-série, 4 & Études et Recherches Archéologiques de l'Université de Liège, 128: 105-148.
- PIRSON S., DRAILY C. & TOUSSAINT M. (dir), 2011. *La grotte Walou à Trooz (Belgique). Fouilles de 1996 à 2004, vol. 1 : Les sciences de la terre*. Namur, Service public de Wallonie, IPW, Études et documents, Archéologie, 20, 208 p.
- ROUGIER H., CREVECOEUR I., BEAUVAL C., FLAS D., BOCHERENS H., WIFING C., GERMONPRÉ M., SEMAL P. & VAN DER PLICHT J., 2014. New fossils at the « Troisième Caverne » of Goyet (Belgium) and the mortuary practices of Late Neandertals. *Middle Palaeolithic in North-West Europe. Multidisciplinary approaches*. Book of Abstracts, Namur, March 20th-21st: 35.
- ROUGIER H., CREVECOEUR I., FIERES E., HAUZEUR A., GERMONPRÉ M., MAUREILLE B. & SEMAL P., 2004. Collections de la Grotte de Spy : re (découvertes) et inventaire anthropologique. *Notae Praehistoricae*, 24: 181-190.
- ROUGIER H. & SEMAL P. (eds.), 2013. *Spy Cave, 125 years of multidisciplinary research at the Betche aux Rotches (Jemeppe-sur-Sambre, Province of Namur, Belgium)*, vol. 1, *Anthropologica et Praehistorica*, 123, 380 p.
- ROUGIER H. & SEMAL P. (eds.), 2014. *Spy Cave, 125 years of multidisciplinary research at the Betche aux Rotches (Jemeppe-sur-Sambre, Province of Namur, Belgium)*, vol. 2, *Anthropologica et Praehistorica*, 124, in press.
- SEMAL P., JUNGELS C., CREVECOEUR I., ROUGIER H. & PIRSON P., 2009. Acquisition de la collection de Spy de François Beaufays (dit « l'Horloger ») par l'Institut Royal des Sciences Naturelles de Belgique. *Notae Praehistoricae*, 29: 157-164.
- SERANGELI J. & BOLUS M., 2008. Out of Europe - The dispersal of a successful European hominin form. *Quartär*, 55: 83-98.
- SKINNER M. M., EVANS A., SMITH T. M., JEMVALL J., TAFFOREAU P. T., KUPCZIK K., OLEJNICZAK A. J., ROSAS A., RADOVČIĆ J., THACKERAY F., TOUSSAINT M. & HUBLIN J.-J., 2010. Brief Communication: Contributions of Enamel-Dentine Junction Shape and Enamel Deposition to Primate Molar Crown Complexity. *American Journal of Physical Anthropology*, 143: 157-163.
- SMITH T. M., TOUSSAINT M., REID D. J., OLEJNICZAK A. J. & HUBLIN J.-J., 2007. Rapid dental development in a Middle Paleolithic Belgian Neanderthal. *Proceedings of the National Academy of Sciences of the United States of America*, 104, 51: 20220-20225.
- TOUSSAINT M., OTTE M., BONJEAN D., BOCHERENS H., FALGUÈRES C. & YOKOYAMA Y., 1998. Les restes humains néandertaliens immatures de la couche 4A de la grotte Scladina (Andenne, Belgique). *Comptes rendus de l'Académie des Sciences de Paris, Sciences de la terre et des planètes*, 326: 737-742.
- TOUSSAINT M. & PIRSON S., 2004. Trooz/Bay-Bonnet : sondages d'évaluation aux grottes de Fonds de Forêt. *Chronique de l'Archéologie wallonne*, Éditions du Service public de Wallonie, Direction générale opérationnelle de l'aménagement du territoire, du logement, du patrimoine et de l'énergie, Département du patrimoine, 12: 99-102.
- TOUSSAINT M. & PIRSON S., 2006. Neandertal Studies in Belgium: 2000-2005. *Periodicum Biologorum*, 108, 3: 373-387.
- TOUSSAINT M., PIRSON S., LACROIX P. & LAMBERMONT S., 2000. Houyet/Hulsonniaux : premières recherches modernes à la caverne de La Naulette. *Chronique de l'Archéologie wallonne*, Éditions du Service public de Wallonie, Direction générale opérationnelle de l'aménagement du territoire, du logement, du patrimoine et de l'énergie, Département du patrimoine, 8 (activités de 1999): 193-195.
- TOUSSAINT M., PIRSON S., LÓPEZ BAYÓN I., BECKER A., LACROIX P. & LAMBERMONT S., 1999. Bilan préliminaire de trois années de fouille à l'Abri Supérieur de Goyet (Gesves, province de Namur). *Notae Praehistoricae*, 19: 39-47.
- VERNA C., TOUSSAINT M., HUBLIN J.-J. & RICHARDS M. P., 2014. Neandertal mobility patterns in the Meuse valley: insights and perspectives through strontium isotope analysis on dental enamel. *Middle Palaeolithic in North-West Europe, Multidisciplinary approaches*. Book of Abstract, Namur, March the 20th-21st: 44.

An excavation journey

Marcel OTTE

Freedom begets creation. For me, the first is linked to the nebulous utopian ideals of those who participated in the events of May 1968. The second drove me to the caves of the Meuse Valley, with a feverish mind mingling with the powerful attraction of the research of my predecessors and the respectful comprehension of our own origins. My doctorate (1970-1975), full of dreams, fragrances, and changes, introduced me to the spirit of adventure that ignited the first Liégeois (Otte, 1979) and to the enchantment of these countless gestures recorded as much in the stone artefacts as in their lithographic plates: yellowed with time but with a fine and faithful drawing style, a damp texture under the hand, as if we entered them (Schmerling, 1833). In the poetic turmoil, mastered with great effort, and held in a tactical repose, several promising situations had already been recorded. So I was brought to touch the sacred deposits on the margins of these celebrated caves, all visited to find in them the spirit of the places where mysterious civilizations had lived in the past: Montaigne, Chaleux, Furfooz, Goyet, Hastière, Modave, Trou Magrite... and Marche-les-Dames, in 1976, directly across the Meuse from Scladina! Examination of the artefacts recovered in the old excavations showed the significance of the bone industry and the homogeneity of the Aurignacian occupations. With Michèle Gustin and Michel Toussaint, we proceeded with meticulous excavations, but the Aurignacian material discovered was dispersed in disturbed deposits, mixed with material from Neolithic burials. The only intact human occupation at the Grotte de la Princesse was attributed to the Early Middle Ages, probably Carolingian, with beautiful painted pottery (Otte et al., 1981). The connection with the opposite bank of the Meuse was established by an ingenious fighter, Commander Hazée, instructor at the center of the commandos of the Belgian army, where, in all innocence, my humble excavations had led me. This Commander had it all: tall and strong, a good drinker, the charisma of an adventurer, long episodes on the hardest fronts (Katanga, Korea, China), and leader of men in combat, both in the bistros and in the caves. We immediately became friends, by the magic of which the stuff of history is woven. Among these military men, devout followers, a speleological group was then found, attempting to explore the rocky entrails on the slopes of the limestone hills on the south side of the Meuse. Training sessions by this circle of brave men were as welcoming as they were demanding, even in the vigor of my twenties. It is not necessary or proper to recount the menu here, but other long evenings were devoted to a limited circle of 'selected friends'. Complete confidence was established in this group and in June 1976 conceived the idea of a collaboration, sharing methods (they wanted to know everything!) and tips on the different cavities found in the rocky massifs surveyed by the Cercle Archéologique Sclaynois (CAS).

Through the incendiary tumult that took place at the Place Saint-Lambert in Liège (June 1977), our enthusiasm did not dampen the dispute and official and efficient excavations only began in August 1978 under the leadership of a local magician, the Mayor of the City of Andenne, Claude Eerdeken. Claude, like myself, believed in this affair and brought to it all of the persuasive determination of his administration for perpetual and untiring support. For example, he

ensured the inspection of the expansion of the quarries neighbouring 'our' caves in the Meuse Valley and reserved exclusive study to our new association. The Ceramic Museum of the city was soon added to the group. Since then, and thanks to the diabolically effective mechanism of this group, systematic excavations have been in progress in this vast complex of chambers, focusing as much on pure scientific research questions as on the training of students and education of school groups and tourists. Meanwhile, having become a professor, several Master's and Doctoral theses were completed under my supervision. Scladina Cave is now renowned worldwide for the quality of the excavations (Bonjean et al., 2011), the innovative research that it has engendered, and the discovery of the remains of a young Neandertal in 1993 (Otte et al., 1993). International collaboration has brought the best specialists in all fields to the site (Ellwood et al., 2004), thus avoiding the narrowness of thought that nationalist schools can impose. The current experienced team, definitive and exclusively focused on the study of this prodigious site, owes its soul and energy to the total dedication of Dominique Bonjean, scientific collaborator at the University of Liège. As a result of his work, he and his team have produced a series of publications, directed the field school and undertaken coordinated research, all within an amicable atmosphere created by each member. Contrary to commonly accepted ideas, the excavations at Scladina have demonstrated that a range of skills were entirely mastered by hominins more than a hundred thousand years ago. Hunting capacities are shown by the flexibility of their adaptations at the base of the Ardennes hills. The frequency of chamois in the range of fauna hunted demonstrates the precision and rapidity of capture methods, probably linked to the mastery of woodworking techniques. Stone artefacts reveal a broad diversity in methods used simultaneously, depending on the intended tools and within very large distribution networks, from local sources to others located many kilometers from the site. Black colorants perhaps indicate a preoccupation with corporal aesthetics. And curious objects (crystals) were brought back to the site, just as 'curiosities' have been throughout human history.



Marcel Otte with some colleagues in Scladina Cave during the summer of 1980s.

Yet the successive discoveries of disarticulated fragments of human remains, all from a single young individual that is clearly Neandertal, have been the most important scientific aspect of this site since 1993. Although the skull was isolated (all fragments come from it), its selection was dictated by obvious elaborate spiritual concerns because it served to incarnate the care given to those within the community: they ensured collective destiny through rituals. The disposition in caves itself corresponds more to a funerary concern than to a domestic occupation; the burial remained protected as if by a vault, by the natural bowels of the earth formed by the rocky envelope, as perpetual as one could desire. The discrete striations seen on the interior of the mandible appeared to reflect specific treatment of the human remains at first glance, as often this part of the body indicates, both among the Neandertals and modern populations dispersed around the world today ('skull cults of primitive peoples') (Gastaut, 1972).

The remains of this young child followed the same logical line of reasoning: an 'unproductive' being in a hunting society was nonetheless honored, with the worth of an adult hunter and fully integrated within its social rank. This simple note clearly indicates the mythical solidarity of the group, by including all of its members, including the most humble.

The Chair of Prehistory that I have occupied since 1980 results from the long chain of consequences that began in 1817 when the University of Liège was founded. My distant colleague, Philippe-Charles Schmerling, was first a generous doctor. He traded his medical care against the discoveries made by quarry workers as the quarries expanded to cut into cavities rich in fossils. With hard work and a lot of bold, insightful, and free reflection, he foresaw human evolution by combining the remains of extinct animals, stone tools made by humans, and human skeletal remains. This fever of discovery and reasoning continued during the 1820s. He presented his arguments in several articles for the Académie des Sciences de Paris and then in a superb volume which included detailed drawings of stone tools and human skulls and bones, including the first Neandertal ever discovered, known as 'Engis Man' or 'Liège Man' following the nomenclature.

Nearly two centuries separate the discoveries of Engis and Sclayn, but the central pivot of Liège research was at Spy in 1885-86, where two Neandertal burials were found by an interdisciplinary team on the large terrace in front of the cave. Once again, their location supports the ritual value of such a cavity, large and opening onto a river and facing an extended plain on the horizon. During these historical excavations, religious activities were demonstrated for these populations who at the time of discovery were barely accorded the status of being human. Burials, human groups, techniques, and rites were finally associated to give this ancient population a dignity comparable to that, while still hesitant, accorded to exotic modern populations.

Sclayn is thus placed a long trajectory of research by the Liège School in the Ardennes caves and their particular abundance in prehistoric human remains. With the new school of thought that has been formed at Scladina, there is no doubt that equivalent productivity will continue.

Bibliographie

- | | |
|---|---|
| <p>Bonjean D., Di Modica K., Abrams G., Pirson S. & Otte M., 2011. La grotte Scladina: bilan 1971-2011. In M. Toussaint, K. Di Modica & S. Pirson (sc. dir.), <i>Le Paléolithique moyen en Belgique. Mélanges Marguerite Ullrich-Closset</i>.</p> | <p>Bulletin de la Société royale belge d'Études Géologiques et Archéologiques <i>Les Chercheurs de la Wallonie</i>, hors-série, 4 & Études et Recherches Archéologiques de l'Université de Liège, 128: 323-334.</p> |
|---|---|

Ellwood B. B., Harrold F. B., Benoist S. L., Thacker P., Otte M., Bonjean D., Long G. J., Shahin A. M., Hermann R. P. & Grandjean F., 2004. Magnetic susceptibility applied as an age-depth-climate relative dating technique using sediments from Scladina Cave, a Late Pleistocene cave site in Belgium, *Journal of Archaeological Science*, 31: 283-293.

Gastaut H., 1972. *Le crâne, objet de culte, objet d'art*, Marseille, Musée Cantini, 59 p. & 206 pl.

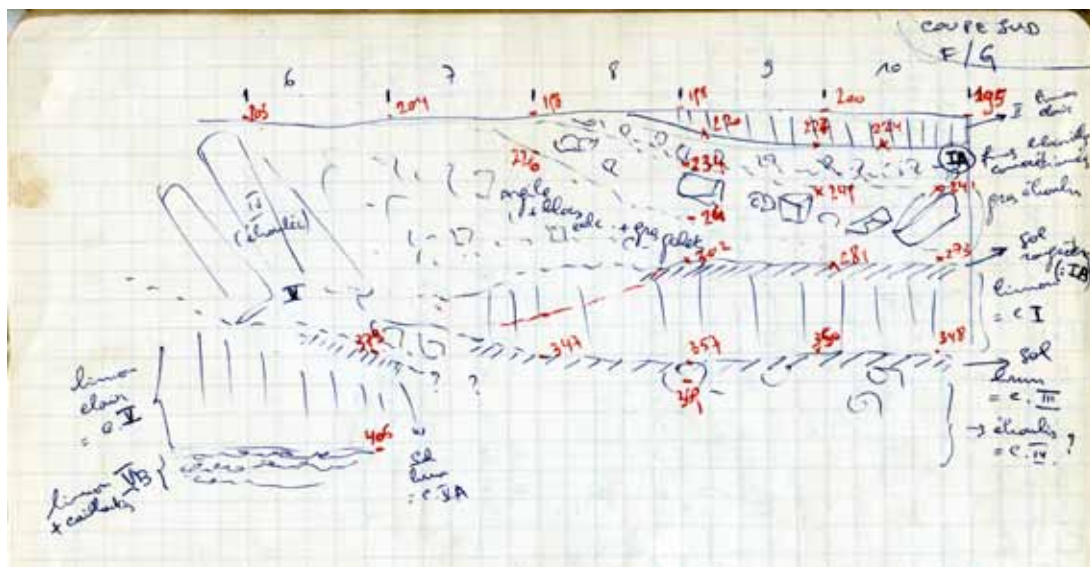
Otte M., 1979. *Le Paléolithique supérieur ancien en Belgique*, Bruxelles, Monographies d'Archéologie Nationale, vol. 5, 684 p.

Otte M., Degbomont J.-M., Hoffsummer P.,

de Coninck J. & Gautier A., 1981. *Sondages à Marches-les-Dames, « Grotte de la Princesse »*. Études et Recherches Archéologiques de l'Université de Liège, 10, 49 p. & 11 pl.

Otte M., Toussaint M. & Bonjean D., 1993. Découverte de restes humains immatures dans les niveaux moustériens de la grotte Scladina à Andenne (Belgique). *Bulletins et Mémoires de la Société d'Anthropologie de Paris*, nouvelle série, 5, 1-2: 327-332.

Schmerling P.-C., 1833-1834. *Recherches sur les ossements fossiles découverts dans les cavernes de la province de Liège*, Liège, P. J. Collardin, 167 & 195 p., 34 & 40 pl.



The south profile (F/G) of the trench dug on the terrace. Sketch of the stratigraphic sequence drawn by Marcel Otte on the 12th of July 1979 (excerpt from the first excavation journal of Scladina).

Scladina Cave from 1971 to 2014

Scladina was discovered in 1971. There were several stages of excavation, beginning with the Cercle Archéologique Sclaynois, followed in 1978 by the Service de Préhistoire de l'Université de Liège, and finally Archéologie Andennaise (now Centre archéologique de la grotte Scladina) from 1985 until the present. This photo album illustrates the important steps of the Scladina project, including the discovery of the Neandertal remains in 1993.



1971: one of the very first pictures of the entrance of Scladina Cave, taken several days after it was discovered on the 15th of June. The cave was filled to the vault with sediment.

1971: the speleologists and amateur archaeologists of the Village of Sclayn unblock the passage, rapidly removing the sediment to allow easier access to the cave.



16.5.1972: to create easier access, two metres of sediment are removed from under the ceiling at the cave's entrance.



1972: the first gate is created. A trench is dug on the terrace to ameliorate both the access to the site and the removal of sediment from the cave.



1978: amateur archaeologists protect the site and contact Marcel Otte of the Department of Prehistory of the University of Liège, who began professional excavation on the 2nd of August.



1981: over a three year period, a longitudinal trench was dug through the terrace and then enlarged to a 16 m² test pit crossing the entire sedimentary sequence of Scladina Cave.



1984: the 3D coordinates of every discovery in former Layer 5 are recorded by the students of the University of Liège during summer excavation.



1983: excavation extends into the cave and focuses on former Layer 5, which has yielded the major Middle Palaeolithic artefact assemblage.



1985: sediment samples are collected from the terrace profile for microfaunal analysis for Jean-Marie Cordy.



1985/2: Archéologie Andennaise formally undertakes year-round excavation and ameliorates the working conditions in the cave.



1986: visitors from the city of Andenne observe the archaeologists and students working in the cave.

1987: excavation has reached twenty metres deep in the cave. Here the excavation must start from the vault and a 5 metre thick sedimentary sequence must be removed to reach former Layer 5.



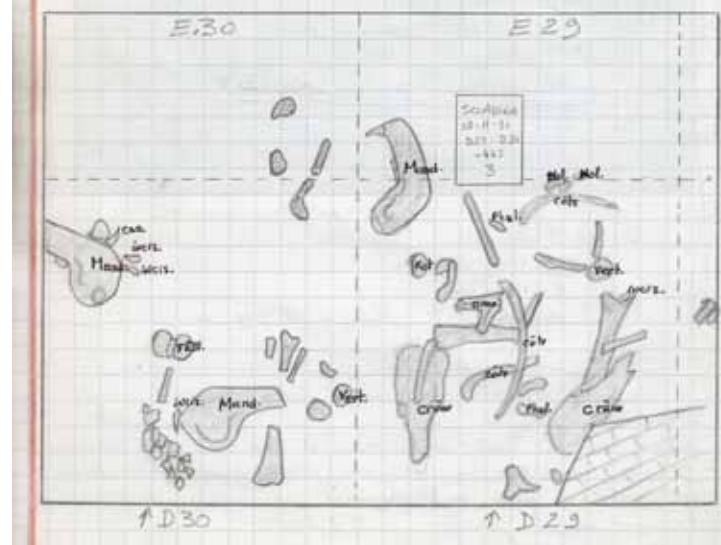


1988: former Layer 5 is completely excavated within the first twelve metres of Scladina Cave, from the porch at metre 11 to metre 22.



1989: deeper in the cave, the top of the sedimentary sequence is covered by a thick Holocene speleothem.

1991: the excavation technique consists of removing 1 or 2 cm of sediment on a 1 m² surface. The 3D coordinates of all the objects are recorded; the finds are also drawn on a plan at the scale of 1/20.



1991: a concentration of cave bear remains found at the bottom part of former Layer 3 in squares D29 and 30 (excerpt of the Scladina excavation journal 15, p. 39).

1992: reference profiles are kept along the north wall of the cave and are still present today.

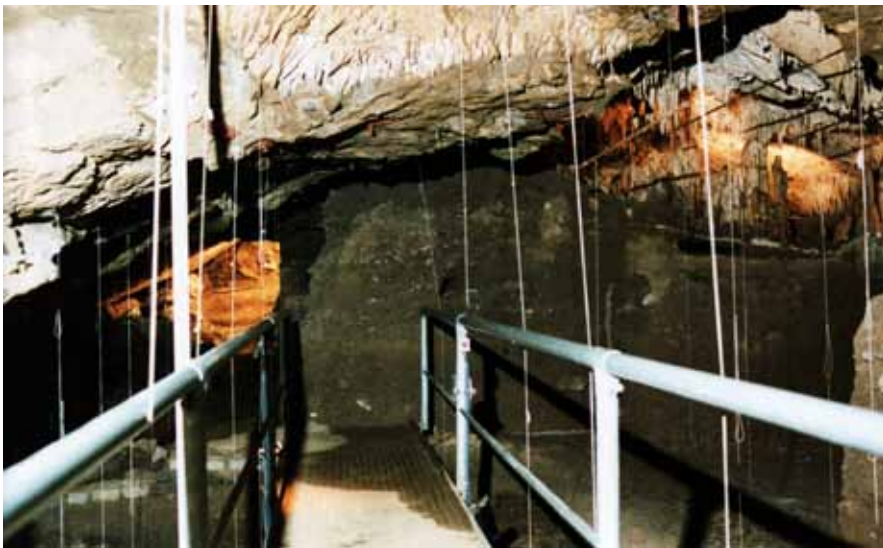




1993: Philippe Frison of Archéologie Andennaise discovers the permanent maxillary first molar Scla 4A-4 on the 14th of December, 1993.



1993: a blue cast representing the position of the right hemimandible Scla 4A-1 in Layer 4A-GX.



1994: with the financial help of the State and the City of Andenne a secure metal bridge was built and two years later the cave is illuminated by lights to develop a tourist programme.



1995: the back Profile 29/28 D-C exhibits the sediments of the 4A-CHE gully reworking speleothem fragments. Those sediments will yield the left hemimandible Scla 4A-9 on the 12th of July 1996.



1997: an aven is identified between metres 43 and 50. Excavation of the aven started from the plateau.



1998: the excavation house has been present on the site since the beginning of the excavations of Archéologie Andennaise in 1985.

2000: the Archaeological Centre of Scladina Cave is enlarged to develop a museum at the site.





2001: again with the help of the State and the City of Andenne, a metal structure is built on the terrace of Scladina Cave to ameliorate the work conditions for archaeologists and to welcome tourists.





2002: to record stratigraphy, profiles are equipped with white elastic ropes.



2002: excavation of former Layer 5 continues on a wide surface to record potential horizontal relationships between objects.



2003: Stéphane Pirson's PhD study between 2003 and 2007 resulted in the reappraisal of Scladina's stratigraphic record.



2004: a 'vertical' excavation strategy is developed to adapt to the complex geometry within the stratigraphy.

2004: The 4A-CHE gully is identified by the speleothem fragments that it reworked (Profile C32/31).





2005: two members of the team of Archéologie Andennaise work in the cave. The team is comprised of nine permanent employees that work year-round on the Scladina Project.



2005: high resolution photographs allow the recording of geometric subtleties, sediment colour, and texture (Profile 32/31 D-B).



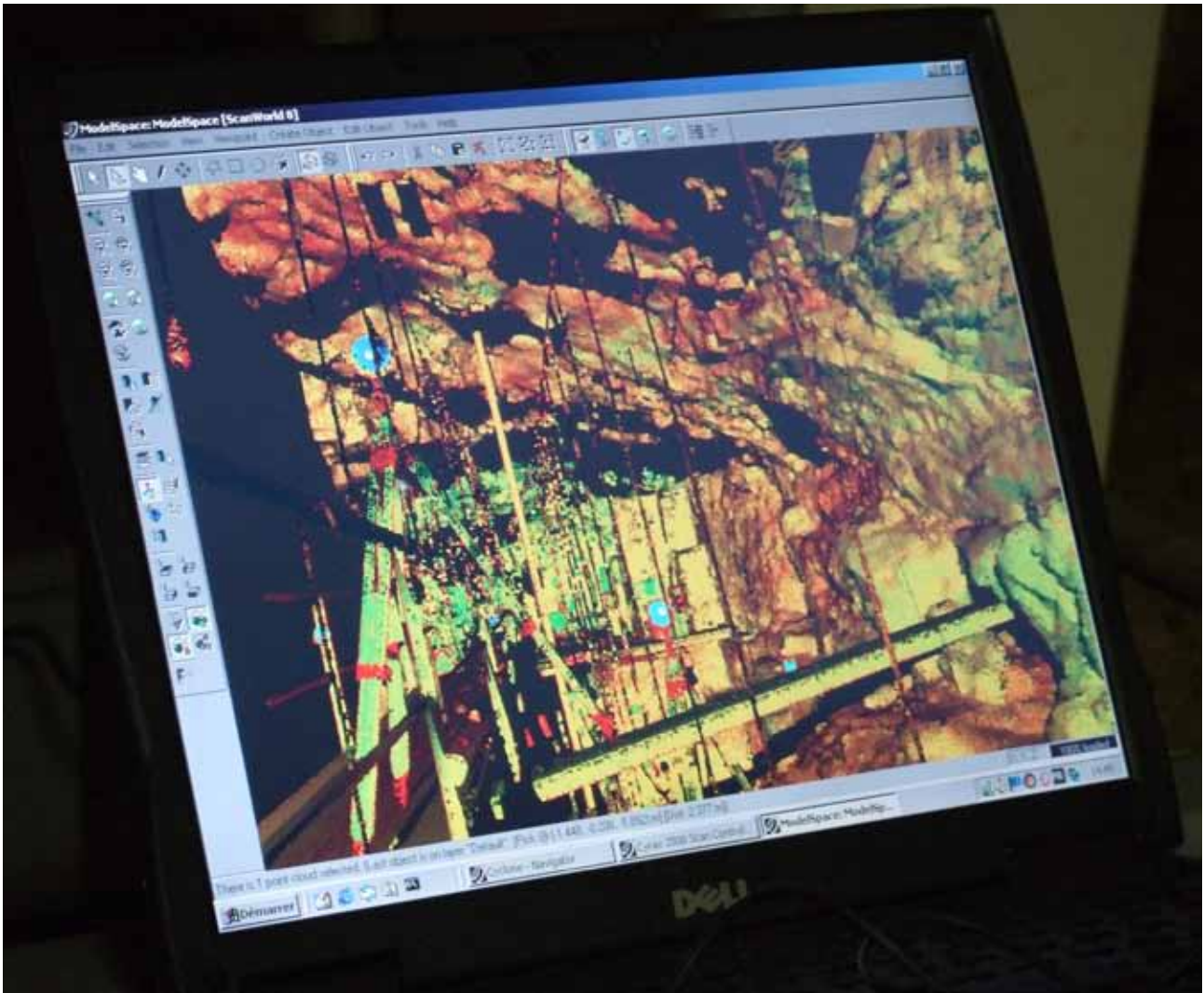
2006: stratigraphic observations require powerful lights. Every archaeologist needs two 500 watt lamps: one fixed over the excavation zone, the other one in front of the Profile H/I 30-23.



2007: throughout the cave, excavation occurs on a small surface of 25 cm x 50 or 100 cm. Every find is stratigraphically provenanced with the use of multiple profiles (Square J27).



2008: with help from the State, a Cyrax 3D scanner records the inner morphology of Scladina Cave in high resolution.



2008: the scan resolution is one dot every 5 mm in 3D.



2009: prior to excavation, the profiles are cleaned, carefully observed, delineated, and annotated on photographs in order to record sedimentary limits (Profile F/G 37-33).



2010: effects of cryoturbation visible on a profile between the layers 1B-OR (top) and 2A-GL (bottom).

2011: Profile 28/27 K-J exhibits a geometrically complex stratigraphic sequence comprised of debris flows, run-off, and cryoturbation.



2010: good lighting, small surfaces, adapted tools, careful observations, and microstratigraphic excavations all help to verify the context.



2012: in this part of the cave bridges are built so that all excavation units can be investigated.



2013: all layers are vertically excavated: those of Unit 4A-POC (below) that may contain Neandertal remains and those of units 1A and T (above) that are yielding numerous artefacts of the MIS 3 assemblage.



2014: a tablet computer is now used to draw stratigraphy on photos as well as locate and annotate artefacts.

Since 1991 Dominique bonjean has been coordinating the Scladina Project, which includes continuous excavation of the cave with the Archéologie Andennaise team, conservation, scientific publications, and student excavation programmes (see more at www.scladina.be).



Photograph credits:

All photos from 1971 to 1978, Cercle Archéologique Sclaynois

All photos from 1981 to 1986, Service de Préhistoire de l'Université de Liège

All photos from 1987 to 2014 (also including 1985/2): Archéologie Andennaise



René Hausman, 2008



Anne-Cécile Derbaudrenghien, 2004



Benoît Clarys, 2013



René Hausman, 2009

Summaries/Résumés

Chapter 1 Overview and context of the Scladina palaeoanthropological project

13

This introduction presents the whole palaeoanthropological project that, since 1993, studied the Neandertal remains discovered in Sedimentary Complex 4A at Scladina Cave. This chapter also briefly discusses the scientific context, including the stratigraphy, archaeology, and palaeoenvironment, within which the 19 remains studied in this monograph (i.e. three bone fragments with teeth as well as 16 isolated teeth) were discovered. In addition to some thoughts on the nature of palaeoanthropology, it also provides a brief overview of all chapters of the book, before concluding with a list of articles written about, or referring to these juvenile remains.

Contexte et évolution du projet paléolithique à la grotte Scladina

Cette introduction a pour objectif de présenter l'ensemble du projet anthropologique qu'a constitué, depuis 1993, l'étude des restes néandertaliens découverts dans le complexe des couches 4A de la grotte Scladina. Le chapitre évoque aussi brièvement le contexte scientifique, notamment stratigraphique, archéologique et paléoenvironnemental, dans lequel se sont produites les découvertes des 19 fossiles qui composent la collection étudiée dans la présente monographie, c'est-à-dire 3 fragments osseux avec dents ainsi que 16 dents isolées. Outre quelques réflexions sur la nature même de la paléolithologie, il propose une brève présentation de tous les chapitres de l'ouvrage, avant de se terminer par une liste des articles concernant les restes juvéniles de l'enfant ou y faisant référence.

Chapter 2 Scladina Cave: archaeological context and history of the discoveries

31

Discovered in 1971, Scladina Cave is located on the west side of a small tributary of the Meuse River in Sclayn, Belgium (Municipality of Andenne, Province of Namur). Facing towards the southeast, the cave is a long cylinder-like karst structure that extends along the axial plane of an anticline. Currently, excavation of the sediment within Scladina extends about 40 m from the cave's entrance. Since the beginning of scientific research at Scladina (1978), multidisciplinary studies have demonstrated that the cave records numerous climatic fluctuations from the Upper Pleistocene. From palaeoclimatic and palaeoenvironmental perspectives, this is one of the most complete sequences available to researchers in Belgium. Presently, more than 120 layers divided into 30 sedimentary units have been identified in a sequence that is approximately 15 m thick. A large number of sedimentary processes and post-depositional processes are recorded, which makes Scladina an excellent reference site. Scladina is also one of the major Palaeolithic archaeological sites in Belgium. Two important Middle Palaeolithic assemblages have been recovered: the one from Unit 5 (attributed to a cold phase of the Weichselian Early Glacial, MIS 5d) and the other from Unit 1A (dated to between 40,210 +400/-350 BP and 37,300 +370/-320 BP, MIS 3). These have been studied from a variety of perspectives, including typology, technology, petrography, spatial distribution, archaeozoology, and statistics. Since 1993, the recovery of a mandible, a maxillary fragment, and 16 isolated teeth of an 8 year-old Neandertal from Sedimentary Complex 4A permitted Scladina to join the 7 other Belgian sites that have yielded Middle Palaeolithic human remains. This discovery is the most important made in Belgium during the 20th century. Dated to approximately 90 ka BP, the oldest Neandertal DNA has been retrieved from this individual.

La grotte Scladina : contexte archéologique et historique des découvertes

Découverte en 1971, la grotte Scladina (Sclayn, Commune d'Andenne, Province de Namur) est localisée sur le versant ouest d'un petit vallon adjacent au cours de la Meuse. Ouverte en direction du sud-est, la grotte se présente sous la forme d'un long boyau qui s'enfonce dans le massif en suivant l'axe d'un anticlinal. Actuellement, la fouille s'étend sur une longueur de 40 m au départ du porche. Depuis le début des recherches scientifiques en 1978, les fréquentes études pluridisciplinaires conduites sur le site ont démontré la présence d'un nombre conséquent de fluctuations climatiques enregistrées dans la stratigraphie au cours du Pléistocène supérieur. De ce point de vue, il s'agit de la séquence la plus complète pour nos régions encore accessible aux chercheurs. À l'heure actuelle, plus de 120 couches, réparties en 30 ensembles sédimentaires, ont été répertoriées sur une séquence qui totalise près de 15 m d'épaisseur. Un grand nombre de processus sédimentaires et post-dépositionnels y sont enregistrés, ce qui en fait un site de référence en la matière. Scladina est un des sites d'occupation majeurs du Paléolithique belge. Deux importantes séries d'artefacts du Paléolithique moyen ont été identifiées dans les ensembles sédimentaires 5 (attribué à une phase froide du Début Glaciaire Weichsélien, MIS 5D) et 1A (daté entre 40,210 ±400/-350 BP and 37,300 ±370/-320 BP, MIS 3) qui ont été étudiées sous de nombreux angles : typologique, technologique, pétrographique, répartition spatiale, calibrages et statistiques. Depuis 1993, une dimension émotionnelle est venue s'ajouter par la mise au jour, dans le complexe des couches 4A, d'une mandibule, d'un fragment de maxillaire et de 16 dents isolées appartenant à un Néandertalien de 8 ans. En Belgique, cette découverte anthropologique est la plus significative du 20^{ème} siècle. Elle permet à Scladina de rejoindre les 7 sites belges ayant livré des restes humains du Paléolithique moyen. Estimée à environ 90 ka BP, cette mandibule a permis l'analyse de l'ADN néandertalien le plus vieux du monde.

Chapter 3 The stratigraphic sequence of Scladina Cave

49

After providing a short history of how the stratigraphic record at Scladina Cave was established, the deposits from Unit 5 to Unit 3-SUP are described. Since 2003, the meticulous study of the sedimentary profiles available at Scladina led to the complete reinterpretation of the stratigraphic sequence. This chapter describes the deposits related to the Neandertal remains, focusing on former Layer 4, referred to here as 'Sedimentary Complex 4'.

Rather than the previous succession of 'Layer 4B/Layer 4A/Speleothem CC4', more than 20 layers with very different lithologies have been identified, and even more importantly a much more complex distribution of the different lithostratigraphic units near Speleothem CC4 became understood. All the layers that comprise Sedimentary Complex 4 are now divided into 5 distinct units: 4B, 4A-AP, 4A-IP (including CC4), 4A-CHE, and 4A-POC. Another major element of the new stratigraphic interpretation is the identification of an important gully in the upper part of Sedimentary Complex 4 (Unit 4A-CHE) that eroded Speleothem CC4 and some subjacent layers.

Sedimentary and diagenetic processes are also discussed for this part of the stratigraphic sequence. A large number of depositional and post-depositional processes have been identified. Sometimes, successive lateral lithofacies that were generated simultaneously by the interaction of different processes in certain areas of the cave were observed.

La séquence stratigraphique de la grotte Scladina

Après un bref historique des relevés stratigraphiques à la grotte Scladina, les dépôts sont décrits, de l'unité 5 à l'unité 3-SUP. L'étude détaillée des coupes disponibles depuis 2003 a conduit à une réinterprétation complète de la séquence stratigraphique. Ce chapitre présente la description des dépôts concernant les restes néandertaliens, mettant l'accent sur l'ancienne couche 4, désormais baptisée « complexe sédimentaire 4 ».

Au lieu de l'ancienne succession « couche 4B/couche 4A/plancher stalagmitique CC4 », plus de 20 couches ont été identifiées, avec des lithologies très variées mais aussi et surtout une distribution des différentes unités lithostratigraphiques autour du plancher CC4 nettement plus complexe que ce qui était précédemment connu. Toutes les couches englobées dans le complexe sédimentaire 4 sont désormais regroupées au sein de 5 unités distinctes : 4B, 4A-AP, 4A-IP (englobant CC4), 4A-CHE et 4A-POC. Un autre élément important de la nouvelle interprétation stratigraphique concerne l'identification d'un important chenal dans la partie supérieure du complexe sédimentaire 4 (unité 4A-CHE), qui érode le spéléothème CC4 ainsi que les couches sous-jacentes.

Les processus sédimentaires et diagénétiques sont également discutés pour la partie de la séquence stratigraphique concernée. Un grand nombre de processus dépositionnels et post-dépositionnels ont été identifiés, avec dans certains cas la présence de lithofaciès se succédant latéralement et générés simultanément par des processus distincts présents dans certaines zones spécifiques de la grotte.

Chapter 4 The palaeoenvironmental context and chronostratigraphic framework of the Scladina Cave sedimentary sequence (units 5 to 3-SUP) 69

Numerous data sets regarding palaeoenvironment and chronostratigraphy have been published since excavation began at Scladina Cave, both before and after the stratigraphic reappraisal. This chapter presents a synthesis of all these studies, focusing on the units related to the Neandertal child (units 5 to 3-SUP).

Recent palaeoenvironmental results indicate a very good relationship between palynology, anthracology, and geology. These are also strongly correlated with the results related to the former stratigraphic record (mainly macrofauna, small mammals, palynology, and magnetic susceptibility), thus strengthening the viability of the recorded climatic fluctuations.

From a chronostratigraphic perspective, the integration of all the available data led most of the Scladina sequence to be confidently positioned in the Upper Pleistocene. These data include biostratigraphy, climatostratigraphy (deduced from palaeontological studies and magnetic susceptibility), numerical dates (more than 60), and the comparison with the loess reference sequence from Middle Belgium. However, the chronostratigraphic framework currently remains rather inaccurate, especially for the lower half of the sequence: the exact position of the beginning and end of MIS 5 is still being debated. The best hypothesis attributes the whole sequence from Unit 6B to Unit 2B to part of MIS 5, and Unit 2B to the end of MIS 5a.

Le contexte paléoenvironnemental et le cadre chronostratigraphique de la séquence sédimentaire (unités 5 à 3-SUP) de la grotte Scladina

De nombreuses données relatives au paléoenvironnement et à la chronostratigraphie ont été publiées depuis le début des fouilles à la grotte Scladina, soit avant, soit après la révision stratigraphique de 2007. Ce chapitre a pour objectif de présenter la synthèse de toutes ces études, en mettant l'accent sur les couches concernées par l'enfant néandertalien (unités 5 à 3-SUP).

Les nouveaux résultats paléoenvironnementaux indiquent une très bonne concordance entre la palynologie, l'anthracologie et la géologie. Ils présentent également une bonne corrélation avec les résultats issus de l'ancien système stratigraphique (principalement macrofaune, microfaune, palynologie et susceptibilité magnétique), ce qui renforce la réalité des fluctuations climatiques enregistrées.

D'un point de vue chronostratigraphique, l'intégration de l'ensemble des données disponibles permet de positionner avec assurance la plus grande partie de la séquence de Scladina dans le Pléistocène supérieur. Ces données concernent surtout la biostratigraphie, la climatostratigraphie (déduite des études paléontologiques et de la susceptibilité magnétique), les dates radiométriques (plus de 60) et la comparaison avec la séquence de référence des loess de Moyenne Belgique. Cependant, à l'heure actuelle, le cadre chronostratigraphique demeure assez imprécis, particulièrement pour l'attribution de la moitié inférieure de la séquence : la position précise du début et de la fin du SIM 5 sont toujours débattus. L'hypothèse la plus probable conduit à positionner l'ensemble de la séquence comprise entre les unités 6B à 2B au sein du SIM 5, et l'unité 2B à la fin du SIM 5a.

Chapter 5 Stratigraphic origin of the juvenile Neandertal remains from Scladina Cave: re-evaluation and consequences for their palaeoenvironmental and chronostratigraphic contexts 93

The 19 remains of the Neandertal juvenile from Scladina Cave were all unearthed before the stratigraphic reappraisal. Therefore, reconsidering the stratigraphic position of these remains within the new stratigraphic record was necessary. In this chapter, all available arguments are re-examined in order to refine the stratigraphic position of each of the Neandertal remains, which were discovered in former Layer 4A. On this basis, 7 fossils could be repositioned with accuracy inside the new stratigraphic record, either to the gully of Unit 4A-CHE or from the deposits that immediately followed (Unit 4A-POC). Three of these 7 fossils were even reattributed to a specific layer. The position of the 12 other remains is still uncertain, as several units are possible candidates, but an attribution to Unit 4A-POC appears most likely.

Given the sedimentary depositional dynamics of Unit 4A-CHE, all the child remains unearthed from there are at least in secondary spatial position. They seemed to have been originally deposited in Unit 4A-CHE. Some of them were subsequently reworked into at least one younger unit (Unit 4A-POC), being therefore at least in tertiary spatial position. The important spatial distribution of the Neandertal remains along the longitudinal axis of the cave makes particular sense in this context of complex subsequent redistribution and reworking phases. However, in the present state of research, the exact primary spatial position of the child is still unknown.

Several arguments, mainly linked with the taphonomical study of the Neandertal juvenile remains, led to the conclusion that the child is contemporaneous with Unit 4A-CHE. Therefore,

given the most probable chronostratigraphic positioning of this unit (i.e. a cold episode of the end of MIS 5), the two best hypotheses for the age of the Neandertal remains are either around 87,000 years ago (MIS 5b), or around 80,000 ago (beginning of second half of MIS 5a), respectively.

Origine stratigraphique des restes néandertaliens juvéniles de la grotte Scladina : réévaluation de leurs contextes paléoenvironnemental et chronostratigraphique

Les 19 vestiges de l'enfant néandertalien de la grotte Scladina ont tous été exhumés avant la révision stratigraphique de 2007. Dès lors, le réexamen de la position stratigraphique de ces vestiges dans la nouvelle séquence stratigraphique était nécessaire. Dans ce chapitre, tous les arguments disponibles ont été revus, pour chaque fossile, afin de préciser la position stratigraphique des restes néandertaliens découverts dans l'ancienne couche 4A. Sur cette base, 7 fossiles ont pu être repositionnés avec précision au sein de la nouvelle séquence ; ils proviennent tous soit du chenal de l'unité 4A-CHE, soit des dépôts immédiatement sus-jacents (unité 4A-POC). Trois de ces 7 fossiles ont même pu être repositionnés dans une couche spécifique. La position des 12 autres vestiges reste incertaine, plusieurs unités demeurant des candidats possibles ; toutefois, leur attribution à l'unité 4A-POC semble être la plus probable.

Etant donné la dynamique sédimentaire de l'unité 4A-CHE, tous les vestiges de l'enfant exhumés dans cette unité sont au minimum dans une position spatiale secondaire. Ils semblent avoir été initialement déposés dans l'unité 4A-CHE. Certains d'entre eux furent ultérieurement remaniés au sein d'au moins une unité plus récente (unité 4A-POC), étant dès lors au minimum dans une position spatiale tertiaire. L'importante dispersion des restes de l'enfant néandertalien dans l'axe longitudinal de la grotte s'explique particulièrement bien dans ce contexte complexe de redistributions et remaniements successifs. Cependant, dans l'état actuel des recherches, la position spatiale primaire de l'enfant demeure inconnue.

Plusieurs arguments, principalement liés à l'étude taphonomique des restes de l'enfant néandertalien, conduisent à la conclusion que l'enfant est contemporain de l'unité 4A-CHE. Dès lors, étant donné la position chronostratigraphique la plus probable de cette unité (un épisode froid de la fin du SIM 5), les deux hypothèses les plus vraisemblables pour l'âge des vestiges néandertaliens sont respectivement soit autour d'il y a 87.000 ans (SIM 5b), soit autour d'il y a 80.000 ans (début de la seconde moitié du SIMS 5a).

Chapter 6 Non-Destructive Gamma-Ray Spectrometry of the Scladina Neandertal mandible (Scla 4A-1)

125

During the early 1980s, developments in the field of gamma-ray spectrometry allowed the observation of long half-life natural radionuclides such as uranium, thorium and protactinium. This paper presents the results obtained, in 1994, from non-destructive gamma-ray spectrometry applied to the right hemimandible Scla 4A-1 of the Neandertal child from Scladina Cave. The fossil was counted during 91 days. The level of uranium in the mandible is low and did not allow the calculation of a date from the $^{231}\text{Pa}/^{235}\text{U}$ ratio. The age obtained via the $^{230}\text{Th}/^{234}\text{U}$ ratio presents an important error range due to the measurement difficulty of ^{234}U which is superimposed with ^{214}Pb at 53.2 keV. The low level of ^{232}Th in the sample indicates correcting the age on the basis of exogenous thorium is not necessary. The age obtained reveals that the child lived at least 100 000 years ago.

La datation non destructive par spectrométrie gamma de la mandibule néandertalienne de Scladina (Scla 4A-1)

Au début des années quatre-vingts, les progrès effectués en spectrométrie gamma ont permis la détermination de radionuclides naturels à longue demi vie tels que l'uranium, le thorium et le protactinium. Le présent article traite des résultats obtenus, en 1994, par spectrométrie gamma non destructive sur l'hémi-mandibule droite Scla 4A-1 de l'enfant néandertalien de la grotte Scladina. Le fossile a été compté pendant 91 jours. La teneur en uranium de cette mandibule est très faible et n'a pas permis de calculer un âge par le rapport $^{231}\text{Pa}/^{235}\text{U}$. L'âge obtenu par le rapport $^{230}\text{Th}/^{234}\text{U}$ présente une erreur importante générée par la difficulté d'enregistrer le taux d' ^{234}U qui se superpose à celui du ^{214}Pb à 53,2 keV. La très faible teneur en ^{232}Th dans l'échantillon indique qu'il n'est pas nécessaire d'effectuer une correction sur l'âge par rapport au thorium exogène. L'âge obtenu montre que cet enfant a vécu il y a au moins 100 000 ans.

Chapter 7 Taphonomy of the juvenile Neandertal remains from Sedimentary Complex 4A, Scladina Cave

127

The 19 fossils (3 bone fragments and 16 isolated teeth) that belong to the 8 year-old juvenile Neandertal exhibit a particular set of various characteristics. Among these attributes is a planimetric dispersal within an elliptical area of around 13 m long by 6 m wide, a stratigraphic dispersal within different layers/units of the Sedimentary Complex 4A, and the relatively complete mandible when the two parts are refitted, which is juxtaposed against the relatively incomplete maxilla.

These fossils have been examined for the presence or absence of numerous taphonomic features. These features include surface colour, surface condition/lustre, weathering traces, degree of fragmentation, abrasion of fractured edges, and the precipitation of MnO_2 . This analysis showed that the majority of the faunal remains that came from the same sedimentary layer seem to exhibit a similar combination of taphonomic attributes.

However, the state of preservation of the Neandertal fossils is exceptional and only a small number of similarities are found among the faunal remains from the sedimentary units analysed in this study (units 6A, 5, and Complex 4A). When all of the physical taphonomic features are combined, the sedimentary units 4A-CHE and 4A-POC have yielded the most bones and teeth that have the most similarities with the Neandertal child. This correlation is in harmony with the stratigraphic analysis that attributed some of the child's bone fragments to the Unit 4A-CHE and some of the isolated teeth to Unit 4A-POC.

How to interpret the presence of the Scladina Neandertal remains? The Scladina Child's cause of death is still unknown. Neither antemortem nor perimortem traces such as pathological stigma, wounds due to human actions, or carnivore predation are present on the remains. Some observable postmortem traces are present on the fossils. The cortices of the three osseous elements exhibit thin cracks that are the first effects of weathering. The fracture located under the alveolus of the permanent mandibular right canine, which has separated the two hemimandibles, is a 'green bone' fracture, indicated by the presence of a small area of cortical peeling on the left hemimandible.

The current hypothesis states that the partial or complete body of the child entered the cave when the bones had not yet undergone fossilization to any degree. Sedimentary processes

linked to the gully most likely caused the mandible to fracture. The low degree of weathering augments this hypothesis; the remains were not directly exposed to atmospheric agents for a long period of time.

There is no evidence that the gully-creating mechanisms brought the maxilla and mandible into the cave; however, the processes that created the gully are known to be responsible for the initial reworking of the bones, for fracturing them, and for their dispersal into different layers within Unit 4A-CHE and in superimposing layers in Unit 4A-POC. The child's remains were distributed in several different sedimentary layers that have differentially altered the bones.

Étude taphonomique des restes néandertaliens juvéniles du complexe sédimentaire 4A de la grotte Scladina

Les 19 restes humains (3 fragments d'os et 16 dents isolées) appartenant au Néandertalien de 8 ans sont caractérisés par une répartition complexe dans le site et un état de conservation hétérogène, opposant une mandibule relativement complète à un maxillaire droit très partiel. Les fossiles sont étalés dans une zone elliptique longue de 13 m et large de 6 et sont stratigraphiquement distribués dans plusieurs couches/ensembles sédimentaires appartenant au complexe sédimentaire 4A.

L'étude de l'état de conservation des fossiles de Scladina vise à mettre en évidence les différentes caractéristiques taphonomiques telles, la teinte de la corticale osseuse, l'état de sa surface (lustre), les traces de météorisation, le degré de fragmentation, les fractures et usures des bords, les dépôts de dioxyde de manganèse. Cette étude met en évidence que la majorité des restes fauniques provenant d'une couche sédimentaire donnée présente un état de conservation similaire.

Néanmoins, l'état de conservation des restes Néandertaliens est exceptionnel et très peu de comparaisons taphonomiques ont été enregistrées parmi les restes de faune provenant des ensembles sédimentaires analysés (ensembles sédimentaires 6A, 5 et le complexe 4A). En combinant certains traits taphonomiques, les restes fauniques (osseux et dentaires) qui présentent les plus grandes affinités avec le Néandertalien juvénile sont ceux qui proviennent des ensembles sédimentaires 4A-CHE et 4A-POC. Cette observation est en harmonie avec les analyses stratigraphiques qui ont attribué certains des restes osseux et dentaires humains aux ensembles 4A-CHE et 4A-POC.

Quelles sont les raisons de la présence des fossiles humains à Scladina? Les causes du décès sont toujours inconnues. Aucune trace antemortem ou perimortem n'a été observée, tels des stigmates pathologiques, des blessures infligées par des actions anthropiques ou encore des marques commises par des prédateurs. Seules quelques traces postmortem sont visibles : la corticale des trois restes osseux de l'enfant présente de très légers fendillements correspondant aux premières actions de la météorisation. La fracture, sous l'alvéole de la canine inférieure droite, qui brisa la mandibule, s'est opérée sur un os frais (un peeling est présent sur l'hémi-mandibule gauche).

L'hypothèse actuelle privilégie l'incorporation du corps partiel ou complet dans la grotte, quand les os n'étaient pas encore reminéralisés par les processus de fossilisation. La mise en place des sédiments du chenal 4A-CHE, est plus que probablement la cause de la fracture de la mandibule. Le faible degré de météorisation soutient cette hypothèse de fraîcheur des ossements, ceux-ci n'ayant pas été exposés longtemps à l'air libre.

La preuve ne peut être faite de l'apport de la mandibule et du maxillaire de l'enfant par le chenal, dans la grotte. Mais les processus qui ont généré le chenal sont tenus pour responsables du premier remaniement des ossements dans la grotte, de leur fracturation et de leur dispersion dans les

différentes couches des ensembles sédimentaires 4A-CHE et 4A-POC sus-jacent. Ainsi enfouis dans des sédiments différents, ils subirent une perminéralisation différenciée.

Chapter 8 Dental development in and age at death of the Scladina I-4A juvenile Neandertal

155

Histological study of tooth growth based on biological rhythms in enamel and dentine facilitates developmental assessments of fossil hominins with greater precision than other skeletal analyses. Quantification of these internal and external incremental features yields ages at crown completion, tooth eruption, and root completion. Recent evidence for developmental differences between modern humans and Neandertals has been ambiguous. By measuring tooth formation in the dentition of the juvenile Neandertal from Scladina, Belgium, we show that most teeth formed over a shorter time than in modern humans, and that dental initiation and eruption were relatively advanced. By registering developmental stress across the dentition we are able to present a precise chronology of Neandertal dental development that differs from modern humans. At eight years of age at death, this juvenile displays a degree of development comparable to modern human children that are several years older. Age at death in juvenile Neandertals should not be assessed by comparison with modern human standards, particularly those derived from populations of European origin. Moreover, evidence from the Scladina Juvenile and other similarly-aged hominins suggests that a prolonged childhood and slow life history are unique to *Homo sapiens*.

Le développement dentaire et l'âge au décès du Néandertalien juvénile Scladina I-4A

L'étude histologique de la croissance dentaire, basée sur les rythmes biologiques enregistrés dans l'émail et la dentine, documente le développement des hominins fossiles avec une précision supérieure à celle fournie par les autres types d'analyses du squelette. La quantification de ces caractéristiques internes et externes de croissance déterminent l'âge de l'individu à chaque étape du développement de la couronne, de la racine et du degré d'éruption des dents. Des résultats récents ont révélé des discordances entre le rythme de croissance dentaire des hommes modernes et celui des Néandertaliens. En examinant le degré d'éruption dentaire du Néandertalien juvénile de Scladina (Belgique), nous avons mis en évidence, pour la plupart de ses dents, un taux de croissance plus rapide que chez les modernes. L'enregistrement de phases de stress dans le développement des dents, nous permet d'établir une chronologie du développement dentaire des Néandertaliens qui diffère nettement de celle des hommes modernes. A huit ans, ce Néandertalien juvénile présente un degré de développement comparable à celui d'enfants modernes plus âgés de quelques années. Il en résulte que l'âge au décès des Néandertaliens juvéniles ne devrait plus être évalué sur base de comparaisons avec les normes établies sur les humains modernes, surtout s'ils sont d'origine européenne. De plus, la preuve apportée par le Néandertalien juvénile de Scladina, renforcée par celles d'autres hominins du même âge, suggère qu'une enfance prolongée et un développement lent sont typiques des Homo sapiens.

Chapitre 9 Is sex determination of the Scladina I-4A juvenile Neandertal possible?

167

Numerous sexing techniques, based either on morphological traits or on metric differences, have been developed for adult bones, but mainly from modern human skeletons of known age and sex. In addition, some bones such as mandibles and maxillae are not as accurate as the pelvic

bones in determining sex. Regarding juveniles, there are no really precise sex diagnosis techniques. At Scladina, three problems are combined: traits commonly used for sexing modern humans are not accurate enough for Neandertals; the remains belonged to an eight-year-old child; all the Scladina remains are fragments of mandibles and maxilla, as well as several teeth.

The statistical dental technique developed by Oxnard avoids the pitfall of applying modern human measurements to other taxa, by using the bimodal appearance of some dimensions of the crowns of the Neandertal corpus, since it is largely acknowledged that the size distribution of some teeth, particularly the canines, shows the greatest differences between males and females. On this basis, it is possible that the Scladina Juvenile was female. The dimensions of the Scladina mandible are relatively small compared with other Neandertal mandibles of similar ages at death; this could tentatively confirm that the fossil is female. Evidence from the histological study are in line with the same interpretation. Finally, the Scladina tooth roots are very short and fall within the lower end of the Neandertal variation, while the pulp cavities are very large. These arguments also support the hypothesis that the Scladina Juvenile would be female. In conclusion, although none of these facts are determinant, the conjunction of the various analyses suggests a female attribution.

La détermination du sexe du Néandertalien juvénile Scladina I-4A est-elle possible?

De nombreuses techniques ont été développées pour déterminer le sexe des restes squelettiques humains, certaines d'ordre morphologique, d'autres d'ordre morphométrique. Elles ont été élaborées à partir d'ossements adultes modernes d'âge et de sexe connus par l'état civil. Certains ossements comme les mandibules et maxillaires ne fournissent cependant pas de résultats aussi précis que les os iliaques, qui sont les seuls à fournir une détermination quasi absolue. L'estimation du sexe de restes d'enfants est une autre question technique qui est loin d'être réglée. À Scladina, les trois problèmes évoqués sont cumulés : les caractères habituellement utilisés pour sexer les ossements modernes ne sont pas extrapolables aux Néandertaliens sans difficultés ; les restes appartiennent à un enfant de 8 ans ; les fossiles découverts sont des hémimandibules, un fragment de maxillaire et des dents.

La méthode statistique développée par Oxnard permet d'éviter l'écueil que constitue la simple application à des hommes fossiles de données provenant d'hommes modernes car la méthode se base sur la répartition bimodale des dimensions de certains diamètres des couronnes dentaires néandertaliennes qui exprime bien que certaines dents, notamment les canines, présentent des différences entre hommes et femmes. Sous cet éclairage, Scladina pourrait s'avérer un sujet féminin. Les dimensions du corps de la mandibule de Scladina sont assez petites par rapport à celles d'autres Néandertaliens d'âge similaire, ce qui pourrait également plaider en faveur du sexe féminin. L'étude histologique des dents va dans le même sens. Enfin, les racines des dents de Scladina sont courtes et se situent dans le bas de la variation néandertalienne, tandis que les cavités pulpaires sont larges. Ces indices supportent également l'hypothèse féminine. En conclusion, et même si aucun argument n'est absolument déterminant, la conjonction de tous les éléments permet d'envisager, avec prudence, une attribution de l'enfant de Scladina au sexe féminin.

Chapter 10 The juvenile Neandertal mandible from Scladina (Scla 4A-1 & Scla 4A-9)

179

In this descriptive chapter, each anatomical region of the Scladina mandible is analyzed according to features from the symphyseal region and the body to the branch and condyle. The

characters are described, illustrated with detailed diagrams, and discussed from the point of view of their taxonomic value while attempting to understand if they are archaic/plesiomorphic, derived, or linked to the young age of the subject. In this context, and based on numerous published studies, it is clear that most of the supposed derived characters from Scladina I-4A as well as other Neandertals are not precisely amenable to careful analysis. By contrast, it is the general morphology of the mandibles, the typical association of many anatomical features, which give fossil remains, including the Scladina mandible, an overall pattern quite characteristic of Neandertals.

La mandibule néandertalienne juvénile de Scladina (Scla 4A-1 & Scla 4A-9)

Dans ce chapitre descriptif, chaque région anatomique de la mandibule de Scladina est analysée faces par faces, depuis la symphyse et le corps de l'os jusqu'à la branche et le condyle. Les caractères sont décrits et illustrés, souvent avec des schémas détaillés, puis discutés du point de vue de leur valeur taxonomique en tentant de décoder s'ils sont archaïques/plésiomorphes, dérivés néandertaliens ou liés au jeune âge du sujet. À ce propos, et en se basant sur les nombreuses études proposées dans la littérature, il apparaît clairement que la plupart des caractères supposés dérivés de Scladina, comme des autres Néandertaliens, résistent mal à une analyse approfondie. C'est par contre la morphologie globale des mandibules, l'association tout à fait typique d'un grand nombre de traits anatomiques, qui confèrent à des fossiles, dont celui de Scladina, un aspect tout à fait caractéristique des Néandertaliens.

Chapter 11 3-D geometric morphometric analysis of the Scladina Neandertal child's mandible in a developmental context 215

This chapter conducts a comparative analysis of the shape of the Scladina mandible in the context of ontogenetic and adult variation of Neandertals and modern humans. Two modern human adult collections are included in the analysis (Inuit and Khoisan), one of which (Khoisan) is also represented by subadults. The fossil sample comprises seven adult and six subadult Neandertal individuals, as well as two *H. heidelbergensis* mandibles. Results show that the Scladina mandible is characterized by the features that distinguish Neandertals from modern humans as reflected by our data. In general, Neandertal juveniles show some of the features differentiating Neandertal from modern human adult mandibles at an early age. Nonetheless both groups are characterized by considerable shape change throughout ontogeny.

Analyse morphométrique géométrique tridimensionnelle de la mandibule de l'enfant de Scladina dans son contexte développemental

*Ce chapitre traite de l'analyse comparée de la forme de la mandibule du Néandertalien de Scladina du point de vue ontogénétique et celui de la variation entre les adultes Néandertaliens et les hommes modernes. Deux séries d'adultes modernes sont concernées par l'analyse (Inuit et Khoisan), dont l'une (Khoisan) est également représentée par des sujets subadultes. Les spécimens fossiles comprennent sept adultes et six subadultes néandertaliens, ainsi que deux mandibules d'*Homo heidelbergensis*. Nos données indiquent que la mandibule de l'enfant de Scladina est porteuse de traits qui permettent de distinguer les Néandertaliens des hommes modernes. En général, les Néandertaliens juvéniles présentent déjà les traits qui différencient les Néandertaliens des hommes modernes adultes à un âge précoce. Néanmoins, les deux groupes sont caractérisés par un changement considérable tout au long de leur ontogénèse.*

Chapter 12 The fragmentary right maxilla of the Scladina I-4A juvenile

223

The Scla 4A-2 maxilla is a small fragment from the right mid-facial region that retains only part of the alveolar and palatine processes as well as a small part of the body. The fossil is consistent with the Neandertal group of maxillae with regards to the bilevel configuration of its internal nasal floor and its rather high estimated subnasal height. The location of its zygoalveolar crest is not as posterior when compared to other similarly aged Neandertals. The anterior part of its dental arcade does not seem very large.

Le maxillaire droit fragmentaire de l'enfant de Scladina I-4A

Le maxillaire droit Scla 4A-2 se réduit à un fragment qui comprend une partie des processus palatin et alvéolaire et une petite partie du corps de l'os. En raison de la morphologie (de type « bileveled ») de son plancher nasal interne et de l'importance de sa hauteur nasale estimée, le fossile s'intègre bien dans le groupe des maxillaires néandertaliens, bien que sa crête zygoalvéolaire soit pas aussi reculée que celle des autres Néandertaliens. Enfin, la partie antérieure de son arcade dentaire ne semble pas très large.

Chapitre 13 The dentition of the Scladina I-4A juvenile Neandertal

233

The purpose of this chapter is to provide a general description of the 24 teeth which belong to the Scladina Juvenile mandible and maxilla that are examined in anatomical and statistical perspectives.

The descriptions focus on diagnostic morphological features of Neandertal teeth, in accordance with recent dental anthropological studies seeking to distinguish the teeth of Neandertals from other taxa. Some non-metric data have been collected following the Arizona State University Dental Anthropology System (ASUDAS). The micro-CT data used were recorded at the University of Antwerp and at the Max Planck Institute in Leipzig. Statistically, the mesiodistal and buccolingual diameters of all crowns have been compared to a sample of similar specimens from different periods: Early Neandertals (EN), Late Neandertals (LN), Middle Palaeolithic Modern Humans (MPMH), Upper Palaeolithic Modern Humans (UPMH) as well as Belgian Middle Ages/ Modern *Homo sapiens sapiens* (MHSS). The univariate analyses employed are 'probabilistic distances' (DP) and "écart centré réduit ajusté" (ECRA). Bivariate biometric comparisons made use of the well-known technique of equiprobable ellipses.

Regarding the taxonomic allocation, the teeth fit very well in the characteristic Neandertal pattern, even if, as other teeth from similar sites, they do not exhibit any character which would be exclusively Neandertal. Whatever the statistical method used, significant differences quite often occur between the Scladina Juvenile and MHSS. Slight differences do sometimes exist with the UPMH comparative sample. By contrast, the Scladina tooth crowns are never different from those of Late Neandertals and rarely different from those of Early Neandertals and MPMH.

La dentition du Néandertalien juvénile Scladina I-4A

Les 24 dents appartenant à la mandibule et au maxillaire de l'enfant de Scladina sont décrites dans une double approche, à la fois anatomique et statistique.

*La description des fossiles se concentre sur les caractères morphologiques et se base sur les études récentes qui cherchent à distinguer les dents néandertaliennes de celles des autres taxons. Divers caractères non-métriques sont enregistrés en utilisant les plaques comparatives du système ASUDAS (Arizona State University Dental Anthropology System), destiné à mieux objectiver les descriptions. Les données microtomographiques des fossiles ont été acquises à l'Université d'Anvers et à l'Institut Max Planck de Leipzig. Sur le plan statistique, les diamètres mésio-distaux et bucco-linguaux des couronnes dentaires sont comparés à des échantillons de Néandertaliens anciens (EN), de Néandertaliens classiques (LN), d'Hommes modernes du Paléolithique moyen (MPMH), d'Hommes modernes du Paléolithique supérieur (UPMH) ainsi que d'*Homo sapiens sapiens* récents (MHSS), provenant de Belgique et remontant principalement au Moyen Âge et aux Temps Modernes. Les techniques statistiques utilisées sont univariées, avec la distance probabiliste (DP) et l'écart centré réduit ajusté (ECRA), et bivariées, avec des ellipses équiprobables.*

*Sur ces bases, il apparaît que la morphologie des dents de Scladina correspond bien au modèle général néandertalien, même si, comme les autres dents de ce taxon, elle ne présente aucun caractère qui serait exclusivement néandertalien. Quel que soit le test statistique utilisé des différences significatives sont enregistrées entre le spécimen de Scladina et les *Homo sapiens sapiens* récents (MHSS). De légères différences apparaissent parfois avec les Hommes modernes du Paléolithique supérieur (UPMH). Les dents de l'enfant de Scladina ne diffèrent par contre jamais de celles des Néandertaliens classiques (LN) et rarement des Néandertaliens anciens (EN) et des Hommes modernes du Paléolithique moyen (MPMH).*

Chapter 14 Enamel thickness in the Scladina I-4A Neandertal teeth 307

Enamel thickness and dental tissue proportions have been recognized as effective taxonomic discriminators between Neandertal and modern human teeth. However, most of the research on this topic focused on molars, and little information is available for other tooth classes. Moreover, the absence of wear is an essential precondition to quantify enamel thickness, but unworn teeth are much less frequent in the fossil record than worn teeth. Therefore, the unworn/slightly worn Scladina teeth represent a valuable sample for the advancement of our knowledge on Neandertal's enamel thickness variability. In particular, we used 3D μ CT data to investigate the 2D and 3D enamel thickness of the Scladina molars, premolars and canines. Our results confirm that Neandertals have lower average enamel thickness (AET) and relative enamel thickness (RET) indices than *Homo sapiens*, and that molars, premolars and canines (and maybe also incisors) have a different and peculiar trend, with premolars having generally larger RET indices than molars, and canines showing the lowest values. We are confident that these results improve our understanding of the Neandertal range of variation for the enamel thickness, and will be useful for future comparative studies between Neandertal and *Homo sapiens*.

L'épaisseur de l'émail dentaire du Néandertalien Scladina I-4A

L'épaisseur de l'émail et les proportions des tissus dentaires se révèlent des facteurs taxonomiques discriminants entre les dents des Néandertaliens et des Hommes modernes. La plupart des études actuelles se focalisent cependant sur les molaires et peu d'informations traitent des autres classes

de dents. En outre, l'absence d'usure est une condition indispensable pour la quantification optimale de l'épaisseur de l'émail, même si, sur les fossiles, les dents intactes se rencontrent moins fréquemment que les dents utilisées. C'est pourquoi les dents intactes ou légèrement usées du sujet juvénile de *Scladina* constituent d'excellents spécimens qui enrichissent nos connaissances sur la variabilité de l'épaisseur de l'émail dentaire chez les Néandertaliens. Nous avons utilisé les données microtomographiques 3D pour examiner, en 2D et en 3D, l'épaisseur de l'émail des molaires, des prémolaires et des canines du fossile de *Scladina*. Nos résultats confirment que les Néandertaliens présentent des indices d'épaisseur moyenne (AET) et relative (RET) d'émail plus faibles que ceux des *Homo sapiens*, et que les molaires, les prémolaires et les canines (peut-être aussi les incisives) ont une tendance différente et particulière : les prémolaires présentent un indice d'épaisseur d'émail relative (RET) généralement plus large que celui des molaires et des canines qui affichent les valeurs les plus basses. Nous sommes convaincus que ces résultats ont amélioré notre compréhension de la variabilité de l'épaisseur de l'émail et stimuleront de nouvelles études comparatives entre les Néandertaliens et les *Homo sapiens*.

Chapter 15 Interspecific and intraspecific taxonomic affinity based on permanent mandibular molar enamel-dentine junction morphology of the *Scladina* I-4A juvenile 315

In this contribution we examine the taxonomic affinity of the *Scladina* specimen based on the morphology of the internal structure of the mandibular molars. Specifically, we use microtomography to image the enamel-dentine junction (EDJ) of the mandibular molars and geometric morphometrics to assess the morphological affinity of the mandibular molars to a comparative sample of *Homo neanderthalensis*, fossil modern humans, and modern humans. In addition to confirming the taxonomic status of the *Scladina* specimen as a Neandertal based on EDJ size and shape, we demonstrate consistent patterns of morphological variation in enamel-dentine morphology of Early (> 100 ka BP) and Classic Neandertals (< 100 ka BP). In this respect, the molar EDJ morphology of *Scladina* shows a stronger affinity with Classic Neandertals compared to its weaker Early Neandertal affinity.

*Comparaisons taxonomiques interspécifiques et intraspécifiques basées sur la morphologie de la jonction émail/dentine des molaires inférieures du Néandertalien *Scladina* I-4A*

*Dans ce chapitre nous examinons les affinités taxonomiques du spécimen néandertalien de *Scladina*, sur base de la morphologie de la structure interne de ses molaires mandibulaires. Nous avons eu recours à la microtomographie pour reconstituer l'image de la jonction entre l'émail et la dentine (« EDJ ») des molaires inférieures ensuite, ainsi qu'à la morphométrie géométrique pour évaluer les affinités morphologiques entre les molaires des *Homo neanderthalensis*, des *Homo sapiens* fossiles et des hommes modernes. Pour confirmer la position taxonomique néandertalienne du spécimen de *Scladina* sur base de la taille et de la forme de la « EDJ », nous apportons des critères pertinents documentant la variation morphologique de la « EDJ » entre les Néandertaliens anciens (>100 ka BP) et les Néandertaliens classiques (< 100 ka BP). Ainsi, la morphologie de la « EDJ » des molaires du spécimen de *Scladina* présente une plus forte affinité avec celle des Néandertaliens classiques qu'avec celle des Néandertaliens anciens.*

Chapter 16 Micro-Computed tomographic quantification of tooth root size and tissue proportions in the Scladina I-4A juvenile, a short-rooted Neandertal 325

Tooth root morphology has been shown to taxonomically differentiate Neandertals from modern humans, for both anterior (incisors and canines) and posterior (molars) teeth.

In the present study, the tooth root morphology of the Scladina Child has been investigated using micro-computed tomography. The dental tissues were segmented and metric, surface, and volumetric measurements were taken on the 3D models of the roots.

Compared to other MIS 5 Neandertals (Krapina, Regourdou 1 and Abri Bourgeois-Delaunay), the Scladina individual has the shortest root dimensions for given crown sizes, for both anterior and posterior teeth. The large Krapina sample shows a noticeable variability in dental dimensions, the teeth being overall robust and large. We discuss these results in terms of geographical variability, sexual dimorphism, modification of dental tissues with age and individual variability. In addition, we place the Scladina Child in a broader comparative context covering a large sample of Lower and Middle Pleistocene hominins. We show that Scladina has an anterior tooth root shape similar to other Neandertals and that its tooth root dimensions plot amongst the smallest Neandertals. Moreover, the Scladina molar roots are lacking any degree of taurodontism.

We draw attention to the fact that, despite its large sample size, the Krapina Neandertals do not fully represent the variability in dental dimensions among MIS 5 Neandertals, and that caution should be considered for taxonomical diagnosis relying on dental measurements alone, as shown here by the particularly short-rooted Scladina outlier that could be misclassified as a modern human.

Quantification tomographique de la taille des racines et de la proportion des tissus des dents de Scladina I-4A, un Néandertalien juvénile dotés de courtes racines

La morphologie des racines dentaires a été reconnue comme particulièrement pertinente pour discriminer taxonomiquement les Néandertaliens des hommes modernes et ce, à la fois pour les dents antérieures (incisives et canines) et postérieures (molaires).

Dans la présente étude, la morphologie racinaire de l'enfant de Scladina a été étudiée en microtomographie. Les tissus dentaires ont été segmentés et des mesures linéaires, surfaciques et volumiques ont été prises sur les modèles 3D des racines.

Comparé à d'autres Néandertaliens du stade isotopique 5 (Krapina, Regourdou 1 et Abri Bourgeois-Delaunay), l'individu de Scladina présente, sur les dents antérieures et postérieures, les dimensions racinaires les plus petites pour une taille de couronne comparable. L'échantillon de Krapina montre une variabilité notable en dimensions dentaires, les dents étant en général robustes et grandes. Nous discutons ces résultats en termes de variabilité géographique, de dimorphisme sexuel, de modification des tissus dentaires avec l'âge et de variabilité individuelle en développement dentaire. De plus, nous replaçons Scladina dans un contexte comparatif plus large, impliquant un vaste échantillon d'hominidés du Pléistocène inférieur et moyen. Nous montrons que Scladina a une forme [shape en anglais] de racine, pour les dents antérieures, similaire à celle des autres Néandertaliens et que ses dimensions racinaires le placent parmi les plus petits Néandertaliens. Enfin, les racines des molaires de l'enfant de Sclayn montrent une absence de taurodontisme.

Nous attirons l'attention sur le fait qu'en dépit d'un grand nombre d'échantillon, les Néandertaliens de Krapina ne représentent pas idéalement la variabilité en dimensions dentaires des Néandertaliens du stade isotopique 5. Toute attribution taxonomique basée seulement sur des mesures dentaires doit être considérée avec prudence, comme le prouve ici le cas particulier des racines dentaires courtes de l'enfant de Sclayn qui, sur cette base, pourrait être classifié de façon erronée parmi les hommes modernes.

Chapter 17 Diet and ecology of the Scladina I-4A Neandertal Child: insights from stable isotopes

351

The Neandertal child from former Layer 4 in Scladina Cave is so far the oldest Neandertal that yielded well preserved collagen suitable for stable isotopic analysis ($^{13}\text{C}/^{12}\text{C}$, $^{15}\text{N}/^{14}\text{N}$). Although the complexity regarding the stratigraphic origin of this specimen makes it difficult to perform a quantitative palaeodietary reconstruction, interesting conclusions could be reached. The $\delta^{13}\text{C}$ values of herbivores found in former layers 4 and 5 in Scladina Cave indicate a mixture of dense forest and open habitat, although it is not clear whether this situation reflects a real mosaic or changes of vegetation through time. Some species traditionally considered to reflect open and cold environment, such as reindeer, exhibit $\delta^{13}\text{C}$ values indicative of dwelling in dense forest conditions while species traditionally considered to be linked to open environments such as horses exhibit $\delta^{13}\text{C}$ values indicative of dense-forest habitat. These results exemplify the ecological flexibility of large herbivorous mammals at the beginning of the Upper Pleistocene. The palaeodietary reconstruction of the Neandertal child from former Layer 4 in Scladina Cave points to the consumption of open environment herbivores, similar to the majority of European Neandertals analysed so far. However, it is not possible to tell if this selection was due to the absence of dense forest herbivores when this specimen was living, or if such animals were present but not consumed.

L'alimentation et l'écologie de l'enfant néandertalien Scladina I-4A: le message des isotopes stables

L'enfant néandertalien de l'ancienne couche 4 de la grotte Scladina est le plus vieux spécimen de cette espèce ayant livré à ce jour du collagène bien conservé permettant l'analyse de la teneur relative en isotopes stables ($^{13}\text{C}/^{12}\text{C}$, $^{15}\text{N}/^{14}\text{N}$). Bien que la position stratigraphique complexe de ce spécimen ne permette pas une reconstitution paléalimentaire quantitative, des conclusions intéressantes ont pu être établies. Les valeurs de $\delta^{13}\text{C}$ des herbivores des anciennes couches 4 et 5 de la grotte Scladina indiquent un mélange d'habitats de types ouverts et forestiers denses, sans qu'il soit possible de trancher entre une mosaïque d'habitats contemporains et une succession rapide d'habitats changeant au cours du temps. Une espèce traditionnellement considérée comme reflétant un environnement ouvert et froid, comme le renne, présente des valeurs de $\delta^{13}\text{C}$ indiquant un habitat de type forestier dense tandis qu'une autre traditionnellement considérée comme liée à un milieu ouvert, tel le cheval, présente des valeurs de $\delta^{13}\text{C}$ indiquant un milieu forestier dense. Ces résultats démontrent la flexibilité écologique des grands mammifères herbivores au début du Pléistocène supérieur. La reconstitution paléalimentaire de l'enfant néandertalien de l'ancienne couche 4 de la grotte Scladina indique la consommation d'herbivores de milieu ouvert, comparable à celle de la majorité des spécimens de Néandertaliens d'Europe analysés à ce jour. Il n'est cependant pas possible de déterminer si cette sélection est due à l'absence d'herbivores de forêt dense au moment où vivait ce Néandertalien, ou si de tels animaux étaient effectivement présents mais non consommés.

Chapter 18 Dental microwear texture analysis and the diet of the Scladina I-4A Neandertal Child

363

Microwear analyses have been shown to be an important tool for the reconstruction of tooth use for dietary as well as non-dietary purposes for a variety of species including fossil hominins. The results of the analysis of the microwear textures of the anterior and of post-canine dentitions of the Scladina Neandertal child are presented here. Overall, these results shed further light on the dietary and behavioral strategies of Neandertals. In addition, they provide a rare glimpse into such strategies among subadult Neandertals.

Analyse des micro-usures dentaires et alimentation du Néandertalien juvénile Scladina I-4A

Les analyses des micro-usures se sont révélées un outil important pour la reconstitution du mode d'utilisation des dents tant à des fins alimentaires que non alimentaires et ce pour plusieurs espèces dont les hominés fossiles. Les résultats obtenus sur la texture des micro-usures de la dentition antérieure et postérieure aux canines de l'enfant néandertalien de Scladina sont présentés ici. Principalement, ils ont apporté des éléments significatifs sur les stratégies alimentaires et comportementales des Néandertaliens. De plus, ils offrent un premier aperçu de ces stratégies actuellement peu documentées chez les Néandertaliens subadultes.

Chapter 19 Neandertal evolution and human origins: a tale from the Scladina I-4A Child

379

Ancient DNA offers the unique opportunity to catch evolution red-handed and to document the past with genetic information. We used ancient DNA methods to reconstruct short mitochondrial sequences from the Scladina Child. Its comparison to orthologous sequences from other Neandertal specimens from Croatia, Germany, Italy, and the Caucasus confirmed Neandertals as our closest relatives. The Neandertal child from Scladina appeared surprisingly more distantly related to modern humans than younger Neandertals. This suggests that the Neandertal population experienced a significant demographic bottleneck in the last 30-50 ka BP preceding its extinction. In the future, new methodological approaches tailored to the molecular preservation state of ancient DNA molecules will likely enable the sequencing of the whole genome of the Scladina Child and provide further insights about its evolutionary origins.

Évolution des Néandertaliens et origines de l'homme : histoire de l'enfant Scladina I-4A

L'ADN ancien offre une chance exceptionnelle de pouvoir appréhender l'évolution en pleine action et documente le passé grâce aux données génétiques. En employant les méthodes d'analyses de l'ADN ancien nous avons pu reconstituer de courtes séquences mitochondriales du Néandertalien juvénile de Scladina. Sa comparaison avec les séquences orthologues d'autres spécimens néandertaliens de Croatie, Allemagne, Italie et du Caucase a confirmé que les Néandertaliens étaient nos plus proches parents. De façon surprenante, le Néandertalien de Scladina est apparu moins apparenté avec les hommes modernes que l'étaient les autres Néandertaliens plus récents. La population néandertalienne semble donc avoir subi un goulet d'étranglement démographique durant les derniers 30 à 50 ka BP, avant son extinction. Dans un futur proche, de nouvelles méthodes d'étude mieux adaptées à l'état de conservation de molécules de l'ADN ancien seront probablement capables de

séquencer le génome complet de l'enfant de Scladina et préciseront sa place dans l'évolution des hominidés.

Chapter 20 Scladina I-4A in the chronological context of the Neandertals from the Belgian Meuse Valley and northwest Europe

395

The anthropological discoveries that occurred over the past quarter of a century at Scladina Cave are far from being the only Neandertal remains from the Meuse River Basin, in southern Belgium. Indeed, at least seven other karstic sites yielded Neandertal fossils (five during the 19th century): Engis (1829-30), La Naulette (1866), Goyet (around 1870), Spy (1886) and Fonds de Forêt (1895). Three of these finds (Engis, La Naulette and Spy) have played a primary role in the genesis and initial developments of palaeoanthropology and prehistory. After nine decades without new discoveries, the end of the 20th century was marked by three discoveries of Neandertal remains, all of them important because they occurred during excavation campaigns that yielded contextual data of quality: an isolated deciduous tooth at Trou de l'Abîme in Couvin (1984), the Scladina Juvenile remains from 1990 onwards, and a premolar in Walou Cave (1997). Like other Neandertal remains found in the neighbouring regions (France, Great Britain, Germany and the Netherlands), these 'Belgian' fossils provide the juvenile of Scladina with an anthropological context only analysed, in this chapter, from a chronological perspective.

After discussing the variable quality of information available from the stratigraphic, archaeological, chronological and palaeoenvironmental contexts of the remains found in the Meuse River Basin, the chapter provides a simplified chronology of the regional Neandertals. In the current state of research, there are two main groups of fossils. La Naulette mandible might well be the oldest fossil, dating from the MIS 5 or even earlier whereas the Scladina Juvenile remains belong to a Classic Neandertal (MIS 5b or 5a). During the second part of MIS 4, there are no occupations of the Belgian Meuse River Basin, due to a major climatic deterioration. The second group is composed of Late/Classic Neandertals from the MIS 3, associated with late Mousterian industries from around 45 ka BP at Couvin to 36 ka BP at Spy, where the associated lithic industry is imprecise, possibly transitional L.R.J., or even late Mousterian.

La position chronologique de Scladina I-4A dans le contexte des Néandertaliens de la vallée de la Meuse belge et du Nord-Ouest de l'Europe

Les découvertes anthropologiques réalisées à la grotte Scladina depuis un quart de siècle sont loin de représenter les seuls restes néandertaliens exhumés dans le bassin mosan belge. En effet, sept autres sites karstiques ont livré de tels fossiles. Cinq de ces trouvailles furent effectuées au 19e siècle : Engis (1829-30), La Naulette (1866), Goyet (vers 1870), Spy (1886) et Fonds de Forêt (1895). Trois d'entre elles, Engis, La Naulette et Spy ont joué un rôle de premier plan dans la genèse et les développements initiaux de la paléontologie humaine et de la Préhistoire. Après neuf décennies infructueuses, la fin du 20e siècle est marquée par trois mises au jour de restes néandertaliens, toutes de grandes importance en raison de la qualité des informations contextuelles obtenues dans les fouilles qui les ont livrées : une molaire déciduale inférieure au Trou de l'Abîme à Couvin (1984), les restes de l'enfant de Scladina à partir de 1990 et une prémolaire à la grotte Walou (1997). Comme d'autres fossiles néandertaliens provenant des régions voisines (France, Grande-Bretagne, Allemagne et Pays-Bas), ces spécimens "belges" permettent de donner à l'enfant de Scladina un contexte anthropologique qui est analysé, dans ce chapitre, uniquement dans une optique chronologique.

Après une évaluation de la qualité variable des informations relatives au contexte stratigraphique, archéologique, chronologique et paléoenvironnemental des découvertes réalisées dans le bassin mosan, ce chapitre propose un modèle chronologique des Néandertaliens régionaux. Dans l'état actuel de la recherche, deux grands groupes de fossiles apparaissent. La mandibule de La Naulette pourrait bien être le plus ancien fossile, remontant au SIM 5 ou auparavant, tandis que les restes de l'enfant de Scladina appartiennent à un Néandertalien classique ancien, au cours du SIM 5b ou 5a. Aucune occupation humaine ne semble avoir été présente au cours de la seconde partie du SIM 4, en raison d'une péjoration climatique majeure. Le second groupe se compose de Néandertaliens classiques tardifs du SIM 3, associés à de l'industrie moustérienne qui s'échelonnent des alentours de 45 ka BP (50-47 ka cal BP) à Couvin, aux alentours de 36 ka BP (42-40 ka cal BP) à Spy où l'industrie associée est difficilement identifiable, peut-être un moustérien très tardif ou alors l'industrie de transition que représente le L.R.J.

Chapter 21 The Scladina I-4A juvenile Neandertal: synthesis

409

This concluding chapter of the Scladina monograph comprises two parts. The first synthesizes, from an interdisciplinary perspective, some key aspects regarding the context of the Neandertal remains from former Layer 4A, discussed through their stratigraphic position, their palaeoenvironment and chronostratigraphy. In the field of palaeoanthropology, some questions concerning the attribution of Scladina to Early or Late Neandertals, the individual age of the remains, their sexual attribution as well as the diet are raised. The second part of this final chapter discusses various ideas concerning the future of regional Neandertal research, both at Scladina and at the other sites of the Meuse River Basin.

Le Néandertalien juvénile Scladina I-4A : synthèse

Le chapitre final de la monographie comprend deux parties. La première partie synthétise, dans une optique interdisciplinaire, le contexte des fossiles Néandertaliens de l'ancienne couche 4A qui est ainsi abordé par le biais de leur position stratigraphique, de leur paléoenvironnement et de leur chronostratigraphie. Dans le domaine plus strictement paléoanthropologique, les questions soulevées concernent l'attribution de l'enfant de Scladina à un Néandertalien ancien ou classique, son âge individuel, son sexe ou encore son régime alimentaire. La seconde partie du chapitre aborde certaines perspectives de la recherche néandertalienne régionale, tant à propos de Scladina que des autres sites du bassin mosan.

Figures and Tables

Chapter 1. Overview and context of the Scladina palaeoanthropological project

Fig. 1: Refitting of all Scladina Neandertal fossils.	13
Fig. 2: 3D representation of the Meuse Valley.	14
Fig. 3: 3D reconstruction positioning the fossils.	15
Tab. 1: List of all Scladina Neandertal remains.	17
Fig. 4: Technical sheet and field plan of the hemimandible.	18
Fig. 5: Left half of the mandible in situ.	19
Fig. 6: Permanent maxillary first right molar.	19
Fig. 7: Evocation of the Scladina Child (B. Clarys).	21

Chapter 2. Scladina Cave: archaeological context and history of the discoveries

Fig. 1: Situation of the village of Sclayn.	31
Fig. 2: Situation of Scladina Cave.	32
Fig. 3: Map of Scladina Cave with the excavated areas.	32
Fig. 4: In 1971, the cave was filled to the vault with sediments.	33
Fig. 5: Longitudinal schematic section of Scladina Cave.	33
Fig. 6: Scladina Cave and the evolution of the site excavation.	34-35
Fig. 7: View of a longitudinal section in Square F34.	36
Fig. 8: Stratigraphic log of Scladina Cave.	38
Fig. 9: The raw material types from Unit 5.	39
Fig. 10: The flint nodules are roughly prepared with low standardization.	40
Fig. 11: Simple convex side scraper.	40
Fig. 12: The refitting of a quartzite pebble.	41
Fig. 13: A massive quartzite asymmetrical knife from Unit 5.	41
Fig. 14: Hare coxal fragment with 18 cut marks.	41
Fig. 15: Debitage of an alluvial flint pebble following the Quina conception.	42
Fig. 16: Two cave bear canines.	43
Fig. 17: The patinated flint artefacts of Unit 2A and the sharp ones from Unit 6A.	44
Fig. 18: Recreation of the geographic and stratigraphic position of Scla 4A-1.	45
Fig. 19: The permanent maxillary right first molar in situ.	45
Fig. 20: The left hemimandible Scla 4A-9 in situ.	46
Fig. 21: The deciduous molar Scla 4A-13 in situ.	46

Chapter 3. The stratigraphic sequence of Scladina Cave

Fig. 1: The complexity of cave entrance sedimentary sequences.	49
Fig. 2: The former stratigraphic sequence of Scladina Cave.	50
Fig. 3: The new stratigraphic sequence of Scladina Cave.	52
Fig. 4: Map of the squares where Sedimentary Complex 4 has been excavated.	53
Fig. 5: Section H/I.	54
Fig. 6: Section 30/31.	54
Fig. 7: Section 32/31.	55
Fig. 8: Diagrams presenting the 5 distinct units of Sedimentary Complex 4.	56

Tab. 1: Correlation between the former stratigraphic system and the new one.	59
Fig. 9: Previous stratigraphic records of profiles H/I and 30/31.	60
Fig. 10: Picture of Section 32/31 showing units 4A-CHE and 4A-POC.	61

Chapter 4. The palaeoenvironmental context and chronostratigraphic framework of the Scladina Cave

Fig. 1: The former and the new stratigraphic sequences of Scladina.	70
Fig. 2: Magnetic susceptibility data.	71
Fig. 3: Scladina Cave's stratigraphic log including the palaeoenvironmental and chronostratigraphical data.	74-75
Fig. 4: The Middle Belgium loess reference sequence.	81
Tab. 1: Synthesis of the green amphibole data from the Middle Belgian loess belt.	83

Chapter 5. Stratigraphic origin of the juvenile Neandertal remains from Scladina Cave

Fig. 1: The former stratigraphic record.	93
Fig. 2: The new stratigraphic record.	94
Tab. 1: List of the 19 Neandertal remains.	95
Fig. 3: Plan of the cave with location of Fig. 4.	96
Fig. 4: Spatial distribution of the 19 juvenile Neandertal remains.	97
Fig. 5: Orthogonal projections of Scla 4A-1 to 4 on Cross-Section 30/31 B-E.	98
Fig. 6: Orthogonal projections of Scla 4A-1 and 9 on Cross-Section E/D.	98
Fig. 7 & 8: Pictures of a cast showing the discovery position of the mandible Scla 4A-1.	99
Fig. 9: Course and extent of the gully structure of Unit 4A-CHE.	100
Fig. 10: Small profiles threatened by the collapse of large stone slabs.	100
Tab. 2: Possible stratigraphic origin of the 19 remains.	100
Fig. 11: Left half of the mandible in its discovery position.	101
Fig. 12: The permanent maxillary right first molar in situ.	103
Fig. 13: Orthogonal projections of Scla 4A-8 & 19 on Cross-Section 32/31.	104
Fig. 14: The deciduous molar Scla 4A-13 in situ.	105
Fig. 15: Orthogonal projections of Scla 4A-13 & 19 on Profile E/F.	106
Fig. 16: Orthogonal projections of 10 teeth on Profile H/I.	107
Fig. 17: The extrapolated depth of the bottom of Unit 4A-IP and of Layer 3-EMO.	109
Fig. 18: Profile 30/31 showing the bottom of Layer 3-EMO.	109
Fig. 19: Profile E/F showing the badger burrows.	111
Fig. 20: Evocation of the depositional history of the remains.	112
Fig. 21: Hypotheses attributing the Scladina I-4A to MIS 5b or MIS 5a.	121

Chapter 6. Non-Destructive Gamma-Ray Spectrometry of the Scladina Neandertal mandible (Scla 4A-1)

Tab. 1. Measured uranium content and age of the Scladina mandible.	126
--	-----

Chapter 7. Taphonomy of the juvenile Neandertal remains from Sedimentary Complex 4A, Scladina Cave

Fig. 1: Stratigraphic log of units 6A to 4A-POC.	128
Fig. 2: Spatial distribution of the Neandertal and animal remains.	130
Fig. 3: The 19 juvenile Neandertal fossils.	131
Fig. 4: The left hemimandible Scla 4A-9.	132
Fig. 5: Cracks on Scla 4A-9.	132
Fig. 6: The manganese deposits on Scla 4A-9.	132
Fig. 7: The peeling adjacent to the anterior fracture of Scla 4A-9.	133
Fig. 8: Excavation damage on Scla 4A-9.	133
Fig. 9: The right hemimandible Scla 4A-1.	134
Fig. 10: Thin horizontal cracks on Scla 4A-1.	134
Fig. 11: Comparison of the anterior break of Scla 4A-1 & 9.	134
Fig. 12: The eroded gonion of Scla 4A-1.	135
Fig. 13: The star-shaped fracture of Scla 4A-1.	135
Fig. 14: The straight thin groove caused by sedimentary processes.	135
Fig. 15: The splinter broken off from Scla 4A-1 during excavation.	136
Fig. 16: The maxilla Scla 4A-2.	136
Fig. 17: The crenulated margin of Scla 4A-2.	136
Fig. 18: The thin cracks of Scla 4A-2.	137
Tab. 1: Taphonomic results.	139
Fig. 19: The greyishgreen colour of Scla 4A-1 & 2.	140
Fig. 20: The orange colour of the hemimandible Scla 4A-9.	141
Fig. 21: The doubly coloured splinter Sc 2006-341-1.	142
Fig. 22: An example of typical weathering marks.	143
Fig. 23: The tiny light grey spots on Scla 4A-1.	144
Fig. 24: 26 <i>Ursus spelaeus</i> teeth and Scla 4A-19.	145
Tab. 2: Synthesis of stratigraphic and taphonomic features.	146

Chapter 8. Dental development in and age at death of the Scladina I-4A juvenile Neandertal

Fig. 1: Incremental features found in enamel and dentine.	155
Fig. 2: Long-period incremental growth lines.	156
Fig. 3: Virtual model of the molar crown Scla 4A-4.	157
Fig. 4: Histological section of the molar crown Scla 4A-4.	157
Fig. 5: The embedded molar Scla 4A-4 on the annular saw.	158
Fig. 6: The Scladina molar Scla 4A-4 before and after reconstruction.	158
Fig. 7: Scan of the incisor Scla 4A-11.	159
Fig. 8: Reconstruction of protocone crown formation time (Scla 4A-4).	160
Tab. 1: Developmental variables for the Scladina tooth crowns.	161
Fig. 9: Developmental stress matched across the anterior dentition.	162

Fig. 10: Developmental chronology of the Scladina Juvenile.	162
Tab. 2: Cumulative mean root extension rates for the Scladina individual's dentition.	162
Tab. 3: Comparison of perikymata number in the Scladina dentition with other Neandertals.	163
Fig. 11: Permanent maxillary canine size variation: Scla 4A-18 and Obi Rakhmat Grotto.	163

Chapter 9. Is sex determination of the Scladina I-4A juvenile Neandertal possible?

Fig. 1: Canine and lateral incisor breadths.	171
Tab. 1: Ranges and means of some Neandertal teeth.	172
Tab. 2: Height, thickness and index of robusticity of mandibles.	173

Chapter 10. The juvenile Neandertal mandible from Scladina (Scla 4A-1 & Scla 4A-9)

Fig. 1: Scladina mandible (Scla4A-1 & 9) without the refitted teeth.	179
Fig. 2: Scladina 4A-1 right hemimandible.	180
Fig. 3: Scladina 4A-9 left hemimandible.	181
Fig. 4: Scla 4A-1 & 9 viewed from the right side.	181
Fig. 5: Scla 4A-1 & 9 in superior view.	182
Fig. 6: Scla 4A-1 & 9, anterior face of the symphyseal region.	182
Fig. 7: Scla 4A-1 & 9, posterior views.	183
Fig. 8: Scla 4A-1 & 9, schematic drawing of the posterior surface of the symphysis.	183
Fig. 9: Scla 4A-1 & 9, different sections.	184
Fig. 10: Scladina mandible (Scla 4A-1 & 9), inferior border.	185
Fig. 11: Scladina 4A-1 right hemimandible, external aspect.	186
Fig. 12: Scladina 4A-9 left hemimandible, external aspect.	186
Fig. 13: Right hemimandible, schematic drawing.	187
Fig. 14: Scladina mandible, mental foramen.	187
Tab. 1: Position of the mental foramen of Scladina I-4A and comparisons.	188
Fig. 15: Scladina right hemimandible (Scla 4A-1), internal aspect.	189
Fig. 16: Scladina left hemimandible (Scla 4A-9), internal aspect.	189
Fig. 17: Mandible, internal aspect of the bodies, schematic drawing.	189
Fig. 18: Ramus of the right hemimandible, schematic drawing.	191
Fig. 19: Scladina mandible, right mandibular foramen.	192
Fig. 20: Tubercles of the right ramus.	193
Fig. 21: Tubercles of the right ramus, schematic drawing.	193
Fig. 22: Lateral surface of the right ramus.	194
Fig. 23: Scladina mandible (Scla 4A-1), condyle in superior view.	195
Tab. 2: Features of the mandible compared with Neandertal characteristics.	197
Tab. 3: Measurements of the Scladina mandible.	198
Tab. 4: Dimensions and comparisons of the right ramus.	198-199
Tab. 5: Dimensions of the corpus and comparisons.	200-201
Fig. 24: Infradentale-pogonion and infradentale-gnathion angles, graph.	202

Tab. 6: Infradentale-pogonion angle and infradental-gnathion angle of the Scladina symphysis and comparisons.	202	Fig. 1: Scla 4A-11 maxillary right central incisor.	236
Tab. 7: Height and thickness of the Scladina symphysis and comparisons.	203	Tab. 3: Distinctive anatomical features on maxillary central incisors.	237
Fig. 25: Height and thickness of the symphysis, graph.	203	Tab. 4: Scla 4A-11: MD and BL dimensions and comparisons.	238
Tab. 8: Height and thickness of the mandible at the canine and comparisons.	204	Fig. 2: Bivariate analysis of the MD and BL diameters of maxillary central incisors.	238
Fig. 26: Height and thickness of the mandible at the canine, graph.	204	Fig. 3: Scla 4A-17 maxillary left lateral incisor.	239
Tab. 9: Height and thickness of the mandible at the P ₃ and comparisons.	205	Fig. 4: Scla 4A-14 maxillary right lateral incisor.	241
Fig. 27: Height and thickness of the mandible at the P ₃ , graph.	205	Tab. 5: Distinctive anatomical features on maxillary lateral incisors.	242
Tab. 10: Height and thickness of the mandible at the M ₁ and comparisons.	206	Tab. 6: Scla 4A-14 & 17: MD and BL dimensions and comparisons.	243
Fig. 28: Height and thickness of the mandible at the M ₁ , graph.	206	Fig. 5: Bivariate analysis of the MD and BL diameters of maxillary lateral incisors.	243
Tab. 11: Ramus minimum breadth of the mandible and comparisons.	207	Fig. 6: Scla 4A-15 mandibular right central incisor.	245
Tab. 12: Ramus height of the mandible and comparisons.	207	Tab. 7: Scla 4A-15: MD and BL dimensions and comparisons.	246
Fig. 29: Minimum breadth of the ramus and the gonion-condyle height, graph.	207	Fig. 7: Bivariate analysis of the MD and BL diameters of mandibular central incisors.	246
Fig. 30: ECRA of the symphysis angles and of the height and thickness of the mandible.	208	Fig. 8: Scla 4A-20 mandibular right lateral incisor.	248
Tab. 13: Mandibular angle of the Scla 4A-1 and comparisons.	209	Fig. 9: Scla 4A-19 mandibular left lateral incisor.	249
<i>Chapter 11. 3-D geometric morphometric analysis of the Scladina Neandertal child's mandible</i>			
Fig. 1: The Scladina mandible.	215	Tab. 8: Scla 4A-19 & 20: MD and BL dimensions and comparisons.	250
Tab. 1: 70 mandibles of the comparative study.	216	Fig. 10: Bivariate analysis of MD and BL diameters of mandibular lateral incisors.	251
Tab. 2: Landmarks used and their definitions.	216	Fig. 11: Scla 4A-16 maxillary right canine.	252
Fig. 2: Landmarks used in the analysis.	217	Fig. 12: Scla 4A-18 maxillary left canine.	254
Fig. 3: Shape-space analysis. Principal components 1 and 2.	218	Tab. 9: Distinctive anatomical features on maxillary canines of different taxa.	255
Fig. 4: Principal component 1 and 2 plotted against centroid size.	219	Tab. 10: Scla 4A-16 & 18: MD and BL dimensions and comparisons.	255
Fig. 5: Size-shape space principal components analysis.	219	Fig. 13: Bivariate analysis of the MD and BL diameters of maxillary canines.	256
Fig. 6: PC 1 plotted against log centroid size.	220	Fig. 14: Scla 4A-12 mandibular right canine.	257
Fig. 7: The modern human and Neandertal growth trajectories along PC 1.	220	Tab. 11: Scla 4A-12: MD and BL dimensions and comparisons.	258
<i>Chapter 12. The fragmentary right maxilla of the Scladina I-4A juvenile</i>			
Fig. 1: Scla 4A-2 right maxilla.	224	Fig. 15: Bivariate analysis of MD and BL diameters of mandibular canines.	259
Tab. 1: Internasal floor pattern and nasal margin configuration.	225	Fig. 16: Scla 4A-2/P ⁴ unerupted maxillary right second premolar.	260
Tab. 2: Subnasal height and arcade length measurements.	226	Tab. 12: Distinctive anatomical features on maxillary second premolars of different taxa.	261
Fig. 2: Subnasal height, anterior arcade length LA2 and posterior length LP2.	227	Tab. 13: Scla 4A-2/P ⁴ : MD and BL dimensions and comparisons.	261
Fig. 3: Superior and inferior views of the Scladina maxilla.	228	Fig. 17: Bivariate analysis of the MD and BL diameters of maxillary second premolars.	262
Fig. 4: Micro-CT scans data showing the premaxillary suture.	229	Fig. 18: Scla 4A-6 mandibular right first premolar.	263
Tab. 3: Expression of the premaxillary suture.	230	Tab. 14: Distinctive anatomical features on mandibular first premolars of different taxa.	264
<i>Chapter 13. The dentition of the Scladina I-4A juvenile Neandertal</i>			
Tab. 1: List of all the Scladina juvenile teeth.	233	Tab. 15: Scla 4A-6: MD and BL dimensions and comparisons.	265
Tab. 2: Variations in the identification of the teeth.	234	Fig. 19: Bivariate analysis of MD and BL diameters of mandibular first premolars.	265
		Fig. 20: Scla 4A-9/P ₄ unerupted mandibular left second premolar.	267
		Fig. 21: Scla 4A-1/P ₄ unerupted mandibular right second premolar.	268
		Tab. 16: Distinctive anatomical features on mandibular second premolars of different taxa.	269
		Tab. 17: Scla 4A-1/P ₄ & Scla 4A-9/P ₄ : MD and BL dimensions and comparisons.	270

Fig. 22: Bivariate analysis of the MD and BL diameters of mandibular second premolars.	270	Tab. 32: Scla 4A-13: MD and BL dimensions and comparisons.	301
Fig. 23: Scla 4A-4 maxillary right first molar.	272	Fig. 44: Bivariate analysis of the BL and MD diameters of deciduous mandibular second molars.	301
Tab. 18: Distinctive anatomical features on maxillary first molars of different taxa.	273	Fig. 45: Mandible and maxilla with the refitted teeth.	302
Tab. 19: Scla 4A-4: MD and BL dimensions and comparisons.	273	Fig. 46: ECRA of both MD and BL diameters of the maxillary teeth.	303
Fig. 24: Bivariate analysis of the MD and BL diameters of maxillary first molars.	274	Fig. 47: ECRA of both MD and BL diameters of the mandibular teeth.	303
Fig. 25: Scla 4A-3 maxillary right second molar.	275		
Tab. 20: Distinctive anatomical features on maxillary second molars of different taxa.	276	<i>Chapter 14. Enamel thickness in the Scladina I-4A Neandertal teeth</i>	
Tab. 21: Scla 4A-3: MD and BL dimensions and comparisons.	276	Fig. 1-4: Four figures explaining the methodology.	308-309
Fig. 26: Bivariate analysis of MD and BL diameters of maxillary second molars.	277	Tab. 1: Values of the components of 2D enamel thickness measurements.	310
Fig. 27: Scla 4A-8 maxillary right third molar.	278	Tab. 2: Values of the components of 3D enamel thickness measurements.	311
Tab. 22: Distinctive anatomical features on maxillary third molars of different taxa.	279	Tab. 3: 2D enamel thickness in the molar sample and comparisons.	311
Tab. 23: Scla 4A-8: MD and BL dimensions and comparisons.	279	Tab. 4: 3D enamel thickness in the molars and comparisons.	312
Fig. 28: Bivariate analysis of MD and BL diameters of maxillary third molars.	280	Tab. 5: 2D enamel thickness in the canines and premolars and comparisons.	312
Fig. 29: Scla 4A-7 deciduous maxillary right first molar.	281		
Fig. 30: Comparison of the wear of maxillary right dm ¹ , dm ² and M ¹ of Scladina I-4A and La Quina 18.	281	<i>Chapter 15. Molar enamel-dentine junction morphology of the Scladina I-4A juvenile</i>	
Tab. 24: Scla 4A-7: MD and BL dimensions and comparisons.	282	Tab. 1: Comparative sample.	316
Fig. 31: Bivariate analysis of MD and BL diameters of deciduous maxillary first molars.	282	Fig. 1: Three landmark sets on the EDJ surface of Scla 4A-1/M ₂ .	317
Fig. 32: Scla 4A-5 deciduous maxillary right second molar.	284	Fig. 2: Scladina EDJ morphology of mandibular right molars.	318
Tab. 25: Scla 4A-5: MD and BL dimensions and comparisons.	285	Tab. 2: Classification accuracy of Late Pleistocene <i>Homo</i> .	318
Fig. 33: Bivariate analysis of MD and BL diameters of deciduous maxillary second molars.	285	Tab. 3: Classification accuracy when Early and Classic Neandertals are treated separately.	318
Fig. 34: Scla 4A-1/M ₁ mandibular right first molar.	286	Fig. 3: PCA and canonical variate analysis of EDJ shape in different taxa for each mandibular molar.	319
Fig. 35: Scla 4A-9/M ₁ mandibular left first molar.	288	Fig. 4: PCA and canonical variate analysis of EDJ shape for each mandibular molar.	320
Tab. 26: Distinctive anatomical features on mandibular first molars of different taxa.	289	Fig. 5: EDJ mean shape comparison between Scladina, EN and CN, shown from buccal side.	321
Tab. 27: Scla 4A-1/M ₁ & 4A-9/M ₁ : MD and BL dimensions and comparisons.	290	Appendix 1: Classification results for the Neandertal sample using PC 5-20.	324
Fig. 36: Bivariate analysis of the BL and MD diameters of mandibular first molars.	290		
Fig. 37: Scla 4A-1/M ₂ mandibular right second molar.	292	<i>Chapter 16. The Scladina I-4A juvenile, a short-rooted Neandertal</i>	
Fig. 38: Scla 4A-9/M ₂ mandibular left second molar.	293	Tab. 1: Samples of permanent teeth of MIS 5 Neandertals.	326
Tab. 28: Distinctive anatomical features on mandibular second molars of different taxa.	295	Tab. 2a: Root length estimation for missing root apical portions.	327
Tab. 29: Scla 4A-1/M ₂ & 4A-9/M ₂ : MD and BL dimensions and comparisons.	295	Tab. 2b: Root surface area and volume estimations for missing root apical portions.	327
Fig. 39: Bivariate analysis of the BL and MD diameters of mandibular second molars.	296	Fig. 1: Crown and root measurements used in this study.	328
Fig. 40: Scla 4A-1/M ₃ mandibular right third molar.	297	Tab. 3: Description of the external root in the Scladina mixed dentition.	330-331-332-333
Tab. 30: Distinctive anatomical features on mandibular third molars of different taxa.	298	Fig. 2: Maxillary lateral incisor root shape and comparisons.	331
Tab. 31: Scla 4A-1/M ₃ : MD and BL dimensions and comparisons.	298	Fig. 3: 3D surface models of right teeth from Scladina and other Neandertals.	333
Fig. 41: Bivariate analysis of the BL and MD diameters of mandibular third molars.	298	Tab. 4: Descriptive statistics for the labiolingual crown diameter.	334
Fig. 42: Scla 4A-13 deciduous mandibular right second molar.	299	Tab. 5: Descriptive statistics for the root length.	334
Fig. 43: Plot depicting the range of lateral relative enamel thickness index values in different taxa.	301		

Tab. 6: Descriptive statistics for the root surface area.	334	Tab. 2: Raw data for the Scladina Neandertal anterior teeth microwear texture.	366
Tab. 7: Descriptive statistics for the cervical surface area.	334	Tab. 3: Raw data for the Scladina Neandertal molar microwear texture.	367
Tab. 8: Descriptive statistics for the root volume.	335	Fig. 1: Representative 2D photosimulations of the anterior dentitions.	368
Tab. 9: Descriptive statistics for the root pulp volume.	335	Fig. 2: Representative 2D photosimulations of the occlusal molar surfaces.	369
Fig. 4: Adjusted z-scores comparing Scladina and the Krapina variability.	336	Fig. 3: Means of anterior dental microwear texture variables.	370
Fig. 5: Total root volume of the incisors, canines and first molars of different taxa.	336	Fig. 4: Means of molar microwear texture variables.	371
Fig. 6: Proportions of tooth root dentine and pulp volumes.	336	Chapter 19. Neandertal evolution and human origins: a tale from the Scladina I-4A Child	
Fig. 7: Intra-individual proportions in root length of I ₁ , I ₂ and C, compared to M ₁ .	337	Fig. 1: Phylogenetic trees of Neandertal and modern human lineages.	387
Fig. 8: Proportion of the maximum BL crown diameter to the root length.	337	Fig. 2: Pairwise mismatch distributions.	387
Fig. 9: Scla 4A-15 in the broader context of mandibular central incisors.	341	Fig. 3: D. Bonjean and L. Orlando proceed to the amputation of one molar root.	388
Fig. 10: Scla 4A-20 in the broader context of mandibular lateral incisors.	342	Chapter 20. Scladina I-4A in the chronological context of the Neandertals from the Belgium and northwest Europe	
Fig. 11: Scla 4A-12 in the broader context of mandibular canines.	342	Fig. 1: Map of the Belgian Neandertal remains.	395
Fig. 12: Scla 4A-11 in the broader context of maxillary central incisors.	343	Tab. 1: Assessing the quality of data.	396
Fig. 13: Scla 4A-14 in the broader context of maxillary lateral incisors.	343	Fig. 2: La Naulette: sedimentary profile.	397
Fig. 14: Scla 4A-16 in the broader context of maxillary canines.	344	Fig. 3: La Naulette: mandible ulna and third metacarpal.	398
Fig. 15: Molar root morphology and taurodontism.	345	Fig. 4: The Couvin deciduous mandibular right second molar.	399
Chapter 17. Diet and ecology of the Scladina I-4A Neandertal Child: insights from stable isotopes		Fig. 5: Walou: mandibular left first premolar.	399
Tab. 1: Bone nitrogen analysis, collagen extraction, isotopic, and carbon isotopic analysis.	354	Fig. 6: Spy: two skullcaps.	400
Tab. 2: Collagen and bioapatite $\delta^{13}\text{C}$ values of large herbivores from Scladina and comparisons.	355	Fig. 7: Goyet: fragment of mandible and a tooth.	400
Fig. 1: Reconstruction of vegetation type based on $\delta^{13}\text{C}$ of collagen and bioapatite.	356	Fig. 8: Engis 2 skullcap.	401
Fig. 2: H. Bocherens samples the maxillary Scla 4A-2.	356	Fig. 9: Fonds de Forêt: the Neandertal femur.	401
Fig. 3: Isotopic values of bone collagen from Neandertal and faunal remains.	357	Fig. 10: Map of the Classic Neandertal remains of NW Europe.	402
Tab. 3: Isotopic results of different Neandertal specimens from Europe.	358	Fig. 11: Hypothetical chronology of the Meuse River Basin Neandertals.	404
Fig. 4: Comparison of carbon and nitrogen isotopic signatures of European Neandertal collagen.	359	Chapter 21. The Scladina I-4A juvenile Neandertal: a synthesis	
Chapter 18. Dental microwear texture analysis and the diet of the Scladina I-4A Neandertal Child		Fig. 1: The Scladina I-4A juvenile Neandertal remains.	409
Tab. 1: Neandertal specimens compared to the Scladina Child.	365	Fig. 2: Hypotheses attributing Scladina I-4A to MIS 5b or MIS 5a.	411

Authors' addresses



ABRAMS Grégory, MA

Centre archéologique de la grotte Scladina, Archéologie Andennaise. 339d rue Fond des Vaux, 5300 Sclayn, Belgium
direction@scladina.be



Court-Picon Mona, Dr

Belgian Royal Institute of Natural Sciences. 29 rue Vautier, 1000 Bruxelles, Belgium
mcourtpicon@naturalsciences.be



BALESCU Sanda, Dr

Université Lille 1, Sciences et Technologies, Bâtiment de Géographie, Laboratoire Halma-Ipel (CNRS, UMR 8164). 59655 Villeneuve d'Ascq Cedex, France
sanda.balescu@univ-lille1.fr



DAMBLON Freddy, Dr

Belgian Royal Institute of Natural Sciences. 29 rue Vautier, 1000 Bruxelles, Belgium
fdamblon@naturalsciences.be



BENAZZI Stefano, Dr

Department of Cultural Heritage, University of Bologna, 1 Via degli Ariani, 48121 Ravenna, Italy & Department of Human Evolution, Max Planck Institute for Evolutionary Anthropology, 6 Deutscher Platz, 04103 Leipzig, Germany
stefano.benazzi@unibo.it



DELAUNOIS Élise, MA

Musée de la préhistoire en Wallonie/Préhistosite de Ramioul. 128 rue de la Grotte, 4400 Flémalle, Belgium
leptixi@gmail.com



BOCHERENS Hervé, Prof. Dr

Fachbereich Geowissenschaften, Forschungsbereich Paläobiologie – Biogeologie Senckenberg. Center for Human Evolution and Palaeoecology (HEP). Universität Tübingen. 12 Hölderlinstrasse, 72074 Tübingen, Germany
herve.bocherens@uni-tuebingen.de



DE VRIES Dorien, MA

Interdepartmental Doctoral Program in Anthropological Sciences, Stony Brook University, Stony Brook, NY 11794-4364, United States of America
dorien.devries@stonybrook.edu



BONJEAN Dominique, MA

Centre archéologique de la grotte Scladina, Archéologie Andennaise. 339d rue Fond des Vaux, 5300 Sclayn, Belgium
direction@scladina.be



DI MODICA Kévin, Dr

Centre archéologique de la grotte Scladina, Archéologie Andennaise. 339d rue Fond des Vaux, 5300 Sclayn, Belgium
direction@scladina.be

EL ZAATARI Sireen, Dr

Department of Early Prehistory and Quaternary Ecology, Paleoanthropology, Senckenberg Center for Human, Evolution and Paleoecology, Eberhard-Karls-Universität Tübingen. 23 Rümelinstraße, 72070 Tübingen, Germany & Department of Human Evolution, Max Planck Institute for Evolutionary Anthropology, 6 Deutscher Platz, 04103 Leipzig, Germany
sireen_elzaatari@eva.mpg.de



Institute for Evolutionary Anthropology, 6 Deutscher Platz, 04103 Leipzig, Germany
Katerina.harvati@ifu.uni-tuebingen.de

HUBLIN Jean-Jacques, Prof. Dr

Department of Human Evolution, Max Planck Institute for Evolutionary Anthropology, 6 Deutscher Platz, 04103 Leipzig, Germany
hublin@eva.mpg.de

**FALGUÈRES Christophe, Dr**

Département de Préhistoire du Museum National d'Histoire Naturelle, UMR7194 du CNRS. 1 rue R. Panhard, 75013, Paris, France
falguere@mnhn.fr

**KUPCZIK Kornelius, Dr**

Max Planck Weizmann Center for Integrative Archaeology and Anthropology. Max Planck Institute for Evolutionary Anthropology, 6 Deutscher Platz, 04103 Leipzig, Germany
kornelius_kupczik@eva.mpg.de

**HAESAERTS Paul, Dr**

Belgian Royal Institute of Natural Sciences. 29 rue Vautier, 1000 Bruxelles, Belgium
phaesaerts@skynet.be

**KRUEGER Kristin L., Dr**

Department of Anthropology, Loyola University Chicago, 1032 West Sheridan Road, Chicago, Illinois 60660, United States of America
kkrueger4@luc.edu

**HÄNNI Catherine, Dr**

Paléogénomique et Evolution Moléculaire, UMR 5242 CNRS/ Lyon/ ENS de Lyon. Institut de Génomique Fonctionnelle de Lyon, École Normale Supérieure de Lyon. 46, Allée d'Italie, 69364 Lyon Cedex 07, France
catherine.hanni@ens-lyon.fr

**LE CABEC Adeline, Dr**

ESRF – European Synchrotron Radiation Facility. 71 avenue des Martyrs, CS-40220, 38043 Grenoble cedex 09, France & Department of Human Evolution, Max Planck Institute for Evolutionary Anthropology, 6 Deutscher Platz, 04103 Leipzig, Germany
adeline.le-cabec@esrf.fr

**HARVATI Katerina, Prof. Dr**

Department of Early Prehistory and Quaternary Ecology, Paleoanthropology, Senckenberg Center for Human, Evolution and Paleoecology, Eberhard-Karls-Universität Tübingen. 23 Rümelinstraße, 72070 Tübingen, Germany & Department of Human Evolution, Max Planck

**McMILLAN Rhylan, BA (Distinction)**

Vancouver Island University, Nanaimo Campus. 900 Fifth Street, Nanaimo, BC V9R 5S5, Canada
rhy.mcmillan@viu.ca





OLEJNICZAK Anthony J., Dr

605 North High Street,
Columbus OH 43215, United
States of America
anthony.olejniczak@gmail.com



SKINNER Matthew M., Dr

Department of Anthropology,
University College London.
14 Taviton Street, Office 241,
London, WC1H 0BW, United
Kingdom
m.skinner@ucl.ac.uk



ORLANDO Ludovic, Dr

Centre for GeoGenetics,
Paleomix Group. Natural
History Museum of Denmark.
University of Copenhagen,
Øster Voldgade 5-7, 1350
Copenhagen K, Denmark
lorlando@snm.ku.dk



SMITH Tanya M., Dr

Department of Human
Evolutionary Biology. Harvard
University. 11 Divinity Avenue,
Cambridge, MA 02138, United
States of America
tsmith@fas.harvard.edu



OTTE Marcel, Prof. Dr

Service de Préhistoire de
l'Université de Liège. 7 place du
XX Août, bât. A1, 4000 Liège,
Belgium
marcel.otte@ulg.ac.be



TAFFOREAU Paul T., Dr

ESRF - European Synchrotron
Radiation Facility. 71 avenue
des Martyrs, CS-40220, 38043
Grenoble cedex 09, France
paul.tafforeau@esrf.fr



PIRSON Stéphane, Dr

Direction de l'Archéologie,
Service public de Wallonie. 1
rue des Brigades d'Irlande, 5100
Namur
stephane.pirson@spw.wallonie.be



TOUSSAINT Michel, Dr

Direction de l'Archéologie,
Service public de Wallonie. 1
rue des Brigades d'Irlande, 5100
Namur
mtoussaint1866@hotmail.com



REID Donald J., Dr

Department of Anthropology &
Center for the Advanced Study
of Hominid Paleobiology, The
George Washington University,
Washington D.C., United States
of America
donald.reid14@gmail.com



VERNA Christine, Dr

Dynamique de l'Evolution
Humaine : Individus,
Populations, Espèces, CNRS,
UPR 2147. 44 rue de l'Amiral
Mouchez, 75014 Paris
christine.verna@cnr.fr



ROY Cheryl A., MA

Faculty of Social Sciences,
Anthropology Department.
Vancouver Island University,
Nanaimo Campus. 900 Fifth
Street, Nanaimo, BC V9R 5S5,
Canada
caroy@shaw.ca



YOKOYAMA Yuji, Dr

Département de Préhistoire du
Museum National d'Histoire
Naturelle, UMR7194 du CNRS.
1 rue R. Panhard, 75013, Paris,
France



2014

Professional archaeological excavations have been conducted without interruption at Scladina Cave (Andenne, Belgium) for over 30 years. Since 1990, several Neandertal remains have been found: 16 isolated teeth, two hemimandibles, and a maxillary fragment, all belonging to an 8-year-old juvenile. These are the most important Middle Palaeolithic human remains found in Belgium in the 20th century. The aim of this multidisciplinary work, involving 32 researchers from many different countries and institutions, is to present these remains in detail using new methods, such as micro-CT data acquisition, histology, and biogeochemistry. The stratigraphic and palaeoenvironmental context of the remains is also analyzed.

The Scladina I-4A Juvenile Neandertal

Palaeoanthropology and Context

Andenne, Belgium

